SILVERSTEIN □ BASSLER □ MORRILL

SPECTROMETRIC IDENTIFICATION OF ORGANIC COMPOUNDS

FIFTH EDITION

SPECTROMETRIC IDENTIFICATION OF ORGANIC COMPOUNDS

SPECTROMETRIC IDENTIFICATION OF ORGANIC COMPOUNDS

SPECTROMETRIC IDENTIFICATION OF ORGANIC COMPOUNDS

FIFTH EDITION

R. M. Silverstein
SUNY College of Environmental Science and Forestry

G. Clayton Bassler
Los Altos, California

Terence C. Morrill
Rochester Institute of Technology

JOHN WILEY & SONS, INC.

New York ■ Chichester ■ Brisbane ■ Toronto ■ Singapore

ACQUISITIONS EDITOR: Dennis Sawicki
PRODUCTION MANAGER: Joe Ford
PRODUCTION SUPERVISOR: Elizabeth Austin
COPY EDITOR: Jeannette Stiefel
ILLUSTRATION: Edward T. Starr

Library of Congress Cataloging in Publication Data:

Silverstein, R. M. (Robert Milton), 1916–
Spectrometric identification of organic compounds /
R.M. Silverstein, G. Clayton Bassler, Terence C. Morrill. — 5th ed.
p. cm.
Includes bibliographical references and indexes.

1. Spectrum analysis. 2. Organic compounds—Spectra.
I. Bassler, G. Clayton. II. Morrill, Terence C. III. Title.
QD272.S6S55 1991
543'.0858—dc20

90-15514
CIP

Printed in Singapore

10 9 8 7 6 5 4 3 2

PREFACE

The application to spectrometry of Fourier transform procedures together with advances in computer technology require updating of the fourth edition of this textbook. Yet, the format evolved in the first edition (1963) remains intact: discussions of mass, infrared, nuclear magnetic resonance, and ultraviolet spectrometry, followed by problems that involve translations of sets of spectra into chemical structures.

All of the chapters have been extensively revised with outmoded material deleted and relevant new material inserted. Nuclear magnetic resonance (NMR), in particular, has been revised and material has been added in the form of Chapter 6, "New Dimensions in NMR." New problems follow each chapter. Major changes are summarized as follows:

MASS SPECTROMETRY (CHAPTER 2)

The major change in the mass spectrometry chapter is a greatly lessened reliance on the M + 1 and M + 2 isotope peaks for developing the molecular formula, although the use of M + 2 in calculating the number of S, Cl, and Br atoms is retained. The molecular ion peak together with the proton and carbon count from NMR, as well as information from other spectra, frequently serve to postulate a molecular formula; this can, of course, be confirmed by high-resolution mass spectrometry, which in recent years has become more available. New instrumentation and the newer methods of ionizing less volatile molecules are briefly described.

INFRARED (CHAPTER 3)

A brief description of Fourier transform IR (FT IR) spectrometry has been added. Most spectra, many FT IR, are calibrated linear in wavenumbers (cm^{-1}); the nonlinear wavelength (μm) scale is also shown in several spectra with a brief explanation so that older references in the literature can be used.

NUCLEAR MAGNETIC RESONANCE (CHAPTERS 4–6)

For pedagogical reasons and for convenience in using the charts and tables, the ^{1}H and the ^{13}C chapters (Chapters 4 and 5) remain separate. A brief introduction to pulsed NMR was inserted in the ^{1}H chapter. Details of the virtually outmoded off-resonance decoupling technique were deleted from the ^{13}C chapter, as was the discussion of the "crossover" experiment, which has been completely displaced by correlation spectra. The new chapter (Chapter 6) provides a brief introduction to 2-D NMR, and describes the currently useful techniques, both one and two dimensional, with each spectrum illustrated; a brief section (Section 6.6) entitled "Options and How to Use Them" discusses basic strategies for effective use of the new techniques in determining the structure of organic compounds.

ULTRAVIOLET (CHAPTER 7)

The chapter on UV spectrometry is retained despite suggestions that its utility for structure elucidation has been diminished by the increased sophistication of NMR spectrometry. The argument that students should understand structure–UV absorption relationships, the ready access to UV instrumentation, and its ability to give a quick answer to questions of electron delocalization combined in favor of retention.

PROBLEMS (CHAPTERS 8 AND 9)

Chapter 8 comprises three problem sets worked out in detail as preparation for the 58 problem sets in Chapter 9, which are presented in a graded sequence of increasing difficulty. The types of spectra for each problem set are selected to match the level of difficulty; thus, the NMR spectra range from 60 to 500 MHz, and a number of 2-D spectra are included in the more difficult problem sets. Most students enjoy problem solving and rise to the challenge. They also begin to appreciate the elegance of chemical structure as they interpret spectra.

ACKNOWLEDGMENTS

It is a pleasure to acknowledge stimulating discussions with Dr. F. X. Webster, Dr. R. T. LaLonde, and Mr. D. J. Kiemle (SUNY College of Environmental Science and Forestry), Dr. J. Hornak (Rochester Institute of Technology), Dr. H. M. Fales (NIH), and Dr. J. Wronka (Bruker Instruments). High-field NMR spectra, including 2-D spectra, were obtained and processed by Dr. Hornak, Ms. Eileen George, and Ms. Garland Jen (RIT), and by Mr. Kiemle with the help and advice of Dr. P. Borer, Mr. G. J. Heffron, and Dr. Istvan Pelczer, in Dr. G. C. Levy's laboratory (Syracuse University). Dr. D. D. Traficante and Dr. M. A. McGregor (University of Rhode Island) provided us with several 2-D spectra. Dr. LaLonde and Dr. Webster supplied research samples and spectra. Mr. Scott Lee (RIT) obtained GC–MS spectra, and Ms. Joanne Yeh (RIT) and Ms. Garland Jen (RIT) carried out literature searches. Dr. C. J. Pouchert (Aldrich Chemical Co.) furnished the FT IR spectra in Chapter 3. We are indebted to those who allowed us to use their figures and spectra; individual acknowledgments are made at the appropriate place in the text. We thank Mrs. Pauline Tonnesen, Mrs. Shirley Thomas, and Ms. Ragan Feidt (ESF) for their patience with unending revisions to the manuscript; Ms. Marion Bleiler (RIT), who typed Chapter 2, also has our gratitude.

Mr. Dennis Sawicki, our editor at Wiley, has been highly supportive throughout, and the other members of the Wiley staff have been most cooperative. Our many interactions with Jeannette Stiefel, our copy-editor, have resulted in improvements in both the style and the technical content of this edition.

Numerous perceptive comments by the following reviewers resulted in much fine tuning, and we are most grateful: Dr. Albert Burgstrahler (University of Kansas), Dr. William Closson (SUNY Albany), Dr. Henry Fales (NIH), Dr. John Marx (Texas Technological University), Dr. L. G. Wade, Jr. (Whitman College), and Dr. F. X. Webster (ESF).

Finally, how does one adequately thank wives (Olive, Gaylene) who sustain husbands through five editions of a textbook!

R. M. Silverstein
Terence C. Morrill

PREFACE TO FIRST EDITION

During the past several years, we have been engaged in isolating small amounts of organic compounds from complex mixtures and identifying these compounds spectrometrically.

At the suggestion of Dr. A. J. Castro of San Jose State College, we developed a one unit course entitled "Spectrometric Identificiation of Organic Compounds," and presented it to a class of graduate students and industrial chemists during the 1962 spring semester. This book has evolved largely from the material gathered for the course and bears the same title as the course.

We should first like to acknowledge the financial support we received from two sources: The Perkin-Elmer Corporation and Stanford Research Institute.

A large debt of gratitude is owed to our colleagues at Stanford Research Institute. We have taken advantage of the generosity of too many of them to list them individually, but we should like to thank Dr. S. A. Fuqua, in particular, for many helpful discussions of NMR spectrometry. We wish to acknowledge also the cooperation at the management level, of Dr. C. M. Himel, chairman of the Organic Research Department, and Dr. D. M. Coulson, chairman of the Analytical Research Department.

Varian Associates contributed the time and talents of its NMR Applications Laboratory. We are indebted to Mr. N. S. Bhacca, Mr. L. F. Johnson, and Dr. J. N. Shoolery for the NMR spectra and for their generous help with points of interpretation.

The invitation to teach at San Jose State College was extended by Dr. Bert M. Morris, head of the Department of Chemistry, who kindly arranged the administrative details.

The bulk of the manuscript was read by Dr. R. H. Eastman of the Stanford University whose comments were most helpful and are deeply appreciated.

Finally, we want to thank our wives. As a test of a wife's patience, there are few things to compare with an author in the throes of composition. Our wives not only endured, they also encouraged, assisted, and inspired.

R. M. Silverstein
G. C. Bassler

Menlo Park, California
April 1963

CONTENTS

CHAPTER ONE

INTRODUCTION

Our purpose in writing this book is to teach the organic chemist how to identify organic compounds from the complementary information afforded by four types of spectra: mass, infrared, nuclear magnetic resonance, and ultraviolet. Essentially, the molecule in question is subjected to energy probes, and the molecule's responses are recorded as spectra.

The small amounts of pure compounds that can be isolated from complex mixtures by chromatography present a challenge to the chemist concerned with identification and structure elucidation of organic compounds. These techniques have two characteristics: they are rapid, and they are most effective in milligram and microgram quantities. There is neither enough time nor enough material to accommodate the classical manipulations involving sodium fusion, boiling point, refractive index, solubility tests, functional group tests, derivative preparation, mixture melting point, combustion analysis, molecular weight, and degradation with similar manipulations of the degradation products.

Our goal in this book is a rather modest level of sophistication and expertise in each of the four areas of spectrometry. Even this level will permit solution of a gratifying number of identification problems with *no history and no other chemical or physical data*. Of course, in practice other information is usually available: the sample source, details of isolation, a synthesis sequence, or information on analogous material. Often, complex molecules can be identified because partial structures are known, and specific questions can be formulated; the process is more confirmation than identification. In practice, however, difficulties arise in physical handling of minute amounts of compound: trapping, elution from adsorbents, solvent removal, prevention of contamination, and decomposition of unstable compounds. Water, air, stopcock greases, solvent impurities, and plasticizers have frustrated many investigations. The quality of spectra obtained in practice is usually inferior to that presented here.

For pedagogical reasons, we deal only with pure organic compounds. *Pure* in this context is a relative term, and all we can say is the purer, the better. A good criterion of purity for a sufficiently volatile compound (no nonvolatile impurities present) is gas chromatographic homogeneity on both polar and nonpolar substrates in capillary columns. Various forms of liquid-phase chromatography (adsorption and liquid–liquid columns, paper, and thin-layer) are applicable to less volatile compounds. The spectra presented in this book were obtained on purified samples.

In many cases, identification can be made on a fraction of a milligram, or even on several micrograms, of sample. Identification on the milligram scale is routine. Of course, not all molecules yield so easily. Chemical manipulations may be necessary but the information obtained from the four types of spectra will permit intelligent selection of chemical treatment, and the energy probe methodology can be applied to the resulting products.

When we proposed in the first edition of this book that the complementary combination of four types of spectra sufficed to identify organic compounds, we did so in 177 pages, after having explored the possibilities in a series of lectures at San Jose State College, CA, in 1962. The methodology thus elaborated was being rapidly adopted by practicing organic chemists, and we predicted that "in one form or another, such material would soon become part of the training of every organic chemist." In fact, every first year organic textbook now provides an introduction to the four areas of spectrometry. Although our goal is still a *rather modest level of expertise,* there has been some escalation since the first edition, notably ^{13}C NMR and various new one-dimensional (1-D) and two-dimensional (2-D) forms of NMR.

We spend only a minimum amount of time on spectrometric theory and instrumentation, but we do describe the incredible development of computerized instrumentation and the consequences thereof. References and problems are provided at the end of each chapter.

The charts and tables provided throughout the text are quite extensive and are designed for rapid, convenient access. They, together with the large number of spectra—including those of the problem sets—should furnish useful reference material.

CHAPTER TWO

MASS SPECTROMETRY

2.1. INTRODUCTION

In the commonly used electron-impact (EI)mode, a mass spectrometer bombards molecules in the vapor phase with a high-energy electron beam and records the result of electron impact as a spectrum of positive ions separated on the basis of mass/charge (m/z); most of these ions are singly charged. The mass spectrum of benzamide $\left(C_6H_5—\overset{\overset{O}{\|}}{C}—NH_2\right)$ is presented as a computer-plot bar graph of abundance (vertical peak intensity) versus m/z (Fig. 2.1). The positive ion peak at m/z 121 represents the intact molecule (M) less one electron removed by the impacting beam and is designated the molecular ion, $M^{\cdot+}$. The molecular ion in turn produces a series of fragment ions as shown for benzamide:

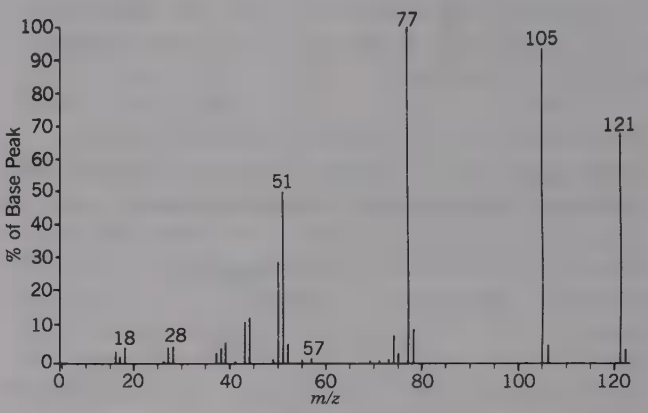

FIGURE 2.1. Computer-generated, electron-impact (EI) mass spectrum of benzamide $\left(C_6H_5—\overset{\overset{O}{\|}}{C}—NH_2\right)$ in bar graph form. Peak abundances as percent of base peak (100%) are reported versus mass to charge (m/z). Peaks of < 0.5% of the base peak were omitted. A Hewlett–Packard HP 5995 96A GC–MS instrument was used.

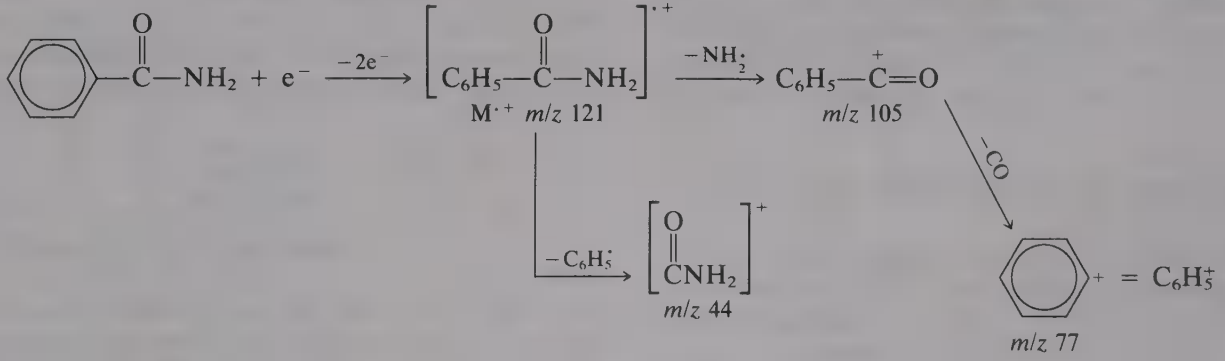

Various methods of producing molecular ions (including the EI method) are discussed in Section 2.5. Details of fragmentation patterns for representative organic compounds are described in Sections 2.7 and 2.10.

In this chapter we describe mass spectrometry (MS) in sufficient detail to appreciate its application to organic structure determination. For more details, mass spectrometry texts and spectral compilations are listed at the end of this chapter.

2.2 INSTRUMENTATION

In this section we describe the EI method for obtaining mass spectra.

The minimum instrumental requirement for the organic chemist is the ability to record the molecular weight of the compound under examination to the nearest whole number. Thus, the recording should show a

peak at, say, mass 400, which is distinguishable from a peak at mass 399 or at mass 401. In order to select possible molecular formulas by measuring isotope peak intensities (see Section 2.4), adjacent peaks must be cleanly separated. Arbitrarily, a valley between two adjacent peaks should not be more than about 10% of the height of the larger peak. This latter degree of resolution is termed "unit" resolution and can be obtained up to masses of approximately 500–2000 on several available instruments.

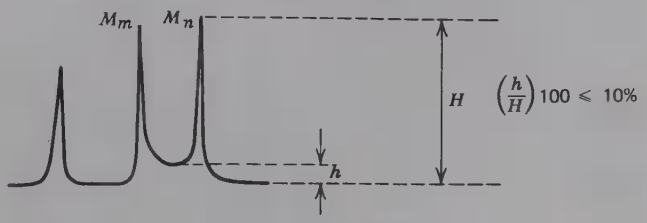

To determine the resolution of an instrument, consider two adjacent peaks of approximately equal intensity. These peaks should be chosen so that the height of the valley between the peaks is less than 10% of the intensity of the peaks. The resolution (R) is

$$R = \frac{M_n}{M_n - M_m}$$

where M_n is the higher mass number of the two peaks, and M_m corresponds to the mass of a peak of one unit less than M_n.

There are two important categories of magnetic-deflection mass spectrometers: low (unit) resolution and high resolution. Low-resolution instruments can be defined arbitrarily as the instruments that separate unit masses up to m/z 2000 [$R = 2000/(2000 - 1999) = 2000$]. Unit mass (or low-resolution) spectra are obtained from these instruments. An instrument is generally considered high resolution if it can resolve two ions differing *in* mass by at least one part in ten to fifteen thousand ($R = 10{,}000 - 15{,}000$). An instrument with 10,000 res-

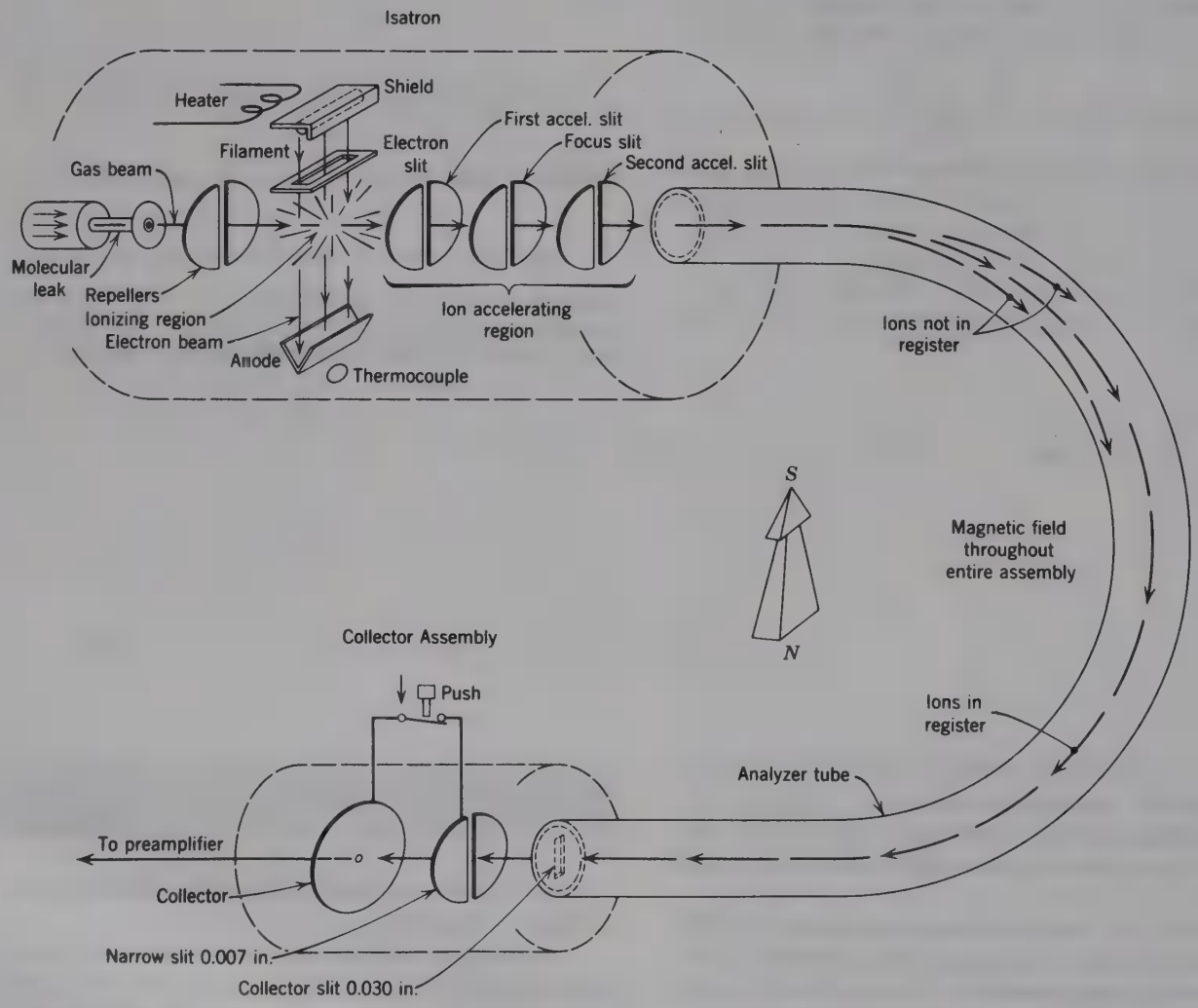

FIGURE 2.2. Schematic diagram of CEC model 21-103 Mass Spectrometer, a single-focusing, 180° sector mass analyzer. The magnetic field is perpendicular to the page.

olution can resolve an ion of mass 500.00 from one of mass 499.95 (R = 500/0.05 = 10,000). This important class of mass spectrometers can measure the mass of an ion with sufficient accuracy to determine its atomic composition. High-resolution mass spectrometry will be discussed only briefly, since the instruments are not available in many laboratories.

A schematic diagram of a 180° single-focusing mass spectrometer is shown in Figure 2.2. There are five component parts in this low-resolution system.

2.2.1 Sample Handling System

This includes a heated inlet and a pumping system so that samples are vaporized under vacuum. Liquids are introduced by hypodermic needle injection into the sample handling system where they are vaporized and bled into the ionization chamber through a small orifice. Insertion of the liquid or solid sample directly into the ionization chamber through a direct inlet probe ("DIP" probe) reduces the limitations imposed by lack of volatility and of thermal stability. Since ionization must take place in the vapor state, some degree of volatility and thermal stability is still required. Reproducible breakdown patterns have been obtained on high molecular weight terpenoids, steroids, polysaccharides, peptides, and alkaloids. Even with these special techniques, a compound must be stable at a temperature at which its vapor pressure is of the order of 10^{-7}–10^{-6} torr. Sample sizes for liquids and solids range from several milligrams to less than a nanogram, depending on the method of introduction and the detector. Special ionization procedures, discussed below, allow direct ionization of solids and solutions. Introduction of a sample through gas chromatography is very convenient and widely used (GC–MS, Section 2.2.9).

2.2.2. Ionization and Accelerating Chambers

The gas stream from the inlet system enters the ionization chamber (operated at a pressure of about 10^{-6}–10^{-5} torr) in which it is bombarded at right angles by an electron beam emitted from a hot filament. Positive ions produced by interaction with the electron beam are forced through the first accelerating slit by a weak electrostatic field. A strong electrostatic field then accelerates the ions to their final velocities. To obtain a spectrum, the applied magnetic field is increased, bringing successively heavier ions into the collector slit. In most instruments, a scan from mass (strictly m/z; see below) 12–500 may be performed in seconds.

2.2.3. Analyzer Tube and Magnet

The analyzer tube is an evacuated (10^{-7}–10^{-8} torr), curved, metal tube through which the ion beam passes from the ion source to the collector. The magnetic field is imposed perpendicular to the plane of the diagram (Fig. 2.2). The main requirement is a uniform magnetic field that can be smoothly varied in strength.

2.2.4. Ion Collector, Amplifier, and Recorder

A typical ion collector consists of collimating slits that direct only one set of ions at a time into the collector where they are detected and amplified by an electron multiplier.

Mass spectrometers provide computer output as bar graphs (Fig. 2.1) and as tabular data. Minor peaks, many of them due to possible impurities, occur at almost every mass unit. The minor peaks are frequently deleted in the bar graph (those < 0.5% have been omitted in Fig. 2.1). A search of the computer's library and a fit to these peaks may either identify the compound or suggest "near structures." Peak heights are proportional to the number of ions of each mass.

As mentioned previously, most ions are singly charged, but multiple ionization does occur and this is indicated by peaks at half-mass units. These represent odd-numbered masses that carry a double charge. For example, a doubly charged ion of mass 89 gives rise to a peak at 89/2 or m/z 44.5.

Sometimes the peaks at the high end of the spectrum may be weak and the background trace indistinct; in this case, a calibration compound may be added to the sample. Perfluorokerosene, which gives a large number of peaks, is often used for calibration.

2.2.5. Mass Spectrometer Classifications

Mass spectrometers for structure elucidation can be classified according to the method of separating the charged particles:

A. Magnetic Field Deflection (Direction Focusing, Section 2.2.6)
   1. Magnetic Field Only (Unit Resolution, Section 2.2.6.1)
   2. Double Focusing (Electrostatic Field and Magnetic Field, High Resolution, Section 2.2.6.2)

B. Quadrupole Mass Spectrometry (Section 2.2.7)
   1. Quadrupole Mass Filter (Section 2.2.7.1)
   2. Quadrupole Ion Storage (Ion Trap) (Section 2.2.7.2)

C. Time of Flight (Section 2.2.8)

2.2.6. Magnetic Field Deflection (Direction Focusing)

2.2.6.1. Magnetic Field Only (Unit Resolution)

In the magnetic-field-deflection mass spectrometer (Fig. 2.2), ions formed in the source are deflected in a curved path by a magnetic field and focused into the detector. Mass separation depends on the strength of the magnetic field, the radius of curvature of the path, and the magnitude of the acceleration voltage.

2.2.6.2. Double Focusing (Electrostatic and Magnetic Field, High Resolution)

The introduction of an electrostatic field after (or before) the magnetic field permits high resolution so that the mass of a particle can be obtained to four decimal places. Figure 2.3 shows a double-focusing instrument. Ions generated in the source are accelerated toward the analyzer. The magnetic field provides directional focusing. The path of the positive ion is again curved by the electric field applied perpendicular to the flight path of the ions. This double focusing provides resolution on the order of 40,000.

2.2.7. Quadrupole Mass Spectrometry

2.2.7.1. Quadrupole Mass Filter

This mass filter uses four voltage-carrying rods (the "quadrupole") (Fig. 2.4*a*). Ions entering from one end travel with constant velocity in the direction parallel to the poles (z direction), but acquire complex oscillations in the x and y directions by application of both a direct current (dc) voltage (V_{dc}) and a radio frequency (rf) voltage (V_{rf}) to the poles. There is a "stable oscillation" that allows a particular ion to pass from one end of the quadrupole to the other without striking the poles; this oscillation is dependent on the m/z ratio of an ion. Therefore, ions of only a single m/z value will traverse the entire length of the filter at a given set of conditions. All other ions will have unstable oscillations and will strike the poles and be lost. Mass scanning is carried out by varying each of the rf and dc frequencies while keeping their ratios constant.

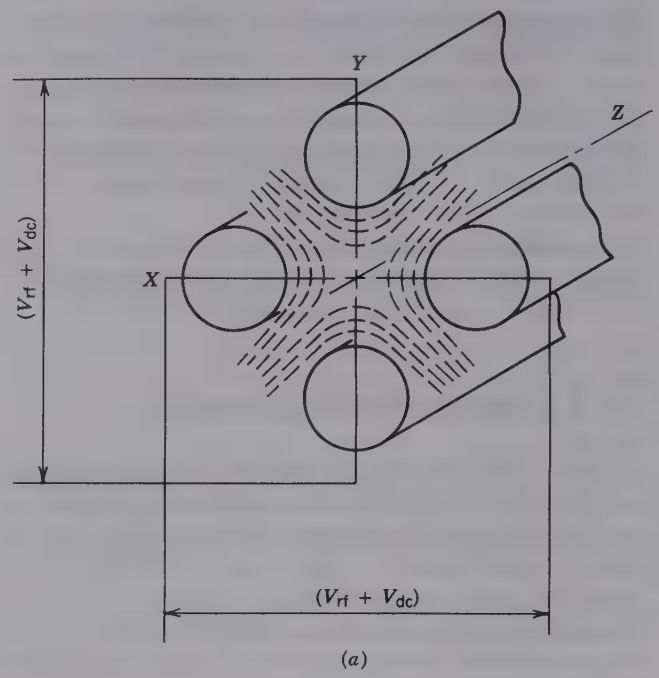

FIGURE 2.4(*a*). Schematic of quadrupole mass filter. Courtesy of Finnigan Corporation.

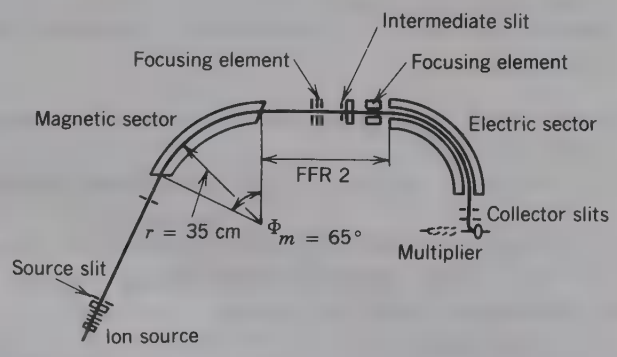

FIGURE 2.3. Schematic of double-focusing mass spectrometer. Courtesy of Finnigan Corporation.

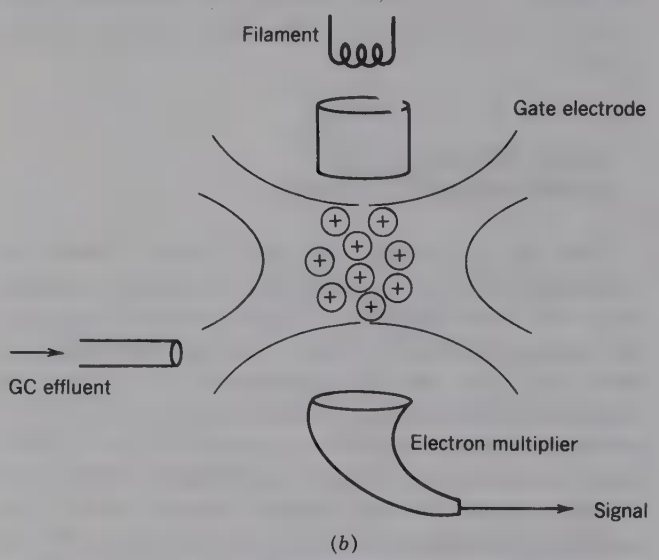

FIGURE 2.4(*b*). Schematic of ion-trap mass spectrometer. Courtesy of Finnigan Corporation.

2.2.7.2. Quadrupole Ion Storage (Ion Trap)

In the ion trap configuration (Fig. 2.4*b*), ionization and mass analysis occur in the same place. Electrons emitted by the filament ionize the sample molecules in the trap; these ions can be scanned over a mass range of 20–650 in a period of one tenth to a few seconds. One electrode is a donut-shaped piece horizontally encircling the chamber, and the other two are hemispherical caps on the top and the bottom of the chamber (Fig. 2.4*c*). The ion trap is widely used as the MS component of a bench top GC–MS unit; it is simple, compact, rugged, and easy to use, but it has at present a 650-dalton upper limit to the mass range. It is easily adapted to chemical ionization (CI, see Section 2.5), but it does not tolerate large samples.

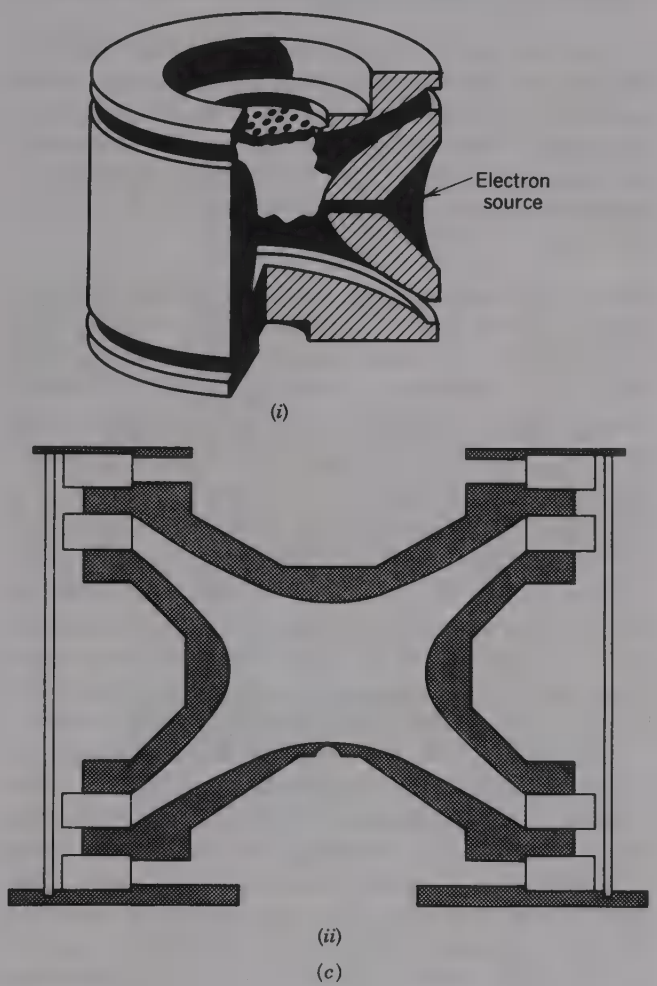

FIGURE 2.4(c). Drawing of an ion-trap mass spectrometer. (*i*) The electrode structure required to produce the 3-D rotationally symmetric quadrupole fields used in the quadrupole ion trap (reproduced by permission of General Electric Corporate Research and Development); (*ii*) cross-sectional view of quadrupole ion trap electrode structure.

2.2.8. Time of Flight

In the time-of-flight (TOF) mass spectrometers, all singly charged particles subjected to a potential difference V attain the same translational energy in electron volts (eV). Thus lighter particles have the shorter TOF over a given distance. The accelerated praticles are passed into a field-free region where they are separated in time by their m/z values and collected. Since arrival times between successive ions can be less than 10^{-7} s, fast electronics are necessary for adequate resolution. Time-of-flight devices are now largely used with sophisticated ionizing methods (FAB, etc.; see Section 2.5) for high-mass measurements.

2.2.9. Gas Chromatography–Mass Spectrometry (GC–MS)

Several firms offer a gas chromatograph coupled to a mass spectrometer (GC–MS) through an interface that enriches the concentration of the sample in the carrier gas by taking advantage of the higher diffusivity of the carrier gas. Scan times are rapid enough so that several MS can be obtained during the elution of a single peak from the GC unit. Capillary GC columns can be connected directly to the mass spectrometer without an enriching device and this allows MS scans to be carried out rapidly to provide several analyses at different points of a GC peak to test for homogeneity. Thus, partially overlapping chromatography peaks can be resolved. High-performance liquid chromatography–mass spectrometry (HPLC–MS) is also available.

2.3. THE MASS SPECTRUM

Mass spectra (EI) are routinely obtained at an electron beam energy of 70 eV. The simplest event that occurs is the removal of a single electron from the molecule in the gas phase by an electron of the electrom beam to form the molecular ion, which is a radical cation ($M^{\cdot +}$). For example, methanol forms a molecular ion.

$$CH_3OH + e \longrightarrow \underset{m/z\ 32}{CH_3OH^{\cdot +}} + 2e$$

When the charge can be localized on one particular atom, the charge is shown on that atom.

$$CH_3\overset{\cdot\cdot}{\underset{\cdot\cdot}{O}}H^{\cdot+}$$

The single dot represents the odd electron. Many of these molecular ions disintegrate in 10^{-10}–10^{-3} s to give, in the simplest case, a positively charged fragment and a radical. A number of fragment ions are thus formed, and each of these can cleave to yield smaller fragments. Again, illustrating with methanol

$$CH_3OH^{\cdot+} \longrightarrow CH_2OH^+ \ (m/z\ 31) + H^\cdot$$

$$CH_3OH^+ \longrightarrow CH_3^+ \ (m/z\ 15) + {\cdot}OH$$

$$CH_2OH^+ \longrightarrow CHO^+ \ (m/z\ 29) + H_2$$

If some of the molecular (parent) ions remain intact long enough to reach the detector, we see a molecular ion peak. It is important to recognize the molecular ion peak because this gives the molecular weight of the compound. With unit resolution, this weight is the molecular weight to the nearest whole number, and not merely the approximation obtained by other molecular weight determinations familiar to the organic chemist.

A mass spectrum is a presentation of the masses of the positively charged fragments (including the molecular ion) versus their relative concentrations. The most intense peak in the spectrum, called the base peak, is assigned a value of 100%, and the intensities (height × sensitivity factor) of the other peaks, including the molecular ion peak, are reported as percentages of the base peak. Of course, the molecular ion peak may sometimes be the base peak. In Figure 2.1, the molecular ion peak is *m/z* 121, and the base peak is *m/z* 77.

A tabular or graphic presentation of a spectrum may be used. A graph has the advantage of presenting patterns that, with experience, can be quickly recognized. However, a graph must be drawn so that there is no difficulty in distinguishing mass units. Mistaking a peak at, say, *m/z* 79 for *m/z* 80 can result in total confusion. Computer programs are available for printing out good line graphs. The grid that we use permits ready recognition of individual mass units as well as patterns. Except for isotope peaks and molecular ion peaks, peaks of very low intensity are not shown unless they have special significance. The molecular ion peak is usually the peak of highest mass number except for the isotope peaks. These isotope peaks are present because a certain number of molecules contain heavier isotopes than the common isotopes. If an ion (m_1) fragments after acceleration but before entering the magnetic field, it was accelerated as mass m_1 but dispersed in the magnetic field as m_2. The resulting ion current will be recorded as a low-intensity, broad peak at apparent mass m^* and is given by

$$m^* = \frac{(m_2)^2}{m_1}$$

The peak caused by the ion current corresponding to mass m^* is called a *metastable ion peak*. Measurement of the mass of the metastable peak affords information that m_2 is derived directly from m_1 by loss of a neutral fragment. Computer displays normally omit metastable ion peaks.

2.4. DETERMINATION OF A MOLECULAR FORMULA

A unique molecular formula (or fragment formula) can often be derived from a sufficiently accurate mass measurement alone (high-resolution mass spectrometry). This is possible because the atomic masses are not integers (see Table 2.1). For example, we can distinguish at a nominal mass of 28 among CO, N_2, CH_2N, and C_2H_4.

^{12}C 12.0000	$^{14}N_2$ 28.0062	^{12}C 12.0000	$^{12}C_2$ 24.0000
^{16}O 15.9949		$^1H_2$ 2.0156	$^1H_4$ 4.0312
27.9949		^{14}N 14.0031	28.0312
		28.0187	

Thus, the mass observed for the molecular ion of CO is the sum of the exact masses of the most abundant isotope of carbon and of oxygen. This differs from a molecular weight of CO based on atomic weights that are the average of weights of all natural isotopes of an element (e.g., C = 12.01, O = 15.999). It is a tedious task to find a molecular formula by arithmetic trial and error from the output of a high-resolution mass spectrometer. Tables (Appendix A), algorithms, and computer programs have been assembled for this purpose.

Appendix A lists the formulas that correspond to either molecules or fragments of mass 12–250. Also listed is the exact formula mass (FM) for each; this mass is obtained by summing the exact mass (Table 2.1) of the most abundant isotope of each element. The mass of the molecular ion is the sum of the masses of the most abundant isotopes (e.g., ^{12}C, ^1H, ^{16}O, etc.) in the molecule. Thus the molecular ion for methane occurs at *m/z* 16 in a unit-resolution spectrum (the molecule has the formula $^{12}C^1H_4$). In addition, molecular species exist that contain less abundant isotopes: $^{13}C^1H_4$ (*m/z* 17, M + 1 peak), $^{12}C^2H^1H_3$(*m/z* 17, M + 1 peak), $^{13}C^2H_1{}^1H_3$ (*m/z* 18, M + 2 peak), and so on. These give rise to peaks at *m/z* 17, 18, and so on. The intensity

TABLE 2.1

Exact Masses of Isotopes

Element	Atomic Weight	Nuclide	Mass
Hydrogen	1.00794	^{1}H	1.00783
		D(^{2}H)	2.01410
Carbon	12.01115	^{12}C	12.00000 (std)
		^{13}C	13.00336
Nitrogen	14.0067	^{14}N	14.0031
		^{15}N	15.0001
Oxygen	15.9994	^{16}O	15.9949
		^{17}O	16.9991
		^{18}O	17.9992
Fluorine	18.9984	^{19}F	18.9984
Silicon	28.0855	^{28}Si	27.9769
		^{29}Si	28.9765
		^{30}Si	29.9738
Phosphorus	30.9738	^{31}P	30.9738
Sulfur	32.066	^{32}S	31.9721
		^{33}S	32.9715
		^{34}S	33.9679
Chlorine	35.4527	^{35}Cl	34.9689
		^{37}Cl	36.9659
Bromine	79.9094	^{79}Br	78.9183
		^{81}Br	80.9163
Iodine	126.9045	^{127}I	126.9045

of these isotope peaks is much less than that of the M peak except when Cl or Br is present: the M + 1 peak for methane, for example, should be 1.14% of the M peak, and the M + 2 peak is negligible. In principle the intensities of the M + 1 and M + 2 peaks can be used to generate formulas. In practice, the observed M + 1 and M + 2 peak intensities are frequently inaccurate, especially in fast scan instruments, and their intensities are often higher than expected because of ion–molecule reactions (see Section 2.5). Moreover, beyond about mass 250, the (M + 1)/(M + 2) data do not differentiate sufficiently among formulas. Therefore, high-resolution, rather than unit mass resolution mass spectrometry should be used to determine molecular formulas. For fairly simple molecules, the low-resolution M peak together with other information (e.g., NMR, Chapters 4–6) often can be used to determine molecular formulas.

Table 2.2 lists the principal stable isotopes of the common elements and their relative abundance cal-

TABLE 2.2

Relative Isotope Abundances of Common Elements

Elements	Isotope	Relative Abundance	Isotope	Relative Abundance	Isotope	Relative Abundance
Carbon	^{12}C	100	^{13}C	1.11		
Hydrogen	^{1}H	100	^{2}H	0.016		
Nitrogen	^{14}N	100	^{15}N	0.38		
Oxygen	^{16}O	100	^{17}O	0.04	^{18}O	0.20
Fluorine	^{19}F	100				
Silicon	^{28}Si	100	^{29}Si	5.10	^{30}Si	3.35
Phosphorus	^{31}P	100				
Sulfur	^{32}S	100	^{33}S	0.78	^{34}S	4.40
Chlorine	^{35}Cl	100			^{37}Cl	32.5
Bromine	^{79}Br	100			^{81}Br	98.0
Iodine	^{127}I	100				

culated on the basis of 100 molecules containing the most common isotope. Note that this presentation differs from many isotope abundance tables in which the sum of all the isotopes of an element adds up to 100%.

Suppose that a compound contains 1 carbon atom. Then for every 100 molecules containing a ^{12}C atom, about 1.11 "molecules" contain a ^{13}C atom, and these molecules will produce an M + 1 peak of about 1.1% the intensity of the molecular ion peak; the ^{2}H atoms present will make an additional very small contribution to the M + 1 peak. If a compound contains 1 sulfur atom, the M + 2 peak will be about 4.4% of the molecular ion peak.

There are special cases in which unit resolution MS can be used to obtain information about molecular formulas. The presence of S, Si, Cl, or Br is usually readily apparent because of a large isotope contribution to M + 2. We shall see that the number of sulfur, silicon, chlorine, and bromine atoms can be determined. Iodine, fluorine, and phosphorus are monoisotopic. Their presence can be deduced from a suspiciously small M + 1 peak relative to the molecular ion peak, from the fragmentation pattern, from the other spectra with which we are concerned, or from the history of the compound.

If only C, H, N, O, F, P, I are present, the approximate expected % (M + 1) and % (M + 2) intensities can be calculated by use of the following formulas:

$$\%\,(M+1) = 100\left[\frac{(M+1)}{(M)}\right]$$

$$\simeq 1.1 \times \text{number of C atoms} + 0.36 \times \text{number of N atoms}$$

$$\%\,(M+2) = 100\left[\frac{(M+2)}{(M)}\right]$$

$$\simeq \frac{(1.1 \times \text{number of C atoms})^2}{200} + 0.20 \times \text{number of O atoms}$$

These equations are useful for cases in which we have a preconceived notion about the molecular formula for the compound of interest. To utilize M + 1 and M + 2 data, the relevant portion of the spectrum should be run at slow scan on very pure samples, and the results of several runs should be averaged.

It is difficult to overemphasize the importance of locating the molecular ion peak. It will be stressed again that this gives an exact numerical molecular weight. Even in cases in which the molecular ion peak is very small, extra information can often lead to identification. This information may be available from the source and history of the sample, from the fragmentation pattern, and from other spectra.

When elements other than C, H, O, and N are present, their kind and number must be determined (see the discussion under the appropriate chemical class in Section 2.10) and their mass subtracted from the molecular weight. The composition of the remainder of the molecule is then determined from Appendix A.

Other types of spectra (IR, NMR, and UV) greatly aid the determination of a molecular formula. For example, as we shall see in Chapter 5, a ^{13}C NMR spectrum is a powerful aid in establishing the molecular formula since it frequently reveals the number of carbon atoms and protons in a molecule.

2.5. RECOGNITION OF THE MOLECULAR ION PEAK

Quite often, recognition of the molecular ion peak (M) poses a problem. The peak may be very weak or it may not appear at all; how can we be sure that it is the molecular ion peak and not a fragment peak or an impurity? Often the best solution is to obtain a chemical ionization spectrum (see below in this section). The usual result is an intense peak at M + 1 and little fragmentation.

Many peaks can be ruled out as possible molecular ions simply on grounds of reasonable structure requirements. The "nitrogen rule" is often helpful. It states that a molecule of even-numbered molecular weight must contain either no nitrogen or an even number of nitrogen atoms; an odd-numbered molecular weight requires an odd number of nitrogen atoms. This rule holds for all compounds containing carbon, hydrogen, oxygen, nitrogen, sulfur, and the halogens, as well as many of the less usual atoms such as phosphorus, boron, silicon, arsenic, and the alkaline earths. A useful corollary states that fragmentation at a single bond gives an odd-numbered ion fragment from an even-numbered molecular ion, and an even-numbered ion fragment from an odd-numbered molecular ion. For this corollary to hold, the ion fragment must contain all of the nitrogen (if any) of the molecular ion. Consideration of the breakdown pattern coupled with other information will also assist in identifying molecular ions. It should be kept in mind that Appendix A contains fragment formulas as well as molecular formulas. Some of the formulas may be regarded as trivial when used in attempts to solve practical problems.

The intensity of the molecular ion peak depends on the stability of the molecular ion. The most stable molecular ions are those of purely aromatic systems. If

substituents that have favorable modes of cleavage are present, the molecular ion peak will be less intense, and the fragment peaks relatively more intense. In general, the following group of compounds will, in order of decreasing ability, give prominent molecular ion peaks: aromatic compounds > conjugated alkenes > cyclic compounds > organic sulfides > short, normal alkanes > mercaptans. Recognizable molecular ions are usually produced for these compound in order of decreasing ability: ketones > amines > esters > ethers > carboxylic acids ~ aldehydes ~ amides ~ halides. The molecular ion is frequently not detectable in aliphatic alcohols, nitrites, nitrates, nitro compounds, nitriles, and in highly branched compounds.

The presence of an M − 15 peak (loss of CH_3), or an M − 18 peak (loss of H_2O), or an M − 31 peak (loss of OCH_3 from methyl esters), and so on, is taken as confirmation of a molecular ion peak. An M − 1 peak is common, and occasionally an M − 2 peak (loss of H_2 by either fragmentation or thermolysis), or even a rare M − 3 peak (from alcohols) is reasonable. Peaks in the range of M − 3 to M − 14, however, indicate that contaminants may be present or that the presumed molecular ion peak is actually a fragment ion peak. Losses of fragments of masses 19–25 are also unlikely (except for loss of F = 19 or HF = 20 from fluorinated compounds). Loss of 16 (O), 17 (OH), or 18 (H_2O) are likely only if an oxygen atom is in the molecule.

In addition to the EI method described above, several promising techniques were developed for obtaining and locating the molecular ion peak for compounds that give very weak or nonexistant molecular ions by EI.

In chemical ionization (CI), the sample is introduced at about 1-torr pressure with a carrier gas, such as methane. The methane is ionized by electron impact to the primary ions: CH_4^+ + CH_3^+, and so on. These react with the excess methane to give secondary ions.

$$CH_4^+ + CH_4 \longrightarrow CH_5^+ \quad \text{and} \quad CH_3\cdot$$

$$CH_3^+ + CH_4 \longrightarrow C_2H_5^+ \quad \text{and} \quad H_2$$

$$CH_4 + C_2H_5^+ \longrightarrow C_3H_5^+ + 2H_2$$

The secondary ions react with the sample (RH).

$$CH_5^+ + RH \longrightarrow RH_2^+ + CH_4$$

$$C_2H_5^+ + RH \longrightarrow RH_2^+ + C_2H_4$$

These CI M + 1 ions (*quasimolecular ions*) are often prominent. Chemical ionization spectra sometimes have prominent M − 1 ions because of hydride ion abstraction by CH_5^+. Since the M + 1 ions are chemically produced, they do not have the great excess of energy associated with ionization by electron impact, and they undergo less fragmentation. For example, the EI spectrum of 3,4-dimethoxyacetophenone shows, in addition to the molecular ion at *m/z* 180, 49 fragment peaks in the range of *m/z* 40–167; these include the base peak at *m/z* 165 and prominent peaks at *m/z* 137 and *m/z* 77. The CH_4 induced CI spectrum shows the quasimolecular ion (MH^+, *m/z* 181) as the base peak (100%), and virtually the only other peaks, each of just a few percent intensity, are the molecular ion peak, *m/z* 180, and *m/z* 209 and 221 peaks due to reaction with carbocations.

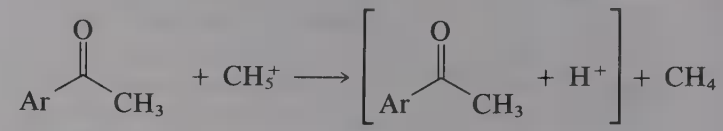

Ar = 3,4-Dimethoxyphenyl *m/z* 181 (base peak)

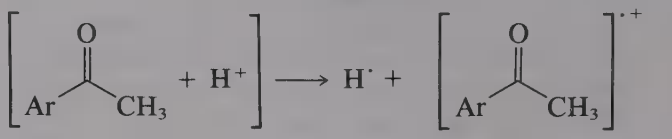

m/z 180 (molecular ion)

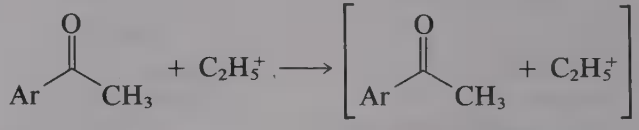

m/z 209

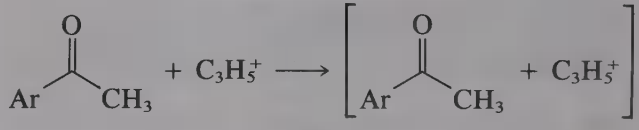

m/z 221

The energy content of the various secondary ions (from, respectively, CH_4, isobutane, and ammonia) decreases in this order:

$$CH_5^+ > t\text{-}C_4H_9^+ > NH_4^+$$

Thus by choice of carrier gas, we can control the tendency of the CI-produced MH^+ ion to fragment. For example, when methane is the carrier gas, dioctyl phthalate shows its MH^+ peak (*m/z* 391) as the base peak; more importantly, the fragment peaks (e.g., *m/z* 113 and 149) are 30–60% of the intensity of the base peak. When isobutane is used, the MH^+ peak is large and the fragment peaks are only roughly 5% as intense as the MH^+ peak.

Molecular ions can be obtained from samples of very low volatility by the field desorption (FD) technique. Here the solid sample is placed directly on the

field ion emitter. This ion source is operated only slightly above room temperature, and the ions produced thus have little or no internal energy. Since the internal energy necessary for fragmentation is not present, observable molecular ions are formed. Sometimes $(M + H)^+$ or $(M + Na)^+$ peaks are observed. These ions are desorbed from the solid by a strong electric field. Field desorption techniques have been used for analyzing nonpolar synthetic polymers with molecular weights of the order of 10,000 dalton, but there is a much lower molecular weight limit for polar biopolymers; here fast-atom bombardment procedures (below) are superior.

Polar molecules, such as peptides, with molecular weights up to 10,000 daltons can be analyzed by a "soft" ionization technique called fast-atom bombardment (FAB, Fig. 2.5). The bombarding beam consists of xenon (or argon) atoms of high translational energy

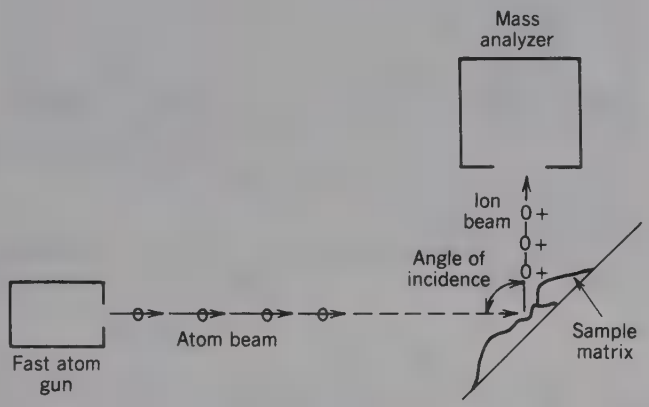

FIGURE 2.5 Schematic for FAB Mass Spectrometry. The intense activity at the surface of the sample produces neutrals, sample ions, ions from the matrix, etc. Only the ions are accelerated toward the analyzer.

(Xe). This beam is produced by first ionizing xenon atoms with electrons to give xenon radical cations:

$$Xe \xrightarrow{e} Xe^{\cdot +} + 2e$$

The radical cations are accelerated to 6–10 keV to give radical cations of high translational energy $(Xe)^{\cdot +}$, which are then passed through xenon. During this passage, the charged high energy xenon obtain electrons from the atoms to become high-energy xenon atoms ($\vec{Xe}$).

$$Xe^{\cdot +} \text{ accelerate } \vec{Xe}^{\cdot +}$$

$$\vec{Xe}^{\cdot +} + Xe \longrightarrow \vec{Xe} + Xe^{\cdot +}$$

The compound of interest is dissolved in a high-boiling viscous solvent such as glycerol and the compound is ionized by the high-energy beam of xenon atoms ($\vec{Xe}$). Ionization by translational energy minimizes the amount of vibrational excitation and this results in less destruction of the ionized molecules. The polar solvent promotes ionization and allows diffusion of fresh sample to the surface. Thus ions are produced which last 20–30 minutes, in contrast to a few seconds for ions produced from solid samples.

The molecular ion itself is usually not seen, but adduct ions such as $[M+H]^+$ are prominent. Other adduct ions can be formed from salt impurities or upon addition of salts such as NaCl or KCl, which give $[M+Na]^+$ and $[M+K]^+$ adduct ions. Glycerol adduct ions are prominent and do not complicate the spectrum. Fragment ions are prominent and useful. Watson (see references) may be consulted for a good discussion of the interpretation of FAB spectra.

2.6. USE OF THE MOLECULAR FORMULA

If organic chemists had to choose a single item of information above all others that are usually available from spectra or from chemical manipulations, they would certainly choose the molecular formula.

In addition to the kinds and numbers of atoms, the molecular formula gives the index of hydrogen deficiency. The index of hydrogen deficiency is the number of *pairs* of hydrogen atoms that must be removed from the "saturated" formula (e.g., C_nH_{2n+2} for alkanes) to produce the molecular formula of the compound of interest. The index of hydrogen deficiency is also called the number of "sites (or degrees) of unsaturation"; this description is incomplete since hydrogen deficiency can be due to cyclic structure features as well as to multiple bonds. The index is thus the sum of the number of rings, the number of double bonds, and twice the number of triple bonds.

The index of hydrogen deficiency can be calculated for compounds containing carbon, hydrogen, nitrogen, halogen, oxygen, and sulfur from the formula

$$\text{Index} = \text{carbons} - \frac{\text{hydrogens}}{2} - \frac{\text{halogens}}{2} + \frac{\text{nitrogens}}{2} + 1$$

Thus, the compound C_7H_7NO has an index of $7 - 3.5 + 0.5 + 1 = 5$. Note that divalent atoms (oxygen and sulfur) are not counted in the formula.

For the generalized molecular formula $\alpha_I\beta_{II}\gamma_{III}\delta_{IV}$, the index = IV $-$ $\frac{1}{2}$I + $\frac{1}{2}$III + 1, where

α is H, D, or halogen (i.e., any monovalent atom)
β is O, S, or any other bivalent atom
γ is N, P, or any other trivalent atom
δ is C, Si, or any other tetravalent atom

The numerals I–IV designate the numbers of the mono-, di-, tri-, and tetravalent atoms, respectively.

For simple molecular formulas, we can arrive at the index by comparison of the formula of interest with the molecular formula of the corresponding saturated compound. Compare C_6H_6 and C_6H_{14}; the index is 4 for the former and 0 for the latter.

Polar structures must be used for compounds containing an atom in a higher valence state, such as sulfur or phosphorus. Thus, if we treat sulfur in dimethyl sulfoxide (DMSO) formally as a divalent atom, the calculated index, 0, is compatible with the structure

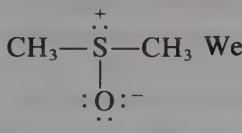

We must use only formulas with filled valence shells; that is, the Lewis octet rule must be obeyed.

Similarly, if we treat the nitrogen in nitromethane as a trivalent atom, the index is 1, which is compatible with

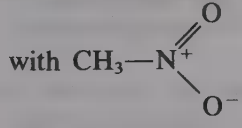

. If we treat phosphorus in triphenylphosphine oxide as trivalent, the index is 12, which fits $(C_6H_5)_3P^+—O^-$. As an example, let us consider the molecular formula $C_{13}H_9N_2O_4BrS$. The index of hydrogen deficiency would be $13 - \frac{10}{2} + \frac{2}{2} + 1 = 10$ and a consistent structure would be

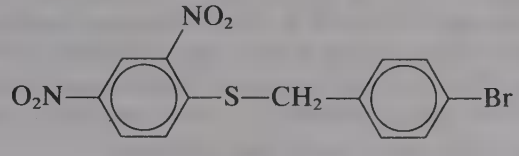

(Index of hydrogen deficiency = 4 per benzene ring and 1 per NO_2 group.)

The formula above for the index can be applied to fragment ions as well as to the molecular ion. When it is applied to even-electron (all electrons paired) ions, the result is always an odd multiple of 0.5. As an example, consider $C_7H_5O^+$ with an index of 5.5. A reasonable structure is

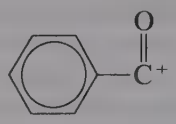

since $5\frac{1}{2}$ pairs of hydrogen atoms would be necessary to obtain the corresponding saturated formula $C_7H_{16}O$ ($C_nH_{2n+2}O$). Odd-electron fragment ions will always give integer values of the index.

Terpenes often present a choice between a double bond and a ring structure. This question can readily be resolved on a microgram scale by catalytically hydrogenating the compound and rerunning the mass spectrum. If no other easily reducible groups are present, the increase in the mass of the molecular ion peak is a measure of the number of double bonds; and other "unsaturated sites" must be rings.

Such simple considerations give the chemist very ready information about structure. As another example, a compound containing a single oxygen atom might quickly be determined to be an ether or a carbonyl compound simply by counting "unsaturated sites."

2.7. FRAGMENTATION

As a first impression, fragmenting a molecule with a huge excess of energy would seem a brute-force approach to molecular structure. The rationalizations used to correlate spectral patterns with structure, however, can only be described as elegant, though sometimes arbitrary. The insight of such pioneers as McLafferty, Beynon, Stenhagen, Ryhage, and Meyerson led to a number of rational mechanisms for fragmentation. These were masterfully summarized and elaborated by Biemann, Djerassi, Budzikiewicz, and others.

Generally, the tendency is to represent the molecular ion with a delocalized charge. Djerassi's approach is to localize the positive charge on either a π bond (except in conjugated systems), or on a heteroatom. Whether or not this concept is totally rigorous, it is at the least a *pedagogic tour de force*. We shall use such locally charged molecular ions in this book.

Structures **A** and **B**, for example, represent the molecular ion of cyclohexadiene. Compound **A** is a de-

localized structure with one less electron than the original uncharged diene; both the electron and the positive charge are delocalized over the π system. Since the electron removed to form the molecular ion is a π electron, other structures, such as **B** or **C** (valence bond structures) can be used. Structures such as **B** and **C** localize the electron and the positive charge, and thus are useful for describing fragmentation processes.

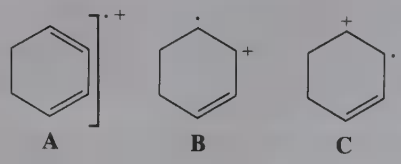

A **B** **C**

Fragmentation is initiated by electron impact. Only a small part of the driving force for fragmentation is energy transferred as the result of the impact. The major driving force is the cation–radical character that is imposed upon the structure.

Fragmentation of the odd-electron molecular ion (radical–cation, $M^{\cdot +}$) may occur by homolytic or heterolytic cleavage of a single bond. In homolytic cleavage, each electron "moves" independently as shown by a (single-barbed) fishhook; the fragments here are an even-electron cation and a free radical (odd electron).

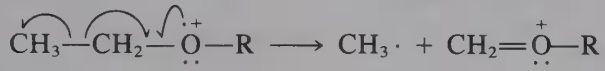

To prevent clutter, only one of each pair of fishhooks need be shown:

In heterolytic cleavage, a pair of electrons "move" together toward the charged site as shown by the conventional curved arrow; the fragments are again an even-electron cation and a radical, but here the final charge site is on the alkyl product.

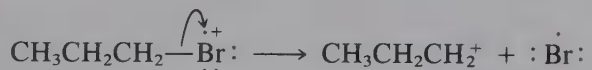

In the absence of rings (whose fragmentation requires cleavage of two or more bonds), most of the prominent fragments in a mass spectrum are even-electron cations formed as above by a single cleavage. Further fragmentation of an even-electron cation usually results in another even-electron cation and an even-electron neutral molecule or fragment.

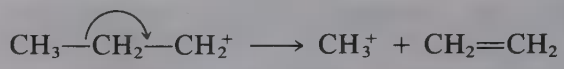

Simultaneous or consecutive cleavage of several bonds may occur when energy benefits accrue from formation of a highly stabilized cation and/or a stable radical, or a neutral molecule, often through a well-defined low-energy pathway. These are treated in Section 2.8 (rearrangements) and in Section 2.10 under individual chemical classes.

The probability of cleavage of a particular bond is related to the bond strength, to the possibility of low-energy transitions, and to the stability of the fragments both charged and uncharged formed in the fragmentation process. Our knowledge of pyrolytic cleavages can be used, to some extent, in order to predict likely modes of cleavage of the molecular ion. Because of the extremely low pressure in the mass spectrometer, there are very few fragment collisions; we are dealing largely with unimolecular decompositions. This assumption, backed by a file of reference spectra, is the basis for the vast amount of information available from the fragmentation pattern of a molecule. Whereas conventional organic chemistry deals with reactions initiated by chemical reagents, by thermal energy, or by light, mass spectrometry is concerned with the consequences suffered by an organic molecule at a vapor pressure of about 10^{-5} mm Hg struck by an ionizing electron beam.

A number of general rules for predicting prominent peaks in EI spectra can be written and rationalized by using standard concepts of physical organic chemistry.

1. The relative height of the molecular ion peak is greatest for the straight-chain compound and decreases as the degree of branching increases (see Rule 3).
2. The relative height of the molecular ion peak usually decreases with increasing molecular weight in a homologous series. Fatty esters appear to be an exception.
3. Cleavage is favored at alkyl substituted carbon atoms; the more substituted, the more likely is cleavage. This is a consequence of the increased stability of a tertiary carbocation over a secondary, which in turn is more stable than a primary.

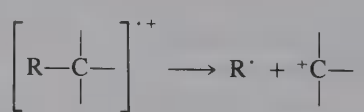

Cation stability order:

$$CH_3^+ < R'CH_2^+ < R_2'CH^+ < R_3'C^+$$

Generally, the largest substituent at a branch is eliminated most readily as a radical, presumably because a long-chain radical can achieve some stability by delocalization of the lone electron.

4. Double bonds, cyclic structures, and especially aromatic (or heteroaromatic) rings stabilize the molecular ion, and thus increase the probability of its appearance.
5. Double bonds favor allylic cleavage and give the resonance-stabilized allylic carbocation. This rule does not hold for simple alkenes because of the ready migration of the double bond, but it does hold for cycloalkenes.

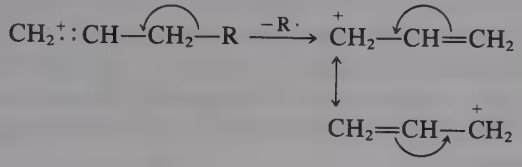

6. Saturated rings tend to lose alkyl side chains at the α bond. This is merely a special case of branching (Rule 3). The positive charge tends to stay with the ring fragment.

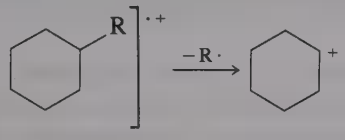

Unsaturated rings can undergo a *retro*-Diels–Alder reaction:

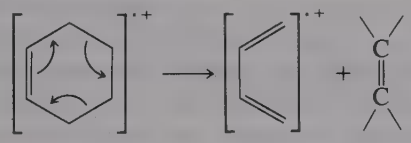

7. In alkyl-substituted aromatic compounds, cleavage is very probable at the bond β to the ring, giving the resonance-stabilized benzyl ion or, more likely, the tropylium ion:

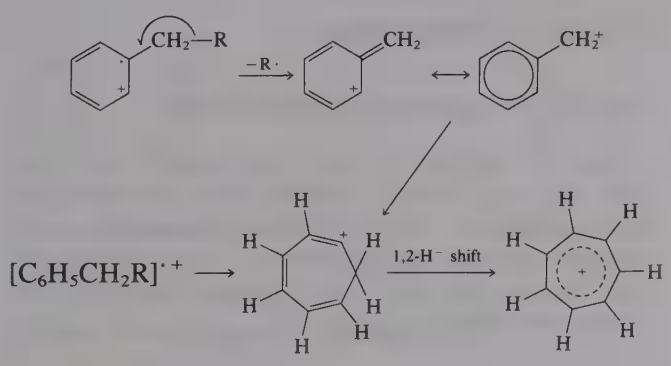

8. The C—C bonds next to a heteroatom are frequently cleaved, leaving the charge on the fragment containing the heteroatom whose nonbonding electrons provide resonance stabilization.

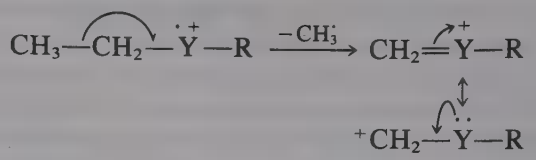

Y = O, N, or S

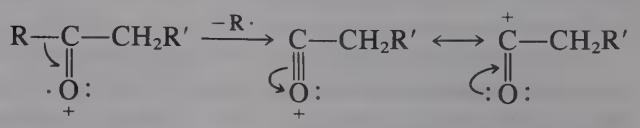

9. Cleavage is often associated with elimination of small stable neutral molecules, such as carbon monoxide, olefins, water, ammonia, hydrogen sulfide, hydrogen cyanide, mercaptans, ketene or alcohols, often with rearrangement (Section 2.8).

It should be kept in mind that the fragmentation rules above apply to EI mass spectrometry. Since other ionizing (CI, etc.) techniques often produce molecular ions with much lower energy or quasimolecular ions with very different fragmentation patterns, different rules govern the fragmentation of these molecular ions.

2.8. REARRANGEMENTS

Rearrangement ions are fragments whose origin cannot be described by simple cleavage of bonds in the molecular ion, but are a result of intramolecular atomic rearrangement during fragmentation. Rearrangements involving migration of hydrogen atoms in molecules that contain a heteroatom are especially common. One important example is the so-called McLafferty rearrangement.

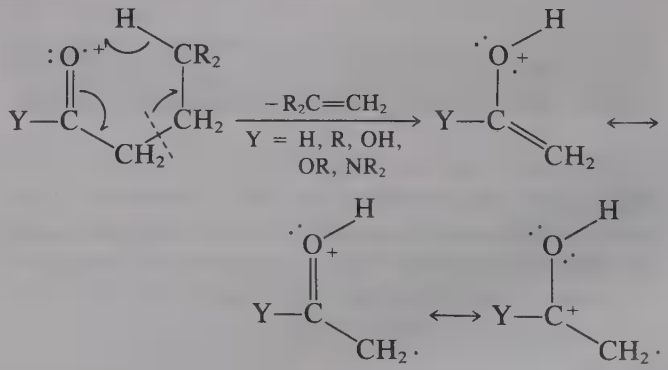

To undergo a McLafferty rearrangement, a molecule must possess an appropriately located heteroatom (e.g., O), a π system (usually a double bond), and an abstractable hydrogen atom γ to the C=O system.

Such rearrangements often account for prominent characteristic peaks and are consequently very useful for our purpose. They can frequently be rationalized on the basis of low-energy transitions and increased stability of the products. Rearrangements resulting in elimination of a stable neutral molecule are common (e.g., the alkene product in the McLafferty rearrangement) and will be encountered in the discussion of mass spectra of chemical classes.

Rearrangement peaks can be recognized by considering the mass (m/z) number for fragment ions and for their corresponding molecular ions. A simple (no rearrangement) cleavage of an even-numbered molecular ion gives an odd-numbered fragment ion and simple cleavage of an odd-numbered molecular ion gives an even-numbered fragment. Observation of a fragment ion mass different by 1 unit from that expected for a fragment resulting from simple cleavage (e.g., an even-numbered fragment mass from an even-numbered molecular ion mass) indicates rearrangement of hydrogen has accompanied fragmentation. Rearrangement peaks may be recognized by considering the corollary to the "nitrogen rule" (Section 2.5). Thus, an even-numbered peak derived from an even-numbered molecular ion is a result of two cleavages, which may involve a rearrangement.

"Random" rearrangements of hydrocarbons were noted by the early mass spectrometrists in the petroleum industry. For example,

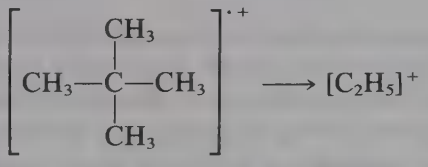

These rearrangements defy straightforward explanations.

2.9. DERIVATIVES

If a compound has low volatility or if the parent mass cannot be determined, it may be possible to prepare a suitable derivative. The derivative selected should provide enhanced volatility, a predictable mode of cleavage, a simplified fragmentation pattern, or an increased stability of the molecular ion.

Compounds containing several polar groups may have very low volatility (e.g., sugars, peptides, and dibasic carboxylic acids). Acetylation of hydroxyl and amino groups and methylation of free acids are obvious and effective choices to increase volatility and give characteristic peaks. Perhaps less immediately obvious is the use of trimethylsilyl derivatives of hydroxyl, amino, sulfhydryl, and carboxylic acid groups. Trimethylsilyl derivatives of sugars and of amino acids are volatile enough to pass through GC columns. The molecular ion peak of trimethylsilyl derivatives may not always be present, but the M − 15 peak due to cleavage of one of the Si—CH_3 bonds is often prominent.

Reduction of ketones to hydrocarbons has been used to elucidate the carbon skeleton of the ketone molecule. Polypeptides have been reduced with $LiAlH_4$ to give volatile polyamino alcohols with predictable fragmentation patterns. Methylation and trifluoroacetylation of tri- and tetrapeptides have lead to useful mass spectra.

2.10. MASS SPECTRA OF SOME CHEMICAL CLASSES

Mass spectra of a number of chemical classes are briefly described in this section in terms of the most useful generalizations for identification. For more details, the references cited (in particular, the thorough treatment by Budzikiewicz, Djerassi, and Williams) should be consulted. Databases are available both from publishers and as part of instrument capabilities. The references are selective rather than comprehensive. A table of frequently encountered fragment ions is given in Appendix B. A table of fragments (uncharged) that are commonly eliminated and some structural inferences are presented in Appendix C. More exhaustive listings of common fragment ions have been compiled in the books by Hamming and Foster and by McLafferty. The cleavage patterns described here in Section 2.10 are for EI spectra, unless stated otherwise.

2.10.1. Hydrocarbons

2.10.1.1. Saturated Hydrocarbons

Most of the work in mass spectrometry has been done on hydrocarbons of interest to the petroleum industry. Rules 1–3 (p. 14) apply quite generally; rearrangement peaks, though common, are not usually intense (random rearrangements), and numerous reference spectra are available.

The molecular ion peak of a straight-chain, saturated hydrocarbon is always present, though of low intensity for long-chain compounds. The fragmentation pattern is characterized by clusters of peaks, and the corresponding peaks of each cluster are 14 (CH_2) mass units apart. The largest peak in each cluster represents a C_nH_{2n+1} fragment and thus occurs at $m/z = 14n + 1$; this is accompanied by C_nH_{2n} and C_nH_{2n-1} fragments. The most abundant fragments are at C_3 and C_4, and the fragment abundances decrease in a smooth curve down to M − C_2H_5; the M − CH_3 peak is characteristically very weak or missing. Compounds containing more than 8 carbon atoms show fairly similar spectra; identification then depends on the molecular ion peak.

Spectra of branched saturated hydrocarbons are grossly similar to those of straight-chain compounds, but the smooth curve of decreasing intensities is broken by preferred fragmentation at each branch. The smooth curve for the *n*-alkane in Figure 2.6*a* is in contrast to the discontinuity at C_{10} for the branched alkane (Fig. 2.6*b*). This discontinuity indicates that the longest branch of 5-methylpentadecane has 10 carbon atoms.

In Figure 2.6*b*, the peaks at *m/z* 169 and 85 represent cleavage on either side of the branch with charge retention on the substituted carbon atom. Subtraction of the molecular weight from the sum of these fragments accounts for the fragment —CH—CH_3. Again, we appreciate the absence of a C_{11} unit, which cannot form by a single cleavage. Finally, the presence of a distinct M − 15 peak also indicates a methyl branch. The fragment resulting from cleavage at a branch tends to lose a single hydrogen atom so that the resulting C_nH_{2n} peak is prominent and sometimes more intense than the corresponding C_nH_{2n+1} peak. Random rearrangements are common, and the use of reference compounds and GC retention time for final identification is good practice.

A saturated ring in a hydrocarbon increases the relative intensity of the molecular ion peak and favors cleavage at the bond connecting the ring to the rest of the molecule (Rule 6, p. 15). Fragmentation of the ring is usually characterized by loss of two carbon atoms as C_2H_4 (28) and C_2H_5 (29). This tendency to lose even numbered fragments, such as C_2H_4, gives a spectrum that contains a greater proportion of even-numbered mass ions than the spectrum of an acyclic hydrocarbon. As in branched hydrocarbons, C—C

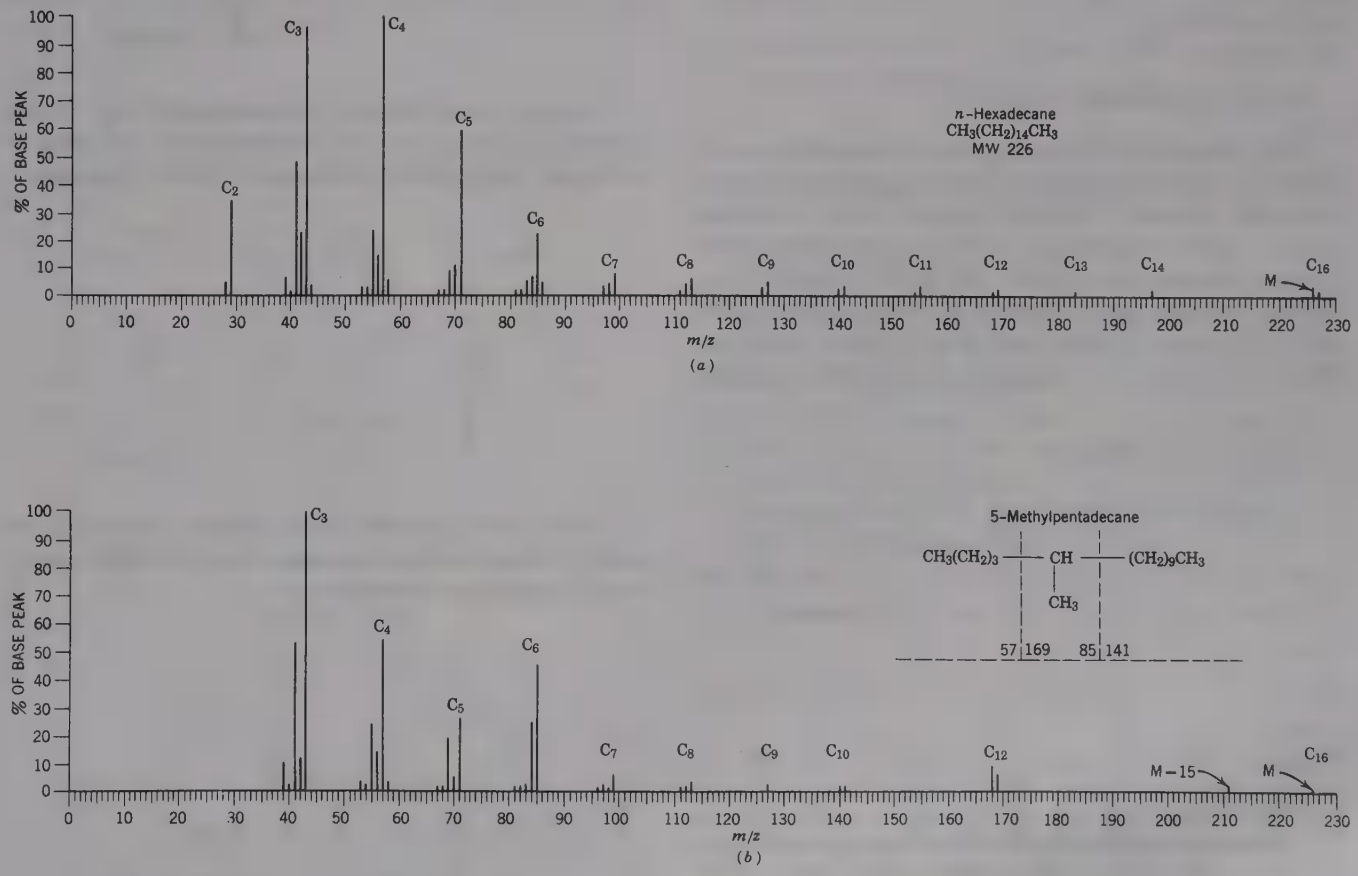

FIGURE 2.6(*a*–*b*). Isomeric C_{16} hydrocarbons.

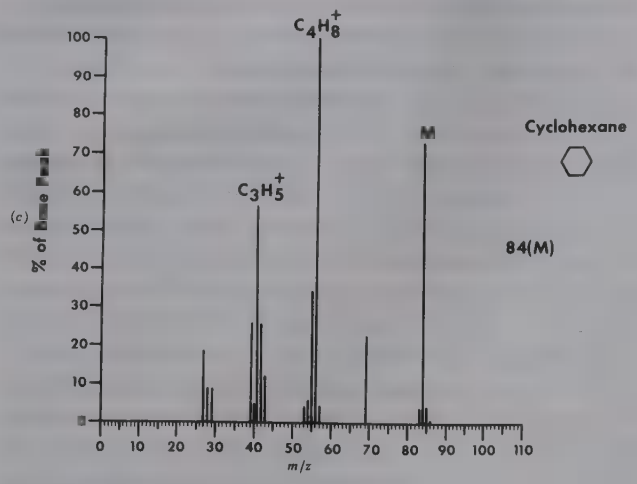

FIGURE 2.6c. Cyclohexane.

cleavage is accompanied by loss of a hydrogen atom. The characteristic peaks are therefore in the C_nH_{2n-1} and C_nH_{2n-2} series.

The mass spectrum of cyclohexane (Fig. 2.6*c*) shows a much more intense molecular ion than those of acyclic compounds, since fragmentation requires the cleavage of two carbon–carbon bonds. This spectrum has its base peak at *m/z* 56 (due to loss of C_2H_4) and a large peak at *m/z* 41, which is a fragment in the C_nH_{2n-1} series with $n = 3$.

2.10.1.2. Alkenes (Olefins)

The molecular ion peak of alkenes, especially polyalkenes, is usually distinct. Location of the double bond in acyclic alkenes is difficult because of its facile migration in the fragments. In cyclic (especially polycyclic) alkenes, location of the double bond is frequently evident as a result of a strong tendency for allylic cleavage without much double-bond migration (Rule 5, Section 2.7). Conjugation with a carbonyl group also fixes the position of the double bond. As with saturated hydrocarbons, acyclic alkenes are characterized by clusters of peaks at intervals of 14 units. In these clusters the C_nH_{2n-1} and C_nH_{2n} peaks are more intense than the C_nH_{2n+1} peaks.

The mass spectrum of β-myrcene, a terpene, is shown in Figure 2.7. The peaks at *m/z* 41, 55, and 69 correspond to the formula C_nH_{2n-1} with $n = 3$, 4, and 5, respectively. Formation of the *m/z* 41 peak must involve rearrangement. The peaks at *m/z* 67 and 69 are the fragments from cleavage of a biallylic bond.

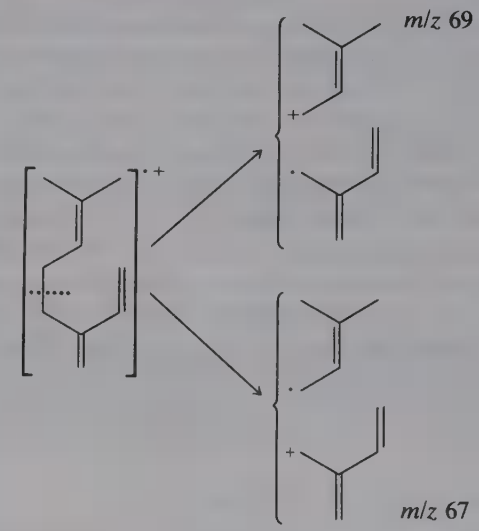

The peak at *m/z* 93 may be rationalized as a structure of formula $C_7H_9^+$ formed by isomerization (resulting in increased conjugation), followed by allylic cleavage.

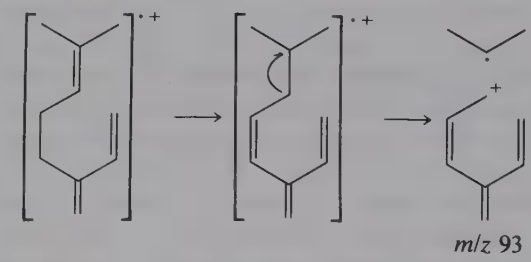

Cyclic alkenes usually show a distinct molecular ion peak. A unique mode of cleavage is the *retro*-Diels–Alder reaction shown by limonene:

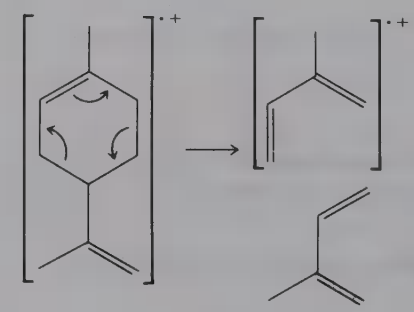

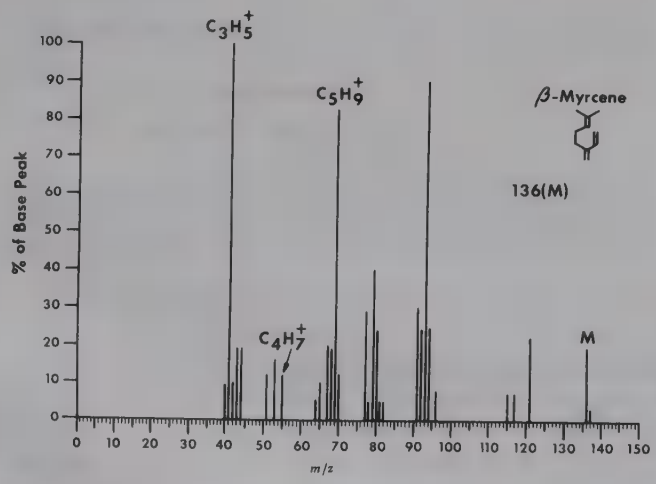

FIGURE 2.7. β-Myrcene.

2.10.1.3. Aromatic and Aralkyl Hydrocarbons

An aromatic ring in a molecule stabilizes the molecular ion peak (Rule 4, p. 15), which is usually sufficiently large that accurate intensity measurements can be made on the M + 1 and M + 2 peaks.

Figure 2.8 is the mass spectrum of naphthalene. The molecular ion peak is also the base peak, and the largest fragment peak, *m/z* 51, is only 12.5% as intense as the molecular ion peak.

A prominent peak (often the base peak) at *m/z* 91 ($C_6H_5CH_2^+$) is indicative of an alkyl substituted benzene ring. Branching at the α carbon leads to masses higher than 91 by increments of 14, the largest substituent being eliminated most readily (Rule 3, p. 14). The mere presence of a peak at mass 91, however, does not preclude branching at the α carbon because this highly stabilized fragment may result from rearrangements. A distinct and sometimes prominent M − 1 peak results from similar benzylic cleavage of a C—H bond.

It has been proposed that, in most cases, the ion of mass 91 is a tropylium rather than a benzylic cation. This explains the ready loss of a methyl group from xylenes although toluene does not easily lose a methyl group. The incipient molecular ion rearranges to the parent tropylium radical ion, which then cleaves to the simple tropylium ion ($C_7H_7^+$).

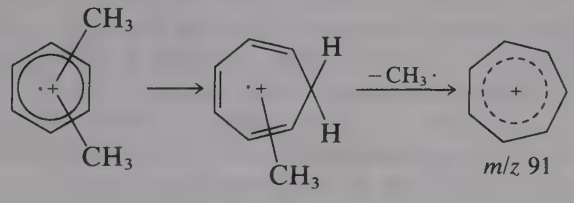

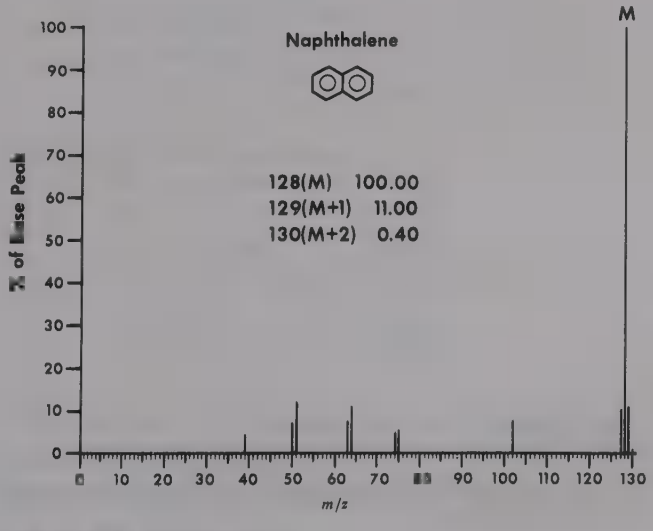

FIGURE 2.8. Naphthalene.

The frequently observed peak at *m/z* 65 results from elimination of a neutral acetylene molecule from the tropylium ion.

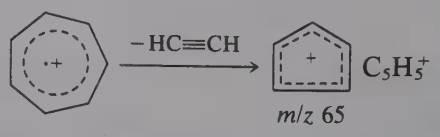

Hydrogen migration with elimination of a neutral alkene molecule accounts for the peak at *m/z* 92 observed when the alkyl group is longer than C_2.

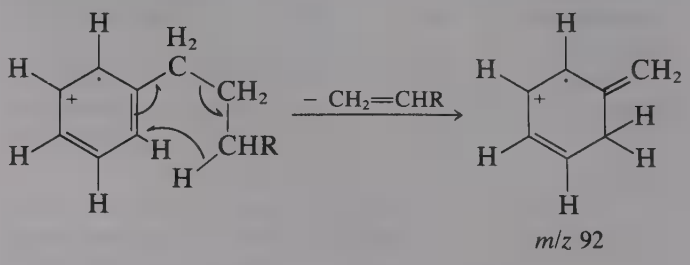

A characteristic cluster of ions due to a α cleavage and hydrogen migration in monalkylbenzenes appears at *m/z* 77 ($C_6H_5^+$), 78 ($C_6H_6^+$), and 79 ($C_6H_7^+$).

Alkylated polyphenyls and alkylated polycyclic aromatic hydrocarbons exhibit the same β cleavage as alkylbenzene compounds.

2.10.2. Hydroxy Compounds

2.10.2.1. Alcohols

The molecular ion peak of a primary or secondary alcohol is quite small and for a tertiary alcohol is undetectable. The molecular ion of 1-pentanol is extremely weak compared with its near homologs. Expedients such as CI, or derivatization, may be used to obtain the molecular weight.

Cleavage of the C—C bond next to the oxygen atom is of general occurrence (Rule 8, p. 15). Thus, primary alcohols show a prominent peak due to $CH_2{=}\dot{\ddot{O}}H$ (*m/z* 31). Secondary and tertiary alcohols cleave analogously to give a prominent peak due to

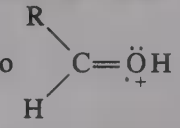

(*m/z* 45, 59, 73, etc.), and

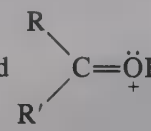

(*m/z* 59, 73, 87, etc.), respectively. The largest substituent is expelled most readily (Rule 3).

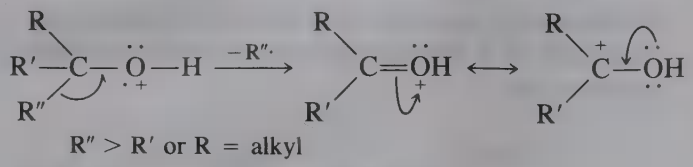

R″ > R′ or R = alkyl

When R and/or R′ = H, an M − 1 peak can usually be seen.

Primary alcohols, in addition to the principal C—C cleavage next to the oxygen atom, show a homologous series of peaks of progressively decreasing intensity resulting from cleavage at C—C bonds successively removed from the oxygen atom. In long-chain (>C_6) alcohols, the fragmentation becomes dominated by the hydrocarbon pattern; in fact, the spectrum resembles that of the corresponding alkene.

The spectrum in the vicinity of the very weak or missing molecular ion peak of a primary alcohol is sometimes complicated by weak M − 2 (R—CH=$\overset{+}{\ddot{O}}$) and M − 3 (R—C≡$\overset{+}{\ddot{O}}$) peaks.

A distinct and sometimes prominent peak can usually be found at M − 18 from loss of water. This peak is most noticeable in spectra of primary alcohols. This elimination by electron impact has been rationalized as follows:

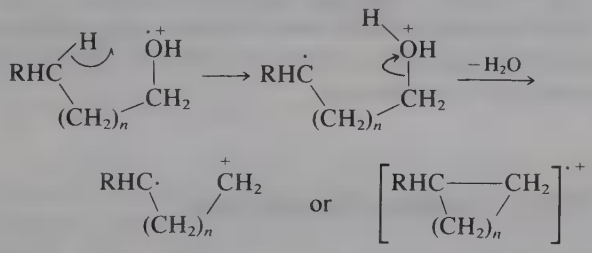

This pathway is consistent with the loss of the OH and γ hydrogen (n = 1) or δ hydrogen (n = 2); the ring structure is not proven by the observations and is merely one possible structure for the product radical cation. The M − 18 peak is frequently exaggerated by thermal decomposition of higher alcohols on hot inlet surfaces. Elimination of water, together with elimination of an alkene from primary alcohols, accounts for the presence of a peak at M − (alkene + H_2O), that is, a peak at M − 46, M − 74, M − 102, ...

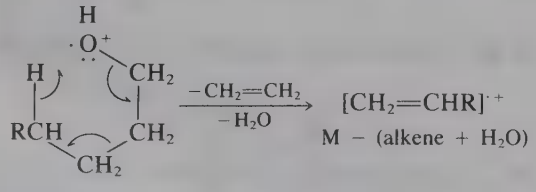

The alkene ion then decomposes by successive eliminations of ethylene.

Alcohols containing branched methyl groups (e.g., terpene alcohols) frequently show a fairly strong peak at M − 33 resulting from loss of CH_3 and H_2O.

Cyclic alcohols undergo fragmentation by complicated pathways; for example, cyclohexanol (M = m/z 100) forms $C_6H_{11}O^+$ by simple loss of the α hydrogen, loses H_2O to form $C_6H_{10}^+$ (which appears to have more than one possible bridged bicyclic structure), and forms $C_3H_5O^+$ (m/z 57) by a complex ring cleavage pathway.

A peak at m/z 31 (see above) is quite diagnostic for a primary alcohol provided it is more intense than peaks at m/z 45, 59, 73. . . . However, the first-formed ion of a secondary alcohol can decompose further to give a moderately intense m/z 31 ion.

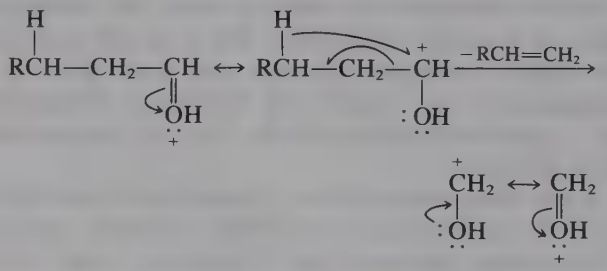

Figure 2.9 gives the characteristic spectra of isomeric primary, secondary, and tertiary C_5 alcohols.

Benzyl alcohols and their substituted homologs and analogs constitute a distinct class. Generally the parent peak is strong. A moderate benzylic peak (M − OH) is present as expected from cleavage β to the ring. A complicated sequence leads to prominent M − 1, M − 2, and M − 3 peaks. Benzyl alcohol itself fragments to give sequentially the M − 1 ion, the C_6H_7 ion by loss of CO, and the C_6H_5 ion by loss of H_2.

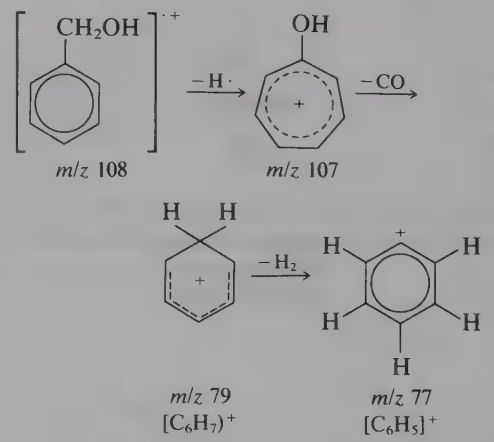

Loss of H_2O to give a distinct M − 18 peak is a common feature, especially pronounced and mechanistically straightforward in some ortho-substituted benzyl alcohols.

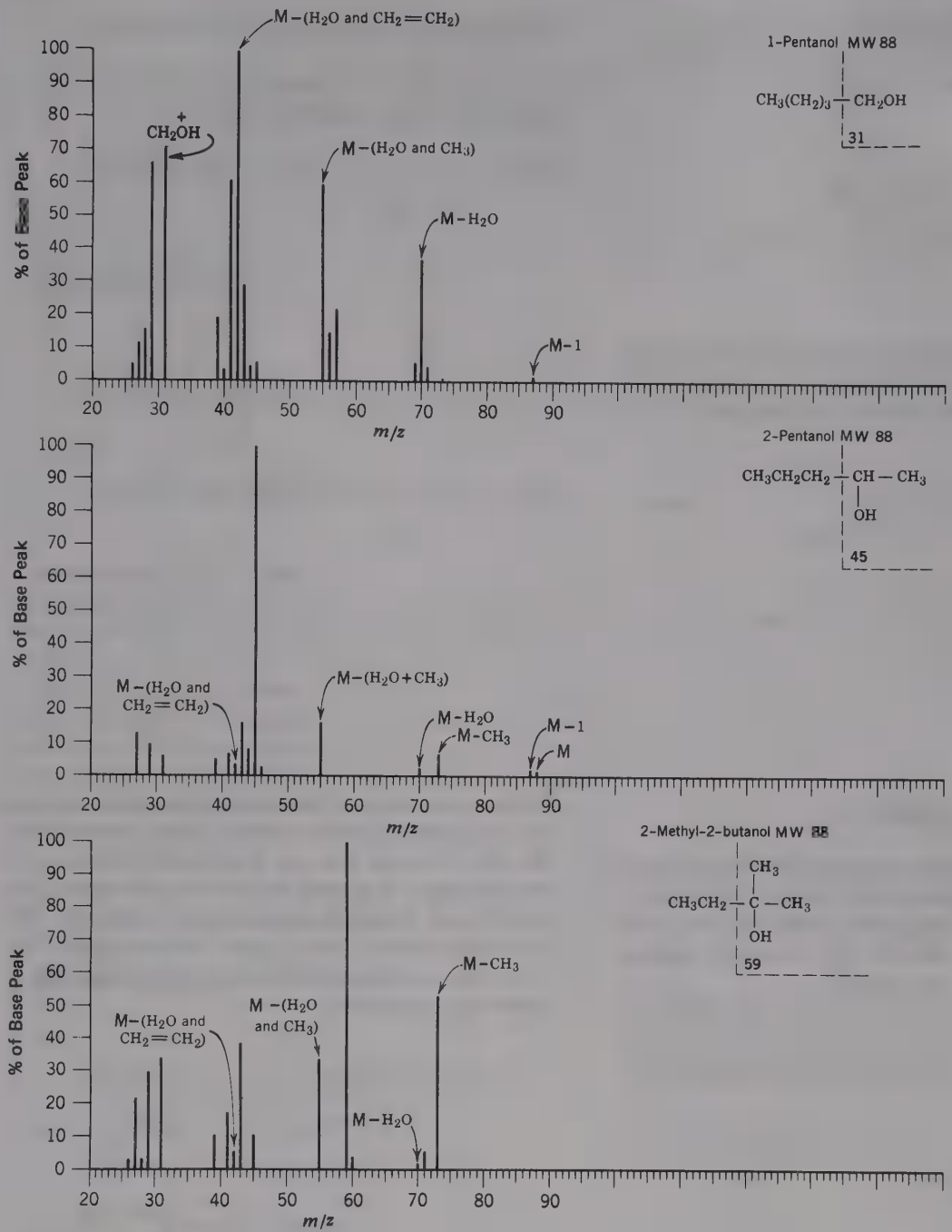

FIGURE 2.9. Isomeric pentanols.

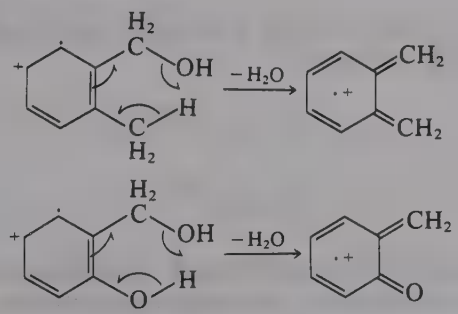

The aromatic cluster at *m/z* 77, 78, and 79 resulting from complex degradation is prominent here also.

2.10.2.2. Phenols

A conspicuous molecular ion peak facilitates identification of phenols. In phenol itself, the molecular ion peak is the base peak, and the M − 1 peak is small. In cresols, the M − 1 peak is larger than the molecular

ion as a result of a facile benzylic C—H cleavage. A rearrangement peak at *m/z* 77 and peaks resulting from loss of CO (M − 28) and CHO (M − 29) are usually found in phenols.

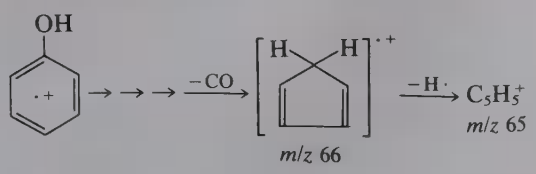

The mass spectrum of a typical phenol is shown in Figure 2.10. This spectrum shows that a methyl group is lost much more readily than an α hydrogen.

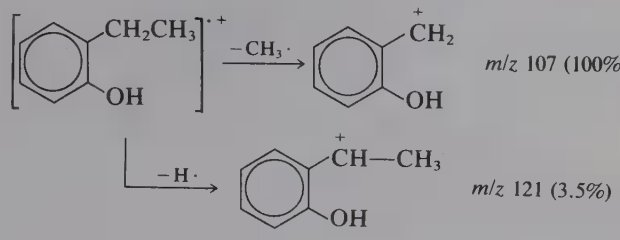

2.10.3. Ethers

2.10.3.1. Aliphatic Ethers

The molecular ion peak (two mass units larger than that of an analogous hydrocarbon) is small, but larger sample size usually will make the molecular ion peak or the M + 1 peak obvious (H· transfer during ion–molecule collision, see Section 2.5).

The presence of an oxygen atom can be deduced from strong peaks at *m/z* 31, 45, 59, 73, ... These peaks represent the RO^+ and $ROCH_2^+$ fragments.

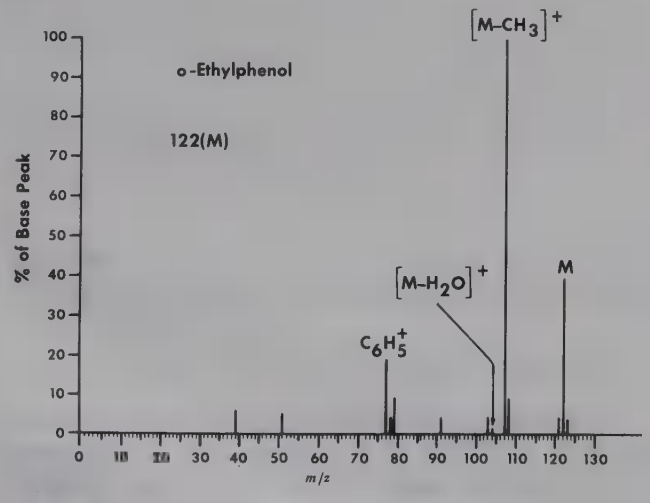

FIGURE 2.10. *o*-Ethylphenol.

Fragmentation occurs in two principal ways:

1. Cleavage of the C—C bond next to the oxygen atom (α,β bond, Rule 8, Section 2.7)

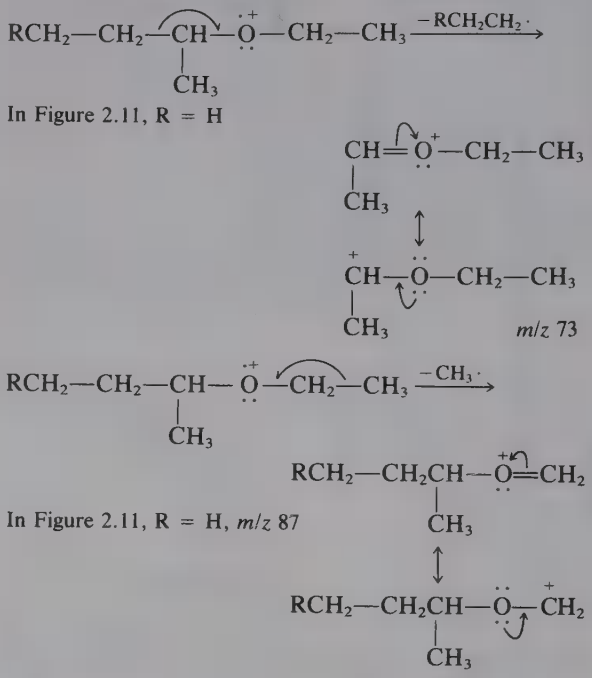

One or the other of these oxygen-containing ions may account for the base peak. In the case shown, the first cleavage (i.e., at the branch positions to lose the larger fragment) is preferred. However, the first-formed fragment decomposes further by the following process, often to give the base peak (Fig. 2.11); the decomposition is important when the α carbon is substituted.

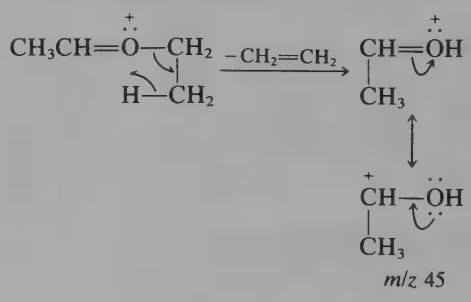

2. C—O bond cleavage with the charge remaining on the alkyl fragment.

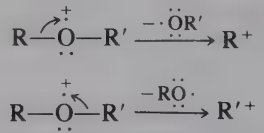

As expected, the spectrum of long-chain ethers becomes dominated by the hydrocarbon pattern.

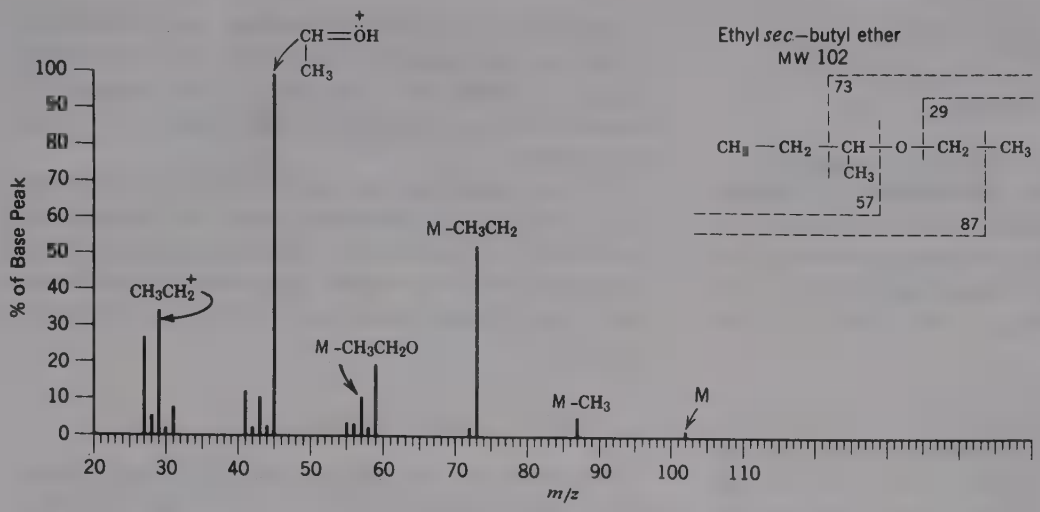

FIGURE 2.11. Ethyl *sec*-butyl ether.

Acetals are a special class of ethers. Their mass spectra are characterized by an extremely weak molecular ion peak, by the prominent peaks at M − R, and M − OR, and a weak peak at M − H. Each of these cleavages is mediated by an oxygen atom and thus facile. As usual elimination of the largest group is preferred. As with aliphatic ethers, the first-formed oxygen-containing fragments can decompose further with hydrogen migration and alkene elimination.

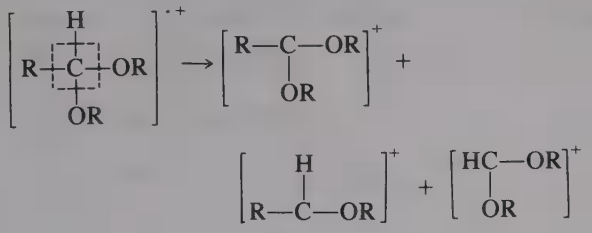

Ketals behave similarly.

2.10.3.2. Aromatic Ethers

The molecular ion peak of aromatic ethers is prominent. Primary cleavage occurs at the bond β to the ring, and the first-formed ion can decompose further. Thus anisole, MW 108, gives ions of *m/z* 93 and 65.

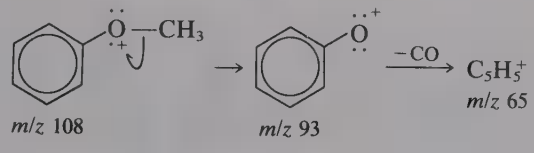

The characteristic aromatic peaks at *m/z* 78 and 77 may arise from anisole as follows:

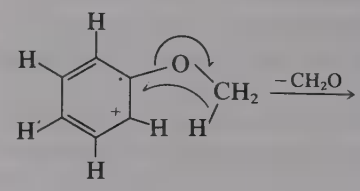

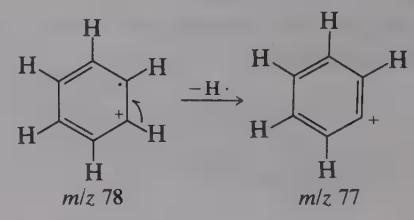

When the alkyl portion of an aromatic alkyl ether is C_2 or larger, cleavage β to the ring is accompanied by hydrogen migration as noted above for alkylbenzenes. Clearly, cleavage is mediated by the ring rather than by the oxygen atom; C—C cleavage next to the oxygen atom is insignificant.

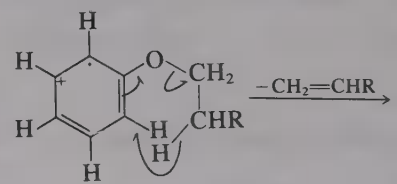

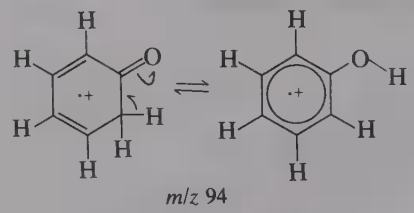

Diphenyl ethers show peaks at M − H, M − CO, and M − CHO by complex rearrangements.

2.10.4. Ketones

2.10.4.1. Aliphatic Ketones

The molecular ion peak of ketones is usually quite pronounced. Major fragmentation peaks of aliphatic ketones result from cleavage at the C—C bonds adjacent to the oxygen atom, the charge remaining with the resonance-stabilized acylium ion. Thus, as with alcohols and ethers, cleavage is mediated by the oxygen atom.

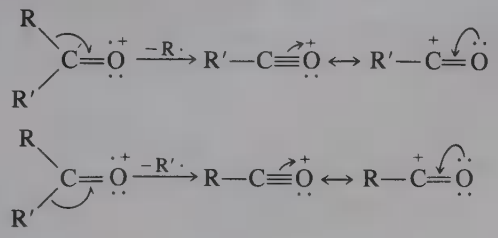

This cleavage gives rise to a peak at *m/z* 43 or 57 or 71. . . . The base peak very often results from loss of the larger alkyl group.

When one of the alkyl chains attached to the C=O group is C_3 or longer, cleavage of the C—C bond once removed (α, β bond) from the C=O group occurs with hydrogen migration to give a major peak (McLafferty rearrangement).

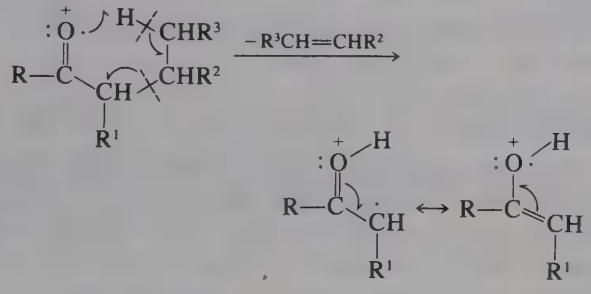

Simple cleavage of the α, β bond, which does not occur to any extent, would give an ion of low stability with two adjacent positive centers $R-\overset{\delta+}{\underset{\underset{\delta-}{O}}{\overset{\|}{C}}}-\overset{+}{C}H_2$. When R is C_3 or longer, the first-formed ion can cleave again with hydrogen migration:

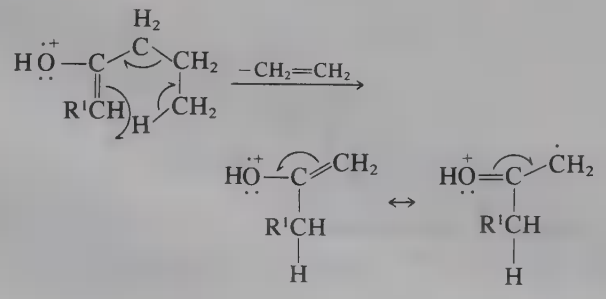

Note that in long-chain ketones the hydrocarbon peaks are indistinguishable (without the aid of high-resolution techniques) from the acyl peaks, since the mass of the C=O unit (28) is the same as two methylene units.

The multiple cleavage modes in ketones sometimes make difficult the determination of the carbon chain configuration. Reduction of the carbonyl group to a methylene group yields the corresponding hydrocarbon whose fragmentation pattern leads to the carbon skeleton.

2.10.4.2. Cyclic Ketones

The molecular ion peak in cyclic ketones is prominent. As with aliphatic ketones, the primary cleavage of cyclic ketones is adjacent to the C=O group, but the ion thus formed must undergo further cleavage in order to produce a fragment. The base peak in the spectrum of cyclopentanone and of cyclohexanone is *m/z* 55. The mechanisms are similar in both cases: hydrogen shift to convert a primary radical to a conjugated secondary radical followed by formation of the resonance-stabilized ion, *m/z* 55.

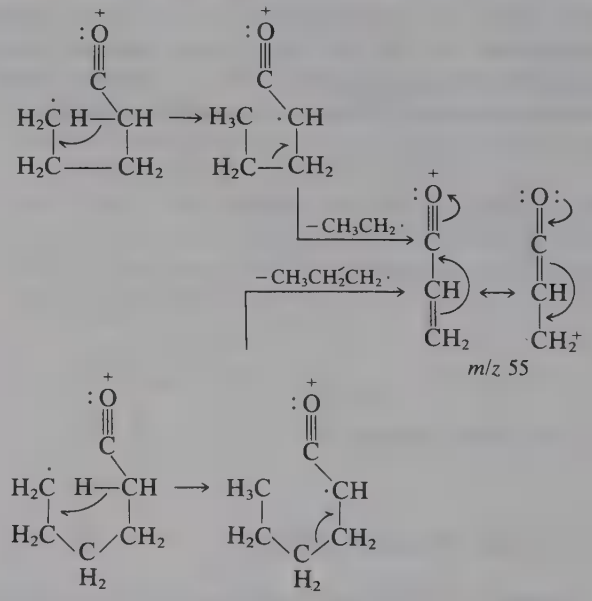

The other distinctive peaks at *m/z* 83 and 42 in the spectrum of cyclohexanone have been rationalized as follows:

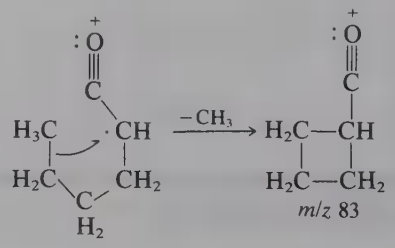

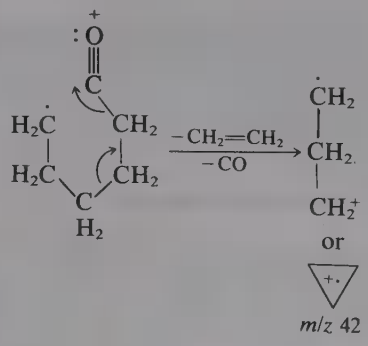

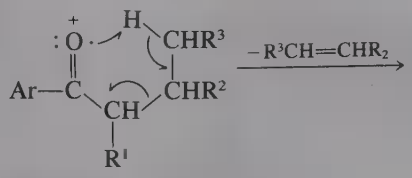

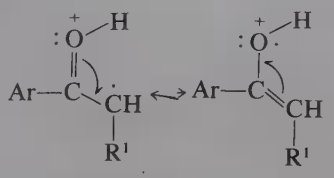

2.10.4.3. Aromatic Ketones

The molecular ion peak of aromatic ketones is prominent. Cleavage of aryl alkyl ketones occurs at the bond β to the ring, leaving a characteristic $ArC{\equiv}\overset{+}{O}$: fragment, which usually accounts for the base peak. Loss of CO from this fragment gives the "aryl" ion (*m/z* 77 in the case of acetophenone). Cleavage of the bond adjacent to the ring to form a $RC{\equiv}\overset{+}{O}$: fragment is less important though somewhat enhanced by electron-withdrawing groups (and diminished by electron-donating groups) in the para position of the Ar group.

When the alkyl chain is C_3 or longer, cleavage of the C—C bond once-removed from the C=O group occurs with hydrogen migration. This is the same cleavage noted for aliphatic ketones that proceeds through a cyclic transition state and results in elimination of an alkene and formation of a stable ion.

The mass spectrum of an unsymmetrical diaryl ketone, *p*-chlorobenzophenone, is displayed in Figure 2.12. The molecular ion peak (*m/z* 216) is prominent and the intensity (33.99%) of the M + 2 peak (relative to the molecular ion peak) demonstrates that chlorine is in the structure (see the discussion of Table 2.3 and Fig. 2.16).

Since the intensity of the *m/z* 141 peaks is about $\frac{1}{3}$ the intensity of the *m/z* 139 peak, these peaks correspond to fragments containing 1 chlorine each. The same can be said about the fragments producing the *m/z* 111 and 113 peaks.

The major peaks in Figure 2.12 arise as follows:

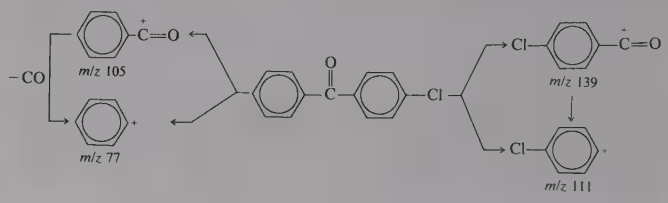

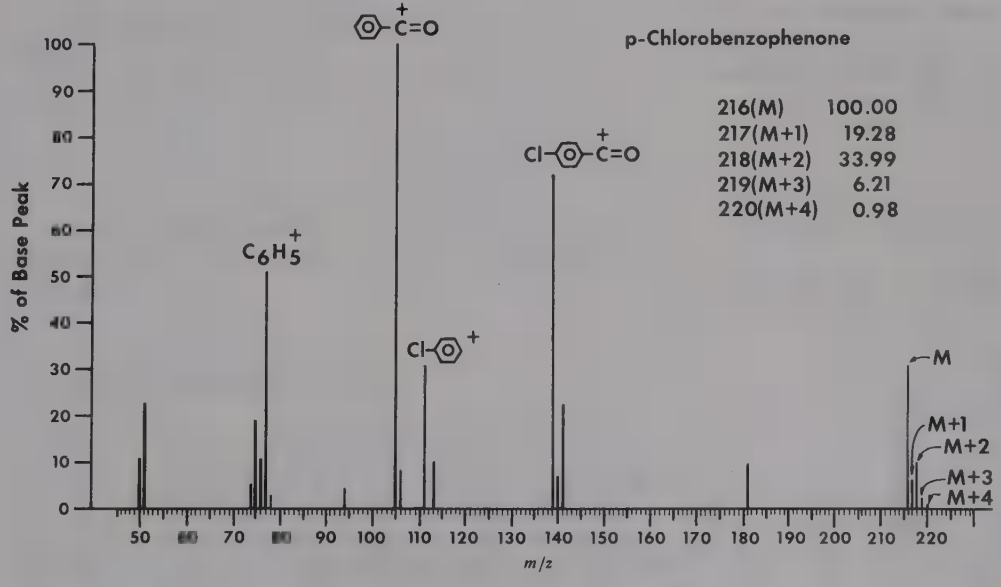

FIGURE 2.12. *p*-Chlorobenzophenone. The M peak is arbitrarily set in the table above at intensity 100% for discussion of the molecular ion cluster.

The observed peak intensities make it clear that formation of a $ArCO^+$ fragment occurs more readily than does Ar^+ formation. In addition, for either of these two types of fragments, the structure bearing the chlorine is less favored than that bearing no chlorine because the electron-withdrawal effect of the chlorine destabilizes positive charge.

2.10.5. Aldehydes

2.10.5.1. Aliphatic Aldehydes

The molecular ion peak of aliphatic aldehydes is usually discernible. Cleavage of the C—H and C—C bonds next to the oxygen atom results in an M − 1 peak and in an M − R peak (*m/z* 29, CHO^+). The M − 1 peak is a good diagnostic peak even for long-chain aldehydes, but the *m/z* 29 peak present in C_4 and higher aldehydes is due to the hydrocarbon $C_2H_5^+$ ion.

In the C_4 and higher aldehydes, McLafferty cleavage of the α,β C—C bond occurs to give a major peak at *m/z* 44, 58, or 72, . . . , depending on the α substituents. This is the resonance-stabilized ion formed through the cyclic transition state as shown above for aliphatic ketones (R = H).

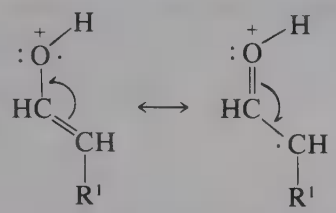

In straight-chain aldehydes, the other unique, diagnostic peaks are at M − 18 (loss of water), M − 28 (loss of ethylene), M − 43 (loss of $CH_2{=}CH{-}O\cdot$), and M − 44 (loss of $CH_2{=}CH{-}OH$). The rearrangements leading to these peaks have been rationalized (see Budzikiewicz et al.). As the chain lengthens, the hydrocarbon pattern (*m/z* 29, 43, 57, 71, . . .) becomes dominant. These features are evident in the spectrum of nonanal (Fig. 2.13).

2.10.5.2. Aromatic Aldehydes

Aromatic aldehydes are characterized by a large molecular ion peak and by an M − 1 peak ($Ar{-}C{\equiv}\overset{+}{O}$) that is always large and may be larger than the molecular ion peak. The M − 1 ion $C_6H_5C{\equiv}\overset{+}{O}$ eliminates CO to give the phenyl ion (*m/z* 77), which in turn eliminates $HC{\equiv}CH$ to give the $C_4H_3^+$ ion (*m/z* 51).

2.10.6. Carboxylic Acids

2.10.6.1. Aliphatic Acids

The molecular ion peak of a straight-chain monocarboxylic acid is weak but usually discernible. The most characteristic (sometimes the base) peak is *m/z* 60 due to the McLafferty rearrangement. Branching at the α carbon enhances this cleavage.

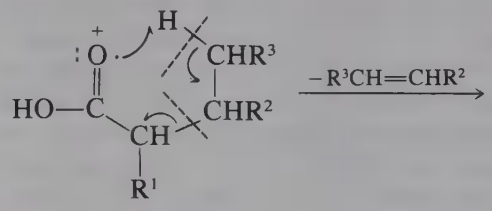

McLafferty rearrangement

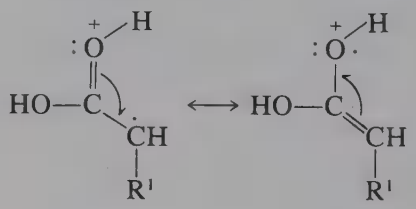

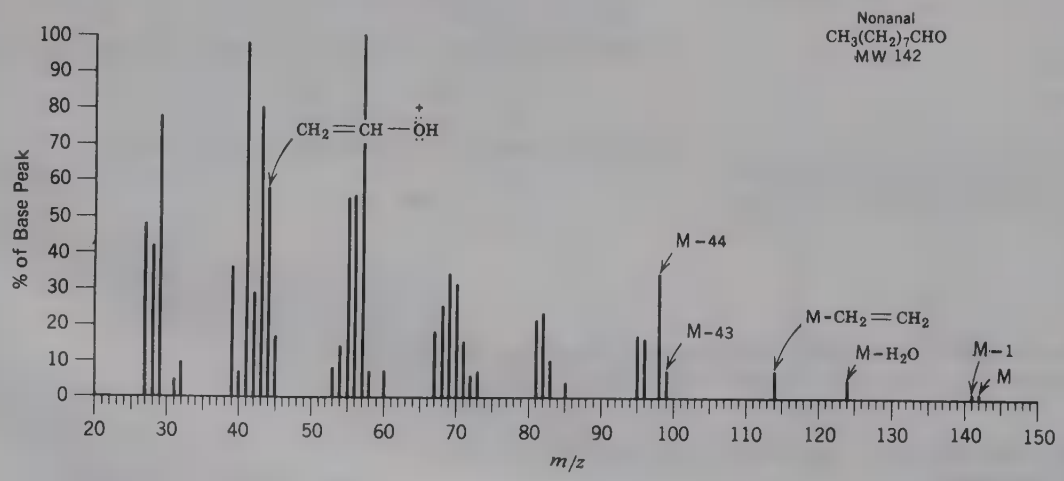

FIGURE 2.13. Nonanal.

In short-chain acids, peaks at M − OH and M − CO_2H are prominent; these represent cleavage of bonds next to C=O. In long-chain acids, the spectrum consists of two series of peaks resulting from cleavage at each C—C bond with retention of charge either on the oxygen-containing fragment (*m/z* 45, 59, 73, 87, . . .) or on the alkyl fragment (*m/z* 29, 43, 57, 71, 85, . . .). As previously discussed, the hydrocarbon pattern also shows peaks at *m/z* 27, 28; 41, 42; 55, 56; 69, 70; . . . . In summary, besides the McLafferty rearrangement peak, the spectrum of a long-chain acid resembles the series of "hydrocarbon" clusters at interval of 14 mass units. In each cluster, however, is a prominent peak at $C_nH_{2n-1}O_2$. Hexanoic acid (mw 116), for example, cleaves as follows:

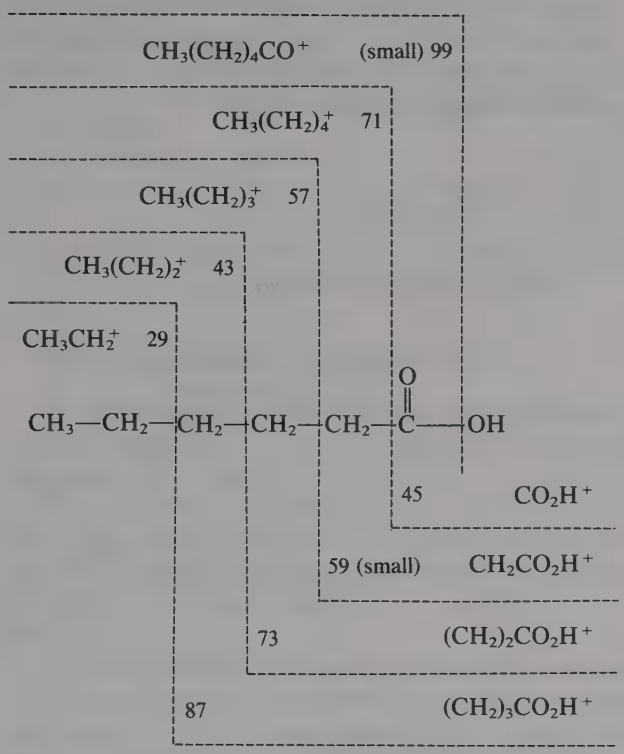

Dibasic acids are usually converted to esters to increase volatility. Trimethylsilyl esters are often successful.

2.10.6.2. Aromatic Acids

The molecular ion peak of aromatic acids is large. The other prominent peaks are formed by loss of OH (M − 17) and of CO_2H (M − 45). Loss of H_2O (M − 18) is noted if a hydrogen-bearing ortho group is available. This is one example of the general "ortho effect" noted when the substituents can be in a six-membered transition state to facilitate loss of a neutral molecule of H_2O, ROH, or NH_3.

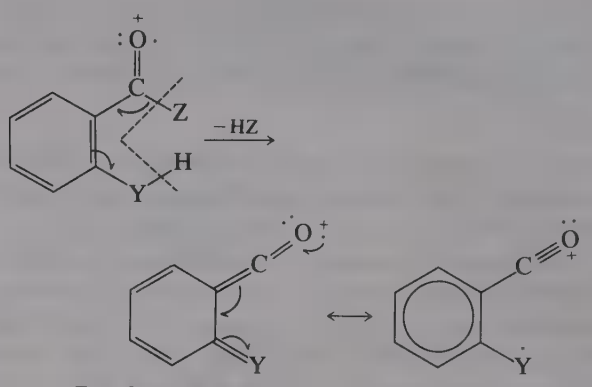

2.10.7. Carboxylic Esters

2.10.7.1. Aliphatic Esters

The molecular ion peak of a methyl ester of a straight-chain aliphatic acid is usually distinct. Even waxes usually show a discernible molecular ion peak. The molecular ion peak is weak in the range *m/z* 130 to ~200, but becomes somewhat more intense beyond this range. The most characteristic peak is due to the familiar McLafferty rearrangement and cleavage one bond removed from the C=O group. Thus a methyl ester of an aliphatic acid unbranched at the α carbon gives a strong peak at *m/z* 74, which, in fact, is the base peak in straight-chain methyl esters from C_6–C_{26}. The alcohol moiety and/or the α substituent can often be deduced by the location of the peak resulting from this cleavage.

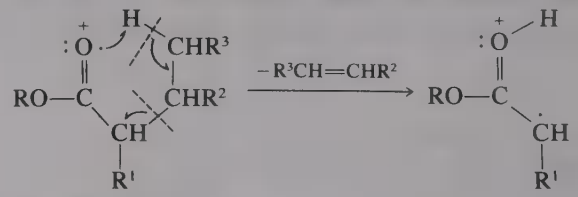

McLafferty rearrangement

Four ions can result from bond cleavage next to C=O.

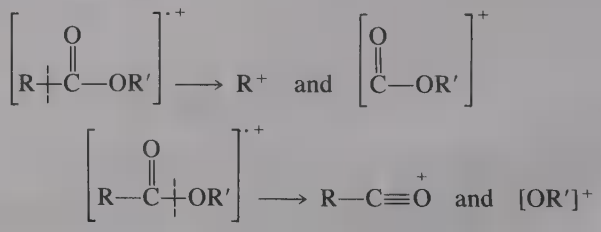

The ion R^+ is prominent in the short chain esters, but diminishes rapidly with increasing chain length and is barely perceptible in methyl hexanoate. The ion

$R—C\equiv\overset{+}{O}$ gives an easily recognizable peak for esters. In methyl esters it occurs at M − 31. It is the base peak in methyl acetate, and is still 4% of the base peak in the C_{26} methyl ester. The ions $[OR']^+$ and $[\overset{O}{\overset{\|}{C}}OR']^+$ are usually of little importance. The latter is discernible when R′ = CH_3 (see *m/z* 59 peak of Fig. 2.14).

First, consider esters in which the acid portion is the predominant portion of the molecule. The fragmentation pattern for methyl esters of straight-chain acids can be described in the same terms used for the pattern of the free acid. Cleavage at each C—C bond gives an alkyl ion (*m/z* 29, 43, 57, . . .) and an oxygen-containing ion, $C_nH_{2n-1}O_2^+$ (59, 73, 87, . . .). Thus, there are hydrocarbon clusters at intervals of 14 mass units; in each cluster is a prominent peak at $C_nH_{2n-1}O_2$. The peak (*m/z* 87) formally represented by the ion $[CH_2CH_2COOCH_3]^+$ is always more intense than its homologs, but the reason is not immediately obvious. However, it seems clear that the $C_nH_{2n-1}O_2$ ions do not at all arise from simple cleavage.

The spectrum of methyl octanoate is presented as Figure 2.14. This spectrum illustrates one difficulty previously mentioned (Section 2.5) in using the M + 1 peak to arrive at a molecular formula. The measured value for the M + 1 peak is 12.9%. The calculated value is 10.0%. The measured value is high due to an ion–molecule reaction because a relatively large sample was used in order to see the weak molecular ion peak.

Now let us consider esters in which the alcohol portion is the predominant portion of the molecule. Esters of fatty alcohols (except methyl esters) eliminate a molecule of acid in the same manner that alcohols eliminate water. A scheme similar to that described earlier for alcohols, involving a single hydrogen transfer to the alcohol oxygen of the ester, can be written. An alternative mechanism involves a hydride transfer to the carbonyl oxygen (McLafferty rearrangement).

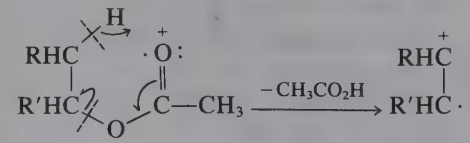

The preceding loss of acetic acid is so facile in steroidal acetates that they frequently show no detectable molecular ion peak. Steroidal systems also seem unusual in that they often display significant molecular ions as alcohols, even when the corresponding acetates do not.

Esters of long-chain alcohols show a diagnostic peak at *m/z* 61, 75, or 89, . . . from elimination of the alkyl moiety and transfer to *two* hydrogen atoms to the fragment containing the oxygen atoms.

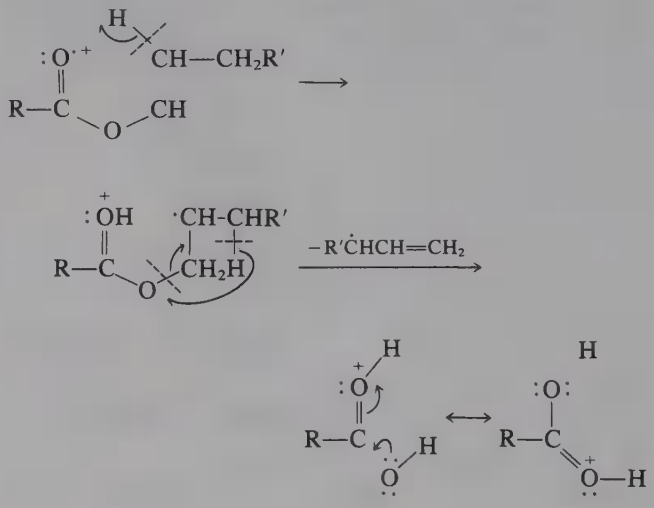

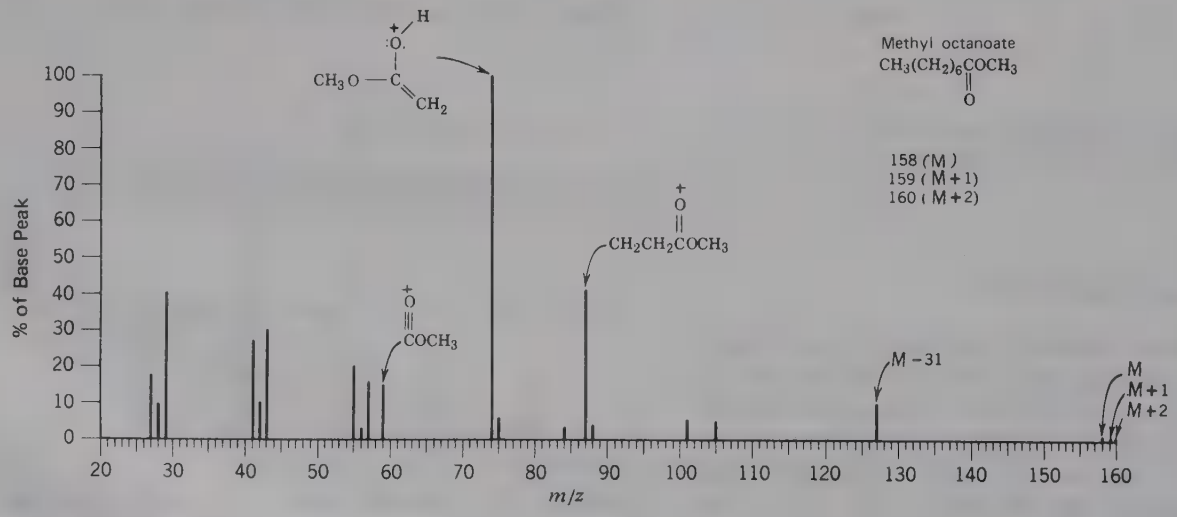

FIGURE 2.14. Methyl octanoate.

Esters of dibasic acids $ROC(CH_2)_nCOR$, in general, give recognizable molecular ion peaks. Intense peaks are found at $(ROC(CH_2)_nC)^+$ and at $(ROC(CH_2)_n)^+$.

2.10.7.2. Benzyl and Phenyl Esters

Benzyl acetate (also furfuryl acetate and other similar acetates) and phenyl acetate eliminate the neutral molecule ketene; frequently this gives rise to the base peak.

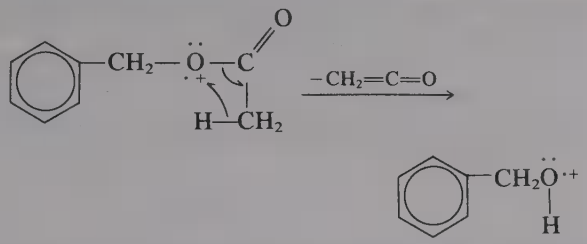

Of course, the *m/z* 43 peak ($CH_3C{\equiv}\overset{+}{O}$) and *m/z* 91 ($C_7H_7^+$) peaks are prominent for benzyl acetate.

2.10.7.3. Esters of Aromatic Acids

The molecular ion peak of methyl esters of aromatic acids is prominent. As the size of the alcohol moiety increases, the intensity of the molecular ion peak decreases rapidly to practically zero at C_5. The base peak results from elimination of $\cdot OR$, and elimination of $\cdot COOR$ accounts for another prominent peak. In methyl esters, these peaks are at M − 31, and M − 59, respectively.

As the alkyl moiety increases in length, three modes of cleavage become important: (1) McLafferty rearrangement, (2) rearrangement of two hydrogen atoms with elimination of an allylic radical, and (3) retention of the positive charge by the alkyl group.

Appropriately, ortho-substituted benzoates eliminate ROH through the general "ortho" effect described above under aromatic acids. Thus, the base peak in the spectrum of methyl salicylate is *m/z* 120; this ion eliminates carbon monoxide to give a strong peak at *m/z* 92.

A strong characteristic peak at mass 149 is found in the spectra of all esters of phthalic acid, starting with the diethyl ester. This peak is not significant in the dimethyl or methyl ethyl ester of phthalic acid, nor in esters of isophthalic or terephthalic acids, all of which give the expected peaks at M − R, M − 2R, M − CO_2R, and M − $2CO_2R$. Since long-chain phthalate

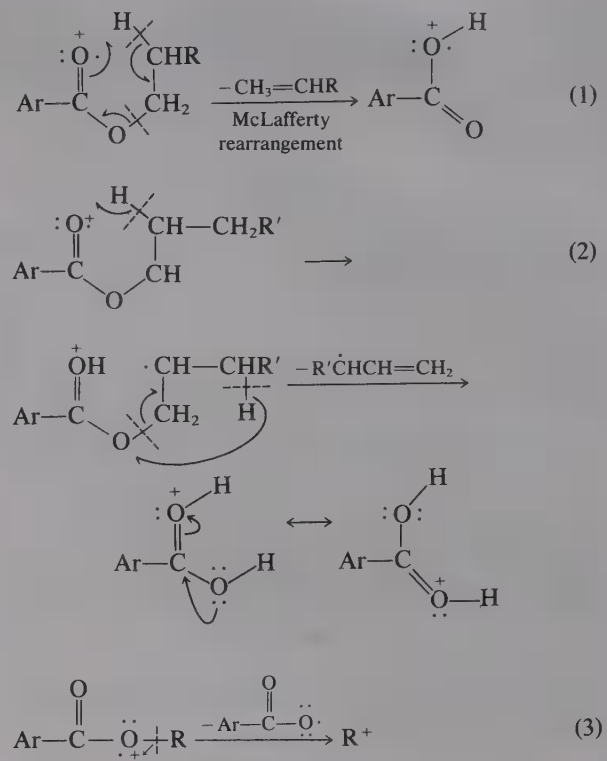

esters are widely used as plasticizers, a strong peak at *m/z* 149 may indicate contamination. The *m/z* 149 fragment is probably formed by two ester cleavages involving the shift of two hydrogen atoms and then another hydrogen atom, followed by elimination of H_2O.

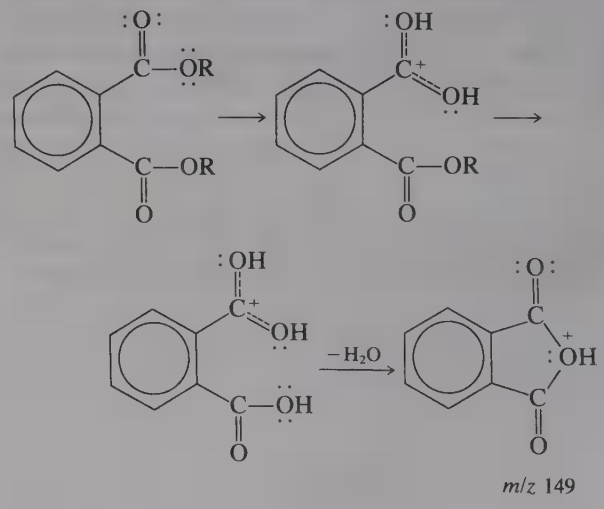

2.10.8. Lactones

The molecular ion peak of five-membered ring lactones is distinct but is weaker when an alkyl substitutent is present at C_4. Facile cleavage of the side chain at C_4 (Rules 3 and 8, pp. 14–15) gives a strong peak at M − alkyl.

The base peak (*m/z* 56) of γ-valerolactone and the same strong peak of butyrolactone probably arise as follows:

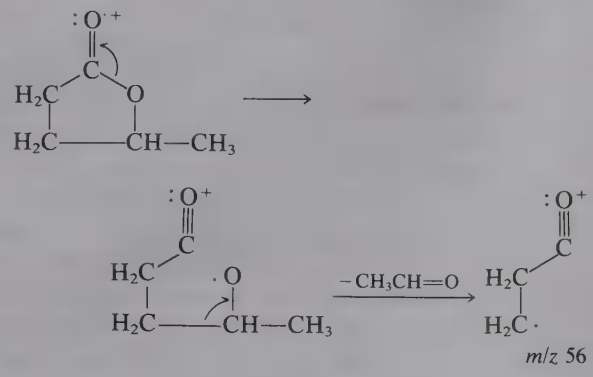

m/z 56

Labeling experiments indicate that some of the *m/z* 56 peak in γ-valerolactone arises from the $C_4H_8^+$ ion. The other intense peaks in γ-valerolactone are at *m/z* 27 ($C_2H_3^+$), 28 ($C_2H_4^+$), 29 ($C_2H_5^+$), 41 ($C_3H_5^+$), and 43 ($C_3H_7^+$), and 85 ($C_4H_5O_2^+$, loss of the methyl group). In butyrolactone, there are strong peaks at *m/z* 27, 28, 29, 41, and 42 ($C_3H_6^+$).

2.10.9. Amines

2.10.9.1. Aliphatic Amines

The molecular ion peak of an aliphatic monoamine is an odd number, but it is usually quite weak and, in long-chain or highly branched amines, undetectable. The base peak frequently results from C—C cleavage next (α, β) to the atom (Rule 8, Section 2.7); for primary amines unbranched at the α carbon, this is *m/z* 30 ($CH_2NH_2^+$). This cleavage accounts for the base peak in all primary amines and secondary and tertiary amines that are not branched at the α carbon. Loss of the largest branch from the α-C atom is preferred.

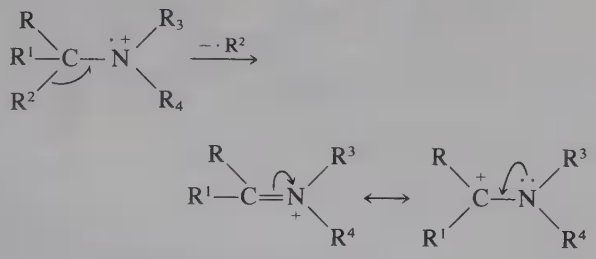

$R^2 > R^1$ or R = alkyl group sizes

When R and/or R^1 = H, an M − 1 peak is usually visible. This is the same type of cleavage noted above for alcohols. The effect is more pronounced in amines because of the better resonance stabilization of the ion fragment by the less electronegative N atom compared with the O atom.

Primary straight-chain amines show a homologous series of peaks of progressively decreasing intensity (the cleavage at the ε bond is slightly more important than at the neighboring bonds) at *m/z* 30, 44, 58, . . . resulting from cleavage at C—C bonds successively removed from the nitrogen atom with retention of the charge on the N-containing fragment. These peaks are accompanied by the hydrocarbon pattern of C_nH_{2n+1}, C_nH_{2n}, and C_nH_{2n-1} ions. Thus, we note characteristic clusters at intervals of 14 mass units, each cluster containing a peak due to a $C_nH_{2n+2}N$ ion. Because of the very facile cleavage to form the base peak, the fragmentation pattern in the high mass region becomes extremely weak.

Cyclic fragments apparently occur during the fragmentation of longer chain amines.

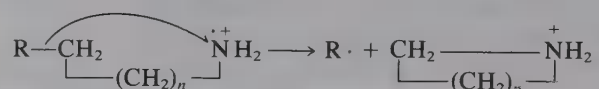

n = 3,4 *m/z* 72, 86

A peak at *m/z* 30 is good though not conclusive evidence for a straight-chain primary amine. Further decomposition of the first-formed ion from a secondary or tertiary amine leads to a peak at *m/z* 30, 44, 58, 72, ... This is a process similar to that described for aliphatic alcohols and ethers above, and similarly is enhanced by branching at one of the α-carbon atoms:

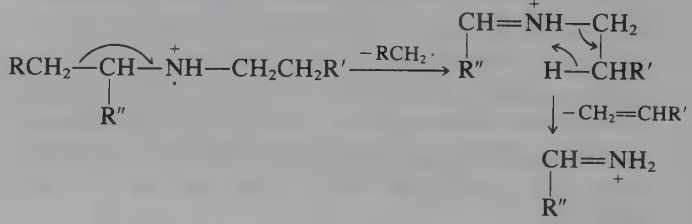

R″ = CH_3, *m/z* 44, more intense
R″ = H, *m/z* 30, less intense

Cleavage of amino acid esters occurs at both C—C bonds (*a*, *b* below) next to the nitrogen atom, loss of the carbalkoxy group being preferred (*a*). The aliphatic amine fragment decomposes further to give a peak at *m/z* 30.

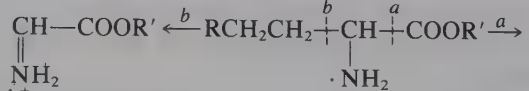

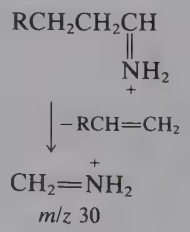

m/z 30

2.10.9.2. Cyclic Amines

In contrast to acyclic amines, the molecular ion peaks of cyclic amines are usually intense unless there is substitution at the α position; for example, the molecular ion peak of pyrrolidine is strong. Primary cleavage at the bonds next to the N atom leads either to loss of an α-hydrogen atom to give a strong M − 1 peak or to opening of the ring; the latter event is followed by elimination of ethylene to give $\cdot CH_2\overset{+}{N}H{=}CH_2$ (*m/z* 43, base peak), hence by loss of a hydrogen atom to give $CH_2{=}\overset{+}{N}{=}CH_2$ (*m/z* 42). *N*-Methyl pyrrolidine also gives a $C_2H_4N^+$ (*m/z* 42) peak, apparently by more than one pathway.

Piperidine likewise shows a strong molecular ion and M − 1 (base) peak. Ring opening followed by several available sequences leads to characteristic peaks at *m/z* 70, 57, 56, 44, 43, 42, 30, 29, and 28. Substituents are cleaved from the ring (Rule 6, Section 2.7).

2.10.9.3. Anilines

The molecular ion peak (odd number) of an aromatic monoamine is intense. Loss of one of the amino H atoms of aniline gives a moderately intense M − 1 peak; loss of a neutral molecule of HCN followed by loss of a hydrogen atom gives prominent peaks at *m/z* 66 and 65, respectively.

It was noted above that cleavage of alkyl aryl ethers occurs with rearrangement involving cleavage of the ArO—R bond; that is, cleavage was controlled by the ring rather than by the oxygen atom. In the case of alkylarylamines, cleavage of the C—C bond next to the nitrogen atom is dominant; that is, the heteroatom controls cleavage.

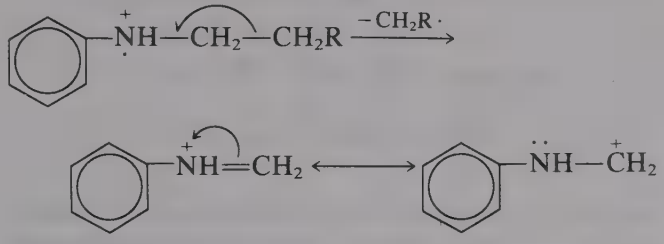

2.10.10. Amides

2.10.10.1. Aliphatic Amides

The molecular ion peak of straight-chain monoamides is usually discernible. The dominant modes of cleavage depend on the length of the acyl moiety, and on the lengths and number of the alkyl groups attached to the nitrogen atom.

The base peak in all straight-chain primary amides higher than propionamide results from the familiar McLafferty rearrangement.

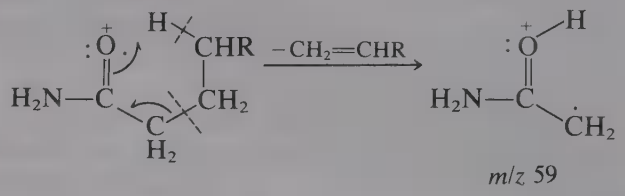

Branching at the α carbon (CH_3, etc.) gives a homologous peak at *m/z* 73 or 87, ...

Primary amides give a strong peak at *m/z* 44 from cleavage of the R—$CONH_2$ bond: $(\overset{+}{O}{\equiv}C{-}\ddot{N}H_2 \leftrightarrow \ddot{O}{=}C{=}\overset{+}{N}H_2)$; this is the base peak in C_1—C_3 primary amides and in isobutyramide. A moderate peak at *m/z* 86 results from $\gamma\delta$ C—C cleavage, possibly accompanied by cyclization.

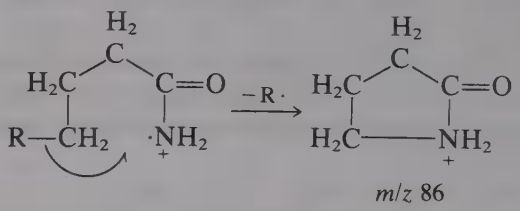

Secondary and tertiary amides with an available hydrogen on the γ carbon of the acyl moiety and methyl groups on the N atom show the dominant peak resulting from the McLafferty rearrangement. When the N-alkyl groups are C_2 or longer and the acyl moiety is shorter than C_3, another mode of cleavage predominates. This is cleavage of the N-alkyl group β to the N atom, and cleavage of the carbonyl C—N bond with migration of an α-hydrogen atom of the acyl moiety.

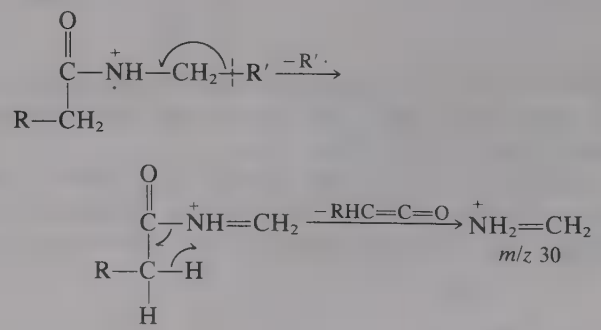

2.10.10.2. Aromatic Amides

Benzamide (Fig. 2.1) is a typical example. Loss of NH_2 from the molecular ion yields a resonance-stabilized benzoyl cation that in turn undergoes cleavage to a phenyl cation.

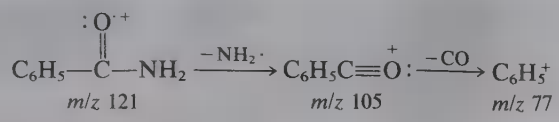

A separate fragmentation pathway gives rise to a modest *m/z* 44 peak.

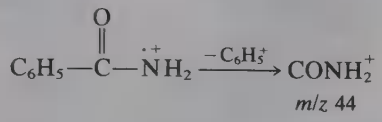

2.10.11. Aliphatic Nitriles

The molecular ion peaks of aliphatic nitriles (except for acetonitrile and propionitrile) are weak or absent, but the M + 1 peak can usually be located by its behavior on increasing inlet pressure or decreasing repeller voltage (Section 2.5). A weak but diagnostically useful M − 1 peak is formed by loss of an α hydrogen to form the stable ion: $RCH{-}C{\equiv}N^{\cdot+} \leftrightarrow RCH{=}C{=}N^{\cdot+}$

The base peak of straight-chain nitriles between C_4 and C_9 is *m/z* 41. This peak is the ion resulting from hydrogen rearrangement in a six-membered transition state.

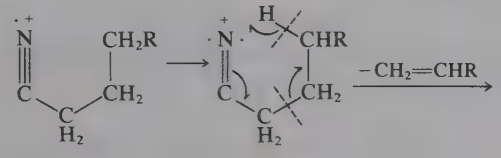

McLafferty rearrangement

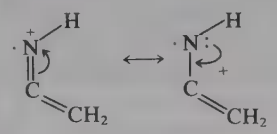

However, this peak lacks diagnostic value because of the presence of the C_3H_5 (*m/z* 41) for all molecules containing a hydrocarbon chain.

A peak at *m/z* 97 is characteristic and intense (sometimes the base peak) in straight-chain nitriles C_8 and higher. The following mechanism has been depicted:

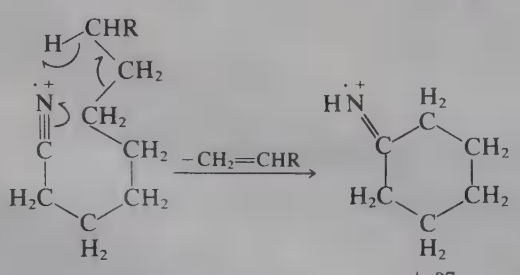

Simple cleavage at each C—C bond (except the one next to the N atom) gives a characteristic series of homologous peaks of even mass number down the entire length of the chain (*m/z* 40, 54, 68, 82, . . .) due to the $(CH_2)_nC{\equiv}N^+$ ions. Accompanying these peaks are the usual peaks of the hydrocarbon pattern.

2.10.12. Nitro Compounds

2.10.12.1. Aliphatic Nitro Compounds

The molecular ion peak (odd number) of an aliphatic mononitro compound is weak or absent (except in the lower homologs). The main peaks are attributable to the hydrocarbon fragments up to M − NO_2. Presence of a nitro group is indicated by an appreciable peak at *m/z* 30 (NO^+) and a smaller peak at mass 46 (NO_2^+).

2.10.12.2. Aromatic Nitro Compounds

The molecular ion peak of aromatic nitro compounds (odd number for one N atom) is strong. Prominent peaks result from elimination of an NO_2 radical (M − 46, the base peak in nitrobenzene), and of a neutral NO molecule with rearrangement to form the phenoxy cation (M − 30); both are good diagnostic peaks. Loss of HC≡CH from the M − 46 ion accounts for a strong peak at M − 72; loss of CO from the M − 30 ion gives a peak at M − 58. A diagnostic peak at *m/z* 30 results from the NO^+ ion.

The isomeric *o*-, *m*-, and *p*-nitroanilines each give a strong molecular ion (even number). They all give prominent peaks resulting from two sequences.

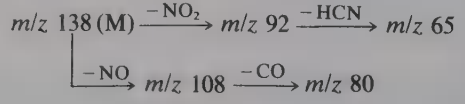

Aside from differences in intensities, the three isomers give very similar spectra. The meta and para compounds give a small peak at *m/z* 122 from loss of an O atom, whereas the ortho compound eliminates ·OH as follows to give a small peak at *m/z* 121.

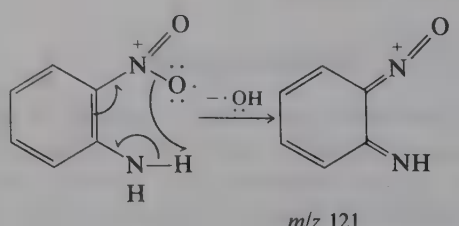

2.10.13. Aliphatic Nitrites

The molecular ion peak (odd number) of aliphatic nitrites (one N present) is weak or absent. The peak at *m/z* 30 (NO^+) is always large and is often the base peak. There is a large peak at *m/z* 60 ($CH_2{=}\overset{+}{O}NO$) in all nitrites unbranched at the α carbon; this represents cleavage of the C—C bond next to the ONO group. An α branch can be identified by a peak at *m/z* 74, 88, or 102, ... Absence of a large peak at *m/z* 46 permits differentiation from nitro compounds. Hydrocarbon peaks are prominent, and their distribution and intensities describe the arrangement of the carbon chain.

2.10.14. Aliphatic Nitrates

The molecular ion peak (odd number) of aliphatic nitrates (one nitrogen present) is weak or absent. A prominent (frequently the base) peak is formed by cleavage of the C—C bond next to the ONO_2 group with loss of the heaviest alkyl group attached to the α carbon.

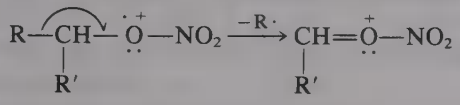

$R > R'$

The NO_2^+ peak at *m/z* 46 is also prominent. As in the case of aliphatic nitrites, the hydrocarbon fragment ions are distinct.

2.10.15. Sulfur Compounds

The contribution (4.4%, see Table 2.2 and Fig. 2.15) of the ^{34}S isotope to the M + 2 peak, and often to a (fragment + 2) peak, affords ready recognition of sulfur-containing compounds. A homologous series of sulfur-containing fragments is four mass units higher than the hydrocarbon fragment series. The number of sulfur atoms can be determined from the size of the contribution of the ^{34}S isotope to the M + 2 peak. The mass of the sulfur atom(s) present is subtracted from the molecular weight. In diisopentyl disulfide, for example, the molecular weight is 206, and the molecule contains two sulfur atoms. The formula for the rest of the molecule is therefore found under mass 142, that is, 206 − (2 × 32).

2.10.15.1. Aliphatic Mercaptans (Thiols)

The molecular ion peak of aliphatic mercaptans, except for higher tertiary mercaptans, is usually strong enough so that the M + 2 peak can be accurately measured. In general, the cleavage modes resemble those of alcohols. Cleavage of the C—C bond (α,β bond) next to the SH group gives the characteristic ion $CH_2{=}\overset{+}{S}H \leftrightarrow \overset{+}{C}H_2{-}SH$ (*m/z* 47). Sulfur is poorer than nitrogen, but better than oxygen, at stabilizing such a fragment. Cleavage at the β,γ bond gives a peak at *m/z* 61 of about one-half the intensity of the *m/z* 47 peak. Cleavage at the γ,δ bond gives a small peak at *m/z* 75, and cleavage at the δ,ϵ bond gives a peak at *m/z* 89 that is more intense than the peak at *m/z* 75; presumably the *m/z* 89 ion is stabilized by cyclization:

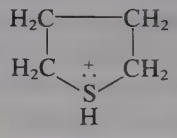

Again analogous to alcohols, primary mercaptans split out H_2S to give a strong M − 34 peak, the resulting

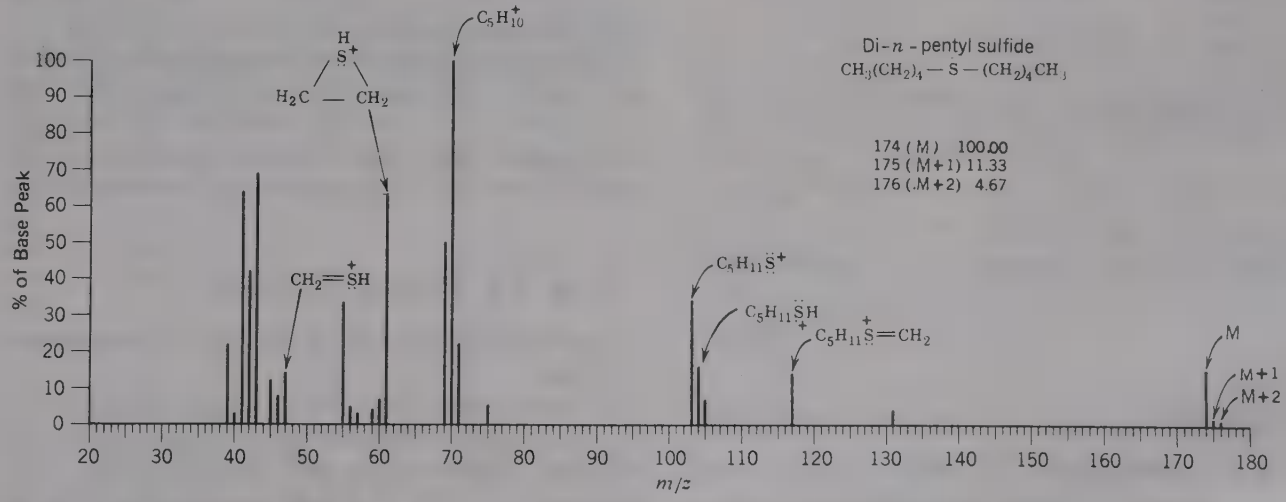

FIGURE 2.15. Di-*n*-pentyl sulfide. The table (upper right) has reset the molecular ion at an intensity of 100% for discussion of the molecular ion cluster.

ion then eliminating ethylene; thus the homologous series M − H_2S − $(CH_2{=}CH_2)_n$ arises.

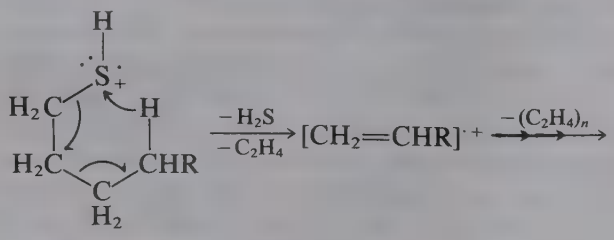

Secondary and tertiary mercaptans cleave at the α-carbon atom with loss of the largest group to give a prominent peak M − CH_3, M − C_2H_5, M − C_3H_7, ... However, a peak at *m/z* 47 may also appear as a rearrangement peak of secondary and tertiary mercaptans. A peak at M − 33 (loss of HS) is usually present for secondary mercaptans.

In long-chain mercaptans, the hydrocarbon pattern is superimposed on the mercaptan pattern. As for alcohols, the alkenyl peaks (i.e., *m/z* 41, 55, 69, . . .) are as large or larger than the alkyl peaks (*m/z* 43, 57, 71, . . .).

2.10.15.2. Aliphatic Sulfides

The molecular ion peak of aliphatic sulfides is usually intense enough so that the M + 2 peak can be accurately measured. The cleavage modes generally resemble those of ethers. Cleavage of one or the other of the α,β C—C bonds occurs, with loss of the largest group being favored. These first-formed ions decompose further with hydrogen transfer and elimination of an alkene. The steps for aliphatic ethers also occur for sulfides; the end result is the ion $RCH{=}\overset{+}{S}H$ (see Fig. 2.15, p. 33 for an example.)

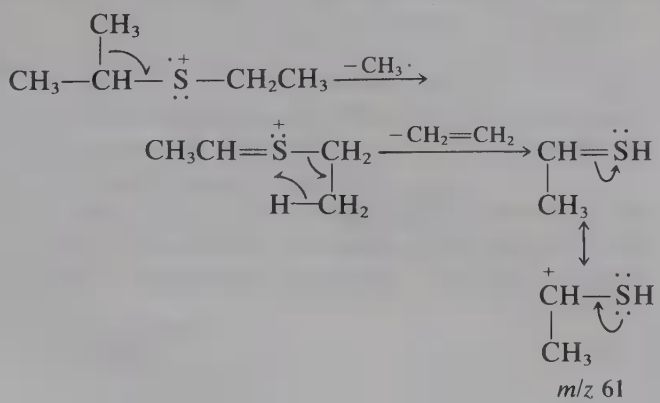

m/z 61

For a sulfide unbranched at either δ-carbon atom, this ion is $CH_2{=}\overset{+}{S}H$ (*m/z* 47), and its intensity may lead to confusion with the same ion derived from a mercaptan. However, the absence of M − H_2S or M − SH peaks in sulfide spectra makes the distinction.

A moderate to strong peak at *m/z* 61 is present (see alkyl sulfide cleavage above) in the spectrum of all except tertiary sulfides. When an α-methyl substituent is present, *m/z* 61 is the ion $CH_3CH{=}\overset{+}{S}H$ resulting from the double cleavage described above. Methyl primary sulfides cleave at the α,β bond to give the *m/z* 61 ion, $CH_3{-}\overset{+}{S}{=}CH_2$.

However, a strong *m/z* 61 peak in the spectrum of a straight-chain sulfide calls for a different explanation. The following rationalization is offered:

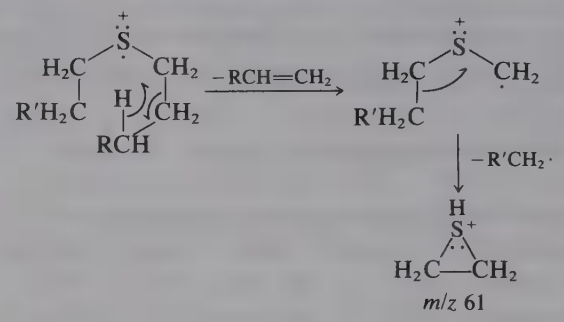

m/z 61

Sulfides give a characteristic ion by cleavage of the C—S bond with retention of charge on sulfur. The resulting $R\overset{+}{S}$ ion gives a peak at *m/z* 32 + CH_3, 32 + C_2H_5, 32 + C_3H_7, ... The ion of *m/z* 103 seems especially favored possibly because of formation of a rearranged cyclic ion.

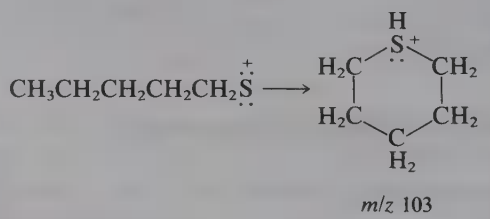

m/z 103

These features are illustrated by the spectrum of di-*n*-pentyl sulfide (Fig. 2.15).

As with long-chain ethers, the hydrocarbon pattern may dominate the spectrum of long-chain sulfides; the C_nH_{2n} peaks seem especially prominent. In branched-chain sulfides, cleavage at the branch may reduce the relative intensity of the characteristic sulfide peaks.

2.10.15.3. Aliphatic Disulfides

The molecular ion peak, at least up to C_{10} disulfides, is strong.

A major peak results from cleavage of one of the C—S bonds with retention of the charge on the alkyl fragment. Another major peak results from the same cleavage with shift of a hydrogen atom to form the RSSH fragment, which retains the charge. Other peaks apparently result from cleavage between the sulfur at-

oms without rearrangement, and with migration of one or two hydrogen atoms to give, respectively, $R\overset{+}{S}$, $R\overset{+}{S} - 1$, and $R\overset{+}{S} - 2$.

2.10.16. Halogen Compounds

A compound that contains one chlorine atom will have an M + 2 peak approximately one-third the intensity of the molecular ion peak because of the presence of a molecular ion containing the ^{37}Cl isotope (see Table 2.2). A compound that contains one bromine atom will have an M + 2 peak almost equal in intensity to the molecular ion because of the presence of a molecular ion containing the ^{81}Br isotope. A compound that contains two chlorines, or two bromines, or one chlorine and one bromine, will show a distinct M + 4 peak, in addition to the M + 2 peak, because of the presence of a molecular ion containing two atoms of the heavy isotope. In general, the number of chlorine and/or bromine atoms in a molecule can be ascertained by the number of alternate peaks beyond the molecular ion peak. Thus, three chlorine atoms in a molecule will give peaks at M + 2, M + 4, and M + 6; in polychloro compounds, the peak of highest mass may be so weak as to escape notice.

The relative abundances of the peaks (molecular ion, M + 2, M + 4, and so on) have been calculated by Beynon et al. for compounds containing chlorine and bromine (atoms other than chlorine and bromine were ignored). A portion of these results is presented here, somewhat modified, as Table 2.3. We can now tell what combination of chlorine and bromine atoms is present. It should be noted that Table 2.3 presents the isotope contributions in terms of percent of the molecular ion peak. Figure 2.16*a* provides the corresponding bar graphs.

TABLE 2.3

Intensities of Isotope Peaks (Relative to the Molecular Ion) for Combinations of Bromine and Chlorine

Halogen Present	% M + 2	% M + 4	% M + 6	% M + 8	% M + 10	% M + 12
Br	97.9					
Br_2	195.0	95.5				
Br_3	293.0	286.0	93.4			
Cl	32.6					
Cl_2	65.3	10.6				
Cl_3	97.8	31.9	3.47			
Cl_4	131.0	63.9	14.0	1.15		
Cl_5	163.0	106.0	34.7	5.66	0.37	
Cl_6	196.0	161.0	69.4	17.0	2.23	0.11
BrCl	130.0	31.9				
Br_2Cl	228.0	159.0	31.2			
Cl_2Br	163.0	74.4	10.4			

As required by Table 2.3, the M + 2 peak in the spectrum of *p*-chlorobenzophenone (Fig. 2.12) is about one-third the intensity of the molecular ion peak (*m/z* 218). As mentioned earlier, the chlorine-containing fragments (*m/z* 141 and 113) show (fragment + 2) peaks of the proper intensity.

Unfortunately, the application of isotope contributions, though generally useful for aromatic halogen compounds, is limited by the weak molecular ion peak of many aliphatic halogen compounds of more than about six carbon atoms for a straight chain, or fewer for a branched chain. However, the halogen-containing fragments are recognizable by the ratio of the (fragment + 2) peaks to fragment peaks in monochlorides or monobromides. In polychloro or bromo compounds, these (fragment + isotope) peaks form a distinctive series of multiplets (Fig. 2.16*b*). Coincidence of fragment ion with one of the isotope fragments, with another disruption of the characteristic ratios, must always be kept in mind.

Neither fluorine nor iodine has a heavier isotope.

2.10.16.1. Aliphatic Chlorides

The molecular ion peak is detectable only in the lower monochlorides. Fragmentation of the molecular ion is mediated by the chlorine atom but to a much lesser degree than is the case in oxygen-, nitrogen-, or sulfur-containing compounds. Thus, cleavage of a straight-chain monochloride at the C—C bond adjacent to the chlorine atom accounts for a small peak at *m/z* 49 (and, of course, the isotope peak at *m/z* 51).

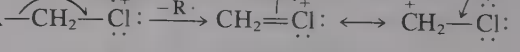

Cleavage of the C—Cl bond leads to a small Cl^+ peak and to a R^+ peak which is prominent in the lower chlorides, but quite small when the chain is longer than about C_5.

Straight-chain chlorides longer than C_6 give $C_3H_6\overset{+}{Cl}$, $C_4H_8\overset{+}{Cl}$, and $C_5H_{10}\overset{+}{Cl}$ ions. Of these the $C_4H_8\overset{+}{Cl}$ ion forms the most intense (sometimes the base) peak; a five-membered cyclic structure may explain its stability.

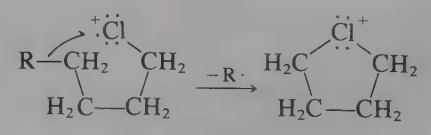

Loss of HCl occurs, possibly by 1,3-elimination, to give a peak (weak or moderate) at M − 36.

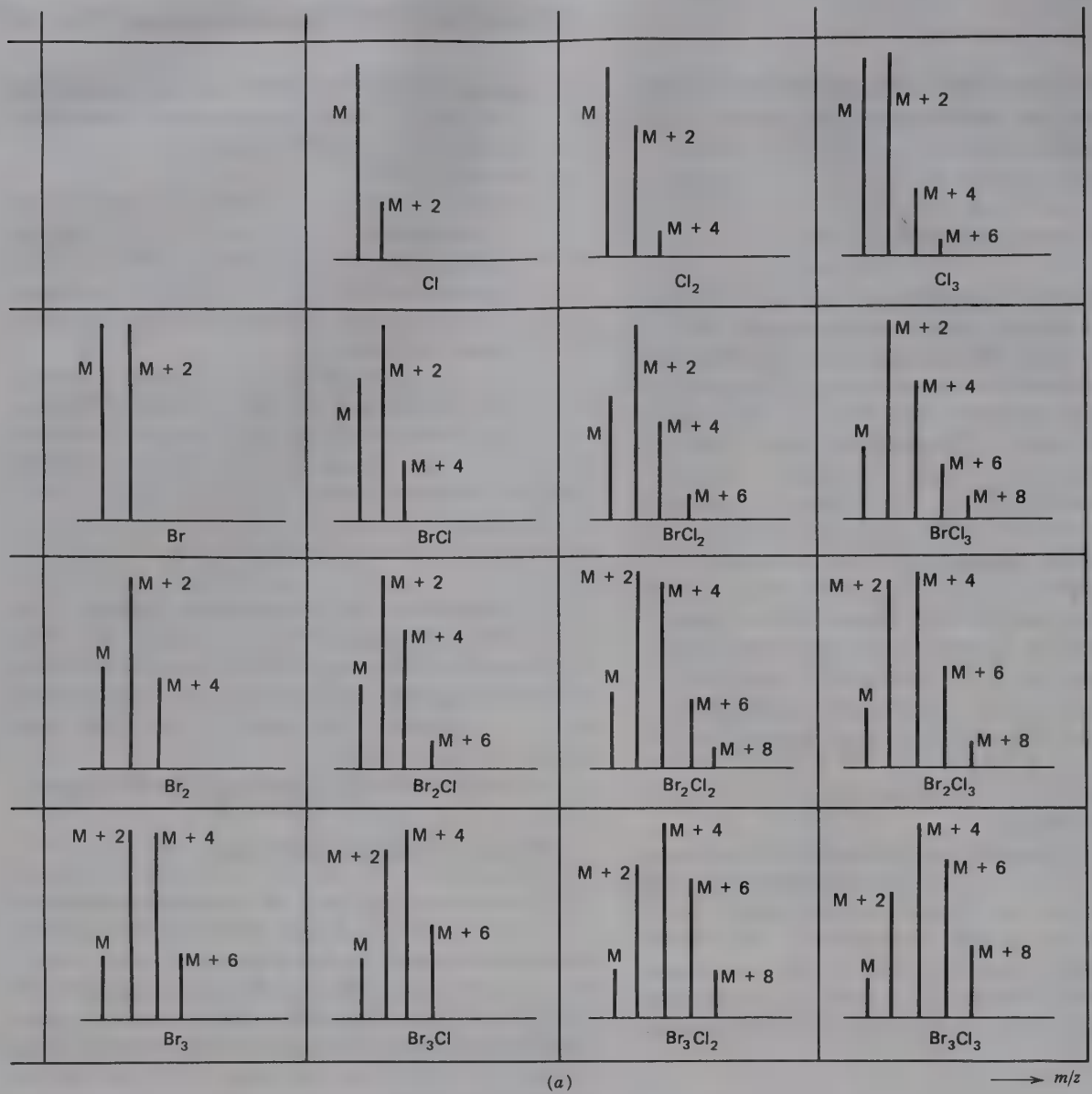

FIGURE 2.16(*a*). Peaks in the molecular ion region of bromo and chloro compounds. Contributions due to C, H, N, and O are usually small compared to those for Br and Cl.

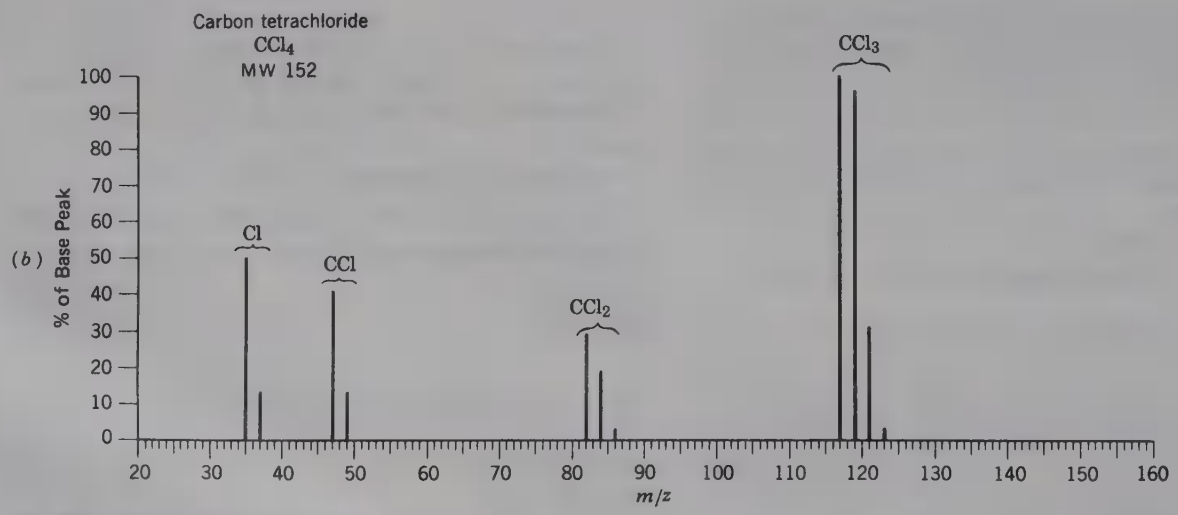

FIGURE 2.16(*b*). Carbon tetrachloride (cf. Fig. 2.16*a*).

In general, the spectrum of an aliphatic monochloride is dominated by the hydrocarbon pattern to a greater extent than that of a corresponding alcohol, amine, or mercaptan.

2.10.16.2. Aliphatic Bromides

The remarks under aliphatic chlorides apply quite generally to the corresponding bromides.

2.10.16.3. Aliphatic Iodides

Aliphatic iodides give the strongest molecular ion peak of the aliphatic halides. Since iodine is monoisotopic, there is no distinctive isotope peak. The presence of an iodine atom can sometimes be deduced from isotope peaks that are suspiciously low in relation to the molecular ion peaks, and from several distinctive peaks; in polyiodo compounds, the large interval between major peaks is characteristic.

Iodides cleave much as do chlorides and bromides, but the $C_4H_8\overset{+}{I}$ ion is not as evident as the corresponding chloride and bromide ions.

2.10.16.4. Aliphatic Fluorides

Aliphatic fluorides give the weakest molecular ion peak of the aliphatic halides. Fluorine is monoisotopic, and its detection in polyfluoro compounds depends on suspiciously small isotopic peaks relative to the molecular ion, on the intervals between peaks, and on characteristic peaks. Of these, the most characteristic is *m/z* 69 due to the ion CF_3^+, which is the base peak in all perfluorocarbons. Prominent peaks are noted at *m/z* 119, 169, 219. . . ; these are increments of CF_2. The stable ions $C_3F_5^+$ and $C_4F_7^+$ give large peaks at *m/z* 131 and 181. The M − F peak is frequently visible in perfluorinated compounds. In monofluorides, cleavage of the α,β C—C bond is less important than in the other monohalides, but cleavage of a C—H bond on the α-carbon atom is more important. This reversal is a consequence of the high electronegativity of the F atom, and is rationalized by placing the positive charge on the α-carbon atom. The secondary carbonium ion thus depicted by a loss of a hydrogen atom is more stable than the primary carbonium ion resulting from loss of an alkyl radical.

62

$$[R{-}CH_2{-}F]^{\cdot+} \xrightarrow{-H\cdot} R{-}\overset{+}{C}H{-}F$$
$$\qquad\qquad \xrightarrow{-R\cdot} \overset{+}{C}H_2{-}F$$

2.10.16.5. Benzyl Halides

The molecular ion peak of benzyl halides is usually detectable. The benzyl (or tropylium) ion from loss of the halide (Section 2.7, Rule 8) is favored even over β-bond cleavage of an alkyl substituent. A substituted phenyl ion (α-bond cleavage) is prominent when the ring is polysubstituted.

2.10.16.6. Aromatic Halides

The molecular ion peak of an aryl halide is readily apparent. The M − X peak is large for all compounds in which X is attached directly to the ring.

2.10.17. Heteroaromatic Compounds

The molecular ion peak of heteroaromatics and alkylated heteroaromatics is intense. Cleavage of the bond β to the ring, as in alkylbenzenes, is the general rule; in pyridine, the position of substitution determines the ease of cleavage of the β bond (see below).

Localizing the charge of the molecular ion on the heteroatom, rather than in the ring π structure, provides a satisfactory rationale for the observed mode of cleavage. The present treatment follows that used by Djerassi.

The five-membered ring heteroaromatics (furan, thiophene, and pyrrole) show very similar ring cleavage patterns. The first step in each case is cleavage of the carbon–heteroatom bond.

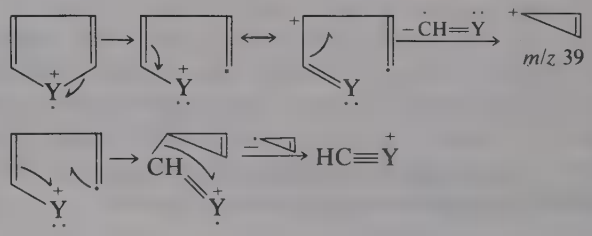

Y = O, S, NH

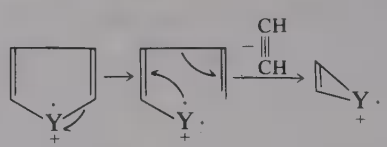

Y = S, NH

Thus furan exhibits two principal peaks: $C_3H_3^+$ (*m/z* 39) and $HC{\equiv}\overset{+}{O}$ (*m/z* 29). For thiophene, there are three peaks: $C_3H_3^+$ (*m/z* 39), $HC{\equiv}\overset{+}{S}$ (*m/z* 45), and $C_2H_2\overset{+}{S}$ (*m/z* 58). And for pyrrole, there are three peaks: $C_3H_3^+$ (*m/z* 39), $HC{\equiv}\overset{+}{N}H$ (*m/z* 28) and $C_2H_2\overset{+}{N}H$ (*m/z* 41). Pyrrole also eliminates a neutral molecule of HCN

to give an intense peak at *m/z* 40. The base peak of 2,5-dimethylfuran is *m/z* 43 ($CH_3C{\equiv}\overset{+}{O}$).

Cleavage of the β C—C bond in alkylpyridines depends on the position of the ring substitution, being more pronounced when the alkyl group is in the 3 position. An alkyl group of more than three carbon atoms in the 2 position can undergo migration of a hydrogen atom to the ring nitrogen.

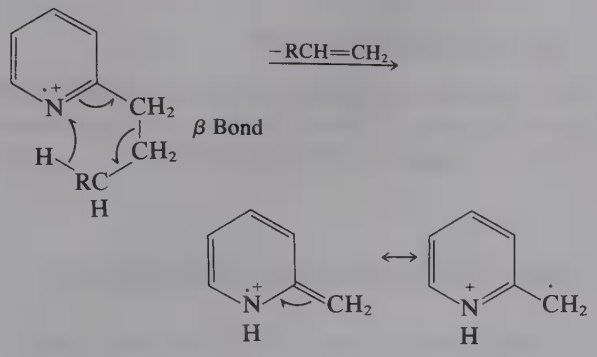

A similar cleavage is found in pyrazines since all ring substituents are necessarily ortho to one of the nitrogen atoms.

2.10.18. Natural Products

2.10.18.1. Amino Acids

Detection of the molecular ion peaks of amino acids can be difficult. If we examine the mass spectra of amino acids, as well as of steroids and triglycerides, by a variety of ionization techniques, we can appreciate their relative merits.

The EI spectra of amino acids (Fig. 2.17*a*) or their esters give weak or nonexistent molecular ion peaks, but CI and FD (Fig. 2.17*b* and *c*) give either molecular or quasi-molecular ion peaks. The weak molecular ions in the EI spectra arise since amino acids easily lose their carboxyl group and the esters easily lose their carboalkoxyl group upon electron impact.

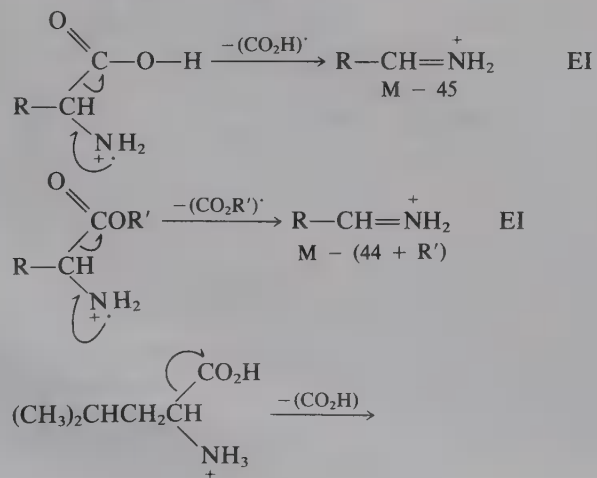

The FD fragmentation pattern for leucine shows an MH^+ (*m/z* 132) ion, that readily loses a carboxyl group

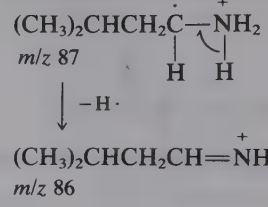

to form the *m/z* 87 ion, which in turn loses a hydrogen atom to form the *m/z* 86 ion.

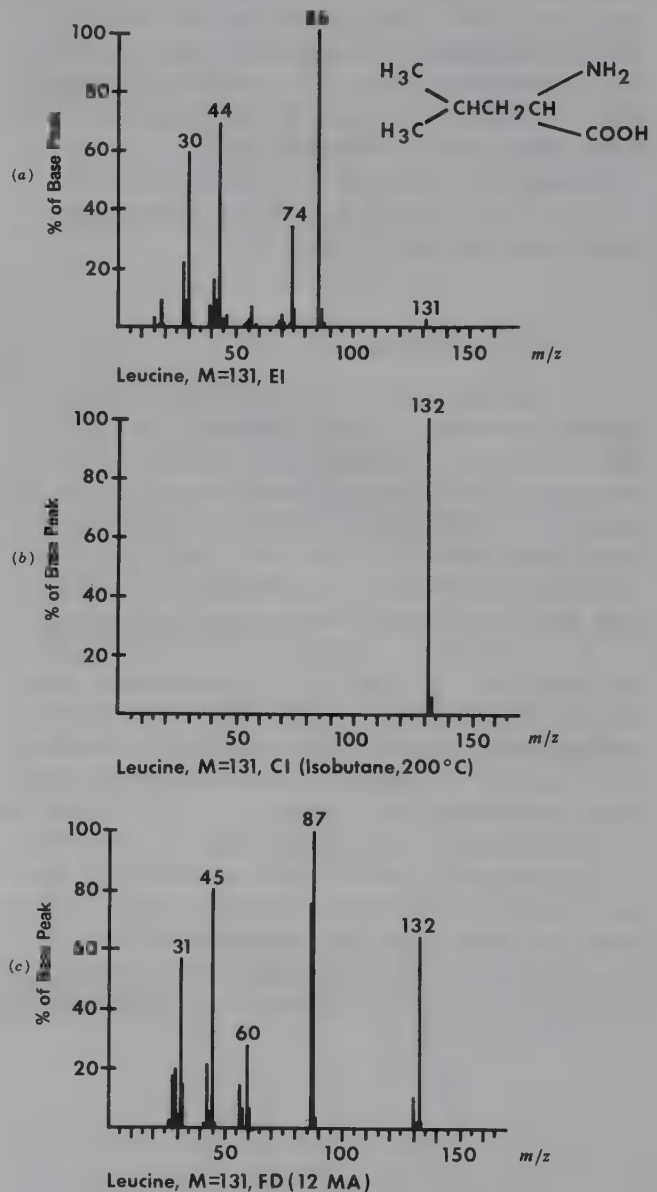

FIGURE 2.17. Mass spectra of leucine. (*a*) Electron impact (EI). (*b*) Chemical ionization (CI). (*c*) Field desorption (FD).

2.10.19. Steroids

Polyhydroxy steroids (e.g., the tetrol for which spectra are shown in Fig. 2.18) give EI spectra that often show weak or nonexistent molecular ion peaks. For this tetrol facile dehydration is only partly caused by heating.

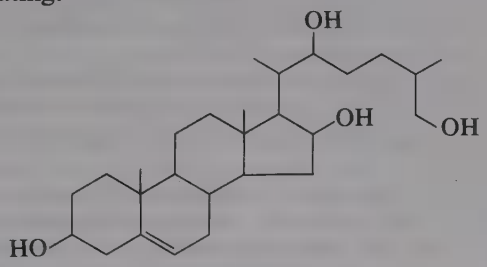

Cholesten-5-ene-3,16,22,26-tetrol

Chemical ionization (Fig. 2.18*b*) is not useful since the protonated molecular ion also readily dehydrates. Dehydration is not observed at all in the FD spectrum (Fig. 18*c*), which shows only a molecular ion peak.

Triglycerides give rise to characteristic [M − O_2CR] ions arising from positive charge stabilization by neighboring oxygen.

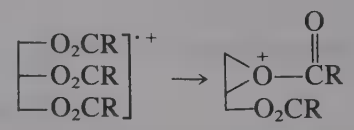

Thus the loss of the RCO_2 fragment and the appearance of $(RCO_2H + H)^+$ fragments reveal the identity of their acid components.

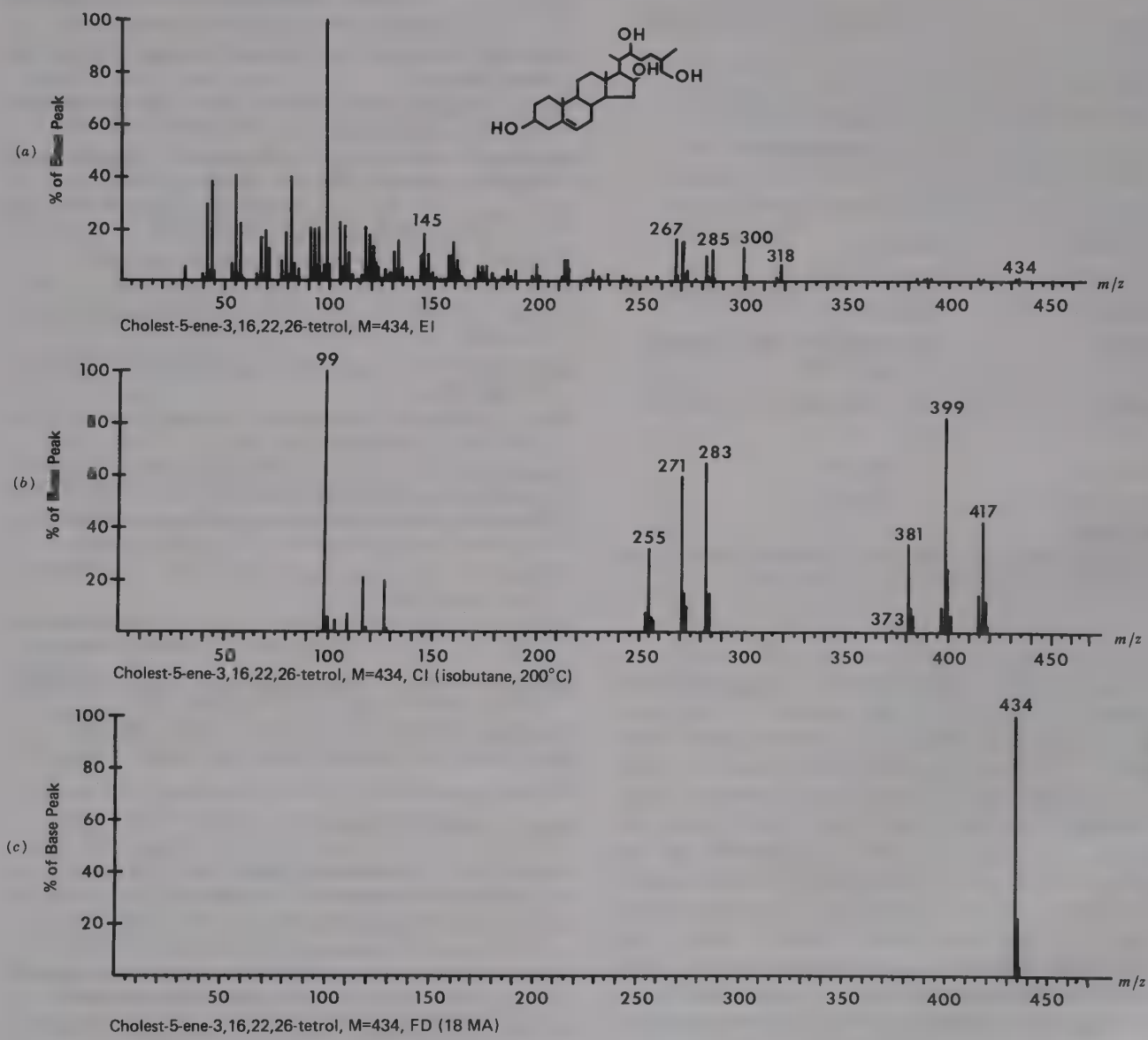

FIGURE 2.18. Mass spectra of cholest-5-ene-3,16,22,26-tetrol. (*a*) Electron impact (EI). (*b*) Chemical ionization (CI). (*c*) Field desorption (FD).

2.10.19.1. Triglycerides

Naturally occurring triglycerides, which have high molecular weights and low volatility, give weak or nonexistent molecular ion (or MH^+) peaks by EI and CI techniques.

2.10.20. Miscellaneous Classes

The following classes of organic compounds are discussed in Biemann's book (B) or in Djerassi's books (D, DI, DII).*

Alkaloids	D, Chapter 5; DI; DII, Chapter 17; B, p. 305
Amino acids and peptides	DII, Chapter 26; B, Chapter 7
Antibiotics	DII, p, 172
Carbohydrates	DII, Chapter 27
Cyanides and isothiocyanates	D, Chapter 11
Estrogens	DII, Chapter 19
Glycerides	B, p. 255
Sapogenins	DII, Chapter 22
Silicones	B, p. 172
Steroids	B, Chapter 9; DII, Chapters 17, 20, 21, 22
Terpenes	B, p. 334; DII, Chapters 23, 24
Thioketals	D, Chapter 7
Tropone and tropolones	D, Chapter 18

*B: Biemann (1962). D: Djerassi, et al., (1967). DI: Djerassi, et al. (1964, Vol. 1). DII: Djerassi, et al., (1964, Vol. II).

In this chapter we have covered a large amount of information. Now let us apply some of it to the spectrum of benzamide (Fig. 2.1) as if it were an "unknown." The intense molecular ion peak (*m/z* 121) suggests aromaticity. The fact that 121 is an odd number indicates an odd number of nitrogen atoms in the structure. Aromatic character is supported and its identity clarified by the intense phenyl cation peak at *m/z* 77: We are clearly dealing with a monosubstituted benzene ring. The nitrogen rule corollary suggests that neither the *m/z* 77 nor 105 peak contain nitrogen. Since the IR spectrum indicates that the compound is a primary amide, we use the *m/z* 44 peak as confirmation of this functional group.

REFERENCES

Beynon, J. H. *Mass Spectrometry and Its Application to Organic Chemistry*. Amsterdam: Elsevier, 1960.

Beynon, J. H., Saunders, R. A., Williams A. E. *The Mass Spectra of Organic Molecules*. New York: Elsevier, 1968.

Biemann, K. *Mass Spectrometry, Applications to Organic Chemistry*. New York: McGraw–Hill, 1962.

Budzikiewicz, H., Djerassi, C., Williams, D. H. *Mass Spectrometry of Organic Compounds*. San Francisco: Holden–Day, 1967. Written for the organic chemist who uses mass spectrometry in structure determination.

Budzikiewicz, H., Djerassi, C., Williams, D. H. *Structure Elucidation of Natural Products by Mass Spectrometry*. San Francisco: Holden–Day, 1964, Vols. I and II.

Beynon, J. H. *Mass Spectrometry and Its Application to Organic Chemistry*. Amsterdam: Elsevier, 1960.

Beynon, J. H., Saunders, R. A., Williams A. E. *The Mass Spectra of Organic Molecules*. New York: Elsevier, 1968.

Chapman, J. R. *Practical Organic Mass Spectrometry*, New York: Wiley, 1985.

Howe, I., Williams, D. H., and Bowen, R. D. *Mass Spectrometry-Principles and Application*, New York: Wiley, 1981.

Hamming, M. and Foster, N. *Interpretation of Mass Spectra of Organic Compounds*. New York: Academic, 1972.

McLafferty, F. W. *Interpretation of Mass Spectra*, 3rd ed., Mill Valley, CA. University Scientific Books, 1980.

McLafferty, F. W. and Venkataraghavan, R. *Mass Spectral Correlations*, Washington, DC: American Chemical Society, 1982.

McNeal, C. J., (Ed.) *Mass Spectrometry in the Analysis of Large Molecules*, New York: Wiley, 1986.

Middeditch, B. S. (Ed.) *Practical Mass Spectrometry*, New York: Plenum, 1979.

Milne, G. W. A. *Mass Spectrometry: Techniques and Applications*. New York: Wiley–Interscience, 1971.

Rose, M. and Johnston, R. A. W. *Mass Spectrometry for Chemists and Biochemists*, New York, Cambridge University Press, 1982.

Shrader, S. R. *Introduction to Mass Spectrometry*, Boston: Allyn and Bacon, 1971.

Watson, J. T. *Introduction to Mass Spectrometry*, 2nd ed., New York: Raven Press, 1985.

Williams, D. H. *Mass Spectrometry, A Specialist Periodical Report*, Vols. I–V. London: Chemical Society, June 1968–June 1979.

Advances in Mass Spectrometry: Applications in Organic and Analytical Chemistry; New York: Pergamon, 1980.

Mass Spectrometry Reviews, New York: Wiley, 1982–date.

Mass Spectrometry Bulletin, Aldermaston, England, 1966–date.

Data and Spectral Compilations

ASTM (1963). "Index of Mass Spectral Data," American Society for Testing and Materials. STP-356, 244 pp.

ASTM (1969). "Index of Mass Spectral Data," American Society for Testing and Materials, AMD 11, 632 pp.

Beynon, J. H. and Williams, A. E. *Mass and Abundance Tables for Use in Mass Spectrometry*, Amsterdam: Elsevier, 1963.

Beynon, J. H., Saunders, R. A., and Williams, A. E. *Table of Meta-Stable Transitions*, New York: Elsevier, 1965.

Catalog of Selected Mass Spectral Data (1947 to date), American Petroleum Institute Research Project 44 and Thermodynamics Research Center (formerly MCA Research Project), College Station, Texas, Texas A & M University, Dr. Bruno Zwolinski, Director.

Cornu, A. and Massot, R. *Compilation of Mass Spectral Data.* London: Heyden, 1966. First and second supplements issued.

Eight Peak Index of Mass Spectral Vols. 1–3 (5 books, 66,720 spectra), Chemical Society: London, 1983.

Handbook of Spectroscopy Vol. II. Cleveland: CRC Press, 1974, pp. 317–330. Electron impact data for 15 compounds in each of 16 classes of organic compounds.

Heller, S. R. and Milne, G. W. EPA/NIH Mass Spectral Search System (MSSS), A Division of CIS, Washington: US Government Printing Office. An interactive computer searching system containing the spectra of over 32,000 compounds. These can be searched on the basis of peak intensities as well as by Biemann and probability matching techniques.

McLafferty, F. S. *Mass Spectral Correlations,* 2nd ed., Washington, DC: American Chemical Society, 1982.

McLafferty, F. S. and Penzelik, J. *Index and Bibliography of Mass Spectrometry 1963–1965,* New York: Interscience–Wiley, 1967.

McLafferty, F. W. and Stauffer, D. B. *The Wiley/NBS Registry of Mass Spectral Data,* New York: Wiley–Interscience, 1988 (7 Volumes, 15,000 Spectra).

McLafferty, F. W. and Stauffer, D. B. *Registry of Mass Spectral Data,* 5th ed. (Magnetic Disc, Hard Disc, or CD-Rom) New York: Wiley, 193,859 Spectra.

Stenhagen, E., Abrahamsson, S., and McLafferty, F. (Eds.) *Atlas of Mass Spectral Data,* New York: Interscience–Wiley, 1969. Vol. 1: Molecular Weight: 16.313–142.0089; Vol. 2: Molecular Weight: 142.0185–213.2456; Vol. 3: Molecular Weight: 213,8629–702.7981. The three volumes have complete EI data for about 6000 compounds.

Stenhagen, E., Abrahamsson, S., and McLafferty, F. (Eds.) *Registry of Mass Spectral Data,* New York: Wiley–Interscience, 1974. Vol. I: MW 16.0313–187.1572, Formula CH_4–$C_{10}H_{21}NO_2$; Vol. II: MW 187.1572–270.1256, Formula $C_{10}H_{21}NO_2$–$C_{17}H_{18}O_3$; Vol. III: MW 270.2671–402.3305, Formula $C_{16}H_{34}N_2O$–$C_{25}H_{13}O_3B$; Vol. IV: MW 40.3305–1519.806, Formula $C_{25}H_3O_3B$–$(C_9H_{18}D_3O_3Al)_n$. The four volumes contain bar graphs of 18,806 compounds. Volume IV also contains the index for all four volumes.

Special Monographs

Adams, F., Grijbis, R., and VanGriekan, R. (Eds.) *Inorganic Mass Spectrometry,* New York: Wiley, 1988.

Dawson, P. H. *Quadrupole Mass Spectrometry,* New York: Elsevier, 1976.

Linskens, H. F. and Berlin, J. (Eds.) *Gas Chromatography-Mass Spectrometry,* New York: Springer–Verlag, 1986.

March, R. E. and Hughes, R. J. *Quadrupole Storage Mass Spectrometry,* New York: Wiley–Interscience, 1989.

McFadden, W. H. *Techniques of Combined Gas Chromatography/Mass Spectrometry: Applications in Organic Analysis,* New York: Wiley–Interscience, 1973.

McLafferty, F. S. *Tandem Mass Spectrometry,* 2nd ed., New York: Wiley–Interscience, 1983.

Message, G. M. *Practical Aspects of Gas Chromatography–Mass Spectrometry,* New York: Wiley, 1984.

Porter, Q. N. and Baldas, J. *Mass Spectrometry of Heterocyclic Compounds* in General Heterocycle Chemistry Series, A. Weissberger and E. C. Taylor (Eds.) New York: Wiley–Interscience, 1971.

Safe, S. and Hutzinger, O. *Mass Spectrometry of Pesticides and Pollutants.* Cleveland: CRC Press, 1973.

Waller, G. R. (Ed.) *Biochemical Applications of Mass Spectrometry.* New York: Wiley–Interscience, 1972.

Waller, G. R. and Dermer, O. C., (Eds.) *Biochemical Applications of Mass Spectrometry,* First Supplementary Volume, New York: Wiley–Interscience, 1980.

PROBLEMS

All spectra were determined by EI methods.

2.1 The exact mass of a compound determined by high-resolution mass spectrometry is 212.0833. What is the molecular formula of the compound?

2.2 The compound whose molecular formula is deduced in Problem 2.1 gives rise to the mass spectrum shown below. Deduce the structure of this compound.

PROBLEM 2.2.

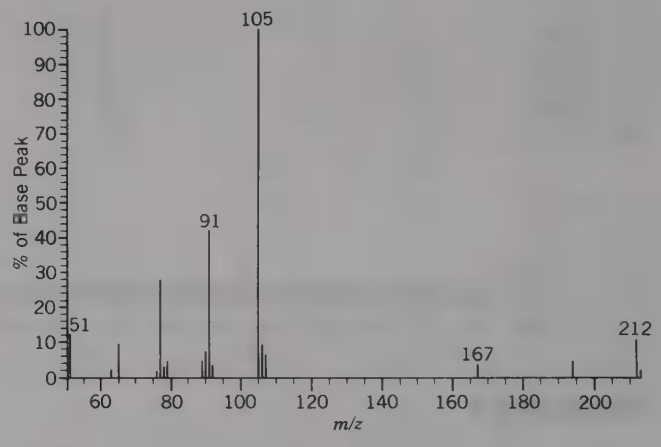

2.3 The mass spectrum of 2-butenal shows a peak at *m/z* 69 that is 28.9% as intense as the base peak. Propose at least one fragmentation route to account for this peak, and explain why this fragment would be reasonably stable.

2.4 The mass spectrum of 3-butyn-2-ol shows the base peak at *m/z* 55. Explain why the fragment giving rise to this peak would be very stable.

2.5 Consider the mass spectra on p. 42 (nominal mass resolution) of two isomers (**A** and **B**) of molecular formula $C_{10}H_{14}$. Determine their structures and explain the major spectral features for each.

2.6 The mass spectrum of *o*-nitrotoluene shows a substantial peak at *m/z* 120. Similar analysis of α,α,α-tri-deutero-*o*-nitrotoluene does not give a peak at *m/z* 120 but rather at *m/z* 122. Explain.

2.7 Determine the structure for the mass spectrum shown below.

2.8 Below find mass spectra for compounds **C–F**. Compound **C** has an M + 1 peak that is 2.5% of M (where M = 100%). Compound **F** can easily be converted to compounds **D** and **E**. Compounds **C–E** each give precipitates when treated with alcoholic silver nitrate. The precipitate from **D** is white, the other two are varying shades of yellow. Deduce the structures of **C–F**.

PROBLEM 2.5, isomer A.

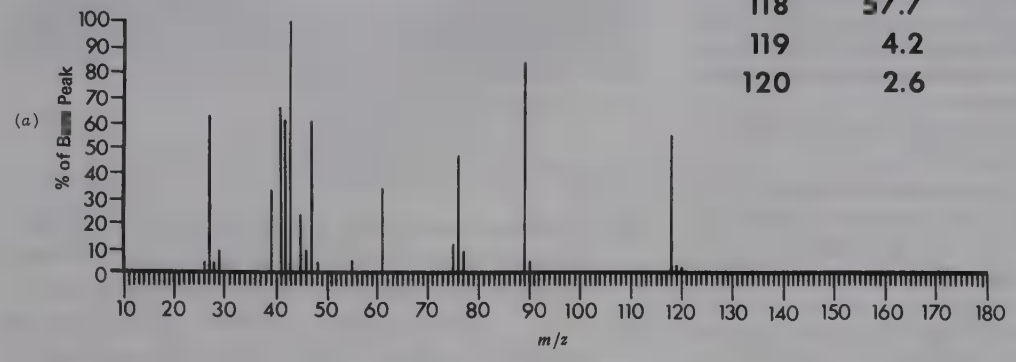

Isomer A *m/z*	Relative Intensity
118	57.7
119	4.2
120	2.6

PROBLEM 2.5, isomer B.

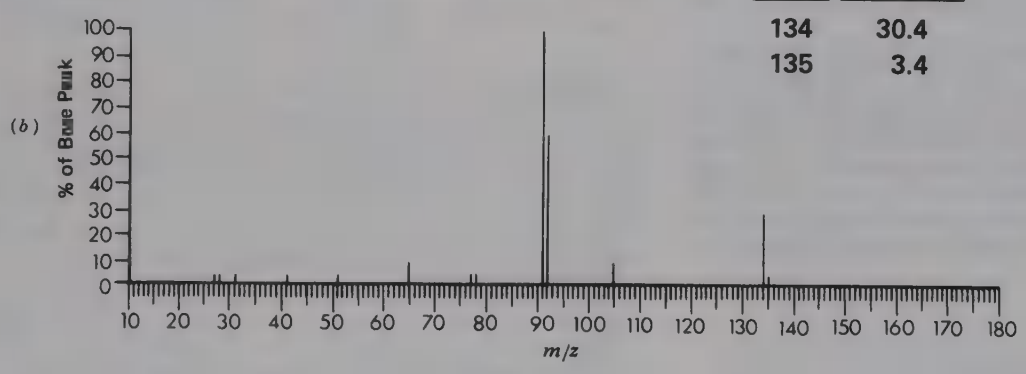

Isomer B *m/z*	Relative Intensity
134	30.4
135	3.4

PROBLEM 2.7.

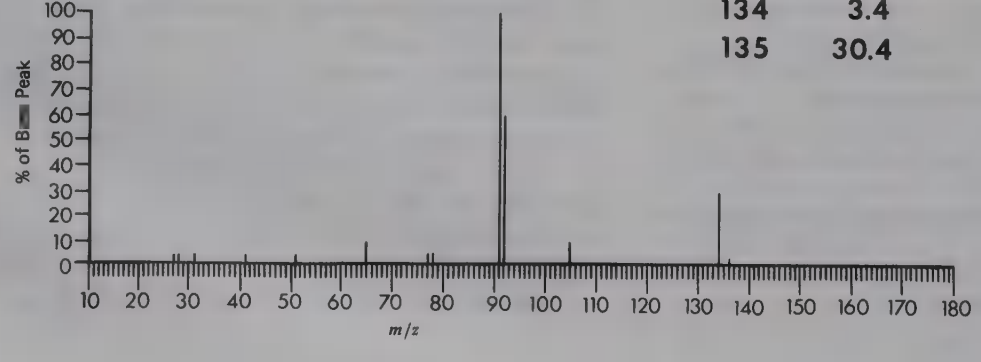

m/z	Relative Intensity
134	3.4
135	30.4

PROBLEM 2.8, Compound C.

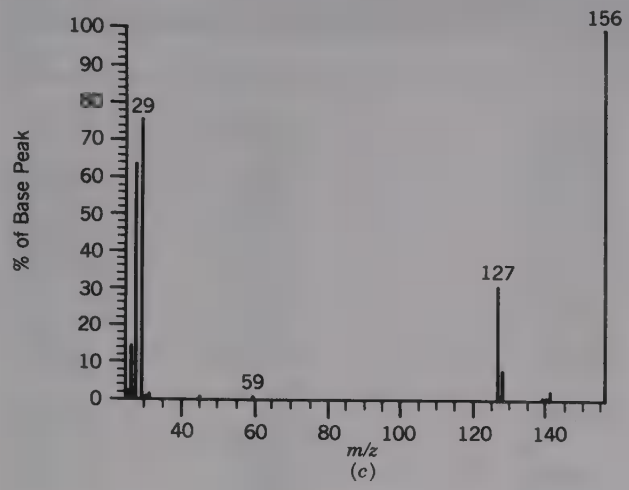

(c)

PROBLEM 2.8, Compound D.

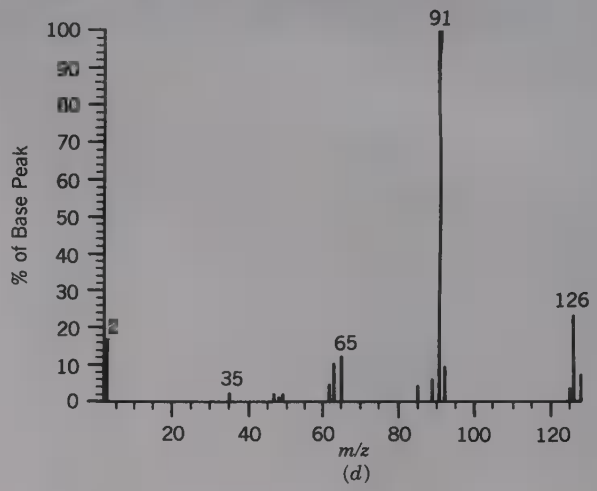

(d)

PROBLEM 2.8, Compound E.

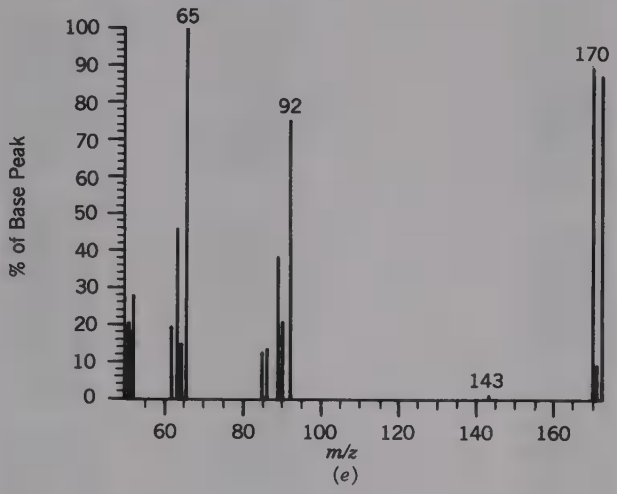

(e)

PROBLEM 2.8, Compound F.

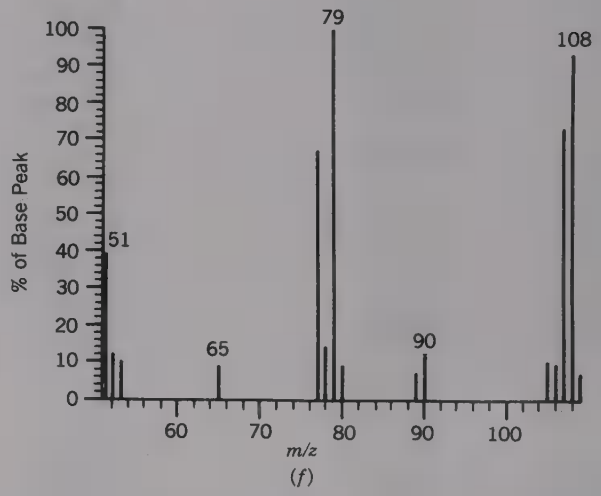

(f)

Appendix A Masses and Isotopic Abundance Ratios for Various Combinations of Carbon, Hydrogen, Nitrogen and Oxygen[a]

	FM		FM		FM
12		O_2	31.9898	C_3H_8	44.0626
C	12.0000	H_2NO	32.0136	**45**	
13		H_4N_2	32.0375	HN_2O	45.0089
CH	13.0078	CH_4O	32.0262	H_3N_3	45.0328
14		**33**		CHO_2	44.9976
N	14.0031	HO_2	32.9976	CH_3NO	45.0215
CH_2	14.0157	H_3NO	33.0215	CH_5N_2	45.0453
15		**34**		C_2H_5O	45.0340
HN	15.0109	H_2O_2	34.0054	C_2H_7N	45.0579
CH_3	15.0235	**36**		**46**	
16		C_3	36.0000	NO_2	45.9929
O	15.9949	**37**		H_2N_2O	46.0167
H_2N	16.0187	C_3H	37.0078	H_4N_3	46.0406
CH_4	16.0313	**38**		CH_2O_2	46.0054
17		C_2N	38.0031	CH_4NO	46.0293
HO	17.0027	C_3H_2	38.0157	CH_6N_2	46.0532
H_3N	17.0266	**39**		C_2H_6O	46.0419
18		C_2HN	39.0109	**47**	
H_2O	18.0106	C_3H_3	39.0235	HNO_2	47.0007
24		**40**		H_3N_2O	47.0246
C_2	24.0000	CN_2	40.0062	H_5N_3	47.0484
25		C_2O	39.9949	CH_3O_2	47.0133
C_2H	25.0078	C_2H_2N	40.0187	CH_5NO	47.0371
26		C_3H_4	40.0313	**48**	
CN	26.0031	**41**		O_3	47.9847
C_2H_2	26.0157	CHN_2	41.0140	H_2NO_2	48.0085
27		C_2HO	41.0027	H_4N_2O	48.0324
CHN	27.0109	C_2H_3N	41.0266	CH_4O_2	48.0211
C_2H_3	27.0235	C_3H_5	41.0391	C_4	48.0000
28		**42**		C_4N	62.0031
N_2	28.0062	N_3	42.0093	C_5H_2	62.0157
CO	27.9949	CNO	41.9980	**49**	
CH_2N	28.0187	CH_2N_2	42.0218	HO_3	48.9925
C_2H_4	28.0313	C_2H_2O	42.0106	H_3NO_2	49.0164
29		C_2H_4N	42.0344	C_4H	49.0078
HN_2	29.0140	C_3H_6	42.0470	**50**	
CHO	29.0027	**43**		H_2O_3	50.0003
CH_3N	29.0266	HN_3	43.0171	C_3N	50.0031
C_2H_5	29.0391	CHNO	43.0058	C_4H_2	50.0157
30		CH_3N_2	43.0297	**51**	
NO	29.9980	C_2H_3O	43.0184	C_3HN	51.0109
H_2N_2	30.0218	C_2H_5N	43.0422	C_4H_3	51.0235
CH_2O	30.0106	C_3H_7	43.0548	**52**	
CH_4N	30.0344	**44**		C_2N_2	52.0062
C_2H_6	30.0470	N_2O	44.0011	C_3O	51.9949
31		H_2N_3	44.0249	C_3H_2N	52.0187
HNO	31.0058	CO_2	43.9898	C_4H_4	52.0313
H_3N_2	31.0297	CH_2NO	44.0136	**53**	
CH_3O	31.0184	CH_4N_2	44.0375	C_2HN_2	53.0140
CH_5N	31.0422	C_2H_4O	44.0262	C_3HO	53.0027
32		C_2H_6N	44.0501	C_3H_3N	53.0266

[a]M + 1 and M + 2 intensities may be calculated (p. 10) or may be taken from J.H. Beynon, *Mass Spectrometry and its Application to Organic Chemistry*, Elsevier, Amsterdam, 1960.

Those data form a self-consistent set and can be used regardless of the mass standard. The columns headed FM contain the formula masses based on the exact mass of the most abundant isotope of each element; these masses are based on the most abundant isotope of carbon having a mass of 12.0000.

Appendix A (continued)

	FM		FM		FM
C_4H_5	53.0391	**60**		H_2O_4	65.9953
54		N_2O_2	59.9960	C_2N_3	66.0093
CN_3	54.0093	H_2N_3O	60.0198	C_3NO	65.9980
C_2NO	53.9980	H_4N_4	60.0437	$C_3H_2N_2$	66.0218
$C_2H_2N_2$	54.0218	CO_3	59.9847	C_4H_2O	66.0106
C_3H_2O	54.0106	CH_2NO_2	60.0085	C_4H_4N	66.0344
C_3H_4N	54.0344	CH_4N_2O	60.0324	C_5H_6	66.0470
C_4H_6	54.0470	CH_6N_3	60.0563	**67**	
55		$C_2H_4O_2$	60.0211	C_2HN_3	67.0171
CHN_3	55.0171	C_2H_6NO	60.0449	C_3HNO	67.0058
C_2HNO	55.0058	$C_2H_8N_2$	60.0688	$C_3H_3N_2$	67.0297
$C_2H_3N_2$	55.0297	C_3H_8O	60.0575	C_4H_3O	67.0184
C_3H_3O	55.0184	C_5	60.0000	C_4H_5N	67.0422
C_3H_5N	55.0422	**61**		C_5H_7	67.0548
C_4H_7	55.0548	HN_2O_2	61.0038	**68**	
56		H_3N_3O	61.0277	CN_4	68.0124
N_4	56.0124	H_5N_4	61.0515	C_2N_2O	68.0011
CN_2O	56.0011	CHO_3	60.9925	$C_2H_2N_3$	68.0249
CH_2N_3	56.0249	CH_3NO_2	61.0164	C_3O_2	67.9898
C_2O_2	55.9898	CH_5N_2O	61.0402	C_3H_2NO	68.0136
C_2H_2NO	56.0136	CH_7N_3	61.0641	$C_3H_4N_2$	68.0375
$C_2H_4N_2$	56.0375	$C_2H_5O_2$	61.0289	C_4H_4O	68.0262
C_3H_4O	56.0262	C_2H_7NO	61.0528	C_4H_6N	68.0501
C_3H_6N	56.0501	C_5H	61.0078	C_5H_8	68.0626
C_4H_8	56.0626	**62**		**69**	
57		NO_3	61.9878	CHN_4	69.0202
HN_4	57.0202	$H_2N_2O_2$	82.0116	C_2HN_2O	69.0089
CHN_2O	57.0089	H_4N_3O	62.0355	$C_2H_3N_3$	69.0328
CH_3N_3	57.0328	H_6N_4	62.0594	C_3HO_2	68.9976
C_2HO_2	56.9976	CH_2O_3	62.0003	C_3H_3NO	69.0215
C_2H_3NO	57.0215	CH_4NO_2	62.0242	$C_3H_5N_2$	69.0453
$C_2H_5N_2$	57.0453	CH_6N_2O	62.0480	C_4H_5O	69.0340
C_3H_5O	57.0340	$C_2H_6O_2$	62.0368	C_4H_7N	69.0579
C_3H_7N	57.0579	**63**		C_5H_9	69.0705
C_4H_9	57.0705	HNO_3	62.9956	**70**	
58		$H_3N_2O_2$	63.0195	CN_3O	70.0042
N_3O	58.0042	H_5N_3O	63.0433	CH_2N_4	70.0280
H_2N_4	58.0280	CH_3O_3	63.0082	C_2NO_2	69.9929
CNO_2	57.9929	CH_5NO_2	63.0320	$C_2H_2N_2O$	70.0167
CH_2N_2O	58.0167	C_4HN	63.0109	$C_2H_4N_3$	70.0406
CH_4N_3	58.0406	C_5H_3	63.0235	$C_3H_2O_2$	70.0054
$C_2H_2O_2$	58.0054	**64**		C_3H_4NO	70.0293
C_2H_4NO	58.0293	O_4	63.9796	$C_3H_6N_2$	70.0532
$C_2H_6N_2$	58.0532	H_2NO_3	64.0034	C_4H_6O	70.0419
C_3H_6O	58.0419	$H_4N_2O_2$	64.0273	C_4H_8N	70.0657
C_3H_8N	58.0657	CH_4O_3	64.0160	C_5H_{10}	70.0783
C_4H_{10}	58.0783	C_3N_2	64.0062	**71**	
59		C_4O	63.9949	CHN_3O	71.0120
HN_3O	59.0120	C_4H_2N	64.0187	CH_3N_4	71.0359
H_3N_4	59.0359	C_5H_4	64.0313	C_2HNO_2	71.0007
$CHNO_2$	59.0007	**65**		$C_2H_3N_2O$	71.0246
CH_3N_2O	59.0246	HO_4	64.9874	$C_2H_5N_3$	71.0484
CH_5N_3	59.0484	H_3NO_3	65.0113	$C_3H_3O_2$	71.0133
$C_2H_3O_2$	59.0133	C_3HN_2	65.0140	C_3H_5NO	71.0371
C_2H_5NO	59.0371	C_4HO	65.0027	$C_3H_7N_2$	71.0610
$C_2H_7N_2$	59.0610	C_4H_3N	65.0266	C_4H_7O	71.0497
C_3H_7O	59.0497	C_5H_5	65.0391	C_4H_9N	71.0736
C_3H_9N	59.0736	**66**		C_5H_{11}	71.0861

Appendix A (continued)

FM		FM		FM	
72		$C_2H_7N_2O$	75.0559	CH_5NO_3	79.0269
N_4O	72.0073	$C_2H_9N_3$	75.0798	C_3HN_3	79.0171
CN_2O_2	71.9960	$C_3H_7O_2$	75.0446	C_4HNO	79.0058
CH_2N_3O	72.0198	C_3H_9NO	75.0684	$C_4H_3N_2$	79.0297
CH_4N_4	72.0437	C_5HN	75.0109	C_5H_3O	79.0184
C_2O_3	71.9847	C_6H_3	75.0235	C_5H_5N	79.0422
$C_2H_2NO_2$	72.0085	**76**		C_6H_7	79.0548
$C_2H_4N_2O$	72.0324	N_2O_3	75.9909	**80**	
$C_2H_6N_3$	72.0563	$H_2N_3O_2$	76.0147	H_2NO_4	79.9983
$C_3H_4O_2$	72.0211	H_4N_4O	76.0386	$H_4N_2O_3$	80.0222
C_3H_6NO	72.0449	CO_4	75.9796	CH_4O_4	80.0109
$C_3H_8N_2$	72.0688	CH_2NO_3	76.0034	C_2N_4	80.0124
C_4H_8O	72.0575	$CH_4N_2O_2$	76.0273	C_3N_2O	80.0011
$C_4H_{10}N$	72.0814	CH_6N_3O	76.0511	$C_3H_2N_3$	80.0249
C_5H_{12}	72.0939	CH_8N_4	76.0750	C_4O_2	79.9898
C_6	72.0000	$C_2H_4O_3$	76.0160	C_4H_2NO	80.0136
73		$C_2H_6NO_2$	76.0399	$C_4H_4N_2$	80.0375
HN_4O	73.0151	$C_2H_8N_2O$	76.0637	C_5H_4O	80.0262
CHN_2O_2	73.0038	$C_3H_8O_2$	76.0524	C_5H_6N	80.0501
CH_3N_3O	73.0277	C_4N_2	76.0062	C_6H_8	80.0626
CH_5N_4	73.0515	C_5O	75.9949	**81**	
C_2HO_3	72.9925	C_5H_2N	76.0187	H_3NO_4	81.0062
$C_2H_3NO_2$	73.0164	C_6H_4	76.0313	C_2HN_4	81.0202
$C_2H_5N_2O$	73.0402	**77**		C_3HN_2O	81.0089
$C_2H_7N_3$	73.0641	HN_2O_3	76.9987	$C_3H_3N_3$	81.0328
$C_3H_5O_2$	73.0289	$H_3N_3O_2$	77.0226	C_4HO_2	80.9976
C_3H_7NO	73.0528	H_5N_4O	77.0464	C_4H_3NO	81.0215
$C_3H_9N_2$	73.0767	CHO_4	76.9874	$C_4H_5N_2$	81.0453
C_4H_9O	73.0653	CH_3NO_3	77.0113	C_5H_5O	81.0340
$C_4H_{11}N$	73.0892	$CH_5N_2O_2$	77.0351	C_5H_7N	81.0579
C_6H	73.0078	CH_7N_3O	77.0590	C_6H_8	81.0705
74		$C_2H_5O_3$	77.0238	**82**	
N_3O_2	73.9991	$C_2H_7NO_2$	77.0477	C_2N_3O	82.0042
H_2N_4O	74.0229	C_4HN_2	77.0140	$C_2H_2N_4$	82.0280
CNO_3	73.9878	C_5HO	77.0027	C_3NO_2	81.9929
$CH_2N_2O_2$	74.0116	C_5H_3N	77.0266	$C_3H_2N_2O$	82.0167
CH_4N_3O	74.0355	C_6H_5	77.0391	$C_3H_4N_3$	82.0406
CH_6N_4	74.0594	**78**		$C_4H_2O_2$	82.0054
$C_2H_2O_3$	74.0003	NO_4	77.9827	C_4H_4NO	82.0293
$C_2H_4NO_2$	74.0242	$H_2N_2O_3$	78.0065	$C_4H_6N_2$	82.0532
$C_2H_6N_2O$	74.0480	$H_4N_3O_2$	78.0304	C_5H_6O	82.0419
$C_2H_8N_3$	74.0719	H_6N_4O	78.0542	C_5H_8N	82.0657
$C_3H_6O_2$	74.0368	CH_2O_4	77.9953	C_6H_{10}	82.0783
C_3H_8NO	74.0606	CH_4NO_3	78.0191	**83**	
$C_3H_{10}N_2$	74.0845	$CH_6N_2O_2$	78.0429	C_2HN_3O	83.0120
$C_4H_{10}O$	74.0732	$C_2H_6O_3$	78.0317	$C_2H_3N_4$	83.0359
C_5N	74.0031	C_3N_3	78.0093	C_3HNO_2	83.0007
C_6H_2	74.0157	C_4NO	77.9980	$C_3H_3N_2O$	83.0246
75		$C_4H_2N_2$	78.0218	$C_3H_5N_3$	83.0484
HN_3O_2	75.0069	C_5H_2O	78.0106	$C_4H_3O_2$	83.0133
H_3N_4O	75.0308	C_5H_4N	78.0344	C_4H_5NO	83.0371
$CHNO_3$	74.9956	C_6H_6	78.0470	$C_4H_7N_2$	83.0610
$CH_3N_2C_2$	75.0195	**79**		C_5H_7O	83.0497
CH_5N_3O	75.0433	HNO_4	78.9905	C_5H_9N	83.0736
CH_7N_4	75.0672	$H_3N_2O_3$	79.0144	C_6H_{11}	83.0861
$C_2H_3O_3$	75.0082	$H_5N_3O_2$	79.0382	**84**	
$C_2H_5NO_2$	75.0320	CH_3O_4	79.0031	CN_4O	84.0073

Appendix A (continued)

	FM		FM		FM
$C_2N_2O_2$	83.9960	$C_3H_5NO_2$	87.0320	$CH_4N_3O_2$	90.0304
$C_2H_2N_3O$	84.0198	$C_3H_7N_2O$	87.0559	CH_6N_4O	90.0542
$C_2H_4N_4$	84.0437	$C_3H_9N_3$	87.0798	$C_2H_2O_4$	89.9953
C_3O_3	83.9847	$C_4H_7O_2$	87.0446	$C_2H_4NO_3$	90.0191
$C_3H_2NO_2$	84.0085	C_4H_9NO	87.0684	$C_2H_6N_2O_2$	90.0429
$C_3H_4N_2O$	84.0324	$C_4H_{11}N_2$	87.0923	$C_2H_8N_3O$	90.0668
$C_3H_6N_3$	84.0563	$C_5H_{11}O$	87.0810	$C_2H_{10}N_4$	90.0907
$C_4H_4O_2$	84.0211	$C_5H_{13}N$	87.1049	$C_3H_6O_3$	90.0317
C_4H_6NO	84.0449	C_6HN	87.0109	$C_3H_8NO_2$	90.0555
$C_4H_8N_2$	84.0688	C_7H_3	87.0235	$C_3H_{10}N_2O$	90.0794
C_5H_8O	84.0575	**88**		$C_4H_{10}O_2$	90.0681
$C_5H_{10}N$	84.0814	N_4O_2	88.0022	C_4N_3	90.0093
C_6H_{12}	84.0939	CN_2O_3	87.9909	C_5NO	89.9980
C_7	84.0000	$CH_2N_3O_2$	88.0147	$C_5H_2N_2$	90.0218
85		CH_4N_4O	88.0386	C_6H_2O	90.0106
CHN_4O	85.0151	C_2O_4	87.9796	C_6H_4N	90.0344
$C_2HN_2O_2$	85.0038	$C_2H_2NO_3$	88.0034	C_7H_6	90.0470
$C_2H_3N_3O$	85.0277	$C_2H_4N_2O_2$	88.0273	**91**	
$C_2H_5N_4$	85.0515	$C_2H_6N_3O$	88.0511	HN_3O_3	91.0018
C_3HO_3	84.9925	$C_2H_8N_4$	88.0750	$H_3N_4O_2$	91.0257
$C_3H_3NO_2$	85.0164	$C_3H_4O_3$	88.0160	$CHNO_4$	90.9905
$C_3H_5N_2O$	85.0402	$C_3H_6NO_2$	88.0399	$CH_3N_2O_3$	91.0144
$C_3H_7N_3$	85.0641	$C_3H_8N_2O$	88.0637	$CH_5N_3O_2$	91.0382
$C_4H_5O_2$	85.0289	$C_3H_{10}N_3$	88.0876	CH_7N_4O	91.0621
C_4H_7NO	85.0528	$C_4H_8O_2$	88.0524	$C_2H_3O_4$	91.0031
$C_4H_9N_2$	85.0767	$C_4H_{10}NO$	88.0763	$C_2H_5NO_3$	91.0269
C_5H_9O	85.0653	$C_4H_{12}N_2$	88.1001	$C_2H_7N_2O_2$	91.0508
$C_5H_{11}N$	85.0892	$C_5H_{12}O$	88.0888	$C_2H_9N_3O$	91.0746
C_6H_{13}	85.1018	C_5N_2	88.0062	$C_3H_7O_3$	91.0395
C_7H	85.0078	C_6O	87.9949	$C_3H_9NO_2$	91.0634
86		C_6H_2N	88.0187	C_4HN_3	91.0171
CN_3O_2	85.9991	C_7H_4	88.0313	C_5HNO	91.0058
CH_2N_4O	86.0229	**89**		$C_5H_3N_2$	91.0297
C_2NO_3	85.9878	HN_4O_2	89.0100	C_6H_3O	91.0184
$C_2H_2N_2O_2$	86.0116	CHN_2O_3	88.9987	C_6H_5N	91.0422
$C_2H_4N_3O$	86.0355	$CH_3N_3O_2$	89.0226	C_7H_7	91.0548
$C_2H_6N_4$	86.0594	CH_5N_4O	89.0464	**92**	
$C_3H_2O_3$	86.0003	C_2HO_4	88.9874	N_2O_4	91.9858
$C_3H_4NO_2$	86.0242	$C_2H_3NO_3$	89.0113	$H_2N_3O_3$	92.0096
$C_3H_6N_2O$	86.0480	$C_2H_5N_2O_2$	89.0351	$H_4N_4O_2$	92.0335
$C_3H_8N_3$	86.0719	$C_2H_7N_3O$	89.0590	CH_2NO_4	91.9983
$C_4H_6O_2$	86.0368	$C_2H_9N_4$	89.0829	$CH_4N_2O_3$	92.0222
C_4H_8NO	86.0606	$C_3H_5O_3$	89.0238	$CH_6N_3O_2$	92.0460
$C_4H_{10}N_2$	86.0845	$C_3H_7NO_2$	89.0477	CH_8N_4O	92.0699
$C_5H_{10}O$	86.0732	$C_3H_9N_2O$	89.0715	$C_2H_4O_4$	92.0109
$C_5H_{12}N$	86.0970	$C_3H_{11}N_3$	89.0954	$C_2H_6NO_3$	92.0348
C_6H_{14}	86.1096	$C_4H_9O_2$	89.0603	$C_2H_8N_2O_2$	92.0586
C_6N	86.0031	$C_4H_{11}NO$	89.0841	$C_3H_8O_3$	92.0473
C_7H_2	86.0157	C_5HN_2	89.0140	C_3N_4	92.0124
87		C_6HO	89.0027	C_4N_2O	92.0011
CHN_3O_2	87.0069	C_6H_3N	89.0266	$C_4H_2N_3$	92.0249
CH_3N_4O	87.0308	C_7H_5	89.0391	C_5O_2	91.9898
C_2HNO_3	86.9956	**90**		C_5H_2NO	92.0136
$C_2H_3N_2O_2$	87.0195	N_3O_3	89.9940	$C_5H_4N_2$	92.0375
$C_2H_5N_3O$	87.0433	$H_2N_4O_2$	90.0178	C_6H_4O	92.0262
$C_2H_7N_4$	87.0672	CNO_4	89.9827	C_6H_6N	92.0501
$C_3H_3O_3$	87.0082	$CH_2N_2O_3$	90.0065	C_7H_8	92.0626

Appendix A (continued)

	FM		FM		FM
93		C_4O_3	95.9847	$C_5H_7O_2$	99.0446
HN_2O_4	92.9936	$C_4H_2NO_2$	96.0085	C_5H_9NO	99.0684
$H_3N_3O_3$	93.0175	$C_4H_4N_2O$	96.0324	$C_5H_{11}N_2$	99.0923
$H_5N_4O_2$	93.0413	$C_4H_6N_3$	96.0563	$C_6H_{11}O$	99.0810
CH_3NO_4	93.0062	$C_5H_4O_2$	96.0211	$C_6H_{13}N$	99.1049
$CH_5N_2O_3$	93.0300	C_5H_6NO	96.0449	C_7H_{15}	99.1174
$CH_7N_3O_2$	93.0539	$C_5H_8N_2$	96.0688	C_7HN	99.0109
$C_2H_5O_4$	93.0187	C_6H_8O	96.0575	C_8H_3	99.0235
$C_2H_7NO_3$	93.0426	$C_6H_{10}N$	96.0814	**100**	
C_3HN_4	93.0202	C_7H_{12}	96.0939	CN_4O_2	100.0022
C_4HN_2O	93.0089	C_8	96.0000	$C_2N_2O_3$	99.9909
$C_4H_3N_3$	93.0328	**97**		$C_2H_2N_3O_2$	100.0147
C_5HO_2	92.9976	C_2HN_4O	97.0151	$C_2H_4N_4O$	100.0386
C_5H_3NO	93.0215	$C_3HN_2O_2$	97.0038	C_3O_4	99.9796
$C_5H_5N_2$	93.0453	$C_3H_3N_3O$	97.0277	$C_3H_2NO_3$	100.0034
C_6H_5O	93.0340	$C_3H_5N_4$	97.0515	$C_3H_4N_2O_2$	100.0273
C_6H_7N	93.0579	C_4HO_3	96.9925	$C_3H_6N_3O$	100.0511
C_7H_9	93.0705	$C_4H_3NO_2$	97.0164	$C_3H_8N_4$	100.0750
94		$C_4H_5N_2O$	97.0402	$C_4H_4O_3$	100.0160
$H_2N_2O_4$	94.0014	$C_4H_7N_3$	97.0641	$C_4H_6NO_2$	100.0399
$H_4N_3O_3$	94.0253	$C_5H_5O_2$	97.0289	$C_4H_8N_2O$	100.0637
$H_6N_4O_2$	94.0491	C_5H_7NO	97.0528	$C_4H_{10}N_3$	100.0876
CH_4NO_4	94.0140	$C_5H_9N_2$	97.0767	$C_5H_8O_2$	100.0524
$CH_6N_2O_3$	94.0379	C_6H_9O	97.0653	$C_5H_{10}NO$	100.0763
$C_2H_6O_4$	94.0266	$C_6H_{11}N$	97.0892	$C_5H_{12}N_2$	100.1001
C_3N_3O	94.0042	C_7H_{13}	97.1018	$C_6H_{12}O$	100.0888
$C_3H_2N_4$	94.0280	C_8H	97.0078	$C_6H_{14}N$	100.1127
C_4NO_2	93.9929	**98**		C_6N_2	100.0062
$C_4H_2N_2O$	94.0167	$C_2N_3O_2$	97.9991	C_7H_{16}	100.1253
$C_4H_4N_3$	94.0406	$C_2H_2N_4O$	98.0229	C_7O	99.9949
$C_5H_2O_2$	94.0054	C_3NO_3	97.9878	C_7H_2N	100.0187
C_5H_4NO	94.0293	$C_3H_2N_2O_2$	98.0116	C_8H_4	100.0313
$C_5H_6N_2$	94.0532	$C_3H_4N_3O$	98.0355	**101**	
C_6H_6O	94.0419	$C_3H_6N_4$	98.0594	CHN_4O_2	101.0100
C_6H_8N	94.0657	$C_4H_2O_3$	98.0003	$C_2HN_2O_3$	100.9987
C_7H_{10}	94.0783	$C_4H_4NO_2$	98.0242	$C_2H_3N_3O_2$	101.0226
95		$C_4H_6N_2O$	98.0480	$C_2H_5N_4O$	101.0464
$H_3N_2O_4$	95.0093	$C_4H_8N_3$	98.0719	C_3HO_4	100.9874
$H_5N_3O_3$	95.0331	$C_5H_6O_2$	98.0368	$C_3H_3NO_3$	101.0113
CH_5NO_4	95.0218	C_5H_8NO	98.0606	$C_3H_5N_2O_2$	101.0351
C_3HN_3O	95.0120	$C_5H_{10}N_2$	98.0845	$C_3H_7N_3O$	101.0590
$C_3H_3N_4$	95.0359	$C_6H_{10}O$	98.0732	$C_3H_9N_4$	101.0829
C_4HNO_2	95.0007	$C_6H_{12}N$	98.0970	$C_4H_5O_3$	101.0238
$C_4H_3N_2O$	95.0246	C_7H_{14}	98.1096	$C_4H_7NO_2$	101.0477
$C_4H_5N_3$	95.0484	C_7N	98.0031	$C_4H_9N_2O$	101.0715
$C_5H_3O_2$	95.0133	C_8H_2	98.0157	$C_4H_{11}N_3$	101.0954
C_5H_5NO	95.0371	**99**		$C_5H_9O_2$	101.0603
$C_5H_7N_2$	95.0610	$C_2HN_3O_2$	99.0069	$C_5H_{11}NO$	101.0841
C_6H_7O	95.0497	$C_2H_3N_4O$	99.0308	$C_5H_{13}N_2$	101.1080
C_6H_9N	95.0736	C_3HNO_3	98.9956	$C_6H_{13}O$	101.0967
C_7H_{11}	95.0861	$C_3H_3N_2O_2$	99.0195	$C_6H_{15}N$	101.1205
96		$C_3H_5N_3O$	99.0433	C_6HN_2	101.0140
$H_4N_2O_4$	96.0171	$C_3H_7N_4$	99.0672	C_7HO	101.0027
C_2N_4O	96.0073	$C_4H_3O_3$	99.0082	C_7H_3N	101.0266
$C_3N_2O_2$	95.9960	$C_4H_5NO_2$	99.0320	C_8H_5	101.0391
$C_3H_2N_3O$	96.0198	$C_4H_7N_2O$	99.0559	**102**	
$C_3H_4N_4$	96.0437	$C_4H_9N_3$	99.0798	CN_3O_3	101.9940

Appendix A (continued)

	FM		FM		FM
$CH_2N_4O_2$	102.0178	$C_3H_6NO_3$	104.0348	$C_6H_2O_2$	106.0054
C_2NO_4	101.9827	$C_3H_8N_2O_2$	104.0586	C_6H_4NO	106.0293
$C_2H_2N_2O_3$	102.0065	$C_3H_{10}N_3O$	104.0825	$C_6H_6N_2$	106.0532
$C_2H_4N_3O_2$	102.0304	$C_3H_{12}N_4$	104.1063	C_7H_6O	106.0419
$C_2H_6N_4O$	102.0542	$C_4H_8O_3$	104.0473	C_7H_8N	106.0657
$C_3H_2O_4$	101.9953	$C_4H_{10}NO_2$	104.0712	C_8H_{10}	106.0783
$C_3H_4NO_3$	102.0191	$C_4H_{12}N_2O$	104.0950	**107**	
$C_3H_6N_2O_2$	102.0429	C_4N_4	104.0124	$CH_3N_2O_4$	107.0093
$C_3H_8N_3O$	102.0668	$C_5H_{12}O_2$	104.0837	$CH_5N_3O_3$	107.0331
$C_3H_{10}N_4$	102.0907	C_5N_2O	104.0011	$CH_7N_4O_2$	107.0570
$C_4H_6O_3$	102.0317	$C_5H_2N_3$	104.0249	$C_2H_5NO_4$	107.0218
$C_4H_8NO_2$	102.0555	C_6O_2	103.9898	$C_2H_7N_2O_3$	107.0457
$C_4H_{10}N_2O$	102.0794	C_6H_2NO	104.0136	$C_2H_9N_3O_2$	107.0695
$C_4H_{12}N_3$	102.1032	$C_6H_4N_2$	104.0375	$C_3H_7O_4$	107.0344
$C_5H_{10}O_2$	102.0681	C_7H_4O	104.0262	$C_3H_9NO_3$	107.0583
$C_5H_{12}NO$	102.0919	C_7H_6N	104.0501	C_4HN_3O	107.0120
$C_5H_{14}N_2$	102.1158	C_8H_8	104.0626	$C_4H_3N_4$	107.0359
C_5N_3	102.0093	**105**		C_5HNO_2	107.0007
$C_6H_{14}O$	102.1045	CHN_2O_4	104.9936	$C_5H_3N_2O$	107.0246
C_6NO	101.9980	$CH_3N_3O_3$	105.0175	$C_5H_5N_3$	107.0484
$C_6H_2N_2$	102.0218	$CH_5N_4O_2$	105.0413	$C_6H_3O_2$	107.0133
C_7H_2O	102.0106	$C_2H_3NO_4$	105.0062	C_6H_5NO	107.0371
C_7H_4N	102.0344	$C_2H_5N_2O_3$	105.0300	$C_6H_7N_2$	107.0610
C_8H_6	102.0470	$C_2H_7N_3O_2$	105.0539	C_7H_7O	107.0497
103		$C_2H_9N_4O$	105.0777	C_7H_9N	107.0736
CHN_3O_3	103.0018	$C_3H_5O_4$	105.0187	C_8H_{11}	107.0861
$CH_3N_4O_2$	103.0257	$C_3H_7NO_3$	105.0426	**108**	
C_2HNO_4	102.9905	$C_3H_9N_2O_2$	105.0664	$CH_4N_2O_4$	108.0171
$C_2H_3N_2O_3$	103.0144	$C_3H_{11}N_3O$	105.0903	$CH_6N_3O_3$	108.0410
$C_2H_5N_3O_2$	103.0382	$C_4H_9O_3$	105.0552	$CH_8N_4O_2$	108.0648
$C_2H_7N_4O$	103.0621	$C_4H_{11}NO_2$	105.0790	$C_2H_6NO_4$	108.0297
$C_3H_3O_4$	103.0031	C_4HN_4	105.0202	$C_2H_8N_2O_3$	108.0535
$C_3H_5NO_3$	103.0269	C_5HN_2O	105.0089	$C_3H_8O_4$	108.0422
$C_3H_7N_2O_2$	103.0508	$C_5H_3N_3$	105.0328	C_3N_4O	108.0073
$C_3H_9N_3O$	103.0746	C_6HO_2	104.9976	$C_4N_2O_2$	107.9960
$C_3H_{11}N_4$	103.0985	C_6H_3NO	105.0215	$C_4H_2N_3O$	108.0198
$C_4H_7O_3$	103.0395	$C_6H_5N_2$	105.0453	$C_4H_4N_4$	108.0437
$C_4H_9NO_2$	103.0634	C_7H_5O	105.0340	C_5O_3	107.9847
$C_4H_{11}N_2O$	103.0872	C_7H_7N	105.0579	$C_5H_2NO_2$	108.0085
$C_4H_{13}N_3$	103.1111	C_8H_9	105.0705	$C_5H_4N_2O$	108.0324
$C_5H_{11}O_2$	103.0759	**106**		$C_5H_6N_3$	108.0563
$C_5H_{13}NO$	103.0998	$CH_2N_2O_4$	106.0014	$C_6H_4O_2$	108.0211
C_5HN_3	103.0171	$CH_4N_3O_3$	106.0253	C_6H_6NO	108.0449
C_6HNO	103.0058	$CH_6N_4O_2$	106.0491	$C_6H_8N_2$	108.0688
$C_6H_3N_2$	103.0297	$C_2H_4NO_4$	106.0140	C_7H_8O	108.0575
C_7H_3O	103.0184	$C_2H_6N_2O_3$	106.0379	$C_7H_{10}N$	108.0814
C_7H_5N	103.0422	$C_2H_8N_3O_2$	106.0617	C_8H_{12}	108.0939
C_8H_7	103.0548	$C_2H_{10}N_4O$	106.0856	C_9	108.0000
104		$C_3H_6O_4$	106.0266	**109**	
CN_2O_4	103.9858	$C_3H_8NO_3$	106.0504	$CH_5N_2O_4$	109.0249
$CH_2N_3O_3$	104.0096	$C_3H_{10}N_2O_2$	106.0743	$CH_7N_3O_3$	109.0488
$CH_4N_4O_2$	104.0335	$C_4H_{10}O_3$	106.0630	$C_2H_7NO_4$	109.0375
$C_2H_2NO_4$	103.9983	C_4N_3O	106.0042	C_3HN_4O	109.0151
$C_2H_4N_2O_3$	104.0222	$C_4H_2N_4$	106.0280	$C_4HN_2O_2$	109.0038
$C_2H_6N_3O_2$	104.0460	C_5NO_2	105.9929	$C_4H_3N_3O$	109.0277
$C_2H_8N_4O$	104.0699	$C_5H_2N_2O$	106.0167	$C_4H_5N_4$	109.0515
$C_3H_4O_4$	104.0109	$C_5H_4N_3$	106.0406	C_5HO_3	108.9925

Appendix A (continued)

FM		FM		FM	
$C_5H_3NO_2$	109.0164	$C_4H_8N_4$	112.0750	C_6N_3	114.0093
$C_5H_5N_2O$	109.0402	$C_5H_4O_3$	112.0160	$C_7H_{14}O$	114.1045
$C_5H_7N_3$	109.0641	$C_5H_6NO_2$	112.0399	$C_7H_{16}N$	114.1284
$C_6H_5O_2$	109.0289	$C_5H_8N_2O$	112.0637	C_7NO	113.9980
C_6H_7NO	109.0528	$C_5H_{10}N_3$	112.0876	$C_7H_2N_2$	114.0218
$C_6H_9N_2$	109.0767	$C_6H_8O_2$	112.0524	C_8H_{18}	114.1409
C_7H_9O	109.0653	$C_6H_{10}NO$	112.0763	C_8H_2O	114.0106
$C_7H_{11}N$	109.0892	$C_6H_{12}N_2$	112.1001	C_8H_4N	114.0344
C_8H_{13}	109.1018	$C_7H_{12}O$	112.0888	C_9H_6	114.0470
C_9H	109.0078	$C_7H_{14}N$	112.1127	**115**	
110		C_7N_2	112.0062	$C_2HN_3O_3$	115.0018
$CH_6N_2O_4$	110.0328	C_8H_{16}	112.1253	$C_2H_3N_4O_2$	115.0257
$C_3N_3O_2$	109.9991	C_8O	111.9949	C_3HNO_4	114.9905
$C_3H_2N_4O$	110.0229	C_8H_2N	112.0187	$C_3H_3N_2O_3$	115.0144
C_4NO_3	109.9878	C_9H_4	112.0313	$C_3H_5N_3O_2$	115.0382
$C_4H_2N_2O_2$	110.0116	**113**		$C_3H_7N_4O$	115.0621
$C_4H_4N_3O$	110.0355	$C_2HN_4O_2$	113.0100	$C_4H_3O_4$	115.0031
$C_4H_6N_4$	110.0594	$C_3HN_2O_3$	112.9987	$C_4H_5NO_3$	115.0269
$C_5H_2O_3$	110.0003	$C_3H_3N_3O_2$	113.0226	$C_4H_7N_2O_2$	115.0508
$C_5H_4NO_2$	110.0242	$C_3H_5N_4O$	113.0464	$C_4H_9N_3O$	115.0746
$C_5H_6N_2O$	110.0480	C_4HO_4	112.9874	$C_4H_{11}N_4$	115.0985
$C_5H_8N_3$	110.0719	$C_4H_3NO_3$	113.0113	$C_5H_7O_3$	115.0395
$C_6H_6O_2$	110.0368	$C_4H_5N_2O_2$	113.0351	$C_5H_9NO_2$	115.0634
C_6H_8NO	110.0606	$C_4H_7N_3O$	113.0590	$C_5H_{11}N_2O$	115.0872
$C_6H_{10}N_2$	110.0845	$C_4H_9N_4$	113.0829	$C_5H_{13}N_3$	115.1111
$C_7H_{10}O$	110.0732	$C_5H_5O_3$	113.0238	$C_6H_{11}O_2$	115.0759
$C_7H_{12}N$	110.0970	$C_5H_7NO_2$	113.0477	$C_6H_{13}NO$	115.0998
C_8H_{14}	110.1096	$C_5H_9N_2O$	113.0715	$C_6H_{15}N_2$	115.1236
C_8N	110.0031	$C_5H_{11}N_3$	113.0954	C_6HN_3	115.0171
C_9H_2	110.0157	$C_6H_9O_2$	113.0603	$C_7H_{15}O$	115.1123
111		$C_6H_{11}NO$	113.0841	$C_7H_{17}N$	115.1362
$C_3HN_3O_2$	111.0069	$C_6H_{13}N_2$	113.1080	C_7HNO	115.0058
$C_3H_3N_4O$	111.0308	$C_7H_{13}O$	113.0967	$C_7H_3N_2$	115.0297
C_4HNO_3	110.9956	$C_7H_{15}N$	113.1205	C_8H_3O	115.0184
$C_4H_3N_2O_2$	111.0195	C_7HN_2	113.0140	C_8H_5N	115.0422
$C_4H_5N_3O$	111.0433	C_8H_{17}	113.1331	C_9H_7	115.0548
$C_4H_7N_4$	111.0672	C_8HO	113.0027	**116**	
$C_5H_3O_3$	111.0082	C_8H_3N	113.0266	$C_2N_2O_4$	115.9858
$C_5H_5NO_2$	111.0320	C_9H_5	113.0391	$C_2H_2N_3O_3$	116.0096
$C_5H_7N_2O$	111.0559	**114**		$C_2H_4N_4O_2$	116.0335
$C_5H_9N_3$	111.0798	$C_2N_3O_3$	113.9940	$C_3H_2NO_4$	115.9983
$C_6H_7O_2$	111.0446	$C_2H_2N_4O_2$	114.0178	$C_3H_4N_2O_3$	116.0222
C_6H_9NO	111.0684	C_3NO_4	113.9827	$C_3H_6N_3O_2$	116.0460
$C_6H_{11}N_2$	111.0923	$C_3H_2N_2O_3$	114.0065	$C_3H_8N_4O$	116.0699
$C_7H_{11}O$	111.0810	$C_3H_4N_3O_2$	114.0304	$C_4H_4O_4$	116.0109
$C_7H_{13}N$	111.1049	$C_3H_6N_4O$	114.0542	$C_4H_6NO_3$	116.0348
C_8H_{15}	111.1174	$C_4H_2O_4$	113.9953	$C_4H_8N_2O_2$	116.0586
C_8HN	111.0109	$C_4H_4NO_3$	114.0191	$C_4H_{10}N_3O$	116.0825
C_9H_3	111.0235	$C_4H_6N_2O_2$	114.0429	$C_4H_{12}N_4$	116.1063
112		$C_4H_8N_3O$	114.0668	$C_5H_8O_3$	116.0473
$C_2N_4O_2$	112.0022	$C_4H_{10}N_4$	114.0907	$C_5H_{10}NO_2$	116.0712
$C_3N_2O_3$	111.9909	$C_5H_6O_3$	114.0317	$C_5H_{12}N_2O$	116.0950
$C_3H_2N_3O_2$	112.0147	$C_5H_8NO_2$	114.0555	$C_5H_{14}N_3$	116.1189
$C_3H_4N_4O$	112.0386	$C_5H_{10}N_2O$	114.0794	C_5N_4	116.0124
C_4O_4	111.9796	$C_5H_{12}N_3$	114.1032	$C_6H_{12}O_2$	116.0837
$C_4H_2NO_3$	112.0034	$C_6H_{10}O_2$	114.0681	$C_6H_{14}NO$	116.1076
$C_4H_4N_2O_2$	112.0273	$C_6H_{12}NO$	114.0919	$C_6H_{16}N_2$	116.1315
$C_4H_6N_3O$	112.0511	$C_6H_{14}N_2$	114.1158	C_6N_2O	116.0011

Appendix A (continued)

FM		FM		FM	
$C_6H_2N_3$	116.0249	$C_7H_2O_2$	118.0054	**121**	
$C_7H_{16}O$	116.1202	C_7H_4NO	118.0293	$C_2H_5N_2O_4$	121.0249
C_7O_2	115.9898	$C_7H_6N_2$	118.0532	$C_2H_7N_3O_3$	121.0488
C_7H_2NO	116.0136	C_8H_6O	118.0419	$C_2H_9N_4O_2$	121.0726
$C_7H_4N_2$	116.0375	C_8H_8N	118.0657	$C_3H_7NO_4$	121.0375
C_8H_4O	116.0262	C_9H_{10}	118.0783	$C_3H_9N_2O_3$	121.0614
C_8H_6N	116.0501	**119**		$C_3H_{11}N_3O_2$	121.0852
C_9H_8	116.0626	$C_2H_3N_2O_4$	119.0093	$C_4H_9O_4$	121.0501
117		$C_2H_5N_3O_3$	119.0331	$C_4H_{11}NO_3$	121.0739
$C_2HN_2O_4$	116.9936	$C_2H_7N_4O_2$	119.0570	C_4HN_4O	121.0151
$C_2H_3N_3O_3$	117.0175	$C_3H_5NO_4$	119.0218	$C_5HN_2O_2$	121.0038
$C_2H_5N_4O_2$	117.0413	$C_3H_7N_2O_3$	119.0457	$C_5H_3N_3O$	121.0277
$C_3H_3NO_4$	117.0062	$C_3H_9N_3O_2$	119.0695	$C_5H_5N_4$	121.0515
$C_3H_5N_2O_3$	117.0300	$C_3H_{11}N_4O$	119.0934	C_6HO_3	120.9925
$C_3H_7N_3O_2$	117.0539	$C_4H_7O_4$	119.0344	$C_6H_3NO_2$	121.0164
$C_3H_9N_4O$	117.0777	$C_4H_9NO_3$	119.0583	$C_6H_5N_2O$	121.0402
$C_4H_5O_4$	117.0187	$C_4H_{11}N_2O_2$	119.0821	$C_6H_7N_3$	121.0641
$C_4H_7NO_3$	117.0426	$C_4H_{13}N_3O$	119.1060	$C_7H_5O_2$	121.0289
$C_4H_9N_2O_2$	117.0664	$C_5H_{11}O_3$	119.0708	C_7H_7NO	121.0528
$C_4H_{11}N_3O$	117.0903	$C_5H_{13}NO_2$	119.0947	$C_7H_9N_2$	121.0767
$C_4H_{13}N_4$	117.1142	C_5HN_3O	119.0120	C_8H_9O	121.0653
$C_5H_9O_3$	117.0552	$C_5H_3N_4$	119.0359	$C_8H_{11}N$	121.0892
$C_5H_{11}NO_2$	117.0790	C_6HNO_2	119.0007	C_9H_{13}	121.1018
$C_5H_{13}N_2O$	117.1029	$C_6H_3N_2O$	119.0246	$C_{10}H$	121.0078
$C_5H_{15}N_3$	117.1267	$C_6H_5N_3$	119.0484	**122**	
C_5HN_4	117.0202	$C_7H_3O_2$	119.0133	$C_2H_6N_2O_4$	122.0328
$C_6H_{13}O_2$	117.0916	C_7H_5NO	119.0371	$C_2H_8N_3O_3$	122.0566
$C_6H_{15}NO$	117.1154	$C_7H_7N_2$	119.0610	$C_2H_{10}N_4O_2$	122.0805
C_6HN_2O	117.0089	C_8H_7O	119.0497	$C_3H_8NO_4$	122.0453
$C_6H_3N_3$	117.0328	C_8H_9N	119.0736	$C_3H_{10}N_2O_3$	122.0692
C_7HO_2	116.9976	C_9H_{11}	119.0861	$C_4H_{10}O_4$	122.0579
C_7H_3NO	117.0215	**120**		$C_4N_3O_2$	121.9991
$C_7H_5N_2$	117.0453	$C_2H_4N_2O_4$	120.0171	$C_4H_2N_4O$	122.0229
C_8H_5O	117.0340	$C_2H_6N_3O_3$	120.0410	C_5NO_3	121.9878
C_8H_7N	117.0579	$C_2H_8N_4O_2$	120.0648	$C_5H_2N_2O_2$	122.0116
C_9H_9	117.0705	$C_3H_6NO_4$	120.0297	$C_5H_4N_3O$	122.0355
118		$C_3H_8N_2O_3$	120.0535	$C_5H_6N_4$	122.0594
$C_2H_2N_2O_4$	118.0014	$C_3H_{10}N_3O_2$	120.0774	$C_6H_2O_3$	122.0003
$C_2H_4N_3O_3$	118.0253	$C_3H_{12}N_4O$	120.1012	$C_6H_4NO_2$	122.0242
$C_2H_6N_4O_2$	118.0491	$C_4H_8O_4$	120.0422	$C_6H_6N_2O$	122.0480
$C_3H_4NO_4$	118.0140	$C_4H_{10}NO_3$	120.0661	$C_6H_8N_3$	122.0719
$C_3H_6N_2O_3$	118.0379	$C_4H_{12}N_2O_2$	120.0899	$C_7H_6O_2$	122.0368
$C_3H_8N_3O_2$	118.0617	C_4N_4O	120.0073	C_7H_8NO	122.0606
$C_3H_{10}N_4O$	118.0856	$C_5H_{12}O_3$	120.0786	$C_7H_{10}N_2$	122.0845
$C_4H_6O_4$	118.0266	$C_5N_2O_2$	119.9960	$C_8H_{10}O$	122.0732
$C_4H_8NO_3$	118.0504	$C_5H_2N_3O$	120.0198	$C_8H_{12}N$	122.0970
$C_4H_{10}N_2O_2$	118.0743	$C_5H_4N_4$	120.0437	C_9H_{14}	122.1096
$C_4H_{12}N_3O$	118.0981	C_6O_3	119.9847	C_9N	122.0031
$C_4H_{14}N_4$	118.1220	$C_6H_2NO_2$	120.0085	$C_{10}H_2$	122.0157
$C_5H_{10}O_3$	118.0630	$C_6H_4N_2O$	120.0324	**123**	
$C_5H_{12}NO_2$	118.0868	$C_6H_6N_3$	120.0563	$C_2H_7N_2O_4$	123.0406
$C_5H_{14}N_2O$	118.1107	$C_7H_4O_2$	120.0211	$C_2H_9N_3O_3$	123.0644
C_5N_3O	118.0042	C_7H_6NO	120.0449	$C_3H_9NO_4$	123.0532
$C_5H_2N_4$	118.0280	$C_7H_8N_2$	120.0688	$C_4HN_3O_2$	123.0069
$C_6H_{14}O_2$	118.0994	C_8H_8O	120.0575	$C_4H_3N_4O$	123.0308
C_6NO_2	117.9929	$C_8H_{10}N$	120.0814	C_5HNO_3	122.9956
$C_6H_2N_2O$	118.0167	C_9H_{12}	120.0939	$C_5H_3N_2O_2$	123.0195
$C_6H_4N_3$	118.0406	C_{10}	120.0000	$C_5H_5N_3O$	123.0433

Appendix A (continued)

	FM		FM		FM
$C_5H_7N_4$	123.0672	C_8HN_2	125.0140	C_9H_{19}	127.1488
$C_6H_3O_3$	123.0082	C_9H_{17}	125.1331	C_9H_3O	127.0184
$C_6H_5NO_2$	123.0320	C_9HO	125.0027	C_9H_5N	127.0422
$C_6H_7N_2O$	123.0559	C_9H_3N	125.0266	$C_{10}H_7$	127.0548
$C_6H_9N_3$	123.0798	$C_{10}H_5$	125.0391	**128**	
$C_7H_7O_2$	123.0446	**126**		$C_3N_2O_4$	127.9858
C_7H_9NO	123.0684	$C_3N_3O_3$	125.9940	$C_3H_2N_3O_3$	128.0096
$C_7H_{11}N_2$	123.0923	$C_3H_2N_4O_2$	126.0178	$C_3H_4N_4O_2$	128.0335
$C_8H_{11}O$	123.0810	C_4NO_4	125.9827	$C_4H_2NO_4$	127.9983
$C_8H_{13}N$	123.1049	$C_4H_2N_2O_3$	126.0065	$C_4H_4N_2O_3$	128.0222
C_9H_{15}	123.1174	$C_4H_4N_3O_2$	126.0304	$C_4H_6N_3O_2$	128.0460
C_9HN	123.0109	$C_4H_6N_4O$	126.0542	$C_4H_8N_4O$	128.0699
$C_{10}H_3$	123.0235	$C_5H_2O_4$	125.9953	$C_5H_4O_4$	128.0109
124		$C_5H_4NO_3$	126.0191	$C_5H_6NO_3$	128.0348
$C_2H_8N_2O_4$	124.0484	$C_5H_6N_2O_2$	126.0429	$C_5H_8N_2O_2$	128.0586
$C_3N_4O_2$	124.0022	$C_5H_8N_3O$	126.0668	$C_5H_{10}N_3O$	128.0825
$C_4N_2O_3$	123.9909	$C_5H_{10}N_4$	126.0907	$C_5H_{12}N_4$	128.1063
$C_4H_2N_3O_2$	124.0147	$C_6H_6O_3$	126.0317	$C_6H_8O_3$	128.0473
$C_4H_4N_4O$	124.0386	$C_6H_8NO_2$	126.0555	$C_6H_{10}NO_2$	128.0712
C_5O_4	123.9796	$C_6H_{10}N_2O$	126.0794	$C_6H_{12}N_2O$	128.0950
$C_5H_2NO_3$	124.0034	$C_6H_{12}N_3$	126.1032	$C_6H_{14}N_3$	128.1189
$C_5H_4N_2O_2$	124.0273	$C_7H_{10}O_2$	126.0681	C_6N_4	128.0124
$C_5H_6N_3O$	124.0511	$C_7H_{12}NO$	126.0919	$C_7H_{12}O_2$	128.0837
$C_5H_8N_4$	124.0750	$C_7H_{14}N_2$	126.1158	$C_7H_{14}NO$	128.1076
$C_6H_4O_3$	124.0160	C_7N_3	126.0093	$C_7H_{16}N_2$	128.1315
$C_6H_6NO_2$	124.0399	$C_8H_{14}O$	126.1045	C_7N_2O	128.0011
$C_6H_8N_2O$	124.0637	$C_8H_{16}N$	126.1284	$C_7H_2N_3$	128.0249
$C_6H_{10}N_3$	124.0876	C_8NO	125.9980	$C_8H_{16}O$	128.1202
$C_7H_8O_2$	124.0524	$C_8H_2N_2$	126.0218	C_8O_2	127.9898
$C_7H_{10}NO$	124.0763	C_9H_{18}	126.1409	$C_8H_{18}N$	128.1440
$C_7H_{12}N_2$	124.1001	C_9H_2O	126.0106	C_8H_2NO	128.0136
$C_8H_{12}O$	124.0888	C_9H_4N	126.0344	$C_8H_4N_2$	128.0375
$C_8H_{14}N$	124.1127	$C_{10}H_6$	126.0470	C_9H_{20}	128.1566
C_8N_2	124.0062	**127**		C_9H_4O	128.0262
C_9H_{16}	124.1253	CHN_3O_3	127.0018	C_9H_6N	128.0501
C_9O	123.9949	$C_3H_3N_4O_2$	127.0257	$C_{10}H_8$	128.0626
C_9H_2N	124.0187	C_4HNO_4	126.9905	**129**	
$C_{10}H_4$	124.0313	$C_4H_3N_2O_3$	127.0144	$C_3HN_2O_4$	128.9936
125		$C_4H_5N_3O_2$	127.0382	$C_3H_3N_3O_3$	129.0175
$C_3HN_4O_2$	125.0100	$C_4H_7N_4O$	127.0621	$C_3H_5N_4O_2$	129.0413
$C_4HN_2O_3$	124.9987	$C_5H_3O_4$	127.0031	$C_4H_3NO_4$	129.0062
$C_4H_3N_3O_2$	125.0226	$C_5H_5NO_3$	127.0269	$C_4H_5N_2O_3$	129.0300
$C_4H_5N_4O$	125.0464	$C_5H_7N_2O_2$	127.0508	$C_4H_7N_3O_2$	129.0539
C_5HO_4	124.9874	$C_5H_9N_3O$	127.0746	$C_4H_9N_4O$	129.0777
$C_5H_3NO_3$	125.0113	$C_5H_{11}N_4$	127.0985	$C_5H_5O_4$	129.0187
$C_5H_5N_2O_2$	125.0351	$C_6H_7O_3$	127.0395	$C_5H_7NO_3$	129.0426
$C_5H_7N_3O$	125.0590	$C_6H_9NO_2$	127.0634	$C_5H_9N_2O_2$	129.0664
$C_5H_9N_4$	125.0829	$C_6H_{11}N_2O$	127.0872	$C_5H_{11}N_3O$	129.0903
$C_6H_5O_3$	125.0238	$C_6H_{13}N_3$	127.1111	$C_5H_{13}N_4$	129.1142
$C_6H_7NO_2$	125.0477	$C_7H_{11}O_2$	127.0759	$C_6H_9O_3$	129.0552
$C_6H_9N_2O$	125.0715	$C_7H_{13}NO$	127.0998	$C_6H_{11}NO_2$	129.0790
$C_6H_{11}N_3$	125.0954	$C_7H_{15}N_2$	127.1236	$C_6H_{13}N_2O$	129.1029
$C_7H_9O_2$	125.0603	C_7HN_3	127.0171	$C_6H_{15}N_3$	129.1267
$C_7H_{11}NO$	125.0841	$C_8H_{15}O$	127.1123	C_6HN_4	129.0202
$C_7H_{13}N_2$	125.1080	$C_8H_{17}N$	127.1362	$C_7H_{13}O_2$	129.0916
$C_8H_{13}O$	125.0967	C_8HNO	127.0058	$C_7H_{15}NO$	129.1154
$C_8H_{15}N$	125.1205	$C_8H_3N_2$	127.0297	$C_7H_{17}N_2$	129.1393

Appendix A (continued)

FM		FM		FM	
C_7HN_2O	129.0089	$C_6H_{15}N_2O$	131.1185	$C_5H_{13}N_2O_2$	133.0978
$C_7H_3N_3$	129.0328	$C_6H_{17}N_3$	131.1424	$C_5H_{15}N_3O$	133.1216
$C_8H_{17}O$	129.1280	C_6HN_3O	131.0120	C_5HN_4O	133.0151
C_8HO_2	128.9976	$C_6H_3N_4$	131.0359	$C_6H_{13}O_3$	133.0865
$C_8H_{19}N$	129.1519	$C_7H_{15}O_2$	131.1072	$C_6H_{15}NO_2$	133.1103
C_8H_3NO	129.0215	$C_7H_{17}NO$	131.1311	$C_6HN_2O_2$	133.0038
$C_8H_5N_2$	129.0453	C_7HNO_2	131.0007	$C_6H_3N_3O$	133.0277
C_9H_5O	129.0340	$C_7H_3N_2O$	131.0246	$C_6H_5N_4$	133.0515
C_9H_7N	129.0579	$C_7H_5N_3$	131.0484	C_7HO_3	132.9925
$C_{10}H_9$	129.0705	$C_8H_3O_2$	131.0133	$C_7H_3NO_2$	133.0164
130		C_8H_5NO	131.0371	$C_7H_5N_2O$	133.0402
$C_3H_2N_2O_4$	130.0014	$C_8H_7N_2$	131.0610	$C_7H_7N_3$	133.0641
$C_3H_4N_3O_3$	130.0253	C_9H_7O	131.0497	$C_8H_5O_2$	133.0289
$C_3H_6N_4O_2$	130.0491	C_9H_9N	131.0736	C_8H_7NO	133.0528
$C_4H_4NO_4$	130.0140	$C_{10}H_{11}$	131.0861	$C_8H_9N_2$	133.0767
$C_4H_6N_2O_3$	130.0379	**132**		C_9H_9O	133.0653
$C_4H_8N_3O_2$	130.0617	$C_3H_4N_2O_4$	132.0171	$C_9H_{11}N$	133.0892
$C_4H_{10}N_4O$	130.0856	$C_3H_6N_3O_3$	132.0410	$C_{10}H_{13}$	133.1018
$C_5H_6O_4$	130.0266	$C_3H_8N_4O_2$	132.0648	$C_{11}H$	133.0078
$C_5H_8NO_3$	130.0504	$C_4H_6NO_4$	132.0297	**134**	
$C_5H_{10}N_2O_2$	130.0743	$C_4H_8N_2O_3$	132.0535	$C_3H_6N_2O_4$	134.0328
$C_5H_{12}N_3O$	130.0981	$C_4H_{10}N_3O_2$	132.0774	$C_3H_8N_3O_3$	134.0566
$C_5H_{14}N_4$	130.1220	$C_4H_{12}N_4O$	132.1012	$C_3H_{10}N_4O_2$	134.0805
$C_6H_{10}O_3$	130.0603	$C_5H_8O_4$	132.0422	$C_4H_8NO_4$	134.0453
$C_6H_{12}NO_2$	130.0868	$C_5H_{10}NO_3$	132.0661	$C_4H_{10}N_2O_3$	134.0692
$C_6H_{14}N_2O$	130.1107	$C_5H_{12}N_2O_2$	132.0899	$C_4H_{12}N_3O_2$	134.0930
$C_6H_{16}N_3$	130.1346	$C_5H_{14}N_3O$	132.1138	$C_4H_{14}N_4O$	134.1169
C_6N_3O	130.0042	$C_5H_{16}N_4$	132.1377	$C_5H_{10}O_4$	134.0579
$C_6H_2N_4$	130.0280	C_5N_4O	132.0073	$C_5H_{12}NO_3$	134.0817
$C_7H_{14}O_2$	130.0994	$C_6H_{12}O_3$	132.0786	$C_5H_{14}N_2O_2$	134.1056
$C_7H_{16}NO$	130.1233	$C_6H_{14}NO_2$	132.1025	$C_5N_3O_2$	133.9991
C_7NO_2	129.9929	$C_6H_{16}N_2O$	132.1264	$C_5H_2N_4O$	134.0229
$C_7H_{18}N_2$	130.1471	$C_6N_2O_2$	131.9960	$C_6H_{14}O_3$	134.0943
$C_7H_2N_2O$	130.0167	$C_6H_2N_3O$	132.0198	C_6NO_3	133.9878
$C_7H_4N_3$	130.0406	$C_6H_4N_4$	132.0437	$C_6H_2N_2O_2$	134.0116
$C_8H_{18}O$	130.1358	$C_7H_{16}O_2$	132.1151	$C_6H_4N_3O$	134.0355
$C_8H_2O_2$	130.0054	C_7O_3	131.9847	$C_6H_6N_4$	134.0594
C_8H_4NO	130.0293	$C_7H_2NO_2$	132.0085	$C_7H_2O_3$	134.0003
$C_8H_6N_2$	130.0532	$C_7H_4N_2O$	132.0324	$C_7H_4NO_2$	134.0242
C_9H_6O	130.0419	$C_7H_6N_3$	132.0563	$C_7H_6N_2O$	134.0480
C_9H_8N	130.0657	$C_8H_4O_2$	132.0211	$C_7H_8N_3$	134.0719
$C_{10}H_{10}$	130.0783	C_8H_6NO	132.0449	$C_8H_6O_2$	134.0368
131		$C_8H_8N_2$	132.0688	C_8H_8NO	134.0606
$C_3H_3N_2O_4$	131.0093	C_9H_8O	132.0575	$C_8H_{10}N_2$	134.0845
$C_3H_5N_3O_3$	131.0331	$C_9H_{10}N$	132.0814	$C_9H_{10}O$	134.0732
$C_3H_7N_4O_2$	131.0570	$C_{10}H_{12}$	132.0939	$C_9H_{12}N$	134.0970
$C_4H_5NO_4$	131.0218	C_{11}	132.0000	$C_{10}H_{14}$	134.1096
$C_4H_7N_2O_3$	131.0457	**133**		$C_{10}N$	134.0031
$C_4H_9N_3O_2$	131.0695	$C_3H_5N_2O_4$	133.0249	$C_{11}H_2$	134.0157
$C_4H_{11}N_4O$	131.0934	$C_3H_7N_3O_3$	133.0488	**135**	
$C_5H_7O_4$	131.0344	$C_3H_9N_4O_2$	133.0726	$C_3H_7N_2O_4$	135.0406
$C_5H_9NO_3$	131.0583	$C_4H_7NO_4$	133.0375	$C_3H_9N_3O_3$	135.0644
$C_5H_{11}N_2O_2$	131.0821	$C_4H_9N_2O_3$	133.0614	$C_3H_{11}N_4O_2$	135.0883
$C_5H_{13}N_3O$	131.1060	$C_4H_{11}N_3O_2$	133.0852	$C_4H_9NO_4$	135.0532
$C_5H_{15}N_4$	131.1298	$C_4H_{13}N_4O$	133.1091	$C_4H_{11}N_2O_3$	135.0770
$C_6H_{11}O_3$	131.0708	$C_5H_9O_4$	133.0501	$C_4H_{13}N_3O_2$	135.1009
$C_6H_{13}NO_2$	131.0947	$C_5H_{11}NO_3$	133.0739	$C_5H_{11}O_4$	135.0657

Appendix A (continued)

	FM		FM		FM
$C_5H_{13}NO_3$	135.0896	C_6HO_4	136.9874	$C_6H_7N_2O_2$	139.0508
$C_5HN_3O_2$	135.0069	$C_6H_3NO_3$	137.0113	$C_6H_9N_3O$	139.0746
$C_5H_3N_4O$	135.0308	$C_6H_5N_2O_2$	137.0351	$C_6H_{11}N_4$	139.0985
C_6HNO_3	134.9956	$C_6H_7N_3O$	137.0590	$C_7H_7O_3$	139.0395
$C_6H_3N_2O_2$	135.0195	$C_6H_9N_4$	137.0829	$C_7H_9NO_2$	139.0634
$C_6H_5N_3O$	135.0433	$C_7H_5O_3$	137.0238	$C_7H_{11}N_2O$	139.0872
$C_6H_7N_4$	135.0672	$C_7H_7NO_2$	137.0477	$C_7H_{13}N_3$	139.1111
$C_7H_3O_3$	135.0082	$C_7H_9N_2O$	137.0715	$C_8H_{11}O_2$	139.0759
$C_7H_5NO_2$	135.0320	$C_7H_{11}N_3$	137.0954	$C_8H_{13}NO$	139.0998
$C_7H_7N_2O$	135.0559	$C_8H_9O_2$	137.0603	$C_8H_{15}N_2$	139.1236
$C_7H_9N_3$	135.0798	$C_8H_{11}NO$	137.0841	C_8HN_3	139.0171
$C_8H_7O_2$	135.0446	$C_8H_{13}N_2$	137.1080	$C_9H_{15}O$	139.1123
C_8H_9NO	135.0684	$C_9H_{13}O$	137.0967	$C_9H_{17}N$	139.1362
$C_8H_{11}N_2$	135.0923	$C_9H_{15}N$	137.1205	C_9HNO	139.0058
$C_9H_{11}O$	135.0810	C_9HN_2	137.0140	$C_9H_3N_2$	139.0297
$C_9H_{13}N$	135.1049	$C_{10}H_{17}$	137.1331	$C_{10}H_{19}$	139.1488
$C_{10}H_{15}$	135.1174	$C_{10}HO$	137.0027	$C_{10}H_3O$	139.0184
$C_{10}HN$	135.0109	$C_{10}H_3N$	137.0266	$C_{10}H_5N$	139.0422
$C_{11}H_3$	135.0235	$C_{11}H_5$	137.0391	$C_{11}H_7$	139.0548
136		**138**		**140**	
$C_3H_8N_2O_4$	136.0484	$C_3H_{10}N_2O_4$	138.0641	$C_4N_2O_4$	139.9858
$C_3H_{10}N_3O_3$	136.0723	$C_4N_3O_3$	137.9940	$C_4H_2N_3O_3$	140.0096
$C_3H_{12}N_4O_2$	136.0961	$C_4H_2N_4O_2$	138.0178	$C_4H_4N_4O_2$	140.0335
$C_4H_{10}NO_4$	136.0610	C_5NO_4	137.9827	$C_5H_2NO_4$	139.9983
$C_4H_{12}N_2O_3$	136.0848	$C_5H_2N_2O_3$	138.0065	$C_5H_4N_2O_3$	140.0222
$C_4N_4O_2$	136.0022	$C_5H_4N_3O_2$	138.0304	$C_5H_6N_3O_2$	140.0460
$C_5H_{12}O_4$	136.0735	$C_5H_6N_4O$	138.0542	$C_5H_8N_4O$	140.0699
$C_5N_2O_3$	135.9909	$C_6H_2O_4$	137.9953	$C_6H_4O_4$	140.0109
$C_5H_2N_3O_2$	136.0147	$C_6H_4NO_3$	138.0191	$C_6H_6NO_3$	140.0348
$C_5H_4N_4O$	136.0386	$C_6H_6N_2O_2$	138.0429	$C_6H_8N_2O_2$	140.0586
C_6O_4	135.9796	$C_6H_8N_3O$	138.0668	$C_6H_{10}N_3O$	140.0825
$C_6H_2NO_3$	136.0034	$C_6H_{10}N_4$	138.0907	$C_6H_{12}N_4$	140.1063
$C_6H_4N_2O_2$	136.0273	$C_7H_6O_3$	138.0317	$C_7H_8O_3$	140.0473
$C_6H_6N_3O$	136.0511	$C_7H_8NO_2$	138.0555	$C_7H_{10}NO_2$	140.0712
$C_6H_8N_4$	136.0750	$C_7H_{10}N_2O$	138.0794	$C_7H_{12}N_2O$	140.0950
$C_7H_4O_3$	136.0160	$C_7H_{12}N_3$	138.1032	$C_7H_{14}N_3$	140.1189
$C_7H_8NO_2$	136.0399	$C_8H_{10}O_2$	138.0681	C_7N_4	140.0124
$C_7H_8N_2O$	136.0637	$C_8H_{12}NO$	138.0919	$C_8H_{12}O_2$	140.0837
$C_7H_{10}N_3$	136.0876	$C_8H_{14}N_2$	138.1158	$C_8H_{14}NO$	140.1076
$C_8H_8O_2$	136.0524	C_8N_3	138.0093	$C_8H_{16}N_2$	140.1315
$C_8H_{10}NO$	136.0763	$C_9H_{14}O$	138.1045	C_8N_2O	140.0011
$C_8H_{12}N_2$	136.1001	$C_9H_{16}N$	138.1284	$C_8H_2N_3$	140.0249
$C_9H_{12}O$	136.0888	C_9NO	137.9980	$C_9H_{16}O$	140.1202
$C_9H_{14}N$	136.1127	$C_9H_2N_2$	138.0218	C_9O_2	139.9898
C_9N_2	136.0062	$C_{10}H_{18}$	138.1409	$C_9H_{18}N$	140.1440
$C_{10}H_{16}$	136.1253	$C_{10}H_2O$	138.0106	C_9H_2NO	140.0136
$C_{10}O$	135.9949	$C_{10}H_4N$	138.0344	$C_9H_4N_2$	140.0375
$C_{10}H_2N$	136.0187	$C_{11}H_6$	138.0470	$C_{10}H_{20}$	140.1566
$C_{11}H_4$	136.0313	**139**		$C_{10}H_4O$	140.0262
137		$C_4HN_3O_3$	139.0018	$C_{10}H_6N$	140.0501
$C_3H_9N_2O_4$	137.0563	$C_4H_3N_4O_2$	139.0257	$C_{11}H_8$	140.0626
$C_3H_{11}N_3O_3$	137.0801	C_5HNO_4	138.9905	**141**	
$C_4H_{11}NO_4$	137.0688	$C_5H_3N_2O_3$	139.0144	$C_4HN_2O_4$	140.9936
$C_4HN_4O_2$	137.0100	$C_5H_5N_3O_2$	139.0382	$C_4H_3N_3O_3$	141.0175
$C_5HN_2O_3$	136.9987	$C_5H_7N_4O$	139.0621	$C_4H_5N_4O_2$	141.0413
$C_5H_3N_3O_2$	137.0226	$C_6H_3O_4$	139.0031	$C_5H_3NO_4$	141.0062
$C_5H_5N_4O$	137.0464	$C_6H_5NO_3$	139.0269	$C_5H_5N_2O_3$	141.0300

Appendix A (continued)

FM		FM		FM	
$C_5H_7N_3O_2$	141.0539	$C_{10}H_6O$	142.0419	$C_8H_{16}O_2$	144.1151
$C_5H_9N_4O$	141.0777	$C_{10}H_8N$	142.0657	C_8O_3	143.9847
$C_6H_5O_4$	141.0187	$C_{11}H_{10}$	142.0783	$C_8H_{18}NO$	144.1389
$C_6H_7NO_3$	141.0426	**143**		$C_8H_2NO_2$	144.0085
$C_6H_9N_2O_2$	141.0664	$C_4H_3N_2O_4$	143.0093	$C_8H_{20}N_2$	144.1628
$C_6H_{11}N_3O$	141.0903	$C_4H_5N_3O_3$	143.0331	$C_8H_4N_2O$	144.0324
$C_6H_{13}N_4$	141.1142	$C_4H_7N_4O_2$	143.0570	$C_8H_6N_3$	144.0563
$C_7H_9O_3$	141.0552	$C_5H_5NO_4$	143.0218	$C_9H_{20}O$	144.1515
$C_7H_{11}NO_2$	141.0790	$C_5H_7N_2O_3$	143.0457	$C_9H_4O_2$	144.0211
$C_7H_{13}N_2O$	141.1029	$C_5H_9N_3O_2$	143.0695	C_9H_6NO	144.0449
$C_7H_{15}N_3$	141.1267	$C_5H_{11}N_4O$	143.0934	$C_9H_8N_2$	144.0688
C_7HN_4	141.0202	$C_6H_7O_4$	143.0344	$C_{10}H_8O$	144.0575
$C_8H_{13}O_2$	141.0916	$C_6H_9NO_3$	143.0583	$C_{10}H_{10}N$	144.0814
$C_8H_{15}NO$	141.1154	$C_6H_{11}N_2O_2$	143.0821	$C_{11}H_{12}$	144.0939
$C_8H_{17}N_2$	141.1393	$C_6H_{13}N_3O$	143.1060	C_{12}	144.0000
C_8HN_2O	141.0089	$C_6H_{15}N_4$	143.1298	**145**	
$C_8H_3N_3$	141.0328	$C_7H_{11}O_3$	143.0708	$C_4H_5N_2O_4$	145.0249
$C_9H_{17}O$	141.1280	$C_7H_{13}NO_2$	143.0947	$C_4H_7N_3O_3$	145.0488
C_9HO_2	140.9976	$C_7H_{15}N_2O$	143.1185	$C_4H_9N_4O_2$	145.0726
$C_9H_{19}N$	141.1519	$C_7H_{17}N_3$	143.1424	$C_5H_7NO_4$	145.0375
C_9H_3NO	141.0215	C_7HN_3O	143.0120	$C_5H_9N_2O_3$	145.0614
$C_9H_5N_2$	141.0453	$C_7H_3N_4$	143.0359	$C_5H_{11}N_3O_2$	145.0852
$C_{10}H_{21}$	141.1644	$C_8H_{15}O_2$	143.1072	$C_5H_{13}N_4O$	145.1091
$C_{10}H_5O$	141.0340	$C_8H_{17}NO$	143.1311	$C_6H_9O_4$	145.0501
$C_{10}H_7N$	141.0579	C_8HNO_2	143.0007	$C_6H_{11}NO_3$	145.0739
$C_{11}H_9$	141.0705	$C_8H_{19}N_2$	143.1549	$C_6H_{13}N_2O_2$	145.0978
142		$C_8H_3N_2O$	143.0246	$C_6H_{15}N_3O$	145.1216
$C_4H_2N_2O_4$	142.0014	$C_8H_5N_3$	143.0484	$C_6H_{17}N_4$	145.1455
$C_4H_4N_3O_3$	142.0253	$C_9H_{19}O$	143.1436	C_6HN_4O	145.0151
$C_4H_6N_4O_2$	142.0491	$C_9H_3O_2$	143.0133	$C_7H_{13}O_3$	145.0865
$C_5H_4NO_4$	142.0140	$C_9H_{21}N$	143.1675	$C_7H_{15}NO_2$	145.1103
$C_5H_6N_2O_3$	142.0379	C_9H_5NO	143.0371	$C_7H_{17}N_2O$	145.1342
$C_5H_8N_3O_2$	142.0617	$C_9H_7N_2$	143.0610	$C_7HN_2O_2$	145.0038
$C_5H_{10}N_4O$	142.0856	$C_{10}H_7O$	143.0497	$C_7H_{19}N_3$	145.1580
$C_6H_6O_4$	142.0266	$C_{10}H_9N$	143.0736	$C_7H_3N_3O$	145.0277
$C_6H_8NO_3$	142.0504	$C_{11}H_{11}$	143.0861	$C_7H_5N_4$	145.0515
$C_6H_{10}N_2O_2$	142.0743	**144**		$C_8H_{17}O_2$	145.1229
$C_6H_{12}N_3O$	142.0981	$C_4H_4N_2O_4$	144.0171	C_8HO_3	144.9925
$C_6H_{14}N_4$	142.1220	$C_4H_6N_3O_3$	144.0410	$C_8H_{19}NO$	145.1467
$C_7H_{10}O_3$	142.0630	$C_4H_8N_4O_2$	144.0648	$C_8H_3NO_2$	145.0164
$C_7H_{12}NO_2$	142.0868	$C_5H_6NO_4$	144.0297	$C_8H_5N_2O$	145.0402
$C_7H_{14}N_2O$	142.1107	$C_5H_8N_2O_3$	144.0535	$C_8H_7N_3$	145.0641
$C_7H_{16}N_3$	142.1346	$C_5H_{10}N_3O_2$	144.0774	$C_9H_5O_2$	145.0289
C_7N_3O	142.0042	$C_5H_{12}N_4O$	144.1012	C_9H_7NO	145.0528
$C_7H_2N_4$	142.0280	$C_6H_8O_4$	144.0422	$C_9H_9N_2$	145.0767
$C_8H_{14}O_2$	142.0994	$C_6H_{10}NO_3$	144.0661	$C_{10}H_9O$	145.0653
$C_8H_{16}NO$	142.1233	$C_6H_{12}N_2O_2$	144.0899	$C_{10}H_{11}N$	145.0892
C_8NO_2	141.9929	$C_6H_{14}N_3O$	144.1138	$C_{11}H_{13}$	145.1018
$C_8H_{18}N_2$	142.1471	$C_6H_{16}N_4$	144.1377	$C_{12}H$	145.0078
$C_8H_2N_2O$	142.0167	C_6N_4O	144.0073	**146**	
$C_8H_4N_3$	142.0406	$C_7H_{12}O_3$	144.0786	$C_4H_6N_2O_4$	146.0328
$C_9H_{18}O$	142.1358	$C_7H_{14}NO_2$	144.1025	$C_4H_8N_3O_3$	146.0566
$C_9H_2O_2$	142.0054	$C_7H_{16}N_2O$	144.1264	$C_4H_{10}N_4O_2$	146.0805
$C_9H_{20}N$	142.1597	$C_7N_2O_2$	143.9960	$C_5H_8NO_4$	146.0453
C_9H_4NO	142.0293	$C_7H_{18}N_3$	144.1502	$C_5H_{10}N_2O_3$	146.0692
$C_9H_6N_2$	142.0532	$C_7H_2N_3O$	144.0198	$C_5H_{12}N_3O_2$	146.0930
$C_{10}H_{22}$	142.1722	$C_7H_4N_4$	144.0437	$C_5H_{14}N_4O$	146.1169

Appendix A (continued)

	FM		FM		FM
$C_6H_{10}O_4$	146.0579	$C_{11}HN$	147.0109	$C_8H_9N_2O$	149.0715
$C_6H_{12}NO_3$	146.0817	$C_{12}H_3$	147.0235	$C_8H_{11}N_3$	149.0954
$C_6H_{14}N_2O_2$	146.1056	**148**		$C_9H_9O_2$	149.0603
$C_6H_{16}N_3O$	146.1295	$C_4H_8N_2O_4$	148.0484	$C_9H_{11}NO$	149.0841
$C_6N_3O_2$	145.9991	$C_4H_{10}N_3O_3$	148.0723	$C_9H_{13}N_2$	149.1080
$C_6H_{18}N_4$	146.1533	$C_4H_{12}N_4O_2$	148.0961	$C_{10}H_{13}O$	149.0967
$C_6H_2N_4O$	146.0229	$C_5H_{10}NO_4$	148.0610	$C_{10}H_{15}N$	149.1205
$C_7H_{14}O_3$	146.0943	$C_5H_{12}N_2O_3$	148.0848	$C_{10}HN_2$	149.0140
$C_7H_{16}NO_2$	146.1182	$C_5H_{14}N_3O_2$	148.1087	$C_{11}H_{17}$	149.1331
C_7NO_3	145.9878	$C_5H_{16}N_4O$	148.1325	$C_{11}HO$	149.0027
$C_7H_{18}N_2O$	146.1420	$C_5N_4O_2$	148.0022	$C_{11}H_3N$	149.0266
$C_7H_2N_2O_2$	146.0116	$C_6H_{12}O_4$	148.0735	$C_{12}H_5$	149.0391
$C_7H_4N_3O$	146.0355	$C_6H_{14}NO_3$	148.0974	**150**	
$C_7H_6N_4$	146.0594	$C_6H_{16}N_2O_2$	148.1213	$C_4H_{10}N_2O_4$	150.0641
$C_8H_{18}O_2$	146.1307	$C_6N_2O_3$	147.9909	$C_4H_{12}N_3O_3$	150.0879
$C_8H_2O_3$	146.0003	$C_6H_2N_3O_2$	148.0147	$C_4H_{14}N_4O_2$	150.1118
$C_8H_4NO_2$	146.0242	$C_6H_4N_4O$	148.0386	$C_5H_{12}NO_4$	150.0766
$C_8H_8N_2O$	146.0480	$C_7H_{16}O_3$	148.1100	$C_5H_{14}N_2O_3$	150.1005
$C_8H_8N_3$	146.0719	C_7O_4	147.9796	$C_5N_3O_3$	149.9940
$C_9H_6O_2$	146.0368	$C_7H_2NO_3$	148.0034	$C_5H_2N_4O_2$	150.0178
C_9H_8NO	146.0606	$C_7H_4N_2O_2$	148.0273	$C_6H_{14}O_4$	150.0892
$C_9H_{10}N_2$	146.0845	$C_7H_6N_3O$	148.0511	C_6NO_4	149.9827
$C_{10}H_{10}O$	146.0732	$C_7H_8N_4$	148.0750	$C_6H_2N_2O_3$	150.0065
$C_{10}H_{12}N$	146.0970	$C_8H_4O_3$	148.0160	$C_6H_4N_3O_2$	150.0304
$C_{11}H_{14}$	146.1096	$C_8H_6NO_2$	148.0399	$C_6H_6N_4O$	150.0542
$C_{11}N$	146.0031	$C_8H_8N_2O$	148.0637	$C_7H_2O_4$	149.9953
$C_{12}H_2$	146.0157	$C_8H_{10}N_3$	148.0876	$C_7H_4NO_3$	150.0191
147		$C_9H_8O_2$	148.0524	$C_7H_6N_2O_2$	150.0429
$C_4H_7N_2O_4$	147.0406	$C_9H_{10}NO$	148.0763	$C_7H_8N_3O$	150.0668
$C_4H_9N_3O_3$	147.0644	$C_9H_{12}N_2$	148.1001	$C_7H_{10}N_4$	150.0907
$C_4H_{11}N_4O_2$	147.0883	$C_{10}H_{12}O$	148.0888	$C_8H_6O_3$	150.0317
$C_5H_9NO_4$	147.0532	$C_{10}H_{14}N$	148.1127	$C_8H_8NO_2$	150.0555
$C_5H_{11}N_2O_3$	147.0770	$C_{10}N_2$	148.0062	$C_8H_{10}N_2O$	150.0794
$C_5H_{13}N_3O_2$	147.1009	$C_{11}H_{16}$	148.1253	$C_8H_{12}N_3$	150.1032
$C_5H_{15}N_4O$	147.1247	$C_{11}O$	147.9949	$C_9H_{10}O_2$	150.0681
$C_6H_{11}O_4$	147.0657	$C_{11}H_2N$	148.0187	$C_9H_{12}NO$	150.0919
$C_6H_{13}NO_3$	147.0896	$C_{12}H_4$	148.0313	$C_9H_{14}N_2$	150.1158
$C_6H_{15}N_2O_2$	147.1134	**149**		C_9N_3	150.0093
$C_6H_{17}N_3O$	147.1373	$C_4H_9N_2O_4$	149.0563	$C_{10}H_{14}O$	150.1045
$C_6HN_3O_2$	147.0069	$C_4H_{11}N_3O_3$	149.0801	$C_{10}H_{16}N$	150.1284
$C_6H_3N_4O$	147.0308	$C_4H_{13}N_4O_2$	149.1040	$C_{10}NO$	149.9980
$C_7H_{15}O_3$	147.1021	$C_5H_{11}NO_4$	149.0688	$C_{10}H_2N_2$	150.0218
$C_7H_{17}NO_2$	147.1260	$C_5H_{13}N_2O_3$	149.0927	$C_{11}H_{18}$	150.1409
C_7HNO_3	146.9956	$C_5H_{15}N_3O_2$	149.1165	$C_{11}H_2O$	150.0106
$C_7H_3N_2O_2$	147.0195	$C_5HN_4O_2$	149.0100	$C_{11}H_4N$	150.0344
$C_7H_5N_3O$	147.0433	$C_6H_{13}O_4$	149.0814	$C_{12}H_6$	150.0470
$C_7H_7N_4$	147.0672	$C_6H_{15}NO_3$	149.1052	**151**	
$C_8H_3O_3$	147.0082	$C_6HN_2O_3$	148.9987	$C_4H_{11}N_2O_4$	151.0719
$C_8H_5NO_2$	147.0320	$C_6H_3N_3O_2$	149.0226	$C_4H_{13}N_3O_3$	151.0958
$C_8H_7N_2O$	147.0559	$C_6H_5N_4O$	149.0464	$C_5H_{13}NO_4$	151.0845
$C_8H_9N_3$	147.0798	C_7HO_4	148.9874	$C_5HN_3O_3$	151.0018
$C_9H_7O_2$	147.0446	$C_7H_3NO_3$	149.0113	$C_5H_3N_4O_2$	151.0257
C_9H_9NO	147.0684	$C_7H_5N_2O_2$	149.0351	C_6HNO_4	150.9905
$C_9H_{11}N_2$	147.0923	$C_7H_7N_3O$	149.0590	$C_6H_3N_2O_3$	151.0144
$C_{10}H_{11}O$	147.0810	$C_7H_9N_4$	149.0829	$C_6H_5N_3O_2$	151.0382
$C_{10}H_{13}N$	147.1049	$C_8H_5O_3$	149.0238	$C_6H_7N_4O$	151.0621
$C_{11}H_{15}$	147.1174	$C_8H_7NO_2$	149.0477	$C_7H_3O_4$	151.0031

Appendix A (continued)

FM		FM		FM	
$C_7H_5NO_3$	151.0269	$C_6H_3NO_4$	153.0062	$C_{10}H_6N_2$	154.0532
$C_7H_7N_2O_2$	151.0508	$C_6H_5N_2O_3$	153.0300	$C_{11}H_{22}$	154.1722
$C_7H_9N_3O$	151.0746	$C_6H_7N_3O_2$	153.0539	$C_{11}H_6O$	154.0419
$C_7H_{11}N_4$	151.0985	$C_6H_9N_4O$	153.0777	$C_{11}H_8N$	154.0657
$C_8H_7O_3$	151.0395	$C_7H_5O_4$	153.0187	$C_{12}H_{10}$	154.0783
$C_8H_9NO_2$	151.0634	$C_7H_7NO_3$	153.0426	**155**	
$C_8H_{11}N_2O$	151.0872	$C_7H_9N_2O_2$	153.0664	$C_5H_3N_2O_4$	155.0093
$C_8H_{13}N_3$	151.1111	$C_7H_{11}N_3O$	153.0903	$C_5H_5N_3O_3$	155.0331
$C_9H_{11}O_2$	151.0759	$C_7H_{13}N_4$	153.1142	$C_5H_7N_4O_2$	155.0570
$C_9H_{13}NO$	151.0998	$C_8H_9O_3$	153.0552	$C_6H_5NO_4$	155.0218
$C_9H_{15}N_2$	151.1236	$C_8H_{11}NO_2$	153.0790	$C_6H_7N_2O_3$	155.0457
C_9HN_3	151.0171	$C_8H_{13}N_2O$	153.1029	$C_6H_9N_3O_2$	155.0695
$C_{10}H_{15}O$	151.1123	$C_8H_{15}N_3$	153.1267	$C_6H_{11}N_4O$	155.0934
$C_{10}H_{17}N$	151.1362	C_8HN_4	153.0202	$C_7H_7O_4$	155.0344
$C_{10}HNO$	151.0058	$C_9H_{13}O_2$	153.0916	$C_7H_9NO_3$	155.0583
$C_{10}H_3N_2$	151.0297	$C_9H_{15}NO$	153.1154	$C_7H_{11}N_2O_2$	155.0821
$C_{11}H_{19}$	151.1488	$C_9H_{17}N_2$	153.1393	$C_7H_{13}N_3O$	155.1060
$C_{11}H_3O$	151.0184	C_9HN_2O	153.0089	$C_7H_{15}N_4$	155.1298
$C_{11}H_5N$	151.0422	$C_9H_3N_3$	153.0328	$C_8H_{11}O_3$	155.0708
$C_{12}H_7$	151.0548	$C_{10}H_{17}O$	153.1280	$C_8H_{13}NO_2$	155.0947
152		$C_{10}HO_2$	152.9976	$C_8H_{15}N_2O$	155.1185
$C_4H_{12}N_2O_4$	152.0797	$C_{10}H_{19}N$	153.1519	$C_8H_{17}N_3$	155.1424
$C_5N_2O_4$	151.9858	$C_{10}H_3NO$	153.0215	C_8HN_3O	155.0120
$C_5H_2N_3O_3$	152.0096	$C_{10}H_5N_2$	153.0453	$C_8H_3N_4$	155.0359
$C_5H_4N_4O_2$	152.0335	$C_{11}H_{21}$	153.1644	$C_9H_{15}O_2$	155.1072
$C_6H_2NO_4$	151.9983	$C_{11}H_5O$	153.0340	$C_9H_{17}NO$	155.1311
$C_6H_4N_2O_3$	152.0222	$C_{11}H_7N$	153.0579	C_9HNO_2	155.0007
$C_6H_6N_3O_2$	152.0460	$C_{12}H_9$	153.0705	$C_9H_{19}N_2$	155.1549
$C_6H_8N_4O$	152.0699	**154**		$C_9H_3N_2O$	155.0246
$C_7H_4O_4$	152.0109	$C_5H_2N_2O_4$	154.0014	$C_9H_5N_3$	155.0484
$C_7H_6NO_3$	152.0348	$C_5H_4N_3O_3$	154.0253	$C_{10}H_{19}O$	155.1436
$C_7H_8N_2O_2$	152.0586	$C_5H_6N_4O_2$	154.0491	$C_{10}H_3O_2$	155.0133
$C_7H_{10}N_3O$	152.0825	$C_6H_4NO_4$	154.0140	$C_{10}H_{21}N$	155.1675
$C_7H_{12}N_4$	152.1063	$C_6H_6N_2O_3$	154.0379	$C_{10}H_5NO$	155.0371
$C_8H_8O_3$	152.0473	$C_6H_8N_3O_2$	154.0617	$C_{10}H_7N_2$	155.0610
$C_8H_{10}NO_2$	152.0712	$C_6H_{10}N_4O$	154.0856	$C_{11}H_{23}$	155.1801
$C_8H_{12}N_2O$	152.0950	$C_7H_6O_4$	154.0266	$C_{11}H_7O$	155.0497
$C_8H_{14}N_3$	152.1189	$C_7H_8NO_3$	154.0504	$C_{11}H_9N$	155.0736
C_8N_4	152.0124	$C_7H_{10}N_2O_2$	154.0743	$C_{12}H_{11}$	155.0861
$C_9H_{12}O_2$	152.0837	$C_7H_{12}N_3O$	154.0981	**156**	
$C_9H_{14}NO$	152.1076	$C_7H_{14}N_4$	154.1220	$C_5H_4N_2O_4$	156.0171
$C_9H_{16}N_2$	152.1315	$C_8H_{10}O_3$	154.0630	$C_5H_6N_3O_3$	156.0410
C_9N_2O	152.0011	$C_8H_{12}NO_2$	154.0868	$C_5H_8N_4O_2$	156.0648
$C_9H_2N_3$	152.0249	$C_8H_{14}N_2O$	154.1107	$C_6H_6NO_4$	156.0297
$C_{10}H_{16}O$	152.1202	$C_8H_{16}N_3$	154.1346	$C_6H_8N_2O_3$	156.0535
$C_{10}O_2$	151.9898	C_8N_3O	154.0042	$C_6H_{10}N_3O_2$	156.0774
$C_{10}H_{18}N$	152.1440	$C_8H_2N_4$	154.0280	$C_6H_{12}N_4O$	156.1012
$C_{10}H_2NO$	152.0136	$C_9H_{14}O_2$	154.0994	$C_7H_8O_4$	156.0422
$C_{10}H_4N_2$	152.0375	$C_9H_{16}NO$	154.1233	$C_7H_{10}NO_3$	156.0661
$C_{11}H_{20}$	152.1566	C_9NO_2	153.9929	$C_7H_{12}N_2O_2$	156.0899
$C_{11}H_4O$	152.0262	$C_9H_{18}N_2$	154.1471	$C_7H_{14}N_3O$	156.1138
$C_{11}H_6N$	152.0501	$C_9H_2N_2O$	154.0167	$C_7H_{16}N_4$	156.1377
$C_{12}H_8$	152.0626	$C_9H_4N_3$	154.0406	C_7N_4O	156.0073
153		$C_{10}H_{18}O$	154.1358	$C_8H_{12}O_3$	156.0786
$C_5HN_2O_4$	152.9936	$C_{10}H_2O_2$	154.0054	$C_8H_{14}NO_2$	156.1025
$C_5H_3N_3O_3$	153.0175	$C_{10}H_{20}N$	154.1597	$C_8H_{16}N_2O$	156.1264
$C_5H_5N_4O_2$	153.0413	$C_{10}H_4NO$	154.0293	$C_8N_2O_2$	155.9960

Appendix A (continued)

FM		FM		FM	
$C_8H_{18}N_3$	156.1502	**158**		$C_8H_{19}N_2O$	159.1498
$C_8H_2N_3O$	156.0198	$C_5H_6N_2O_4$	158.0328	$C_8H_3N_2O_2$	159.0195
$C_8H_4N_4$	156.0437	$C_5H_8N_3O_3$	158.0566	$C_8H_{21}N_3$	159.1737
$C_9H_{16}O_2$	156.1151	$C_5H_{10}N_4O_2$	158.0805	$C_8H_5N_3O$	159.0433
C_9O_3	155.9847	$C_6H_8NO_4$	158.0453	$C_8H_7N_4$	159.0672
$C_9H_{18}NO$	156.1389	$C_6H_{10}N_2O_3$	158.0692	$C_9H_{19}O_2$	159.1385
$C_9H_2NO_2$	156.0085	$C_6H_{12}N_3O_2$	158.0930	$C_9H_3O_3$	159.0082
$C_9H_{20}N_2$	156.1628	$C_6H_{14}N_4O$	158.1169	$C_9H_{21}NO$	159.1624
$C_9H_4N_2O$	156.0324	$C_7H_{10}O_4$	158.0579	$C_9H_5NO_2$	159.0320
$C_9H_6N_3$	156.0563	$C_7H_{12}NO_3$	158.0817	$C_9H_7N_2O$	159.0559
$C_{10}H_{20}O$	156.1515	$C_7H_{14}N_2O_2$	158.1056	$C_9H_9N_3$	159.0798
$C_{10}H_4O_2$	156.0211	$C_7H_{16}N_3O$	158.1295	$C_{10}H_7O_2$	159.0446
$C_{10}H_{22}N$	156.1753	$C_7N_3O_2$	157.9991	$C_{10}H_9NO$	159.0684
$C_{10}H_6NO$	156.0449	$C_7H_{18}N_4$	158.1533	$C_{10}H_{11}N_2$	159.0923
$C_{10}H_8N_2$	156.0688	$C_7H_2N_4O$	158.0229	$C_{11}H_{11}O$	159.0810
$C_{11}H_{24}$	156.1879	$C_8H_{14}O_3$	158.0943	$C_{11}H_{13}N$	159.1049
$C_{11}H_8O$	156.0575	$C_8H_{16}NO_2$	158.1182	$C_{12}H_{15}$	159.1174
$C_{11}H_{10}N$	156.0814	C_8NO_3	157.9878	$C_{12}HN$	159.0109
$C_{12}H_{12}$	156.0939	$C_8H_{18}N_2O$	158.1420	$C_{13}H_3$	158.0235
C_{13}	156.0000	$C_8H_2N_2O_2$	158.0116	**160**	
157		$C_8H_{20}N_3$	158.1659	$C_5H_8N_2O_4$	160.0484
$C_5H_5N_2O_4$	157.0249	$C_8H_4N_3O$	158.0355	$C_5H_{10}N_3O_3$	160.0723
$C_5H_7N_3O_3$	157.0488	$C_8H_6N_4$	158.0594	$C_5H_{12}N_4O_2$	160.0961
$C_5H_9N_4O_2$	157.0726	$C_9H_{18}O_2$	158.1307	$C_6H_{10}NO_4$	160.0610
$C_6H_7NO_4$	157.0375	$C_9H_2O_3$	158.0003	$C_6H_{12}N_2O_3$	160.0848
$C_6H_9N_2O_3$	157.0614	$C_9H_{20}NO$	158.1546	$C_6H_{14}N_3O_2$	160.1087
$C_6H_{11}N_3O_2$	157.0852	$C_9H_4NO_2$	158.0242	$C_6H_{16}N_4O$	160.1325
$C_6H_{13}N_4O$	157.1091	$C_9H_{22}N_2$	158.1784	$C_6N_4O_2$	160.0022
$C_7H_9O_4$	157.0501	$C_9H_6N_2O$	158.0480	$C_7H_{12}O_4$	160.0735
$C_7H_{11}NO_3$	157.0739	$C_9H_8N_3$	158.0719	$C_7H_{14}NO_3$	160.0974
$C_7H_{13}N_2O_2$	157.0978	$C_{10}H_{22}O$	158.1671	$C_7H_{16}N_2O_2$	160.1213
$C_7H_{15}N_3O$	157.1216	$C_{10}H_6O_2$	158.0368	$C_7N_2O_3$	159.9909
$C_7H_{17}N_4$	157.1455	$C_{10}H_8NO$	158.0606	$C_7H_{18}N_3O$	160.1451
C_7HN_4O	157.0151	$C_{10}H_{10}N_2$	158.0845	$C_7H_2N_3O_2$	160.0147
$C_8H_{13}O_3$	157.0865	$C_{11}H_{10}O$	158.0732	$C_7H_{20}N_4$	160.1690
$C_8H_{15}NO_2$	157.1103	$C_{11}H_{12}N$	158.0970	$C_7H_4N_4O$	160.0386
$C_8H_{17}N_2O$	157.1342	$C_{12}H_{14}$	158.1096	$C_8H_{16}O_3$	160.1100
$C_8HN_2O_2$	157.0038	$C_{12}N$	158.0031	C_8O_4	159.9796
$C_8H_{19}N_3$	157.1580	$C_{13}H_2$	158.0157	$C_8H_{18}NO_2$	160.1338
$C_8H_3N_3O$	157.0277	**159**		$C_8H_2NO_3$	160.0034
$C_8H_5N_4$	157.0515	$C_5H_7N_2O_4$	159.0406	$C_8H_{20}N_2O$	160.1577
$C_9H_{17}O_2$	157.1229	$C_5H_9N_3O_3$	159.0644	$C_8H_4N_2O_2$	160.0273
C_9HO_3	156.9925	$C_5H_{11}N_4O_2$	159.0883	$C_8H_6N_3O$	160.0511
$C_9H_{19}NO$	157.1467	$C_6H_9NO_4$	159.0532	$C_8H_8N_4$	160.0750
$C_9H_3NO_2$	157.0164	$C_6H_{11}N_2O_3$	159.0770	$C_9H_{20}O_2$	160.1464
$C_9H_{21}N_2$	157.1706	$C_6H_{13}N_3O_2$	159.1009	$C_9H_4O_3$	160.0160
$C_9H_5N_2O$	157.0402	$C_6H_{15}N_4O$	159.1247	$C_9H_6NO_2$	160.0399
$C_9H_7N_3$	157.0641	$C_7H_{11}O_4$	159.0657	$C_9H_8N_2O$	160.0637
$C_{10}H_{21}O$	157.1593	$C_7H_{13}NO_3$	159.0896	$C_9H_{10}N_3$	160.0876
$C_{10}H_5O_2$	157.0289	$C_7H_{15}N_2O_2$	159.1134	$C_{10}H_8O_2$	160.0524
$C_{10}H_{23}N$	157.1832	$C_7H_{17}N_3O$	159.1373	$C_{10}H_{10}NO$	160.0763
$C_{10}H_7NO$	157.0528	$C_7HN_3O_2$	159.0069	$C_{10}H_{12}N_2$	160.1001
$C_{10}H_9N_2$	157.0767	$C_7H_{19}N_4$	159.1611	$C_{11}H_{12}O$	160.0888
$C_{11}H_9O$	157.0653	$C_7H_3N_4O$	159.0308	$C_{11}H_{14}N$	160.1127
$C_{11}H_{11}N$	157.0892	$C_8H_{15}O_3$	159.1021	$C_{11}N_2$	160.0062
$C_{12}H_{13}$	157.1018	$C_8H_{17}NO_2$	159.1260	$C_{12}H_{16}$	160.1253
$C_{13}H$	157.0078	C_8HNO_3	158.9956	$C_{12}O$	159.9949

Appendix A (continued)

FM		FM		FM	
$C_{12}H_2N$	160.0187	$C_8H_2O_4$	161.9953	**164**	
$C_{13}H_4$	160.0313	$C_8H_4NO_3$	162.0191	$C_5H_{12}N_2O_4$	164.0797
161		$C_8H_6N_2O_2$	162.0429	$C_5H_{14}N_3O_3$	164.1036
$C_5H_9N_2O_4$	161.0563	$C_8H_8N_3O$	162.0668	$C_5H_{16}N_4O_2$	164.1275
$C_5H_{11}N_3O_3$	161.0801	$C_8H_{10}N_4$	162.0907	$C_6H_{14}NO_4$	164.0923
$C_5H_{13}N_4O_2$	161.1040	$C_9H_6O_3$	162.0317	$C_6H_{16}N_2O_3$	164.1162
$C_6H_{11}NO_4$	161.0688	$C_9H_8NO_2$	162.0555	$C_6N_2O_4$	163.9858
$C_6H_{13}N_2O_3$	161.0927	$C_9H_{10}N_2O$	162.0794	$C_6H_2N_3O_3$	164.0096
$C_6H_{15}N_3O_2$	161.1165	$C_9H_{12}N_3$	162.1032	$C_6H_4N_4O_2$	164.0335
$C_6H_{17}N_4O$	161.1404	$C_{10}H_{10}O_2$	162.0681	$C_7H_{16}O_4$	164.1049
$C_6HN_4O_2$	161.0100	$C_{10}H_{12}NO$	162.0919	$C_7H_2NO_4$	163.9983
$C_7H_{13}O_4$	161.0814	$C_{10}H_{14}N_2$	162.1158	$C_7H_4N_2O_3$	164.0222
$C_7H_{15}NO_3$	161.1052	$C_{10}N_3$	162.0093	$C_7H_6N_3O_2$	164.0460
$C_7H_{17}N_2O_2$	161.1291	$C_{11}H_{14}O$	162.1045	$C_7H_8N_4O$	164.0699
$C_7HN_2O_3$	160.9987	$C_{11}H_{16}N$	162.1284	$C_8H_4O_4$	164.0109
$C_7H_{19}N_3O$	161.1529	$C_{11}NO$	161.9980	$C_8H_6NO_3$	164.0348
$C_7H_3N_3O_2$	161.0226	$C_{11}H_2N_2$	162.0218	$C_8H_8N_2O_2$	164.0586
$C_7H_5N_4O$	161.0464	$C_{12}H_{18}$	162.1409	$C_8H_{10}N_3O$	164.0825
$C_8H_{17}O_3$	161.1178	$C_{12}H_2O$	162.0106	$C_8H_{12}N_4$	164.1063
C_8HO_4	160.9874	$C_{12}H_4N$	162.0344	$C_9H_8O_3$	164.0473
$C_8H_{19}NO_2$	161.1416	$C_{13}H_6$	162.0470	$C_9H_{10}NO_2$	164.0712
$C_8H_3NO_3$	161.0113	**163**		$C_9H_{12}N_2O$	164.0950
$C_8H_5N_2O_2$	161.0351	$C_5H_{11}N_2O_4$	163.0719	$C_9H_{14}N_3$	164.1189
$C_8H_7N_3O$	161.0590	$C_5H_{13}N_3O_3$	163.0958	C_9N_4	164.0124
$C_8H_9N_4$	161.0829	$C_5H_{15}N_4O_2$	163.1196	$C_{10}H_{12}O_2$	164.0837
$C_9H_5O_3$	161.0238	$C_6H_{13}NO_4$	163.0845	$C_{10}H_{14}NO$	164.1076
$C_9H_7NO_2$	161.0477	$C_6H_{15}N_2O_3$	163.1083	$C_{10}H_{16}N_2$	164.1315
$C_9H_9N_2O$	161.0715	$C_6H_{17}N_3O_2$	163.1322	$C_{10}N_2O$	164.0011
$C_9H_{11}N_3$	161.0954	$C_6HN_3O_3$	163.0018	$C_{10}H_2N_3$	164.0249
$C_{10}H_9O_2$	161.0603	$C_6H_3N_4O_2$	163.0257	$C_{11}H_{16}O$	164.1202
$C_{10}H_{11}NO$	161.0841	$C_7H_{15}O_4$	163.0970	$C_{11}O_2$	163.9898
$C_{10}H_{13}N_2$	161.1080	$C_7H_{17}NO_3$	163.1209	$C_{11}H_{18}N$	164.1440
$C_{11}H_{13}O$	161.0967	C_7HNO_4	162.9905	$C_{11}H_2NO$	164.0136
$C_{11}H_{15}N$	161.1205	$C_7H_3N_2O_3$	163.0144	$C_{11}H_4N_2$	164.0375
$C_{11}HN_2$	161.0140	$C_7H_5N_3O_2$	163.0382	$C_{12}H_{20}$	164.1566
$C_{12}H_{17}$	161.1331	$C_7H_7N_4O$	163.0621	$C_{12}H_4O$	164.0262
$C_{12}HO$	161.0027	$C_8H_3O_4$	163.0031	$C_{12}H_6N$	164.0501
$C_{12}H_3N$	161.0266	$C_8H_5NO_3$	163.0269	$C_{13}H_8$	164.0626
$C_{13}H_5$	161.0391	$C_8H_7N_2O_2$	163.0508	**165**	
162		$C_8H_9N_3O$	163.0746	$C_5H_{13}N_2O_4$	165.0876
$C_5H_{10}N_2O_4$	162.0641	$C_8H_{11}N_4$	163.0985	$C_5H_{15}N_3O_3$	165.1114
$C_5H_{12}N_3O_3$	162.0879	$C_9H_7O_3$	163.0395	$C_6H_{15}NO_4$	165.1001
$C_5H_{14}N_4O_2$	162.1118	$C_9H_9NO_2$	163.0634	$C_6HN_2O_4$	164.9936
$C_6H_{12}NO_4$	162.0766	$C_9H_{11}N_2O$	163.0872	$C_6H_3N_3O_3$	165.0175
$C_6H_{14}N_2O_3$	162.1005	$C_9H_{13}N_3$	163.1111	$C_6H_5N_4O_2$	165.0413
$C_6H_{16}N_3O_2$	162.1244	$C_{10}H_{11}O_2$	163.0759	$C_7H_3NO_4$	165.0062
$C_6N_3O_3$	161.9940	$C_{10}H_{13}NO$	163.0998	$C_7H_5N_2O_3$	165.0300
$C_6H_{18}N_4O$	162.1482	$C_{10}H_{15}N_2$	163.1236	$C_7H_7N_3O_2$	165.0539
$C_6H_2N_4O_2$	162.0178	$C_{10}HN_3$	163.0171	$C_7H_9N_4O$	165.0777
$C_7H_{14}O_4$	162.0892	$C_{11}H_{15}O$	163.1123	$C_8H_5O_4$	165.0187
$C_7H_{16}NO_3$	162.1131	$C_{11}H_{17}N$	163.1362	$C_8H_7NO_3$	165.0426
C_7NO_4	161.9827	$C_{11}HNO$	163.0058	$C_8H_9N_2O_2$	165.0664
$C_7H_{18}N_2O_2$	162.1369	$C_{11}H_3N_2$	163.0297	$C_8H_{11}N_3O$	165.0903
$C_7H_2N_2O_3$	162.0065	$C_{12}H_{19}$	163.1488	$C_8H_{13}N_4$	165.1142
$C_7H_4N_3O_2$	162.0304	$C_{12}H_3O$	163.0184	$C_9H_9O_3$	165.0552
$C_7H_6N_4O$	162.0542	$C_{12}H_5N$	163.0422	$C_9H_{11}NO_2$	165.0790
$C_8H_{18}O_3$	162.1256	$C_{13}H_7$	163.0548	$C_9H_{13}N_2O$	165.1029

Appendix A (continued)

FM		FM		FM	
$C_9H_{15}N_3$	165.1267	$C_7H_7N_2O_3$	167.0457	$C_{10}H_6N_3$	168.0563
C_9HN_4	165.0202	$C_7H_9N_3O_2$	167.0695	$C_{11}H_{20}O$	168.1515
$C_{10}H_{13}O_2$	165.0916	$C_7H_{11}N_4O$	167.0934	$C_{11}H_4O_2$	168.0211
$C_{10}H_{15}NO$	165.1154	$C_8H_7O_4$	167.0344	$C_{11}H_{22}N$	168.1753
$C_{10}H_{17}N_2$	165.1393	$C_8H_9NO_3$	167.0583	$C_{11}H_6NO$	168.0449
$C_{10}HN_2O$	165.0089	$C_8H_{11}N_2O_2$	167.0821	$C_{11}H_8N_2$	168.0688
$C_{10}H_3N_3$	165.0328	$C_8H_{13}N_3O$	167.1060	$C_{12}H_{24}$	168.1879
$C_{11}H_{17}O$	165.1280	$C_8H_{15}N_4$	167.1298	$C_{12}H_8O$	168.0575
$C_{11}HO_2$	164.9976	$C_9H_{11}O_3$	167.0708	$C_{12}H_{10}N$	168.0814
$C_{11}H_{19}N$	165.1519	$C_9H_{13}NO_2$	167.0947	$C_{13}H_{12}$	168.0939
$C_{11}H_3NO$	165.0215	$C_9H_{15}N_2O$	167.1185	C_{14}	168.0000
$C_{11}H_5N_2$	165.0453	$C_9H_{17}N_3$	167.1424	**169**	
$C_{12}H_{21}$	165.1644	C_9HN_3O	167.0120	$C_6H_5N_2O_4$	169.0249
$C_{12}H_5O$	165.0340	$C_9H_3N_4$	167.0359	$C_6H_7N_3O_3$	169.0488
$C_{12}H_7N$	165.0579	$C_{10}H_{15}O_2$	167.1072	$C_6H_9N_4O_2$	169.0726
$C_{13}H_9$	165.0705	$C_{10}H_{17}NO$	167.1311	$C_7H_7NO_4$	169.0375
166		$C_{10}HNO_2$	167.0007	$C_7H_9N_2O_3$	169.0614
$C_5H_{14}N_2O_4$	166.0954	$C_{10}H_{19}N_2$	167.1549	$C_7H_{11}N_3O_2$	169.0852
$C_6H_2N_2O_4$	166.0014	$C_{10}H_3N_2O$	167.0246	$C_7H_{13}N_4O$	169.1091
$C_6H_4N_3O_3$	166.0253	$C_{10}H_5N_3$	167.0484	$C_8H_9O_4$	169.0501
$C_6H_6N_4O_2$	166.0491	$C_{11}H_{19}O$	167.1436	$C_8H_{11}NO_3$	169.0739
$C_7H_4NO_4$	166.0140	$C_{11}H_3O_2$	167.0133	$C_8H_{13}N_2O_2$	169.0978
$C_7H_6N_2O_3$	166.0379	$C_{11}H_{21}N$	167.1675	$C_8H_{15}N_3O$	169.1216
$C_7H_8N_3O_2$	166.0617	$C_{11}H_5NO$	167.0371	$C_8H_{17}N_4$	169.1455
$C_7H_{10}N_4O$	166.0856	$C_{11}H_7N_2$	167.0610	C_8HN_4O	169.0151
$C_8H_6O_4$	166.0266	$C_{12}H_{23}$	167.1801	$C_9H_{13}O_3$	169.0865
$C_8H_8NO_3$	166.0504	$C_{12}H_7O$	167.0497	$C_9H_{15}NO_2$	169.1103
$C_8H_{10}N_2O_2$	166.0743	$C_{12}H_9N$	167.0736	$C_9H_{17}N_2O$	169.1342
$C_8H_{12}N_3O$	166.0981	$C_{13}H_{11}$	167.0861	$C_9HN_2O_2$	169.0038
$C_8H_{14}N_4$	166.1220	**168**		$C_9H_{19}N_3$	169.1580
$C_9H_{10}O_3$	166.0630	$C_6H_4N_2O_4$	168.0171	$C_9H_3N_3O$	169.0277
$C_9H_{12}NO_2$	166.0868	$C_6H_6N_3O_3$	168.0410	$C_9H_5N_4$	169.0515
$C_9H_{14}N_2O$	166.1107	$C_6H_8N_4O_2$	168.0648	$C_{10}H_{17}O_2$	169.1229
$C_9H_{16}N_3$	166.1346	$C_7H_6NO_4$	168.0297	$C_{10}HO_3$	168.9925
C_9N_3O	166.0042	$C_7H_8N_2O_3$	168.0535	$C_{10}H_{19}NO$	169.1467
$C_9H_2N_4$	166.0280	$C_7H_{10}N_3O_2$	168.0774	$C_{10}H_3NO_2$	169.0164
$C_{10}H_{14}O_2$	166.0994	$C_7H_{12}N_4O$	168.1012	$C_{10}H_{21}N_2$	169.1706
$C_{10}H_{16}NO$	166.1233	$C_8H_8O_4$	168.0422	$C_{10}H_5N_2O$	169.0402
$C_{10}NO_2$	165.9929	$C_8H_{10}NO_3$	168.0661	$C_{10}H_7N_3$	169.0641
$C_{10}H_{18}N_2$	166.1471	$C_8H_{12}N_2O_2$	168.0899	$C_{11}H_{21}O$	169.1593
$C_{10}H_2N_2O$	166.0167	$C_8H_{14}N_3O$	168.1138	$C_{11}H_5O_2$	169.0289
$C_{10}H_4N_3$	166.0406	$C_8H_{16}N_4$	168.1377	$C_{11}H_{23}N$	169.1832
$C_{11}H_{18}O$	166.1358	C_8N_4O	168.0073	$C_{11}H_7NO$	169.0528
$C_{11}H_2O_2$	166.0054	$C_9H_{12}O_3$	168.0786	$C_{11}H_9N_2$	169.0767
$C_{11}H_{20}N$	166.1597	$C_9H_{14}NO_2$	168.1025	$C_{12}H_{25}$	169.1957
$C_{11}H_4NO$	166.0293	$C_9H_{16}N_2O$	168.1264	$C_{12}H_9O$	169.0653
$C_{11}H_6N_2$	166.0532	$C_9N_2O_2$	167.9960	$C_{12}H_{11}N$	169.0892
$C_{12}H_{22}$	166.1722	$C_9H_{18}N_3$	168.1502	$C_{13}H_{13}$	169.1018
$C_{12}H_6O$	166.0419	$C_9H_2N_3O$	168.0198	$C_{14}H$	169.0078
$C_{12}H_8N$	166.0657	$C_9H_4N_4$	168.0437	**170**	
$C_{13}H_{10}$	166.0783	$C_{10}H_{16}O_2$	168.1151	$C_6H_6N_2O_4$	170.0328
167		$C_{10}O_3$	167.9847	$C_6H_8N_3O_3$	170.0566
$C_6H_3N_2O_4$	167.0093	$C_{10}H_{18}NO$	168.1389	$C_6H_{10}N_4O_2$	170.0805
$C_6H_5N_3O_3$	167.0331	$C_{10}H_2NO_2$	168.0085	$C_7H_8NO_4$	170.0453
$C_6H_7N_4O_2$	167.0570	$C_{10}H_{20}N_2$	168.1628	$C_7H_{10}N_2O_3$	170.0692
$C_7H_5NO_4$	167.0218	$C_{10}H_4N_2O$	168.0324	$C_7H_{12}N_3O_2$	170.0930

Appendix A (continued)

FM		FM		FM	
$C_7H_{14}N_4O$	170.1169	$C_9H_7N_4$	171.0672	$C_{12}H_{14}N$	172.1127
$C_8H_{10}O_4$	170.0579	$C_{10}H_{19}O_2$	171.1385	$C_{12}N_2$	172.0062
$C_8H_{12}NO_3$	170.0817	$C_{10}H_3O_3$	171.0082	$C_{13}H_{16}$	172.1253
$C_8H_{14}N_2O_2$	170.1056	$C_{10}H_{21}NO$	171.1624	$C_{13}O$	171.9949
$C_8H_{16}N_3O$	170.1295	$C_{10}H_5NO_2$	171.0320	$C_{13}H_2N$	172.0187
$C_8N_3O_2$	169.9991	$C_{10}H_{23}N_2$	171.1863	$C_{14}H_4$	172.0313
$C_8H_{18}N_4$	170.1533	$C_{10}H_7N_2O$	171.0559	**173**	
$C_8H_2N_4O$	170.0229	$C_{10}H_9N_3$	171.0798	$C_6H_9N_2O_4$	173.0563
$C_9H_{14}O_3$	170.0943	$C_{11}H_{23}O$	171.1750	$C_6H_{11}N_3O_3$	173.0801
$C_9H_{16}NO_2$	170.1182	$C_{11}H_7O_2$	171.0446	$C_6H_{13}N_4O_2$	173.1040
C_9NO_3	169.9878	$C_{11}H_{25}N$	171.1988	$C_7H_{11}NO_4$	173.0688
$C_9H_{18}N_2O$	170.1420	$C_{11}H_9NO$	171.0684	$C_7H_{13}N_2O_3$	173.0927
$C_9H_2N_2O_2$	170.0116	$C_{11}H_{11}N_2$	171.0923	$C_7H_{15}N_3O_2$	173.1165
$C_9H_{20}N_3$	170.1659	$C_{12}H_{11}O$	171.0810	$C_7H_{17}N_4O$	173.1404
$C_9H_4N_3O$	170.0355	$C_{12}H_{13}N$	171.1049	$C_7HN_4O_2$	173.0100
$C_9H_6N_4$	170.0594	$C_{13}H_{15}$	171.1174	$C_8H_{13}O_4$	173.0814
$C_{10}H_{18}O_2$	170.1307	$C_{13}HN$	171.0109	$C_8H_{15}NO_3$	173.1052
$C_{10}H_2O_3$	170.0003	$C_{14}H_3$	171.0235	$C_8H_{17}N_2O_2$	173.1291
$C_{10}H_{20}NO$	170.1546	**172**		$C_8HN_2O_3$	172.9987
$C_{10}H_4NO_2$	170.0242	$C_6H_8N_2O_4$	172.0484	$C_8H_{19}N_3O$	173.1529
$C_{10}H_{22}N_2$	170.1784	$C_6H_{10}N_3O_3$	172.0723	$C_8H_3N_3O_2$	173.0226
$C_{10}H_6N_2O$	170.0480	$C_6H_{12}N_4O_2$	172.0961	$C_8H_{21}N_4$	173.1768
$C_{10}H_8N_3$	170.0719	$C_7H_{10}NO_4$	172.0610	$C_8H_5N_4O$	173.0464
$C_{11}H_{22}O$	170.1671	$C_7H_{12}N_2O_3$	172.0848	$C_9H_{17}O_3$	173.1178
$C_{11}H_6O_2$	170.0368	$C_7H_{14}N_3O_2$	172.1087	C_9HO_4	172.9874
$C_{11}H_{24}N$	170.1910	$C_7H_{16}N_4O$	172.1325	$C_9H_{19}NO_2$	173.1416
$C_{11}H_8NO$	170.0606	$C_7N_4O_2$	172.0022	$C_9H_3NO_3$	173.0113
$C_{11}H_{10}N_2$	170.0845	$C_8H_{12}O_4$	172.0735	$C_9H_{21}N_2O$	173.1655
$C_{12}H_{26}$	170.2036	$C_8H_{14}NO_3$	172.0974	$C_9H_5N_2O_2$	173.0351
$C_{12}H_{10}O$	170.0732	$C_8H_{16}N_2O_2$	172.1213	$C_9H_{23}N_3$	173.1894
$C_{12}H_{12}N$	170.0970	$C_8N_2O_3$	171.9909	$C_9H_7N_3O$	173.0590
$C_{13}H_{14}$	170.1096	$C_8H_{18}N_3O$	172.1451	$C_9H_9N_4$	173.0829
$C_{13}N$	170.0031	$C_8H_2N_3O_2$	172.0147	$C_{10}H_{21}O_2$	173.1542
$C_{14}H_2$	170.0157	$C_8H_{20}N_4$	172.1690	$C_{10}H_5O_3$	173.0238
171		$C_8H_4N_4O$	172.0386	$C_{10}H_{23}NO$	173.1781
$C_6H_7N_2O_4$	171.0406	$C_9H_{16}O_3$	172.1100	$C_{10}H_7NO_2$	173.0477
$C_6H_9N_3O_3$	171.0644	C_9O_4	171.9796	$C_{10}H_9N_2O$	173.0715
$C_6H_{11}N_4O_2$	171.0883	$C_9H_{18}NO_2$	172.1338	$C_{10}H_{11}N_3$	173.0954
$C_7H_9NO_4$	171.0532	$C_9H_2NO_3$	172.0034	$C_{11}H_9O_2$	173.0603
$C_7H_{11}N_2O_3$	171.0770	$C_9H_{20}N_2O$	172.1577	$C_{11}H_{11}NO$	173.0841
$C_7H_{13}N_3O_2$	171.1009	$C_9H_4N_2O_2$	172.0273	$C_{11}H_{13}N_2$	173.1080
$C_7H_{15}N_4O$	171.1247	$C_9H_{22}N_3$	172.1815	$C_{12}H_{13}O$	173.0967
$C_8H_{11}O_4$	171.0657	$C_9H_6N_3O$	172.0511	$C_{12}H_{15}N$	173.1205
$C_8H_{13}NO_3$	171.0896	$C_9H_8N_4$	172.0750	$C_{12}HN_2$	173.0140
$C_8H_{15}N_2O_2$	171.1134	$C_{10}H_{20}O_2$	172.1464	$C_{13}H_{17}$	173.1331
$C_8H_{17}N_3O$	171.1373	$C_{10}H_4O_3$	172.0160	$C_{13}HO$	173.0027
$C_8HN_3O_2$	171.0069	$C_{10}H_{22}NO$	172.1702	$C_{13}H_3N$	173.0266
$C_8H_{19}N_4$	171.1611	$C_{10}H_6NO_2$	172.0399	$C_{14}H_5$	173.0391
$C_8H_3N_4O$	171.0308	$C_{10}H_{24}N_2$	172.1941	**174**	
$C_9H_{15}O_3$	171.1021	$C_{10}H_8N_2O$	172.0637	$C_6H_{10}N_2O_4$	174.0641
$C_9H_{17}NO_2$	171.1260	$C_{10}H_{10}N_3$	172.0876	$C_6H_{12}N_3O_3$	174.0879
C_9HNO_3	170.9956	$C_{11}H_{24}O$	172.1828	$C_6H_{14}N_4O_2$	174.1118
$C_9H_{19}N_2O$	171.1498	$C_{11}H_8O_2$	172.0524	$C_7H_{12}NO_4$	174.0766
$C_9H_3N_2O_2$	171.0195	$C_{11}H_{10}NO$	172.0763	$C_7H_{14}N_2O_3$	174.1005
$C_9H_{21}N_3$	171.1737	$C_{11}H_{12}N_2$	172.1001	$C_7H_{16}N_3O_2$	174.1244
$C_9H_5N_3O$	171.0433	$C_{12}H_{12}O$	172.0888	$C_7N_3O_3$	173.9940

Appendix A (continued)

FM		FM		FM	
$C_7H_{18}N_4O$	174.1482	$C_9H_5NO_3$	175.0269	$C_{12}H_2NO$	176.0136
$C_7H_2N_4O_2$	174.0178	$C_9H_7N_2O_2$	175.0508	$C_{12}H_4N_2$	176.0375
$C_8H_{14}O_4$	174.0892	$C_9H_9N_3O$	175.0746	$C_{13}H_{20}$	176.1566
$C_8H_{16}NO_3$	174.1131	$C_9H_{11}N_4$	175.0985	$C_{13}H_4O$	176.0262
C_8NO_4	173.9827	$C_{10}H_7O_3$	175.0395	$C_{13}H_6N$	176.0501
$C_8H_{18}N_2O_2$	174.1369	$C_{10}H_9NO_2$	175.0634	$C_{14}H_8$	176.0626
$C_8H_2N_2O_3$	174.0065	$C_{10}H_{11}N_2O$	175.0872	**177**	
$C_8H_{20}N_3O$	174.1608	$C_{10}H_{13}N_3$	175.1111	$C_6H_{13}N_2O_4$	177.0876
$C_8H_4N_3O_2$	174.0304	$C_{11}H_{11}O_2$	175.0759	$C_6H_{15}N_3O_3$	177.1114
$C_8H_{22}N_4$	174.1846	$C_{11}H_{13}NO$	175.0998	$C_6H_{17}N_4O_2$	177.1353
$C_8H_6N_4O$	174.0542	$C_{11}H_{15}N_2$	175.1236	$C_7H_{15}NO_4$	177.1001
$C_9H_{18}O_3$	174.1256	$C_{11}HN_3$	175.0171	$C_7H_{17}N_2O_3$	177.1240
$C_9H_2O_4$	173.9953	$C_{12}H_{15}O$	175.1123	$C_7HN_2O_4$	176.9936
$C_9H_{20}NO_2$	174.1495	$C_{12}H_{17}N$	175.1362	$C_7H_{19}N_3O_2$	177.1478
$C_9H_4NO_3$	174.0191	$C_{12}HNO$	175.0058	$C_7H_3N_3O_3$	177.0175
$C_9H_{22}N_2O$	174.1733	$C_{12}H_3N_2$	175.0297	$C_7H_5N_4O_2$	177.0413
$C_9H_6N_2O_2$	174.0429	$C_{13}H_{19}$	175.1488	$C_8H_{17}O_4$	177.1127
$C_9H_8N_3O$	174.0668	$C_{13}H_3O$	175.0184	$C_8H_{19}NO_3$	177.1365
$C_9H_{10}N_4$	174.0907	$C_{13}H_5N$	175.0422	$C_8H_3NO_4$	177.0062
$C_{10}H_{22}O_2$	174.1620	$C_{14}H_7$	175.0548	$C_8H_5N_2O_3$	177.0300
$C_{10}H_6O_3$	174.0317	**176**		$C_8H_7N_3O_2$	177.0539
$C_{10}H_8NO_2$	174.0555	$C_6H_{12}N_2O_4$	176.0797	$C_8H_9N_4O$	177.0777
$C_{10}H_{10}N_2O$	174.0794	$C_6H_{14}N_3O_3$	176.1036	$C_9H_5O_4$	177.0187
$C_{10}H_{12}N_3$	174.1032	$C_6H_{16}N_4O_2$	176.1275	$C_9H_7NO_3$	177.0426
$C_{11}H_{10}O_2$	174.0681	$C_7H_{14}NO_4$	176.0923	$C_9H_9N_2O_2$	177.0664
$C_{11}H_{12}NO$	174.0919	$C_7H_{16}N_2O_3$	176.1162	$C_9H_{11}N_3O$	177.0903
$C_{11}H_{14}N_2$	174.1158	$C_7N_2O_4$	175.9858	$C_9H_{13}N_4$	177.1142
$C_{11}N_3$	174.0093	$C_7H_{18}N_3O_2$	176.1400	$C_{10}H_9O_3$	177.0552
$C_{12}H_{14}O$	174.1045	$C_7H_2N_3O_3$	176.0096	$C_{10}H_{11}NO_2$	177.0790
$C_{12}H_{16}N$	174.1284	$C_7H_{20}N_4O$	176.1639	$C_{10}H_{13}N_2O$	177.1029
$C_{12}NO$	173.9980	$C_7H_4N_4O_2$	176.0335	$C_{10}H_{15}N_3$	177.1267
$C_{12}H_2N_2$	174.0218	$C_8H_{16}O_4$	176.1049	$C_{10}HN_4$	177.0202
$C_{13}H_{18}$	174.1409	$C_8H_{18}NO_3$	176.1287	$C_{11}H_{13}O_2$	177.0916
$C_{13}H_2O$	174.0106	$C_8H_2NO_4$	175.9983	$C_{11}H_{15}NO$	177.1154
$C_{13}H_4N$	174.0344	$C_8H_{20}N_2O_2$	176.1526	$C_{11}H_{17}N_2$	177.1393
$C_{14}H_6$	174.0470	$C_8H_4N_2O_3$	176.0222	$C_{11}HN_2O$	177.0089
175		$C_8H_6N_3O_2$	176.0460	$C_{11}H_3N_3$	177.0328
$C_6H_{11}N_2O_4$	175.0719	$C_8H_8N_4O$	176.0699	$C_{12}H_{17}O$	177.1280
$C_6H_{13}N_3O_3$	175.0958	$C_9H_{20}O_3$	176.1413	$C_{12}HO_2$	176.9976
$C_6H_{15}N_4O_2$	175.1196	$C_9H_4O_4$	176.0109	$C_{12}H_{19}N$	177.1519
$C_7H_{13}NO_4$	175.0845	$C_9H_6NO_3$	176.0348	$C_{12}H_3NO$	177.0215
$C_7H_{15}N_2O_3$	175.1083	$C_9H_8N_2O_2$	176.0586	$C_{12}H_5N_2$	177.0453
$C_7H_{17}N_3O_2$	175.1322	$C_9H_{10}N_3O$	176.0825	$C_{13}H_{21}$	177.1644
$C_7HN_3O_3$	175.0018	$C_9H_{12}N_4$	176.1063	$C_{13}H_5O$	177.0340
$C_7H_{19}N_4O$	175.1560	$C_{10}H_8O_3$	176.0473	$C_{13}H_7N$	177.0579
$C_7H_3N_4O_2$	175.0257	$C_{10}H_{10}NO_2$	176.0712	$C_{14}H_9$	177.0705
$C_8H_{15}O_4$	175.0970	$C_{10}H_{12}N_2O$	176.0950	**178**	
$C_8H_{17}NO_3$	175.1209	$C_{10}H_{14}N_3$	176.1189	$C_6H_{14}N_2O_4$	178.0954
C_8HNO_4	174.9905	$C_{10}N_4$	176.0124	$C_6H_{16}N_3O_3$	178.1193
$C_8H_{19}N_2O_2$	175.1447	$C_{11}H_{12}O_2$	176.0837	$C_6H_{18}N_4O_2$	178.1431
$C_8H_3N_2O_3$	175.0144	$C_{11}H_{14}NO$	176.1076	$C_7H_{16}NO_4$	178.1080
$C_8H_{21}N_3O$	175.1686	$C_{11}H_{16}N_2$	176.1315	$C_7H_{18}N_2O_3$	178.1318
$C_8H_5N_3O_2$	175.0382	$C_{11}N_2O$	176.0011	$C_7H_2N_2O_4$	178.0014
$C_8H_7N_4O$	175.0621	$C_{11}H_2N_3$	176.0249	$C_7H_4N_3O_3$	178.0253
$C_9H_{19}O_3$	175.1334	$C_{12}H_{16}O$	176.1202	$C_7H_6N_4O_2$	178.0491
$C_9H_3O_4$	175.0031	$C_{12}O_2$	175.9898	$C_8H_{18}O_4$	178.1205
$C_9H_{21}NO_2$	175.1573	$C_{12}H_{18}N$	176.1440	$C_8H_4NO_4$	178.0140

Appendix A (continued)

FM		FM		FM	
$C_8H_6N_2O_3$	178.0379	$C_{12}H_{19}O$	179.1436	$C_9H_{11}NO_3$	181.0739
$C_8H_8N_3O_2$	178.0617	$C_{12}H_3O_2$	179.0133	$C_9H_{13}N_2O_2$	181.0978
$C_8H_{10}N_4O$	178.0856	$C_{12}H_{21}N$	179.1675	$C_9H_{15}N_3O$	181.1216
$C_9H_6O_4$	178.0266	$C_{12}H_5NO$	179.0371	$C_9H_{17}N_4$	181.1455
$C_9H_8NO_3$	178.0504	$C_{12}H_7N_2$	179.0610	C_9HN_4O	181.0151
$C_9H_{10}N_2O_2$	178.0743	$C_{13}H_{23}$	179.1801	$C_{10}H_{13}O_3$	181.0865
$C_9H_{12}N_3O$	178.0981	$C_{13}H_7O$	179.0497	$C_{10}H_{15}NO_2$	181.1103
$C_9H_{14}N_4$	178.1220	$C_{13}H_9N$	179.0736	$C_{10}H_{17}N_2O$	181.1342
$C_{10}H_{10}O_3$	178.0630	$C_{14}H_{11}$	179.0861	$C_{10}HN_2O_2$	181.0038
$C_{10}H_{12}NO_2$	178.0868	**180**		$C_{10}H_{19}N_3$	181.1580
$C_{10}H_{14}N_2O$	178.1107	$C_6H_{16}N_2O_4$	180.1111	$C_{10}H_3N_3O$	181.0277
$C_{10}H_{16}N_3$	178.1346	$C_7H_4N_2O_4$	180.0171	$C_{10}H_5N_4$	181.0515
$C_{10}N_3O$	178.0042	$C_7H_6N_3O_3$	180.0410	$C_{11}H_{17}O_2$	181.1229
$C_{10}H_2N_4$	178.0280	$C_7H_8N_4O_2$	180.0648	$C_{11}HO_3$	180.9925
$C_{11}H_{14}O_2$	178.0994	$C_8H_6NO_4$	180.0297	$C_{11}H_{19}NO$	181.1467
$C_{11}H_{16}NO$	178.1233	$C_8H_8N_2O_3$	180.0535	$C_{11}H_3NO_2$	181.0164
$C_{11}NO_2$	177.9929	$C_8H_{10}N_3O_2$	180.0774	$C_{11}H_{21}N_2$	181.1706
$C_{11}H_{18}N_2$	178.1471	$C_8H_{12}N_4O$	180.1012	$C_{11}H_5N_2O$	181.0402
$C_{11}H_2N_2O$	178.0167	$C_9H_8O_4$	180.0422	$C_{11}H_7N_3$	181.0641
$C_{11}H_4N_3$	178.0406	$C_9H_{10}NO_3$	180.0661	$C_{12}H_{21}O$	181.1593
$C_{12}H_{18}O$	178.1358	$C_9H_{12}N_2O_2$	180.0899	$C_{12}H_5O_2$	181.0289
$C_{12}H_2O_2$	178.0054	$C_9H_{14}N_3O$	180.1138	$C_{12}H_{23}N$	181.1832
$C_{12}H_{20}N$	178.1597	$C_9H_{16}N_4$	180.1377	$C_{12}H_7NO$	181.0528
$C_{12}H_4NO$	178.0293	C_9N_4O	180.0073	$C_{12}H_9N_2$	181.0767
$C_{12}H_6N_2$	178.0532	$C_{10}H_{12}O_3$	180.0786	$C_{13}H_{25}$	181.1957
$C_{13}H_{22}$	178.1722	$C_{10}H_{14}NO_2$	180.1025	$C_{13}H_9O$	181.0653
$C_{13}H_6O$	178.0419	$C_{10}H_{16}N_2O$	180.1264	$C_{13}H_{11}N$	181.0892
$C_{13}H_8N$	178.0657	$C_{10}N_2O_2$	179.9960	$C_{14}H_{13}$	181.1018
$C_{14}H_{10}$	178.0783	$C_{10}H_{18}N_3$	180.1502	$C_{15}H$	181.0078
179		$C_{10}H_2N_3O$	180.0198	**182**	
$C_6H_{15}N_2O_4$	179.1032	$C_{10}H_4N_4$	180.0437	$C_7H_6N_2O_4$	182.0328
$C_6H_{17}N_3O_3$	179.1271	$C_{11}H_{16}O_2$	180.1151	$C_7H_8N_3O_3$	182.0566
$C_7H_{17}NO_4$	179.1158	$C_{11}O_3$	179.9847	$C_7H_{10}N_4O_2$	182.0805
$C_7H_3N_2O_4$	179.0093	$C_{11}H_{18}NO$	180.1389	$C_8H_8NO_4$	182.0453
$C_7H_5N_3O_3$	179.0331	$C_{11}H_2NO_2$	180.0085	$C_8H_{10}N_2O_3$	182.0692
$C_7H_7N_4O_2$	179.0570	$C_{11}H_{20}N_2$	180.1628	$C_8H_{12}N_3O_2$	182.0930
$C_8H_5NO_4$	179.0218	$C_{11}H_4N_2O$	180.0324	$C_8H_{14}N_4O$	182.1169
$C_8H_7N_2O_3$	179.0457	$C_{11}H_6N_3$	180.0563	$C_9H_{10}O_4$	182.0579
$C_8H_9N_3O_2$	179.0695	$C_{12}H_{20}O$	180.1515	$C_9H_{12}NO_3$	182.0817
$C_8H_{11}N_4O$	179.0934	$C_{12}H_4O_2$	180.0211	$C_9H_{14}N_2O_2$	182.1056
$C_9H_7O_4$	179.0344	$C_{12}H_{22}N$	180.1753	$C_9H_{16}N_3O$	182.1295
$C_9H_9NO_3$	179.0583	$C_{12}H_6NO$	180.0449	$C_9N_3O_2$	181.9991
$C_9H_{11}N_2O_2$	179.0821	$C_{12}H_8N_2$	180.0688	$C_9H_{18}N_4$	182.1533
$C_9H_{13}N_3O$	179.1060	$C_{13}H_{24}$	180.1879	$C_9H_2N_4O$	182.0229
$C_9H_{15}N_4$	179.1298	$C_{13}H_8O$	180.0575	$C_{10}H_{14}O_3$	182.0943
$C_{10}H_{11}O_3$	179.0708	$C_{13}H_{10}N$	180.0814	$C_{10}H_{16}NO_2$	182.1182
$C_{10}H_{13}NO_2$	179.0947	$C_{14}H_{12}$	180.0939	$C_{10}NO_3$	181.9878
$C_{10}H_{15}N_2O$	179.1185	C_{15}	180.0000	$C_{10}H_{18}N_2O$	182.1420
$C_{10}H_{17}N_3$	179.1424	**181**		$C_{10}H_2N_2O_2$	182.0116
$C_{10}HN_3O$	179.0120	$C_7H_5N_2O_4$	181.0249	$C_{10}H_{20}N_3$	182.1659
$C_{10}H_3N_4$	179.0359	$C_7H_7N_3O_3$	181.0488	$C_{10}H_4N_3O$	182.0355
$C_{11}H_{15}O_2$	179.1072	$C_7H_9N_4O_2$	181.0726	$C_{10}H_6N_4$	182.0594
$C_{11}H_{17}NO$	179.1311	$C_8H_7NO_4$	181.0375	$C_{11}H_{18}O_2$	182.1307
$C_{11}HNO_2$	179.0007	$C_8H_9N_2O_3$	181.0614	$C_{11}H_2O_3$	182.0003
$C_{11}H_{19}N_2$	179.1549	$C_8H_{11}N_3O_2$	181.0852	$C_{11}H_{20}NO$	182.1546
$C_{11}H_3N_2O$	179.0246	$C_8H_{13}N_4O$	181.1091	$C_{11}H_4NO_2$	182.0242
$C_{11}H_5N_3$	179.0484	$C_9H_9O_4$	181.0501	$C_{11}H_{22}N_2$	182.1784

Appendix A (continued)

FM		FM		FM	
$C_{11}H_6N_2O$	182.0480	$C_{14}H_{15}$	183.1174	$C_7H_{11}N_3O_3$	185.0801
$C_{11}H_8N_3$	182.0719	$C_{14}HN$	183.0109	$C_7H_{13}N_4O_2$	185.1040
$C_{12}H_{22}O$	182.1671	$C_{15}H_3$	183.0235	$C_8H_{11}NO_4$	185.0688
$C_{12}H_6O_2$	182.0368	**184**		$C_8H_{13}N_2O_3$	185.0927
$C_{12}H_{24}N$	182.1910	$C_7H_8N_2O_4$	184.0484	$C_8H_{15}N_3O_2$	185.1165
$C_{12}H_8NO$	182.0606	$C_7H_{10}N_3O_3$	184.0723	$C_8H_{17}N_4O$	185.1404
$C_{12}H_{10}N_2$	182.0845	$C_7H_{12}N_4O_2$	184.0961	$C_8HN_4O_2$	185.0100
$C_9H_{19}N_3O$	185.1529	$C_8H_{10}NO_4$	184.0610	$C_9H_{13}O_4$	185.0814
$C_9H_3N_3O_2$	185.0226	$C_8H_{12}N_2O_3$	184.0848	$C_9H_{15}NO_3$	185.1052
$C_9H_{21}N_4$	185.1768	$C_{10}H_{20}NO_2$	186.1495	$C_9H_{17}N_2O_2$	185.1291
$C_9H_5N_4O$	185.0464	$C_{10}H_4NO_3$	186.0191	$C_9HN_2O_3$	184.9987
$C_{10}H_{17}O_3$	185.1178	$C_{10}H_{22}N_2O$	186.1733	$C_{10}H_9N_3O$	187.0746
$C_{10}HO_4$	184.9874	$C_{10}H_6N_2O_2$	186.0429	$C_{10}H_{11}N_4$	187.0985
$C_{13}H_{26}$	182.2036	$C_{10}H_{24}N_3$	186.1972	$C_{11}H_{23}O_2$	187.1699
$C_{13}H_{10}O$	182.0732	$C_{10}H_8N_3O$	186.0668	$C_{11}H_7O_3$	187.0395
$C_{13}H_{12}N$	182.0970	$C_8H_{14}N_3O_2$	184.1087	$C_{11}H_{25}NO$	187.1937
$C_{14}H_{14}$	182.1096	$C_8H_{16}N_4O$	184.1325	$C_{11}H_9NO_2$	187.0634
$C_{14}N$	182.0031	$C_8N_4O_2$	184.0022	$C_{10}H_{19}NO_2$	185.1416
$C_{15}H_2$	182.0157	$C_9H_{12}O_4$	184.0735	$C_{10}H_3NO_3$	185.0113
183		$C_9H_{14}NO_3$	184.0974	$C_{10}H_{21}N_2O$	185.1655
$C_7H_7N_2O_4$	183.0406	$C_9H_{16}N_2O_2$	184.1213	$C_{10}H_5N_2O_2$	185.0351
$C_7H_9N_3O_3$	183.0644	$C_9N_2O_3$	183.9909	$C_{10}H_{23}N_3$	185.1894
$C_7H_{11}N_4O_2$	183.0883	$C_9H_{18}N_3O$	184.1451	$C_{10}H_7N_3O$	185.0590
$C_8H_9NO_4$	183.0532	$C_9H_2N_3O_2$	184.0147	$C_{10}H_9N_4$	185.0829
$C_8H_{11}N_2O_3$	183.0770	$C_9H_{20}N_4$	184.1690	$C_{11}H_{21}O_2$	185.1542
$C_8H_{13}N_3O_2$	183.1009	$C_9H_4N_4O$	184.0386	$C_{11}H_5O_3$	185.0238
$C_8H_{15}N_4O$	183.1247	$C_{10}H_{16}O_3$	184.1100	$C_{11}H_{23}NO$	185.1781
$C_9H_{11}O_4$	183.0657	$C_{10}O_4$	183.9796	$C_{11}H_7NO_2$	185.0477
$C_9H_{13}NO_3$	183.0896	$C_{10}H_{18}NO_2$	184.1338	$C_{11}H_{25}N_2$	185.2019
$C_9H_{15}N_2O_2$	183.1134	$C_{10}H_2NO_3$	184.0034	$C_{11}H_9N_2O$	185.0715
$C_9H_{17}N_3O$	183.1373	$C_{10}H_{20}N_2O$	184.1577	$C_{11}H_{11}N_3$	185.0954
$C_9HN_3O_2$	183.0069	$C_{10}H_4N_2O_2$	184.0273	$C_{12}H_{25}O$	185.1906
$C_9H_{19}N_4$	183.1611	$C_{10}H_{22}N_3$	184.1815	$C_{12}H_9O_2$	185.0603
$C_9H_3N_4O$	183,0308	$C_{10}H_6N_3O$	184.0511	$C_{12}H_{27}N$	185.2145
$C_{10}H_{15}O_3$	183.1021	$C_{10}H_8N_4$	184.0750	$C_{12}H_{11}NO$	185.0841
$C_{10}H_{17}NO_2$	183.1260	$C_{11}H_{20}O_2$	184.1464	$C_{12}H_{13}N_2$	185.1080
$C_{10}HNO_3$	182.9956	$C_{11}H_4O_3$	184.0160	$C_{13}H_{13}O$	185.0967
$C_{10}H_{19}N_2O$	183.1498	$C_{11}H_{22}NO$	184.1702	$C_{13}H_{15}N$	185.1205
$C_{10}H_3N_2O_2$	183.0195	$C_{11}H_6NO_2$	184.0399	$C_{13}HN_2$	185.0140
$C_{10}H_{21}N_3$	183.1737	$C_{11}H_{24}N_2$	184.1941	$C_{14}H_{17}$	185.1331
$C_{10}H_5N_3O$	183.0433	$C_{11}H_8N_2O$	184.0637	$C_{14}HO$	185.0027
$C_{10}H_7N_4$	183.0672	$C_{11}H_{10}N_3$	184.0876	$C_{14}H_3N$	185.0266
$C_{11}H_{19}O_2$	183.1385	$C_{12}H_{24}O$	184.1828	$C_{15}H_5$	185.0391
$C_{11}H_3O_3$	183.0082	$C_{12}H_8O_2$	184.0524	**186**	
$C_{11}H_{21}NO$	183.1624	$C_{12}H_{26}N$	184.2067	$C_7H_{10}N_2O_4$	186.0641
$C_{11}H_5NO_2$	183.0320	$C_{12}H_{10}NO$	184.0763	$C_7H_{12}N_3O_3$	186.0879
$C_{11}H_{23}N_2$	183.1863	$C_{12}H_{12}N_2$	184.1001	$C_7H_{14}N_4O_2$	186.1118
$C_{11}H_7N_2O$	183.0559	$C_{13}H_{28}$	184.2192	$C_8H_{12}NO_4$	186.0766
$C_{11}H_9N_3$	183.0798	$C_{13}H_{12}O$	184.0888	$C_8H_{14}N_2O_3$	186.1005
$C_{12}H_{23}O$	183.1750	$C_{13}H_{14}N$	184.1127	$C_8H_{16}N_3O_2$	186.1244
$C_{12}H_7O_2$	183.0446	$C_{13}N_2$	184.0062	$C_8N_3O_3$	185.9940
$C_{12}H_{25}N$	183.1988	$C_{14}H_{16}$	184.1253	$C_8H_{18}N_4O$	186.1482
$C_{12}H_9NO$	183.0684	$C_{14}O$	183.9949	$C_8H_2N_4O_2$	186.0178
$C_{12}H_{11}N_2$	183.0923	$C_{14}H_2N$	184.0187	$C_9H_{14}O_4$	186.0892
$C_{13}H_{27}$	183.2114	$C_{15}H_4$	184.0313	$C_9H_{16}NO_3$	186.1131
$C_{13}H_{11}O$	183.0810	**185**		C_9NO_4	185.9827
$C_{13}H_{13}N$	183.1049	$C_7H_9N_2O_4$	185.0563	$C_9H_{18}N_2O_2$	186.1369

Appendix A (continued)

FM		FM		FM	
$C_9H_2N_2O_3$	186.0065	$C_{12}H_{13}NO$	187.0998	$C_{14}H_6N$	188.0501
$C_9H_{20}N_3O$	186.1608	$C_{12}H_{15}N_2$	187.1236	$C_{15}H_8$	188.0626
$C_9H_4N_3O_2$	186.0304	$C_{12}HN_3$	187.0171	**189**	
$C_9H_{22}N_4$	186.1846	$C_{13}H_{15}O$	187.1123	$C_7H_{13}N_2O_4$	189.0876
$C_9H_6N_4O$	186.0542	$C_{13}H_{17}N$	187.1362	$C_7H_{15}N_3O_3$	189.1114
$C_{10}H_{18}O_3$	186.1256	$C_{13}HNO$	187.0058	$C_7H_{17}N_4O_2$	189.1353
$C_{10}H_2O_4$	185.9953	$C_{13}H_3N_2$	187.0297	$C_8H_{15}NO_4$	189.1001
$C_{10}H_{10}N_4$	186.0907	$C_{14}H_{19}$	187.1488	$C_8H_{17}N_2O_3$	189.1240
$C_{11}H_{22}O_2$	186.1620	$C_{14}H_3O$	187.0184	$C_8HN_2O_4$	188.9936
$C_{11}H_6O_3$	186.0317	$C_{14}H_5N$	187.0422	$C_8H_{19}N_3O_2$	189.1478
$C_{11}H_{24}NO$	186.1859	$C_{15}H_7$	187.0548	$C_8H_3N_3O_3$	189.0175
$C_{11}H_8NO_2$	186.0555	**188**		$C_8H_{21}N_4O$	189.1717
$C_{11}H_{26}N_2$	186.2098	$C_7H_{12}N_2O_4$	188.0797	$C_8H_5N_4O_2$	189.0413
$C_{11}H_{10}N_2O$	186.0794	$C_7H_{14}N_3O_3$	188.1036	$C_9H_{17}O_4$	189.1127
$C_{11}H_{12}N_3$	186.1032	$C_7H_{16}N_4O_2$	188.1275	$C_9H_{19}NO_3$	189.1365
$C_{12}H_{26}O$	186.1985	$C_8H_{14}NO_4$	188.0923	$C_9H_3NO_4$	189.0062
$C_{12}H_{10}O_2$	186.0681	$C_8H_{16}N_2O_3$	188.1162	$C_9H_{21}N_2O_2$	189.1604
$C_{12}H_{12}NO$	186.0919	$C_8N_2O_4$	187.9858	$C_9H_5N_2O_3$	189.0300
$C_{12}H_{14}N_2$	186.1158	$C_8H_{18}N_3O_2$	188.1400	$C_9H_{23}N_3O$	189.1842
$C_{12}N_3$	186.0093	$C_8H_2N_3O_3$	188.0096	$C_9H_7N_3O_2$	189.0539
$C_{13}H_{14}O$	186.1045	$C_8H_{20}N_4O$	188.1639	$C_9H_9N_4O$	189.0777
$C_{13}H_{16}N$	186.1284	$C_8H_4N_4O_2$	188.0335	$C_{10}H_{21}O_3$	189.1491
$C_{13}NO$	185.9980	$C_9H_{16}O_4$	188.1049	$C_{10}H_5O_4$	189.0187
$C_{13}H_2N_2$	186.0218	$C_9H_{18}NO_3$	188.1287	$C_{10}H_{23}NO_2$	189.1730
$C_{14}H_{18}$	186.1409	$C_9H_2NO_4$	187.9983	$C_{10}H_7NO_3$	189.0426
$C_{14}H_2O$	186.0106	$C_9H_{20}N_2O_2$	188.1526	$C_{10}H_9N_2O_2$	189.0664
$C_{14}H_4N$	186.0344	$C_9H_4N_2O_3$	188.0222	$C_{10}H_{11}N_3O$	189.0903
$C_{15}H_6$	186.0470	$C_9H_{22}N_3O$	188.1764	$C_{10}H_{13}N_4$	189.1142
187		$C_9H_6N_3O_2$	188.0460	$C_{11}H_9O_3$	189.0552
$C_7H_{11}N_2O_4$	187.0719	$C_9H_{24}N_4$	188.2003	$C_{11}H_{11}NO_2$	189.0790
$C_7H_{13}N_3O_3$	187.0958	$C_9H_8N_4O$	188.0699	$C_{11}H_{13}N_2O$	189.1029
$C_7H_{15}N_4O_2$	187.1196	$C_{10}H_{20}O_3$	188.1413	$C_{11}H_{15}N_3$	189.1267
$C_8H_{13}NO_4$	187.0845	$C_{10}H_4O_4$	188.0109	$C_{11}HN_4$	189.0202
$C_8H_{15}N_2O_3$	187.1083	$C_{10}H_{22}NO_2$	188.1651	$C_{12}H_{13}O_2$	189.0916
$C_8H_{17}N_3O_2$	187.1322	$C_{10}H_6NO_3$	188.0348	$C_{12}H_{15}NO$	189.1154
$C_8HN_3O_3$	187.0018	$C_{10}H_{24}N_2O$	188.1890	$C_{12}H_{17}N_2$	189.1393
$C_8H_{19}N_4O$	817.1560	$C_{10}H_8N_2O_2$	188.0586	$C_{12}HN_2O$	189.0089
$C_8H_3N_4O_2$	187.0257	$C_{10}H_{10}N_3O$	188.0825	$C_{12}H_3N_3$	189.0328
$C_9H_{15}O_4$	187.0970	$C_{10}H_{12}N_4$	188.1063	$C_{13}H_{17}O$	189.1280
$C_9H_{17}NO_3$	187.1209	$C_{11}H_{24}O_2$	188.1777	$C_{13}HO_2$	188.9976
C_9HNO_4	186.9905	$C_{11}H_8O_3$	188.0473	$C_{13}H_{19}N$	189.1519
$C_9H_{19}N_2O_2$	187.1447	$C_{11}H_{10}NO_2$	188.0712	$C_{13}H_3NO$	189.0215
$C_9H_3N_2O_3$	187.0144	$C_{11}H_{12}N_2O$	188.0950	$C_{13}H_5N_2$	189.0453
$C_9H_{21}N_3O$	187.1686	$C_{11}H_{14}N_3$	188.1189	$C_{14}H_{21}$	189.1644
$C_9H_5N_3O_2$	187.0382	$C_{11}N_4$	188.0124	$C_{14}H_5O$	189.0340
$C_9H_{23}N_4$	187.1925	$C_{12}H_{12}O_2$	188.0837	$C_{14}H_7N$	189.0579
$C_9H_7N_4O$	187.0621	$C_{12}H_{14}NO$	188.1076	$C_{15}H_9$	189.0705
$C_{10}H_{19}O_3$	187.1334	$C_{12}H_{16}N_2$	188.1315	**190**	
$C_{10}H_3O_4$	187.0031	$C_{12}N_2O$	188.0011	$C_7H_{14}N_2O_4$	190.0954
$C_{10}H_{21}NO_2$	187.1573	$C_{12}H_2N_3$	188.0249	$C_7H_{16}N_3O_3$	190.1193
$C_{10}H_5NO_3$	187.0269	$C_{13}H_{16}O$	188.1202	$C_7H_{18}N_4O_2$	190.1431
$C_{10}H_{23}N_2O$	187.1811	$C_{13}O_2$	187.9898	$C_8H_{16}NO_4$	190.1080
$C_{10}H_7N_2O_2$	187.0508	$C_{13}H_{18}N$	188.1440	$C_8H_{18}N_2O_3$	190.1318
$C_{10}H_{25}N_3$	187.2050	$C_{13}H_2NO$	188.0136	$C_8H_2N_2O_4$	190.0014
$C_{11}H_{11}N_2O$	187.0872	$C_{13}H_4N_2$	188.0375	$C_8H_{20}N_3O_2$	190.1557
$C_{11}H_{13}N_3$	187.1111	$C_{14}H_{20}$	188.1566	$C_8H_4N_3O_3$	190.0253
$C_{12}H_{11}O_2$	187.0759	$C_{14}H_4O$	188.0262	$C_8H_{22}N_4O$	190.1795

Appendix A (continued)

	FM		FM		FM
$C_8H_6N_4O_2$	190.0491	$C_{11}H_{13}NO_2$	191.0947	$C_{13}H_6NO$	192.0449
$C_9H_{18}O_4$	190.1205	$C_{11}H_{15}N_2O$	191.1185	$C_{13}H_8N_2$	192.0688
$C_9H_{20}NO_3$	190.1444	$C_{11}H_{17}N_3$	191.1424	$C_{14}H_{24}$	192.1879
$C_9H_4NO_4$	190.0140	$C_{11}HN_3O$	191.0120	$C_{14}H_8O$	192.0575
$C_9H_{22}N_2O_2$	190.1682	$C_{11}H_3N_4$	191.0359	$C_{14}H_{10}N$	192.0814
$C_9H_6N_2O_3$	190.0379	$C_{12}H_{15}O_2$	191.1072	$C_{15}H_{12}$	192.0939
$C_9H_8N_3O_2$	190.0617	$C_{12}H_{17}NO$	191.1311	C_{16}	192.0000
$C_9H_{10}N_4O$	190.0856	$C_{12}HNO_2$	191.0007	**193**	
$C_{10}H_{22}O_3$	190.1569	$C_{12}H_{19}N_2$	191.1549	$C_7H_{17}N_2O_4$	193.1189
$C_{10}H_6O_4$	190.0266	$C_{12}H_3N_2O$	191.0246	$C_7H_{19}N_3O_3$	193.1427
$C_{10}H_8NO_3$	190.0504	$C_{12}H_5N_3$	191.0484	$C_8H_{19}NO_4$	193.1315
$C_{10}H_{10}N_2O_2$	190.0743	$C_{13}H_{19}O$	191.1436	$C_8H_5N_2O_4$	193.0249
$C_{10}H_{12}N_3O$	190.0981	$C_{13}H_3O_2$	191.0133	$C_8H_7N_3O_3$	193.0488
$C_{10}H_{14}N_4$	190.1220	$C_{13}H_{21}N$	191.1675	$C_8H_9N_4O_2$	193.0726
$C_{11}H_{10}O_3$	190.0630	$C_{13}H_5NO$	191.0371	$C_9H_7NO_4$	193.0375
$C_{11}H_{12}NO_2$	190.0868	$C_{13}H_7N_2$	191.0610	$C_9H_9N_2O_3$	193.0614
$C_{11}H_{14}N_2O$	190.1107	$C_{14}H_{23}$	191.1801	$C_9H_{11}N_3O_2$	193.0852
$C_{11}H_{16}N_3$	190.1346	$C_{14}H_7O$	191.0497	$C_9H_{13}N_4O$	193.1091
$C_{11}N_3O$	190.0042	$C_{14}H_9N$	191.0736	$C_{10}H_9O_4$	193.0501
$C_{11}H_2N_4$	190.0280	$C_{15}H_{11}$	191.0861	$C_{10}H_{11}NO_3$	193.0739
$C_{12}H_{14}O_2$	190.0994	**192**		$C_{10}H_{13}N_2O_2$	193.0978
$C_{12}H_{16}NO$	190.1233	$C_7H_{16}N_2O_4$	192.1111	$C_{10}H_{15}N_3O$	193.1216
$C_{12}NO_2$	189.9929	$C_7H_{18}N_3O_3$	192.1349	$C_{10}H_{17}N_4$	193.1455
$C_{12}H_{18}N_2$	190.1471	$C_7H_{20}N_4O_2$	192.1588	$C_{10}HN_4O$	193.0151
$C_{12}H_2N_2O$	190.0167	$C_8H_{18}NO_4$	192.1236	$C_{11}H_{13}O_3$	193.0865
$C_{12}H_4N_3$	190.0406	$C_8H_{20}N_2O_3$	192.1475	$C_{11}H_{15}NO_2$	193.1103
$C_{13}H_{18}O$	190.1358	$C_8H_4N_2O_4$	192.0171	$C_{11}H_{17}N_2O$	193.1342
$C_{13}H_2O_2$	190.0054	$C_8H_6N_3O_3$	192.0410	$C_{11}HN_2O_2$	193.0038
$C_{13}H_{20}N$	190.1597	$C_8H_8N_4O_2$	192.0648	$C_{11}H_{19}N_3$	193.1580
$C_{13}H_4NO$	190.0293	$C_9H_{20}O_4$	192.1362	$C_{11}H_3N_3O$	193.0277
$C_{13}H_6N_2$	190.0532	$C_9H_6NO_4$	192.0297	$C_{11}H_5N_4$	193.0515
$C_{14}H_{22}$	190.1722	$C_9H_8N_2O_3$	192.0535	$C_{12}H_{17}O_2$	193.1229
$C_{14}H_6O$	190.0419	$C_9H_{10}N_3O_2$	192.0774	$C_{12}HO_3$	192.9925
$C_{14}H_8N$	190.0657	$C_9H_{12}N_4O$	192.1012	$C_{12}H_{19}NO$	193.1467
$C_{15}H_{10}$	190.0783	$C_{10}H_8O_4$	192.0422	$C_{12}H_3NO_2$	193.0164
191		$C_{10}H_{10}NO_3$	192.0661	$C_{12}H_{21}N_2$	193.1706
$C_7H_{15}N_2O_4$	191.1032	$C_{10}H_{12}N_2O_2$	192.0899	$C_{12}H_5N_2O$	193.0402
$C_7H_{17}N_3O_3$	191.1271	$C_{10}H_{14}N_3O$	192.1138	$C_{12}H_7N_3$	193.0641
$C_7H_{19}N_4O_2$	191.1509	$C_{10}H_{16}N_4$	192.1377	$C_{13}H_{21}O$	193.1593
$C_8H_{17}NO_4$	191.1158	$C_{10}N_4O$	192.0073	$C_{13}H_5O_2$	193.0289
$C_8H_{19}N_2O_3$	191.1396	$C_{11}H_{12}O_3$	192.0786	$C_{13}H_{23}N$	193.1832
$C_8H_3N_2O_4$	191.0093	$C_{11}H_{14}NO_2$	192.1025	$C_{13}H_7NO$	193.0528
$C_8H_{21}N_3O_2$	191.1635	$C_{11}H_{16}N_2O$	192.1264	$C_{13}H_9N_2$	193.0767
$C_8H_5N_3O_3$	191.0331	$C_{11}N_2O_2$	191.9960	$C_{14}H_{25}$	193.1957
$C_8H_7N_4O_2$	191.0570	$C_{11}H_{18}N_3$	192.1502	$C_{14}H_9O$	193.0653
$C_9H_{19}O_4$	191.1284	$C_{11}H_2N_3O$	192.0198	$C_{14}H_{11}N$	193.0892
$C_9H_{21}NO_3$	191.1522	$C_{11}H_4N_4$	192.0437	$C_{15}H_{13}$	193.1018
$C_9H_5NO_4$	191.0218	$C_{12}H_{16}O_2$	192.1151	$C_{16}H$	193.0078
$C_9H_7N_2O_3$	191.0457	$C_{12}O_3$	191.9847	**194**	
$C_9H_9N_3O_2$	191.0695	$C_{12}H_{18}NO$	192.1389	$C_7H_{18}N_2O_4$	194.1267
$C_9H_{11}N_4O$	191.0934	$C_{12}H_2NO_2$	192.0085	$C_8H_6N_2O_4$	194.0328
$C_{10}H_7O_4$	191.0344	$C_{12}H_{20}N_2$	192.1628	$C_8H_8N_3O_3$	194.0566
$C_{10}H_9NO_3$	191.0583	$C_{12}H_4N_2O$	192.0324	$C_8H_{10}N_4O_2$	194.0805
$C_{10}H_{11}N_2O_2$	191.0821	$C_{12}H_6N_3$	192.0563	$C_9H_8NO_4$	194.0453
$C_{10}H_{13}N_3O$	191.1060	$C_{13}H_{20}O$	192.1515	$C_9H_{10}N_2O_3$	194.0692
$C_{10}H_{15}N_4$	191.1298	$C_{13}H_4O_2$	192.0211	$C_9H_{12}N_3O_2$	194.0930
$C_{11}H_{11}O_3$	191.0708	$C_{13}H_{22}N$	192.1753	$C_9H_{14}N_4O$	194.1169

Appendix A (continued)

FM		FM		FM	
$C_{10}H_{10}O_4$	194.0579	$C_{12}H_3O_3$	195.0082	$C_{14}H_{14}N$	196.1127
$C_{10}H_{12}NO_3$	194.0817	$C_{12}H_{21}NO$	195.1624	$C_{14}N_2$	196.0062
$C_{10}H_{14}N_2O_2$	194.1056	$C_{12}H_5NO_2$	195.0320	$C_{15}H_{16}$	196.1253
$C_{10}H_{16}N_3O$	194.1295	$C_{12}H_{23}N_2$	195.1863	$C_{15}O$	195.9949
$C_{10}N_3O_2$	193.9991	$C_{12}H_7N_2O$	195.0559	$C_{15}H_2N$	196.0187
$C_{10}H_{18}N_4$	194.1533	$C_{12}H_9N_3$	195.0798	$C_{16}H_4$	196.0313
$C_{10}H_2N_4O$	194.0229	$C_{13}H_{23}O$	195.1750	**197**	
$C_{11}H_{14}O_3$	194.0943	$C_{13}H_7O_2$	195.0446	$C_8H_9N_2O_4$	197.0563
$C_{11}H_{16}NO_2$	194.1182	$C_{13}H_{25}N$	195.1988	$C_8H_{11}N_3O_3$	197.0801
$C_{11}NO_3$	193.9878	$C_{13}H_9NO$	195.0684	$C_8H_{13}N_4O_2$	197.1040
$C_{11}H_{18}N_2O$	194.1420	$C_{13}H_{11}N_2$	195.0923	$C_9H_{11}NO_4$	197.0688
$C_{11}H_2N_2O_2$	194.0116	$C_{14}H_{27}$	195.2114	$C_9H_{13}N_2O_3$	197.0927
$C_{11}H_{20}N_3$	194.1659	$C_{14}H_{11}O$	195.0810	$C_9H_{15}N_3O_2$	197.1165
$C_{11}H_4N_3O$	194.0355	$C_{14}H_{13}N$	195.1049	$C_9H_{17}N_4O$	197.1404
$C_{11}H_6N_4$	194.0594	$C_{15}H_{15}$	195.1174	$C_9HN_4O_2$	197.0100
$C_{12}H_{18}O_2$	194.1307	$C_{15}HN$	195.0109	$C_{10}H_{13}O_4$	197.0814
$C_{12}H_2O_3$	194.0003	$C_{16}H_3$	195.0235	$C_{10}H_{15}NO_3$	197.1052
$C_{12}H_{20}NO$	194.1546	**196**		$C_{10}H_{17}N_2O_2$	197.1291
$C_{12}H_4NO_2$	194.0242	$C_8H_8N_2O_4$	196.0484	$C_{10}HN_2O_3$	196.9987
$C_{12}H_{22}N_2$	194.1784	$C_8H_{10}N_3O_3$	196.0723	$C_{10}H_{19}N_3O$	197.1529
$C_{12}H_6N_2O$	194.0480	$C_8H_{12}N_4O_2$	196.0961	$C_{10}H_3N_3O_2$	197.0226
$C_{12}H_8N_3$	194.0719	$C_9H_{10}NO_4$	196.0610	$C_{10}H_{21}N_4$	197.1768
$C_{13}H_{22}O$	194.1671	$C_9H_{12}N_2O_3$	196.0848	$C_{10}H_5N_4O$	197.0464
$C_{13}H_6O_2$	194.0368	$C_9H_{14}N_3O_2$	196.1087	$C_{11}H_{17}O_3$	197.1178
$C_{13}H_{24}N$	194.1910	$C_9H_{16}N_4O$	196.1325	$C_{11}HO_4$	196.9874
$C_{13}H_8NO$	194.0606	$C_9N_4O_2$	196.0022	$C_{11}H_{19}NO_2$	197.1416
$C_{13}H_{10}N_2$	194.0845	$C_{10}H_{12}O_4$	196.0735	$C_{11}H_3NO_3$	197.0113
$C_{14}H_{26}$	194.2036	$C_{10}H_{14}NO_3$	196.0974	$C_{11}H_{21}N_2O$	197.1655
$C_{14}H_{10}O$	194.0732	$C_{10}H_{16}N_2O_2$	196.1213	$C_{11}H_5N_2O_2$	197.0351
$C_{14}H_{12}N$	194.0970	$C_{10}N_2O_3$	195.9909	$C_{11}H_{23}N_3$	197.1894
$C_{15}H_{14}$	194.1096	$C_{10}H_{18}N_3O$	196.1451	$C_{11}H_7N_3O$	197.0590
$C_{15}N$	194.0031	$C_{10}H_2N_3O_2$	196.0147	$C_{11}H_9N_4$	197.0829
$C_{16}H_2$	194.0157	$C_{10}H_{20}N_4$	196.1690	$C_{12}H_{21}O_2$	197.1542
195		$C_{10}H_4N_4O$	196.0386	$C_{12}H_5O_3$	197.0238
$C_8H_7N_2O_4$	195.0406	$C_{11}H_{16}O_3$	196.1100	$C_{12}H_{23}NO$	197.1781
$C_8H_9N_3O_3$	195.0644	$C_{11}O_4$	195.9796	$C_{12}H_7NO_2$	197.0477
$C_8H_{11}N_4O_2$	195.0883	$C_{11}H_{18}NO_2$	196.1338	$C_{12}H_{25}N_2$	197.2019
$C_9H_9NO_4$	195.0532	$C_{11}H_2NO_3$	196.0034	$C_{12}H_9N_2O$	197.0715
$C_9H_{11}N_2O_3$	195.0770	$C_{11}H_{20}N_2O$	196.1577	$C_{12}H_{11}N_3$	197.0954
$C_9H_{13}N_3O_2$	195.1009	$C_{11}H_4N_2O_2$	196.0273	$C_{13}H_{25}O$	197.1906
$C_9H_{15}N_4O$	195.1247	$C_{11}H_{22}N_3$	196.1815	$C_{13}H_9O_2$	197.0603
$C_{10}H_{11}O_4$	195.0657	$C_{11}H_6N_3O$	196.0511	$C_{13}H_{27}N$	197.2145
$C_{10}H_{13}NO_3$	195.0896	$C_{11}H_8N_4$	196.0750	$C_{13}H_{11}NO$	197.0841
$C_{10}H_{15}N_2O_2$	195.1134	$C_{12}H_{20}O_2$	196.1464	$C_{13}H_{13}N_2$	197.1080
$C_{10}H_{17}N_3O$	195.1373	$C_{12}H_4O_3$	196.0160	$C_{14}H_{29}$	197.2270
$C_{10}HN_3O_2$	195.0069	$C_{12}H_{22}NO$	196.1702	$C_{14}H_{13}O$	197.0967
$C_{10}H_{19}N_4$	195.1611	$C_{12}H_6NO_2$	196.0399	$C_{14}H_{15}N$	197.1205
$C_{10}H_3N_4O$	195.0308	$C_{12}H_{24}N_2$	196.1941	$C_{14}HN_2$	197.0104
$C_{11}H_{15}O_3$	195.1021	$C_{12}H_8N_2O$	196.0637	$C_{15}H_{17}$	197.1331
$C_{11}H_{17}NO_2$	195.1260	$C_{12}H_{10}N_3$	196.0876	$C_{15}HO$	197.0027
$C_{11}HNO_3$	194.9956	$C_{13}H_{24}O$	196.1828	$C_{15}H_3N$	197.0266
$C_{11}H_{19}N_2O$	195.1498	$C_{13}H_8O_2$	196.0524	$C_{16}H_5$	197.0391
$C_{11}H_3N_2O_2$	195.0195	$C_{13}H_{26}N$	196.2067	**198**	
$C_{11}H_{21}N_3$	195.1737	$C_{13}H_{10}NO$	196.0763	$C_8H_{10}N_2O_4$	198.0641
$C_{11}H_5N_3O$	195.0433	$C_{13}H_{12}N_2$	196.1001	$C_8H_{12}N_3O_3$	198.0879
$C_{11}H_7N_4$	195.0672	$C_{14}H_{28}$	196.2192	$C_8H_{14}N_4O_2$	198.1118
$C_{12}H_{19}O_2$	195.1385	$C_{14}H_{12}O$	196.0888	$C_9H_{12}NO_4$	198.0766

Appendix A (continued)

FM		FM		FM	
$C_9H_{14}N_2O_3$	198.1005	$C_{10}HNO_4$	198.9905	$C_{11}H_{20}O_3$	200.1413
$C_9H_{16}N_3O_2$	198.1244	$C_{10}H_{19}N_2O_2$	199.1447	$C_{11}H_4O_4$	200.0109
$C_9N_3O_3$	197.9940	$C_{10}H_3N_2O_3$	199.0144	$C_{11}H_{22}NO_2$	200.1651
$C_9H_{18}N_4O$	198.1482	$C_{10}H_{21}N_3O$	199.1686	$C_{11}H_6NO_3$	200.0348
$C_9H_2N_4O_2$	198.0178	$C_{10}H_5N_3O_2$	199.0382	$C_{11}H_{24}N_2O$	200.1890
$C_{10}H_{14}O_4$	198.0892	$C_{10}H_{23}N_4$	199.1925	$C_{11}H_8N_2O_2$	200.0586
$C_{10}H_{16}NO_3$	198.1131	$C_{10}H_7N_4O$	199.0621	$C_{11}H_{26}N_3$	200.2129
$C_{10}NO_4$	197.9827	$C_{11}H_{19}O_3$	199.1334	$C_{11}H_{10}N_3O$	200.0825
$C_{10}H_{18}N_2O_2$	198.1369	$C_{11}H_3O_4$	199.0031	$C_{11}H_{12}N_4$	200.1063
$C_{10}H_2N_2O_3$	198.0065	$C_{11}H_{21}NO_2$	199.1573	$C_{12}H_{24}O_2$	200.1777
$C_{10}H_{20}N_3O$	198.1608	$C_{11}H_5NO_3$	199.0269	$C_{12}H_8O_3$	200.0473
$C_{10}H_4N_3O_2$	198.0304	$C_{11}H_{23}N_2O$	199.1811	$C_{12}H_{26}NO$	200.2015
$C_{10}H_{22}N_4$	198.1846	$C_{11}H_7N_2O_2$	199.0508	$C_{12}H_{10}NO_2$	200.0712
$C_{10}H_6N_4O$	198.0542	$C_{11}H_{25}N_3$	199.2050	$C_{12}H_{28}N_2$	200.2254
$C_{11}H_{18}O_3$	198.1256	$C_{11}H_9N_3O$	199.0746	$C_{12}H_{12}N_2O$	200.0950
$C_{11}H_2O_4$	197.9953	$C_{11}H_{11}N_4$	199.0985	$C_{12}H_{14}N_3$	200.1189
$C_{11}H_{20}NO_2$	198.1495	$C_{12}H_{23}O_2$	199.1699	$C_{12}N_4$	200.0124
$C_{11}H_4NO_3$	198.0191	$C_{12}H_7O_3$	199.0395	$C_{13}H_{28}O$	200.2141
$C_{11}H_{22}N_2O$	198.1733	$C_{12}H_{25}NO$	199.1937	$C_{13}H_{12}O_2$	200.0837
$C_{11}H_6N_2O_2$	198.0429	$C_{12}H_9NO_2$	199.0634	$C_{13}H_{14}NO$	200.1076
$C_{11}H_{24}N_3$	198.1972	$C_{12}H_{27}N_2$	199.2176	$C_{13}H_{16}N_2$	200.1315
$C_{11}H_8N_3O$	198.0668	$C_{12}H_{11}N_2O$	199.0872	$C_{13}N_2O$	200.0011
$C_{11}H_{10}N_4$	198.0907	$C_{12}H_{13}N_3$	199.1111	$C_{13}H_2N_3$	200.0249
$C_{12}H_{22}O_2$	198.1620	$C_{13}H_{27}O$	199.2063	$C_{14}H_{16}O$	200.1202
$C_{12}H_6O_3$	198.0317	$C_{13}H_{11}O_2$	199.0759	$C_{14}O_2$	199.9898
$C_{12}H_{24}NO$	198.1859	$C_{13}H_{29}N$	199.2301	$C_{14}H_{18}N$	200.1440
$C_{12}H_8NO_2$	198.0555	$C_{13}H_{13}NO$	199.0998	$C_{14}H_2NO$	200.0136
$C_{12}H_{26}N_2$	198.2098	$C_{13}H_{15}N_2$	199.1236	$C_{14}H_4N_2$	200.0375
$C_{12}H_{10}N_2O$	198.0794	$C_{13}HN_3$	199.0171	$C_{15}H_{20}$	200.1566
$C_{12}H_{12}N_3$	198.1032	$C_{14}H_{15}O$	199.1123	$C_{15}H_4O$	200.0262
$C_{13}H_{26}O$	198.1985	$C_{14}H_{17}N$	199.1362	$C_{15}H_6N$	200.0501
$C_{13}H_{10}O_2$	198.0681	$C_{14}HNO$	199.0058	$C_{16}H_8$	200.0626
$C_{13}H_{28}N$	198.2223	$C_{14}H_3N_2$	199.0297	**201**	
$C_{13}H_{12}NO$	198.0919	$C_{15}H_{19}$	199.1488	$C_8H_{13}N_2O_4$	201.0876
$C_{13}H_{14}N_2$	198.1158	$C_{15}H_3O$	199.0184	$C_8H_{15}N_3O_3$	201.1114
$C_{13}N_3$	198.0093	$C_{15}H_5N$	199.0422	$C_8H_{17}N_4O_2$	201.1353
$C_{14}H_{30}$	198.2349	$C_{16}H_7$	199.0548	$C_9H_{15}NO_4$	201.1001
$C_{14}H_{14}O$	198.1045	**200**		$C_9H_{17}N_2O_3$	201.1240
$C_{14}H_{16}N$	198.1284	$C_8H_{12}N_2O_4$	200.0797	$C_9HN_2O_4$	200.9936
$C_{14}NO$	197.9980	$C_8H_{14}N_3O_3$	200.1036	$C_9H_{19}N_3O_2$	201.1478
$C_{14}H_2N_2$	198.0218	$C_8H_{16}N_4O_2$	200.1275	$C_9H_3N_3O_3$	201.0175
$C_{15}H_{18}$	198.1409	$C_9H_{14}NO_4$	200.0923	$C_9H_{21}N_4O$	201.1717
$C_{15}H_2O$	198.0106	$C_9H_{16}N_2O_3$	200.1162	$C_9H_5N_4O_2$	201.0413
$C_{15}H_4N$	198.0344	$C_9N_2O_4$	199.9858	$C_{10}H_{17}O_4$	201.1127
$C_{16}H_6$	198.0470	$C_9H_{18}N_3O_2$	200.1400	$C_{10}H_{19}NO_3$	201.1365
199		$C_9H_2N_3O_3$	200.0096	$C_{10}H_3NO_4$	201.0062
$C_8H_{11}N_2O_4$	199.0719	$C_9H_{20}N_4O$	200.1639	$C_{10}H_{21}N_2O_2$	201.1604
$C_8H_{13}N_3O_3$	199.0958	$C_9H_4N_4O_2$	200.0335	$C_{10}H_5N_2O_3$	201.0300
$C_8H_{15}N_4O_2$	199.1196	$C_{10}H_{16}O_4$	200.1049	$C_{10}H_{23}N_3O$	201.1842
$C_9H_{13}NO_4$	199.0845	$C_{10}H_{18}NO_3$	200.1287	$C_{10}H_7N_3O_2$	201.0539
$C_9H_{15}N_2O_3$	199.1083	$C_{10}H_2NO_4$	199.9983	$C_{10}H_{25}N_4$	201.2081
$C_9H_{17}N_3O_2$	199.1322	$C_{10}H_{20}N_2O_2$	200.1526	$C_{10}H_9N_4O$	201.0777
$C_9HN_3O_3$	199.0018	$C_{10}H_4N_2O_3$	200.0222	$C_{11}H_{21}O_3$	201.1491
$C_9H_{19}N_4O$	199.1560	$C_{10}H_{22}N_3O$	200.1764	$C_{11}H_5O_4$	201.0187
$C_9H_3N_4O_2$	199.0257	$C_{10}H_6N_3O_2$	200.0460	$C_{11}H_{23}NO_2$	201.1730
$C_{10}H_{15}O_4$	199.0970	$C_{10}H_{24}N_4$	200.2003	$C_{11}H_7NO_3$	201.0426
$C_{10}H_{17}NO_3$	199.1209	$C_{10}H_8N_4O$	200.0699	$C_{11}H_{25}N_2O$	201.1968

Appendix A (continued)

FM		FM		FM	
$C_{11}H_9N_2O_2$	201.0664	$C_{12}H_{16}N_3$	202.1346	$C_{14}H_3O_2$	203.0133
$C_{11}H_{27}N_3$	201.2207	$C_{12}N_3O$	202.0042	$C_{14}H_{21}N$	203.1675
$C_{11}H_{11}N_3O$	201.0903	$C_{12}H_2N_4$	202.0280	$C_{14}H_5NO$	203.0371
$C_{11}H_{13}N_4$	201.1142	$C_{13}H_{14}O_2$	202.0994	$C_{14}H_7N_2$	203.0610
$C_{12}H_{25}O_2$	201.1855	$C_{13}H_{16}NO$	202.1233	$C_{15}H_{23}$	203.1801
$C_{12}H_9O_3$	201.0552	$C_{13}NO_2$	201.9929	$C_{15}H_7O$	203.0497
$C_{12}H_{27}NO$	201.2094	$C_{13}H_{18}N_2$	202.1471	$C_{15}H_9N$	203.0736
$C_{12}H_{11}NO_2$	201.0790	$C_{13}H_2N_2O$	202.0167	$C_{16}H_{11}$	203.0861
$C_{12}H_{13}N_2O$	201.1029	$C_{13}H_4N_3$	202.0406	**204**	
$C_{12}H_{15}N_3$	201.1267	$C_{14}H_{18}O$	202.1358	$C_8H_{16}N_2O_4$	204.1111
$C_{12}HN_4$	201.0202	$C_{14}H_2O_2$	202.0054	$C_8H_{18}N_3O_3$	204.1349
$C_{13}H_{13}O_2$	201.0916	$C_{14}H_{20}N$	202.1597	$C_8H_{20}N_4O_2$	204.1588
$C_{13}H_{15}NO$	201.1154	$C_{14}H_4NO$	202.0293	$C_9H_{18}NO_4$	204.1236
$C_{13}H_{17}N_2$	201.1393	$C_{14}H_6N_2$	202.0532	$C_9H_{20}N_2O_3$	204.1475
$C_{13}HN_2O$	201.0089	$C_{15}H_{22}$	202.1722	$C_9H_4N_2O_4$	204.0171
$C_{13}H_3N_3$	201.0328	$C_{15}H_6O$	202.0419	$C_9H_{22}N_3O_2$	204.1713
$C_{14}H_{17}O$	201.1280	$C_{15}H_8N$	202.0657	$C_9H_6N_3O_3$	204.0410
$C_{14}HO_2$	200.9976	$C_{16}H_{10}$	202.0783	$C_9H_{24}N_4O$	204.1952
$C_{14}H_{19}N$	201.1519	**203**		$C_9H_8N_4O_2$	204.0648
$C_{14}H_3NO$	201.0215	$C_8H_{15}N_2O_4$	203.1032	$C_{10}H_{20}O_4$	204.1362
$C_{14}H_5N_2$	201.0453	$C_8H_{17}N_3O_3$	203.1271	$C_{10}H_{22}NO_3$	204.1600
$C_{15}H_{21}$	201.1644	$C_8H_{19}N_4O_2$	203.1509	$C_{10}H_6NO_4$	204.0297
$C_{15}H_5O$	201.0340	$C_9H_{17}NO_4$	203.1158	$C_{10}H_{24}N_2O_2$	204.1839
$C_{15}H_7N$	201.0579	$C_9H_{19}N_2O_3$	203.1396	$C_{10}H_8N_2O_3$	204.0535
$C_{16}H_9$	201.0705	$C_9H_3N_2O_4$	203.0093	$C_{10}H_{10}N_3O_2$	204.0774
202		$C_9H_{21}N_3O_2$	203.1635	$C_{10}H_{12}N_4O$	204.1012
$C_8H_{14}N_2O_4$	202.0954	$C_9H_5N_3O_3$	203.0331	$C_{11}H_{24}O_3$	204.1726
$C_8H_{16}N_3O_3$	202.1193	$C_9H_{23}N_4O$	203.1873	$C_{11}H_8O_4$	204.0422
$C_8H_{18}N_4O_2$	202.1431	$C_9H_7N_4O_2$	203.0570	$C_{11}H_{10}NO_3$	204.0661
$C_9H_{16}NO_4$	202.1080	$C_{10}H_{19}O_4$	203.1284	$C_{11}H_{12}N_2O_2$	204.0899
$C_9H_{18}N_2O_3$	202.1318	$C_{10}H_{21}NO_3$	203.1522	$C_{11}H_{14}N_3O$	204.1138
$C_9H_2N_2O_4$	202.0014	$C_{10}H_5NO_4$	203.0218	$C_{11}H_{16}N_4$	204.1377
$C_9H_{20}N_3O_2$	202.1557	$C_{10}H_{23}N_2O_2$	203.1761	$C_{11}N_4O$	204.0073
$C_9H_4N_3O_3$	202.0253	$C_{10}H_7N_2O_3$	203.0457	$C_{12}H_{12}O_3$	204.0786
$C_9H_{22}N_4O$	202.1795	$C_{10}H_{25}N_3O$	203.1999	$C_{12}H_{14}NO_2$	204.1025
$C_9H_6N_4O_2$	202.0491	$C_{10}H_9N_3O_2$	203.0695	$C_{12}H_{18}N_2O$	204.1264
$C_{10}H_{18}O_4$	202.1205	$C_{10}H_{11}N_4O$	203.0934	$C_{12}N_2O_2$	203.9960
$C_{10}H_{20}NO_3$	202.1444	$C_{11}H_{23}O_3$	203.1648	$C_{12}H_{18}N_3$	204.1502
$C_{10}H_4NO_4$	202.0140	$C_{11}H_7O_4$	203.0344	$C_{12}H_2N_3O$	204.0198
$C_{10}H_{22}N_2O_2$	202.1682	$C_{11}H_{25}NO_2$	203.1886	$C_{12}H_4N_4$	204.0437
$C_{10}H_6N_2O_3$	202.0379	$C_{11}H_9NO_3$	203.0583	$C_{13}H_{16}O_2$	204.1151
$C_{10}H_{24}N_3O$	202.1921	$C_{11}H_{11}N_2O_2$	203.0821	$C_{13}O_3$	203.9847
$C_{10}H_8N_3O_2$	202.0617	$C_{11}H_{13}N_3O$	203.1060	$C_{13}H_{18}NO$	204.1389
$C_{10}H_{26}N_4$	202.2160	$C_{11}H_{15}N_4$	203.1298	$C_{13}H_2NO_2$	204.0085
$C_{10}H_{10}N_4O$	202.0856	$C_{12}H_{11}O_3$	203.0708	$C_{13}H_{20}N_2$	204.1628
$C_{11}H_{22}O_3$	202.1569	$C_{12}H_{13}NO_2$	203.0947	$C_{13}H_4N_2O$	204.0324
$C_{11}H_6O_4$	202.0266	$C_{12}H_{15}N_2O$	203.1185	$C_{13}H_6N_3$	204.0563
$C_{11}H_{24}NO_2$	202.1808	$C_{12}H_{17}N_3$	203.1424	$C_{14}H_{20}O$	204.1515
$C_{11}H_8NO_3$	202.0504	$C_{12}HN_3O$	203.0120	$C_{14}H_4O_2$	204.0211
$C_{11}H_{26}N_2O$	202.2046	$C_{12}H_3N_4$	203.0359	$C_{14}H_{22}N$	204.1753
$C_{11}H_{10}N_2O_2$	202.0743	$C_{13}H_{15}O_2$	203.1072	$C_{14}H_6NO$	204.0449
$C_{11}H_{12}N_3O$	202.0981	$C_{13}H_{17}NO$	203.1311	$C_{14}H_8N_2$	204.0688
$C_{11}H_{14}N_4$	202.1220	$C_{13}HNO_2$	203.0007	$C_{15}H_{24}$	204.1879
$C_{12}H_{26}O_2$	202.1934	$C_{13}H_{19}N_2$	203.1549	$C_{15}H_8O$	204.0575
$C_{12}H_{10}O_3$	202.0630	$C_{13}H_3N_2O$	203.0246	$C_{15}H_{10}N$	204.0814
$C_{12}H_{12}NO_2$	202.0868	$C_{13}H_5N_3$	203.0484	$C_{16}H_{12}$	204.0939
$C_{12}H_{14}N_2O$	202.1107	$C_{14}H_{19}O$	203.1436	C_{17}	204.0000

Appendix A (continued)

FM		FM		FM	
205		$C_{10}H_{10}N_2O_3$	206.0692	$C_{12}H_{19}N_2O$	207.1498
$C_8H_{17}N_2O_4$	205.1189	$C_{10}H_{12}N_3O_2$	206.0930	$C_{12}H_3N_2O_2$	207.0195
$C_8H_{19}N_3O_3$	205.1427	$C_{10}H_{14}N_4O$	206.1169	$C_{12}H_{21}N_3$	207.1737
$C_8H_{21}N_4O_2$	205.1666	$C_{11}H_{10}O_4$	206.0579	$C_{12}H_5N_3O$	207.0433
$C_9H_{19}NO_4$	205.1315	$C_{11}H_{12}NO_3$	206.0817	$C_{12}H_7N_4$	207.0672
$C_9H_{21}N_2O_3$	205.1553	$C_{11}H_{14}N_2O_2$	206.1056	$C_{13}H_{19}O_2$	207.1385
$C_9H_5N_2O_4$	205.0249	$C_{11}H_{16}N_3O$	206.1295	$C_{13}H_3O_3$	207.0082
$C_9H_{23}N_3O_2$	205.1791	$C_{11}N_3O_2$	205.9991	$C_{13}H_{21}NO$	207.1624
$C_9H_7N_3O_3$	205.0488	$C_{11}H_{18}N_4$	206.1533	$C_{13}H_5NO_2$	207.0320
$C_9H_9N_4O_2$	205.0726	$C_{11}H_2N_4O$	206.0229	$C_{13}H_{23}N_2$	207.1863
$C_{10}H_{21}O_4$	205.1440	$C_{12}H_{14}O_3$	206.0943	$C_{13}H_7N_2O$	207.0559
$C_{10}H_{23}NO_3$	205.1679	$C_{12}H_{16}NO_2$	206.1182	$C_{13}H_9N_3$	207.0798
$C_{10}H_7NO_4$	205.0375	$C_{12}NO_3$	205.9878	$C_{14}H_{23}O$	207.1750
$C_{10}H_9N_2O_3$	205.0614	$C_{12}H_{18}N_2O$	206.1420	$C_{14}H_7O_2$	207.0446
$C_{10}H_{11}N_3O_2$	205.0852	$C_{12}H_2N_2O_2$	206.0116	$C_{14}H_{25}N$	207.1988
$C_{10}H_{13}N_4O$	205.1091	$C_{12}H_{20}N_3$	206.1659	$C_{14}H_9NO$	207.0684
$C_{11}H_9O_4$	205.0501	$C_{12}H_4N_3O$	206.0355	$C_{14}H_{11}N_2$	207.0923
$C_{11}H_{11}NO_3$	205.0739	$C_{12}H_6N_4$	206.0594	$C_{15}H_{27}$	207.2114
$C_{11}H_{13}N_2O_2$	205.0978	$C_{13}H_{18}O_2$	206.1307	$C_{15}H_{11}O$	207.0810
$C_{11}H_{15}N_3O$	205.1216	$C_{13}H_2O_3$	206.0003	$C_{15}H_{13}N$	207.1049
$C_{11}H_{17}N_4$	205.1455	$C_{13}H_{20}NO$	206.1546	$C_{16}H_{15}$	207.1174
$C_{11}HN_4O$	205.0151	$C_{13}H_4NO_2$	206.0242	$C_{16}HN$	207.0109
$C_{12}H_{13}O_3$	205.0865	$C_{13}H_{22}N_2$	206.1784	$C_{17}H_3$	207.0235
$C_{12}H_{15}NO_2$	205.1103	$C_{13}H_6N_2O$	206.0480	**208**	
$C_{12}H_{17}N_2O$	205.1342	$C_{13}H_8N_3$	206.0719	$C_8H_{20}N_2O_4$	208.1424
$C_{12}HN_2O_2$	205.0038	$C_{14}H_{22}O$	206.1671	$C_9H_8N_2O_4$	208.0484
$C_{12}H_{19}N_3$	205.1580	$C_{14}H_6O_2$	206.0368	$C_9H_{10}N_3O_3$	208.0723
$C_{12}H_3N_3O$	205.0277	$C_{14}H_{24}N$	206.1910	$C_9H_{12}N_4O_2$	208.0961
$C_{12}H_5N_4$	205.0515	$C_{14}H_8NO$	206.0606	$C_{10}H_{10}NO_4$	208.0610
$C_{13}H_{17}O_2$	205.1229	$C_{14}H_{10}N_2$	206.0845	$C_{10}H_{12}N_2O_3$	208.0848
$C_{13}HO_3$	204.9925	$C_{15}H_{26}$	206.2036	$C_{10}H_{14}N_3O_2$	208.1087
$C_{13}H_{19}NO$	205.1467	$C_{15}H_{10}O$	206.0732	$C_{10}H_{16}N_4O$	208.1325
$C_{13}H_3NO_2$	205.0164	$C_{15}H_{12}N$	206.0970	$C_{10}N_4O_2$	208.0022
$C_{13}H_{21}N_2$	205.1706	$C_{16}H_{14}$	206.1096	$C_{11}H_{12}O_4$	208.0735
$C_{13}H_5N_2O$	205.0402	$C_{16}N$	206.0031	$C_{11}H_{14}NO_3$	208.0974
$C_{13}H_7N_3$	205.0641	$C_{17}H_2$	206.0157	$C_{11}H_{16}N_2O_2$	208.1213
$C_{14}H_{21}O$	205.1593	**207**		$C_{11}N_2O_3$	207.9909
$C_{14}H_5O_2$	205.0289	$C_8H_{19}N_2O_4$	207.1345	$C_{11}H_{18}N_3O$	208.1451
$C_{14}H_{23}N$	205.1832	$C_8H_{21}N_3O_3$	207.1584	$C_{11}H_2N_3O_2$	208.0147
$C_{14}H_7NO$	205.0528	$C_9H_{21}NO_4$	207.1471	$C_{11}H_{20}N_4$	208.1690
$C_{14}H_9N_2$	205.0767	$C_9H_7N_2O_4$	207.0406	$C_{11}H_4N_4O$	208.0386
$C_{15}H_{25}$	205.1957	$C_9H_9N_3O_3$	207.0644	$C_{12}H_{16}O_3$	208.1100
$C_{15}H_9O$	205.0653	$C_9H_{11}N_4O_2$	207.0883	$C_{12}O_4$	207.9796
$C_{15}H_{11}N$	205.0892	$C_{10}H_9NO_4$	207.0532	$C_{12}H_{18}NO_2$	208.1338
$C_{16}H_{13}$	205.1018	$C_{10}H_{11}N_2O_3$	207.0770	$C_{12}H_2NO_3$	208.0034
$C_{17}H$	205.0078	$C_{10}H_{13}N_3O_2$	207.1009	$C_{12}H_{20}N_2O$	208.1577
206		$C_{10}H_{15}N_4O$	207.1247	$C_{12}H_4N_2O_2$	208.0273
$C_8H_{18}N_2O_4$	206.1267	$C_{11}H_{11}O_4$	207.0657	$C_{12}H_{22}N_3$	208.1815
$C_8H_{20}N_3O_3$	206.1506	$C_{11}H_{13}NO_3$	207.0896	$C_{12}H_6N_3O$	208.0511
$C_8H_{22}N_4O_2$	206.1744	$C_{11}H_{15}N_2O_2$	207.1134	$C_{12}H_8N_4$	208.0750
$C_9H_{20}NO_4$	206.1393	$C_{11}H_{17}N_3O$	207.1373	$C_{13}H_{20}O_2$	208.1464
$C_9H_{22}N_2O_3$	206.1631	$C_{11}HN_3O_2$	207.0069	$C_{13}H_4O_3$	208.0160
$C_9H_6N_2O_4$	206.0328	$C_{11}H_{19}N_4$	207.1611	$C_{13}H_{22}NO$	208.1702
$C_9H_8N_3O_3$	206.0566	$C_{11}H_3N_4O$	207.0308	$C_{13}H_6NO_2$	208.0399
$C_9H_{10}N_4O_2$	206.0805	$C_{12}H_{15}O_3$	207.1021	$C_{13}H_{24}N_2$	208.1941
$C_{10}H_{22}O_4$	206.1518	$C_{12}H_{17}NO_2$	207.1260	$C_{13}H_8N_2O$	208.0637
$C_{10}H_8NO_4$	206.0453	$C_{12}HNO_3$	206.9956	$C_{13}H_{10}N_3$	208.0876

Appendix A (continued)

FM		FM		FM	
$C_{14}H_{24}O$	208.1828	$C_{16}H_3N$	209.0266	$C_{10}H_{15}N_2O_3$	211.1083
$C_{14}H_8O_2$	208.0524	$C_{17}H_5$	209.0391	$C_{10}H_{17}N_3O_2$	211.1322
$C_{14}H_{26}N$	208.2067	**210**		$C_{10}HN_3O_3$	211.0018
$C_{14}H_{10}NO$	208.0763	$C_9H_{10}N_2O_4$	210.0641	$C_{10}H_{19}N_4O$	211.1560
$C_{14}H_{12}N_2$	208.1001	$C_9H_{12}N_3O_3$	210.0879	$C_{10}H_3N_4O_2$	211.0257
$C_{15}H_{28}$	208.2192	$C_9H_{14}N_4O_2$	210.1118	$C_{11}H_{15}O_4$	211.0970
$C_{15}H_{12}O$	208.0888	$C_{10}H_{12}NO_4$	210.0766	$C_{11}H_{17}NO_3$	211.1209
$C_{15}H_{14}N$	208.1127	$C_{10}H_{14}N_2O_3$	210.1005	$C_{11}HNO_4$	210.9905
$C_{15}N_2$	208.0062	$C_{10}H_{16}N_3O_2$	210.1244	$C_{11}H_{19}N_2O_2$	211.1447
$C_{16}H_{16}$	208.1253	$C_{10}N_3O_3$	209.9940	$C_{11}H_3N_2O_3$	211.0144
$C_{16}O$	207.9949	$C_{10}H_{18}N_4O$	210.1482	$C_{11}H_{21}N_3O$	211.1686
$C_{16}H_2N$	208.0187	$C_{10}H_2N_4O_2$	210.0178	$C_{11}H_5N_3O_2$	211.0382
$C_{17}H_4$	208.0313	$C_{11}H_{14}O_4$	210.0892	$C_{11}H_{23}N_4$	211.1925
209		$C_{11}H_{16}NO_3$	210.1131	$C_{11}H_7N_4O$	211.0621
$C_9H_9N_2O_4$	209.0563	$C_{11}NO_4$	209.9827	$C_{12}H_{19}O_3$	211.1334
$C_9H_{11}N_3O_3$	209.0801	$C_{11}H_{18}N_2O_2$	210.1369	$C_{12}H_3O_4$	211.0031
$C_9H_{13}N_4O_2$	209.1040	$C_{11}H_2N_2O_3$	210.0065	$C_{12}H_{21}NO_2$	211.1573
$C_{10}H_{11}NO_4$	209.0688	$C_{11}H_{20}N_3O$	210.1608	$C_{12}H_5NO_3$	211.0269
$C_{10}H_{13}N_2O_3$	209.0927	$C_{11}H_4N_3O_2$	210.0304	$C_{12}H_{23}N_2O$	211.1811
$C_{10}H_{15}N_3O_2$	209.1165	$C_{11}H_{22}N_4$	210.1846	$C_{12}H_7N_2O_2$	211.0508
$C_{10}H_{17}N_4O$	209.1404	$C_{11}H_6N_4O$	210.0542	$C_{12}H_{25}N_3$	211.2050
$C_{10}HN_4O_2$	209.0100	$C_{12}H_{18}O_3$	210.1256	$C_{12}H_9N_3O$	211.0746
$C_{11}H_{13}O_4$	209.0814	$C_{12}H_2O_4$	209.9953	$C_{12}H_{11}N_4$	211.0985
$C_{11}H_{15}NO_3$	209.1052	$C_{12}H_{20}NO_2$	210.1495	$C_{13}H_{23}O_2$	211.1699
$C_{11}H_{17}N_2O_2$	209.1291	$C_{12}H_4NO_3$	210.0191	$C_{13}H_7O_3$	211.0395
$C_{11}HN_2O_3$	208.9987	$C_{12}H_{22}N_2O$	210.1733	$C_{13}H_{25}NO$	211.1937
$C_{11}H_{19}N_3O$	209.1529	$C_{12}H_6N_2O_2$	210.0429	$C_{13}H_9NO_2$	211.0634
$C_{11}H_3N_3O_2$	209.0226	$C_{12}H_{24}N_3$	210.1972	$C_{13}H_{27}N_2$	211.2176
$C_{11}H_{21}N_4$	209.1768	$C_{12}H_8N_3O$	210.0668	$C_{13}H_{11}N_2O$	211.0872
$C_{11}H_5N_4O$	209.0464	$C_{12}H_{10}N_4$	210.0907	$C_{13}H_{13}N_3$	211.1111
$C_{12}H_{17}O_3$	209.1178	$C_{13}H_{22}O_2$	210.1620	$C_{14}H_{27}O$	211.2063
$C_{12}HO_4$	208.9874	$C_{13}H_6O_3$	210.0317	$C_{14}H_{11}O_2$	211.0759
$C_{12}H_{19}NO_2$	209.1416	$C_{13}H_{24}NO$	210.1859	$C_{14}H_{29}N$	211.2301
$C_{12}H_3NO_3$	209.0113	$C_{13}H_8NO_2$	210.0555	$C_{14}H_{13}NO$	211.0998
$C_{12}H_{21}N_2O$	209.1655	$C_{13}H_{26}N_2$	210.2098	$C_{14}H_{15}N_2$	211.1236
$C_{12}H_5N_2O_2$	209.0351	$C_{13}H_{10}N_2O$	210.0794	$C_{14}HN_3$	211.0171
$C_{12}H_{23}N_3$	209.1894	$C_{13}H_{12}N_3$	210.1032	$C_{15}H_{31}$	211.2427
$C_{12}H_7N_3O$	209.0590	$C_{14}H_{26}O$	210.1985	$C_{15}H_{15}O$	211.1123
$C_{12}H_9N_4$	209.0829	$C_{14}H_{10}O_2$	210.0681	$C_{15}H_{17}N$	211.1362
$C_{13}H_{21}O_2$	209.1542	$C_{14}H_{28}N$	210.2223	$C_{15}HNO$	211.0058
$C_{13}H_5O_3$	209.0238	$C_{14}H_{12}NO$	210.0919	$C_{15}H_3N_2$	211.0297
$C_{13}H_{23}NO$	209.1781	$C_{14}H_{14}N_2$	210.1158	$C_{16}H_{19}$	211.1488
$C_{13}H_7NO_2$	209.0477	$C_{14}N_3$	210.0093	$C_{16}H_3O$	211.0184
$C_{13}H_{25}N_2$	209.2019	$C_{15}H_{30}$	210.2349	$C_{16}H_5N$	211.0422
$C_{13}H_9N_2O$	209.0715	$C_{15}H_{14}O$	210.1045	$C_{17}H_7$	211.0548
$C_{13}H_{11}N_3$	209.0954	$C_{15}H_{16}N$	210.1284	**212**	
$C_{14}H_{25}O$	209.1906	$C_{15}NO$	209.9980	$C_9H_{12}N_2O_4$	212.0797
$C_{14}H_9O_2$	209.0603	$C_{15}H_2N_2$	210.0218	$C_9H_{14}N_3O_3$	212.1036
$C_{14}H_{27}N$	209.2145	$C_{16}H_{18}$	210.1409	$C_9H_{16}N_4O_2$	212.1275
$C_{14}H_{11}NO$	209.0841	$C_{16}H_2O$	210.0106	$C_{10}H_{14}NO_4$	212.0923
$C_{14}H_{13}N_2$	209.1080	$C_{16}H_4N$	210.0344	$C_{10}H_{16}N_2O_3$	212.1162
$C_{15}H_{29}$	209.2270	$C_{17}H_6$	210.0470	$C_{10}N_2O_4$	211.9858
$C_{15}H_{13}O$	209.0967	**211**		$C_{10}H_{18}N_3O_2$	212.1400
$C_{15}H_{15}N$	209.1205	$C_9H_{11}N_2O_4$	211.0719	$C_{10}H_2N_3O_3$	212.0096
$C_{15}HN_2$	209.0140	$C_9H_{13}N_3O_3$	211.0958	$C_{10}H_{20}N_4O$	212.1639
$C_{16}H_{17}$	209.1331	$C_9H_{15}N_4O_2$	211.1196	$C_{10}H_4N_4O_2$	212.0335
$C_{16}HO$	209.0027	$C_{10}H_{13}NO_4$	211.0845	$C_{11}H_{16}O_4$	212.1049

Appendix A (continued)

	FM		FM		FM
$C_{11}H_{18}NO_3$	212.1287	$C_{11}H_5N_2O_3$	213.0300	$C_{11}H_{10}N_4O$	214.0856
$C_{11}H_2NO_4$	211.9983	$C_{11}H_{23}N_3O$	213.1842	$C_{12}H_{22}O_3$	214.1569
$C_{11}H_{20}N_2O_2$	212.1526	$C_{11}H_7N_3O_2$	213.0539	$C_{12}H_6O_4$	214.0266
$C_{11}H_4N_2O_3$	212.0222	$C_{11}H_{25}N_4$	213.2081	$C_{12}H_{24}NO_2$	214.1808
$C_{11}H_{22}N_3O$	212.1764	$C_{11}H_9N_4O$	213.0777	$C_{12}H_8NO_3$	214.0504
$C_{11}H_6N_3O_2$	212.0460	$C_{12}H_{21}O_3$	213.1491	$C_{12}H_{26}N_2O$	214.2046
$C_{11}H_{24}N_4$	212.2003	$C_{12}H_5O_4$	213.0187	$C_{12}H_{10}N_2O_2$	214.0743
$C_{11}H_8N_4O$	212.0699	$C_{12}H_{23}NO_2$	213.1730	$C_{12}H_{28}N_3$	214.2285
$C_{12}H_{20}O_3$	212.1413	$C_{12}H_7NO_3$	213.0426	$C_{12}H_{12}N_3O$	214.0981
$C_{12}H_4O_4$	212.0109	$C_{12}H_{25}N_2O$	213.1968	$C_{12}H_{14}N_4$	214.1220
$C_{12}H_{22}NO_2$	212.1651	$C_{12}H_9N_2O_2$	213.0664	$C_{13}H_{26}O_2$	214.1934
$C_{12}H_6NO_3$	212.0348	$C_{12}H_{27}N_3$	213.2207	$C_{13}H_{10}O_3$	214.0630
$C_{12}H_{24}N_2O$	212.1890	$C_{12}H_{11}N_3O$	213.0903	$C_{13}H_{28}NO$	214.2172
$C_{12}H_8N_2O_2$	212.0586	$C_{12}H_{13}N_4$	213.1142	$C_{13}H_{12}NO_2$	214.0859
$C_{12}H_{26}N_3$	212.2129	$C_{13}H_{25}O_2$	213.1855	$C_{13}H_{30}N_2$	214.2411
$C_{12}H_{10}N_3O$	212.0825	$C_{13}H_9O_3$	213.0552	$C_{13}H_{14}N_2O$	214.1107
$C_{12}H_{12}N_4$	212.1063	$C_{13}H_{27}NO$	213.2094	$C_{13}H_{16}N_3$	214.1345
$C_{13}H_{24}O_2$	212.1777	$C_{13}H_{11}NO_2$	213.0790	$C_{13}N_3O$	214.0042
$C_{13}H_8O_3$	212.0473	$C_{13}H_{29}N_2$	213.2332	$C_{13}H_2N_4$	214.0280
$C_{13}H_{26}NO$	212.2015	$C_{13}H_{13}N_2O$	213.1029	$C_{14}H_{30}O$	214.2298
$C_{13}H_{10}NO_2$	212.0712	$C_{13}H_{15}N_3$	213.1267	$C_{14}H_{14}O_2$	214.0994
$C_{13}H_{28}N_2$	212.2254	$C_{13}HN_4$	213.0202	$C_{14}H_{16}NO$	214.1233
$C_{13}H_{12}N_2O$	212.0950	$C_{14}H_{29}O$	213.2219	$C_{14}NO_2$	213.9929
$C_{13}H_{14}N_3$	212.1189	$C_{14}H_{13}O_2$	213.0916	$C_{14}H_{18}N_2$	214.1471
$C_{13}N_4$	212.0124	$C_{14}H_{31}N$	213.2458	$C_{14}H_2N_2O$	214.0167
$C_{14}H_{28}O$	212.2141	$C_{14}H_{15}NO$	213.1154	$C_{14}H_4N_3$	214.0406
$C_{14}H_{12}O_2$	212.0837	$C_{14}H_{17}N_2$	213.1393	$C_{15}H_{18}O$	214.1358
$C_{14}H_{30}N$	212.2380	$C_{14}HN_2O$	213.0089	$C_{15}H_2O_2$	214.0054
$C_{14}H_{14}NO$	212.1076	$C_{14}H_3N_3$	213.0328	$C_{15}H_{20}N$	214.1597
$C_{14}H_{16}N_2$	212.1315	$C_{15}H_{17}O$	213.1280	$C_{15}H_4NO$	214.0293
$C_{14}N_2O$	212.0011	$C_{15}HO_2$	212.9976	$C_{15}H_6N_2$	214.0532
$C_{14}H_2N_3$	212.0249	$C_{15}H_{19}N$	213.1519	$C_{16}H_{22}$	214.1722
$C_{15}H_{32}$	212.2505	$C_{15}H_3NO$	213.0215	$C_{16}H_6O$	214.0419
$C_{15}H_{16}O$	212.1202	$C_{15}H_5N_2$	213.0453	$C_{16}H_8N$	214.0657
$C_{15}O_2$	211.9898	$C_{16}H_{21}$	213.1644	$C_{17}H_{10}$	214.0783
$C_{15}H_{18}N$	212.1440	$C_{16}H_5O$	213.0340	**215**	
$C_{15}H_2NO$	212.0136	$C_{16}H_7N$	213.0579	$C_9H_{15}N_2O_4$	215.1032
$C_{15}H_4N_2$	212.0375	$C_{17}H_9$	213.0705	$C_9H_{17}N_3O_3$	215.1271
$C_{16}H_{20}$	212.1566	**214**		$C_9H_{19}N_4O_2$	215.1509
$C_{16}H_4O$	212.0262	$C_9H_{14}N_2O_4$	214.0954	$C_{10}H_{17}NO_4$	215.1158
$C_{16}H_6N$	212.0501	$C_9H_{16}N_3O_3$	214.1193	$C_{10}H_{19}N_2O_3$	215.1396
$C_{17}H_8$	212.0626	$C_9H_{18}N_4O_2$	214.1431	$C_{10}H_3N_2O_4$	215.0093
213		$C_{10}H_{16}NO_4$	214.1080	$C_{10}H_{21}N_3O_2$	215.1635
$C_9H_{13}N_2O_4$	213.0876	$C_{10}H_{18}N_2O_3$	214.1318	$C_{10}H_5N_3O_3$	215.0331
$C_9H_{15}N_3O_3$	213.1114	$C_{10}H_2N_2O_4$	214.0014	$C_{10}H_{23}N_4O$	215.1873
$C_9H_{17}N_4O_2$	213.1353	$C_{10}H_{20}N_3O_2$	214.1557	$C_{10}H_7N_4O_2$	215.0570
$C_{10}H_{15}NO_4$	213.1001	$C_{10}H_4N_3O_3$	214.0253	$C_{11}H_{19}O_4$	215.1284
$C_{10}H_{17}N_2O_3$	213.1240	$C_{10}H_{22}N_4O$	214.1795	$C_{11}H_{21}NO_3$	215.1522
$C_{10}HN_2O_4$	212.9936	$C_{10}H_6N_4O_2$	214.0491	$C_{11}H_5NO_4$	215.0218
$C_{10}H_{19}N_3O_2$	213.1478	$C_{11}H_{18}O_4$	214.1205	$C_{11}H_{23}N_2O_2$	215.1761
$C_{10}H_3N_3O_3$	213.0175	$C_{11}H_{20}NO_3$	214.1444	$C_{11}H_7N_2O_3$	215.0457
$C_{10}H_{21}N_4O$	213.1717	$C_{11}H_4NO_4$	214.0140	$C_{11}H_{25}N_3O$	215.1999
$C_{10}H_5N_4O_2$	213.0413	$C_{11}H_{22}N_2O_2$	214.1682	$C_{11}H_9N_3O_2$	215.0695
$C_{11}H_{17}O_4$	213.1127	$C_{11}H_6N_2O_3$	214.0379	$C_{11}H_{27}N_4$	215.2238
$C_{11}H_{19}NO_3$	213.1365	$C_{11}H_{24}N_3O$	214.1921	$C_{11}H_{11}N_4O$	215.0934
$C_{11}H_3NO_4$	213.0062	$C_{11}H_8N_3O_2$	214.0617	$C_{12}H_{23}O_3$	215.1648
$C_{11}H_{21}N_2O_2$	213.1604	$C_{11}H_{26}N_4$	214.2160	$C_{12}H_7O_4$	215.0344

Appendix A (continued)

FM		FM		FM	
$C_{12}H_{25}NO_2$	215.1886	$C_{12}H_{16}N_4$	216.1377	$C_{13}HN_2O_2$	217.0038
$C_{12}H_9NO_3$	215.0583	$C_{12}N_4O$	216.0073	$C_{13}H_{19}N_3$	217.1580
$C_{12}H_{27}N_2O$	215.2125	$C_{13}H_{28}O_2$	216.2090	$C_{13}H_3N_3O$	217.0277
$C_{12}H_{11}N_2O_2$	215.0821	$C_{13}H_{12}O_3$	216.0786	$C_{13}H_5N_4$	217.0515
$C_{12}H_{29}N_3$	215.2363	$C_{13}H_{14}NO_2$	216.1025	$C_{14}H_{17}O_2$	217.1229
$C_{12}H_{13}N_3O$	215.1060	$C_{13}H_{16}N_2O$	216.1264	$C_{14}HO_3$	216.9925
$C_{12}H_{15}N_4$	215.1298	$C_{13}N_2O_2$	215.9960	$C_{14}H_{19}NO$	217.1467
$C_{13}H_{27}O_2$	215.2012	$C_{13}H_{18}N_3$	216.1502	$C_{14}H_3NO_2$	217.0164
$C_{13}H_{11}O_3$	215.0708	$C_{13}H_2N_3O$	216.0198	$C_{14}H_{21}N_2$	217.1706
$C_{13}H_{29}NO$	215.2250	$C_{13}H_4N_4$	216.0437	$C_{14}H_5N_2O$	217.0402
$C_{13}H_{13}NO_2$	215.0947	$C_{14}H_{16}O_2$	216.1151	$C_{14}H_7N_3$	217.0641
$C_{13}H_{15}N_2O$	215.1185	$C_{14}O_3$	215.9847	$C_{15}H_{21}O$	217.1593
$C_{13}H_{17}N_3$	215.1424	$C_{14}H_{18}NO$	216.1389	$C_{15}H_5O_2$	217.0289
$C_{13}HN_3O$	215.0120	$C_{14}H_2NO_2$	216.0085	$C_{15}H_{23}N$	217.1832
$C_{13}H_3N_4$	215.0359	$C_{14}H_{20}N_2$	216.1628	$C_{15}H_7NO$	217.0528
$C_{14}H_{15}O_2$	215.1072	$C_{14}H_4N_2O$	216.0324	$C_{15}H_9N_2$	217.0767
$C_{14}H_{17}NO$	215.1311	$C_{14}H_6N_3$	216.0563	$C_{16}H_{25}$	217.1957
$C_{14}HNO_2$	215.0007	$C_{15}H_{20}O$	216.1515	$C_{16}H_9O$	217.0653
$C_{14}H_{19}N_2$	215.1549	$C_{15}H_4O_2$	216.0211	$C_{16}H_{11}N$	217.0892
$C_{14}H_3N_2O$	215.0246	$C_{15}H_{22}N$	216.1753	$C_{17}H_{13}$	217.1018
$C_{14}H_5N_3$	215.0484	$C_{15}H_6NO$	216.0449	$C_{18}H$	217.0078
$C_{15}H_{19}O$	215.1436	$C_{15}H_8N_2$	216.0688	**218**	
$C_{15}H_3O_2$	215.0133	$C_{16}H_{24}$	216.1879	$C_9H_{18}N_2O_4$	218.1267
$C_{15}H_{21}N$	215.1675	$C_{16}H_8O$	216.0575	$C_9H_{20}N_3O_3$	218.1506
$C_{15}H_5NO$	215.0371	$C_{16}H_{10}N$	216.0814	$C_9H_{22}N_4O_2$	218.1744
$C_{15}H_7N_2$	215.0610	$C_{17}H_{12}$	216.0939	$C_{10}H_{20}NO_4$	218.1393
$C_{16}H_{23}$	215.1801	C_{18}	216.0000	$C_{10}H_{22}N_2O_3$	218.1631
$C_{16}H_7O$	215.0497	**217**		$C_{10}H_6N_2O_4$	218.0328
$C_{16}H_9N$	215.0736	$C_9H_{17}N_2O_4$	217.1189	$C_{10}H_{24}N_3O_2$	218.1870
$C_{17}H_{11}$	215.0861	$C_9H_{19}N_3O_3$	217.1427	$C_{10}H_8N_3O_3$	218.0566
216		$C_9H_{21}N_4O_2$	217.1666	$C_{10}H_{26}N_4O$	218.2108
$C_9H_{16}N_2O_4$	216.1111	$C_{10}H_{19}NO_4$	217.1315	$C_{10}H_{10}N_4O_2$	218.0805
$C_9H_{18}N_3O_3$	216.1349	$C_{10}H_{21}N_2O_3$	217.1553	$C_{11}H_{22}O_4$	218.1518
$C_9H_{20}N_4O_2$	216.1588	$C_{10}H_5N_2O_4$	217.0249	$C_{11}H_{24}NO_3$	218.1757
$C_{10}H_{18}NO_4$	216.1236	$C_{10}H_{23}N_3O_2$	217.1791	$C_{11}H_8NO_4$	218.0453
$C_{10}H_{20}N_2O_3$	216.1475	$C_{10}H_7N_3O_3$	217.0488	$C_{11}H_{26}N_2O_2$	218.1996
$C_{10}H_4N_2O_4$	216.0171	$C_{10}H_{25}N_4O$	217.2030	$C_{11}H_{10}N_2O_3$	218.0692
$C_{10}H_{22}N_3O_2$	216.1713	$C_{10}H_9N_4O_2$	217.0726	$C_{11}H_{12}N_3O_2$	218.0930
$C_{10}H_6N_3O_3$	216.0410	$C_{11}H_{21}O_4$	217.1440	$C_{11}H_{14}N_4O$	218.1169
$C_{10}H_{24}N_4O$	216.1952	$C_{11}H_{23}NO_3$	217.1679	$C_{12}H_{26}O_3$	218.1883
$C_{10}H_8N_4O_2$	216.0648	$C_{11}H_7NO_4$	217.0375	$C_{12}H_{10}O_4$	218.0579
$C_{11}H_{20}O_4$	216.1362	$C_{11}H_{25}N_2O_2$	217.1917	$C_{12}H_{12}NO_3$	218.0817
$C_{11}H_{22}NO_3$	216.1600	$C_{11}H_9N_2O_3$	217.0614	$C_{12}H_{14}N_2O_2$	218.1056
$C_{11}H_6NO_4$	216.0297	$C_{11}H_{27}N_3O$	217.2156	$C_{12}H_{16}N_3O$	218.1295
$C_{11}H_{24}N_2O_2$	216.1839	$C_{11}H_{11}N_3O_2$	217.0852	$C_{12}N_3O_2$	217.9991
$C_{11}H_8N_2O_3$	216.0535	$C_{11}H_{13}N_4O$	217.1091	$C_{12}H_{18}N_4$	218.1533
$C_{11}H_{26}N_3O$	216.2077	$C_{12}H_{25}O_3$	217.1804	$C_{12}H_2N_4O$	218.0229
$C_{11}H_{10}N_3O_2$	216.0774	$C_{12}H_9O_4$	217.0501	$C_{13}H_{14}O_3$	218.0943
$C_{11}H_{28}N_4$	216.2316	$C_{12}H_{27}NO_2$	217.2043	$C_{13}H_{16}NO_2$	218.1182
$C_{11}H_{12}N_4O$	216.1012	$C_{12}H_{11}NO_3$	217.0739	$C_{13}NO_3$	217.9878
$C_{12}H_{24}O_3$	216.1726	$C_{12}H_{13}N_2O_2$	217.0978	$C_{13}H_{18}N_2O$	218.1420
$C_{12}H_8O_4$	216.0422	$C_{12}H_{15}N_3O$	217.1216	$C_{13}H_2N_2O_2$	218.0116
$C_{12}H_{26}NO_2$	216.1965	$C_{12}H_{17}N_4$	217.1455	$C_{13}H_{20}N_3$	218.1659
$C_{12}H_{10}NO_3$	216.0661	$C_{12}HN_4O$	217.0151	$C_{13}H_4N_3O$	218.0355
$C_{12}H_{28}N_2O$	216.2203	$C_{13}H_{13}O_3$	217.0865	$C_{13}H_6N_4$	218.0594
$C_{12}H_{12}N_2O_2$	216.0899	$C_{13}H_{15}NO_2$	217.1103	$C_{14}H_{18}O_2$	218.1307
$C_{12}H_{14}N_3O$	216.1138	$C_{13}H_{17}N_2O$	217.1342	$C_{14}H_2O_3$	218.0003

Appendix A (continued)

	FM		FM		FM
$C_{14}H_{20}NO$	218.1546	$C_{15}H_9NO$	219.0684	$C_{17}O$	219.9949
$C_{14}H_4NO_2$	218.0242	$C_{15}H_{11}N_2$	219.0923	$C_{17}H_2N$	220.0187
$C_{14}H_{22}N_2$	218.1784	$C_{16}H_{27}$	219.2114	$C_{18}H_4$	220.0313
$C_{14}H_6N_2O$	218.0480	$C_{16}H_{11}O$	219.0810	**221**	
$C_{14}H_8N_3$	218.0719	$C_{16}H_{13}N$	219.1049	$C_9H_{21}N_2O_4$	221.1502
$C_{15}H_{22}O$	218.1671	$C_{17}H_{15}$	219.1174	$C_9H_{23}N_3O_3$	221.1741
$C_{15}H_6O_2$	218.0368	$C_{17}HN$	219.0109	$C_{10}H_{23}NO_4$	221.1628
$C_{15}H_{24}N$	218.1910	$C_{18}H_3$	219.0235	$C_{10}H_9N_2O_4$	221.0563
$C_{15}H_8NO$	218.0606	**220**		$C_{10}H_{11}N_3O_3$	221.0801
$C_{15}H_{10}N_2$	218.0845	$C_9H_{20}N_2O_4$	220.1424	$C_{10}H_{13}N_4O_2$	221.1040
$C_{16}H_{26}$	218.2036	$C_9H_{22}N_3O_3$	220.1662	$C_{11}H_{11}NO_4$	221.0688
$C_{16}H_{10}O$	218.0732	$C_9H_{24}N_4O_2$	220.1901	$C_{11}H_{13}N_2O_3$	221.0927
$C_{16}H_{12}N$	218.0970	$C_{10}H_{22}NO_4$	220.1549	$C_{11}H_{15}N_3O_2$	221.1165
$C_{17}H_{14}$	218.1096	$C_{10}H_{24}N_2O_3$	220.1788	$C_{11}H_{17}N_4O$	221.1404
$C_{17}N$	218.0031	$C_{10}H_8N_2O_4$	220.0484	$C_{11}HN_4O_2$	221.0100
$C_{18}H_2$	218.0157	$C_{10}H_{10}N_3O_3$	220.0723	$C_{12}H_{13}O_4$	221.0814
219		$C_{10}H_{12}N_4O_2$	220.0961	$C_{12}H_{15}NO_3$	221.1052
$C_9H_{19}N_2O_4$	219.1345	$C_{11}H_{24}O_4$	220.1675	$C_{12}H_{17}N_2O_2$	221.1291
$C_9H_{21}N_3O_3$	219.1584	$C_{11}H_{10}NO_4$	220.0610	$C_{12}HN_2O_3$	220.9987
$C_9H_{23}N_4O_2$	219.1822	$C_{11}H_{12}N_2O_3$	220.0848	$C_{12}H_{19}N_3O$	221.1529
$C_{10}H_{21}NO_4$	219.1471	$C_{11}H_{14}N_3O_2$	220.1087	$C_{12}H_3N_3O_2$	221.0226
$C_{10}H_{23}N_2O_3$	219.1710	$C_{11}H_{16}N_4O$	220.1325	$C_{12}H_{21}N_4$	221.1768
$C_{10}H_7N_2O_4$	219.0406	$C_{11}N_4O_2$	220.0022	$C_{12}H_5N_4O$	221.0464
$C_{10}H_{25}N_3O_2$	219.1948	$C_{12}H_{12}O_4$	220.0735	$C_{13}H_{17}O_3$	221.1178
$C_{10}H_9N_3O_3$	219.0644	$C_{12}H_{14}NO_3$	220.0974	$C_{13}HO_4$	220.9874
$C_{10}H_{11}N_4O_2$	219.0883	$C_{12}H_{16}N_2O_2$	220.1213	$C_{13}H_{19}NO_2$	221.1416
$C_{11}H_{23}O_4$	219.1597	$C_{12}N_2O_3$	219.9909	$C_{13}H_3NO_3$	221.0113
$C_{11}H_{25}NO_3$	219.1835	$C_{12}H_{18}N_3O$	220.1451	$C_{13}H_{21}N_2O$	221.1655
$C_{11}H_9NO_4$	219.0532	$C_{12}H_2N_3O_2$	220.0147	$C_{13}H_5N_2O_2$	221.0351
$C_{11}H_{11}N_2O_3$	219.0770	$C_{12}H_{20}N_4$	220.1690	$C_{13}H_{23}N_3$	221.1894
$C_{11}H_{13}N_3O_2$	219.1009	$C_{12}H_4N_4O$	220.0386	$C_{13}H_7N_3O$	221.0590
$C_{11}H_{15}N_4O$	219.1247	$C_{13}H_{16}O_3$	220.1100	$C_{13}H_9N_4$	221.0829
$C_{12}H_{11}O_4$	219.0657	$C_{13}O_4$	219.9796	$C_{14}H_{21}O_2$	221.1542
$C_{12}H_{13}NO_3$	219.0896	$C_{13}H_{18}NO_2$	220.1338	$C_{14}H_5O_3$	221.0238
$C_{12}H_{15}N_2O_2$	219.1134	$C_{13}H_2NO_3$	220.0034	$C_{14}H_{23}NO$	221.1781
$C_{12}H_{17}N_3O$	219.1373	$C_{13}H_{20}N_2O$	220.1577	$C_{14}H_7NO_2$	221.0477
$C_{12}HN_3O_2$	219.0069	$C_{13}H_4N_2O_2$	220.0273	$C_{14}H_{25}N_2$	221.2019
$C_{12}H_{19}N_4$	219.1611	$C_{13}H_{22}N_3$	220.1815	$C_{14}H_9N_2O$	221.0715
$C_{12}H_3N_4O$	219.0308	$C_{13}H_6N_3O$	220.0511	$C_{14}H_{11}N_3$	221.0954
$C_{13}H_{15}O_3$	219.1021	$C_{13}H_8N_4$	220.0750	$C_{15}H_{25}O$	221.1906
$C_{13}H_{17}NO_2$	219.1260	$C_{14}H_{20}O_2$	220.1464	$C_{15}H_9O_2$	221.0603
$C_{13}HNO_3$	218.9956	$C_{14}H_4O_3$	220.0160	$C_{15}H_{27}N$	221.2145
$C_{13}H_{19}N_2O$	219.1498	$C_{14}H_{22}NO$	220.1702	$C_{15}H_{11}NO$	221.0841
$C_{13}H_3N_2O_2$	219.0195	$C_{14}H_6NO_2$	220.0399	$C_{15}H_{13}N_2$	221.1080
$C_{13}H_{21}N_3$	219.1737	$C_{14}H_{24}N_2$	220.1941	$C_{16}H_{29}$	221.2270
$C_{13}H_5N_3O$	219.0433	$C_{14}H_8N_2O$	220.0637	$C_{16}H_{13}O$	221.0967
$C_{13}H_7N_4$	219.0672	$C_{14}H_{10}N_3$	220.0876	$C_{16}H_{15}N$	221.1205
$C_{14}H_{19}O_2$	219.1385	$C_{15}H_{24}O$	220.1828	$C_{16}HN_2$	221.0140
$C_{14}H_3O_3$	219.0082	$C_{15}H_8O_2$	220.0524	$C_{17}H_{17}$	221.1331
$C_{14}H_{21}NO$	219.1624	$C_{15}H_{26}N$	220.2067	$C_{17}HO$	221.0027
$C_{14}H_5NO_2$	219.0320	$C_{15}H_{10}NO$	220.0763	$C_{17}H_3N$	221.0266
$C_{14}H_{23}N_2$	219.1863	$C_{15}H_{12}N_2$	220.1001	$C_{18}H_5$	221.0391
$C_{14}H_7N_2O$	219.0559	$C_{16}H_{28}$	220.2192	**222**	
$C_{14}H_9N_3$	219.0798	$C_{16}H_{12}O$	220.0888	$C_9H_{22}N_2O_4$	222.1580
$C_{15}H_{23}O$	219.1750	$C_{16}H_{14}N$	220.1127	$C_{10}H_{10}N_2O_4$	222.0641
$C_{15}H_7O_2$	219.0446	$C_{16}N_2$	220.0062	$C_{10}H_{12}N_3O_3$	222.0879
$C_{15}H_{25}N$	219.1988	$C_{17}H_{16}$	220.1253	$C_{10}H_{14}N_4O_2$	222.1118

Appendix A (continued)

FM		FM		FM	
$C_{11}H_{12}NO_4$	222.0766	$C_{12}H_{17}NO_3$	223.1209	$C_{12}H_{24}N_4$	224.2003
$C_{11}H_{14}N_2O_3$	222.1005	$C_{12}HNO_4$	222.9905	$C_{12}H_8N_4O$	224.0699
$C_{11}H_{16}N_3O_2$	222.1244	$C_{12}H_{19}N_2O_2$	223.1447	$C_{13}H_{20}O_3$	224.1413
$C_{11}N_3O_3$	221.9940	$C_{12}H_3N_2O_3$	223.0144	$C_{13}H_4O_4$	224.0109
$C_{11}H_{18}N_4O$	222.1482	$C_{12}H_{21}N_3O$	223.1686	$C_{13}H_{22}NO_2$	224.1651
$C_{11}H_2N_4O_2$	222.0178	$C_{12}H_5N_3O_2$	223.0382	$C_{13}H_6NO_3$	224.0348
$C_{12}H_{14}O_4$	222.0892	$C_{12}H_{23}N_4$	223.1925	$C_{13}H_{24}N_2O$	224.1890
$C_{12}H_{16}NO_3$	222.1131	$C_{12}H_7N_4O$	223.0621	$C_{13}H_8N_2O_2$	224.0586
$C_{12}NO_4$	221.9827	$C_{13}H_{19}O_3$	223.1334	$C_{13}H_{26}N_3$	224.2129
$C_{12}H_{18}N_2O_2$	222.1369	$C_{13}H_3O_4$	223.0031	$C_{13}H_{10}N_3O$	224.0825
$C_{12}H_2N_2O_3$	222.0065	$C_{13}H_{21}NO_2$	223.1573	$C_{13}H_{12}N_4$	224.1063
$C_{12}H_{20}N_3O$	222.1608	$C_{13}H_5NO_3$	223.0269	$C_{14}H_{24}O_2$	224.1777
$C_{12}H_4N_3O_2$	222.0304	$C_{13}H_{23}N_2O$	223.1811	$C_{14}H_8O_3$	224.0473
$C_{12}H_{22}N_4$	222.1846	$C_{13}H_7N_2O_2$	223.0508	$C_{14}H_{26}NO$	224.2015
$C_{12}H_6N_4O$	222.0542	$C_{13}H_{25}N_3$	223.2050	$C_{14}H_{10}NO_2$	224.0712
$C_{13}H_{18}O_3$	222.1256	$C_{13}H_9N_3O$	223.0746	$C_{14}H_{28}N_2$	224.2254
$C_{13}H_2O_4$	221.9953	$C_{13}H_{11}N_4$	223.0985	$C_{14}H_{12}N_2O$	224.0950
$C_{13}H_{20}NO_2$	222.1495	$C_{14}H_{23}O_2$	223.1699	$C_{14}H_{14}N_3$	224.1189
$C_{13}H_4NO_3$	222.0191	$C_{14}H_7O_3$	223.0395	$C_{14}N_4$	224.0124
$C_{13}H_{22}N_2O$	222.1733	$C_{14}H_{25}NO$	223.1937	$C_{15}H_{28}O$	224.2141
$C_{13}H_6N_2O_2$	222.0429	$C_{14}H_9NO_2$	223.0634	$C_{15}H_{12}O_2$	224.0837
$C_{13}H_{24}N_3$	222.1972	$C_{14}H_{27}N_2$	223.2176	$C_{15}H_{30}N$	224.2380
$C_{13}H_8N_3O$	222.0668	$C_{14}H_{11}N_2O$	223.0872	$C_{15}H_{14}NO$	224.1076
$C_{13}H_{10}N_4$	222.0907	$C_{14}H_{13}N_3$	223.1111	$C_{15}H_{16}N_2$	24.1315
$C_{14}H_{22}O_2$	222.1620	$C_{15}H_{27}O$	223.2063	$C_{15}N_2O$	224.0011
$C_{14}H_6O_3$	222.0317	$C_{15}H_{11}O_2$	223.0759	$C_{15}H_2N_3$	224.0249
$C_{14}H_{24}NO$	222.1859	$C_{15}H_{29}N$	223.2301	$C_{16}H_{32}$	224.2505
$C_{14}H_8NO_2$	222.0555	$C_{15}H_{13}NO$	223.0998	$C_{16}H_{16}O$	224.1202
$C_{14}H_{26}N_2$	222.2098	$C_{15}H_{15}N_2$	223.1236	$C_{16}O_2$	223.9898
$C_{14}H_{10}N_2O$	222.0794	$C_{15}HN_3$	223.0171	$C_{16}H_{18}N$	224.1440
$C_{14}H_{12}N_3$	222.1032	$C_{16}H_{31}$	223.2427	$C_{16}H_2NO$	224.0136
$C_{15}H_{26}O$	222.1985	$C_{16}H_{15}O$	223.1123	$C_{16}H_4N_2$	224.0375
$C_{15}H_{10}O_2$	222.0681	$C_{16}H_{17}N$	223.1362	$C_{17}H_{20}$	224.1566
$C_{15}H_{28}N$	222.2223	$C_{16}HNO$	223.0058	$C_{17}H_4O$	224.0262
$C_{15}H_{12}NO$	222.0919	$C_{16}H_3N_2$	223.0297	$C_{17}H_6N$	224.0501
$C_{15}H_{14}N_2$	222.1158	$C_{17}H_{19}$	223.1488	$C_{18}H_8$	224.0626
$C_{15}N_3$	222.0093	$C_{17}H_3O$	223.0184	**225**	
$C_{16}H_{30}$	222.2349	$C_{17}H_5N$	223.0422	$C_{10}H_{13}N_2O_4$	225.0876
$C_{16}H_{14}O$	222.1045	$C_{18}H_7$	223.0548	$C_{10}H_{15}N_3O_3$	225.1114
$C_{16}H_{16}N$	222.1284	**224**		$C_{10}H_{17}N_4O_2$	225.1353
$C_{16}NO$	221.9980	$C_{10}H_{12}N_2O_4$	224.0797	$C_{11}H_{15}NO_4$	225.1001
$C_{16}H_2N_2$	222.0218	$C_{10}H_{14}N_3O_3$	224.1036	$C_{11}H_{17}N_2O_3$	225.1240
$C_{17}H_{18}$	222.1409	$C_{10}H_{16}N_4O_2$	224.1275	$C_{11}HN_2O_4$	224.9936
$C_{17}H_2O$	222.0106	$C_{11}H_{14}NO_4$	224.0923	$C_{11}H_{19}N_3O_2$	225.1478
$C_{17}H_4N$	222.0344	$C_{11}H_{16}N_2O_3$	224.1162	$C_{11}H_3N_3O_3$	225.0175
$C_{18}H_6$	222.0470	$C_{11}N_2O_4$	223.9858	$C_{11}H_{21}N_4O$	225.1717
223		$C_{11}H_{18}N_3O_2$	224.1400	$C_{11}H_5N_4O_2$	225.0413
$C_{10}H_{11}N_2O_4$	223.0719	$C_{11}H_2N_3O_3$	224.0096	$C_{12}H_{17}O_4$	225.1127
$C_{10}H_{13}N_3O_3$	223.0958	$C_{11}H_{20}N_4O$	224.1639	$C_{12}H_{19}NO_3$	225.1365
$C_{10}H_{15}N_4O_2$	223.1196	$C_{11}H_4N_4O_2$	224.0335	$C_{12}H_3NO_4$	225.0062
$C_{11}H_{13}NO_4$	223.0845	$C_{12}H_{16}O_4$	224.1049	$C_{12}H_{21}N_2O_2$	225.1604
$C_{11}H_{15}N_2O_3$	223.1083	$C_{12}H_{18}NO_3$	224.1287	$C_{12}H_5N_2O_3$	225.0300
$C_{11}H_{17}N_3O_2$	223.1322	$C_{12}H_2NO_4$	223.9983	$C_{12}H_{23}N_3O$	225.1842
$C_{11}HN_3O_3$	223.0018	$C_{12}H_{20}N_2O_2$	224.1526	$C_{12}H_7N_3O_2$	225.0539
$C_{11}H_{19}N_4O$	223.1560	$C_{12}H_4N_2O_3$	224.0222	$C_{12}H_{25}N_4$	225.2081
$C_{11}H_3N_4O_2$	223.0257	$C_{12}H_{22}N_3O$	224.1764	$C_{12}H_9N_4O$	225.0777
$C_{12}H_{15}O_4$	223.0970	$C_{12}H_6N_3O_2$	224.0460	$C_{13}H_{21}O_3$	225.1491

Appendix A (continued)

FM		FM		FM	
$C_{13}H_5O_4$	225.0187	$C_{13}H_{26}N_2O$	226.2046	$C_{13}H_{11}N_2O_2$	227.0821
$C_{13}H_{23}NO_2$	225.1730	$C_{13}H_{10}N_2O_2$	226.0743	$C_{13}H_{29}N_3$	227.2363
$C_{13}H_7NO_3$	225.0426	$C_{13}H_{28}N_3$	226.2285	$C_{13}H_{13}N_3O$	227.1060
$C_{13}H_{25}N_2O$	225.1968	$C_{13}H_{12}N_3O$	226.0981	$C_{13}H_{15}N_4$	227.1298
$C_{13}H_9N_2O_2$	225.0664	$C_{13}H_{14}N_4$	226.1220	$C_{14}H_{27}O_2$	227.2012
$C_{13}H_{27}N_3$	225.2207	$C_{14}H_{26}O_2$	226.1934	$C_{14}H_{11}O_3$	227.0708
$C_{13}H_{11}N_3O$	225.0903	$C_{14}H_{10}O_3$	226.0630	$C_{14}H_{29}NO$	227.2250
$C_{13}H_{13}N_4$	225.1142	$C_{14}H_{28}NO$	226.2172	$C_{14}H_{13}NO_2$	227.0947
$C_{14}H_{25}O_2$	225.1855	$C_{14}H_{12}NO_2$	226.0868	$C_{14}H_{31}N_2$	227.2489
$C_{14}H_9O_3$	225.0552	$C_{14}H_{30}N_2$	226.2411	$C_{14}H_{15}N_2O$	227.1185
$C_{14}H_{27}NO$	225.2094	$C_{14}H_{14}N_2O$	226.1107	$C_{14}H_{17}N_3$	227.1424
$C_{14}H_{11}NO_2$	225.0790	$C_{14}H_{16}N_3$	226.1346	$C_{14}HN_3O$	227.0120
$C_{14}H_{29}N_2$	225.2332	$C_{14}N_3O$	226.0042	$C_{14}H_3N_4$	227.0359
$C_{14}H_{13}N_2O$	225.1029	$C_{14}H_2N_4$	226.0280	$C_{15}H_{31}O$	227.2376
$C_{14}H_{15}N_3$	225.1267	$C_{15}H_{30}O$	226.2298	$C_{15}H_{15}O_2$	227.1072
$C_{14}HN_4$	225.0202	$C_{15}H_{14}O_2$	226.0994	$C_{15}H_{33}N$	227.2615
$C_{15}H_{29}O$	225.2219	$C_{15}H_{32}N$	226.2536	$C_{15}H_{17}NO$	227.1311
$C_{15}H_{13}O_2$	225.0916	$C_{15}H_{16}NO$	226.1233	$C_{15}HNO_2$	227.0007
$C_{15}H_{31}N$	225.2458	$C_{15}NO_2$	225.9929	$C_{15}H_{19}N_2$	227.1549
$C_{15}H_{15}NO$	225.1154	$C_{15}H_{18}N_2$	226.1471	$C_{15}H_3N_2O$	227.0246
$C_{15}H_{17}N_2$	225.1393	$C_{15}H_2N_2O$	226.0167	$C_{15}H_5N_3$	227.0484
$C_{15}HN_2O$	225.0089	$C_{15}H_4N_3$	226.0406	$C_{16}H_{19}O$	227.1436
$C_{15}H_3N_3$	225.0328	$C_{16}H_{34}$	226.2662	$C_{16}H_3O_2$	227.0133
$C_{16}H_{33}$	225.2584	$C_{16}H_{18}O$	226.1358	$C_{16}H_{21}N$	227.1675
$C_{16}H_{17}O$	225.1280	$C_{16}H_2O_2$	226.0054	$C_{16}H_5NO$	227.0371
$C_{16}HO_2$	224.9976	$C_{16}H_{20}N$	226.1597	$C_{16}H_7N_2$	227.0610
$C_{16}H_{19}N$	225.1519	$C_{16}H_4NO$	226.0293	$C_{17}H_{23}$	227.1801
$C_{16}H_3NO$	225.0215	$C_{16}H_6N_2$	226.0532	$C_{17}H_7O$	227.0497
$C_{16}H_5N_2$	225.0453	$C_{17}H_{22}$	226.1722	$C_{17}H_9N$	227.0736
$C_{17}H_{21}$	225.1644	$C_{17}H_6O$	226.0419	$C_{18}H_{11}$	227.0861
$C_{17}H_5O$	225.0340	$C_{17}H_8N$	226.0657	**228**	
$C_{17}H_7N$	225.0579	$C_{18}H_{10}$	226.0783	$C_{10}H_{16}N_2O_4$	228.1111
$C_{18}H_9$	225.0705	**227**		$C_{10}H_{18}N_3O_3$	228.1349
226		$C_{10}H_{15}N_2O_4$	227.1032	$C_{10}H_{20}N_4O_2$	228.1588
$C_{10}H_{14}N_2O_4$	226.0954	$C_{10}H_{17}N_3O_3$	227.1271	$C_{11}H_{18}NO_4$	228.1236
$C_{10}H_{16}N_3O_3$	226.1193	$C_{10}H_{19}N_4O_2$	227.1509	$C_{11}H_{20}N_2O_3$	228.1475
$C_{10}H_{18}N_4O_2$	226.1431	$C_{11}H_{17}NO_4$	227.1158	$C_{11}H_4N_2O_4$	228.0171
$C_{11}H_{16}NO_4$	226.1080	$C_{11}H_{19}N_2O_3$	227.1396	$C_{11}H_{22}N_3O_2$	228.1713
$C_{11}H_{18}N_2O_3$	226.1318	$C_{11}H_3N_2O_4$	227.0093	$C_{11}H_6N_3O_3$	228.0410
$C_{11}H_2N_2O_4$	226.0014	$C_{11}H_{21}N_3O_2$	227.1635	$C_{11}H_{24}N_4O$	228.1952
$C_{11}H_{20}N_3O_2$	226.1557	$C_{11}H_5N_3O_3$	227.0331	$C_{11}H_8N_4O_2$	228.0648
$C_{11}H_4N_3O_3$	226.0253	$C_{11}H_{23}N_4O$	227.1873	$C_{12}H_{20}O_4$	228.1362
$C_{11}H_{22}N_4O$	226.1795	$C_{11}H_7N_4O_2$	227.0570	$C_{12}H_{22}NO_3$	228.1600
$C_{11}H_6N_4O_2$	226.0491	$C_{12}H_{19}O_4$	227.1284	$C_{12}H_6NO_4$	228.0297
$C_{12}H_{18}O_4$	226.1205	$C_{12}H_{21}NO_3$	227.1522	$C_{12}H_{24}N_2O_2$	228.1839
$C_{12}H_{20}NO_3$	226.1444	$C_{12}H_5NO_4$	227.0218	$C_{12}H_8N_2O_3$	228.0535
$C_{12}H_4NO_4$	226.0140	$C_{12}H_{23}N_2O_2$	227.1761	$C_{12}H_{26}N_3O$	228.2077
$C_{12}H_{22}N_2O_2$	226.1682	$C_{12}H_7N_2O_3$	227.0457	$C_{12}H_{10}N_3O_2$	228.0774
$C_{12}H_6N_2O_3$	226.0379	$C_{12}H_{25}N_3O$	227.1999	$C_{12}H_{28}N_4$	228.2316
$C_{12}H_{24}N_3O$	226.1929	$C_{12}H_9N_3O_2$	227.0695	$C_{12}H_{12}N_4O$	228.1012
$C_{12}H_8N_3O_2$	226.0617	$C_{12}H_{27}N_4$	227.2238	$C_{13}H_{24}O_3$	228.1726
$C_{12}H_{26}N_4$	226.2160	$C_{12}H_{11}N_4O$	227.0934	$C_{13}H_8O_4$	228.0422
$C_{12}H_{10}N_4O$	226.0856	$C_{13}H_{23}O_3$	227.1648	$C_{13}H_{26}NO_2$	228.1965
$C_{13}H_{22}O_3$	226.1569	$C_{13}H_7O_4$	227.0344	$C_{13}H_{10}NO_3$	228.0661
$C_{13}H_6O_4$	226.0266	$C_{13}H_{25}NO_2$	227.1886	$C_{13}H_{28}N_2O$	228.2203
$C_{13}H_{24}NO_2$	226.1808	$C_{13}H_9NO_3$	227.0583	$C_{13}H_{12}N_2O_2$	228.0899
$C_{13}H_8NO_3$	226.0504	$C_{13}H_{27}N_2O$	227.2125	$C_{13}H_{30}N_3$	228.2442

Appendix A (continued)

FM		FM		FM	
$C_{13}H_{14}N_3O$	228.1138	$C_{13}H_{31}N_3$	229.2520	$C_{13}N_3O_2$	229.9991
$C_{13}H_{16}N_4$	228.1377	$C_{13}H_{15}N_3O$	229.1216	$C_{13}H_{18}N_4$	230.1533
$C_{13}N_4O$	228.0073	$C_{13}H_{17}N_4$	229.1455	$C_{13}H_2N_4O$	230.0229
$C_{14}H_{28}O_2$	228.2090	$C_{13}HN_4O$	229.0151	$C_{14}H_{30}O_2$	230.2247
$C_{14}H_{12}O_3$	228.0786	$C_{14}H_{29}O_2$	229.2168	$C_{14}H_{14}O_3$	230.0943
$C_{14}H_{30}NO$	228.2329	$C_{14}H_{13}O_3$	229.0865	$C_{14}H_{16}NO_2$	230.1182
$C_{14}H_{14}NO_2$	228.1025	$C_{14}H_{31}NO$	229.2407	$C_{14}NO_3$	229.9878
$C_{14}H_{32}N_2$	228.2567	$C_{14}H_{15}NO_2$	229.1103	$C_{14}H_{18}N_2O$	230.1420
$C_{14}H_{16}N_2O$	228.1264	$C_{14}H_{17}N_2O$	229.1342	$C_{14}H_2N_2O_2$	230.0116
$C_{14}N_2O_2$	227.9960	$C_{14}HN_2O_2$	229.0038	$C_{14}H_{20}N_3$	230.1659
$C_{14}H_{18}N_3$	228.1502	$C_{14}H_{19}N_3$	229.1580	$C_{14}H_4N_3O$	230.0355
$C_{14}H_2N_3O$	228.0198	$C_{14}H_3N_3O$	229.0277	$C_{14}H_6N_4$	230.0594
$C_{14}H_4N_4$	228.0437	$C_{14}H_5N_4$	229.0515	$C_{15}H_{18}O_2$	230.1307
$C_{15}H_{32}O$	228.2454	$C_{15}H_{17}O_2$	229.1229	$C_{15}H_2O_3$	230.0003
$C_{15}H_{16}O_2$	228.1151	$C_{15}HO_3$	228.9925	$C_{15}H_{20}NO$	230.1546
$C_{15}O_3$	227.9847	$C_{15}H_{19}NO$	229.1467	$C_{15}H_4NO_2$	230.0242
$C_{15}H_{18}NO$	228.1389	$C_{15}H_3NO_2$	229.0164	$C_{15}H_{22}N_2$	230.1784
$C_{15}H_2NO_2$	228.0085	$C_{15}H_{21}N_2$	229.1706	$C_{15}H_6N_2O$	230.0480
$C_{15}H_{20}N_2$	228.1628	$C_{15}H_5N_2O$	229.0402	$C_{15}H_8N_3$	230.0719
$C_{15}H_4N_2O$	228.0324	$C_{15}H_7N_3$	229.0641	$C_{16}H_{22}O$	230.1671
$C_{15}H_6N_3$	228.0563	$C_{16}H_{21}O$	229.1593	$C_{16}H_6O_2$	230.0368
$C_{16}H_{20}O$	228.1515	$C_{16}H_5O_2$	229.0289	$C_{16}H_{24}N$	230.1910
$C_{16}H_4O_2$	228.0211	$C_{16}H_{23}N$	229.1832	$C_{16}H_8NO$	230.0606
$C_{16}H_{22}N$	228.1753	$C_{16}H_7NO$	229.0528	$C_{16}H_{10}N_2$	230.0845
$C_{16}H_6NO$	228.0449	$C_{16}H_9N_2$	229.0767	$C_{17}H_{26}$	230.2036
$C_{16}H_8N_2$	228.0688	$C_{17}H_{25}$	229.1957	$C_{17}H_{10}O$	230.0732
$C_{17}H_{24}$	228.1879	$C_{17}H_9O$	229.0653	$C_{17}H_{12}N$	230.0970
$C_{17}H_8O$	228.0575	$C_{17}H_{11}N$	229.0892	$C_{18}H_{14}$	230.1096
$C_{17}H_{10}N$	228.0814	$C_{18}H_{13}$	229.1018	$C_{18}N$	230.0031
$C_{18}H_{12}$	228.0939	$C_{19}H$	229.0078	$C_{19}H_2$	230.0157
C_{19}	228.0000	**230**		**231**	
229		$C_{10}H_{18}N_2O_4$	230.1267	$C_{10}H_{19}N_2O_4$	231.1345
$C_{10}H_{17}N_2O_4$	229.1189	$C_{10}H_{20}N_3O_3$	230.1506	$C_{10}H_{21}N_3O_3$	231.1584
$C_{10}H_{19}N_3O_3$	229.1427	$C_{10}H_{22}N_4O_2$	230.1744	$C_{10}H_{23}N_4O_2$	231.1822
$C_{10}H_{21}N_4O_2$	229.1666	$C_{11}H_{20}NO_4$	230.1393	$C_{11}H_{21}NO_4$	231.1471
$C_{11}H_{19}NO_4$	229.1315	$C_{11}H_{22}N_2O_3$	230.1631	$C_{11}H_{23}N_2O_3$	231.1710
$C_{11}H_{21}N_2O_3$	229.1553	$C_{11}H_6N_2O_4$	230.0328	$C_{11}H_7N_2O_4$	231.0406
$C_{11}H_5N_2O_4$	229.0249	$C_{11}H_{24}N_3O_2$	230.1870	$C_{11}H_{25}N_3O_2$	231.1948
$C_{11}H_{23}N_3O_2$	229.1791	$C_{11}H_8N_3O_3$	230.0566	$C_{11}H_9N_3O_3$	231.0644
$C_{11}H_7N_3O_3$	229.0488	$C_{11}H_{26}N_4O$	230.2108	$C_{11}H_{27}N_4O$	231.2187
$C_{11}H_{25}N_4O$	229.2030	$C_{11}H_{10}N_4O_2$	230.0805	$C_{11}H_{11}N_4O_2$	231.0883
$C_{11}H_9N_4O_2$	229.0726	$C_{12}H_{22}O_4$	230.1518	$C_{12}H_{23}O_4$	231.1597
$C_{12}H_{21}O_4$	229.1440	$C_{12}H_{24}NO_3$	230.1757	$C_{12}H_{25}NO_3$	231.1835
$C_{12}H_{23}NO_3$	229.1679	$C_{12}H_8NO_4$	230.0453	$C_{12}H_9NO_4$	231.0532
$C_{12}H_7NO_4$	229.0375	$C_{12}H_{26}N_2O_2$	230.1996	$C_{12}H_{27}N_2O_2$	231.2074
$C_{12}H_{25}N_2O_2$	229.1917	$C_{12}H_{10}N_2O_3$	230.0692	$C_{12}H_{11}N_2O_3$	231.0770
$C_{12}H_9N_2O_3$	229.0614	$C_{12}H_{28}N_3O$	230.2234	$C_{12}H_{29}N_3O$	231.2312
$C_{12}H_{27}N_3O$	229.2156	$C_{12}H_{12}N_3O_2$	230.0930	$C_{12}H_{13}N_3O_2$	231.1009
$C_{12}H_{11}N_3O_2$	229.0852	$C_{12}H_{30}N_4$	230.2473	$C_{12}H_{15}N_4O$	231.1247
$C_{12}H_{29}N_4$	229.2394	$C_{12}H_{14}N_4O$	230.1169	$C_{13}H_{27}O_3$	231.1961
$C_{12}H_{13}N_4O$	229.1091	$C_{13}H_{26}O_3$	230.1883	$C_{13}H_{11}O_4$	231.0657
$C_{13}H_{25}O_3$	229.1804	$C_{13}H_{10}O_4$	230.0579	$C_{13}H_{29}NO_2$	231.2199
$C_{13}H_9O_4$	229.0501	$C_{13}H_{28}NO_2$	230.2121	$C_{13}H_{13}NO_3$	231.0896
$C_{13}H_{27}NO_2$	229.2043	$C_{13}H_{12}NO_3$	230.0817	$C_{13}H_{15}N_2O_2$	231.1134
$C_{13}H_{11}NO_3$	229.0739	$C_{13}H_{30}N_2O$	230.2360	$C_{13}H_{17}N_3O$	231.1373
$C_{13}H_{29}N_2O$	229.2281	$C_{13}H_{14}N_2O_2$	230.1056	$C_{13}HN_3O_2$	231.0069
$C_{13}H_{13}N_2O_2$	229.0978	$C_{13}H_{16}N_3O$	230.1295	$C_{13}H_{19}N_4$	231.1611

Appendix A (continued)

FM		FM		FM	
$C_{13}H_3N_4O$	231.0308	$C_{14}H_{18}NO_2$	232.1338	$C_{14}H_5N_2O_2$	233.0351
$C_{14}H_{15}O_3$	231.1021	$C_{14}H_2NO_3$	232.0034	$C_{14}H_{23}N_3$	233.1894
$C_{14}H_{17}NO_2$	231.1260	$C_{14}H_{20}N_2O$	232.1577	$C_{14}H_7N_3O$	233.0590
$C_{14}HNO_3$	230.9956	$C_{14}H_4N_2O_2$	232.0273	$C_{14}H_9N_4$	233.0829
$C_{14}H_{19}N_2O$	231.1498	$C_{14}H_{22}N_3$	232.1815	$C_{15}H_{21}O_2$	233.1542
$C_{14}H_3N_2O_2$	231.0195	$C_{14}H_6N_3O$	232.0511	$C_{15}H_5O_3$	233.0238
$C_{14}H_{21}N_3$	231.1737	$C_{14}H_8N_4$	232.0750	$C_{15}H_{23}NO$	233.1781
$C_{14}H_5N_3O$	231.0433	$C_{15}H_{20}O_2$	232.1464	$C_{15}H_7NO_2$	233.0477
$C_{14}H_7N_4$	231.0672	$C_{15}H_4O_3$	232.0160	$C_{15}H_{25}N_2$	233.2019
$C_{15}H_{19}O_2$	231.1385	$C_{15}H_{22}NO$	232.1702	$C_{15}H_9N_2O$	233.0715
$C_{15}H_3O_3$	231.0082	$C_{15}H_6NO_2$	232.0399	$C_{15}H_{11}N_3$	233.0954
$C_{15}H_{21}NO$	231.1624	$C_{15}H_{24}N_2$	232.1941	$C_{16}H_{25}O$	233.1906
$C_{15}H_5NO_2$	231.0320	$C_{15}H_8N_2O$	232.0637	$C_{16}H_9O_2$	233.0603
$C_{15}H_{23}N_2$	231.1863	$C_{15}H_{10}N_3$	232.0876	$C_{16}H_{27}N$	233.2145
$C_{15}H_7N_2O$	231.0559	$C_{16}H_{24}O$	232.1828	$C_{16}H_{11}NO$	233.0841
$C_{15}H_9N_3$	231.0798	$C_{16}H_8O_2$	232.0524	$C_{16}H_{13}N_2$	233.1080
$C_{16}H_{23}O$	231.1750	$C_{16}H_{26}N$	232.2067	$C_{17}H_{29}$	233.2270
$C_{16}H_7O_2$	231.0446	$C_{16}H_{10}NO$	232.0768	$C_{17}H_{13}O$	233.0967
$C_{16}H_{25}N$	231.1988	$C_{16}H_{12}N_2$	232.1001	$C_{17}H_{15}N$	233.1205
$C_{16}H_9NO$	231.0684	$C_{17}H_{28}$	232.2192	$C_{17}HN_2$	233.0140
$C_{16}H_{11}N_2$	231.0923	$C_{17}H_{12}O$	232.0888	$C_{18}H_{17}$	233.1331
$C_{17}H_{27}$	231.2114	$C_{17}H_{14}N$	232.1127	$C_{18}HO$	233.0027
$C_{17}H_{11}O$	231.0810	$C_{17}N_2$	232.0062	$C_{18}H_3N$	233.0266
$C_{17}H_{13}N$	231.1049	$C_{18}H_{16}$	232.1253	$C_{19}H_5$	233.0391
$C_{18}H_{15}$	231.1174	$C_{18}O$	231.9949	**234**	
$C_{18}HN$	231.0109	$C_{18}H_2N$	232.0187	$C_{10}H_{22}N_2O_4$	234.1580
$C_{19}H_3$	231.0235	$C_{19}H_4$	232.0313	$C_{10}H_{24}N_3O_3$	234.1819
232		**233**		$C_{10}H_{26}N_4O_2$	234.2057
$C_{10}H_{20}N_2O_4$	232.1424	$C_{10}H_{21}N_2O_4$	233.1502	$C_{11}H_{24}NO_4$	234.1706
$C_{10}H_{22}N_3O_3$	232.1662	$C_{10}H_{23}N_3O_3$	233.1741	$C_{11}H_{26}N_2O_3$	234.1945
$C_{10}H_{24}N_4O_2$	232.1901	$C_{10}H_{25}N_4O_2$	233.1979	$C_{11}H_{10}N_2O_4$	234.0641
$C_{11}H_{22}NO_4$	232.1549	$C_{11}H_{23}NO_4$	233.1628	$C_{11}H_{12}N_3O_3$	234.0879
$C_{11}H_{24}N_2O_3$	232.1788	$C_{11}H_{25}N_2O_3$	233.1866	$C_{11}H_{14}N_4O_2$	234.1118
$C_{11}H_8N_2O_4$	232.0484	$C_{11}H_9N_2O_4$	233.0563	$C_{12}H_{26}O_4$	234.1832
$C_{11}H_{26}N_3O_2$	232.2026	$C_{11}H_{27}N_3O_2$	233.2105	$C_{12}H_{12}NO_4$	234.0766
$C_{11}H_{10}N_3O_3$	232.0723	$C_{11}H_{11}N_3O_3$	233.0801	$C_{12}H_{14}N_2O_3$	234.1005
$C_{11}H_{28}N_4O$	232.2265	$C_{11}H_{13}N_4O_2$	233.1040	$C_{12}H_{16}N_3O_2$	234.1244
$C_{11}H_{12}N_4O_2$	232.0961	$C_{12}H_{25}O_4$	233.1753	$C_{12}N_3O_3$	233.9940
$C_{12}H_{24}O_4$	232.1675	$C_{12}H_{27}NO_3$	233.1992	$C_{12}H_{18}N_4O$	234.1482
$C_{12}H_{26}NO_3$	232.1914	$C_{12}H_{11}NO_4$	233.0688	$C_{12}H_2N_4O_2$	234.0178
$C_{12}H_{10}NO_4$	232.0610	$C_{12}H_{13}N_2O_3$	233.0927	$C_{13}H_{14}O_4$	234.0892
$C_{12}H_{28}N_2O_2$	232.2152	$C_{12}H_{15}N_3O_2$	233.1165	$C_{13}H_{16}NO_3$	234.1131
$C_{12}H_{12}N_2O_3$	232.0848	$C_{12}H_{17}N_4O$	233.1404	$C_{13}NO_4$	233.9827
$C_{12}H_{14}N_3O_2$	232.1087	$C_{12}HN_4O_2$	233.0100	$C_{13}H_{18}N_2O_2$	234.1369
$C_{12}H_{16}N_4O$	232.1325	$C_{13}H_{13}O_4$	233.0814	$C_{13}H_2N_2O_3$	234.0065
$C_{12}N_4O_2$	232.0022	$C_{13}H_{15}NO_3$	233.1052	$C_{13}H_{20}N_3O$	234.1608
$C_{13}H_{28}O_3$	232.2039	$C_{13}H_{17}N_2O_2$	233.1291	$C_{13}H_4N_3O_2$	234.0304
$C_{13}H_{12}O_4$	232.0735	$C_{13}HN_2O_3$	232.9987	$C_{13}H_{22}N_4$	234.1846
$C_{13}H_{14}NO_3$	232.0974	$C_{13}H_{19}N_3O$	233.1529	$C_{13}H_6N_4O$	234.0542
$C_{13}H_{16}N_2O_2$	232.1213	$C_{13}H_3N_3O_2$	233.0226	$C_{14}H_{18}O_3$	234.1256
$C_{13}N_2O_3$	231.9909	$C_{13}H_{21}N_4$	233.1768	$C_{14}H_2O_4$	233.9953
$C_{13}H_{18}N_3O$	232.1451	$C_{13}H_5N_4O$	233.0464	$C_{14}H_{20}NO_2$	234.1495
$C_{13}H_2N_3O_2$	232.0147	$C_{14}H_{17}O_3$	233.1178	$C_{14}H_4NO_3$	234.0191
$C_{13}H_{20}N_4$	232.1690	$C_{14}HO_4$	232.9874	$C_{14}H_{22}N_2O$	234.1733
$C_{13}H_4N_4O$	232.0386	$C_{14}H_{19}NO_2$	233.1416	$C_{14}H_6N_2O_2$	234.0429
$C_{14}H_{16}O_3$	232.1100	$C_{14}H_3NO_3$	233.0113	$C_{14}H_{24}N_3$	234.1972
$C_{14}O_4$	231.9796	$C_{14}H_{21}N_2O$	233.1655	$C_{14}H_8N_3O$	234.0668

Appendix A (continued)

FM		FM		FM	
$C_{14}H_{10}N_4$	234.0907	$C_{15}H_9NO_2$	235.0634	$C_{16}H_{28}O$	236.2141
$C_{15}H_{22}O_2$	234.1620	$C_{15}H_{27}N_2$	235.2176	$C_{16}H_{12}O_2$	236.0837
$C_{15}H_6O_3$	234.0317	$C_{15}H_{11}N_2O$	235.0872	$C_{16}H_{30}N$	236.2380
$C_{15}H_{24}NO$	234.1859	$C_{15}H_{13}N_3$	235.1111	$C_{16}H_{14}NO$	236.1076
$C_{15}H_8NO_2$	234.0555	$C_{16}H_{27}O$	235.2063	$C_{16}H_{16}N_2$	236.1315
$C_{15}H_{26}N_2$	234.2098	$C_{16}H_{11}O_2$	235.0759	$C_{16}N_2O$	236.0011
$C_{15}H_{10}N_2O$	234.0794	$C_{16}H_{29}N$	235.2301	$C_{16}H_2N_3$	236.0249
$C_{15}H_{12}N_3$	234.1032	$C_{16}H_{13}NO$	235.0998	$C_{17}H_{32}$	236.2505
$C_{16}H_{26}O$	234.1985	$C_{16}H_{15}N_2$	235.1236	$C_{17}H_{16}O$	236.1202
$C_{16}H_{10}O_2$	234.0681	$C_{16}HN_3$	235.0171	$C_{17}O_2$	235.9898
$C_{16}H_{28}N$	234.2223	$C_{17}H_{31}$	235.2427	$C_{17}H_{18}N$	236.1440
$C_{16}H_{12}NO$	234.0919	$C_{17}H_{15}O$	235.1123	$C_{17}H_2NO$	236.0136
$C_{16}H_{14}N_2$	234.1158	$C_{17}H_{17}N$	235.1362	$C_{17}H_4N_2$	236.0375
$C_{16}N_3$	234.0093	$C_{17}HNO$	235.0058	$C_{18}H_{20}$	236.1566
$C_{17}H_{30}$	234.2349	$C_{17}H_3N_2$	235.0297	$C_{18}H_4O$	236.0262
$C_{17}H_{14}O$	234.1045	$C_{18}H_{19}$	235.1488	$C_{18}H_6N$	236.0501
$C_{17}H_{16}N$	234.1284	$C_{18}H_3O$	235.0184	$C_{19}H_8$	236.0626
$C_{17}NO$	233.9980	$C_{18}H_5N$	235.0422	**237**	
$C_{17}H_2N_2$	234.0218	$C_{19}H_7$	235.0548	$C_{11}H_{13}N_2O_4$	237.0876
$C_{18}H_{18}$	234.1409	**236**		$C_{11}H_{15}N_3O_3$	237.1114
$C_{18}H_2O$	234.0106	$C_{10}H_{24}N_2O_4$	236.1737	$C_{11}H_{17}N_4O_2$	237.1353
$C_{18}H_4N$	234.0344	$C_{11}H_{12}N_2O_4$	236.0797	$C_{12}H_{15}NO_4$	237.1001
$C_{19}H_6$	234.0470	$C_{11}H_{14}N_3O_3$	236.1036	$C_{12}H_{17}N_2O_3$	237.1240
235		$C_{11}H_{16}N_4O_2$	236.1275	$C_{12}HN_2O_4$	236.9936
$C_{10}H_{23}N_2O_4$	235.1659	$C_{12}H_{14}NO_4$	236.0923	$C_{12}H_{19}N_3O_2$	237.1478
$C_{10}H_{25}N_3O_3$	235.1897	$C_{12}H_{16}N_2O_3$	236.1162	$C_{12}H_3N_3O_3$	237.0175
$C_{11}H_{25}NO_4$	235.1784	$C_{12}N_2O_4$	235.9858	$C_{12}H_{21}N_4O$	237.1717
$C_{11}H_{11}N_2O_4$	235.0719	$C_{12}H_{18}N_3O_2$	236.1400	$C_{12}H_5N_4O_2$	237.0413
$C_{11}H_{13}N_3O_3$	235.0958	$C_{12}H_2N_3O_3$	236.0096	$C_{13}H_{17}O_4$	237.1127
$C_{11}H_{15}N_4O_2$	235.1196	$C_{12}H_{20}N_4O$	236.1639	$C_{13}H_{19}NO_3$	237.1365
$C_{12}H_{13}NO_4$	235.0845	$C_{12}H_4N_4O_2$	236.0335	$C_{13}H_3NO_4$	237.0062
$C_{12}H_{15}N_2O_3$	235.1083	$C_{13}H_{16}O_4$	236.1049	$C_{13}H_{21}N_2O_2$	237.1604
$C_{12}H_{17}N_3O_2$	235.1322	$C_{13}H_{18}NO_3$	236.1287	$C_{13}H_5N_2O_3$	237.0300
$C_{12}HN_3O_3$	235.0018	$C_{13}H_2NO_4$	235.9983	$C_{13}H_{23}N_3O$	237.1842
$C_{12}H_{19}N_4O$	235.1560	$C_{13}H_{20}N_2O_2$	236.1526	$C_{13}H_7N_3O_2$	237.0539
$C_{12}H_3N_4O_2$	235.0257	$C_{13}H_4N_2O_3$	236.0222	$C_{13}H_{25}N_4$	237.2081
$C_{13}H_{15}O_4$	235.0970	$C_{13}H_{22}N_3O$	236.1764	$C_{13}H_9N_4O$	237.0777
$C_{13}H_{17}NO_3$	235.1209	$C_{13}H_6N_3O_2$	236.0460	$C_{14}H_{21}O_3$	237.1491
$C_{13}HNO_4$	234.9905	$C_{13}H_{24}N_4$	236.2003	$C_{14}H_5O_4$	237.0187
$C_{13}H_{19}N_2O_2$	235.1447	$C_{13}H_8N_4O$	236.0699	$C_{14}H_{23}NO_2$	237.1730
$C_{13}H_3N_2O_3$	235.0144	$C_{14}H_{20}O_3$	236.1413	$C_{14}H_7NO_3$	237.0426
$C_{13}H_{21}N_3O$	235.1686	$C_{14}H_4O_4$	236.0109	$C_{14}H_{25}N_2O$	237.1968
$C_{13}H_5N_3O_2$	235.0382	$C_{14}H_{22}NO_2$	236.1651	$C_{14}H_9N_2O_2$	237.0664
$C_{13}H_{23}N_4$	235.1925	$C_{14}H_6NO_3$	236.0348	$C_{14}H_{27}N_3$	237.2207
$C_{13}H_7N_4O$	235.0621	$C_{14}H_{24}N_2O$	236.1890	$C_{14}H_{11}N_3O$	237.0903
$C_{14}H_{19}O_3$	235.1334	$C_{14}H_8N_2O_2$	236.0586	$C_{14}H_{13}N_4$	237.1142
$C_{14}H_3O_4$	235.0031	$C_{14}H_{26}N_3$	236.2129	$C_{15}H_{25}O_2$	237.1855
$C_{14}H_{21}NO_2$	235.1573	$C_{14}H_{10}N_3O$	236.0825	$C_{15}H_9O_3$	237.0552
$C_{14}H_5NO_3$	235.0269	$C_{14}H_{12}N_4$	236.1063	$C_{15}H_{27}NO$	237.2094
$C_{14}H_{23}N_2O$	235.1811	$C_{15}H_{24}O_2$	236.1777	$C_{15}H_{11}NO_2$	237.0790
$C_{14}H_7N_2O_2$	235.0508	$C_{15}H_8O_3$	236.0473	$C_{15}H_{29}N_2$	237.2332
$C_{14}H_{25}N_3$	235.2050	$C_{15}H_{26}NO$	236.2015	$C_{15}H_{13}N_2O$	237.1029
$C_{14}H_9N_3O$	235.0746	$C_{15}H_{10}NO_2$	236.0712	$C_{15}H_{15}N_3$	237.1267
$C_{14}H_{11}N_4$	235.0985	$C_{15}H_{28}N_2$	236.2254	$C_{15}HN_4$	237.0202
$C_{15}H_{23}O_2$	235.1699	$C_{15}H_{12}N_2O$	236.0950	$C_{16}H_{29}O$	237.2219
$C_{15}H_7O_3$	235.0395	$C_{15}H_{14}N_3$	236.1189	$C_{16}H_{13}O_2$	237.0916
$C_{15}H_{25}NO$	235.1937	$C_{15}N_4$	236.0124	$C_{16}H_{31}N$	237.2458

Appendix A (continued)

FM		FM		FM	
$C_{16}H_{15}NO$	237.1154	$C_{16}H_{18}N_2$	238.1471	$C_{16}H_3N_2O$	239.0246
$C_{16}H_{17}N_2$	237.1393	$C_{16}H_2N_2O$	238.0167	$C_{16}H_5N_3$	239.0484
$C_{16}HN_2O$	237.0089	$C_{16}H_4N_3$	238.0406	$C_{17}H_{35}$	239.2740
$C_{16}H_3N_3$	237.0328	$C_{17}H_{34}$	238.2662	$C_{17}H_{19}O$	239.1436
$C_{17}H_{33}$	237.2584	$C_{17}H_{18}O$	238.1358	$C_{17}H_3O_2$	239.0133
$C_{17}H_{17}O$	237.1280	$C_{17}H_2O_2$	238.0054	$C_{17}H_{21}N$	239.1675
$C_{17}HO_2$	236.9976	$C_{17}H_{20}N$	238.1597	$C_{17}H_5NO$	239.0371
$C_{17}H_{19}N$	237.1519	$C_{17}H_4NO$	238.0293	$C_{17}H_7N_2$	239.0610
$C_{17}H_3NO$	237.0215	$C_{17}H_6N_2$	238.0532	$C_{18}H_{23}$	239.1801
$C_{17}H_5N_2$	237.0453	$C_{18}H_{22}$	238.1722	$C_{18}H_7O$	239.0497
$C_{18}H_{21}$	237.1644	$C_{18}H_6O$	238.0419	$C_{18}H_9N$	239.0736
$C_{18}H_5O$	237.0340	$C_{18}H_8N$	238.0657	$C_{19}H_{11}$	239.0861
$C_{18}H_7N$	237.0579	$C_{19}H_{10}$	238.0783	**240**	
$C_{19}H_9$	237.0705	**239**		$C_{11}H_{16}N_2O_4$	240.1111
238		$C_{11}H_{15}N_2O_4$	239.1032	$C_{11}H_{18}N_3O_3$	240.1349
$C_{11}H_{14}N_2O_4$	238.0954	$C_{11}H_{17}N_3O_3$	239.1271	$C_{11}H_{20}N_4O_2$	240.1588
$C_{11}H_{16}N_3O_3$	238.1193	$C_{11}H_{19}N_4O_2$	239.1509	$C_{12}H_{18}NO_4$	240.1236
$C_{11}H_{18}N_4O_2$	238.1431	$C_{12}H_{17}NO_4$	239.1158	$C_{12}H_{20}N_2O_3$	240.1475
$C_{12}H_{16}NO_4$	238.1080	$C_{12}H_{19}N_2O_3$	239.1396	$C_{12}H_4N_2O_4$	240.0171
$C_{12}H_{18}N_2O_3$	238.1318	$C_{12}H_3N_2O_4$	239.0093	$C_{12}H_{22}N_3O_2$	240.1713
$C_{12}H_2N_2O_4$	238.0014	$C_{12}H_{21}N_3O_2$	239.1635	$C_{12}H_6N_3O_3$	240.0410
$C_{12}H_{20}N_3O_2$	238.1557	$C_{12}H_5N_3O_3$	239.0331	$C_{12}H_{24}N_4O$	240.1952
$C_{12}H_4N_3O_3$	238.0253	$C_{12}H_{23}N_4O$	239.1873	$C_{12}H_8N_4O_2$	240.0648
$C_{12}H_{22}N_4O$	238.1795	$C_{12}H_7N_4O_2$	239.0570	$C_{13}H_{20}O_4$	240.1362
$C_{12}H_6N_4O_2$	238.0491	$C_{13}H_{19}O_4$	239.1284	$C_{13}H_{22}NO_3$	240.1600
$C_{13}H_{18}O_4$	238.1205	$C_{13}H_{21}NO_3$	239.1522	$C_{13}H_6NO_4$	240.0297
$C_{13}H_{20}NO_3$	238.1444	$C_{13}H_5NO_4$	239.0218	$C_{13}H_{24}N_2O_2$	240.1839
$C_{13}H_4NO_4$	238.0140	$C_{13}H_{23}N_2O_2$	239.1761	$C_{13}H_8N_2O_3$	240.0535
$C_{13}H_{22}N_2O_2$	238.1682	$C_{13}H_7N_2O_3$	239.0457	$C_{13}H_{26}N_3O$	240.2077
$C_{13}H_6N_2O_3$	238.0379	$C_{13}H_{25}N_3O$	239.1999	$C_{13}H_{10}N_3O_2$	240.0774
$C_{13}H_{24}N_3O$	238.1921	$C_{13}H_9N_3O_2$	239.0695	$C_{13}H_{28}N_4$	240.2316
$C_{13}H_8N_3O_2$	238.0617	$C_{13}H_{27}N_4$	239.2238	$C_{13}H_{12}N_4O$	240.1012
$C_{13}H_{26}N_4$	238.2160	$C_{13}H_{11}N_4O$	239.0934	$C_{14}H_{24}O_3$	240.1726
$C_{13}H_{10}N_4O$	238.0856	$C_{14}H_{23}O_3$	239.1648	$C_{14}H_8O_4$	240.0422
$C_{14}H_{22}O_3$	238.1569	$C_{14}H_7O_4$	239.0344	$C_{14}H_{26}NO_2$	240.1965
$C_{14}H_6O_4$	238.0266	$C_{14}H_{25}NO_2$	239.1886	$C_{14}H_{10}NO_3$	240.0661
$C_{14}H_{24}NO_2$	238.1808	$C_{14}H_9NO_3$	239.0583	$C_{14}H_{28}N_2O$	240.2203
$C_{14}H_8NO_3$	238.0504	$C_{14}H_{27}N_2O$	239.2125	$C_{14}H_{12}N_2O_2$	240.0899
$C_{14}H_{26}N_2O$	238.2046	$C_{14}H_{11}N_2O_2$	239.0821	$C_{14}H_{30}N_3$	240.2442
$C_{14}H_{10}N_2O_2$	238.0743	$C_{14}H_{29}N_3$	239.2363	$C_{14}H_{14}N_3O$	240.1138
$C_{14}H_{28}N_3$	238.2285	$C_{14}H_{13}N_3O$	239.1060	$C_{14}H_{16}N_4$	240.1377
$C_{14}H_{12}N_3O$	238.0981	$C_{14}H_{15}N_4$	239.1298	$C_{14}N_4O$	240.0073
$C_{14}H_{14}N_4$	238.1220	$C_{15}H_{27}O_2$	239.2012	$C_{15}H_{28}O_2$	240.2090
$C_{15}H_{26}O_2$	238.1934	$C_{15}H_{11}O_3$	239.0708	$C_{15}H_{12}O_3$	240.0786
$C_{15}H_{10}O_3$	238.0630	$C_{15}H_{29}NO$	239.2250	$C_{15}H_{30}NO$	240.2329
$C_{15}H_{28}NO$	238.2172	$C_{15}H_{13}NO_2$	239.0947	$C_{15}H_{14}NO_2$	240.1025
$C_{15}H_{12}NO_2$	238.0868	$C_{15}H_{31}N_2$	239.2489	$C_{15}H_{32}N_2$	240.2567
$C_{15}H_{30}N_2$	238.2411	$C_{15}H_{15}N_2O$	239.1185	$C_{15}H_{16}N_2O$	240.1264
$C_{15}H_{14}N_2O$	238.1107	$C_{15}H_{17}N_3$	239.1424	$C_{15}N_2O_2$	239.9960
$C_{15}H_{16}N_3$	238.1346	$C_{15}HN_3O$	239.0120	$C_{15}H_{18}N_3$	240.1502
$C_{15}N_3O$	238.0042	$C_{15}H_3N_4$	239.0359	$C_{15}H_2N_3O$	240.0198
$C_{15}H_2N_4$	238.0280	$C_{16}H_{31}O$	239.2376	$C_{15}H_4N_4$	240.0437
$C_{16}H_{30}O$	238.2298	$C_{16}H_{15}O_2$	239.1072	$C_{16}H_{32}O$	240.2454
$C_{16}H_{14}O_2$	238.0994	$C_{16}H_{33}N$	239.2615	$C_{16}H_{16}O_2$	240.1151
$C_{16}H_{32}N$	238.2536	$C_{16}H_{17}NO$	239.1311	$C_{16}O_3$	239.9847
$C_{16}H_{16}NO$	238.1233	$C_{16}HNO_2$	239.0007	$C_{16}H_{34}N$	240.2693
$C_{16}NO_2$	237.9929	$C_{16}H_{19}N_2$	239.1549	$C_{16}H_{18}NO$	240.1389

Appendix A (continued)

FM		FM		FM	
$C_{16}H_2NO_2$	240.0085	$C_{16}HO_3$	240.9925	$C_{15}H_4N_3O$	242.0355
$C_{16}H_{20}N_2$	240.1628	$C_{16}H_{35}N$	241.2771	$C_{15}H_6N_4$	242.0594
$C_{16}H_4N_2O$	240.0324	$C_{16}H_{19}NO$	241.1467	$C_{16}H_{34}O$	242.2611
$C_{16}H_6N_3$	240.0563	$C_{16}H_3NO_2$	241.0164	$C_{16}H_{18}O_2$	242.1307
$C_{17}H_{36}$	240.2819	$C_{16}H_{21}N_2$	241.1706	$C_{16}H_2O_3$	242.0003
$C_{17}H_{20}O$	240.1515	$C_{16}H_5N_2O$	241.0402	$C_{16}H_{20}NO$	242.1546
$C_{17}H_4O_2$	240.0211	$C_{16}H_7N_3$	241.0641	$C_{16}H_4NO_2$	242.0242
$C_{17}H_{22}N$	240.1753	$C_{17}H_{21}O$	241.1593	$C_{16}H_{22}N_2$	242.1784
$C_{17}H_6NO$	240.0449	$C_{17}H_5O_2$	241.0289	$C_{16}H_6N_2O$	242.0480
$C_{17}H_8N_2$	240.0688	$C_{17}H_{23}N$	241.1832	$C_{16}H_8N_3$	242.0719
$C_{18}H_{24}$	240.1879	$C_{17}H_7NO$	241.0528	$C_{17}H_{22}O$	242.1671
$C_{18}H_8O$	240.0575	$C_{17}H_9N_2$	241.0767	$C_{17}H_6O_2$	242.0368
$C_{18}H_{10}N$	240.0814	$C_{18}H_{25}$	241.1957	$C_{17}H_{24}N$	242.1910
$C_{19}H_{12}$	240.0939	$C_{18}H_9O$	241.0653	$C_{17}H_8NO$	242.0606
C_{20}	240.0000	$C_{18}H_{11}N$	241.0892	$C_{17}H_{10}N_2$	242.0845
241		$C_{19}H_{13}$	241.1018	$C_{18}H_{26}$	242.2036
$C_{11}H_{17}N_2O_4$	241.1189	$C_{20}H$	241.0078	$C_{18}H_{10}O$	242.0732
$C_{11}H_{19}N_3O_3$	241.1427	**242**		$C_{18}H_{12}N$	242.0970
$C_{11}H_{21}N_4O_2$	241.1666	$C_{11}H_{18}N_2O_4$	242.1267	$C_{19}H_{14}$	242.1096
$C_{12}H_{19}NO_4$	241.1315	$C_{11}H_{20}N_3O_3$	242.1506	$C_{19}N$	242.0031
$C_{12}H_{21}N_2O_3$	241.1553	$C_{11}H_{22}N_4O_2$	242.1744	$C_{20}H_2$	242.0157
$C_{12}H_5N_2O_4$	241.0249	$C_{12}H_{20}NO_4$	242.1393	**243**	
$C_{12}H_{23}N_3O_2$	241.1791	$C_{12}H_{22}N_2O_3$	242.1631	$C_{11}H_{19}N_2O_4$	243.1345
$C_{12}H_7N_3O_3$	241.0488	$C_{12}H_6N_2O_4$	242.0328	$C_{11}H_{21}N_3O_3$	243.1584
$C_{12}H_{25}N_4O$	241.2030	$C_{12}H_{24}N_3O_2$	242.1870	$C_{11}H_{23}N_4O_2$	243.1822
$C_{12}H_9N_4O_2$	241.0726	$C_{12}H_8N_3O_3$	242.0566	$C_{12}H_{21}NO_4$	243.1471
$C_{13}H_{21}O_4$	241.1440	$C_{12}H_{26}N_4O$	242.2108	$C_{12}H_{23}N_2O_3$	243.1710
$C_{13}H_{23}NO_3$	241.1679	$C_{12}H_{10}N_4O_2$	242.0805	$C_{12}H_7N_2O_4$	243.0406
$C_{13}H_7NO_4$	241.0375	$C_{13}H_{22}O_4$	242.1518	$C_{12}H_{25}N_3O_2$	243.1948
$C_{13}H_{25}N_2O_2$	241.1917	$C_{13}H_{24}NO_3$	242.1757	$C_{12}H_9N_3O_3$	243.0644
$C_{13}H_9N_2O_3$	241.0614	$C_{13}H_8NO_4$	242.0453	$C_{12}H_{27}N_4O$	243.2187
$C_{13}H_{27}N_3O$	241.2156	$C_{13}H_{26}N_2O_2$	242.1996	$C_{12}H_{11}N_4O_2$	243.0883
$C_{13}H_{11}N_3O_2$	241.0852	$C_{13}H_{10}N_2O_3$	242.0692	$C_{13}H_{23}O_4$	243.1597
$C_{13}H_{29}N_4$	241.2394	$C_{13}H_{28}N_3O$	242.2234	$C_{13}H_{25}NO_3$	243.1835
$C_{13}H_{13}N_4O$	241.1091	$C_{13}H_{12}N_3O_2$	242.0930	$C_{13}H_9NO_4$	243.0532
$C_{14}H_{25}O_3$	241.1804	$C_{13}H_{30}N_4$	242.2473	$C_{13}H_{27}N_2O_2$	243.2074
$C_{14}H_9O_4$	241.0501	$C_{13}H_{14}N_4O$	242.1169	$C_{13}H_{11}N_2O_3$	243.0770
$C_{14}H_{27}NO_2$	241.2043	$C_{14}H_{26}O_3$	242.1883	$C_{13}H_{29}N_3O$	243.2312
$C_{14}H_{11}NO_3$	241.0739	$C_{14}H_{10}O_4$	242.0579	$C_{13}H_{13}N_3O_2$	243.1009
$C_{14}H_{29}N_2O$	241.2281	$C_{14}H_{28}NO_2$	242.2121	$C_{13}H_{31}N_4$	243.2551
$C_{14}H_{13}N_2O_2$	241.0978	$C_{14}H_{12}NO_3$	242.0817	$C_{13}H_{15}N_4O$	243.1247
$C_{14}H_{31}N_3$	241.2520	$C_{14}H_{30}N_2O$	242.2360	$C_{14}H_{27}O_3$	243.1961
$C_{14}H_{15}N_3O$	241.1216	$C_{14}H_{14}N_2O_2$	242.1056	$C_{14}H_{11}O_4$	243.0657
$C_{14}H_{17}N_4$	241.1455	$C_{14}H_{32}N_3$	242.2598	$C_{14}H_{29}NO_2$	243.2199
$C_{14}HN_4O$	241.0151	$C_{14}H_{16}N_3O$	242.1295	$C_{14}H_{13}NO_3$	243.0896
$C_{15}H_{29}O_2$	241.2168	$C_{14}N_3O_2$	241.9991	$C_{14}H_{31}N_2O$	243.2438
$C_{15}H_{13}O_3$	241.0865	$C_{14}H_{18}N_4$	242.1533	$C_{14}H_{15}N_2O_2$	243.1134
$C_{15}H_{31}NO$	241.2407	$C_{14}H_2N_4O$	242.0229	$C_{14}H_{33}N_3$	243.2677
$C_{15}H_{15}NO_2$	241.1103	$C_{15}H_{30}O_2$	242.2247	$C_{14}H_{17}N_3O$	243.1373
$C_{15}H_{33}N_2$	241.2646	$C_{15}H_{14}O_3$	242.0943	$C_{14}HN_3O_2$	243.0069
$C_{15}H_{17}N_2O$	241.1342	$C_{15}H_{32}NO$	242.2485	$C_{14}H_{19}N_4$	243.1611
$C_{15}HN_2O_2$	241.0038	$C_{15}H_{16}NO_2$	242.1182	$C_{14}H_3N_4O$	243.0308
$C_{15}H_{19}N_3$	241.1580	$C_{15}NO_3$	241.9878	$C_{15}H_{31}O_2$	243.2325
$C_{15}H_3N_3O$	241.0277	$C_{15}H_{34}N_2$	242.2724	$C_{15}H_{15}O_3$	243.1021
$C_{15}H_5N_4$	241.0515	$C_{15}H_{18}N_2O$	242.1420	$C_{15}H_{33}NO$	243.2564
$C_{16}H_{33}O$	241.2533	$C_{15}H_2N_2O_2$	242.0116	$C_{15}H_{17}NO_2$	243.1260
$C_{16}H_{17}O_2$	241.1229	$C_{15}H_{20}N_3$	242.1659	$C_{15}HNO_3$	242.9956

Appendix A (continued)

	FM		FM		FM
$C_{15}H_{19}N_2O$	243.1498	$C_{15}O_4$	243.9796	$C_{14}H_5N_4O$	245.0464
$C_{15}H_3N_2O_2$	243.0195	$C_{15}H_{18}NO_2$	244.1338	$C_{15}H_{17}O_3$	245.1178
$C_{15}H_{21}N_3$	243.1737	$C_{15}H_2NO_3$	244.0034	$C_{15}HO_4$	244.9874
$C_{15}H_5N_3O$	243.0433	$C_{15}H_{20}N_2O$	244.1577	$C_{15}H_{19}NO_2$	245.1416
$C_{15}H_7N_4$	243.0672	$C_{15}H_4N_2O_2$	244.0273	$C_{15}H_3NO_3$	245.0113
$C_{16}H_{19}O_2$	243.1385	$C_{15}H_{22}N_3$	244.1815	$C_{15}H_{21}N_2O$	245.1655
$C_{16}H_3O_3$	243.0082	$C_{15}H_6N_3O$	244.0511	$C_{15}H_5N_2O_2$	245.0351
$C_{16}H_{21}NO$	243.1624	$C_{15}H_8N_4$	244.0750	$C_{15}H_{23}N_3$	245.1894
$C_{16}H_5NO_2$	243.0320	$C_{16}H_{20}O_2$	244.1464	$C_{15}H_7N_3O$	245.0590
$C_{16}H_{23}N_2$	243.1863	$C_{16}H_4O_3$	244.0160	$C_{15}H_9N_4$	245.0829
$C_{16}H_7N_2O$	243.0559	$C_{16}H_{22}NO$	244.1702	$C_{16}H_{21}O_2$	245.1542
$C_{16}H_9N_3$	243.0798	$C_{16}H_6NO_2$	244.0399	$C_{16}H_5O_3$	245.0238
$C_{17}H_{23}O$	243.1750	$C_{16}H_{24}N_2$	244.1941	$C_{16}H_{23}NO$	245.1781
$C_{17}H_7O_2$	243.0446	$C_{16}H_8N_2O$	244.0637	$C_{16}H_7NO_2$	245.0477
$C_{17}H_{25}N$	243.1988	$C_{16}H_{10}N_3$	244.0876	$C_{16}H_{25}N_2$	245.2019
$C_{17}H_9NO$	243.0684	$C_{17}H_{24}O$	244.1828	$C_{16}H_9N_2O$	245.0715
$C_{17}H_{11}N_2$	243.0923	$C_{17}H_8O_2$	244.0524	$C_{16}H_{11}N_3$	245.0954
$C_{18}H_{27}$	243.2114	$C_{17}H_{26}N$	244.2067	$C_{17}H_{25}O$	245.1906
$C_{18}H_{11}O$	243.0810	$C_{17}H_{10}NO$	244.0763	$C_{17}H_9O_2$	245.0603
$C_{18}H_{13}N$	243.1049	$C_{17}H_{12}N_2$	244.1001	$C_{17}H_{27}N$	245.2145
$C_{19}H_{15}$	243.1174	$C_{18}H_{28}$	244.2192	$C_{17}H_{11}NO$	245.0841
$C_{19}HN$	243.0109	$C_{18}H_{12}O$	244.0888	$C_{17}H_{13}N_2$	245.1080
$C_{20}H_3$	243.0235	$C_{18}H_{14}N$	244.1127	$C_{18}H_{29}$	245.2270
244		$C_{18}N_2$	244.0062	$C_{18}H_{13}O$	245.0967
$C_{11}H_{20}N_2O_4$	244.1424	$C_{19}H_{16}$	244.1253	$C_{18}H_{15}N$	245.1205
$C_{11}H_{22}N_3O_3$	244.1662	$C_{19}O$	243.9949	$C_{18}HN_2$	245.0140
$C_{11}H_{24}N_4O_2$	244.1901	$C_{19}H_2N$	244.0187	$C_{19}H_{17}$	245.1331
$C_{12}H_{22}NO_4$	244.1549	$C_{20}H_4$	244.0313	$C_{19}HO$	245.0027
$C_{12}H_{24}N_2O_3$	244.1788	**245**		$C_{19}H_3N$	245.0266
$C_{12}H_8N_2O_4$	244.0484	$C_{11}H_{21}N_2O_4$	245.1502	$C_{20}H_5$	245.0391
$C_{12}H_{26}N_3O_2$	244.2026	$C_{11}H_{23}N_3O_3$	245.1741	**246**	
$C_{12}H_{10}N_3O_3$	244.0723	$C_{11}H_{25}N_4O_2$	245.1979	$C_{11}H_{22}N_2O_4$	246.1580
$C_{12}H_{28}N_4O$	244.2265	$C_{12}H_{23}NO_4$	245.1628	$C_{11}H_{24}N_3O_3$	246.1819
$C_{12}H_{12}N_4O_2$	244.0961	$C_{12}H_{25}N_2O_3$	245.1866	$C_{11}H_{26}N_4O_2$	246.2057
$C_{13}H_{24}O_4$	244.1675	$C_{12}H_9N_2O_4$	245.0563	$C_{12}H_{24}NO_4$	246.1706
$C_{13}H_{26}NO_3$	244.1914	$C_{12}H_{27}N_3O_2$	245.2105	$C_{12}H_{26}N_2O_3$	246.1945
$C_{13}H_{10}NO_4$	244.0610	$C_{12}H_{11}N_3O_3$	245.0801	$C_{12}H_{10}N_2O_4$	246.0641
$C_{13}H_{28}N_2O_2$	244.2152	$C_{12}H_{29}N_4O$	245.2343	$C_{12}H_{28}N_3O_2$	246.2183
$C_{13}H_{12}N_2O_3$	244.0848	$C_{12}H_{13}N_4O_2$	245.1040	$C_{12}H_{12}N_3O_3$	246.0879
$C_{13}H_{30}N_3O$	244.2391	$C_{13}H_{25}O_4$	245.1753	$C_{12}H_{30}N_4O$	246.2422
$C_{13}H_{14}N_3O_2$	244.1087	$C_{13}H_{27}NO_3$	245.1992	$C_{12}H_{14}N_4O_2$	246.1118
$C_{13}H_{32}N_4$	244.2629	$C_{13}H_{11}NO_4$	245.0688	$C_{13}H_{26}O_4$	246.1832
$C_{13}H_{16}N_4O$	244.1325	$C_{13}H_{29}N_2O_2$	245.2230	$C_{13}H_{28}NO_3$	246.2070
$C_{13}N_4O_2$	244.0022	$C_{13}H_{13}N_2O_3$	245.0927	$C_{13}H_{12}NO_4$	246.0766
$C_{14}H_{28}O_3$	244.2039	$C_{13}H_{31}N_3O$	245.2469	$C_{13}H_{30}N_2O_2$	246.2309
$C_{14}H_{12}O_4$	244.0735	$C_{13}H_{15}N_3O_2$	245.1165	$C_{13}H_{14}N_2O_3$	246.1005
$C_{14}H_{30}NO_2$	244.2278	$C_{13}H_{17}N_4O$	245.1404	$C_{13}H_{16}N_3O_2$	246.1244
$C_{14}H_{14}NO_3$	244.0974	$C_{13}HN_4O_2$	245.0100	$C_{13}N_3O_3$	245.9940
$C_{14}H_{32}N_2O$	244.2516	$C_{14}H_{29}O_3$	245.2117	$C_{13}H_{18}N_4O$	246.1482
$C_{14}H_{16}N_2O_2$	244.1213	$C_{14}H_{13}O_4$	245.0814	$C_{13}H_2N_4O_2$	246.0178
$C_{14}N_2O_3$	243.9909	$C_{14}H_{31}NO_2$	245.2356	$C_{14}H_{30}O_3$	246.2196
$C_{14}H_{18}N_3O$	244.1451	$C_{14}H_{15}NO_3$	245.1052	$C_{14}H_{14}O_4$	246.0892
$C_{14}H_2N_3O_2$	244.0147	$C_{14}H_{17}N_2O_2$	245.1291	$C_{14}H_{16}NO_3$	246.1131
$C_{14}H_{20}N_4$	244.1690	$C_{14}HN_2O_3$	244.9987	$C_{14}NO_4$	245.9827
$C_{14}H_4N_4O$	244.0386	$C_{14}H_{19}N_3O$	245.1529	$C_{14}H_{18}N_2O_2$	246.1369
$C_{15}H_{32}O_2$	244.2403	$C_{14}H_3N_3O_2$	245.0226	$C_{14}H_2N_2O_3$	246.0065
$C_{15}H_{16}O_3$	244.1100	$C_{14}H_{21}N_4$	245.1768	$C_{14}H_{20}N_3O$	246.1608

Appendix A (continued)

FM		FM		FM	
$C_{14}H_4N_3O_2$	246.0304	$C_{14}H_{21}N_3O$	247.1686	$C_{14}H_{22}N_3O$	248.1764
$C_{14}H_{22}N_4$	246.1846	$C_{14}H_5N_3O_2$	247.0382	$C_{14}H_6N_3O_2$	248.0460
$C_{14}H_6N_4O$	246.0542	$C_{14}H_{23}N_4$	247.1925	$C_{14}H_{24}N_4$	248.2003
$C_{15}H_{18}O_3$	246.1256	$C_{14}H_7N_4O$	247.0621	$C_{14}H_8N_4O$	248.0699
$C_{15}H_2O_4$	245.9953	$C_{15}H_{19}O_3$	247.1334	$C_{15}H_{20}O_3$	248.1413
$C_{15}H_{20}NO_2$	246.1495	$C_{15}H_3O_4$	247.0031	$C_{15}H_4O_4$	248.0109
$C_{15}H_4NO_3$	246.0191	$C_{15}H_{21}NO_2$	247.1573	$C_{15}H_{22}NO_2$	248.1651
$C_{15}H_{22}N_2O$	246.1733	$C_{15}H_5NO_3$	247.0269	$C_{15}H_6NO_3$	248.0348
$C_{15}H_6N_2O_2$	246.0429	$C_{15}H_{23}N_2O$	247.1811	$C_{15}H_{24}N_2O$	248.1890
$C_{15}H_{24}N_3$	246.1972	$C_{15}H_7N_2O_2$	247.0508	$C_{15}H_8N_2O_2$	248.0586
$C_{15}H_8N_3O$	246.0668	$C_{15}H_{25}N_3$	247.2050	$C_{15}H_{26}N_3$	248.2129
$C_{15}H_{10}N_4$	246.0907	$C_{15}H_9N_3O$	247.0746	$C_{15}H_{10}N_3O$	248.0825
$C_{16}H_{22}O_2$	246.1620	$C_{15}H_{11}N_4$	247.0985	$C_{15}H_{12}N_4$	248.1063
$C_{16}H_6O_3$	246.0317	$C_{16}H_{23}O_2$	247.1699	$C_{16}H_{24}O_2$	248.1777
$C_{16}H_{24}NO$	246.1859	$C_{16}H_7O_3$	247.0395	$C_{16}H_8O_3$	248.0473
$C_{16}H_8NO_2$	246.0555	$C_{16}H_{25}NO$	247.1937	$C_{16}H_{26}NO$	248.2015
$C_{16}H_{26}N_2$	246.2098	$C_{16}H_9NO_2$	247.0634	$C_{16}H_{10}NO_2$	248.0712
$C_{16}H_{10}N_2O$	246.0794	$C_{16}H_{27}N_2$	247.2176	$C_{16}H_{28}N_2$	248.2254
$C_{16}H_{12}N_3$	246.1032	$C_{16}H_{11}N_2O$	247.0872	$C_{16}H_{12}N_2O$	248.0950
$C_{17}H_{26}O$	246.1985	$C_{16}H_{13}N_3$	247.1111	$C_{16}H_{14}N_3$	248.1189
$C_{17}H_{10}O_2$	246.0681	$C_{17}H_{27}O$	247.2063	$C_{16}N_4$	248.0124
$C_{17}H_{28}N$	246.2223	$C_{17}H_{11}O_2$	247.0759	$C_{17}H_{28}O$	248.2141
$C_{17}H_{12}NO$	246.0919	$C_{17}H_{29}N$	247.2301	$C_{17}H_{12}O_2$	248.0837
$C_{17}H_{14}N_2$	246.1158	$C_{17}H_{13}NO$	247.0998	$C_{17}H_{30}N$	248.2380
$C_{17}N_3$	246.0093	$C_{17}H_{15}N_2$	247.1236	$C_{17}H_{14}NO$	248.1076
$C_{18}H_{30}$	246.2349	$C_{17}HN_3$	247.0171	$C_{17}H_{16}N_2$	248.1315
$C_{18}H_{14}O$	246.1045	$C_{18}H_{31}$	247.2427	$C_{17}N_2O$	248.0011
$C_{18}H_{16}N$	246.1284	$C_{18}H_{15}O$	247.1123	$C_{17}H_2N_3$	248.0249
$C_{18}NO$	245.9980	$C_{18}H_{17}N$	247.1362	$C_{18}H_{32}$	248.2505
$C_{18}H_2N_2$	246.0218	$C_{18}HNO$	247.0058	$C_{18}H_{16}O$	248.1202
$C_{19}H_{18}$	246.1409	$C_{18}H_3N_2$	247.0297	$C_{18}O_2$	247.9898
$C_{19}H_2O$	246.0106	$C_{19}H_{19}$	247.1488	$C_{18}H_{18}N$	248.1440
$C_{19}H_4N$	246.0344	$C_{19}H_3O$	247.0184	$C_{18}H_2NO$	248.0136
$C_{20}H_6$	246.0470	$C_{19}H_5N$	247.0422	$C_{18}H_4N_2$	248.0375
247		$C_{20}H_7$	247.0548	$C_{19}H_{20}$	248.1566
$C_{11}H_{23}N_2O_4$	247.1659	**248**		$C_{19}H_4O$	248.0262
$C_{11}H_{25}N_3O_3$	247.1897	$C_{11}H_{24}N_2O_4$	248.1737	$C_{19}H_6N$	248.0501
$C_{11}H_{27}N_4O_2$	247.2136	$C_{11}H_{26}N_3O_3$	248.1976	$C_{20}H_8$	248.0626
$C_{12}H_{25}NO_4$	247.1784	$C_{11}H_{28}N_4O_2$	248.2214	**249**	
$C_{12}H_{27}N_2O_3$	247.2023	$C_{12}H_{26}NO_4$	248.1863	$C_{11}H_{25}N_2O_4$	249.1815
$C_{12}H_{11}N_2O_4$	247.0719	$C_{12}H_{28}N_2O_3$	248.2101	$C_{11}H_{27}N_3O_3$	249.2054
$C_{12}H_{29}N_3O_2$	247.2261	$C_{12}H_{12}N_2O_4$	248.0797	$C_{12}H_{27}NO_4$	249.1941
$C_{12}H_{13}N_3O_3$	247.0958	$C_{12}H_{14}N_3O_3$	248.1036	$C_{12}H_{13}N_2O_4$	249.0876
$C_{12}H_{15}N_4O_2$	247.1196	$C_{12}H_{16}N_4O_2$	248.1275	$C_{12}H_{15}N_3O_3$	249.1114
$C_{13}H_{27}O_4$	247.1910	$C_{13}H_{28}O_4$	248.1988	$C_{12}H_{17}N_4O_2$	249.1353
$C_{13}H_{29}NO_3$	247.2148	$C_{13}H_{14}NO_4$	248.0923	$C_{13}H_{15}NO_4$	249.1001
$C_{13}H_{13}NO_4$	247.0845	$C_{13}H_{16}N_2O_3$	248.1162	$C_{13}H_{17}N_2O_3$	249.1240
$C_{13}H_{15}N_2O_3$	247.1083	$C_{13}N_2O_4$	247.9858	$C_{13}HN_2O_4$	248.9936
$C_{13}H_{17}N_3O_2$	247.1322	$C_{13}H_{18}N_3O_2$	248.1400	$C_{13}H_{19}N_3O_2$	249.1478
$C_{13}HN_3O_3$	247.0018	$C_{13}H_2N_3O_3$	248.0096	$C_{13}H_3N_3O_3$	249.0175
$C_{13}H_{19}N_4O$	247.1560	$C_{13}H_{20}N_4O$	248.1639	$C_{13}H_{21}N_4O$	249.1717
$C_{13}H_3N_4O_2$	247.0257	$C_{13}H_4N_4O_2$	248.0335	$C_{13}H_5N_4O_2$	249.0413
$C_{14}H_{15}O_4$	247.0970	$C_{14}H_{16}O_4$	248.1049	$C_{14}H_{17}O_4$	249.1127
$C_{14}H_{17}NO_3$	247.1209	$C_{14}H_{18}NO_3$	248.1287	$C_{14}H_{19}NO_3$	249.1365
$C_{14}HNO_4$	246.9905	$C_{14}H_2NO_4$	247.9983	$C_{14}H_3NO_4$	249.0062
$C_{14}H_{19}N_2O_2$	247.1447	$C_{14}H_{20}N_2O_2$	248.1526	$C_{14}H_{21}N_2O_2$	249.1604
$C_{14}H_3N_2O_3$	247.0144	$C_{14}H_4N_2O_3$	248.0222	$C_{14}H_5N_2O_3$	249.0300

Appendix A (continued)

	FM		FM		FM
$C_{14}H_{23}N_3O$	249.1842	$C_{18}H_3NO$	249.0215	$C_{15}H_{10}N_2O_2$	250.0743
$C_{14}H_7N_3O_2$	249.0539	$C_{18}H_5N_2$	249.0453	$C_{15}H_{28}N_3$	250.2285
$C_{14}H_{25}N_4$	249.2081	$C_{19}H_{21}$	249.1644	$C_{15}H_{12}N_3O$	250.0981
$C_{14}H_9N_4O$	249.0777	$C_{19}H_5O$	249.0340	$C_{15}H_{14}N_4$	250.1220
$C_{15}H_{21}O_3$	249.1491	$C_{19}H_7N$	249.0579	$C_{16}H_{26}O_2$	250.1934
$C_{15}H_5O_4$	249.0187	$C_{20}H_9$	249.0705	$C_{16}H_{10}O_3$	250.0630
$C_{15}H_{23}NO_2$	249.1730	**150**		$C_{16}H_{28}NO$	250.2172
$C_{15}H_7NO_3$	249.0426	$C_{11}H_{26}N_2O_4$	250.1894	$C_{16}H_{12}NO_2$	250.0868
$C_{15}H_{25}N_2O$	249.1968	$C_{12}H_{14}N_2O_4$	250.0954	$C_{16}H_{30}N_2$	250.2411
$C_{15}H_9N_2O_2$	249.0664	$C_{12}H_{16}N_3O_3$	250.1193	$C_{16}H_{14}N_2O$	250.1107
$C_{15}H_{27}N_3$	249.2207	$C_{12}H_{18}N_4O_2$	250.1431	$C_{16}H_{16}N_3$	250.1346
$C_{15}H_{11}N_3O$	249.0903	$C_{13}H_{16}NO_4$	250.1080	$C_{16}N_3O$	250.0042
$C_{15}H_{13}N_4$	249.1142	$C_{13}H_{18}N_2O_3$	250.1318	$C_{16}H_2N_4$	250.0280
$C_{16}H_{25}O_2$	249.1855	$C_{13}H_2N_2O_4$	250.0014	$C_{17}H_{30}O$	250.2298
$C_{16}H_9O_3$	249.0552	$C_{13}H_{20}N_3O_2$	250.1557	$C_{17}H_{14}O_2$	250.0994
$C_{16}H_{27}NO$	249.2094	$C_{13}H_4N_3O_3$	250.0253	$C_{17}H_{32}N$	250.2536
$C_{16}H_{11}NO_2$	249.0790	$C_{13}H_{22}N_4O$	250.1795	$C_{17}H_{16}NO$	250.1233
$C_{16}H_{29}N_2$	249.2332	$C_{13}H_6N_4O_2$	250.0491	$C_{17}NO_2$	249.9929
$C_{16}H_{13}N_2O$	249.1029	$C_{14}H_{18}O_4$	250.1205	$C_{17}H_{18}N_2$	250.1471
$C_{16}H_{15}N_3$	249.1267	$C_{14}H_{20}NO_3$	250.1444	$C_{17}H_2N_2O$	250.0167
$C_{16}HN_4$	249.0202	$C_{14}H_4NO_4$	250.0140	$C_{17}H_4N_3$	250.0406
$C_{17}H_{29}O$	249.2219	$C_{14}H_{22}N_2O_2$	250.1682	$C_{18}H_{34}$	250.2662
$C_{17}H_{13}O_2$	249.0916	$C_{14}H_6N_2O_3$	250.0379	$C_{18}H_{18}O$	250.1358
$C_{17}H_{31}N$	249.2458	$C_{14}H_{24}N_3O$	250.1921	$C_{18}H_2O_2$	250.0054
$C_{17}H_{15}NO$	249.1154	$C_{14}H_8N_3O_2$	250.0617	$C_{18}H_{20}N$	250.1597
$C_{17}H_{17}N_2$	249.1393	$C_{14}H_{26}N_4$	250.2160	$C_{18}H_4NO$	250.0293
$C_{17}HN_2O$	249.0089	$C_{14}H_{10}N_4O$	250.0856	$C_{18}H_6N_2$	250.0532
$C_{17}H_3N_3$	249.0328	$C_{15}H_{22}O_3$	250.1569	$C_{19}H_{22}$	250.1722
$C_{18}H_{33}$	249.2584	$C_{15}H_6O_4$	250.0266	$C_{19}H_6O$	250.0419
$C_{18}H_{17}O$	249.1280	$C_{15}H_{24}NO_2$	250.1808	$C_{19}H_8N$	250.0657
$C_{18}HO_2$	248.9976	$C_{15}H_8NO_3$	250.0504	$C_{20}H_{10}$	250.0783
$C_{18}H_{19}N$	249.1519	$C_{15}H_{26}N_2O$	250.2046		

Appendix B Common Fragment Ions

All fragments listed bear +1 charges. To be used in conjunction with Appendix C. Not all members of homologous and isomeric series are given. The list is meant to be suggestive rather than exhaustive. Appendix II of Hamming and Foster, Table A-7 of McLafferty's Interpretative book, and the high-resolution ion data of McLafferty are recommended as supplements. Structural inferences are listed in parentheses.

m/z Ions[a]	(Structural Inference)
14	CH_2
15	CH_3
16	O
17	OH
18	H_2O, NH_4
19	F, H_3O
26	$C{\equiv}N$, C_2H_2
27	C_2H_3
28	C_2H_4, CO, N_2 (air), CH=NH
29	C_2H_5, CHO
30	CH_2NH_2 (RCH_2NH_2), NO
31	CH_2OH (RCH_2OH), OCH_3
32	O_2 (air)
33	SH, CH_2F
34	H_2S
35	Cl (^{37}Cl at 37)
36	HCl (H ^{37}Cl at 38)
39	C_3H_3
40	$CH_2C{\equiv}N$, Ar(air)
41	C_3H_5, $CH_2C{\equiv}N$ + H,[a] C_2H_2NH
42	C_3H_6, C_2H_2O
43	C_3H_7, $CH_3C{=}O$, $CH_3C{=}OG$, G = R, Ar, NH_2, OR, OH, C_2H_5N
44	$CH_2C{=}O$ + H (Aldehydes, McLafferty Rearrangement), CH_3CHNH_2, CO_2, $NH_2C{=}O$ ($RC{=}ONH_2$), $(CH_3)_2N$
45	$CHOH$, CH_2CH_2OH, CH_2OCH_3 (RCH_2OCH_3), $C{-}OH$, $CH_3CH{-}O$ + H (CH_3CHOHR)
46	NO_2
47	CH_2SH (RCH_2SH), CH_3S
48	CH_3S + H
49	CH_2Cl (CH_2 ^{37}Cl at 51)
51	CHF_2, C_4H_3
53	C_4H_5
54	$CH_2CH_2C{\equiv}N$
55	C_4H_7, $CH_2{=}CHC{=}O$
56	C_4H_8
57	C_4H_9, $C_2H_5C{=}O$

m/z Ions[a]	(Structural Inference)
58	$CH_3{-}C(=O){-}CH_2$ + H, $C_2H_5CHNH_2$, $(CH_3)_2NCH_2$, $C_2H_5NHCH_2$, C_2H_2S
59	$(CH_3)_2COH$, $CH_2OC_2H_5$, $C{-}OCH_3$ (RCO_2CH_3), $NH_2C{=}O$ + H, CH_3OCHCH_3, CH_3CHCH_2OH, C_2H_5CHOH
60	$CH_2C(=O){-}OH$ + H, CH_2ONO
61	$CH_3C(=O){-}O$ + 2H, CH_2CH_2SH, CH_2SCH_3
65	C_5H_5
66	≡ C_5H_6, H_2S_2 (RSSR)
67	C_5H_7
68	$CH_2CH_2CH_2C{\equiv}N$
69	C_5H_9, CF_3, $CH_3CH{=}CHC{=}O$, $CH_2{=}C(CH_3)C{=}O$
70	C_5H_{10}
71	C_5H_{11}, $C_3H_7C{=}O$
72	$C_2H_5C(=O){-}CH_2$ + H, $C_3H_7CHNH_2$, $(CH_3)_2N{=}C{=}O$, $C_2H_5NHCHCH_3$ and isomers
73	Homologs of 59, $(CH_3)_3Si$
74	$CH_2{-}C(=O){-}OCH_3$ + H
75	$C(=O){-}OC_2H_5$ + 2H, C_2H_5CO + 2H, $CH_2SC_2H_5$, $(CH_3)_2CSH$, $(CH_3O)_2CH$, $(CH_3)_2SiOH$
76	C_6H_4 (C_6H_5X, C_6H_4XY)
77	C_6H_5 (C_6H_5X)
78	C_6H_5 + H
79	C_6H_5 + 2H, Br (^{81}Br at 81)

[a]Ions inidicated as a fragment + nH (n = 1, 2, 3, . . .) are ions that arise via rearrangement involving hydrogen transfer.

80 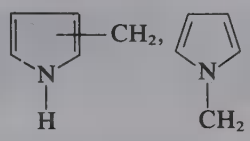

CH_3SS + H, HBr ($H^{81}Br$ at 82)

81 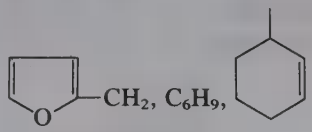

82 $CH_2CH_2CH_2CH_2C{\equiv}N$,

CCl_2 ($C^{35}Cl^{37}Cl$ at 84, $C^{37}Cl_2$ at 86), C_6H_{10}

83 C_6H_{11}, $CHCl_2$ ($CH^{35}Cl^{37}Cl$ at 85,

$CH^{37}Cl_2$ at 87), 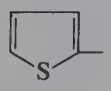

85 C_6H_{13}, $C_4H_9C{=}O$,

$CClF_2$ ($C^{37}ClF_2$ at 87), 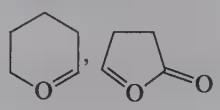

86 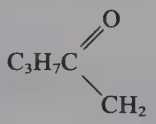 + H, $C_4H_9CHNH_2$ and isomers

87 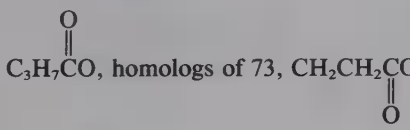 , homologs of 73, $CH_2CH_2COCH_3$

89 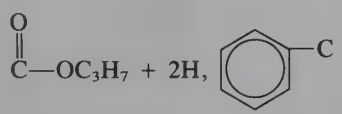

90 CH_3CHONO_2, 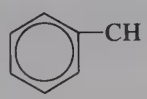

91 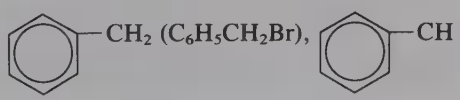

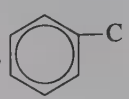

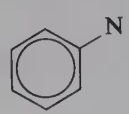

92 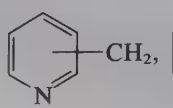

93 CH_2Br ($CH_2{}^{81}Br$ at 95, RCH_2Br), C_7H_9,

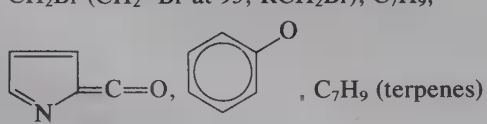 , C_7H_9 (terpenes)

94 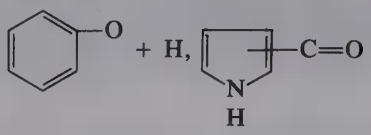

95 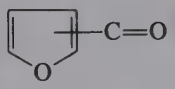

96 $CH_2CH_2CH_2CH_2CH_2C{\equiv}N$

97 C_7H_{13}, 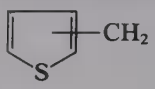

98 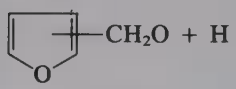

99 C_7H_{15}, $C_6H_{11}O$, 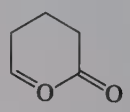

100 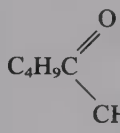 + H, $C_5H_{11}CHNH_2$

101 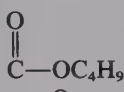

102 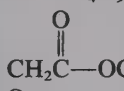 + H

103 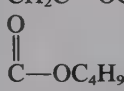 + 2H, $C_5H_{11}S$, $CH(OCH_2CH_3)_2$

104 $C_2H_5CHONO_2$

105 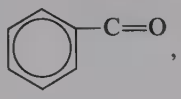 ,

$[C_6H_5(C{=}O)G$, G = OH, OR, OAr, halogen, $NH_2]$,

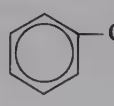 , 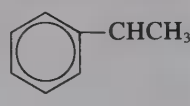

106 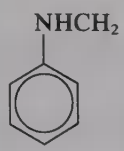

107 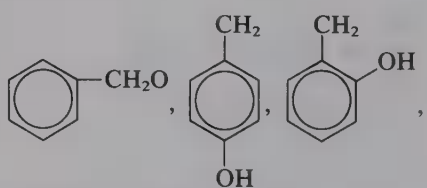 ,

C_2H_4Br ($C_2H_4{}^{81}Br$ at 109)

108 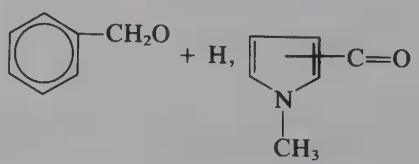 + H,

109 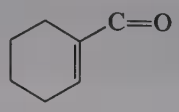

111 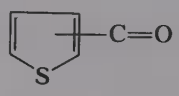

119 CF_3CF_2, 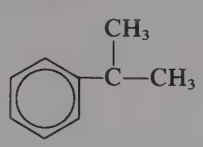 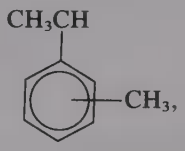 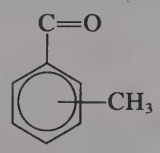

120 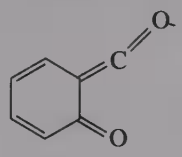

121 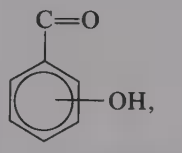 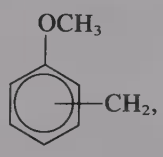 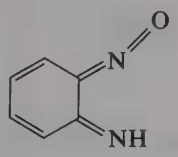

C_9H_{13} (terpenes)

122 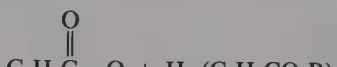

123 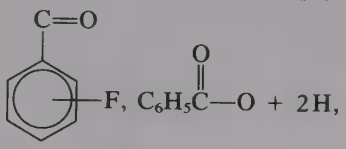

125 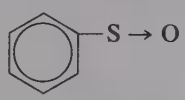

127 I

128 HI

130 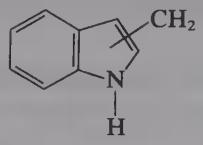

131 C_3F_5, 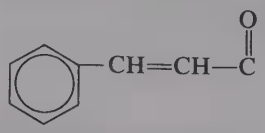

135 $(CH_2)_4Br$ [$(CH_2)_4{}^{81}Br$ at 137]

138 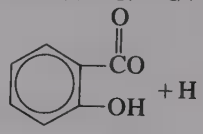

139 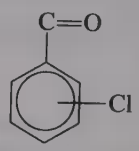

141 CH_2I (RCH_2I)

147 $(CH_3)_2Si{=}O{-}Si(CH_3)_3$

149 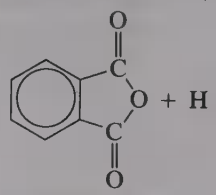

154 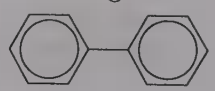

Appendix C Common Fragments Lost

This list is suggestive rather than comprehensive. It should be used in conjunction with Appendix B. Table 5-19 of Hamming and Foster and Table A-5 of McLafferty are recommended as supplements. All of these fragments are lost as neutral species.

Molecular Ion Minus	Fragment Lost Inference Structure
1	H·
2	2H·
15	CH_3·
16	O ($ArNO_2$, amine oxides, sulfoxides); · NH_2 (carboxamides, sulfonamides)
17	HO·
18	H_2O (alcohols, aldehydes, ketones)
19	F·
20	HF
26	CH≡CH, ·CH≡N
27	CH_2=CH·, HC≡N (aromatic nitrites, nitrogen heterocycles)
28	CH_2=CH_2, CO, (quinones) (HCN + H)
29	CH_3CH_2·, (ethyl ketones, $ArCH_2CH_2CH_3$), ·CHO
30	NH_2CH_2·, CH_2O ($ArOCH_3$), NO ($ArNO_2$), C_2H_6
31	·OCH_3(methyl esters), ·CH_2OH, CH_3NH_2
32	CH_3OH, S
33	HS· (thiols), (·CH_3 and H_2O)
34	H_2S (thiols)
35	Cl·
36	HCl, $2H_2O$
37	H_2Cl (or HCl + H)
38	C_3H_2, C_2N, F_2
39	C_3H_3, HC_2N
40	CH_3C≡CH
41	CH_2=$CHCH_2$·
42	CH_2=$CHCH_3$, CH_2=C=O, 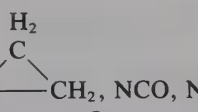 , NCO, $NCNH_2$
43	C_3H_7·(propyl ketones, $ArCH_2$—C_3H_7), CH_3C(=O)·(methyl ketones, CH_3CG, where G = various functional groups), CH_2=CH—O·, (CH_3· and CH_2=CH_2), HCNO
44	CH_2=CHOH, CO_2 (esters, anhydrides), N_2O, $CONH_2$, $NHCH_2CH_3$
45	CH_3CHOH, CH_3CH_2O·(ethyl esters), CO_2H, $CH_3CH_2NH_2$
46	(H_2O and CH_2=CH_2), CH_3CH_2OH, ·NO_2 ($ArNO_2$)
47	CH_3S·
48	CH_3SH, SO (sulfoxides), O_3
49	·CH_2Cl
51	·CHF_2
52	C_4H_4, C_2N_2
53	C_4H_5
54	CH_2=CH—CH=CH_2
55	CH_2=$CHCHCH_3$
56	CH_2=$CHCH_2CH_3$, CH_3CH=$CHCH_3$, 2CO
57	C_4H_9· (butyl ketones), C_2H_5CO (ethyl ketones, EtC=OG, G = various structural units)
58	·NCS, (NO + CO), CH_3COCH_3, C_4H_{10}

Appendix C (continued)

59	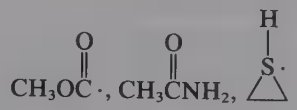
60	C_3H_7OH, $CH_2{=}C(OH)_2$ (acetate esters)[a]
61	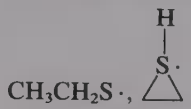
62	(H_2S and $CH_2{=}CH_2$)
63	$\cdot CH_2CH_2Cl$
64	C_5H_4, S_2, SO_2
68	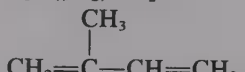
69	$CF_3\cdot$, $C_5H_9\cdot$
71	$C_5H_{11}\cdot$
73	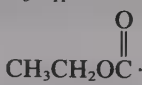
74	C_4H_9OH
75	C_6H_3
76	C_6H_4, CS_2
77	C_6H_5, CS_2H
78	C_6H_6, CS_2H_2, C_5H_4N
79	$Br\cdot$, C_5H_5N
80	HBr
85	$\cdot CClF_2$
100	$CF_2{=}CF_2$
119	$CF_3{-}CF_2\cdot$
122	C_6H_5COOH
127	$I\cdot$
128	HI

[a]McLafferty Rearrangement.

CHAPTER THREE

INFRARED SPECTROMETRY

3.1. INTRODUCTION

Infrared (IR) radiation refers broadly to that part of the electromagnetic spectrum between the visible and microwave regions. Of greatest practical use to the organic chemist is the limited portion between 4000 and 400 cm^{-1}. There has been some interest in the near-IR (14,290–4000 cm^{-1}) and the far-IR regions, 700–200 cm^{-1}.

From the brief theoretical discussion that follows, it is clear that even a very simple molecule can give an extremely complex spectrum. The organic chemist takes advantage of this complexity when he matches the spectrum of an unknown compound against that of an authentic sample. A peak-by-peak correlation is excellent evidence for identity. It is unlikely that any two compounds, except enantiomers, give exactly the same IR spectrum.

Although the IR spectrum is characteristic of the entire molecule, it is true that certain groups of atoms give rise to bands at or near the same frequency regardless of the structure of the rest of the molecule. It is the persistence of these characteristic bands that permits the chemist to obtain useful structural information by simple inspection and reference to generalized charts of characteristic group frequencies. We shall rely heavily on these characteristic group frequencies.

Since we are not solely dependent on IR spectra for identification, a detailed analysis of the spectrum will not be required. Following our general plan, we shall present only sufficient theory to accomplish our purpose: utilization of IR spectra in conjunction with other spectral data in order to determine molecular structure.

Because most academic and industrial laboratories make IR spectrometers available as bench tools for the organic chemist, we shall describe instrumentation and sample preparation in somewhat more detail than is given in the other chapters.

The importance of IR spectrometry as a tool of the practicing organic chemist is readily apparent from the number of books devoted wholly or in part to discussions of applications of IR spectrometry (see the references at the end of this chapter). There are many compilations of spectra as well as indexes to spectral collections and to the literature. Among the more commonly used compilations are those published by Sadtler and by Aldrich.

3.2. THEORY

Infrared radiation of frequencies less than about 100 cm^{-1} is absorbed and converted by an organic molecule into energy of molecular rotation. This absorption is quantized; thus a molecular rotation spectrum consists of discrete lines.

Infrared radiation in the range from about 10,000–100 cm^{-1} is absorbed and converted by an organic molecule into energy of molecular vibration. This absorption is also quantized, but vibrational spectra appear as bands rather than as lines because a single vibrational energy change is accompanied by a number of rotational energy changes. It is with these vibrational–rotational bands, particularly those occurring between 4000 and 400 cm^{-1} that we shall be concerned. The frequency or wavelength of absorption depends on the relative masses of the atoms, the force constants of the bonds, and the geometry of the atoms.

Band positions in IR spectra are presented here as wavenumbers ($\bar{\nu}$) whose unit is the reciprocal centimeter (cm^{-1}); this unit is proportional to the energy of vibration and modern instruments are linear in reciprocal centimeters. Wavelength (λ) was used in the

older literature in units of micrometers ($\mu m = 10^{-6}$ m; earlier called microns). Wavenumbers are reciprocally related to wavelength.

$$cm^{-1} = 10^4/\mu m$$

Notice also that wavenumbers ($\bar{\nu}$) are often called "frequencies"; this is not rigorously correct, since wavenumbers are $1/\lambda$ and the frequency (ν) is c/λ, c being the speed of light (3×10^{10} cm/s). Most of our spectra are linear in reciprocal centimeters with the exception of a few linear in micrometers. A spectrum linear in wavenumbers has a very different appearance from one linear in wavelength (Fig. 3.7).

Band intensities can be expressed either as transmittance (T) or absorbance (A). Transmittance is the ratio of the radiant power transmitted by a sample to the radiant power incident on the sample. Absorbance is the logarithm, to the base 10, of the reciprocal of the transmittance; $A = \log_{10}(1/T)$. Organic chemists usually report intensity in semiquantitative terms (s = strong, m = medium, w = weak).

There are two types of molecular vibrations: stretching and bending. A stretching vibration is a rhythmical movement along the bond axis such that the interatomic distance is increasing or decreasing. A bending vibration may consist of a change in bond angle between bonds with a common atom or the movement of a group of atoms with respect to the remainder of the molecule without movement of the atoms in the group with respect to one another. For example, twisting, rocking, and torsional vibrations involve a change in bond angles with reference to a set of coordinates arbitrarily set up within the molecule.

Only those vibrations that result in a rhythmical change in the dipole moment of the molecule are observed in the IR. The alternating electric field, produced by the changing charge distribution accompanying a vibration, couples the molecule vibration with the oscillating electric field of the electromagnetic radiation.

A molecule has as many degrees of freedom as the total degrees of freedom of its individual atoms. Each atom has three degrees of freedom corresponding to the Cartesian coordinates (x, y, z) necessary to describe its position relative to other atoms in the molecule. A molecule of n atoms therefore has $3n$ degrees of freedom. For nonlinear molecules, three degrees of freedom describe rotation and three describe translation; the remaining $3n - 6$ degrees of freedom are vibrational degrees of freedom or fundamental vibrations. Linear molecules have $3n - 5$ vibrational degrees of freedom, for only two degrees of freedom are required to describe rotation.

Fundamental vibrations involve no change in the center of gravity of the molecule.

The three fundamental vibrations of the nonlinear, triatomic water molecule can be depicted as follows:

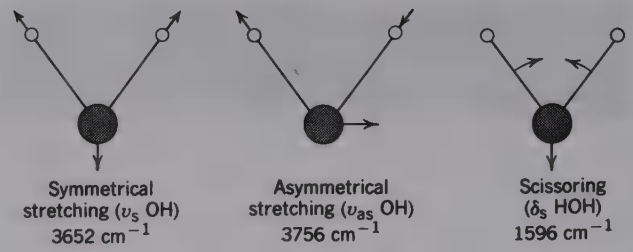

Note the very close spacing of the interacting or coupled asymmetric and symmetric stretching above compared with the far-removed scissoring mode. This will be shown to be useful later in classification of absorptions and application to structure determination.

The CO_2 molecule is linear and contains three atoms; therefore it has four fundamental vibrations [$(3 \times 3) - 5$].

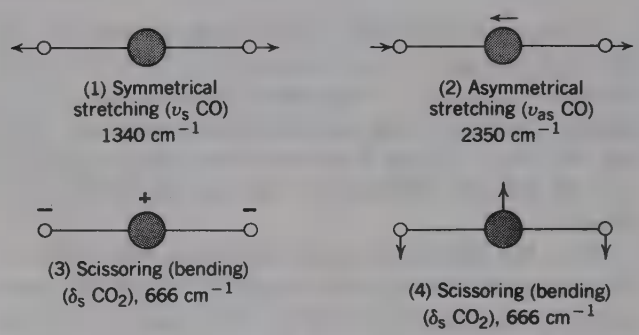

+ and − indicate movement perpendicular to the plane of the page.

The symmetrical stretching vibration in (1) above is inactive in the IR since it produces no change in the dipole moment of the molecule. The bending vibrations in (3) and (4) above are equivalent, and are the resolved components of bending motion oriented at any angle to the internuclear axis; they have the same frequency and are said to be doubly degenerate.

The various stretching and bending modes for an AX_2 group appearing as a portion of a molecule, for example, the CH_2 group in a hydrocarbon molecule, are shown in Figure 3.1. The $3n - 6$ rule does not apply since the CH_2 group represents only a portion of a molecule.

The theoretical number of fundamental vibrations (absorption frequencies) will seldom be observed because overtones (multiples of a given frequency) and combination tones (sum of two other vibrations) increase the number of bands, whereas other phenomena reduce the number of bands. The following will reduce the theoretical number of bands.

1. Fundamental frequencies that fall outside of the 4000–400 cm region^{-1}.

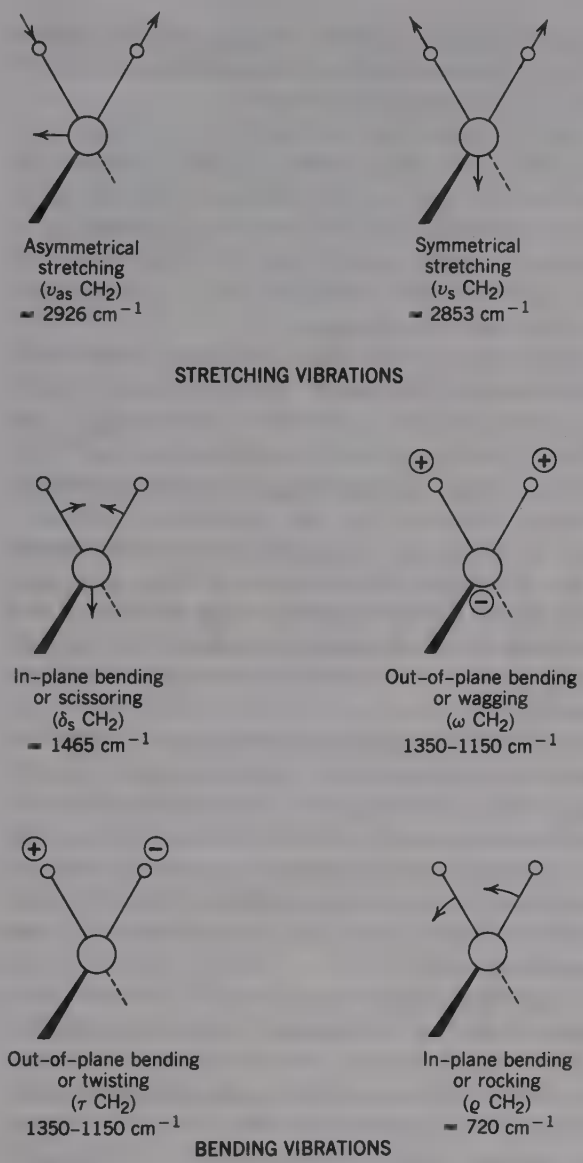

FIGURE 3.1. Vibrational modes for a CH_2 group. (+ and − indicate movement perpendicular to the plane of the page.)

2. Fundamental bands that are too weak to be observed.
3. Fundamental vibrations that are so close that they coalesce.
4. The occurrence of a degenerate band from several absorptions of the same frequency in highly symmetrical molecules.
5. The failure of certain fundamental vibrations to appear in the IR because of the lack of change in molecular dipole.

Assignments for stretching frequencies can be approximated by the application of Hooke's law. In the application of the law, two atoms and their connecting bond are treated as a simple harmonic oscillator composed of two masses joined by a spring. The following equation, derived from Hooke's law, states the relationship between frequency of oscillation, atomic masses, and the force constant of the bond.

$$\bar{\nu} = \frac{1}{2\pi c}\left[\frac{f}{(MxMy)/(Mx + My)}\right]^{1/2}$$

where $\bar{\nu}$ = the vibrational frequency (cm^{-1})
c = velocity of light (cm/s)
f = force constant of bond (dyne/cm)
Mx and My = mass (g) of atom x and atom y, respectively.

The value of f is approximately 5×10^5 dyne/cm for single bonds and approximately two and three times this value for double and triple bonds, respectively.

Application of the formula to C—H stretching using 19.8×10^{-24} and 1.64×10^{-24} g as mass values for C and H, respectively, places the frequency of the C—H bond vibration at 3040 cm^{-1}. Actually, C—H stretching vibrations, associated with methyl and methylene groups, are generally observed in the region between 2960 and 2850 cm^{-1}. The calculation is not highly accurate because effects arising from the environment of the C—H within a molecule have been ignored. The frequency of IR absorption is commonly used to calculate the force constants of bonds.

The shift in absorption frequency following deuteration is often employed in the assignment of C—H stretching frequencies. The above equation can be used to estimate the change in stretching frequency as the result of deuteration. The term $MxMy/(Mx + My)$ will be equal to $M_CM_H/(M_C + M_H)$ for the C—H compound. Since $M_C >> M_H$, this term is approximately equal to M_CM_H/M_C or to M_H. Thus, for the C—D compound the term is equal to M_D, and the frequency by Hooke's law application is inversely proportional to the square root of the mass of the isotope of hydrogen, and the ratio of the C—H to C—D stretching frequencies should equal $\sqrt{2}$. If the ratio of the frequencies, following deuteration, is much less than $\sqrt{2}$, we can assume that the vibration is not simply a C—H stretching vibration, but rather a mixed vibration involving interaction (coupling) with another vibration.

Calculations place the stretching frequencies of the following bonds in the general absorption regions indicated:

Bond Type	Absorption Region (cm^{-1})
C—C, C—O, C—N	1300–800
C=C, C=O, C=N, N=O	1900–1500
C≡C, C≡N	2300–2000
C—H, O—H, N—H	3800–2700

To approximate the vibrational frequencies of bond stretching by Hooke's law, the relative contributions of bond strengths and atomic masses must be considered. For example, a superficial comparison of the C—H group with the F—H group, on the basis of atomic masses, might lead to the conclusion that the stretching frequency of the F—H bond should occur at a lower frequency than that for the C—H bond. However, the increase in the force constant from left to right across the first two rows of the periodic table has a greater effect than the mass increase. Thus, the F—H group absorbs at a higher frequency (4138 cm^{-1}) than the C—H group (3040 cm^{-1}).

In general, functional groups that have a strong dipole give rise to strong absorptions in the IR.

3.2.1. Coupled Interactions

When two bond oscillators share a common atom, they seldom behave as individual oscillators unless the individual oscillation frequencies are widely different. This is because there is mechanical coupling interaction between the oscillators. For example, the carbon dioxide molecule, which consists of two C=O bonds with a common carbon atom, has two fundamental stretching vibrations: an asymmetrical and a symmetrical stretching mode. The symmetrical stretching mode consists of an in-phase stretching or contracting of the C—O bonds, and absorption occurs at a wavelength longer than that observed for the carbonyl group in an aliphatic ketone. The symmetrical stretching mode produces no change in the dipole moment (μ) of the molecule and is therefore "inactive" in the IR, but is easily observed in the Raman spectrum* near 1340 cm^{-1}. In the asymmetrical stretching mode, the two C—O bonds stretch out of phase; one C=O bond stretches as the other contracts. The asymmetrical stretching mode, since it produces a change in the dipole moment, is IR active; the absorption (2350 cm^{-1}) is at a higher frequency (shorter wavelength) than observed for a carbonyl group in aliphatic ketones.

$\longleftarrow O{=}C{=}O \longrightarrow$	$\longleftarrow O{=}\overrightarrow{C}{=}O \longleftarrow$
Symmetrical	Asymmetrical
$\mu = 0$	$\mu \neq 0$

This difference in carbonyl absorption frequencies displayed by the carbon dioxide molecule results from strong mechanical coupling or interaction. In contrast, two ketonic carbonyl groups separated by one or more carbon atoms show normal carbonyl absorption near 1715 cm^{-1} because appreciable coupling is prevented by the intervening carbon atom(s).

Coupling accounts for the two N—H stretching bands in the 3497–3077 cm^{-1} region in primary amine and primary amide spectra, for the two C=O stretching bands in the 1818–1720 cm^{-1} region in carboxylic anhydride and imide spectra, and for the two C—H stretching bands in the 3000–2760 cm^{-1} region for both methylene and methyl groups.

Useful characteristic group frequency bands often involve coupled vibrations. The spectra of alcohols have a strong band in the region between 1212 and 1000 cm^{-1}, which is usually designated as the "C—O stretching band." In the spectrum of methanol this band is at 1034 cm^{-1}; in the spectrum of ethanol it occurs at 1053 cm^{-1}. Branching and unsaturation produce absorption characteristic of these structures (see alcohols). It is evident that we are not dealing with an isolated C—O stretching vibration, but rather a coupled asymmetric vibration involving C—C—O stretching.

Vibrations resulting from bond angle changes frequently couple in a manner similar to stretching vibrations. Thus, the ring C—H out-of-plane bending frequencies of aromatic molecules depend on the number of adjacent hydrogen atoms on the ring; coupling between the hydrogen atoms is affected by the bending of the C—C bond in the ring to which the hydrogen atoms are attached.

Interaction arising from coupling of stretching and bending vibrations is illustrated by the absorption of secondary acyclic amides. Secondary acyclic amides, which exist predominantly in the trans conformation, show strong absorption in the 1563–1515 cm^{-1} region; this absorption involves coupling of the N—H bending and C—N stretching vibrations.

The requirements for effective coupling interaction may be summarized as follows:

1. The vibrations must be of the same symmetry species if interaction is to occur.
2. Strong coupling between stretching vibrations requires a common atom between the groups.
3. Interaction is greatest when the coupled groups absorb, individually, near the same frequency.
4. Coupling between bending and stretching vibrations can occur if the stretching bond forms one side of the changing angle.
5. A common bond is required for coupling of bending vibrations.
6. Coupling is negligible when groups are separated by one or more carbon atoms and the vibrations are mutually perpendicular.

*Band intensity in Raman spectra depends on bond polarizability rather than molecular dipole changes.

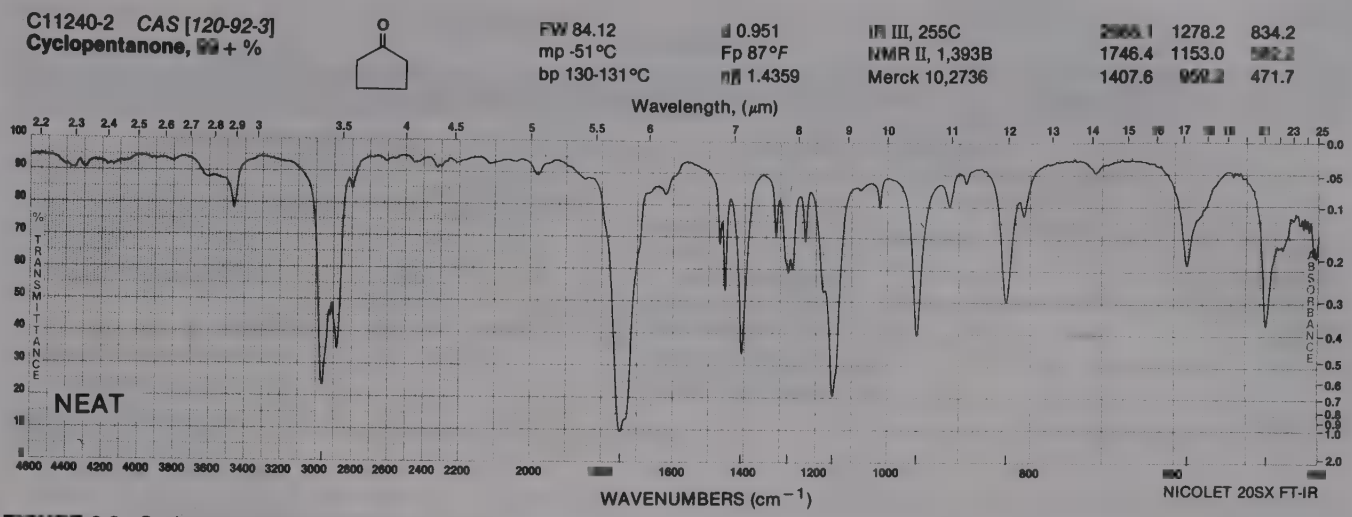

FIGURE 3.2. Cyclopentanone, thin film.

As we have seen in our discussion of interaction, coupling of two fundamental vibrational modes will produce two new modes of vibration, with frequencies higher and lower than that observed when interaction is absent. Interaction can also occur between fundamental vibrations and overtones or combination–tone vibrations. Such interaction is known as Fermi resonance. One example of Fermi resonance is afforded by the absorption pattern of carbon dioxide. In our discussion of interaction, we indicated that the symmetrical stretching band of CO_2 appears in the Raman spectrum near 1340 cm^{-1}. Actually two bands are observed; one at 1286 cm^{-1} and one at 1388 cm^{-1}. The splitting results from coupling between the fundamental C=O stretching vibration, near 1340 cm^{-1}, and the first overtone of the bending vibration. The fundamental bending vibration occurs near 666 cm^{-1}, the first overtone near 1334 cm^{-1}.

Fermi resonance is a common phenomenon in IR and Raman spectra. It requires that the vibrational levels be of the same symmetry species and that the interacting groups be located in the molecule so that mechanical coupling is appreciable.

An example of Fermi resonance in an organic structure is the "doublet" appearance of the C=O stretch of cyclopentanone under sufficient resolution conditions. Figure 3. 2 shows the appearance of the spectrum of cyclopentanone under the usual conditions. With adequate resolution (Fig. 3.3), Fermi resonance with an overtone or combination band of an α-methylene group shows two absorptions in the carbonyl stretch region.

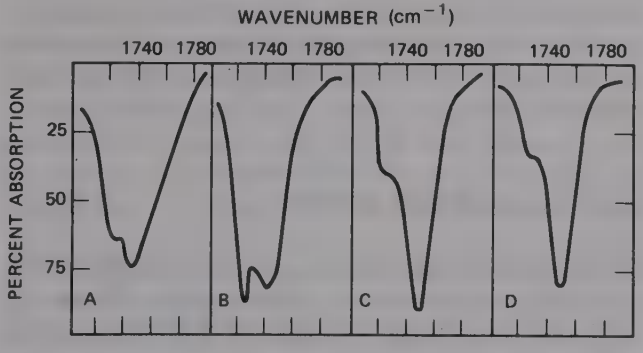

FIGURE 3.3. Infrared spectrum of cyclopentanone in various media. A. Carbon tetrachloride solution (0.15 *M*). B. Carbon disulfide solution (0.023 *M*). C. Chloroform solution (0.025 *M*). D. Liquid state (thin films). (Computed spectral slit width 2 cm^{-1}.)

3.2.2. Hydrogen Bonding

Hydrogen bonding can occur in any system containing a proton donor group (X—H) and a proton acceptor ($\ddot{Y}$) if the *s* orbital of the proton can effectively overlap the *p* or π orbital of the acceptor group. Atoms X and $\ddot{Y}$ are electronegative with $\ddot{Y}$ possessing lone pair electrons. The common proton donor groups in organic molecules are carboxyl, hydroxyl, amine, or amide groups. Common proton acceptor atoms are oxygen, nitrogen, and the halogens. Unsaturated groups, such as the C=C linkage, can also act as proton acceptors.

The strength of the hydrogen bond is at a maximum when the proton donor group and the axis of the lone pair orbital are collinear. The strength of the bond decreases as the distance between X and Y increases.

Hydrogen bonding alters the force constant of both groups; thus, the frequencies of both stretching and bending vibrations are altered. The X—H stretching bands move to lower frequencies (longer wavelengths) usually with increased intensity and band widening. The stretching frequency of the acceptor group, for example, C=O, is also reduced but to a lesser degree

TABLE 3.1

Stretching Frequencies in Hydrogen Bonding

	Intermolecular Bonding			Intramolecular Bonding		
X—H · · · Y Strength	Frequency Reduction (cm^{-1}) ν_{OH}	$\nu_{C=O}$	Compound Class	Frequency Reduction (cm^{-1}) ν_{OH}	$\nu_{C=O}$	Compound Class
Weak	300[a]	15[b]	Alcohols, phenols, and intermolecular hydroxyl to carbonyl bonding.	<100[a]	10	1,2-Diols; α- and most β-hydroxy ketones; *o*-chloro and *o*-alkoxy phenols
Medium				100–300[a]	50	1,3-Diols; some β-hydroxy ketones; β-hydroxy amino compounds; β-hydroxy nitro compounds
Strong	>500[a]	50[b]	RCO_2H dimers	>300[a]	100	*o*-Hydroxy aryl ketones; *o*-hydroxy aryl acids; *o*-hydroxy aryl esters; β-diketones; tropolones.

[a]Frequency shift relative to "free" stretching frequencies.
[b]Carbonyl stretching only where applicable.

than the proton donor group. The H—X bending vibration usually shifts to a shorter wavelength when bonding occurs; this shift is less pronounced than that of the stretching frequency.

*Inter*molecular hydrogen bonding involves association of two or more molecules of the same or different compounds. Intermolecular bonding may result in dimer molecules (as observed for carboxylic acids) or in polymeric molecular chains, which exist in neat samples or concentrated solutions of monohydroxy alcohols. *Intra*molecular hydrogen bonds are formed when the proton donor and acceptor are present in a single molecule under spatial conditions that allow the required overlap of orbitals, for example, the formation of a five- or six-membered ring. The extent of both inter- and intramolecular bonding is temperature dependent. The effect of concentration on intermolecular and intramolecular hydrogen bonding is markedly different. The bands that result from intermolecular bonding generally disappear at low concentrations (less than about 0.01 *M* in nonpolar solvents). Intramolecular hydrogen bonding is an internal effect and persists at very low concentrations.

The change in frequency between "free" OH absorption and bonded OH absorption is a measure of the strength of the hydrogen bond. Ring strain, molecular geometry, and the relative acidity and basicity of the proton donor and acceptor groups affect the strength of bonding. Intramolecular bonding involving the same bonding groups is stronger when a six-membered ring is formed than when a smaller ring results from bonding. Hydrogen bonding is strongest when the bonded structure is stabilized by resonance.

The effects of hydrogen bonding on the stretching frequencies of hydroxyl and carbonyl groups are summarized in Table 3.1. Figure 3.17 (spectrum of cyclohexylcarbinol in the stretch region) clearly illustrates this effect.

An important aspect of hydrogen bonding involves interaction between functional groups of solvent and solute. If the solute is polar, then it is important to note the solvent used and the solute concentration.

3.3. INSTRUMENTATION

The modern double-beam IR spectrophotometer consists of five principal sections: source (radiation), sampling area, photometer, grating (monochromator), and detector (thermocouple). A diagram of the optical system of a double-beam IR spectrophotometer is shown in Figure 3.4*a*.

3.3.1. Radiation Source

Infrared radiation is produced by electrically heating a source, often a Nernst filament or a Globar, to 1000–1800°C. The Nernst filament is fabricated from a binder and oxides of zirconium, thorium, and cerium. The Globar is a small rod of silicon carbide. The image of the source must be wider than the maximum width of the slits. The maximum radiation for the Globar occurs in the 5500–5000 cm^{-1} region and drops off by

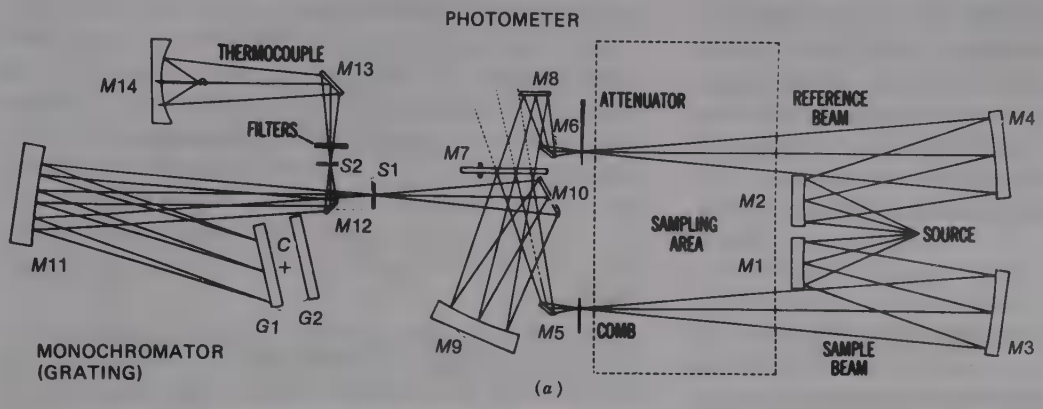

FIGURE 3.4(*a*). Optical system of double-beam IR spectrophotometer.

a factor of about 600 as the 600 cm^{-1} region is approached. The Nernst filament furnishes maximum radiation energy at about 7100 cm^{-1} and drops by a factor of about 1000 as the lower frequency region is approached.

The radiation from the source is divided into two beams by mirrors *M*1 and *M*2. The two beams, reference beam and sample beam, are focused into the sample area by mirrors *M*3 and *M*4.

3.3.2. Sampling Area

Reference and sample beams enter the sampling area and pass through the reference cell and sampling cell, respectively. Opaque shutters, mounted on the source housing, permit blocking of either beam independently. The sampling area of a precision spectrophotometer accommodates a wide variety of sampling accessories varying from gas cells of 40-m effective path to microcells.

3.3.3. Photometer

The reference beam passes through the attenuator (see below) and is reflected by mirrors *M*6 and *M*8 to the rotating sector mirror *M*7, which alternately reflects the reference beam out of the optical system and transmits the beam to mirror *M*9. The reference beam is now an intermittent beam with a "frequency" of from 8 to 13 cps (cycles per second) depending on the particular instrument. This beam is focused by mirror *M*10 on the slit *S*1. The sample beam passes through the comb (see below) and is reflected by mirror *M*5 to the rotating sector mirror *M*7, which alternately transmits the beam out of the optical system and reflects it to mirror *M*9, thence to mirror *M*10 and slit *S*1.

At any given moment, the beam focused on slit *S*1 is either the reference beam, which was transmitted by the rotating sector mirror *M*7, or the sample beam, which was reflected by *M*7. In other words, the reference beam and the sample beam have been combined into a single beam of alternating segments; this establishes a switching frequency at the detector equal to the speed of rotation of *M*7.

When the beams are of equal intensity, the instrument is at an optical null. The comb in the sample beam permits balancing the beams. The recording pen is then at 100% transmittance when no sample is present.

The attenuator is driven in and out of the reference beam in response to the signal created at the detector by the sample beam. Thus, when the sample beam is absorbed by the sample, the attenuator is driven into the reference beam until its intensity matches that of the sample beam.

3.3.4. Monochromator

The combined beam passes through the monochromator entrance slit *S*1 to the mirror *M*11, which reflects it to the diffraction grating *G*1. This beam is dispersed into various frequencies, and it is reflected back to mirror *M*11, and then on to mirror *M*12. Mirror *M*12 focuses the beam on exit slit *S*2. The width of the frequency range focused on slit *S*2 is determined by the width of entrance slit *S*1 and the dispersing power of the grating. The frequency band of one dispersed beam focused on slit *S*2 at any moment is determined by the angle of grating *G*1 at that moment. Rotation of grating *G*1 produces a scan of frequency bands at exit slit *S*2 and thus at the detector. Filters are automatically inserted into the radiation path at the exit slit in a sequence during scanning to eliminate all unwanted radiation; this unwanted radiation corresponds to harmonic multiples of the frequency to be measured.

Maximum resolution is obtained by using gratings only in the range of greatest dispersing effectiveness. Therefore, often in a high-resolution instrument, two or more gratings are used (*G*1 and *G*2 of Fig. 3.4*a*).

The narrower the slit width, the greater is the resolution. Here again, some compromise is necessary because of the decreased energy output of the source at lower frequencies (longer wavelengths). On most instruments, the slit width is programmed to increase as the emitted source energy decreases, so that constant reference beam energy enters the monochromator.

3.3.5. Detector (Thermocouple)

After leaving the exit slit of the monochromator, the beam is reflected by a flat mirror *M*13 to an ellipsoidal mirror *M*14. The foci of the ellipsoidal mirror are the exit slit *S*2 and the detector.

The detector is a device that measures radiant energy by means of its heating effect. Two common types of detectors are the thermocouple and bolometer. In the thermocouple detector, the radiant energy heats one of two bimetallic junctions, and an electromotive force (emf) is produced between the two junctions proportional to the degree of heating. The bolometer changes its resistance upon heating. It serves as one arm of a bridge so that a change in temperature will cause an unbalanced signal across the circuit. The unbalanced signal can be amplified and recorded or used to activate a servomechanism to reestablish a balance.

Since the detector sees alternately the reference and the sample beam at a switching frequency determined by the rotation of the sector mirror, any change in the intensity of the radiation due to absorption is detected as an off-null signal.

The amplified off-null signal of the detector is used to position the optical attenuator so that the reference and sample beams are kept at equal intensity. The amount of attenuation required is a direct measure of the absorption by the sample. The movement of the attenuator is recorded by the recording chart pen.

Fourier Transform Infrared (FT IR) spectrometry has been extensively developed over the past few years and provides a number of advantages. Radiation containing all IR wavelengths (e.g., 5000–400 cm^{-1}) is split into two beams (Fig. 3.4*b*). One beam is of fixed length, the other of variable length (movable mirror). When the difference in the corresponding wavelengths is an integer multiple of the invariant beam, there is constructive interference; destructive interference occurs when the difference is an odd integer multiple of one quarter of the wavelength. The result of a complete variation of wavelengths is an oscillatory series of destructive or constructive combinations, or interferogram. Fourier transformation converts this interferogram from the time domain into one spectral point on the more familiar form of the frequency domain. Smooth

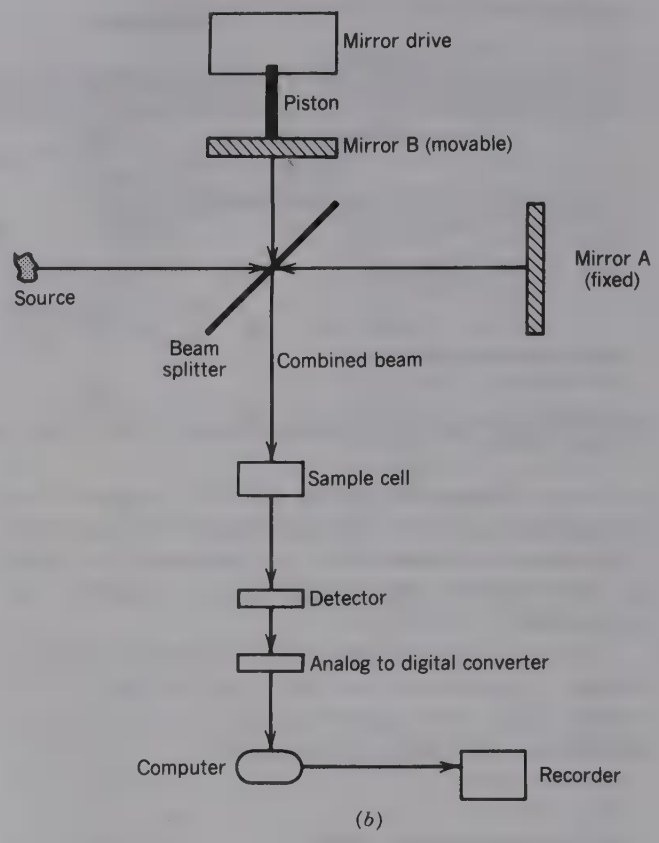

FIGURE 3.4(*b*). Schematic of an FT IR spectrometer.

and continuous variation of the length of the piston adjusts the position of Mirror B and varies the length of beam *B*; Fourier transformation at successive points throughout this variation gives rise to the complete IR spectrum. Passage of this radiation through a sample subjects the compound to a broadband of energies. In principle the analysis of one broadbanded pass of radiation through the sample will give rise to a complete IR spectrum.

There are a number of advantages to FT IR methods. Since a monochromator is not used, the entire radiation range is passed through the sample simultaneously and much time is saved (Felgett's advantage); FT IR instruments can have very high resolution ($\leq$0.001 cm^{-1}). Moreover since the data undergo analog-to-digital conversion, IR results are easily manipulated: Results of several scans are combined to average out random absorption artifacts, and excellent spectra from very small samples can be obtained. An FT IR unit can therefore be used in conjunction with HPLC or GC. As with any computer-aided spectrometer, spectra of pure samples or solvents (stored in the computer) can be subtracted from mixtures. Flexibility in spectral print-out is also available: for example, spectra linear in either wavenumber or wavelength can be obtained from the same data set.

Several manufacturers offer GC–FT IR instruments with which a vapor phase spectrum can be obtained on nanogram amounts of a compound eluting from a capillary GC column. Vapor phase spectra resemble those obtained at high dilution in a nonpolar solvent: Concentration-dependent peaks are shifted to higher frequency compared with those obtained from concentrated solutions, thin films, or the solid state.

3.4. SAMPLE HANDLING

Infrared spectra may be obtained for gases, liquids, or solids. The spectra of gases or low-boiling liquids may be obtained by expansion of the sample into an evacuated cell. Gas cells are available in lengths of a few centimeters to 40 m. The sampling area of a standard IR spectrophotometer will not accommodate cells much longer than 10 cm; long paths are achieved by multiple reflection optics.

Liquids may be examined neat or in solution. Neat liquids are examined between salt plates usually without a spacer. Pressing a liquid sample between flat plates produces a film of 0.01 mm or less in thickness, the plates being held together by capillary action. Samples of 1–10 mg are required. Thick samples of neat liquids usually absorb too strongly to produce a satisfactory spectrum. Volatile liquids are examined in sealed cells with very thin spacers. Silver chloride plates may be used for samples that dissolve sodium chloride plates.

Solutions are handled in cells of 0.1–1 mm thickness. Volumes of 0.1–1 mL of 0.05–10% solutions are required for readily available cells (Fig. 3.5). A compensating cell, containing pure solvent, is placed in the reference beam. The spectrum thus obtained is that of the solute except in those regions in which the solvent absorbs strongly. For example, thick samples of carbon tetrachloride absorb strongly near 800 cm^{-1}; compensation for this band is ineffective since strong absorption prevents any radiation from reaching the detector.

The solvent selected must be dry and transparent in the region of interest. When the entire spectrum is of interest, several solvents must be used. A common pair of solvents is carbon tetrachloride (CCl_4) and carbon disulfide (CS_2). Carbon tetrachloride is relatively free of absorption at frequencies above 1333 cm^{-1}, whereas CS_2 shows little absorption below 1333 cm^{-1}. Solvent and solute combinations that react must be avoided. For example, CS_2 cannot be used as a solvent for primary or secondary amines. Amino alcohols react slowly with CS_2 and CCl_4.

When only very small samples are available, ultramicrocavity cells are used in conjunction with a beam condenser. A spectrum can be obtained on a few micrograms of sample in solution. When volatility permits, the solute can be recovered for examination by other spectrometric techniques. The absorption patterns of selected solvents and mulling oils are presented in Appendix A.

Solids are usually examined as a mull, a pressed disk, or as a deposited glassy film. Mulls are prepared by thoroughly grinding 2–5 mg of a solid in a smooth agate mortar. Grinding is continued after the addition of 1 or 2 drops of the mulling oil. The suspended particles must be less than 2 μm to avoid excessive scattering of radiation. The mull is examined as a thin film between flat salt plates. Nujol® (a high-boiling petroleum oil) is commonly used as a mulling agent. When hydrocarbon bands interfere with the spectrum, Fluorolube® (a completely halogenated polymer containing F and Cl) or hexachlorobutadiene may be used. The use of both Nujol® and Fluorolube® mulls makes possible a scan, essentially free of interfering bands, over the 4000–250 cm^{-1} region.

The pellet (pressed-disk) technique depends on the fact that dry, powdered potassium bromide (or other alkali metal halides) can be compacted under pressure *in vacuo* to form transparent disks. The sample (0.5–1.0 mg) is intimately mixed with approximately 100 mg of dry, powdered KBr. Mixing can be effected by thorough grinding in a smooth agate mortar or, more efficiently, with a small vibrating ball mill, or by lyophilization. The mixture is pressed with special dies under a pressure of 10,000–15,000 psi into a transparent disk.

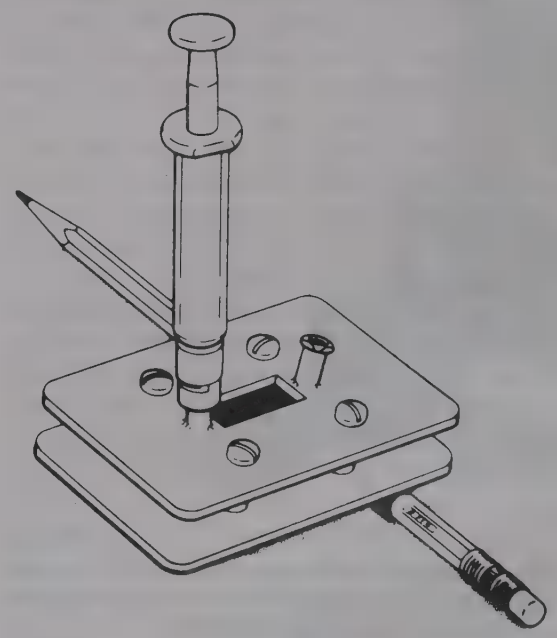

FIGURE 3.5. Correct way to fill a sealed cell.

The quality of the spectrum depends on intimacy of mixing and the reduction of the suspended particles to 2 μm or less. Microdisks, 0.5–1.5 mm in diameter, can be used with a beam condenser. The microdisk technique permits examination of samples as small as 1 μg. Bands near 3448 and 1639 cm^{-1}, due to moisture, frequently appear in spectra obtained by the pressed-disk technique.

The use of KBr disks or pellets has often been avoided because of the demanding task of making good pellets. Such KBr techniques can be less formidable through the Mini-Press (Fig. 3.6) that affords a simple procedure; the KBr-sample mixture is placed in the nut portion of the assembly with one bolt in place. The second bolt is introduced, and pressure is applied by tightening the bolts. Removal of the bolts leaves a pellet in the nut that now serves as a cell.

Deposited films are useful only when the material can be deposited from solution or cooled from a melt as microcrystals or as a glassy film. Crystalline films generally lead to excessive light scattering. Specific crystal orientation may lead to spectra differing from those observed for randomly oriented particles such as exist in a mull or halide disk. The deposited film technique is particularly useful for obtaining spectra of resins and plastics. Care must be taken to free the sample of solvent by vacuum treatment or gentle heating.

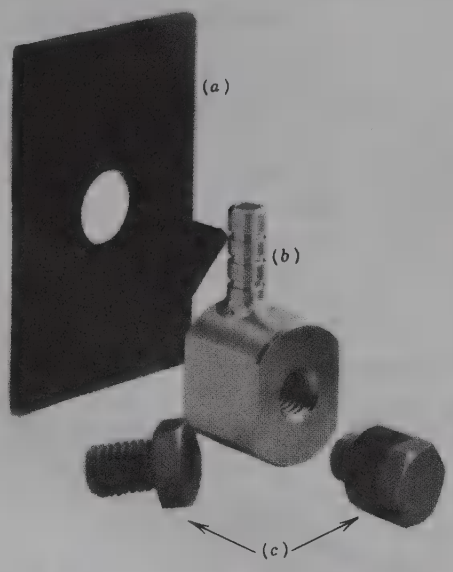

FIGURE 3.6. Mini-Press: (*a*) Cell holder. (*b*) Nut = cell. (*c*) Bolts. Side-arm (b) permits pellet formation under reduced pressure. Photo used with permission of Perkin-Elmer Corporation.

A technique known as attenuated total reflection or internal reflection spectroscopy is now available for obtaining qualitative spectra of solids regardless of thickness. The technique depends on the fact that a beam of light that is internally reflected from the surface of a transmitting medium passes a short distance beyond the reflecting boundary and returns to the transmitting medium as a part of the process of reflection. If a material (i.e., the sample) of lower refractive index than the transmitting medium is brought in contact with the reflecting surface, the light passes through the material to the depth of a few micrometers, producing an absorption spectrum. An extension of the technique provides for multiple internal reflections along the surface of the sample. The multiple internal reflection technique results in spectra with intensities comparable to transmission spectra.

In general, a dilute solution in a nonpolar solvent furnishes the best (i.e., least distorted) spectrum. Nonpolar compounds give essentially the same spectra in the condensed phase (i.e., neat liquid, a mull, a KBr disk, or a thin film) as they give in nonpolar solvents. Polar compounds, however, often show hydrogen-bonding effects in the condensed phase. Unfortunately, polar compounds are frequently insoluble in nonpolar solvents, and the spectrum must be obtained either in a condensed phase or in a polar solvent; the latter introduces the possibility of solute–solvent hydrogen bonding.

Reasonable care must be taken in handling salt cells and plates. Moisture-free samples should be used. Fingers should not come in contact with the optical surfaces. Care should be taken to prevent contamination with silicones, which are hard to remove and have strong absorption patterns.

3.5. INTERPRETATION OF SPECTRA

There are no rigid rules for interpreting an IR spectrum. Certain requirements, however, must be met before an attempt is made to interpret a spectrum.

1. The spectrum must be adequately resolved and of adequate intensity.
2. The spectrum should be that of a reasonably pure compound.
3. The spectrophotometer should be calibrated so that the bands are observed at their proper frequencies

or wavelengths. Proper calibration can be made with reliable standards, such as poly(styrene) film.

4. The method of sample handling must be specified. If a solvent is employed, the solvent, concentration, and the cell thickness should be indicated.

A precise treatment of the vibrations of a complex molecule is not feasible; thus, the IR spectrum must be interpreted from empirical comparison of spectra, and extrapolation of studies of simpler molecules. Many questions arising in the interpretation of an IR spectrum can be answered by data obtained from the mass, UV, and NMR spectra.

Infrared absorption of organic molecules is summarized in the chart of characteristic group absorptions in Appendix C. Many of the group absorptions vary over a wide range because the bands arise from complex interacting vibrations within the molecule. Absorption bands may, however, represent predominantly a single vibrational mode. Certain absorption bands, for example, those arising from the C—H, O—H, and C=O stretching modes, remain within fairly narrow regions of the spectrum. Important details of structure may be revealed by the exact position of an absorption band within these narrow regions. Shifts in absorption position and changes in band contours, accompanying changes in molecular environment, may also suggest important structural details.

The two important areas for a preliminary examination of a spectrum are the regions 4000–1300 and 900–650 cm^{-1}. The high-frequency portion of the spectrum is called the functional group region. The characteristic stretching frequencies for important functional groups such as OH, NH, and C=O occur in this portion of the spectrum. The absence of absorption in the assigned ranges for the various functional groups can usually be used as evidence for the absence of such groups in the molecule. Care must be exercised, however, in such interpretations since certain structural characteristics may cause a band to become extremely broad so that it may go unnoticed. For example, intramolecular hydrogen bonding in the enolic form of acetylacetone results in a broad OH band, which may be overlooked. The absence of absorption in the 1850–1540 cm^{-1} region excludes a structure containing a carbonyl group. Weak bands in the high-frequency region, resulting from the fundamental absorption of functional groups, such as S—H and C≡C, are extremely valuable in the determination of structure. Such weak bands would be of little value in the more complicated regions of the spectrum. Overtones and combination tones of lower frequency bands frequently appear in the high-frequency region of the spectrum. Overtone and combination-tone bands are characteristically weak except when Fermi resonance occurs. Strong skeletal bands for aromatics and heteroaromatics fall in the 1600–1300 cm^{-1} region of the spectrum.

The lack of strong absorption bands in the 900–650 cm^{-1} region generally indicates a nonaromatic structure. Aromatic and heteroaromatic compounds display strong out-of-plane C—H bending and ring bending absorption bands in this region that can frequently be correlated with the substitution pattern. Broad, moderately intense absorption in the low-frequency region suggests the presence of carboxylic acid dimers, amines, or amides, all of which show out-of-plane bending in this region. If the region is extended to 1000 cm^{-1}, absorption bands characteristic of alkene structures are included.

The intermediate portion of the spectrum, 1300–900 cm^{-1}, is usually referred to as the "fingerprint" region. The absorption pattern in this region is frequently complex, with the bands originating in interacting vibrational modes. This portion of the spectrum is extremely valuable when examined in reference to the other regions. For example, if alcoholic or phenolic O—H stretching absorption appears in the high-frequency region of the spectrum, the position of the C—C—O absorption band in the 1260–1000 cm^{-1} region frequently makes it possible to assign the O—H absorption to alcohols and phenols with highly specific structures. Absorption in this intermediate region is probably unique for every molecular species.

Any conclusions reached after examination of a particular band should be confirmed where possible by examination of other portions of the spectrum. For example, the assignment of a carbonyl band to an aldehyde should be confirmed by the appearance of a band or a pair of bands in the 2900–2695 cm^{-1} region of the spectrum, arising from the C—H stretching vibrations of the aldehyde group. Similarly, the assignment of a carbonyl band to an ester should be confirmed by observation of a strong band in the C—O stretching region, 1300–1100 cm^{-1}.

Similar compounds may give virtually identical spectra under normal conditions, but fingerprint differences can be detected with an expanded vertical scale or with a very large sample (major bands off-scale). For example, pentane and hexane are essentially indistinguishable under normal conditions and can be differentiated only at very high recorder sensitivity.

Finally, in a "fingerprint" comparison of spectra, or any other situation in which the *shapes* of peaks are important, we should be aware of the substantial differences in the appearance of the spectrum in changing

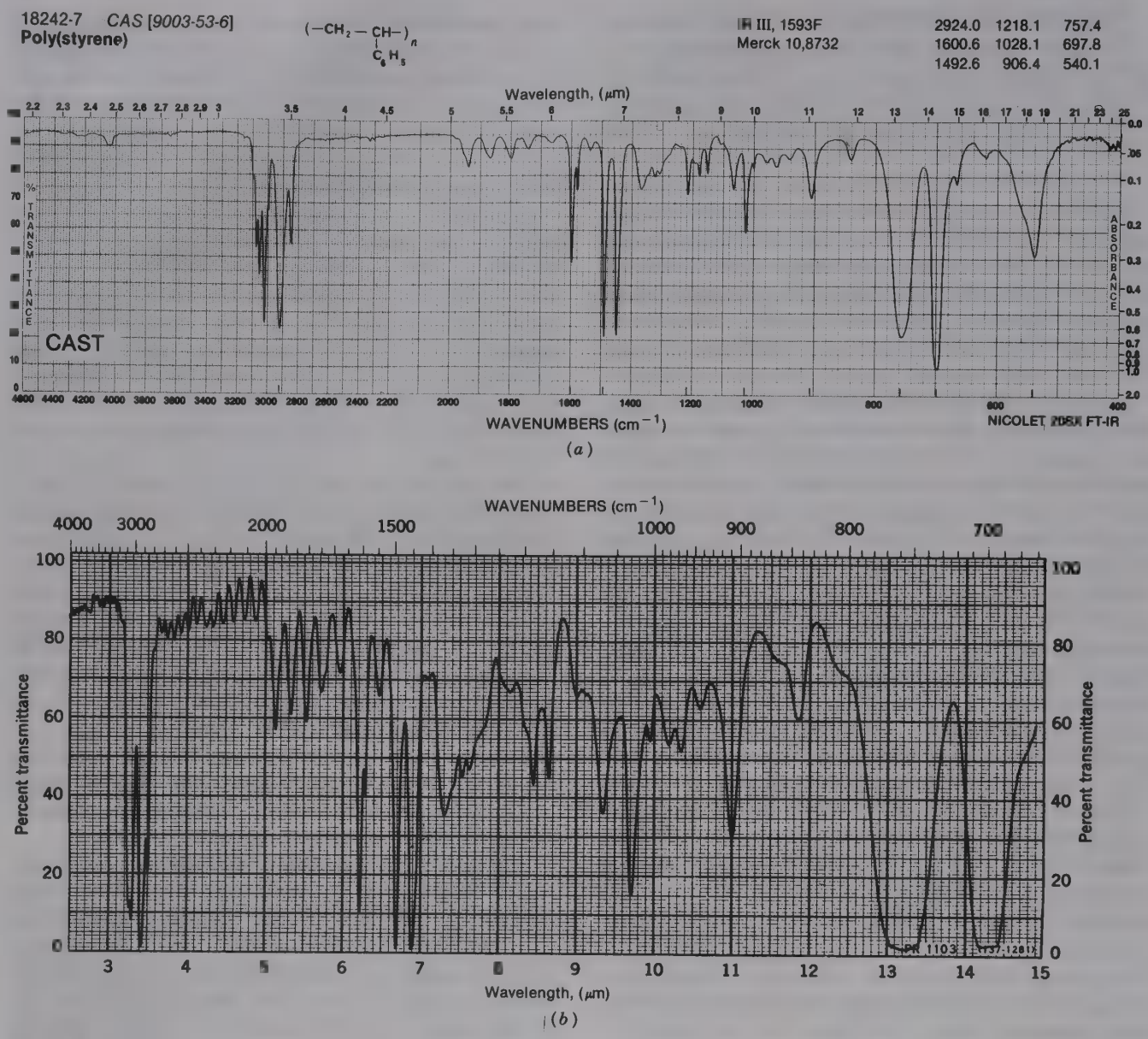

FIGURE 3.7. Polystyrene, same sample for both (*a*) and (*b*). Spectrum (*a*) Linear in wavenumber (cm^{-1}); spectrum (*b*) linear in wavelength (μm).

from a spectrum that is linear in wavenumber to one that is linear in wavelength (Fig. 3.7).

3.6. CHARACTERISTIC GROUP ABSORPTIONS OF ORGANIC MOLECULES

A table of characteristic group absorptions is presented as Appendix C. The ranges presented for group absorptions have been assigned following the examination of many compounds in which the groups occur. Although the ranges are quite well defined, the precise frequency or wavelength at which a specific group absorbs is dependent on its environment within the molecule and on its physical state.

This section is concerned with a comprehensive look at these characteristic group absorptions and their relationship to molecular structure. As a major type or class of molecule or functional group is introduced in the succeeding sections, an example of an IR spectrum with the important peak assignments will be given. Spectra of common laboratory substances, representing many of the chemical classes listed below, are shown in Appendix B. Characteristic group absorptions are found in Appendix C.

3.6.1. Normal Alkanes (Paraffins)

The spectra of normal alkanes (paraffins) can be interpreted in terms of four vibrations, namely, the stretching and bending of C—H and C—C bonds. Detailed analysis of the spectra of the lower members of the alkane series has made detailed assignments of the spectral positions of specific vibrational modes possible.

Not all of the possible absorption frequencies of the paraffin molecule are of equal value in the assignment of structure. The C—C bending vibrations occur at very low frequencies (below 500 cm^{-1}) and therefore do not appear in our spectra. The bands assigned to C—C stretching vibrations are weak and appear in the broad region of 1200–800 cm^{-1}; they are generally of little value for identification.

The most characteristic vibrations are those arising from C—H stretching and bending. Of these vibrations, those arising from methylene twisting and wagging are usually of limited diagnostic value because of their weakness and instability. This instability is a result of strong coupling to the remainder of the molecule.

The vibrational modes of alkanes are common to many organic molecules. Although the positions of C—H stretching and bending frequencies of methyl and methylene groups remain nearly constant in hydrocarbons, the attachment of CH_3 or CH_2 to atoms other than carbon, or to a carbonyl group or aromatic ring, may result in appreciable shifts of the C—H stretching and bending frequencies.

The spectrum of dodecane, Figure 3.8, is that of a typical straight-chain hydrocarbon.

3.6.1.1. C—H Stretching Vibrations

Absorption arising from C—H stretching in the alkanes occurs in the general region of 3000–2840 cm^{-1}. The positions of the C—H stretching vibrations are among the most stable in the spectrum. When a spectrum is obtained with an instrument using a sodium chloride prism, the bands in this region are frequently unresolved (as in Fig. 3.7*b*). Resolution (Fig. 3.7*a*) is achieved through the use of a grating instrument or FTIR.

METHYL GROUPS. An examination of a large number of saturated hydrocarbons containing methyl groups showed, in all cases, two distinct bands occurring at 2962 and 2872 cm^{-1}. The first of these results from the asymmetrical (as) stretching mode in which two C—H bonds of the methyl group are extending while the third one is contracting ($\nu_{as}CH_3$). The second arises from symmetrical (s) stretching (ν_sCH_3) in which all three of the C—H bonds extend and contract in phase. The presence of several methyl groups in a molecule results in strong absorption at these positions.

METHYLENE GROUPS. The asymmetrical stretching ($\nu_{as}CH_2$) and symmetrical stretching (ν_sCH_2) occur, respectively, near 2926 and 2853 cm^{-1}. The positions of these bands do not vary more than ± 10 cm^{-1} in the aliphatic and nonstrained cyclic hydrocarbons. The frequency of methylene stretching is increased when the methylene group is part of a strained ring.

3.6.1.2. C—H Bending Vibrations

METHYL GROUPS. Two bending vibrations can oc-

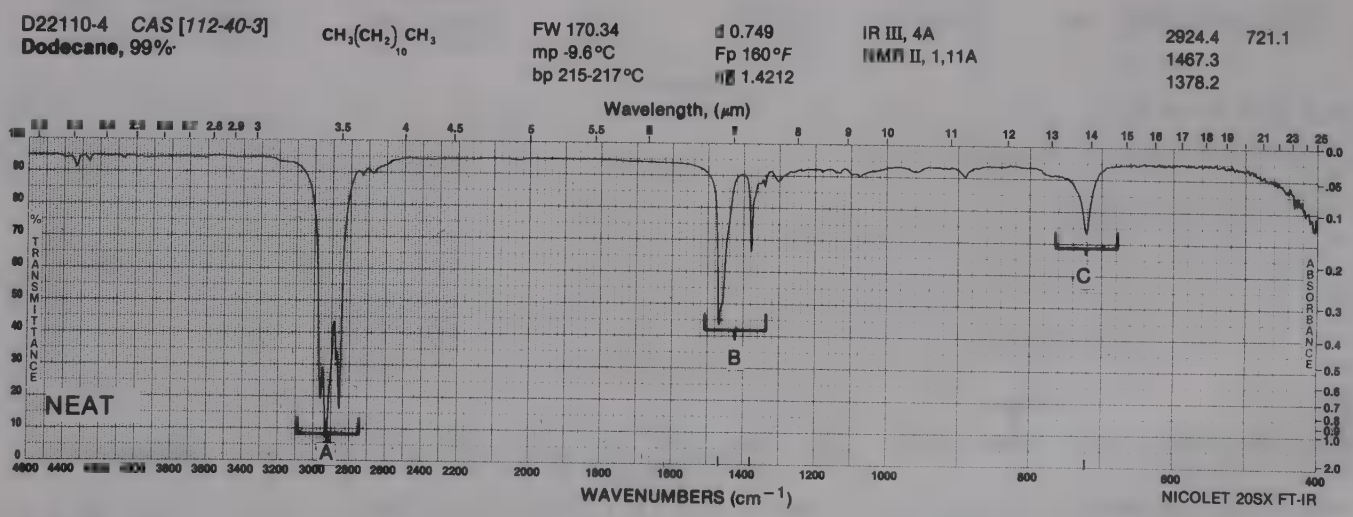

FIGURE 3.8. Dodecane. A. The C—H stretch: 2962 cm^{-1} ν_{as} CH_3, 2872 cm^{-1} ν_s CH_3, 2924 cm^{-1} ν_{as} CH_2, 2853 cm^{-1} ν_s CH_2. B. The C—H bend: 1467 cm^{-1} δ_s CH_2, 1450 cm^{-1} δ_{as} CH_3, 1378 cm^{-1} δ_s CH_3. C. The CH_2 rock: 721 cm^{-1} ρ CH_2.

cur within a methyl group. The first of these, the symmetrical bending vibration, involves the in-phase bending of the C—H bonds (**I**). The second, the asymmetrical bending vibration, involves out-of-phase bending of the C—H bonds (**II**).

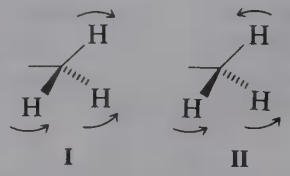

In **I**, the C—H bonds are moving like the closing petals of a flower; in **H**, one petal opens as two petals close.

The symmetrical bending vibration ($\delta_s CH_3$) occurs near 1375 cm^{-1}, the asymmetrical bending vibration ($\delta_{as} CH_3$) near 1450 cm^{-1}.

The asymmetrical vibration generally overlaps the scissoring vibration of the methylene groups (see below). Two distinct bands are observed, however, in compounds such as diethyl ketone, in which the methylene scissoring band has been shifted to a lower frequency, 1439–1399 cm^{-1} and increased in intensity because of its proximity to the carbonyl group.

The absorption band near 1375 cm^{-1}, arising from the symmetrical bending of the methyl C—H bonds, is very stable in position when the methyl group is attached to another carbon atom. The intensity of this band is greater for each methyl group in the compound than that for the asymmetrical methyl bending vibration or the methylene scissoring vibration.

METHYLENE GROUPS. The bending vibrations of the C—H bonds in the methylene group have been shown schematically in Figure 1. The four bending vibrations are referred to as *scissoring, rocking, wagging,* and *twisting*.

The scissoring band ($\delta_s CH_2$) in the spectra of hydrocarbons occurs at a nearly constant position near 1465 cm^{-1}.

The band resulting from the methylene rocking vibration (ρ CH_2), in which all of the methylene groups rock in phase, appears near 720 cm^{-1} for straight-chain alkanes of seven or more carbon atoms. This band may appear as a doublet in the spectra of solid samples. In the lower members of the *n*-alkane series, the band appears at somewhat higher frequencies.

Absorption of hydrocarbons, due to methylene twisting and wagging vibrations, is observed in the 1350–1150 cm^{-1} region. These bands are generally appreciably weaker than those resulting from methylene scissoring. A series of bands in this region, arising from the methylene group, is characteristic of the spectra of solid samples of long-chain acids, amides, and esters.

3.6.2. Branched-Chain Alkanes

In general, the changes brought about in the spectrum of a hydrocarbon by branching result from changes in skeletal stretching vibrations and methyl bending vibrations; these occur below 1500 cm^{-1}. The spectrum of Figure 3.9 is that of a typical branched alkane.

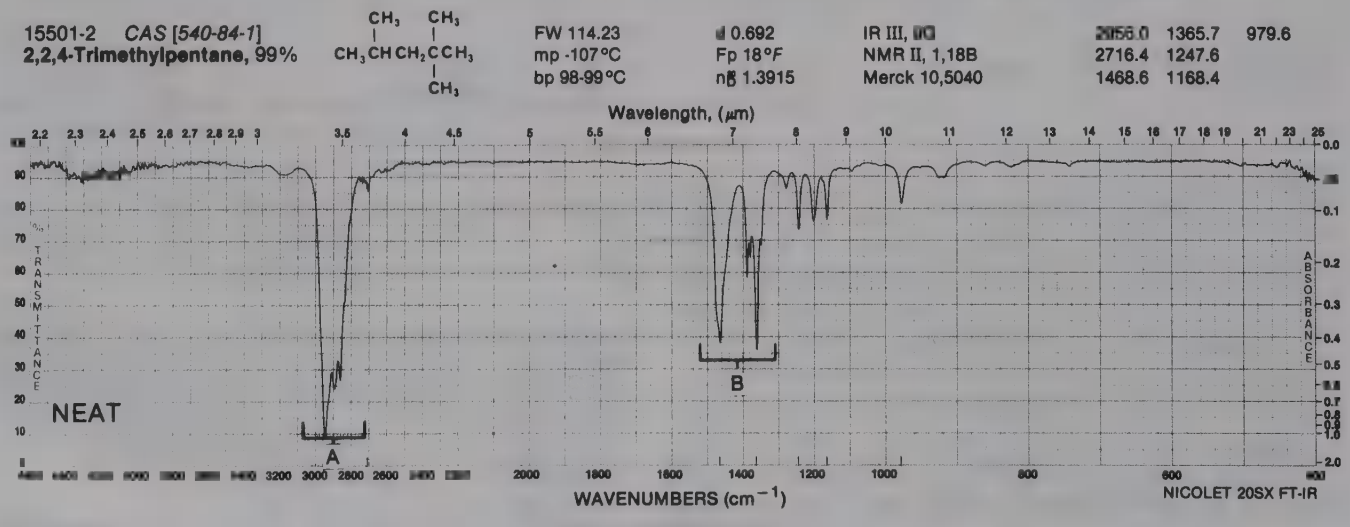

FIGURE 3.9. 2,2,4-Trimethylpentane.* A. The C—H stretch (see Fig. 3.8). B. The C—H bend (see Fig. 3.8). There are overlapping doublets for the *t*-butyl and the isopropyl groups at 1340–1400 cm^{-1}. Compare the absence of methylene rocking band(s) 800–1000 cm^{-1} to Figure 3.8.

*Isooctane is another name for 2,2,4-trimethylpentane.

3.6.2.1. C—H Stretching Vibrations

TERTIARY C—H GROUPS. Absorption resulting from this vibrational mode is very weak and is usually lost in other aliphatic C—H absorption. Absorption in hydrocarbons occurs near 2890 cm^{-1}.

3.6.2.2. C—H Bending Vibrations

gem-DIMETHYL GROUPS. Configurations in which two methyl groups are attached to the same carbon atom exhibit distinctive absorption in the C—H bending region. The isopropyl group shows a strong doublet, with peaks of almost equal intensity at 1385–1380 and 1370–1365 cm^{-1}. The tertiary butyl group gives rise to two C—H bending bands, one in the 1395–1385 cm^{-1} region and one near 1370 cm^{-1}. In the *t*-butyl doublet, the long wavelength band is more intense. When the *gem*-dimethyl group occurs at an internal position, a doublet is observed in essentially the same region where absorption occurs for the isopropyl and *t*-butyl groups. Doublets are observed for *gem*-dimethyl groups because of interaction between the in-phase and out-of-phase symmetrical CH_3 bending of the two methyl groups attached to a common carbon atom.

Weak bands result from methyl rocking vibrations in isopropyl and *t*-butyl groups. These vibrations are sensitive to mass and interaction with skeletal stretching modes and are generally less reliable than the C—H bending vibrations. The following assignments have been made: isopropyl group, 922–919 cm^{-1}, and *t*-butyl group, 932–926 cm^{-1}.

3.6.3. Cyclic Alkanes

3.6.3.1. C—H Stretching Vibrations

The methylene stretching vibrations of unstrained cyclic poly(methylene) structures are much the same as those observed for acyclic paraffins. Increasing ring strain moves the C—H stretching bands progressively to high frequencies. The ring CH_2 and CH groups in a monoalkylcyclopropane ring absorb in the region of 3100–2990 cm^{-1}.

3.6.3.2. C—H Bending Vibrations

Cyclization decreases the frequency of the CH_2 scissoring vibration. Cyclohexane absorbs at 1452 cm^{-1}, whereas *n*-hexane absorbs at 1468 cm^{-1}. Cyclopentane absorbs at 1455 cm^{-1}, cyclopropane absorbs at 1442 cm^{-1}. This shift frequently makes it possible to observe distinct bands for methylene and methyl absorption in this region. Spectra of other saturated hydrocarbons appear in Appendix B: hexane (No. 1), Nujol® (No. 2), and cyclohexane (No. 3).

3.6.4. Alkenes

Alkene (olefinic) structures introduce several new modes of vibration into a hydrocarbon molecule: a C=C stretching vibration, C—H stretching vibrations in which the carbon atom is present in the alkene linkage, and in-plane and out-of-plane bending of the alkene C—H bond. The spectrum of Figure 3.10 is that of a typical terminal alkene.

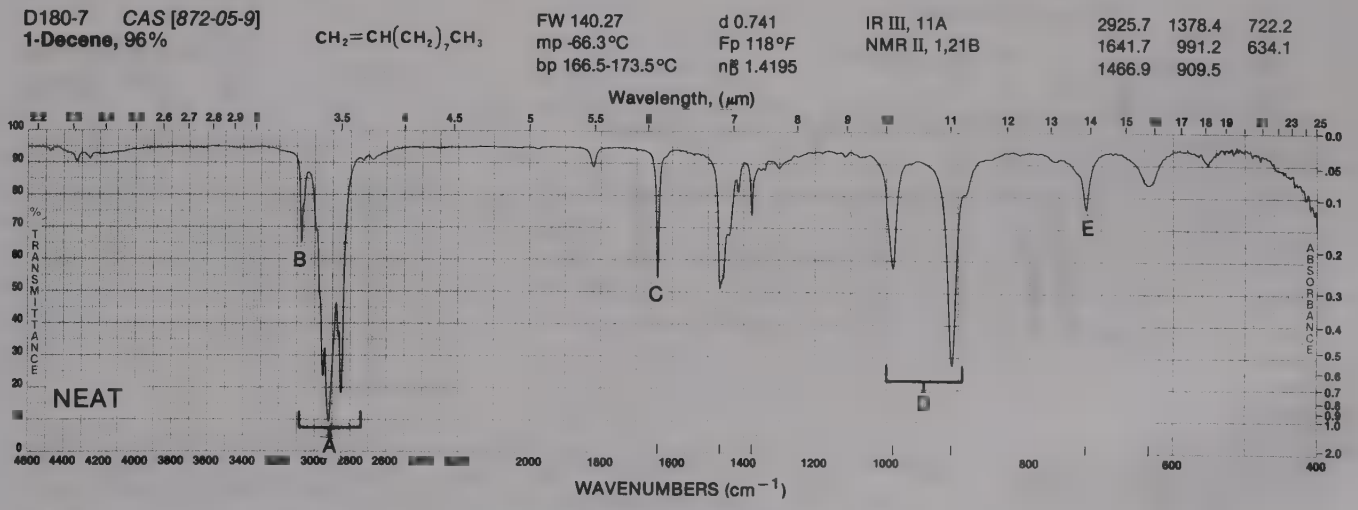

FIGURE 3.10. 1-Decene. A. The C—H stretch (see Fig. 3.8). Note alkene C—H stretch (B) at 3049 cm^{-1}. C. The C=C stretch, 1642 cm^{-1}, see Appendix Table D-1. D. Out-of-plane C—H bend: 991 cm^{-1}, (alkene) 909.5 cm^{-1}. E. Methylene rock: 722 cm^{-1}.

3.6.4.1. C=C Stretching Vibrations

UNCONJUGATED LINEAR ALKENES. The C=C stretching mode of unconjugated alkenes usually shows moderate to weak absorption at 1667–1640 cm^{-1}. Monosubstituted alkenes, that is, vinyl groups, absorb near 1640 cm^{-1}, with moderate intensity. Disubstituted trans-alkenes, tri-, and tetraalkyl substituted alkenes absorb at or near 1670 cm^{-1}; disubstituted cis-alkenes and vinylidene alkenes absorb near 1650 cm^{-1}.

The absorption of symmetrical disubstituted trans-alkenes or tetrasubstituted alkenes may be extremely weak or absent. The cis-alkenes, which lack the symmetry of the trans structure, absorb more strongly than trans-alkenes. Internal double bonds generally absorb more weakly than terminal double bonds because of pseudosymmetry.

Abnormally high absorption frequency is observed for $—CH=CF_2$ and $—CF=CF_2$ groups. The former absorbs near 1754 cm^{-1}, the latter near 1786 cm^{-1}. In contrast, the absorption frequency is reduced by the attachment of chlorine, bromine, or iodine.

CYCLOALKENES. Absorption of the internal double bond in the unstrained cyclohexene system is essentially the same as that of a cis isomer in an acyclic system. The C=C stretch vibration is coupled with the C—C stretching of the adjacent bonds. As the angle α 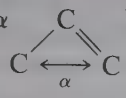 becomes smaller the interaction becomes less until it is at a minimum at 90° in cyclobutene (1566 cm^{-1}). In the cyclopropene structure, interaction again becomes appreciable, and the absorption frequency increases (1641 cm^{-1}).

The substitution of alkyl groups for an α-hydrogen atom in strained ring systems serves to increase the frequency of C=C absorption. Cyclobutene absorbs at 1566 cm^{-1}, 1-methylcyclobutene at 1641 cm^{-1}.

The absorption frequency of external exocyclic bonds increases with decreasing ring size. Methylenecyclohexane absorbs at 1650 cm^{-1}, methylenecyclopropane at 1781 cm^{-1}.

CONJUGATED SYSTEMS. The alkene bond stretching vibrations in conjugated dienes without a center of symmetry interact to produce two C=C stretching bands. The spectrum of an unsymmetrical conjugated diene, such as 1,3-pentadiene, shows absorption near 1650 and 1600 cm^{-1}. The symmetrical molecule 1,3-butadiene shows only one band near 1600 cm^{-1}, resulting from asymmetric stretching; the symmetrical stretching band is inactive in the IR. The IR spectrum of isoprene (Fig. 3.11) illustrates many of these features.

Conjugation of an alkene double bond with an aromatic ring produces enhanced alkene absorption near 1625 cm^{-1}.

The absorption frequency of the alkene bond in conjugation with a carbonyl group is lowered by about 30 cm^{-1}; the intensity of absorption is increased. In *s*-cis structures, the alkene absorption may be as intense as that of the carbonyl group. *s*-Trans structures absorb more weakly than *s*-cis structures.

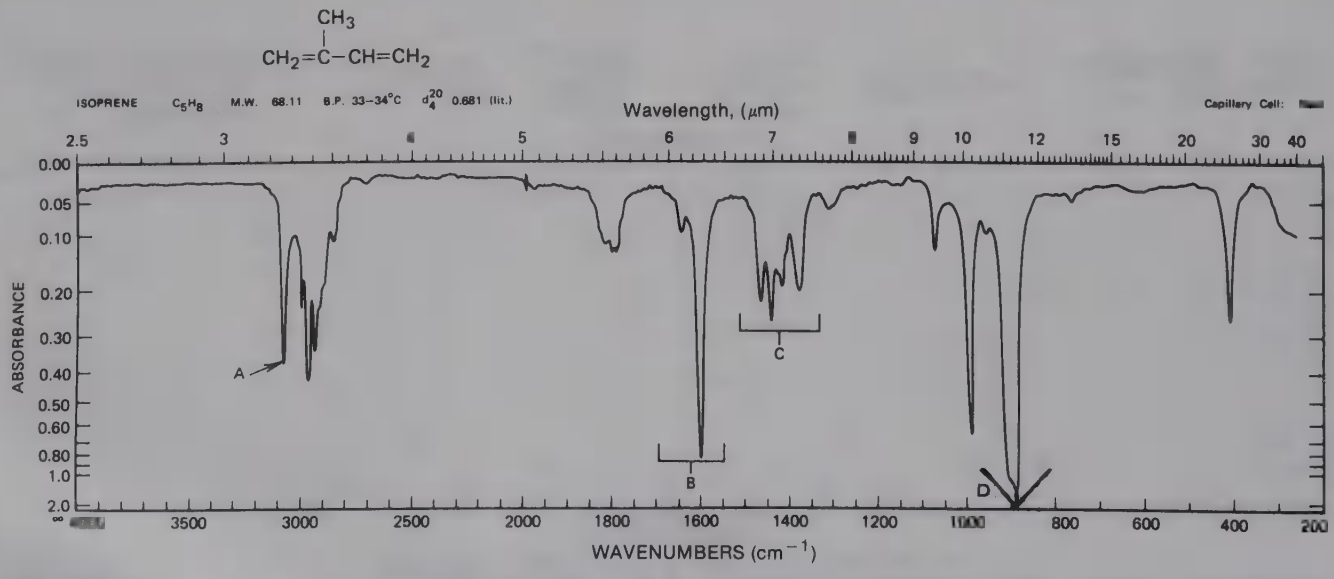

FIGURE 3.11. Isoprene. A. The C—H stretch: =C—H 3090 cm^{-1}. B. Coupled C=C—C=C stretch: symmetric 1640 cm^{-1} (weak), asymmetric 1598 cm^{-1} (strong). C. The C—H bend (saturated, alkene in-plane). D. The C—H out-of-plane bend: 990 cm^{-1}, 892 cm^{-1} (see vinyl, Appendix Table D-1.)

CUMULATED ALKENES. A cumulated double-bond system, as occurs in the allenes $\left(\rangle C{=}C{=}CH_2\right)$, absorbs near 2000–1900 cm^{-1}. The absorption results from asymmetric C=C=C stretching. The absorption may be considered an extreme case of exocyclic C=C absorption.

3.6.4.2. Alkene C—H Stretching Vibrations

In general, any C—H stretching bands above 3000 cm^{-1} result from aromatic, heteroaromatic, alkyne, or alkene C—H stretching. Also found in the same region are the C—H stretching in small rings, such as cyclopropane, and the C—H in halogenated alkyl groups. The frequency and intensity of alkene C—H stretching absorption are influenced by the pattern of substitution. With proper resolution, multiple bands are observed for structures in which stretching interaction may occur. For example, the vinyl group produces three closely spaced C—H stretching bands. Two of these result from symmetrical and asymmetrical stretching of the terminal C—H groups, and the third from the stretching of the remaining single C—H.

3.6.4.3. Alkene C—H Bending Vibrations

Alkene C—H bonds can undergo bending either in the same plane as the C=C bond or perpendicular to it; the bending vibrations can be either in phase or out of phase with respect to each other.

Assignments have been made for a few of the more prominent and reliable in-plane bending vibrations. The vinyl group absorbs near 1416 cm^{-1} due to a scissoring vibration of the terminal methylene. The C—H rocking vibration of a cis-disubstituted alkene occurs in the same general region.

The most characteristic vibrational modes of alkenes are the out-of-plane C—H bending vibrations between 1000 and 650 cm^{-1}. These bands are usually the strongest in the spectra of alkenes. The most reliable bands are those of the vinyl group, the vinylidene group, and the trans-disubstituted alkene. Alkene absorption is summarized in Tables D-1 and D-2.

In allene structures, strong absorption is observed near 850 cm^{-1}, arising from $=CH_2$ wagging. The first overtone of this band may also be seen. Some spectra showing alkene features are shown in Appendix B: trichloroethylene (No. 12) and tetrachloroethylene (No. 13).

3.6.5. Alkynes

The two stretching vibrations in alkynes (acetylenes) involve C≡C and C—H stretching. Absorption due to C—H bending is characteristic of acetylene and monosubstituted alkynes. The spectrum of Figure 3.12 is that of a typical terminal alkyne.

3.6.5.1. C≡C Stretching Vibrations

The weak C≡C stretching band of alkyne molecules occurs in the region of 2260–2100 cm^{-1}. Because of symmetry, no C≡C band is observed in the IR for alkynes and symmetrically substituted alkynes. In the IR spectra of monosubstituted alkynes, the band appears at 2140–2100 cm^{-1}. Disubstituted alkynes, in which the substitutents are different, absorb near 2260–2190 cm^{-1}. When the substituents are similar in mass, or produce similar inductive and resonance ef-

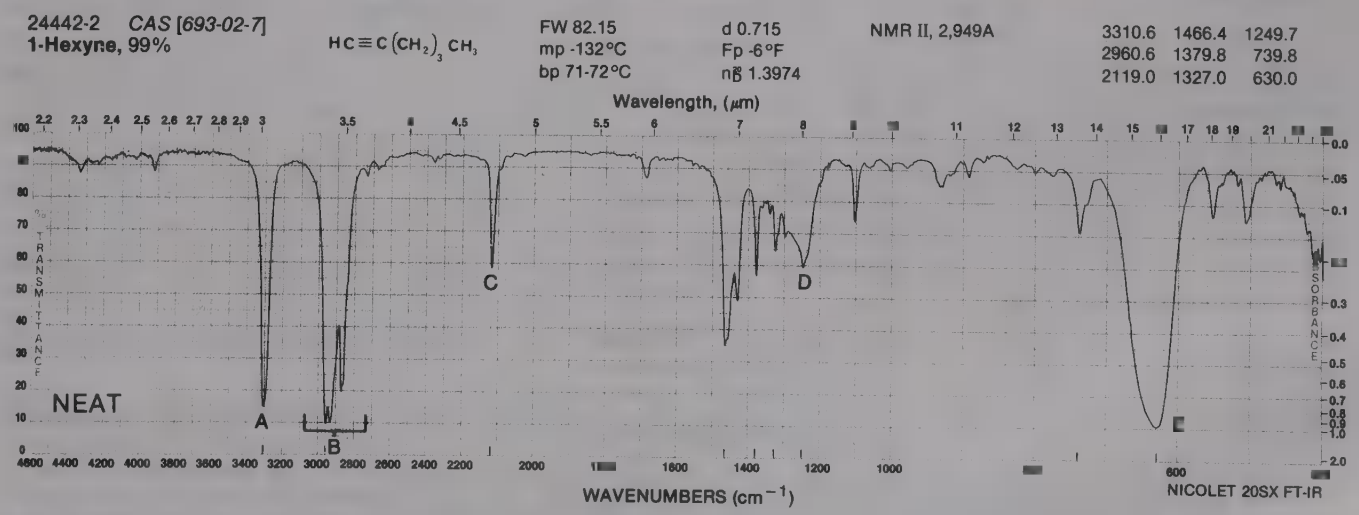

FIGURE 3.12. 1-Hexyne. A. The ≡C—H stretch, 3310 cm^{-1}. B. Normal C—H stretch (see Fig. 3.8), 2857–2941 cm^{-1}. C. The C≡C stretch, 2119 cm^{-1}. D. The ≡C—H bend overtone, 1250 cm^{-1}. E. The ≡C—H bend fundamental, 630 cm^{-1}.

fects, the band may be so weak as to be unobserved in the IR spectrum. For reasons of symmetry, a terminal C≡C produces a stronger band than an internal C≡C (pseudosymmetry). The intensity of the C≡C stretching band is increased by conjugation with a carbonyl group.

3.6.5.2. C—H Stretching Vibrations

The C—H stretching band of monosubstituted alkynes occurs in the general region of 3333–3267 cm^{-1}. This is a strong band and is narrower than the hydrogen-bonded OH and NH bands occurring in the same region.

3.6.5.3. C—H Bending Vibrations

The C—H bending vibration of alkynes or monosubstituted alkynes leads to strong, broad absorption in the 700–610 cm^{-1} region. The first overtone of the C—H bending vibration appears as a weak, broadband in the 1370–1220 cm^{-1} region.

3.6.6. Mononuclear Aromatic Hydrocarbons

The most prominent and most informative bands in the spectra of aromatic compounds occur in the low-frequency range between 900 and 675 cm^{-1}. These strong absorption bands result from the out-of-plane ("oop") bending of the ring C—H bonds. In-plane bending bands appear in the 1300–1000 cm^{-1} region. Skeletal vibrations, involving carbon–carbon stretching within the ring, absorb in the 1600–1585 and 1500–1400 cm^{-1} regions. The skeletal bands frequently appear as doublets, depending on the nature of the ring substituents.

Aromatic C—H stretching bands occur between 3100 and 3000 cm^{-1}.

Weak combination and overtone bands appear in the 2000–1650 cm^{-1} region. The pattern of the overtone bands is characteristic of the substitution pattern of the ring. Because they are weak, the overtone and combination bands are most readily observed in spectra obtained from thick samples. The spectrum of Figure 3.13 is that of a typical aromatic (benzenoid) compound.

3.6.6.1. Out-of-Plane C—H Bending Vibrations

The in-phase, out-of-plane bending of a ring hydrogen atom is strongly coupled to adjacent hydrogen atoms. The position of absorption of the out-of-plane bending bands is, therefore, characteristic of the number of adjacent hydrogen atoms on the ring. The bands are frequently intense, and may be used for the quantitative determination of the relative concentrations of isomers in mixtures.

Assignments for C—H out-of-plane bending bands in the spectra of substituted benzenes appear in the chart of characteristic group absorptions (Appendix C). These assignments are usually reliable for alkyl-substituted benzenes, but caution must be observed in the interpretation of spectra when polar groups are

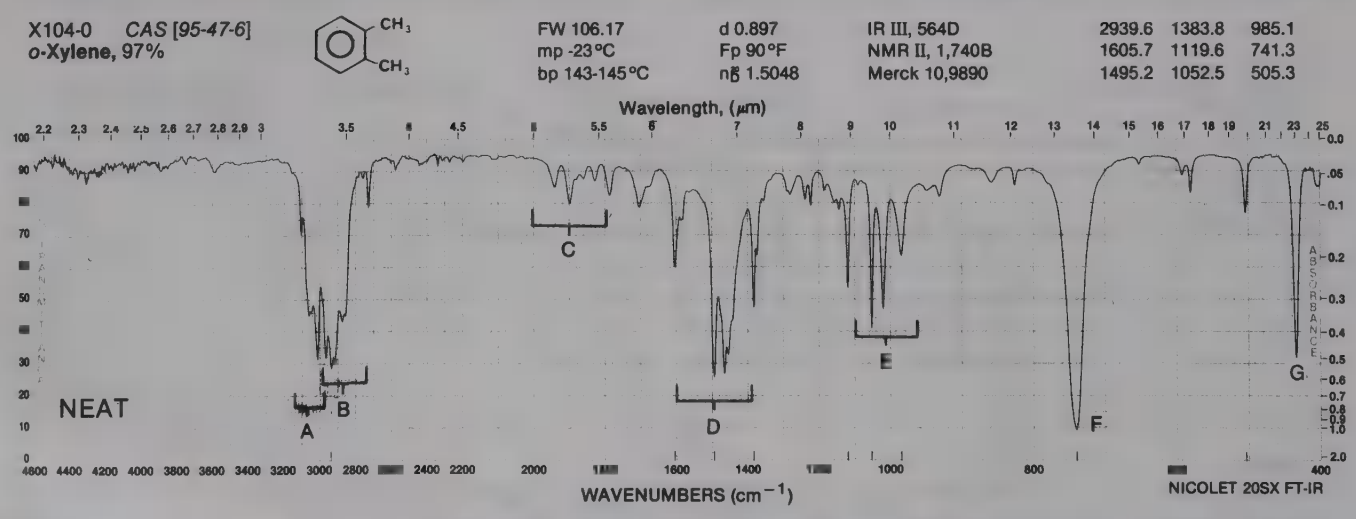

FIGURE 3.13. *o*-Xylene. A. Aromatic C—H stretch, 3008 cm^{-1}. B. Methyl C—H stretch, 2965, 2940, 2918, 2875 cm^{-1} (see Fig. 3.8). C. Overtone or combination bands, 2000–1667 cm^{-1} (see Fig. 3.14.) D. The C=C ring stretch, 1605, 1495, 1466 cm^{-1}. E. In-plane C—H bend, 1052, 1022 cm^{-1}. F. Out-of-plane =C—H bend, 741 cm^{-1}. G. Out-of-plane ring C=C bend, 438 cm^{-1}.

attached directly to the ring, for example, in nitrobenzenes, aromatic acids, and esters or amides of aromatic acids.

The absorption band that frequently appears in the spectra of substituted benzenes near 710–675 cm^{-1} is attributed to out-of-plane ring bending. Some spectra showing typical aromatic absorption are shown in Appendix B: benzene (No. 4), indene (No. 8), diethyl phthalate (No. 21), and *m*-xylene (No. 6).

m di 690 - 710 p di 810 - 840
o di 735 - 770

3.6.7. Polynuclear Aromatic Hydrocarbons

Polynuclear aromatic compounds, like the mononuclear aromatics, show characteristic absorption in three regions of the spectrum.

The aromatic C—H stretching and the skeletal vibrations absorb in the same regions as observed for the mononuclear aromatics. The most characteristic absorption of polynuclear aromatics results from C—H out-of-plane bending in the 900–675-cm^{-1} region. These bands can be correlated with the number of adjacent hydrogen atoms on the rings. Most β-substituted naphthalenes, for example, show three absorption bands due to out-of-plane C—H bending; these correspond to an isolated hydrogen atom and two adjacent hydrogen atoms on one ring and four adjacent hydrogen atoms on the other ring.

In the spectra of α-substituted naphthalenes the bands for the isolated hydrogen and the two adjacent hydrogen atoms of β-naphthalenes are replaced by a band for three adjacent hydrogen atoms. This band is near 810–785 cm^{-1}.

C—H Out-of-Plane Bending Vibrations of a β-Substituted Naphthalene

Substitution Pattern	Absorption Range (cm^{-1})
Isolated hydrogen	862–835
2 Adjacent hydrogen atoms	835–805
4 Adjacent hydrogen atoms	760–735

Additional bands may appear because of ring bending vibrations. The position of absorption bands for more highly substituted naphthalenes and other polynuclear aromatics are summarized by Colthup and by Conley.

3.6.8. Alcohols and Phenols

The characteristic bands observed in the spectra of alcohols and phenols result from O—H stretching and C—O stretching. These vibrations are sensitive to hydrogen bonding. The C—O stretching and O—H bending modes are not independent vibrational modes because they couple with the vibrations of adjacent groups. Some typical spectra of alcohols and a phenol are shown in Figures 3.14–3.16.

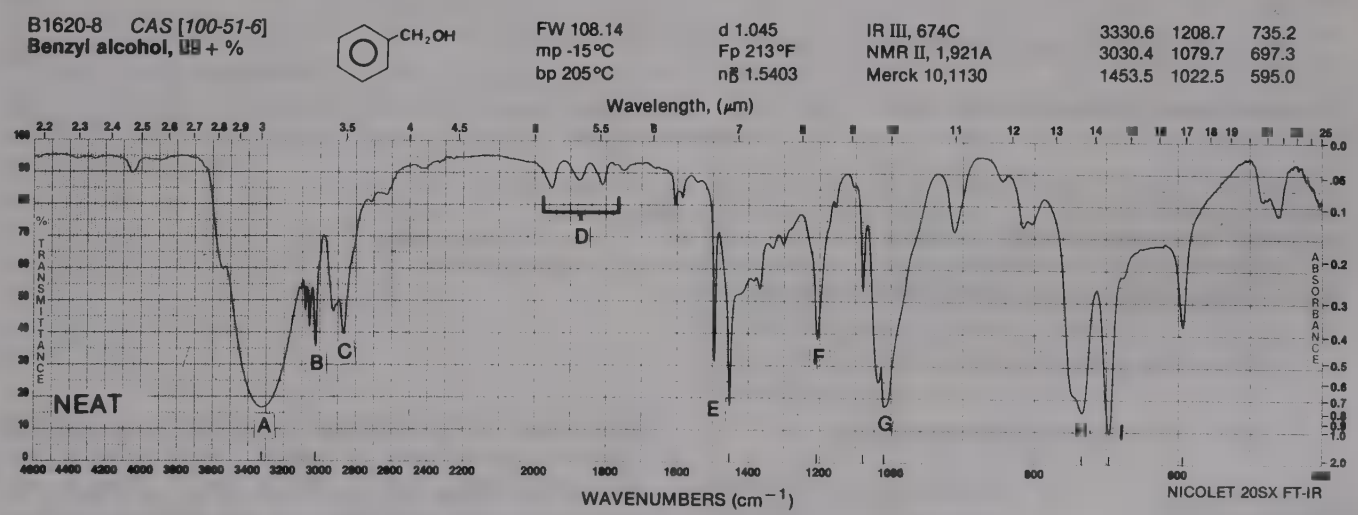

FIGURE 3.14. Benzyl alcohol. A. O—H stretch: intermolecular hydrogen bonded, 3331 cm^{-1}. B. The C—H stretch: aromatic 3100–3000 cm^{-1}. C. The C—H stretch: methylene, 2980–2840 cm^{-1}. D. Overtone or combination bands, 2000–1667 cm^{-1}. E. The C=C ring stretch, 1497, 1454 cm^{-1}, overlapped by CH_2 scissoring, about 1471 cm^{-1}. F. The O—H bend, possibly augmented by C—H in-plane bend, 1209 cm^{-1}. G. The C—O stretch, primary alcohol (see Table 3.2) 1023 cm^{-1}. H. Out-of-plane aromatic C—H bend, 735 cm^{-1}. I. Ring C=C bend, 697 cm^{-1}.

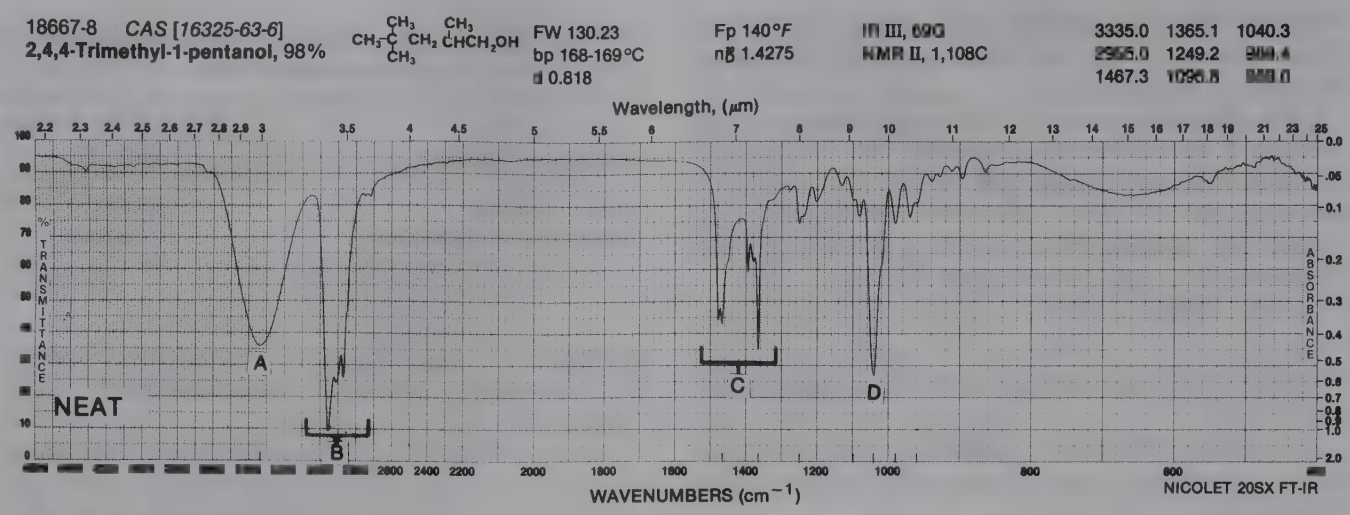

FIGURE 3.15. 2,4,4-Trimethyl-1-pentanol. A. The O—H stretch, intermolecular hydrogen bonding 3335 cm^{-1}. B. The C—H stretch (see Fig. 3.8, 3000–2800 cm^{-1}). C. The C—H bend (see Fig. 3.8). Note the pair of bands for the *gem*-dimethyl group at 1395 and 1365 cm^{-1}. D. The C—O stretch 1040 cm^{-1}.

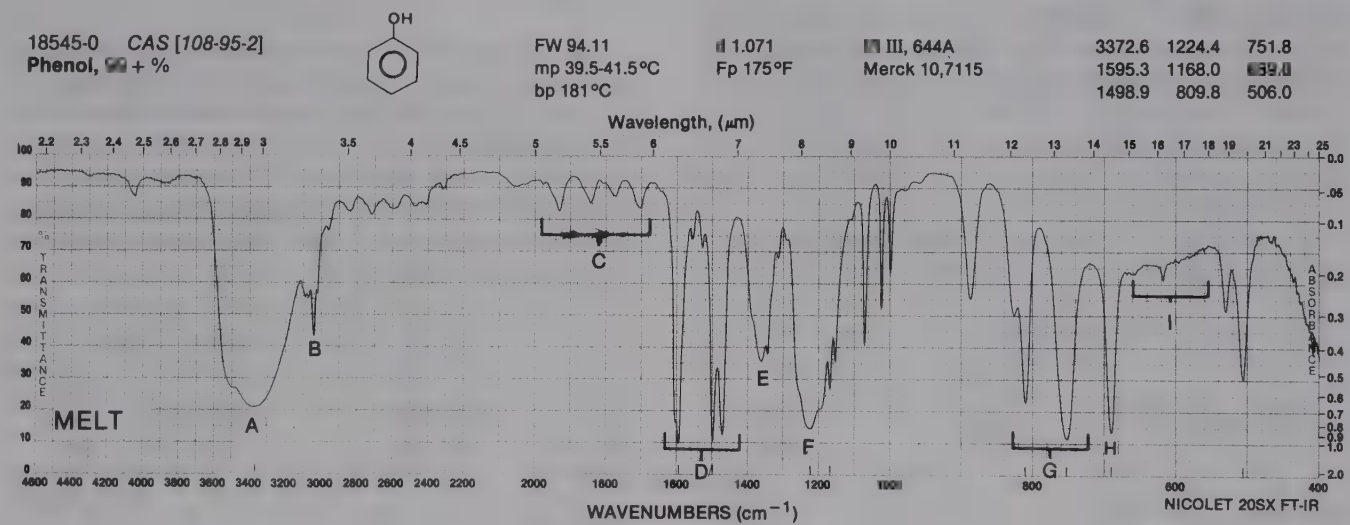

FIGURE 3.16. Phenol. A. Broad intermolecular hydrogen bonded, O—H stretch, 3373 cm^{-1}. B. Aromatic C—H stretch, 3045 cm^{-1}. C. Overtone or combination bands, 2000–1667 cm^{-1}. D. The C=C ring stretch, 1595, 1499, 1470 cm^{-1}. E. In-plane O—H bend, 1360 cm^{-1}. F. The C—O stretch, 1224 cm^{-1}. G. Out-of-plane C—H bend, 810, 752 cm^{-1}. H. Out-of-plane ring C=C bend, 690 cm^{-1}. I. (Broad) hydrogen-bonded, out-of-plane O—H bend, about 650 cm^{-1}.

3.6.8.1. O—H Stretching Vibrations

The unbonded or "free" hydroxyl group of alcohols and phenols absorbs strongly in the 3650–3584 cm^{-1} region. Sharp, "free" hydroxyl bands are observed only in the vapor phase or in very dilute solution in nonpolar solvents. Intermolecular hydrogen bonding increases as the concentration of the solution increases, and additional bands start to appear at lower frequencies, 3550–3200 cm^{-1}, at the expense of the "free" hydroxyl band. This effect is illustrated in Figure 3.17 in which the absorption bands in the O—H stretching region are shown for two different concentrations of cyclohexylcarbinol in carbon tetrachloride. For comparisons of this type, the path length of the cell must be altered with changing concentration, so that the same number of absorbing molecules will be present in the IR beam at each concentration. The band

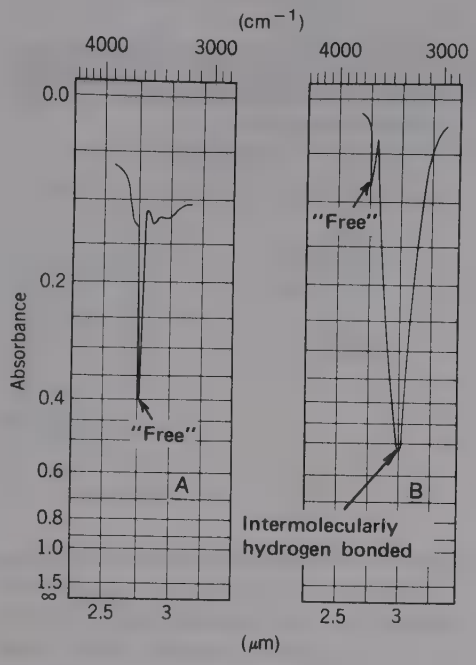

FIGURE 3.17. Infrared spectrum of the O—H stretching region of cyclohexylcarbinol in CCl_4. Peak A at 0.03 *M* (0.406 mm cell); Peak B at 1.00 *M* (0.014 mm cell).

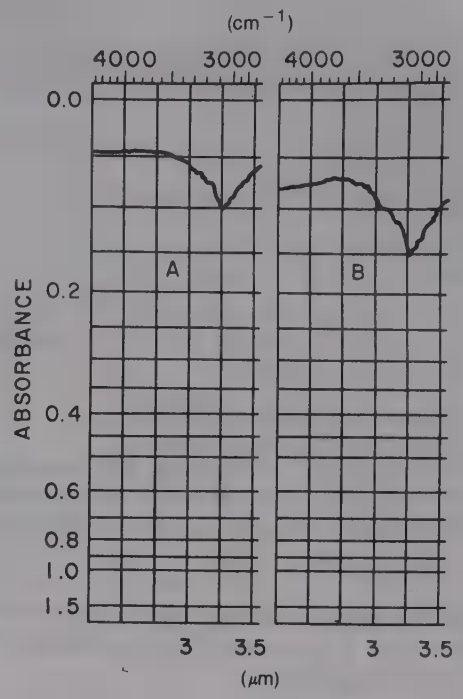

FIGURE 3.18. A portion of the IR spectra of *o*-hydroxyacetophenone. Peak A at 0.03 *M*, cell thickness: 0.41 mm. Peak B at 1.0 *M*, cell thickness: 0.015 mm.

at 3623 cm^{-1} results from the monomer, whereas the broad absorption near 3333 cm^{-1} arises from "polymeric" structures.

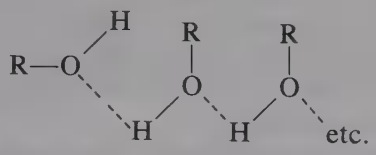

Strong intramolecular hydrogen bonding occurs in *o*-hydroxyacetophenone. The resulting absorption at 3077 cm^{-1} is broad, shallow, and independent of concentration (Fig. 3.18).

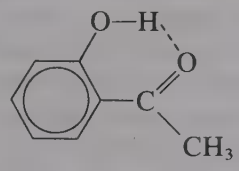

In contrast, *p*-hydroxyacetophenone

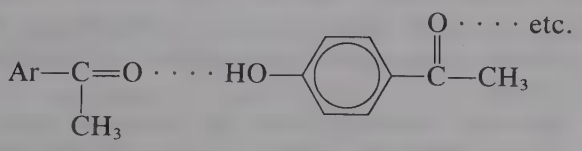

shows a sharp "free" hydroxyl peak at 3600 cm^{-1} in dilute CCl_4 solution as well as a broad strong intermolecular peak at 3100 cm^{-1} in the spectrum of a neat sample.

In structures, such as 2,6-di-*t*-butylphenol, in which steric hindrance prevents hydrogen bonding, no bonded hydroxyl band is observed, not even in spectra of neat samples.

3.6.8.2. C—O Stretching Vibrations

The C—O stretching vibrations in alcohols and phenols produce a strong band in the 1260–1000 cm^{-1} region of the spectrum. The C—O stretching mode is coupled with the adjacent C—C stretching vibration; thus in primary alcohols the vibration might better be described as an asymmetric C—C—O stretching vibration. The vibrational mode is further complicated by branching and α,β unsaturation. These effects are summarized as follows for a series of secondary alcohols (neat samples).

Secondary Alcohol	Absorption (cm^{-1})
2-Butanol	1105
3-Methyl-2-butanol	1091
1-Phenylethanol	1073
3-Buten-2-ol	1058
Diphenylmethanol	1014

TABLE 3.2

Alcoholic C—O Stretch Absorptions

Alcohol Type	Absorption Range (cm^{-1})
(1) Saturated tertiary (2) Secondary, highly symmetrical	1205–1124
(1) Saturated secondary (2) α-Unsaturated or cyclic tert.	1124–1087
(1) Secondary, α-unsaturated (2) Secondary, alicyclic five- or six-membered ring (3) Saturated primary	1085–1050
(1) Tertiary, highly α-unsaturated (2) Secondary, di-α-unsaturated (3) Secondary, α-unsaturated and α-branched (4) Secondary, alicyclic seven- or eight-membered ring (5) Primary, α-unsaturated and/or α-branched	<1050

The absorption ranges of the various types of alcohols appear in Table 3.2, above. These values are for neat samples of the alcohols.

Mulls, pellets, or melts of phenols absorb at 1390–1330 and 1260–1180 cm^{-1}. These bands apparently result from interaction between O—H bending and C—O stretching. The long wavelength band is the stronger and both bands appear at longer wavelengths in spectra observed in solution. The spectrum of Figure 3.16 was determined on a melt, to show a high degree of association.

3.6.8.3. O—H Bending Vibrations

The O—H in-plane bending vibration occurs in the general region of 1420–1330 cm^{-1}. In primary and secondary alcohols, the O—H in-plane bending couples with the C—H wagging vibrations to produce two bands; the first near 1420 cm^{-1}, the second near 1330 cm^{-1}. These bands are of little diagnostic value. Tertiary alcohols, in which no coupling can occur, show a single band in this region, the position depending on the degree of hydrogen bonding.

The spectra of alcohols and phenols determined in the liquid state, show a broad absorption band in the 769–650-cm^{-1} region because of out-of-plane bending of the bonded O—H group. Some spectra showing typical alcoholic absorptions are shown in Appendix B: ethyl alcohol (No. 16) and methanol (No. 15).

3.6.9. Ethers, Epoxides, and Peroxides

3.6.9.1. C—O Stretching Vibrations

The characteristic response of ethers in the IR is associated with the stretching vibration of the C—O—C system. Since the vibrational characteristics of this system would not be expected to differ greatly from the C—C—C system, it is not surprising to find the response to C—O—C stretching in the same general region. However, since vibrations involving oxygen atoms result in greater dipole moment changes than those involving carbon atoms, more intense IR bands are observed for ethers. The C—O—C stretching bands of ethers, as is the case with the C—O stretching bands of alcohols, involve coupling with other vibrations within the molecule. The spectrum of Figure 3.19 is that of a typical aryl alkyl ether. In addition, the spectra of ethyl ether (No. 22) and *p*-dioxane (a cyclic diether, No. 23) are shown in Appendix B.

In the spectra of aliphatic ethers, the most characteristic absorption is a strong band in the 1150–1085 cm^{-1} region because of asymmetrical C—O—C stretching; this band usually occurs near 1125 cm^{-1}. The symmetrical stretching band is usually weak and is more readily observed in the Raman spectrum.

The C—O—C group in a six-membered ring absorbs at the same frequency as in an acyclic ether. As the ring becomes smaller, the asymmetrical C—O—C stretching vibration moves progressively to lower wavenumbers (longer wavelengths), whereas the symmetrical C—O—C stretching vibration (ring breathing frequency) moves to higher wavenumbers.

Branching on the carbon atoms adjacent to the oxygen usually leads to splitting of the C—O—C band. Isopropyl ether shows a triplet structure in the 1170–1114-cm^{-1} region, the principal band occurring at 1114 cm^{-1}.

Spectra of aryl alkyl ethers display an asymmetrical C—O—C stretching band at 1275–1200 cm^{-1} with symmetrical stretching near 1075–1020 cm^{-1}. Strong absorption due to asymmetrical C—O—C stretching in vinyl ethers occurs in the 1225–1200 cm^{-1} region

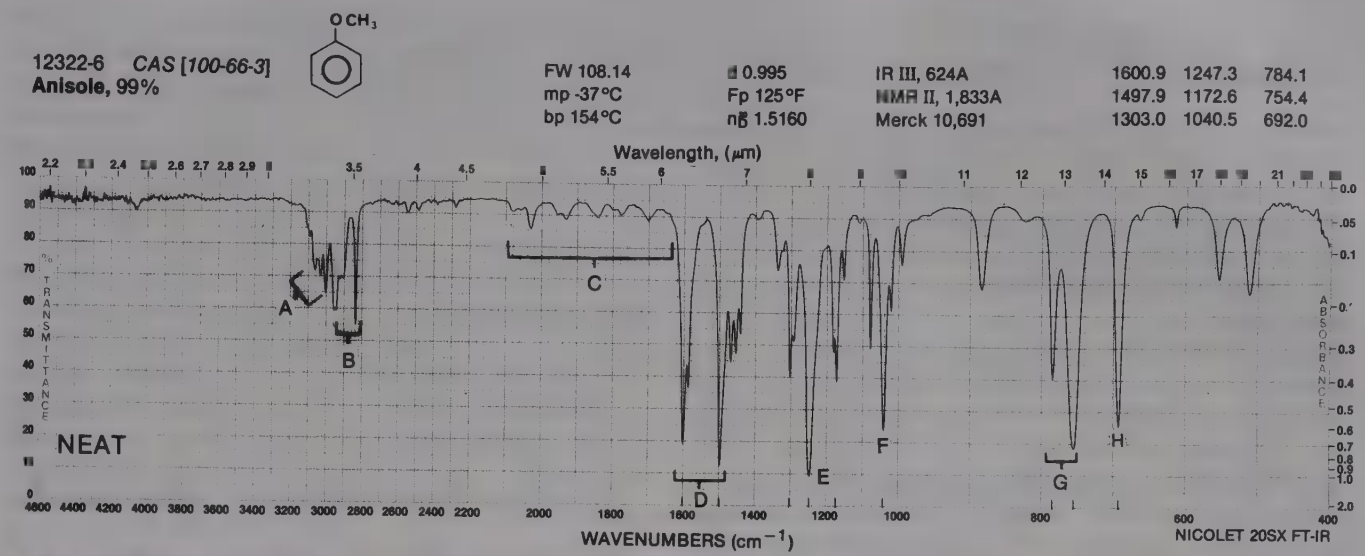

FIGURE 3.19. Anisole. A. Aromatic C—H stretch, 3060, 3030, 3000 cm^{-1}. B. Methyl C—H stretch, 2950, 2835 cm^{-1}. C. Overtone–combination region, 2000–1650 cm^{-1}. D. The C=C ring stretch, 1600, 1498 cm^{-1}. E. Asymmetric C—O—C stretch, 1247 cm^{-1}. F. Symmetric C—O—C stretch, 1040 cm^{-1}. G. Out-of-plane C—H bend, 784, 754 cm^{-1}. H. Out-of-plane ring C=C bend, 692 cm^{-1}.

with a strong symmetrical band at 1075–1020 cm^{-1}. Resonance, which results in strengthening of the C—O bond, is responsible for the shift in the asymmetric absorption band of aryl alkyl and vinyl ethers.

The C=C stretching band of vinyl ethers occurs in the 1660–1610 cm^{-1} region. This alkene band is characterized by its higher intensity compared with the C=C stretching band in alkenes. This band frequently appears as a doublet resulting from absorption of rotational isomers.

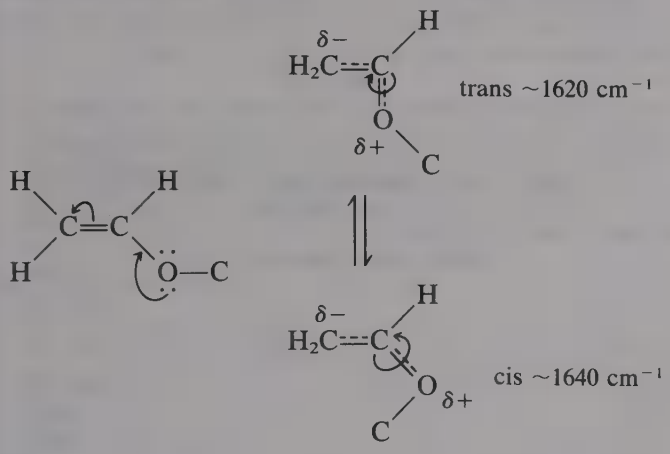

Coplanarity in the trans isomer allows maximum resonance, thus more effectively reducing the double-bond character of the alkene linkage. Steric hindrance reduces resonance in the cis isomer.

The two bands arising from =C—H wagging in terminal alkenes occur near 1000 and 909 cm^{-1}. In the spectra of vinyl ethers, these bands are shifted to longer wavelengths because of resonance.

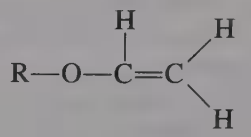

terminal CH_3 wag, 813 cm^{-1}
trans CH wag, 960 cm^{-1}

Alkyl and aryl peroxides display C—C—O absorption in the 1198–1176 cm^{-1} region. Acyl and aroyl peroxides display two carbonyl absorption bands in the 1818–1754 cm^{-1} region. Two bands are observed because of mechanical interaction between the stretching modes of the two carbonyl groups.

The symmetrical stretching, or ring breathing frequency, of the epoxy ring, all ring bonds stretching and contracting in phase, occurs near 1250 cm^{-1}. Another band appears in the 950–810 cm^{-1} region attributed to asymmetrical ring stretching in which the C—C bond is stretching during contraction of the C—O bond. A third band, referred to as the "12 micron band," appears in the 840–750 cm^{-1} region. The C—H stretching vibrations of epoxy rings occur in the 3050–2990 cm^{-1} region of the spectrum.

3.6.10. Ketones

3.6.10.1. C=O Stretching Vibrations

Ketones, aldehydes, carboxylic acids, carboxylic esters, lactones, acid halides, anhydrides, amides, and lactams show a strong C=O stretching absorption band in the region of 1870–1540 cm^{-1}. Its relatively constant

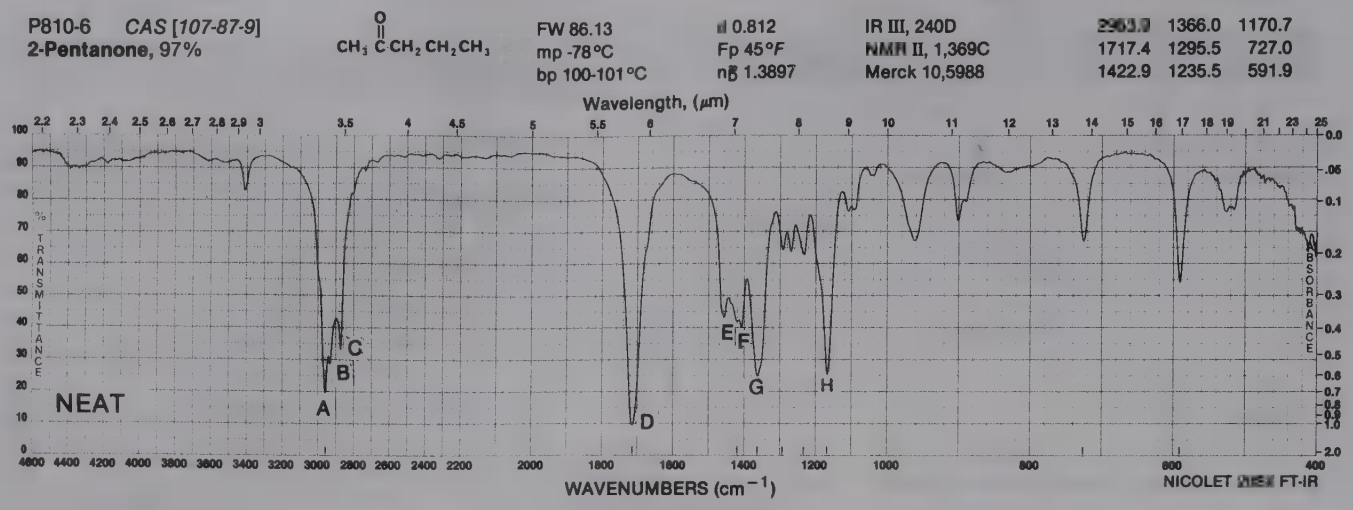

FIGURE 3.20. 2-Pentanone. A. ν_{as}, Methyl, 2964 cm^{-1}. B. ν_{as}, Methylene, 2935 cm^{-1}. C. ν_s, Methyl, 2870 cm^{-1}. D. Normal* C=O stretch, 1717 cm^{-1}. E. δ_{as}, CH_3, ~1423 cm^{-1}. F. δ_s, CH_2, ~1410 cm^{-1}. G. δ_s, CH_3 of CH_3CO unit, 1366 cm^{-1}. H. The C—CO—C stretch and bend, 1171 cm^{-1}.
*See Section 3.6.10 for a definition of normal.

position, high intensity, and relative freedom from interfering bands make this one of the easiest bands to recognize in IR spectra.

Within its given range, the position of the C=O stretching band is determined by the following factors: (1) the physical state, (2) electronic and mass effects of neighboring substituents, (3) conjugation, (4) hydrogen bonding (intermolecular and intramolecular), and (5) ring strain. Consideration of these factors leads to a considerable amount of information about the environment of the C=O group.

In a discussion of these effects, it is customary to refer to the absorption frequency of a neat sample of a saturated aliphatic ketone, 1715 cm^{-1}, as "normal." For example, acetone and cyclohexanone absorb at 1715 cm^{-1}. Changes in the environment of the carbonyl can either lower or raise the absorption frequency from this "normal" value. A typical ketone spectrum is displayed in Figure 3.20.

The absorption frequency observed for a neat sample is increased when absorption is observed in nonpolar solvents. Polar solvents reduce the frequency of absorption. The overall range of solvent effects does not exceed 25 cm^{-1}.

Replacement of an alkyl group of a saturated aliphatic ketone by a hetero atom (G) shifts the carbonyl absorption. The direction of the shift depends on whether the inductive effect (a) or resonance effect (b) predominates.

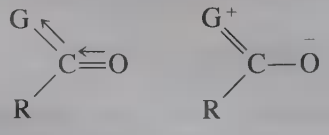

(a) (b)

The inductive effect reduces the length of the C=O bond and thus increases its force constant and the frequency of absorption. The resonance effect increases the C=O bond length and reduces the frequency of absorption.

The absorptions of several carbonyl compound classes are summarized in Table 3.3.

Conjugation with a C=C bond results in delocalization of the π electrons of both unsaturated groups. Delocalization of the π electrons of the C=O group

TABLE 3.3

The Carbonyl Absorption of Various RCG Compounds

G Effect Predominantly Inductive	
G	ν C=O (cm^{-1})
Cl	1815–1785
F	~1869
Br	1812
OH (monomer)	1760
OR	1750–1735
G Effect Predominantly Resonance	
G	ν C=O (cm^{-1})
NH_2	1695–1650
SR	1720–1690

reduces the double-bond character of the C—O bond, causing absorption at lower wavenumbers (longer wavelengths). Conjugation with an alkene or phenyl group causes absorption in the 1685–1666 cm^{-1} region. Additional conjugation may cause a slight further reduction in frequency. This effect of conjugation is illustrated in Figure 3.21.

Steric effects that reduce the coplanarity of the conjugated system reduce the effect of conjugation. In the absence of steric hindrance, a conjugated system will tend toward a planar conformation. Thus, α,β-unsaturated ketones may exist in *s*-cis and *s*-trans conformations. When both forms are present, absorption for each of the forms is observed. The absorption of benzalacetone in CS_2 serves as an example; both the *s*-cis and *s*-trans forms are present at room temperature.

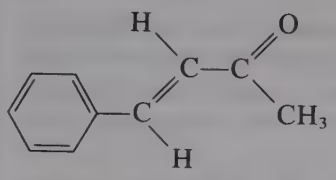

s-trans
1674 cm^{-1}

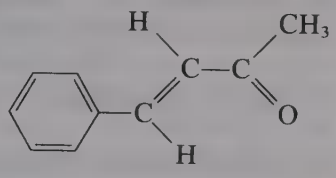

s-cis
1699 cm^{-1}

The absorption of the alkene bond in conjugation with the carbonyl group occurs at a lower frequency than that of an isolated C=C bond; the intensity of the conjugated double-bond absorption, when in an *s*-cis system, is greater than that of an isolated double bond.

Intermolecular hydrogen bonding between a ketone and a hydroxylic solvent such as methanol causes a slight decrease in the absorption frequency of the carbonyl group. For example, a neat sample of ethyl methyl ketone absorbs at 1715 cm^{-1}, whereas a 10% solution of the ketone in methanol absorbs at 1706 cm^{-1}.

β-Diketones usually exist as mixtures of tautomeric keto and enol forms. The enolic form does not show the normal absorption of conjugated ketones. Instead, a broad band appears in the 1640–1580 cm^{-1} region, many times more intense than normal carbonyl absorption. The intense and displaced absorption results from intramolecular hydrogen bonding, the bonded structure being stabilized by resonance.

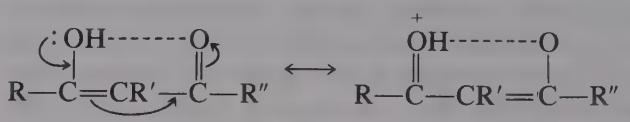

Acetylacetone as a liquid at 40°C exists to the extent of 64% in the enolic form that absorbs at 1613 cm^{-1}. The keto form and a small amount of unbonded enolic form may be responsible for two bands centering near 1725 cm^{-1}. Interaction between the two carbonyl groups in the keto form was suggested as a cause for this doublet. The enolic O—H stretching absorption is seen as a broad shallow band at 3000–2700 cm^{-1}.

α-Diketones, in which carbonyl groups exist in formal conjugation, show a single absorption band near the frequency observed for the corresponding monoketone. Biacetyl absorbs at 1718 cm^{-1}, benzil at 1681

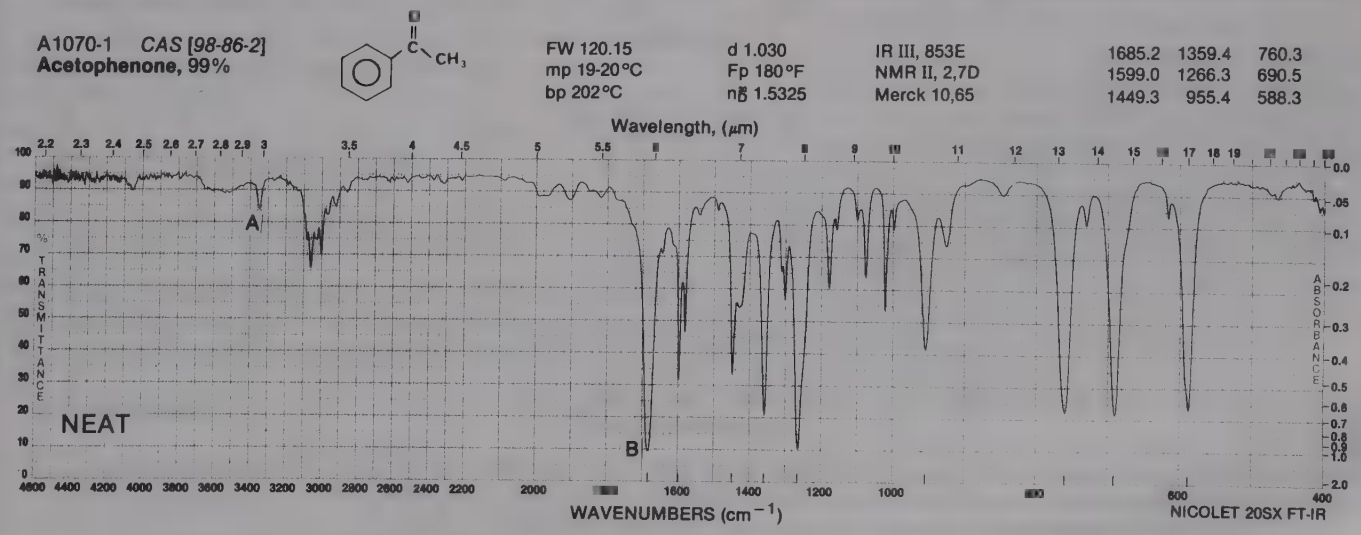

FIGURE 3.21. Acetophenone. A. Overtone of C=O stretch ~3350 cm^{-1}; frequency about twice that of C=O stretch. B. The C=O stretch, 1685 cm^{-1}, lower frequency than observed in Figure 3.20 because of the conjugation with the phenyl group.

cm^{-1}. Conjugation is ineffective for α-diketones and the C=O groups of these diketones do not couple as do, for example, the corresponding groups in acid anhydrides (see below).

Quinones, which have both carbonyl groups in the same ring, absorb in the 1690–1655-cm^{-1} region. With extended conjugation, in which the carbonyl groups appear in different rings, the absorption shifts to the 1655–1635-cm^{-1} region.

Acyclic α-chloro ketones absorb at two frequencies due to rotational isomerism. When the chlorine atom is near the oxygen, its negative field repels the nonbonding electrons of the oxygen atom, thus increasing the force constant of the C=O bond. This conformation absorbs at a higher frequency (1745 cm^{-1}) than that in which the carbonyl oxygen and chlorine atom are widely separated (1725 cm^{-1}). In rigid molecules such as the monoketo steroids, α-halogenation results in equatorial or axial substitution. In the equatorial orientation, the halogen atom is near the carbonyl group and the "field effect" causes an increase in the C=O stretching frequency. In the isomer in which the halogen atom is axial to the ring, and distant from the C=O, no shift is observed.

In cyclic ketones, the bond angle of the 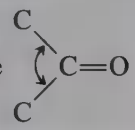 group influences the absorption frequency of the carbonyl group. The C=O stretching undoubtedly is affected by adjacent C—C stretching. In acyclic ketones and in ketones with a six-membered ring, the angle is near 120°. In strained rings in which the angle is less than 120°, interaction with C—C bond stretching increases the energy required to produce C=O stretching and thus increases the stretching frequency. Cyclohexanone absorbs at 1715 cm^{-1}, cyclopentanone absorbs at 1751 cm^{-1}, and cyclobutanone absorbs at 1775 cm^{-1}.

3.6.10.2. C—C—C Stretching and Bending Vibrations

Ketones show moderate absorption in the 1300–1100 cm^{-1} region as a result of C—C—C stretching and bending in the C—C—C group. The absorption may consist of multiple bands. Aliphatic ketones absorb in the 1230–1100 cm^{-1} region; aromatic ketones absorb at the higher frequency end of the general absorption region.

The spectra of 2-butanone (ethyl methyl ketone, No. 18), acetone (No. 17), and cyclohexanone (No. 19) in Appendix B illustrate ketonic absorptions.

3.6.11. Aldehydes

The spectrum of 2-phenylpropionaldehyde, illustrating typical aldehydic absorption characteristics, is shown in Figure 3.22.

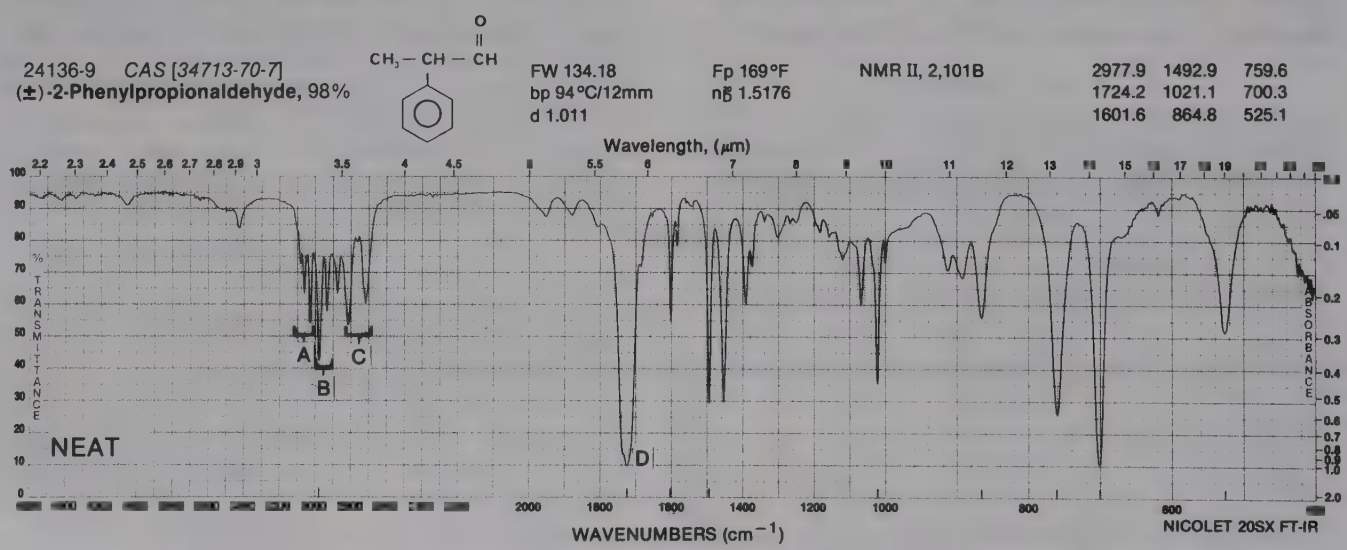

FIGURE 3.22. (±)-2-Phenylpropionaldehyde. A.* Aromatic, 3070, 3040 cm^{-1} (see Fig. 3.13). B.* Aliphatic, 2978, 2940, 2875 cm^{-1} (see Figs. 3.8 and 3.13). C.* Aldehydic, C—H stretch, 2825, 2720 cm^{-1}. Doublet due to Fermi resonance with overtone of band at F. D. Normal aldehydic C=O stretch, 1724 cm^{-1}. Conjugated C=O stretch would be about 1700 cm^{-1}, for example, as for C_6H_5CHO. E. Ring C=C stretch, 1602, 1493, 1455 cm^{-1}. F. Aldehydic C—H bend, 1390 cm^{-1}. G. Out-of-plane C—H bend, 760 cm^{-1}. H. Out-of-plane C=C bend, 700 cm^{-1}.

*Bands A–C are C—H stretch absorptions

Source: Courtesy of Aldrich Chemical Company.

3.6.11.1. C=O Stretching Vibrations

The carbonyl groups of aldehydes absorb at slightly higher frequencies than that of the corresponding methyl ketones. Aliphatic aldehydes absorb near 1740–1720 cm^{-1}. Aldehydic carbonyl absorption responds to structural changes in the same manner as ketones. Electronegative substitution on the α carbon increases the frequency of carbonyl absorption. Acetaldehyde absorbs at 1730 cm^{-1}, trichloroacetaldehyde absorbs at 1768 cm^{-1}. Conjugate unsaturation, as in α,β-unsaturated aldehydes and benzaldehydes, reduces the frequency of carbonyl absorption. α,β-Unsaturated aldehydes and benzaldehydes absorb in the region of 1710–1685 cm^{-1}. Internal hydrogen bonding, such as occurs in salicylaldehyde, shifts the absorption (1666 cm^{-1} for salicylaldehyde) to lower wavenumbers. Glyoxal, like the α-diketones, shows only one carbonyl absorption peak with no shift from the normal absorption position of monoaldehydic absorption.

3.6.11.2. C—H Stretching Vibrations

The majority of aldehydes show aldehydic C—H stretching absorption in the 2830–2695 cm^{-1} region. Two moderately intense bands are frequently observed in this region. The appearance of two bands is attributed to Fermi resonance between the fundamental aldehydic C—H stretch and the first overtone of the aldehydic C—H bending vibration that usually appears near 1390 cm^{-1}. Only one C—H stretching band is observed for aldehydes whose C—H bending band has been shifted appreciably from 1390 cm^{-1}.

Some aromatic aldehydes with strongly electronegative groups in the ortho position may absorb as high as 2900 cm^{-1}.

An absorption of medium intensity near 2720 cm^{-1}, accompanied by a carbonyl absorption band is good evidence for the presence of an aldehyde group.

3.6.12. Carboxylic Acids

3.6.12.1 O—H Stretching Vibrations

In the liquid or solid state, and in CCl_4 solution at concentrations much over 0.01 M, carboxylic acids exist as dimers due to strong hydrogen bonding.

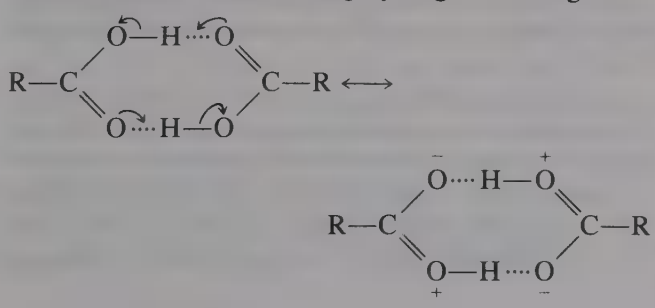

The exceptional strength of the hydrogen bonding is explained on the basis of the large contribution of the ionic resonance structure. Because of the strong bonding, a free hydroxyl stretching vibration (near 3520 cm^{-1}) is observed only in very dilute solution in nonpolar solvents or in the vapor phase. In each case, however, there is a mixture of monomer and dimer.

Carboxylic acid dimers display very broad, intense O—H stretching absorption in the region of 3300–2500 cm^{-1}. The band usually centers near 3000 cm^{-1}. The weaker C—H stretching bands are generally seen superimposed upon the broad O—H band. Fine structure observed on the long-wavelength side of the broad O—H band represents overtones and combination tones of fundamental bands occurring at longer wavelengths. The spectrum of a typical aliphatic carboxylic acid is displayed in Figure 3.23.

Other structures with strong hydrogen bonding, such as β-diketones, also absorb in the 3300–2500-cm^{-1} region, but the absorption is usually less intense. Also, the C=O stretching vibrations of structures such as β-diketones are shifted to lower frequencies than those observed for carboxylic acids.

Carboxylic acids can bond intermolecularly with ethers, such as dioxane and tetrahydrofuran, or with other solvents that can act as proton acceptors. Spectra determined in such solvents show bonded O—H absorption near 3100 cm^{-1}.

3.6.12.2. C=O Stretching Vibrations

The C=O stretching bands of acids are considerably more intense than ketonic C=O stretching bands. The monomers of saturated aliphatic acids absorb near 1760 cm^{-1}.

The carboxylic dimer has a center of symmetry; only the asymmetrical C=O stretching mode absorbs in the IR. Hydrogen bonding and resonance weaken the C=O bond, resulting in absorption at a lower frequency than the monomer. The C=O group in dimerized saturated aliphatic acids absorbs in the region of 1720–1706 cm^{-1}.

Internal hydrogen bonding reduces the frequency of the carbonyl stretching absorption to a greater degree than does intermolecular hydrogen bonding. For example, salicylic acid absorbs at 1665 cm^{-1}, whereas p-hydroxybenzoic acid absorbs at 1680 cm^{-1}.

Unsaturation in conjugation with the carboxylic carbonyl group decreases the frequency (increases the wavelength) of absorption of both the monomer and dimer forms only slightly. In general, α,β-unsaturated and aryl conjugated acids show absorption for the dimer in the 1710–1680 cm^{-1} region. Extension of conjugation beyond the α,β-position results in very little additional shifting of the C=O absorption.

Substitution in the α position with electronegative groups, such as the halogens, brings about a slight

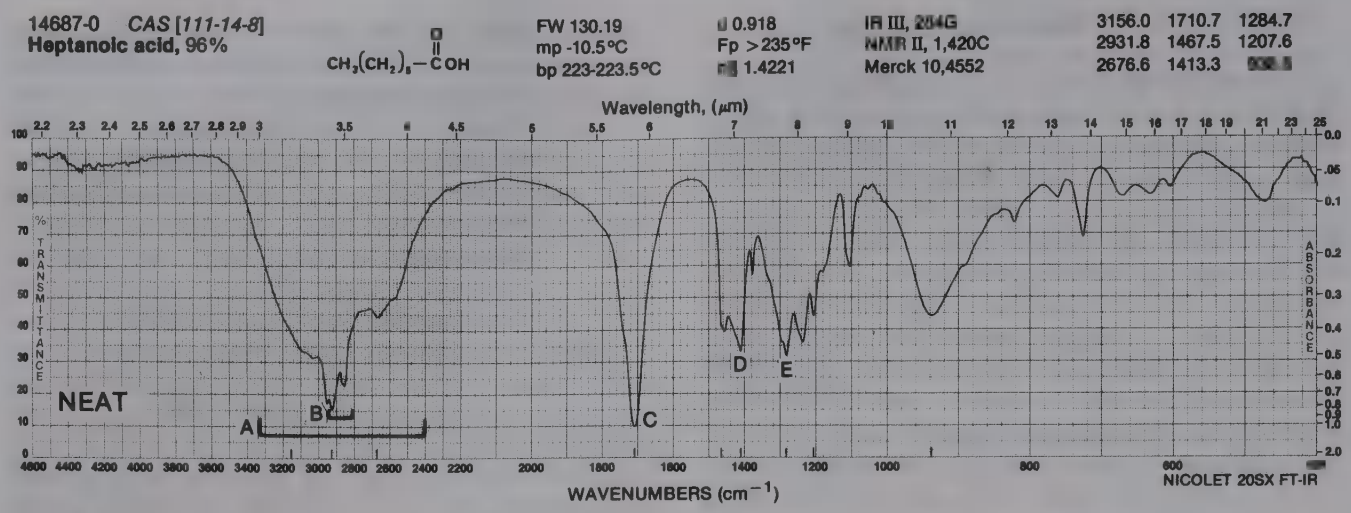

FIGURE 3.23. Heptanoic Acid. A. Broad O—H stretch, 3300–2500 cm^{-1}. B. The C—H stretch, (see Fig. 3.8) 2950, 2932, 2855 cm^{-1}. Superimposed upon O—H stretch. C. Normal, dimeric carboxylic C=O stretch, 1711 cm^{-1}. D. The C—O—H in-plane bend,* 1413 cm^{-1}. E. The C—O stretch,* dimer, 1285 cm^{-1}. F. The O—H out-of-plane bend, 939 cm^{-1}.

*Bands at D and E involve C—O—H interaction.

increase in the C=O absorption frequency (10–20 cm^{-1}). The spectra of acids with halogens in the α position, determined in the liquid state or in solution, show dual carbonyl bands due to rotational isomerism (field effect). The higher frequency band corresponds to the conformation in which the halogen is in proximity to the carbonyl group.

3.6.12.3. C—O Stretching and O—H Bending Vibrations

Two bands arising from C—O stretching and O—H bending appear in the spectra of carboxylic acids near 1320–1210 and 1440–1395 cm^{-1}, respectively. Both of these bands involve some interaction between C—O stretching and in-plane C—O—H bending. The more intense band, near 1315–1280 cm^{-1} for dimers, is generally referred to as the C—O stretching band and usually appears as a doublet in the spectra of long-chain fatty acids. The C—O—H bending band near 1440–1395 cm^{-1} is of moderate intensity and occurs in the same region as the CH_2 scissoring vibration of the CH_2 group adjacent to the carbonyl.

One of the characteristic bands in the spectra of dimeric carboxylic acids results from the out-of-plane bending of the bonded O—H. The band appears near 920 cm^{-1} and is characteristically broad with medium intensity.

3.6.13. Carboxylate Anion

The carboxylate anion has two strongly coupled C=O bonds with bond strengths intermediate between C=O and C—O.

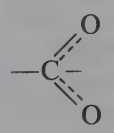

The carboxylate ion gives rise to two bands: a strong asymmetrical stretching band near 1650–1550 cm^{-1} and a weaker, symmetrical stretching band near 1400 cm^{-1}.

The conversion of a carboxylic acid to a salt can serve as confirmation of the acid structure. This is conveniently done by the addition of a tertiary, aliphatic amine, such as triethylamine, to a solution of the carboxylic acid in chloroform (no reaction occurs in CCl_4). The carboxylate ion, thus formed, shows the two characteristic carbonyl absorption bands in addition to an "ammonium" band in the 2700–2200 cm^{-1} region. The O—H stretching band, of course, disappears. The spectrum of ammonium benzoate, Figure 3.24, demonstrates most of these features.

3.6.14. Esters and Lactones

Esters and lactones have two characteristically strong absorption bands arising from C=O and C—O stretching. The intense C=O stretching vibration occurs at higher frequencies (shorter wavelength) than that of normal ketones. The force constant of the carbonyl bond is increased by the electron-attracting nature of the adjacent oxygen atom (inductive effect). Overlapping occurs between esters in which the carbonyl frequency is lowered, and ketones in which the normal ketone frequency is raised. A distinguishing feature of esters and lactones, however, is the strong C—O stretching band in the region where a weaker

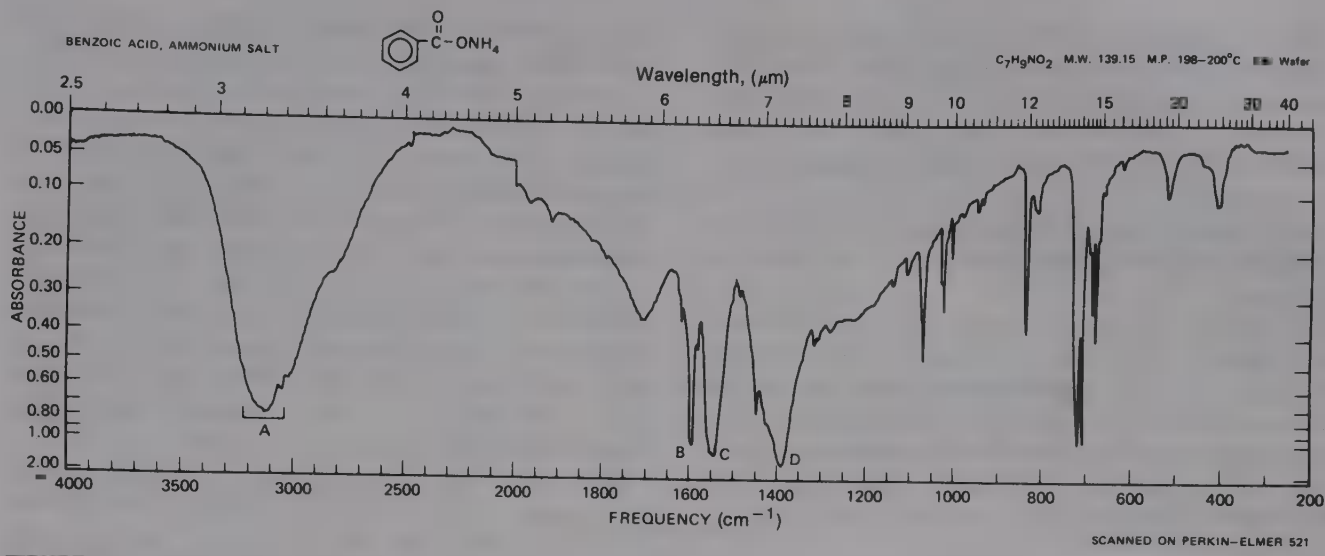

FIGURE 3.24. Benzoic acid, ammonium salt. A. N—H and C—H stretch, 3600–2500 cm^{-1}. B. Ring C=C stretch 1600 cm^{-1}. C. Asymmetric carboxylate anion C $(=O)_2^-$ stretch 1550 cm^{-1}. D. Symmetric carboxylate C$(=O)_2^-$ stretch 1385 cm^{-1}.

band occurs for ketones. There is overlapping in the C=O frequency of esters or lactones and acids, but the OH stretching and bending vibrations and the possibility of salt formation distinguish the acids.

The frequency of the ester carbonyl responds to environmental changes in the vicinity of the carbonyl group in much the same manner as ketones. The spectrum of phenyl acetate, Figure 3.25, illustrates most of the important absorption characteristics for esters.

3.6.14.1. C=O Stretching Vibrations

The C=O absorption band of saturated aliphatic esters (except formates) is in the 1750–1735 cm^{-1} region. The C=O absorption bands of formates, α,β unsaturated, and benzoate esters are in the region of 1730–1715 cm^{-1}. Further conjugation has little or no additional effect upon the frequency of the carbonyl absorption.

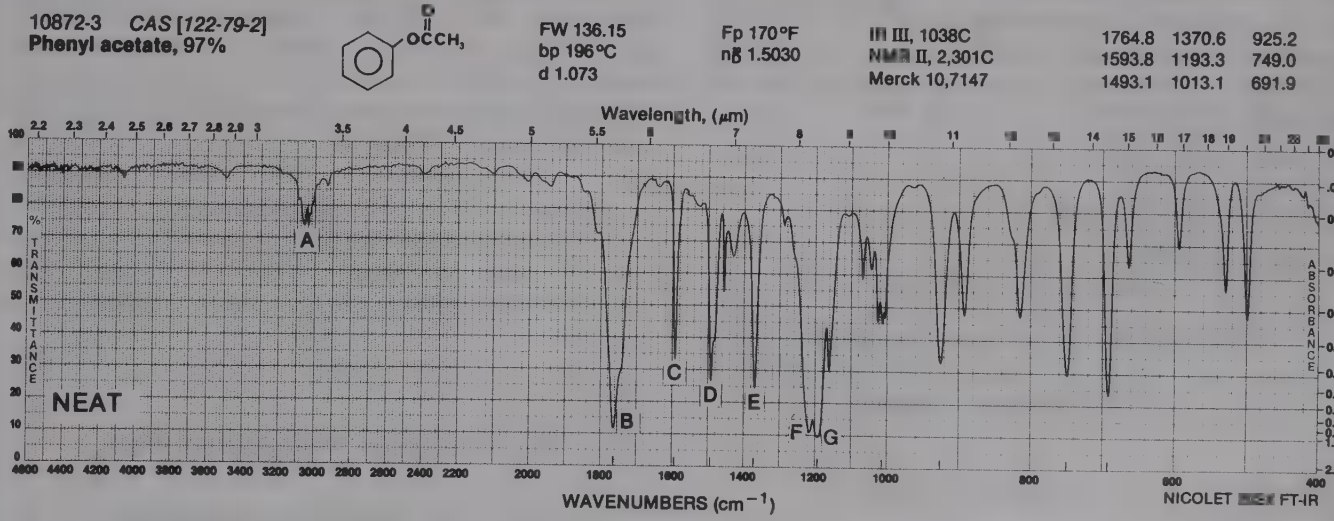

FIGURE 3.25. Phenyl acetate. A. Aromatic C—H stretch, 3070, 3040 cm^{-1}. B. The C=O stretch, 1765 cm^{-1}; this is higher frequency than that due to normal ester C=O stretch (~1740 cm^{-1}, see Table 3.3), due to phenyl conjugation with alcohol oxygen; conjugation of an aryl group or other unsaturation with the carbonyl group causes this C=O stretch to be at lower than normal frequency (e.g., benzoates absorb at about 1724 cm^{-1}. C. Ring C=C stretch, 1594 cm^{-1}. D. δ_{as}, CH_3, 1493 cm^{-1}. E. δ_s, CH_3, 1371 cm^{-1}. F. Acetate CC(=O)—O stretch, 1215 cm^{-1}. G. The O—C=C asym stretch, 1193 cm^{-1}.

In the spectra of vinyl or phenyl esters, with unsaturation adjacent to the C—O— group, a marked rise in the carbonyl frequency is observed along with a lowering of the C—O frequency. Vinyl acetate has a carbonyl band at 1776 cm^{-1}; phenyl acetate absorbs at 1770 cm^{-1}.

α-Halogen substitution results in a rise in the C=O stretching frequency. Ethyl trichloroacetate absorbs at 1770 cm^{-1}.

In oxalates and α-keto esters, as in α-diketones, there appears to be little or no interaction between the two carbonyl groups so that normal absorption occurs in the region of 1755–1740 cm^{-1}. In the spectra of β-keto esters, however, where enolization can occur, a band is observed near 1650 cm^{-1} that results from bonding between the ester C=O and the enolic hydroxyl group.

The carbonyl absorption of saturated δ-lactones (six-membered ring) occurs in the same region as straight-chain, unconjugated esters. Unsaturation α to the C=O

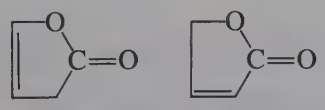

1800 cm^{-1} 1750 cm^{-1}

reduces the C=O absorption frequency. Unsaturation α to the —O— group increases it.

α-Pyrones frequently display two carbonyl absorption bands in the 1775–1715 cm^{-1} region, probably due to Fermi resonance.

Saturated γ-lactones (five-membered ring) absorb at shorter wavelengths than esters or δ-lactones: 1795–1760 cm^{-1}; γ-valerolactone absorbs at 1770 cm^{-1}. Unsaturation in the γ-lactone molecule affects the carbonyl absorption in the same manner as unsaturation in δ-lactones.

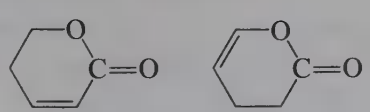

1720 cm^{-1} 1760 cm^{-1}

In unsaturated lactones, when the double bond is adjacent to the —O—, a strong C=C absorption is observed in the 1685–1660 cm^{-1} region.

3.6.14.2. C—O Stretching Vibrations

The "C—O stretching vibrations" of esters actually consists of two asymmetric coupled vibrations: C—C(=O)—O and O—C—C, the former being more important. These bands occur in the region of 1300–1000 cm^{-1}. The corresponding symmetric vibrations are of little importance. The C—O stretch correlations are less reliable than the C=O stretch correlations.

The C—C(=O)—O band of saturated esters, except for acetates, shows strongly in the 1210–1163 cm^{-1} region. It is often broader and stronger than the C=O stretch absorption. Acetates of saturated alcohols display this band at 1240 cm^{-1}. Vinyl and phenyl acetates absorb at a somewhat lower frequency, 1190–1140 cm^{-1}; for example, see Figure 3.25. The C—C(=O)—O stretch of esters of α,β-unsaturated acids results in multiple bands in the 1300–1160 cm^{-1} region. Esters of aromatic acids absorb strongly in the 1310–1250 cm^{-1} region. The analogous type of stretch in lactones is observed in the 1250–1111 cm^{-1} region.

The O—C—C band of esters ("alcohol" carbon–oxygen stretch) of primary alcohols occurs at about 1064–1031 cm^{-1} and that of esters of secondary alcohols occurs at about 1100 cm^{-1}. Aromatic esters of primary alcohols show this absorption near 1111 cm^{-1}.

Methyl esters of long-chain fatty acids present a three-band pattern with bands near 1250, 1205, and 1175 cm^{-1}. The band near 1175 cm^{-1} is the strongest.

Spectra showing typical ester absorptions are shown in Appendix B: ethyl acetate (No. 20) and diethyl phthalate (No. 21).

3.6.15. Acid Halides

3.6.15.1. C=O Stretching Vibrations

Acid halides show strong absorption in the C=O stretching region. Unconjugated acid chlorides absorb in the 1815–1785 cm^{-1} region. Acetyl fluoride in the gas phase absorbs near 1869 cm^{-1}. Conjugated acid halides absorb at a slightly lower frequency because resonance reduces the force constant of the C=O bond; aromatic acid chlorides absorb strongly at 1800–1770 cm^{-1}. A weak band near 1750–1735 cm^{-1} appearing in the spectra of aroyl chlorides probably results from Fermi resonance between the C=O band and the overtone of a lower wavenumber band near 875 cm^{-1}. The annotated spectrum of benzoyl chloride is given in Figure 3.26.

3.6.16. Carboxylic Acid Anhydrides

3.6.16.1. C=O Stretching Vibrations

Anhydrides display two stretching bands in the carbonyl region. The two bands result from asymmetrical and symmetrical C=O stretching modes. Saturated acyclic anhydrides absorb near 1818 and 1750 cm^{-1}.

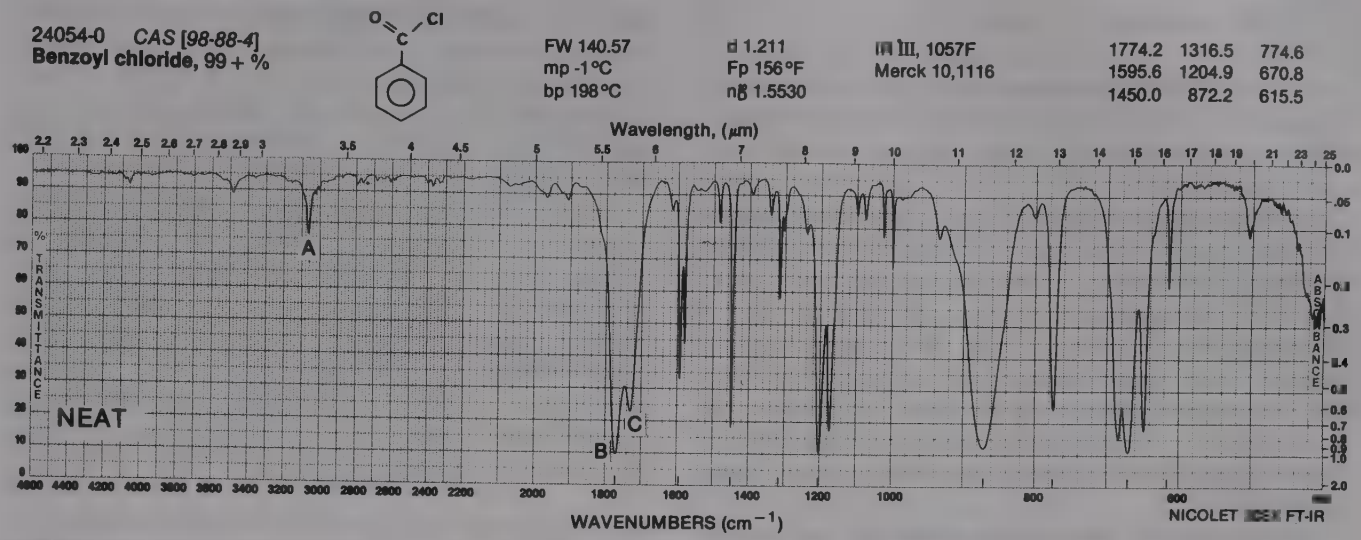

FIGURE 3.26. Benzoyl chloride. A. Aromatic C—H stretch, 3065 cm^{-1}. B. The C=O stretch, 1774 cm^{-1} (see Table 3.3, p. 114). (Acid chloride C=O stretch position shows very small dependence on conjugation; aroyl chlorides identified by band such as at C.) C. Fermi resonance band (of C=O stretch and overtone of 872-cm^{-1} band), 1730 cm^{-1}.

Source: Courtesy of Aldrich Chemical Co.

Conjugated acyclic anhydrides show absorption near 1775 and 1720 cm^{-1}; the decrease in the frequency of absorption is due to resonance. The higher frequency band is the more intense.

Cyclic anhydrides with five-membered rings show absorption at higher frequencies (lower wavelengths) than acyclic anhydrides because of ring strain; succinic anhydride absorbs at 1865 and 1782 cm^{-1}. The lower frequency (longer wavelength) C=O band is the stronger of the two carbonyl bands in five-membered ring cyclic anhydrides.

3.6.16.2. C—O Stretching Vibrations

Other strong bands appear in the spectra of anhydrides as a result of

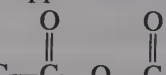

C—O—C stretching vibrations. Unconjugated straight-chain anhydrides absorb near 1047 cm^{-1}. Cyclic anhydrides display bands near 952–909 and 1299–1176 cm^{-1}. The C—O stretching band for acetic anhydride is at 1125 cm^{-1}.

The spectrum of Figure 3.27 is that of a typical aliphatic anhydride.

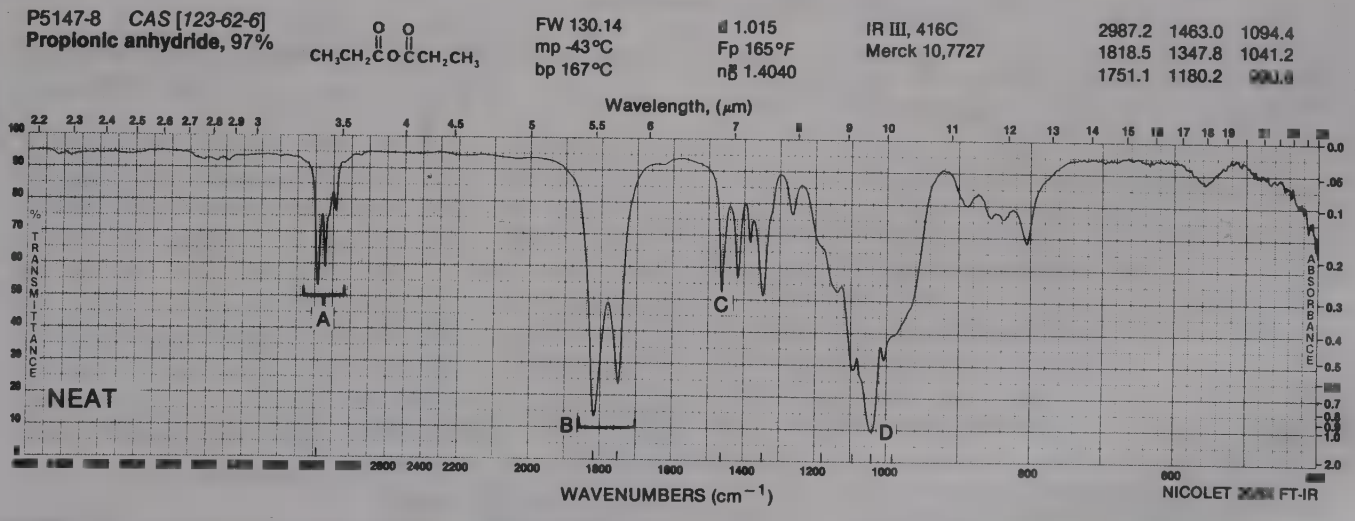

FIGURE 3.27. Propionic anhydride A. The C—H stretch, 2987, 2940, 2880 cm^{-1}. B. Asymmetric and symmetric C=O coupled stretching, respectively: 1818, 1751 cm^{-1}. See Table 3.3. C. δ_s CH_2 (scissoring), 1463 cm^{-1}. D. C—CO—O—CO—C stretch, 1041 cm^{-1}.

3.6.17. Amides

All amides show a carbonyl absorption band known as the amide I band. Its position depends on the degree of hydrogen bonding and, thus, on the physical state of the compound.

Primary amides show two N—H stretching bands resulting from symmetrical and asymmetrical N—H stretching. Secondary amides and lactams show only one N—H stretching band. As in the case of O—H stretching, the frequency of the N—H stretching is reduced by hydrogen bonding, though to a lesser degree. Overlapping occurs in the observed position of N—H and O—H stretching frequencies so that an unequivocal differentiation in structure is sometimes impossible.

Primary amides and secondary amides, and a few lactams, display a band or bands in the region of 1650–1515 cm^{-1} due primarily to NH_2 or NH bending: the amide II band. This absorption involves coupling between N—H bending and other fundamental vibrations and requires a trans geometry.

Out-of-plane NH wagging is responsible for a broad band of medium intensity in the 800–666 cm^{-1} region.

The spectrum of Figure 3.28 is that of a typical primary amide of an aliphatic acid. The spectrum of DMF (*N*,*N*-dimethylformamide, Appendix B, No. 28) displays typical amide absorptions.

3.6.17.1. N—H Stretching Vibrations

In dilute solution in nonpolar solvents, primary amides show two moderately intense NH stretching frequencies corresponding to the asymmetrical and symmetrical NH stretching vibrations. These bands occur near 3520 and 3400 cm^{-1} respectively. In the spectra of solid samples, these bands are observed near 3350 and 3180 cm^{-1} because of hydrogen bonding.

In IR spectra of secondary amides, which exist mainly in the trans conformation, the free NH stretching vibration observed in dilute solutions occurs near 3500–3400 cm^{-1}. In more concentrated solutions and in solid samples, the free NH band is replaced by multiple bands in the 3330–3060 cm^{-1} region. Multiple bands are observed since the amide group can bond to produce dimers, with an *s*-cis conformation, and polymers with an *s*-trans conformation.

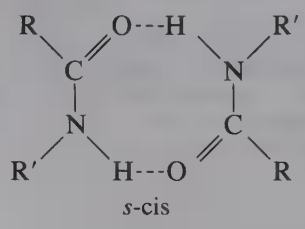

s-cis

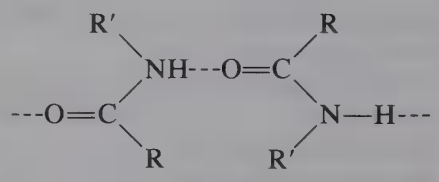

s-trans

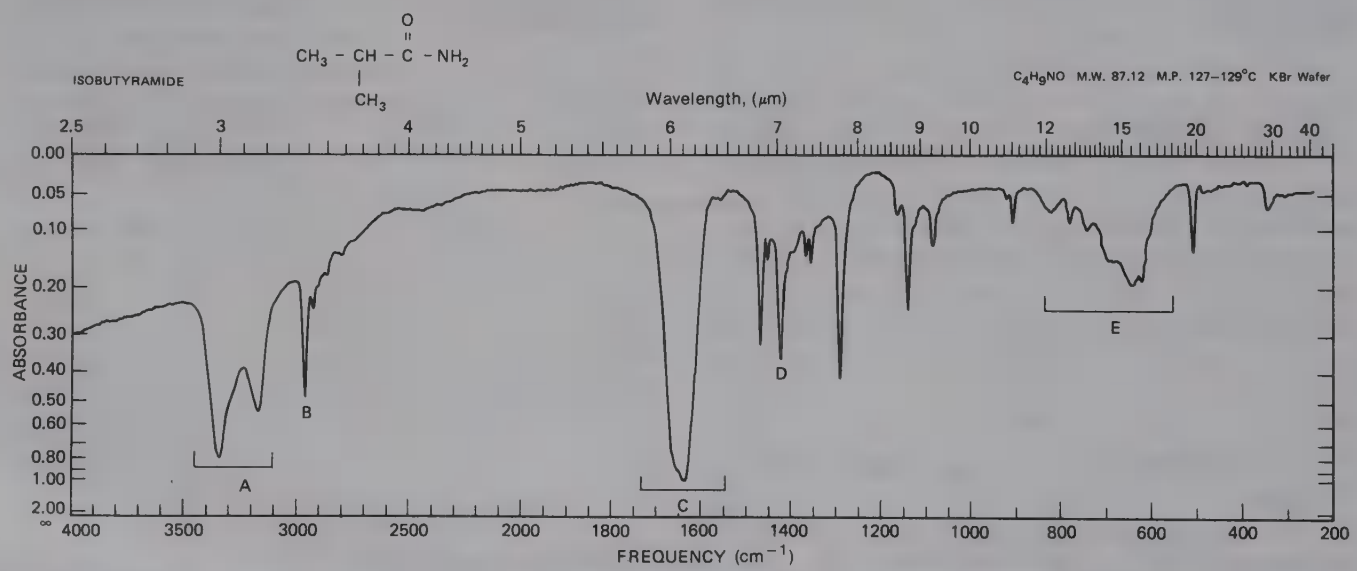

FIGURE 3.28. 2-Methylbutanamide.* A. The N—H stretch, coupled, primary amide, hydrogen bonded; asymmetric, 3352 cm^{-1}; symmetric, 3170 cm^{-1}. B. Aliphatic C—H stretch, 2960 cm^{-1}. C. Overlap C=O stretch, amide I band, 1640 cm^{-1}, ▪▪▪ Table 3.3. N—H bend, amide II band, 1640 cm^{-1}. D. The C—N stretch, 1425 cm^{-1}. E. Broad N—H out-of-plane bend, 700–600 cm^{-1}.

*The CA name for isobutyramide is 2-methylbutanamide.

3.6.17.2. C=O Stretching Vibrations (Amide I Band)

The C=O absorption of amides occurs at lower frequencies than "normal" carbonyl absorption due to the resonance effect (see p. 114). The position of absorption depends on the same environmental factors as the carbonyl absorption of other compounds.

Primary amides (except acetamide, whose C=O bond absorbs at 1694 cm^{-1}) have a strong amide I band in the region of 1650 cm^{-1} when examined in the solid phase. When the amide is examined in dilute solution, the absorption is observed at a higher frequency, near 1690 cm^{-1}. In more concentrated solutions, the C=O frequency is observed at some intermediate value, depending on the degree of hydrogen bonding.

Simple, open-chain, secondary amides absorb near 1640 cm^{-1} when examined in the solid state. In dilute solution, the frequency of the amide I band may be raised to 1680 cm^{-1} and even to 1700 cm^{-1} in the case of the anilides. In the anilide structure there is competition between the ring and the C=O for the nonbonded electron pair of the nitrogen.

The carbonyl frequency of tertiary amides is independent of the physical state since hydrogen bonding with another tertiary amide group is impossible. The C=O absorption occurs in the range of 1680–1630 cm^{-1}. The absorption range of tertiary amides in solution is influenced by hydrogen bonding with the solvent: *N,N*-Diethylacetamide absorbs at 1647 cm^{-1} in dioxane and at 1615 cm^{-1} in methanol.

Electron-attracting groups attached to the nitrogen increase the frequency of absorption since they effectively compete with the carbonyl oxygen for the electrons of the nitrogen, thus increasing the force constant of the C=O bond.

3.6.17.3. N—H Bending Vibrations (Amide II Band)

All primary amides show a sharp absorption band in dilute solution (amide II band) resulting from NH_2 bending at a somewhat lower frequency than the C=O band. This band has an intensity of one-half to one-third of the C=O absorption band. In mulls and pellets the band occurs near 1655–1620 cm^{-1} and is usually under the envelope of the amide I band. In dilute solutions, the band appears at lower frequency, 1620–1590 cm^{-1}, and normally is separated from the amide I band. Multiple bands may appear in the spectra of concentrated solutions, arising from the free and associated states. The nature of the R group $\left(R—\overset{\overset{O}{\|}}{C}—NH_2\right)$ has little effect upon the amide II band.

Secondary acyclic amides in the solid state display an amide II band in the region of 1570–1515 cm^{-1}. In dilute solution, the band occurs in the 1550–1510-cm^{-1} region. This band results from interaction between the N—H bending and the C—N stretching of the C—N—H group. A second, weaker band near 1250 cm^{-1} also results from interaction between the N—H bending and C—N stretching.

3.6.17.4. Other Vibration Bands

The C—N stretching band of primary amides occurs near 1400 cm^{-1}. A broad, medium band in the 800–666 cm^{-1} region in the spectra of primary and secondary amides results from out-of-plane N—H wagging.

In lactams of medium ring size, the amide group is forced into the *s*-cis conformation. Solid lactams absorb strongly near 3200 cm^{-1} because of the N—H stretching vibration. This band does not shift appreciably with dilution since the *s*-cis form remains associated at relatively low concentrations.

3.6.17.5. C=O Stretching Vibrations

The C=O absorption of lactams with six-membered rings or larger is near 1650 cm^{-1}. Five-membered ring (γ) lactams absorb in the 1750–1700 cm^{-1} region. Four-membered ring (β) lactams, unfused, absorb at 1760–1730 cm^{-1}. Fusion of the lactam ring to another ring generally increases the frequency by 20–50 cm^{-1}.

Most lactams do not show a band near 1550 cm^{-1} that is characteristic of *s*-trans noncyclic secondary amides. The N—H out-of-plane wagging in lactams causes broad absorption in the 800–700-cm^{-1} region.

3.6.18. Amines

The spectrum of a typical primary, aliphatic amine appears in Figure 3.29.

3.6.18.1. N—H Stretching Vibrations

Primary amines, examined in dilute solution, display two weak absorption bands: one near 3500 cm^{-1} and the other near 3400 cm^{-1}. These bands represent, respectively, the "free" asymmetrical and symmetrical N—H stretching modes. Secondary amines show a single weak band in the 3350–3310 cm^{-1} region. These bands are shifted to longer wavelengths by hydrogen bonding. The associated N—H bands are weaker and frequently sharper than the corresponding O—H bands. Aliphatic primary amines (neat) absorb at 3400–3330 and 3330–3250 cm^{-1}. Aromatic primary amines absorb at slightly higher frequencies (shorter wavelengths). In the spectra of liquid primary and secondary amines, a

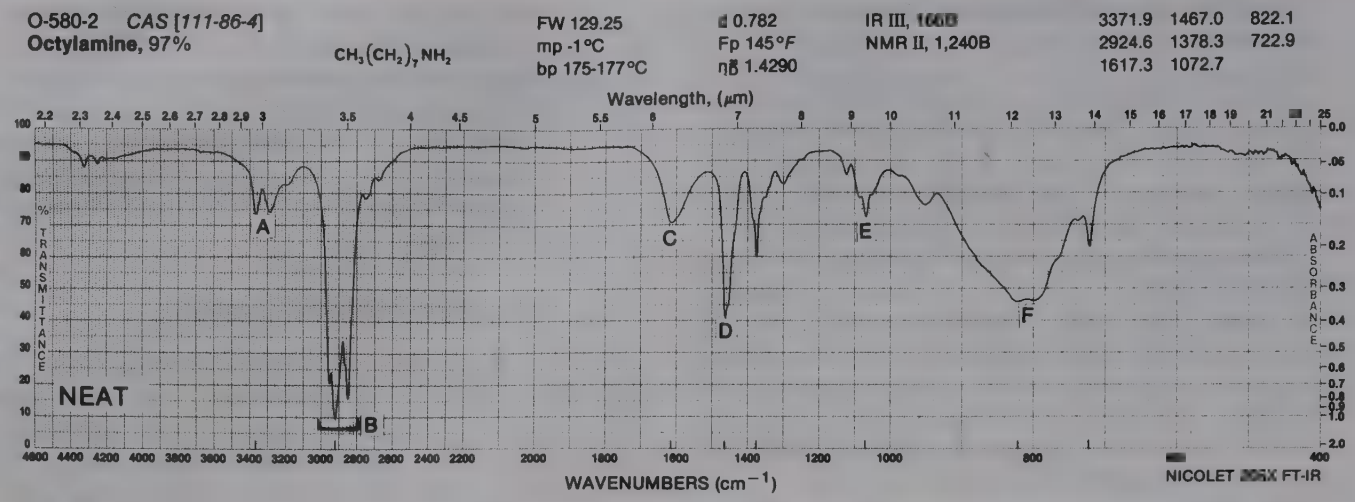

FIGURE 3.29. Octylamine.* A. The N—H stretch, hydrogen-bonded, primary amine coupled doublet: Asymmetric, 3372 cm^{-1}. Symmetric, 3290 cm^{-1}. (Shoulder at about 3200 cm^{-1}, Fermi resonance band with overtone of band at C.) B. Aliphatic C—H stretch, 2925, 2850 cm^{-1}; ν_s, CH_2, 2817 cm^{-1}. C. The N—H bend (scissoring) 1617 cm^{-1}. D. δ_s, CH_2 (scissoring), 1467 cm^{-1}. E. The C—N stretch, 1073 cm^{-1}. F. The N—H wag (neat sample), ~900–700 cm^{-1}.

*The CA name for octylamine is octanamine.

shoulder usually appears on the low-frequency side of the N—H stretching band, arising from the overtone of the NH bending band intensified by Fermi resonance. Tertiary amines do not absorb in this region.

3.6.18.2. N—H Bending Vibrations

The N—H bending (scissoring) vibration of primary amines is observed in the 1650–1580 cm^{-1} region of the spectrum. The band is medium to strong in intensity and is moved to slightly higher frequencies when the compound is associated. The N—H bending band is seldom detectable in the spectra of aliphatic secondary amines, whereas secondary aromatic amines absorb near 1515 cm^{-1}.

Liquid samples of primary and secondary amines display medium-to-strong broad absorption in the 909–666 cm^{-1} region of the spectrum arising from NH wagging. The position of this band depends on the degree of hydrogen bonding.

3.6.18.3. C—N Stretching Vibrations

Medium-to-weak absorption bands for the unconjugated C—N linkage in primary, secondary, and tertiary aliphatic amines appear in the region of 1250–1020 cm^{-1}. The vibrations responsible for these bands involve C—N stretching coupled with the stretching of adjacent bonds in the molecule. The position of absorption in this region depends on the class of the amine and the pattern of substitution on the α carbon.

Aromatic amines display strong C—N stretching absorption in the 1342–1266 cm^{-1} region. The absorption appears at higher frequencies (shorter wavelengths) than the corresponding absorption of aliphatic amines because the force constant of the C—N bond is increased by resonance with the ring.

Characteristic strong C—N stretching bands in the spectra of aromatic amines have been assigned as in Table 3.4.

3.6.19. Amine Salts

3.6.19.1. N—H Stretching Vibrations

The ammonium ion displays strong, broad absorption in the 3300–3030 cm^{-1} region because of N—H stretching vibrations (see Fig. 3.24). There is also a combination band in the 2000–1709 cm^{-1} region.

TABLE 3.4

C—N Stretch of Primary, Secondary, and Tertiary Aromatic Amines

Aromatic Amine	Absorption Region (cm^{-1})
Primary	1340–1250
Secondary	1350–1280
Tertiary	1360–1310

Salts of primary amines show strong, broad absorption between 3000 and 2800 cm^{-1} arising from asymmetrical and symmetrical stretching in the NH_3^+ group. In addition, multiple combination bands of medium intensity occur in the 2800–2000 cm^{-1} region, the most prominent being the band near 2000 cm^{-1}. Salts of secondary amines absorb strongly in the 3000–2700 cm^{-1} region with multiple bands extending to 2273 cm^{-1}. A medium band near 2000 cm^{-1} may be observed. Tertiary amine salts absorb at longer wavelengths than the salts of primary and secondary amines (2700–2250 cm^{-1}). Quaternary ammonium salts can have no N—H stretching vibrations.

3.6.19.2. N—H Bending Vibrations

The ammonium ion displays a strong, broad NH_4^+ bending band near 1429 cm^{-1}. The NH_3^+ group of the salt of a primary amine absorbs near 1600–1575 and 1550–1504 cm^{-1}. These bands originate in asymmetrical and symmetrical NH_3^+ bending, analogous to the corresponding bands of the CH_3 group. Salts of secondary amines absorb near 1620–1560 cm^{-1}. The N—H bending band of the salts of tertiary amines is weak and of no practical value.

3.6.20. Amino Acids and Salts of Amino Acids

Amino acids are encountered in three forms:

1. The free amino acid (zwitterion).

Guide—Msp. 178

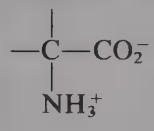

2. The hydrochloride (or other salt).

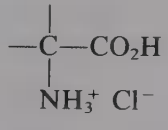

3. The sodium (or other cation) salt.

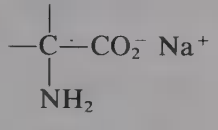

Free primary amino acids are characterized by the following absorptions (most of the work was done with α-amino acids, but the relative positions of the amino and carboxyl groups seem to have little effect):

1. A broad, strong NH_3^+ stretching band in the 3100–2600 cm^{-1} region. Multiple combination and overtone bands extend the absorption to about 2000 cm^{-1}. This overtone region usually contains a prominent band near 2222–2000 cm^{-1} assigned to a combination of the asymmetrical NH_3^+ bending vibration and the torsional oscillation of the NH_3^+ group. The torsional oscillation occurs near 500 cm^{-1}. The 2000 cm^{-1} band is absent if the nitrogen atom of the amino acid is substituted.
2. A weak asymmetric NH_3^+ bending band near 1660–1610 cm^{-1}, a fairly strong symmetrical bending band near 1550–1485 cm^{-1}.
3. The carboxylate ion group 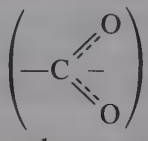 absorbs strongly near 1600–1590 cm^{-1} and more weakly near 1400 cm^{-1}. These bands result, respectively, from asymmetrical and symmetrical $C(=O)_2$ stretching.

The spectrum of the amino acid leucine, including assignments corresponding to the preceding three categories, is shown in Figure 3.30.

Hydrochlorides of amino acids present the following patterns:

1. Broad strong absorption in the 3333–2380-cm^{-1} region resulting from superimposed O—H and NH_3^+ stretching bands. Absorption in this region is characterized by multiple fine structure on the low wavenumber side of the band.
2. A weak, asymmetrical NH_3^+ bending band near 1610–1590 cm^{-1}; a relatively strong, symmetrical NH_3^+ bending band at 1550–1481 cm^{-1}.
3. A strong band at 1220–1190 cm^{-1} arising from  stretching.
4. Strong carbonyl absorption at 1755–1730 cm^{-1} for α-amino acid hydrochlorides, and at 1730–1700 cm^{-1} for other amino acid hydrochlorides.

Sodium salts of amino acids show the normal N—H stretching vibrations at 3400–3200 cm^{-1} common to other amines. The characteristic carboxylate ion bands appear near 1600–1590 cm^{-1} and near 1400 cm^{-1}.

3.6.21. Nitriles

The spectra of nitriles (R—C≡N) are characterized by weak to medium absorption in the triple-bond

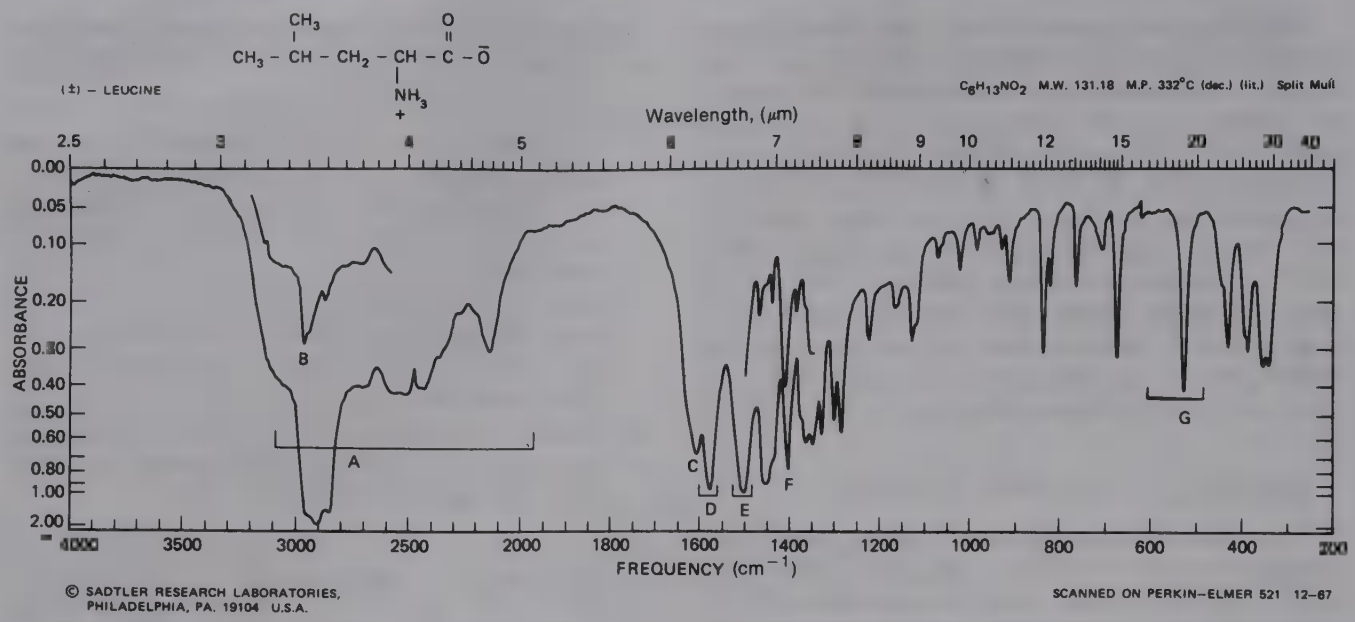

FIGURE 3.30. (±)-Leucine. A. Broad (—NH_3^+) N—H stretch, 3100–2000 cm^{-1}, extended by combination band at 2140 cm^{-1}, and other combination–overtone bands. B. Aliphatic C—H stretch (superimposed on N—H stretch), 2967 cm^{-1}. C. Asymmetric (—NH_3^+) N—H bend, 1610 cm^{-1}. D. Asymmetric carboxylate $(C{=}O)_2$ stretch, 1580 cm^{-1}. E. Symmetric (—NH_3^+) N—H bend, 1505 cm^{-1}. F. Symmetric carboxylate $(C{=}O)_2$ stretch, 1405 cm^{-1}. G. Torsional (—NH_3^+) N—H oscillation, 525 cm^{-1}.

stretching region of the spectrum. Aliphatic nitriles absorb near 2260–2240 cm^{-1}. Electron-attracting atoms, such as oxygen or chlorine, attached to the carbon atom α to the C≡N group reduce the intensity of absorption. Conjugation, such as occurs in aromatic nitriles, reduces the frequency of absorption to 2240–2222 cm^{-1} and enhances the intensity. The spectrum of a typical nitrile, with an aryl group in conjugation with the cyano function, is shown in Figure 3.31.

3.6.22. Compounds Containing C≡N, C=N, —N=C=O and —N=C=S Groups

Isocyanides (isonitriles), isocyanates, thiocyanates, and isothiocyanates all show C≡N stretch or cumulated double bond (—Y=C=X; X, Y = N, S or O) stretch in the 2273–2000-cm^{-1} region (Appendix C). Schiff's bases (RCH=NR, imines), oximes, thiazoles,

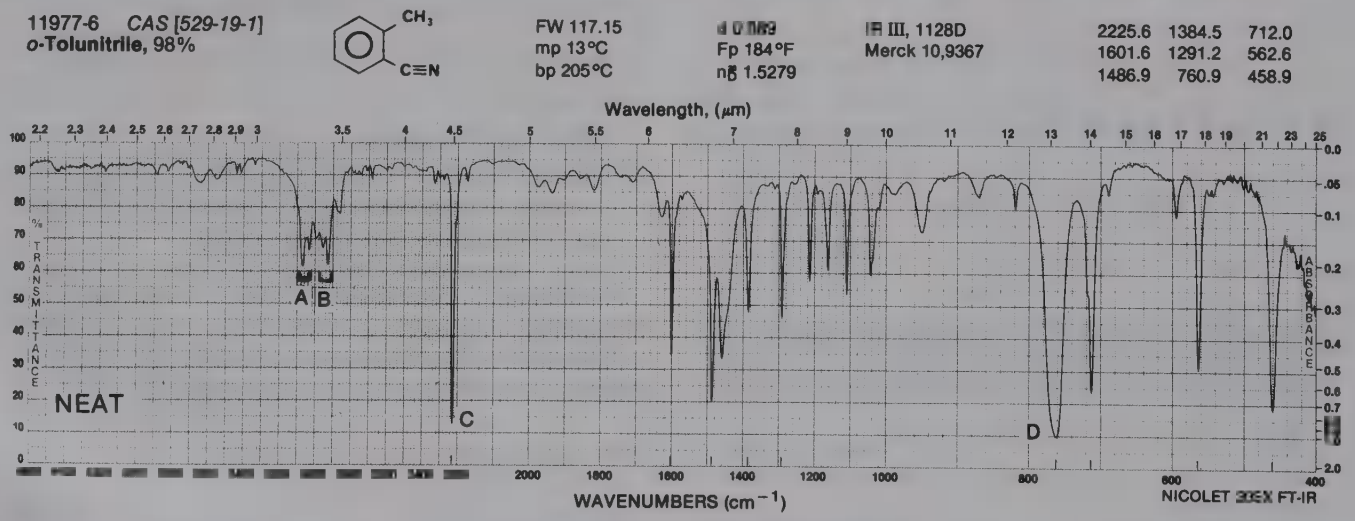

FIGURE 3.31. *o*-Tolunitrile. A. Aromatic C—H stretch, 3070, 3030 cm^{-1}. B. Aliphatic C—H stretch, 2960, 2930 cm^{-1}. C. The C≡N stretch, 2226 cm^{-1} (intensified by aryl conjugation; aliphatic nitriles absorb at higher frequency). D. Out-of-plane C—H bend (aromatic ring) D, 761 cm^{-1}.

iminocarbonates, guanidines, and so on, show the C=N stretch in the 1689–1471 cm^{-1} region. Although the intensity of the C=N stretch is variable, it is usually more intense than the C=C stretch. Azides show bands near 2140 cm^{-1} suggestive of the resonance form with cumulated double bonds: $R—N=\overset{+}{N}=N:^-$

3.6.23. Compounds Containing —N=N— Group

The N=N stretching vibration of a symmetrical trans azo compound is forbidden in the IR but absorbs in the 1576 cm^{-1} region of the Raman spectrum. Unsymmetrical para-substituted azobenzenes in which the substituent is an electron donating group absorb near 1429 cm^{-1}. The bands are weak because of the nonpolar nature of the bond.

3.6.24. Covalent Compounds Containing Nitrogen–Oxygen Bonds

Nitro compounds, nitrates, and nitramines contain an NO_2 group. Each of these classes shows absorption due to asymmetrical and symmetrical stretching of the NO_2 group. Asymmetrical absorption results in a strong band in the 1661–1499 cm^{-1} region; symmetrical absorption occurs in the region between 1389–1259 cm^{-1}. The exact position of the bands is dependent on substitution and unsaturation in the vicinity of the NO_2 group.

3.6.24.1. N⋯O Stretching Vibrations

NITRO COMPOUNDS. In the nitroalkanes, the bands occur near 1550 and 1372 cm^{-1}. Conjugation lowers the frequency of both bands, resulting in absorption near 1550–1500 and 1360–1290 cm^{-1}. Attachment of electronegative groups to the α carbon of a nitro compound causes an increase in the frequency of the asymmetrical NO_2 band and a reduction in the frequency of the symmetrical band; chloropicrin, Cl_3CNO_2, absorbs at 1610 and 1307 cm^{-1}.

Aromatic nitro groups absorb near the same frequencies as observed for conjugated aliphatic nitro compounds. Interaction between the NO_2 out-of-plane bending and ring C—H out-of-plane bending frequencies destroys the reliability of the substitution pattern observed for nitroaromatics in the long wavelength region of the spectrum. Nitroaromatic compounds show a C—N stretching vibration near 870 cm^{-1}. The spectrum of nitrobenzene, with assignments corresponding to the preceding discussion, is shown in Figure 3.32.

Because of strong resonance in aromatic systems containing NO_2 groups and electron-donating groups such as the amino group, ortho or para to one another, the symmetrical NO_2 vibration is shifted to lower frequencies and increases in intensity. *p*-Nitroaniline absorbs at 1475 and 1310 cm^{-1}.

The positions of asymmetric and symmetric NO_2 stretching bands of nitramines $\left(\diagdown\!\!>N—NO_2\right)$ and the NO stretch of nitrosoamines are given in Appendix C.

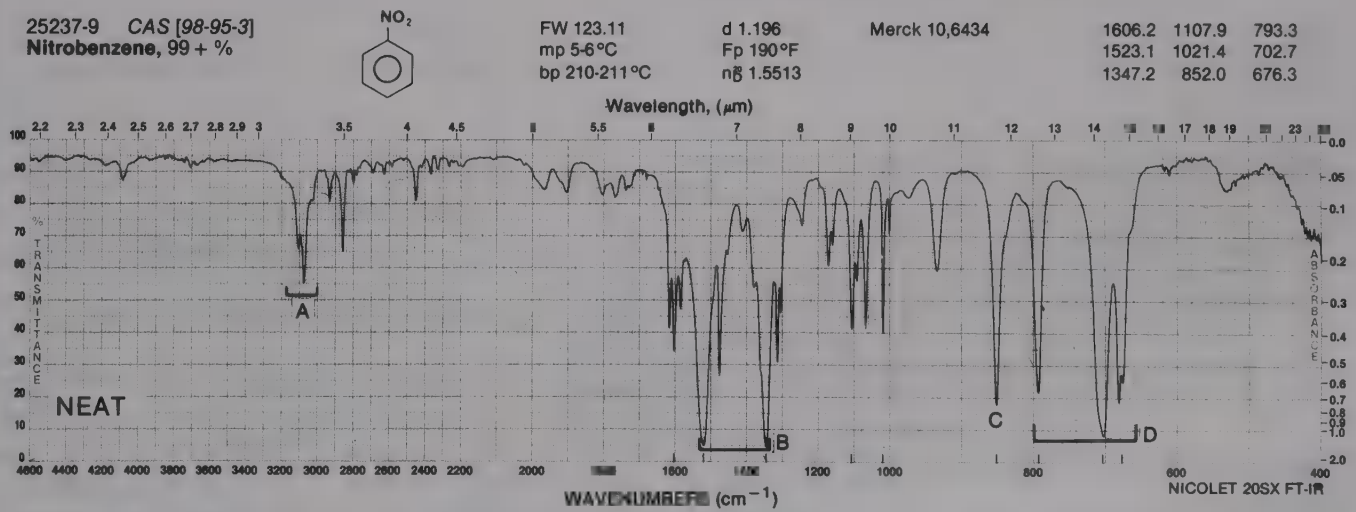

FIGURE 3.32. Nitrobenzene. A. Aromatic C—H stretch, 3100, 3080 cm^{-1}. B. Asymmetric ($ArNO_2$) (N=O)$_2$ stretch, 1523 cm^{-1}. Symmetric ($ArNO_2$) (N=O)$_2$ stretch 1347 cm^{-1}. C. C—N stretch for $ArNO_2$, 852 cm^{-1}. D. Low-frequency bands are of little use in determining the nature of ring substitution since these absorption patterns are due to interaction of NO_2 and C—H out-of-plane bending frequencies. The inability of the "oop" region to reveal structural information is typical of aromatic compounds with highly polar substituents.

NITRATES. Organic nitrates show absorption for N—O stretching vibrations of the NO_2 group and for the O—N linkage. Asymmetrical stretching in the NO_2 group results in strong absorption in the 1660–1625-cm^{-1} region; the symmetrical vibration absorbs strongly near 1300–1255 cm^{-1}. Stretching of the π bonds of the N—O linkage produces absorption near 870–833 cm^{-1}. Absorption observed at longer wavelengths, near 763–690 cm^{-1}, likely results from NO_2 bending vibrations.

NITRITES. Nitrites display two strong N=O stretching bands. The band near 1680–1650 cm^{-1} is attributed to the trans isomer; the cis isomer absorbs in the 1625–1610-cm^{-1} region. The N—O stretching band appears in the region between 850 and 750 cm^{-1}. The nitrite absorption bands are among the strongest observed in IR spectra.

NITROSO COMPOUNDS. Primary and secondary aliphatic *C*-nitroso compounds are usually unstable and rearrange to oximes or dimerize. Tertiary and aromatic nitroso compounds are reasonably stable, existing as monomers in the gaseous phase or in dilute solution and as dimers in neat samples. Monomeric, tertiary, aliphatic nitroso compounds show N=O absorption in the 1585–1539 cm^{-1} region; aromatic monomers absorb between 1511 and 1495 cm^{-1}.

The N → O stretching absorption of dimeric nitroso compounds are categorized in Appendix C as to cis versus trans and aliphatic versus aromatic. Nitrosoamine absorptions are given in Appendix C.

3.6.25. Organic Sulfur Compounds

3.6.25.1. S—H Stretching Vibrations

MERCAPTANS. Aliphatic mercaptans and thiophenols, as liquids or in solution, show S—H stretching absorption in the range of 2600–2550 cm^{-1}. The S—H stretching band is characteristically weak and may go undetected in the spectra of dilute solutions or thin films. However, since few other groups show absorption in this region, it is useful in detecting S—H groups. The spectrum of benzyl mercaptan in Figure 3.33 is that of a mercaptan with a detectable S—H stretch band. The band may be obscured by strong carboxyl absorption in the same region. Hydrogen bonding is much weaker for S—H groups than for O—H and N—H groups.

The S—H group of thiol acids absorbs in the same region as mercaptans and thiophenols.

3.6.25.2. C—S and C=S Stretching Vibrations

SULFIDES. The stretching vibrations assigned to the C—S linkage occur in the region of 700–600 cm^{-1}. The weakness of absorption and variability of position make this band of little value in structural determination.

DISULFIDES. The S—S stretching vibration is very weak and falls between 500–400 cm^{-1}.

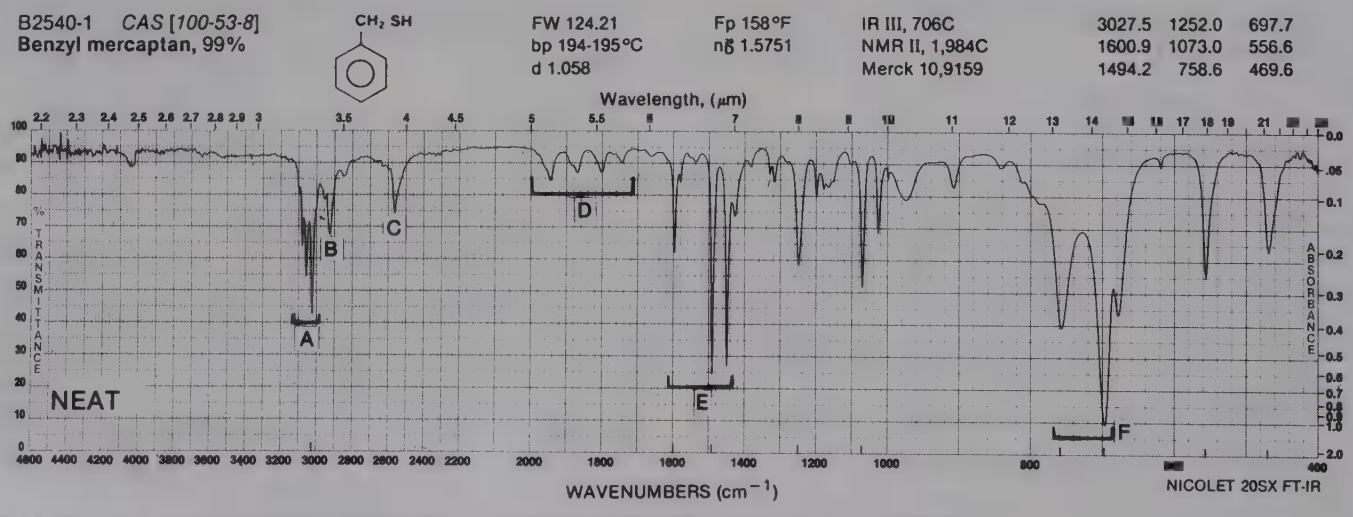

FIGURE 3.33. Benzyl mercaptan.* A. Aromatic C—H stretch, 3085, 3060, 3027.5 cm^{-1}. B. Aliphatic C—H stretch, 2930 cm^{-1}. C. Moderately weak S—H stretch, 2565 cm^{-1}. D. Overtone or combination band pattern indicative of monosubstituted aromatic 2000–1667 cm^{-1}. E. The C=C ring stretch, 1601, 1495, 1455 cm^{-1}. F. Out-of-plane aromatic C—H bend (monosubstituted benzene ring), 759, 698 cm^{-1}.

*Benzyl mercaptan is another common name for α-toluenethiol.

THIOCARBONYL COMPOUNDS. Aliphatic thials or thiones exist as trimeric, cyclic sulfides. Aralkyl thiones may exist either as monomers or trimers, whereas diaryl. thiones, such as thiobenzophenone, exist only as monomers. The C=S group is less polar than the C=O group and has a considerably weaker bond. In consequence, the band is not intense, and it falls at lower frequencies, where it is much more susceptible to coupling effects. Identification is therefore difficult and uncertain.

Compounds that contain a thiocarbonyl group show absorption in the 1250–1020 cm^{-1} region. Thiobenzophenone and its derivatives absorb moderately in the 1224–1207-cm^{-1} region. Since the absorption occurs in the same general region as C—O and C—N stretching, considerable interaction can occur between these vibrations within a single molecule.

Spectra of compounds in which the C=S group is attached to a nitrogen atom show an absorption band in the general C=S stretching region. In addition, several other bands in the broad region of 1563–700 cm^{-1} can be attributed to vibrations involving interaction between C=S stretching and C—N stretching.

Thioketo compounds that can undergo enolization exist as thioketo–thioenol tautomeric systems; such systems show S—H stretching absorption. The thioenol tautomer of ethyl thiobenzoylacetate,

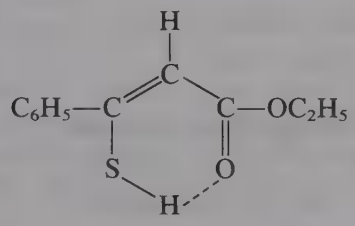

absorbs broadly at 2415 cm^{-1} due to hydrogen-bonded S—H stretching absorption.

3.6.26. Compounds Containing Sulfur–Oxygen Bonds

3.6.26.1. S=O Stretching Vibrations

SULFOXIDES. Alkyl and aryl sulfoxides as liquids or in solution show strong absorption in the 1070–1030 cm^{-1} region. This absorption occurs at 1050 cm^{-1} for dimethyl sulfoxide (DMSO, methyl sulfoxide) as may be seen in Appendix B, No. 26. Conjugation brings about a small change in the observed frequency in contrast to the marked reduction in frequency of the C=O bond accompanying conjugation. Diallyl sulfoxide absorbs at 1047 cm^{-1}. Phenyl methyl sulfoxide and cyclohexyl methyl sulfoxide absorb at 1055 cm^{-1} in dilute solution in carbon tetrachloride. The sulfoxide group is susceptible to hydrogen bonding, the absorption shifting to slightly lower frequencies from dilute solution to the liquid phase. The frequency of S=O absorption is increased by electronegative substitution.

SULFONES. Spectra of sulfones show strong absorption bands at 1350–1300 and 1160–1120 cm^{-1}. These bands arise from asymmetric and symmetric SO_2 stretching, respectively. Hydrogen bonding results in absorption near 1300 and 1125 cm^{-1}. Splitting of the high-frequency band often occurs in CCl_4 solution or in the solid state.

SULFONYL CHLORIDES. Sulfonyl chlorides absorb strongly in the regions of 1410–1380 and 1204–1177 cm^{-1}. This increase in frequency, compared with the sulfones, results from the electronegativity of the chlorine atom.

SULFONAMIDES. Solutions of sulfonamides absorb strongly at 1370–1335 and 1170–1155 cm^{-1}. In the solid phase, these frequencies are lowered by 10–20 cm^{-1}. In solid samples, the high-frequency band is broadened and several submaxima usually appear.

Primary sulfonamides show strong N—H stretching bands at 3390–3330 and 3300–3247 cm^{-1} in the solid state; secondary sulfonamides absorb near 3265 cm^{-1}.

SULFONATES, SULFATES, and SULFONIC ACIDS. The asymmetric (higher frequency, shorter wavelength) and symmetric S=O stretching frequency ranges for these compounds are as follows:

Class	Stretching Frequencies (cm^{-1})
Sulfonates (covalent)	1372–1335, 1195–1168
Sulfates (organic)	1415–1380, 1200–1185
Sulfonic acids	1350–1342, 1165–1150
Sulfonate salts	~1175 ~1055

The spectrum of a typical alkyl arenesulfonate is given in Figure 3.34. In virtually all sulfonates, the asymmetric stretch occurs as a doublet. Alkyl and aryl sulfonates show negligible differences; electron-donating groups in the para position of arenesulfonates cause higher frequency absorption.

Sulfonic acids are listed in narrow ranges above; these apply only to anhydrous forms. Such acids hy-

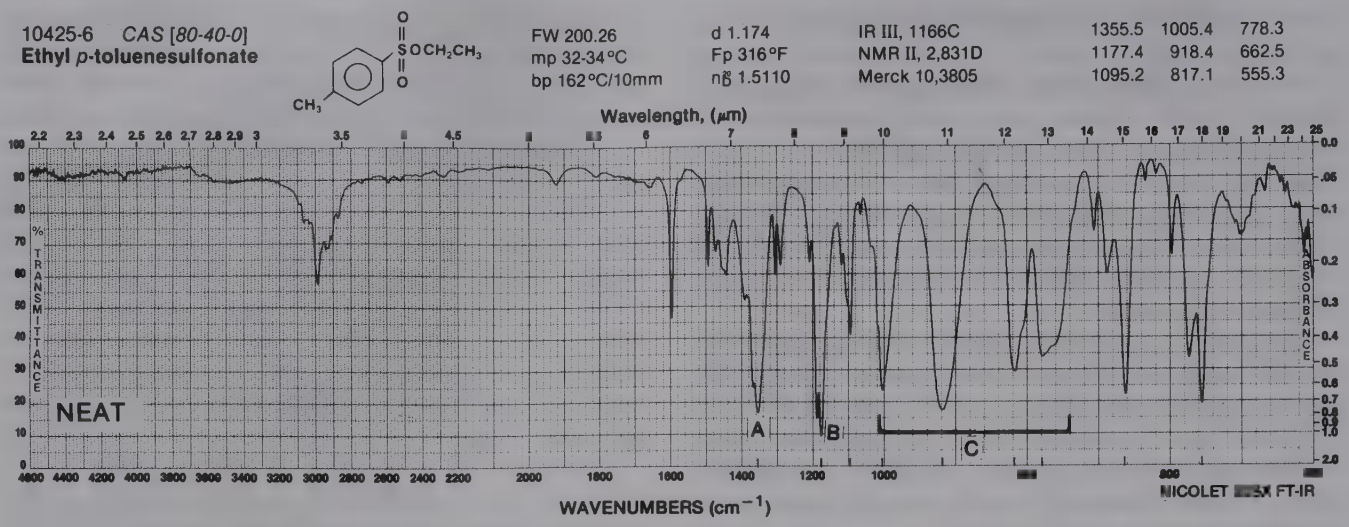

FIGURE 3.34. Ethyl *p*-toluenesulfonate. A. Asymmetric $S(=O)_2$ stretch, 1355.5 cm^{-1}. B. Symmetric $S(=O)_2$ stretch, 1177 cm^{-1}. C. Various strong S—O—C stretching, 1000–769 cm^{-1}.

drate readily to give bands that are probably a result of the formation of hydronium sulfonate salts, in the 1230–1120 cm^{-1} range.

3.6.27. Organic Halogen Compounds

The strong absorption of halogenated hydrocarbons arises from the stretching vibrations of the carbon–halogen bond.

Aliphatic C—Cl absorption is observed in the broad region between 850 and 550 cm^{-1}. When several chlorine atoms are attached to one carbon atom, the band is usually more intense and at the high-frequency end of the assigned limits. Carbon tetrachloride (see Appendix B, No. 10) shows an intense band at 797 cm^{-1}. The first overtones of the intense fundamental bands are frequently observed. Spectra of typical chlorinated hydrocarbons are shown in Appendix B: Nos. 10–13. Brominated compounds absorb in the 690–515 cm^{-1} region, iodo-compounds in the 600–500-cm^{-1} region. A strong CH_2 wagging band is observed for the CH_2X (X = Cl, Br, and I) group in the 1300–1150 cm^{-1} region.

Fluorine-containing compounds absorb strongly over a wide range between 1400 and 730 cm^{-1} due to C—F stretching modes. A monofluoroalkane shows a strong band in the 1100–1000 cm^{-1} region. As the number of fluorine atoms in an aliphatic molecule increases, the band pattern becomes more complex, with multiple strong bands appearing over the broad region of C—F absorption. The CF_3 and CF_2 groups absorb strongly in the 1350–1120-cm^{-1} region. The spectrum of Fluorolube®, Appendix B, No. 14, illustrates many of the preceding absorption characteristics.

Chlorobenzenes absorb in the 1096–1089 cm^{-1} region. The position within this region depends on the substitution pattern. Aryl fluorides absorb in the 1250–110 cm^{-1} region of the spectrum. A monofluorinated benzene ring displays a strong, narrow absorption band near 1230 cm^{-1}.

3.6.28. Silicon Compounds

3.6.28.1. Si—H Vibrations

Vibrations for the Si—H bond include the Si—H stretch (~2200 cm^{-1}) and the Si—H bend (800–950 cm^{-1}). The Si—H stretching frequencies are increased by the attachment of an electronegative group to the silicon.

3.6.28.2. SiOH Vibrations

The OH stretching vibrations of the SiOH group absorb in the same region as the alcohols, 3700–3200 cm^{-1}, and strong Si—O bands are at 830–1110 cm^{-1}. As in alcohols, the absorption characteristics depend on the degree of hydrogen bonding.

3.6.28.3. Silicon–Halogen Stretching Vibrations

Absorption due to Si—F stretch is in the 800–1000 region.

Bands resulting from Si—Cl stretching occur at frequencies below 666 cm^{-1}.

The spectrum of silicone lubricant, Appendix B (No. 27), illustrates some of the preceding absorptions.

3.6.29. Phosphorus Compounds

3.6.29.1. P=O and P—O Stretching Vibrations

Such absorptions are listed in Appendix E, Table E-1.

3.6.30. Heteroaromatic Compounds

The spectra of heteroaromatic compounds result primarily from the same vibrational modes as observed for the aromatics.

3.6.30.1. C—H Stretching Vibrations

Heteroaromatics, such as pyridines, pyrazines, pyrroles, furans, and thiophenes, show C—H stretching bands in the 3077–3003 cm^{-1} region.

3.6.30.2. N—H Stretching Frequencies

Heteroaromatics containing an N—H group show N—H stretching absorption in the region of 3500–3220 cm^{-1}. The position of absorption within this general region depends on the degree of hydrogen bonding, and hence upon the physical state of the sample or the polarity of the solvent. Pyrrole and indole in dilute solution in nonpolar solvents show a sharp band near 3495 cm^{-1}; concentrated solutions show a widened band near 3400 cm^{-1}. Both bands may be seen at intermediate concentrations.

3.6.30.3. Ring Stretching Vibrations (Skeletal Bands)

Ring stretching vibrations occur in the general region between 1600 and 1300 cm^{-1}. The absorption involves stretching and contraction of all of the bonds in the ring and interaction between these stretching modes. The band pattern and the relative intensities depend on the substitution pattern and the nature of the substituents.

Pyridine (Fig. 3.35) shows four bands in this region and, in this respect, closely resembles a monosubstituted benzene. Furans, pyrroles, and thiophenes display two to four bands in this region.

3.6.30.4. C—H Out-of-Plane Bending

The C—H out-of-plane bending (γ-CH) absorption pattern of the heteroaromatics is determined by the number of adjacent hydrogen atoms bending in phase. The C—H out-of-plane and ring bending (β ring) absorption of the alkylpyridines are summarized in Table E-1.

Absorption data for the out-of-phase C—H bending (γ-CH) and ring bending (β ring) modes of three common five-membered heteroaromatic rings are presented in Table E-3. The ranges in Table E-3 (p. 164) include polar as well as nonpolar substituents on the ring.

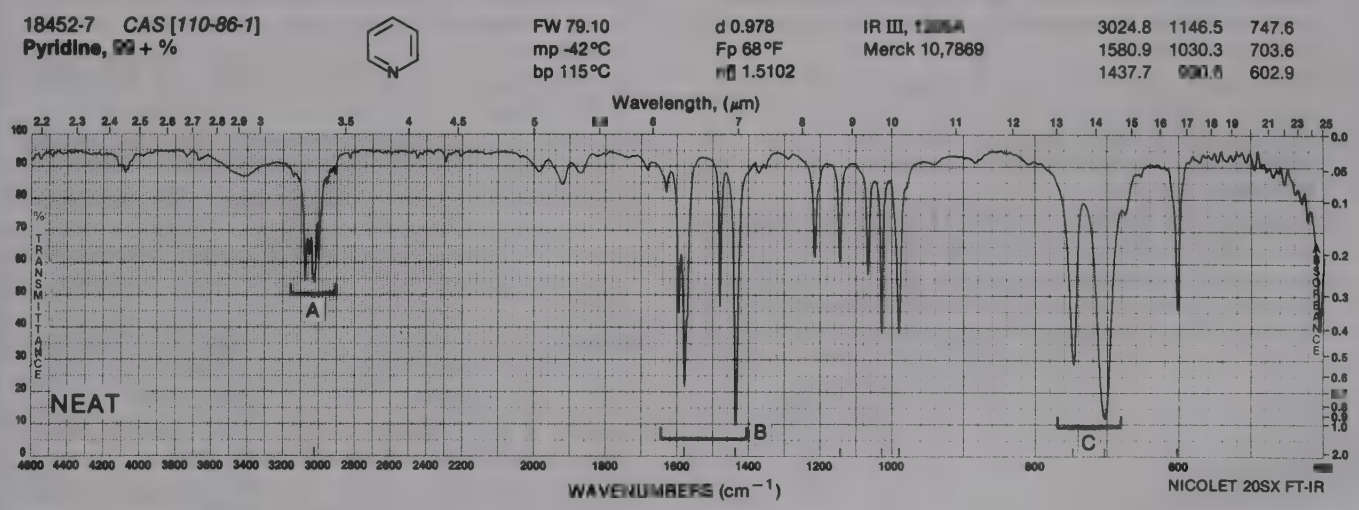

FIGURE 3.35. Pyridine. A. Aromatic C—H stretch, 3080–3010 cm^{-1}. B. C=C, C=N ring stretching (skeletal bands), 1600–1430 cm^{-1}. C. The C—H out-of-plane bending, 748, 704 cm^{-1}. See Table E-2, for patterns in region C for substituted pyridines.

REFERENCES

Introductory and Theoretical

Conley, R. T. *Infrared Spectroscopy*. 2nd ed. Boston: Allyn and Bacon, 1972.

Nakanishi, Koji and Solomon, P. H. *Infrared Absorption Spectroscopy–Practical*. 2nd ed. San Francisco: Holden–Day, 1977.

Colthup, N. B., Daly, L. H., and Wiberley, S. E. *Introduction to Infrared and Raman Spectroscopy*. 3rd ed. New York and London: Academic, 1990.

Dyer, J. R. *Applications of Absorption Spectroscopy of Organic Compounds*. Englewood Cliffs, NJ: Prentice–Hall, 1965.

Miller, K. G. J. and Stace, B. C. (Eds.) *Laboratory Methods in Infrared Spectroscopy*. 2nd ed., New York: Heyden, 1972.

Herzberg, G. *Infrared and Raman Spectra of Polyatomic Molecules*. New York: Van Nostrand, 1945.

Compilations of Spectra or Data

Pouchert, C. J. (Ed.) *The Aldrich Library of Infrared Spectra*. Milwaukee, WI: Aldrich, 1975.

Bellamy, L. J. *The Infrared Spectra of Complex Molecules*. 3rd ed. London: Chapman and Hall, New York: Halsted–Wiley, 1975.

Bellamy, L. J. *Advances in Infrared Group Frequencies*. London: Methuen, 1968.

Flett, M. St. C. *Characteristic Frequencies of Chemical Groups in the Infrared*. New York: American Elsevier, 1969.

Dolphin, D. and Wick, A. E. *Tabulation of Infrared Spectral Data*. New York: Wiley, 1977.

Catalog of Infrared Spectrograms, American Petroleum Institute Research Project 44. Pittsburgh, PA: Carnegie Institute of Technology.

Catalog of Infrared Spectral Data, Manufacturing Chemists Association Research Project, Chemical and Petroleum Research Laboratories. Pittsburgh, PA: Carnegie Institute of Technology, to June 30, 1960; College Station, TX.: Chemical Thermodynamics Properties Center, Agriculture and Mechanical College of Texas, from July 1, 1960.

ASTM-Wyandotte Index, Molecular Formula List of Compounds, Names and References to Published Infrared Spectra. Philadelphia, PA: ASTM Special Technical Publications 131 (1962) and 131-A (1963). Lists about 57,000 compounds. Covers IR, near-IR, and far-IR spectra.

Hershenson, H. H. *Infrared Absorption Spectra Index*. New York and London: Academic, 1959, 1964. Two volumes cover 1945–1962.

Documentation of Molecular Spectroscopy (DMS), London: Butterworths Scientific Publications, and Weinheim/Bergstrasse, West Germany: Verlag Chemie GMBH, in cooperation with the infrared Absorption Data Joint Committee, London, and the Institut für Spectrochemie und Angewandte Spectroskopie, Dortmund. Spectra are presented on coded cards. Coded cards containing abstracts of articles relating to IR spectrometry are also issued.

IRDC Cards: *Infrared Data Committee of Japan* (S. Mizushima). Haruki-cho, Tokyo: Handled by Nankodo Co.

The NRC–NBS (Creitz) File of Spectrograms, issued by National Research Council–National Bureau of Standards Committee on Spectral Absorption Data, National Bureau of Standards, Washington 25, DC. Spectra presented on edge-punched cards.

Bentley, F. F., L. D. Smithson, and Rozek, A. L. *Infrared Spectra and Characteristic Frequencies ~700 to 300 cm^{-1}, A Collection of Spectra, Interpretation and Bibliography*. New York: Wiley–Interscience, 1968.

Ministry of Aviation Technical Information and Library Services (ed.) *An Index of Published Infra-Red Spectra*. Vols. 1 and 2: London: Her Majesty's Stationery Office, 1960.

Brown, C. R., Ayton, M. W., Goodwin, T. C., and Derby, T. J. *Infrared—A Bibliography*. Washington, DC: Library of Congress, Technical Information Division, 1954.

Dobriner, K., Katzenellenbogen, E. R., and Jones, R. N. *Infrared Absorption Spectra of Steroids—An Atlas*. Vol. 1. New York: Wiley–Interscience, 1953.

Szymanski, H. A. *Correlation of Infrared and Raman Spectra of Organic Compounds*. Hertillon Press, 1969.

Szymanski, H. A. *IR Theory and Practice of Infrared Spectroscopy*. New York: Plenum, 1964.

Szymanski, H. A. *Interpreted Infrared Spectra*. Vols. I–III. New York: Plenum, 1964–1967.

Szymanski, H. A. *Infrared Band Handbook*. New York: Plenum, 1963.

Infrared Band Handbook. Supplements 1 and 2. New York: Plenum, 1964, 259 pp.

Infrared Band Handbook. Supplements 3 and 4. New York: Plenum, 1965.

Infrared Band Handbook. 2nd rev. ed. New York: IFI/Plenum, 1970, 2 volumes.

Catalog of Infrared Spectrograms. Philadelphia: Sadtler Research Laboratories, PA. 19104. Spectra are indexed by name and by the Spec-Finder. The latter is an index that tabulates major bands by wavelength intervals. This allows quick identification of unknown compounds.

Sadtler Standard Infrared Grating Spectra. Philadelphia: Sadtler Research Laboratories, Inc., 1972. 26,000 spectra in 26 volumes.

Sadtler Standard Infrared Prism Spectra. Philadelphia: Sadtler Research Laboratories, Inc., 1972. 43,000 spectra in 43 volumes.

Sadtler Reference Spectra—Commonly Abused Drugs IR & UV Spectra. Philadelphia: Sadtler Research Laboratories, Inc., 1972. 600 IR Spectra, 300 UV.

Sadtler Reference Spectra—Gases & Vapors High Resolution Infrared. Philadelphia: Sadtler Research Laboratories, Inc., 1972. 150 Spectra.

Sadtler Reference Spectra—Inorganics IR Grating. Philadelphia: Sadtler Research Laboratories, Inc., 1967. 1300 spectra.

Sadtler Reference Spectra—Organometallics IR Grating. Philadelphia: Sadtler Research Laboratories, Inc., 1966. 400 spectra.

Socrates, G. *IR Characteristic Group Frequencies*. New York: Wiley, 1980.

Pouchert, C. J., *Aldrich Library of FTIR Spectra,* Vols. I–III, Aldrich, Milwaukee, WI, 1985. Volume III consists of vapor-phase spectra.

Griffiths, P. R. and DeHaseth, J. A. *FTIR,* New York: Wiley, 1986.

Herres, W. *HRGC–FTIR, Capillary GC, and FTIR Spectroscopy: Theory and Applications*. New York: Huthig, 1987.

Mattson, J. S. (Ed.). *Infrared, Correlation and Fourier Transform Spectroscopy*. New York: Marcel Dekker, 1977.

Durig, J. R. *Chemical, Biological, and Industrial Applications of Infrared Spectra*. New York: Wiley, 1985.

Maslowsky, E. *Vibrational Spectra of Organometallic Compounds*. New York: Wiley–Interscience, 1977.

Katritzky, A. R. (Ed.) *Physical Methods in Heterocyclic Chemistry*. Vol. II. New York and London: Academic, 1963.

Szymanski, H. A. (Ed.) *Raman Spectroscopy: Theory and Practice*. Vols. 1, 2. New York: Plenum, 1969, 1970.

Loader, E. J. *Basic Laser Raman Spectroscopy*. London, New York: Heyden–Sadtler, 1970.

Finch, A., Gates, P. N., Radcliffe, K., Dickson, F. N., and Bentley, F. F. *Chemical Applications of Far Infrared Spectroscopy*. New York: Academic, 1970.

Stewart, J. E. "Far Infrared Spectroscopy" in *Interpretive Spectroscopy*. Freeman, S. K. (Ed.) New York: Reinhold, 1965, p. 131.

Tichy, M. "The Determination of Intramolecular Hydrogen Bonding by Infrared Spectroscopy and Its Applications in Stereochemistry," in *Advances in Organic Chemistry: Methods and Results*. Vol. 5. R. R. Raphael (Ed.) New York: Wiley–Interscience, 1964.

PROBLEMS

3.1 Either benzonitrile or phenylacetonitrile shows a band of medium intensity at 2940 cm^{-1}; the other compound shows nothing in the range 3000–2500 cm^{-1}. Explain.

3.2 Select a compound that best fits each of the following sets of IR bands (in cm^{-1}). Each set corresponds to a list of just a few important bands for each compound.

a. 3080 (w), nothing 3000–2800, 2230 (s), 1450 (s), 760 (s), 688 (s)

b. 3380 (m), 3300 (m), nothing 3200–3000, 2980 (s), 2870 (m)

c. 3080 (w), nothing 3000–2800, 1315 (s), 1300 (s), 1155 (s)

d. 2955 (s), 2850 (s), 1120 (s)

e. 2970 (s), 2930 (m), 1600 (s), 1360 (m)

f. 2900 (b,s), 1720 (b,s)

g. 3030 (m), 730 (s), 690 (s)

h. 3200–2400 (s), 1685 (b,s), 705 (s)

i. 3350 (s), 3060 (m), 1635 (s)

s = strong, m = medium, w = weak, b = broad

Benzamide
Benzoic acid
Benzonitrile
Biphenyl
Dioxane
Diphenyl sulfone
Formic acid
Isobutylamine
1-Nitropropane

For Problems 3.3–3.6, match the name from each list to the proper IR spectrum. Identify the diagnostic bands in each spectrum. These spectra are on pp. 133–139.

3.3. SPECTRA A–D
1,3-Cyclohexadiene
Diphenylacetylene
1-Octene
2-Pentene

3.4. SPECTRA E–I
Butyl acetate
Butyramide
Isobutylamine
Lauric acid
Sodium propionate

3.5. SPECTRA J–M
Allyl phenyl ether
Benzaldehyde
o-Cresol
m-Toluic acid

3.6. SPECTRA N–R
Aniline
Azobenzene
Benzophenone oxime
Benzylamine
Dimethylamine hydrochloride

PROBLEM 3.3 SPECTRUM A

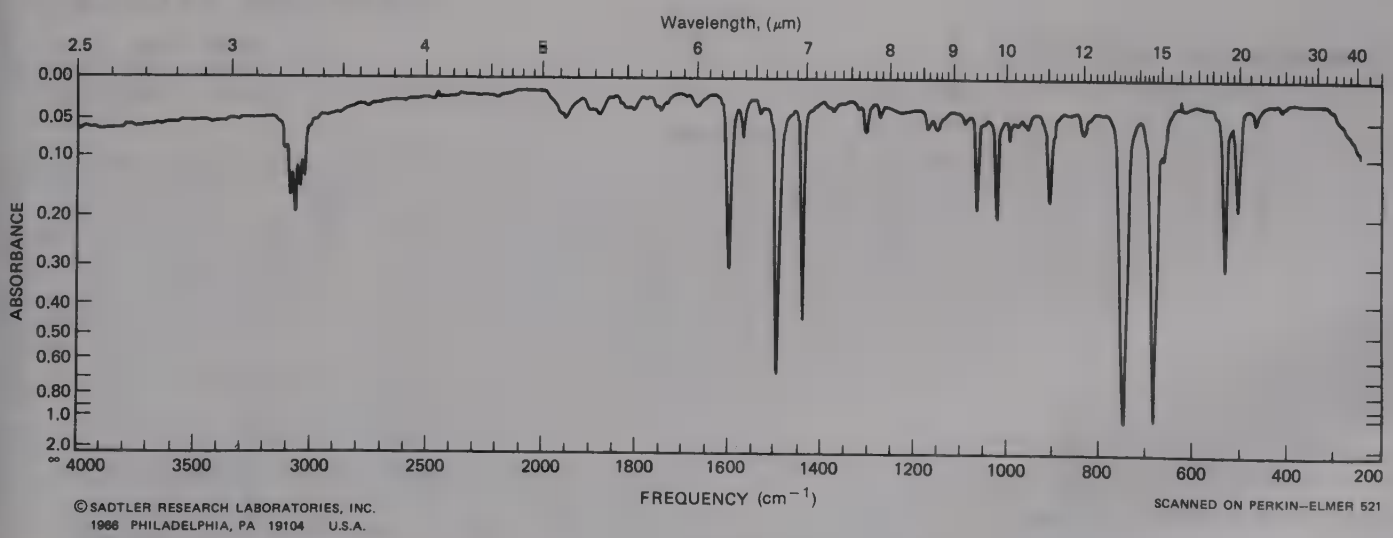

PROBLEM 3.3 SPECTRUM B

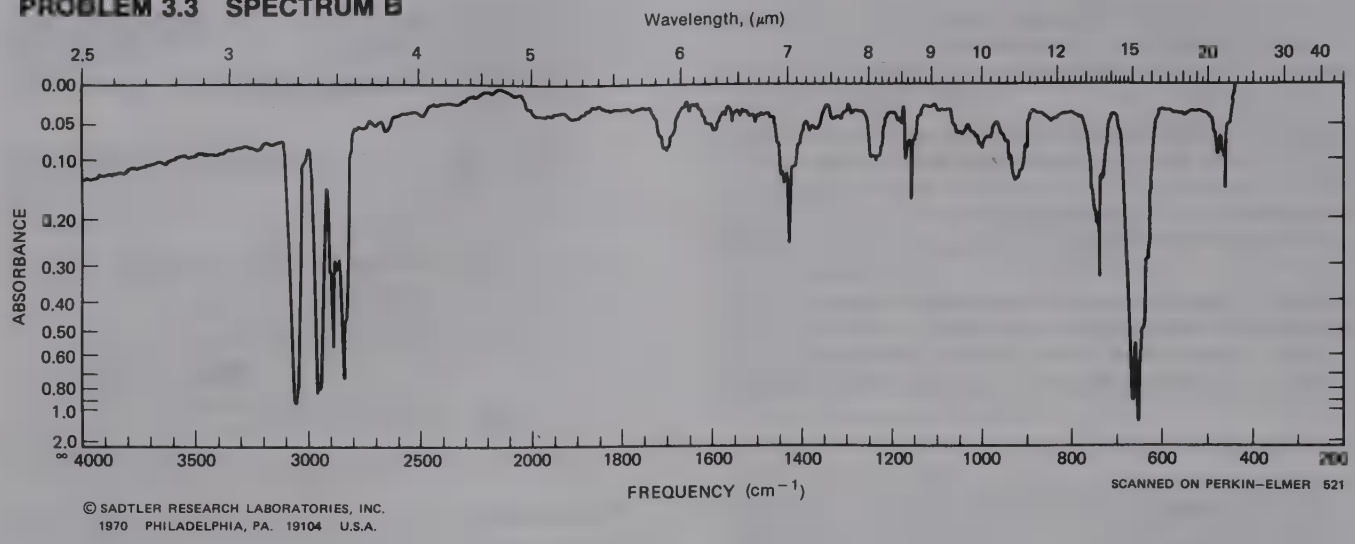

PROBLEM 3.3 SPECTRUM C

2966.4 1404.1 965.0
1657.8 1306.1 933.2
1455.5 1069.7 697.1

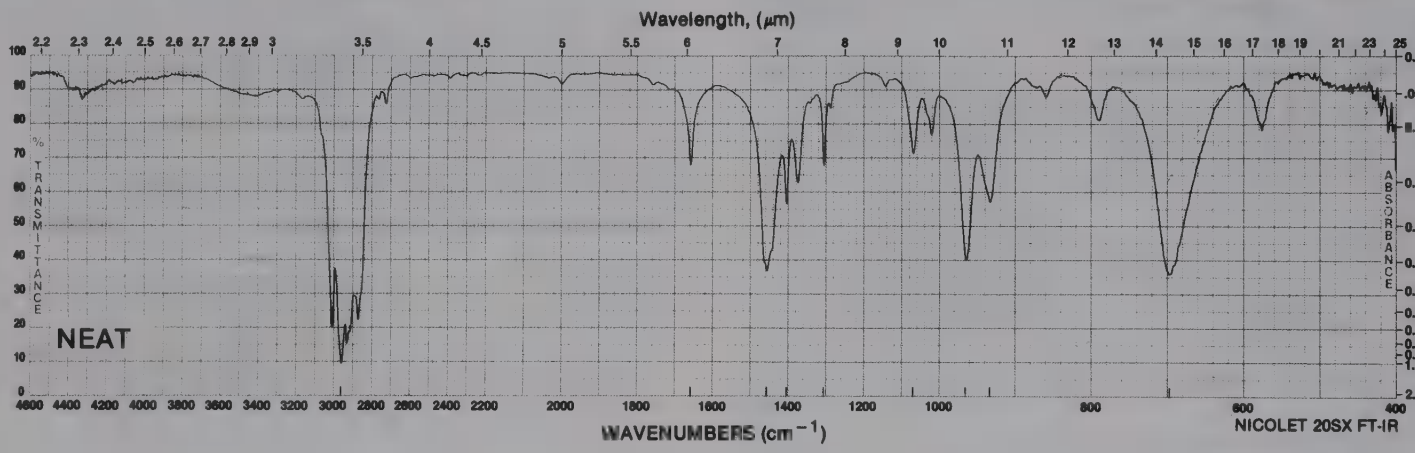

PROBLEM 3.3 SPECTRUM D

2927.1 1467.1 909.8
1822.5 1378.9 724.5
1641.7 [illegible] 634.5

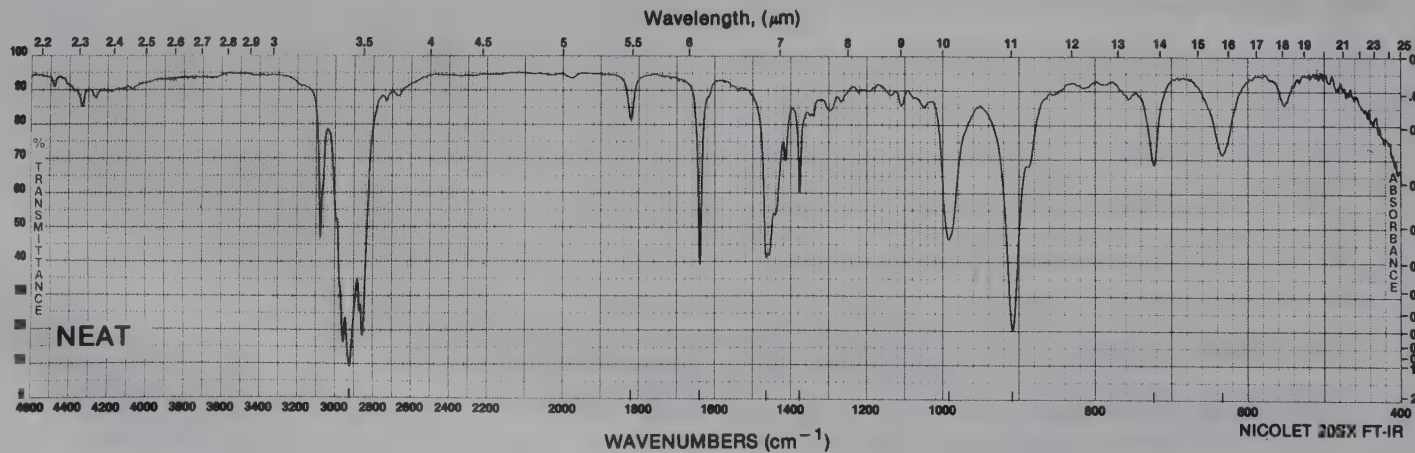

PROBLEM 3.4 SPECTRUM E

2962.1 1366.3 1031.3
1743.1 1303.6
1466.5 1243.2

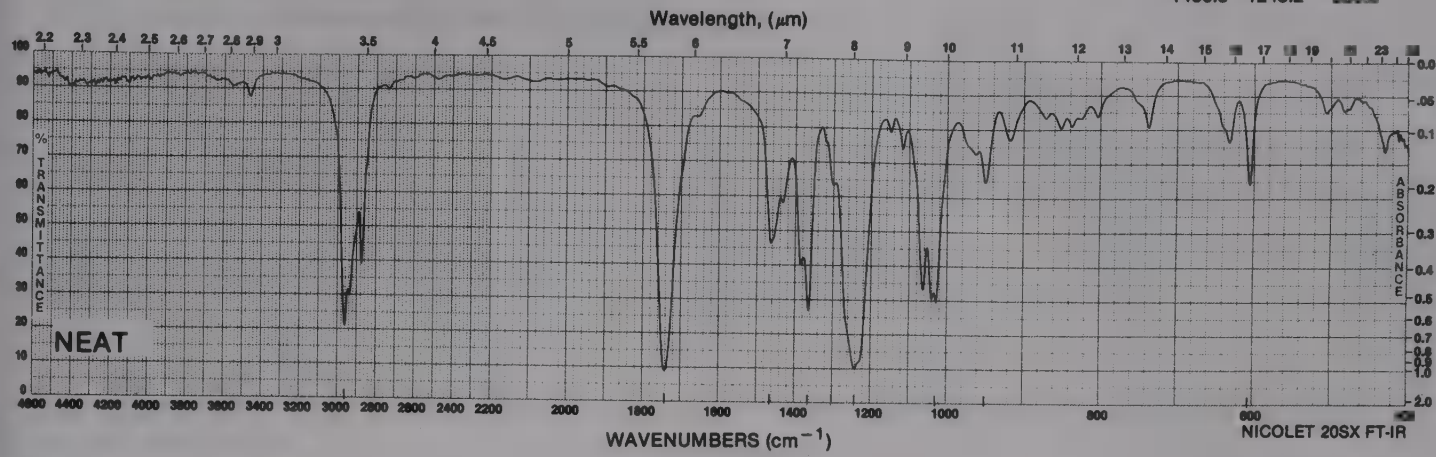

PROBLEM 3.4 SPECTRUM F

3148.2 1712.1 1285.0
2925.9 1466.3 1218.9
2870.8 1412.3

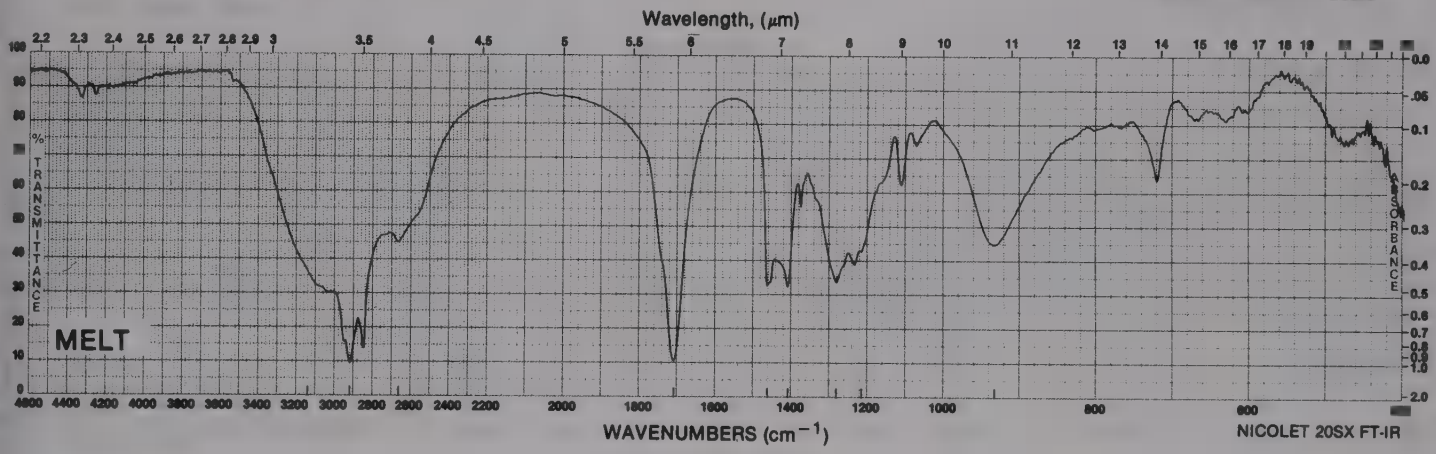

PROBLEM 3.4 SPECTRUM G

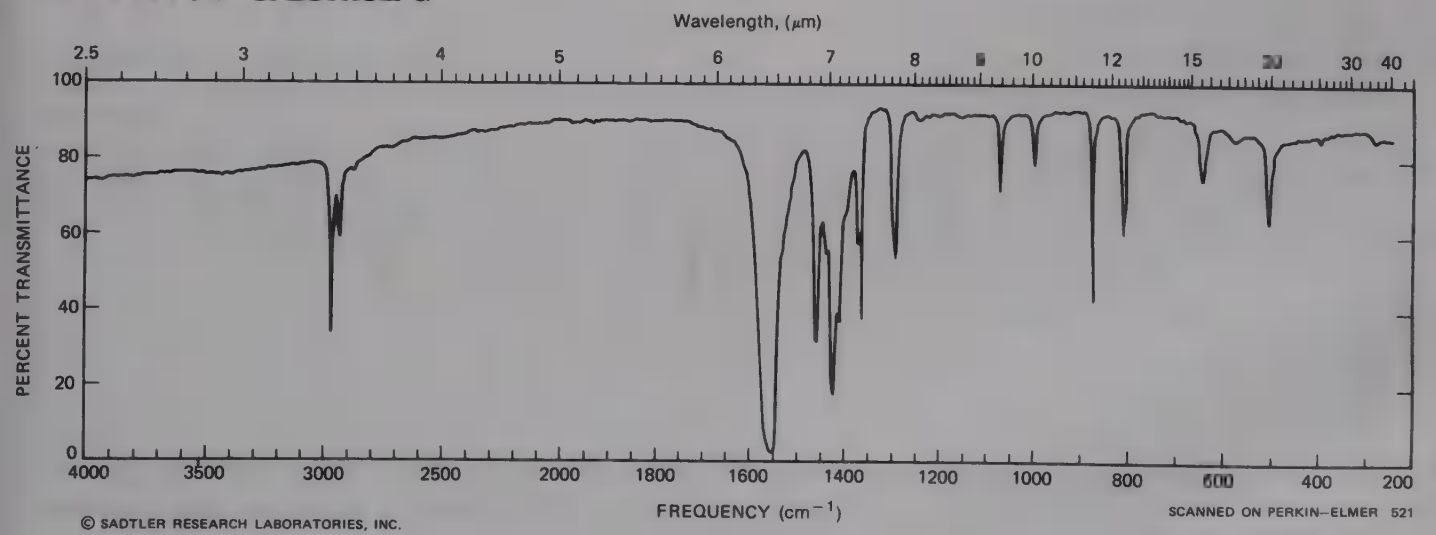

PROBLEM 3.4 SPECTRUM H

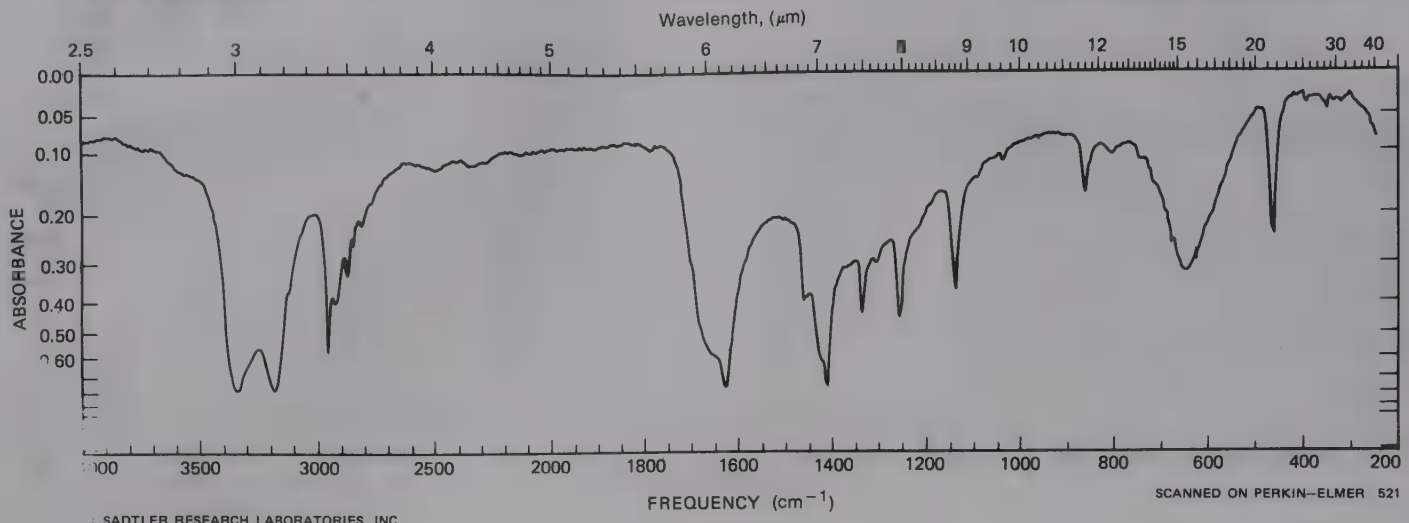

PROBLEM 3.4 SPECTRUM I

3375.8	1366.4	903.6
2955.6	1065.7	839.0
1470.0	939.6	778.0

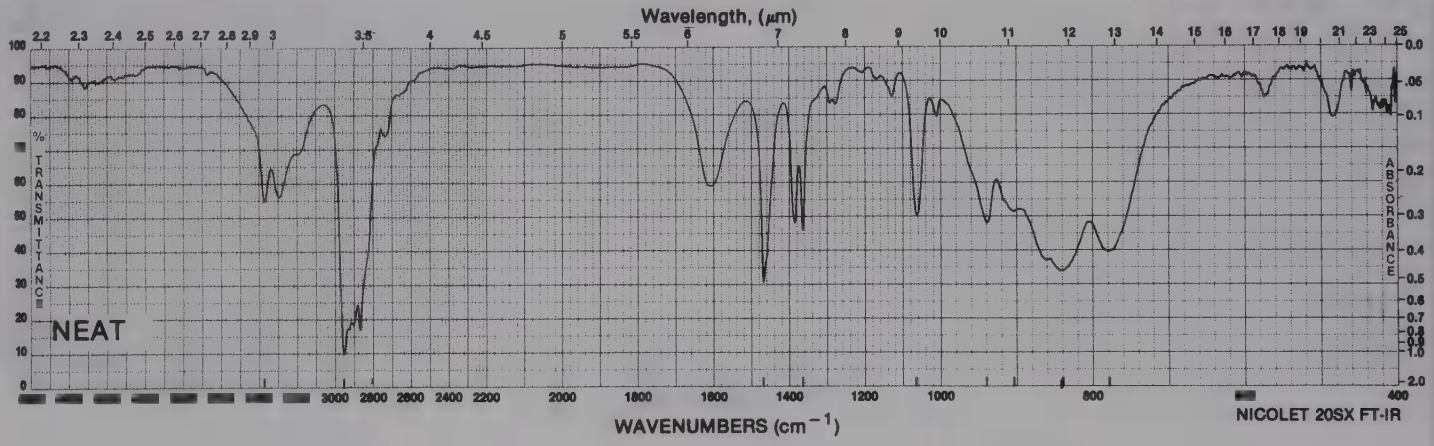

PROBLEM 3.5 SPECTRUM J

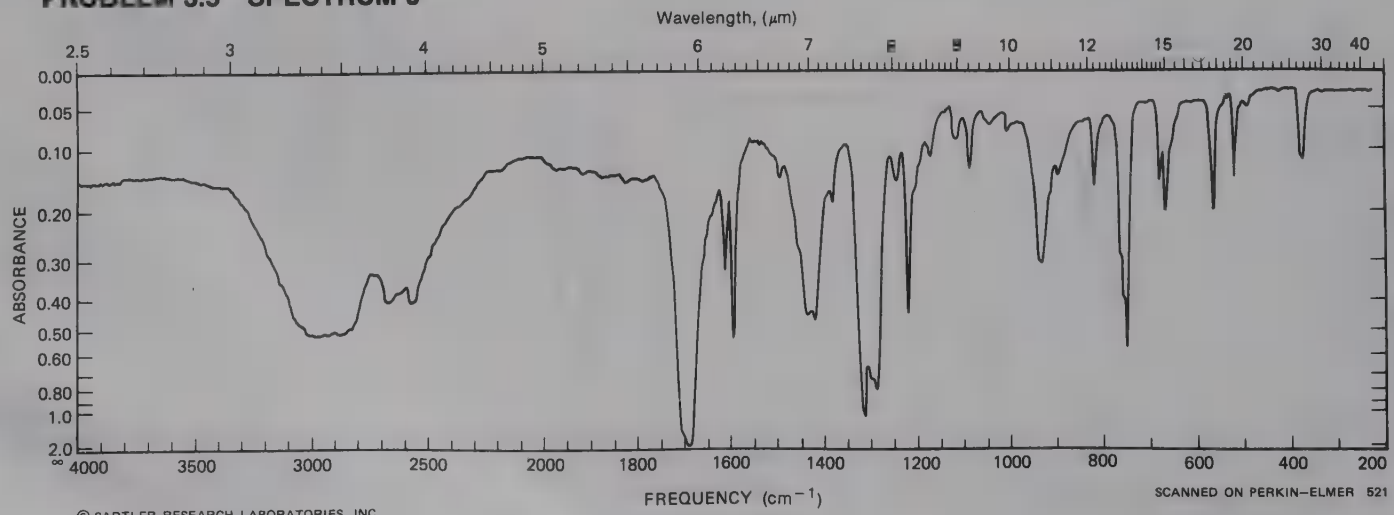

PROBLEM 3.5 SPECTRUM K

3447.7 1327.7 1106.2
1592.6 1239.7 843.1
1464.2 1170.0 751.3

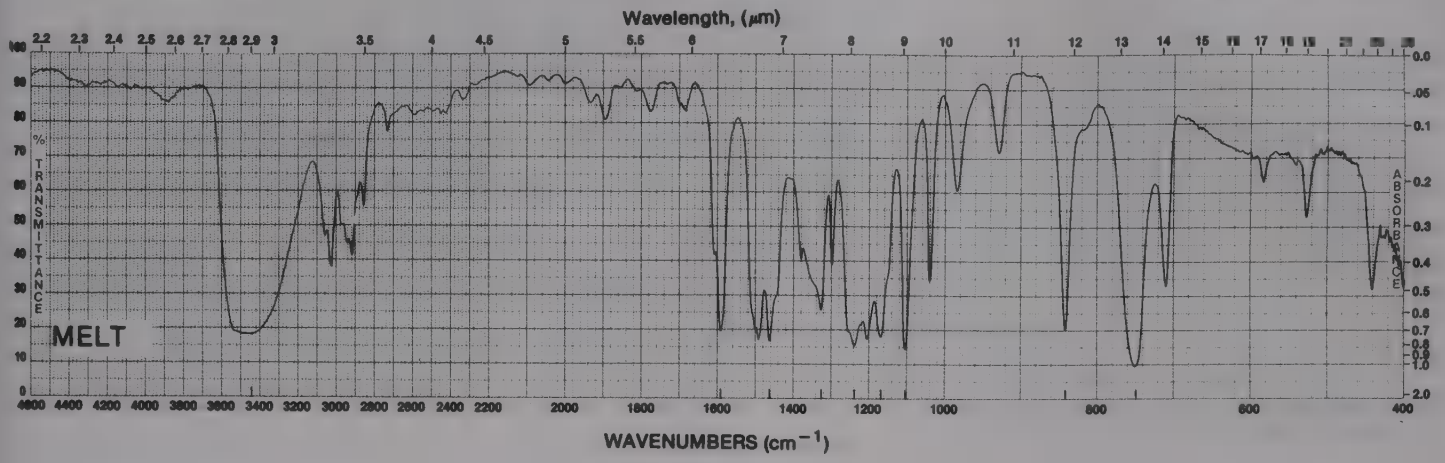

PROBLEM 3.5 SPECTRUM L

1599.2 1173.0
1495.8 1033.3 753.8
1242.5 991.7 691.3

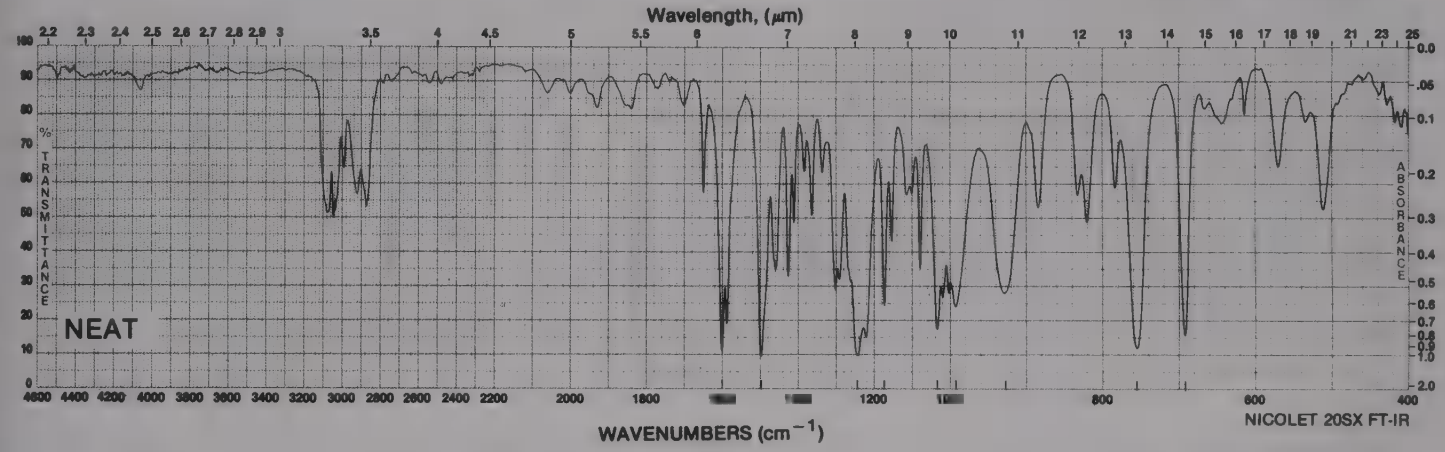

PROBLEM 3.5 SPECTRUM M

1702.5 1310.7 745.4
1596.9 1203.7 688.3
1455.7 827.9 650.0

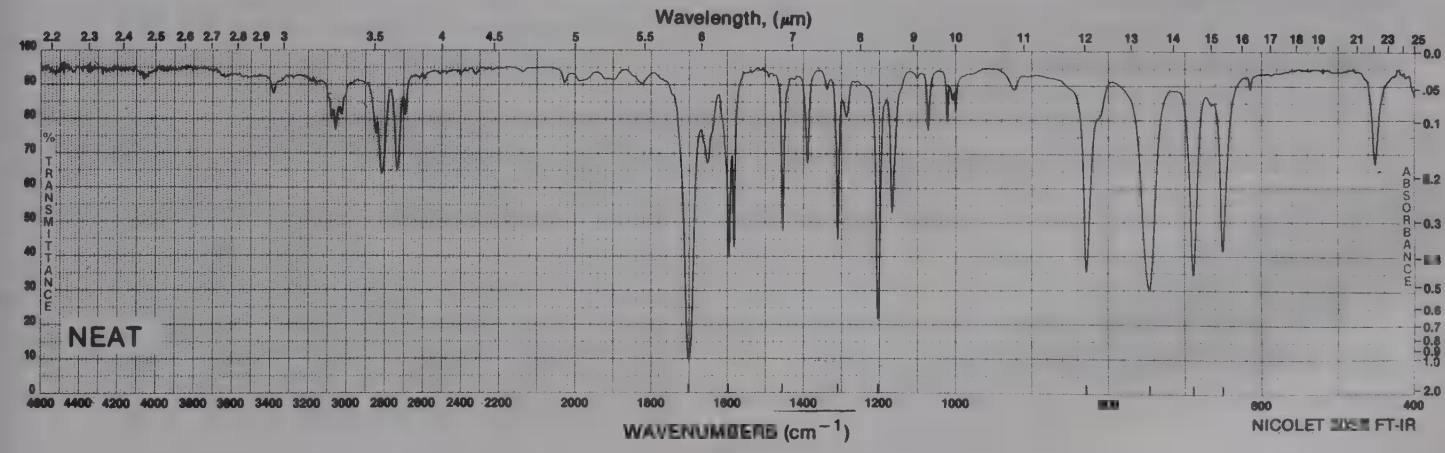

PROBLEM 3.6 SPECTRUM N

Merck 10,1131

3370.1 1452.3 779.2
3025.9 [illegible] 735.9
1604.5 [illegible] [illegible]

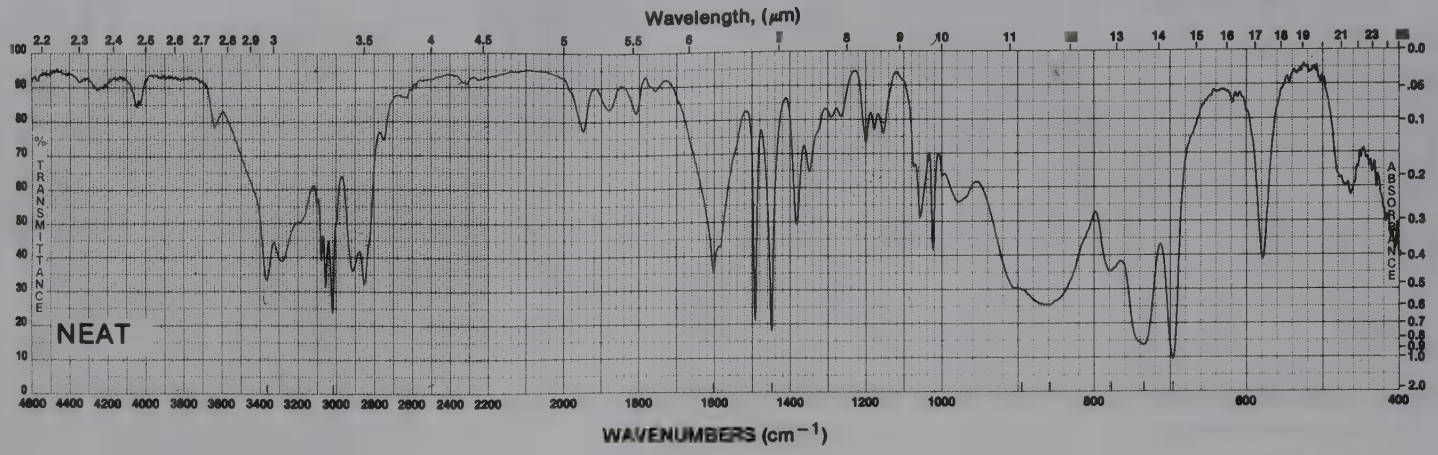

PROBLEM 3.6 SPECTRUM O

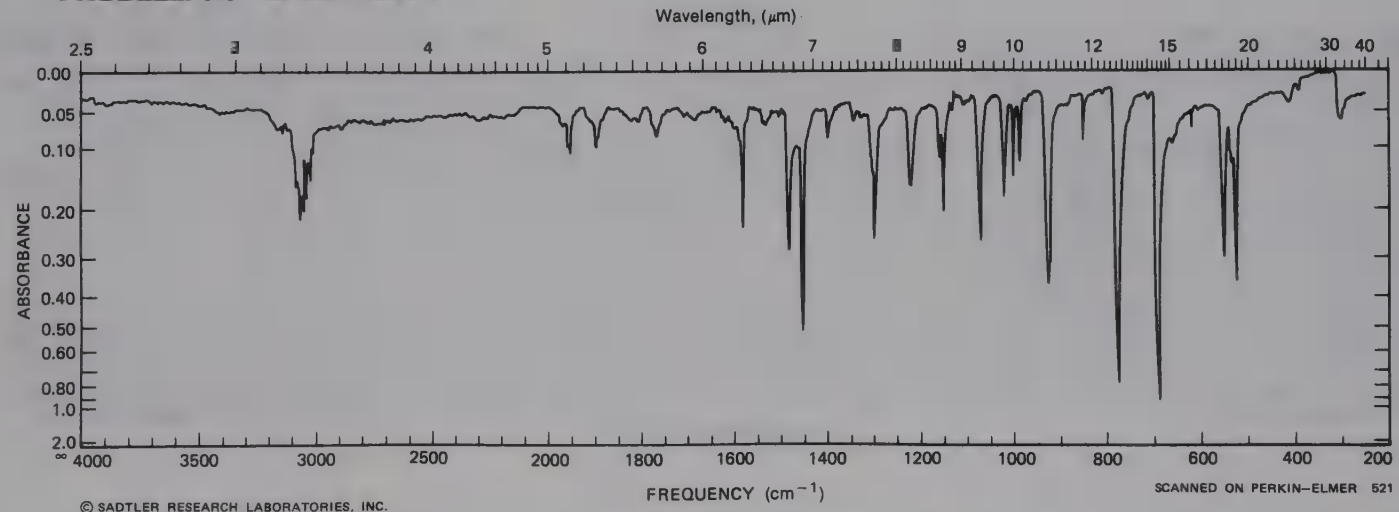

PROBLEM 3.6 SPECTRUM P

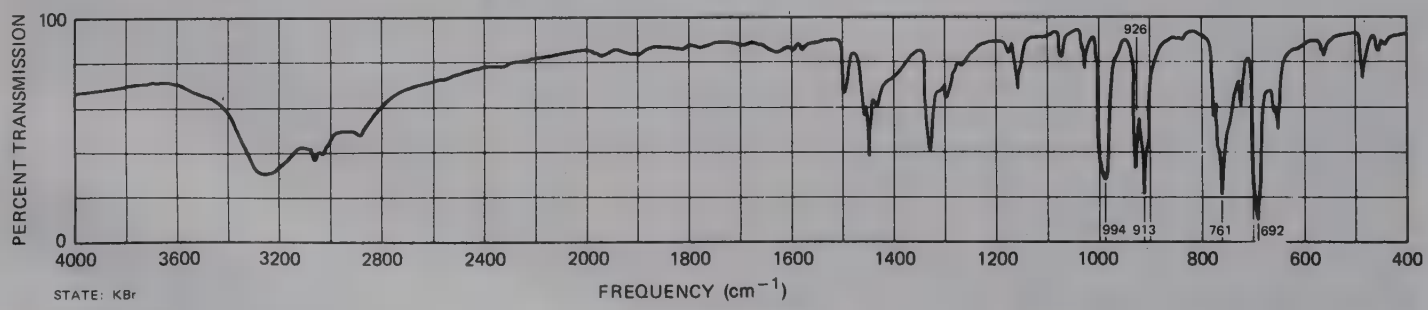

PROBLEM 3.6 SPECTRUM Q

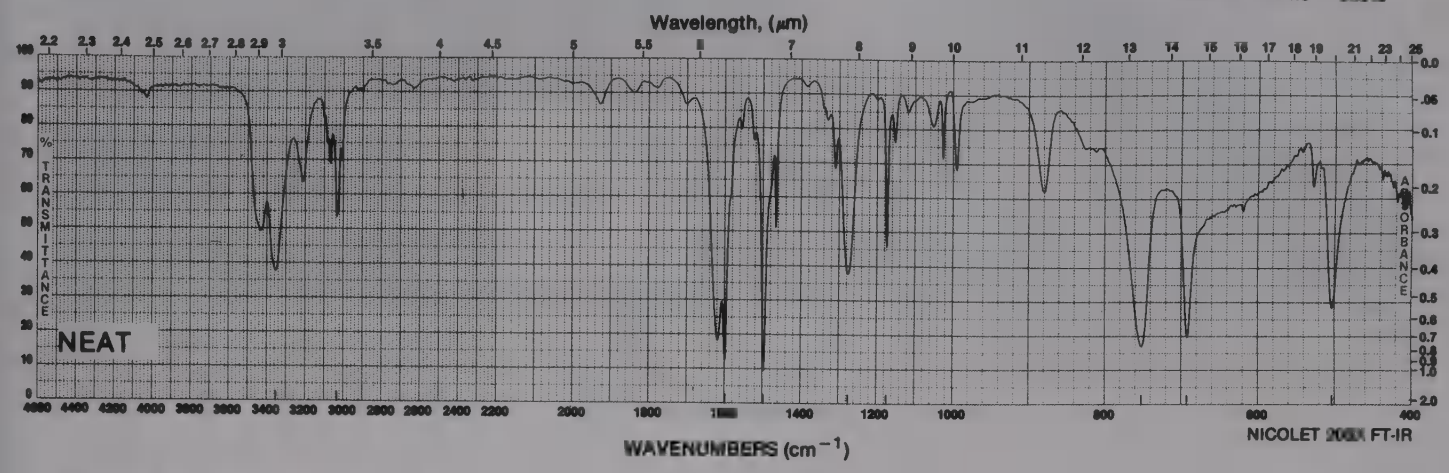

PROBLEM 3.6 SPECTRUM R

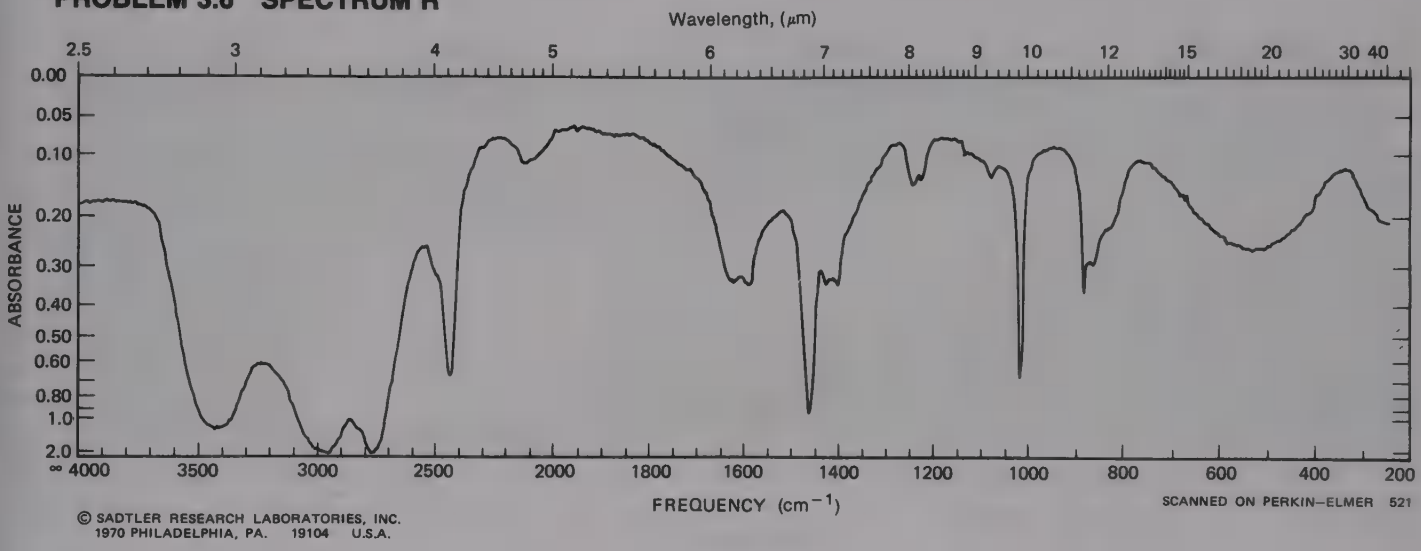

3.7 Deduce the structure of a compound(S) whose formula is C_2H_3NS from the spectrum below.

3.8 Point out evidence for enol formation (IR, p. 140) of 2,4-pentanedione. Include explanations of the two bands in the 1700–1750-cm^{-1} range, the 1650 band and the very broad band with multiple maxima running from 3400 to 2600 cm^{-1} (only the peaks at 3000–2900 are due to C—H stretching).

3.9 The IR spectrum of Compound T, of molecular formula $C_6H_{12}O$, is provided below. This compound yields a positive 2,4-dinitrophenylhydrazone test result, and when treated with iodine in aqueous NaOH gives rise to a yellow precipitate with an obnoxious odor. Deduce the structure of Compound T.

3.10 The IR spectrum of Compound U, of molecular formula $C_4H_{11}N$, is provided below. This compound when treated with benzenesulfonyl chloride mixed with aqueous NaOH gives rise to a chemical reaction that produces a homogeneous solution. Treatment of this solution with aqueous HCl yields a precipitate. Deduce the structure of Compound U.

3.11 The IR spectrum of Compound V, of molecular formula C_8H_9NO, is provided below. Partial hydrolysis of phenylacetonitrile results in Compound V. Deduce the structure of Compound V.

3.12 The IR spectrum of Compound W, of molecular formula $C_4H_{10}O$, is provided below. Treatment of Compound W with Lucas reagent (HCl, $ZnCl_2$) results in a very slow reaction. The NMR spectra show that this compound contains three kinds of carbon atoms and four kinds of hydrogen atoms. Deduce the structure of Compound W.

2934.5	1413.4	563.1
2113.1	1089.7	531.1
1517.4	647.6	458.2

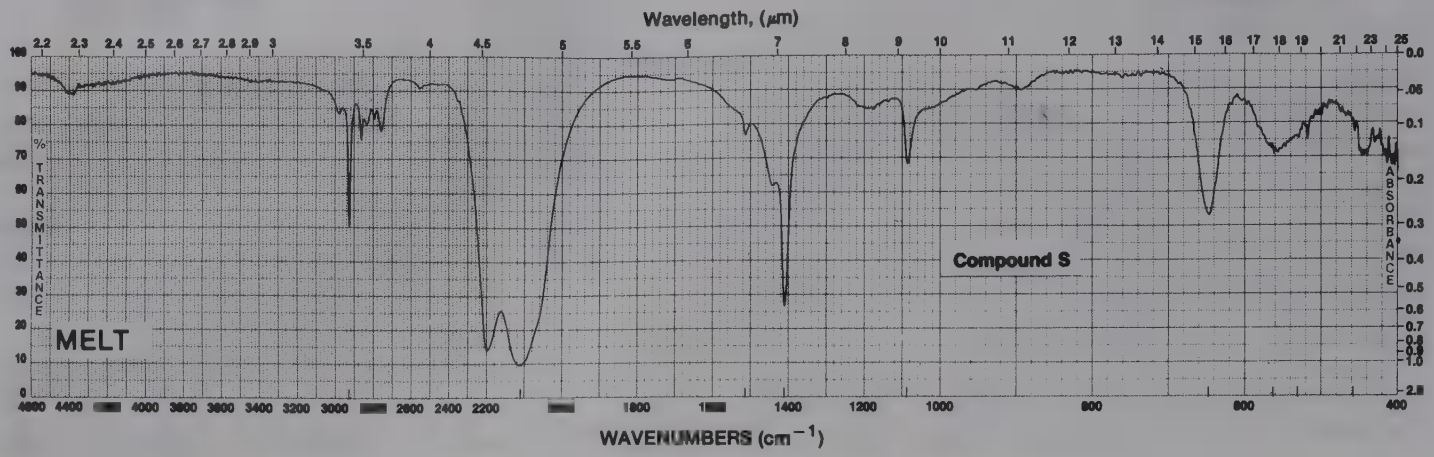

P775-4 *CAS [123-54-6]*
2,4-Pentanedione, 90 + %

FW 100.12
mp -23°C
bp 140.4°C

d 0.975
Fp 94°F
nβ 1.4510

IR III, 252C
NMR II, 1,388B
Merck 10,76

1710.0	1418.8	1249.4
1622.3	1360.9	914.7
1516.8	1304.5	780.7

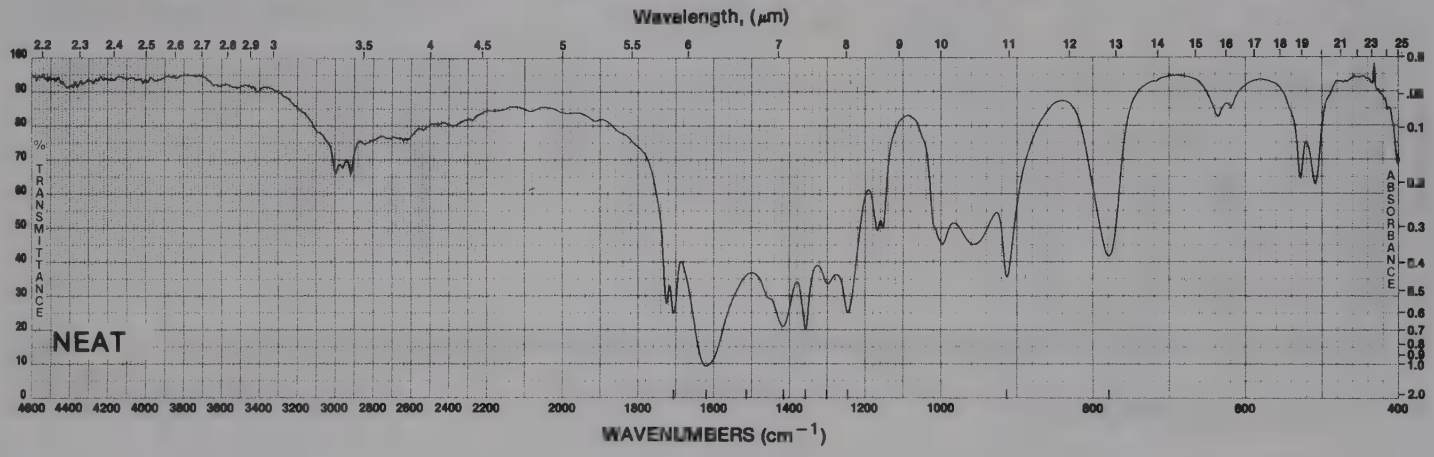

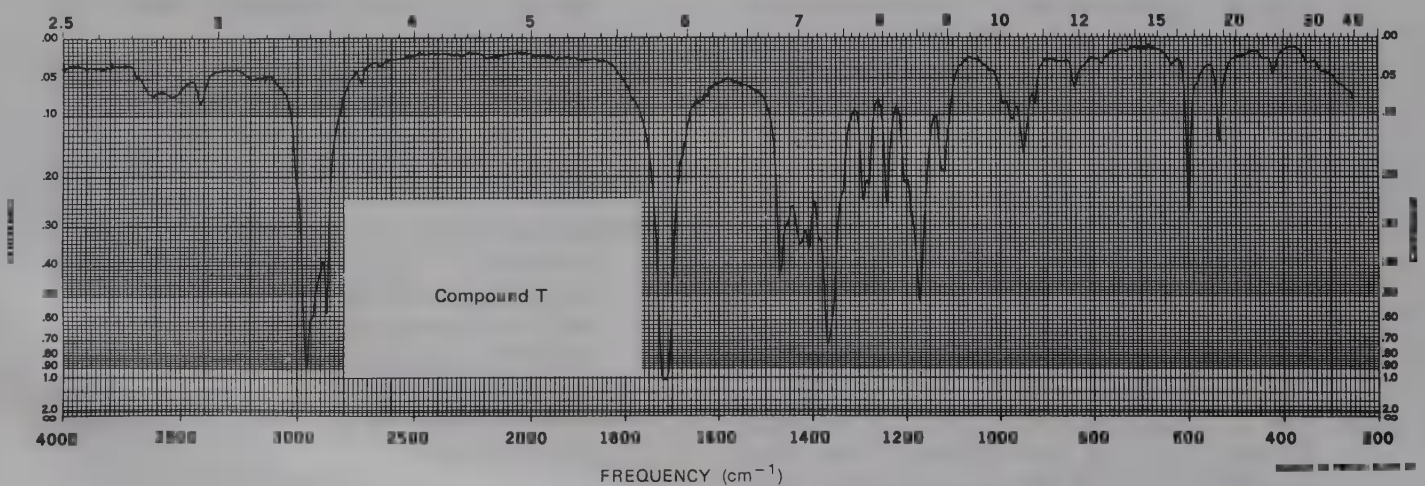

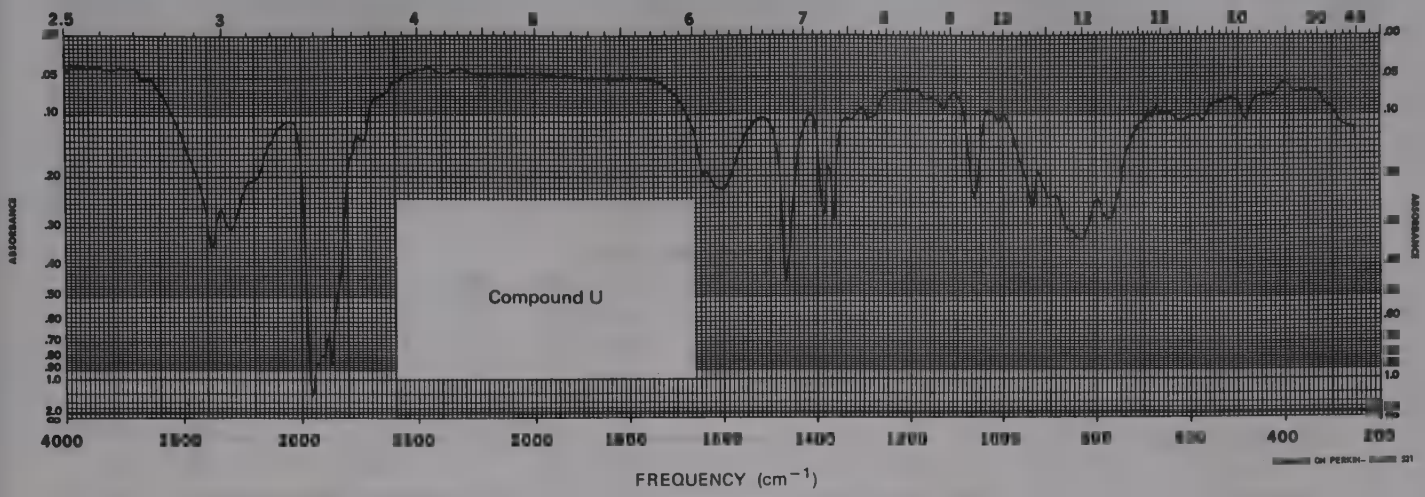
Compound U
FREQUENCY (cm^{-1})

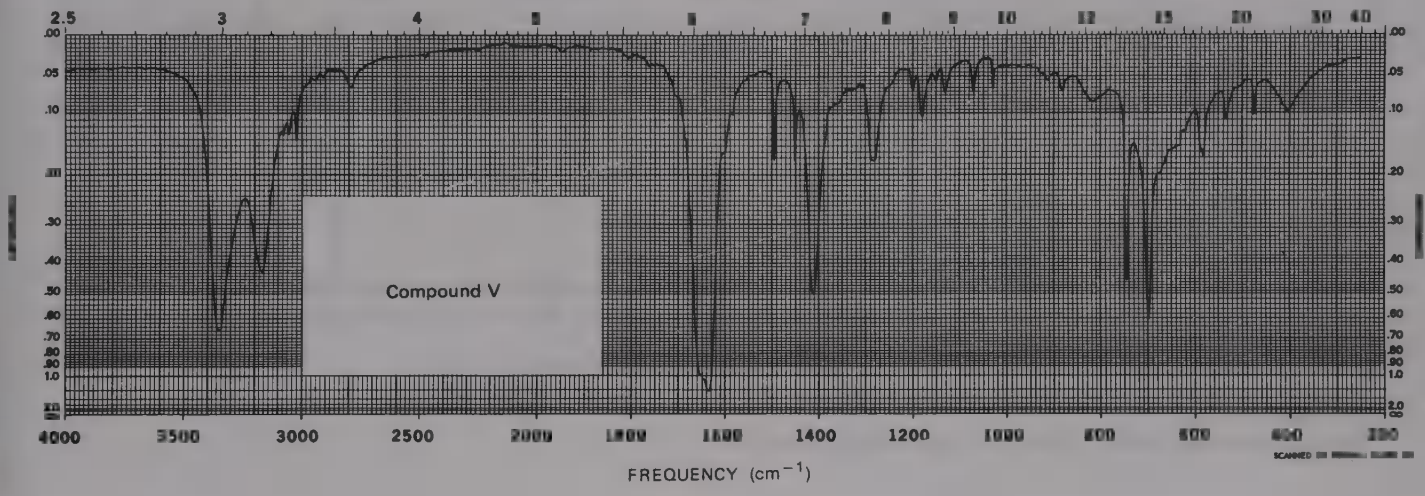
Compound V
FREQUENCY (cm^{-1})

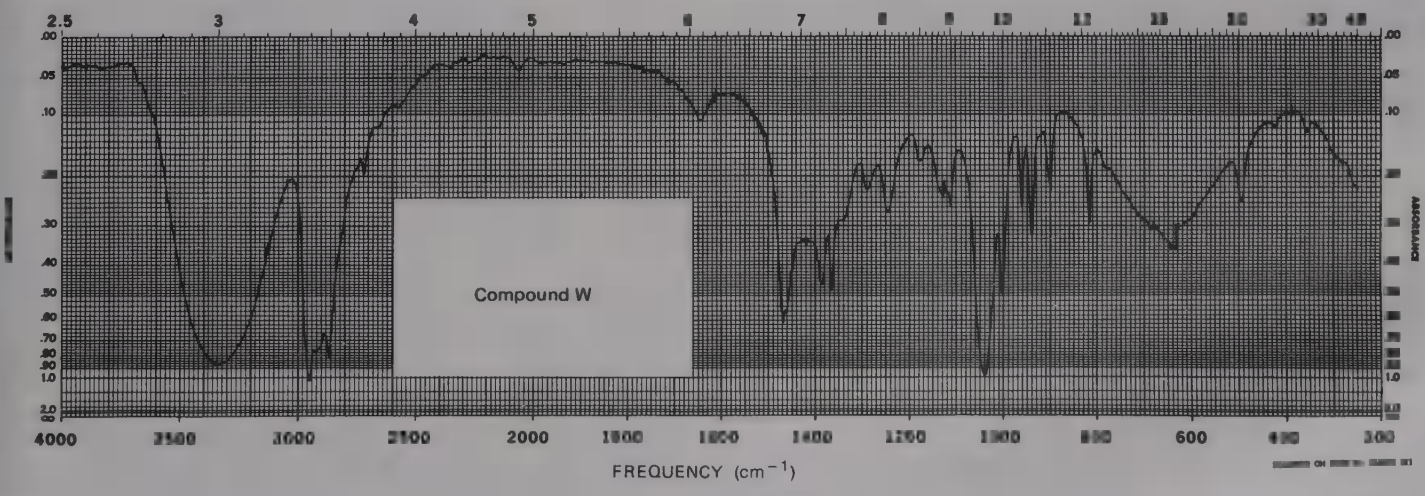
Compound W
FREQUENCY (cm^{-1})

Chart and Spectral Presentations of Organic Solvents, Mulling Oils, and Other Common Laboratory Substances

Appendix A Transparent Regions of Solvents and Mulling Oils.

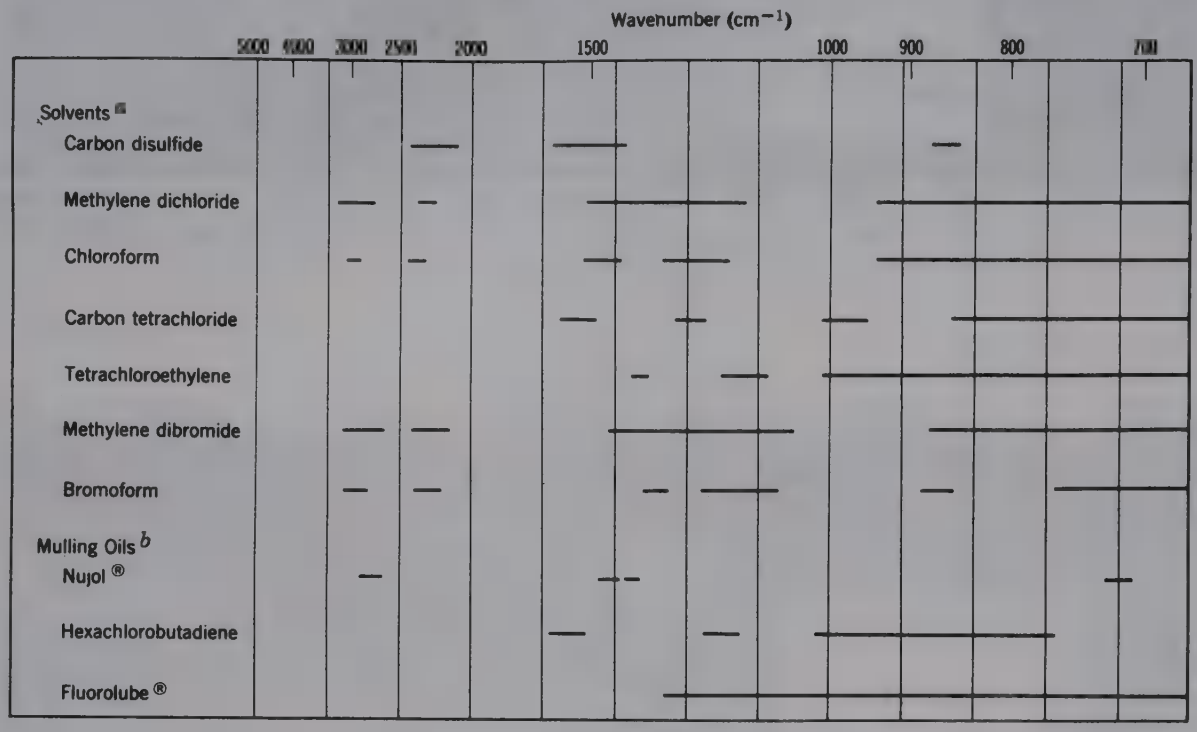

[a]The open regions are those in which the solvent transmits more than 25% of the incident light at 1 mm thickness.

[b]The open regions for mulling oils indicate transparency of thin films.

Appendix B Spectra of Common Laboratory Substances[a]

Alphabetical Listing of Spectra Shown on Succeeding Pages (pp. 144–157).

	Spectrum No. (p. no.)		Spectrum No. (p. no.)
Acetone	17 (152)	Ethyl ether	22 (154)
Benzene	4 (145)	Fluorolube®	14 (150)
2-Butanone	18 (152)	Hexane	1 (144)
Carbon disulfide	25 (156)	Indene	8 (147)
Carbon tetrachloride	10 (148)	Methanol	15 (151)
Chloroform	9 (148)	Nujol®	2 (144)
Cyclohexane	3 (145)	Petroleum ether	24 (155)
Cyclohexanone	19 (153)	Phthalic acid, diethyl ester	21 (154)
1,2-Dichloroethane	11 (149)	Polystyrene	7 (147)
N,N-Dimethylformamide (DMF)	28 (157)	Silicone lubricant	27 (157)
Dimethyl sulfoxide (DMSO)	26 (156)	Tetrachloroethylene	13 (150)
p-Dioxane	23 (155)	Toluene	5 (146)
Ethyl acetate	20 (153)	Trichloroethylene	12 (149)
Ethanol	16 (151)	*m*-Xylene	6 (146)

Source: Spectra courtesy of Sadtler Laboratories and Aldrich Chemical Co.

[a]Carbon dioxide (Sadtler Prism Spectrum No. 1924) has bands in the 3700–3550 and 2380–2222-cm^{-1} regions and at ~720 cm^{-1}.

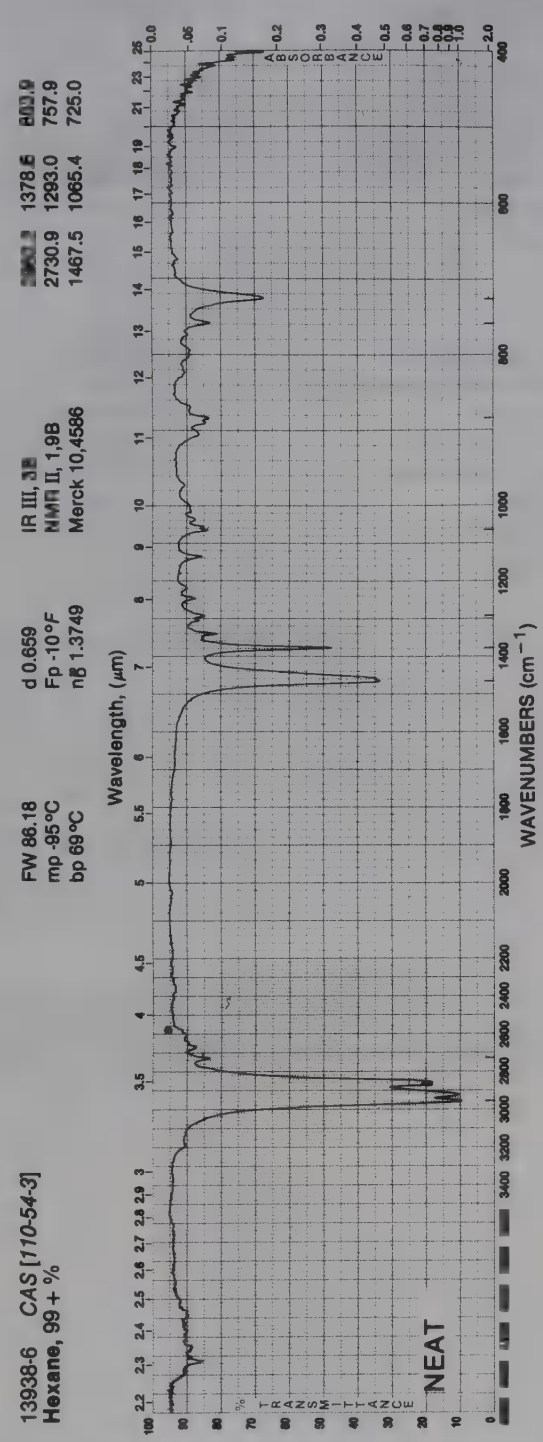

NO. 1

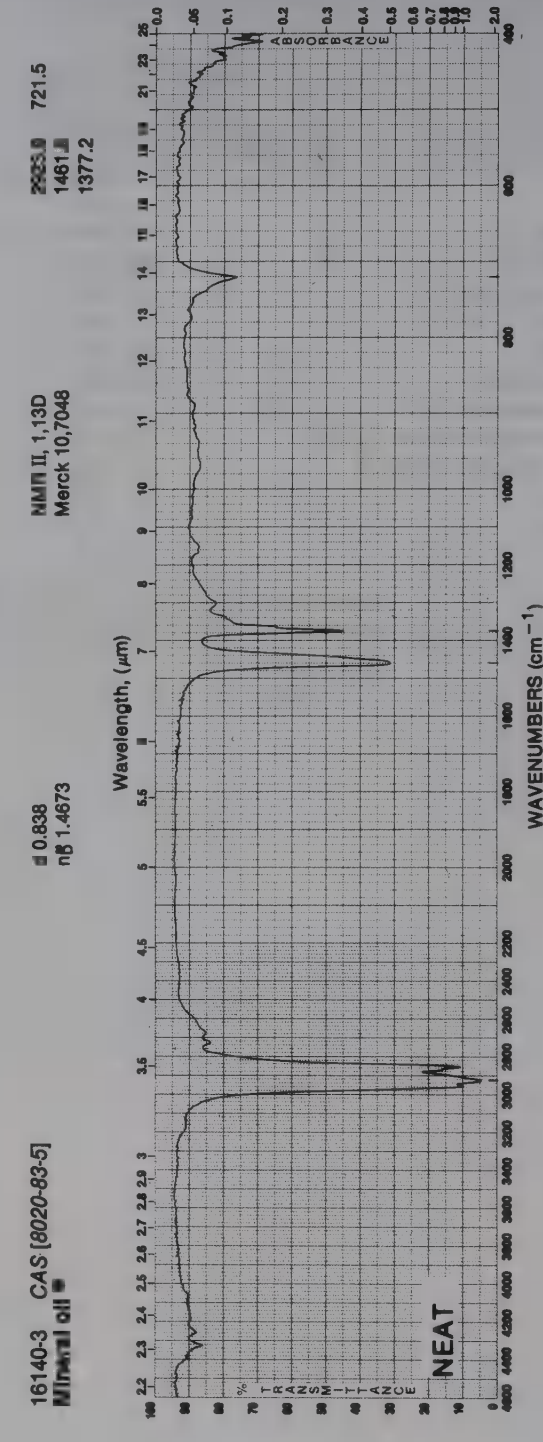

NO. 2

*Nujol® is another name for mineral oil.

NO. 3

15474-1 *CAS [110-82-7]*
Cyclohexane, [illegible] + %

FW 84.16 | d 0.779 | IR III, [illegible]
mp 6.5°C | Fp -1°F | Merck 10,2717
bp 80.7-81°C | n[illegible] 1.4260

2926.7 [illegible]
[illegible]
1449.9 [illegible]

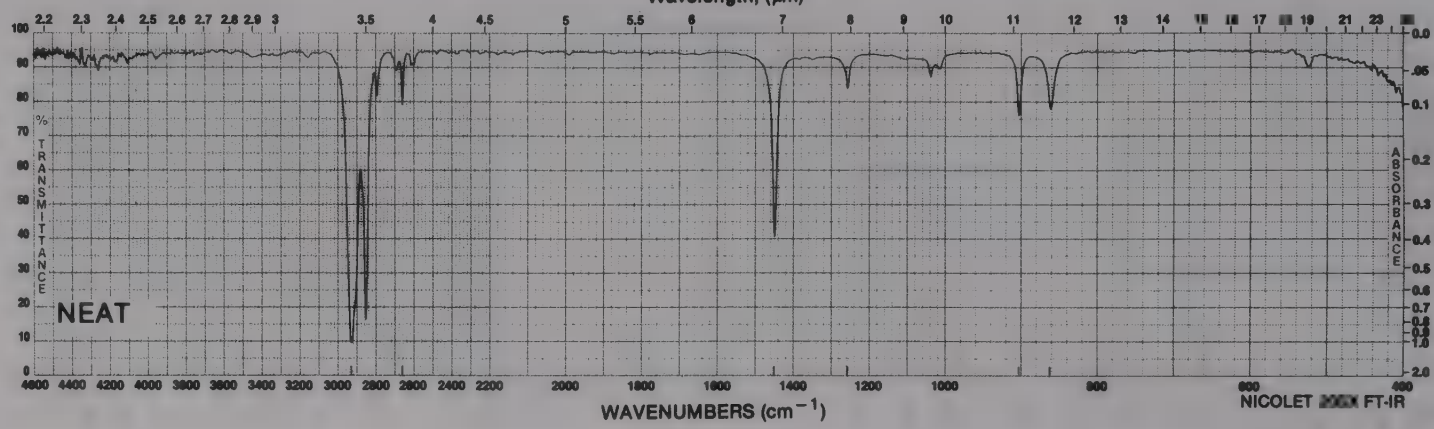

NO. 4

15462-8 *CAS [71-43-2]*
Benzene, [illegible] + %

FW 78.11 | d 0.874 | IR III, 561A
mp 5.5°C | Fp 12°F | NMR II, 1,733A
bp 80.2°C | n[illegible] 1.5010 | Merck 10,1063

[illegible] 1815.0 673.3
3035.7 1478.8
1960.4 [illegible]

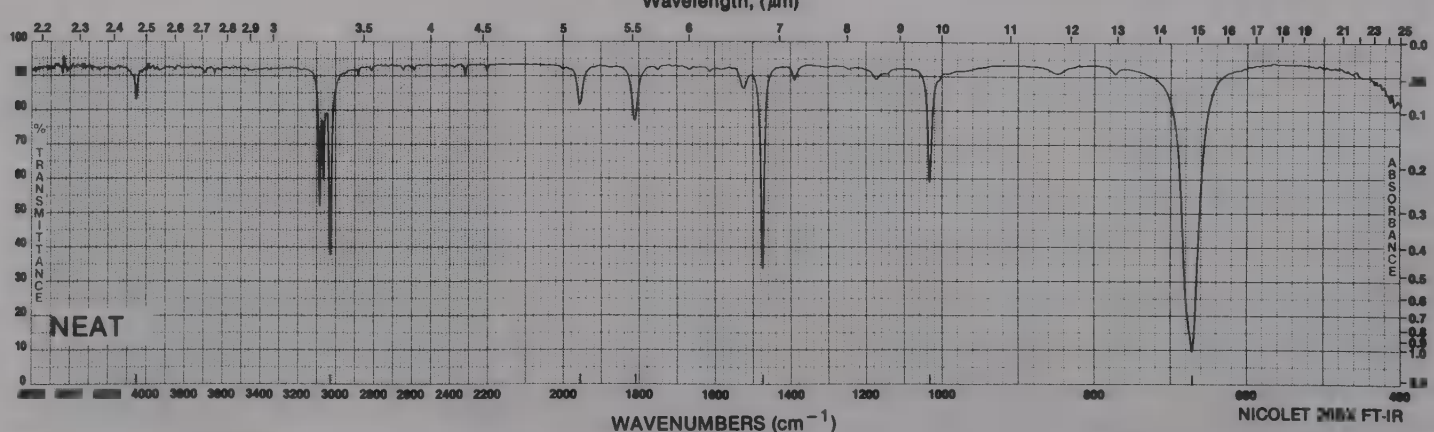

NO. 5

15500-4 *CAS [108-88-3]*
Toluene, 99 + %

FW 92.14 | d 0.867 | IR III, 561B | 3025.4 1378.6 728.4
mp -93°C | Fp 40°F | NMR II, 1,733B | 1604.3 1081.2 694.4
bp 111°C | n_D^{20} 1.4968 | Merck 10,9357 | 1495.4 1029.9 464.1

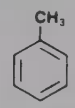

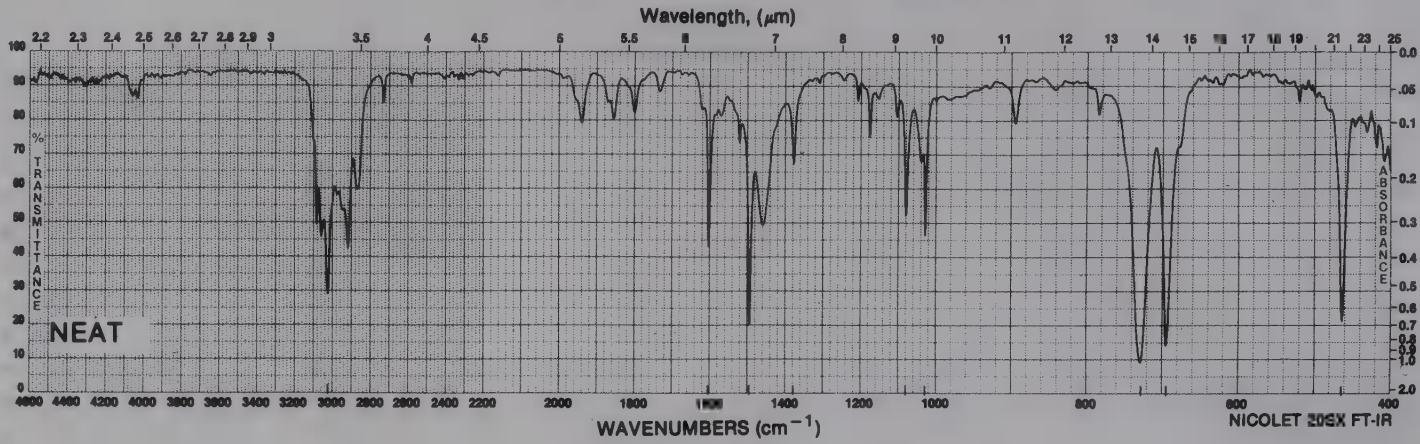

NO. 6

18556-8 *CAS [108-38-3]*
***m*-Xylene, 99%**

FW 106.17 | Fp 77°F | IR III, 565A | 2921.2 1376.3 1039.7
bp 138-139°C | n_D^{20} 1.4970 | Merck 10,9890 | 1613.9 1170.0 768.3
d 0.864 | | | 1491.8 1094.5 691.1

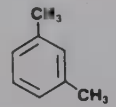

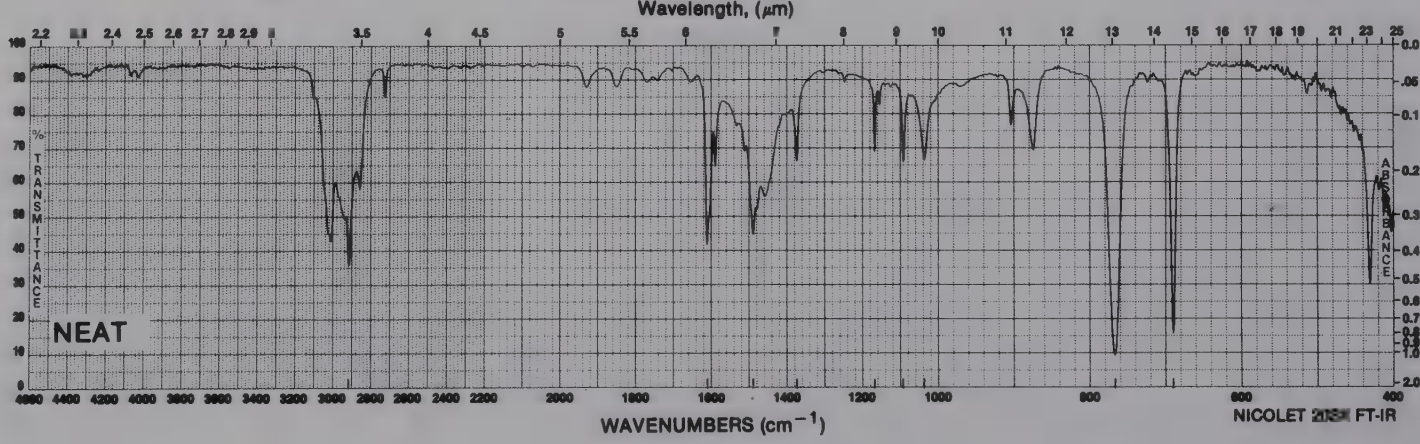

NO. 7

18243-5 *CAS [9003-53-6]*
Poly(styrene), secondary standard

IR III, 1593F
Merck 10,8732

2924.3 1218.0 698.0
1600.7 1028.1 667.8
1492.7 756.3 538.8

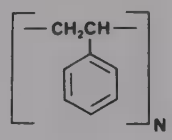

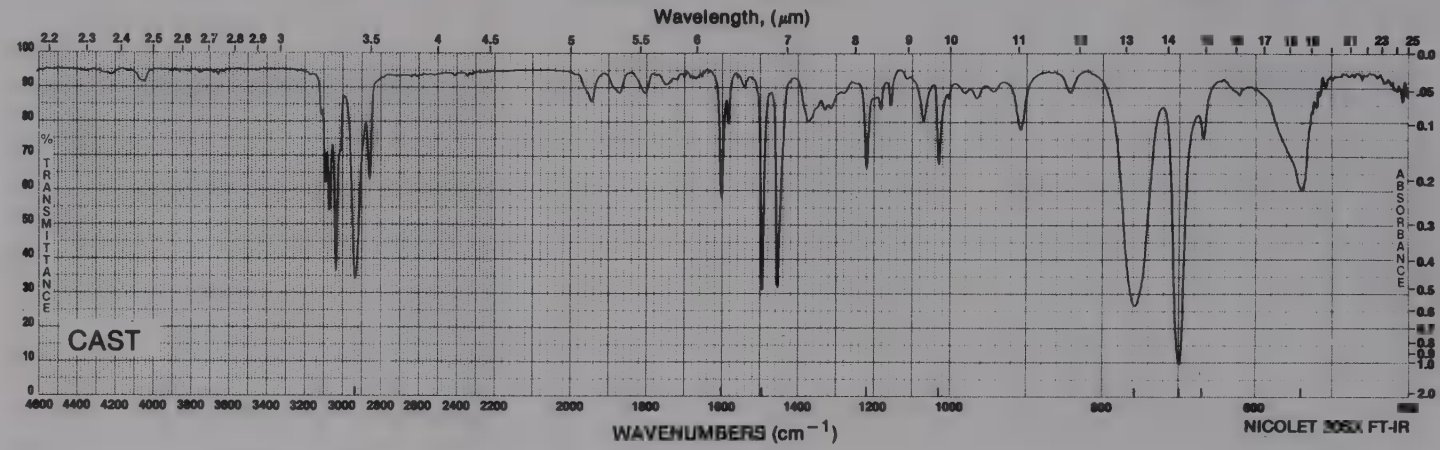

NO. 8

19352-8 *CAS [95-13-6]*
Indene, 99 + %

FW 116.16
mp -2°C
bp 181.6°C

d [illegible]
Fp 138°F
n[illegible] 1.5762

IR III, 575H
NMR II, 1,759C
Merck 10,4830

3058.7 946.9 718.0
1457.2 914.4 682.6
1393.1 765.1 550.6

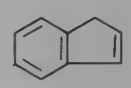

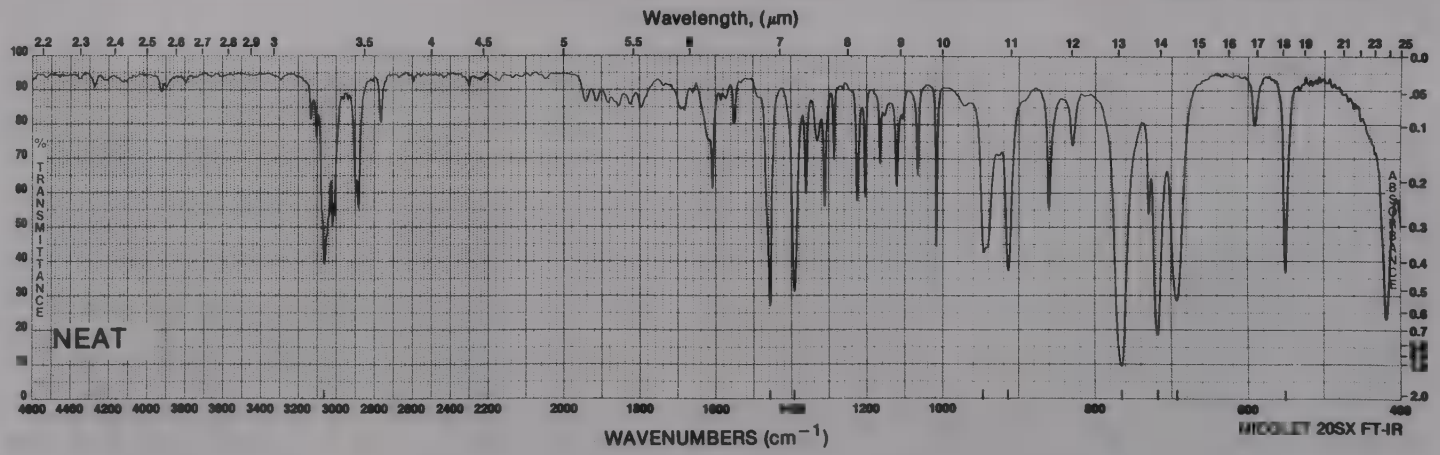

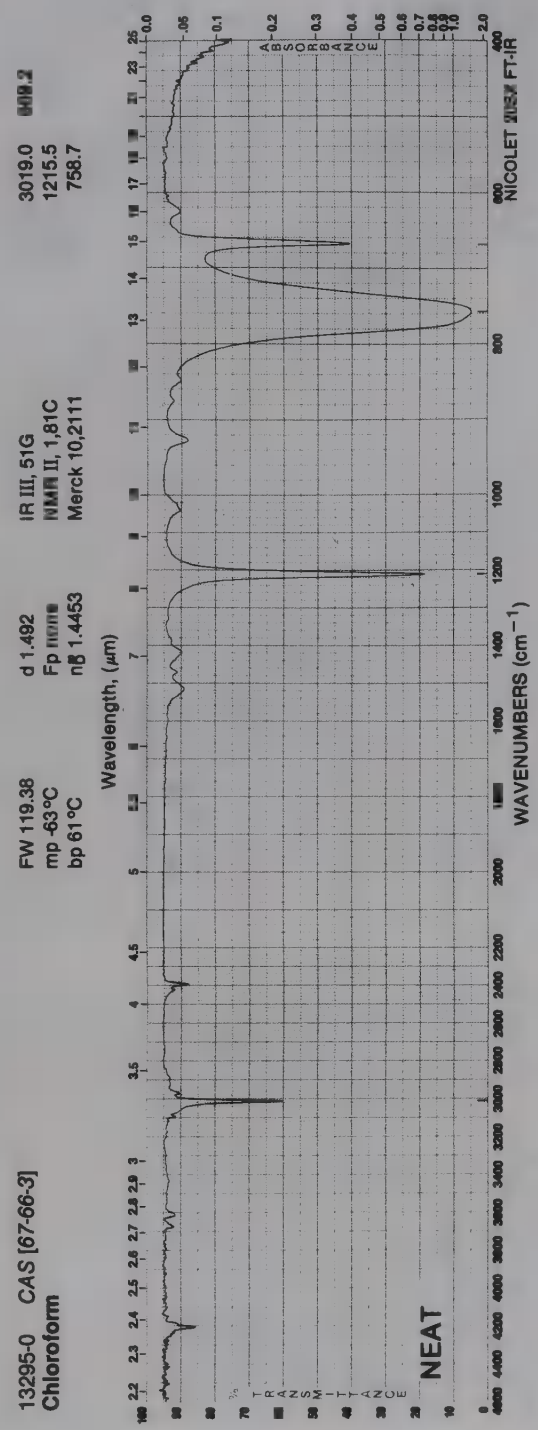
13295-0 CAS [67-66-3]
Chloroform
FW 119.38
mp -63°C
bp 61°C
d 1.492
Fp none
nD 1.4453
IR III, 51G
NMR II, 1,81C
Merck 10,2111
3019.0
1215.5
758.7
Wavelength, (μm)
WAVENUMBERS (cm⁻¹)
NICOLET 20SX FT-IR
NEAT
TRANSMITTANCE
ABSORBANCE

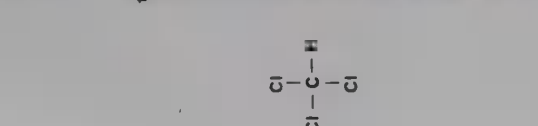

NO. 9

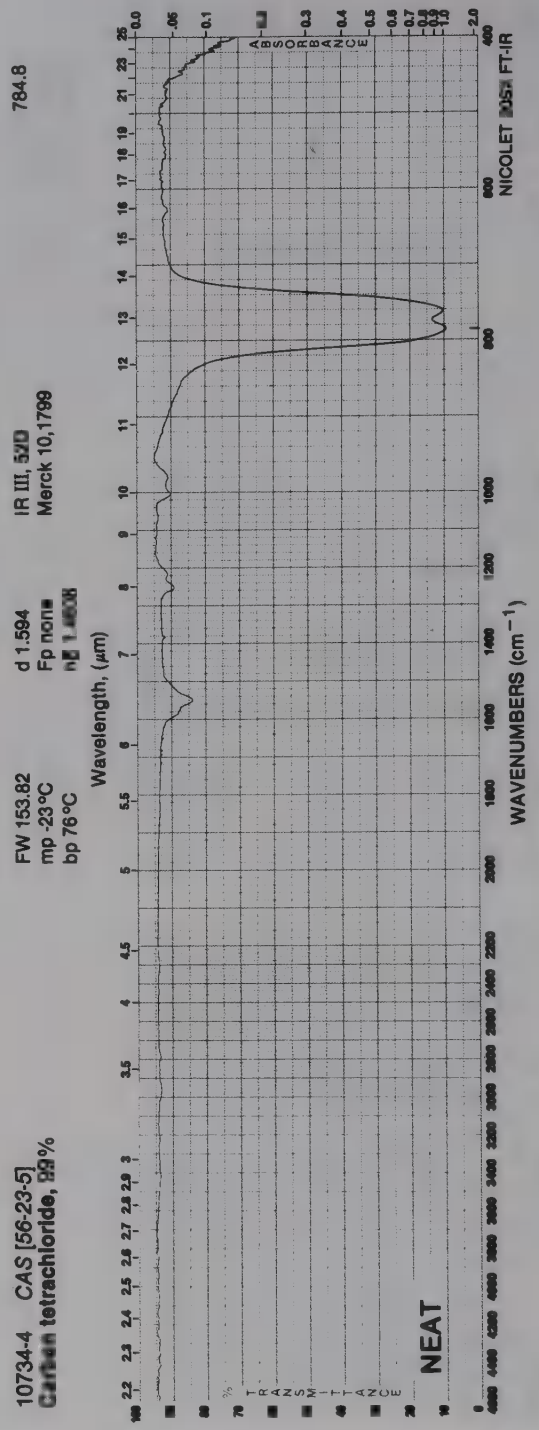
10734-4 CAS [56-23-5]
Carbon tetrachloride, 99%
FW 153.82
mp -23°C
bp 76°C
d 1.594
Fp none
IR III, 52D
Merck 10,1799
784.8
Wavelength, (μm)
WAVENUMBERS (cm⁻¹)
NICOLET 20SX FT-IR
NEAT
TRANSMITTANCE
ABSORBANCE

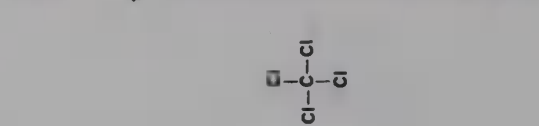

NO. 10

NO. 11

15478-4 *CAS [107-06-2]*
1,2-Dichloroethane, 99 + %

FW 98.96 | d 1.256 | IR III, 43A
mp -35°C | Fp 60°F | Merck 10,3743
bp 83°C | n_D^{20} 1.4438

2957.3 1233.2 881.5
1429.5 1031.9 710.8
1285.2 944.2 655.8

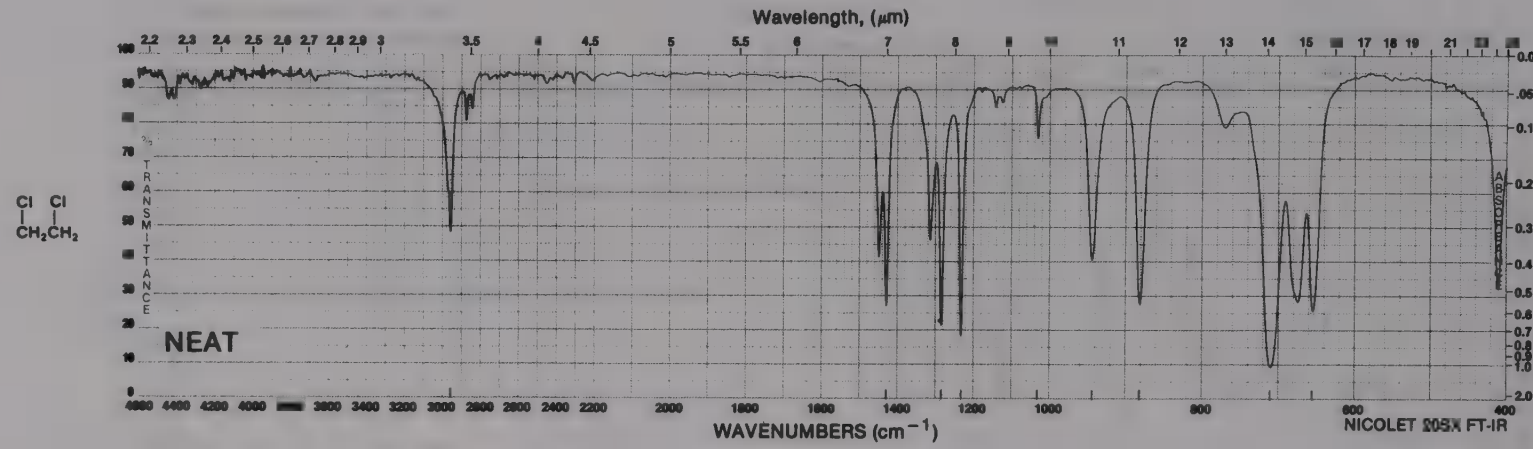

NO. 12

13312-4 *CAS [79-01-6]*
Trichloroethylene, 98%

FW 131.39 | d 1.462 | IR III, 59H
mp -87°C | Fp none | NMR II, 192D
bp 87°C | n_D^{20} 1.4760 | Merck 10,9452

3082.7 1015.3 781.5
1585.8 931.2 650.0
1247.1 841.4 453.4

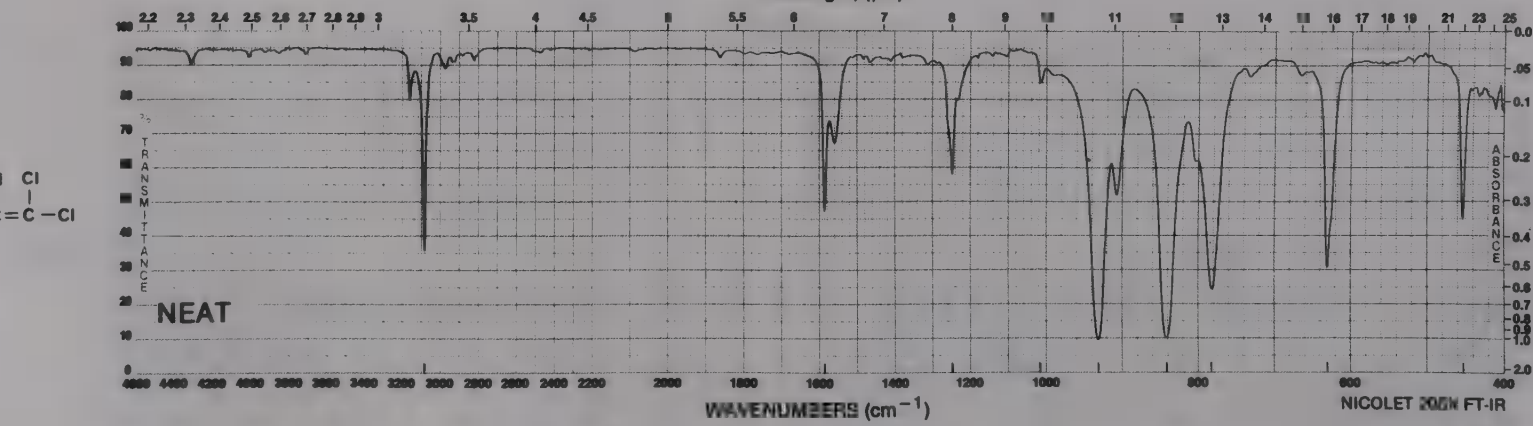

15499-7 CAS [127-18-4]
Tetrachloroethylene, 99 + %
FW 165.83
mp -22°C
bp 121°C
d 1.623
Fp none
nD 1.5058
IR III, 80A
Merck 10,9017
1123.7 777.5
979.7
908.6
Wavelength, (μm)
WAVENUMBERS (cm⁻¹)
% TRANSMITTANCE
ABSORBANCE
NEAT
NICOLET FT-IR
Cl2C=CCl2

NO. 13

FLUOROLUBE ®
Capillary Cell
Wavelength, (μm)
FREQUENCY (cm⁻¹)
ABSORBANCE
© SADTLER RESEARCH LABORATORIES, INC
PHILADELPHIA, PA., U.S.A.

NO. 14

15490-3 *CAS [67-56-1]*
Methyl alcohol, 99.9%

FW 32.04 | d 0.791 | IR III, 66A | 3342.0 | 1114.8 | 669.5
mp -98°C | Fp 52°F | NMR II, 1,101A | 2942.3 | 1033.1 | 643.3
bp 64.6°C | n_D^{20} 1.3290 | Merck 10,5816 | 1449.9 | 1017.4 | 615.9

CH_3OH

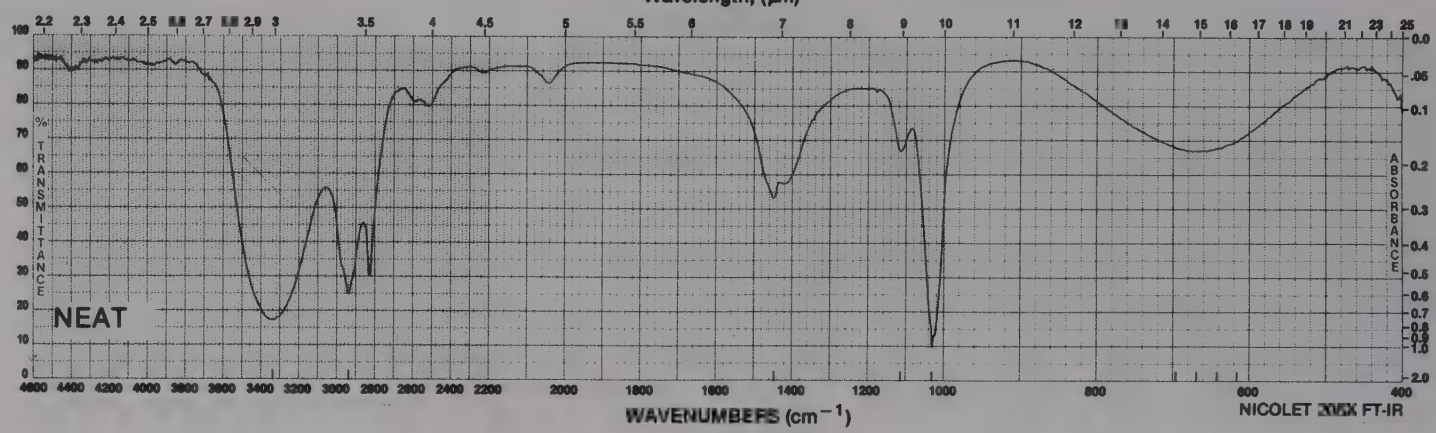

18738-0 *CAS [64-17-5]*
Ethyl alcohol, anhydrous,

FW 46.07 | n_D^{20} 1.3610 | IR III, 660 | 3331.5 | 1379.9 | 881.1
d 0.789 | | Merck 10,213 | 2974.7 | 1274.4 | 665.2
Fp 48°F | | | 1455.4 | 1050.0 | 638.0

CH_3CH_2OH

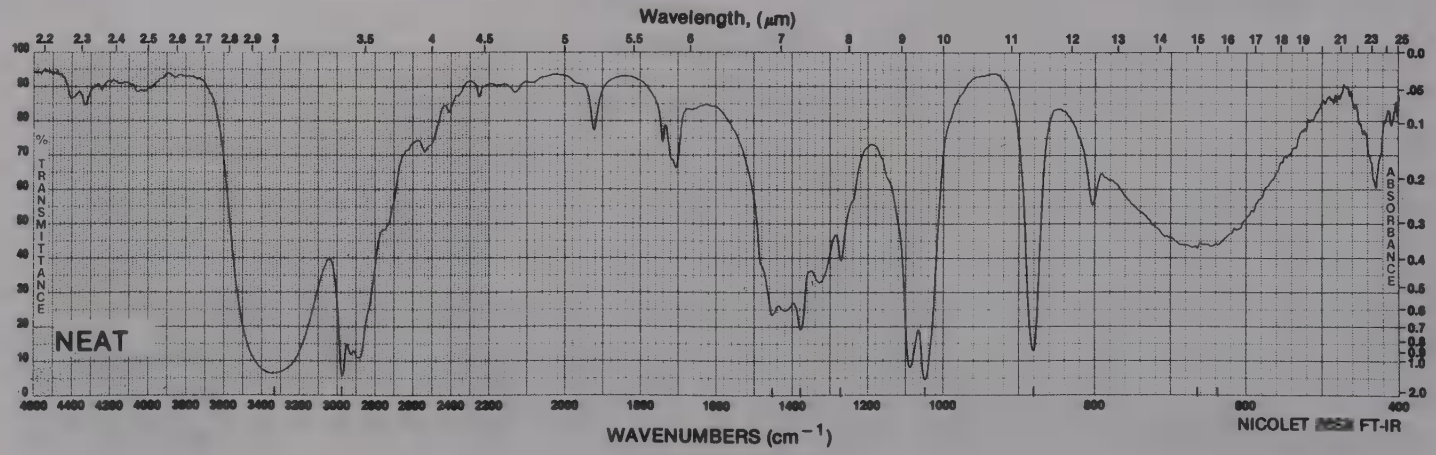

NO. 17

15459-8 *CAS [67-64-1]*
Acetone, 99 + %

FW 58.08
mp -94°C
bp 56°C

d 0.791
Fp 1°F
n_D^{20} 1.3585

IR III, 240A
NMR II, 1,369A
Merck 10,58

3004.6 1363.0 902.4
1715.1 1222.2 530.3
1421.7 1092.6

CH_3CCH_3 (O)

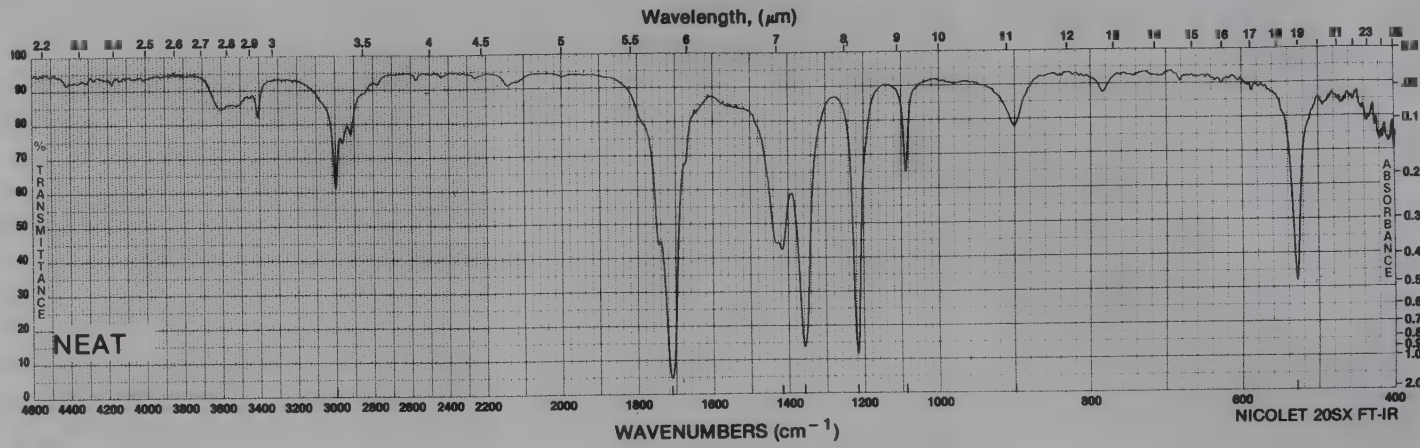

NO. 18

23029-4 *CAS [78-93-3]*
2-Butanone, 99 + %

FW 72.11
mp -87°C
bp 80°C

d 0.805
Fp 26°F
n_D^{20} 1.3788

IR III, 240B
Merck 10,5945

2979.8 1366.3 944.9
1717.5 1171.7 760.7
1417.0 1086.7 588.7

$CH_3CH_2-C(=O)-CH_3$

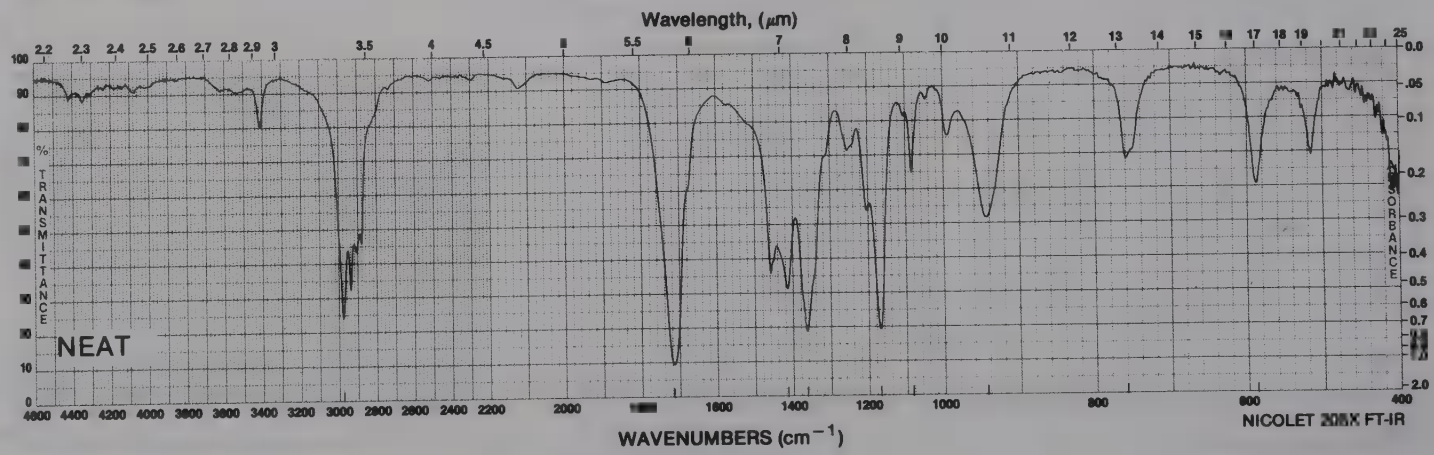

C10218-0 *CAS [108-94-1]*
Cyclohexanone, 99.8%

FW 98.15 | d 0.947 | IR III, 2589 | 2937.8 | 1311.2 | 908.4
mp -47°C | Fp 116°F | NMR II, 1,394C | 1714.0 | 1221.7 | 740.8
bp 155°C | n_D^{20} 1.4500 | Merck 10,2720 | 1449.5 | 1118.8 | 489.7

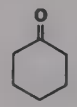

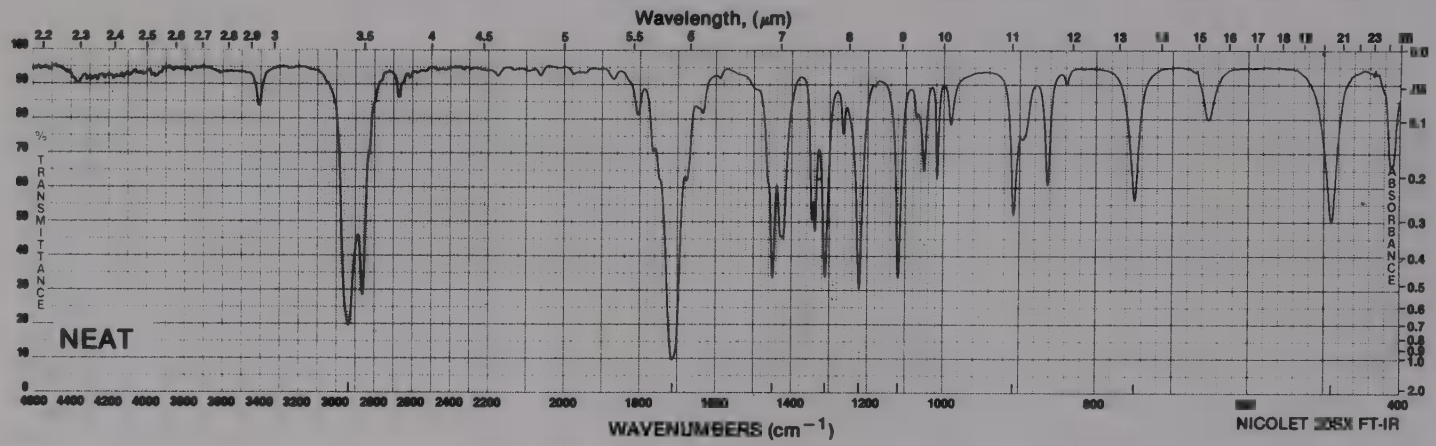

15485-7 *CAS [141-78-6]*
Ethyl acetate, 99.5 + %

FW 88.11 | d 0.902 | IR III, 359F | 2985.2 | 1373.7 | 1097.9
mp -84°C | Fp 28°F | Merck 10,3706 | 1742.3 | 1360.8 | 1047.7
bp 76.5-77.5°C | n_D^{20} 1.3720 | | 1447.6 | 1240.9 | 907.0

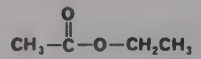

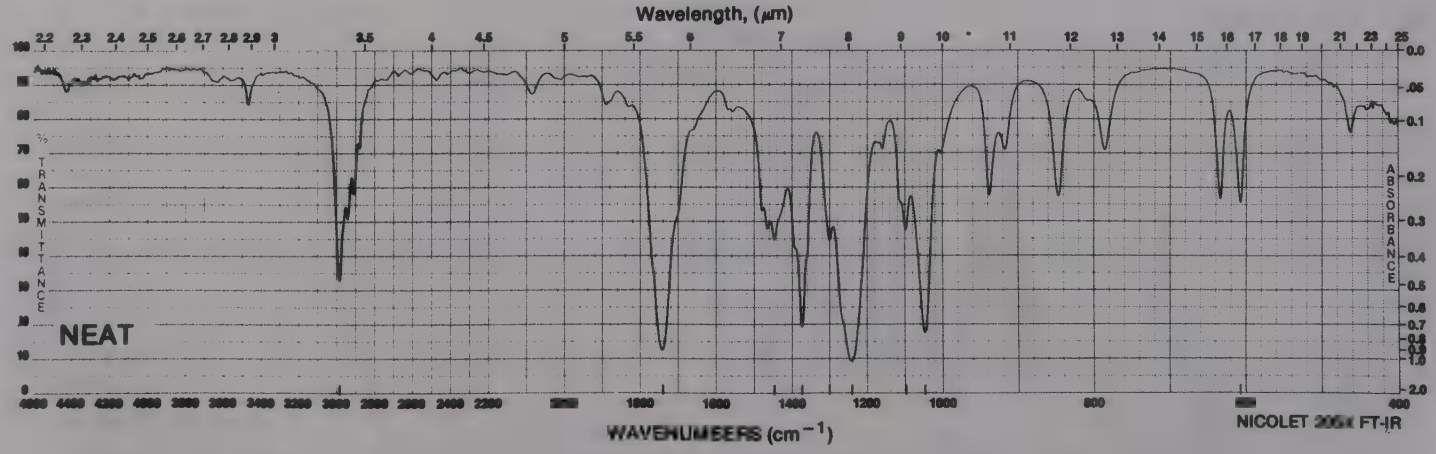

NO. 21

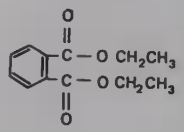

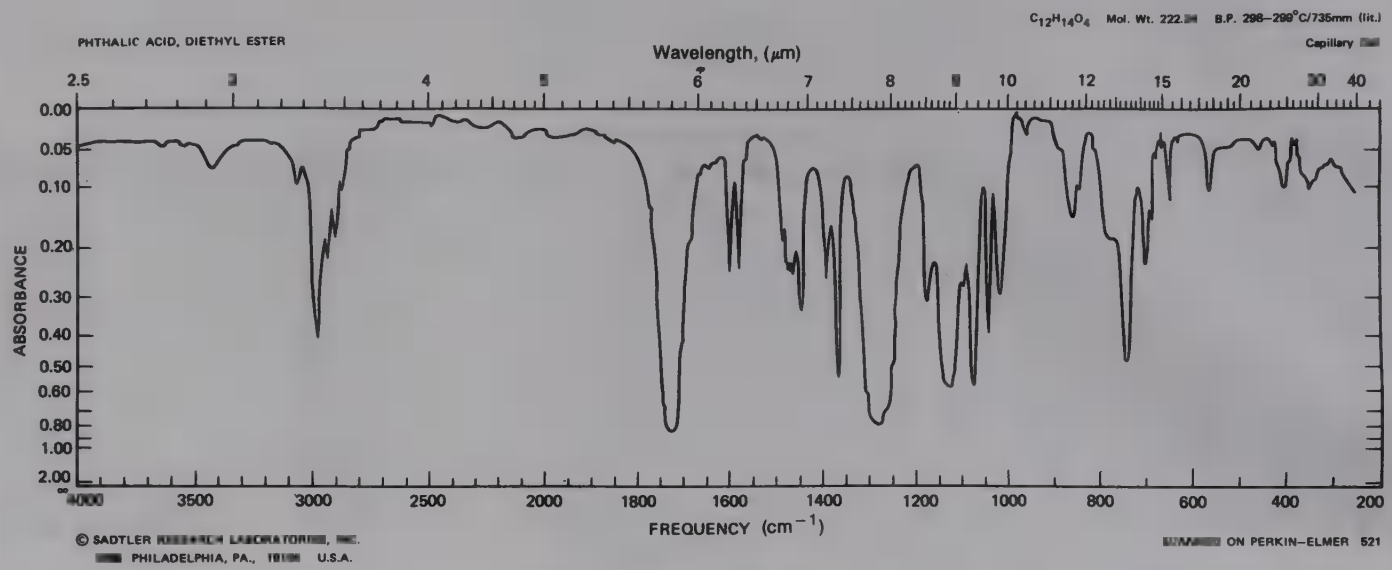

NO. 22

17926-4 *CAS [60-29-7]*
Ether, A.C.S. reagent, absolute

FW 74.12	d 0.706	IR III, 124A	2977.2	1382.5	1123.2
mp -116°C	Fp -40°F	NMR II, 1,173A	2776.1	1297.3	1043.8
bp 34.6°C	n 1.3506	Merck 10,3751	1444.2	1181.3	845.6

$CH_3CH_2—O—CH_2CH_3$

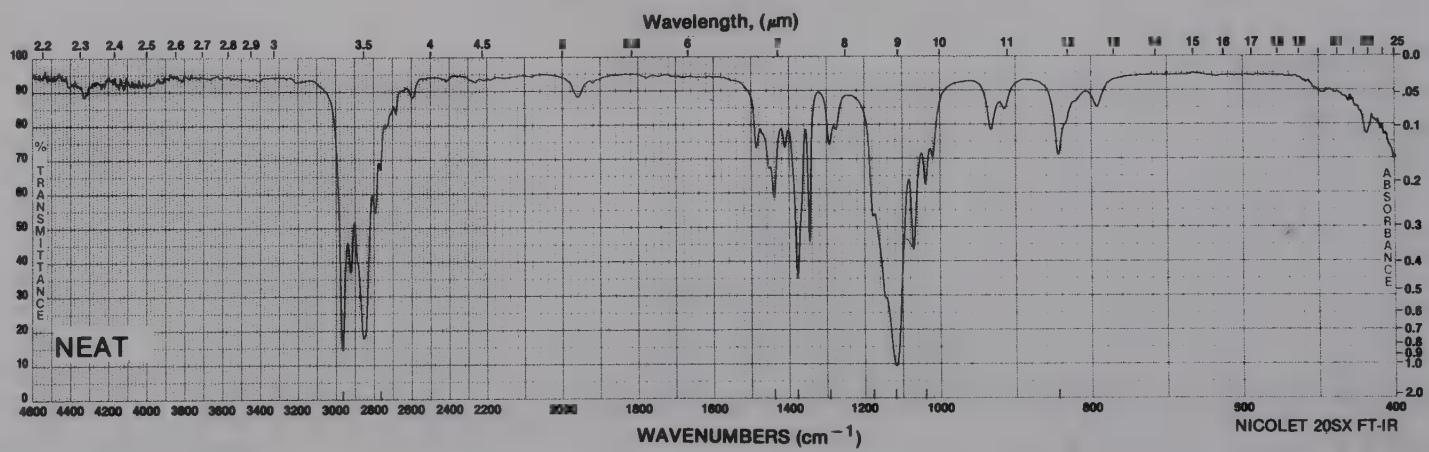

NO. 23

15482-2 *CAS [123-91-1]*
1,4-Dioxane, 99 + %

FW 88.11 | d 1.034 | IR III, 145F | 2851.8 1368.0 1045.8
mp 11.8°C | Fp 54°F | Merck 10,3304 | 1990.1 1254.6 879.0
bp 100-102°C | n$_D^{20}$ 1.4215 | | 1454.4 1121.1 613.3

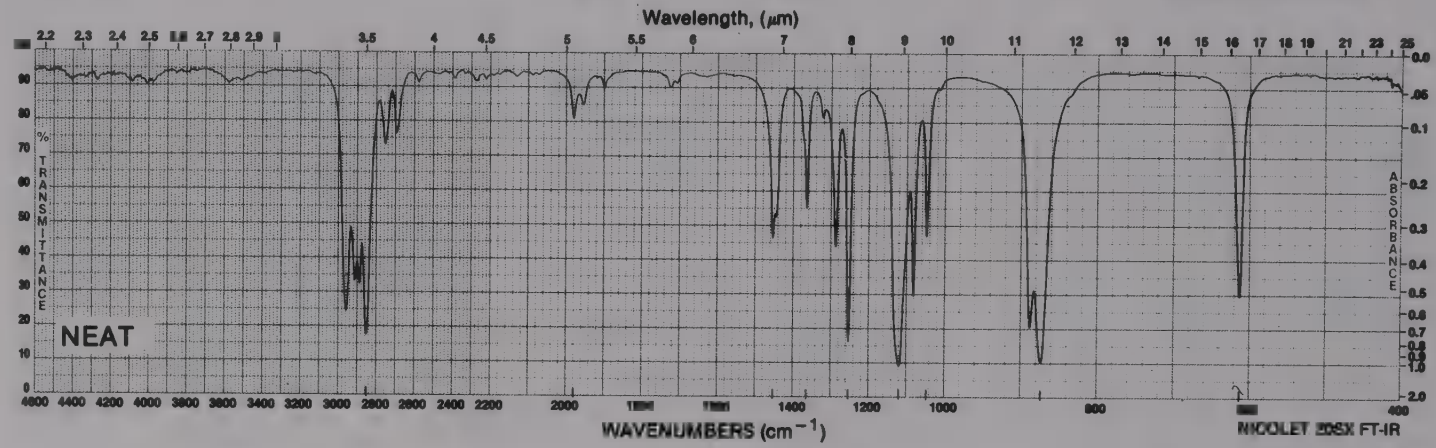

NO. 24

18451-9 *CAS [8032-32-4]*
Petroleum ether, A.C.S. reagent

bp 30-60°C | IR III, 5G | 2961.4 1146.1 808.2
d 0.640 | NMR II, 1,13C | 1453.2 1025.4 731.9
Fp -57°F | Merck 10,7050 | 1380.1 888.0 450.1

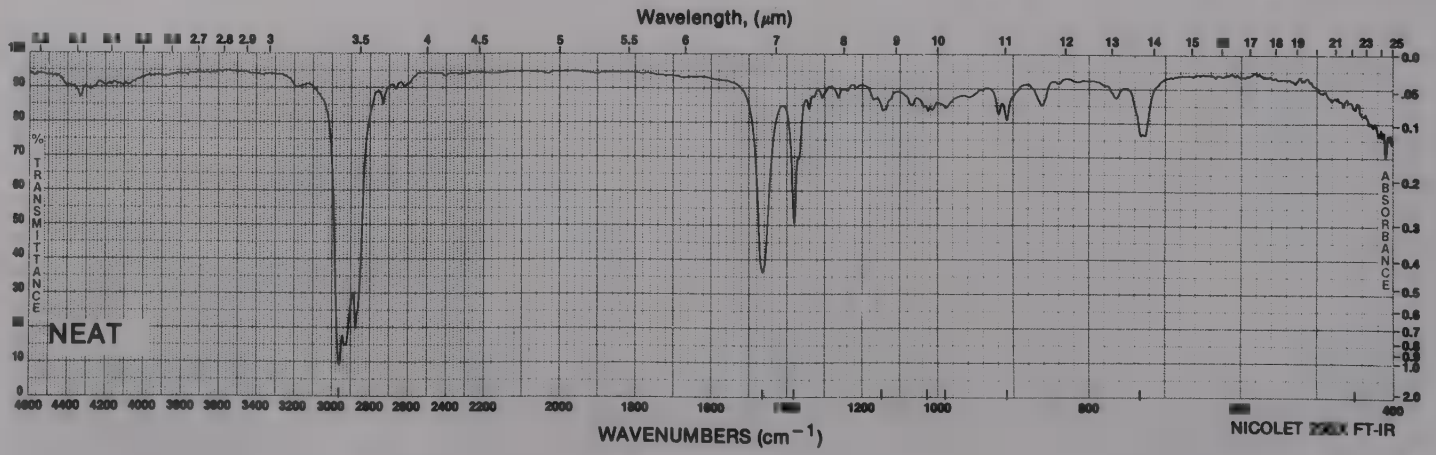

NO. 25

15470-9 *CAS [75-15-0]*
Carbon disulfide, 99 + %

FW 76.14 | d 1.266 | IR III, 162D | 2154.5
mp -111.5°C | Fp -22°F | Merck 10,1795 | 1524.6
bp 46.3-46°C | n_D^{20} 1.6270 | | 1462.9

$S{=}C{=}S$

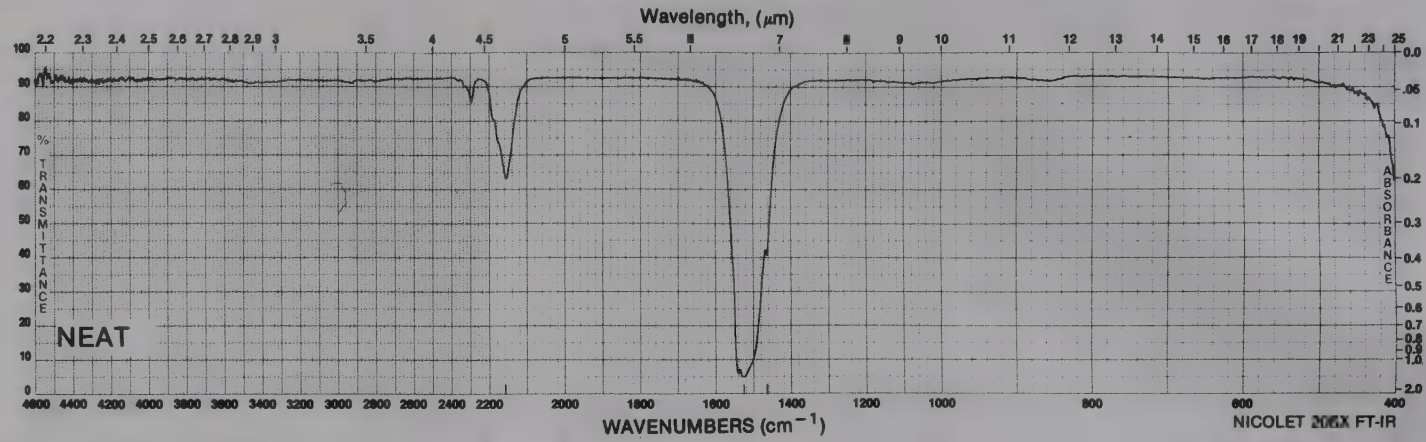

NO. 26

15493-8 *CAS [67-68-5]*
Methyl sulfoxide,* 99.9%

FW 78.13 | d 1.101 | IR III, 529A | 2994.5 1056.6 696.6
mp 18.4°C | Fp 203°F | Merck 10,3255 | 1437.1 [illegible] [illegible]
bp 189°C | n_D^{20} 1.4787 | | 1310.1 [illegible]

$CH_3{-}\overset{\overset{O}{\|}}{S}{-}CH_3$

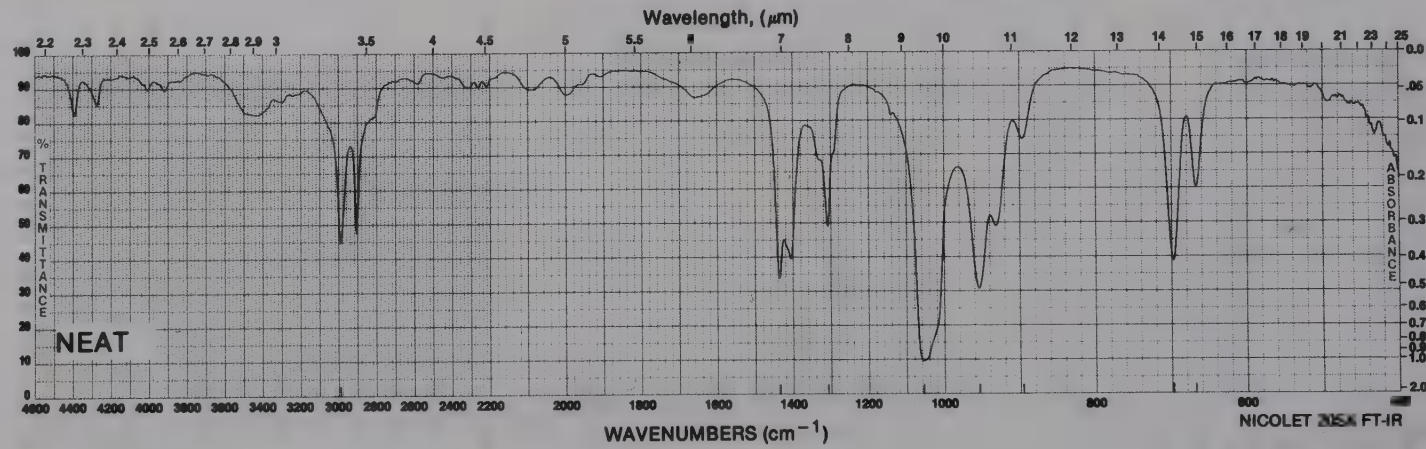

*Dimethyl sulfoxide (DMSO) is another name for methyl sulfoxide.

14615-3
Silicone oil, for melting point and boiling point apparatuses

bp >140°C/.002mm nD 1.4040
d 0.9[illegible]
Fp 600°F

IR III, 1537E
NMR II, 2,990C

2962.5 1092.5 800.3
1412.6 1022.5 754.4
1260.9 [illegible] 702.3

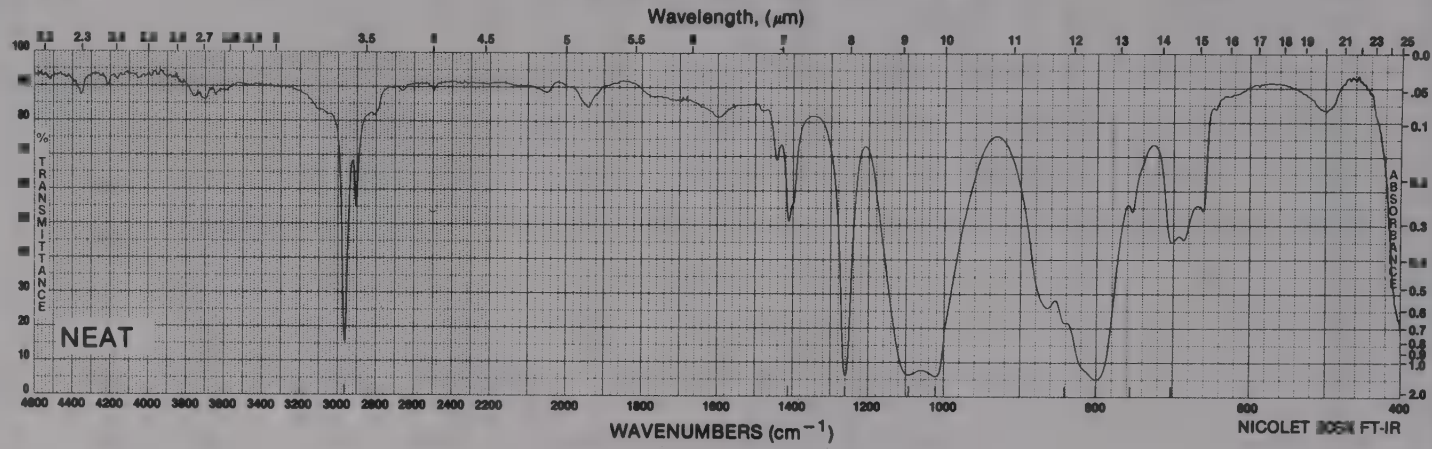

15481-4 *CAS [68-12-2]*
***N,N*-Dimethylformamide,* 99+ %**

FW 73.10
mp -61°C
bp 153°C

d 0.944
Fp 136°F
nD 1.4305

IR III, 443D
Merck 10,3237

2928.4 1438.4 1[illegible]
1676.3 1387.7 6[illegible]
1505.6 1257.0

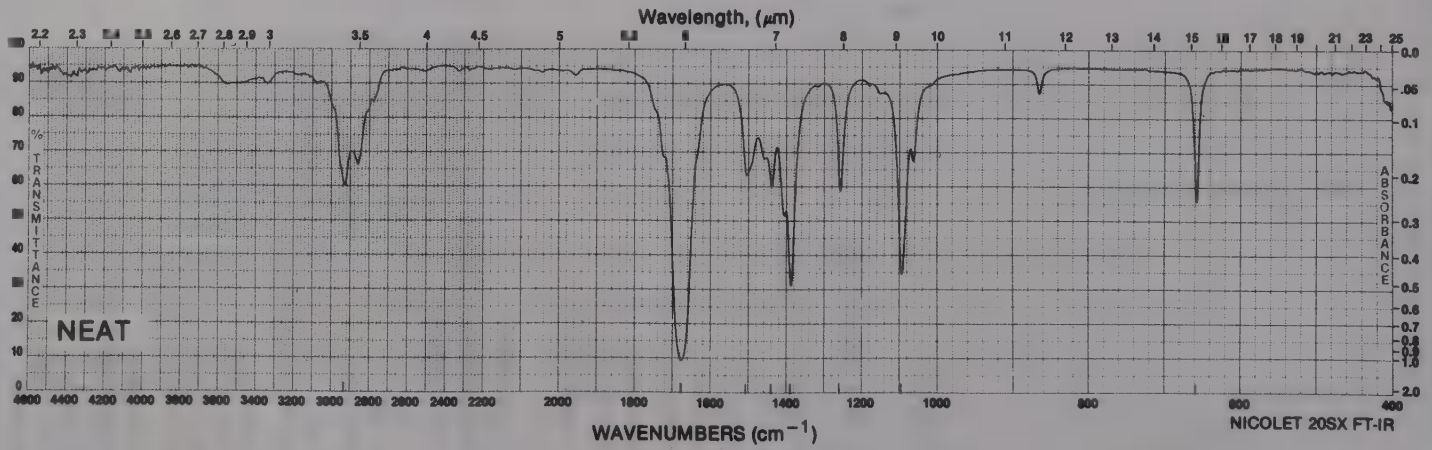

*The abbreviation for *N,N*-dimethylformamide is DMF.

Appendix C Characteristic Group Absorptions

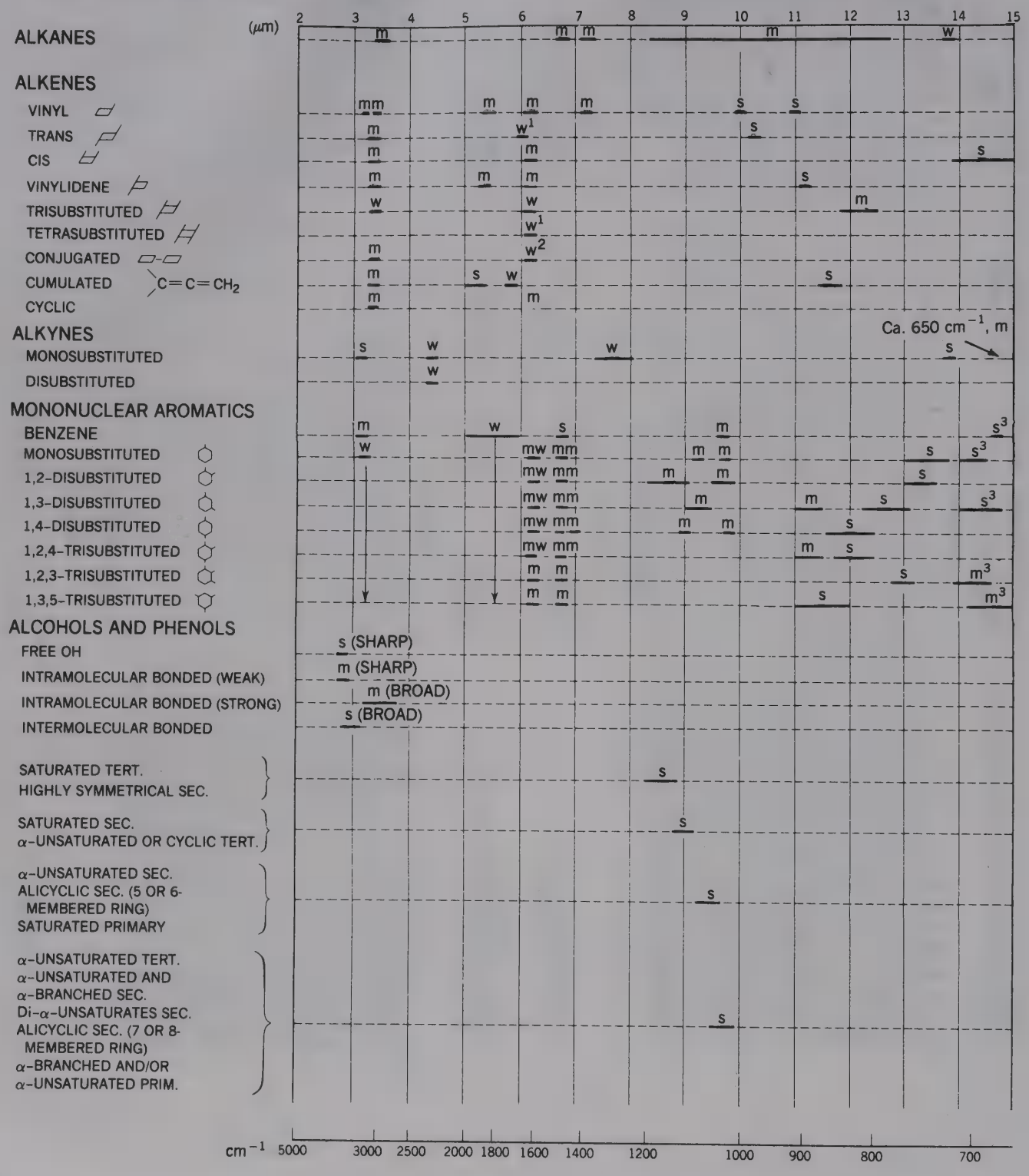

[1]May be absent
[2]Frequently a doublet
[3]Ring bending bands

Characteristic group frequencies. Absorption regions are indicated by ▪ heavy bar. s = strong, m = medium, w = weak. For example, a monosubstituted mononuclear aromatic may have four bands between 1667 and 1429 cm^{-1}, three of medium intensity, and one weak.

Appendix C continued

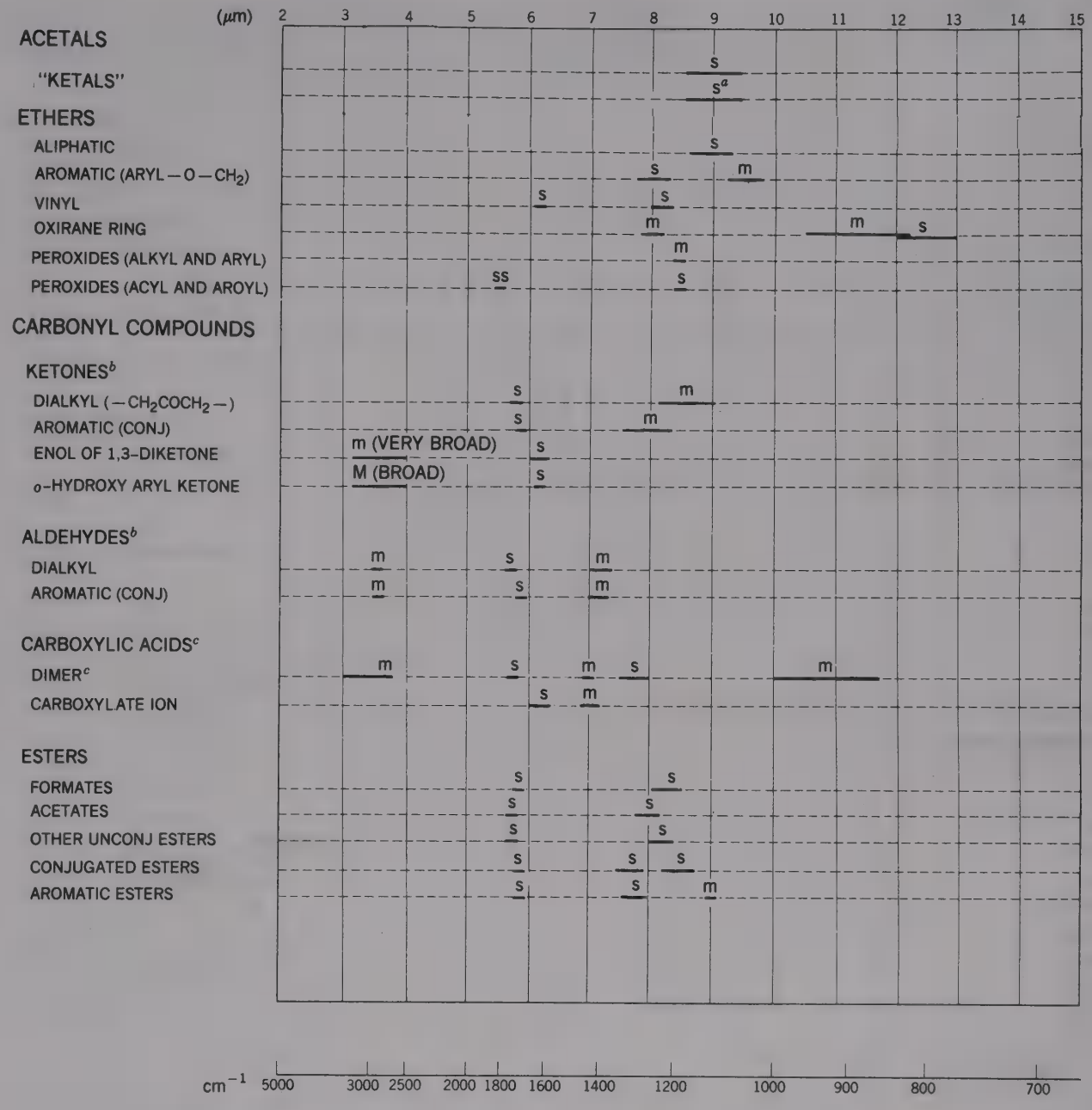

[a]Three bands, sometimes ■ fourth band for ketals and ■ fifth band for acetals.
[b]Conjugated aliphatic examples show C=O stretch at virtually the same position as conjugated aromatic structures.
[c]Conjugated examples show C=O stretch at lower wavenumbers (1710–1680 cm^{-1}). The O—H stretch (3300–2600 cm^{-1}) is very broad.

Appendix C continued

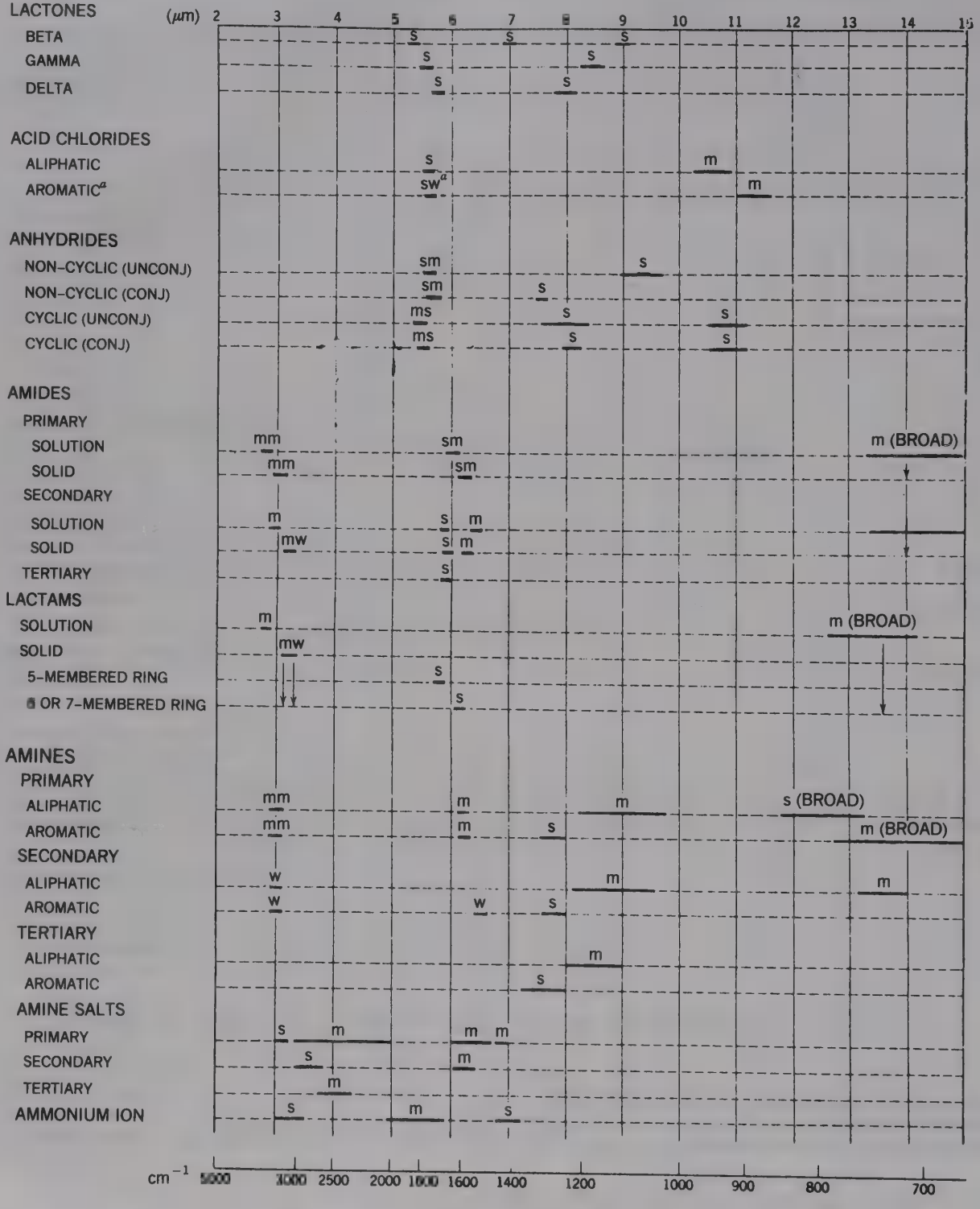

[a]Weaker band at 1750–1735 cm^{-1} (split due to Fermi resonance); conjugated aliphatic acyl halides show C=O stretch at virtually same position as (conjugated) aromatic entry.

Appendix C continued

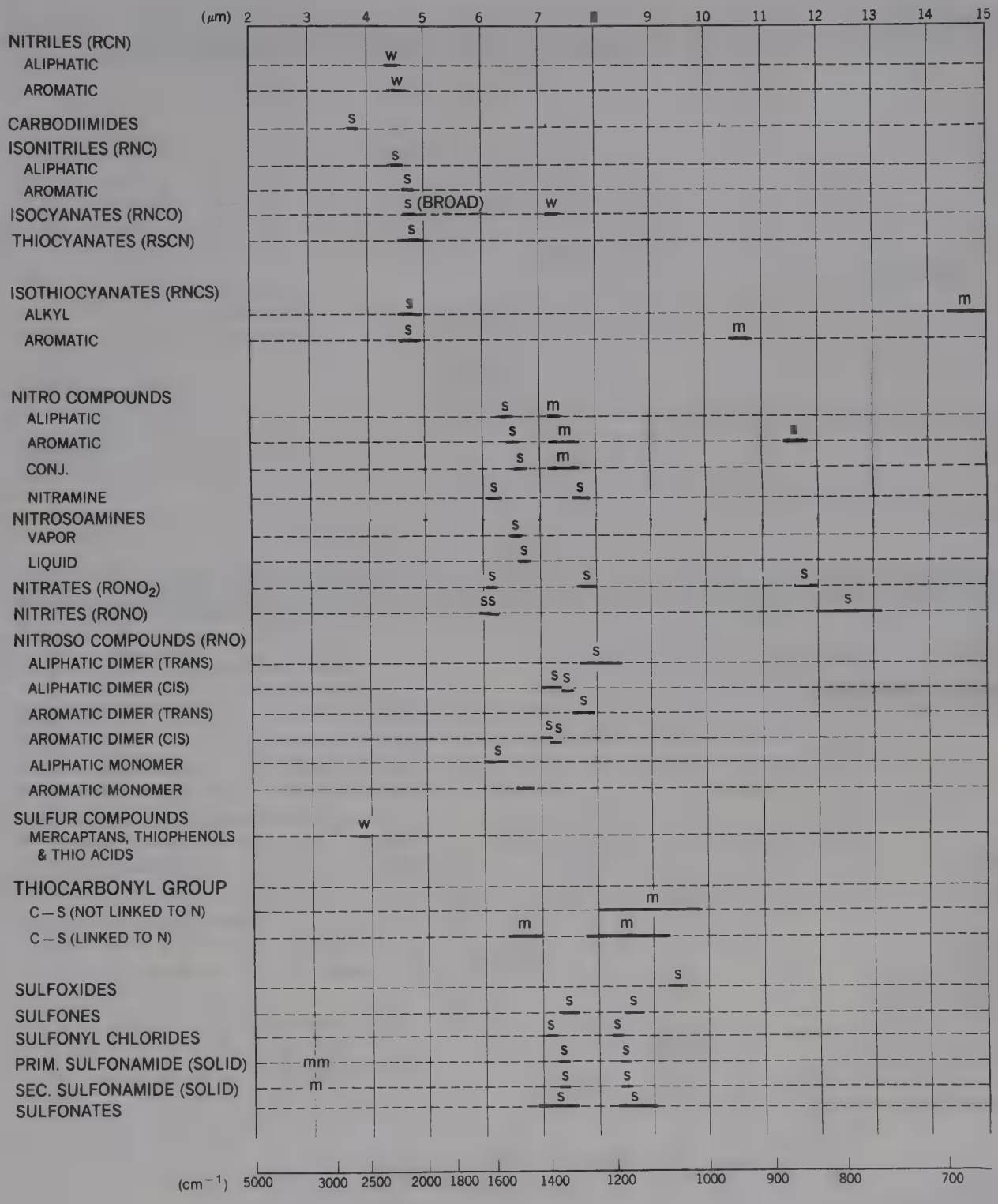

Appendix C continued

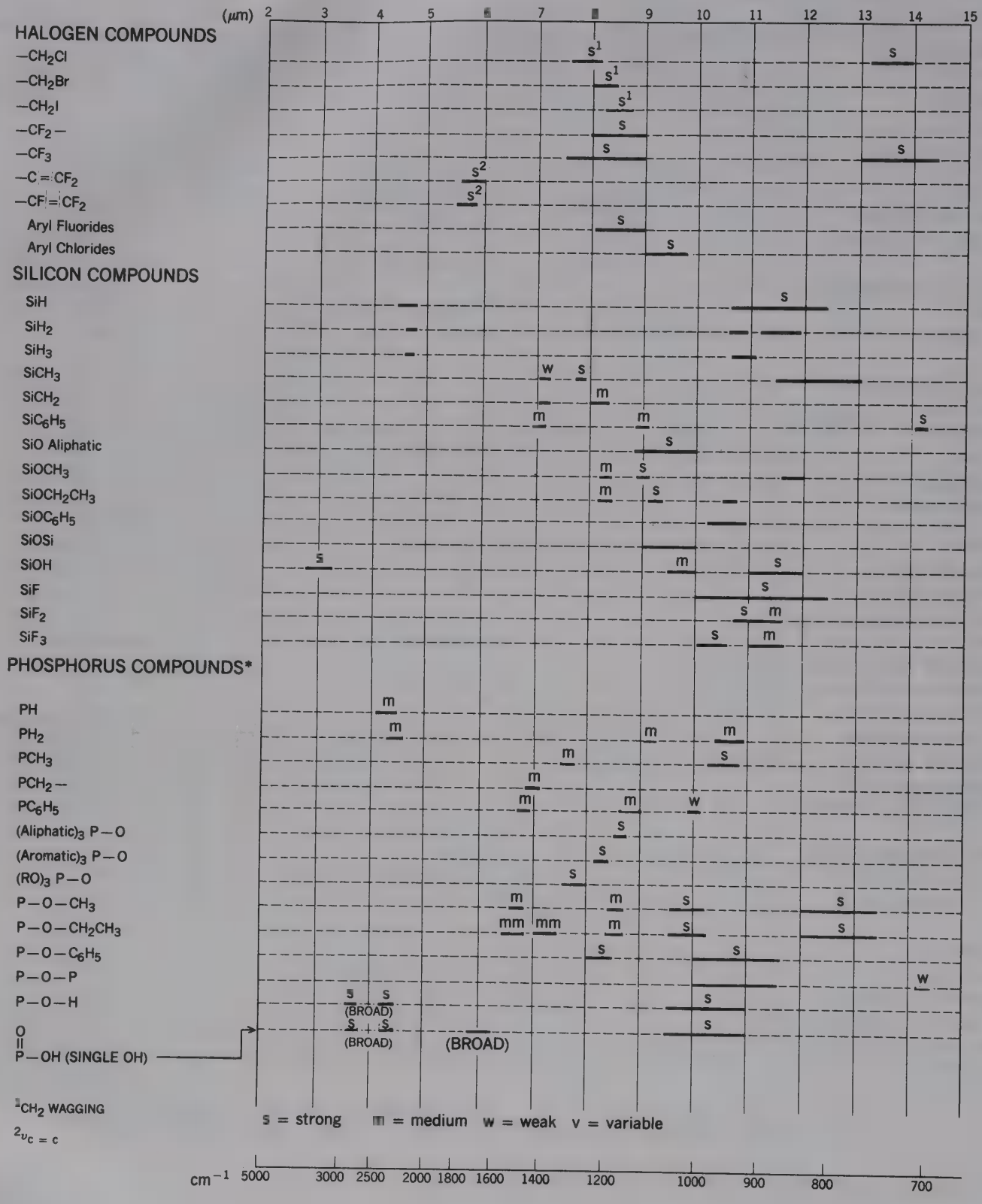

Appendix D

Table D-1

Alkene Absorptions[a]

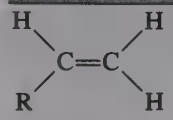

Vinyl
1648–1638 cm^{-1}
995–985 cm^{-1}(s)[b]
915–905 cm^{-1} (s)

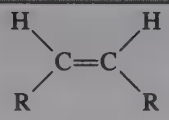

cis
1662–1626 cm^{-1} (ν)
730–665 cm^{-1} (s)

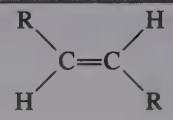

trans
1678–1668 cm^{-1} (v)
980–960 cm^{-1} (s)[c]

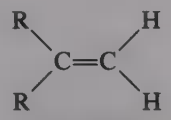

Vinylidine
1658–1648 cm^{-1} (m)
895–885 cm^{-1} (s)

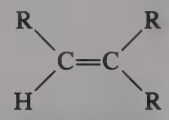

Trisubstituted
1675–1665 cm^{-1} (w)
840–790 cm^{-1} (m)

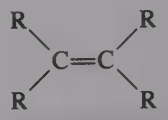

Tetrasubstituted
1675–1665 cm^{-1} very weak
or absent.

[a]s = strong, m = medium, w = weak, v = variable.
[b]This band also shows a strong overtone band.
[c]This band occurs near 1000 cm^{-1} in conjugated trans–trans systems such as the esters of sorbic acid.

Table D-2

C=C Stretching Frequencies in Cyclic and Acyclic Systems (cm^{-1})

Ring or Chain	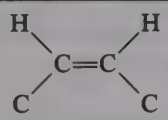	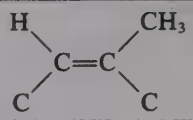	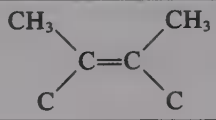	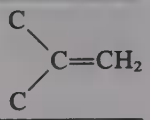
Chain cis	1661	1681	1672	1661
Chain trans	1676			
Three-membered ring	1641		1890	1780
Four-membered ring	1566		1685	1678
Five-membered ring	1611	1658	1686	1657
Six-membered ring	1649	1678	1685	1651
Seven-membered ring	1651	1673		
Eight-membered ring	1653			

All rings have cis double bonds.

Appendix E Absorptions for Phosphorus Compounds

TABLE E-1

P=O and P—O Stretching Vibrations

Group	Position cm^{-1} Intensity[a]	ν_{P-O} Bands[a] (cm^{-1})
P=O stretch		
phosphine oxides		
aliphatic	~1150	
aromatic	~1190	
phosphate esters[b]	1299–1250	
P—OH	1040–910 (s)	
P—O—P	1000–870 (s)	~700 w
P—O—C (aliph)	1050–970 (s)[c]	830–740 (s)[d]
P—O—C (arom)	1260–1160 (s)	994–855 (s)

[a]s = strong; w = weak
[b]The increase in P=O stretching frequency of the ester, relative to the oxides, results from the electronegativity of the attached alkoxy groups.
[c]May be a doublet.
[d]May be absent.

TABLE E-2

γ-CH and Ring Bending (β Ring) Bands of Pyridines[a]

Substitution	Number Adjacent H Atoms	γ-CH (cm^{-1})	β-Ring
2-	4	781–740	752–746
3-	3	810–789	715–712
4-	2	820–794	775–709

[a]The γ and β (p. 131) notations are explained in the text and in the book by Katritzky (References).

TABLE E-3

Characteristic γ-CH or β-Ring Bands of Furans, Thiophenes, and Pyrroles

Ring	Position of Substitution	Phase	γ-CH or β-Ring Modes[a]			
			cm^{-1}	cm^{-1}	cm^{-1}	cm^{-1}
Furan	2-	$CHCl_3$	~925	~884	835–780	
	2-	Liquid	960–915	890–875		780–725
	2-	Solid	955–906	887–860	821–793	750–723
	3-	Liquid		885–870	741	
Thiophene	2-	$CHCl_3$	~925	~853	843–803	
	3-	Liquid				755
Pyrrole	2-Acyl	Solid			774–740	~755

[a]The γ and β (p. 131) notations are explained in the text and in the book by Katritzky (References).

CHAPTER FOUR

PROTON MAGNETIC RESONANCE SPECTROMETRY

4.1. INTRODUCTION

Nuclear magnetic resonance (NMR) spectrometry is basically another form of absorption spectrometry, akin to IR or UV spectrometry. Under appropriate conditions in a magnetic field, a sample can absorb electromagnetic radiation in the radio frequency (rf) region at frequencies governed by the characteristics of the sample. Absorption is a function of certain nuclei in the molecule. A plot of the frequencies of the absorption peaks versus peak intensities constitutes an NMR spectrum. This chapter covers proton magnetic resonance (^{1}H NMR) spectrometry.

With some mastery of basic theory, interpretation of NMR spectra merely by inspection is usually feasible in greater detail than is the case for IR or UV spectra. The present account will suffice for the immediate limited objective: identification of organic compounds in conjunction with other spectrometric information. References are given at the end of this chapter.

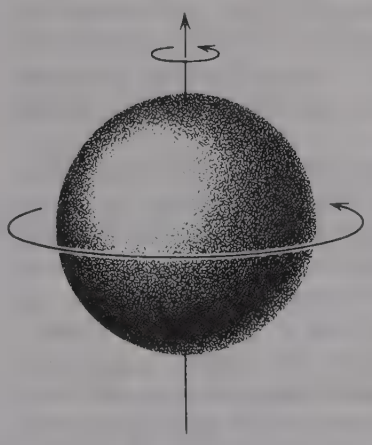

FIGURE 4.1. Spinning charge in proton generates magnetic dipole.

We begin by describing some magnetic properties of nuclei. All nuclei carry a charge. In some nuclei this charge "spins" on the nuclear axis, and this circulation of nuclear charge generates a magnetic dipole along the axis (Fig. 4.1). The angular momentum of the spinning charge can be described in terms of spin numbers I; these numbers have values of 0, $\frac{1}{2}$, 1, $\frac{3}{2}$, and so on ($I = 0$ denotes no spin). The intrinsic magnitude of the generated dipole is expressed in terms of nuclear magnetic moment, μ.

Relevant properties, including the spin number I, of several nuclei are given in Appendix H. The spin number I can be determined from the atomic mass and the atomic number as follows:

I	Atomic Mass	Atomic Number	Example (I)
Half-integer	Odd	Odd or even	$^1_1$H($\frac{1}{2}$), $^{17}_8$O($\frac{5}{2}$), $^{15}_7$N($\frac{1}{2}$)
Integer	Even	Odd	$^2_1$H(1), $^{14}_7$N(1), $^{10}_5$B(3)
Zero	Even	Even	$^{12}_6$C(0), $^{16}_8$O(0), $^{34}_{16}$S(0)

Several nuclei (e.g., $^1_1$H, $^3_1$H, $^{13}_6$C, $^{15}_7$N, $^{19}_9$F, $^{31}_{15}$P) have spin numbers I of $\frac{1}{2}$ and a uniform spherical charge distribution (Fig. 4.1). Of these, by far the most widely used in NMR spectrometry are ^{1}H (this chapter) and ^{13}C (Chapter 5). Nuclei with a spin number I of 1 or higher have a nonspherical charge distribution. This asymmetry is described by an electrical quadrupole moment which, as we shall see later, affects the relaxation time and, consequently, the coupling with neighboring nuclei. In quantum mechanical terms, the spin number I determines the number of orientations a nucleus may assume in an external uniform magnetic field in accordance with the formulas $2I + 1$. We are concerned with the proton whose spin number I is $\frac{1}{2}$;

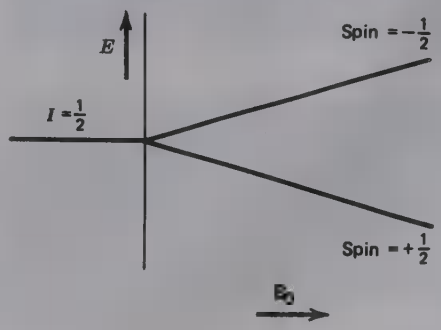

FIGURE 4.2. Two energy levels for a proton in a magnetic field $\mathbf{B}_0$.

thus, there are two energy levels, and a slight excess population in the lower energy state (Fig. 4.2).

Once two energy levels for the proton have been established, it should be possible to introduce quanta of energy $h\nu$ (h is Planck's constant; ν is the frequency of electromagnetic radiation) to effect a transition between these energy levels in a magnetic field of given strength $\mathbf{B}_0$. The fundamental NMR equation correlating electromagnetic frequency with magnetic field strength is*

$$\nu = \frac{\gamma \mathbf{B}_0}{2\pi}$$

A frequency of 100 megahertz (MHz)† is needed at a magnetic field $\mathbf{B}_0$ of 2.33 tesla (T) for the proton (or any other desired combination in the same ratio (see Appendix H). The constant γ is called the magnetogyric ratio and is a fundamental nuclear constant; it is the proportionality constant between the magnetic moment μ and the spin number I.

$$\gamma = \frac{2\pi\mu}{hI}$$

The problem is how to transfer radio frequency (rf) electromagnetic energy to protons aligned in a magnetic field, and how to measure the energy thus absorbed as the proton is raised to the higher spin state. This can best be explained in classical mechanical terms, wherein we visualize the proton as spinning in an external magnetic field: The magnetic axis of the proton will precess about the axis of the external magnetic field in the same manner in which an off-perpendicular spinning top precesses under the influence of gravity

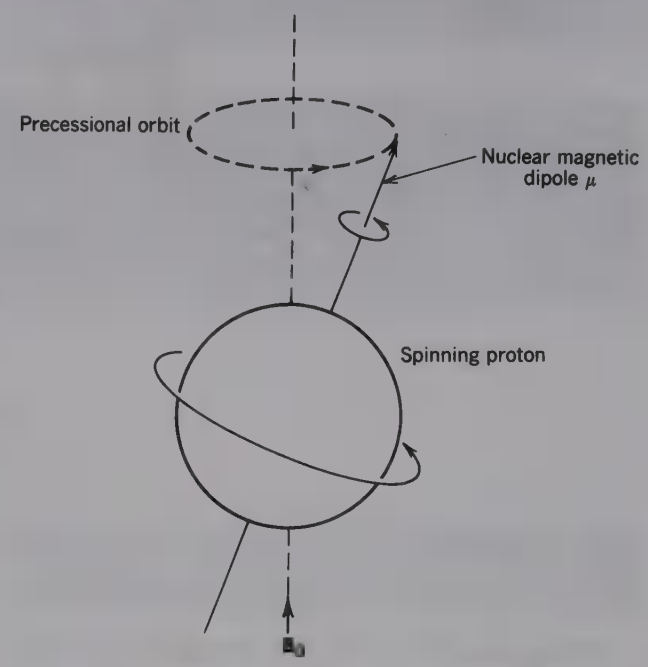

FIGURE 4.3. Proton precessing in a magnetic field $\mathbf{B}_0$.

(Fig. 4.3). The precessional angular velocity (Larmor frequency ω_0) is equal to the product of the magnetogyric ratio and the strength of the applied magnetic field $\mathbf{B}_0$.

$$\omega_0 = \gamma \mathbf{B}_0$$

We recall from the fundamental NMR equation that

$$\gamma \mathbf{B}_0 = 2\pi\nu$$

Therefore,

$$\omega_0 = 2\pi\nu$$

We start with an assemblage of such nuclei precessing in random phase around the z axis designating the direction of the stationary applied magnetic field $\mathbf{B}_0$. This randomly phased assemblage has a net magnetization ($\mathbf{M}_0$) along the z axis but not in the x–y plane (Fig. 4.4).

The assemblage shown represents the slight excess population over the assemblage aligned against the applied field $\mathbf{B}_0$ (not shown) in accordance with the Boltzmann distribution. Thus, we can equate the quantum description of the lower energy level (spin = $+\frac{1}{2}$) and the higher energy level (spin = $-\frac{1}{2}$) with the classical description of precessing nuclei aligned, respectively, with and against the applied field (see Fig. 4.2).

The aim now is to tip the net magnetization $\mathbf{M}_0$ toward the horizontal plane (x–y plane in Fig. 4.4) and measure the resulting component of magnetization in

*The designations $\mathbf{B}$ (magnetic induction or flux density) and $\mathbf{H}$ (magnetic intensity) are often used interchangeably in NMR spectrometry; the distinction is not important for our purpose. The SI term tesla supercedes the cgs term gauss (1 tesla = 10^4 G).

†Hz = hertz, which was formerly cycles per second (cps).

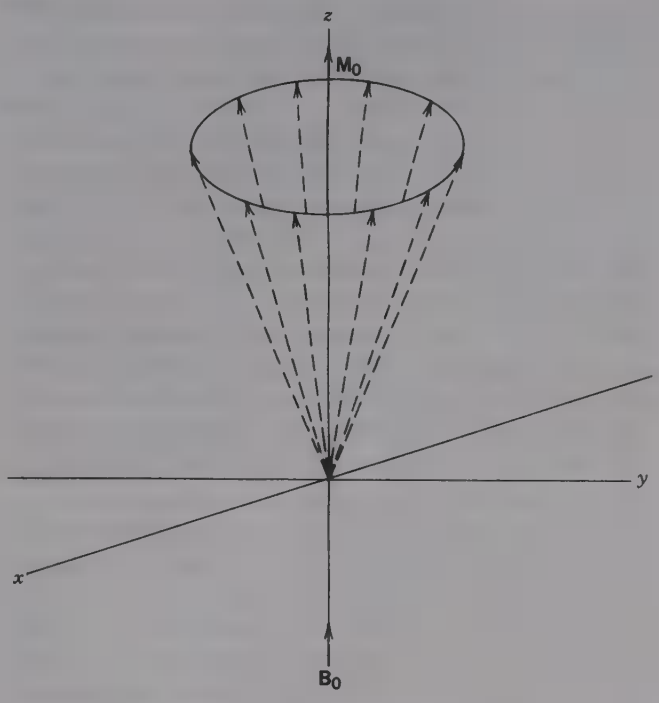

FIGURE 4.4. Assemblage of excess precessing nuclei with net magnetization $\mathbf{M_0}$ in the direction of the stationary applied magnetic field $\mathbf{B_0}$.

that plane (see Fig. 4.5). Rf electromagnetic energy is applied in such a way that its magnetic component $\mathbf{B_1}$ is at right angles to the main magnetic field $\mathbf{B_0}$ and is rotating with the precessing proton. This is accomplished by a coil with its axis at right angles to the axis of the main magnetic field $\mathbf{B_0}$. Such a coil will generate an oscillating magnetic field $\mathbf{B_1}$ along the direction of the coil axis as shown in Figure 4.4. An oscillating magnetic field can be resolved into two components rotating in opposite directions. One of these components is rotating in the same direction as the precessional orbit of the nuclear magnetic dipole (the proton); the oppositely rotating component of $\mathbf{B_1}$ is essentially ineffective. If $\mathbf{B_0}$ is held constant and the oscillator frequency is varied, the angular velocity of the component of rotating magnetic field $\mathbf{B_1}$ will vary until it is equal to (in resonance with) the angular velocity ω_0 of the precessing proton. At this point, the absorbed energy is at a maximum, and the net magnetization $\mathbf{M_0}$ is tilted away from alignment with $\mathbf{B_0}$ toward the horizontal plane in Figure 4.5. The magnetic component thus generated in that plane can be detected. Alternatively, the oscillator frequency is held constant, and $\mathbf{B_0}$ is swept over a narrow range. Conventionally, the oscillator is placed on the x axis and the receiver on the y axis of the Cartesian coordinates (Fig. 4.5).

Now that we have briefly discussed how a nucleus is excited to a higher energy state by absorption of energy, we need to describe a mechanism for the return of the nucleus to the ground state. In the absence of such a mechanism, all of the small excess population of nuclei in the lower energy state will be raised to the high-energy state, and no more energy could be absorbed. Fortunately, there exist mechanisms whereby the nucleus in the higher energy state can lose energy to its environment and thus return to its lower energy state. One mechanism is called a spin–lattice or longitudinal relaxation process and involves transfer of energy from the nucleus in its high-energy state to the surrounding molecules (molecular lattice). The relaxation efficiency is characterized by the time constant T_1 (Fig. 4.5c). The other mechanism, called spin–spin or transverse relaxation, is characterized by the time constant T_2. This relaxation involves a transfer of en-

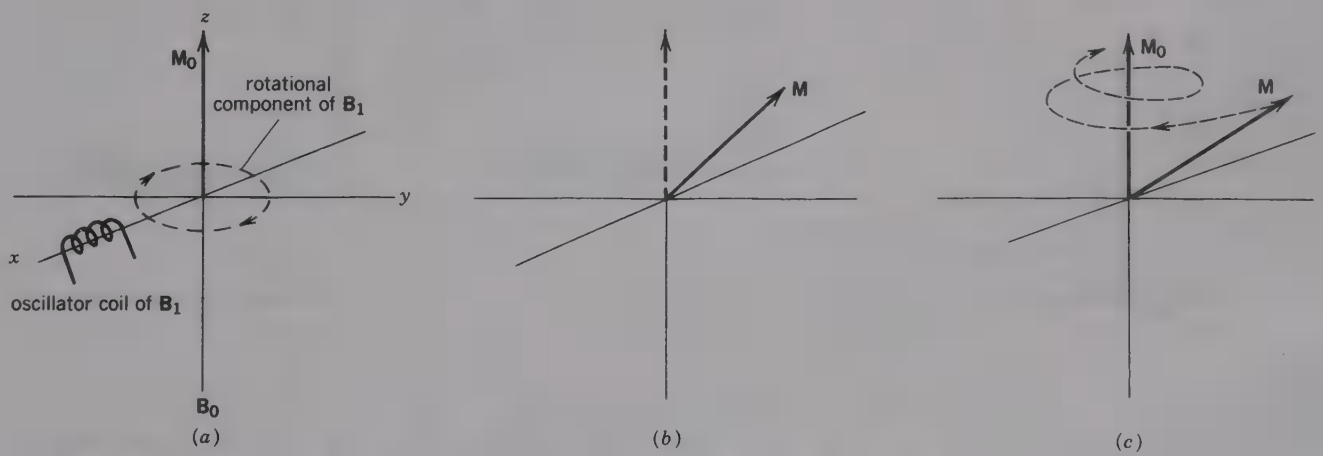

FIGURE 4.5 (*a* and *b*). Oscillator generates rotating component of applied magnetic field $\mathbf{B_1}$. The net magnetization $\mathbf{M_0}$ is tipped to $\mathbf{M}$, which precesses about the z axis generating a component of magnetization in the horizontal plane. (*c*) Longitudinal relaxation of $\mathbf{M}$ to $\mathbf{M_0}$ follows a decreasing spiral. The assemblage of nuclei precessing about $\mathbf{M_0}$ and $\mathbf{M}$ is omitted (see Fig. 4.4). Transverse relaxation T_2 (dephasing of $\mathbf{M}$) is also omitted.

ergy from one nucleus to another. There is no net loss of energy, but the spread of energy (dephasing) among the nuclei results in signal loss and line broadening. The designation T_2^* is often used to denote the time constant for the signal loss. This term includes both T_2 (the time constant of the actual spin dynamics) and the effect of the magnetic field inhomogeneity; the latter frequently dominates. The terms R_1 and R_2 are the rate constants corresponding to the time constants T_1 and T_2.

$$R_1 = \frac{1}{T_1} \qquad R_2 = \frac{1}{T_2}$$

Thus far, we have described the interaction between the net magnetization ($\mathbf{M_0}$ and $\mathbf{M}$) of an assemblage of nuclei in a strong, static, homogeneous, magnetic field $\mathbf{B_0}$ and an oscillating rf field (actually one of the circular components of the generated magnetic field $\mathbf{B_1}$). To obtain a spectrum, either the oscillator frequency or the magnetic field $\mathbf{B_0}$ may be scanned over a narrow range. Historically, the early instruments employed this mode, known as continuous wave (CW); it has in turn been superceded almost completely by pulsed Fourier transform (FT). Since the CW scan mode is grasped more readily because of its similarity to IR, visible, or UV spectrometry, we have described this older technique first and used the familiar stationary *xyz* Cartesian frame of reference. This is followed by a brief introduction to pulsed FT spectrometry and the rotating frame of reference; details are deferred to

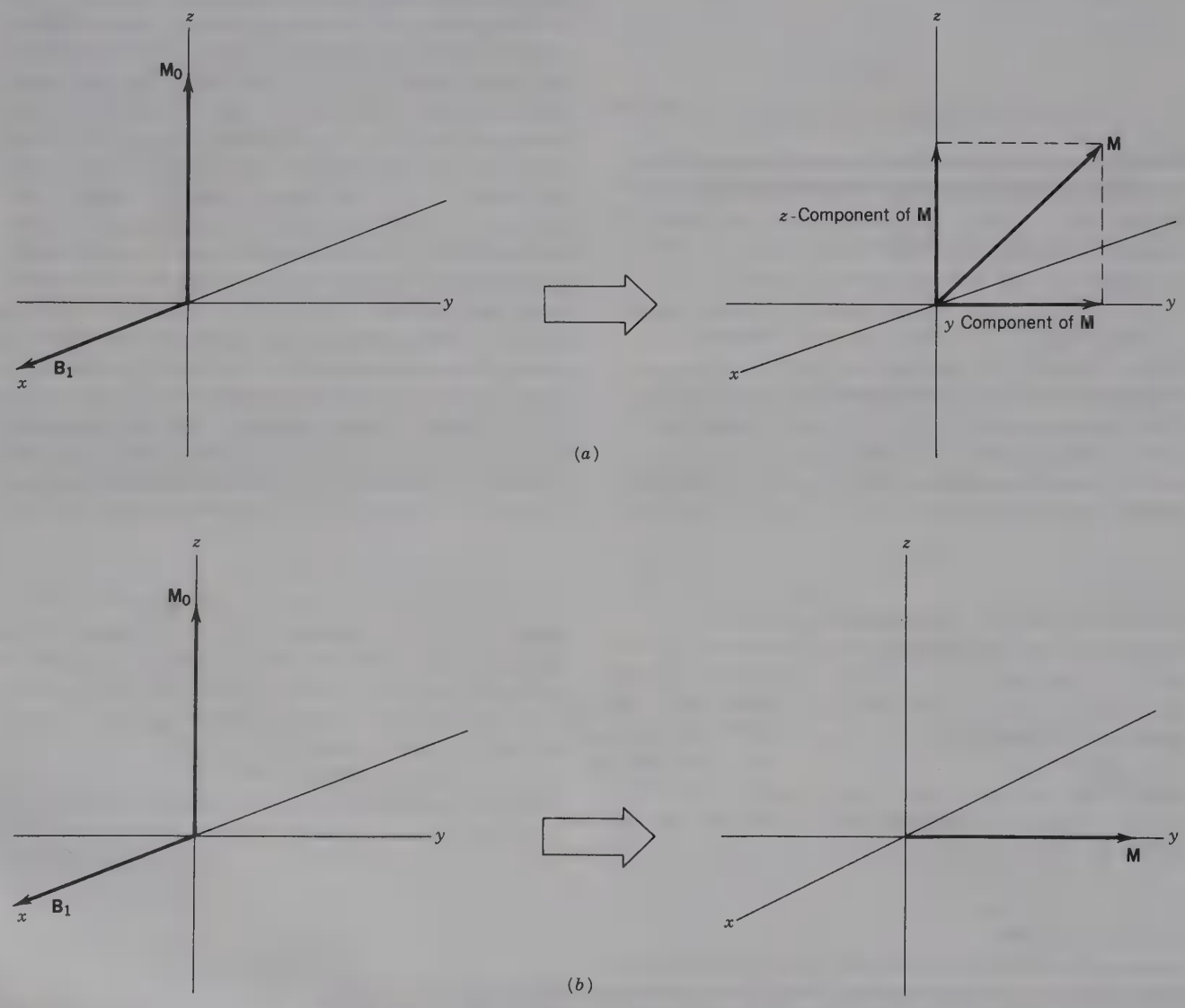

FIGURE 4.6. In the rotating frame, $\mathbf{B_1}$ and $\mathbf{M}$ are static. (*a*) A 45° pulse along the *x* axis and (*b*) a 90° pulse. At the end of the pulse, the signal decays as $\mathbf{M}$ returns to the *z* axis (longitudinal relaxation) and also as $\mathbf{M}$ fans out in the *x*–*y* plane. Recall from Figure 4.5 that the actual path of longitudinal relaxation is a decreasing spiral around the *z* axis.

Chapter 5, which covers ^{13}C NMR spectrometry since, historically, the pulsed technique was developed largely in response to the need for much higher sensitivity in ^{13}C spectrometry.

This higher sensitivity is achieved by exciting, and then collecting signals from, all of the nuclei (in this chapter, protons) simultaneously, rather than sequentially as in the CW scan. A short (microseconds, μs), powerful rf pulse applied along the x axis provides the entire frequency range, generates the rotating magnetic field $\mathbf{B_1}$, and has essentially the same effect as the scanning oscillator: It tips the net magnetization $\mathbf{M_0}$ toward the xy plane but does so for all of the protons simultaneously. The amplitude of $\mathbf{B_1}$ is much less than that of $\mathbf{B_0}$.

By using a frame of reference that is rotating at the Larmor frequency ω_0, we eliminate the rotation of the generated magnetic field $\mathbf{B_1}$ and the precessional movement, and show a simplified version of Figure 4.5 (see Fig. 4.6). The observer is moving with the rotating frame, and can be compared with an observer who has mounted a moving carousel and no longer sees the rotation. In the pulsed mode, the degree of tipping is described by the pulse width (i.e., the time in microseconds), or in terms of the angle through which the magnetization is tipped (e.g., a 90° pulse, also called a $\pi/2$ pulse).

Figure 4.6 shows a 45° and a 90° pulse. Longitudinal relaxation (spin–lattice relaxation) is represented by the return of $\mathbf{M}$ to the z axis with time constant T_1. Transverse relaxation can be represented by a "fanning out" of the $\mathbf{M}$ component (loss of phase) in the x–y plane with time constant T_2, with loss of signal. Magnetic field inhomogeneity also contributes to transverse relaxation.

Bear in mind that the simplified picture permitted by the artificial device of the rotating frame obscures the fact of precession of $\mathbf{M}$ about the z axis.

4.2. INSTRUMENTATION AND SAMPLE HANDLING

Beginning in 1953 with the first commercial NMR spectrometer, the early instruments used permanent magnets or electromagnets with fields of 1.41, 1.87, 2.20, or 2.35 T corresponding to 60, 80, 90, or 100 MHz, respectively, for proton resonance (the usual way of describing an instrument).

The "horsepower race," driven by the need for higher resolution and sensitivity, has culminated in wide use of 200–500-MHz instruments and in the production of

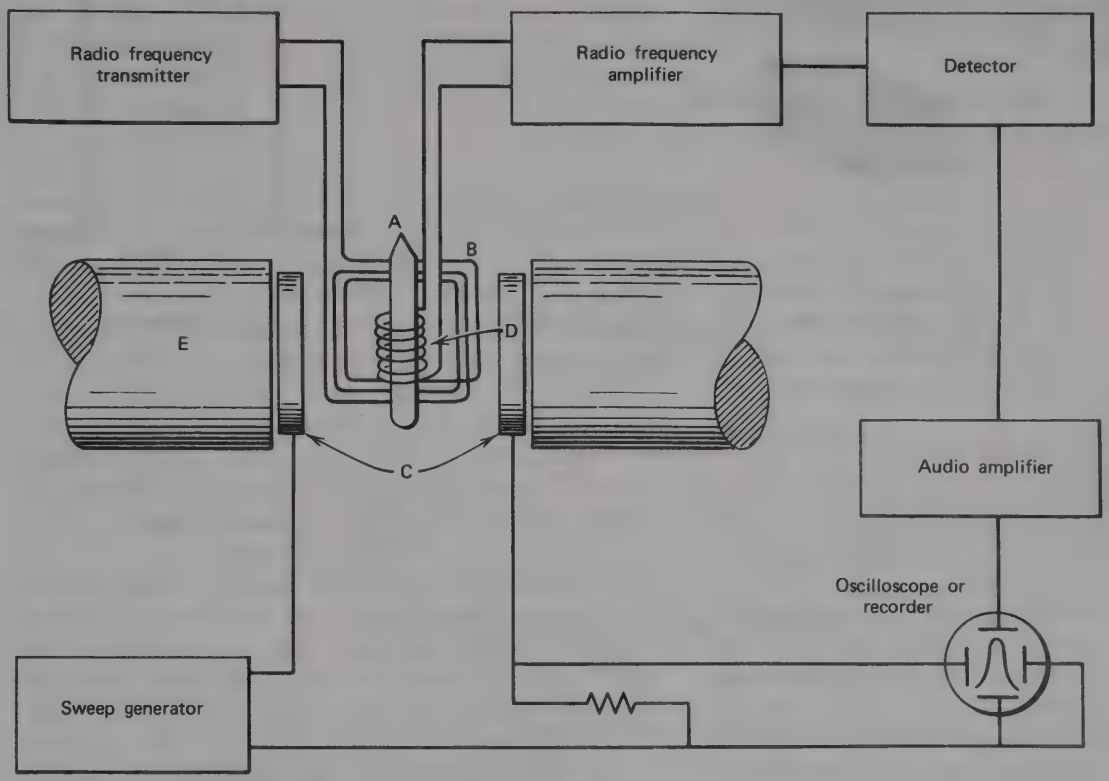

FIGURE 4.7. Schematic diagram of an NMR spectrometer. The tube is perpendicular to the z axis of the magnet. A, sample tube; B, transmitter coil; C, sweep coils; D, receiver coil; E, magnet. Courtesy of Varian Associates, Palo Alto, California.

600-MHz instruments. All of the instruments above 100 MHz are based on helium-cooled superconducting magnets (solenoids) and operate in the pulsed FT mode. The other basic requirements besides high field are frequency–field stability and field homogeneity.

The sample (routinely a solution in a deuterated solvent in a 5-mm tube) is placed in the probe, which contains the transmitter and receiver coils and a spinner to spin the tube about its vertical axis in order to average out field inhomogeneities. Figure 4.7 shows the probe elements between the poles of an electromagnet or permanent magnet, and Figure 4.8 shows the arrangement for a superconducting magnet. Note that in the electromagnet the tube spins at right angles to the z axis, which is horizontal, whereas in the superconducting magnet, the tube fits in the bore of the solenoid and spins about the z axis, which is vertical. The transmitter and receiver are coupled through the sample nuclei (protons in this chapter).

The spectrum obtained either by CW scan or pulse FT is shown as a series of peaks whose areas are proportional to the number of protons they represent. Peak areas are measured by an electronic integrator that traces a series of steps with heights proportional to the peak areas (see Fig. 4.30). A proton count from the integration is useful to determine or confirm molecular formulas, detect hidden peaks, determine sample purity, and do quantitative analysis. Peak positions (chemical shifts, Section 4.3) are measured in frequency units from a reference peak.

A routine sample for proton NMR on a scanning 60-MHz instrument consists of about 5–20 mg of the compound in about 0.4 mL of solvent in a 5-mm o.d. glass tube. Under favorable conditions, it is possible to obtain a spectrum on less than 1 μg of a compound of modest molecular weight in a microtube in a 500-MHz pulsed instrument.

The ideal solvent should contain no protons and be

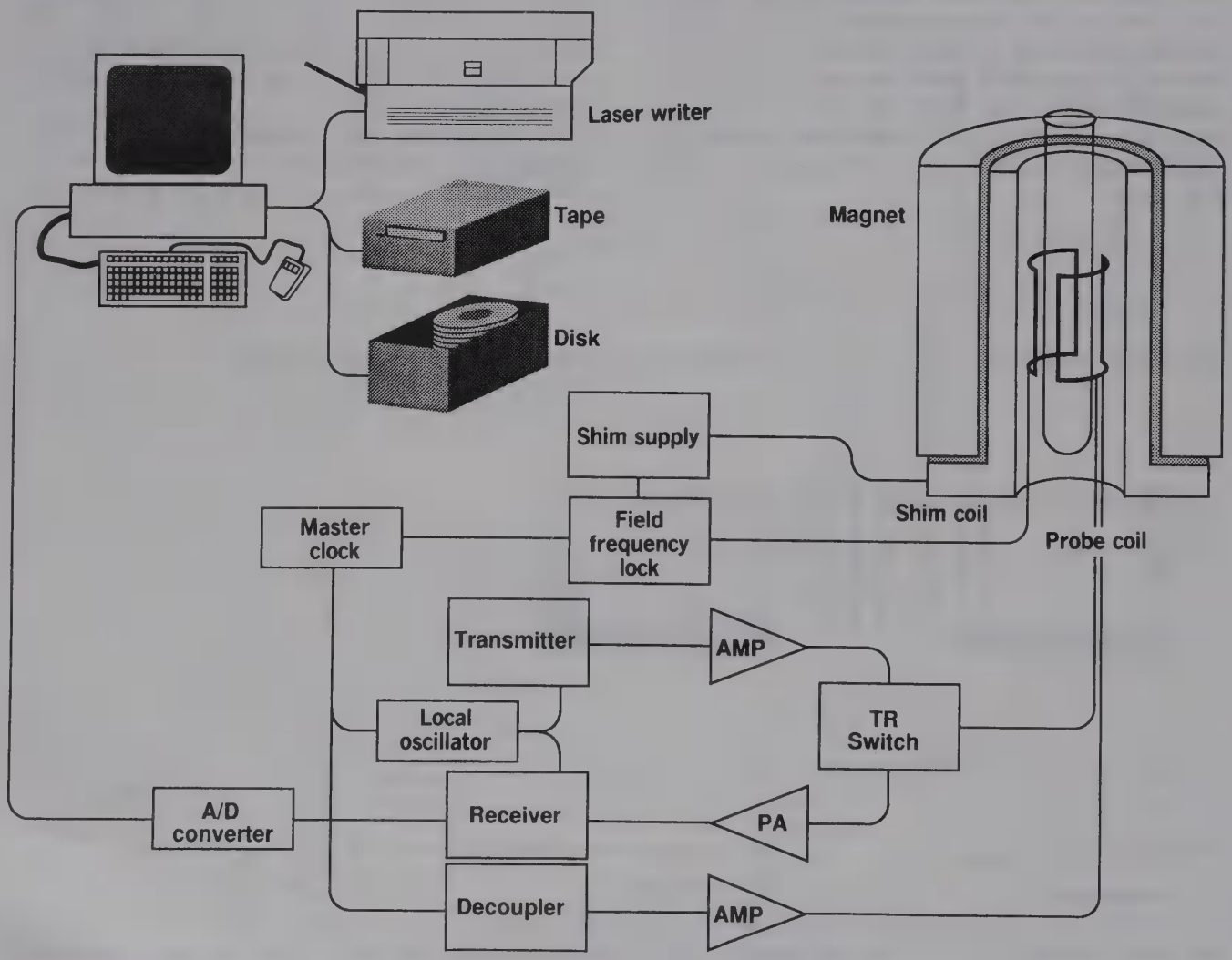

FIGURE 4.8. Schematic diagram of a GE WMR series cryogenic NMR spectrometer. The probe is parallel with the z axis of the magnet, which is cooled by liquid helium surrounded by liquid nitrogen in a large Dewar flask. With permission from GE NMR Instruments.

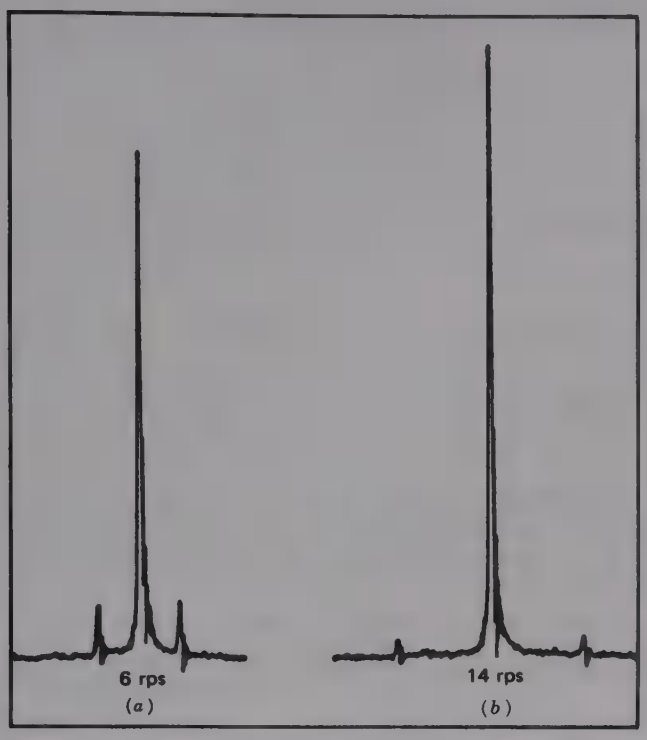

FIGURE 4.9. Signal of neat chloroform with spinning side bands produced by spinning rate of (*a*) 6 rps and (*b*) 14 rps. From Bovey, F. A. *NMR Spectroscopy,* New York: Academic 1969. With permission.

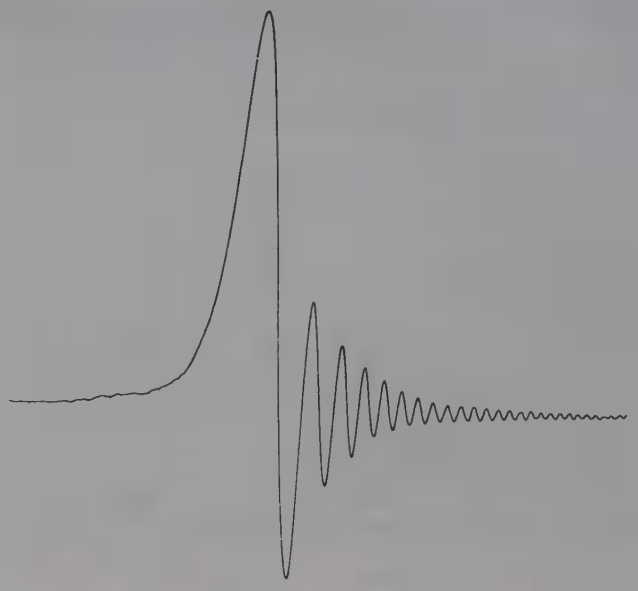

FIGURE 4.10. Ringing (or wiggles) seen after passage through resonance. Direction of scan is from left to right. With permission, see Figure 4.9.

inert, nonpolar, low-boiling, and inexpensive. Carbon tetrachloride meets these requirements and can be used in a scanning instrument. Since pulsed instruments depend on deuterium in the field–frequency lock (see Section 5.1), deuterated solvents are necessary. Deuterated chloroform ($CDCl_3$) is used whenever circumstances permit—in fact most of the time. The small sharp proton peak from $CHCl_3$ impurity present at δ 7.24 rarely interferes seriously. For very dilute samples, $CDCl_3$ can be obtained in "100% purity." A list of common, commercially available solvents with the positions of proton impurities is given in Appendix G.

Small "spinning side bands" (see Fig. 4.9) are often seen, symmetrically disposed on both sides of a strong absorption peak; these result from inhomogeneities in the magnetic field and in the spinning tube. They are readily recognized because of their symmetrical appearance and because their separation from the absorption peak is equal to the rate of spinning. The oscillations often seen in scanned spectra at the high-field end of a strong sharp peak are called "ringing" (Fig. 4.10). These are "beat" frequencies resulting from "fast" (normal operation) passage through the absorption peak.

Traces of ferromagnetic impurities cause severe broadening of absorption peaks. Common sources are tap water, steel wool, Raney nickel, and particles from metal spatulas or fittings (Fig. 4.11). These impurities can be removed by dipping a thin bar magnet into the NMR tube, by filtration, or by centrifugation.

4.3. CHEMICAL SHIFT

Only a single peak should be obtainable from the interaction of rf energy and a strong magnetic field on a proton in accordance with the basic NMR equation in which γ, the magnetogyric ratio, is an intrinsic property of the nucleus. The peak area (measured by the integrator) is proportional to the number of protons it represents. Fortunately, the situation is not quite so simple. The nucleus is shielded to a small extent by its electron cloud whose density varies with the environment. This variation gives rise to different absorption positions usually within the range of about 750 Hz in a magnetic field corresponding to 60 MHz or about 3750 Hz in a field corresponding to 300 MHz. The ability to discriminate among the individual absorptions describes high-resolution NMR spectrometry.

Electrons under the influence of a magnetic field will circulate, and, in circulating, will generate their own magnetic field opposing the applied field, in accordance with the "right-hand rule"; hence, the shielding effect (Fig. 4.12). This effect accounts for the diamagnetism exhibited by all organic materials. In the case of materials with an unpaired electron, the paramagnetism associated with the net electron spin far overrides the diamagnetism of the circulating, paired electrons.

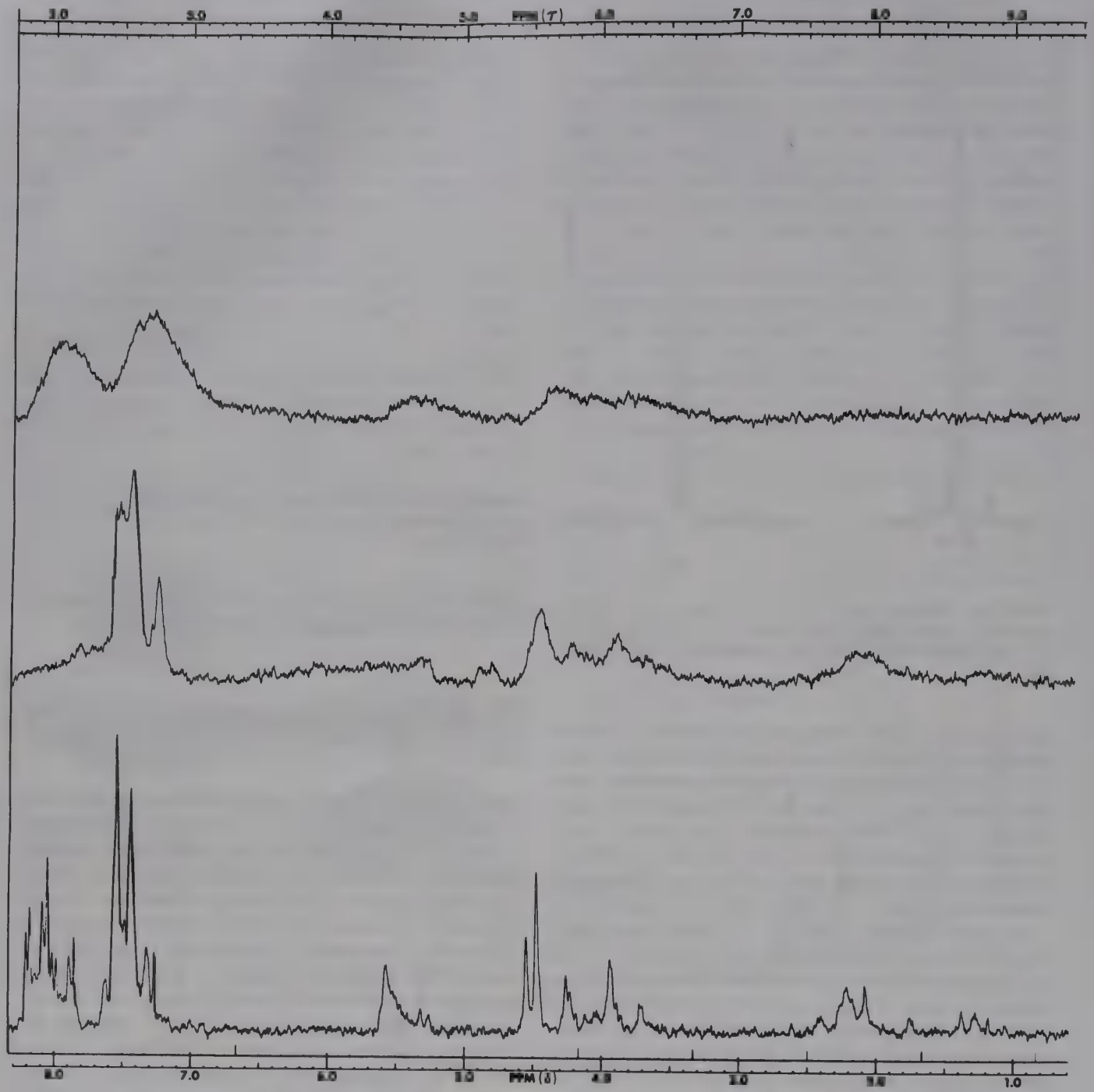

FIGURE 4.11. The effect of a tiny ferromagnetic particle on the proton resonance spectrum of a benzoylated sugar. The top and middle curves are repeated runs with the particle present; the bottom curve is the spectrum with the particle removed. (From Becker, E. D. *High Resolution NMR.* New York: Academic, 2nd ed., 1980. With permission.)

The degree of shielding depends on the density of the circulating electrons, and, as a first, very rough approximation, the degree of shielding of a proton on a carbon atom will depend on the inductive effect of other groups attached to the carbon atom. The difference in the absorption position of a particular proton from the absorption position of a reference proton is called the *chemical shift* of the particular proton.

We now have the concept that protons in "different" chemical environments have different chemical shifts. Conversely, protons in the "same" chemical environment have the same chemical shift. But what

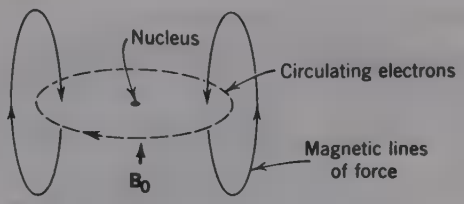

FIGURE 4.12. Diamagnetic shielding of nucleus by circulating electrons.

do we mean by "different" and "same"? While it is intuitively obvious that the chemically different methylene groups of $ClCH_2CH_2OH$ have different chemical shifts and that the protons in either one of the methylene groups have the same chemical shift, it may not be so obvious, for example, that the protons of the methylene group of $C_6H_5CH_2CHBrCl$ do not have the same chemical shift. For the present, we shall deal with obvious cases and postpone a more rigorous treatment of chemical shift equivalence to Section 4.7.

The most generally useful reference compound is tetramethylsilane (TMS).

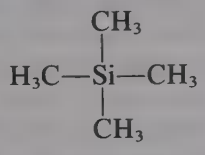

This has several advantages: it is chemically inert, symmetrical, volatile (bp. 27°C), and soluble in most organic solvents; it gives a single sharp absorption peak, and absorbs at higher field (shielded) than almost all organic protons. When water or deuterium oxide is the solvent, TMS can be used as an "external reference" in a concentric capillary. The methyl protons of sodium 2,2-dimethyl-2-silapentane-5-sulfonate (DSS)

$$(CH_3)_3SiCH_2CH_2CH_2SO_3Na$$

are sometimes used as an internal reference in aqueous solution. Acetonitrile and dioxane are also used as references in aqueous solution.

Let us set up an NMR scale (Fig. 4.13) and set the TMS peak at 0 Hz at the right-hand edge. The magnetic field increases toward the right. When chemical shifts are given in hertz (designated ν), the applied frequency must be specified. Chemical shifts can be expressed in dimensionless units, independent of the applied frequency, by dividing ν by the applied frequency and multiplying by 10^6. Thus, a peak at 60 Hz (ν 60) from TMS at an applied frequency of 60 MHz would be at δ 1.00 (δ scale).

$$\frac{60}{60 \times 10^6} \times 10^6 = \delta\ 1.00$$

Since δ units are expressed in parts per million, the expression ppm is often used. The same peak at an applied frequency of 100 MHz would be at 100 Hz but would still be at δ 1.00 or at 1.00 ppm.

$$\frac{100}{100 \times 10^6} \times 10^6 = \delta\ 1.00$$

An alternative system assigns a value of 10.00 for TMS, and describes chemical shifts in terms of τ values.

$$\tau = 10.00 - \delta$$

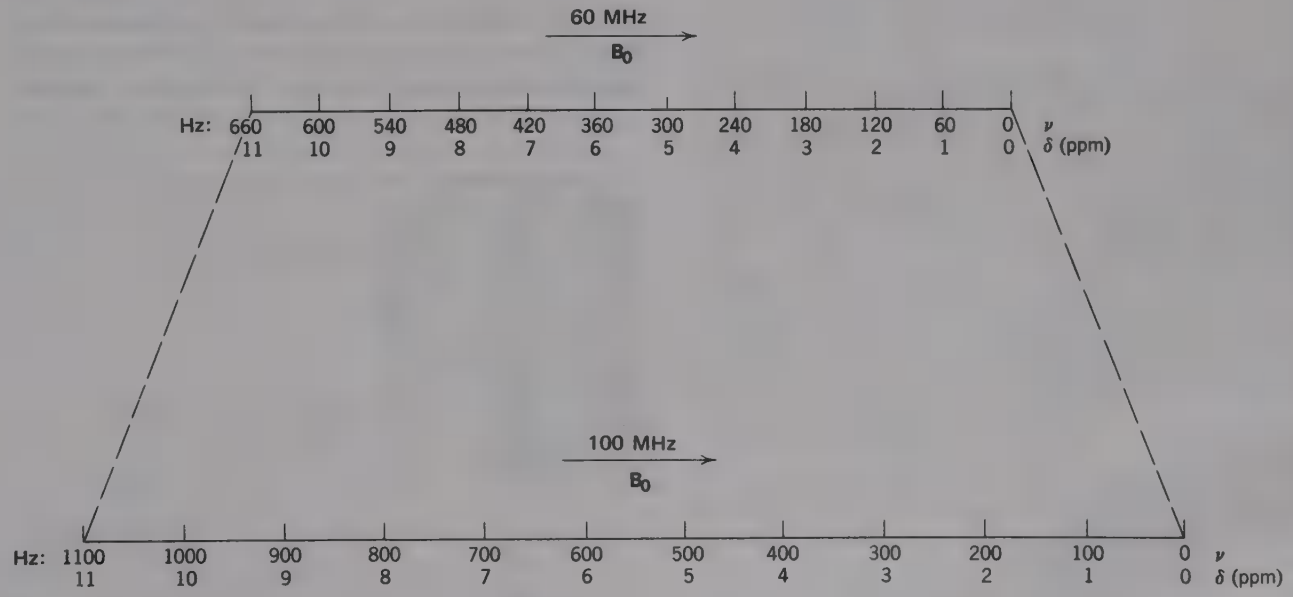

FIGURE 4.13. NMR Scale at 60 and 100 MHz. Higher magnetic field (more shielding) is to the right.

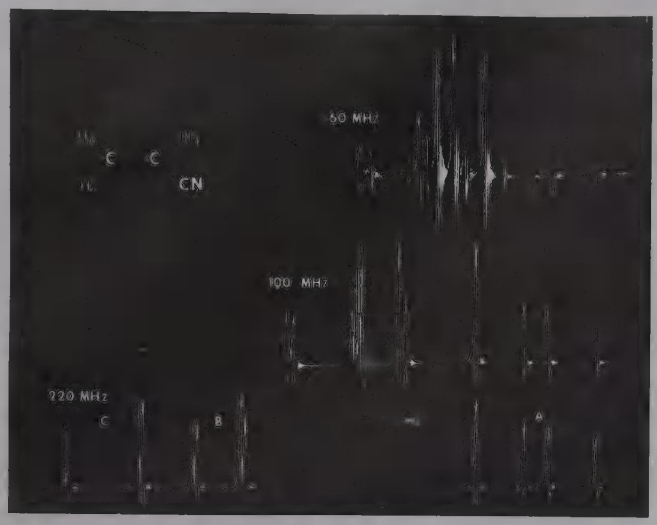

FIGURE 4.14. The 60-, 100-, and 220-MHz spectra of acrylonitrile. Reprinted from *Anal. Chem.* Copyright © 1971 by the American Chemical Society. Reprinted by permission of the copyright owner.

Shifts at higher field than TMS (δ 0.00, τ 10.00) will be encountered very rarely; δ values are then shown with a negative sign, and τ values merely increase numerically. The δ system is now used almost universally, and will be used here. The τ system in the older literature may cause confusion.

It is important to realize that the chemical shift in hertz is directly proportional to the strength of the applied field $\mathbf{B_0}$ and therefore to the applied frequency. This is understandable because the chemical shift is dependent on the diamagnetic shielding induced by $\mathbf{B_0}$. The strongest magnetic field consistent with field homogeneity should be used to spread out the chemical shifts. This is made clear in Figure 4.13 and in Figure 4.14 in which increased applied magnetic field in the NMR spectrum of acrylonitrile means increased separation of signals.

The concept of electronegativity is a dependable guide, up to a point, to chemical shifts. It tells us that the electron density around the protons of TMS is high (silicon is electropositive relative to carbon), and these protons will therefore be highly shielded and their peak will be found at high field. Since C is more electronegative than H, the sequence of proton absorptions in the series CH_4, RCH_3, R_2CH_2, and R_3CH is from more shielding to less (Chart A.1). We could make a number of good estimates as to chemical shifts, using concepts of electronegativity and proton acidity. For example, the following values are reasonable on these grounds:

Compound	δ
$(CH_3)_2O$	3.27
CH_3F	4.30
RCO_2H	~10.8

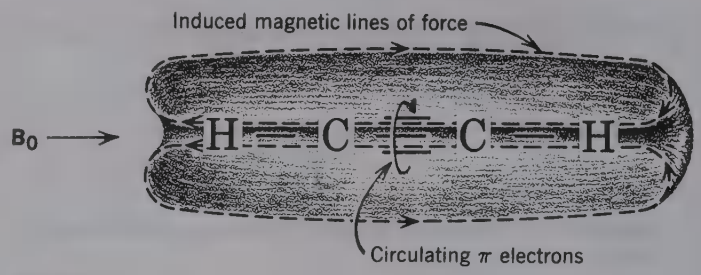

FIGURE 4.15. Shielding of alkyne protons.

But finding the protons of acetylene at δ 1.80, that is, more shielded than ethylene protons (δ 5.25), is unsettling. Finding the aldehydic proton of acetaldehyde at δ 9.97 definitely calls for some augmentation of the electronegativity concept. We shall use diamagnetic anisotropy to explain these and other apparent anomalies, such as the unexpectedly large deshielding effect of the benzene ring (benzene protons δ 7.27).

Let us begin with acetylene. The molecule is linear, and the triple bond is symmetrical about the axis. If this axis is aligned with the applied magnetic field, the π electrons of the bond can circulate at right angles to the applied field, thus inducing their own magnetic field opposing the applied field. Since the protons lie along the magnetic axis, the magnetic lines of force induced by the circulating electrons act to shield the protons (Fig. 4.15), and the NMR peak is found further upfield than electronegativity would predict. Of course, only a small number of the rapidly tumbling molecules are aligned with the magnetic field, but the overall average shift is affected by the aligned molecules.

This effect depends on diamagnetic anisotropy, which means that shielding and deshielding depend on the orientation of the molecule with respect to the applied magnetic field. Similar arguments can be adduced to rationalize the unexpected low-field position of the aldehydic proton. In this case, the effect of the applied magnetic field is greatest along the transverse axis of

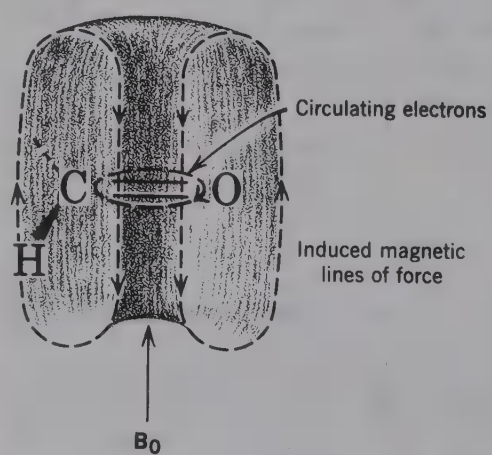

FIGURE 4.16. Deshielding of aldehydic protons.

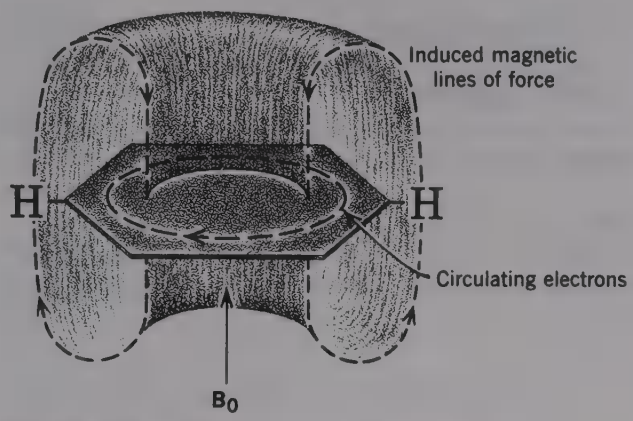

FIGURE 4.17. Ring current effects in benzene.

the C=O bond (i.e., in the plane of the page in Fig. 4.16). The geometry is such that the aldehydic proton, which lies in front of the page, is in the deshielding portion of the induced magnetic field. The same argument can be used to account for at least part of the rather large amount of deshielding of alkene protons.

The so-called "ring-current effect" is another example of diamagnetic anisotropy and accounts for the large deshielding of benzene ring protons. Figure 4.17 shows this effect. It also indicates that a proton held directly above or below the ring should be shielded. This has actually been found to be the case for some of the methylene protons in 1,4-polymethylenebenzenes.

All the ring protons of acetophenone are found downfield because of the ring current effect. Moreover, the ortho protons are shifted slightly further downfield (meta, para $\delta \sim 7.40$, ortho $\delta \sim 7.85$) because of the additional deshielding effect of the carbonyl group. In Figure 4.18 the carbonyl bond and the benzene ring are coplanar. If the molecule is oriented so that the applied magnetic field $\mathbf{B_0}$ is perpendicular to the plane of the molecule, the circulating π electrons of the C=O bond shield the conical zones above and below them, and deshield the lateral zones in which the ortho proton is located. Both ortho protons are equally deshielded since another, equally populated, conformation can be written in which the "left-hand" ortho proton is de-

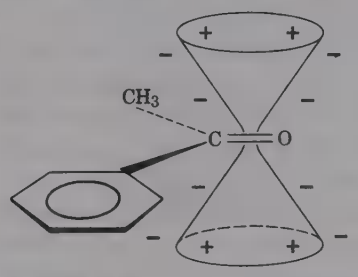

FIGURE 4.18. Shielding (+) and deshielding (−) zones of acetophenone.

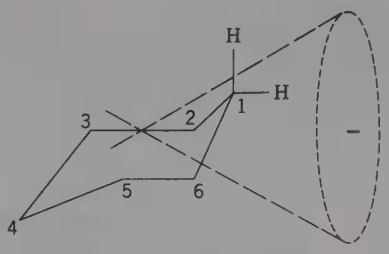

FIGURE 4.19. Deshielding of equatorial proton of a rigid six-membered ring.

shielded by the anisotropy cone. Nitrobenzene shows a similar effect.

A spectacular example of shielding and deshielding by ring currents is furnished by some of the annulenes.

At low temperatures, the protons outside the ring of [18]annulene are strongly deshielded (δ 9.3) and those inside are strongly shielded (δ −3.0, i.e., upfield of TMS).

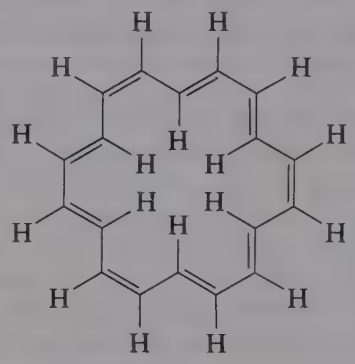

[18]Annulene

Demonstration of such a ring current is probably the best evidence available for aromaticity.

In contrast with the striking anisotropic effects of circulating π electrons, the σ electrons of a C—C bond produce a small effect. The axis of the C—C bond is the axis of the deshielding cone (Fig. 4.19). The observation that an equatorial proton is consistently found further downfield by 0.1–0.7 ppm than the axial proton on the same carbon atom in a rigid six-membered ring can thus be rationalized. The axial and equatorial protons on C_1 are oriented similarly with respect to C_1—C_2 and C_1—C_6, but the equatorial proton is within the deshielding cone of the C_2—C_3 bond (and C_5—C_6).

Extensive tables and charts of chemical shifts in the appendices give the useful impression that chemical shifts of protons in organic compounds fall roughly into eight regions as shown in Figure 4.20.

To demonstrate the use of some of the material in the appendices, we predict the chemical shifts of the protons in benzyl acetate (Fig. 4.21).

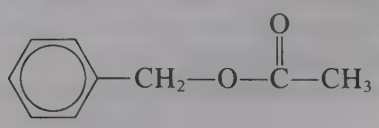

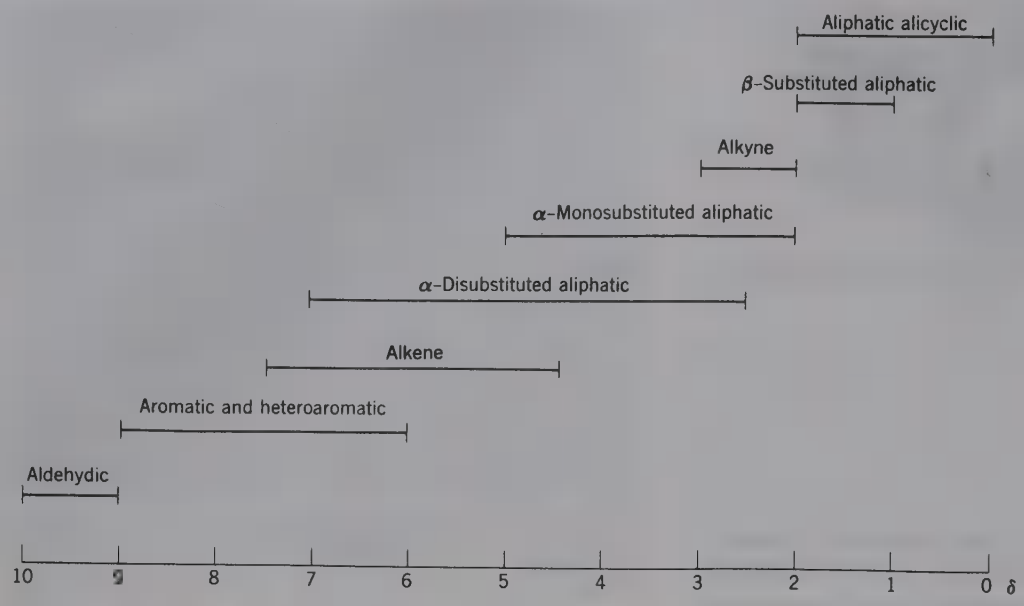

FIGURE 4.20. General regions of chemical shifts.

In Chart A.1, we see that the chemical shift of the CH_3 group is $\sim\delta$ 2.0. In the "mileage chart", Chart B.1, the CH_2 group is at $\sim\delta$ 5.08. In Chart D.1, the aromatic protons are at $\sim\delta$ 7.2. In the spectrum of benzyl acetate (Fig. 4.21), we see three sharp peaks from right to left at δ 1.96, δ 5.00, and δ 7.22; the integration steps are in the ratio 3:2:5 corresponding to CH_3, CH_2, and five-ring protons. The peaks are all singlets. This means that the CH_3 and CH_2 groups are isolated; that is, there are no protons on the adjacent carbon atoms for coupling (see Section 4.4). But there is a problem with the apparent singlet representing the ring protons, which are not chemical shift equivalent (Section 4.7.1) and do couple with one another. In fact, at higher resolution, we would see a multiplet rather than an apparent singlet.

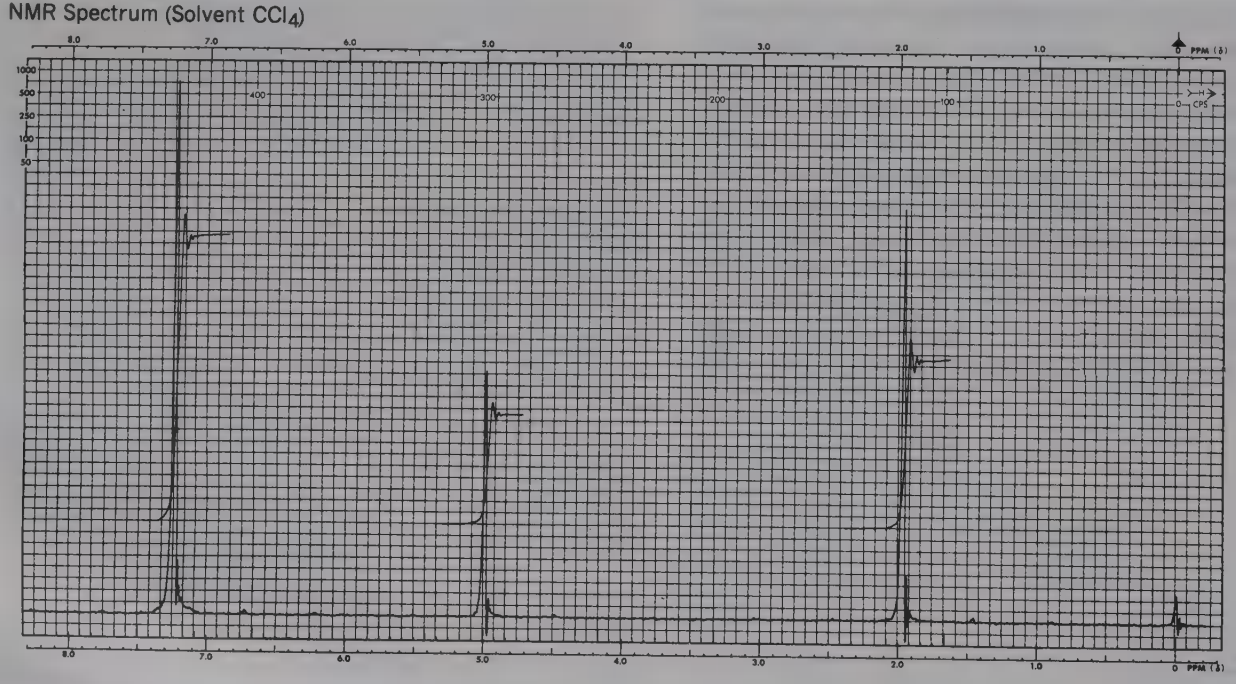

FIGURE 4.21. NMR spectrum of benzylacetate in carbon tetrachloride at 60 MHz.

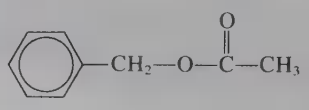

We point out again that an appreciation of the concepts of electronegativity (inductive effects) and of electron delocalization—combined with an understanding of diamagnetic anisotropy—permits both rationalization and prediction of chemical shift. Several examples make the point:

1. The β proton of an α,β-unsaturated ketone is further downfield than the α proton because delocalization results in a lower electron density at the β proton.

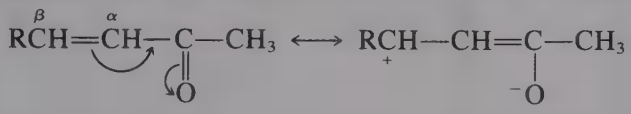

2. The β proton of a vinylic ether is further upfield than the α proton because of a higher electron density.

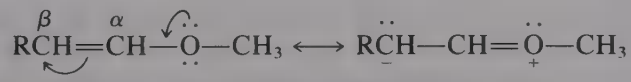

3. The shifts of protons ortho, meta, or para to a substituent on an aromatic ring are correlated with electron densities and with the effects of electrophilic reagents (Chart D.1). For example, the ortho and para protons of phenol are at higher field because of the higher electron density that also accounts for the predominance of ortho and para substitution by electrophilic reagents. Conversely, the ortho and para protons of nitrobenzene are deshielded and thus are at lower field.

4.4. SIMPLE SPIN COUPLING

We have obtained a series of absorption peaks representing protons in different chemical environments, each absorption area being proportional to the number of protons it represents. We have now to consider one further phenomenon, spin coupling. This can be described as the indirect coupling of proton spins through the intervening bonding electrons. Very briefly, it occurs because there is some tendency for a bonding electron to pair its spin with the spin of the nearest proton; the spin of a bonding electron having been thus influenced, the electron will affect the spin of the other bonding electron, and so on, through to the next proton. Coupling is ordinarily not important beyond three bonds unless there is ring strain as in small rings or bridged systems, or bond delocalization as in aromatic or unsaturated systems.

Suppose that two vicinal protons are in very different chemical environments from one another as in the compound $RO—\underset{|}{\overset{OR}{CH}}—\underset{|}{\overset{CR_3}{CH}}—CR_3$. Each proton will give rise to an absorption, and the absorptions will be quite widely separated, but the spin of each proton is affected slightly by the two orientations of the other proton through the intervening electrons so that each absorption appears as a doublet (Fig. 4.22). The frequency difference between the component peaks of a doublet is proportional to the effectiveness of the coupling and is denoted by a coupling constant, J, which is independent of the applied magnetic field $\mathbf{B_0}$. Whereas chemical shifts usually range over about 1250 Hz at 100 MHz, coupling constants between protons rarely exceed 20 Hz (see Appendix F).

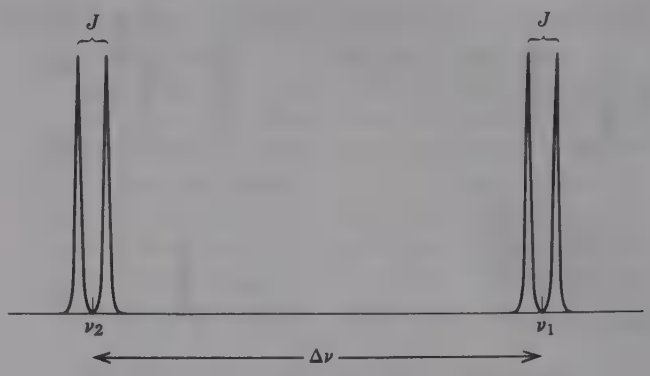

FIGURE 4.22. Spin coupling between two protons with very different chemical shifts.

So long as the chemical shift difference in hertz ($\Delta\nu$) is much larger than the coupling constant ($\Delta\nu/J$ is greater than about 10), the simple pattern of two doublets appears. As $\Delta\nu/J$ becomes smaller, the doublets approach one another, the inner two peaks increase in intensity, and the outer two peaks decrease (Fig. 4.23). The shift position of each proton is no longer midway between its two peaks as in Figure 4.22 but is at the "center of gravity" (Fig. 4.24); it can be estimated with fair accuracy by inspection or determined precisely by the following formula in which the peak positions (1, 2, 3, and 4 from left to right) are given in hertz from TMS.

$$(1 - 3) = (2 - 4) = \sqrt{(\Delta\nu)^2 + J^2}$$

The shift position of each proton is $\Delta\nu/2$ from the midpoint of the pattern. When $\Delta\nu = J\sqrt{3}$, the two pairs could be mistaken for a quartet, which results from splitting by three equivalent vicinal protons (Fig. 4.23*d* is almost at this stage). Failure to note the small outer peaks (i.e., 1 and 4) may lead to mistaking the two large inner peaks for a doublet (Fig. 4.23*e*). When the chemical shift difference becomes zero, the middle peaks coalesce to give a single peak, and the end peaks vanish; that is, the protons are equivalent. (Equivalent protons do spin couple with one another, but splitting is not observed.)

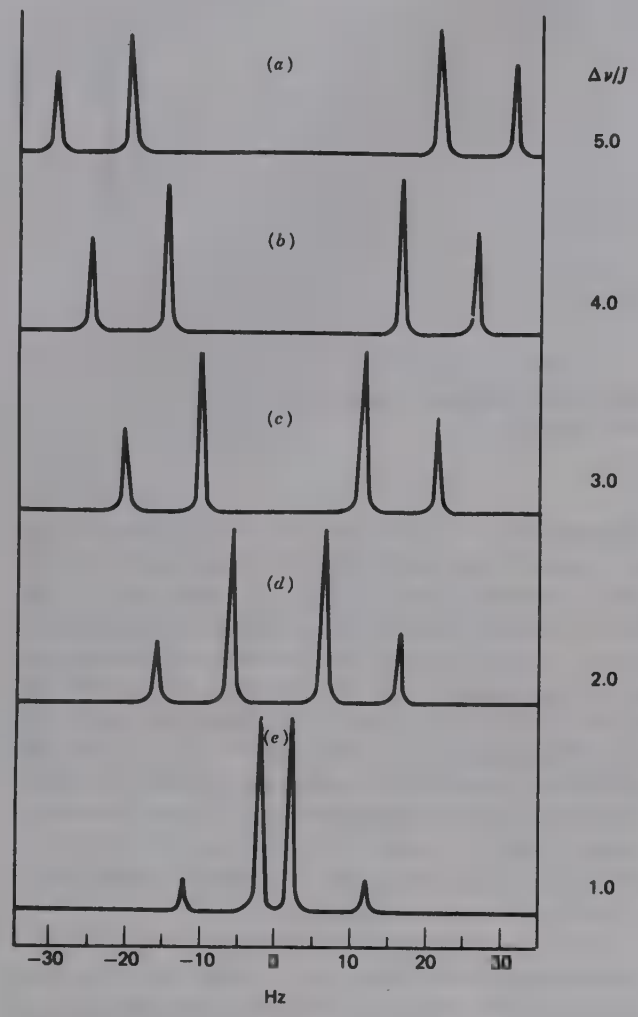

FIGURE 4.23. A two-proton system spin coupling with a decreasing difference in chemical shifts and a large J value (10 Hz); the difference between AB and AX notation is explained in the text (p. 179).

Note that the inner lines of coupled protons merge but do not cross. A further point to be noted is the obvious one that the spacing between the peaks of two coupled multiplets is the same.

The dependence of chemical shift on the applied magnetic field and the independence of the spin coupling afford a method of distinguishing between them. The spectrum is merely run on two different instruments, for example, at 100 and 300 MHz. Chemical shifts are also solvent dependent, but J values are usually only slightly affected by change of solvent, at least to a far lesser degree than are chemical shifts.

FIGURE 4.24. "Center of gravity," instead of linear midpoints, for shift position location (due to "low" $\Delta\nu/J$ ratio).

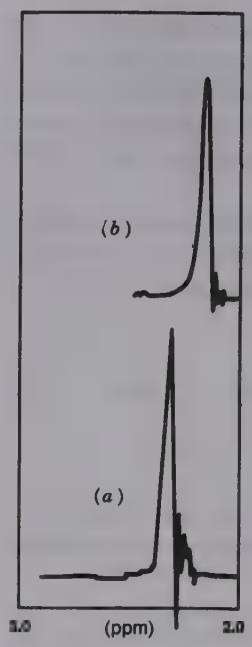

FIGURE 4.25. The NMR spectrum of biacetyl(2,3-butanedione): (*a*) in $CDCl_3$; (*b*) in C_6D_6.

The chemical shifts of the methyl and alkyne protons of methylacetylene are (fortuitously) coincident (δ 1.80) when the spectrum is obtained in a $CDCl_3$ solvent, whereas the spectrum of a neat sample of this alkyne shows the alkyne proton at δ 1.80 and the methyl protons at δ 1.76. Figure 4.25 illustrates the chemical shift dependence of the protons of biacetyl on solvent. The change from a chlorinated solvent (e.g., $CDCl_3$) to an aromatic solvent (e.g., C_6D_6) often drastically influences the position and appearance of NMR signals.

Look at the next stage in complexity of spin coupling (Fig. 4.26). Consider the system —HC—CH_2— in the

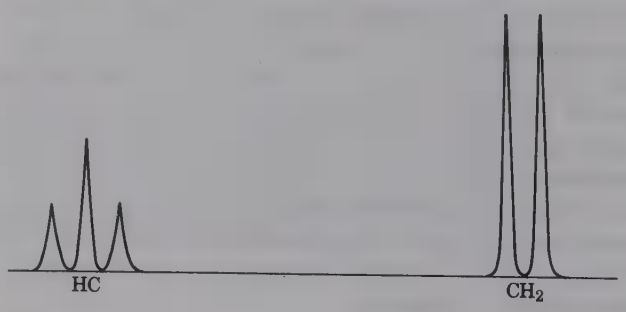

FIGURE 4.26. Spin coupling between CH and CH_2 with very different chemical shifts.

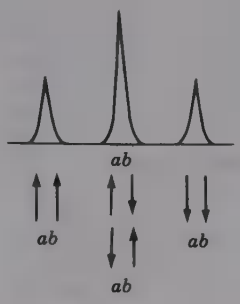

FIGURE 4.27. Energy levels for the three spin states of the methylene group (protons *a* and *b*) that produce the triplet shown in Figure 4.26.

compound RO—CH(OR)—CH_2—CR_3 in which the single methine proton is in a very different chemical environment from the two methylene protons. As before, we see two sets of absorptions widely separated, and now the absorption areas are in the ratio of 1:2. The methine proton couples with the methylene protons and splits the methylene proton absorption into a symmetrical doublet, as explained above. The two methylene protons split the methine proton absorption into a triplet because three combinations of proton spins exist in the two methylene protons (*a* and *b*) of Figure 4.27. Since there are two equivalent combinations of spin that do not produce any net opposing or concerted field relative to the applied field, there is an absorption of relative intensity two at the center of the multiplet. Since there are single pairs, respectively, opposed and in concert with the applied field, there are equally spaced lines of relative intensity one upfield and one downfield from the center line. In summary, the intensities of the peaks in the triplet are in the ratio 1:2:1.

When the methine and methylene protons in the system —CH—CH_2— are in similar environments (i.e., $\Delta\nu/J$ is small), the simple doublet–triplet pattern degenerates to a complex pattern of from seven to nine lines as a result of second-order splitting; analysis by inspection is no longer possible, since the peak spacings may not correspond to the coupling constants.

Simple splitting patterns that are produced by the coupling of protons that have very different chemical shifts ($\Delta\nu/J$ is greater than about 10 or so) are called *first-order* splitting patterns. These can usually be interpreted by using two rules.

1. Splitting of a proton absorption is done by neighboring protons, and the multiplicity of the split is determined by the number of these protons. Thus, one proton causes a doublet, and two equally coupled neighboring protons cause a triplet. The multiplicity then is $n + 1$, n being the number of neighboring equally coupled protons. The general formula, which covers all nuclei, is $2nI + 1$, I being the spin number.
2. The relative intensities of the peaks of a multiplet also depend on n. We have seen that doublet ($n = 1$) peaks are in the ratio 1:1, and triplet peaks are in the ratio 1:2:1. Quartets are in the ratio 1:3:3:1. The general formula is $(a + b)^n$; when this is expanded to the desired value of n, the coefficients give the relative intensities. The multiplicity and relative intensities may be easily obtained from Pascal's triangle (Fig. 4.28), in which n is the number of equivalently coupled protons.

In the Pople notation,* we place protons that have the same chemical shift into sets (see Section 4.7), and we designate sets of protons separated by a small chemical shift with the letters A, B, and C, and sets separated by a large chemical shift ($\Delta\nu/J > \sim 10$) with the letters A, M, and X. The number of protons in each set is denoted by a subscript number. Thus, the first case we examined (Fig. 4.22) is an AX system. The second case (Fig. 4.24 is an AB system, and the third case (Fig. 4.26) is an A_2X system. As $\Delta\nu/J$ decreases, the A_2X system approaches an A_2B system, and the simple first-order splitting of the A_2X system becomes more complex (see Section 4.7).

Thus far, we have dealt with two sets of protons; every proton in each set is equally coupled to every proton in the other set, that is, a single coupling constant is involved. Given these conditions and the conditions that $\Delta\nu/J$ be large (~ 10), the two rules above apply, and we obtain a first-order pattern. In general, these are the A_aX_x systems (a and x are the number of protons in each set); the first-order rules apply only to these systems, but as we have seen, there is a gradual change in the appearances of spectra changing from an AX to an AB pattern. In a similar way, it is frequently possible to relate complex patterns back to first-order patterns. With practice, a fair amount of deviation from first order may be tolerated. Wiberg's and Bovey's collections of calculated spectra can be used to match fairly complex splitting patterns (see the reference section).

A system of three sets of protons, each set separated by a large chemical shift, can be designated $A_aM_mX_x$. If two sets are separated from each other by a small chemical shift, and the third set is widely separated from the other two, we use an $A_aB_bX_x$ designation. If all shift positions are close, the system is $A_aB_bC_c$. Both end sets may be coupled to the middle set with the same or different coupling constants, whereas the end sets may or may not be coupled to one another. The AMX systems are first order; ABX systems approximate first order, but ABC systems cannot be analyzed

*J. A. Pople, W. G. Schneider, H. J. Bernstein. *High Resolution NMR*. New York: McGraw–Hill, 1959.

n	Relative Intensity
0	1
1	1 1
2	1 2 1
3	1 3 3 1
4	1 4 6 4 1
5	1 5 10 10 5 1
6	1 6 15 20 15 6 1
7	1 7 21 35 35 21 7 1
8	1 8 28 56 70 56 28 8 1

FIGURE 4.28. Pascal's triangle. Relative intensities of first-order multiplets; n = No. of equivalent coupling nuclei of spin $\frac{1}{2}$ (e.g., protons).

by inspection. These more complex patterns are treated in Section 4.8.

We can now appreciate the three main features of an NMR spectrum: chemical shifts, peak intensities, and spin couplings that are first order or that approximate first-order patterns. We can now analyze first-order NMR spectra.

The 60 MHz NMR spectrum of ethyl chloride is shown in Figure 4.29. The peak at δ 0.00 is the internal reference TMS and that at δ 7.25 is the $CHCl_3$ impurity in the $CDCl_3$ solvent. The methylene group (α)

$$\overset{\beta}{CH_3}—\overset{\alpha}{CH_2}—Cl$$

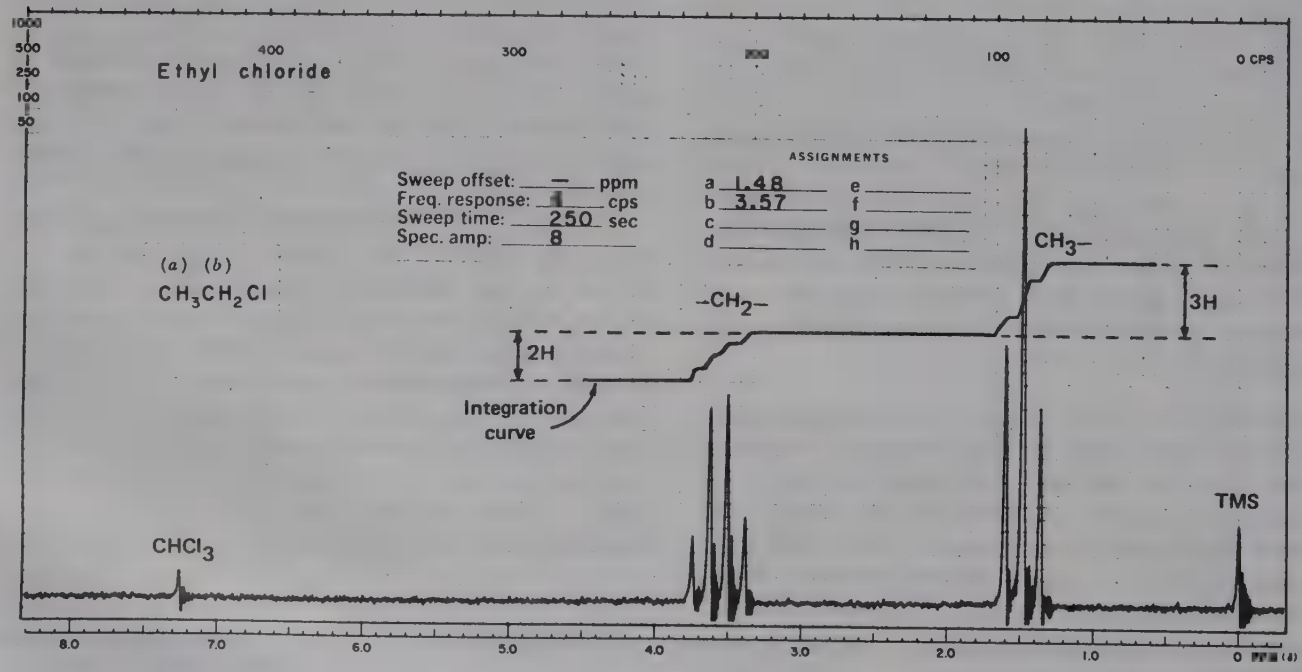

FIGURE 4.29. Ethyl chloride in $CDCl_3$ at 60 MHz. (Courtesy of Varian Associates, Palo Alto, CA.)

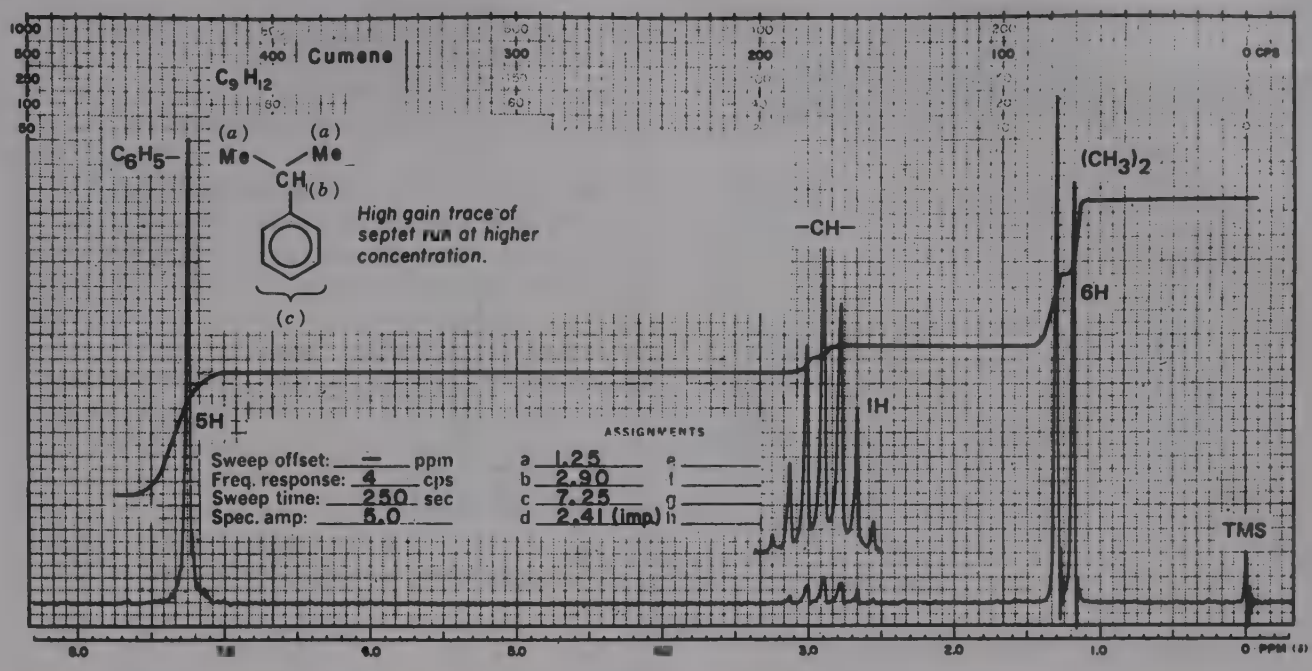

FIGURE 4.30. Cumene in $CDCl_3$ at 60 MHz. (Courtesy of Varian Associates, Palo Alto, CA.)

(δ 3.57) is more deshielded by the chlorine than is the methyl group (δ 1.48), and thus the methylene group is downfield (higher δ) from the methyl by 2.09 ppm or about 125 Hz. Since the coupling is about 9 Hz, $\Delta\nu/J$ is about 14, a large enough ratio for first-order analysis. The system is A_3X_2, and the first-order rules correctly predict a triplet and a quartet with relative intensities (see integration "steps") of 3:2 corresponding to the number of protons causing the absorptions. Note that even at $\Delta\nu/J = 14$ there is a "leaning" of the two interacting signals toward each other; that is, the intensity of the upfield lines of the methylene signal and the downfield lines of the methyl signal are somewhat larger than they would be if these signals were perfectly symmetrical. This fact, together with the same spacing in both multiplets, is valuable in identifying interacting proton signals in more complex spectra.

We stated earlier that "the peak area (measured by the integrator) is proportional to the number of protons it represents." The "steps" in the integration curve in Figure 4.29 thus provide the ratios of the different kinds of protons in the molecule. This count can be compared with the proton count obtained from the off-resonance decoupled ^{13}C spectrum (Chapter 5).

Consider the NMR spectrum of cumene in Figure 4.30. The five aromatic protons, δ 7.25, although actually not chemical shift equivalent (see Section 4.7), are fortuitously equivalent and occur as a single absorption downfield from the remaining absorptions (because of the benzene ring current, Fig. 4.16). The side chain is treated as an A_6X system. The methyl signal occurs as a doublet at δ 1.25, the methine proton as a 1:6:15:20:15:6:1 septet at δ 2.90. Note that this signal is completely seen only when the sample is run at high gain (upper lines). Outer lines of complex multiplets may be overlooked, especially when these lines are part of a single proton absorption and when base line noise is substantial.

The vicinal coupling described (H—C—C—H) involves three bonds and can be designated by J_{HCCH} or ^3J. When geminal protons are not chemical shift equivalent to one another (Section 4.7), we see coupling designated as J_{HCH} or ^2J.

4.5. PROTONS ON HETEROATOMS

Protons on a heteroatom differ from protons on a carbon atom in that: (1) they are exchangeable, (2) they are subject to hydrogen bonding, and (3) they are subject to partial or complete decoupling by electrical quadrupole effects of some heteroatoms. Shift ranges for protons on heteroatoms are given in Appendix E.

4.5.1. Protons on Oxygen

4.5.1.1. Alcohols

Unless special precautions are taken (see below) the spectrum of neat ethanol usually shows the hydroxylic proton as a slightly broadened peak at δ 5.35. At the commonly used concentration of about 5–20% in a nonpolar solvent, such as carbon tetrachloride or deu-

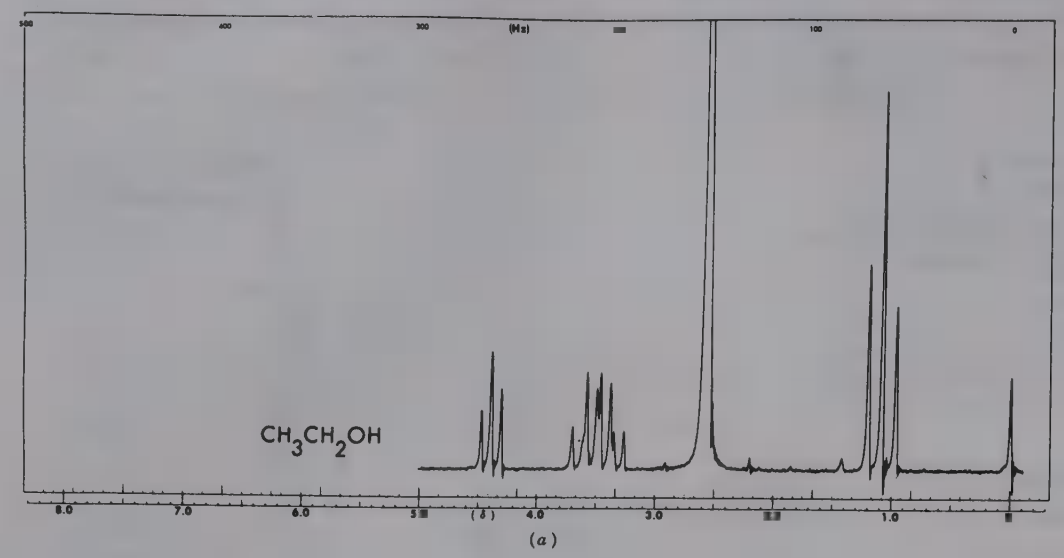

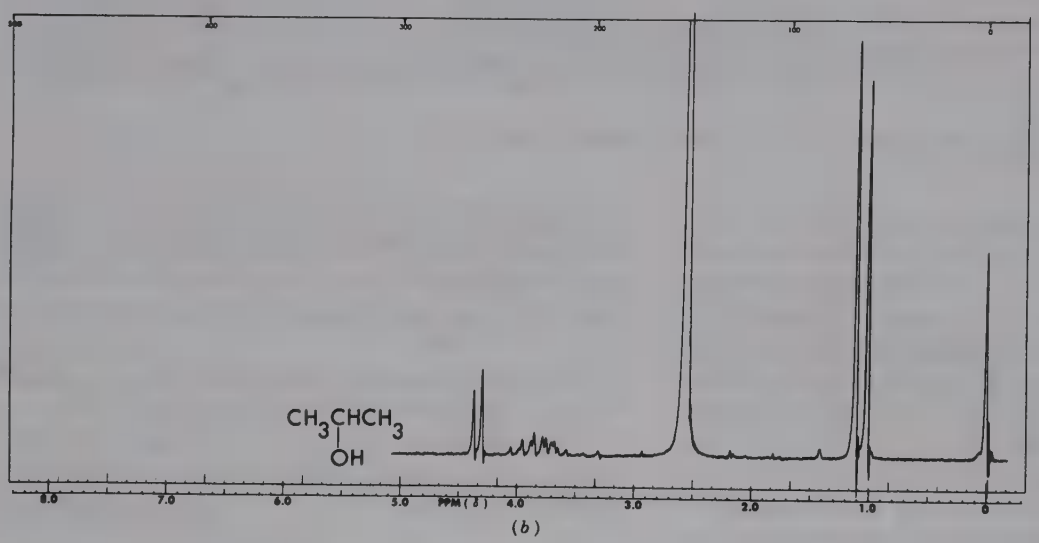

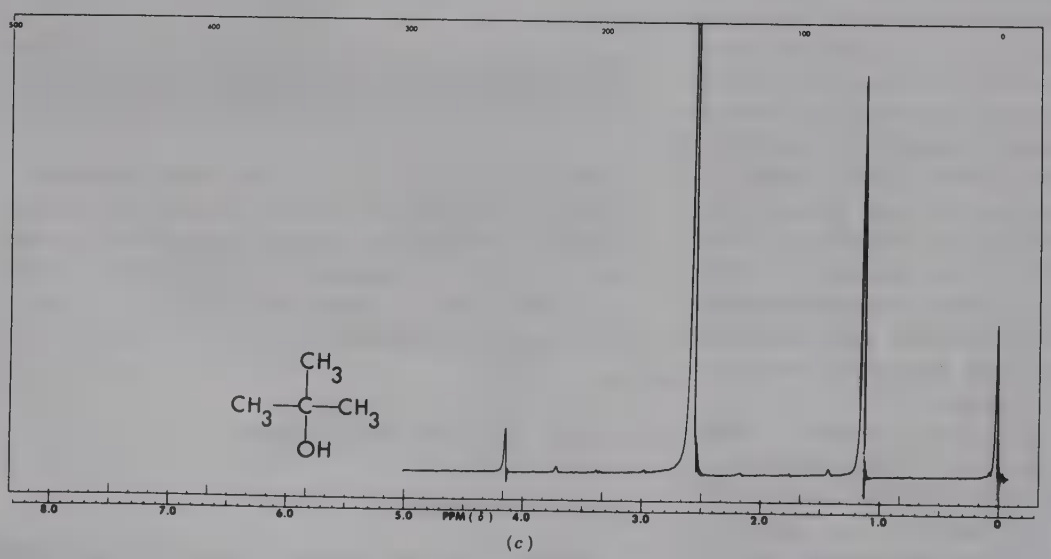

FIGURE 4.31. NMR spectra of typical (*a*) primary, (*b*) secondary, and (*c*) tertiary alcohols run in DMSO. Absorption at δ 2.6 is due to DMSO.

Source: Daniel J. Pasto and Carl R. Johnson, *Organic Structure Determination,* copyright © 1969, pp. 358–359. (Reprinted by permission of Prentice–Hall, Englewood Cliffs, NJ.)

terochloroform, the hydroxylic peak is found between δ 2 and δ 4. On extrapolation to infinite dilution or in the vapor phase, the peak is near δ 0.5. A change in solvent or temperature will also shift the hydroxylic peak.

Hydrogen bonding explains why the shift position of the hydroxylic proton depends on concentration, temperature, and solvent. Hydrogen bonding decreases the electron density around the proton, and thus moves the proton absorption to lower field. The extent of intermolecular hydrogen bonding is decreased by dilution with a nonpolar solvent and with increased temperature. Polar solvents introduce the additional complication of hydrogen bonding between the hydroxylic proton and the solvent. Intramolecular hydrogen bonds are less affected by their environment than are intermolecular hydrogen bonds. In fact the enolic, hydroxylic absorption of β-diketones

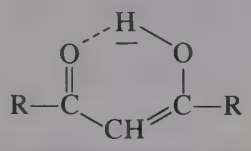

for example, is hardly affected by change of concentration or solvent, though it can be shifted upfield somewhat by warming. Nuclear magnetic resonance spectrometry is a powerful tool for studying hydrogen bonding.

Exchangeability explains why the hydroxylic peak of ethanol is usually seen as a singlet. Under ordinary conditions, enough acidic impurities are present in solution to catalyze rapid exchange of the hydroxylic proton. The proton is not on the oxygen atom long enough for it to be affected by the three states of the methylene protons, and there is no coupling. The rate of exchange can be decreased by treating the solvent with anhydrous sodium carbonate, alumina, or molecular sieves immediately before obtaining the spectrum. Purified deuterated DMSO or acetone, in addition to allowing a lower rate of exchange, shifts the hydroxylic proton to lower field, even in dilute solution, by hydrogen bonding between solute and solvent.* Since the hydroxylic proton can now couple with the protons on the α carbon, a primary alcohol will show a triplet, a secondary alcohol a doublet, and a tertiary alcohol a singlet. This is illustrated in Figure 4.31, and a list of successful applications is given in Table 4.1. Exceptions have been reported, but these may be due to the concentration dependence of this phenomenon. At intermediate rates of exchange, the multiplet merges into a broad absorption band; at this point, the exchange rate in hertz is equal to approximately $\pi J/\sqrt{2}$.

If water is present in the alcohol solution, rapid interchange results in a single peak at a position intermediate between the actual shift positions of the HOH and ROH peaks. Of course, the presence of water is reflected in the integration for the single peak.

TABLE 4.1

Hydroxyl Proton Resonances in DMSO

Compound[a]	Chemical Shift (δ)	Multiplicity
Methanol	4.08	q
Ethanol	4.35	t
2-Propanol	4.35	d
2-Methyl-2-propanol	4.16	s
2-Methyl-2-butanol	3.99	s
Propylene glycol, 1-OH	4.45	t
2-OH	4.38	d
Cyclohexanol	4.38	d
cis-4-*t*-Butylcyclohexyl alcohol	4.11	d
trans-4-*t*-Butylcyclohexyl alcohol	4.45	d
Benzyl alcohol	5.16	t
Phenol	9.25	s
β-L-Arabinopyranose, O—C—OH	5.98	d
α-D-Glucopyranose, O—C—OH	6.16	d
α-D-Fructopyranose, O—C—OH	5.12	s

[a] All spectra were taken of DMSO solutions with concentrations 10 mol % or less.

Source: O. L. Chapman and R. W. King, *J. Am. Chem. Soc.*, **86**, 1256 (1964).

A dihydroxy alcohol may show separate absorption peaks for each hydroxylic proton; in this case, the rate of exchange in hertz is much less than the difference in hertz between the separate absorptions. As the rate increases (trace of acid catalyst), the two absorption peaks broaden, then merge to form a single broad peak; at this point, the exchange rate in hertz is equal to the original separation in hertz. As the rate increases, the single peak becomes sharper. The relative position of each peak depends on the extent of hydrogen bonding of each hydroxylic proton; steric hindrance to hydrogen bonding frequently accounts for a relative upfield absorption.

The spectrum of a compound containing exchangeable protons can be simplified, and the exchangeable proton absorption removed, simply by shaking the solution with excess deuterium oxide or by obtaining a spectrum in deuterium oxide solution if the compound is soluble. A peak due to HOD will appear, generally between δ 5 and δ 4.5 in nonpolar solvents, and near δ 3.3 in DMSO (see Appendix E). A $CDCl_3$ or CCl_4 solution in the NMR tube may be shaken vigorously

*O. L. Chapman and R. W. King, *J. Am. Chem. Soc.*, **86**, 1256 (1964). D. E. McGreer and M. M. Mocek, *J. Chem. Educ.* **40**, 358 (1963).

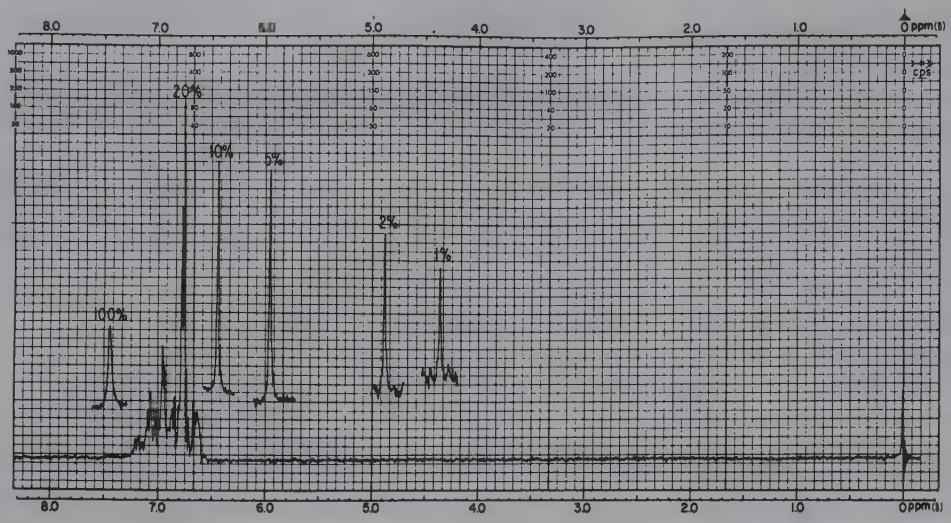

FIGURE 4.32. Phenol, in CCl_4, at various w/v %, at 60 MHz. Complete sweep is at 20%; single absorptions represent the OH proton at the indicated w/v %.

Source: J. R. Dyer, *Applications of Absorption Spectroscopy of Organic Compounds,* copyright © 1965, p. 90. Reprinted by permission of Prentice–Hall, Inc., Englewood Cliffs, NJ.

for several seconds with 1 or 2 drops of D_2O, and the mixture allowed to stand (or centrifuged) until the layers are clearly separated. The top aqueous layer does not interfere.

Acetylation or benzoylation of a hydroxyl group moves the absorption of the carbinyl protons of a primary alcohol downfield about 0.5 ppm, and that of a secondary alcohol about 1.0–1.2 ppm. Such shifts provide a confirmation of the presence of a primary or secondary alcohol.

4.5.1.2. Water

Aside from the problems of exchangeability, as just discussed, water is an ubiquitous impurity that faithfully obeys Murphy's law by interfering with critically important peaks. "Bulk" water as suspended droplets or wall films gives a peak at $\sim\delta$ 4.7 in $CDCl_3$ (HOD occurs in the D_2O exchange experiment mentioned previously). Dissolved (monomeric) water absorbs at $\sim\delta$ 1.5 in $CDCl_3$ and can be a serious interference in a critical region of the spectrum in dilute solutions.* Use of C_6D_6 (H_2O at δ 0.4) avoids this interference. A table of water peaks in the common deuterated solvents appears in Appendix E.

4.5.1.3. Phenols

The behavior of a phenolic proton resembles that of an alcoholic proton. The phenolic proton peak is usually a sharp singlet (rapid exchange, no coupling), and its range, depending on concentration, solvent, and temperature, is generally downfield ($\delta \sim 7.5$–$\delta \sim 4.0$) compared with the alcoholic proton. This is illustrated in Figure 4.32. Note the concentration dependence of the OH peak. A carbonyl group in the ortho position shifts the phenolic proton absorption downfield to the range of about δ 12.0–δ 10.0 because of intramolecular hydrogen bonding. Thus, *o*-hydroxyacetophenone shows a peak at about δ 12.05 almost completely invariant with concentration. The much weaker intramolecular hydrogen bonding in *o*-chlorophenol explains its shift range ($\delta \sim 6.3$ at 1 *M* concentration to $\delta \sim 5.6$ at infinite dilution), which is broad compared with that of *o*-hydroxyacetophenone but narrow compared with that of phenol.

4.5.1.4. Enols

Enols are usually stabilized by intramolecular hydrogen bonding, which varies from very strong in aliphatic β-diketones to weak in cyclic α-diketones. The enolic proton is downfield relative to alcohol protons and, in the case of the enolic form of some β-diketones, may be found as far downfield as δ 16.6 (the enolic proton of acetylacetone absorbs at δ 15.0 and that of dibenzoylmethane at δ 16.6). The enolic proton peak is frequently broad at room temperature because of slow exchange. Furthermore, the keto–enol conversion is slow enough so that absorption peaks of both forms can be observed, and the equilibrium measured.

*F. X. Webster and R. M. Silverstein *Aldrichimica Acta* **18** (No. 3), 58 (1985).

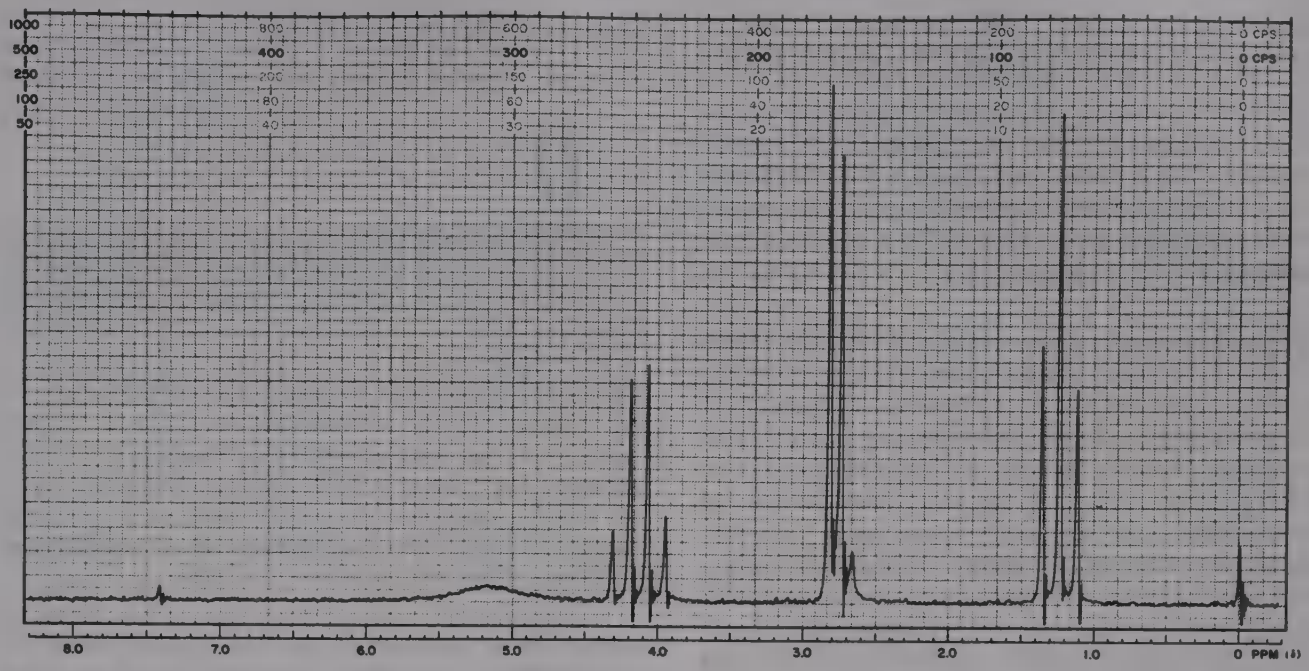

FIGURE 4.33. Ethyl *N*-methylcarbamate, $CH_3NHCOCH_2CH_3$, at 60 MHz.

When strong intramolecular bonding is not involved, the enolic proton absorbs in about the same range as the phenolic proton.

4.5.1.5. Carboxylic Acids

Carboxylic acids exist as stable hydrogen-bonded dimers in nonpolar solvents even at high dilution. The carboxylic proton therefore absorbs in a characteristically narrow range $\delta \sim 13.2$–$\delta \sim 10.0$ and is affected only slightly by concentration. Polar solvents partially disrupt the dimer and shift the peak accordingly.

The peak width at room temperature ranges from sharp to broad, depending on the exchange rate of the particular acid. The carboxylic proton exchanges quite rapidly with protons of water and alcohols (or hydroxyl groups of hydroxy acids) to give a single peak whose position depends on concentration. Sulfhydryl or enolic protons do not exchange rapidly with carboxylic protons, and individual peaks are observed.

4.5.2. Protons on Nitrogen

The ^{14}N nucleus has a spin number I of 1 and, in accordance with the formula $2I + 1$, should cause a proton attached to it and a proton on an adjacent carbon atom to show three equally intense peaks. There are two factors, however, that complicate the picture: the rate of exchange of the proton on the nitrogen atom and the electrical quadrupole moment of the ^{14}N nucleus.

The proton on a nitrogen atom may undergo rapid, intermediate, or slow exchange. If the exchange is rapid, the NH proton(s) is decoupled from the N atom and from protons on adjacent carbon atoms. The NH peak is therefore a sharp singlet, and the adjacent CH protons are not split by NH. Such is the case for most aliphatic amines.* At an intermediate rate of exchange, the NH proton is partially decoupled, and a broad NH peak results. The adjacent CH protons are not split by the NH proton. Such is the case for *N*-methyl-*p*-nitroaniline. If the NH exchange rate is low, the NH peak is still broad because the electrical quadrupole moment of the nitrogen nucleus induces a moderately efficient spin relaxation and, thus, an intermediate lifetime for the spin states of the nitrogen nucleus. The proton thus sees three spin states of the nitrogen nucleus (spin number = 1), which are changing at a moderate rate, and the proton responds by giving a broad peak. In this case, coupling of the NH proton to the adjacent protons is observed. Such is the case for pyrroles, indoles, secondary and primary amides, and carbamates (Fig. 4.33). Note that H—N—C—H coupling takes place through the C—H, C—N, and N—H bonds, but coupling between nitrogen and protons on adjacent carbon atoms is negligible. The proton-proton coupling is observed in the signal due to hydrogen on carbon; the N—H proton signal is severely broadened by the

*H—C—N—H coupling in several amines was observed following rigorous removal (with Na–K alloy) of traces of water. This effectively stops proton exchange on the NMR time scale (K. L. Henold, *Chem. Commun.*, 1340 (1970).

quadrupolar interaction. In the spectrum of ethyl *N*-methylcarbamate (Fig. 4.33), $CH_3NHCOCH_2CH_3$, the

NH proton shows a broad absorption centered about δ 5.16, and the N—CH_3 absorption at δ 2.78 is split into a doublet ($J \sim 5$ Hz) by the NH proton. The ethoxy protons are represented by the triplet at δ 1.23 and the quartet at δ 4.14. The small peak at δ 2.67 is an impurity.

Aliphatic and cyclic amine NH protons absorb from $\sim\delta$ 3.0–0.5; aromatic amines absorb from $\sim\delta$ 5.0–3.0. Because amines are subject to hydrogen bonding, the shift position depends on concentration, solvent, and temperature. Amides, pyrroles, and indoles absorb from $\sim\delta$ 8.5–5.0; the effect on the absorption position of concentration, solvent, and temperature is generally smaller than in the case of amines. The nonequivalence of the protons on the nitrogen atom of a primary amide and of the methyl groups of *N,N*-dimethylamides is caused by hindered rotation around the C—N bond

because of the contribution of the resonance form

Protons on the nitrogen atom of an amine salt exchange at a low rate; they are seen as a broad peak downfield ($\delta \sim 8.5$–$\delta \sim 6.0$), and they are coupled to protons on adjacent carbon atoms ($J \sim 7$ Hz); the α protons are recognized by their downfield position in the salt compared with that in the free amine. The use of trifluoroacetic acid as both a protonating agent and a solvent frequently allows classification of amines as primary, secondary, or tertiary. This is illustrated in Table 4.2 in which the number of protons on nitrogen determines the multiplicity of the methylene unit in the salt (Fig. 4.34). Sometimes the broad ^+NH, $^+NH_2$, or $^+NH_3$ absorption can be seen to consist of three broad humps. These humps represent splitting by the nitrogen nucleus ($J \sim 50$ Hz). With good resolution, it is sometimes possible to observe splitting of each of the humps by the protons on adjacent carbon atoms ($J \sim 7$ Hz).

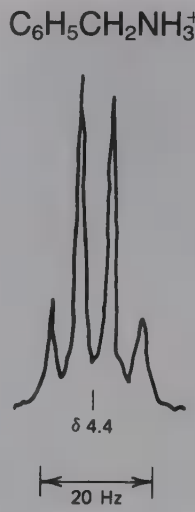

FIGURE 4.34. NMR spectrum of α methylene unit of a primary amine in CF_3CO_2H; corresponds to Table 4.2, first line.

TABLE 4.2

Classification of Amines by hNMR of Their Ammonium Salts in Trifluoroacetic Acid

Amine Precursor Class	Ammonium Salt Structure	Multiplicity of Methylene Unit
Primary	$C_6H_5CH_2NH_3^+$	Quartet (Fig. 4.34)
Secondary	$C_6H_5CH_2NH_2R^+$	Triplet
Tertiary	$C_6H_5CH_2NHR_2^+$	Doublet

Source: W. R. Anderson, Jr. and R. M. Silverstein, *Anal. Chem.*, 37, 1417 (1965).

4.5.3. Protons on Sulfur

Sulfhydryl protons usually exchange at a low rate so that at room temperature they are coupled to protons on adjacent carbon atoms ($J \sim 8$ Hz). Nor do they exchange rapidly with hydroxyl, carboxylic, or enolic protons on the same or on other molecules; thus, separate peaks are seen. However, exchange is rapid enough that shaking for a few minutes with deuterium oxide replaces sulfhydryl protons with deuterium. The absorption range for aliphatic sulfhydryl protons is δ 1.6–δ 1.2; for aromatic sulfhydryl protons, δ 3.6–δ 2.8. Concentration, solvent, and temperature affect the position within these ranges.

4.5.4. Protons on or near Halogens

Chlorine, bromine, and iodine nuclei are completely decoupled from protons directly attached, or on adjacent carbon atoms, because of strong electrical quadrupole moments.

The ^{19}F atom has a spin number of $\frac{1}{2}$ and couples strongly with protons (see Appendix F). The rules for coupling of protons with fluorine are the same as for proton–proton coupling; in general, the proton–fluorine coupling constants are somewhat larger, and long-range effects are frequently found. The ^{19}F nucleus can be observed at 56.4 MHz at 14,092 G. Of

course, its spin is split by proton and fluorine spins, and the multiplicity rules are the same as those observed in proton spectra.

4.6. COUPLING OF PROTONS TO OTHER NUCLEI

The organic chemist may encounter proton coupling with such other nuclei (besides ^{1}H, ^{19}F, and ^{14}N) as ^{31}P, ^{13}C, ^{2}H, and ^{29}Si. Three factors must be considered: natural abundance, spin number, and electrical quadrupole moment; the nuclear magnetic moment and relative sensitivity are important when a spectrum of the particular nucleus is considered. These properties are listed for a number of nuclei in Appendix H.

The magnetogyric ratio, γ, describes the combined effect of the magnetic moment and spin number of a given type of nucleus. The ratio of the magnetogyric ratios of one type of nucleus to that of another type of nucleus is a measure of the relative coupling constants of those two nuclei to a given reference nucleus. Consider the relative magnitudes of coupling of hydrogen and of deuterium, D, to a particular nucleus, X. Since

$$\frac{J_{HX}}{J_{DX}} = \sim\frac{\gamma_H}{\gamma_D}$$

we calculate from the magnetogyric ratios in Appendix H that for chemically identical structures

$$\frac{J_{HX}}{J_{DX}} = \sim\frac{26.753}{4.107} = \sim 6.5$$

Thus, it is anticipated that deuterium coupling is less than the corresponding hydrogen coupling by a factor of about 6.5.

The nucleus ^{31}P has a natural abundance of 100% and a spin number of $\frac{1}{2}$ (therefore no electrical quadrupole moment). The multiplicity rules for proton–phosphorus splitting are the same as those for proton–proton splitting. The coupling constants are large ($J_{H—P} \sim 200$–700 Hz, and $J_{HC—P}$ is 0.5–20 Hz) and are observable through at least four bonds. The ^{31}P nucleus can be observed at the appropriate frequency and magnetic field.

The isotope ^{13}C has a natural abundance relative to ^{12}C of 1.1% and a spin number of $\frac{1}{2}$. Protons directly attached to ^{13}C are split into a doublet with a large coupling constant—for example, about 120 Hz for $^{13}CH_3$. The CH_3—CH_2 group is predominantly $^{12}CH_3$—$^{12}CH_2$ but contains a small amount of $^{13}CH_3$—$^{12}CH_2$. Thus, the $^{13}CH_3$ protons are split into a doublet by ^{13}C ($J \sim 120$ Hz), and each peak of the doublet is split into a triplet by the ^{12}C protons ($J \sim 7$ Hz) as shown below. These "^{13}C satellite" peaks are small because of the low abundance of $^{13}CH_3$ in a molecule and can usually be seen disposed on both sides of a large $^{12}CH_n$ peak (e.g., the large $^{12}CH_3$ triplet shown below). The chemical shift of the $^{12}CH_3$ protons is midway between the satellites.

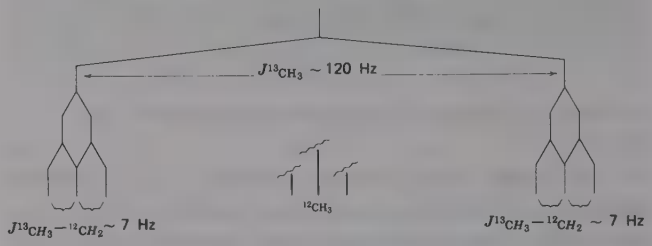

Deuterium (^{2}H or D) usually is introduced into a molecule to detect a group or to simplify a spectrum. Deuterium has a spin number of 1, a small coupling constant with protons, and a small electrical quadrupole moment. A proton–deuterium coupling constant is approximately 15% of the corresponding proton–proton constant. Suppose the protons on the α-carbon atom of a ketone

$$X—\overset{\gamma}{C}H_2—\overset{\beta}{C}H_2—\overset{\alpha}{C}H_2—\overset{O}{\overset{\|}{C}}—$$

were replaced by deuterium:

$$X—\overset{\gamma}{C}H_2—\overset{\beta}{C}H_2—\overset{\alpha}{C}D_2—\overset{O}{\overset{\|}{C}}—$$

The original spectrum would consist of a triplet for the α protons, a quintet (assuming equal coupling) for the β protons, and a triplet for the γ protons. In the deuterated compound, the α-proton absorption would be absent, the β protons would appear as a slightly broadened triplet, and the γ protons would be unaffected. Actually, each peak of the β-proton triplet is a very closely spaced quintet ($J_{CH—CD} \sim 1$ Hz or less), but the effect under ordinary resolution is peak broadening. Even this modest broadening due to the deuterium coupling can be removed by double resonance experiments (see below) involving irradiation at the deuterium resonance; this technique was used to obtain a more exact measurement of the remaining proton–proton coupling. Most deuterated solvents have residual protonated impurities; the CHD_2 group in deuterated acetone or DMSO, for example, is frequently encountered as a closely spaced quintet ($J \sim 2$ Hz, intensities 1:2:3:2:1), in accordance with $n2I + 1$.

The ^{29}Si isotope has a natural abundance of 4.70% (based on $^{28}Si = 92.28\%$), and a spin number of $\frac{1}{2}$. The value of $J_{^{29}Si-CH}$ is about 6 Hz. The small doublet caused by the $^{29}Si—CH_3$ coupling can often be seen straddling (± 3 Hz) an amplified peak of TMS; the $^{13}C—H_3$ doublet can also be seen at ± 59 Hz.

4.7. CHEMICAL SHIFT EQUIVALENCE AND MAGNETIC EQUIVALENCE

4.7.1. Chemical Shift Equivalence

The Pople notation (Section 4.4) is based on the concept of *sets* of nuclei within a *spin system*. A set of nuclei consists of *chemical shift equivalent* (defined below) nuclei. A spin system consists of sets of nuclei that interact (spin couple) among each other but do not ineract with any nuclei outside the spin system. It is not necessary for all nuclei within a spin system to be coupled with all the other nuclei in the spin system. Spin systems are "insulated" from one another; for example, the ethyl protons in ethyl isopropyl ether constitute one spin system, and the isopropyl protons another.

If nuclei are interchangeable by a symmetry operation or a rapid process, they are chemical shift equivalent (isochronous); that is, they have exactly the same chemical shift under all achiral conditions. Nuclei are interchangeable if the structures before and after the operation are indistinguishable. A rapid process means one that occurs faster than once in about 10^{-3} s. Pople proposed that the chemical shift equivalent nuclei be ordered into sets designated A_3, B, X_2, and so on.

The symmetry operations are rotation about a symmetry axis (C_n); inversion at a center of symmetry (i); reflection at a plane of symmetry (σ); or higher orders of rotation about an axis followed by reflection in a plane normal to this axis (S_n). The symmetry element (axis, center, or plane) must be a symmetry element for the entire molecule. The term "interchange" will be clarified by the examples below.

Protons *a* and *b* in *trans*-1,2-dichlorocyclopropane are chemical shift equivalent, as are the protons *c* and *d* (Fig. 4.35). The molecule has an axis of symmetry passing through C_3 and bisecting the $C_1—C_2$ bond. Rotation of the molecule by 180° around the axis of symmetry interchanges proton H_a for H_b and H_c for H_d. If the protons were not labeled, it would not be possible to tell if the symmetry operation had been performed merely by inspecting the molecule before and after the operation; the rotated structure is superimposable on the original structure.

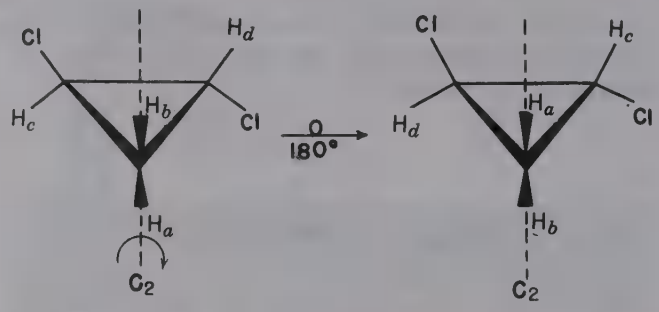

FIGURE 4.35. *trans*-1,2-Dichlorocyclopropane showing axis of symmetry and effect of rotation around the axis.

Protons that are interchangeable through an axis of symmetry are *homotopic*: that is, they are chemical shift equivalent in any environment (solvent or reagent) whether achiral or chiral. Protons that are interchangeable through any other symmetry operation are called *enantiotopic* (nonsuperimposable mirror images), and these are chemical shift equivalent only in an achiral environment. Noninterchangeable geminal protons are termed *diastereotopic*, and they are not chemical shift equivalent in any environment. Noninterchangeable protons on different carbon atoms are termed *heterotopic*, and they are not chemical shift equivalent in any environment. However, enantiotopic protons in a chiral environment, or diastereotopic or heterotopic protons, may fortuitously absorb at the same position for a given instrument resolution.

The concept of interchange through a rapid mechanism can be illustrated by the rapidly interchanging protons on some heteroatoms and by protons in some groups in molecules that are rapidly changing conformations. If the interchange is rapid enough, a single peak will result from, say, the carboxylic acid proton and the hydroxylic proton of a hydroxy carboxylic acid. Chemical shift equivalence of protons on a CH_3 group results from rapid rotation around a carbon–carbon single bond even in the absence of a symmetry element. Figure 4.36 shows Newman projections of the three staggered rotamers of a molecule containing a methyl group attached to another sp^3 carbon atom having four different substituents, that is, a chiral center. In any single rotamer, none of the protons can be interchanged by a symmetry operation. However, the protons are rapidly changing position. The time spent in any one rotamer is short ($\sim 10^{-6}$ s), because the energy barrier for rotation around a C—C single bond is small. The chemical shift of the methyl group is an average of the shifts of each of the three protons. In other words, each proton can be interchanged with the others by a rapid rotational operation. Thus, without the *a*, *b*, *c* labels, the rotamers are indistinguishable.

The chemical shift of cyclohexane protons is an average of the shifts of the axial and the equatorial pro-

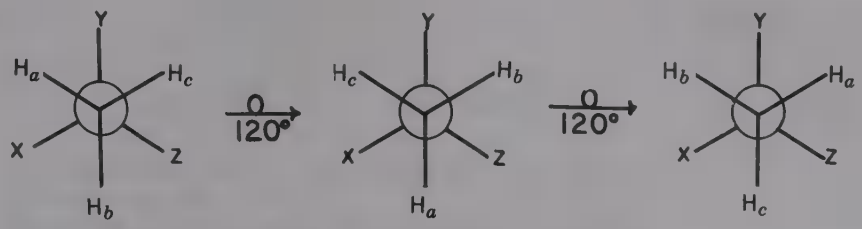

FIGURE 4.36. Newman projection of the staggered rotamers of a molecule with a methyl group attached to a chiral sp^3 carbon atom.

tons. The chemical shift equivalence of the cyclohexane protons results from rapid interchange of axial and equatorial protons as the molecule flips between chair forms.

At room temperature, DMF shows two CH_3 peaks (which merge at ~123°) because the rate of rotation around the hindered C=N bond is slow.

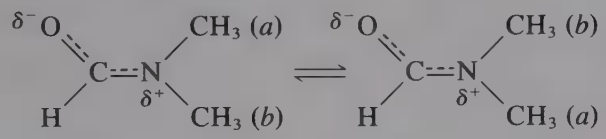

4.7.2. Magnetic Equivalence

A further refinement involves the concept of *magnetic equivalent* nuclei. If nuclei in the same set (i.e, chemical shift equivalent nuclei) couple equally to each nucleus (probe nucleus) in every other set of the spin system, they are magnetic equivalent, and the designations A_2, X_2, and so on apply. However, if the nuclei are not magnetic equivalent, the designations AA', XX' are used.

Magnetic equivalence presupposes chemical shift equivalence. To determine whether chemical shift equivalent nuclei are magnetic equivalent, it must be determined whether they are coupled equally to each nucleus (probe nucleus) in every other set in the spin system. This is done by examining geometrical relationships. If the bond distances and angles from each nucleus in relation to the probe nucleus are identical, the nuclei in question are magnetic equivalent. In other words, two chemical shift equivalent nuclei are magnetic equivalent if they are symmetrically disposed with respect to each nucleus (probe) in any other set in the spin system. This means that the two nuclei under consideration can be interchanged through a reflection plane passing through the probe nucleus and perpendicular to a line joining the chemical shift equivalent nuclei. Note that a test for magnetic equivalence is valid only when the *two nuclei are chemical shift equivalent*. The latter point bears repeating: Only chemical shift equivalent nuclei are tested for magnetic equivalence.

These rules are applied readily to conformationally rigid structures. Thus, in *p*-chloronitrobenzene (Fig. 4.37) the protons ortho to the nitro group (H_A and $H_{A'}$) are chemical shift equivalent to each other, and the protons ortho to the chlorine group (H_X and $H_{X'}$) are chemical shift equivalent to each other. In general for *p*-disubstituted benzene rings, J_{AX} and $J_{A'X'}$ are the same, approximately 7–10 Hz; $J_{A'X}$ and $J_{AX'}$ are also

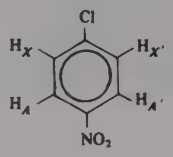

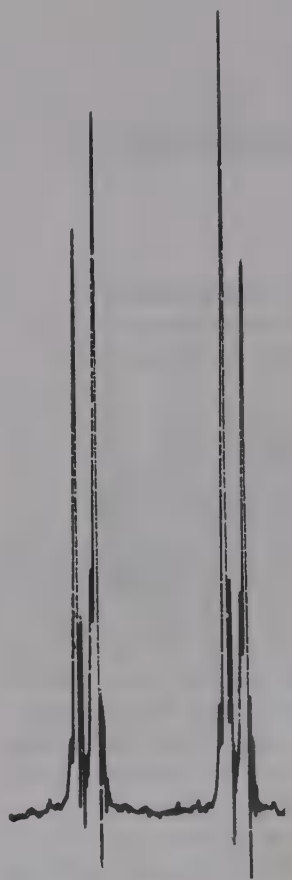

FIGURE 4.37. *p*-Chloronitrobenzene, 100 MHz in CCl_4.

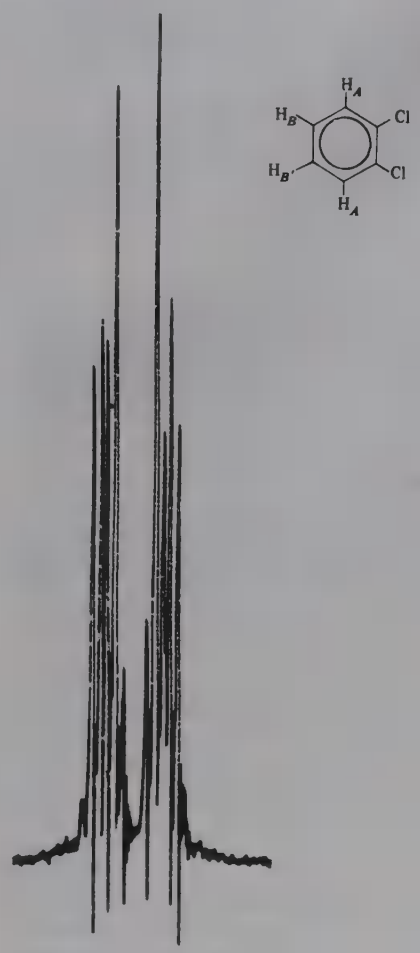

FIGURE 4.38. *o*-Dichlorobenzene, 100 MHz in CCl_4.

the same but much smaller, approximately 0–1 Hz. Since H_A and $H_{A'}$ couple differently to another specific proton, they are not magnetic equivalent, and first-order rules do not apply. (Similarly, H_X is not magnetic equivalent to $H_{X'}$.) The system is described as $AA'XX'$, and the spectrum is very complex (Fig. 4.37). Fortunately the pattern is readily recognized because of its near symmetry and apparent simplicity; under moderate resolution, it resembles an AB pattern of two distorted doublets. Closer inspection reveals many additional splittings. As the para substituents become more similar to each other (in their shielding properties), the system tends toward $AA'BB'$; even these absorptions resemble AB patterns until they overlap.

The aromatic protons of symmetrically ortho-disubstituted benzenes also give $AA'BB'$ spectra. An example is *o*-dichlorobenzene (Fig. 4.38).

The three isomeric difluoroethylenes furnish additional examples of chemical shift equivalent nuclei that are not magnetic equivalent.

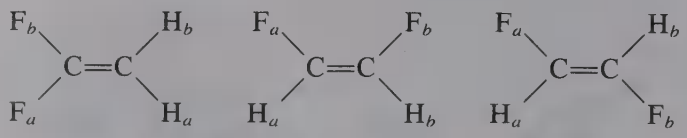

In each case, the protons H_a and H_b comprise a set, and fluorines F_a and F_b comprise a set (of chemical shift equivalent nuclei), but the nuclei in each set are not magnetic equivalent and the spectra are complex.

In conformationally mobile systems, the situation becomes involved. We have seen that the CH_3 protons are chemical shift equivalent, even when the molecule has no symmetry element, by rapid rotational interchange. If one of the substituents on the chiral center is a proton (Y = H in Fig. 4.36), the CH_3 protons are still magnetic equivalent by rapid rotational averaging of the coupling constants among identical rotamers; the system is A_3B or A_3X. Consider, in contrast with the methyl group, a methylene group next to a chiral center, as in 1-bromo-1,2-dichloroethane (Fig. 4.39). Protons H_a and H_b are not chemical shift equivalent, since they cannot be interchanged by a symmetry operation or by rapid rotation. The molecule has no axis, plane, center, or reflection axis of symmetry. Although there is a rapid rotation around the carbon–carbon single bond, the protons are not interchangeable by a rotational operation. An observer can detect the difference before and after rotating the methylene group; the rotamers are not superimposable.

The question of magnetic equivalence does not arise since there is no chemical shift equivalence; the system is ABX.

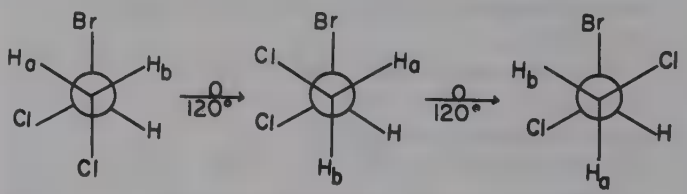

FIGURE 4.39. Newman projection of the rotamers of 1-bromo-1,2-dichloroethane.

In ZCH_2CH_2Y molecules, we are dealing with an anti rotamer and two enantiomeric gauche rotamers (Fig. 4.40). The analysis is quite complex, but in essence, these are $AA'XX'$ systems, which usually give apparent A_2X_2 spectra. The spectrum of 2-dimethylaminoethyl acetate (Fig. 4.41*a*) is a case in point. Figure 4.41*b–d* shows the progressive distortions as $AA'XX' \rightarrow AA'BB'$ (i.e., $\Delta\nu/J$ decreases) in compounds of the type ZCH_2CH_2Y. As the absorptions move closer together, the inner peaks increase in intensity, additional splitting occurs, and some of the outer peaks disappear in the baseline noise. The general appearance of sym-

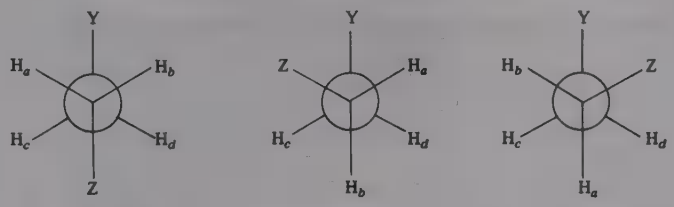

FIGURE 4.40. Newman projection of the rotamers of the YCH_2CH_2Z system.

Source: R. M. Silverstein and R. T. LaLonde, *J. Chem. Educ.*, 57, 343 (1980).

metry throughout aids recognition of the type of spin system involved. At the extreme, the two methylene groups become chemical shift equivalent and a single A_4 peak results. Although 1,3-dichloropropane (Fig. 4.42) is properly described as $XX'AA'XX'$, it presents an apparent A_2X_4 system (triplet and quintet).

A_2B_2 or A_2X_2 systems are quite rare (examples include difluoromethane, 1,1-difluoroallene, and 1,1,3,3-tetrachloropropane); most systems described in the literature as A_2X_2 are really $AA'XX'$.

It turns out that the question of magnetic equivalence in rotamers is readily resolved by examining the individual rotamers in which the protons in question are chemical shift equivalent by a symmetry operation. If the protons are magnetic equivalent in these rotamers, they are so for the molecule.

An interesting situation occurs in a molecule such as 1,3-dibromo-1,3-diphenylpropane, which has a methylene group between two chiral centers (Fig. 4.43). In (1*R*,3*R*)-1,3-dibromo-1,3-diphenylpropane (one of a racemic pair), H_a and H_b are chemical shift equivalent and so are H_c and H_d, because of an axis of symmetry (C_2) in the molecule. Rotation around the axis interchanges H_a with H_b, and H_c with H_d. On the other hand, in (1*S*,3*R*)-1,3-dibromo-1,3,-diphenylpropane (a meso compound), H_c and H_d are not chemical shift equivalent: They cannot be interchanged by a symmetry operation. (1*S*,3*R*)-1,3-Dibromo-1,3-diphenylpropane does have a plane of symmetry (σ), but both H_c and H_d are in that plane and cannot be interchanged. Both H_a and H_b are chemical shift equivalent because they can be interchanged by reflection through the plane of symmetry shown in Figure 4.43.

In the (1*R*,3*R*) compound, H_a and H_b are not magnetic equivalent since they do not identically couple

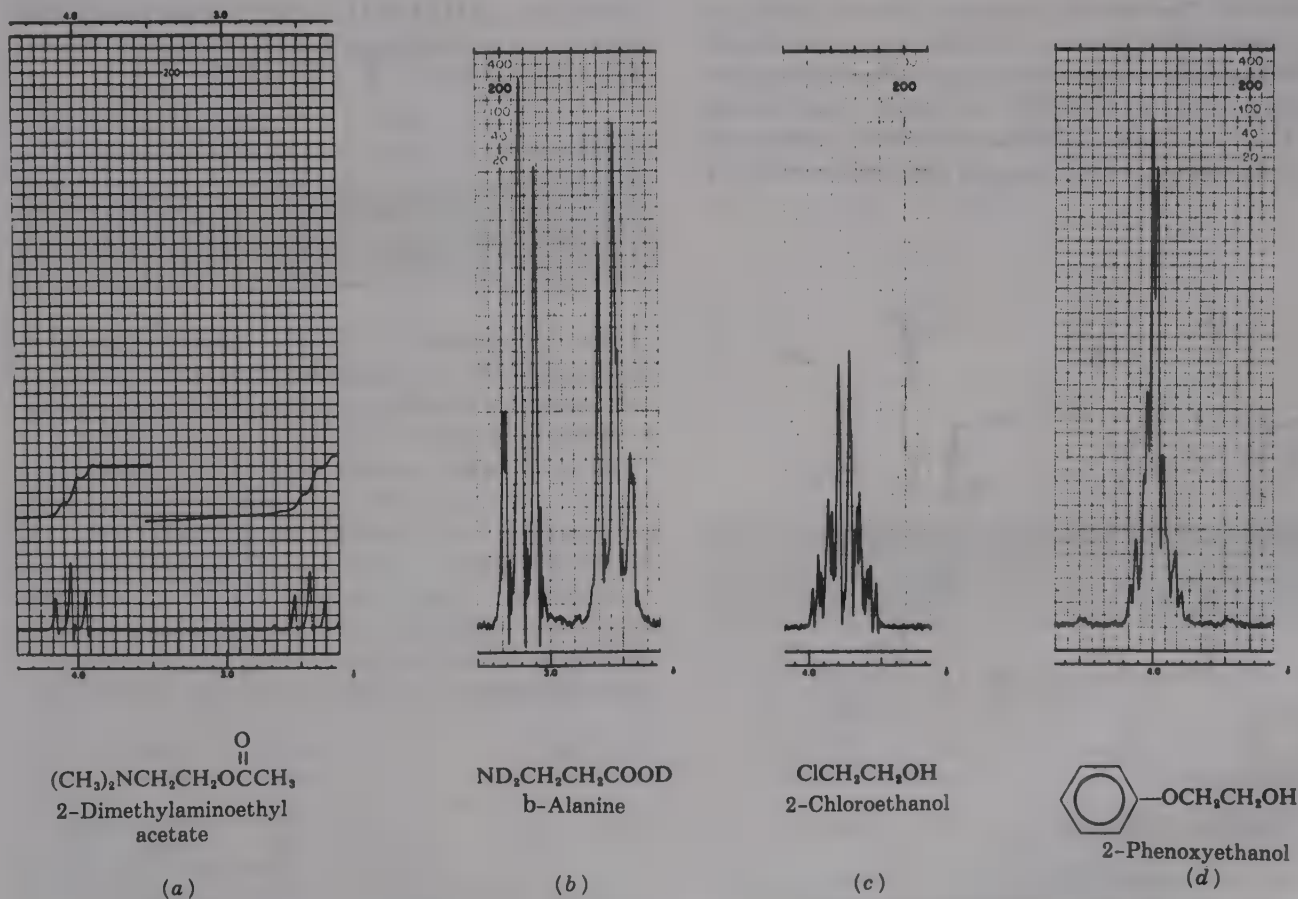

FIGURE 4.41. Progressive distortions as $AA'XX' \rightarrow AA'BB'$ in ZCH_2CH_2Y at 60 MHz.

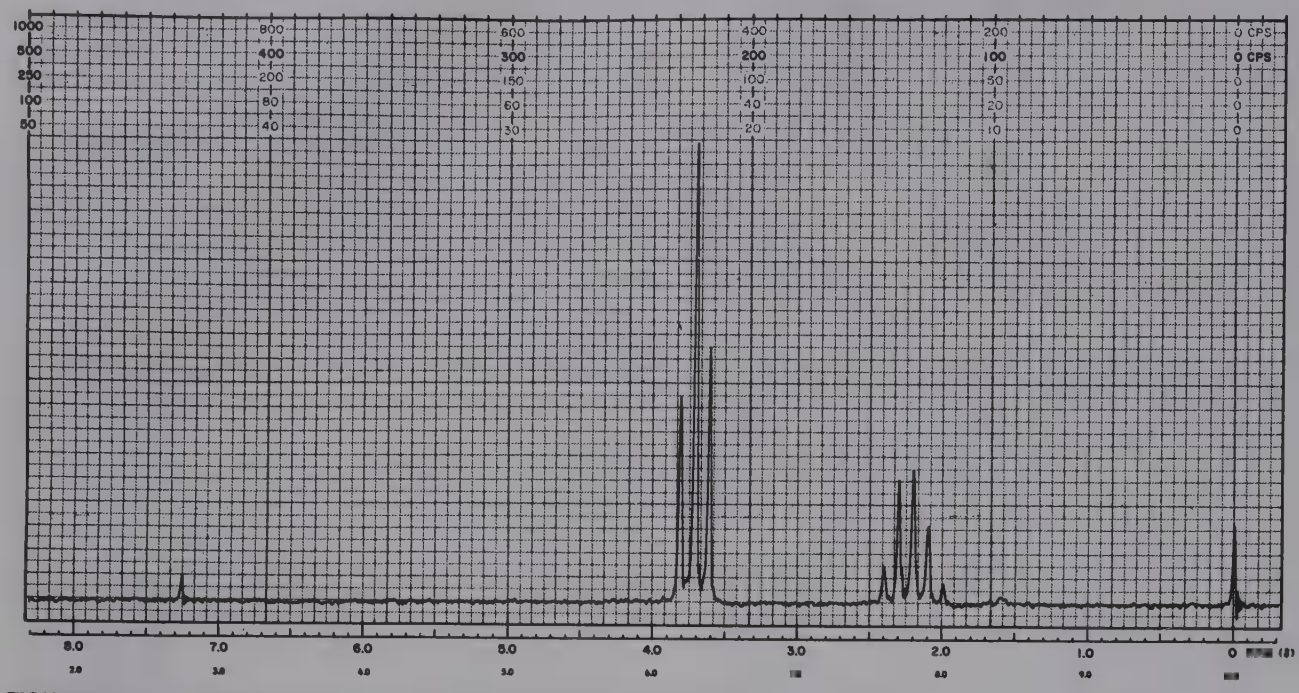

FIGURE 4.42. 1,3-Dichloropropane in $CDCl_3$ at 60 MHz, *XX'AA'XX'* system.

to H_c or to H_d; H_c and H_d also are not magnetic equivalent since they do not identically couple to H_a or H_b. Note that only those rotamers are examined in which the protons in question were chemical shift equivalent. The system is *AA'XX'* or more descriptively *A—XX'—A'*. In the (1*S*,3*R*) compound of Figure 4.43, $J_{ad} = J_{bd}$ and $J_{ac} = J_{bc}$; thus, in this molecule, H_aH_b are magnetic equivalent. The question of magnetic equivalence of H_c and H_d is not relevant since they are not chemical shift equivalent. The system is ABX_2 or more descriptively, *X—AB—X*.

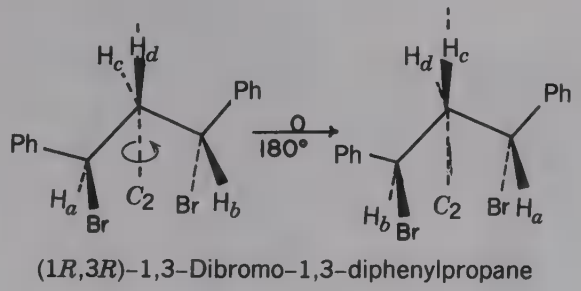

(1*R*,3*R*)-1,3-Dibromo-1,3-diphenylpropane

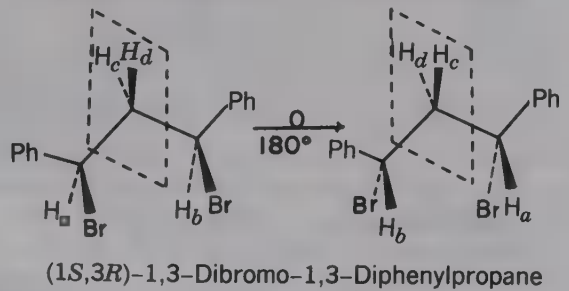

(1*S*,3*R*)-1,3-Dibromo-1,3-Diphenylpropane

FIGURE 4.43. Two isomers of 1,3-dibromo-1,3-diphenylpropane. In the (1*R*,3*R*) isomer, H_a and H_b are chemical shift equivalent, as are H_c and H_d. In the (1*S*,3*R*) isomer, H_a and H_b are chemical shift equivalent, but H_c and H_d are not.

4.8. *AMX*, *ABX*, and *ABC* SYSTEMS WITH THREE COUPLING CONSTANTS

The ring protons of methyl 2-furoate (Chapter 8, Compound 8.2) represent a nearly first-order *AMX* system with three coupling constants. Each proton is represented by a pair of doublets.

Although *ABX* systems with three coupling constants are not first order, these patterns are frequently recognized if the distortions are not too severe. The degree of distortion depends on the ratios of the separation of the *A* and *B* protons to their coupling constants. The vinylic structure gives an *ABX* or an *ABC* system depending on the nature of the substituent Y, which determines the shift positions of the protons.

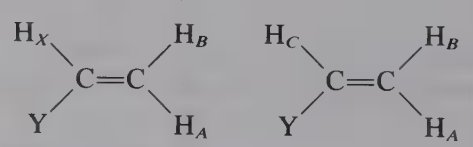

p-Chlorostyrene (Fig. 4.44) shows an *ABX* spectrum that can readily be related to an *AMX* pattern. The following analysis, though not rigorous, is useful.

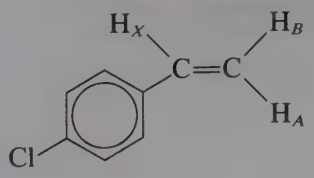

Protons A and B are not chemical shift equivalent. Proton A ($\sim\delta$ 5.70) is deshielded about 25 Hz compared with proton B, because of its relative proximity to the ring. Proton X ($\delta \sim 6.70$) is strongly deshielded by the ring and is split by proton A ($J \sim 18$ Hz) and by proton B ($J \sim 11$ Hz). The A proton signal is split by the X proton ($J \sim 18$ Hz) and by the B proton ($J \sim 2$ Hz). The B proton signal is split by the X proton ($J \sim 11$ Hz) and by the A proton ($J \sim 2$ Hz).

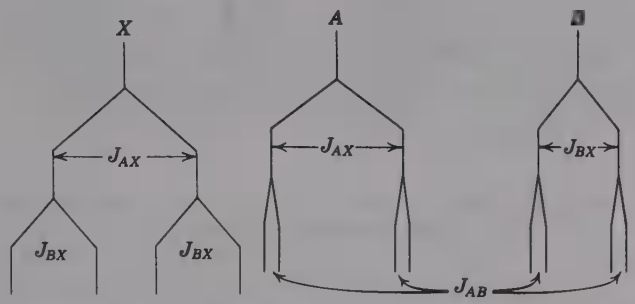

The coupling constants for a vinylic system are characteristic; the trans coupling is larger than the cis, and the geminal coupling is very small.

The preceding analysis lacks rigor in several details. The splittings of proton X do not correspond exactly to J_{BX} and J_{AX}, and although this is a good approximation when $\Delta\nu$ is greater than about 10 Hz for protons AB, the only exact information obtainable from the X pattern is that the spread between the outside peaks is equal to $J_{AX} + J_{BX}$. The distortions in peak intensities from an AMX pattern are obvious. The pattern of two closely spaced pairs should not be confused with the quartet resulting from splitting by three equivalent protons.

As the shift positions of protons A and B approach each other so that $\Delta\nu$ becomes much smaller than 10 Hz, the deviations from a first-order spectrum become severe; the A and B patterns overlap, and the middle peaks of the X pattern merge. In the extreme case that $\nu_A = \nu_B$ and $J_{AX} = J_{BX}$, protons A and B are magnetic equivalent, the spectrum is simply A_2X, and the X proton absorption is a triplet. Note that a very similar spectrum would arise if the A pair were chemical, but not magnetic, equivalent: that is, an $AA'X$ system. As the shift position of the X proton approaches the A and B absorptions, the spectrum degenerates to a very complex ABC pattern.

An equatorial and an axial proton on the same carbon of a conformationally locked six-membered ring may form the AB part of an ABX or an ABC pattern, depending on the nature of Y on an adjacent carbon. Typically, H_A (equatorial) is deshielded relative to H_B (axial) by about 0.1–0.7 ppm (Section 4.3), J_{AB} is about 12–15 Hz, J_{BX} (ax–ax) is about 5–10 Hz, and J_{AX} (eq–ax) is about 2–3 Hz (Section 4.11).

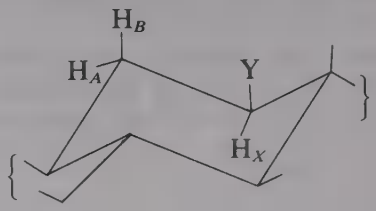

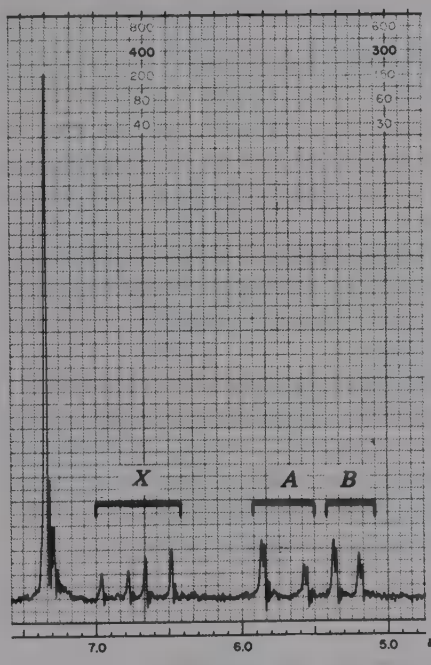

FIGURE 4.44. *p*-Chlorostyrene at 60 MHz.

4.9. STRONGLY AND WEAKLY COUPLED SPIN SYSTEMS

The 60-MHz spectrum of 1-nitropropane (Fig. 4.45) is an $A_3MM'XX'$ system that resembles an $A_3M_2X_2$ system with J_{AM} very similar to J_{MX}. We interpret the upfield triplet as the methyl group split by the adjacent methylene group, the downfield triplet as the methylene group (adjacent to the nitro group) split by the adjacent methylene group that in turn is split by five neighboring protons to give a sextet. We note some broadening of the sextet peaks since J_{AM} is not exactly equal to J_{MX}.

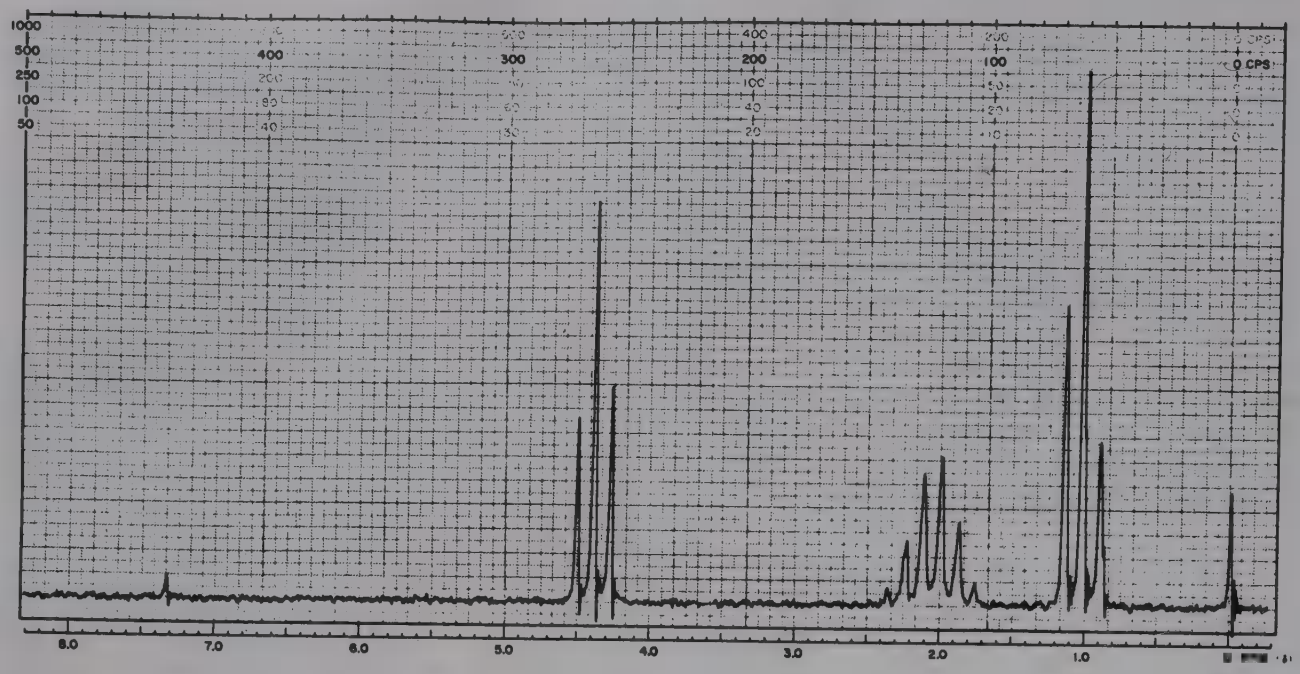

FIGURE 4.45. 1-Nitropropane in $CDCl_3$ at 60 MHz, $CH_3—CH_2—CH_2—NO_2$ ($A_3MM'XX'$).

What we have done, in effect, is to mentally cleave the spin system into segments, and we are successful in rationalizing the spectrum. Why is it that we can use this kind of oversimplified analysis for 1-nitropropane, but we run into trouble when we predict a triplet for the methyl group (Fig. 4.46*a*) of heptanal (A_3B_2 portion of the system), or a doublet for the methyl group (Fig. 4.46*b*) of β-methylglutaric acid, $HOOC—CH_2—\underset{\displaystyle CH_3}{\underset{|}{CH}}—CH_2COOH$ (A_2B portion of the system)?

The answer is that we have weakly coupled protons in 1-nitropropane, but strongly coupled protons in the latter two compounds. Or, to put it another way, the spins of the methyl protons in 1-nitropropane are affected only (or almost entirely) by the adjacent methylene protons. But in heptanal, the methyl proton spins are affected by all of the adjoining methylene groups that have practically the same chemical shift; that is, $\Delta\nu/J$ for four of the methylene protons is almost zero, and they are considered to be strongly coupled.

A similar situation exists in β-methylglutaric acid, in which the methylene groups and the methine group are strongly coupled (the system is $A_3BCC'DD'$). To explain the difficulties arising from attempting to segregate portions of a strongly coupled system, the concept of virtual coupling is invoked. Even though the coupling constant of the methyl group to the methylene group once removed in heptanal or in β-methylglutaric acid is almost zero, the methyl group is considered to be "virtually coupled" to those once removed methylene groups in each compound.

The concept of virtual coupling, then, is convenient but only necessary when one incorrectly considers a portion of a strongly coupled spin system as a separate entity and attempts to apply first-order rules to that portion.

The modus operandi of the organic chemist in interpreting an NMR spectrum is to look initially for first-order absorptions, and then for patterns that can be recognized as distortions of first-order absorptions. There is not usually very much interest in precise solutions of multispin systems. Frequently the emphasis is on portions of spin systems. The above considerations should be of help in setting limits for this convenient, although not rigorous, approach to the interpretation of NMR spectra.

A well-defined multiplet like any one in Figure 4.45 has a chemical shift that is at the midpoint of the signal (e.g., the triplet at δ 4.37). In contrast, an ill-defined multiplet, such as in Figure 4.46*b*, should be reported as the range, in hertz from the reference, over which the signal extends; the instrument frequency must also be reported.*

*G. Slomp, *J. Am. Chem. Soc.*, **84**, 673 (1962).

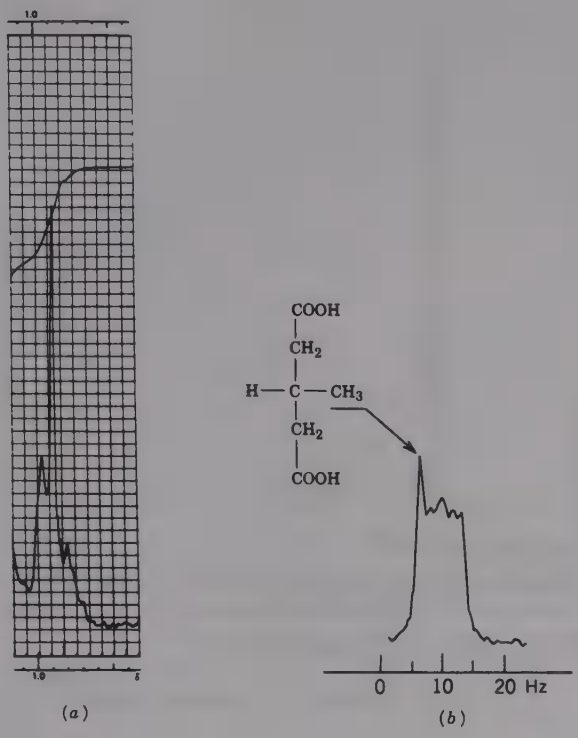

FIGURE 4.46. (*a*) Methyl group of heptanal at 60 MHz. (*b*) Methyl group of β-methylglutaric acid at 60 MHz, expanded.

4.10. EFFECTS OF A CHIRAL CENTER

The protons of any methylene group in a molecule containing one chiral center are not chemical shift equivalent, as explained in Section 4.7. They couple with each other, and each may have a different coupling to a vicinal proton. Even assuming fast rotation around the C—C bond, the methylene protons of a compound R—C(H_a)(M)—C(H_b)(S)—L show an *AB* or *AX* pattern; that is, they are diastereotopic since they cannot be interchanged (Section 4.7). The resolution available determines whether the differences in chemical shift can be observed.

However, a large part of the nonequivalence may result from unequal populations of conformers even at fast rotation. The spectrum may be further complicated by slow rotation caused by low temperature or bulky substituents. Nonequivalence of the methylene protons occurs in a compound such as R—C(H_a)(M)—C(H_b)(S)—C(H_b)—R even though the middle carbon atom is not a chiral center. H_A and H_B are not interchangeable.

The methylene group may display detectable nonequivalence even though it is distant from the chiral center. Examples of the type R—C(H_a)—O—C(M)—L (H_b, S) have been reported. The chiral center need not be a carbon atom. The phenomenon has been reported for the methylene protons in quaternary ammonium salts, sulfites, sulfoxides, diethyl sulfide–borane complexes, and thiophosphonates.

Chemical shift nonequivalence of the methyl groups of an isopropyl moiety near a chiral center is frequently observed; the effect has been measured through as many as seven bonds between the chiral center and the methyl protons.

The methyl groups in the terpene alcohol 2-methyl-6-methylene-7-octen-4-ol are not chemical shift equivalent (Fig. 4.47), and even though the protons are four

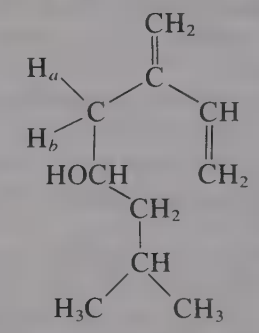

2-Methyl-6-methylene-7-octen-4-ol

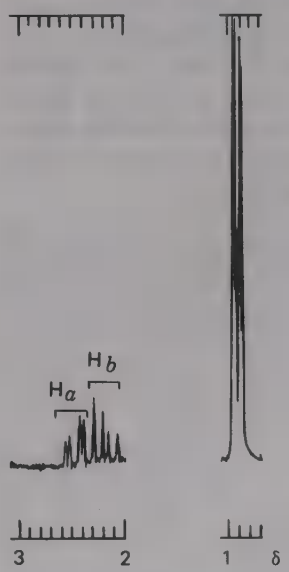

FIGURE 4.47. 5-Methylene and methyl protons of 2-methyl-6-methylene-7-octen-4-ol, 100 MHz.

bonds removed from the chiral center, the nonequivalence is detectable at 100 MHz (δ 0.92 and δ 0.90); each absorption is split by the vicinal CH, giving rise to two overlapping doublets (J = 7 Hz). The nonequivalent protons of the CH_2 (a and b) between the

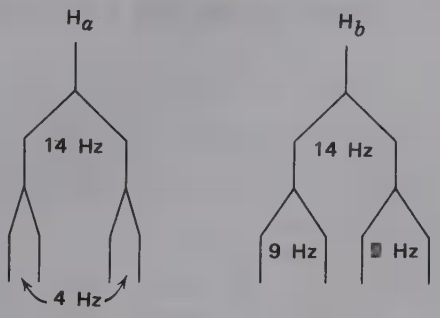

CH_2=C and CHOH groups absorb, individually, at ~δ2.47 and ~δ2.18. Each proton is split by the other (J_{gem} = ~14 Hz) and unequally by the neighboring proton (J_{vic} = ~9 and 4 Hz). The protons of the other CH_2 group are also nonequivalent; additional splitting by the adjacent methine proton results in a partially resolved multiplet.

The methylene protons (upfield absorption) in aspartic acid (Fig. 4.48) in D_2O are nonequivalent, and the shift difference between them is small compared with the geminal coupling constant. Thus, the *AB* pat-

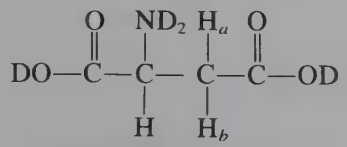

Aspartic acid-*N*-d_2-*O*-*d*

tern from the geminal coupling is quite distorted; the inner peaks are strong, the outer peaks weak. Each methylene proton is also split by the vicinal proton with different coupling constants. Two of the peaks coincide, the end peaks are lost in the baseline noise, and the net result is three peaks. The methine proton absorption consists of two pairs.

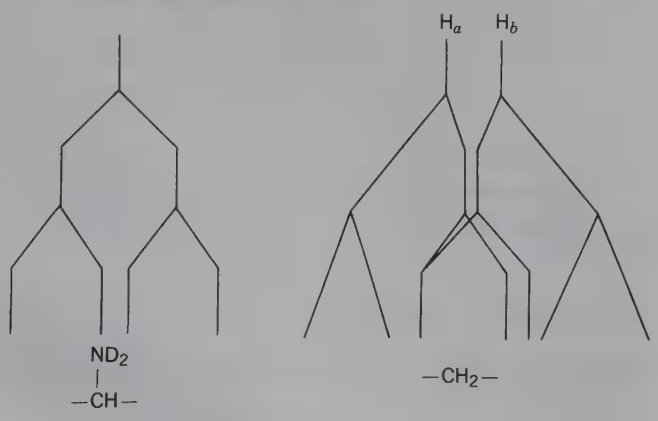

FIGURE 4.48. Aspartic acid in D_2O at 60 MHz.

4.11. VICINAL AND GEMINAL COUPLING IN RIGID SYSTEMS

Coupling between heterotopic protons on vicinal carbon atoms in rigid systems depends primarily on the dihedral angle ϕ between the H—C—C′ and the C—C′—H′ planes. This angle can be visualized by an end-on view of the bond between the vicinal carbon

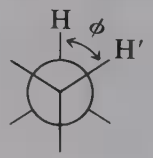

atoms and by the perspective in Figure 4.49 in which the calculated relationship between dihedral angle and vicinal coupling constant is graphed. Karplus emphasized that his calculations are approximations and do not take into account such factors as electronegative substituents, the bond angles Θ ($\angle$H—C—C′ and $\angle$C—C′—H′), and bond lengths. Deductions of dihedral angles from measured coupling constants are safely made only by comparison with closely related compounds. The correlation has been very useful in cyclopentanes, cyclohexanes, carbohydrates, and bridged polycyclic systems. In cyclopentanes, the observed values of about 8 Hz for vicinal cis protons and about 0 Hz for vicinal trans protons are in accord with the corresponding angles of about 0° and about 90°,

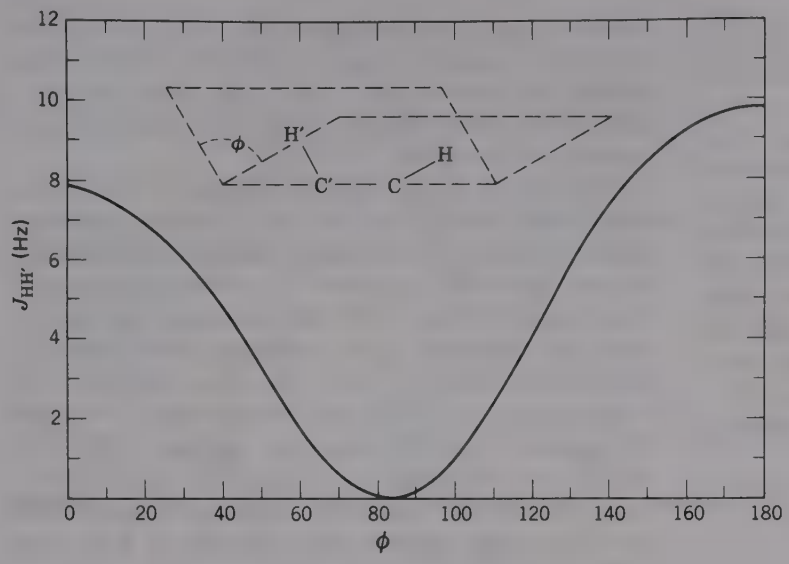

FIGURE 4.49. The vicinal Karplus correlation. Relationship between dihedral angle (ϕ) and coupling constant for vicinal protons.

respectively. In substituted or fused cyclohexane rings, the following relations obtain:

	Calculated J (Hz)	Observed J (Hz)
Axial–axial	9	8–14 (usually 8–10)
Axial–equatorial	1.8	1–7 (usually 2–3)
Equatorial–equatorial	1.8	1–7 (usually 2–3)

A modified Karplus equation can be applied to vicinal coupling in alkenes. The prediction of a larger trans coupling ($\phi = 180°$) than cis coupling ($\phi = 0°$) is borne out. The cis coupling in unsaturated rings decreases with decreasing ring size (increasing bond angle) as follows: cyclohexenes J = 8.8–10.5, cyclopentenes J = 5.1–7.0, cyclobutenes J = 2.5–4.0, and cyclopropenes J = 0.5–2.0.

The calculated relationship due to the H—C—H angle (Θ) jof geminal protons is shown in Figure 4.50. This relationship is quite susceptible to other influences and should be used with due caution. However, it is useful for characterizing methylene groups in a fused cyclohexane ring (approximately tetrahedral, $J \sim$ 12–18), methylene groups of a cyclopropane ring ($J \sim$ 5), or a terminal methylene group ($J \sim$ 0–3). Electronegative substituents reduce the geminal coupling constant (e.g., for CH_2Cl_2, J = 7.5 Hz), whereas sp^2 or sp hybridized carbon atoms increase it (e.g., for NC—CH_2—CN, J = 20.0).

Geminal coupling constants are actually negative numbers, but this can be ignored except for calculations. Note that geminal couplings are seen in routine spectra only when the methylene protons are diastereotopic.

In view of the many factors other than angle dependence that influence coupling constants, it is not surprising that there have been abuses of the Karplus correlation. Direct "reading off" of the angle from the magnitude of the J value is risky. The safest application of the relationships is to structure determinations in which molecular geometries have provided the extrema of the high and low expected J values and for which the 0° and 90° and 180° structures are known for a given system. The limitations of the Karplus correlations are discussed in Jackman and Sternhell (see reference section).

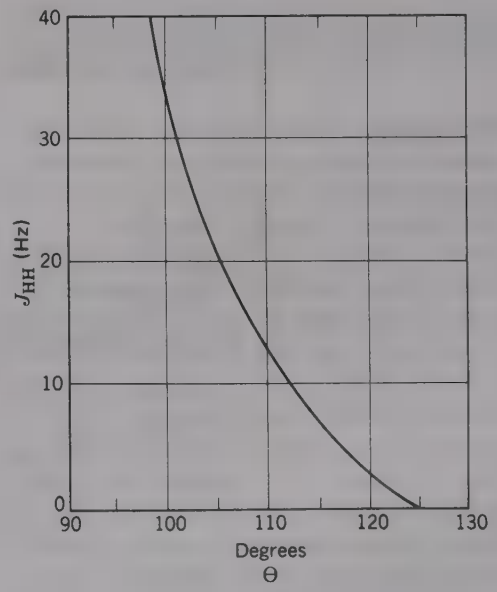

FIGURE 4.50. The geminal Karplus correlation. J_{HH} for CH_2 groups as function of ∠H—C—H.

4.12. LONG-RANGE COUPLING

Proton–proton coupling beyond three bonds may occur in alkenes, alkynes, aromatics, and heteroaromatics, and in strained ring systems (small or bridged rings). Allylic (H—C—C=C—H) coupling constants are about 0–3 Hz. Homoallylic (H—C—C—C=C—H) couplings are usually negligible but may be as much as 1.6 Hz. Coupling through conjugated polyalkyne chains may occur through as many as nine bonds. Meta coupling in a benzene ring is 1–3 Hz, and para, 0–1 Hz. In five-membered heteroaromatic rings, coupling between the 2 and 4 protons is 0–2 Hz.

J_{AB} in the bicyclo[2.1.1]hexane system is about 7 Hz.

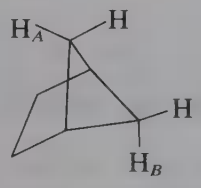

This unusually high long-range coupling constant is attributed to the "W conformation" of the four σ bonds between H_A and H_B.

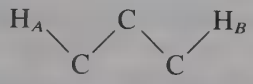

Long-range coupling

4.13. SPIN DECOUPLING

Spin decoupling (double irradiation or double resonance) is a powerful tool for simplifying a spectrum, for determining the relative positions of protons in a molecule, or for locating a buried absorption.

Spin decoupling is simply a technique for irradiating a nucleus with a strong rf signal at its resonance frequency, while scanning other nuclei to detect which ones are affected by decoupling from the irradiated nucleus. The early experiments in spin decoupling were limited to irradiation of other nuclei such as ^{14}N, ^{31}P, or ^{19}F because of the very large frequency difference from the proton resonance. For example, decoupling of the N atom of a pyrrole or an amide was used to sharpen the proton absorption, which can be so broad as to be merely a slight bulge on the baseline. As previously pointed out (Section 4.5), this broadening is a result of partial decoupling by the nitrogen electrical quadrupole moment. Irradiation of the N atom of an amine salt changes the broad ^{+}NH absorption to a sharp absorption whose multiplicity depends on the number of α protons.

Protons can be readily decoupled provided they are more than about 20 Hz apart at 100 MHz. The utility of proton–proton decoupling is shown in the 100-MHz partial spectrum of methyl 2,3,4-tri-*O*-benzoyl-β-L-lyxopyranoside (Fig. 4.51). The integration (not shown) gives the following ratios in Figure 4.51*a* from high field to low field: 3:1:1:1:1:2. The sharp peak at δ 3.53 represents the OCH_3 group. Decoupling the two-proton multiplet at δ 5.75 causes the multiplet at δ 5.45 to collapse to four peaks, and the doublet at δ 5.00 to a sharp singlet (Fig. 4.51*b*). Decoupling the multiplet at δ 5.45 partially collapses the multiplet at δ 5.75 and collapses the two upfield pairs of doublets (at δ 4.45 and δ 3.77) to two doublets (Fig. 4.51*c*). The H_5 absorptions should be relatively upfield since these two protons are deshielded by an ether oxygen, whereas H_2, H_3, and H_4 are deshielded by benzoyl groups. The two H_5 protons are the *AM* portion of an *AMX* pattern; the H_4 proton is the *X* portion (with additional splitting). The pair of doublets at δ 4.45 is 1 (H_{5E}) proton at C_5 strongly deshielded by the benzoyl group on C_4, and the pair of doublets at δ 3.77 is the other (H_{5A}) absorption. Further confirmation is provided by the collapse of each pair of doublets to doublets with the characteristic large geminal coupling (J = 12.5 Hz) on irradiation of the multiplet at δ 5.45, which must therefore be the H_4 absorption (i.e., the *X* proton that was further split). The multiplet at δ 4.75 must therefore represent H_2 and H_3 since irradiation of this multiplet collapsed the multiplet that we identified as H_4 (this now appears as the *X* portion of the *AMX* pattern), and also the doublet at δ 5.00, which must be the H_1 absorption.

A multiplet caused by coupling to two nonequivalent protons can be completely collapsed to a singlet by irradiating both coupling proton frequencies simultaneously. Other methods for establishing $^1H^1H$, $^1H^{13}C$, or $^{13}C^{13}C$ relationships are described in Chapter 6.

4.14. SHIFT REAGENTS

Shift reagents, introduced in 1969, provide a method for spreading out NMR absorption patterns without increasing the strength of the applied magnetic field. Addition of shift reagents to appropriately functionalized samples results in substantial magnification of

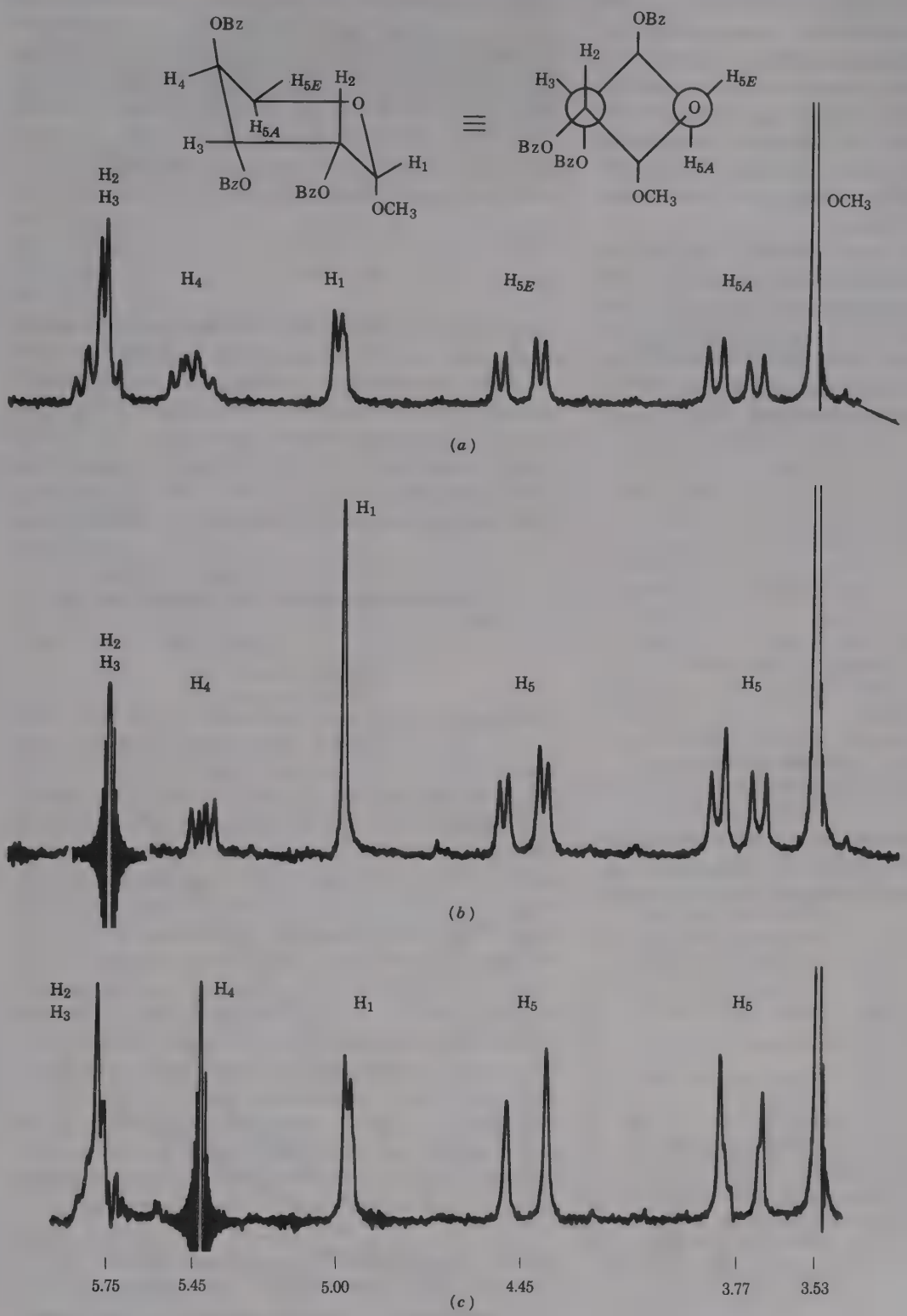

FIGURE 4.51. (*a*) Partial spectrum of methyl 2,3,4-tri-*O*-benzoyl-β-L-lyxopyranoside at 100 MHz in $CDCl_3$. (*b*) H_2 and H_3 decoupled. (*c*) H_4 decoupled. Note that there are two diastereotopic H_5 protons. Bz = C_6H_5CO. Irradiation may cause a detectable change in chemical shift of nearby peaks.

the chemical shift differences of nonequivalent protons. The shift reagents are ions in the rare earth (lanthanide) series coordinated to organic ligands. Although it had been long known that some metal ions caused shifts, it was not until the application of the more recent shift reagents, $Eu(dpm)_3$ and $Eu(fod)_3$ that these shifts could be effected without substantial line broadening; with high-field instruments, line broadening can still be a problem.

The notation for the more commonly used shift reagents, $Eu(dpm)_3$ and $Eu(fod)_3$, come from their names *tris*(*dip*ivalo*m*ethanato)europium and *tris*-(1,1,1,2,2,3,3-hepta*f*luoro-7,7-dimethyl-3,5-*o*-ctane*d*ionato)europium. A more systematic name for the former is *tris*-2,2,6,6-*t*etramethyl-3,5-*h*eptane*d*ionatoeuropium and thus the (less common) substitute $Eu(thd)_3$ for $Eu(dpm)_3$.

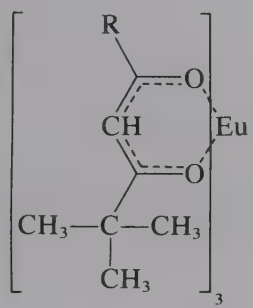

R = *t*-butyl, $Eu(dpm)_3$
R = $CF_2CF_2CF_3$, $Eu(fod)_3$

The use of such shift reagents is illustrated in Figure 4.52 in which the NMR spectrum of 1-heptanol is simplified by the addition of $Eu(dpm)_3$. As is usual for such an alcohol in the absence of shift reagents, the only interpretable signal (Fig. 4.52*a*) is that of the methylene adjacent to OH (proton set *A*, δ 3.7, triplet) and the terminal methyl (distorted set *G*, triplet, δ 0.9). Upon addition of the shift reagent $Eu(dpm)_3$, the signals of the methylene groups closer to the OH group are moved downfield so that a separate signal is available for each of the methylene units (Fig. 4.52*c*):

$$\underset{G}{CH_3}—\underset{F}{CH_2}—\underset{E}{CH_2}—\underset{D}{CH_2}—\underset{C}{CH_2}—\underset{B}{CH_2}—\underset{A}{CH_2}—OH$$

The closer the group to the functional group, the greater is the shift per increment of shift reagent (Fig. 4.53).

There are two major applications of the shift reagent to structure determination: (1) to simplify the spectrum and (2) to assign the protons from data on the response curves as in Figure 4.53. The former is straightforward and is subject only to the limit of the dependence of the coupling constant on shift reagent concentration.

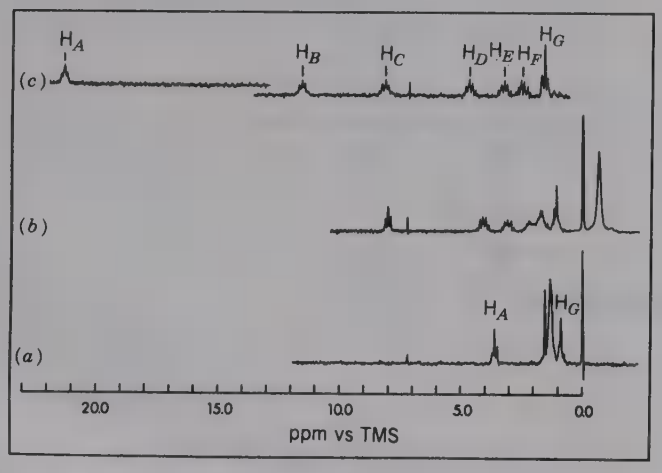

FIGURE 4.52. The 60 MHz proton NMR spectra of 0.40 mL of $CDCl_3$ solution containing 0.300 *M* 1-heptanol at various mole ratios [moles of $Eu(dpm)_3$ per mole of 1-heptanol]: (*a*) 0.00, (*b*) 0.19, (*c*) 0.78. Temperature, 30°C. From *Anal. Chem.*, Vol. 43, p. 1599, Copyright © 1971 by the American Chemical Society. Reprinted by permission of the copyright owner.

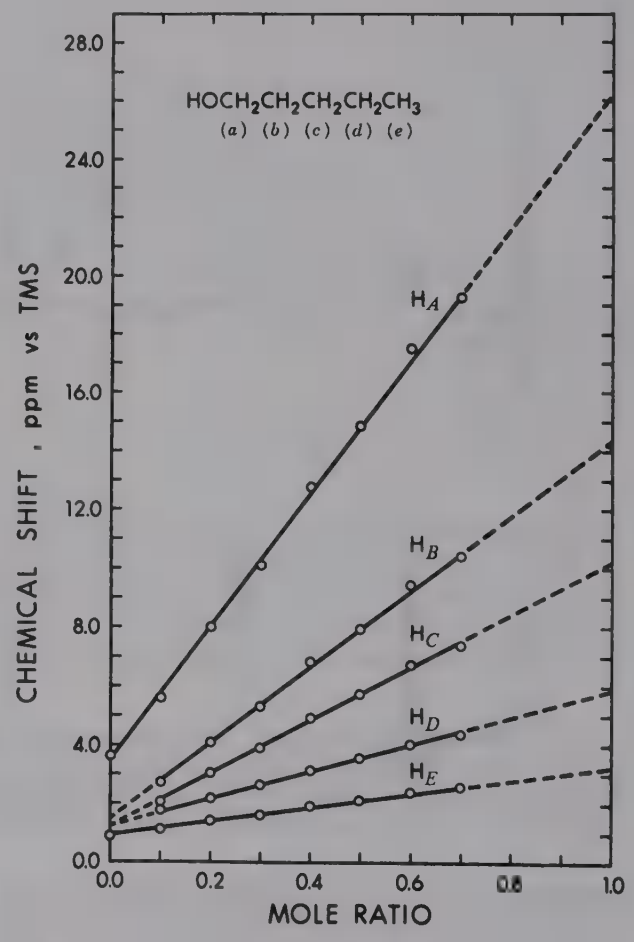

FIGURE 4.53. Variation in chemical shift for carbon-bonded protons of 1-pentanol in $CDCl_3$ (0.40 mL of 0.300 *M* solution) with increasing concentration of $Eu(dpm)_3$. Temperature, 30°C. From *Anal. Chem.*, Vol. 43, p. 1599. Copyright © by the American Chemical Society (1971). Reprinted by permission of the copyright owner.

TABLE 4.3

Variation of the Magnitude of Induced Shift with Functionality

Functional Group	ppm per mol of $Eu(dpm)_3$ per mol of Substrate in CCl_4
$RCH_2\underline{N}H_2$	~150
$RCH_2\underline{O}H$	~100
$R_2C{=}N\underline{O}H$	~40
$RC\underline{H}_2NH_2$	30–40
$RC\underline{H}_2OH$	20–25
$RC\underline{H}{=}NOH$	14–30
$RC\underline{H}_2RC{=}NOH$	14–10
$RC\underline{H}_2COR$	10–17
$RC\underline{H}_2CHO$	11–19
$RC\underline{H}_2SOR$	9–11
$RC\underline{H}_2{-}O{-}C\underline{H}_2R$	10 (17–28 in $CDCl_3$)
$RC\underline{H}_2CO_2Me$	7
$RCH_2CO_2C\underline{H}_3$	6–5
$RC\underline{H}_2CN$	3–7
$RC\underline{H}_2NO_2$	~0
Halides, indoles, alkenes	0
RCO_2H and phenols[a]	Decompose reagent

[a]Phenols can be studied using $Eu(fod)_3$.

The latter is less certain because of the many parameters on which these slopes depend.

It is necessary to report the solvent and the concentration of the substrate and shift reagent for a given shift reagent experiment (see Fig. 4.52 legend).

Table 4.3 shows the general correlation between basicity of the functional group of the substrate and shift magnitude as induced by $Eu(dpm)_3$. The complex $Eu(fod)_3$ is normally a "stronger" shift reagent since it is a stronger Lewis acid; it has the additional advantage of much greater solubility. However, quantitative assessments such as Table 4.3, should be treated with caution, since such data were assembled before it was fully appreciated that shift reagent performance is susceptible to many parameters including the purity of the shift reagent, the method of data handling, and the presence of water. Because of the hygroscopicity of the reagents and the adverse effect of small amounts of water, it is advisable to work in a drybox for quantitative results.

The recent development of binuclear lanthanide(III)–silver(I) shift reagents extends the effectiveness of shift reagents to thioethers, mercaptans, nitro compounds, alkenes, and aromatic hydrocarbons.*

The optical purity (enantiomeric composition) of a chiral substrate may be determined by using a single enantiomer of a chiral shift reagent. Each of the pair of diastereomeric complexes thus formed provides an individual spectrum; given sufficient separation, the enantiomeric composition may be determined.*†

REFERENCES

General

Jackman, L. M. and Sternhell, S. *Applications of NMR Spectroscopy in Organic Chemistry*. 2nd ed. New York: Pergamon, 1969.

Becker, E. D. *High Resolution NMR*. New York: Academic, 2nd ed., 1980.

Ault, A. and Dudek, G. O. *NMR, An Introduction to Proton Nuclear Magnetic Resonance Spectrometry*. San Francisco: Holden–Day, 1976.

Shoolery, J. N. *A Basic Guide to NMR*. Palo Alto: Varian Associates, 1972.

Abraham, R. J., Fisher, J., and Loftus, P. *Introduction to NMR Spectroscopy*, 2nd ed. London–New York: Wiley, 1989.

Paudler, W. W. *Nuclear Magnetic Resonance*. New York: Wiley, 1987.

Atta-ur-Rahman. *Nuclear Magnetic Resonance*. New York: Springer–Verlag, 1986.

Farrar, T. C. *An Introduction to Pulse NMR Spectroscopy*. Chicago: Farragut Press, 1987.

Morrill, T. C. (Ed.). *Lanthanide Shift Reagents in Stereochemical Analysis*. New York: VCH Publishers, 1986.

Bovey, F. A. *Nuclear Magnetic Resonance Spectroscopy*. 2nd ed. New York: Academic, 1988.

Yoder, C. H. and Schaeffer, C. D., Jr. *Introduction to Multinuclear NMR*. Menlo Park, CA: Benjamin–Cummings, 1987.

Sanders, J. K. and Hunter, B. K. *Modern NMR Spectroscopy*. Oxford: Oxford University Press, 1987.

Spectra, Data, and Reviews

Varian Associates. *High Resolution NMR Spectra Catalogue*, Vol. 1, 1962; Vol. 2, 1963.

The Sadtler Collection of High Resolution Spectra. Philadelphia: Sadtler Research Laboratories.

Pouchert, C. J. *Aldrich Library of NMR Spectra*, Vols. 1 and 2, Milwaukee, WI: Aldrich, 1983.

Brugel, W. *Handbook of NMR Spectral Parameters*. Vols. 1–3, Philadelphia: Heyden, 1979.

Bovey, F. A. *NMR Data Tables for Organic Compounds*. Vol. 1, New York: Wiley–Interscience, 1967.

*T. J. Wenzel, Binuclear lanthanide(II)–silver(I) NMR shift reagents. In Morrill, T. C. (Ed.), *Lanthanide Shift Reagents in Stereochemical Analysis*. New York: VCH Publishers, 1986, pp. 151–173.

†K. Mori, The significance of chirality: methods for determining absolute configuration and optical purity of pheromones and related compounds. In Hummel, H. E. and Miller, T. A. (Eds.). *Techniques in Pheromone Research*. New York: Springer–Verlag, 1984, pp. 323–370.

Chamberlain, N. F. *The Practice of NMR Spectroscopy with Spectra–Structure Correlation for ^1H*. New York: Plenum, 1974.

Wiberg, K. B. and Nist, B. J. *The Interpretation of NMR Spectra*. New York: Benjamin, 1962.

Sasaki, S. *Handbook of Proton-NMR Spectra and Data*. Vols. 1–5. New York: Academic, 1985 (4000 spectra).

Schwartz, L. J. *A Step-by-Step Picture of Pulsed (Time-Domain) NMR*. *J. Chem. Educ.* **65**, 752–756 (1988).

PROBLEMS

4.1. Match the underlined protons in the following compounds with the correct chemical shift (δ):

a. $CH_3—CH=C\underline{H}—CH_3$ ( ) 1.20

b. 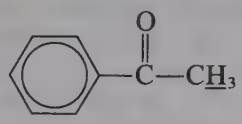 ( ) 2.40

c. $C\underline{H}_3—CH_2—O—CH_3$ ( ) 5.30

d. 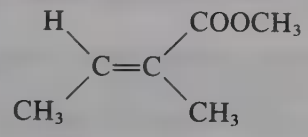 ( ) 8.21

e. 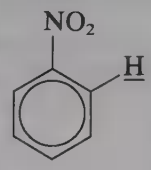 ( ) 5.00

f. 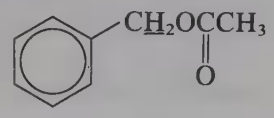 ( ) 6.73

4.2. Draw an ^1H NMR spectrum for each of the following compounds in $CDCl_3$. Assume sufficient resolution to provide a first-order spectrum.

a. 

b. CH_3CH_2Br

c. $CH_3—\overset{\overset{O}{\|}}{C}—O—CH_2CH_3$

d. $Cl—CH_2—\overset{\overset{O}{\|}}{C}—H$

e. 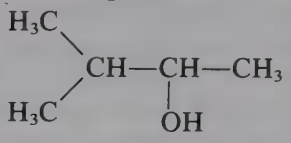

f. $CH_2=CH—\overset{\overset{O}{\|}}{C}—CH_3$

g. 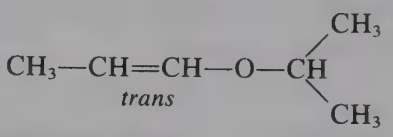

h. 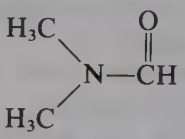

4.3. The pair of protons at C-3 of *cis*-1,2-dichlorocyclopropane are diastereotopic. Explain.

4.4. Give Pople notation (*AX*, etc.) for all of the spin systems of

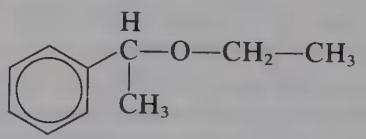

4.5. Deduce the structures of Compounds A–H and assign all ^1H signals (in $CDCl_3$ at 60 MHz).*

*By permission of Sadtler Standard Spectra; all rights reserved by Sadtler Research Laboratories.

PROBLEM 4.5. ***Compound A, $C_5H_{10}O$.***

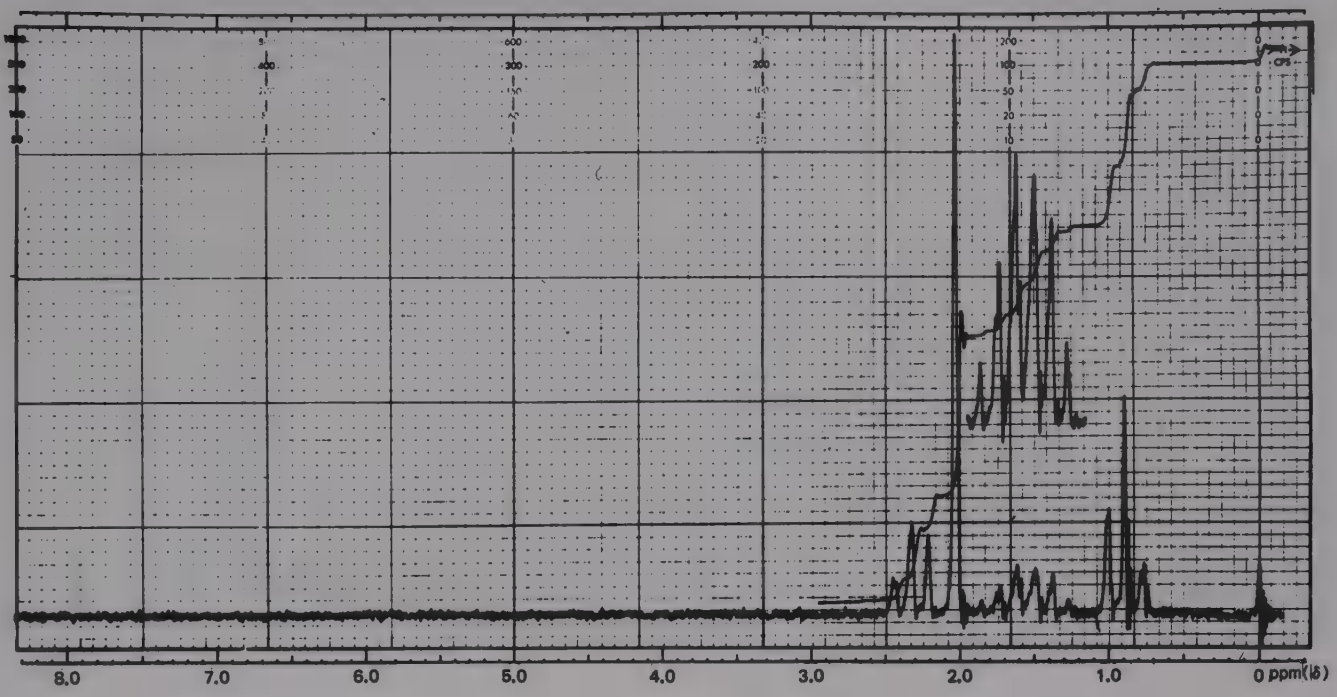

PROBLEM 4.5. ***Compound B, C_4H_8O.***

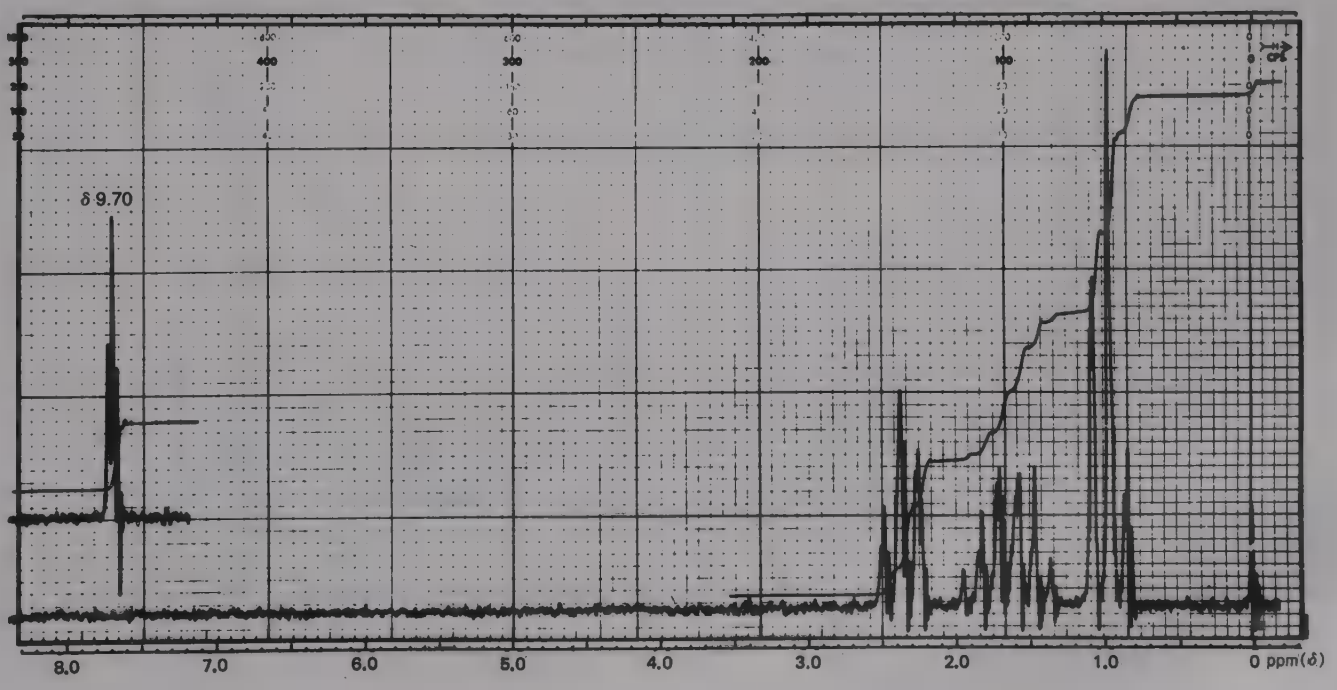

PROBLEM 4.5. *Compound C, $C_5H_{10}O_2$. Absorption at δ 2.40 is sextet.*

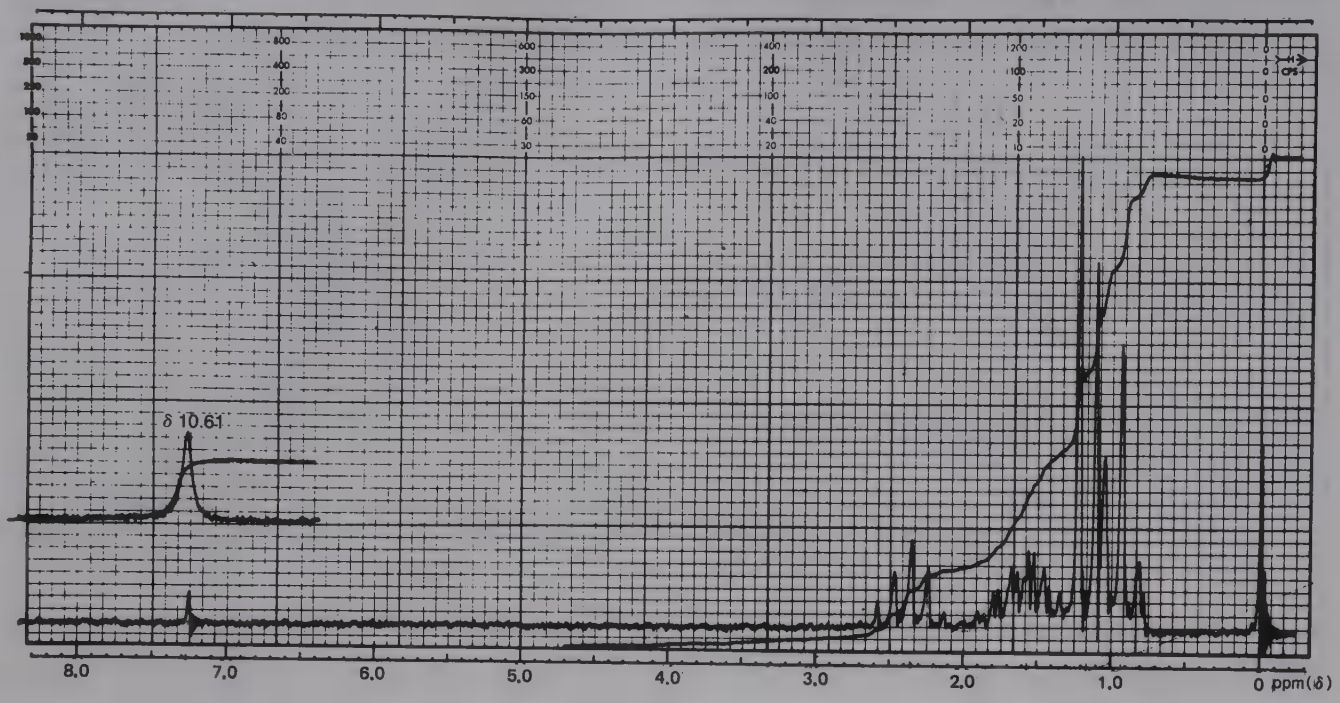

PROBLEM 4.5. *Compound D, C_6H_{12}. Multiplet at δ 2.24 is septet.*

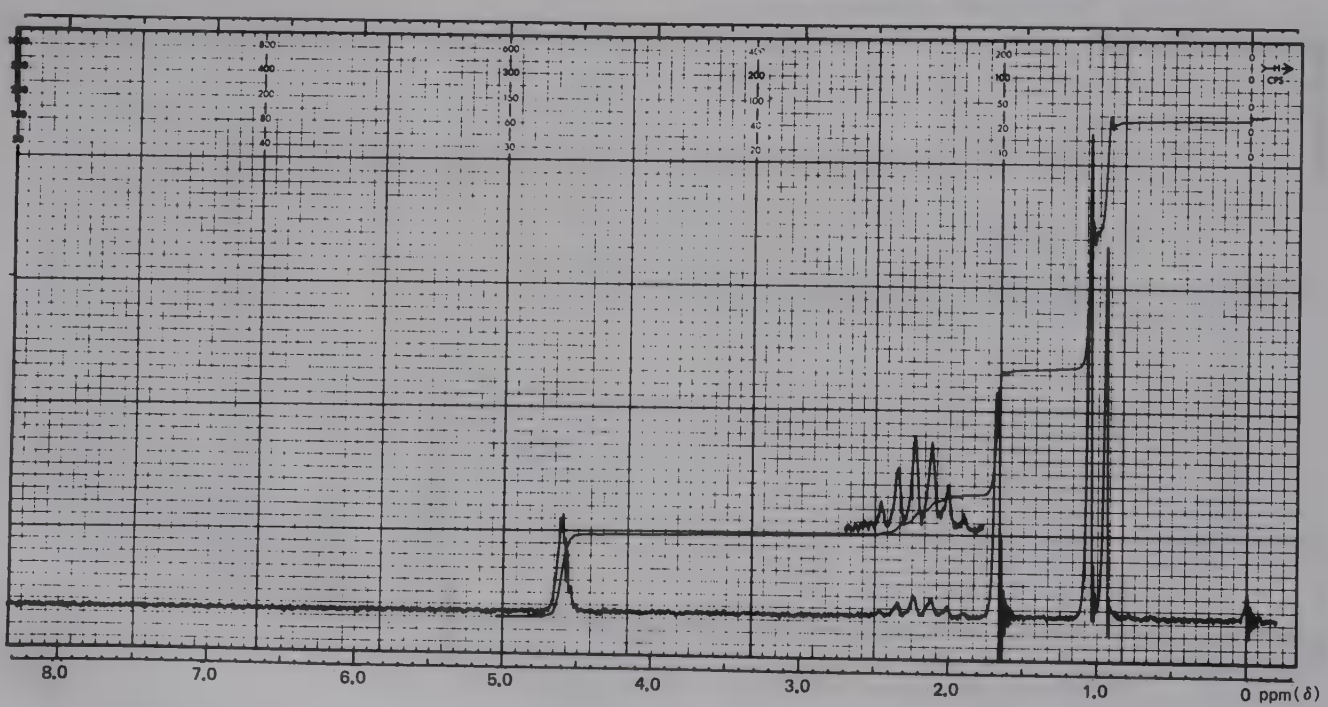

PROBLEM 4.5. ***Compound E, $C_8H_{10}O_2$.***

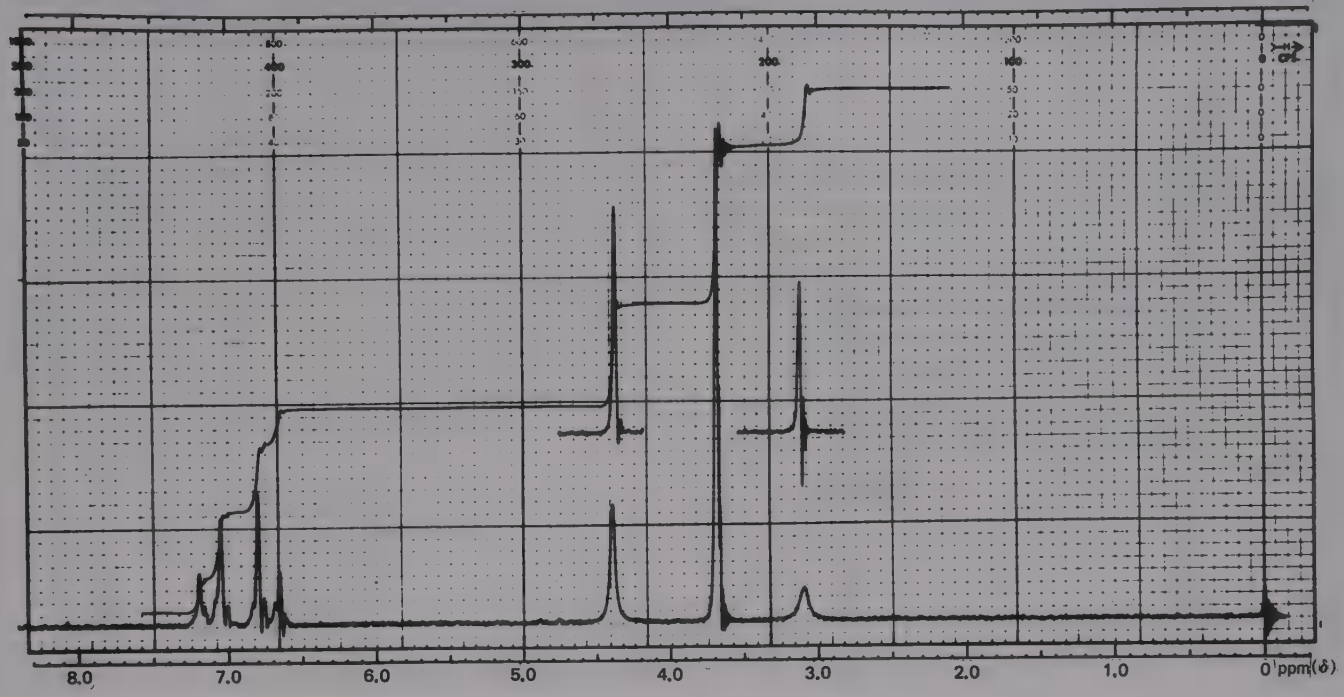

PROBLEM 4.5. ***Compound F, $C_{10}H_{14}O$.***

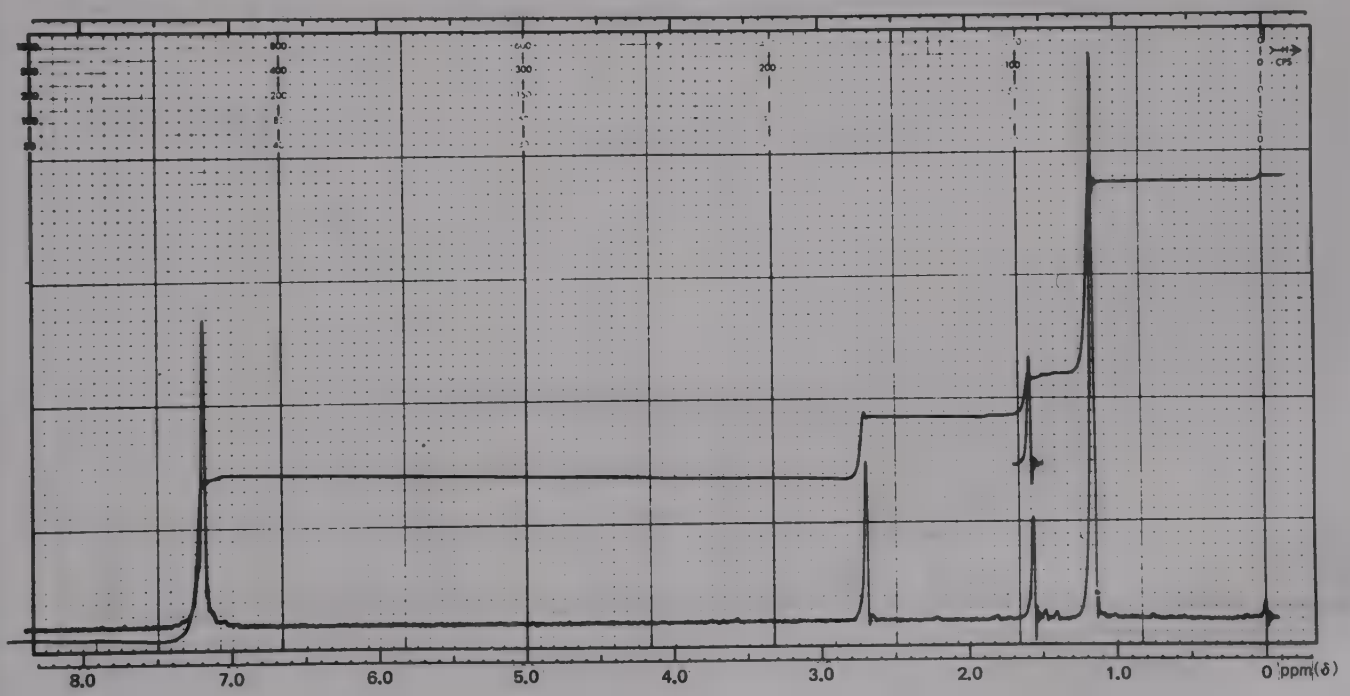

PROBLEM 4.5. ***Compound G, $C_{14}H_{12}O_2$.***

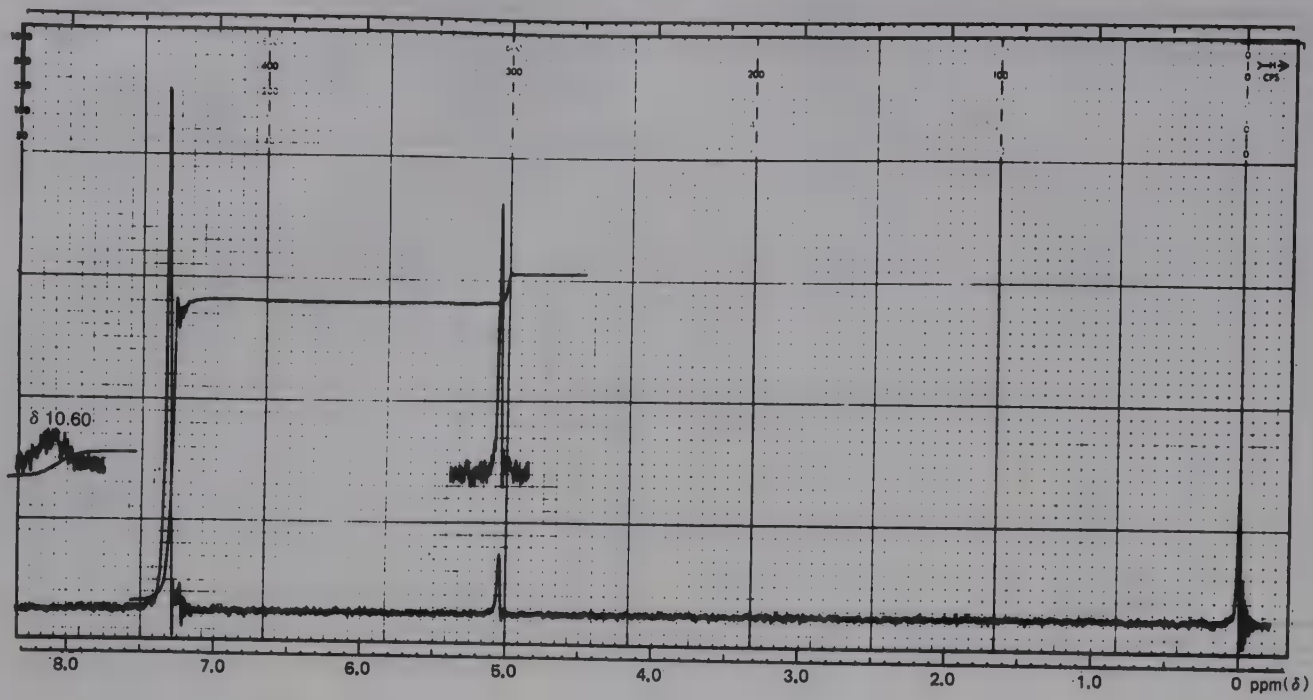

PROBLEM 4.5. ***Compound H, $C_8H_{14}O$. A tertiary alcohol.***

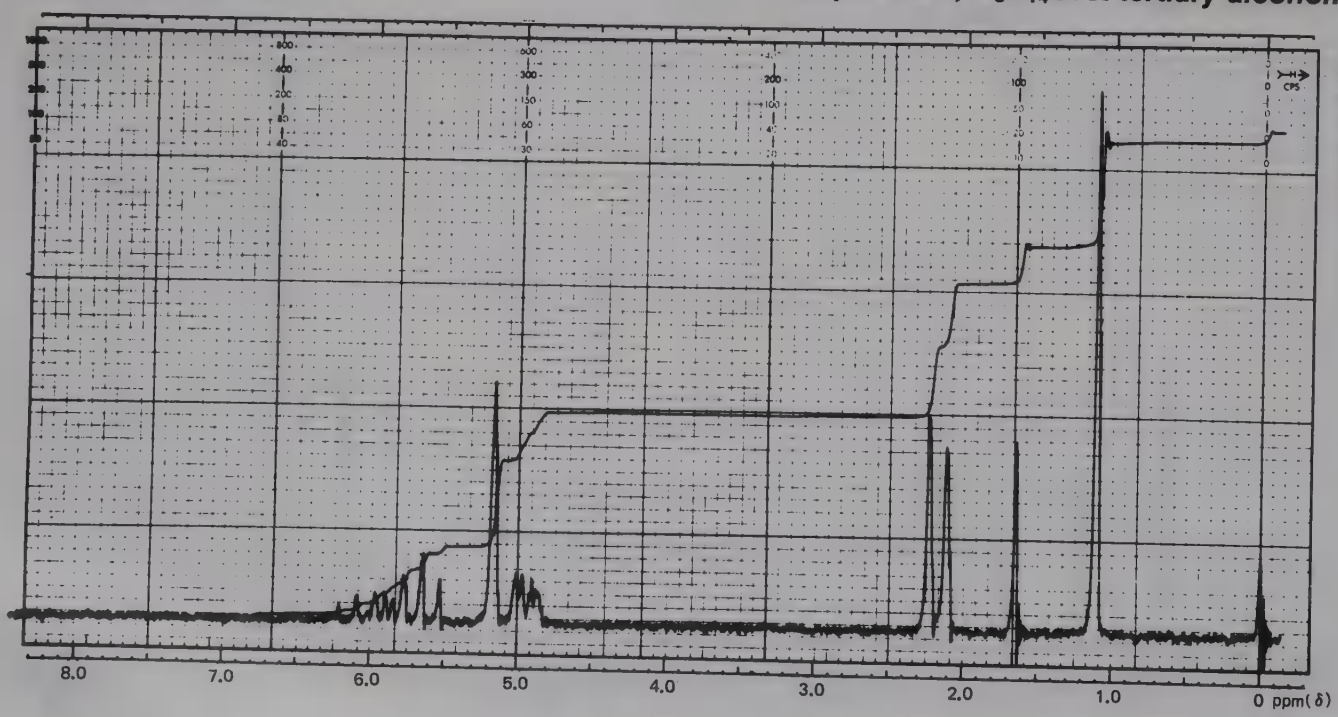

Appendix A Effect on Shift Positions of a Single Functional Group (Data at 60 MHz.)

Charts A.1 and A.2 give the chemical shifts of CH_3, CH_2, and CH groups that are adjacent to, or once removed from, a functional group in aliphatic compounds. In a hydrocarbon, the methyl protons are at about δ 0.90, the methylene protons at about δ 1.25, and the methine protons at about δ 1.50. The first line of the first chart, for example, shows that the protons of CH_3Br absorb at about δ 2.70, the methylene protons of RCH_2Br at about δ 3.40, and the methine protons of R_2CHBr at about δ 4.10.

The shift positions vary with changes in solvent or concentration, but in general these variations are slight in the absence of a very polar solvent or of hydrogen bonding. The positions shown are average values for ranges that are not greater than 0.5 ppm wide if the common solvents CCl_4 or $CDCl_3$ are used. These values were gathered from several sources: Jackman and Sternhell, Chamberlain, Bovey, K. Nukada, et al., *Anal. Chem.* **35**, 1892 (1963), and G. V. D. Tiers (*NMR Summary;* 3M Company, St. Paul, Minnesota).

CHART A.1 Chemical Shifts of Protons on a Carbon Atom Adjacent (α Position) to a Functional Group in Aliphatic Compounds (M—Y)

▮ M = methyl
8 M = methylene
⋮ M = methine

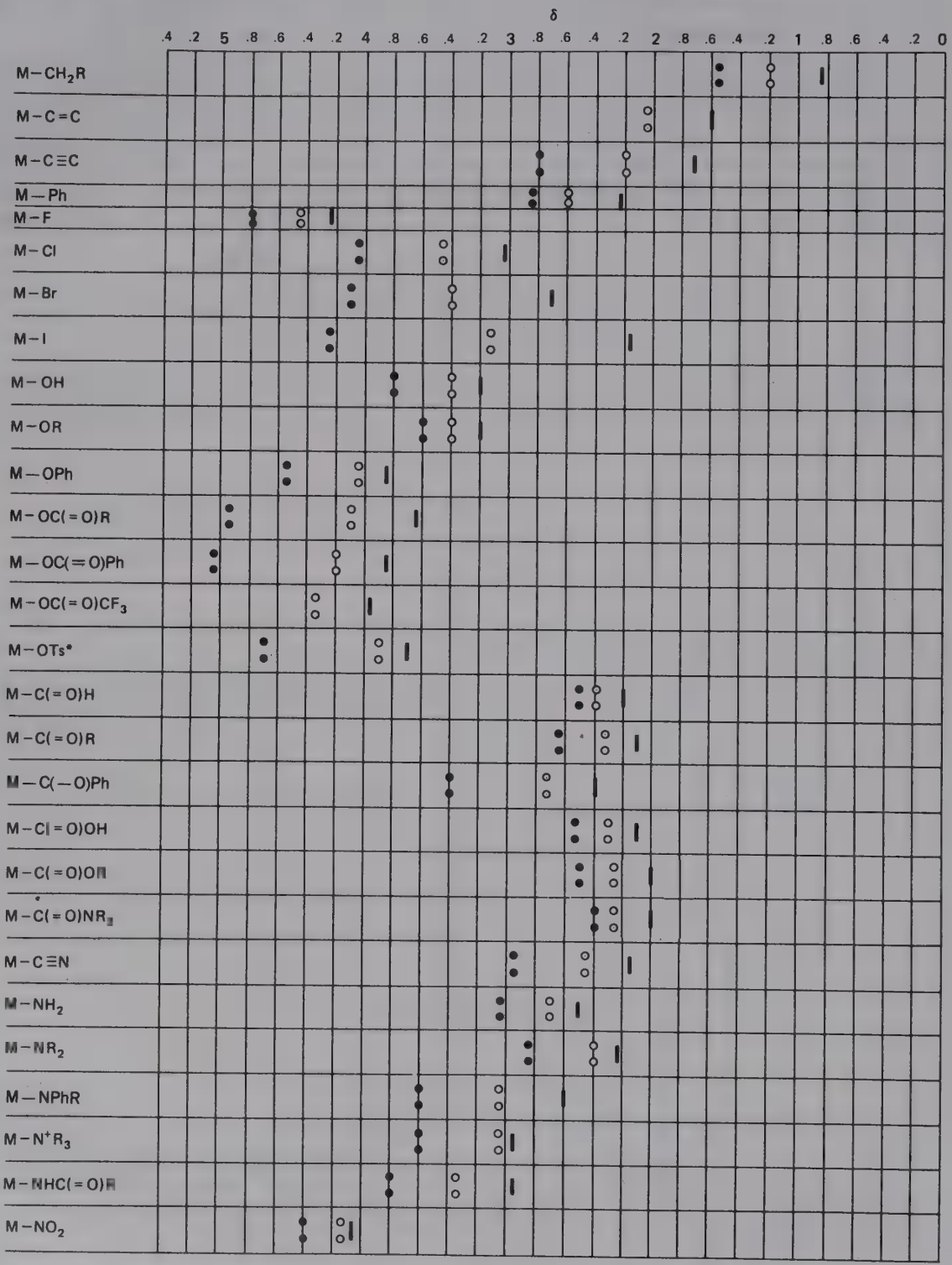

*OTs is —O_2S— CH_3

CHART A.1 (continued)

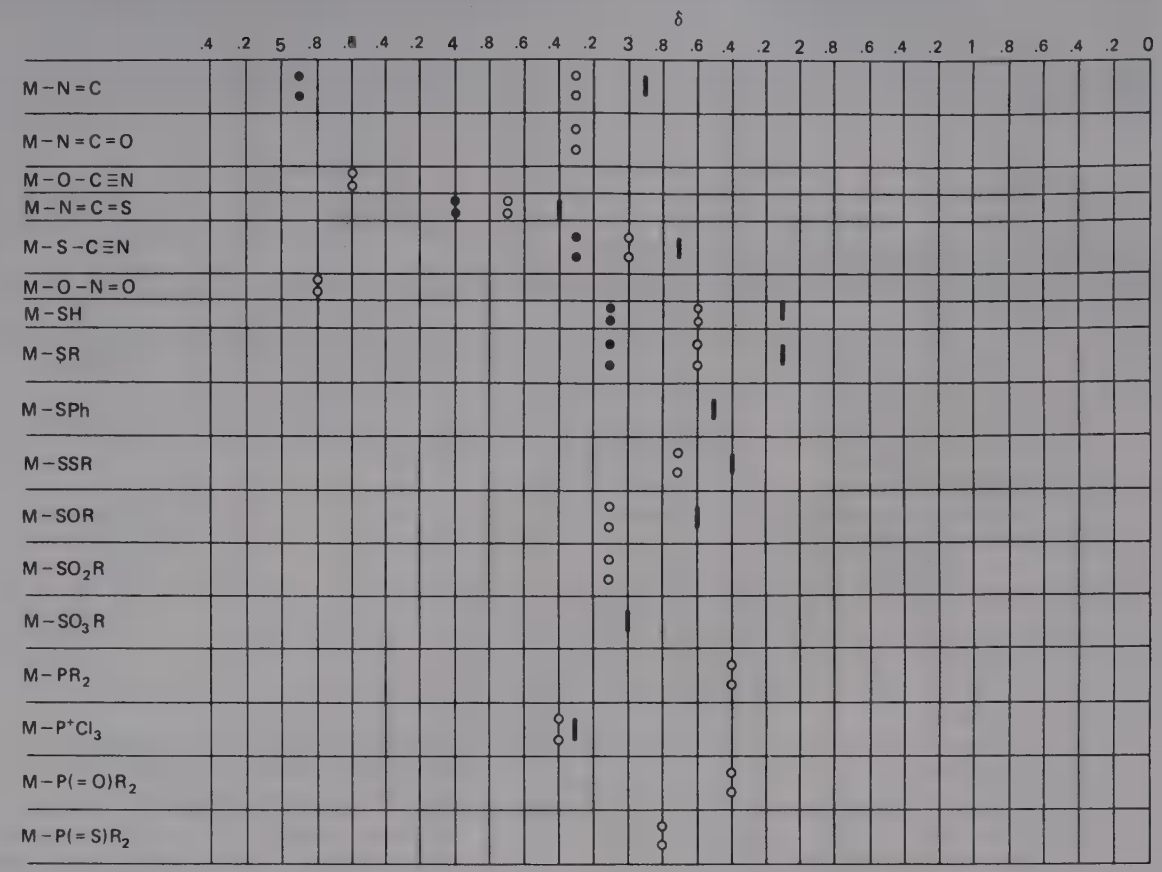

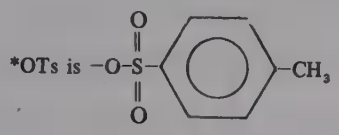

CHART A.2 Chemical Shifts of Protons on a Carbon Atom Once Removed (β POSITION) from a Functional Group in Aliphatic Compounds (M—C—Y)

▮ M = methyl
▮ M = methylene
▮ M = methine

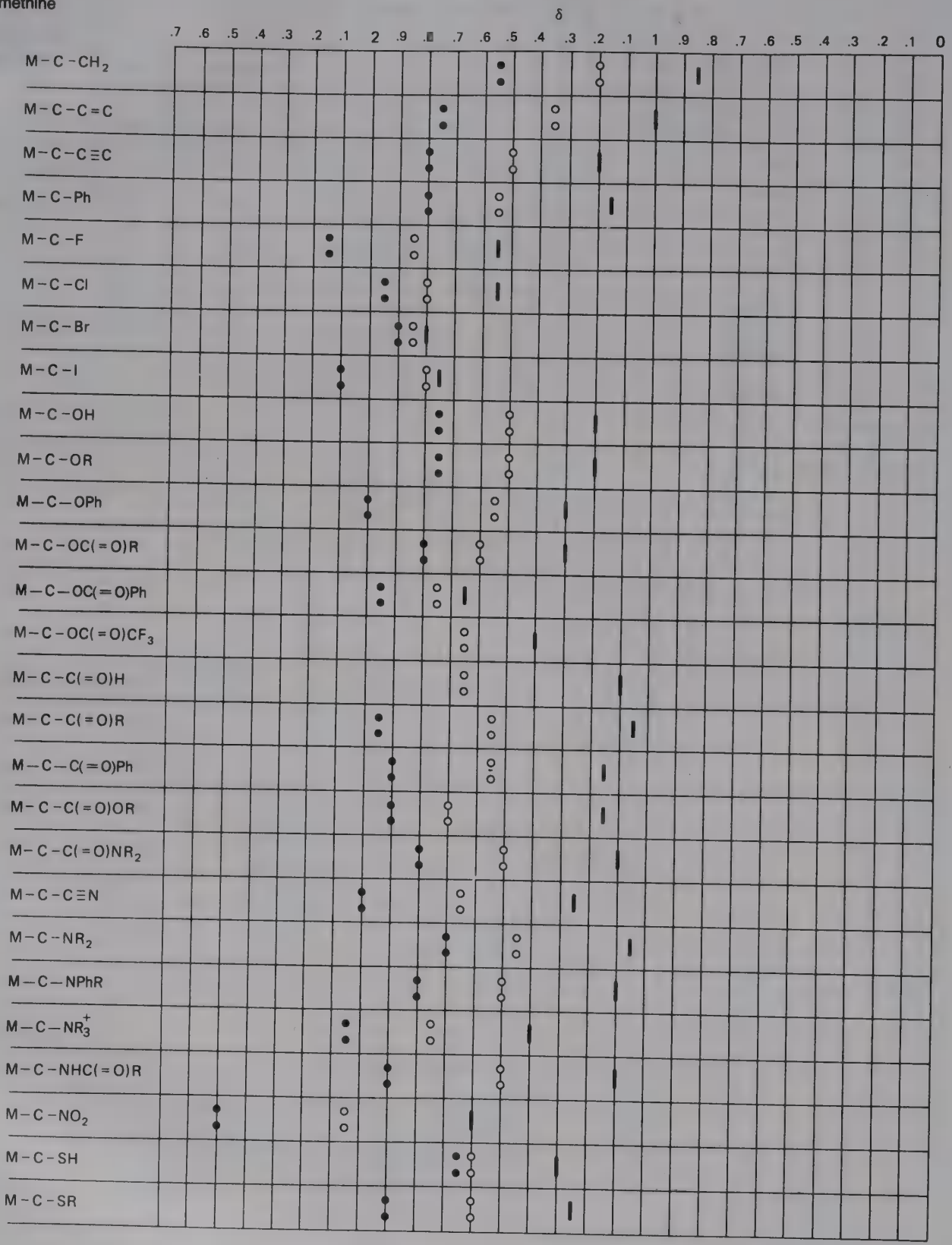

Appendix B Effect on Chemical Shifts of Two or Three Functional Groups (Y—CH_2—Z and Y—C H—Z)
W

Shoolery's rules (J. N. Shoolery, Varian Technical Information Bulletin, Vol. 2, No. 3, Palo Alto, CA, 1959) permit calculation of a shift position of a methylene group attached to two functional groups by the additive effect of the shielding constants in Table B-1. The sum of the constants is added to δ 0.23, the position for CH_4.

Thus, to calculate the shift for the —CH_2— protons of $C_6H_5CH_2Br$

C_6H_5 =	1.85
Br =	2.33
	4.18
add CH_4	0.23
	4.41

The shielding constants were used to prepare the following chart (Chart B-1). Several values were added to the original set of constants. This chart can be used to find the shift position of a methylene group attached to two functional groups from the δ values in the box at the intersection of the horizontal and diagonal groups ("mileage chart"). The upper number in each box is an experimental value; the lower number is calculated from Shoolery's constants.

These shielding constants were revised and extended for methyl, methylene, and methine protons.

TABLE B.1

Shielding Constants

Y or Z	Shielding Constants	Y or Z	Shielding Constants
—CH_3	0.47	—C(=O)NR_2	1.59
—C=C	1.32	—C≡N	1.70
—C≡C	1.44	—NR_2	1.57
—Ph	1.85	—NHC(=O)R	2.27
—CF_2	1.21	—N_3	1.97
—CF_3	1.14	—SR	1.64
—Cl	2.53	—OSO_2R	3.13
—Br	2.33		
—I	1.82		
—OH	2.56		
—OR	2.36		
—OPh	3.23		
—OC(=O)R	3.13		
—C(=O)R	1.70		
—C(=O)Ph	1.84		
—C(=O)OR	1.55		

E. C. Friedrich and K. G. Runkle, *J. Chem. Educ.* **61**, 830 (1984); **63**, 127 (1986).

CHART B.1 Chemical Shifts for Methylene Groups Attached to Two Functional Groups (Y—CH_2—Z)

GROUP	$-CH_3$	$-C{=}C$	$-C{\equiv}C$	$-Ph$	$-CF_2$	$-CF_3$	$-Cl$	$-Br$	$-I$	$-OH$	$-OR$	$-OPh$	$-OC(=O)R$	$-C(=O)R$	$-C(=O)Ph$	$-C(=O)OR$	$-C(=O)NR_2$	$-C{\equiv}N$	$-NR_2$	$-NHC(=O)R$	$-N_3$	$-SR$
$-CH_3$	1.17	1.90 2.02	2.14	2.55	1.91	1.84	3.57 3.23	3.43 3.03	3.20 2.52	3.70 3.26	3.40 3.06	3.93	4.25 3.83	2.47 2.40	2.54	2.25 2.25	2.23 2.29	2.40	2.63 2.27	2.97	2.67	2.53 2.34
$-C{=}C$		2.60 2.87	3.39 2.99	3.30 3.40	2.76	2.69	4.08	3.93 3.88	3.87 3.37	4.13	3.95 3.91	4.78	4.68	3.25	3.39	3.00 3.10	3.14	3.15 3.25	3.30 3.12	3.82	3.52	3.08 3.19
$-C{\equiv}C$			3.11	3.52	2.88	2.81	4.09 4.20	3.90 4.00	3.49	4.28	4.03	4.90	4.71 4.80	3.37	3.51	3.22	3.26	3.37	3.50 3.24	3.97	3.67	3.31
$-Ph$				3.97 3.93	3.29	3.50 3.22	4.50 4.61	4.35 4.41	3.90	4.58	4.70 4.44	4.91 5.31	5.08 5.21	3.55 3.78	3.92	3.40 3.63	3.66	3.65 3.78	3.48 3.65	4.34	4.04	3.68 3.72
$-CF_2$					2.63	2.58	3.97	3.76	3.26	4.01 4.01	3.80	4.67	4.57	3.12	3.28	2.99	3.03	3.12	3.01	3.71	3.41	3.08
$-CF_3$						2.51	3.90	3.70	3.56 3.19	3.93	4.73	4.60	4.54	3.07	3.21	2.92	2.96	3.07	2.94	3.64	3.34	3.01
$-Cl$							4.99 5.29	5.16 5.09	4.99 4.58	5.32	5.40 5.12	5.99	5.89	4.46	4.60	4.05 4.31	4.17 4.35	4.07 4.46	4.37	5.13	4.71	4.40
$-Br$								4.94 4.89	4.38	5.12	4.92	6.36 5.79	5.69	4.26	4.40 3.40	3.70 4.11	3.92 4.15	4.26	4.13	4.83	4.53	4.20
$-I$									3.90 3.87	4.61	4.41	5.16	5.06	3.75	3.89	3.60	3.65 3.64	3.65 3.75	3.62	4.32	4.02	3.69
$-OH$										4.55 4.35	5.15	6.02	5.92	4.49	4.63	4.34	4.38	4.49	4.35	5.06	4.76	4.43
$-OR$											4.55 4.95	5.82	5.72	4.29	4.43	4.13 4.22	4.18	4.20 4.29	4.15	4.94	4.64	4.23
$-OPh$												6.69	6.59	5.16	5.30	5.09	4.45 4.05	5.16	5.03	5.86	5.56	5.10
$-OC(=O)R$													6.46	4.42 5.10	5.20	4.91	4.95	5.10	4.92	5.63	5.37	5.00
$-C(=O)R$														3.60 3.63	3.77	3.37 3.48	3.52	3.63	3.50	4.10 4.20	3.90	3.57
$-C(=O)Ph$															3.91	3.62	3.66	3.77	3.64	4.34	4.02	3.71
$-C(=O)OR$																3.35 3.33	3.37	3.48	3.17 3.35	4.05	3.75	3.42
$-C(=O)NR_2$																	3.30 3.41	3.52	3.39	4.09	3.79	3.46
$-C{\equiv}N$																		3.63	3.50	4.20	3.90	3.57
$-NR_2$																			3.10 3.37	4.07	3.77	3.44
$-NHC(=O)R$																				4.75	4.45	4.14
$-N_3$																					4.15	3.84
$-SR$																						3.51

(a)

Table B-2 can be used to calculate chemical shifts of Y—CH_3, Y—CH_2—Z, or Y—$\underset{\displaystyle W}{\overset{\displaystyle |}{CH}}$—Z groups. Thus, the CH_2 chemical shifts in $Br\overset{2}{C}H_2\overset{1}{C}H_2OCH_2CH_2Br$ can be calculated.

	CH_2 No. 1	CH_2 No. 2
CH_2 (Table B-2, footnote *b*)	1.20	CH_2 1.20
α-OR	2.35	α-Br 2.18
β-Br	0.60	β-OR 0.15
	4.15	3.53

Determined: CH_2 No. 1 at ~δ 3.80; CH_2 No. 2 at ~δ 3.40.

TABLE B.2

Substituent Effects on Chemical Shift[a]

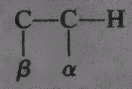

Substituent	Type of Hydrogen[b]	Alpha Shift	Beta Shift
—C=C—	CH_3	0.78	
	CH_2	0.75	0.10
	CH		
—C=C—C(=X)—R (X = C or O)	CH_3	1.08	
Aryl	CH_3	1.40	0.35
	CH_2	1.45	0.53
	CH	1.33	
—Cl	CH_3	2.43	0.63
	CH_2	2.30	0.53
	CH	2.55	0.03
—Br	CH_3	1.80	0.83
	CH_2	2.18	0.60
	CH	2.68	0.25
—I	CH_3	1.28	1.23
	CH_2	1.95	0.58
	CH	2.75	0.00
—OH	CH_3	2.50	0.33
	CH_2	2.30	0.13
	CH	2.20	
—OR (R is saturated)	CH_3	2.43	0.33
	CH_2	2.35	0.15
	CH	2.00	
—OC(=O)—R, —OC(=O)—OR, —OAr	CH_3	2.88	0.38
	CH_2	2.98	0.43
	CH	3.43 (esters only)	
—C(=O)R, where R is alkyl, aryl, OH, OR′, H, CO, or N	CH_3	1.23	0.18
	CH_2	1.05	0.31
	CH	1.05	
—NRR′	CH_3	1.30	0.13
	CH_2	1.33	0.13
	CH	1.33	

[a] From the Ph.D. dissertation of T. J. Curphey, Harvard University, by permission.

[b] Standard positions are CH_3, δ 0.87; CH_2, δ 1.20; CH, δ 1.55.

See also chemical shift correlations for methine proton, *Source:* E. C. Friedrich and K. G. Runkle, *J. Chem. Educ.*, **63**, 127 (1986).

Appendix C Chemical Shifts in Alicyclic and Heterocyclic Rings

TABLE C.1

Chemical Shifts in Alicyclic Rings

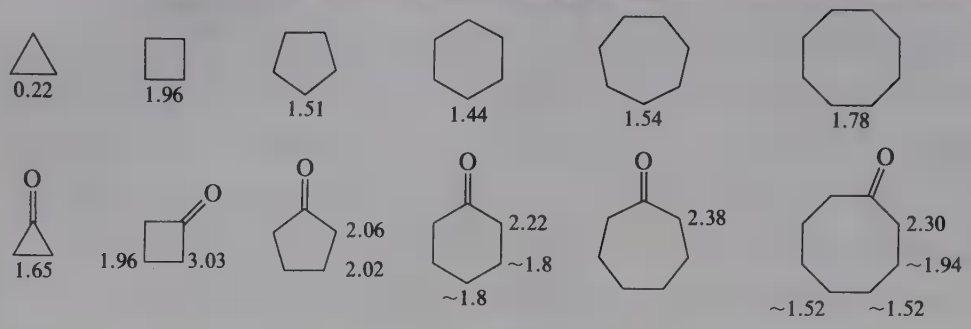

TABLE C.2

Chemical Shifts in Heterocyclic Rings

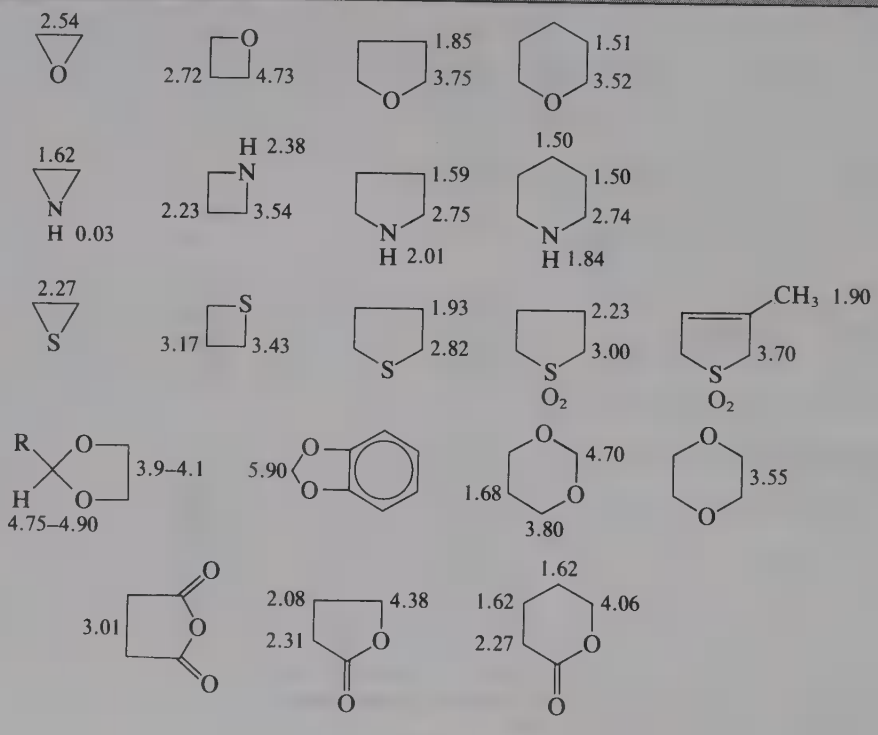

Appendix D Chemical Shifts in Unsaturated and Aromatic Systems

(See Table D.1)

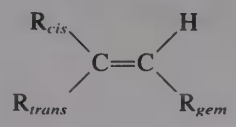

$$\delta_H = 5.25 + Z_{gem} + Z_{cis} + Z_{trans}$$

For example, the chemical shifts of the alkene protons in

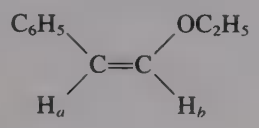

are calculated:

H_a	$C_6H_{5\,gem}$	1.35	5.25
	OR_{trans}	−1.28	0.07
		0.07	δ 5.32
H_b	OR_{gem}	1.18	5.25
	$C_6H_{5\,trans}$	−0.10	1.08
		1.08	δ 6.33

TABLE D.1

Substituent Constants (Z) for Chemical Shifts of Substituted Ethylenes (in CCl_4)

	Z				Z		
Substituent R	gem	cis	trans	Substituent R	gem	cis	trans
—H	0	0	0				
—Alkyl	0.44	−0.26	−0.29	—C=O	1.03	0.97	1.21
—Alkyl-ring[a]	0.71	−0.33	−0.30				
—CH_2O, —CH_2I	0.67	−0.02	−0.07	—C=O	1.37	0.93	0.35
—CH_2S	0.53	−0.15	−0.15				
—CH_2Cl, —CH_2Br	0.72	0.12	0.07	—C=O	1.10	1.41	0.99
—CH_2N	0.66	−0.05	−0.23	—OR, R:aliph	1.18	−1.06	−1.28
—C≡C	0.50	0.35	0.10	—OR, R:conj[b]	1.14	−0.65	−1.05
—C≡N	0.23	0.78	0.58	—OCOR	2.09	−0.40	−0.67
—C=C	0.98	−0.04	−0.21	—Aromatic	1.35	0.37	−0.10
—C=C conj[b]	1.26	0.08	−0.01	—Cl	1.00	0.19	0.03
—C=O	1.10	1.13	0.81	—Br	1.04	0.40	0.55
—C=O conj[b]	1.06	1.01	0.95				
—COOH	1.00	1.35	0.74	—N R:aliph	0.69	−1.19	−1.31
—COOH conj[b]	0.69	0.97	0.39				
				—N R:conj[b]	2.30	−0.73	−0.81
—COOR	0.84	1.15	0.56				
—COOR conj[b]	0.68	1.02	0.33	—SR	1.00	−0.24	−0.04
				—SO_2	1.58	1.15	0.95

[a]Alkyl ring indicates that the double bond is part of the ring 

[b]The Z factor for the conjugated substituent is used when either the substituent or the double bond is further conjugated with other groups.

Source: C. Pascual, J. Meier, and W. Simon, *Helv. Chim. Acta*, **49**, 164 (1966).

TABLE D.2

Chemical Shifts of Miscellaneous Alkenes

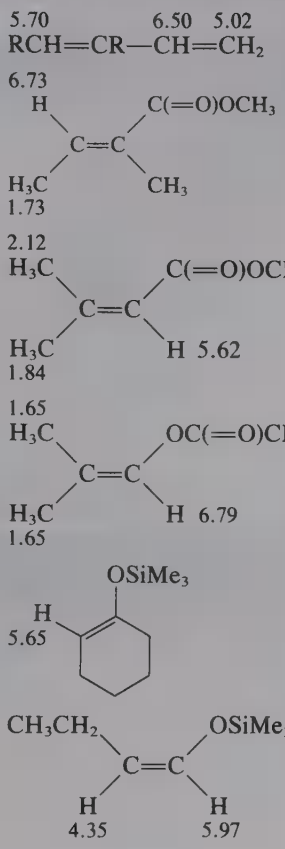

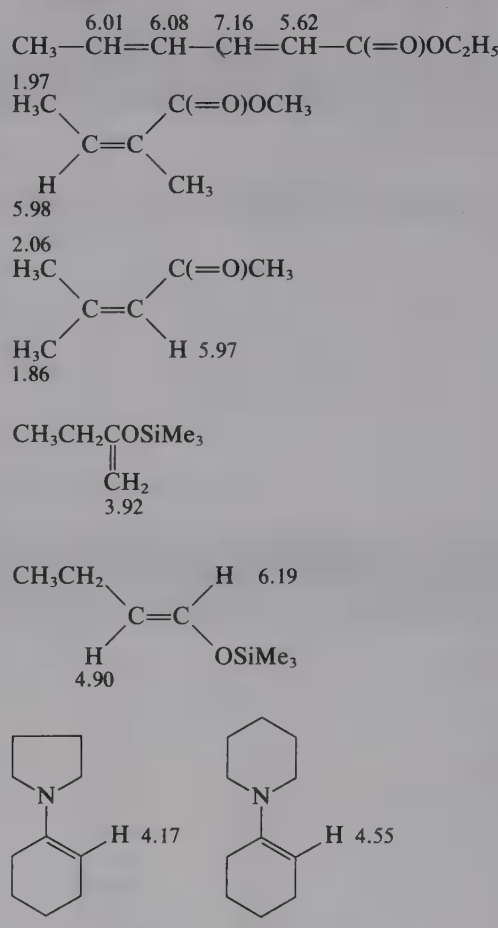

Table D.2 (continued)

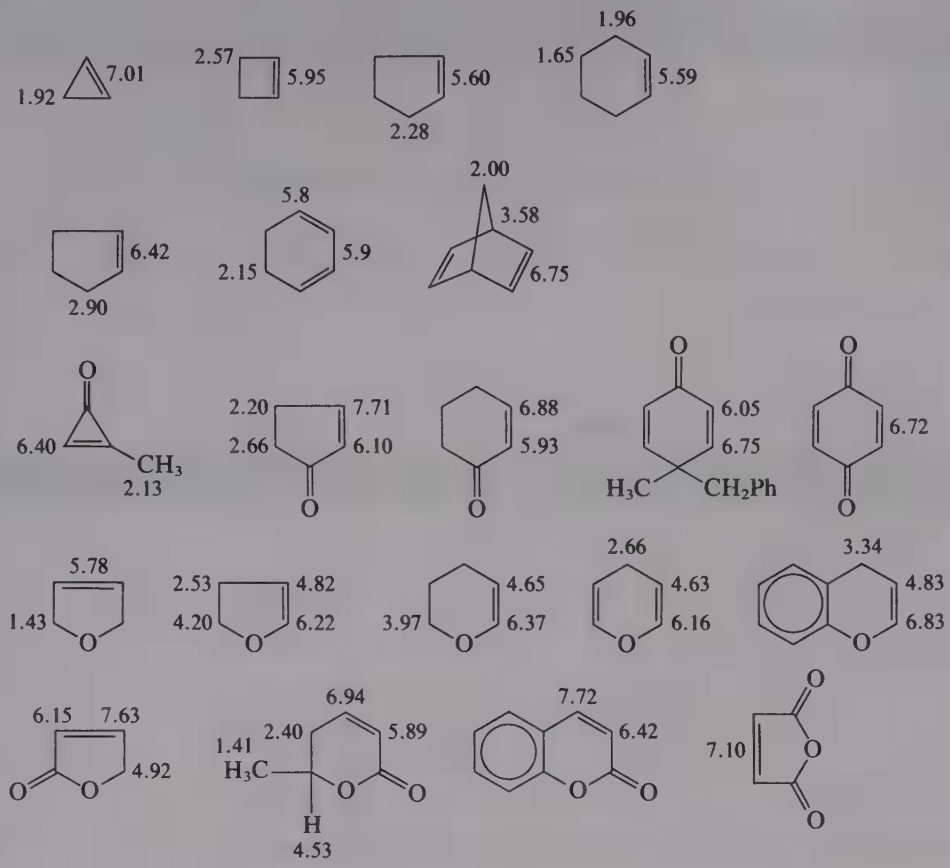

TABLE D.3

Chemical Shifts of Alkyne Protons	
HC≡CR	1.73–1.88
HC≡C—COH	2.23
HC≡C—C≡CR	1.95
HC≡CH	1.80
HC≡CAr	2.71–3.37
HC≡C—C≡CR	2.60–3.10

CHART D.1. Chemical Shifts of Protons on Monosubstituted Benzene Rings

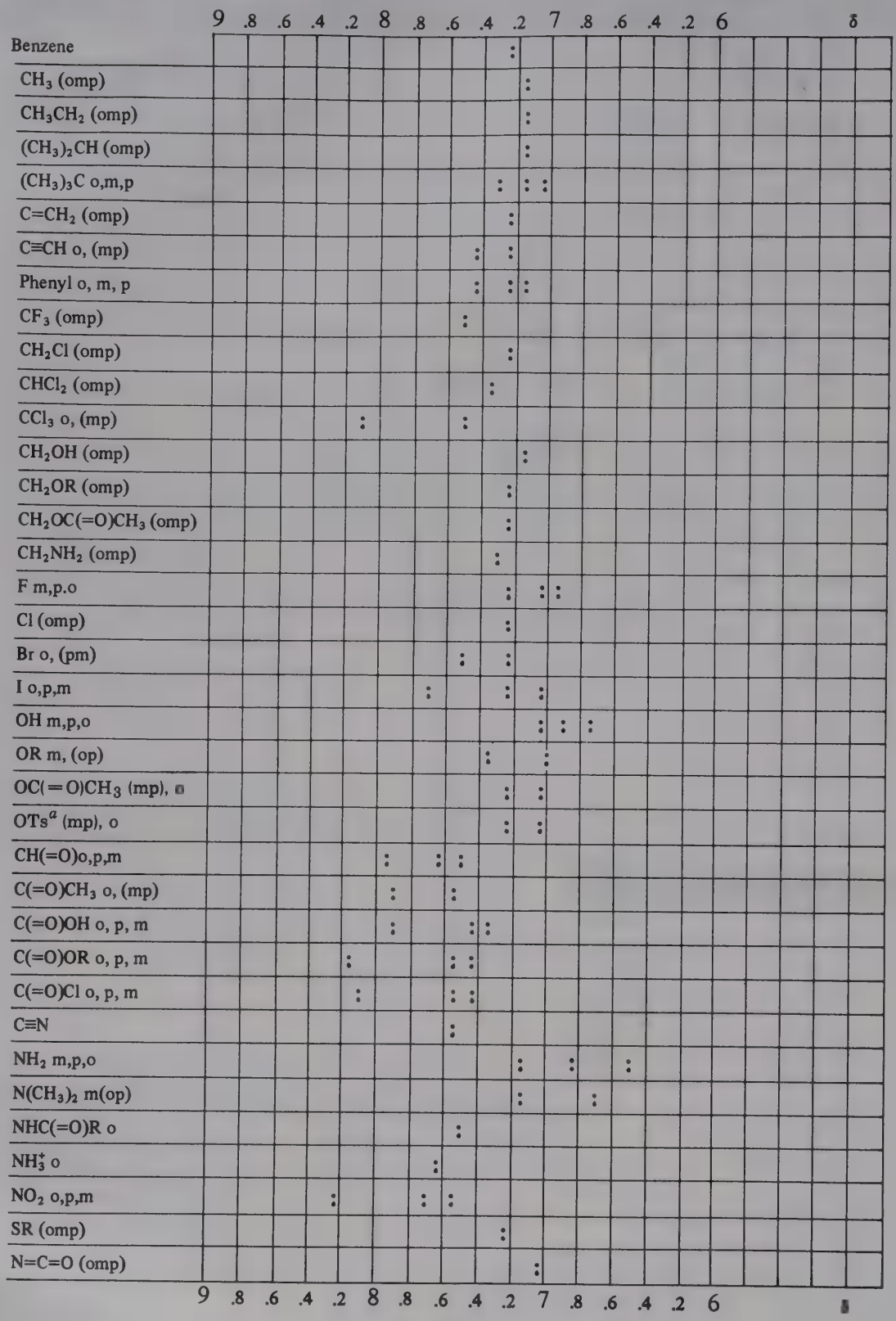

[a]OTs = *p*-Toluenesulfonyloxy group.

TABLE D.4

Chemical Shifts of Protons on Fused Aromatic Rings

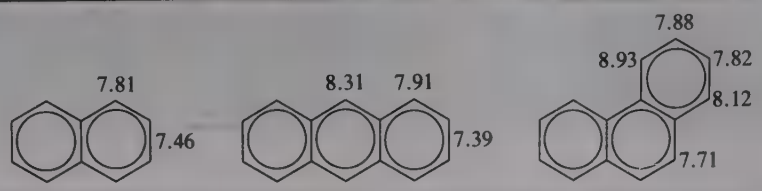

TABLE D.5

Chemical Shifts of Protons on Heteroaromatic Rings

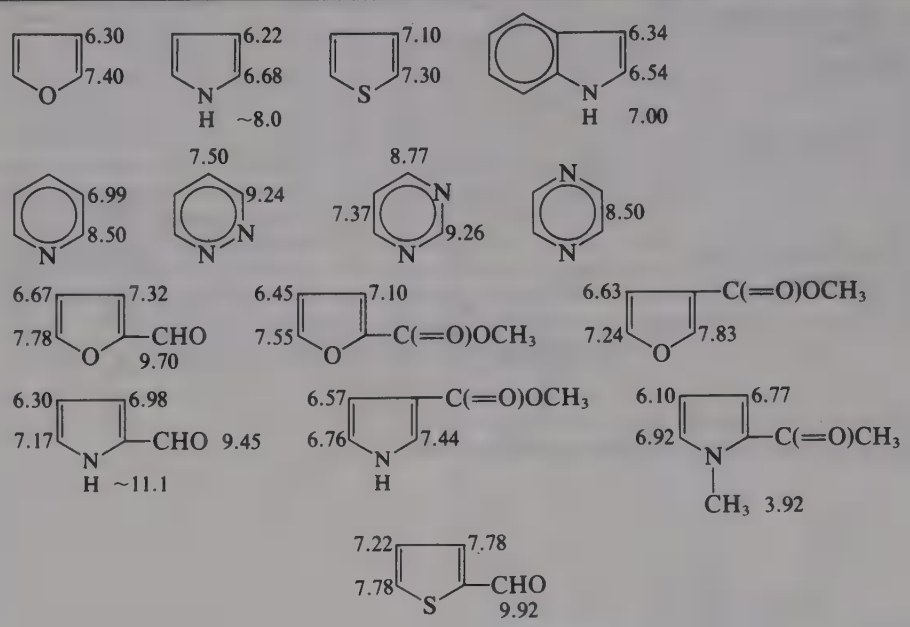

TABLE D.6

Chemical Shifts of HC=O, HC=N, (also HC(OR)2) Protons

RCH=O	9.70	HC(=O)OR	8.05	RCH=NOH *cis*	7.25
PhCH=O	9.98	$HC(=O)NR_2$	8.05	RCH=NOH *trans*	6.65
RCH=CHCH=O	9.78	$HC(OR)_3$	5.00	RCH=N—NH—(2,4-$(NO_2)_2$C$_6$H$_3$)	6.05

Appendix E Protons on Heteroatoms

CHART E.1 Protons Subject to Hydrogen-Bonding Effects (Protons on Heteroatoms)[a]

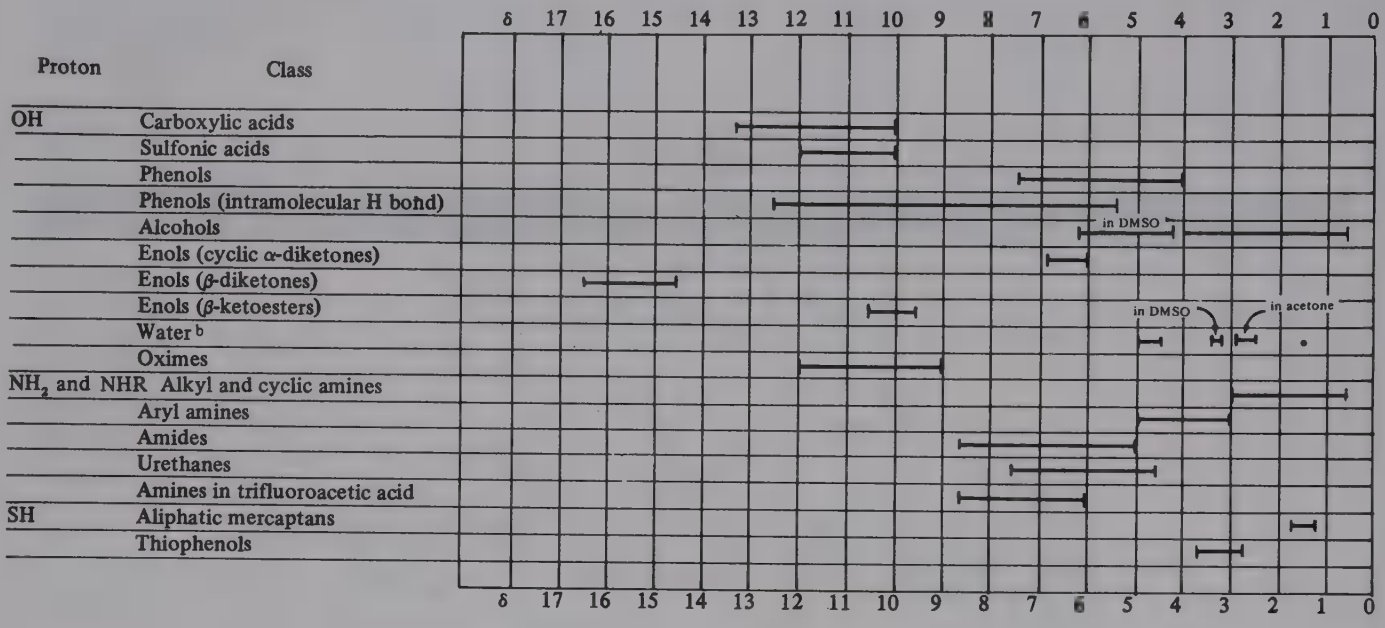

[a]Solvent $CDCl_3$. Chemical shifts within a range are a function of concentration.
[b]See Section 4.5.1.3.

TABLE E.1

Chemical Shift of Dissolved Water in Deuterated Solvents

Solvent	δ
Chloroform–d_3	1.5
Benzene–d_6	0.4
Acetone–d_6	2.75
Methylene chloride–d_2	1.55
Dimethylformamide–d_7	3.0
Pyridine–d_5	5.0
Toluene–d_8	0.1–0.2
Methanol–d_4	4.9
Acetonitrile–d_3	2.1
Dimethyl sulfoxide–d_6	3.35
Water–d_2	~4.75 (HDO)

Appendix F Proton Spin-Coupling Constants[a]

Type	J_{ab} (Hz)	J_{ab} Typical
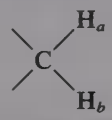	0–30	12–15
$CH_a—CH_b$ (free rotation)	6–8	7
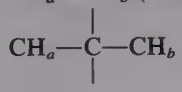	0–1	0
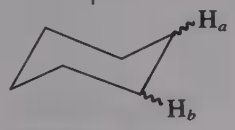		
ax–ax	6–14	8–10
ax–eq	0–5	2–3
eq–eq	0–5	2–3
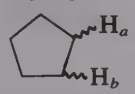 (cis or trans)	*cis* 5–10 *trans* 5–10	
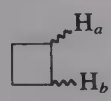 (cis or trans)	*cis* 4–12 *trans* 2–10	
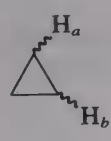 (cis or trans)	*cis* 7–13 *trans* 4–9	
$CH_a—OH_b$ (no exchange)	4–10	5
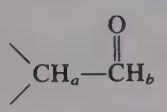	1–3	2–3
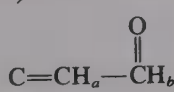	5–8	6
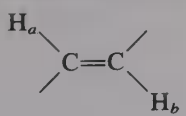	12–18	17
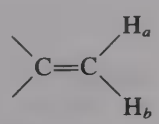	0–3	0–2
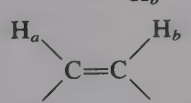	6–12	10
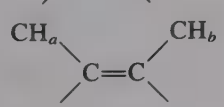	0–3	1–2

Type	J_{ab} (Hz)	J_{ab} Typical
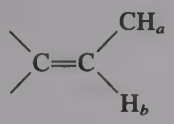	4–10	7
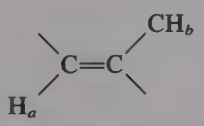	0–3	1.5
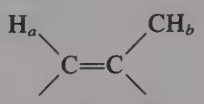	0–3	2
$C=CH_a—CH_b=C$	9–13	10
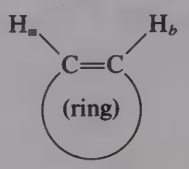	3 member 4 member 5 member 6 member 7 member 8 member	0.5–2.0 2.5–4.0 5.1–7.0 8.8–11.0 9–13 10–13
$CH_a—C\equiv CH_b$	2–3	
$—CH_a—C\equiv C—CH_b—$	2–3	
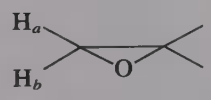		6
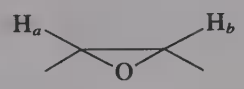		4
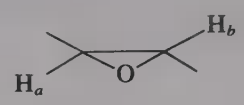		2.5
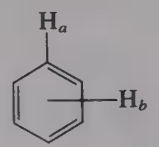	*J* (ortho) *J* (meta) *J* (para)	6–10 1–3 0–1	9 3 ~0
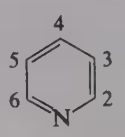	*J* (2–3) *J* (3–4) *J* (2–4) *J* (3–5) *J* (2–5) *J* (2–6)	5–6 7–9 1–2 1–2 0–1 0–1	5 8 1.5 1.5 1 ~0
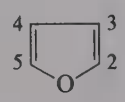	*J* (2–3) *J* (3–4) *J* (2–4) *J* (2–5)	1.3–2.0 3.1–3.8 0–1 1–2	1.8 3.6 ~0 1.5
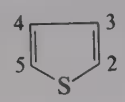	*J* (2–3) *J* (3–4) *J* (2–4) *J* (2–5)	4.9–6.2 3.4–5.0 1.2–1.7 3.2–3.7	5.4 4.0 1.5 3.4

Appendix F (continued)

Type		J_{ab} (Hz)	J_{ab} Typical
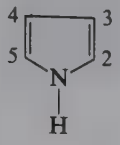	J (1–2)	2–3	
	J (1–3)	2–3	
	J (2–3)	2–3	
	J (3–4)	3–4	
	J (2–4)	1–2	
	J (2–5)	1.5–2.5	
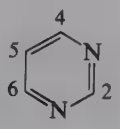	J (4–5)	4–6	
	J (2–5)	1–2	
	J (2–4)	0–1	
	J (4–6)	2–3	
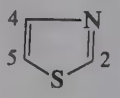	J (4–5)	3–4	
	J (2–5)	1–2	
	J (2–4)	~0	

Proton–Fluorine

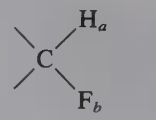	44–81
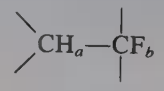	3–25
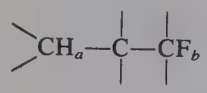	0
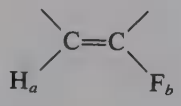	1–8
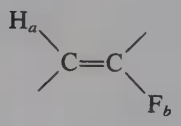	12–40
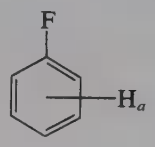	*o* 6–10 *m* 5–6 *p* 2

Proton–Phosphorus

	630–707	
$(CH_3)_3P$	2.7	
$(CH_3)_3P{=}O$	13.4	
$(CH_3CH_2)_3P$	13.7 (HCCP)	0.5 (HCP)
$(CH_3CH_2)_3P{=}O$	16.3 (HCCP)	11.9 (HCP)
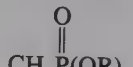	10–13	
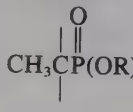	15–20	
$CH_3OP(OR)_2$	10.5–12	
$P[N(CH_3)_2]_3$	8.8	
$O{=}P[N(CH_3)_2]_3$	9.5	

[a]Compiled by Varian Associates. Absolute values.

Appendix G Chemical Shifts, Multiplicities, and Coupling Constants of Residual Protons in Commercially Available Deuterated Solvents (Merck & Co., Inc.)

Compound,[a] Molecular Weight	δ_H (mult)	J_{HD}
Acetic acid-d_4	11.53 (1)	
64.078	2.03 (5)	2
Acetone-d_6		
64.117	2.04 (5)	2.2
Acetonitrile-d_3		
44.071	1.93 (5)	2.5
Benzene-d_6	7.15 (br)	
84.152		
Chloroform-d	7.24 (1)	
120.384		
Cyclohexane-d_{12}	1.38 (br)	
96.236		
Deuterium oxide	4.63	
20.028	(DSS)[b]	
	4.67	
	(TSP)[b]	
1,2-Dichloroethane-d_4	3.72 (br)	
102.985		
Diethyl-d_{10} ether	3.34 (m)	
84.185	1.07 (m)	
Diglyme-d_{14}	3.49 (br)	
148.263	3.40 (br)	
	3.22 (5)	1.5
N,N-Dimethylformamide-d_7	8.01 (br)	
80.138	2.91 (5)	2
	2.74 (5)	2
Dimethyl-d_6 sulphoxide	2.49 (5)	1.7
84.170		
p-Dioxane-d_8	3.53 (m)	
96.156		
Ethyl alcohol-d_6 (anh)	5.19 (1)	
52.106	3.55 (br)	
	1.11 (m)	
Glyme-d_{10}	3.40 (m)	
100.184	3.22 (5)	1.6
Hexafluoroacetone deuterate	5.26 (1)	
198.067		
HMPT-d_{18}	2.53 (2 × 5)	2 (9.5)
197.314		
Methyl alcohol-d_4	4.78 (1)	
36.067	3.30 (5)	1.7
Methylene chloride-d_2	5.32 (3)	1
86.945		
Nitrobenzene-d_5	8.11 (br)	
128.143	7.67 (br)	
	7.50 (br)	

Appendix G (continued)

Nitromethane-d_3 64.059	4.33 (5)	2
Isopropyl alcohol-d_8 68.146	5.12 (1) 3.89 (br) 1.10 (br)	
Pyridine-d_5 84.133	8.71 (br) 7.55 (br) 7.19 (br)	
Tetrahydrofuran-d_8 80.157	3.58 (br) 1.73 (br)	
Toluene-d_8 100.191	7.09 (m) 7.00 (br) 6.98 (m) 2.09 (5)	2.3
Trifluoroacetic acid-d 115.030	11.50 (1)	
2,2,2-Trifluoroethyl alcohol-d_3 103.059	5.02 (1) 3.88 (4 × 3)	2 (9)

[a]Purity (Atom % D) up to 99.96% (''100%'') for several solvents.
[b]DSS is 3-(trimethylsilyl)-1-propane sulfonic acid, sodium salt. TSP is sodium-3-trimethylpropionate-2,2,3,3-d_4. Both are reference standards used in aqueous solutions.

Appendix H Properties of Several Nuclei[a]

Isotope	NMR Frequency MHz for a 1-T Field	Natural Abundance %	Relative Sensitivity at Constant Field	Magnetic Moment (μ)	Spin Number (I)	Electrical Quadrupole Moment ($e \times 10^{-24}$ cm^2)	Magnetogyric Ratio γ (rad) (G^{-1})
^{1}H	42.576	99.9844	1.000	2.79268	$\frac{1}{2}$		26,753
^{2}H	6.5357	1.56×10^{-2}	9.64×10^{-2}	0.85739	1	2.77×10^{-3}	4,107
^{3}H	45.414		1.21	2.9788	$\frac{1}{2}$		
^{10}B	4.575	18.83	1.99×10^{-2}	1.8005	3	7.4×10^{-2}	
^{11}B	13.660	81.17	0.165	2.6880	$\frac{3}{2}$	3.55×10^{-2}	
^{12}C		98.9			0		
^{13}C	10.705	1.108	1.59×10^{-2}	0.70220	$\frac{1}{2}$		6,728
^{14}N	3.076	99.635	1.01×10^{-3}	0.40358	1	7.1×10^{-2}	
^{15}N	4.315	0.365	1.04×10^{-3}	−0.28304	$\frac{1}{2}$		−2,712
^{16}O		99.76			0		
^{17}O	5.772	3.7×10^{-2}	2.91×10^{-2}	−1.8930	$\frac{5}{2}$	-4.0×10^{-3}	−3,628
^{19}F	40.055	100	0.834	2.6273	$\frac{1}{2}$		25,179
^{28}Si		92.28			0		
^{29}Si	8.458	4.70	7.85×10^{-2}	−0.55548	$\frac{1}{2}$		−5,319
^{30}Si		3.02			0		
^{31}P	17.236	100	6.64×10^{-2}	1.1305	$\frac{1}{2}$		10,840
^{32}S		95.06			0		
^{33}S	3.266	0.74	2.26×10^{-3}	0.64274	$\frac{3}{2}$	−0.053	2,054
^{34}S		4.2			0		
^{35}Cl	4.172	75.4	4.71×10^{-3}	0.82091	$\frac{3}{2}$	-7.9×10^{-2}	2,624
^{37}Cl	3.472	24.6	2.72×10^{-3}	0.68330	$\frac{3}{2}$	-6.21×10^{-2}	2,184
^{79}Br	10.667	50.57	7.86×10^{-2}	2.0991	$\frac{3}{2}$	0.34	
^{81}Br	11.499	49.43	9.84×10^{-2}	2.2626	$\frac{3}{2}$	0.28	
^{127}I	8.519	100	9.35×10^{-2}	2.7937	$\frac{5}{2}$	−0.75	

[a] Varian Associates NMR Table, 4th ed., 1964.

CHAPTER FIVE

^{13}C NMR SPECTROMETRY

5.1. INTRODUCTION*

Direct observation of the carbon skeleton has been available on a practical basis only since the early 1970's. The ^{12}C nucleus is not magnetically "active" (spin number, I, is zero), but the ^{13}C nucleus, like the ^{1}H nucleus, has a spin number of $\frac{1}{2}$. However, since the natural abundance of ^{13}C is only 1.1% that of ^{12}C, and its sensitivity is only about 1.6% that of ^{1}H, the overall sensitivity of ^{13}C compared with ^{1}H is about 1/5700.

The earlier, continuous wave, slow-scan procedure requires a large sample and a prohibitively long time to obtain a ^{13}C spectrum, but the availability of FT instrumentation, which permits simultaneous irradiation of all ^{13}C nuclei, has resulted in an increased activity in ^{13}C spectrometry, beginning in the early 1970s, comparable to the burst of activity in ^{1}H spectrometry that began in the late 1950s.

An important development was the use of broadband decoupling of protons. Because of the large J values for ^{13}C—H (~110–320 Hz) and appreciable values for ^{13}C—C—H and ^{13}C—C—C—H, nondecoupled (proton coupled) ^{13}C spectra usually show complex overlapping multiplets that are difficult to interpret, but some nondecoupled spectra such as that of diethyl phthalate (Fig. 5.1*a*) are quite simple. Decoupling (Fig. 5.1*b*) of the protons by means of a broadband generator removes these couplings. The result, in the absence of other coupling nuclei, such as ^{31}P or ^{19}F, is a *single sharp peak† for each chemically nonequivalent ^{13}C atom,* except for the infrequent coincidence of ^{13}C chemical shifts. Furthermore, an increase in signal (up to 200%) accrues from the nuclear Overhauser effect (NOE). This enhancement results from an increase in population of the lower energy level of the ^{13}C nuclei concomitant with the increase in population of the high-energy level of the ^{1}H nuclei on irradiation of the ^{1}H nuclei. The net effect is a very large reduction in the time needed to obtain a noise-decoupled spectrum (Fig. 5.1*b*) as compared with a nondecoupled spectrum (Fig. 5.1*a*).

In the FT mode, a short powerful rf pulse (on the order of a few microseconds) excites all the ^{13}C nuclei simultaneously. Since the central frequency in the pulse is slightly off-resonance for all of the nuclei, each nucleus shows a free induction decay (FID), which is an exponentially decaying sine wave with a frequency equal to the difference between the applied frequency and the resonance frequency for that nucleus. Figure 5.2*a* shows the result for a single carbon compound.

The FID display for a compound containing more than one ^{13}C nucleus consists of superimposed sine waves, each with its characteristic frequency, and an interference (beat) pattern results (Fig. 5.2*b*). These data are automatically digitized and stored in a computer, and a series of repetitive pulses, with signal acquisition and accumulation between pulses, builds up the signal. Fourier transformation by the computer converts this information to the conventional presentation of a ^{13}C NMR spectrum. Figure 5.2*a* represents the FID and the conventional ^{13}C spectra for CH_3OH. Figure 5.2*b* shows the same spectra for C_2H_5OH. The FID is a time domain spectrum (the abscissa is time), whereas the transformed, conventional presentation is a frequency domain spectrum (the abscissa is frequency). The sequence (Fig. 5.2*c*) is pulse, acquisition, and pulse delay if required (see below).

The ^{13}C spectra in this chapter were run on a Varian XL-100 MHz spectrometer. Since this instrument locks on deuterium, the common deuterated solvents (usually $CDCl_3$) are used to furnish the internal lock.‡ (A list of common deuterated solvents is given in Appendix A.) As it is with ^{1}H spectrometry, the common

*Familiarity with Chapter 4 is assumed.

†Because of the low natural abundance of ^{13}C, the occurrence of adjacent ^{13}C atoms has a low probability; thus we are free of the complication of ^{13}C—^{13}C coupling.

‡A field-frequency internal lock provides corresponding changes in the irradiating frequency for minor variations in field strength to furnish a constant field/frequency ratio.

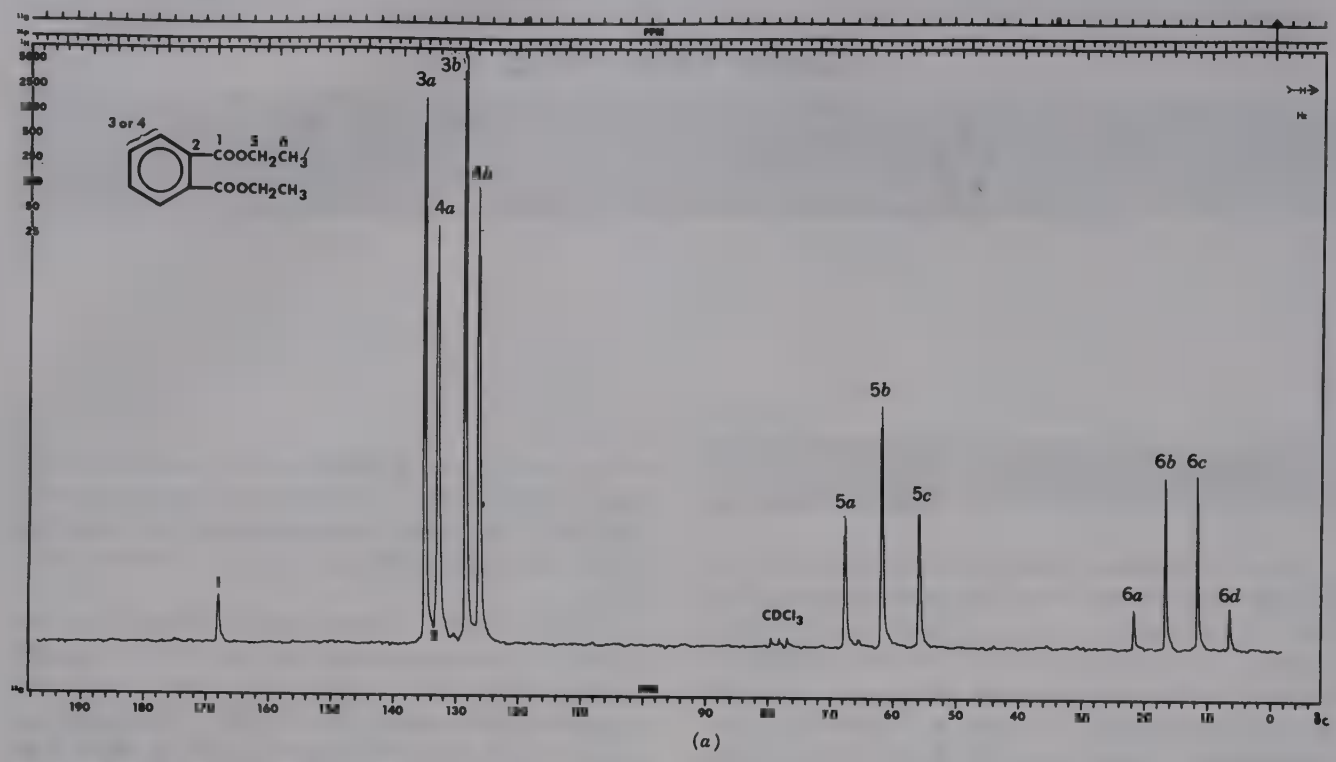

FIGURE 5.1(*a*). The ^{13} C-NMR spectrum of diethyl phthalate with the protons completely coupled. The solvent used was $CDCl_3$ at 25.2 MHz.

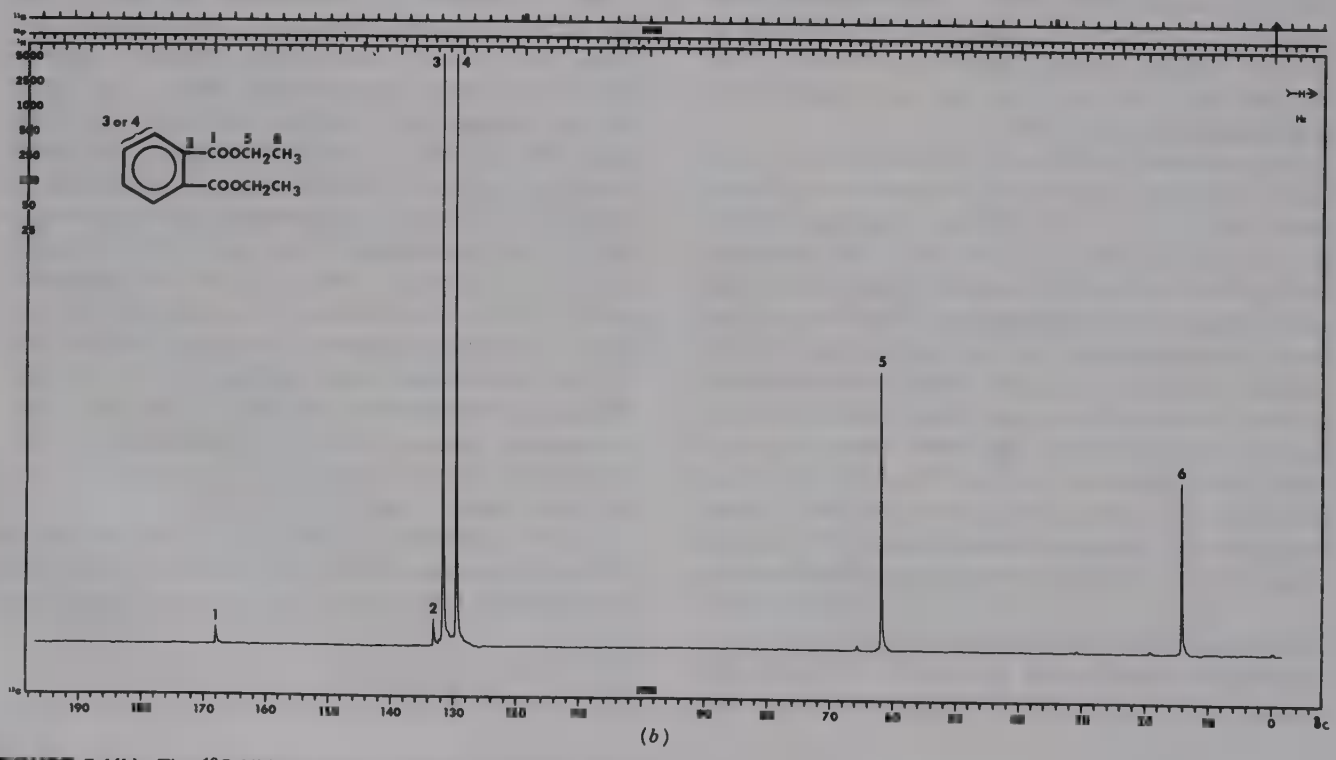

FIGURE 5.1(*b*). The ^{13}C-NMR spectrum of diethyl phthalate with the protons completely decoupled by the broadband decoupler. The solvent used was $CDCl_3$ at 25.2 MHz.

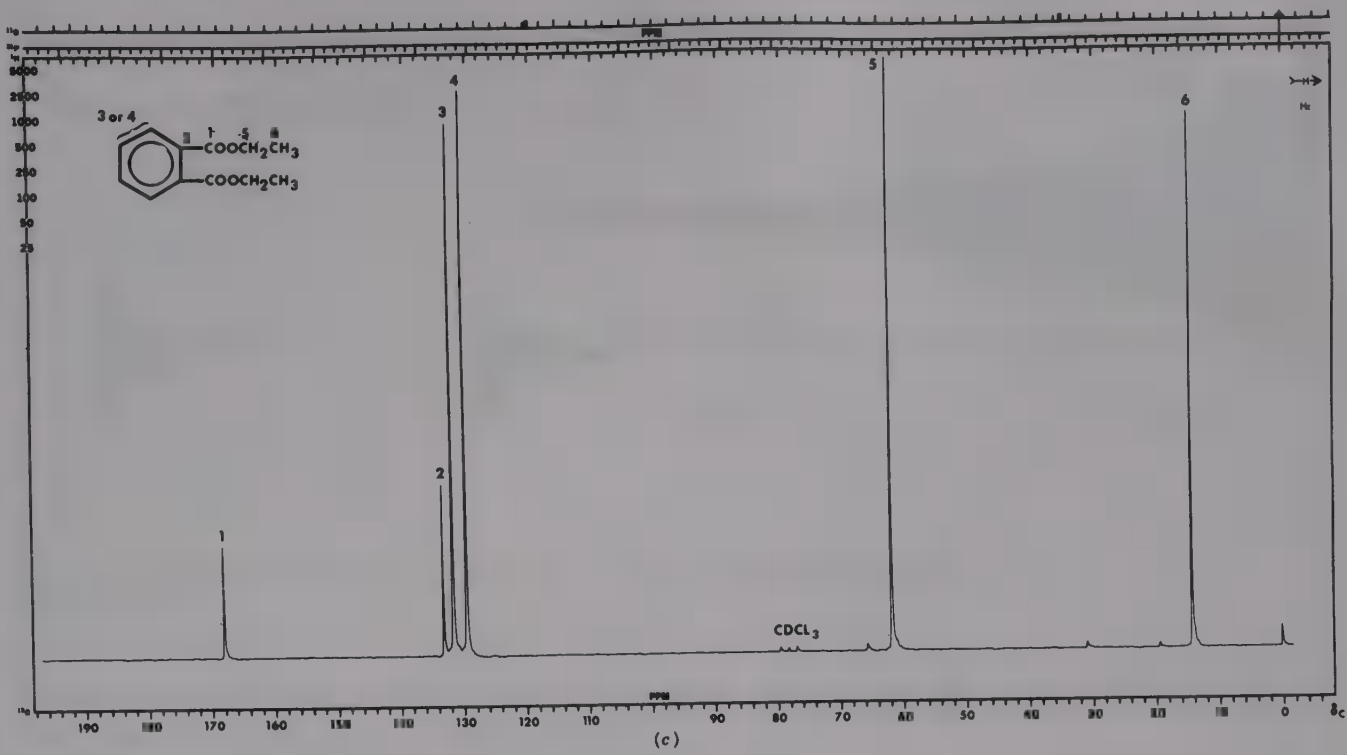

FIGURE 5.1(c). The ^{13}C-NMR spectrum of diethyl phthalate with the protons completely decoupled and a 10-s delay between pulses. The solvent used was $CDCl_3$ at 25.2 MHz.

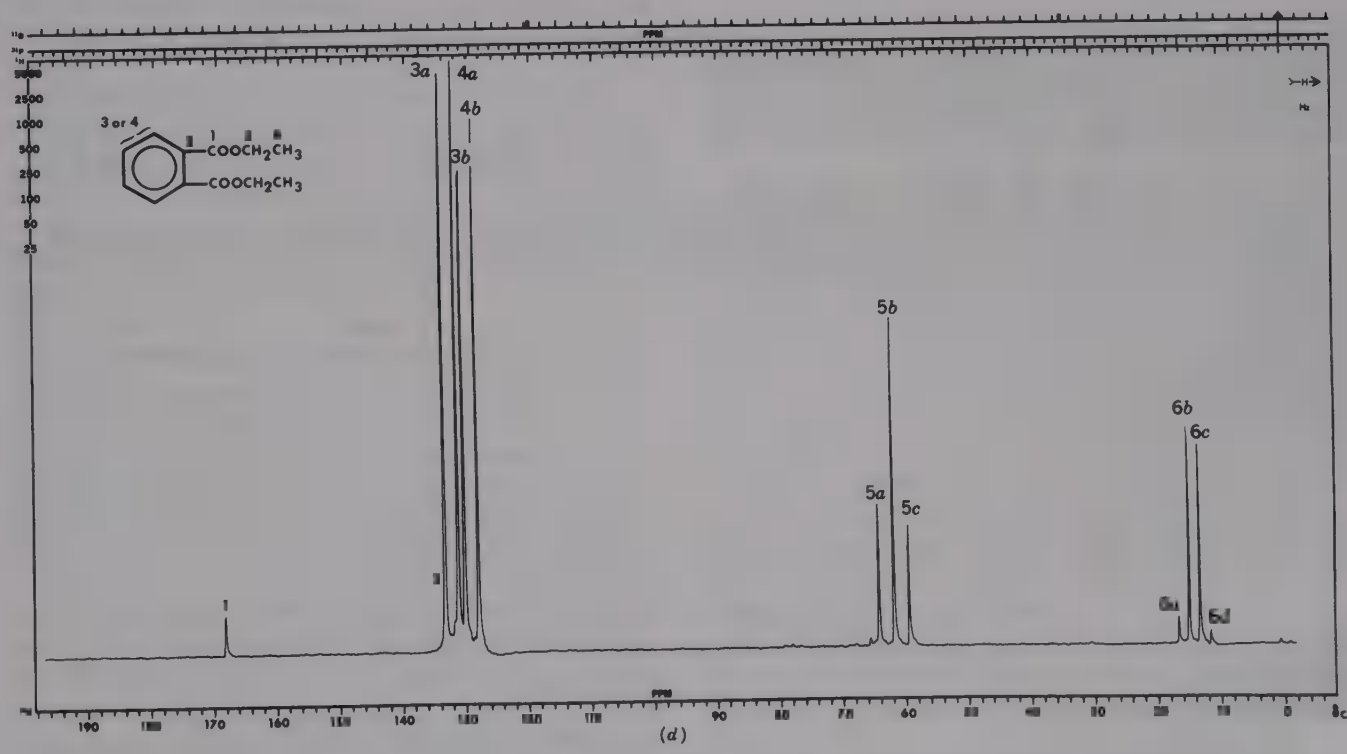

FIGURE 5.1(*d*). The ^{13} C-NMR spectrum of diethyl phthalate with off-resonance decoupled protons. The solvent used was $CDCl_3$ at 25.2 MHz. See Chapter 6 for newer methods.

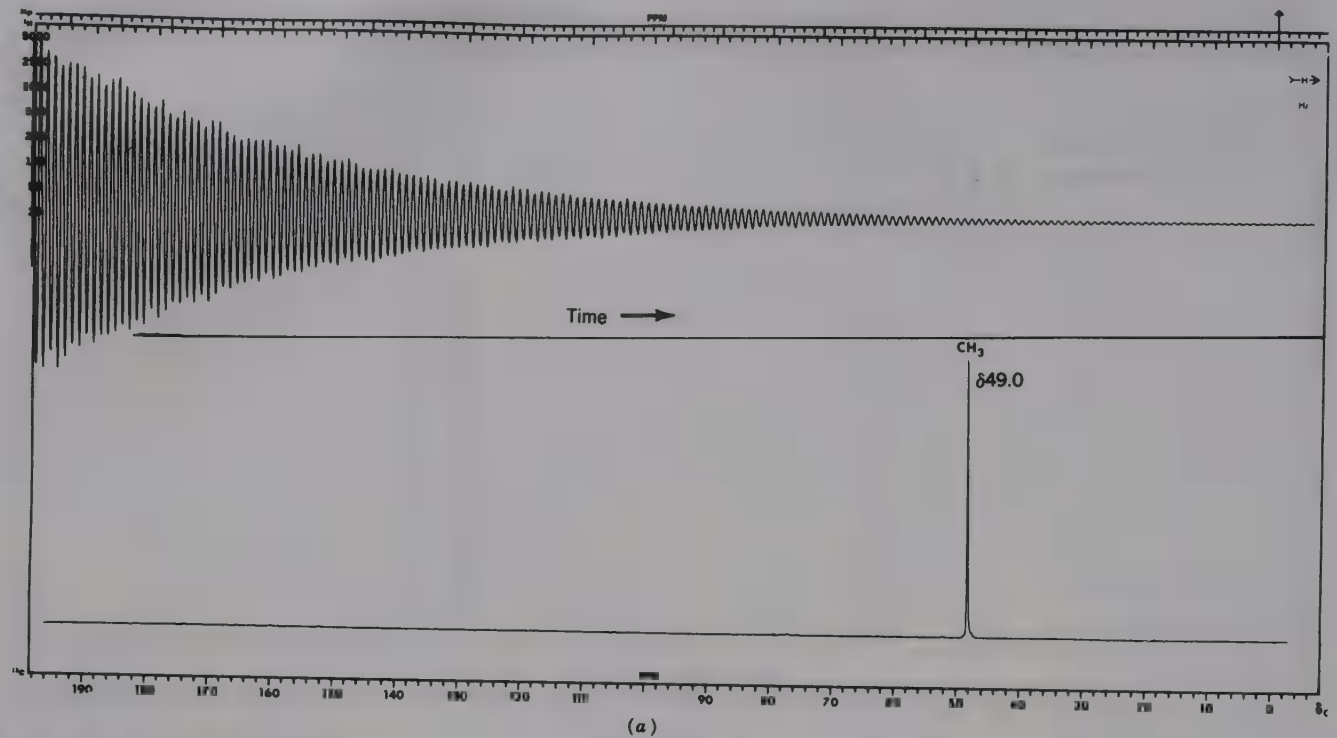

FIGURE 5.2(*a*). Free induction decay (time domain) (above) and transformed ^{13}C-spectrum (frequency domain) of methanol (60% in $CDCl_3$ at 25.2 MHz).

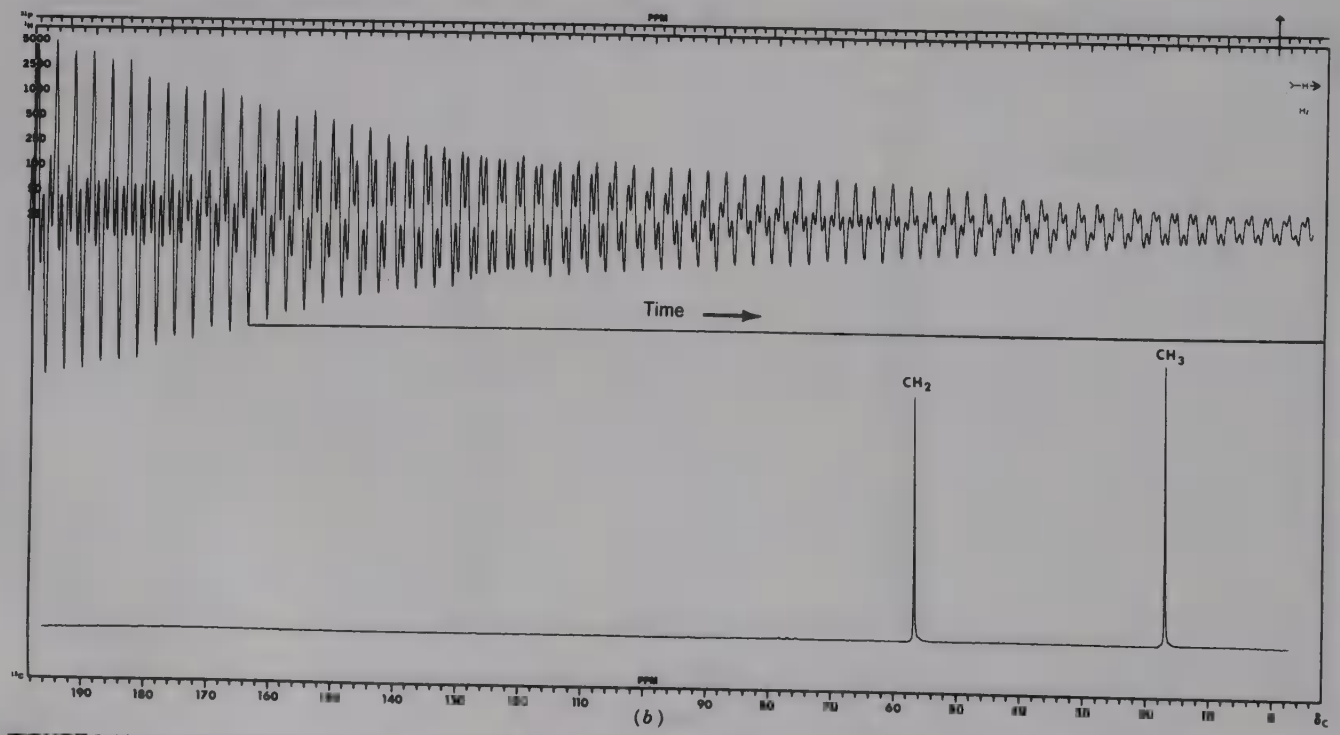

FIGURE 5.2(*b*). Free induction decay (time domain) (above) and transformed ^{13}C-spectrum (frequency domain) of ethanol (60% in $CDCl_3$ at 25.2 MHz).

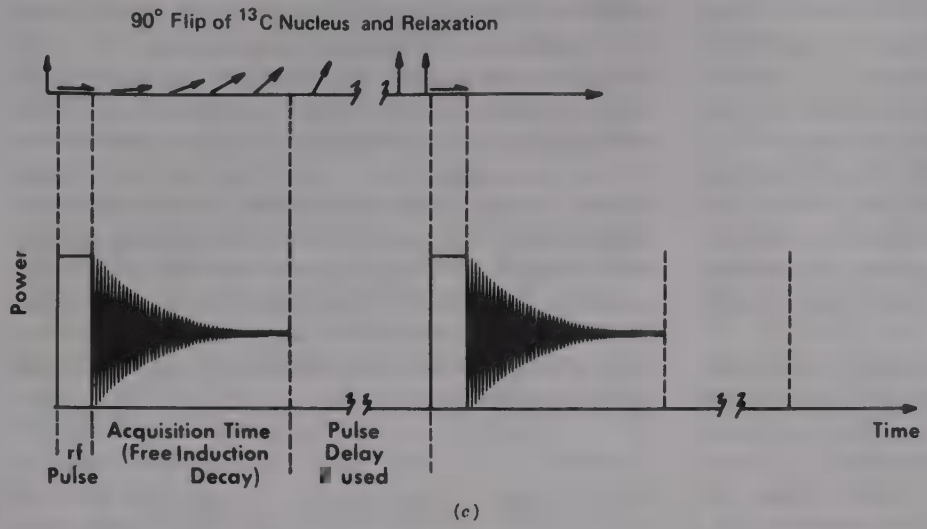

FIGURE 5.2(c). Schematic representation of the rf pulse followed by the FID (acquisition time) and pulse delay.

internal reference is tetramethylsilane (TMS), and the scale is given in δ units (ppm) downfield (deshielding) from TMS in positive numbers, and upfield (shielding) from TMS in negative numbers. The shifts encountered in routine ^{13}C spectra range about 240 ppm downfield from TMS; this is a range of about 20 times that of routine ^{1}H spectra (~12 ppm). Several cations have been recorded at approximately 335 ppm downfield and CI_4 absorbs at approximately −290 ppm (upfield from TMS).

On the Varian XL-100 instrument, the ^{13}C frequency is 25.2 MHz, and the routine spectral width is 5000 Hz (198.4 ppm). Each of the numbered divisions on the bottom scale of the spectrum represents 10 ppm (Fig. 5.1). If the presence of carbon atoms that absorb further downfield is suspected, the sweepwidth is increased accordingly. Returning to the 25.2-MHz spectra of methanol (Fig. 5.2*a*), we can now calculate that the chemical shift of δ 49.0 for CH_3 in the transformed spectrum corresponds to $49.0 \times 25.2 = 1234.8$ Hz (cycles per second, cps) for the frequency of the FID.

As a result of the large sweepwidth and the sharpness of the peaks, impurities (or mixtures) are readily detected. Even stereoisomers that are difficult to separate, or detect by other procedures usually give rise to discrete peaks.

A routine sample (MW ~300) on a 300-MHz instrument would consist of about 100–200 mg in about 0.4 mL of deuterated solvent in a 5-mm tube; such a sample would require perhaps 1 min of instrument time. It is possible to obtain spectra on samples on the order of several hundred micrograms given sufficient instrument time and a highly purified solvent. For small samples, it is advantageous to use the highest quality concentric cell with the inner tube of about 40–100-μL capacity; the annular volume is left empty.

References to further details, collections of spectra, and spectra–structure correlations are appended.

5.2. INTERPRETATION OF ^{13}C SPECTRA (PEAK ASSIGNMENTS)

How are specific peaks assigned in a broadband decoupled ^{13}C spectrum, such as Figure 5.1*b*? First, we do have reference material and empirical relationships to correlate chemical shift with structure. (See discussion under chemical shifts in Section 5.3 for the major chemical classes, and Appendices B and C.) However, we lack coupling information because of decoupling of protons, and we cannot depend on peak integrations for the following reasons.

Repetitive scan (continuous wave) ^{1}H spectrometry usually results in a satisfactory relationship between integrated peak areas and the number of nuclei under those areas because there is sufficient time between irradiations of an individual proton for relaxation to occur. Satisfactory integrations would also result for most ^{13}C spectra under these conditions, but the time needed for the number of scans required is prohibitive for routine work.

In routine FT runs, the repetitive pulses are spaced at intervals of 0.1–1 s (acquisition time) during which

the signal is averaged and stored. Under these conditions, ^{13}C nuclei, whose relaxation time constants (T_1) vary over a wide range, are not equally relaxed between pulses, and the resulting peak areas do not integrate to give the correct number of carbon atoms.* Very long pulse delays (following the acquisition period) can be used, but the time required limits this technique to special situations. Furthermore, there is another complication: the NOE (Section 5.1) is not the same for all nuclei, and this results in further loss of quantitation.

However, one advantage does result. It is usually possible by inspection of a ^{13}C spectrum to recognize the nuclei that do not bear protons by their low intensity (peaks 1 and 2 in Fig. 5.1*b*). The common spin–lattice relaxation mechanism for ^{13}C results from dipole–dipole interaction with directly attached protons. Thus, nonprotonated carbon atoms often have longer relaxation times, which together with little or no NOE, results in small peaks. It is therefore often possible to recognize carbonyl groups (except formyl), nitriles, nonprotonated alkene and aklyne carbon atoms, and other quaternary carbon atoms readily. However, care must be taken to allow a sufficient number of pulses or a long enough interval between pulses (to compensate for the long T_1) so that these weak signals are not completely lost in the baseline noise. In Figure 5.1*c*, a 10 s interval (pulse delay) was used to increase the relative intensities of peaks 1 and 2).

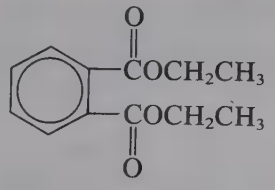

Diethyl phthalete

In the broadband-decoupled spectrum of diethyl phthalate (Fig. 5.1*b*), we can assign the very small peak at 167.75 ppm to the two equivalent C=O groups, the very small peak at 132.85 ppm to the equivalent substituted aromatic carbon atoms, the large peaks at 131.33 and 129.19 ppm to the remaining aromatic carbon atoms, the medium peak at 61.63 ppm to the two equivalent CH_2 groups, and the medium peak at 14.15 ppm to the two equivalent CH_3 groups. These assignments can be made on the basis of Appendices B and C and on the assumption that the quaternary carbon atoms are responsible for the weak peaks; their relative intensity can be increased by inserting a pulse delay (an interval between the acquisition period and the next pulse) as in Figure 5.1*c*. Note that the 10 s pulse delay nearly equalizes the intensities of all the peaks except for those representing the quaternary carbons atoms.

In addition to structure–shift correlations, the most useful technique for assigning peaks has been off-resonance decoupling (Fig. 5.1*d*); however, newer techniques (Chapter 6) for determining the number of protons on each ^{13}C are now available. Limited use is made of lanthanide shift reagents and selective proton decoupling. The effect of deuterium in a molecule (deuterated solvents) should be understood, and the concept of chemical shift equivalence (Chapter 4) should always be kept in mind.

5.2.1. Off-Resonance Decoupling

We have seen that broadband decoupling simplifies the spectrum and increases peak heights, but with the loss of coupling information. Off-resonance decoupling (Fig. 5.1*d*) gives a simplified spectrum, yet retains "residual" ^{13}C—H coupling (J^r) information. Off-resonance decoupling is achieved by offsetting the central frequency of the broadband proton decoupler by about 1000–2000 Hz upfield or about 2000–3000 Hz downfield from the *proton* frequency of TMS, that is, we irradiate upfield or downfield of the usual (1000 Hz sweepwidth) *proton* spectrum. This results in residual coupling from protons directly bonded to the ^{13}C atoms, while long-range coupling is usually lost. The observed residual coupling (J^r), which is determined by the amount of offset and the power of the decoupler, is smaller than the true coupling J.

$$J^r \simeq \frac{2\pi J \Delta\nu}{\gamma \mathbf{B}_2}$$

where γ is the magnetogyric ratio for protons, $\Delta\nu$ is the difference between the resonance frequency of the proton of interest and the decoupler frequency, and $\mathbf{B}_2$ is the strength of the rotating magnetic field generated by the decoupler frequency. Thus, the multiplicities of the ^{13}C bands can be readily observed, often without serious overlap with other ^{13}C bands. Methyl carbon atoms appear as quartets, methylenes as triplets (or as pair of doublets if the protons are not equivalent and their coupling constants are sufficiently different), methines as doublets, and quaternary carbon atoms as singlets.* The procedure, of course, also gives a proton count to corroborate the proton spectrum. A discrep-

*Fourier transform ^{1}H spectra do give satisfactory integrations because their T_1 values are usually shorter and within a smaller range as compared with ^{13}C.

*In practice, the outer peaks are usually weaker than expected from the theoretical 1:2:1 or 1:3:3:1 peak peak height ratios because of decoupler field inhomogeneity. R. Freeman, et al., *J. Am. Chem. Soc.* **100**, 5637 (1979).

ancy between the number of protons obtained from the off-resonance decoupled ^{13}C spectrum and the molecular formula obtained from the mass spectrum results either from elements of symmetry whose presence can be correlated with molecular structure, or from protons attached to heteroatoms.

In Figure 5.1*d*, only the doublets of peaks 3 and 4 overlap. The residual couplings become slightly larger as the offset frequency increases; in this example, the irradiation is upfield of the proton frequency of TMS.

The off-resonance decoupled spectrum of diethyl phthalate (Fig. 5.1*d*) allows us to confirm the assignments made on the basis of chemical shifts and peak heights. The multiplicity of peak 1 is unchanged. Peak 2 is buried under peak 3*a*. Peaks 3 and 4 are overlapping doublets. Peak 5 is a triplet, and peak 6 a quartet. We count six carbon atoms and seven protons, which, given an element of symmetry, corroborates the molecular formula $C_{12}H_{14}O_4$, and the ortho substitution. For this simple molecule, the nondecoupled spectrum (Fig. 5.1*a*) presents no problem, but in more complex molecules, overlapping multiplets are often difficult to interpret. More modern methods are available to determine proton multiplicity on ^{13}C (Chapter 6).

5.2.2. Selective Proton Decoupling

When a specific proton is irradiated at its exact frequency at a lower power level than is used for off-resonance decoupling, the directly bonded ^{13}C absorptions show residual coupling. This technique has been used for peak assignment, but satisfactory results depend on finding the precise frequency of the proton and the appropriate power level for decoupling it, which can be difficult. And, of course, overlapping protons cause problems.

5.2.3. Lanthanide Shift Reagents

The lanthanide shift reagents (see Chapter 4) can be used to "spread out" a ^{13}C spectrum in the same way as they are used in ^1H studies. Two useful results may be obtained: coincident peaks may separate and the proton shifts are also spread out; selective proton decoupling is thus facilitated. However, facile analogies between ^{13}C and ^1H effects are risky.

5.2.4. Deuterium Substitution

Substitution of D for H on a carbon results in a dramatic diminution of the height of the ^{13}C signal in a noise-decoupled spectrum for the following reasons. Since deuterium has a spin number of 1 and a magnetic moment 15% that of ^1H, it will split the ^{13}C absorption into three lines (ratio 1:1:1) with a J value equal to $0.15 \times J_{CH}$. Furthermore, T_1 for ^{13}C—D is longer than that for ^{13}C—H because of decreased dipole–dipole relaxation. Finally, the NOE is lost, since there is no irradiation of deuterium.* A separate peak may also be seen for any residual ^{13}C—H, since the isotope effect usually results in a slight upfield shift of the ^{13}C—D absorption (~0.2 ppm per D atom). The isotope effect may also slightly shift the absorption of the carbon atoms once removed from the deuterated carbon.

5.2.5. Chemical Shift Equivalence

The definition of chemical shift equivalence given for protons also applies to carbon atoms: interchangeability by a symmetry operation or by a rapid mechanism. The presence of equivalent carbon atoms (or coincidence of shift) in a molecule results in a discrepancy between the apparent number of peaks and the actual number of carbon atoms in the molecule.

Thus, ^{13}C atoms of the methyl groups in *t*-butyl alcohol (Fig. 5.3) are equivalent by rapid rotation in the same sense in which the protons of a methyl group are equivalent. The ^{13}C spectrum of *t*-butyl alcohol shows two peaks, one much larger than the other, but not necessarily exactly three times as large; the carbinyl carbon peak (quaternary) is much less than $\frac{1}{3}$ the intensity of the peak representing the carbon atoms of the methyl groups.

In the chiral molecule 2,2,4-trimethyl-1,3-pentanediol (Fig. 5.4), we note that CH_3a and CH_3b are not equivalent, and two peaks are seen. Even though the two methyl groups labeled *c* are not equivalent, they coincidently show only one peak. Two peaks may be seen at higher resolution, or with the help of a shift reagent.

In Section 4.7.1, we noted that the CH_3 protons of $(CH_3)_2NCH{=}O$ gave separate peaks at room temperature, but became chemical shift equivalent at about 123°. Of course, the ^{13}C peaks show the same behavior.

*The same explanation also accounts for the relatively weak signal shown by deuterated solvents. Deuterated chloroform, $CDCl_3$, shows a 1:1:1 *triplet*, deuterated *p*-dioxane a 1:2:3:2:1 *quintet*, and deuterated DMSO $(CD_3)_2SO$, a 1:3:6:7:6:3:1 *septet* in accordance with the $n2I + 1$ rule (Chapter 4). The chemical shifts and multiplicities of the ^{13}C atoms of common NMR solvents are given in Appendix A.

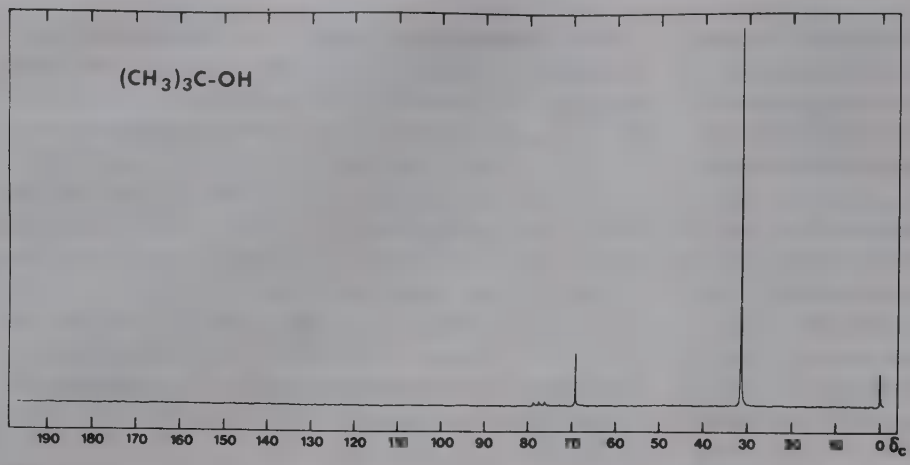

FIGURE 5.3. Decoupled ^{13}C-spectrum of *t*-butyl alcohol. Solvent $CDCl_3$ at 25.2 MHz, 5000-Hz sweepwidth. From Johnson and Jankowski, Spectrum No. 88, with permission.

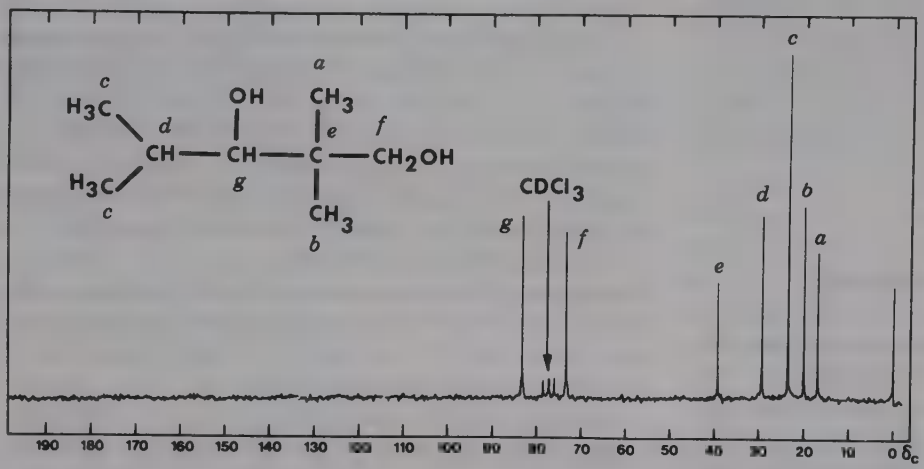

FIGURE 5.4. Decoupled ^{13}C-spectrum of 2,2,4-trimethyl-1,3-pentanediol. Solvent used was $CDCl_3$ at 25.2 MHz, 5000-Hz sweepwidth. From Johnson and Jankowski, spectrum No. 324, with permission.

5.3. CHEMICAL SHIFTS

In this section, chemical shifts will be discussed under the headings of the common chemical classes of organic compounds. As noted earlier, the range of shifts generally encountered in routine ^{13}C studies is about 240 ppm.

As a first reassuring statement, we can say that trends in chemical shifts of ^{13}C are somewhat parallel to those of ^{1}H, so that some of the "feeling" for ^{1}H spectra may carry over to ^{13}C spectra. Furthermore, the concept of *additivity of substituent effects* is useful for both spectra. The ^{13}C shifts are related mainly to hybridization and substituent electronegativity; solvent effects are important in both spectra. Chemical shifts for ^{13}C are affected by substitutions as far removed as the δ position; in the benzene ring, pronounced shifts for ^{13}C are caused by substituents at the ortho, meta, and para positions. The ^{13}C chemical shifts are also moved significantly upfield by the γ-gauche effect, described below. Upfield shifts, as much as several parts per million, may occur on dilution. Hydrogen-bonding effects with polar solvents may cause downfield shifts.

Appendix B gives credence to the statement that ^{13}C chemical shifts somewhat parallel those of ^{1}H, but we note some divergences that are not readily explainable and require development of another set of interpretive skills. In general, in comparison with ^{1}H spectra, it seems more difficult to correlate ^{13}C shifts with substituent electronegativity.

As in other types of spectrometry, peak assignments

are made on the basis of reference compounds. Reference material for many classes of compounds is rapidly accumulating in the literature. The starting point is a general correlation chart for chemical shift regions of ^{13}C atoms in the major chemical classes (see Appendices B and C); then, minor changes within these regions are correlated with structure variations in the particular chemical class. The chemical shift values in the following tables must not be taken too literally because of the use of various solvents and concentration. (Furthermore, much of the early work used various reference compounds, and the values were corrected to give parts per million from TMS.) For example, the C=O absorption of acetophenone in $CDCl_3$ appears at 2.4 ppm further downfield than in CCl_4; the effect on the other carbon atoms of acetophenone ranges from 0.0 to 1.1 ppm.

5.3.1 Alkanes

5.3.1.1. Linear and Branched Alkanes

We know from the general correlation chart (Appendix C) that alkane groups unsubstituted by heteroatoms absorb downfield from TMS to about 60 ppm. (Methane absorbs at 2.5-ppm upfield from TMS.) Within this range, we can predict the chemical shifts of individual ^{13}C atoms in a straight-chain or branched-chain hydrocarbon from the data in Table 5.1 and the formula given below.

This table shows the additive shift parameters (A) in hydrocarbons: the α effect of +9.1 (downfield), the β effect of +9.4 ppm, the γ effect of −2.5 (upfield), the δ effect of +0.3, the ϵ effect of +0.1, and the corrections for branching effects. The calculated (and observed) shifts for the carbon atoms of 3-methylpentane are

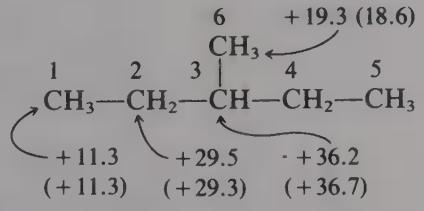

Calculations of shift are made from the formula: $\delta = -2.5 + \Sigma nA$, where δ is the predicted shift for a carbon atom; A is the additive shift parameter; and n is the number of carbon atoms for each shift parameter (−2.5 is the shift of the ^{13}C of methane). Thus, for carbon atom 1, we have 1 α-, 1 β-, 2 γ-, and 1 δ-carbon atoms.

$$\delta_1 = -2.5 + (9.1 \times 1) + (9.4 \times 1) + (-2.5 \times 2) + (0.3 \times 1) = +11.3$$

TABLE 5.1

The ^{13}C Shift Parameters in Some Linear and Branched Hydrocarbons

^{13}C Atoms	Shift (ppm) (A)
α	+9.1
β	+9.4
γ	−2.5
δ	+0.3
ϵ	+0.1
1° (3°)[a]	−1.1
1° (4°)[a]	−3.4
2° (3°)[a]	−2.5
2° (4°)	−7.2
3° (2°)	−3.7
3° (3°)	−9.5
4° (1°)	−1.5
4° (2°)	−8.4

[a]The notations 1° (3°) and 1° (4°) denote a CH_3 group bound to a R_2CH group and to a R_3C group, respectively. The notation 2° (3°) denotes a RCH_2 group bound to a R_2CH group, and so on.

Carbon atom 2 has 2 α-, 2 β-, and 1 γ-carbon atoms. Carbon atom 2 is a 2° carbon with a 3° carbon attached [2°(3°) = −2.5].

$$\delta_2 = -2.5 + (9.1 \times 2) + (9.4 \times 2) + (-2.5 \times 1) + (-2.5 \times 1) = 29.5$$

Carbon atom 3 has 3 α- and 2 β-carbon atoms, and it is a 3° atom with two 2° atoms attached [3°(2°) = −3.7]. Thus,

$$\delta_3 = -2.5 + (9.1 \times 3) + (9.4 \times 2) + (-3.7 \times 2) = +36.2$$

Carbon atom 6 has 1 α-, 2 β-, and 2 γ-carbon atoms, and it is a 1° atom with a 3° atom attached [1°(3°) = −1.1]. Thus,

$$\delta_6 = -2.5 + (9.1 \times 1) + (9.4 \times 2) + (-2.5 \times 2) + (-1.1 \times 1) = +19.3$$

The agreement for such calculations is very good. It is essential that the reference compounds used for such additivity calculations be structurally similar to the compound of interest. Another useful calculation has been given.* The ^{13}C upfield γ shift due to the γ carbon has been attributed to the steric compression of a gauche interaction but has no counterpart in ^1H

*L. P. Lindeman and J. Q. Adams, *Anal. Chem.* **43**, 1245 (1971).

TABLE 5.2

The ^{13}C Shifts for Some Linear and Branched-Chain Alkanes (ppm from TMS)

Compound	C-1	C-2	C-3	C-4	C-5
Methane	−2.3				
Ethane	5.7				
Propane	15.8	16.3	15.8		
Butane	13.4	25.2	25.2		
Pentane	13.9	22.8	34.7	22.8	13.9
Hexane	14.1	23.1	32.2	32.2	23.1
Heptane	14.1	23.2	32.6	29.7	32.6
Octane	14.2	23.2	32.6	29.9	29.9
Nonane	14.2	23.3	32.6	30.0	30.3
Decane	14.2	23.2	32.6	31.1	30.5
Isobutane	24.5	25.4			
Isopentane	22.2	31.1	32.0	11.7	
Isohexane	22.7	28.0	42.0	20.9	14.3
Neopentane	31.7	28.1			
2,2-Dimethylbutane	29.1	30.6	36.9	8.9	
3-Methylpentane	11.5	29.5	36.9	(18.8, 3-CH_3)	
2,3-Dimethylbutane	19.5	34.3			
2,2,3-Trimethylbutane	27.4	33.1	38.3	16.1	
2,3-Dimethylpentane	7.0	25.3	36.3	(14.6, 3-CH_3)	

spectra. It accounts, for example, for the upfield position of an axial methyl substituent on a conformationally rigid cyclohexane ring, relative to an equatorial methyl, and for the upfield shift of the γ carbon atoms of the ring.

Table 5.2 lists the shifts in some linear and branched alkanes.

5.3.2. Effect of Substituents on Alkanes

Table 5.3 shows the effects of a substituent on linear and branched alkanes. The effect on the α carbon parallels electronegativity of the substituent except for bromine and iodine. The effect at the β carbon seems fairly constant for all the substituents except for the carbonyl, cyano, and nitro groups. The upfield shift at the γ carbon results (as above) from steric compression of a gauche interaction. For Y = N, O, and F, there is also an upfield shift with Y in the anti conformation, attributed to hyperconjugation.

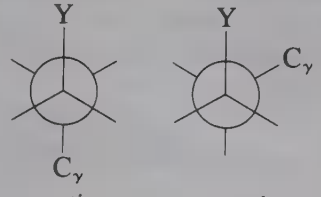

anti *gauche*

From Table 5.3, the approximate shifts for the carbon atoms of, for example, 3-pentanol, may be calculated from the values for pentane in Table 5.2; that is, the increment for the functional group in Table 5.3 is added to the appropriate value in Table 5.2 as follows:

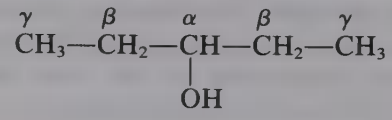

TABLE 5.3

Incremental Substituent Effects (ppm) on Replacement of H by Y in Alkanes. Y is Terminal or Internal[a] (+ downfield, − upfield)

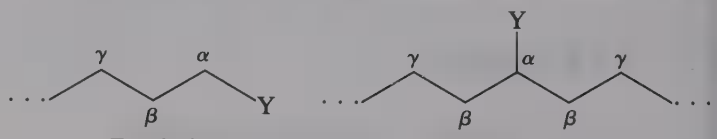

	α		β		γ
Y	Terminal	Internal	Terminal	Internal	
CH_3	+ 9	+ 6	+10	+ 8	−2
$CH{=}CH_2$	+20		+ 6		−0.5
$C{\equiv}CH$	+ 4.5		+ 5.5		−3.5
COOH	+21	+16	+ 3	+ 2	−2
COO^-	+25	+20	+ 5	+ 3	−2
COOR	+20	+17	+ 3	+ 2	−2
COCl	+33	+28		+ 2	
$CONH_2$	+22		+ 2.5		−0.5
COR	+30	+24	+ 1	+ 1	−2
CHO	+31		0		−2
Phenyl	+23	+17	+ 9	+ 7	−2
OH	+48	+41	+10	+ 8	−5
OR	+58	+51	+ 8	+ 5	−4
OCOR	+51	+45	+ 6	+ 5	−3
NH_2	+29	+24	+11	+10	−5
NH_3^+	+26	+24	+ 8	+ 6	−5
NHR	+37	+31	+ 8	+ 6	−4
NR_2	+42		+ 6		−3
NR_3^+	+31		+ 5		−7
NO_2	+63	+57	+ 4	+ 4	
CN	+ 4	+ 1	+ 3	+ 3	−3
SH	+11	+11	+12	+11	−4
SR	+20		+ 7		−3
F	+68	+63	+ 9	+ 6	−4
Cl	+31	+32	+11	+10	−4
Br	+20	+25	+11	+10	−3
I	− 6	+ 4	+11	+12	−1

[a]Add these increments to the shift values of the appropriate carbon atom in Table 5.2 or to the shift value calculated from Table 5.1.

Source: F.W. Wehrli, A.P. Marchand, and S. Wehrli, *Interpretation of Carbon-13 NMR Spectra*. 2nd ed., London: Heyden, 1983.

	Calculated	Found (See Table 5.3)
C_α	34.7 + 41 = 75.8	73.8
C_β	22.8 + 8 = 30.8	30.0
C_γ	13.9 − 5 = 8.9	10.1

5.3.3. Cycloalkanes and Saturated Heterocyclics

The chemical shifts of the CH_2 groups in monocyclic alkanes are given in Table 5.4.

The striking feature here is the strong upfield shift of cyclopropane, analogous to the upfield shift of its proton absorptions.

Each ring skeleton has its own set of shift parameters, but a detailed listing of these is beyond the scope of this text. Rough estimates for substituted rings can be made with the substitution increments in Table 5.3.

One of the striking effects in rigid cyclohexane rings is the upfield shift caused by the γ-gauche steric compression. Thus an axial methyl group at C-1 causes an upfield shift of several parts per million at C-3 and C-5.

Table 5.5 presents chemical shifts for several saturated heterocyclics.

5.3.4. Alkenes

The sp^2 carbon atoms of alkenes substituted only by alkyl groups absorb in the range of about 110–150 ppm downfield from TMS. The double bond has a rather small effect on the shifts of the sp^3 carbon in the molecule as the following comparisons demonstrate.

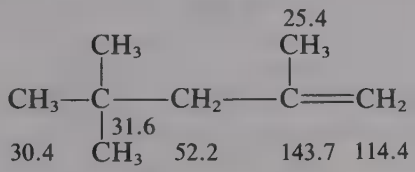

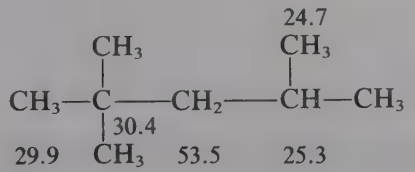

TABLE 5.4

Chemical Shifts of Cycloalkanes (ppm from TMS)

C_3H_6	−2.9	C_7H_{14}	28.4
C_4H_8	22.4	C_8H_{16}	26.9
C_5H_{10}	25.6	C_9H_{18}	26.1
C_6H_{12}	26.9	$C_{10}H_{20}$	25.3

The methyl signal of propene is at 18.7 ppm, and of propane at 15.8 ppm. In *cis*-2-butene, the methyl signals are at 12.1 ppm, compared with 17.6 ppm in *trans*-2-butene, because of the γ effect. (For comparison, the methyl signals of butane are at 13.4 ppm). Note the γ effect on one of the geminal methyl groups in 2-methyl-2-butene (Table 5.6).

In general, the terminal $=CH_2$ group (usually a triplet in an off-resonance decoupled spectrum) absorbs upfield from an internal $=CH-$ group, and cis $-CH=CH-$ signals are upfield from those of corresponding trans groups. Calculations of approximate shifts can be made from the following parameters where α, β, and γ represent substituents on the same end of the double bond as the alkene carbon of interest, and α', β', and γ' represent substituents on the far side.

α	+10.6
β	+ 7.2
γ	− 1.5
α'	− 7.9
β'	− 1.8
γ'	− 1.5
Z (cis) correction	− 1.1

TABLE 5.5

Chemical Shifts for Saturated Heterocyclics (ppm from TMS, neat)

Unsubstituted

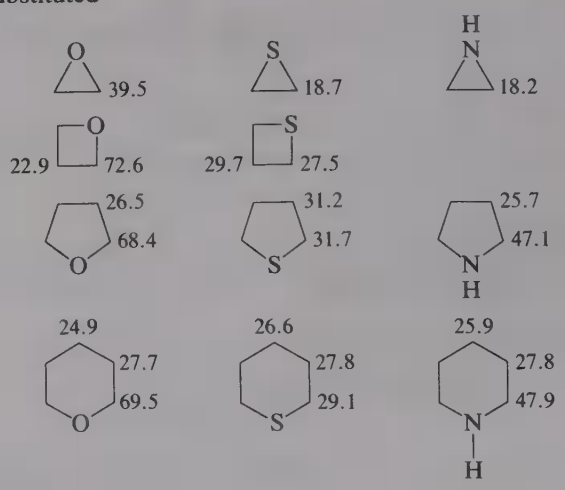

Substituted

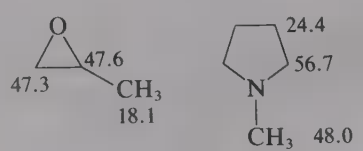

These parameters are added to 123.3 ppm, the shift for ethylene. We can calculate the values for *cis*-3-methyl-2-pentene as follows:

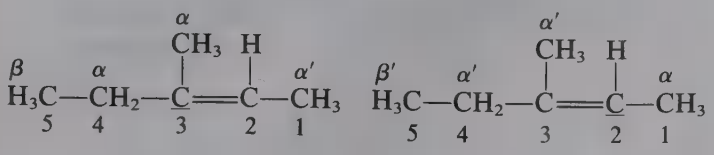

$$\delta_{C\text{-}3} = 123.3 + (2 \times 10.6) + (1 \times 7.2) + (1 \times -7.9) - 1.1 = 142.7 \text{ ppm}$$

$$\delta_{C\text{-}2} = 123.3 + (1 \times 10.6) + (2 \times -7.9) + (1 \times 1.8) - 1.1 = 115.2 \text{ ppm}$$

The measured values are C-3 = 137.2 and C-2 = 116.8. The agreement is fair.

The allylic carbon of a (*Z*) alkene is usually at lower field from that of an (*E*) alkene by about 4–6 ppm (see Section 6.4.1). Alkene carbon atoms in polyenes are treated as though they were alkane carbon substituents on one of the double bonds. Thus, in calculating the shift of C-2 in 1,4-pentadiene, C-4 is treated like a β-sp^3 carbon atom.

Representative alkenes are presented in Table 5.6.

There are no simple rules to handle polar substituents on an alkene carbon. The shifts for vinyl ethers can be rationalized on the basis of electron density of the contributor structures

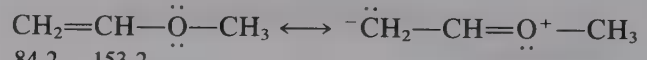

as can the shifts for α,β-unsaturated ketones.

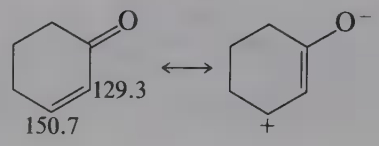

The same rationalization applies to the proton shifts in these compounds. Shifts for several substituted alkenes are presented in Table 5.7.

The central carbon atom (=C=) of alkyl-substi-

TABLE 5.6

Alkene and Cycloalkene Chemical Shifts (ppm from TMS)

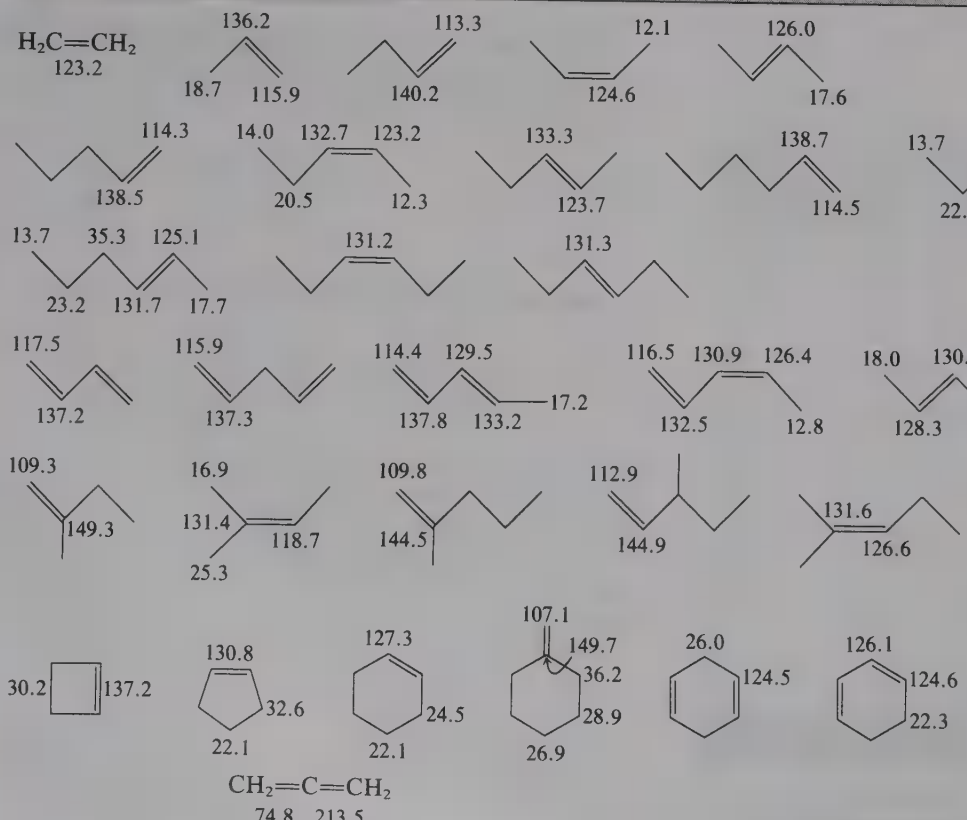

TABLE 5.7

Chemical Shifts of Substituted Alkenes (ppm from TMS)

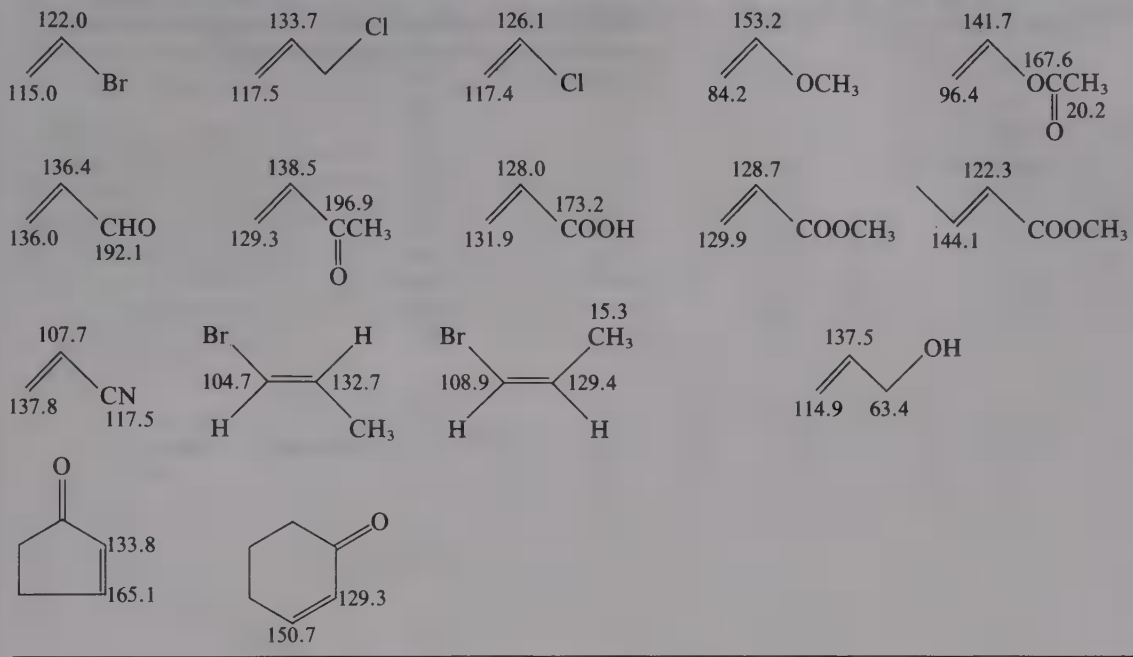

tuted allenes absorbs far downfield in the range of about 200–215 ppm, whereas the terminal atoms (*C*=C=*C*) absorb upfield in the range of about 75–97 ppm.

5.3.5. Alkynes

The *sp* carbon atoms of alkynes substituted only by alkyl groups absorb in the range of approximately 65–90 ppm (Table 5.8). The triple bond shifts the sp^3 carbon atoms directly attached about 5–15 ppm upfield relative to the corresponding alkane. The terminal ≡CH absorbs upfield from the internal ≡CR. Off-resonance decoupling gives a doublet for the terminal ≡CH. Alkyne carbon atoms with a polar group directly attached absorb from about 20–95 ppm.

TABLE 5.8

Alkyne Chemical Shifts (ppm)

Compound	C-1	C-2	C-3	C-4	C-5	C-6
1-Butyne	67.0	84.7				
2-Butyne		73.6				
1-Hexyne	67.4	82.8	17.4	29.9	21.2	12.9
2-Hexyne	1.7	73.7	76.9	19.6	21.6	12.1
3-Hexyne	14.4	12.0	79.9			

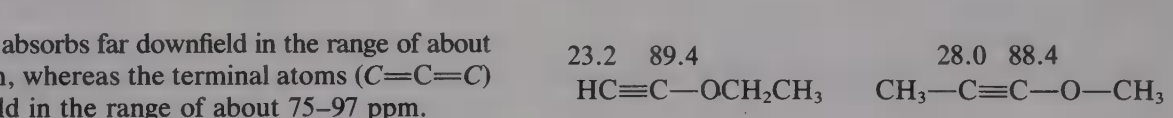

Polar resonance structures explain these shifts as shown above for vinyl ethers.

5.3.6. Aromatic Compounds

Benzene carbon atoms absorb at 128.5 ppm, neat or as a solution in $CDCl_3$ or CCl_4. Substituents shift the attached aromatic carbon atom as much as ±35 ppm. Fused-ring absorptions are as follows:

Naphthalene: C-1, 128.1; C-2, 125.9; C-4a, 133.7.
Anthracene: C-1, 130.1; C-2, 125.4; C-4a, 132.2; C-9, 132.6.
Phenanthrene: C-1, 128.3; C-2, 126.3; C-3, 126.3; C-4, 122.2; C-4a, 131.9*; C-9, 126.6; C-10a, 130.1*.

Shifts of the aromatic carbon atom directly attached to the substituent have been correlated with substituent electronegativity after correcting for magnetic anisotropy effects; shifts at the para aromatic carbon have been correlated with the Hammett σ constant. Ortho shifts are not readily predictable and range over

*Assignment uncertain.

TABLE 5.9

Incremental Shifts of the Aromatic Carbon Atoms of Monosubstituted Benzenes (ppm from Benzene at 128.5 ppm, + downfield, − upfield). Carbon Atom of Substituents in parts per million from TMS[a]

Substituent	C-1 (Attachment)	C-2	C-3	C-4	C of Substituent (ppm from TMS)
H	0.0	0.0	0.0	0.0	
CH_3	9.3	+0.7	−0.1	−2.9	21.3
CH_2CH_3	+15.6	−0.5	0.0	−2.6	29.2 (CH_2), 15.8 (CH_3)
$CH(CH_3)_2$	+20.1	−2.0	0.0	−2.5	34.4 (CH), 24.1 (CH_3)
$C(CH_3)_3$	+22.2	−3.4	−0.4	−3.1	34.5 (C), 31.4 (CH_3)
$CH{=}CH_2$	+9.1	−2.4	+0.2	−0.5	137.1 (CH), 113.3 (CH_2)
$C{\equiv}CH$	−5.8	+6.9	+0.1	+0.4	84.0 (C), 77.8 (CH)
C_6H_5	+12.1	−1.8	−0.1	−1.6	
CH_2OH	+13.3	−0.8	−0.6	−0.4	64.5
CH_2OCCH_3 (O)	+7.7	~0.0	~0.0	~0.0	20.7 (CH_3), 66.1 (CH_2), 170.5 (C=O)
OH	+26.6	−12.7	+1.6	−7.3	
OCH_3	+31.4	−14.4	+1.0	−7.7	54.1
OC_6H_5	+29.0	−9.4	+1.6	−5.3	
$OCCH_3$ (O)	+22.4	−7.1	−0.4	−3.2	23.9 (CH_3), 169.7 (C=O)
CH (O)	+8.2	+1.2	+0.6	+5.8	192.0
CCH_3 (O)	+7.8	−0.4	−0.4	+2.8	24.6 (CH_3), 195.7 (C=O)
CC_6H_5 (O)	+9.1	+1.5	−0.2	+3.8	196.4 (C=O)
CCF_3 (O)	−5.6	+1.8	+0.7	+6.7	
COH (O)	+2.9	+1.3	+0.4	+4.3	168.0
$COCH_3$ (O)	+2.0	+1.2	−0.1	+4.8	51.0 (CH_3), 166.8 (C=O) 168.5
CCl (O)	+4.6	+2.9	+0.6	+7.0	
$C{\equiv}N$	−16.0	+3.6	+0.6	+4.3	119.5
NH_2	+19.2	−12.4	+1.3	−9.5	
$N(CH_3)_2$	+22.4	−15.7	+0.8	−11.8	40.3
$NHCCH_3$ (O)	+11.1	−9.9	+0.2	−5.6	
NO_2	+19.6	−5.3	+0.9	+6.0	
$N{=}C{=}O$	+5.7	−3.6	+1.2	−2.8	129.5
F	+35.1	−14.3	+0.9	−4.5	
Cl	+6.4	+0.2	+1.0	−2.0	
Br	−5.4	+3.4	+2.2	−1.0	
I	−32.2	+9.9	+2.6	−7.3	
CF_3	+2.6	−3.1	+0.4	+3.4	
SH	+2.3	+0.6	+0.2	−3.3	
SCH_3	+10.2	−1.8	+0.4	−3.6	15.9
SO_2NH_2	+15.3	−2.9	+0.4	+3.3	
$Si(CH_3)_3$	+13.4	+4.4	−1.1	−1.1	

[a]See D. E. Ewing, *Org. Magn. Reson.*, **12**, 499 (1979) for chemical shifts of 709 monosubstituted benzenes.

about 15 ppm. Meta shifts are generally small—up to several parts per million for a single substituent.

The substituted aromatic carbon atoms can be distinguished from the unsubstituted aromatic carbon atom by its decreased peak height; that is, it lacks a proton and thus suffers from a longer T_1 and a diminished NOE.

Incremental shifts from benzene for the aromatic carbon atoms of representative monosubstituted benzene rings (and shifts from TMS of carbon-containing substituents) are given in Table 5.9. Shifts from benzene for polysubstituted benzene ring carbon atoms can be approximated by applying the principle of substituent additivity. For example, the shift from benzene for C-2 of the disubstituted compound 4-chlorobenzonitrile is calculated by adding the effect for an ortho CN group (+3.6) to that for a meta Cl group (+1.3):

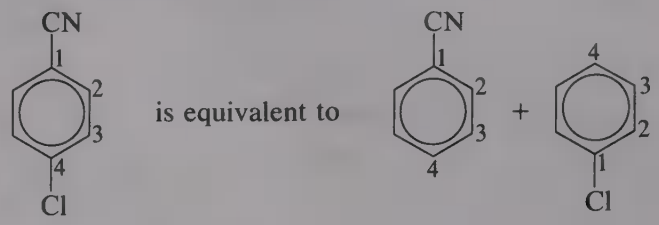

I II III

I			II		III	
C Atom	Calculated	Observed	C Atom	Observed	C Atom	Observed
1	−18.0	−16.6	1	−16.0	4	−2.0
2	+ 4.6	+ 5.1	2	+ 3.6	3	+1.0
3	+ 0.8	+ 1.3	3	+ 0.6	2	+0.2
4	+10.7	+10.8	4	+ 4.3	1	+6.4

5.3.7. Heteroaromatic Compounds

Complex rationalizations have been offered for the shifts of carbon atoms in heteroaromatic compounds. As a general rule, C-2 of oxygen- and nitrogen-containing rings is further downfield than C-3. Large solvent and pH effects have been recorded. Table 5.10 gives values for neat samples of several five- and six-membered heterocyclic compounds.

TABLE 5.10

Shifts for Carbon Atoms of Heteroaromatics (neat, ppm from TMS)

Compound	C-2	C-3	C-4	C-5	C-6	Substituent
Furan	142.7	109.6				
2-Methylfuran	152.2	106.2	110.9	141.2		13.4
Furan-2-carboxaldehyde	153.3	121.7	112.9	148.5		178.2
Methyl 2-furoate	144.8	117.9	111.9	146.4		159.1 (C=O), 51.8 (CH_3)
Pyrrole	118.4	108.0				
2-Methylpyrrole	127.2	105.9	108.1	116.7		12.4
Pyrrole-2-carboxaldehyde	134.0	123.0	112.0	129.0		
Thiophene	124.4	126.2				
2-Methylthiophene	139.0	124.7	126.4	122.6		14.8
Thiophene-2-carboxaldehyde	143.3	136.4	128.1	134.6		182.8
Thiazole	152.2		142.4	118.5		
Imidazole	136.2		122.3	122.3		
Pyridine	150.2	123.9	135.9			
Pyrimidine	159.5		157.4	122.1	157.4	
Pyrazine	145.6					
2-Methylpyrazine	154.0	141.8[a]	143.8[a]	144.7[a]		21.6

[a] Assignment not certain.

TABLE 5.11

Chemical Shifts of Alcohols (neat, ppm from TMS)

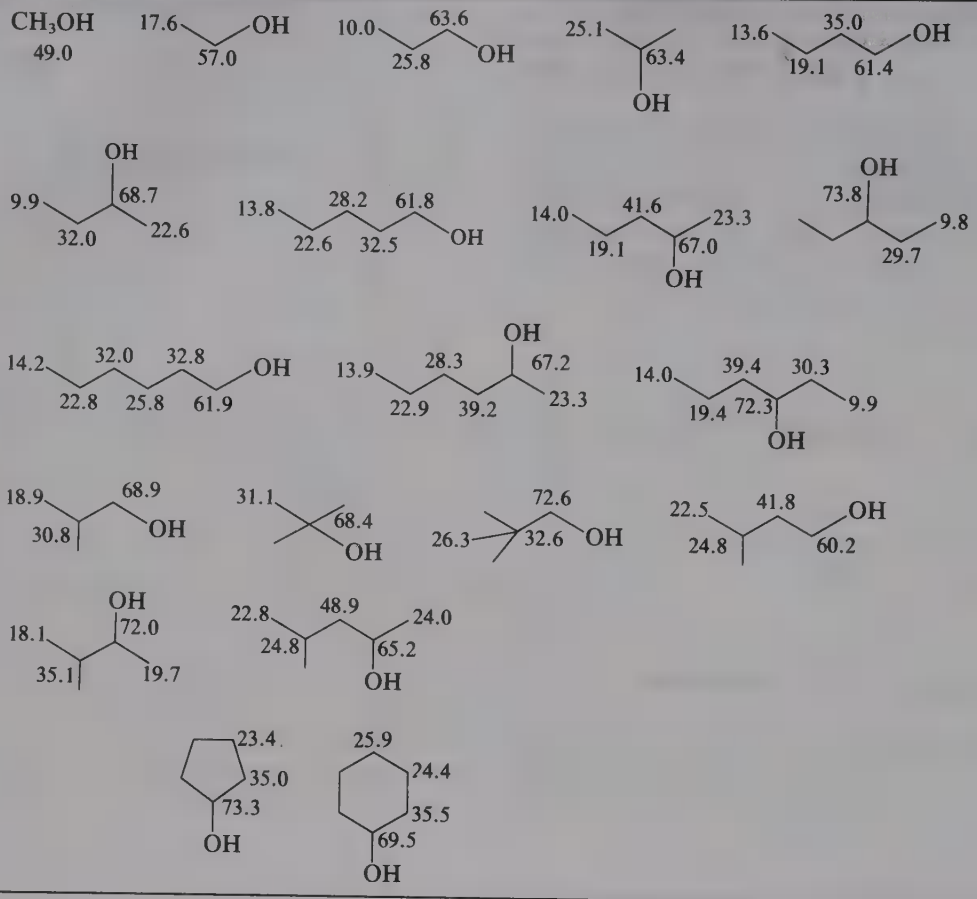

5.3.8. Alcohols

Substitution of H in an alkane by an OH group causes downfield shifts of 35–52 ppm for C-1, 5–12 ppm for C-2, and upfield shifts of about 0–6 ppm for C-3. Shifts for several acyclic and alicyclic alcohols are given in Table 5.11. Acetylation provides a useful diagnostic test for an alcohol, the C-1 absorption moving downfield by about 2.5–4.5 ppm, and the C-2 absorption moving upfield by a similar amount; a 1,3-diaxial interaction may cause a slight (~1 ppm) downfield shift of C-3. Table 5.3 may be used to calculate shifts for alcohols as described earlier.

5.3.9. Ethers, Acetals, and Epoxides

An alkoxy substituent causes a somewhat larger downfield shift at C-1 (~10 ppm larger) than that of a hydroxy substituent. This is attributed to the C-1′ of the alkoxy group having the same effect as a β-C relative to C-1. The O atom is regarded here as an "α-C" to C-1.

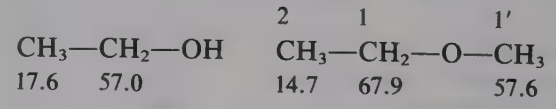

Note also that the "γ effect" (upfield shift) on C-2 is explainable by similar reasoning. Conversely, the ethoxy group affects the OCH_3 group (compare CH_3OH). Table 5.12 gives shifts of several ethers.

The dioxygenated carbon of acetals absorbs in the range of about 88–112 ppm. Oxirane (an epoxide) absorbs at 40.6 ppm.

The alkyl carbon atoms of aralkyl ethers have shifts similar to those of dialkyl ethers. Note the strong upfield shift of the ring ortho carbon resulting from electron delocalization as in the vinyl ethers.

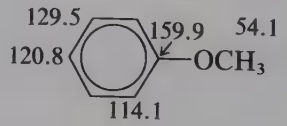

TABLE 5.12

Chemical Shifts of Ethers, Acetals, and Epoxides (ppm from TMS)

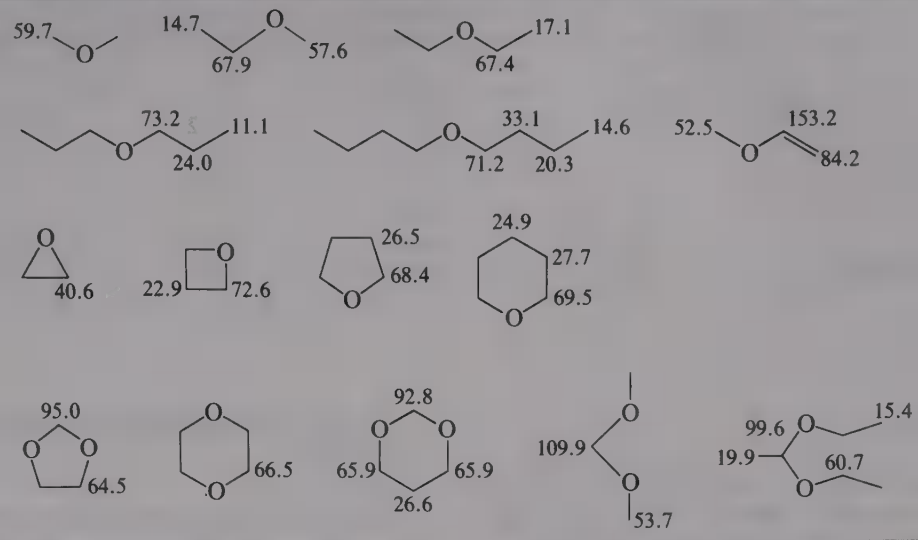

5.3.10. Halides

The effect of halide substitution is complex. A single fluorine atom (in CH_3F) causes a large downfield shift from CH_4 as electronegativity considerations would suggest. Successive geminal substitution by Cl (CH_3Cl, CH_2Cl_2, $CHCl_3$, CCl_4) results in increasing downfield effects—again expected on the basis of electronegativity. But with Br and I, the "heavy atom effect" supervenes. The carbon shifts of CH_3Br and CH_2Br_2 move progressively downfield, but those of $CHBr_3$ and CBr_4 move progressively upfield. A strong upfield progression for I commences with CH_3I, which is upfield from CH_4. There is a progressive downfield effect at C-2 in the order I > Br > F. Chlorine and Br show γ-gauche shielding at C-3, but I does not, presumably because of the low population of the hindered gauche rotamer. Table 5.13 shows these trends.

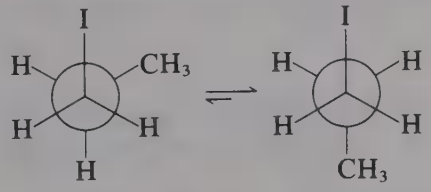

Halides may show large solvent effects; for example, C-1 for iodoethane is at −6.6 in cyclohexane, and at −0.4 in DMF.

TABLE 5.13

Shift Positions for Alkyl Halides (neat, ppm from TMS)

Compound	C-1	C-2	C-3
CH_4	−2.3		
CH_3F	75.4		
CH_3Cl	24.9		
CH_2Cl_2	54.0		
$CHCl_3$	77.5		
CCl_4	96.5		
CH_3Br	10.0		
CH_2Br_2	21.4		
$CHBr_3$	12.1		
CBr_4	− 28.5		
CH_3I	− 20.7		
CH_2I_2	− 54.0		
CHI_3	−139.9		
CI_4	−292.5		
CH_3CH_2F	79.3	14.6	
CH_3CH_2Cl	39.9	18.7	
CH_3CH_2Br	28.3	20.3	
CH_3CH_2I	−0.2	21.6	
$CH_3CH_2CH_2Cl$	46.7	26.5	11.5
$CH_3CH_2CH_2Br$	35.7	26.8	13.2
$CH_3CH_2CH_2I$	10.0	27.6	16.2

TABLE 5.14A

Shift Positions of Acyclic and Alicyclic Amines (neat, ppm from TMS)

Compound	C-1	C-2	C-3	C-4
CH_3NH_2	26.9			
$CH_3CH_2NH_2$	35.9	17.7		
$CH_3CH_2CH_2NH_2$	44.9	27.3	11.2	
$CH_3CH_2CH_2CH_2NH_2$	42.3	36.7	20.4	14.0
$(CH_3)_3N$	47.5			
$CH_3CH_2N(CH_3)_2$	58.2	13.8		
Cyclohexylamine	50.4	36.7	25.7	25.1
N-Methylcyclohexylamine	58.6	33.3	25.1	26.3 (N—CH_3 33.5)

5.3.11. Amines

An NH_2 group attached to an alkyl chain causes a downfield shift of about 30 ppm at C-1, a down field shift of about 11 ppm at C-2, and an upfield shift of about 4.0 ppm at C-3. The NH_3^+ group shows a somewhat smaller effect. N alkylation increases the downfield effect of the NH_2 group at C-1. Shift positions for selected acyclic and alicyclic amines are given in Table 5.14A (see Table 5.5 for heterocyclic amines).

5.3.12. Thiols, Sulfides, and Disulfides

Since the electronegativity of sulfur is considerably less than that of oxygen, sulfur causes a correspondingly smaller chemical shift. Examples of thiols, sulfides, and disulfides are given in Table 5.14B.

5.3.13. Functional Groups Containing Carbon

Carbon-13 NMR spectrometry permits direct observation of carbon-containing functional groups; the shift ranges for these are given in Appendix A. With the exception of CH=O, the presence of these groups could not be directly ascertained by ^1H NMR.

5.3.13.1. Ketones and Aldehydes

The $R_2C{=}O$ and the RCH=O carbon atoms absorb in a characteristic region, downfield. Acetone absorbs at 203.8 ppm and acetaldehyde at 199.3 ppm. Alkyl substitution on the α carbon causes a downfield shift of the C=O absorption of 2–3 ppm until steric effects supervene. Replacement of the CH_3 of acetone or acetaldehyde by a phenyl group causes an upfield shift of the C=O absorption (acetophenone 195.7 ppm, ben-

TABLE 5.14B

Shift Positions of Thiols, Sulfides, and Disulfides (ppm from TMS)

Compounds	C-1	C-2	C-3
CH_3SH	6.5		
CH_3CH_2SH	19.8	17.3	
$CH_3CH_2CH_2SH$	26.4	27.6	12.6
$CH_3CH_2CH_2CH_2SH$	23.7	35.7	21.0
$(CH_3)_2S$	19.3		
$(CH_3CH_2)_2S$	25.5	14.8	
$(CH_3CH_2CH_2)_2S$	34.3	23.2	13.7
$(CH_3CH_2CH_2CH_2)_2S$	34.1	31.4	22.0
CH_3SSCH_3	22.0		
$CH_3CH_2SSCH_2CH_3$	32.8	14.5	

TABLE 5.15

Shift Positions of the C=O Group and Other Carbon Atoms of Ketones and Aldehydes (ppm from TMS)

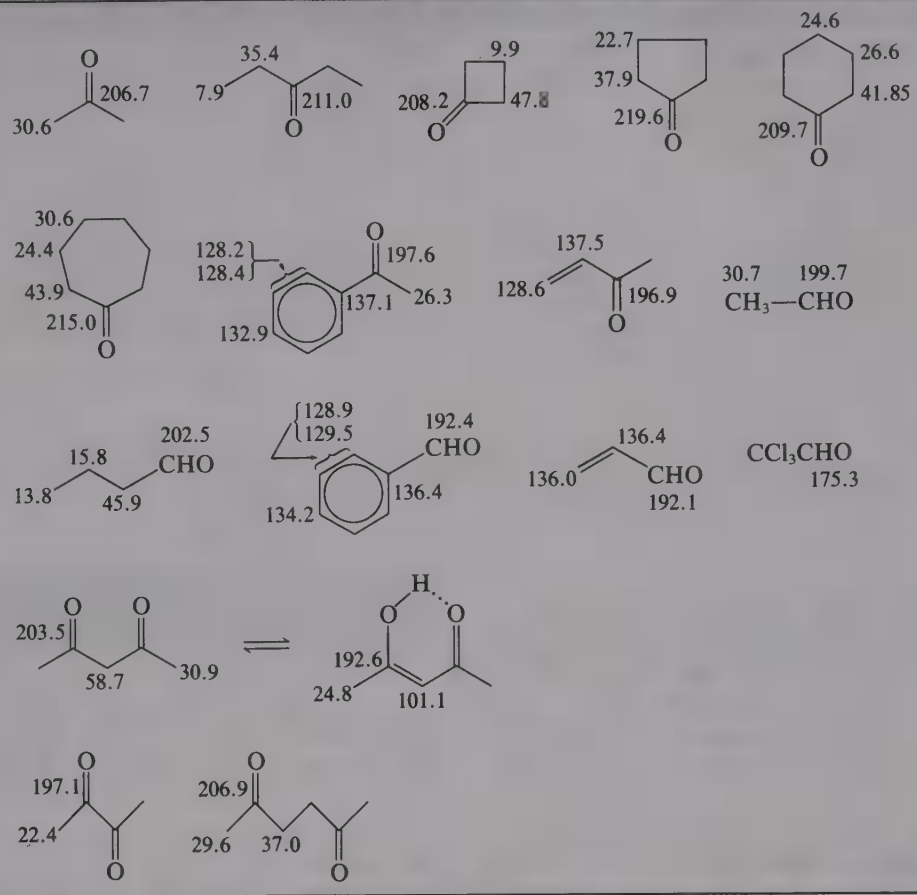

zaldehyde 190.7 ppm); similarly α, β unsaturation causes upfield shifts (acrolein 192.1 ppm, compared with propionaldehyde 201.5 ppm). Presumably, charge delocalization by the benzene ring or the double bond makes the carbonyl carbon less electron deficient. Of the cycloalkanones, cyclopentanone has an anomalously low shift position. Table 5.15 presents chemical shifts of the C=O group of some ketones and aldehydes. Because of rather large solvent effects, there are differences of several parts per million from different literature sources. Replacement of CH_2 of alkanes by C=O causes a downfield shift at the α carbon (~10–14 ppm) and an upfield shift at the β carbon (several ppm in acyclic compounds).

5.3.13.2. Carboxylic Acids, Esters, Chlorides, Anhydrides, Amides, and Nitriles

The C=O groups of carboxylic acids and derivatives are in the range of 150–185 ppm. Dilution and solvent effects are marked for carboxylic acids; anions appear at lower field. The effects of substituents and electron delocalization are generally similar to those for ketones. Nitriles absorb in the range of 115–125 ppm. Alkyl substituents on the nitrogen of amides cause a small (up to several ppm) upfield shift of the C=O group (see Table 5.16).

5.3.13.3. Oximes

The simple oximes absorb in the range of 145–165 ppm. It is possible to distinguish between syn and anti isomers since the C=N shift is upfield in the sterically more compressed form, and the more hindered substituent (syn to the OH) is upfield of the less hindered.

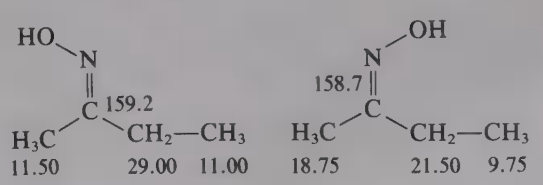

TABLE 5.16

Shift Positions for the C=O group and other Carbon Atoms of Carboxylic Acids, Esters, Lactones, Chlorides Anhydrides, Amides, Carbamates, and Nitriles (ppm from TMS)

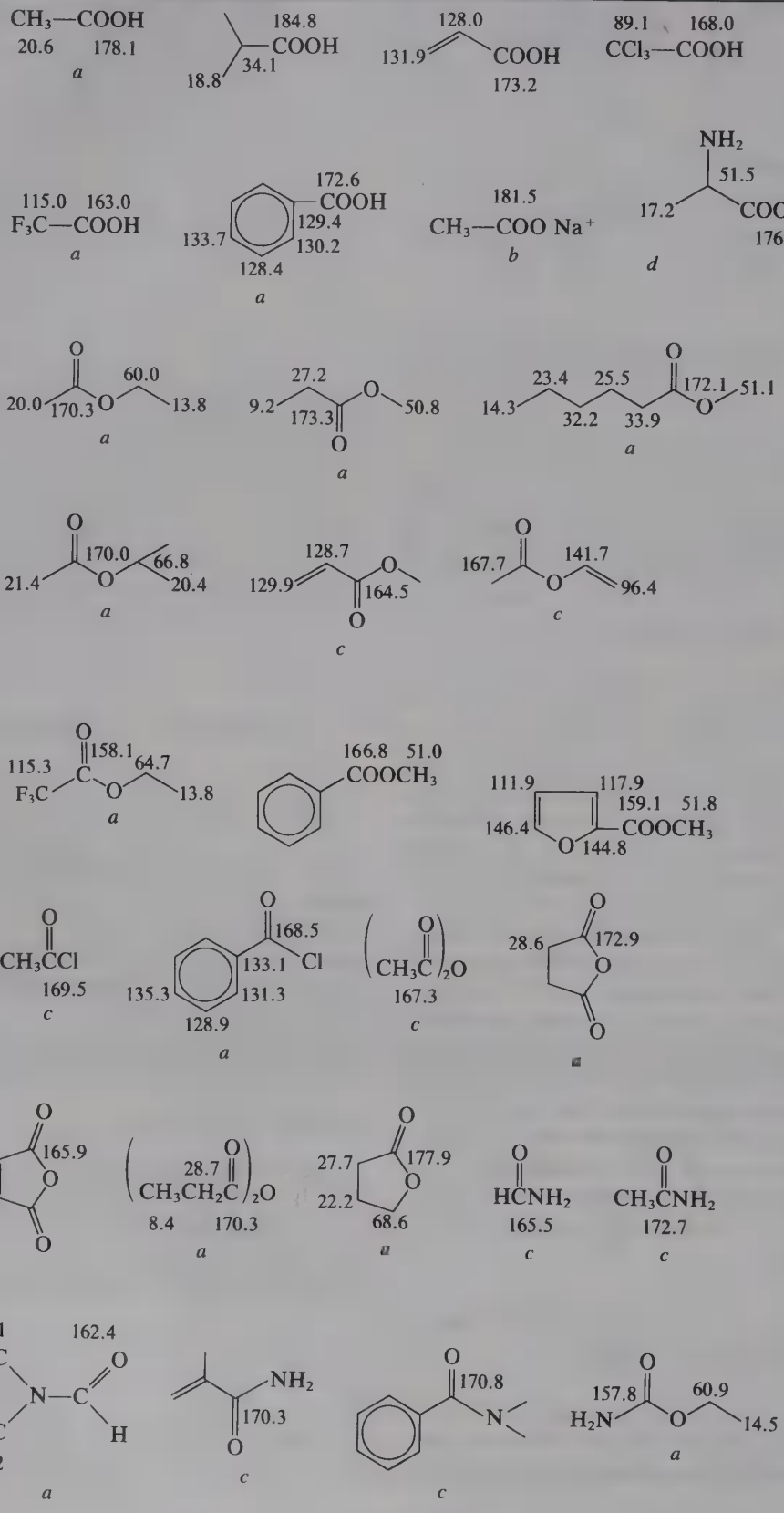

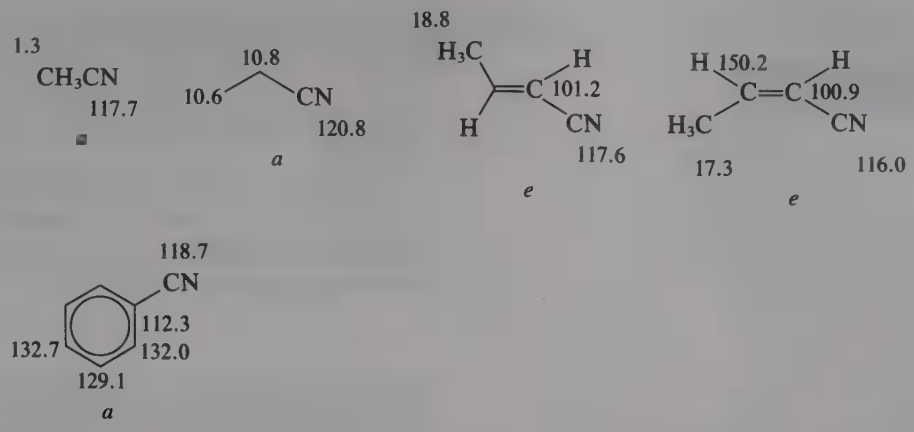

[a]In $CHCl_3$ (~50%)
[b]Saturated aqueous solution of CH_3COONa.
[c]Neat or saturated solution.
[d]In H_2O
[e]In DMSO.
[f]In dioxane (~50%).

5.4. SPIN COUPLING

Coupling—at least as an initial consideration—is less important in ^{13}C NMR than in ^1H NMR, since routine ^{13}C spectra are usually noise decoupled. Thus coupling information is discarded in the interest of obtaining a spectrum in a shorter time or on a smaller sample—a spectrum, furthermore, free of complex overlapping absorptions. However, as mentioned earlier, information from residual coupling can be regained through off-resonance decoupling.

The ^{13}C—^{13}C coupling is usually not observed, except in compounds that have been deliberately enriched with ^{13}C, because of the low probability of two adjacent ^{13}C atoms in a molecule. One-bond ^{13}C—H coupling ($^1J_{CH}$) ranges from about 110 to 320 Hz, increasing with increased *s* character of the ^{13}C—H bond, with substitution on the carbon atom of electron-withdrawing groups, and with angular distortion. Appreciable ^{13}C—H coupling also extends over two or more (*n*) bonds ($^nJ_{CH}$). Table 5.17 gives some representative $^1J_{CH}$ values. Table 5.18 gives some representative $^2J_{CH}$ values, which range from about −5 to 60 Hz.

TABLE 5.17
Some $^1J_{CH}$ Values

Compound	*J* (Hz)
*sp*³	
CH_3CH_3	124.9
$CH_3\underline{C}H_2CH_3$	119.2
$(CH_3)_3\underline{C}H$	114.2
CH_3NH_2	133.0
CH_3OH	141.0
CH_3Cl	150.0
CH_2Cl_2	178.0
$CHCl_3$	209.0
	123.0
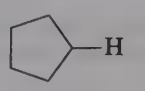	128.0
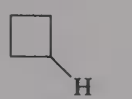	134.0
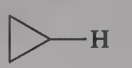	161.0
	205.0
*sp*²	
$CH_2{=}CH_2$	156.2
$CH_3\underline{C}H{=}C(CH_3)_2$	148.4
$CH_3\underline{C}H{=}O$	172.4
$NH_2\underline{C}H{=}O$	188.3
C_6H_6	159.0
sp	
$CH{\equiv}CH$	249.0
$C_6H_5C{\equiv}CH$	251.0
$HC{\equiv}N$	269.0

TABLE 5.18

Some $^2J_{CH}$ Values

Compound	J (Hz)
sp^3	
CH_3CH_3	−4.5
CH_3CCl_3	5.9
$CH_3CH{=}O$	26.7
sp^2	
$CH_2{=}CH_2$	−2.4
$(CH_3)_2C{=}O$	5.5
$CH_2{=}CHCH{=}O$	26.9
C_6H_6	1.0
sp	
$CH{\equiv}CH$	49.3
$C_6H_5OC{\equiv}CH$	61.0

The $^3J_{CH}$ values are roughly comparable to $^2J_{CH}$ values for sp^3 carbon atoms. In aromatic rings, however, the $^3J_{CH}$ values are characteristically larger than $^2J_{CH}$ values. In benzene itself, $^3J_{CH}$ = 7.4 Hz and $^2J_{CH}$ = 1.0 Hz.

Coupling of ^{13}C to several other nuclei, the most important of which are ^{31}P, ^{19}F and D, may be observed in proton-decoupled spectra. Representative coupling constants are given in Table 5.19.

5.5. PEAK ASSIGNMENT PROBLEM

We may review some of the above material by assigning the peaks of *p*-methoxybenzaldehyde in Figure 5.5*a* and *b* by using the chemical shift correlation tables, peak heights, off-resonance decoupling, and the concept of symmetry.

We immediately assign the downfield absorption in Figure 5.5*a* at δ 191.0 (peak 1) to the CHO group (Table 5.15 gives δ 190.7 for benzaldehyde), and the upfield absorption at δ 55.6 (peak 6) to the OCH_3 group (Table

TABLE 5.19

Coupling Constants for ^{31}P, ^{19}F, and D Coupled to ^{13}C

Compound	^1J (Hz)	^2J (Hz)	^3J (Hz)
CH_3CF_3	271		
CF_2H_2	235		
CF_3CO_2H	284	43.7	
C_6H_5F	245	21.0	
$(CH_3CH_2)_3P$	5.4	10.0	
$(CH_3CH_2)_4P^+\ Br^-$	49	4.3	
$(C_6H_5)_3P^+CH_3\ I^-$	88 (CH_3 52)	10.9	
$CH_3CH_2P(OCH_2CH_3)_2$ (O)	143	7.1 (J_{COP} 6.9)	J_{CCOP} 6.2
$CDCl_3$	31.5		
CD_3CCD_3 (O)	19.5		
$(CD_3)_2SO$	22.0		
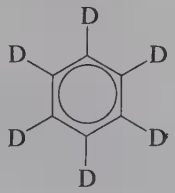	25.5		

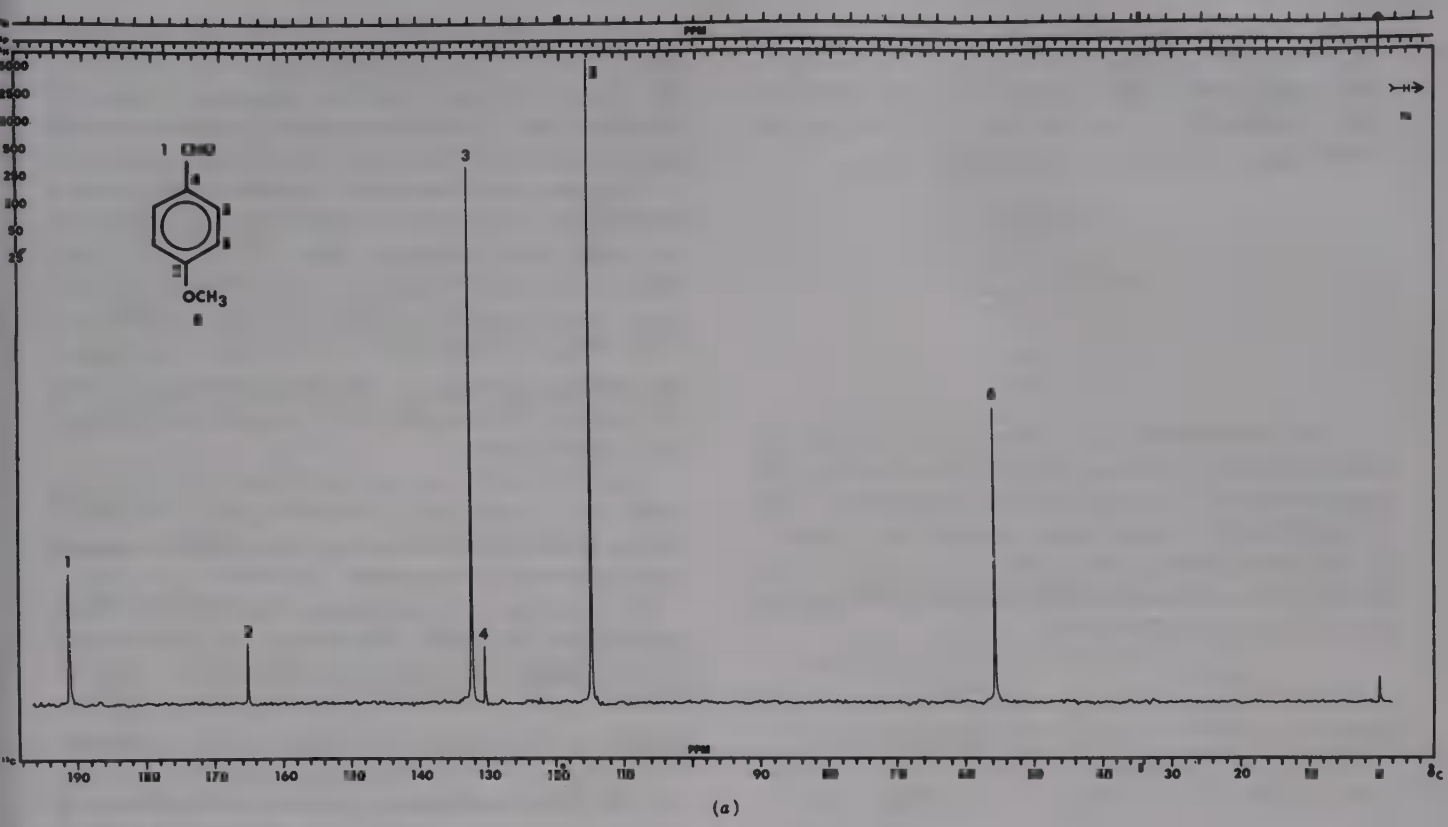

(*a*)

FIGURE 5.5(*a*). Broadband decoupled ^{13}C spectrum of *p*-methoxybenzaldehyde. Solvent $CDCl_3$ at 25.2 MHz, 5000-Hz sweepwidth.

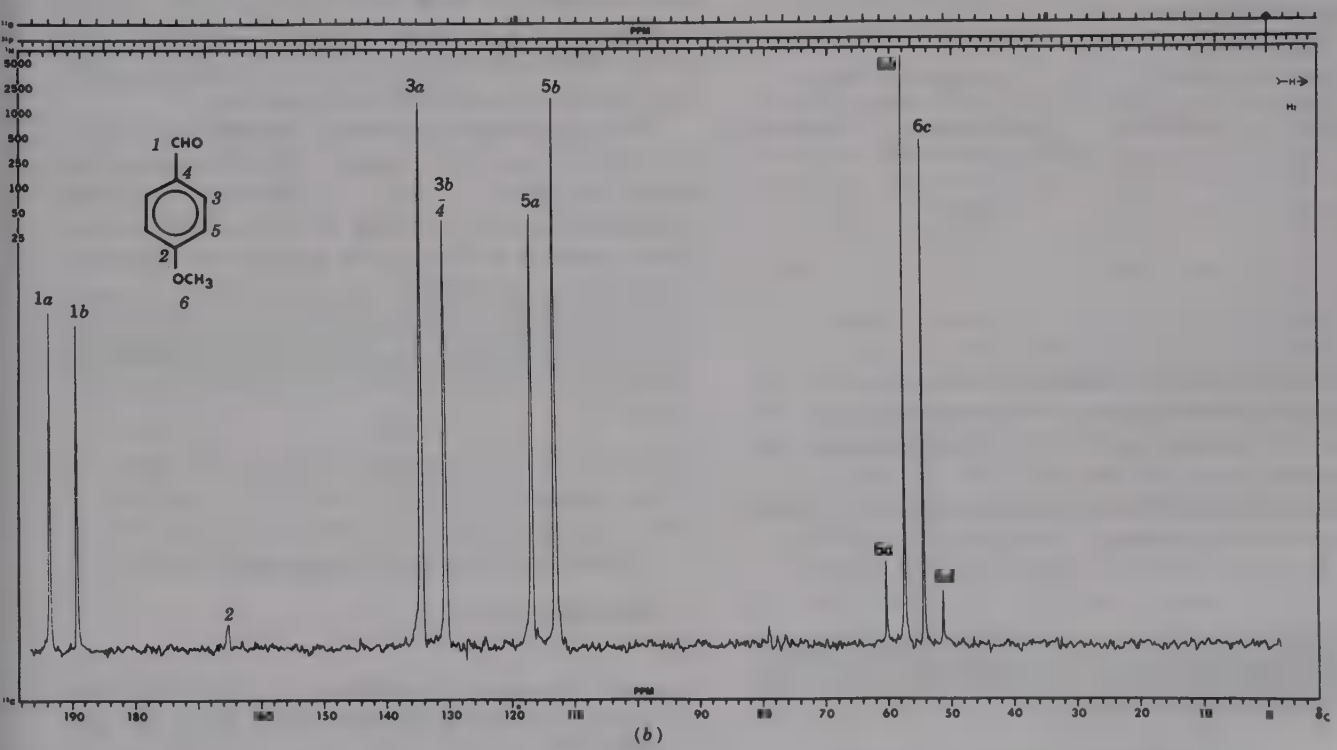

(*b*)

FIGURE 5.5(*b*). Off-resonance decoupled ^{13}C spectrum of *p*-methoxybenzaldehyde. Solvent $CDCl_3$ at 25.2 MHz, 5000-Hz sweepwidth. See Chapter 6 for newer methods.

5.9 gives δ 54.1 for anisole). The small peaks 2 and 4 must represent the quaternary ring carbon atoms, and the 2 large peaks 3 and 5 must each represent the two pairs of equivalent ring carbon atoms. At this point the following assignments are evident.

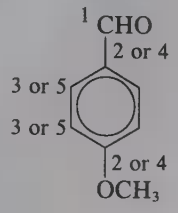

These assignments are confirmed by the off-resonance decoupled spectrum (Fig. 5.5*b*): doublet for CHO, quartet for OCH_3, singlets for the quaternary carbon atoms. Peak 4 is buried under the doublet of peak 3.

The ambiguous assignments can be resolved by applying the principle of substituent additivity and the data of Table 5.9 as follows

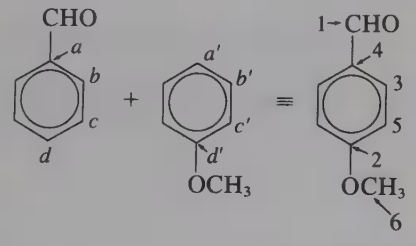

ppm from Benzene (128.5 ppm) (See Table 5.9)		ppm from TMS (δ)			
for CHO	for OCH_3	Calculated		Observed	
a +8.2	*a'* − 7.7	4	129.0	4	130.2
b +1.2	*b'* + 1.0	3	130.7	3	132.1
c +0.6	*c'* −14.4	5	114.7	5	114.5
d +5.8	*d'* +31.4	2	165.7	2	164.9

Note also that we count six carbon atoms in the noise decoupled spectrum and six protons in the off-resonance decoupled spectrum. The discrepancy between this count and the molecular formula $C_8H_8O_2$ confirms the para substitution in the benzene ring, which has an axis of symmetry.

5.6. QUANTITATIVE ANALYSIS

Quantitative ^{13}C NMR is desirable in two situations. First, in structural determinations, it is clearly useful to know if a signal is due to more than one shift-equivalent carbon. Second, quantitative analysis of a mixture of two or more components requires that the area of a signal be proportional to the number of carbon atoms causing that signal.

There are two reasons why noise decoupled spectra are usually not quantitative. First, carbon atoms with long spin–lattice relaxation times (T_1) may not completely return to a Boltzmann's distribution between pulses, and the resulting signals will be considerably weaker than expected from the number of carbon atoms causing those signals. Second, some carbon atoms give rise to exceptionally small signals due to weak NOE enhancement.

Three methods may be employed in an effort to obtain quantitative noise decoupled spectra: long pulse delays, gated decoupling, and the addition of paramagnetic relaxation reagents.

Delays of tens to hundreds of seconds (to allow return of the nuclei to a Boltzmann's distribution) will remove signal area discrepancies caused by long relaxation times; such delays, unfortunately, will frequently require prohibitively long times to obtain the spectrum.

If the noise decoupler is gated on during the pulse and the early part of the FID and then is gated off during the pulse delay, NOE enhancement will be minimized for all carbon atoms. This is true because the free induction signal decays quickly in an exponential fashion, while the NOE factor slowly builds up in an exponential fashion. A weakness of the gated decoupling method is the removal of the NOE factor, whose loss requires extended signal acquisition.

Added paramagnetic relaxation reagents lead to more quantitative spectra by reducing all of the spin–lattice relaxation times (by means of an electronic relaxation mechanism) and by leveling all of the NOE factors. These reagents suffer from the fact that the effects are not complete and from the requirement that the sample must be separated (e.g., by chromatography) if it is to be recovered. Successful quantitative analysis has been carried out by combining two or all three of these procedures.

REFERENCES

General

Levy, G. C., Lichter, R. L., and Nelson, G. L. *Carbon-13 Nuclear Magnetic Resonance for Organic Chemists*, 2nd ed. New York: Wiley, 1980.

Breitmaier, E. and Voelter, W. *Carbon-13 NMR Spectroscopy*, 3rd ed. New York: VCH Publishers, 1987.

Abraham, R. J., Fisher, J., and Loftus, P. *Introduction to NMR Spectroscopy*, New York: Wiley, 1988.

Wehrli, F. W., Marchand, A. P., and Wehrli, S. *Interpretation of Carbon-13 NMR Spectra*, 2nd ed. New York: Wiley, 1988.

Farrar, T. C. *An Introduction to Pulse NMR Spectroscopy*, Chicago: Farragut Press, 1987.

Shaw, D. *Fourier Transform NMR Spectroscopy*, 2nd ed. Amsterdam: Elsevier, 1984.

Muller, K. and Pregosin, P. S. *Fourier Transform NMR: A Practical Approach*, New York: Academic, 1976.

Paudler, W. W. *Nuclear Magnetic Resonance*, New York, Wiley, 1987.

Atta-Ur-Rahman. *Nuclear Magnetic Resonance*, New York: Springer-Verlag, 1986.

Spectra and Data

Pretsch, E., Clerc, T., Seibl, J., and Simon, W. *Spectra Data for Structure Determination of Organic Compounds*, Berlin: Springer–Verlag, 1981.

Bremser, W., Ernst, L., Franke, B., Gerhards, R., and Hardt, A. *Carbon-13 NMR Spectral Data (microfiche)*, New York: VCH Publishers, 4th ed., 1987. (58,108 spectra of 48,357 compounds tabular).

Breitmaier, E., Haas, G., and Voelter, W., *Atlas of C-13 NMR Data*, Vols. 1–3, Philadelphia: Heyden 1979 (3017 compounds).

Sadtler Research Lab. ^{13}C NMR Spectra, Philadelphia: Sadtler Research Laboratories.

Johnson, L. F., and Jankowski, W. C. *Carbon-13 NMR Spectra, a Collection of Assigned, Coded, and Indexed Spectra*, New York: Wiley, 1972.

Bates, R. B. and Beavers, W. A. *C-13 NMR Problems*, Clifton, NJ: Humana Press, 1981.

Fuchs, P. L. and Bunnell, C. A. *Carbon-13 NMR-Based Organic Spectral Problems*, New York: Wiley, 1979.

PROBLEMS

5.1 Draw the ^1H NMR spectrum and the broadband decoupled ^{13}C NMR spectrum (designate multiplicities) for the following compounds (solvent $CDCl_3$). Show peaks in proper proportions.

a. 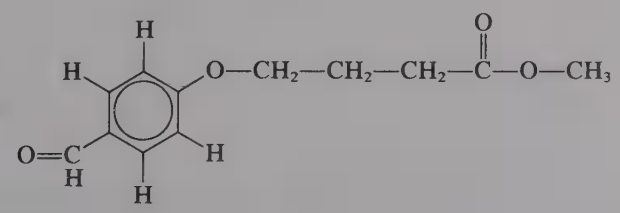

b. $CH_2{=}CH{-}\underset{\displaystyle CH_3}{\underset{|}{CH}}{-}CH_2{-}COOH$

c. $CH_3{-}CH_2{-}CH_2{-}\overset{\displaystyle H}{\overset{|}{N}}{-}CH_2{-}CH_2{-}CH_3$

d. 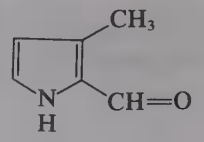

e. 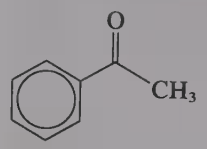

f. $CH_3{-}CH{=}CH{-}\underset{\displaystyle O}{\underset{\|}{C}}{-}O{-}CH_3$ (Z)

g. $CH_3{-}CH{=}CH{-}O{-}CH_3$ (Z)

h. $HC{\equiv}C{-}CH_2{-}CH_2{-}OH$

5.2. How many ^{13}C peaks should be seen in the broadband decoupled spectrum of each of the following compounds? Assign the multiplicity expected for each signal in the off-resonance decoupled spectrum.

a. Benzene
b. Toluene
b. Naphthalene
d. Dodecane

e. 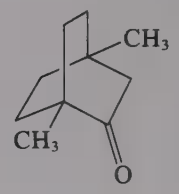

f. 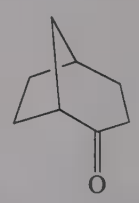

5.3. Because a compound of molecular formula C_6H_8 is highly symmetrical, it shows just two singlets in the broadband decoupled spectrum. The off-resonance decoupled spectrum shows only a triplet and a doublet. Draw the structure.

5.4. Predict the number of lines in ^{13}C spectra for the following compounds. In each case, check your results against the footnote in Section 5.2.4. Recall the $CDCl_3$ signal that appears in many ^{13}C spectra and adapt Pascal's triangle (Fig. 4.28), to ^{13}C—D coupling.

$Cl{-}\overset{\displaystyle Cl}{\overset{|}{\underset{\displaystyle Cl}{\underset{|}{{}^{13}C}}}}{-}D$, $Cl{-}\overset{\displaystyle Cl}{\overset{|}{\underset{\displaystyle D}{\underset{|}{{}^{13}C}}}}{-}D$, $Cl{-}\overset{\displaystyle D}{\overset{|}{\underset{\displaystyle D}{\underset{|}{{}^{13}C}}}}{-}D$.

5.5. What are the symmetry elements in *o*-, *m*-, and *p*-diethyl phthalate, and how many nonequivalent carbon atoms and protons are there in each compound? Draw the broadband-decoupled spectrum of each compound (see Fig. 5.1).

5.6. Deduce the structures of Compounds A–H and assign the ^{13}C signals. The multiplicities are abbreviated: s = singlet, d = doublet, t = triplet, q = quartet. The following spectra were run in $CDCl_3$ at 25.2 MHz.*

*By permission of John Wiley & Sons; See Johnson and Jankowski under References.

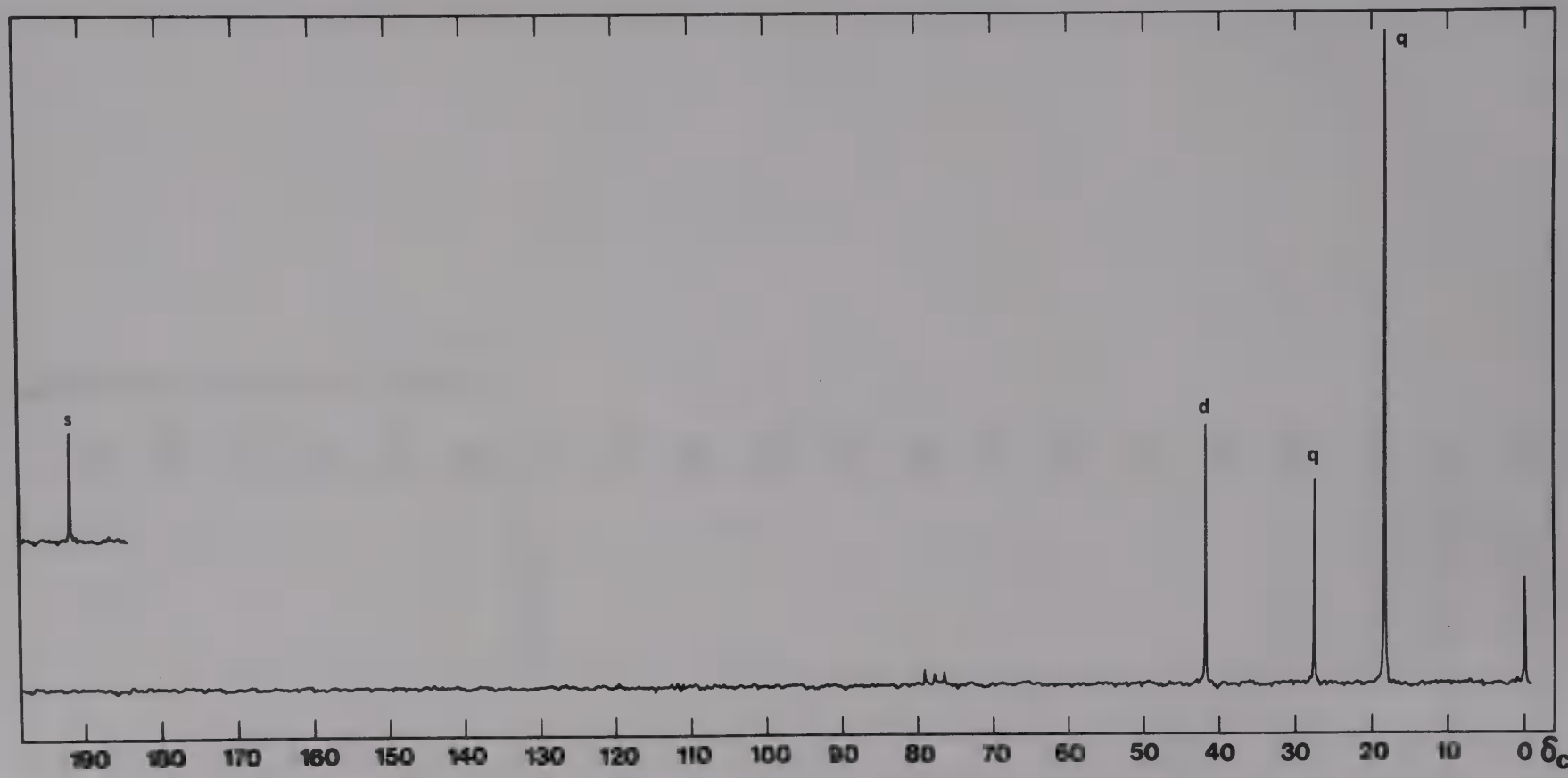

(*a*)

PROBLEM 5.6 COMPOUND A, $C_5H_{10}O$. THE C═O GROUP IS OFFSET AT 211.8 PPM.

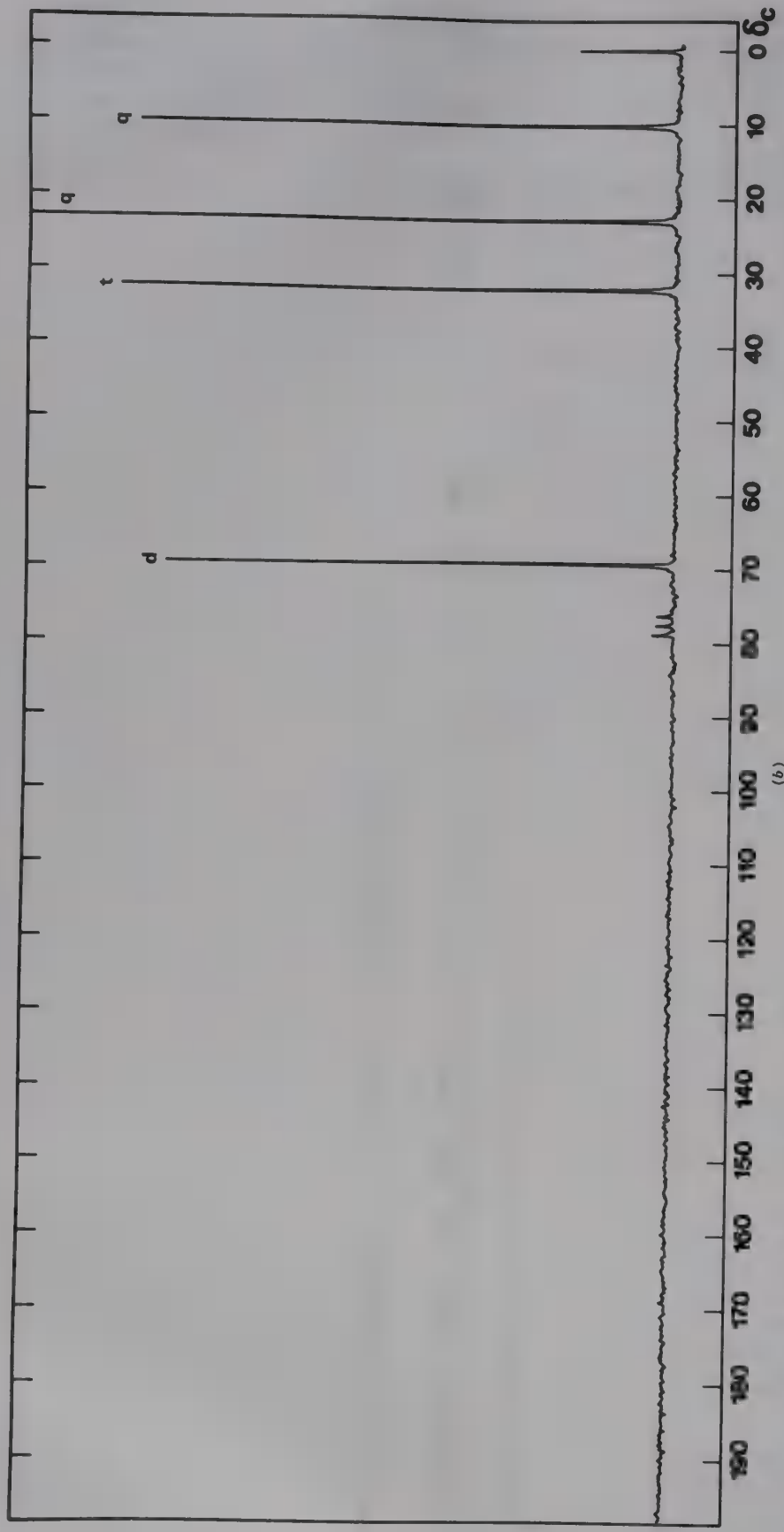

PROBLEM 5.6. COMPOUND B, $C_4H_{10}O$.

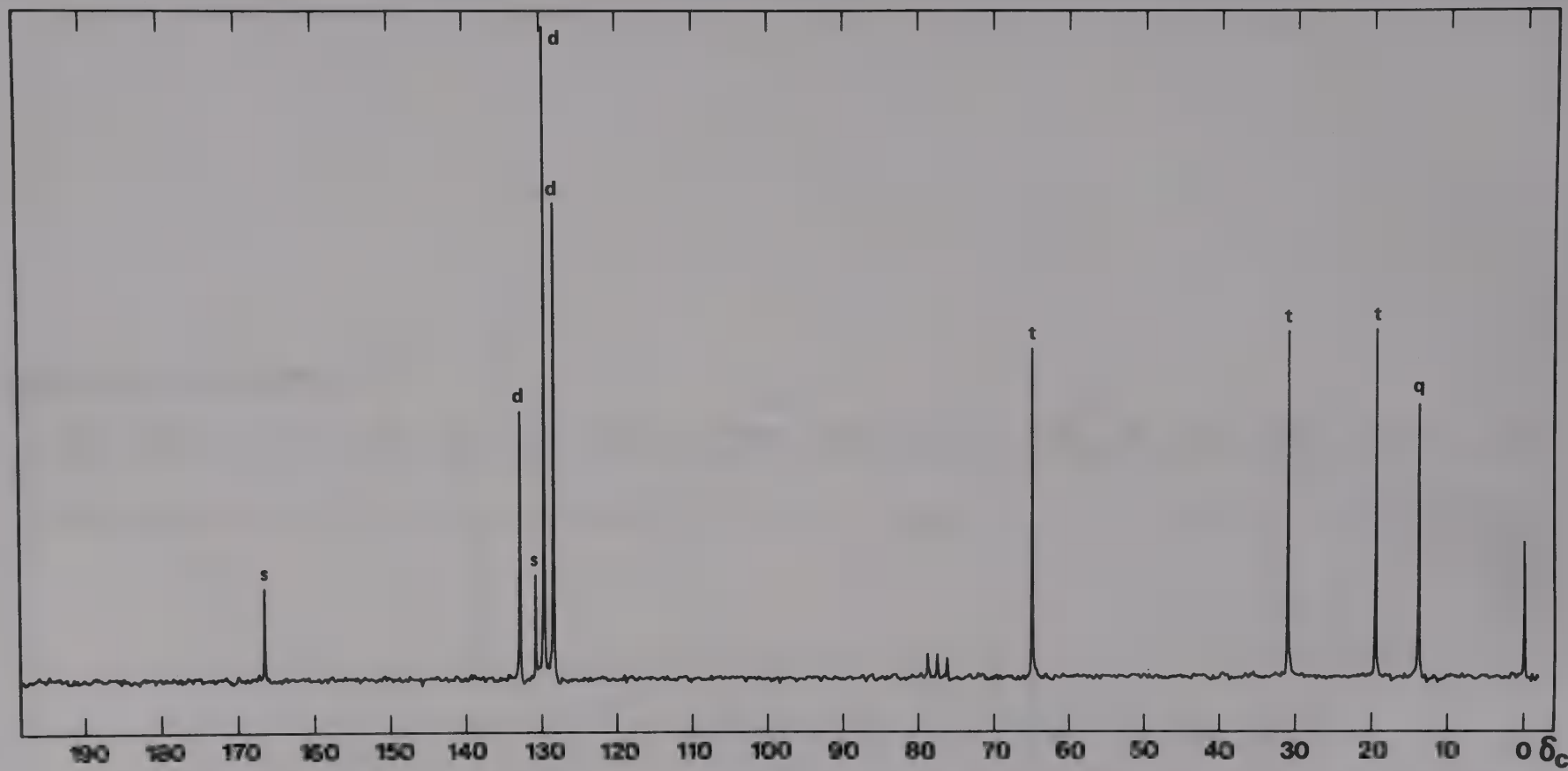

(*c*)

PROBLEM 5.6. COMPOUND C, $C_{11}H_{14}O_2$.

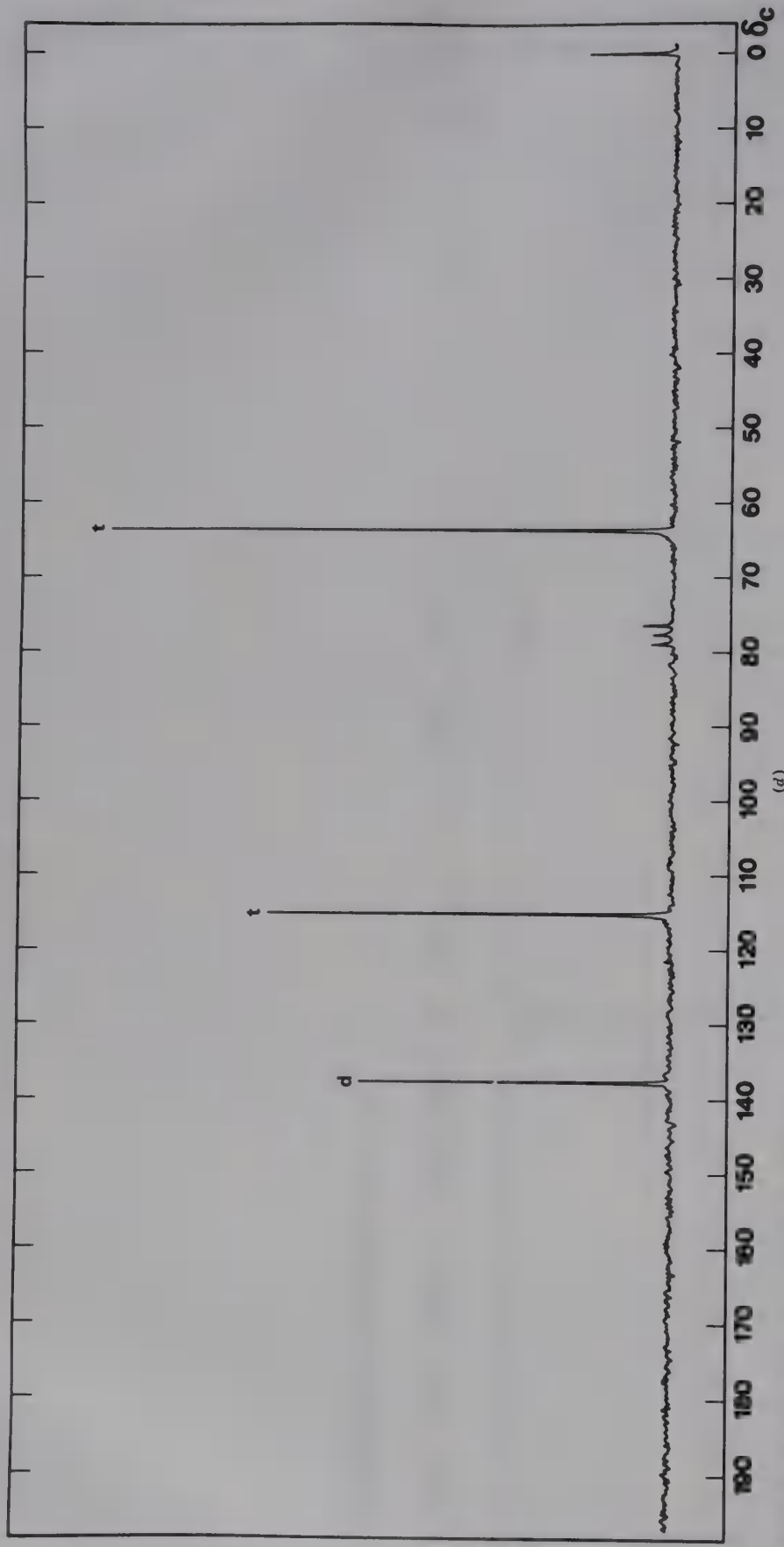

PROBLEM 5.6. COMPOUND D, C_3H_6O.

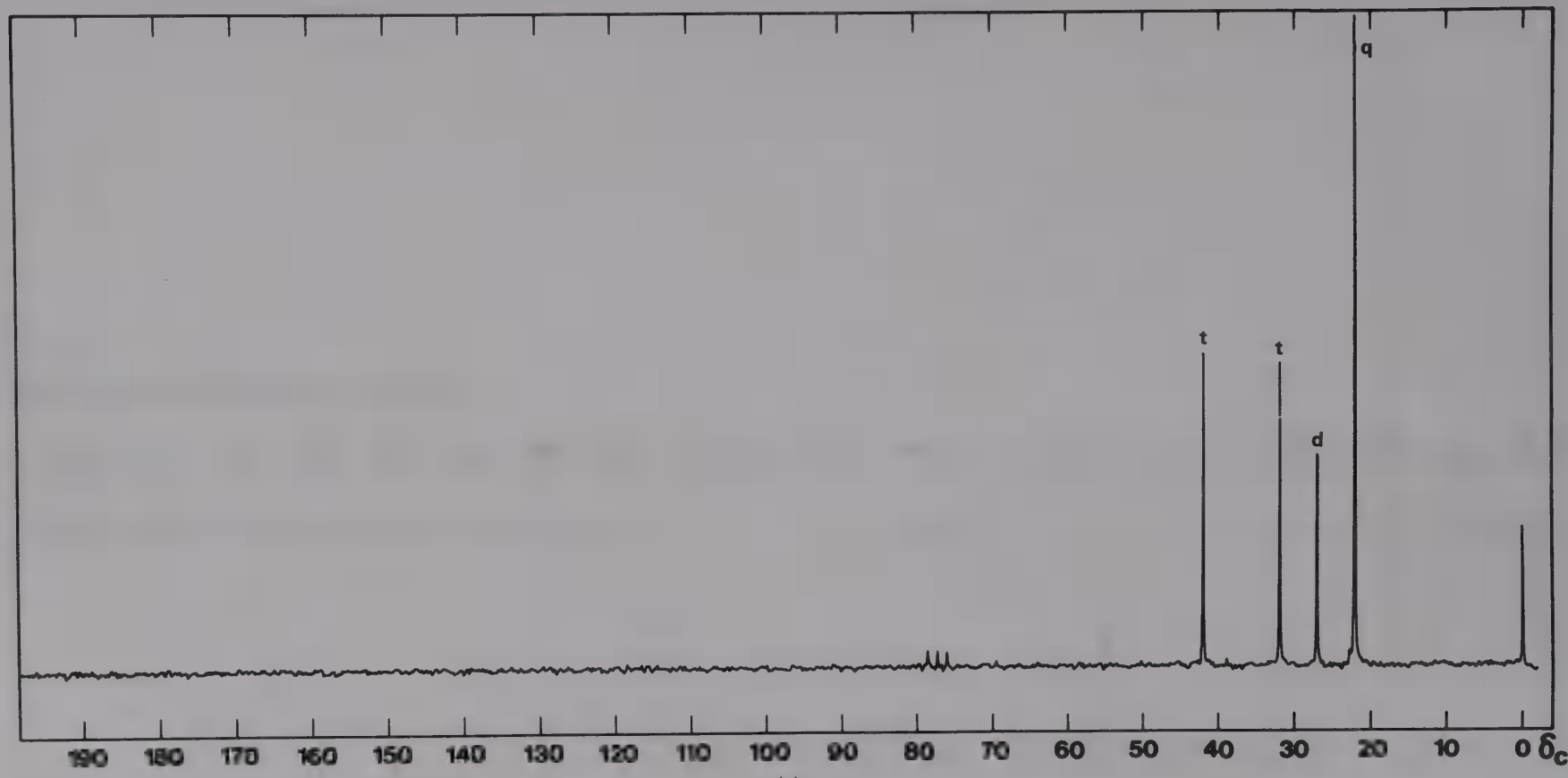

(e)

PROBLEM 5.6. COMPOUND E, $C_5H_{11}Br$.

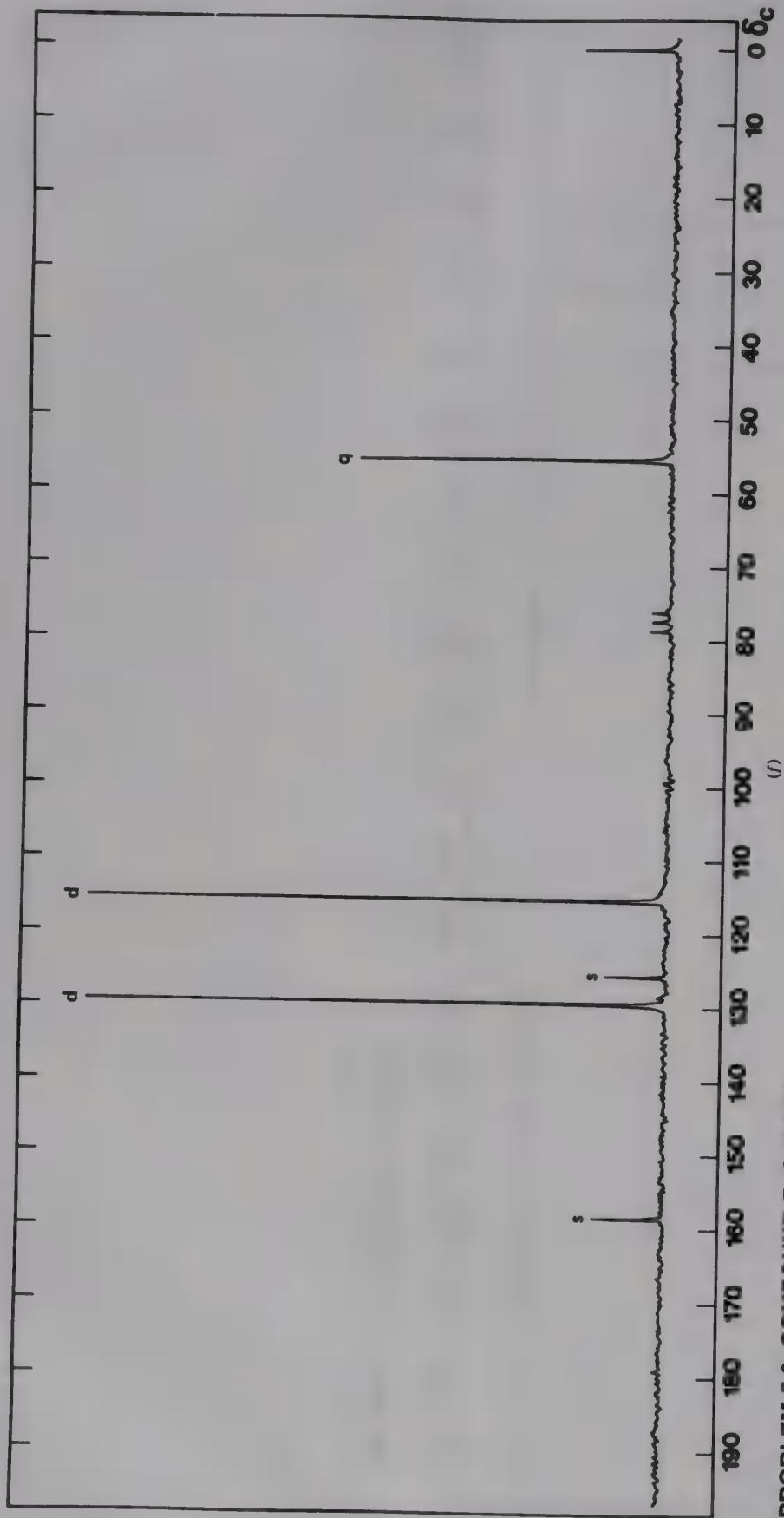

PROBLEM 5.6. COMPOUND F, C_7H_7ClO.

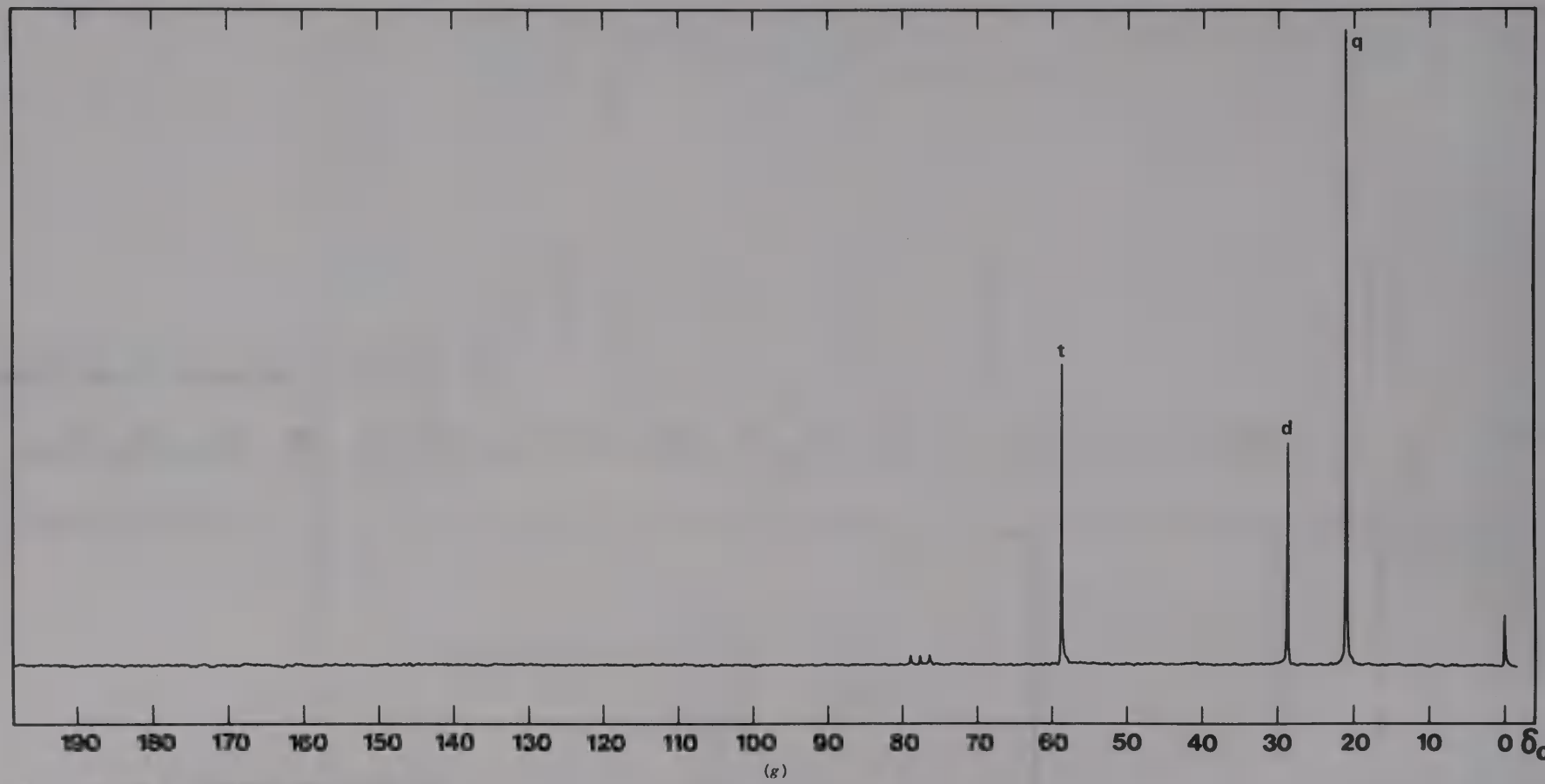

(g)

PROBLEM 5.6. COMPOUND G, $C_8H_{19}N$.

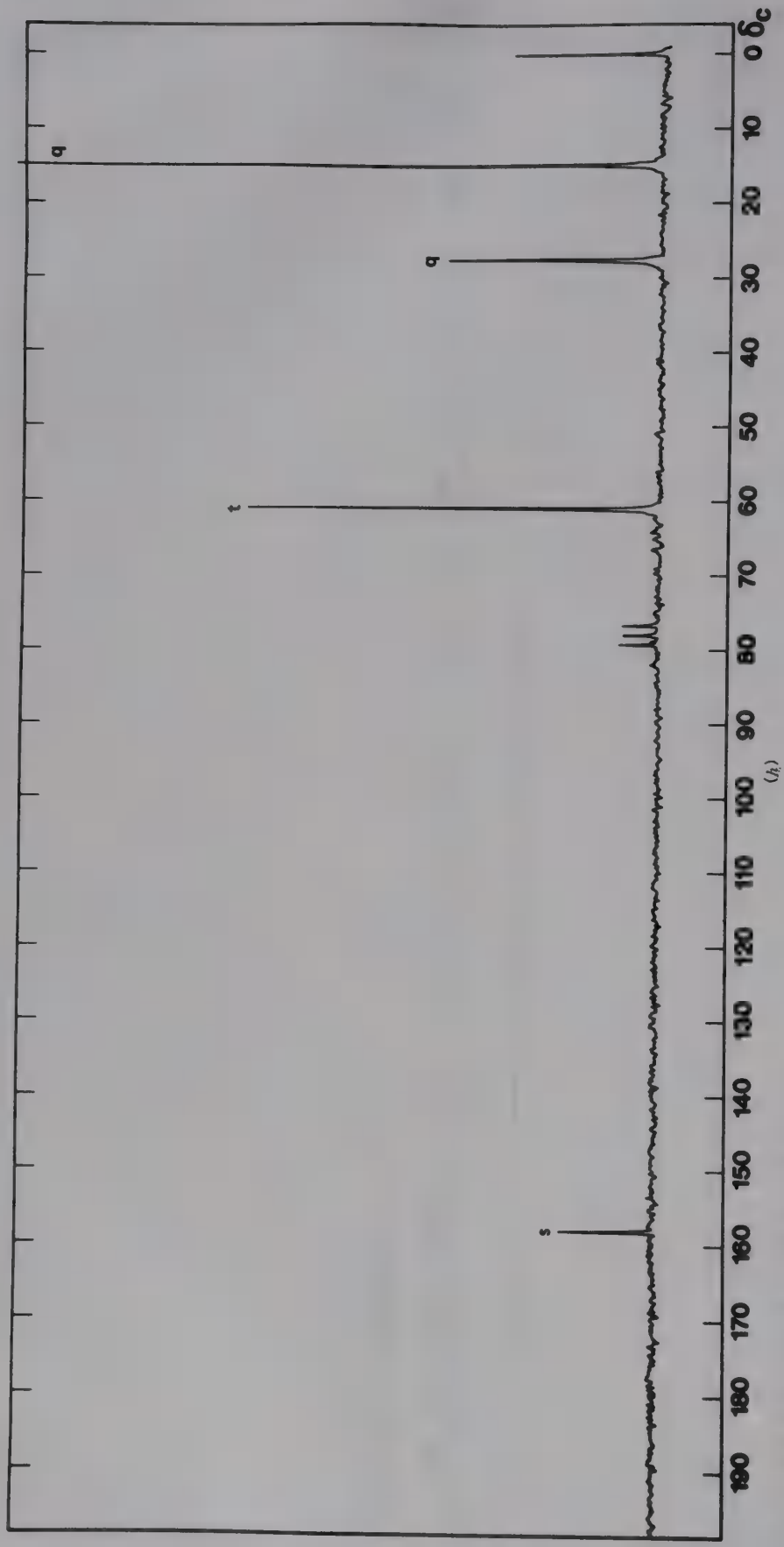

PROBLEM 5.6. COMPOUND H, $C_4H_9NO_2$.

Appendix A The ^{13}C Chemical Shifts, Couplings, and Multiplicities of Common NMR Solvents

Structure	Name	δ(ppm)	J_{C-D} (Hz)	Multiplicity[a]
$CDCl_3$	Chloroform-d_1	77.0	32	Triplet
CD_3OD	Methanol-d_4	49.0	21.5	Septet
CD_3SOCD_3	DMSO-d_6	39.7	21	Septet
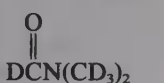	DMF-d_7	30.1	21	Septet
		35.2	21	Septet
		167.7	30	Triplet
C_6D_6	Benzene-d_6	128.0	24	Triplet
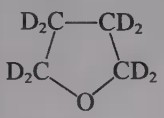	THF-d_8	25.2	20.5	Quintet
		67.4	22	Quintet
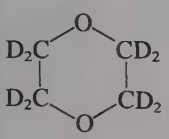	Dioxane-d_8	66.5	22	Quintet
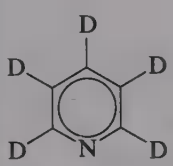	Pyridine-d_5	123.5(C-3,5)	25	Triplet
		135.5(C-4)	24.5	Triplet
		149.2(C-2,6)	27.5	Triplet
		29.8 (methyl)	20	Septet
CD_3CCD_3	Acetone-d_6	206.5(carbonyl)	<1	Septet[b]
CD_3CN	Acetonitrile-d	1.3(methyl)	32	Septet
		118.2(CN)	<1	Septet[b]
CD_3NO_2	Nitromethane-d_3	60.5	23.5	Septet
CD_3CD_2OD	Ethanol-d_6	15.8(C-2)	19.5	Septet
		55.4(C-1)	22	Quintet
$(CD_3CD_2)_2O$	Ether-d_{10}	13.4(C-2)	19	Septet
		64.3(C-1)	21	Quintet
$[(CD_3)_2N]_3P{=}O$	HMPA-d_{18}	35.8	21	Septet
CD_3CO_2D	Acetic acid-d_4	20.0(C-2)	20	Septet
		178.4(C-1)	<1	Septet[b]
CD_2Cl_2	Dichloromethane-d_2 (Methylene chloride-d_2)	53.1	29	Quintet

[a]Triplet intensities = 1:1:1, quintet = 1:2:3:2:1, septet = 1:3:6:7:6:3:1.

[b]Unresolved, long-range coupling.

Source: E. Breitmaier and W. Voelter, "*Carbon-13 NMR Spectroscopy*", 3rd ed., VCH, NY, 1987, p. 109; with permission. Also Merck & Co., Inc.

Appendix B Comparison of ^{1}H and ^{13}C Chemical Shifts

From Application of Fourier Transform NMR to Carbon-13, Varian Associates Lecture Booklet, 1974. Reprinted with permission of Varian Associates, Palo Alto, California.

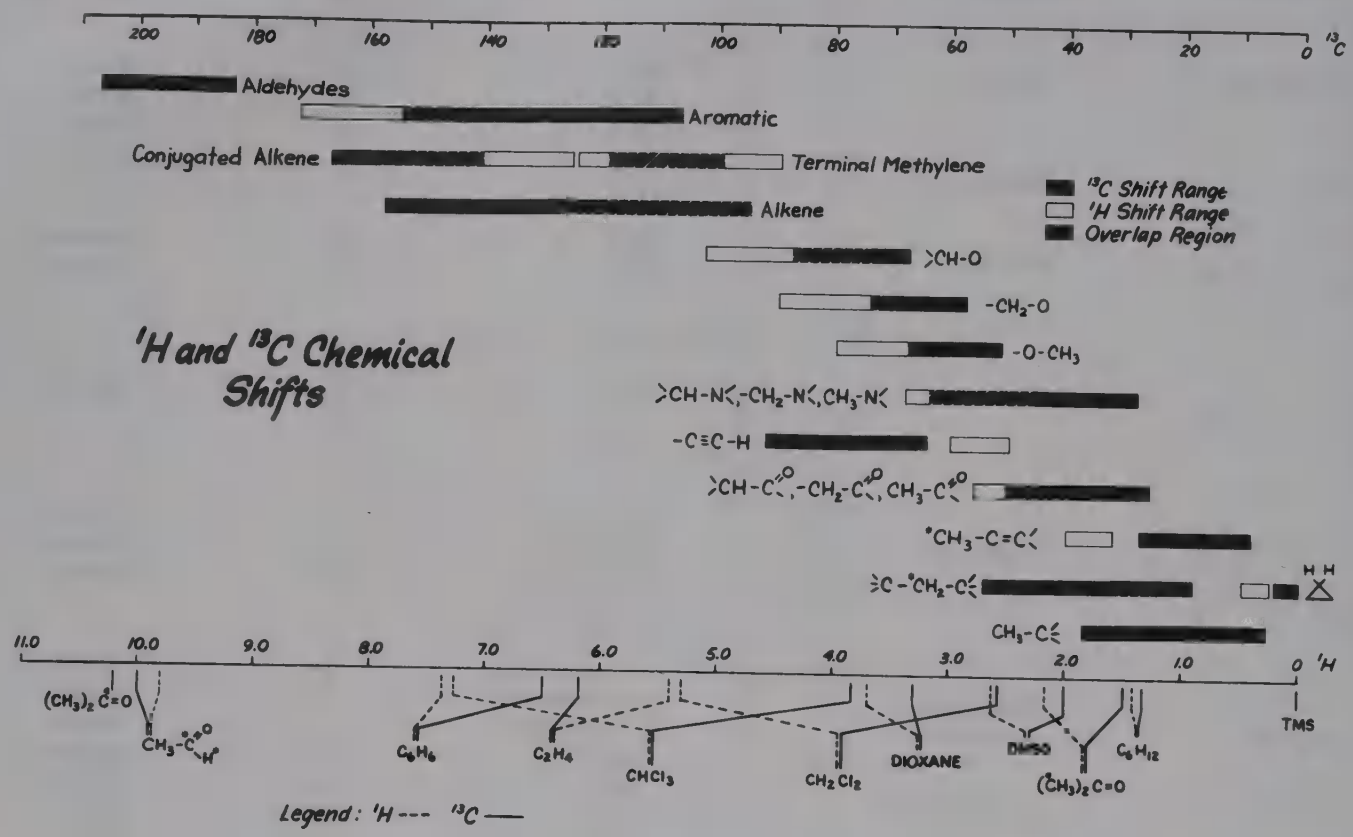

Appendix C The ^{13}C Correlation Chart for Chemical Classes

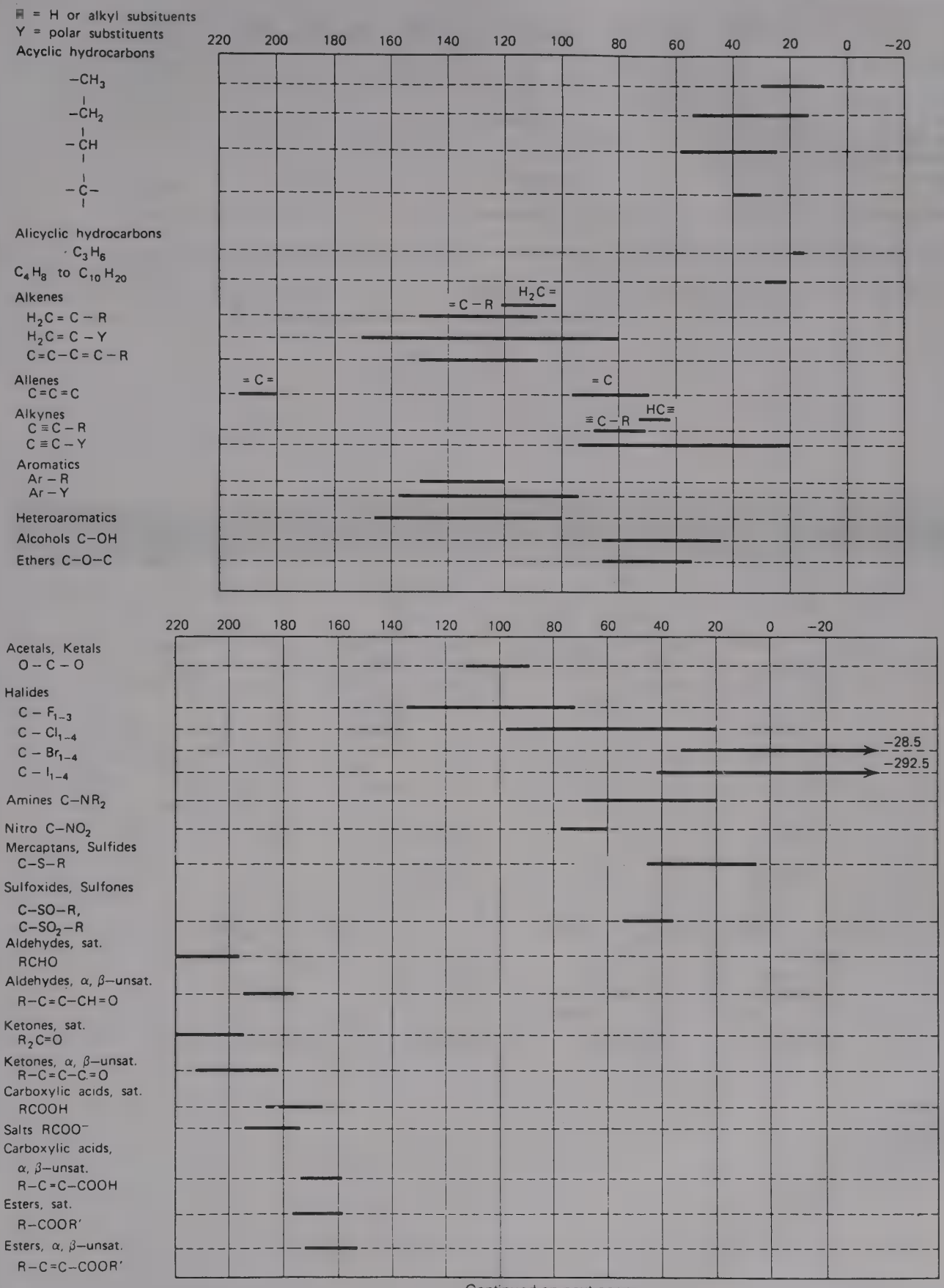

Continued on next page

Appendix C (continued)

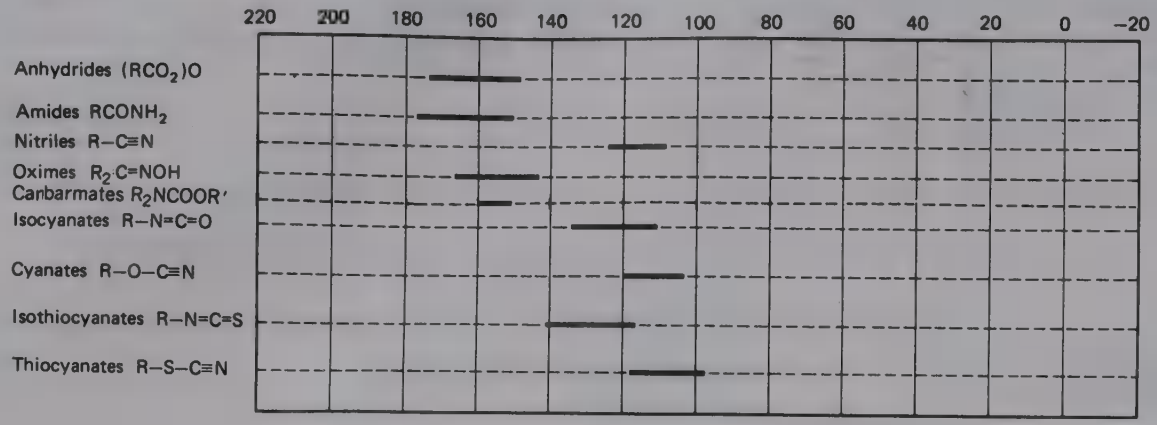

Appendix D ^{13}C NMR Data for Several Natural Products (δ)

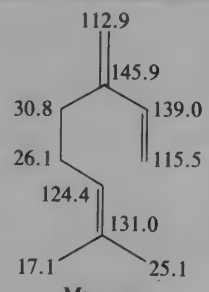

Myrcene

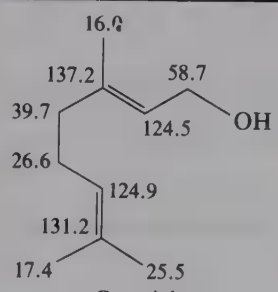

Geraniol

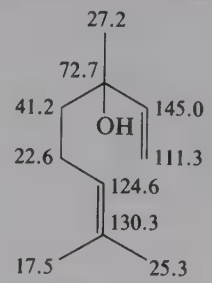

Linalool

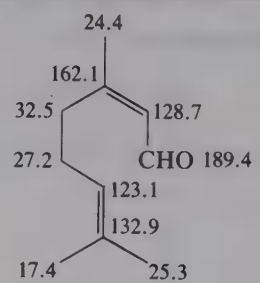

cis-Citral
(Neral, Citral b)

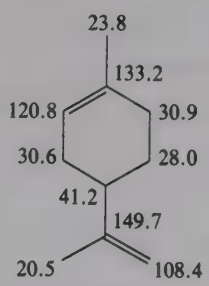

Limonene

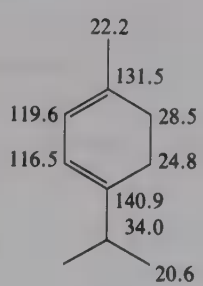

α-Terpinene

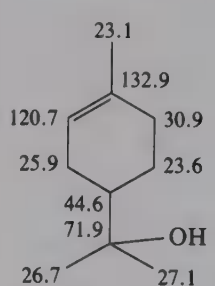

α-Terpineol

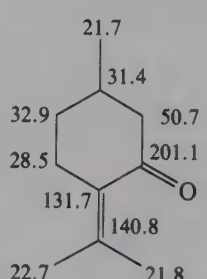

Pulegone

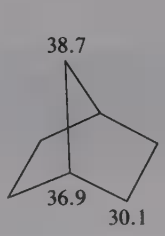

Norbornane

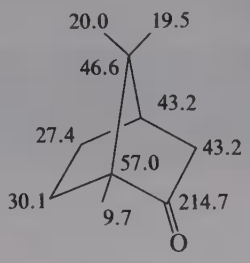

Camphor

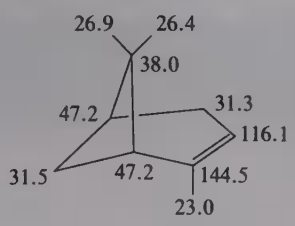

α-Pinene

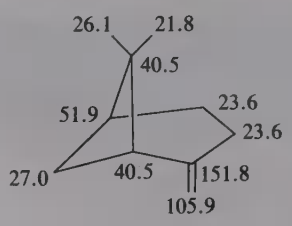

β-Pinene

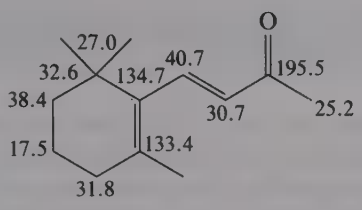

β-Ionone

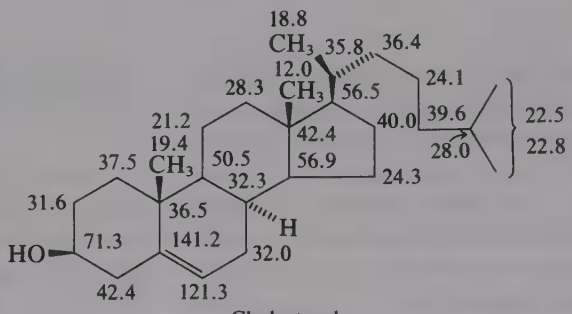

Cholesterol

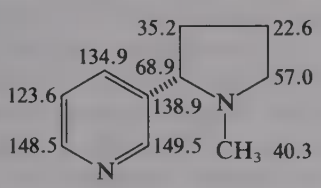

Nicotine

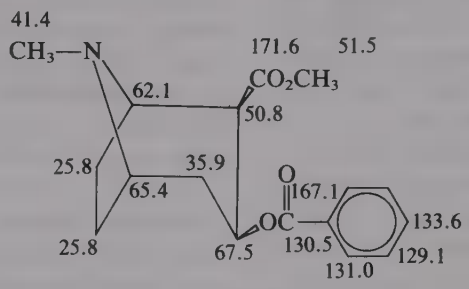

Cocaine

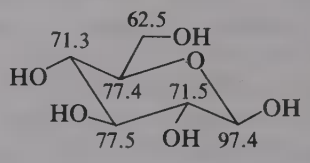

β-D-Glucose

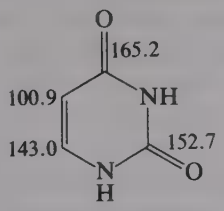

Uracil

CHAPTER SIX

NEW DIMENSIONS IN NMR*

6.1. INTRODUCTION

During the past decade with the remarkable developments in NMR magnets (up to 600 MHz), electronics, and software, a wealth of information for structure determination has become available. Although not every molecule yields a first-order ^1H spectrum, even at 600 MHz, structures of very complex molecules have been elucidated. The amount and kind of information needed depends, of course, on the complexity of the particular molecule, and development of an appropriate strategy comes only with practice. The advent of computer-controlled pulse sequences has resulted in a profusion of ingenious procedures and imaginative acronyms. Pulses of various widths and time intervals introduced between the initial magnetization pulse and the onset of signal acquisition result in either one-dimensional (1-D) or two-dimensional (2-D) spectra. References at the end of this chapter present detailed descriptions of these pulse sequences and, equally important, glossaries for the acronyms.

Obviously the conventional, so-called 1-D NMR spectrum is really 2-D in terms of Cartesian coordinates, the second dimension in the plane of the paper being the peak intensity. That the so-called 2-D spectrum really represents a three-dimensional (3-D) spectrum may not be quite so obvious because the usual presentation is a contour slice through "stacked peaks," that is peaks representing intensities perpendicular to the plane of the page (see Fig. 6.3). However, the 2-D designation in NMR does not refer to Cartesian coordinates but rather to the number of Fourier transformations resulting in the final spectrum; in other words to the number of frequency axes. Treatment of the pulse sequences used in this chapter is beyond the scope of this text, but we furnish a brief introduction to 2-D NMR.

Chapters 4 and 5 deal with experiments that involve an equilibration period (preparation) and a single pulse immediately followed by signal acquisition and Fourier transformation of the FID. We now consider multiple pulse sequences in which the preparation period is followed by two or more pulses with intervening time intervals, the final pulse being the acquisition pulse. Thus, we have inserted an "evolution" period between preparation and acquisition. In the simplest case, we have preparation, pulse, interval (t_1), 90° ($\pi/2$) acquisition pulse, acquisition (t_2), and Fourier transformation of t_1 and t_2; t_1 is the evolution period. In the following 2-D experiment, the first pulse is also a $\pi/2$ pulse. This experiment is repeated a number of times with an increasing t_1 interval. The evolution during t_1 for a noncoupled proton, such as $CHCl_3$, is shown in a rotating frame in Figure 6.1; we ignore spin–lattice relaxation but include transverse relaxation with time constant T_2^* (Section 4.1). The standard $\pi/2$ pulse along the x axis $(\pi/2)_x$ rotates the magnetization $\mathbf{M}_0$ onto the y axis to $\mathbf{M}$. At frequency ν, which is at higher frequency than that of the rotating frame, $\mathbf{M}$ precesses in the xy plane during time interval t_1 through the angle $2\pi\nu t_1$. The y component of $\mathbf{M}$ is $\mathbf{M}\cos 2\pi\nu t_1$, and the x component is $\mathbf{M}\sin 2\pi\nu t_1$. The second pulse $(\pi/2)_x$ rotates the y component downward along the z axis (it therefore contributes no signal) but leaves the x component in the xy plane. The signal acquired from the x component at each successive t_1 interval, when Fourier transformed, gives a peak with frequency ν_2 and amplitude $\mathbf{M}\sin 2\pi\nu t_1$; the signal amplitudes of the series of peaks vary sinusoidally with t_1. A stacked column of this series of peaks (Fig. 6.2*a*) shows the sinusoidal change in amplitude as a function of t_1—a time-domain spectrum. This spectrum is transposed into Figure 6.2*b* (simply by replotting the tops of the peaks as a function of t_1), which now resembles another FID, showing transverse relaxation with time constant T_2^* (Section 4.1). In other words, we have taken a slice parallel to the t_1 axis of Figure 6.2*a* through the tops of the peaks to form Figure 6.2*b*. If we had taken, say, 1 Kb (i.e., 2^{10} or 1024)* increments of t_1, we would

*This gentle pun, suggested by Dr. R. C. Hahn, Syracuse University, was irresistible.

*kb is kilobyte.

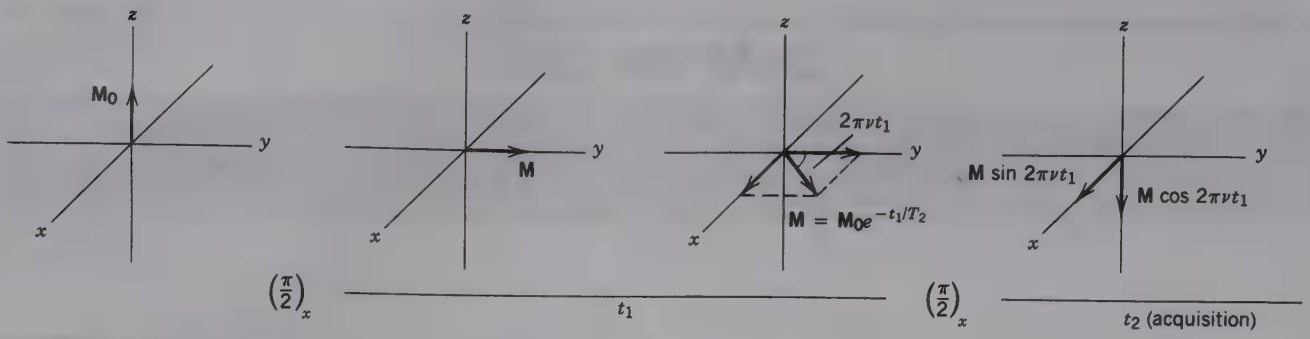

FIGURE 6.1. Evolution in a rotating frame of the $CHCl_3$ proton is shown during time interval t_1 following the first pulse. The second pulse and acquisition give a signal resulting only from the x component of **M**; this signal amplitude varies sinusoidally with t_1. Interval t_1 is of the order of microseconds and milliseconds; t_2 is of the order of seconds. The precessional frequency of the proton is higher than that of the rotating frame. From Derome (see reference section) with permission.

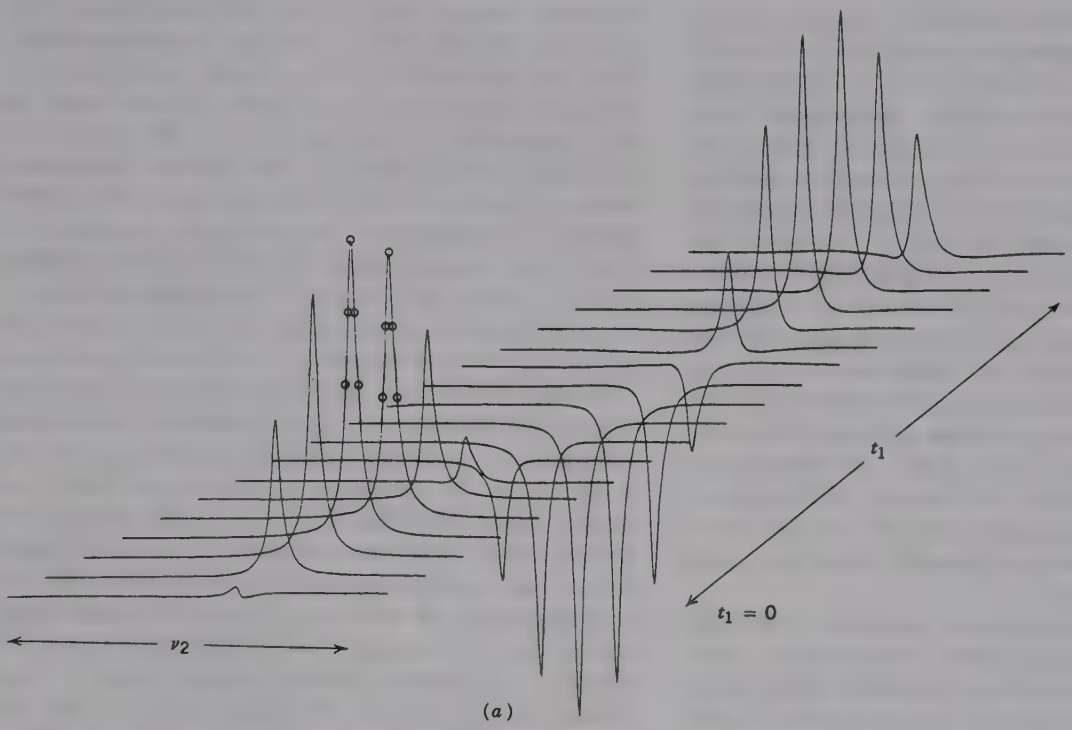

FIGURE 6.2(*a*). Oscillating amplitude of the series of acquired peaks with increasing t_1. Only the first few peaks of the series are shown. Data points are shown on two of the rows. Reprinted with permission from A. E. Derome, *Modern NMR Techniques*, Copyright © 1987, Pergamon Press PLC.

have acquired 1024 rows of FID's, which would give 1024 rows of peaks of different amplitudes, which we have stacked into a column to form Figure 6.2*a* (only the first few peaks are shown). Each peak consists of 1024 data points (for a square matrix), and we have transposed only one point of each peak of the stacked column—the top point—to form Figure 6.2*b*. By repeating the transposition for each column of points, we generate a total of 1024 "FID's." The amplitudes of the "FID's" increase to a maximum at the slice through the peak tops, then decrease. Fourier transformation of these "FID's" produces a transform of a transform—that is, a 2-D FT with two frequency axes ν_1 and ν_2 (Fig. 6.3). The amplitudes of the stacked peaks, each of frequency ν_1, increase to a maximum, then decrease. The maximum amplitude of the stacked peaks is on one of the diagonals of the square plot since ν_1 and ν_2 are identical, this being a 2-D spectrum of the single proton of $CHCl_3$; the proton experiences the same evolution in both t_1 and t_2. The more useful and common contour plot is also shown in Figure 6.3.

This example, though trivial, nonetheless is a pro-

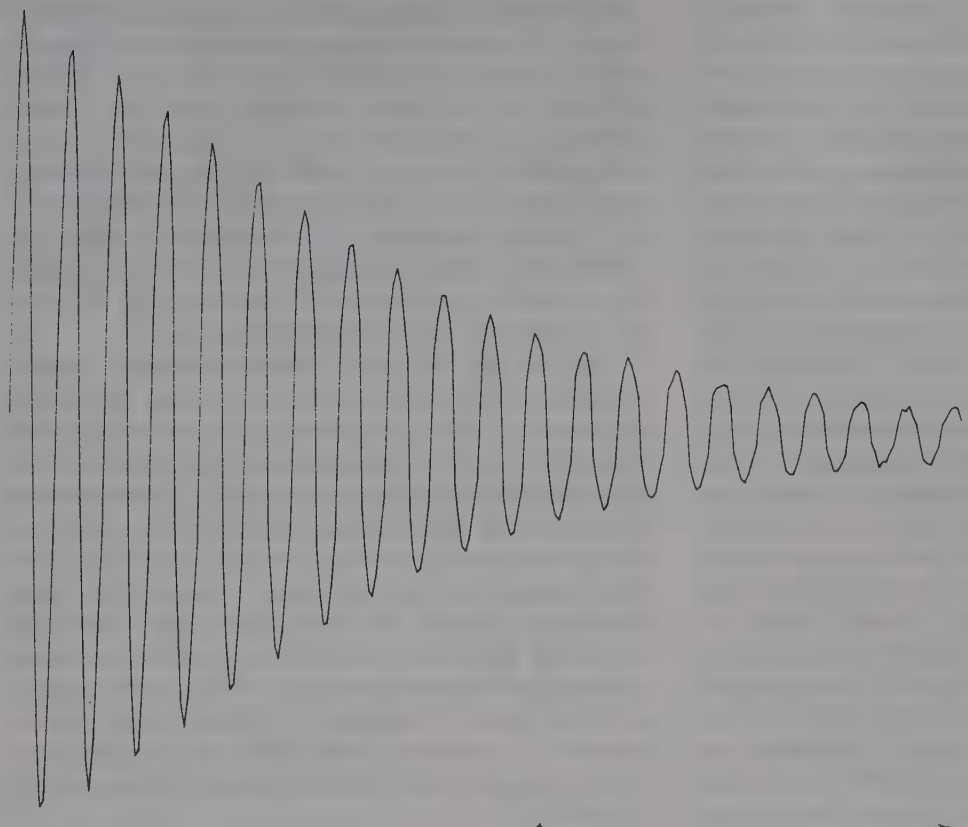

FIGURE 6.2(*b*). Transpositon of Figure 6.2*a*. Slice parallel with t_1 through the tops of peaks in Figure 6.2*a*. Reprinted with permission from A. E. Derome, *Modern NMR Techniques,* Copyright © 1987, Pergamon Press PLC.

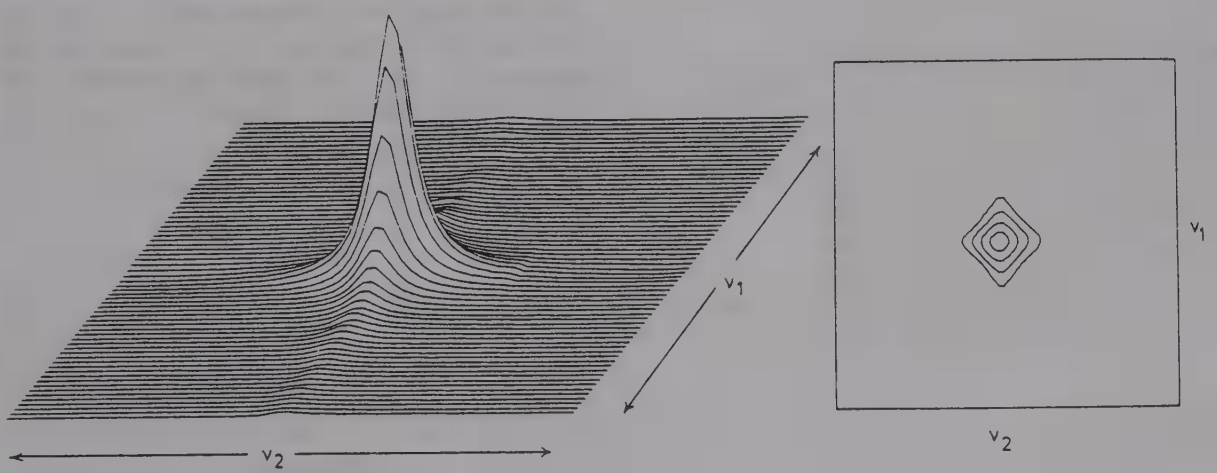

FIGURE 6.3. Fourier transform of a series of FID's like the one in Figure 6.2*b* to give the frequency-domain spectrum as both a peak and a contour. Reprinted with permission from A. E. Derome, *Modern NMR Techniques,* Copyright © 1987, Pergamon Press, PLC.

totype of the very useful COSY spectrum (Fig. 6.8), in which the proton spectrum appears along the diagonal. More accurately, those components of the spin system that remain unperturbed by coupling even in a spin-coupled system appear on the diagonal; ν_1 and ν_2 are identical for each of those components. Consider the same pulse sequence applied to an isolated spin system of two coupled protons: X—CH=CH—Y. In this coupled system, the unperturbed components appear on the diagonal, but some ν_2 frequencies differ from the ν_1 frequencies since ν_2 contains not only the chemical shift frequencies but also the coupling frequencies that evolved during the t_1 period. The contours plotted from these unequal frequencies (i.e., $\nu_2 \neq \nu_1$) are off-diagonal and are termed crosspeaks. These crosspeaks are symmetrically disposed in pairs about the diagonal and indicate which protons are coupled to which, as shown by the dotted lines drawn vertically and horizontally from either one of the paired crosspeaks to the diagonal (Fig. 6.4). Again, a trivial experiment but providing a basis for obvious extrapolation to the COSY spectrum (Fig. 6.8), which was obtained by refinement of the same pulse sequence. The ν_2 axis (also designated F_2) always represents the chemical shift of the observed (acquired) nucleus. The ν_1 axis (F_1) gives information that depends on the pulse sequence and the evolution time. For example, in the HET2DJ spectrum (Fig. 6.13), the F_2 axis gives the chemical shift of the observed ^{13}C atom, and the F_1 axis gives the coupling constant (in hertz) for ^{13}C—^{1}H couplings.

The COSY spectrum gives us, indirectly, all-important information on carbon–carbon connectivities. That is, we can trace the carbon skeleton of the spin system through the ^{1}H—^{1}H couplings; the assumption is that appreciable coupling between protons extends over only two or three bonds—geminal or vicinal—except in cases of electron delocalization. Derome, Bovey, and Sanders and Hunter give more detailed explanations of pulse sequences and their consequences (see reference section).* The general principles outlined here apply to all 2-D spectra: What happens—that is, what modulations occur—during time t_1 is detected (acquired) as a function of t_2. When rereading this highly condensed introduction, remember the somewhat confusing point that the *first* FT gives ν_2, and the *second* transformation gives ν_1.

To sum up the more difficult concepts: Fourier transformation of the FID's gives a series of peaks of frequency ν_2, whose amplitudes vary *sinusoidally* with t_1 as can be seen by looking down the columns of data points in Figure 6.2*a*. Each column of data points is transposed by taking a slice through each column of data points parallel to the t_1 axis of Figure 6.2*a*. The slice through the data points at the tops of the peaks is shown in Figure 6.2*b*, which shows more clearly the sinusoidal variation in amplitudes. In effect, we have created another series of FID's, which on FT gives a series of peaks of frequency ν_1, whose amplitudes increase to a maximum, then decrease. The maximum is on a diagonal of the square plot with axes ν_1 and ν_2 (Fig. 6.3).

We describe the most useful of currently available procedures, classified by the information yielded as follows:

- A first-order (or nearly) integrated ^{1}H spectrum.
- A ^{13}C spectrum.
- ^{1}H—^{1}H connectivity (coupling).
- ^{1}H—^{13}C connectivity (coupling).
- ^{13}C—^{13}C connectivity (coupling).
- Through-space ^{1}H ^{1}H proximity.

To demonstrate and compare the ^{1}H—^{1}H, the ^{1}H—^{13}C, the ^{13}C—^{13}C connectivity procedures, and the through-space ^{1}H ^{1}H proximity data, we use a single, rather simple molecule geraniol.

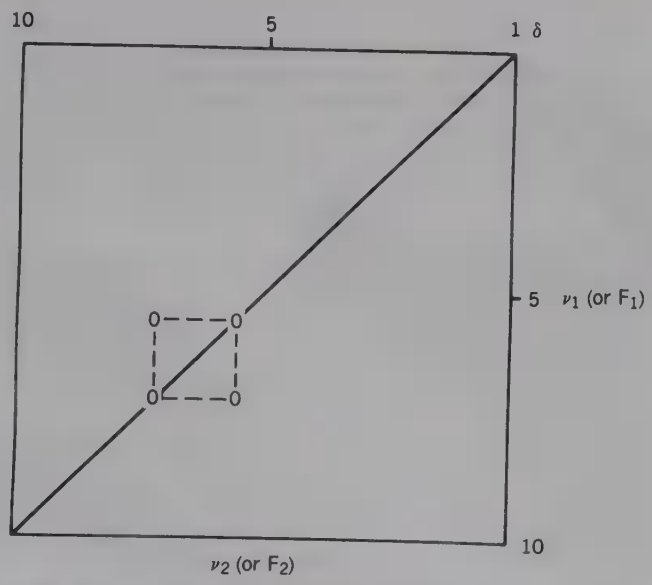

FIGURE 6.4. The COSY spectrum of X—CH=CH—Y.

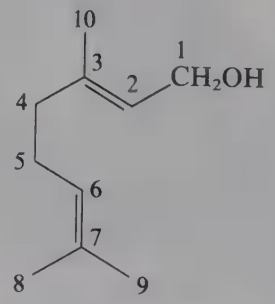

Geraniol

*For a very readable treatment of FT applied to 2-D NMR, see Williams, K. R. and King, R. W., *J. Chem. Educ.*, **67**, A125 (1990). See References therein for previous papers.

For the through-space ^1H ^1H proximity data, we compare geraniol with its (*Z*) isomer, nerol.

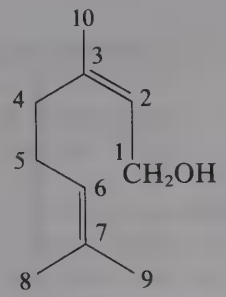

Nerol

Figure 6.5 shows the integrated 500-MHz ^1H spectrum of geraniol. Figure 6.6 shows the broadband decoupled ^{13}C spectrum of geraniol on the same instrument, 127.5 MHz for ^{13}C.

From left to right the integration of the ^1H spectrum shows 1,1,2,5,6,3 protons for a total of 18 protons. The ^{13}C spectrum shows 10 ^{13}C atoms if we assume that each peak represents a single ^{13}C; two of the low-field peaks almost coincide but can readily be separated by expanding the spectrum (see inset). Geraniol is a $C_{10}H_{18}O$ monoterpene, and the concentration-dependent OH singlet is buried under the five-proton absorption at this concentration. Obviously the two low-field absorptions in Figure 6.5 represent the alkene protons, the nine high-field protons comprise three methyl groups (each attached to an alkene carbon), the two-proton doublet represents the H-1 protons, and four protons under the five-proton multiplet represent the two meth-

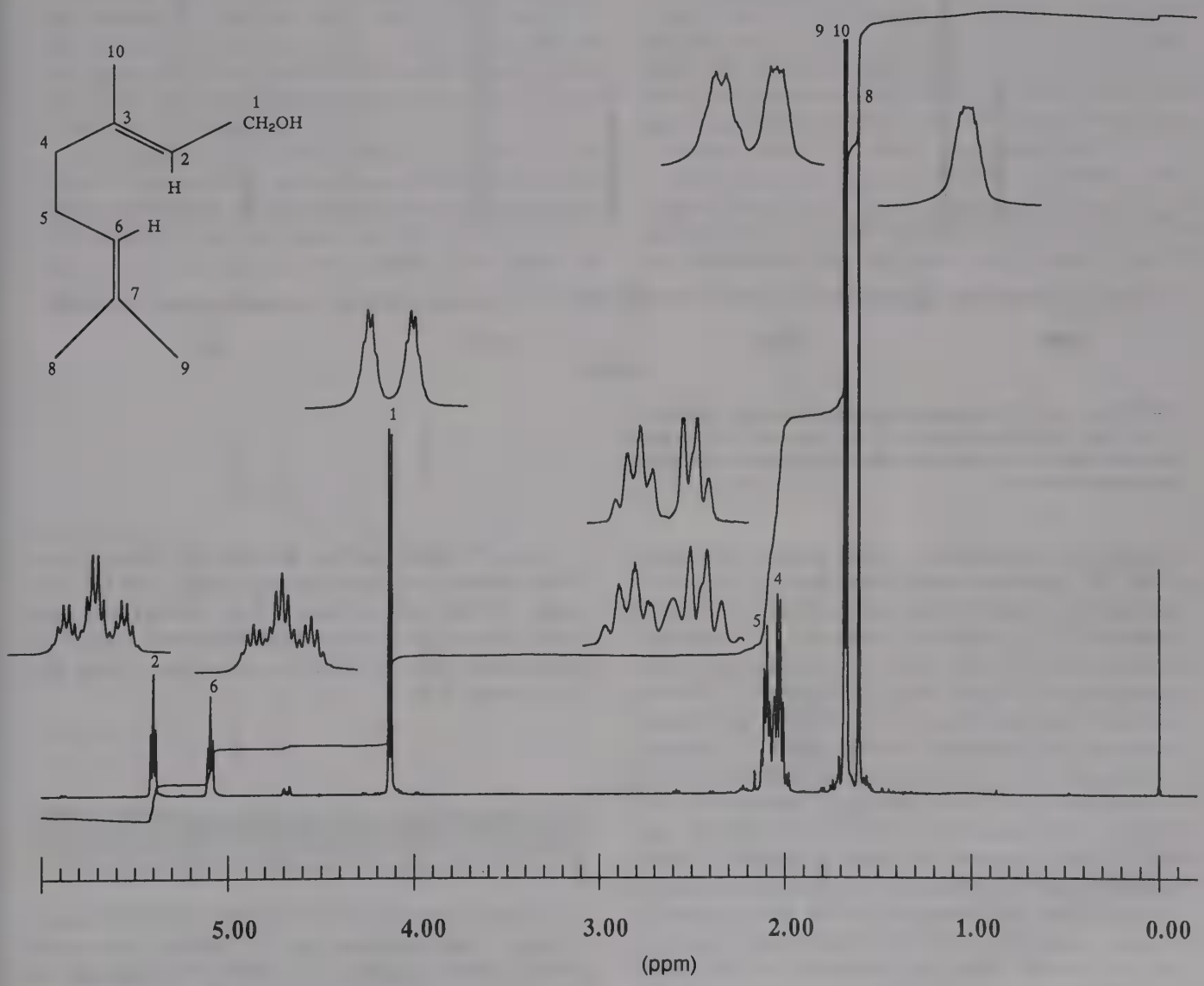

FIGURE 6.5. The ^1H Spectrum of geraniol in $CDCl_3$ at 500 MHz with expanded insets. Lower inset for H-5 and H-4 contains OH peak; upper inset is from a sample in which the OH peak is at higher field.

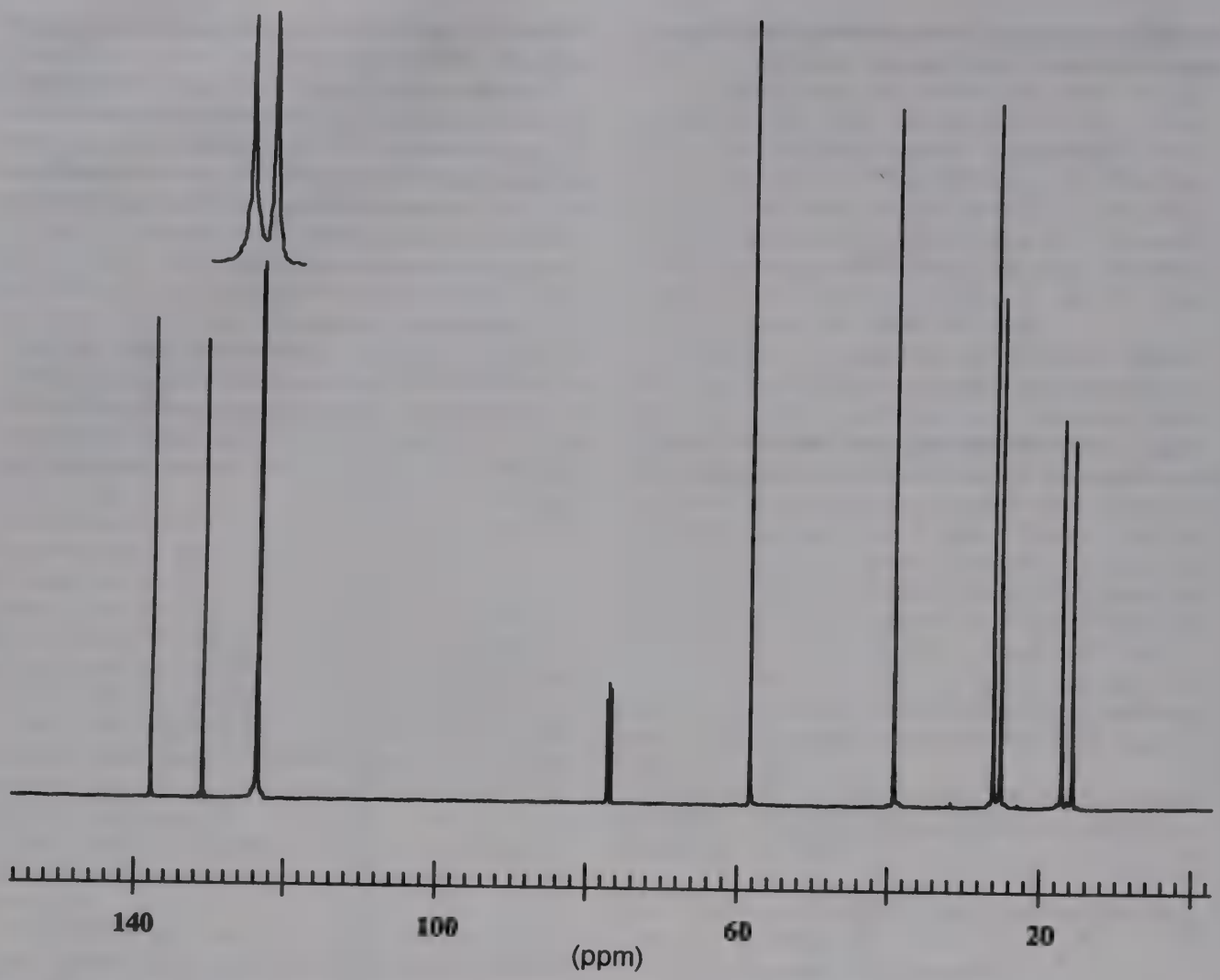

FIGURE 6.6. The ^{13}C broadband-decoupled spectrum of geraniol in $CDCl_3$, using a 500-MHz instrument (125.7 MHz for ^{13}C). The inset is an expansion of two peaks that are almost superimposed in the unexpanded spectrum.

ylene groups at positions 4 and 5. Specific decoupling of the ^1H spectrum would give most of the proton connectivities, but these are more effectively obtained from the COSY spectrum (Section 6.2.3). Further assignments can be made from the fine structure of the expanded peaks in the insets of Figure 6.5. The expanded five-proton inset is still difficult to interpret because of the presence of the OH proton; its removal from the pattern by dilution (inset immediately above) clearly shows a distorted quartet on the low-field side for H-5, and a distorted triplet on the high-field side for H-4. The expanded H-2 inset consists of a triplet (coupled with H-1) of sextets (long-range coupling to H-10 and H-4), and the expanded H-6 inset consists of a triplet (coupled to H-5) of septets (long-range coupling to H-8 and H-9). Assignment of each of the H-8, H-9, and H-10 methyl groups is not possible at this point.

In the ^{13}C spectrum (Fig. 6.6), the four peaks at low field represent the alkene carbon atoms, and the five peaks at high field represent three methyl and two methylene groups, but definite assignments cannot be made on the basis of chemical shifts alone except for C-1 at about δ 58.5.

6.2. ^1H—^1H CONNECTIVITY

Of course, protons are not literally connected as are protons to carbon atoms, or C—C atoms, but we use proton–proton coupling to elucidate the connectivity of the carbon atoms to which the protons are attached. The process is thus an indirect route to working out

the carbon skeleton, and we use the term ^1H—^1H connectivity as a shorthand notation.

6.2.1. Spin Decoupling (1-D)

Spin decoupling to elucidate ^1H—^1H connectivities of protons, discussed in Section 4.13, is still a very useful technique and does not require sophisticated pulse sequences. Its limitations, however, are the need to sequentially decouple individual protons, the need to select the optional decoupling power and frequency, and the difficulty in decoupling strongly coupled protons from one another. Furthermore, if the signal of the observed proton overlaps other signals, the result of decoupling is sometimes not readily apparent. The technique of *difference decoupling* allows direct observation of the decoupled, buried proton signal by subtracting the original undecoupled spectrum from the decoupled spectrum, thus canceling out the unaffected signals. The undecoupled spectrum should be run under the same conditions as the decoupled spectrum but with the decoupler centered in a blank region (Sanders and Hunter, pp. 54–57).

Coupling resulting from the irradiated proton can be cleanly removed with no serious complications, given weak coupling, if the decoupler power and frequency are optimal. The decoupled proton absorption collapses to a singlet or to the multiplicity imposed by other coupled protons. Under less than ideal conditions, distortions occur, but these can be tolerated since merely a definite change in multiplicity is usually sufficient evidence for connectivity. The COSY procedure gives connectivity information without specifically decoupling (Section 6.2.3), and is thus more useful for strongly coupled protons.

6.2.2. Homo *J*-Resolved ^1H—^1H Spectroscopy (HOM2DJ) (2-D)

Overlapping absorptions in a standard 1-D ^1H spectra can sometimes be resolved by presenting chemical shifts on one axis and peak multiplicities (J coupling) on the other axis; the result is a 2-D homo J-resolved spectrum (HOM2DJ) (Fig. 6.3). This display is most useful when the overlapping multiplicities are not coupled to each other or are weakly coupled; the usual complications (extra peaks) in strongly coupled spin systems apply as well to the 2-D presentation. To minimize this problem, a high-field instrument should be used. The contours of weak outer peaks of a multiplet may be missing (Problem 6.4); if this is suspected, the contours should be "sliced" at a lower level.

In practice, the requirement that couplings be first order or nearly so is quite severe, and in the case of geraniol (Fig. 6.7), the HOM2DJ spectrum gives no new information. The OH proton singlet appear at about

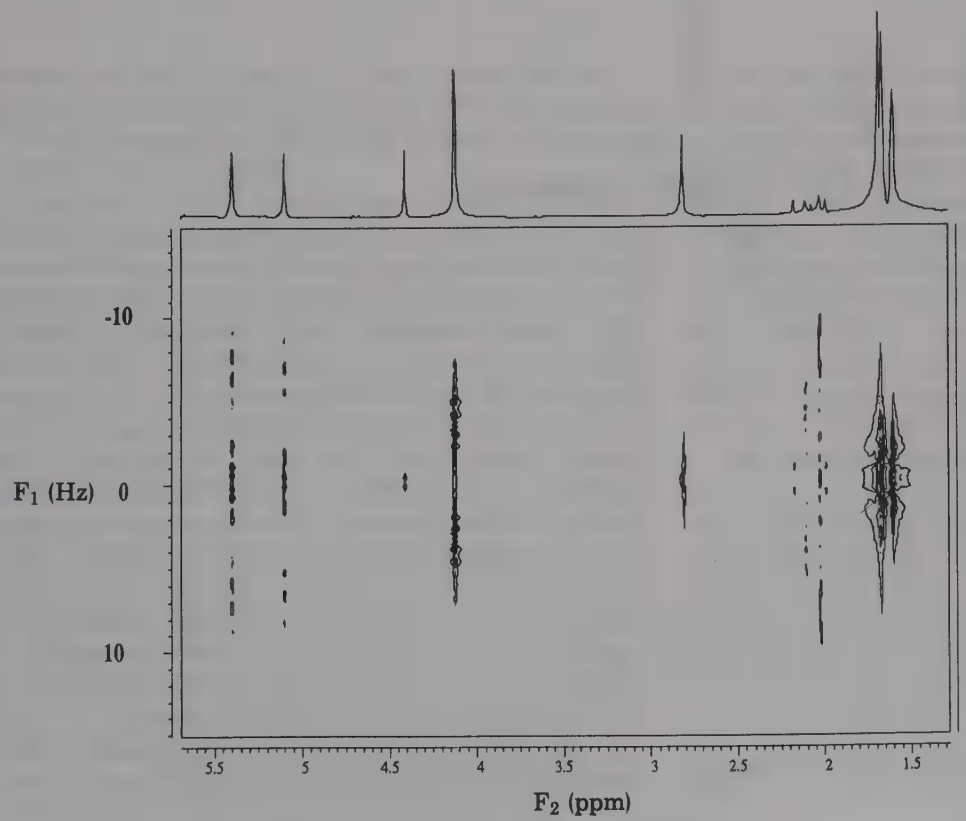

FIGURE 6.7. The HOM2DJ spectrum of geraniol in $CDCl_3$ at 500 MHz.

~δ2.82, but this downfield shift is merely a consequence of the increased concentration compared with that of the sample for the proton spectrum (Fig. 6.5). Since the $—CH_2—CH_2—$ groups (H-4 at ~δ 2.0 and H-5 at ~δ 2.1) are tightly coupled with a $\Delta\nu/J$ ratio of about 3.8, the multiplicities are not clear. Although the separation between the CH_2 vertical rows of contours is quite apparent, extra peaks are present. The HOM2DJ spectrum offers no advantages in separating CH_3 singlets. The H-1 protons give a first-order doublet, but this is much more apparent in the expanded inset of Figure 6.5. Coupling of H-2 and of H-6 with the adjacent methylene results in first-order triplets (J 6.8); long-range couplings of H-2 and of H-6 are also clearer in Figure 6.5. There is an artifact at about δ 4.4, which may be the result of a number of factors such as field inhomogeniety, or imperfect pulses.

A HOM2DJ spectrum would be more useful for a molecule such as XCH_2OCH_2Y where X and Y cause slightly different shifts of the CH_2 groups, which are not coupled to one another. Aside from this rather specialized application, HOM2DJ is mainly of historical and pedagogical interest.

6.2.3. Correlated Spectroscopy (COSY) or Homonuclear Correlated Spectroscopy (HOMCOR) (2-D)

The basic COSY procedure gives a 2-D spectrum (Fig. 6.8) from which almost all of the $^1H—^1H$ connectivities can be determined; this gives the same information obtained through the classical $^1H—^1H$ decoupling procedure without the disadvantages listed above (Section 6.2.1). The ^1H spectrum appears along the diagonal as contours representing peak intensities (Section 6.1). The off-diagonal contours are the so-called crosspeaks. A horizontal line drawn from a crosspeak will intercept a contour on the diagonal, and a vertical line from the same crosspeak will intercept another contour on the diagonal with which the first diagonal contour is "correlated," that is, coupled. Note that the crosspeaks are found symmetrically on both sides of the diagonal. For convenience, the derived ^1H spectrum may be projected along one or both axes. A line drawn perpendicular to a peak in the projected ^1H spectrum will intersect in the diagonal spectrum and indicate the appropriate contour even in an overlapping

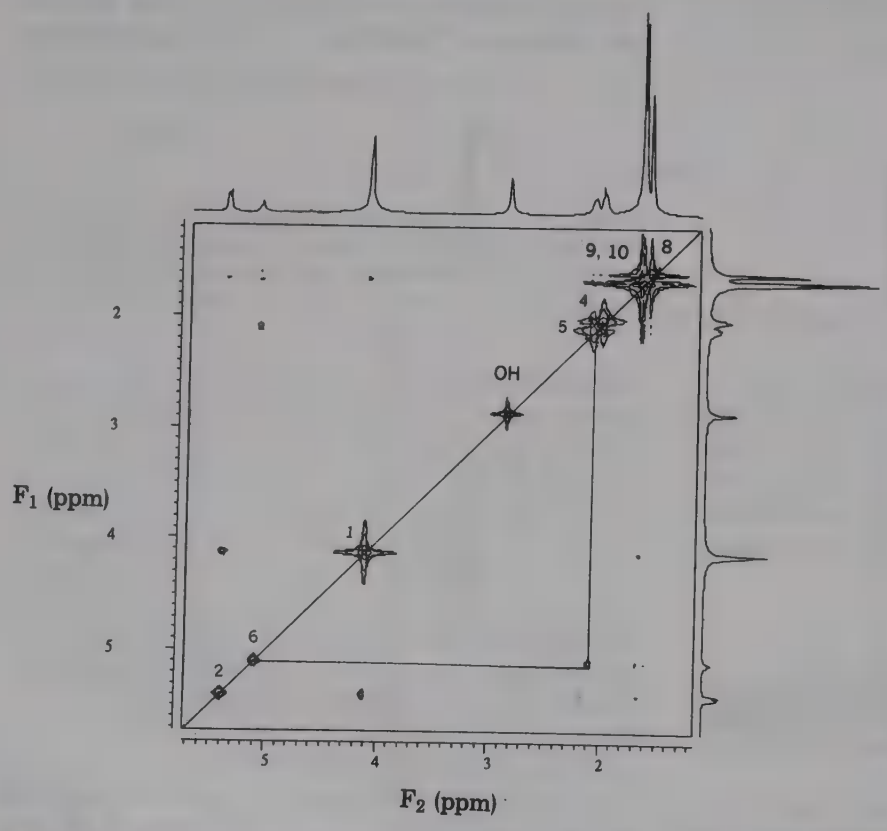

FIGURE 6.8. Basic COSY spectrum of geraniol, in $CDCl_3$ at 500 MHz. The H-5, H-6 coupling is shown.

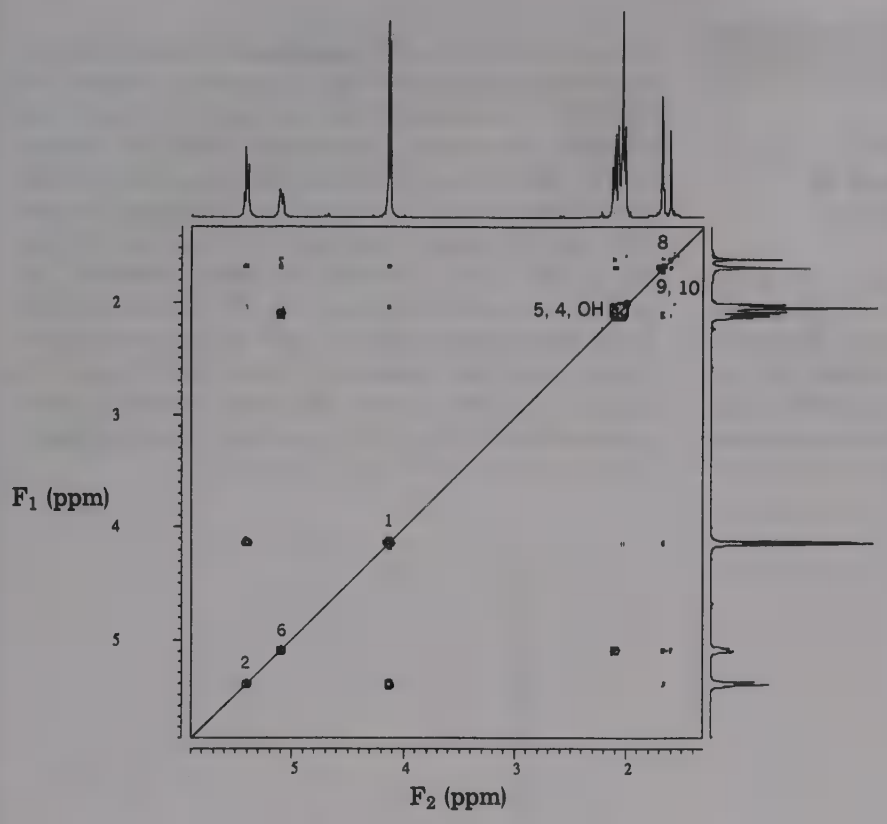

FIGURE 6.9. The DQFCOSY spectrum of geraniol, in $CDCl_3$ at 500 MHz.

region. In general, strongly coupled protons are better handled in a COSY experiment than with conventional $^1H—^1H$ decoupling. The COSY is one of the most useful of all 2-D spectra.

The basic COSY, however, often results in considerable overlap along the diagonal, and thus it is difficult to make assignments. This can be alleviated by a double quantum filtered COSY (DQFCOSY); the intense singlets of noncoupled methyl groups in particular are greatly reduced. In the upper right-hand corner of the basic COSY spectrum of geraniol (Fig. 6.8), the signals for three methyl groups are severely overlapped, as are those for the two methylene groups. In the DQFCOSY spectrum (Fig. 6.9), the H-8 and H-9 methyl proton signals are cleanly separated, and the small allylic coupling to H-6 is apparent through the off-diagonal crosspeak. Also apparent is the long-range coupling of the H-8 and H-9 methyl groups with one another. Both spectra show allylic and homoallylic coupling, but the basic COSY lacks the H-1, H-4, and the H-2–H-4 couplings that are present in the DQFCOSY. The differentiation between H-8 and H-9 is still uncertain. We show the H-5, H-6 coupling in the standard COSY, and the remaining couplings are assigned as a Problem at the end of the chapter.

Actually, the separation between H-4 and H-5 along the diagonal is better in the basic COSY spectrum than in the DQFCOSY spectrum, but this is so because the OH peak has been shifted to lower field in the basic COSY by the use of a more concentrated solution. The OH peak, of course, shows no crosspeak. The separation between H-4 and H-5 is not sufficient to show the crosspeaks for their coupling in either spectrum, but the long range coupling through four single bonds between H-8 and H-9 is visible in the DQFCOSY.

The choice of the optimum contour level in processing a COSY spectrum (or other 2-D spectra) is critical. At too high a level, critical crosspeaks may be missed; at too low a level, confusing long-range couplings—through more than three saturated bonds—may appear. When apparently irreconcilable data result from a COSY spectrum, reprocessing at higher and lower contour levels is advisable. Crosspeak artifacts resulting from crossing of tails of noncoupled protons may occasionally appear and require further processing.

6.3. ^{1}H—^{13}C CONNECTIVITY

6.3.1. Attached Proton Test (APT) (1-D), and Distortionless Enhancement by Polarization Transfer (DEPT) (1-D)

Although off-resonance decoupling has been a useful tool for showing the multiplicities* of ^{13}C peaks, its deficiencies in terms of overlap, spectrum distortion, and loss of J values are a serious problem (Section 5.2.1). The 1-D spectra APT (Fig. 6.10) and DEPT (Fig. 6.11) of geraniol give the number of ^{1}H atoms attached to each C atom in a ^{13}C spectrum without overlap or distortion problems but do not furnish J values (see HET2DJ, Section 6.3.2) or show which ^{1}H atoms are attached to which ^{13}C atoms (see HETCOR, Section 6.3.3). The APT is the simpler procedure, but it is less sensitive than DEPT and does not distinguish between CH_3 and CH peaks (both down) or between CH_2 and quaternary C peaks (both up); often, however, this partial information suffices. The APT spectrum of geraniol differentiates between the CH and quaternary C alkene atoms and between the high-field CH_2 and CH_3 groups. Thus for geraniol, the more specific information furnished by the DEPT spectrum is not necessary.

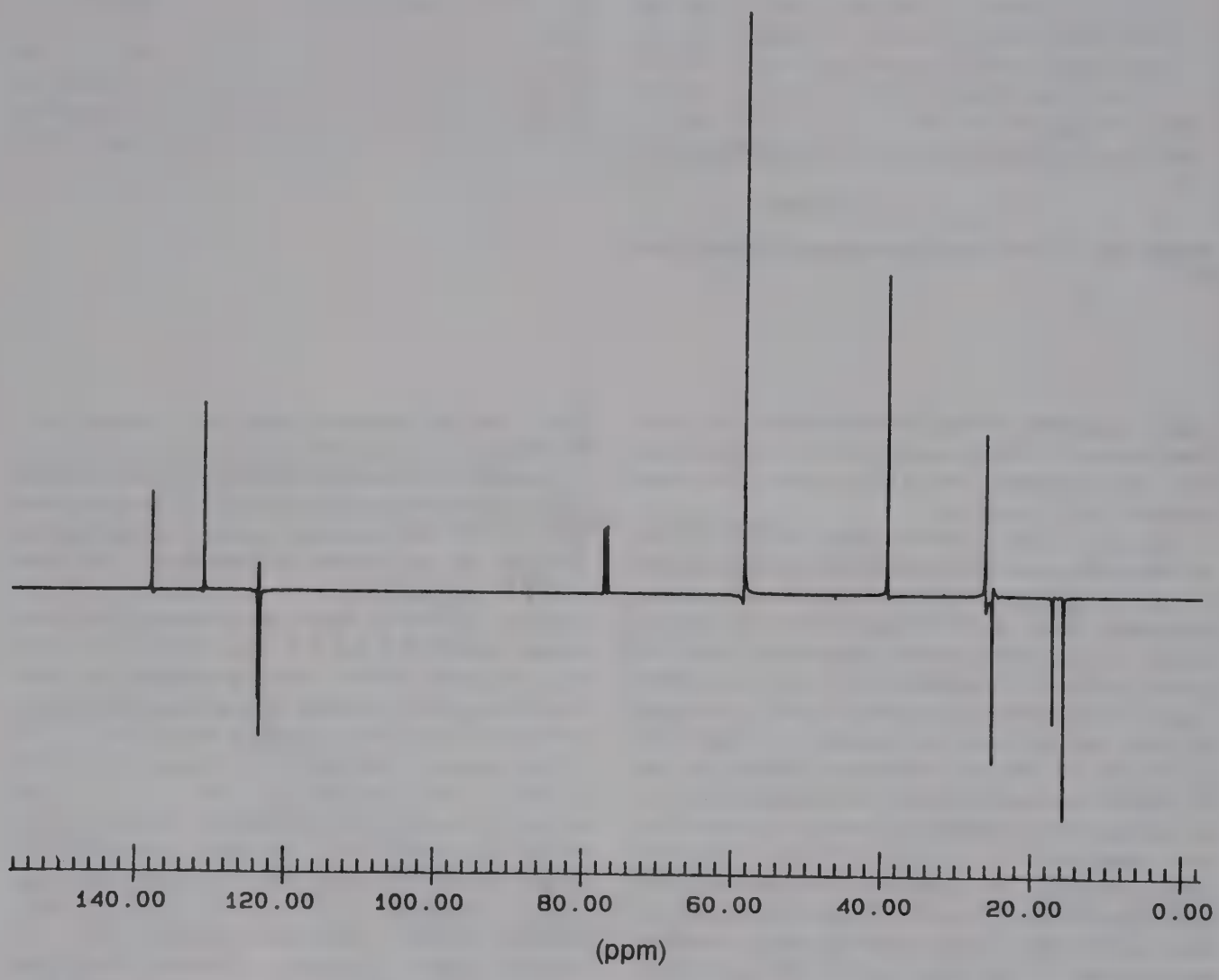

FIGURE 6.10. The APT ^{13}C spectrum of geraniol (peaks CH_3 and CH down, CH_2 and quaternary C up), in $CDCl_3$ at 125.7 MHz for ^{13}C. Compare with ^{13}C spectrum (Fig. 6.2).

*Multiplicity refers to the number of peaks caused by the attached protons.

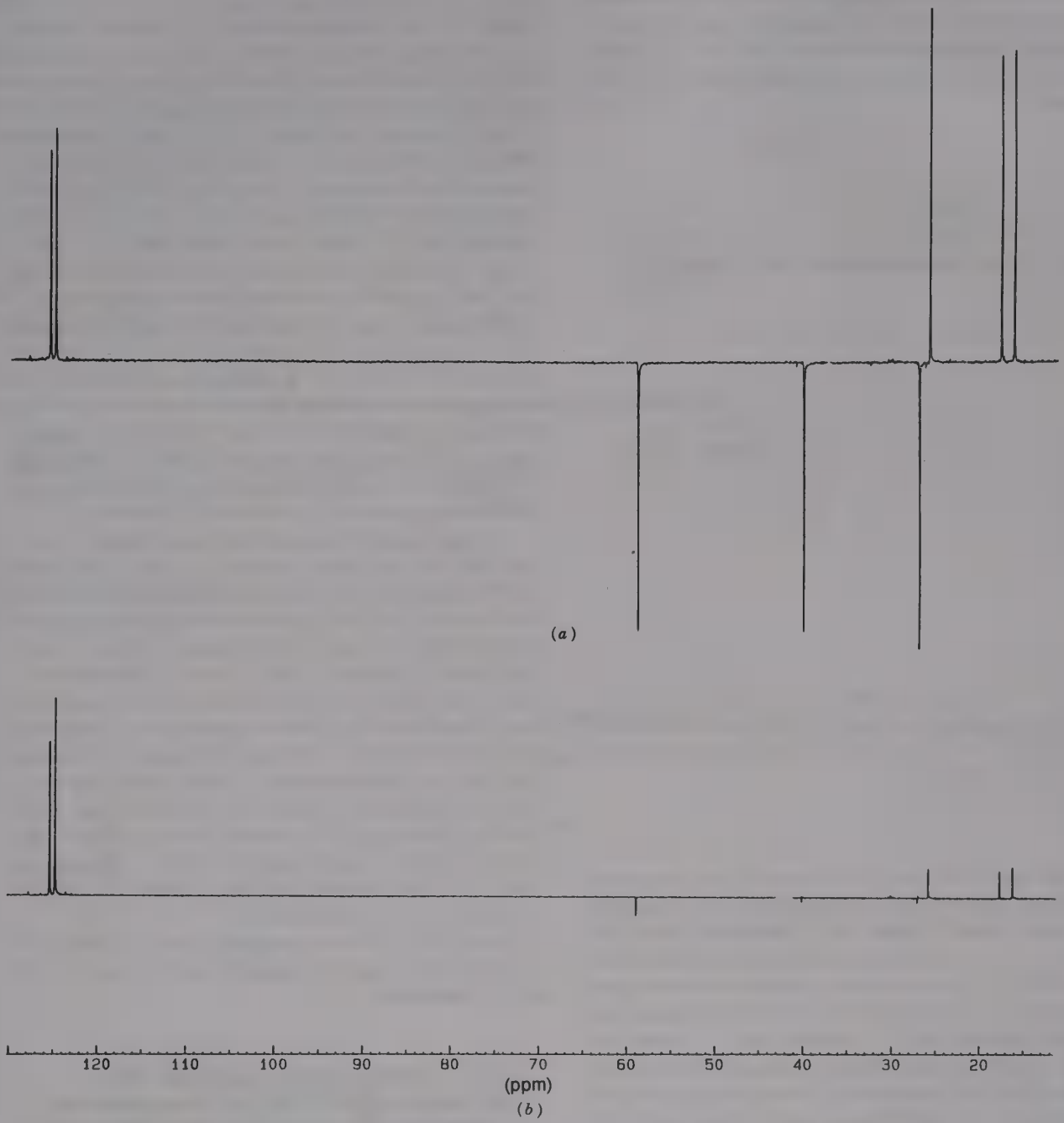

FIGURE 6.11. The DEPT spectrum of geraniol. (*a*) Peaks CH_3 and CH up, CH_2 down. (*b*) Peak CH up (residual CH_3 and CH_2 peaks). In $CDCl_3$ at 75.6 MHz for ^{13}C. Compare with ^{13}C spectrum (Fig. 6.6).

The peaks in the DEPT spectrum are unequivocally sorted as shown in Figure 6.11. Quaternary carbon atoms give no signal in the DEPT procedure but are, of course, obvious in the standard ^{13}C spectrum once the CH_3, CH_2, and CH peaks are identified. As the acronym DEPT implies, the increased sensitivity derives from "polarization transfer" from attached protons, that is, a nuclear Overhauser enhancement.

The APT experiment depends on signal amplitude modulation during two equal evolution periods t_1 and t_2. The amplitude is modulated by the number of protons attached to the ^{13}C atom, the coupling constant,

and the time intervals t_1 and t_2. A series of experiments with increasing time intervals results in a characteristic amplitude variation with time for CH, for CH_2, and for CH_3 as follows (from Sanders and Hunter with permission):

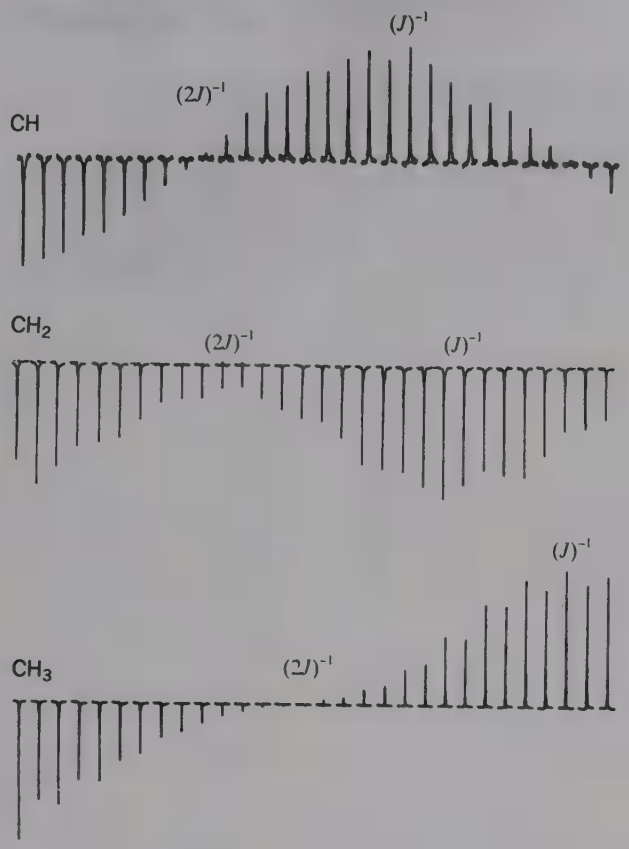

If the amplitudes at time interval $(J)^{-1}$ are compared, the CH and CH_3 peaks will be "up" and the CH_2 peak "down." However, as shown in Figure 6.10, these directions can be reversed by the software program. The ^{13}C atoms without attached protons (quaternary) do not undergo amplitude modulation, and these (including $CDCl_3$) are shown "up" in Figure 6.10.

The DEPT involves the process of polarization transfer from the magnetically more sensitive proton to the less sensitive ^{13}C atom, thus enhancing the ^{13}C spectrum. Excellent accounts of APT and DEPT are given in Sanders and Hunter, and in Derome where APT is indexed under "Spin echoes, *J*-modulated, heteronuclear."

6.3.2. *J*-Resolved ^1H—^{13}C Spectroscopy (HET2DJ) (2-D)

In HOM2DJ (Section 6.2.2), ^1H chemical shifts were presented on one axis and ^1H—^1H *J* coupling on the other. In HET2DJ, ^{13}C chemical shifts are presented on one axis and ^1H—^{13}C *J* coupling on the other. The result of a HET2DJ spectrum is equivalent to that available from a nondecoupled ^{13}C spectrum but without the severe overlap of the latter since the quartet of a CH_3 group, the triplet of a CH_2 group, the doublet of a CH group, or the singlet of a quaternary C atom is each presented at right angles to the conventional broadband decoupled ^{13}C spectrum (Fig. 6.12). In common with off-resonance decoupling, APT, and DEPT, the multiplicity of protons on each carbon is available through HET2DJ, which also shows the ^1H—^{13}C coupling constants; these permit distinction among sp^3, sp^2, and *sp* carbon atoms and indicate attachment of electronegative atoms (Section 5.4). Again in common with off-resonance decoupling, APT, and DEPT, correlation of ^1H with ^{13}C is lacking (see Section 6.3.3). Perhaps the most useful result is the rearrangement of the proton multiplets over the ^{13}C range of approximately 200 ppm in the sequence of the ^{13}C peaks. The ^{13}C shift axis shows a projection, whose intensities differ from those of a standard ^{13}C spectrum.

On the basis of chemical shifts and multiplicities in the HET2DJ spectrum of geraniol (Fig. 6.12), we assign the ^{13}C peaks (see Fig. 6.6) from high field to low field as follows: The three quartets at high field represent the three CH_3 groups, but we cannot be more specific. The three triplets represent C_4 and C_5 methylenes or vice versa (note the wide separation compared with the ^1H spectrum) and the C-1 methylene. Despite the overlap of the alkene methines (C-2 and C-6), it is clear that they are both doublets. The low-field singlets, of course, represent C-3 and C-7 without further specification. Note that the coupling constant for the C-4 and C-5 triplets is approximately 130 Hz, whereas that for the hydroxy-substituted C-1 triplet is approximately 140 Hz, as expected.

Since HET2DJ does not give ^1H—^{13}C correlations, it is used less frequently than the more powerful HETCOR (Section 6.3.3).

6.3.3. Heteronuclear Chemical Shift Correlation (HETCOR), or Heteronuclear Correlated Spectroscopy (HETEROCOSY), or Chemical Shift Correlation Map (CSCM) (2-D)

The HETCOR spectrum (Fig. 6.13) correlates the peaks of an ^1H spectrum with the peaks of a ^{13}C spectrum. Thus it goes beyond the APT, DEPT, and HET2DJ spectra in that it shows the specific protons attached to each ^{13}C. The ^1H spectrum is presented on the vertical axis and the ^{13}C broadband-decoupled spectrum is presented on the horizontal axis. The ^1H—^{13}C correlation is shown by a crosspeak contour at the intersection of a horizontal line drawn from a proton peak

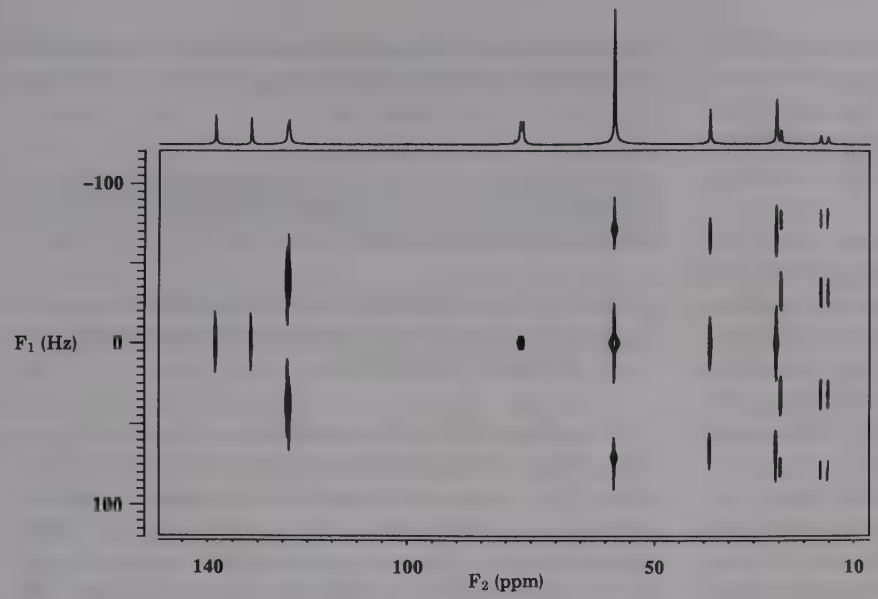

FIGURE 6.12. The HET2DJ spectrum of geraniol, in $CDCl_3$ using a 500-MHz instrument (125.7 MHz for ^{13} C).

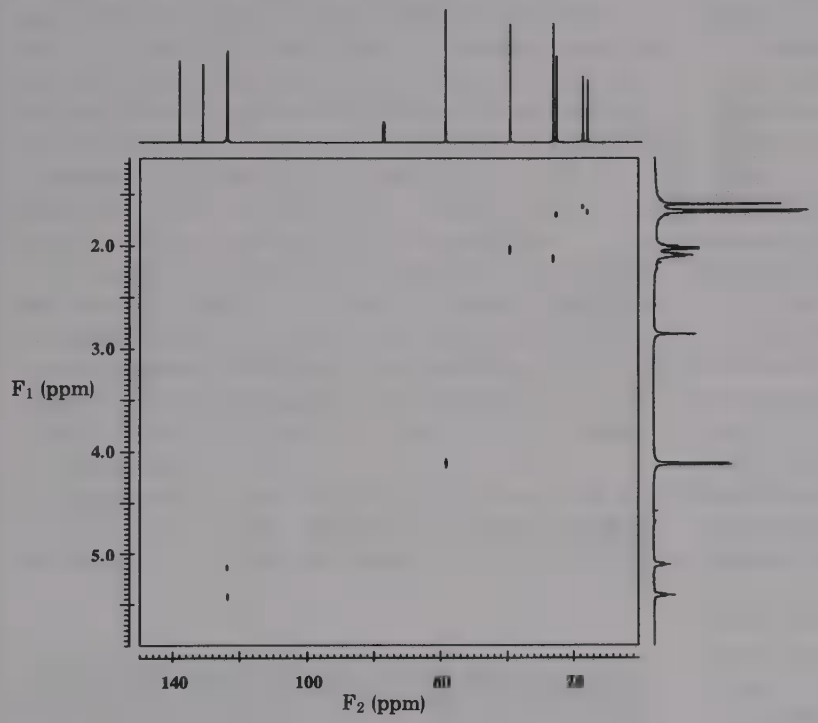

FIGURE 6.13. The HETCOR spectrum of geraniol, in $CDCl_3$ at 500 MHz for ^{1}H and 125.7 for ^{13} C.

or multiplet and a vertical line drawn from a ^{13}C peak. Obviously the combination of the correlation spectra HETCOR and COSY brings tremendous leverage to the task of structure elucidation by correlating both ^{1}H—^{1}H and ^{13}C—^{1}H connectivities.

Since we have the protons assigned from the COSY (HOMCOR) spectrum (Figs. 6.4 and 6.5), (the protons on C-8 and C-9 still being ambiguous), we can now correlate them with the carbon atoms in the HETCOR spectrum of geraniol (Fig. 6.13). Thus, from high-to-low field in the ^{13}C axis, we assign the methyl groups 10, 8, and 9, the methylenes 5, 4, and 1, and the alkene methines 6 and 2. Since the quaternary carbon atoms 3 and 7 are not correlated with protons, we look to the

INADEQUATE spectrum for ^{13}C—^{13}C connectivities (Section 6.4). The C-4 and C-5 methylenes that were partially overlapped in the HOMCOR spectrum are now widely separated in the ^{13}C axis of the HETCOR spectrum. The OH proton peak at δ 2.84, of course, shows no crosspeak.

Note that the quaternary carbon atoms 3 and 7 appear on the horizontal ^{13}C axis, but only because the standard ^{13}C (as well as the ^{1}H spectrum) has been manually superposed. In the other HETCOR spectra in this text, both the ^{1}H and ^{13}C spectra on the axes are projections of the 2-D spectrum. Quaternary carbon atoms do not appear on the projected ^{13}C spectrum since they show no crosspeak contours.

Note also that, as in the HET2DJ spectrum, the proton peaks are distributed on the approximately 200 ppm scale of the ^{13}C spectrum. Furthermore, the occurrence of two crosspeaks on the same carbon atom is a most useful indicator of the presence of diastereotopic methylene protons. See, for example, Chapter 8, Compound 8.3. As with the COSY, the HETCOR can also be modified to give long-range coupling.

6.4. ^{13}C—^{13}C CONNECTIVITY

6.4.1. Incredible Natural Abundance Double Quantum Transfer Experiment (2-D INADEQUATE)

The INADEQUATE experiment, Figure 6.14, detects the connectivities between two adjacent ^{13}C atoms. Each connectivity is shown by a pair of doublets parallel to the horizontal axis. Each doublet lies on the chemical shift of each connected ^{13}C atom; the ^{13}C spectrum is shown on the top horizontal axis. The midpoint of each pair of doublets lies along a diagonal line from lower left to upper right. Since at natural

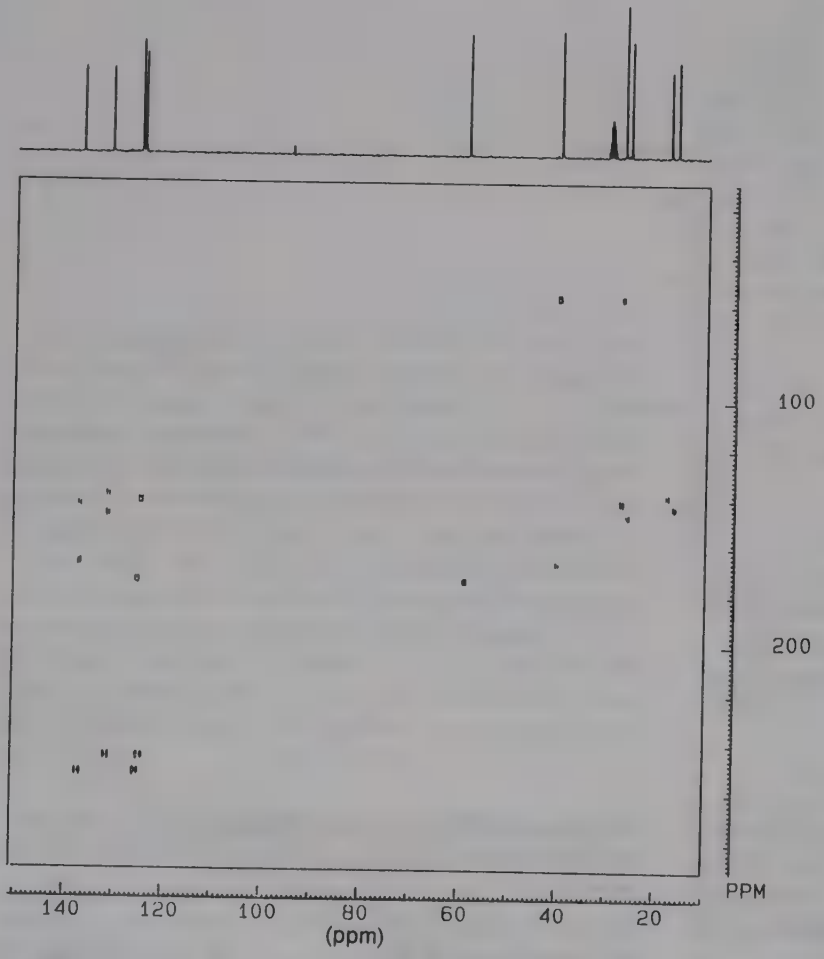

FIGURE 6.14. The INADEQUATE spectrum of geraniol in CD_3COCD_3 at 75.6 MHz for ^{13}C.

abundance, only one molecule in approximately 10,000 contains adjacent ^{13}C atoms, the sensitivity of this experiment is low. It is the very weak satellite doublets resulting from ^{13}C—^{13}C coupling that are observed, while the intense isolated ^{13}C peaks are removed by a double quantum filter. Thus, each horizontal line of doublets consists of the *AX* spin system ^{13}C—^{13}C.

Figure 6.14 is the spectrum of geraniol in hexadeuteroacetone (septet at δ 30.6); the chemical shifts, therefore, differ slightly from those of the ^{13}C spectrum in $CDCl_3$, but the relative shifts are the same. We trace connectivities from any of the already assigned ^{13}C peaks, for example, C-1 at about δ 59.0. Looking horizontally left from this doublet, equidistant across the diagonal, we reach the other doublet of the *AX* system under C-2. Below the latter is another C-2 doublet connected horizontally left to its paired doublet under C-3, above which are two C-3 doublets connected horizontally right to C-4 and to C-10, respectively. The C-10 doublet is terminal since there are no doublets directly above or below, but above the C-4 doublet is another C-4 doublet connected horizontally right to its paired doublet at C-5. Below the C-5 doublet is another C-5 doublet connected horizontally left to C-6. Below the C-6 doublet is another C-6 doublet connected horizontally left to C-7, above which are two C-7 doublets connected horizontally right to C-8 and to C-9, respectively, both of which are terminal. There is, of course, no connectivity for the solvent signal.

We have now established all of the connectivities and have identified the C-3 and C-7 peaks, except for the rather remote possibility that these signals have interchanged in switching solvents from $CDCl_3$ to CD_3COCD_3. An unambiguous distinction between C-8 and C-9 must await the difference NOE experiment in Section 6.5.

The expense of an INADEQUATE spectrum is a deterrent to its routine use, but it remains a powerful tool for tracing the carbon skeleton.

6.5. THROUGH-SPACE ^1H ^1H PROXIMITY

6.5.1. NOE Difference Spectrum (1-D)

We have noted (Section 5.1) that irradiation of a proton results in enhancement of the signal of the ^{13}C to which the proton is directly bonded. This NOE also operates between nonbonded protons through space but only over a short distance and with a smaller effect, which decreases as the inverse of the sixth power of the distance through-space between the nuclei. This effect depends on enhancement of a signal when a nearby resonance is irradiated, the mechanism being nuclear relaxation through-space by dipolar interaction. We are interested in the ^1H ^1H through-space interaction, the usual observable enhancement being less than 20%.

In dealing with these rather small effects, it is most advantageous to obtain an NOE difference spectrum (Fig. 6.15) by obtaining two spectra: one is a specific-proton-irradiated ^1H spectrum, and the other is a conventional ^1H spectrum; the latter is subtracted from the former to obtain the difference NOE spectrum, leaving only the enhanced peak. This procedure is very valuable for distinguishing between stereoisomers, in which case spectra of all of the isomers should be obtained if feasible. A measurable effect can be expected between ^1H atoms over a distance of up to about 4 Å (0.4 nm)—for example, between 1,3-diaxial protons in a fused cyclohexane ring. The ratio of the distance respectively between the C-10 CH_3 group and the C-2 CH of geraniol and that of nerol is about 1.3:1.0. Thus, we should expect a larger NOE enhancement for the C-2 CH of nerol on irradiation of the C-10 CH_3.

Distinguishing between a trisubstituted (*E*) double bond (geraniol) and the corresponding (*Z*) double bond (nerol) is not a trivial assignment. The NOE difference spectrum is indeed a powerful tool for this purpose. Figure 6.15*a* shows the ^1H spectrum for geraniol and the NOE results of irradiating H-9, H-10, and H-8. Figure 6.15*b* shows the NOE results for nerol. These results are recorded as NOE difference spectra. In Figure 6.15*a* (geraniol), we irradiate H-9 and H-10 simultaneously (and unavoidably) and observe that H-2 is not detectably enhanced—equal positive and negative peaks—whereas H-6 is definitely enhanced. These results indicate that H-10 and H-2 are on opposite sides of the 2,3 double bond, which therefore has the (*E*) configuration as drawn. They also indicate that H-9 and H-6 are on the same side of the 6,7 double bond as numbered. This latter result is confirmed by irradiation of H-8 with only slight effect on H-6. In Figure 6.15*b* (nerol), irradiation of H-10 strongly enhances H-2 thus confirming the (*Z*) configuration of the 2,3 double bond in nerol. Irradiation of H-9 gives the same results as for geraniol—enhancement of H-6. Irradiation of H-8 also gives the same results as for geraniol—no pronounced enhancement of either H-2 or H-6, the latter result showing that H-8 and H-6 are on opposite sides of the 6,7 double bond in both geraniol and nerol. Irradiation of C-10 of geraniol also enhances C-1, but this is not shown. It should be noted that a negative NOE peak, usually weak, may be obtained from a proton that receives the irradiation as a "relayed" signal through a proton that shows the usual enhanced, positive peak. Since relaxation rates are very sensitive to the presence of paramagnetic substances, dissolved

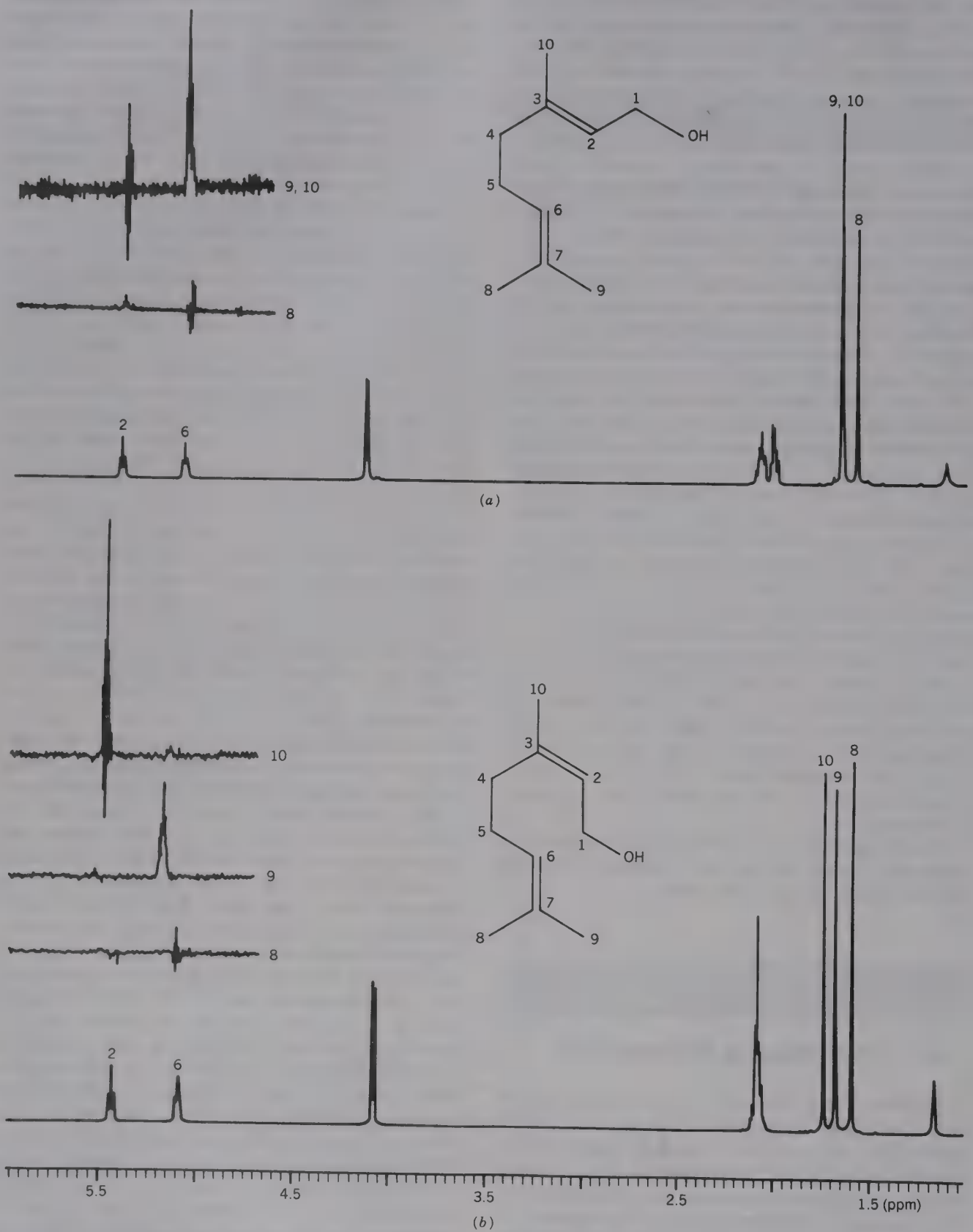

FIGURE 6.15. Difference NOE spectra of (*a*) geraniol and (*b*) nerol in $CDCl_3$ at 500 MHz.

oxygen, a diradical, should be removed by several cycles of freeze, pump, thaw, or by bubbling nitrogen or argon through the solution; the tube should then be sealed.

6.5.2. The NOESY (Nuclear Overhauser and Exchange Spectroscopy) (2-D)

It is possible to assemble all of the ^1H ^1H NOE effects in a molecule into a single spectrum called NOESY, which bears a striking resemblance to the COSY spectrum; the ^1H spectrum is represented by contours along the diagonal, but the off-diagonal contours represent nonbonding ^1H ^1H interactions with protons that are nearby in space. This is a powerful tool for solving questions of configurations and conformations in large molecules with regions of fixed geometry. Our model compounds for this chapter are small and pose only the single problem of the stereochemistry of the double bond, which has been solved by the NOE difference spectrum; we therefore refer to the literature at the end of this chapter.

6.6. OPTIONS AND HOW TO USE THEM

The first step in using NMR for structure elucidation of a completely unknown compound is to obtain, as nearly as possible, a first-order, nonoverlapping, integrated ^1H spectrum. But this is not always possible. In such simple cases as the problems in Chapter 4, satisfactory ^1H spectra were obtained at 60 MHz, but even at 500 or 600 MHz, many molecules may not yield first-order, nonoverlapping spectra. Changing the solvent, for example, from $CDCl_3$ to C_6D_6, or using a lanthanide shift reagent (especially with a low-field instrument) may resolve areas of overlap. Specific decouplings will assist in assigning protons. The next step is to obtain a broadband decoupled ^{13}C spectrum with sufficient resolution to separate all nonequivalent peaks, if possible.

At this point, we can determine the number of protons on each ^{13}C with the 1-D spectra APT or DEPT, or with the 2-D spectrum HET2DJ, which also gives the ^1H—^{13}C coupling constants while spreading the proton multiplets over the ^{13}C range of 200 ppm. Alternatively, recourse can be had to the powerful 2-D HETCOR (HETEROCOSY or SCM) technique, which shows directly the specific protons (including diastereotopic protons) attached to each ^{13}C. This accumulated complementary information will suffice to solve most problems at the level presented in this text. If troublesome areas of overlap remain in the ^1H spectrum, a HOM2DJ spectrum may be useful if the overlapped couplings are either not coupled to one another, or the couplings are first order or nearly so.

Combined use of ^1H and ^{13}C NMR is especially powerful since it furnishes the number of nonequivalent protons and carbon atoms, assuming no peak coincidence. A discrepancy between these numbers and those in the molecular formula indicates one or more symmetry elements.

It is often possible to solve a problem without using the more time-consuming and material-demanding ^{13}C spectra. Thus, the combination of a first-order, nonoverlapping ^1H spectrum and the powerful COSY (HOMCOR) spectrum may suffice. Connectivities are stronger arguments for assignments than those based on chemical shifts alone. Questions of stereoisomerism are investigated by NOE. In the absence of attached protons, ^{13}C ^{13}C connectivities can be established by an INADEQUATE spectrum.

Strategy, of course, is frequently driven by funds available to pay for the spectra. A high-resolution ^1H spectrum can be obtained and processed within minutes on several milligrams, and a broadband decoupled ^{13}C on less than 100 mg; if sample amount is the limiting factor, an ^1H spectrum can be obtained on several micrograms and a ^{13}C spectrum on several milligrams, although several hours on a high-field instrument (possibly overnight) may be necessary. In contrast, tens of milligrams for ^1H 2-D spectra and hundreds of milligrams for ^{13}C 2-D spectra are needed to avoid high costs. As a rough guide, the following minimum amounts are suggested for an overnight run on a 300-MHz instrument:* HOM2DJ, 0.5 mg; HET2DJ, 30 mg; HOMCOR, 5 mg; HETCOR, 10 mg; NOESY, 10 mg; 2-D INADEQUATE 100 mg. These estimates will certainly change as techniques improve. We must also be aware that a good deal of processing is needed to produce high-quality spectra, although this can be done without using instrument time.

Throughout this chapter, we have treated geraniol as a demonstration molecule rather than as a problem, which would obviously require a different approach to the NMR spectra; demonstrating is always easier than solving. How does one approach an unknown NMR spectrum? Almost intuitively, we look for a unique signal as a starting point: unique in chemical shift, multiplicity, or intensity. The IR spectrum of geraniol would have indicated an alcohol. The two-proton doublet at δ 4.10 is highly indicative of the CH—C$\underline{H_2}$OH moiety, and we use it as a starting point in the spectra designed to show connectivities. Since the molecular formula from mass spectrometry would show possible unsaturation, we can use the two low-field proton signals or the four low-field ^{13}C signals as points of entry, and so on, although it is not always so easy.

*G. A. Morris, *Magn. Reson. Chem.*, **24**, 371 (1986).

REFERENCES

Derome, A. *Modern NMR Techniques for Chemistry Research*, Oxford: Pergamon, 1987.

Sanders, J. K. M. and Hunter, B. K. *Modern NMR Spectroscopy*, Oxford: Oxford University Press, 1987.

Croasmum, W. R. and Carlson, R. M. K. (Eds.). *Two-Dimensional NMR Spectroscopy*. New York: VCH, 1987.

Ernst, R. R., Bodenhausen, G., and A. Wokaun. *Principles of Nuclear Magnetic Resonance in One and Two Dimensions*. Oxford: Clarendon, 1987.

Farrar, T. C. *An Introduction to Pulse NMR Spectroscopy*. Chicago: Farragut, 1987.

Chandrakumar, N. and Subramanian, S. *Modern Techniques in High Resolution FT NMR*. New York: Springer–Verlag, 1987.

Kessler H., Gehrke, M., and Griesinger, C. "Two-dimensional NMR Spectroscopy." *Angew. Chem. (Int. Ed., Engl.)* **27**, 490–536 (1988).

Schraml, J. and Bellama, J. M. Two-Dimensional NMR Spectrometry, New York: Wiley, 1988.

Brey, W. (Ed.). *Pulse Methods in 1D and 2D Liquid-Phase NMR*. New York: Academic, 1988.

Martin, G. E. and Zektzer, A. S. *Two-Dimensional NMR Methods for Establishing Molecular Connectivity*, New York: VCH, 1988.

Freibolen, H. Basic One- and Two-Dimensional Spectroscopy. New York: VCH.

PROBLEMS

6.1. For the compounds of Problems 4.1–4.5, 5.1, 5.5, and 5.6, draw the following spectra: spin decoupled ^1H spectra, HOM2DJ, HOMCOR, APT, DEPT, HET2DJ, HETCOR, and INADEQUATE. Assume use of a 300-MHz instrument and $CDCl_3$ as the solvent.

6.2. Show all of the couplings on the DQFCOSY spectrum (Fig. 6.5*b*).

6.3. Identify the compound $C_7H_{14}O$ from its COSY spectrum and show all of the connectivities. The diagonal runs from upper left to lower right. A 1% solution in $CDCl_3$ at 300 MHz. With permission from Varian Associates.

6.4. Identify the compound $C_{11}H_{14}O_2$ from the following spectra: ^1H, ^{13}C, HOM2DJ, and COSY spectra, all in $CDCl_3$ at 300 MHz, except ^{13}C at 75.6 MHz. Courtesy of Dr. Daniel F. Traficante. In the HOM2DJ spectrum, the outer two contours of the sextet at δ 1.40 are missing (see Section 6.2.2).

PROBLEM 6.3. COSY FOR $C_7H_{14}O$

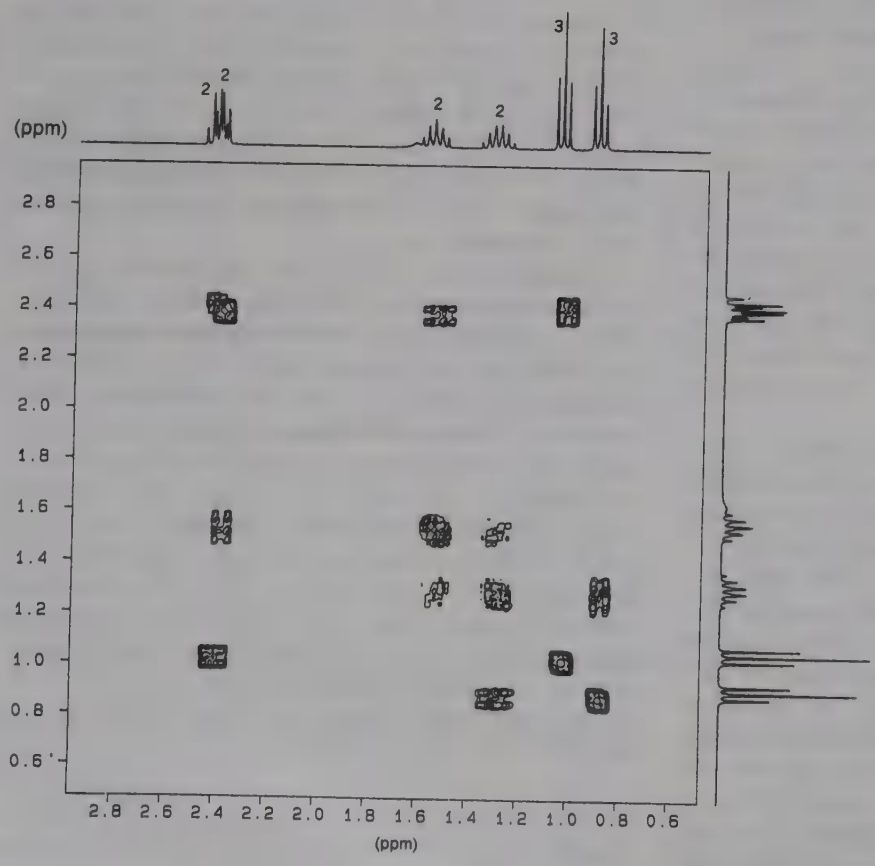

PROBLEM 6.4. 1-D PROTON SPECTRUM. (NUMBERS ABOVE MULTIPLETS INDICATE INTEGRAL VALUES.)

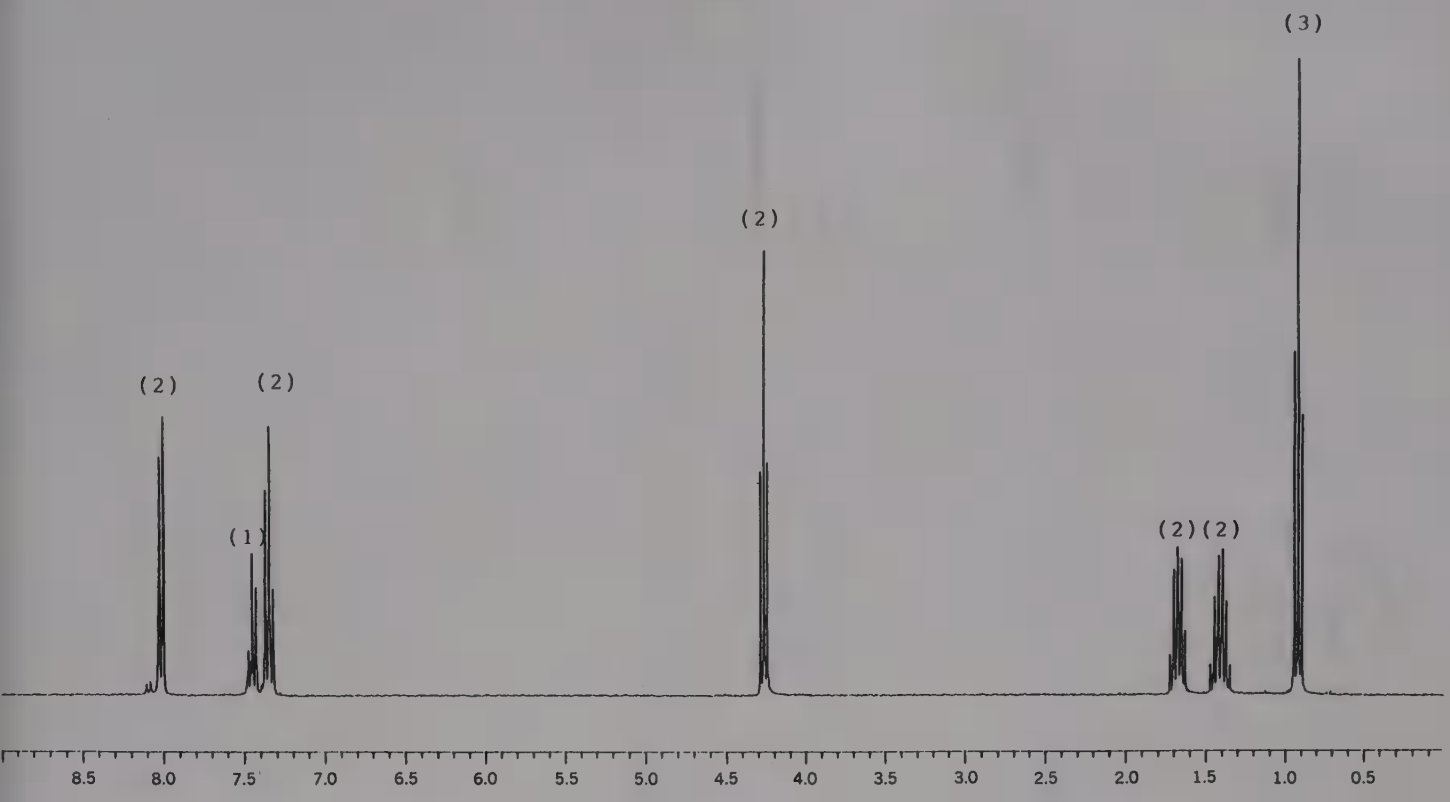

PROBLEM 6.4. 1-D PROTON DECOUPLED CARBON SPECTRUM.

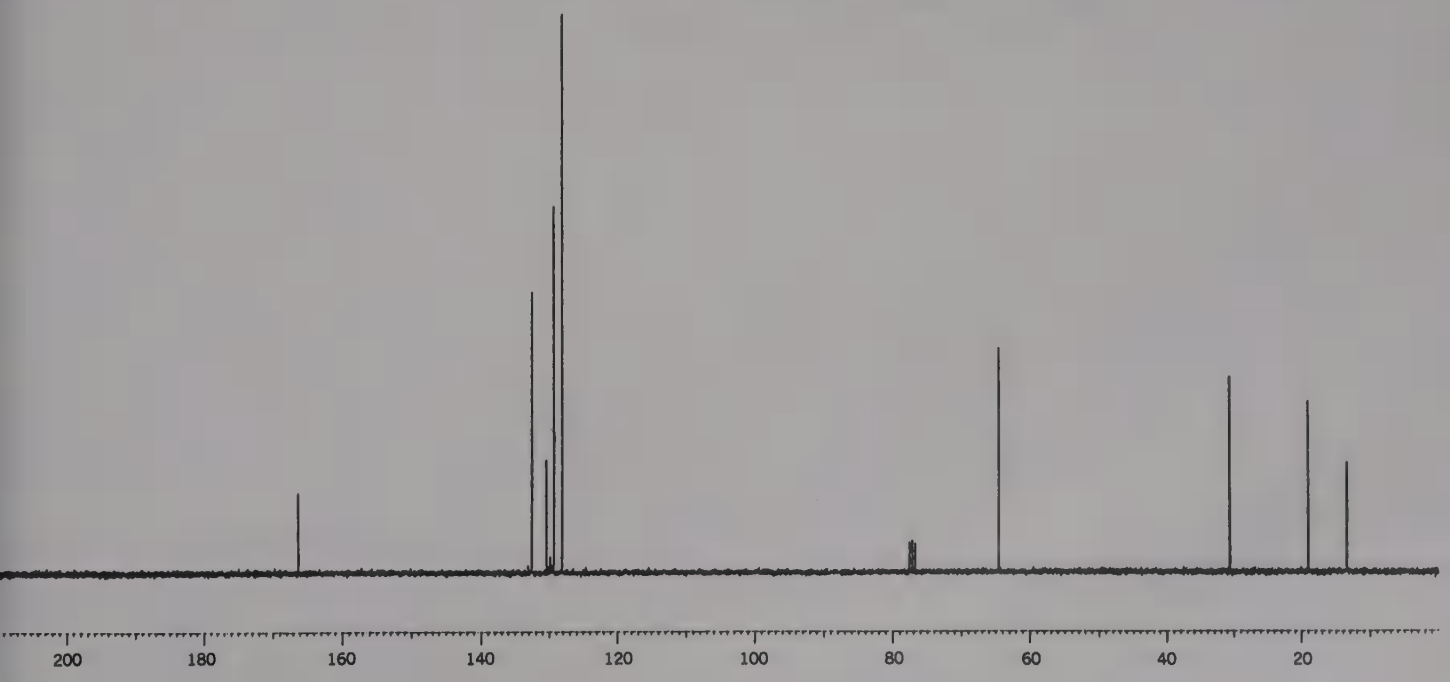

PROBLEM 6.4. HOM2DJ.

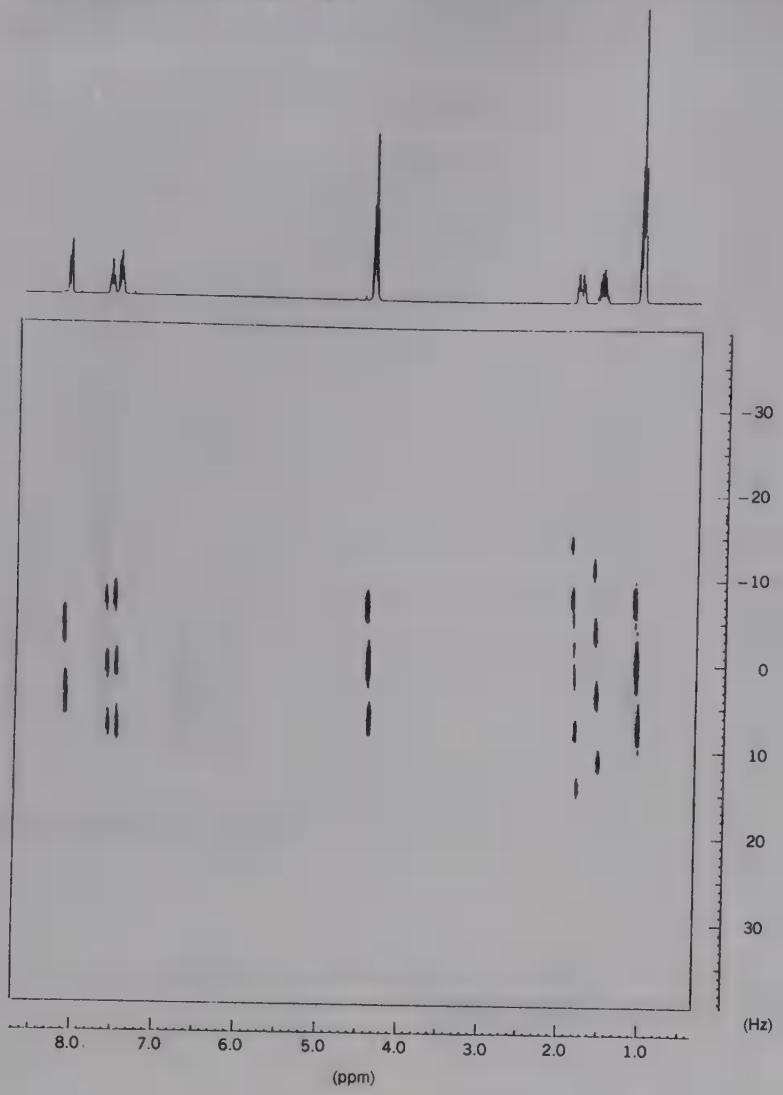

PROBLEM 6.4. COSY.

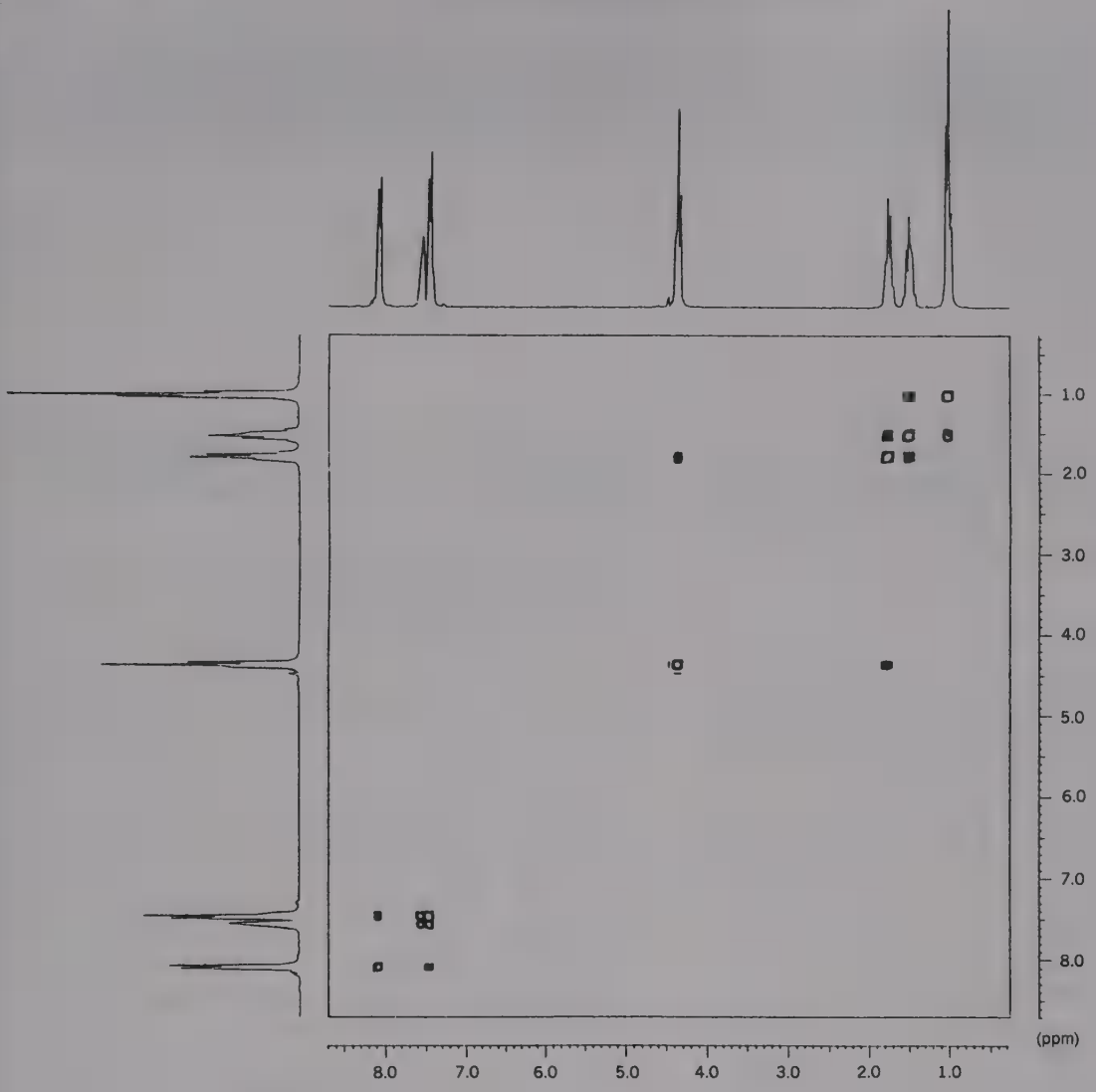

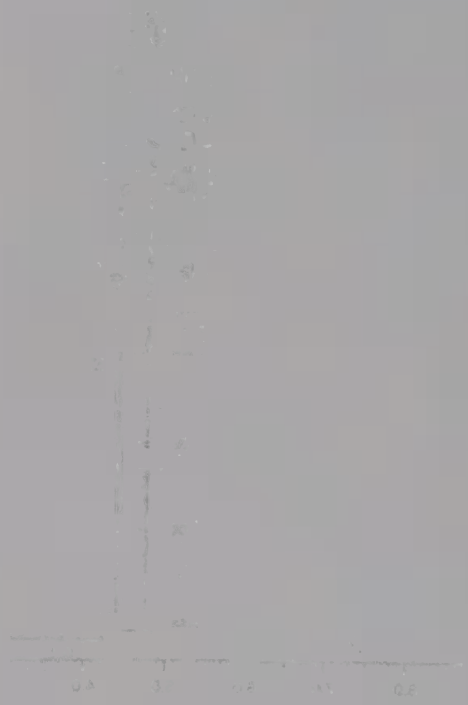

CHAPTER SEVEN

ULTRAVIOLET SPECTROMETRY

7.1. INTRODUCTION

Molecular absorption in the ultraviolet (UV) and visible region of the spectrum is dependent on the electronic structure of the molecule. Absorption of energy is quantized, resulting in the elevation of electrons from orbitals in the ground state to higher energy orbitals in an excited state. For many electronic structures, the absorption does not occur in the readily accessible portion of the UV region. In practice, UV spectrometry is normally limited to conjugated systems.*

There is, however, an advantage to the selectivity of UV absorption: Characteristic groups may be recognized in molecules of widely varying complexities. A large portion of a relatively complex molecule may be transparent in the UV so that we may obtain a spectrum similar to that of a much simpler molecule. Thus, the spectrum of cholest-4-en-3-one closely resembles the spectrum of mesityl oxide. The absorption results from the conjugated enone portion of the two compounds (Fig. 7.1).

A detailed mathematical treatment of the theoretical basis for UV or electronic spectra is beyond the scope of this chapter. Rather, it is our objective to point out correlations between spectra and structure to be used by the organic chemist. However, enough theory to rationalize these correlations will be presented.

A UV spectrum obtained directly from an instrument is simply a plot of wavelength (or frequency) of absorption versus the absorption intensity (absorbance or transmittance). The data are frequently converted to a graphical plot of wavelength versus the molar absorptivity (ϵ_{max} or log ϵ_{max} as in Fig. 7.1). The use of molar absorptivity as the unit of absorption intensity has the advantage that all intensity values refer to the same number of absorbing species. A tabular presentation is used in Chapters 8 and 9.

References to textbooks and compilations of spectra are given at the end of this chapter.

*High-performance liquid chromatography (HPLC) relies heavily on UV detection.

7.2. THEORY

The UV portion of the electromagnetic spectrum is indicated in Figure 7.2. Wavelengths in the UV region are usually expressed in nanometers (1 nm = 10^{-9} m) or angstroms, Å (1 Å = 10^{-10} m). Occasionally, absorption is reported in wavenumbers ($\bar{\nu}$, units = cm^{-1}). We are primarily interested in the near-UV (quartz) region extending from 200 to 380 nm. The atmosphere is transparent in this region and quartz optics may be used to scan from 200 to 380 nm. Atmospheric oxygen absorption starts near 200 nm and extends into the shorter wavelength region, which is accessible through nitrogen flushing (revealing 200–185 nm region) or vacuum UV spectrometry.

The total energy of a molecule is the sum of its electronic energy, its vibrational energy, and its rotational energy. The magnitude of these energies decreases in the following order: E_{elec}, E_{vib}, and E_{rot}. Energy absorbed in the UV region produces changes in the electronic energy of the molecule resulting from transitions of valence electrons in the molecule. These transitions consist of the excitation of an electron from an occupied molecular orbital (usually a nonbonding p or bonding π orbital) to the next higher energy orbital (an antibonding, π^* or σ^*, orbital). The antibonding orbital is designated by an asterisk. Thus, the promotion of an electron from a π-bonding orbital to an antibonding (π^*) orbital is indicated $\pi \rightarrow \pi^*$.

The concept of an antibonding orbital can be explained simply by considering the UV absorption of

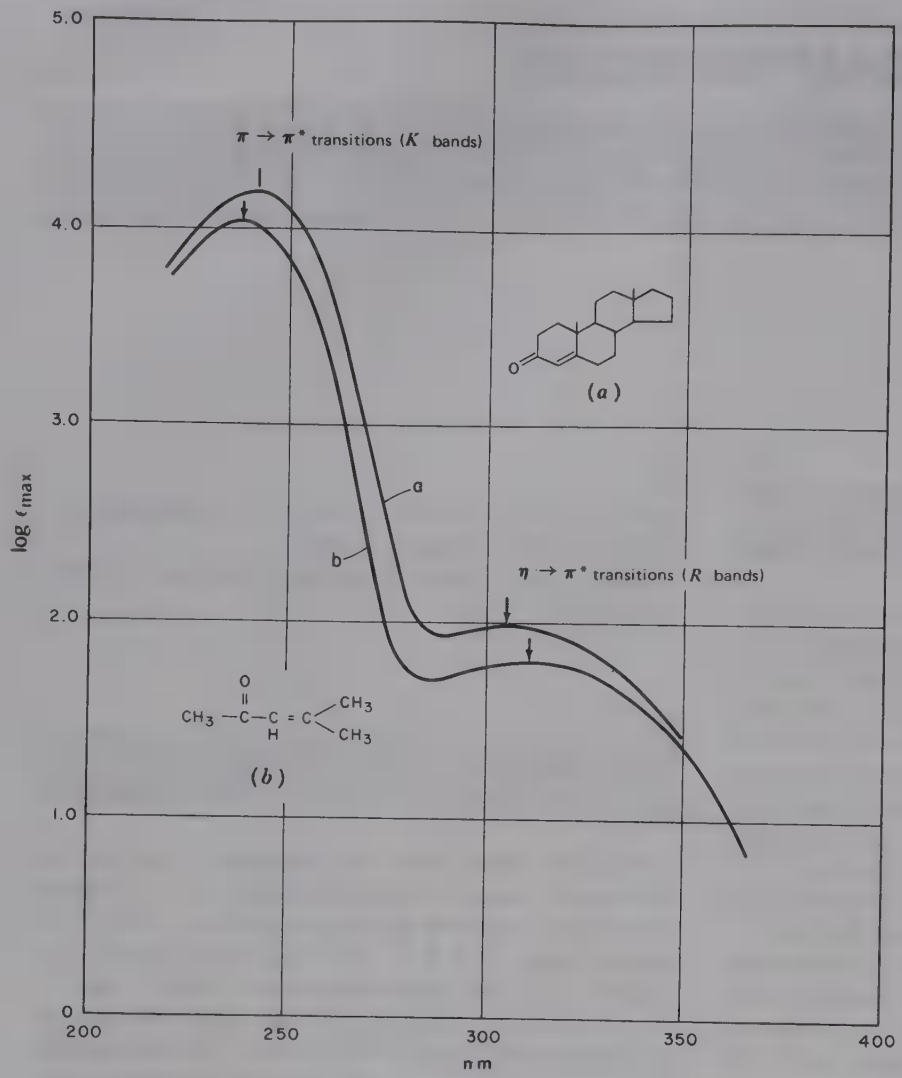

FIGURE 7.1. Ultraviolet spectra of (*a*) cholest-4-en-3-one and (*b*) mesityl oxide. Log ϵ_{max} is calculated from the instrument read out (A or T, see p. 292).

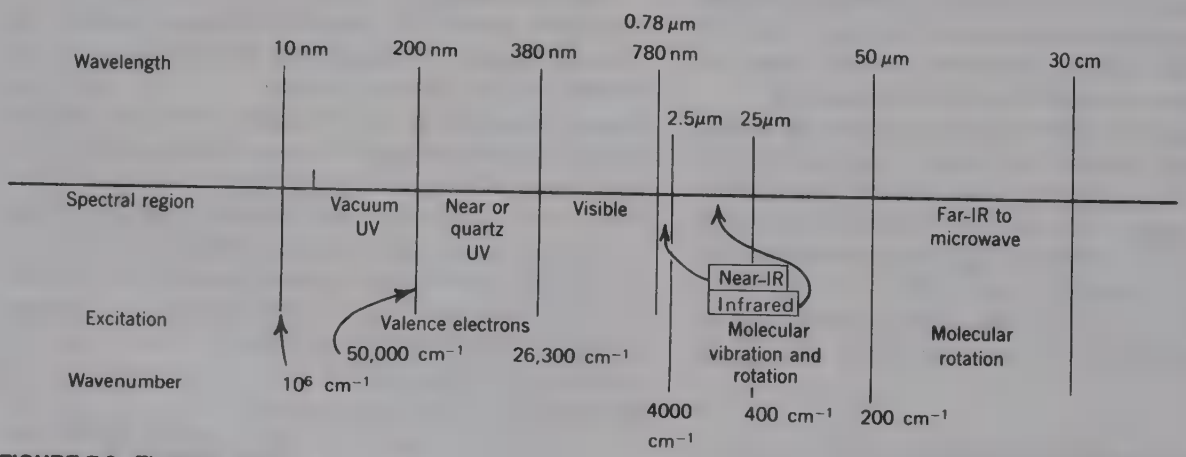

FIGURE 7.2. Electromagnetic spectrum.

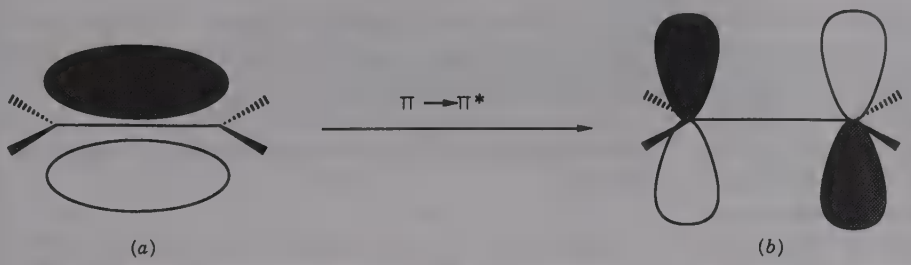

FIGURE 7.3. The π and π^* orbitals of ethylene. (*a*) Bonding orbital, π. Both π electrons occupying bonding orbital. A bonding π orbital has only one nodal plane in the plane of the molecular skeleton. (*b*) Antibonding orbital, π^*. An (antibonding) π^* orbital has an additional nodal plane perpendicular to the plane of the molecule and bisecting the C—C bond.

ethylene. The ethylenic double bond, in the ground state, consists of a pair of bonding σ electrons and a pair of bonding π electrons. On absorption of UV radiation near 165 nm, one of the bonding π electrons is raised to the next higher energy orbital, an antibonding π orbital.

The orbitals occupied by the π electron in the ground state and in the excited state are diagrammed in Figure 7.3. The dark and white areas are regions of maximum electron density. It can be seen that the antibonding π electron no longer contributes appreciably to the overlap of the C—C bond. In fact, it negates the bonding power of the remaining unexcited π electron; the alkene bond has considerable single-bond character in the excited state.

The relationship between the energy absorbed in an electronic transition and the frequency (ν), wavelength (λ), and wavenumber ($\bar{\nu}$) of radiation producing the transition is

$$\Delta E = h\nu = \frac{hc}{\lambda} = h\bar{\nu}c$$

where h is Planck's constant, c is the velocity of light, and ΔE is the energy absorbed in an electronic transition in a molecule from a low-energy state (ground state) to a high-energy state (excited state). The energy absorbed is dependent on the energy difference between the ground state and the excited state; the smaller the difference in energy, the longer the wavelength of absorption. The excess energy in the excited state may result in dissociation or ionization of the molecule, or it may be reemitted as heat or light. The release of energy as light results in fluorescence or phosphorescence.

Since UV energy is quantized, the absorption spectrum arising from a single electronic transition should consist of a single, discrete line. A discrete line is not obtained since electronic absorption is superimposed on rotational and vibrational sublevels. The spectra of simple molecules in the gaseous state consist of narrow absorption peaks, each representing a transition from a particular combination of vibrational and rotational levels in the electronic ground state to a corresponding combination in the excited state. This is shown schematically in Figure 7.4, in which the vibrational levels are designated ν_0, ν_1, ν_2, and so on. At ordinary temperatures, the molecules in the electronic ground state will be largely in the zero vibrational level (G_{ν_0}); consequently, there are many electronic transitions from that level. In molecules containing more atoms, the multiplicity of vibrational sublevels and the closeness of their spacing cause the discrete bands to coalesce, and broad absorption bands or "band envelopes" are obtained.

The principal characteristics of an absorption band are its position and intensity. The position of absorption corresponds to the wavelength of radiation whose energy is equal to that required for an electronic transition. The intensity of absorption is largely dependent on two factors: the probability of interaction between the radiation energy and the electronic system and the

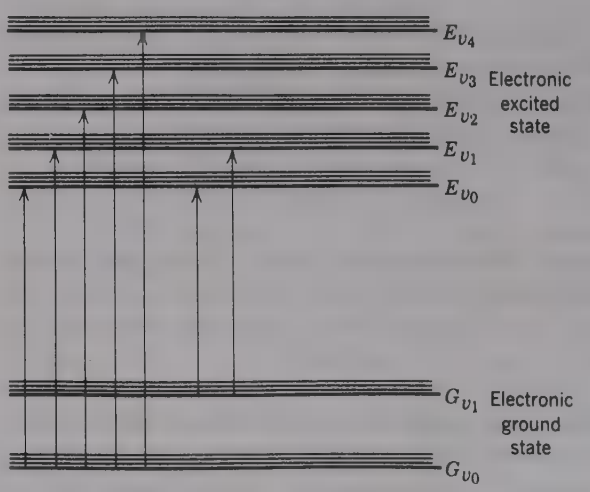

FIGURE 7.4. Energy level diagram of a diatomic molecule.

difference between the ground and the excited state. The probability of transition is proportional to the square of the transition moment. The transition moment, or dipole moment of transition, is proportional to the change in the electronic charge distribution occurring during excitation. Intense absorption occurs when a transition is accompanied by a large change in the transition moment. Absorption with ϵ_{max} values greater than 10^4 is high-intensity absorption; low-intensity absorption corresponds to ϵ_{max} values less than 10^3. Transitions of low probability are "forbidden" transitions. The intensity of absorption may be expressed as transmittance (T), defined by

$$T = I/I_0$$

where I_0 is the intensity of the radiant energy striking the sample, and I is the intensity of the radiation emerging from the sample. A more convenient expression of absorption intensity is that derived from the Lambert–Beer law, which establishes a relationship between the absorbance, the sample thickness, and the concentration of the absorbing species. This relationship is expressed as

$$\log_{10}(I_0/I) = kcb = A$$

where k = a constant characteristic of the solute
c = concentration of solute
b = path length through the sample
A = absorbance (optical density in the older literature)

When c is expressed in moles per liter, and the path length (b) through the sample is expressed in centimeters, the preceding expression becomes

$$A = \epsilon cb$$

The term ϵ is known as the molar absorptivity, formerly called the molar extinction coefficient.

If the concentration (c) of the solute is now defined as grams per liter (g/L), the equation becomes

$$A = abc$$

where a is the absorptivity and is thus related to the molar absorptivity by

$$\epsilon = aM$$

where M is the molecular weight of the solute.

The intensity of an absorption band in the UV spectrum is usually expressed as the molar absorptivity at maximum absorption, ϵ_{max} or log ϵ_{max}.

Each year the journal *Analytical Chemistry* publishes spectroscopy nomenclature and SI units in the January 1 issue.

At this point it is desirable to define certain terms that are frequently used in the discussion of electronic spectra.

Chromophore. A covalently unsaturated group responsible for electronic absorption (e.g., C=C, C=O, and NO_2).

Auxochrome. A saturated group with nonbonded electrons which, when attached to a chromophore, alters both the wavelength and the intensity of the absorption (e.g., $\ddot{O}H$, $\ddot{N}H_2$, and $:\ddot{C}l$).

Bathochromic Shift. The shift of absorption to a longer wavelength due to substitution or solvent effect (a red shift).

Hypsochromic Shift. The shift of absorption to a shorter wavelength due to substitution or solvent effect (a blue shift).

Hyperchromic Effect. An increase in absorption intensity.

Hypochromic Effect. A decrease in absorption intensity.

The absorption characteristics of organic molecules in the UV region depend on the electronic transitions that can occur and the effect of the atomic environment on the transitions. A summary of electronic structures and transitions that are involved in UV absorption is presented in Table 7.1.

Representative UV spectra (plots of log ϵ vs λ) are shown in Figure 7.1. Note that the spectrum of the relatively simple model compound mesityl oxide very closely approximates the spectrum of the more complex steroid. Increased molecular structure complexity normally results in increased spectral complexity in NMR, IR, and mass spectra; Figure 7.1 shows that this is not necessarily true for UV spectra.

The relative ease with which the various transitions can occur is summarized in Figure 7.5. Although the energy changes are not shown in scale, it is readily seen, for example, that an $n \rightarrow \pi^*$ transition requires less energy than a $\pi \rightarrow \pi^*$ or a $\sigma \rightarrow \sigma^*$ transition. Several notation systems are used to designate UV absorption bands (Appendix 1 of Jaffe and Orchin). It seems simplest to use electronic transitions or the letter designation assigned by Burawoy as shown in Table 7.1 and described below.

The $n \rightarrow \pi^*$ transitions (also called R bands) of single chromophoric groups, such as the carbonyl or nitro group are forbidden and the corresponding bands are characterized by low molar absorptivities, ϵ_{max} generally less than 100. They are further characterized by the hypsochromic or blue shift observed with an in-

TABLE 7.1

Summary of Electronic Transitions

Example	Electronic Transition	λ_{max} (nm)	ϵ_{max}	Band[a]
Ethane	$\sigma \rightarrow \sigma^*$	135		
Water	$n \rightarrow \sigma^*$	167	7,000	
Methanol	$n \rightarrow \sigma^*$	183	500	
1-Hexanethiol	$n \rightarrow \sigma^*$	224	126	
n-Butyl iodide	$n \rightarrow \sigma^*$	257	486	
Ethylene	$\pi \rightarrow \pi^*$	165	10,000	
Acetylene	$\pi \rightarrow \pi^*$	173	6,000	
Acetone	$\pi \rightarrow \pi^*$	~150		
	$n \rightarrow \sigma^*$	188	1,860	
	$n \rightarrow \pi^*$	279	15	*R*
1,3-Butadiene	$\pi \rightarrow \pi^*$	217	21,000	*K*
1,3,5-Hexatriene	$\pi \rightarrow \pi^*$	258	35,000	*K*
Acrolein	$\pi \rightarrow \pi^*$	210	11,500	*K*
	$n \rightarrow \pi^*$	315	14	*R*
Benzene	Aromatic $\pi \rightarrow \pi^*$	~180	60,000	E_1
	Aromatic $\pi \rightarrow \pi^*$	~200	8,000	E_2
	Aromatic $\pi \rightarrow \pi^*$	255	215	*B*
Styrene	Aromatic $\pi \rightarrow \pi^*$	244	12,000	*K*
	Aromatic $\pi \rightarrow \pi^*$	282	450	*B*
Toluene	Aromatic $\pi \rightarrow \pi^*$	208	2,460	E_2
	Aromatic $\pi \rightarrow \pi^*$	262	174	*B*
Acetophenone	Aromatic $\pi \rightarrow \pi^*$	240	13,000	*K*
	Aromatic $\pi \rightarrow \pi^*$	278	1,110	*B*
	$n \rightarrow \pi^*$	319	50	*R*
Phenol	Aromatic $\pi \rightarrow \pi^*$	210	6,200	E_2
	Aromatic $\pi \rightarrow \pi^*$	270	1,450	*B*

[a]The *R* band, German *radikalartig; K* band, German, *konjugierte*; *B* band, benzenoid; *E* band, ethylenic; see: A. Burawoy, *Berichte*, **63**, 3155 (1930); *J. Chem. Soc.*, 1177 (1939); also see the chapter by E. A. Braude listed in the reference section.

crease in solvent polarity. They frequently remain in the spectrum when modifications in molecular structure introduce additional bands at shorter wavelengths. When additional bands make their appearance, the $n \rightarrow \pi^*$ transition is shifted to a longer wavelength but may be submerged by more intense bands.

Bands attributed to $\pi \rightarrow \pi^*$ transitions (*K* bands) appear in the spectra of molecules that have conjugated

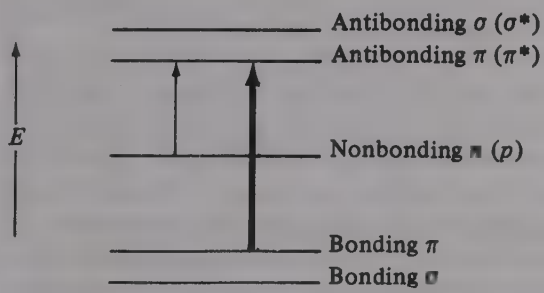

FIGURE 7.5. Summary of electronic energy levels. Both $n \rightarrow \pi^*$ and $\pi \rightarrow \pi^*$ (heavy arrow) transitions are represented.

π systems such as butadiene or mesityl oxide. Such absorptions also appear in the spectra of aromatic molecules possessing chromophoric substitution—styrene, benzaldehyde, or acetophenone. These $\pi \rightarrow \pi^*$ transitions are usually characterized by high molar absorptivity, $\epsilon_{max} > 10{,}000$.

The $\pi \rightarrow \pi^*$ transitions (*K* bands) of conjugated di- or polyene systems can be distinguished from those of enone systems by observing the effect of changing solvent polarity. The $\pi \rightarrow \pi^*$ transitions of diene or polyene systems are essentially unresponsive to solvent polarity; the hydrocarbon double bonds are nonpolar. The corresponding absorptions of enones, however, undergo a bathochromic shift, frequently accompanied by increasing intensity, as the polarity of the solvent is increased. The red shift presumably results from a reduction in the energy level of the excited state accompanying dipole–dipole interaction and hydrogen bonding.

The effect of solvent has been measured for the $n \rightarrow \pi^*$ transition of acetone. This maximum is at

279 nm in hexane, and decreases to 272 and 264.5 nm for the solvents ethanol and water, respectively.

B bands (benzenoid bands) are characteristic of the spectra of aromatic or heteroaromatic molecules. Benzene shows a broad absorption band, containing multiple peaks or fine structure, in the near-UV region between 230 and 270 nm (ϵ of most intense peak ~255 nm). The fine structure arises from vibrational sublevels affecting the electronic transitions. When a chromophoric group is attached to an aromatic ring, the *B* bands are observed at longer wavelengths than the more intense $\pi \rightarrow \pi^*$ transitions. For example, styrene has a $\pi \rightarrow \pi^*$ transition at λ_{max} 244 nm (ϵ_{max} 12,000), and a *B* band at λ_{max} 282 nm (ϵ_{max} 450). When an $n \rightarrow \pi^*$ transition appears in the spectrum of an aromatic compound that contains $\pi \rightarrow \pi^*$ transitions (including *B* bands), the $n \rightarrow \pi^*$ transition is shifted to longer wavelengths. The characteristic fine structure of the *B* bands may be absent in spectra of substituted aromatics. The fine structure is often destroyed by the use of polar solvents.

E bands (ethylenic bands), like the *B* bands, are characteristic of aromatic structures. The E_1 and E_2 bands of benzene are observed near 180 and 200 nm, respectivley. Auxochromic substitution brings the E_2 band into the near-UV region, although in many cases it may not appear at wavelengths much over 210 nm. In auxochromic substitution, the heteroatom with the lone pair of electrons shares these electrons with the π-electron system of the ring, facilitating the $\pi \rightarrow \pi^*$ transition and thus causing a red shift of the *E* bands. The molar absorptivity of *E* bands generally varies between 2000 and 14,000.

A bathochromically displaced E_2 band is probably responsible for the intense, fine-structured bands of polynuclear aromatics. With the appearance of the *E* bands as a results of auxochromic substitution, the *B* band shifts to longer wavelengths and frequently increases in intensity. Molecules such as benzylideneacetone in which more complex conjugated chromophoric substitution occurs, produce spectra with both *E* and *K* bands; the *B* bands are obscured by the displaced *K* bands.

7.3. SAMPLE HANDLING

Ultraviolet spectra of compounds are usually determined either in the vapor phase or in solution.

A variety of quartz cells is available for the determination of spectra in the gas phase. These cells are equipped with gas inlets and outlets and have path lengths from 1.0 to 100 mm. Path lengths of 0.5–120 m can be reached by using cells containing mirrors. Cell jackets are available through which liquids may be circulated for temperature control.

Cells used for the determination of spectra in solution vary in path length from 1 to 10 cm. Quartz cells, 1-cm square, are commonly used. These require about 3 mL of solution. Filler plugs are available to reduce the volume and the path length of the 1-cm square cell. Small-volume cells with 1-cm path lengths are also available. Microcells may be used when only a small amount of solution is available: The use of a beam condenser to minimize the loss of energy is advisable when the microcells are used. Microcells with an internal width of 2 mm and a path length as short as 0.1 mm are available.

In preparing a solution, a sample is accurately weighed and made up to volume in a volumetric flask. Aliquots are then removed, and additional dilutions made until the desired concentration has been acquired. Clean cells are of utmost importance. The cells should be rinsed several times with solvent and checked for absorption between successive determinations. It may be necessary to clean the cells with a detergent or hot nitric acid to remove traces of previous samples.

Many solvents are available for use in the UV region (Fig. 7.6). Three common solvents are cyclohexane, 95% ethanol, and 1,4-dioxane. Cyclohexane may be freed of aromatic and alkene impurities by percolation through activated silica gel and is transparent down to about 210 nm. Aromatic compounds, particularly the polynuclear aromatics, are usually soluble and their spectra generally retain their fine-line structure when determined in cyclohexane. The fine structure is often lost in more polar solvents.

Ninety-five percent ethanol is generally a good choice when a more polar solvent is required. If absolute ethanol contains benzene used in its preparation, the last traces can be removed by careful fractionation. The lower limit of transparency for ethanol is near 210 nm.

1,4-Dioxane can be purified by distillation from sodium. Benzene contamination can be removed by the addition of methanol followed by distillation to remove the benzene–methanol azeotrope. 1,4-Dioxane is transparent down to about 220 nm.

Many types of "spectral grade" solvents for UV analysis are now commercially available. These are usually highly purified and are free of interfering absorptions in the shaded regions indicated in Figure 7.6. Care should be exercised to choose a solvent that will be inert to the solute. For example, the spectra of aldehydes should not be determined in alcohols. Photochemical reactions may be detected by checking for changes in absorbance with time after exposure to the UV beam in the instrument.

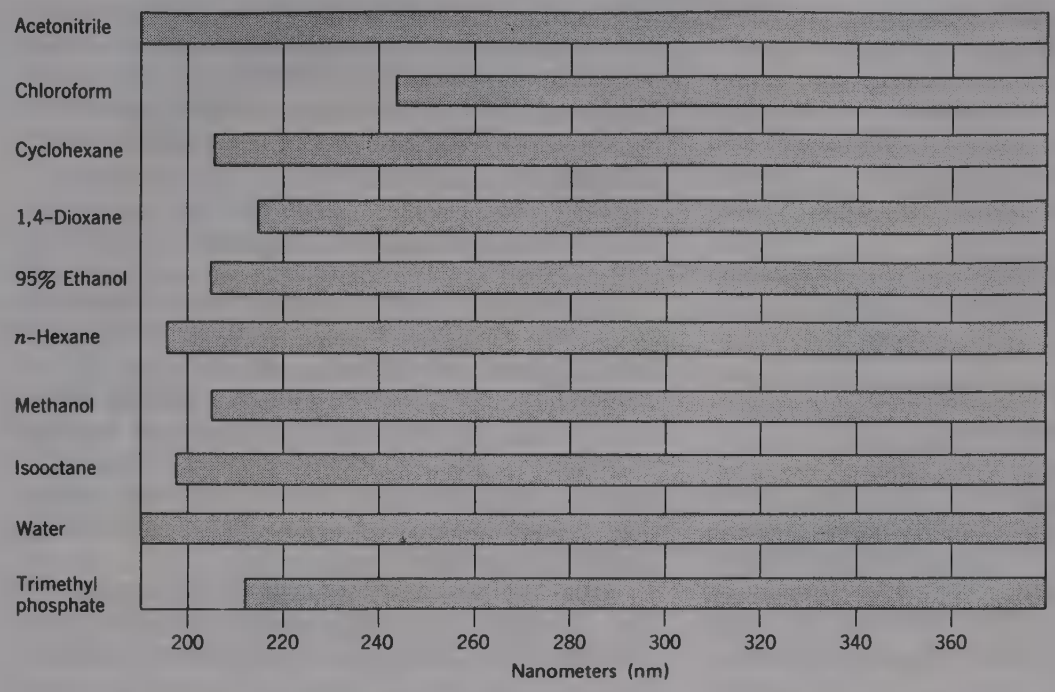

FIGURE 7.6. Useful transparency ranges of solvents in near-UV region.

7.4. CHARACTERISTIC ABSORPTION OF ORGANIC COMPOUNDS

In our discussion of the theory of electronic or UV spectra, it was shown that the ability of an organic compound to absorb UV radiation is dependent on its electronic structure. In the following sections we shall discuss the characteristic absorption of basic electronic structures and the effects of molecular geometry and substitution on the absorption.

7.4.1. Compounds Containing Only σ Electrons

Saturated hydrocarbons contain σ electrons exclusively. Since the energy required to bring about a $\sigma \rightarrow \sigma^*$ transition is of the order of 185 kcal/mol and is available only in the far (vacuum)-UV region, saturated hydrocarbons are transparent in the near-UV region and thus can be used as solvents.

7.4.2. Saturated Compounds Containing n Electrons

Saturated compounds containing heteroatoms, such as oxygen, nitrogen, sulfur, or the halogens, possess nonbonding electrons (n or p electrons) in addition to σ electrons. The $n \rightarrow \sigma^*$ transition requires less energy than the $\sigma \rightarrow \sigma^*$ transition (see Fig. 7.5), but the majority of compounds in this class still show no absorption in the near UV.

Alcohols and ethers absorb at wavelengths shorter than 185 nm (Table 7.2) and therefore are commonly used for work in the near-UV region. When these com-

TABLE 7.2

Absorption Characteristics of Saturated Compounds Containing Heteroatoms ($n \rightarrow \sigma^*$)

Compound	λ_{max} (nm)[a]	ϵ_{max}	Solvent
Methanol	177	200	Hexane
Di-*n*-butyl sulfide	210	1200	Ethanol
	229 (s)		
Di-*n*-butyl disulfide	204	2089	Ethanol
	251	398	
1-Hexanethiol	224 (s)	126	Cyclohexane
Trimethylamine	199	3950	Hexane
N-Methylpiperidine	213	1600	Ether
Methyl chloride	173	200	Hexane
n-Propyl bromide	208	300	Hexane
Methyl iodide	259	400	Hexane
Diethyl ether	188	1995	Gas phase
	171	3981	

[a]Shoulder inflection is represented by (s).

pounds are used as solvents, the intense absorption extends into the near UV, producing end absorption or cut-off in the 200–220 nm region (Fig. 7.6).

Sulfides, disulfides, thiols, amines, bromides, and iodides may show weak absorption in the near UV. Frequently, the absorption appears only as a shoulder or an inflection so that its diagnostic value is questionable.

Absorption data for several saturated compounds bearing heteroatoms are presented in Table 7.2.

7.4.3. Compounds Containing π Electron Chromophores

The absorption characteristics of a list of compounds containing single, isolated chromophoric groups are presented in Table 7.3. All the compounds contain π electrons, and many also contain nonbonding electron pairs. An examination of the absorption data shows that many of these single chromophoric groups absorb strongly in the far-UV region with no absorption in the near UV. Those groups containing both π and n electrons can undergo three transitions: $n \rightarrow \sigma^*$, $\pi \rightarrow \pi^*$, and $\sigma \rightarrow \pi^*$. Weak absorption of single chromophores in the near-UV region results from the low-energy, forbidden $n \rightarrow \pi^*$ transition.

7.4.3.1. Ethylenic Chromophore

The isolated ethylenic chromophore is responsible for intense absorption that almost always occurs in the far-UV region. Absorption is due to a $\pi \rightarrow \pi^*$ transition. Ethylene in the vapor phase absorbs at 165 nm (ϵ_{max} 10,000). A second band near 200 nm has been attributed to the elevation of two π electrons to π^* orbitals. The intensity of alkene absorption is essentially independent of solvent because of the nonpolar nature of the alkene bond.

Alkyl substitution of the parent compound moves the absorption to longer wavelengths. The bathochromic effect is progressive as the number of alkyl

TABLE 7.3

Absorption Data for Isolated Chromophores

Chromophoric Group	System	Example	λ_{max} (nm)	ϵ_{max}	Transition	Solvent
Ethylenic	RCH=CHR	Ethylene	165	15,000	$\pi \rightarrow \pi^*$	Vapor
			193	10,000	$\pi \rightarrow \pi^*$	
Acetylenic	R—C≡C—R	Acetylene	173	6,000	$\pi \rightarrow \pi^*$	Vapor
Carbonyl	$RR_1C{=}O$	Acetone	188	900	$\pi \rightarrow \pi^*$	*n*-Hexane
			279	15	$n \rightarrow \pi^*$	
Carbonyl	RHC=O	Acetaldehyde	290	16	$n \rightarrow \pi^*$	Heptane
Carboxyl	RCOOH	Acetic acid	204	60	$n \rightarrow \pi^*$	Water
Amido	$RCONH_2$	Acetamide	<208		$n \rightarrow \pi^*$	
Azomethine	>C=N—	Acetoxime	190	5,000	$\pi \rightarrow \pi^*$	Water
Nitrile	—C≡N	Acetonitrile	<160		$\pi \rightarrow \pi^*$	
Azo	—N=N—	Azomethane	347	4.5	$n \rightarrow \pi^*$	Dioxane
Nitroso	—N=O	Nitrosobutane	300	100		Ether
			665	20		
Nitrate	$-ONO_2$	Ethyl nitrate	270	12	$n \rightarrow \pi^*$	Dioxane
Nitro	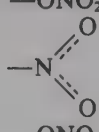	Nitromethane	271	18.6	$n \rightarrow \pi^*$	Alcohol
Nitrite	—ONO	Amyl nitrite	218.5	1,120	$\pi \rightarrow \pi^*$	Petroleum ether
			346.5[a]		$n \rightarrow \pi^*$	
Sulfoxide	S=O	Cyclohexyl methyl sulfoxide	210	1,500		Alcohol
Sulfone	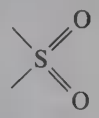	Dimethyl sulfone	<180			

[a]Most intense peak of fine structure group.

Source: A. E. Gillam and E. S. Stern, *An Introduction to Electronic Absorption Spectroscopy in Organic Chemistry*, 2nd ed., London: Edward Arnold, 1957.

groups increases. A double-bond exocyclic to two rings absorbs near 204 nm. The bathochromic shift accompanying alkyl substitution results from hyperconjugation in which the σ electrons of the alkyl group are mobile enough to interact with the chromophoric group.

Attachment of a heteroatom bearing a nonbonded electron pair to the ethylenic linkage brings about a bathochromic shift. Nitrogen and sulfur atoms are most effective, bringing the absorption well into the near-UV region. Methyl vinyl sulfide, for example, absorbs at 228 nm (ϵ_{max} 8000).

The absorption characteristics of cycloalkenes resemble those of the acyclic compounds, the absorption bearing no apparent relationship to ring size.

When two or more ethylenic linkages appear in a single molecule, isolated from one another by at least one methylene group, the molecule absorbs at the same position as the single ethylenic chromophore. The intensity of absorption is proportional to the number of isolated chromophoric groups in the molecule.

Allenes, which possess the C=C=C unit, show a strong absorption band in the far-UV region near 170 nm, with a shoulder on the long wavelength side sometimes extending into the near-UV region.

The alkene bond is described by two π orbitals of different energy, bonding and antibonding. In conjugated diene molecules such as 1,3-butadiene, when coplanarity permits, there is an effective overlap of π orbitals resulting in a π–π conjugated system (I).

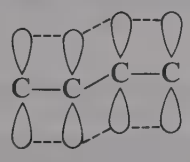

I

This overlap or interaction results in the creation of two new energy levels in butadiene (II). Thus, the $\pi_2 \rightarrow \pi_3^*$ transition of butadiene is bathochromically shifted relative to the $\pi \rightarrow \pi^*$ transition of ethylene.

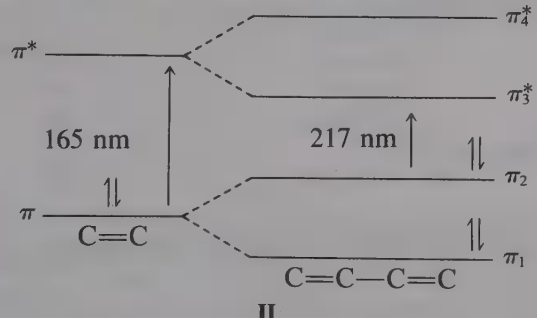

II

There are other $\pi \rightarrow \pi^*$ transitions possible in the conjugated system. Their intensities depend on the "allowedness" of the transitions.

Acyclic conjugated dienes show intense $\pi \rightarrow \pi^*$ transition bands (K bands) in the 215–230-nm region. 1,3-Butadiene absorbs at 217 nm (ϵ_{max} 21,000). Further conjugation, in open-chain trienes and polyenes, results in additional bathochromic shifts accompanied by increases in absorption intensity. The spectra of polyenes are characterized by fine structure, particularly when the spectra are determined in the vapor phase or in nonpolar solvents. Absorption data for several conjugated alkenes are presented in Table 7.4.

The bathochromic effect of alkyl substitution in 1,3-butadiene is apparent from the data for 2,3-dimethyl-1,3-butadiene.

In cases where cis and trans isomers are possible, the trans isomer absorbs at the longer wavelength with the greater intensity (see Table 7.20). This difference becomes more pronounced as the length of the conjugated system increases. Coplanarity is required for the most effective overlap of the π orbitals and lower energy of the $\pi \rightarrow \pi^*$ transition. Of the two isomers, the cis (Z) isomer is more likely to be forced into a nonplanar conformation by steric effects (see discussion of stilbene below). The greater absorption intensity of the trans (E) isomer results from the greater overall magnitude of the transition moment of the excited molecule.

An empirical method for predicting the bathochromic effect of alkyl substitution in 1,3-butadiene has been formulated by Fieser and Woodward. These rules can be summarized as follows: (1) Each alkyl group, or ring residue, attached to the parent diene (1,3-butadiene) shifts the absorption 5 nm toward the long wavelength region. (2) The creation of an exocyclic double bond causes an additional bathochromic shift of 5 nm, the shift being 10 nm if the double bond is exocyclic to two rings. For example, 217 + (2 × 5) is the predicted λ_{max} value for 2,3-dimethyl-1,3-butadiene; the observed λ_{max} is 226 nm.

Examination of the data in Table 7.4 shows a marked

TABLE 7.4.

Absorption Data for Conjugated Alkenes

$\pi \rightarrow \pi^*$ Transition (K Band)

Compound	λ_{max} (nm)	ϵ_{max}	Solvent
1,3-Butadiene	217	21,000	Hexane
2,3-Dimethyl-1,3-butadiene	226	21,400	Cyclohexane
1,3,5-Hexatriene	253	~50,000	Isooctane
	263	52,500	
	274	~50,000	
1,3-Cyclohexadiene	256	8,000	Hexane
1,3-Cyclopentadiene	239	3,400	Hexane

bathochromic shift and a decrease in absorption intensity for the conjugated, monocyclic diene system compared with 1,3-butadiene. Butadiene exists in the preferred *s*-trans (*transoid*) conformation, whereas the cyclic dienes are forced into an *s*-cis (*cisoid*) conformation. The reason for the bathochromic shift in the *s*-cis structure brought about by cyclization is not clear. The decrease in intensity is more easily explained, since the transition moment of the cyclic or homoannular system is less than that of the acyclic or the heteroannular systems.

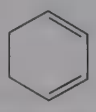

Homoannular

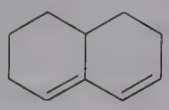

Heteroannular

Heteroannular and acyclic dienes usually display molar absorptivities in the 8000–20,000 range, whereas homoannular dienes usually display molar absorptivities in the 5000–8000 range.

Rules for predicting the position of absorption of homo- and heteroannular systems are due largely to the work of Fieser. These rules are summarized in Table 7.5.

Poor correlations are obtained when the data of Table 7.5 are applied to cross-conjugated polyene systems such as

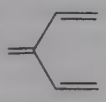

The value of these rules in structural studies of natural products will be obvious from two examples:

EXAMPLE 1

Cholesta-3,5-diene

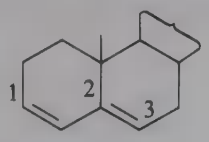

Calc λ_{max}	214 (base)	
	+ 15 (3 ring residues, 1, 2, 3)	
	+ 5 (1 exocyclic C=C)	
	234	

Obs λ_{max} = 235 nm (ϵ_{max} 19,000)

EXAMPLE 2

Cholesta-2,4-diene

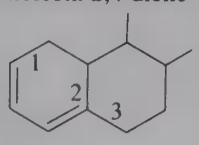

Calc λ_{max}	253 (base)	
	+ 15 (3 ring residues, 1, 2, 3)	
	+ 5 (1 exocyclic C=C)	
	273	

Obs λ_{max} = 275 nm (ϵ_{max} 10,000)

The examples above illustrate the typically much higher molar absorptivity of the heteroannular (*transoid*) diene compared to the homoannular (*cisoid*) diene.

The rules outlined in Table 7.5 work reasonably well for conjugated systems of four double bonds or less. If a conjugated polyene contains more than four double bonds, the Fieser–Kuhn rules are used. In this approach both the λ_{max} and ϵ_{max} are related to the number of conjugated double bonds, as well as other structural units, by the following equations:

$$\lambda_{max} = 114 + 5M + n(48.0 - 1.7n) - 16.5R_{endo} - 10R_{exo}$$

$$\epsilon_{max} = (1.74 \times 10^4)n$$

where n = number of conjugated double bonds
M = number of alkyl or alkyl like substituents on the conjugated system
R_{endo} = number of rings with endocyclic double bonds in the conjugated system
R_{exo} = number of rings with exocyclic double bonds

TABLE 7.5

Rules of Diene Absorption[a]

Base value for heteroannular diene	214
Base value for homoannular diene	253
Increments for	
Double bond extending conjugation	+30
Alkyl substituent or ring residue	+5
Exocyclic double bond	+5
Polar groupings: OAc	+0
OAlk	+6
SAlk	+30
Cl, Br	+5
$N(Alk)_2$	+60
Solvent correction[b]	+0
λ_{calc} = Total	

[a]See L. M. Fieser and M. Fieser, *Steroids*. New York: Reinhold, 1959, pp. 15–24; R. B. Woodward, *J. Am. Chem. Soc.*, **63**, 1123 (1941); **64**, 72, 76 (1942); A. I. Scott, *Interpretation of the Ultraviolet Spectra of Natural Products*. New York: Pergamon (Macmillan), 1964.

[b]Solvents have negligible effects upon the λ_{max} of these $\pi \rightarrow \pi^*$ transitions.

The equations may be applied to lycopene as follows:

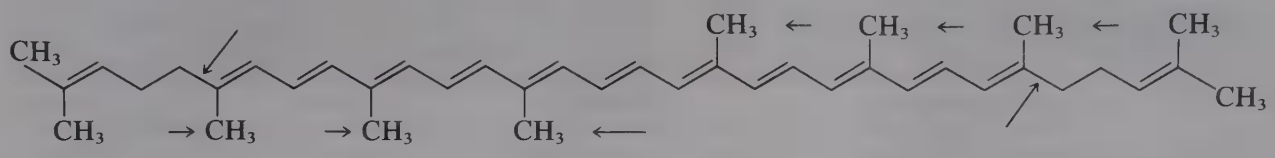

Lycopene

Since only the 11 internal double bonds of the 13 double bonds of lycopene are conjugated, $n = 11$. In addition, since there are 8 substituents (arrows: methyl groups and chain residues) on the polyene system, then $M = 8$. Finally, since there are no ring systems, there are neither exocyclic nor endocyclic double bonds in this conjugated system and $R_{exo} = R_{endo} = 0$. Thus,

$$\lambda_{max}^{calc} = 114 + 5(8) + 11[48.0 - 1.7(11)] - 0 - 0$$
$$= 476 \text{ nm}$$
$$\lambda_{max}^{obs} = 474 \text{ nm (hexane)}$$
$$\epsilon_{max}^{cal} = 1.74 \times 10^4(11) = 19.1 \times 10^4$$
$$\epsilon_{max}^{obs} = 18.6 \times 10^4 \text{ (hexane)}$$

A similar calculation can be carried out for β-carotene:

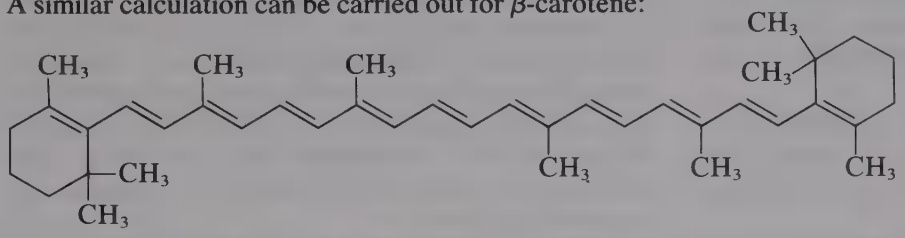

β-Carotene

$\lambda_{max}^{calc} = 453.3$ nm $\quad \epsilon_{max}^{calc} = 19.1 \times 10^4$

$\lambda_{max}^{obs} = 452$ nm (hexane) $\quad \epsilon_{max}^{obs} = 15.2 \times 10^4$

7.4.3.2. Alkyne Chromophore

The absorption characteristics of the alkyne chromophore are more complex than those of the ethylenic chromophore. Acetylene shows a relatively weak band at 173 nm resulting from a $\pi \rightarrow \pi^*$ transition. Conjugated polyynes show two principal bands in the near UV, which are characterized by fine structure. The short-wavelength band is extremely intense, and all of these bands arise from $\pi \rightarrow \pi^*$ transitions. Typical absorption data for conjugated polyynes are shown in Table 7.6.

TABLE 7.6

Absorption Data for Conjugated Polyynes

Polyynes	λ_{max} (nm)	ϵ_{max}	λ_{max} (nm)	ϵ_{max}
2,4-Hexadiyne			227	360
2,4,6-Octatriyne	207	135,000	268	200
2,4,6,8-Decatetrayne	234	281,000	306	180

7.4.3.3. Carbonyl Chromophore

The carbonyl group contains, in addition to a pair of σ electrons, a pair of π electrons and two pairs of nonbonding (n or p) electrons. Saturated ketones and aldehydes display three absorption bands, two of which are observed in the far-UV region. A $\pi \rightarrow \pi^*$ transition absorbs strongly near 150 nm; an $n \rightarrow \sigma^*$ transition absorbs near 190 nm. The third band (R band) appears in the near UV in the 270–300 nm region. The R band is weak ($\epsilon_{max} < 30$) and results from the forbidden transition of a loosely held n electron to the π^* orbital, the lowest unoccupied orbital of the carbonyl group. R bands undergo a blue shift as the polarity of the solvent is increased. Acetone absorbs at 279 nm in hexane; in water the λ_{max} is 264.5 nm. The blue shift results from hydrogen bonding, which lowers the energy of the n orbital. The blue shift can be used as a measure of the strength of the hydrogen bond.

SATURATED KETONES AND ALDEHYDES. Absorption data for several saturated ketones and aldehydes are presented in Table 7.7.

TABLE 7.7

Absorption Data for Saturated Aldehydes and Ketones

	$n \rightarrow \pi^*$ Transition (R Band)		
Compound	λ_{max} (nm)	ϵ_{max}	Solvent
Acetone	279	13	Isooctane
Ethyl methyl ketone	279	16	Isooctane
Diisobutyl ketone	288	24	Isooctane
Hexamethylacetone	295	20	Alcohol
Cyclopentanone	299	20	Hexane
Cyclohexanone	285	14	Hexane
Acetaldehyde	290	17	Isooctane
Propionaldehyde	292	21	Isooctane
Isobutyraldehyde	290	16	Hexane

The bathochromic effect accompanying the introduction of larger and more highly branched alkyl groups in the aliphatic ketones can be seen from the data in Table 7.7.

The $n \rightarrow \pi^*$ absorption of ketones and aldehydes is weak. Spectra of derivatives, such as the semicarbazones or 2,4-dinitrophenylhydrazones, are often used for identification work.

The introduction of an α-halogen atom in an aliphatic ketone has little effect on the $n \rightarrow \pi^*$ transition. However, α substitution of halogen atoms in saturated cyclic ketones has a marked effect on the absorption characteristics (Table 7.8). The λ_{max} of the parent compound is reduced by 5–10 nm when the substituent is equatorial (eq) and a bathochromic shift of 10–30 nm occurs when the substituent is axial. The bathochromic shift is usually accompanied by a strong hyperchromic effect. These effects have been used in the structure determination of halogenated steroids and terpenes. Some sort of conformational rigidity must be present in the cyclohexanone system so that the substituent, X, is clearly either in an equatorial or an axial position.

The attachment of groups containing lone electron pairs to carbonyl groups has a marked effect upon the

TABLE 7.8

Shifts in Absorption Maxima for Substituted Cyclohexanones[a]

X	eq	ax
—Cl	− 7	+22
—Br	− 5	+28
—OH	−12	+17
$—O_2CCH_3$	− 5	+10

[a]eq = equatorial; ax = axial.

TABLE 7.9

$n \rightarrow \pi^*$ Transitions (R Bands) of Simple Carbonyl-Containing Compounds

Compound	λ_{max} (nm)[a]	ϵ_{max}	Solvent[b]
Acetaldehyde	293	11.8	Hexane
Acetic acid	204	41	Ethanol
Ethyl acetate	207	69	Pet. ether[b]
Acetamide	220 (s)		Water
Acetyl chloride	235	53	Hexane
Acetic anhydride	225	47	Isooctane
Acetone	279	15	Hexane

[a]Shoulder inflection is represented by (s).
[b]Pet. ether = petroleum ether.

$n \rightarrow \pi^*$ transition. The R band is shifted to shorter wavelengths with little effect upon intensity. The shift in absorption results from a combination of inductive and resonance effects. Substitution may change the energy levels of both the ground state and the excited state, but the important factor is the relative energies of the two levels. Absorption values for the $n \rightarrow \pi^*$ transitions of several simple carbonyl compounds are presented in Table 7.9.

α-DIKETONES AND α-KETO ALDEHYDES. Acyclic α-diketones, such as biacetyl, exist in the s-trans conformation (with a dihedral angle, ϕ, of 180°).

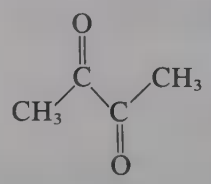

$\phi = \sim 180°$
$\lambda_{max} = 450$ nm
$\epsilon = 10$

s-trans

The spectrum of biacetyl shows the normal weak R band at 275 nm and a weak band near 450 nm resulting from interaction between the carbonyl groups. The position of the long-wavelength band of α-diketones incapable of enolization reflects the effect of coplanarity upon resonance, and hence depends on the dihedral angle ϕ between the carbonyl groups (**I**, **II**, **III**):

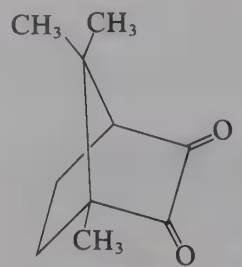

I Camphorquinone
$\phi = 0–10°$ λ_{max} 488 nm
$\epsilon = 17$

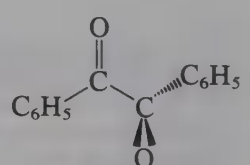

II Benzil
$\phi = 90°$ λ_{max} 370 nm
$\epsilon = 40$

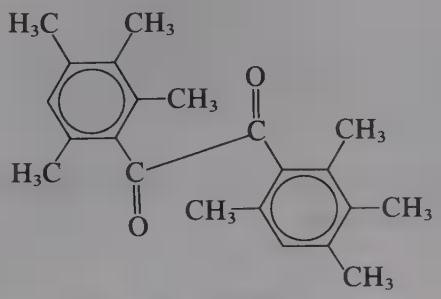

III Isoduril
$\phi = 180°$ λ_{max} 490 nm

Cyclic α-diketones with α-hydrogen atoms exist in the enolic form, for example, diosphenol. The absorption characteristics of diosphenol appear later in this chapter.

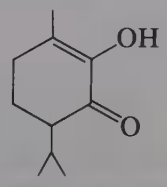

Diosphenol

β-DIKETONES. The UV spectra of β-diketones depend on the degree of enolization. The enolic form is stabilized when steric considerations permit intramolecular hydrogen bonding. Acetylacetone is a classic example. The enolic species exists to the extent of about 15% in aqueous solution and 91–92% in the vapor phase or in solution in nonpolar solvents. The absorption is directly dependent on the concentration of the enol tautomer.

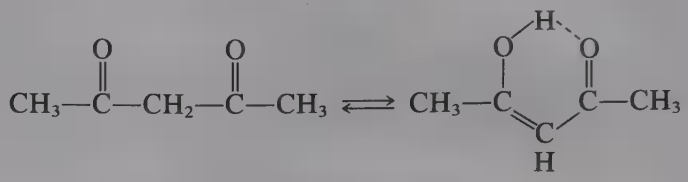

$\lambda_{max}^{H_2O}$ 274 nm, ϵ_{max} 2050

$\lambda_{max}^{isooctane}$ 272 nm, ϵ_{max} 12,000

Cyclic β-diketones, such as 1,3-cyclohexanedione, exist almost exclusively in the enolic form even in polar solvents. The enolic structures show strong absorption in the 230–260 nm region due to the $\pi \rightarrow \pi^*$ transition in the *s*-trans enone system. 1,3-Cyclohexanedione, in ethanol, absorbs at 253 nm (ϵ_{max} 22,000). The formation of the enolate ion, in alkaline solution, shifts the strong absorption band into the 270–300-nm region.

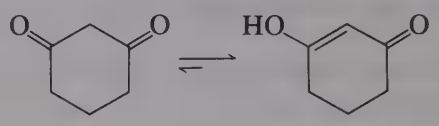

Enone

α,β-UNSATURATED KETONES and ALDEHYDES. Compounds containing a carbonyl group in conjugation with an ethylenic group are called *enones*. Spectra of enones are characterized by an intense absorption band (*K* band) in the 215–250 nm region (ϵ_{max} usually 10,000–20,000), and a weak $n \rightarrow \pi^*$ band (*R* band) at 310–330 nm. The weak *R* band is frequently poorly defined. Absorption data for several conjugated ketones and aldehydes are presented in Table 7.10.

TABLE 7.10

Absorption Data for Conjugated Ketones and Aldehydes

	K Band		*R* Band		
Compound	λ_{max} (nm)	log ϵ_{max}	λ_{max} (nm)[a]	log ϵ_{max}	Solvent
Methyl vinyl ketone	212.5	3.85	320	1.32	Ethanol
Isopropenyl methyl ketone	218	3.90	315	1.4	Ethanol
Acrolein	210	4.06	315	1.41	Water
Crotonaldehyde	220	4.17	322	1.45	Ethanol
Crotonaldehyde	214	4.20	329	1.39	Isooctane
			341	1.38	
			352 (s)	1.25	

[a]Shoulder is represented by (s).

TABLE 7.11

Effect of Solvent Polarity on the Spectrum of Mesityl Oxide

Solvent	Transition $\pi \rightarrow \pi^*$ (λ_{max} nm)[a]	Transition $n \rightarrow \pi^*$ (λ_{max} nm)[b]
Isooctane	230.6	321
Chloroform	237.6	314
Water	242.6	Submerged under *K* band

[a] *K* Band
[b] *R* Band

Since carbonyl compounds are polar, the positions of the *K* and *R* bands of enones are both dependent on the solvent. The hypsochromic effect on the *R* band with increasing solvent polarity has already been discussed.

The *K* bands of enones undergo a bathochromic shift with increasing solvent polarity. The solvent effect on the spectrum of mesityl oxide is summarized in Table 7.11.

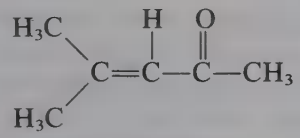

Mesityl oxide

The intensity of the *K* band may be reduced to less than 10^4 where steric hindrance prevents coplanarity. This frequently occurs in cyclic systems, such as **IV**.

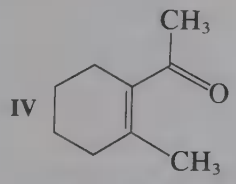

IV

λ_{max} 243 nm, ϵ_{max} 1400

Woodward has derived empirical generalizations for the effect of substitution on the position of the $\pi \rightarrow \pi^*$ transition (*K* band) in the spectra of α,β-unsaturated ketones. Changes in the positions of these bands result from α and β substitution in the basic formula

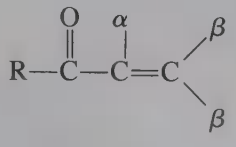

The spectra of α,β-unsaturated aldehydes are similar to those of the α,β-unsaturated ketones. The $n \rightarrow \pi^*$ bands (*R* bands) occur in the 350–370 nm region and exhibit some fine structure when the spectra are determined in nonpolar solvents.

Similar rules apply to the cyclopentenone system.

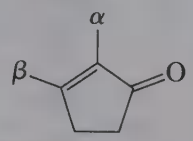

Parent system	214[a]
α or β substituent	224
α, β substituents	236

More extensive rules of enone absorption have been summarized by Fieser. These rules appear as Table 7.12.

TABLE 7.12

Rules of Enone and Dienone Absorption (α,β-Unsaturated Carbonyl Compounds)

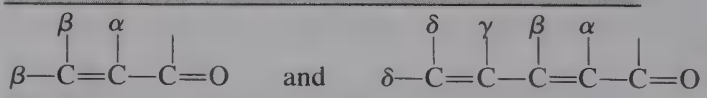

Enone and Dienone

		(nm)
Base values		
Acyclic α,β-unsaturated ketones		215
Six-membered cyclic α,β-unsaturated ketones		215
Five-membered cyclic α,β-unsaturated ketones		202
α,β-Unsaturated aldehydes		210
α,β-Unsaturated carboxylic acids and esters		195
Increments for		
Double bond extending conjugation		+30
Alkyl group, ring residue	α	+10
	β	+12
	γ and higher	+18
Polar groupings: —OH	α	+35
	β	+30
	δ	+50
—OAc	α,β,δ	+ 6
—OMe	α	+35
	β	+30
	γ	+17
	δ	+31
—SAlk	β	+85
—Cl	α	+15
	β	+12
—Br	α	+25
	β	+30
$—NR_2$	β	+95

Exocyclic double bond	+5
Homodiene component[a]	+39
Solvent correction (see table below)	Variable
λ_{calc} = Total[b]	

[a]Two conjugated double bonds, both in the same ring.
[b]The calculated values usually fall within ±3 nm of the observed values. The molar absorptivities of *cisoid* enones are usually less than 10,000, whereas the molar absorptivities of *transoid* enones are greater than 10,000.

Solvent Corrections (Enones)[a]

Solvent	Correction (nm)
Ethanol	0
Methanol	0
Dioxane	+5
Chloroform	+1
Ether	+7
Water	−8
Hexane	+11
Cyclohexane	+11

[a]For example, if the absorption was determined in cyclohexane, 11 nm would be added to the observed $\lambda_{max}^{cyclohexane}$ to compare it to a calculated λ_{max}^{EtOH}.

A few examples will serve to illustrate the usefulness of these correlations.

EXAMPLE 1

1-Acetylcyclohexene

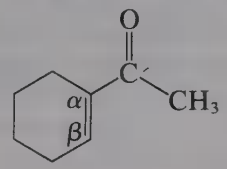

Calc λ_{max}^{EtOH}	215 (base)
	10 (α substituent)
	12 (β substituent)
	237

Obs λ_{max}^{EtOH} = 232 nm

EXAMPLE 2

Cholesta-1,4-dien-3-one

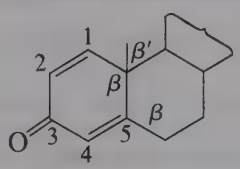

Calc λ_{max}^{EtOH}	215 (base, $\Delta^{4,5}$ system)
	24 (2 β substituents)
	5 (1 exocyclic C=C)
	244

Obs λ_{max}^{EtOH} = 245 nm

Cross-conjugation has little effect on the λ_{max} of cholesta-1,4-diene-3-one. The calculations used were for an enone (β,β disubstituted) with no correction required for the 1,2 double bond or for the β' group. The corresponding calculation using the $\Delta^{1,2}$ system yields 227 nm as the predicted λ_{max}; this is an indication that, when such a choice is presented, the more reliable prediction arises from the system that is more highly substituted (longer wavelength $\pi \rightarrow \pi^*$ transition).

EXAMPLE 3

Enol of 1,2-cyclopentanedione

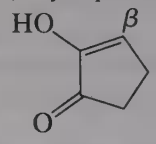

Calc λ_{max}^{EtOH}	202 (base)
	12 (β substituent)
	35 (α-OH)
	249

Obs λ_{max}^{EtOH} = 247 nm

EXAMPLE 4

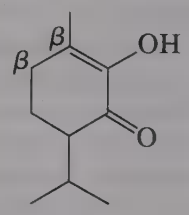

Diosphenol

Calc λ_{max}^{EtOH}	215 (base)
	24 (2β substituents)
	35 (α-OH)
	274

Obs λ_{max}^{EtOH} = 270 nm

The spectrum of *p*-benzoquinone is similar to

p-Benzoquinone

that of a typical α,β-unsaturated ketone, the strong *K* band appearing at 245 nm with a weak *R* band near 435 nm.

There are cases where the C=O and the C=C are nonconjugated in the formal sense but where interaction does occur to produce an absorption band. In structures where this occurs, the C=O and C=C groups must be oriented so that there can be effective overlap of the π orbitals. For example, the structure

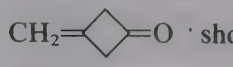

shows a moderately strong band near 214 nm with a normal weak *R* band at 284 nm. Similar effects are observed when there can be effective overlap of the π orbital for the C=O group and the $p(n)$ orbitals of a heteroatom. For example,

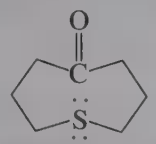

λ_{max} 238 nm, ϵ_{max} 2535

The interaction in these apparently nonconjugated systems is known as transannular conjugation.

CARBOXYLIC ACIDS. Saturated carboxylic acids show a weak absorption band near 200 nm resulting from the forbidden $n \rightarrow \pi^*$ transition. The position of the band undergoes a small bathochromic shift with an increase in chain length. This band is of little diagnostic value.

Ultraviolet analysis of acids is conducted at such a low concentration, the magnitude of the ionization constant may be changed.

α,β-Unsaturated acids display a strong *K*-band characteristic of the conjugated system. In the first member of the series, acrylic acid, the absorption occurs near 200 nm, ϵ_{max} 10,000. Alkyl substitution in this basic structure results in a bathochromic shift of the *K* band in much the same manner as observed for α,β-unsaturated ketones. The extension of conjugation produces further bathochromic shifts accompanied by an increase in the band intensity and the appearance of fine structure. The attachment of an electronegative group on the α carbon also produces a bathochromic shift. We can calculate expected maxima for the compounds described in Table 7.13, utilizing the data of Table 7.12.

The absorption characteristics of several α,β-unsaturated acids are summarized in Table 7.14.

TABLE 7.13

Absorption Maxima of Unsaturated Carboxylic Acids and Esters[a]

	λ_{max}^{EtOH} (±5 nm)
α or β Monosubstituted	208
α,β or β,β Disubstituted	217
α,β,β Trisubstituted	225
exocyclic α,β double bond	+5
endocyclic α,β double bond in five or seven-membered ring	+5

[a]Data of Table 7.12 may be applied here.

Source: A. T. Nielson, *J. Org. Chem.*, **22**, 1539 (1957).

TABLE 7.14

Absorption of α,β-Unsaturated Acids

Compound	λ_{max}^{EtOH} (nm)	ϵ_{max}
$CH_2{=}CH{-}CO_2H$	200	10,000
$CH_3CH{=}CH{-}CO_2H$ (*trans*)	205	14,000
$CH_3CH{=}CH{-}CO_2H$ (*cis*)	205.5	13,500
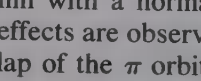	210	
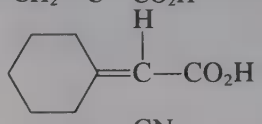	220	14,000
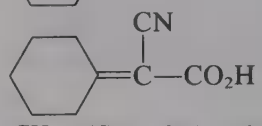	235	12,500
$CH_3{-}(CH{=}CH)_2{-}CO_2H$	254	25,000
$CH_3{-}(CH{=}CH)_3{-}CO_2H$	294	37,000
$CH_3{-}(CH{=}CH)_4{-}CO_2H$	332	49,000

ESTERS AND LACTONES. Esters and sodium salts of carboxylic acids show absorption at wavelengths and intensities comparable to the parent acid. Conjugated, unsaturated lactones display spectra similar to unsaturated esters. The spectra of simple unsaturated lactones show end absorption in the 200–240-nm region. Extended conjugation produces a bathochromic shift of the $\pi \rightarrow \pi^*$ transition (*K* band). Table 7.12 may be used to predict the maxima of such compounds.

AMIDES AND LACTAMS. α,β-Unsaturated amides and lactams show absorption in the near UV at λ_{max} 200–220, $\epsilon_{max} < 10{,}000$. α,β-Unsaturated lactams show a second band near 250 nm ($\epsilon_{max} \sim 1000$).

7.4.3.4. Azomethines (Imines) and Oximes

These structures show only weak absorption in the near UV unless the $\diagdown\!\!\diagup C{=}N{-}$ group is involved in conjugation. In the spectra of conjugated azomethines

and oximes the $\pi \rightarrow \pi^*$ transition (K band) appears in the 220–230 nm region, $\epsilon_{max} > 10{,}000$. Acidification of the azomethines, producing a positive charge on the nitrogen, shifts the absorption to the 270–290 nm region. Simple imines show a weak $n \rightarrow \pi^*$ transition. For example, for $CH_3CH_2CH_2N{=}C(CH_3)_2$

λ_{max} = 246 nm (ϵ = 140, cyclohexane)
λ_{max} = 232 nm (ϵ = 200, EtOH)

7.4.3.5. Nitriles and Azo Compounds

α,β-Unsaturated nitriles absorb just inside the near-UV region, near 213 nm, $\epsilon_{max} \sim 10{,}000$.

The azo group is analogous to the ethylenic linkage with two σ bonds being replaced by two lone pairs of electrons (—$\dot{N}$=$\dot{N}$—). The $\pi \rightarrow \pi^*$ transition occurs in the far (vacuum) UV. The $n \rightarrow \pi^*$ band in aliphatic azo compounds appears near 350 nm with the expected low intensity, $\epsilon_{max} < 30$. *trans*-Azobenzene absorbs at 320 nm (ϵ_{max} 21,000). Comparable absorption for *trans*-stilbene occurs at 295 nm (ϵ_{max} 28,000).

7.4.3.6. Compounds with N to O Bonds

Four groups contain multiple nitrogen–oxygen linkages: nitro, nitroso, nitrates, and nitrites. All of these structures show weak absorption in the near-UV region resulting from an $n \rightarrow \pi^*$ transition.

The absorption of several typical compounds containing nitrogen–oxygen linkages are presented in Table 7.15.

TABLE 7.15

Absorption of Compounds Containing Nitrogen–Oxygen Linkages

	$n \rightarrow \pi^*$ Transition (R Band)		
Compound	λ_{max} (nm)	ϵ_{max}	Solvent
Nitromethane	275	15	Heptane
2-Methyl-2-nitropropane	280.5	23	Heptane
1-Nitro-1-propene	229[a]	9400	Ethanol
	235[a]	9800	
Nitrosobutane	300	100	Ether
	665	20	
Octyl nitrate	270[b]	15	Pentane
Cyclohexyl nitrate	270[b]	22	
n-Butyl nitrite	218	1050	Ethanol
	313–384[c]	17–45	

[a]These are $\pi \rightarrow \pi^*$ transitions.
[b]This is typically a point of inflection in the spectra of nitrates.
[c]This region is one of fine structure with bands roughly 10 nm apart. The band with maximum absorption occurs at 357 nm.

The effect of conjugation upon the absorption characteristics of the nitro group is apparent from the data for 1-nitro-1-propene. The strong $\pi \rightarrow \pi^*$ transition (K band) submerges the weak $n \rightarrow \pi^*$ transition (R band).

7.4.3.7. Multiply Bonded Sulfur Groups

Aliphatic sulfones are transparent in the near-UV region. The sulfur atom in sulfones has no lone-pair electrons, and the lone pairs of electrons associated with the oxygen atoms appear to be tightly bound. In an α,β-unsaturated sulfone, such as ethyl vinyl sulfone, a band appears in the 210 nm region resulting from resonance between the S—O linkage and the ethylenic linkage.

Saturated sulfoxides absorb near 220 nm with intensities of the order of 1500. This absorption involves an $n \rightarrow \pi^*$ transition in the S=O group and thus undergoes a hypsochromic shift as solvent polarity is increased. Aromatic sulfoxides show an intense K band in addition to the displaced B band.

In compounds containing the —S(=O)—X grouping, the position of the $n \rightarrow \pi^*$ band depends on the electronegativity of X; the greater the electronegativity, the shorter will be the wavelength of absorption.

Simple thioketones of the dialkyl or alkylaryl types are unstable and generally exist as trimers. Thiobenzophenone is monomeric as are compounds in which the C=S group is attached to an electron-donating group, such as —NR_2. The $n \rightarrow \pi^*$ transition of the C=S group in thioketones occurs at a longer wavelength than the analogous C=O transition because the energy of the nonbonding electron pair of the sulfur atom lies at a higher level than the corresponding electrons of the oxygen atom. Compounds containing the C=S group also display intense bands in the 250–320 nm region, which presumably arise from $\pi \rightarrow \pi^*$ and $n \rightarrow \sigma^*$ transitions in the C=S group.

The $n \rightarrow \pi^*$ bands of some thiocarbonyl compounds are summarized in Table 7.16.

TABLE 7.16

$n \rightarrow \pi^*$ Transitions in Thiocarbonyl Compounds

	$n \rightarrow \pi^*$ Transition (R Band)	
Compound	λ_{max} (nm)[a]	log ϵ_{max}
Thiobenzophenone	599	2.81
Thioacetamide	358	1.25
Thiourea	291 (s)	1.85

[a]Shoulder is represented by (s).

TABLE 7.17

Benzene Bands			
184 nm	204 nm	256 nm	Reference
E_1	E_2	B	*a*
	K	B	*b*

[a]See E. A. Braude listed in the reference section.
[b]A. Burawoy, *Berichte*, **63**, 3155 (1930); *J. Chem. Soc.*, 1177 (1939).

7.4.3.8. Benzene Chromophore

Benzene displays three absorption bands: 184 nm (ϵ_{max} 60,000), 204 nm (ϵ_{max} 7900), and 256 nm (ϵ_{max} 200). These bands originate from $\pi \rightarrow \pi^*$ transitions. The intense band near 180 nm results from an allowed transition, whereas the weaker bands near 200 and 260 nm result from forbidden transitions in the highly symmetrical benzene molecule. Different notations have been used to designate the absorption bands of benzene; these are summarized in Table 7.17. We shall discuss these bands using Braude's *E* and *B* notation.

The *B* band of benzene and many of its homologs is characterized by considerable fine structure. This is particularly true of spectra determined in the vapor phase or in nonpolar solvents. The fine structure originates from sublevels of vibrational absorption upon which the electronic absorption is superimposed (Fig. 7.7, p. 311). In polar solvents, interactions between solute and solvent tend to reduce the fine structure.

Substitution of alkyl groups on the benzene ring produces a bathochromic shift of the *B* band, but the effect of alkyl substitution upon the *E* bands is not clearly defined. The absorption characteristics of the *B* bands of several alkylbenzenes are presented in Table 7.18.

The bathochromic shift is attributed to hyperconjugation in which the σ electrons of an alkyl C—H bond participate in resonance with the ring. The methyl group is more effective in hyperconjugation than other alkyl groups.

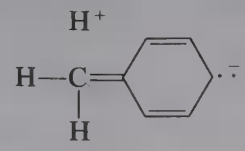

The addition of a second alkyl group to the molecule is most effective in producing a red shift if it is in the para position. The para isomer absorbs at the longest wavelength with the largest ϵ_{max}. The ortho isomer generally absorbs at the shortest wavelength with reduced ϵ_{max}. This effect is attributed to steric interactions between the ortho substituents, which effectively reduce hyperconjugation.

Substitution on the benzene ring of auxochromic groups (OH, NH_2, etc.) shifts the *E* and *B* bands to longer wavelengths, frequently with intensification of the *B* band and loss of its fine structure, because of n–π conjugation (Table 7.19).

Conversion of a phenol to the corresponding anion results in a bathochromic shift of the E_2 and *B* bands and an increase in ϵ_{max} because the nonbonding electrons in the anion are available for interaction with the π-electron system of the ring. When aniline is converted to the anilinium cation, the pair of nonbonding electrons of aniline is no longer available for interaction with the π electrons of the ring, and a spectrum almost identical to that of benzene results.

Confirmation of a suspected phenolic structure may be obtained by comparison of the UV spectra obtained for the compound in neutral and in alkaline solution (pH 13). Similar confirmatory information for a suspected aniline derivative may be obtained by a comparison of spectra determined in neutral and in acid solution (pH 1).

When the spectra of pure acid and of pure conjugate base cross at some point, the spectra of all solutions containing various ratios of these two species (and no other absorbing species) must also go through this point, the isosbestic point, provided that the sum of the concentrations of both species is constant, and that the spectral characteristics (i.e., the absorption coefficients) of both species are insensitive to the effect of pH and of the buffer used. An isosbestic point's presence can be used to verify that one is dealing with a simple acid–base reaction that is not complicated by further equilibria or other phenomena.

Interaction between the nonbonding electron pair(s) of a heteroatom attached to the ring and the π electrons of the ring is most effective when the *p* orbital of the nonbonding electrons is parallel to the π orbitals of the ring. Thus, bulky substitution in the ortho position of molecules such as *N*,*N*-dimethylaniline causes a hyp-

TABLE 7.18

Absorption Data for Alkylbenzenes (*B* Bands)		
Compound	λ_{max} (nm)[a]	ϵ_{max}
Benzene	256	200
Toluene	261	300
m-Xylene	262.5	300
1,3,5-Trimethylbenzene	266	305
Hexamethylbenzene	272	300

[a]The λ_{max} value of the most intense peak in the band with fine structure.

TABLE 7.19

Effect of Auxochromic Substitution on the Spectrum of Benzene

Compound	E_2 Band		B Band		Solvent
	λ_{max} (nm)	ϵ_{max}	λ_{max} (nm)	ϵ_{max}	
Benzene	204	7,900	256	200	Hexane
Chlorobenzene	210	7,600	265	240	Ethanol
Thiophenol	236	10,000	269	700	Hexane
Anisole	217	6,400	269	1,480	Methanol (2%)
Phenol	210.5	6,200	270	1,450	Water
Phenolate anion	235	9,400	287	2,600	Alkali (aq)
o-Catechol	214	6,300	276	2,300	Water (pH 3)
o-Catecholate anion	236.5	6,800	292	3,500	Water (pH 11)
Aniline	230	8,600	280	1,430	Water
Anilinium cation	203	7,500	254	160	Acid (aq)
Diphenyl ether	255	11,000	272	2,000	Cyclohexane
			278	1,800	

sochromic shift in the E_2 band, accompanied by a marked reduction in ϵ_{max}.

N,N-Dimethylaniline	λ_{max} 251 nm	ϵ_{max} 15,500
2-Methyl-*N,N*-dimethylaniline	λ_{max} 248 nm	ϵ_{max} 6,360

Direct attachment of an unsaturated group (chromophore) to the benzene ring produces a strong bathochromic shift of the *B* band, and the appearance of a *K* band ($\epsilon_{max} > 10{,}000$) in the 200–250-nm region (Table 7.20). The overlap of absorption positions of the *K* band, and the displaced *E* bands of auxochromically substituted benzenes, may lead to confusion in the interpretation of UV spectra. Generally *E* bands are less intense. The *B* bands are sometimes buried under the *K* bands.

The data in Table 7.20 show that in certain structures, such as acetophenone and benzaldehyde, displaced *B* and *R* bands can still be recognized.

The data of Table 7.21 allow calculation of an expected maximum for aromatic aldehydes, ketones, carboxylic acids, and esters. Application of Table 7.21 to structure confirmation is illustrated with the following examples:

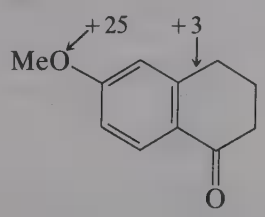

EXAMPLE 1. 6-Methyoxytetralone

Calc λ_{max}^{EtOH} = 246 (parent chromophore) + 3 (*o*-ring residue) + 25 (*p*-OMe)
= 274 nm
Obs λ_{max}^{EtOH} = 276 nm

EXAMPLE 2. 3-Carbethoxy-4-methyl-5-chloro-8-hydroxytetralone

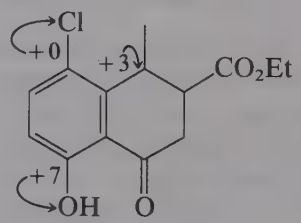

Calc λ_{max}^{EtOH} = 246 + 3 (*o*-ring residue) + 7 (*o*-OH)
= 256 nm
Obs λ_{max}^{EtOH} = 257 nm

EXAMPLE 3. 3,4-Dimethoxy-4*b*,5,6,7,8,8*a*,9,10-octahydrophenanthren-10-one

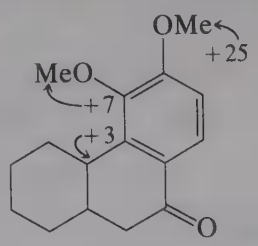

Calc λ_{max}^{EtOH} = 246 + 25 + 7 + 3 = 281 nm
Obs λ_{max}^{EtOH} = 278 nm

TABLE 7.20

Absorption Characteristics of Benzenes Substituted with Chromophores

Compound	$\pi \rightarrow \pi^*$ Transition *K* Band		*B* Band		$n \rightarrow \pi^*$ Transition *R* Band		Solvent
	λ_{max} (nm)	ϵ_{max}	λ_{max} (nm)	ϵ_{max}	λ_{max} (nm)	ϵ_{max}	
Benzene			255	215			Alcohol
Styrene	244	12,000	282	450			Alcohol
Phenylacetylene	236	12,500	278	650			Hexane
Benzaldehyde	244	15,000	280	1,500	328	20	Alcohol
Acetophenone	240	13,000	278	1,100	319	50	Alcohol
Nitrobenzene	252	10,000	280	1,000	330	125	Hexane
Benzoic acid	230	10,000	270	800			Water
Benzonitrile	224	13,000	271	1,000			Water
Diphenyl sulfoxide	232	14,000	262	2,400			Alcohol
Methyl phenyl sulfone	217	6,700	264	977			
Benzophenone	252	20,000			325	180	Alcohol
Biphenyl	246	20,000	Submerged				Alcohol
Stilbene (*cis*)	283	12,300[a]	Submerged				Alcohol
Stilbene (*trans*)	295[b]	25,000[a]	Submerged				Alcohol
1-Phenyl-1,3-butadiene							
cis-	268	18,500					Isooctane
trans-	280	27,000					Isooctane
1,3-Pentadiene							
cis-	223	22,600					Alcohol
trans-	223.5	23,000					Alcohol

[a]Intense bands also occur in the 200–230 nm region.
[b]Most intense band of fine structure.

Application of Table 7.21 does not give accurate predicted maxima for 2,6-disubstituted phenyl carbonyl compounds; that this is due to disruption of the planarity necessary for conjugation of the carbonyl and phenyl groups is supported by the large decrease in molar absorptivity accompanying such substitution.

When auxochromic groups appear on the same ring as the chromophore, both groups influence the absorption. The influence is most pronounced when an electron-donating group and electron-attracting group are para to one another (complementary substitution, Table 7.22).

The red shift and increase in intensity of the *K* band are related to contributions of the following polar resonance forms:

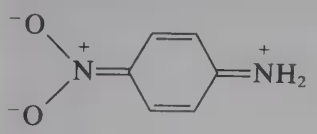

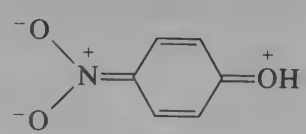

Biphenyl is the parent molecule of a series of compounds in which two aromatic rings are in conjugation. Resonance energy is at a maximum when the rings are coplanar and essentially zero when the rings are at 90° to one another.

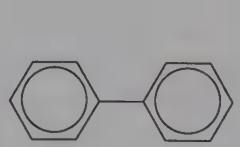

Biphenyl
K Band, λ_{max} 252 nm, ϵ_{max} 19,000

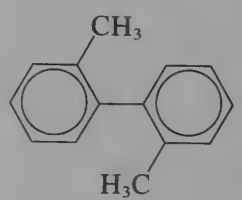

2,2′-Dimethylbiphenyl
B Band, λ_{max} 270 nm, ϵ_{max} 800

The effect of forcing the rings out of coplanarity is readily seen from a comparison of the absorption characteristics of biphenyl and its 2,2′-dimethyl homolog whose absorption characteristics are similar to those of *o*-xylene.

Introduction of a methylene group between two chromophores is capable of disrupting conjugation. Compare the data of diphenylmethane

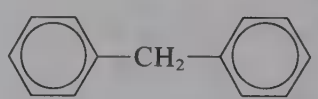

λ_{max} = 262 nm
ϵ_{max} = 5000

with the ϵ_{max} for biphenyl above and the substituted diphenylmethanes below. In some substituted diphen-

TABLE 7.21

Calculation of the Principal Band ($\pi \rightarrow \pi^*$ Transition) of Substituted Benzene Derivatives, Ar—COG (in EtOH)[a]

ArCOR/ArCHO/$ArCO_2H$/$ArCO_2R$		λ_{max}^{EtOH} (nm)
Parent chromophore: Ar = C_6H_5		
G = Alkyl or ring residue, (e.g., ArCOR)		246
G = H, (ArCHO)		250
G = OH, OAlk, ($ArCO_2H$ and $ArCO_2R$)		230
Increment for each substituent on Ar:		
—Alkyl or ring residue	o-, m-	+3
	p-	+10
—OH, —OCH_3, —OAlk	o-, m-	+7
	p-	+25
—O^- (oxyanion)	o-	+11
	m-	+20
	p-	+78[b]
—Cl	o-, m-	+0
	p-	+10
—Br	o-, m-	+2
	p-	+15
—NH_2	o-, m-	+13
	p-	+58
—$NHCOCH_3$	o-, m-	+20
	p-	+45
—$NHCH_3$	p-	+73
—$N(CH_3)_2$	o-, m-	+20
	p-	+85

[a]Use of the table is illustrated by the examples on pp. 000–000 and in A. I. Scott's book listed in the reference section.
[b]This value may be decreased markedly by steric hindrance to coplanarity.

TABLE 7.22

Absorption Characteristics of Disubstituted Benzenes

Compound	$\pi \rightarrow \pi^*$ Transition *K* band λ_{max} (nm)	*K* band ϵ_{max}	*B* Band λ_{max} (nm)	*B* Band ϵ_{max}
o-NO_2 Phenol	279	6,600	351	3,200
m-NO_2 Phenol	274	6,000	333	1,960
p-NO_2 Phenol	318	10,000	Submerged	
o-NO_2 Aniline	283	5,400	412	4,500
m-NO_2 Aniline	280	4,800	358	1,450
p-NO_2 Aniline	381	13,500	Submerged	

ylmethanes, there is an effective overlap of π orbitals of the two rings resulting in homoconjugation. The ϵ_{max} of 4-nitro-4′-methoxydiphenylmethane is not merely the sum of the ϵ_{max} of *p*-nitrotoluene and *p*-methoxytoluene.

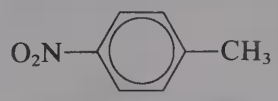

λ_{max} (nm)	ϵ_{max}
274	9490

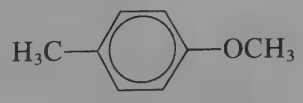

λ_{max} (nm)	ϵ_{max}
277	2190
285.5	1786

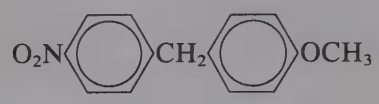

λ_{max} (nm)	ϵ_{max}
280	24,400
287	16,800

Another approach to predicting the λ_{max} of the primary band of substituted benzenes involves the use of Table 7.23. This table has been successfully used with disubstituted compounds when the following rules are used:

1. PARA SUBSTITUTION
   a. Both groups are either electron donating or electron withdrawing: Only the effect of the group causing the larger shift is used. For example, the λ_{max} of *p*-nitrobenzoic acid would be expected to be the same as that of nitrobenzene, ~(203.5 + 65.0) = ~268.5 (in alcohol solvent).
   b. One group is electron donating and the other, electron withdrawing: The calculated λ_{max} here would usually be much lower than the observed λ_{max} for the reasons that were discussed above for *p*-nitrophenol and Table 7.22. Table 7.21 may be used for some of the above compounds for which Table 7.23 cannot be used.
2. ORTHO AND META SUBSTITUTION. The shift effects are additive.

Benzenoid compounds containing three or more substituents have not been thoroughly tested by the method of Table 7.23.

The first homolog in the diphenylpolyene series $[C_6H_5(C{=}C)_nC_6H_5]$ is stilbene. Stilbene offers an interesting example of steric effects in electronic spectra.

TABLE 7.23

Calculation of the Primary Band ($\pi \rightarrow \pi^*$ Transition) of Substituted Benzenes (CH_3OH Solvent). Base Value: 203.5 nm

Substituent	Shift	Substituent	Shift	Substituent	Shift
$-CH_3$	3.0	—Br	6.5	—OH	7.0
—CN	20.5	—Cl	6.0	$-O^-$	31.5
—CHO	46.0	$-NH_2$	26.5	$-OCH_3$	13.5
$-COCH_3$	42.0	$-NHCOCH_3$	38.5		
$-CO_2H$	25.5	$-NO_2$	65.0		

Source: C. N. R. Rao, *J. Sci. Res. (India)*, **17B**, 56 (1958); *Curr. Sci. (India)*, **26**, 276 (1957).

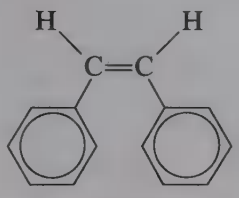

cis-Stilbene

λ_{max}^{EtOH} (nm)	ϵ_{max}
222	25,000
283	12,300

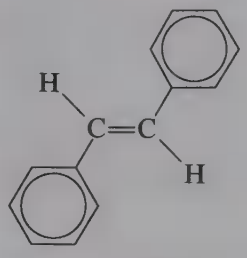

trans-Stilbene

λ_{max}^{EtOH} (nm)	ϵ_{max}
229	15,800
295	25,000
308	25,000
320 (s)	15,800

(s) = shoulder

The destruction of coplanarity by steric interference, in the cis structure, is reflected by the lower intensity of the 283-nm band compared with the corresponding band (295 nm) in the trans isomer. The *B* band appears to be swamped by this intense absorption.

The absorption bands of the parent stilbene molecule move to longer wavelengths and increase in intensity as n, in C_6H_5—$(CH{=}CH)_n$—C_6H_5, increases. When n equals 7, the molecule absorbs in the 400–465 region with ϵ_{max} 135,000.

Two common series of aromatic compounds are the linear series, such as anthracene, and the angular series such as phenanthrene. Although the polynuclear aromatics might well be treated as individual chromophores, a correlation between the bands of benzene and the acenes, as well as naphthalene, can be made. These correlations appear in Table 7.24.

As the number of condensed rings increases in the acene series, the absorption moves to progressively longer wavelengths until it occurs in the visible region.

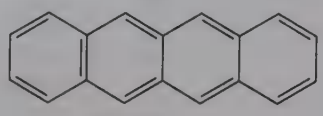

Naphthacene
(yellow)

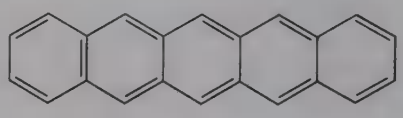

Pentacene
(blue)

The angular polycyclic compounds, the aphenes, also show a bathochromic shift of the three-band system with an increase in the number of rings. However, the increase in λ_{max}, per ring added, is less than for the acenes. The three-band system is still distinct for phenanthrene, but in the spectrum of anthracene the E_2 band has already swamped the *B* band.

TABLE 7.24

Correlation of Aromatic Absorption

Compound	E_1 Band λ_{max} (nm) (ϵ_{max})	E_2 Band λ_{max} (nm) (ϵ_{max})	*B* Band λ_{max} (nm) (ϵ_{max})	λ_{max} (nm) (ϵ_{max})
Benzene	184 (60,000)	204 (7,900)	256 (200)	
Naphthalene	221 (133,000)	286 (9,300)	312 (289)	
Anthracene	256 (180,000)	375 (9,000)	Submerged	221 (14,500)

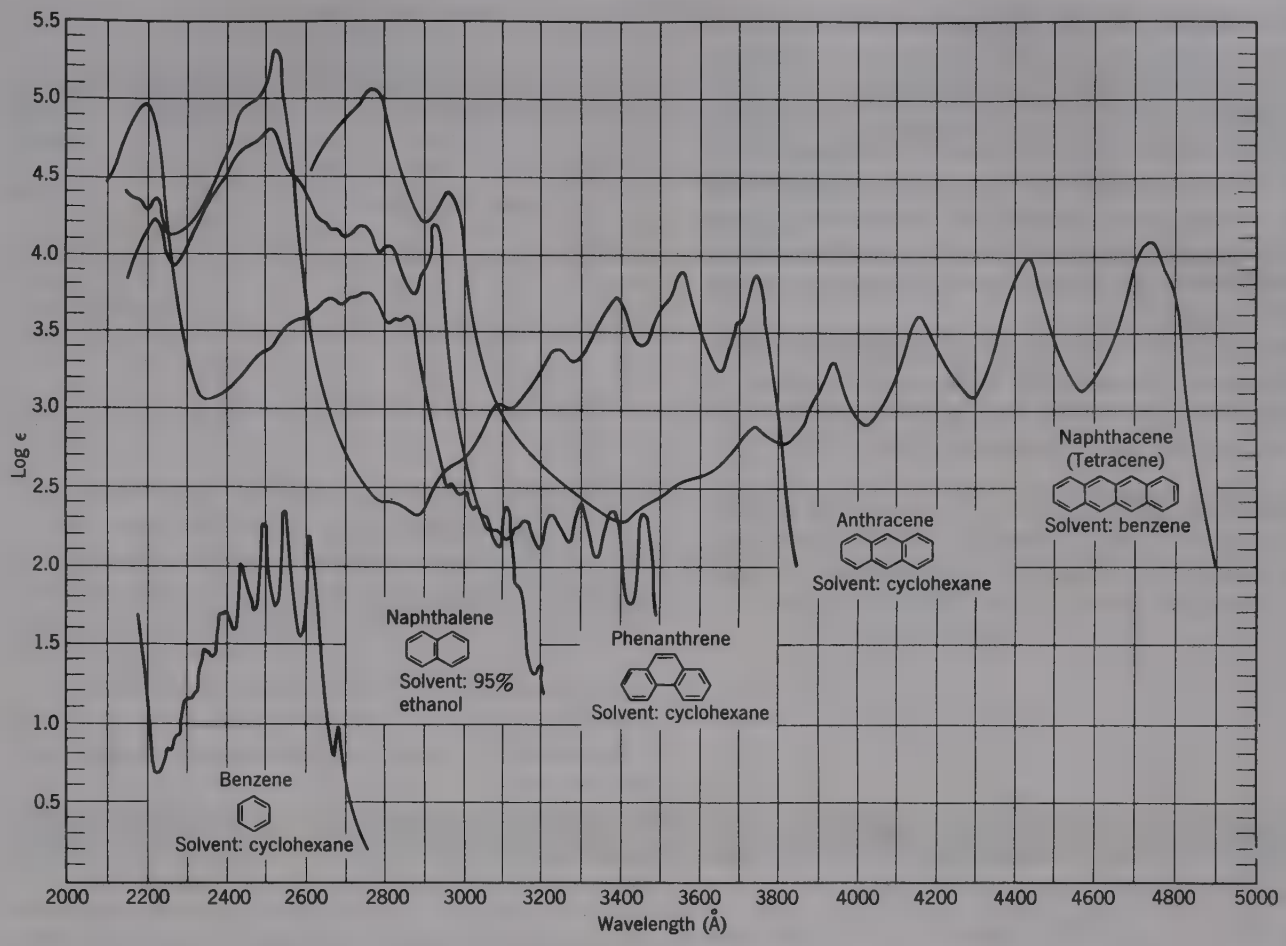

FIGURE 7.7. Electronic absorption spectra of benzene, naphthalene, phenanthrene, anthracene, and naphthacene.

The spectra of polynuclear aromatics are characterized by vibrational fine structure as observed in the spectrum of benzene. Spectra of some polynuclear aromatics are shown in Figure 7.7.

7.4.3.9. Heteroaromatic Compounds

Saturated five- and six-membered heterocyclic compounds are transparent at wavelengths longer than 200 nm. Only the unsaturated heterocyclic compounds (heteroaromatics) show absorption in the near-UV region.

FIVE-MEMBERED RINGS. The theoretical interpretation of the spectra of five-membered ring heteroaromatic compounds is not simple. The absorption of these compounds has been compared to that of cyclopentadiene, the *cis*-diene analog, which shows strong

TABLE 7.25

Absorption Data for Some Five-Membered Heteroaromatics

Compound	Band I		Band II		Solvent
	λ_{max} (nm)	ϵ_{max}	λ_{max} (nm)	ϵ_{max}	
(Cyclopentadiene)	200	10,000	238.5	3,400	Hexane
Furan	200	10,000	252	1[a]	Cyclohexane
Pyrrole	209	6,730	240	300[a]	Hexane
Thiophene	231	7,100	269.5	1.5[a]	Hexane
Pyrazole	214	3,160			Ethanol

[a]These weak bands may be due to impurities rather than a forbidden transition ($n \rightarrow \pi^*$) of a heteroaromatic molecule.

diene absorption near 200 nm, and moderately intense absorption near 238 nm. The aromatic properties increase in the order cyclopentadiene, furan, pyrrole, and thiophene. The absorption of some five-membered heteroaromatics is compared with cyclopentadiene in Table 7.25. No attempt has been made to classify the bands, although the band near 200 nm has been likened to the E_2 band of benzene, and the long-wavelength band frequently has fine structure analogous to that of the B band of benzene.

Auxochromic or chromophoric substitution of the five-membered unsaturated heterocyclics causes a bathochromic shift and an increase in the intensity of the bands of the parent molecule (Table 7.26).

SIX-MEMBERED RINGS. The spectrum of pyridine is similar to that of benzene. The B band of pyridine, however, is somewhat more intense and has less distinct fine structure than that of benzene (Fig. 7.8).

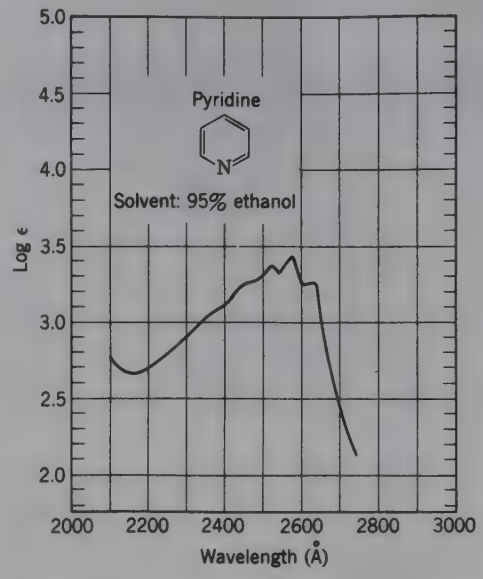

FIGURE 7.8. Ultraviolet spectrum of pyridine.

TABLE 7.26

Absorption Characteristics of Five-Membered Heteroaromatics

		Band I		Band II	
Parent	Substituent[a]	λ_{max} (nm)	ϵ_{max}	λ_{max} (nm)	ϵ_{max}
Furan		200	10,000	252	1
Furan	2-CHO	227	2,200	272	13,000
Furan	2-C(=O)—CH_3	225	2,300	270	12,900
Furan	2-CO_2H	214	3,800	243	10,700
Furan	2-NO_2	225	3,400	315	8,100
Furan	2-Br, 5-NO_2			315	9,600
Pyrrole		183		209	6,730
Pyrrole	2-CHO	252	5,000	290	16,600
Pyrrole	2-C(=O)—CH_3	250	4,400	287	16,000
Pyrrole	2-CO_2H	228	4,500	258	12,600
Pyrrole	1-C(=O)—CH_3	234	10,800	288	760
Thiophene		231	7,100		
Thiophene	2-CHO	265	10,500	279	6,500
Thiophene	2-C(=O)—CH_3	252	10,500	273	7,200
Thiophene	2-CO_2H	249	11,500	269	8,200
Thiophene	2-NO_2	268–272	6,300	294–298	6,000
Thiophene	2-Br	236	9,100		

[a]2-CHO means ■ carboxaldehyde group at the 2-position of the ring.

TABLE 7.27

Absorption Characteristics of 2-Methylpyridine

Solvent	λ_{max} (nm)	ϵ_{max}
Hexane	260	2000
Chloroform	263	4500
Ethanol	260	4000
Water	260	4000
Ethanol/HCl(1:1)	262	5200

This transition is allowed for pyridine, but forbidden for the more symmetrical benzene molecule. The weak *R* band expected for an $n \rightarrow \pi^*$ transition in pyridine has been observed in vapor phase spectra. This band is generally swamped by the more intense *B* band when the spectrum is determined in solution.

An increase in solvent polarity has little or no effect on the position or intensity of the *B* band of benzene, but produces a marked hyperchromic effect on the *B* band of pyridine and its homologs. The hyperchromic effect undoubtedly results from hydrogen bonding through the lone pair of electrons of the nitrogen atom. The extreme case is the absorption of a pyridinium salt. The absorption characteristics of 2-methylpyridine (α-picoline), in several solvents, are shown in Table 7.27.

The effect of substitution on the 257 nm band (*B* band) of pyridine is illustrated in the data presented in Table 7.28.

The absorption of the 2-OH and 4-OH pyridines is attributed to the pyridone structures. Tautomerism in hydroxy- and aminopyridines is discussed in the book by A. I. Scott (see References).

TABLE 7.28

Absorption Characteristics of Pyridine Derivatives

Derivative[a]	$\lambda_{max}^{(pH>7)}$ (nm)	ϵ_{max}
Pyridine	257	2,750
	270	450
2-CH_3	262	3,560
3-CH_3	263	3,110
4-CH_3	255	2,100
2-F	257	3,350
2-Cl	263	3,650
2-Br	265	3,750
2-I	272	400
2-OH	230	10,000
	295	6,300
4-OH	239	14,100
3-OH	260	2,200

[a]2-CH_3 means 2-methylpyridine.

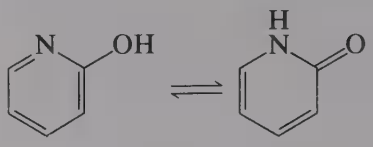

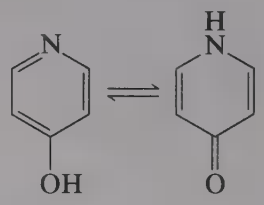

The spectra of heteroaromatics appear to be related to their isocyclic analogs (Table 7.29).

TABLE 7.29

Absorption Characteristics of Some Heteroaromatics Containing Nitrogen and Their Isocyclic Analogs

	E_1 Band[a]		E_2 Band[a]		*B* Band[a]		
Compound	λ_{max} (nm)	ϵ_{max}	λ_{max} (nm)	ϵ_{max}	λ_{max} (nm)	ϵ_{max}	Solvent
Benzene	184	60,000	204	7,900	256	200	
Naphthalene	221	100,000	286	9,300	312	280	
Quinoline	228	40,000	270	3,162	315	2,500	Cyclohexane
Isoquinoline	218	63,000	265	4,170	313	1,800	Cyclohexane
Anthracene	256	180,000	375	9,000			
Acridine	250	200,000	358	10,000			Ethanol

[a]All of the bands contain fine structure.

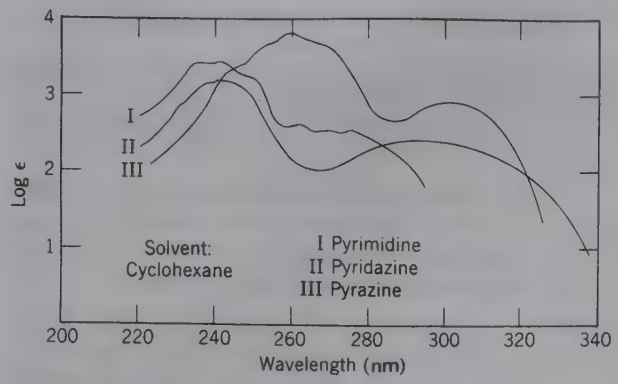

FIGURE 7.9. Ultraviolet spectra for three heteroaromatic compounds.

The spectra of the diazines are similar to those of pyridine (Fig. 7.9). In addition to the enhanced *B* band, still retaining some fine structure, the enhanced $n \rightarrow \pi^*$ bands are quite prominent.

The absorption of the diazines, for example, the pyrazines, respond to solvent polarity in a manner similar to the pyridines. The *B* band undergoes a hyperchromic effect with an increase in solvent polarity with little or no effect upon λ_{max}. The *R* band, of course, disappears in acid solution, since the nonbonding electrons of the free base are now involved in salt formation.

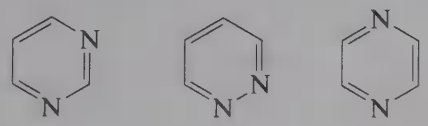

I Pyrimidine

II Pyridazine

III Pyrazine

REFERENCES

General Monographs

Jaffé, H. H. and Orchin, Milton. *Theory and Application of Ultraviolet Spectroscopy*. New York: Wiley, 1962.

Scott, A. I. *Interpretation of the Ultraviolet Spectra of Natural Products*. New York: Pergamon (Macmillan), 1964.

Stern, E. S. and Timmons, T. C. J. *Electronic Absorption Spectroscopy in Organic Chemisty*. New York: St. Martin's Press, 1971 (effectively the third edition of Gillam and Stern).

Selections from Broader References

Ayling, G. M. *Appl. Spec. Rev.*, **8**, 1 (1974).

Braude, E. A., "Ultraviolet and Visible Light Absorption," in *Determination of Organic Structures by Physical Methods*. New York: Academic, 1955, Chapter 4, pp. 131–194.

Braude, E. A. "Ultra-Violet Light Absorption and the Structure of Organic Compounds," *Ann. Rep. Progress Chem.* Chemical Society of London, XLII 105–130 (1945).

Ferguson, L. N. and Nnadi, J. C. "Electronic Interactions between Nonconjugated Groups," *J. Chem. Educ.*, **42**: 529 (1965).

Lambert, J. B., Shurvell, H. F., Verbit, L., Cooks, R. G., and Stout, G. H. *Organic Structural Analysis*. New York: Macmillan, 1976, pp. 317–401.

May, L. "IUPAC Definitions in Ultraviolet Spectroscopy," *Appl. Spectrosc.*, **27**: 419 (1973).

Scheinman, F. *An Introduction to Spectroscopic Methods for Identification of Organic Compounds*. New York: Pergamon, 1973, pp. 93–152.

Schönig, A. G. "A Computer-based UV Storage/Retrieval System," *Anal. Chim. Acta*, **71**: 17 (1974).

"Spectrometry Nomenclature," *Anal. Chem.* annual January 1 issue.

"Ultraviolet Spectrometry," *Anal. Chem.* Periodically this journal publishes literature reviews that include the title subject.

Monographs—Narrow Topics

Bolshakow, G. F., Vatago, V. S., and Agrest, F. B. *Ultraviolet Spectra of Hetero-Organic Compounds*. Leningrad, USSR: Khimia Publishing House, 1969.

Katrizky, A. R. (Ed), *Physical Methods in Heterocyclic Chemistry*. Vol. II, New York and London: Academic, 1963.

Compilations—Data, Spectra, Indexes

American Petroleum Institute Research Project 44, *Selected Ultraviolet Spectral Data*. Vols. I–IV. College Station, Texas: Thermodynamics Research Center, Texas A&M University, 1945–1977, 1178 compounds, 1279 pages.

ASTM Index to Ultraviolet and Visible Spectra. ASTM Technical Publication No. 357, American Society for Testing Materials, 1916 Race St., Philadelphia PA, 1963.

DMS UV Atlas of Organic Compounds. Vols. I–V. New York: Plenum, 1966–1971.

Electronic Spectral Data; Organic Electronic Spectral Data. Vols. I–XIII. New York: Wiley–Interscience, 1946–1968.

Friedel, R. A. and Orchin, Milton. *Ultraviolet Spectra of Aromatic Compounds*. New York: Wiley, 1951.

Graselli, J. G. and Ritchey, W. M. (Eds.) *Atlas of Spectral Data and Physical Constants*. Cleveland: CRC, 1975, pp. 399–408. This includes a listing, in groups by molar absorptivity ($\epsilon <$ 100,000; = 10,000–99,999; 1000-9,999; 0–1,000; and no listed ϵ); of compounds in order of the λ_{max} of their principal absorption, along with all remaining UV maxima for each compound.

Hershenson, H. M. *Ultraviolet Absorption Spectra. Index for 1954–1957*. New York: Academic, 1959.

Hirayama, K. *Handbook of Ultraviolet and Visible Absorption Spectra of Organic Compounds*. New York: Plenum Press Data Div., 1967.

Holubek, J. and Strouf, O. (Eds.) *Spectral Data and Physical Constants of Alkaloids*. New York: Heyden and Sons, 1962.

Lang, L. *Absorption Spectra in the Ultraviolet and Visible Region*. New York: Academic.

UV-Atlas of Organic Compounds. Photoelectric Spectrometry Group, London, and Institut für Spektrochemie und Angewandte Spektroskopie, Dortmund, London: Butterworths.

Ultraviolet Reference Spectra. Philadelphia: Sadtler Research Laboratories, 3314-20 Spring Garden St.

Ultraviolet Spectral Data. Pittsburgh, PA: Manufacturing Chemists Association Research Project, Carnegie Institute of Technology.

PROBLEMS

7.1. Match the three steroid structures shown below to the following values for λ_{max}^{hexane}: Compound A, 275 nm; B, 304 nm, and C, 356 nm.

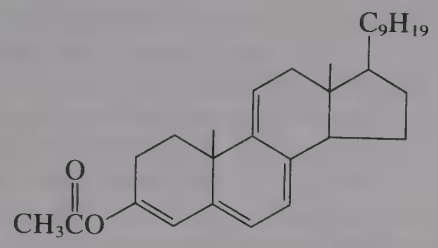

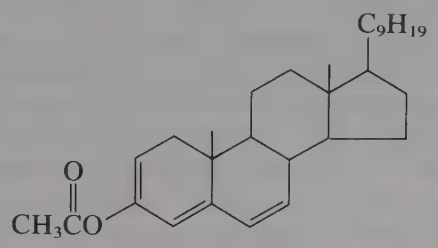

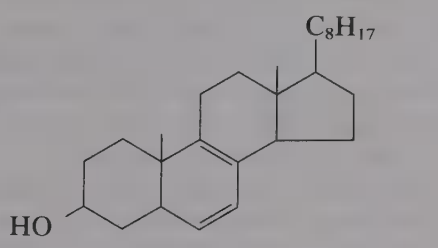

7.2. Partial hydrogenation of the triene shown below results in two compounds, D and E, both of molecular formula $C_{10}H_{14}$. Compound D shows a λ_{max}^{hexane} = 235 nm and E, 275 nm. Assign the structures.

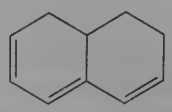

7.3. Compound F ($C_7H_{10}O$) gives a positive test with 2,4-dinitrophenylhydrazine, with sodium hydroxide/iodine and with bromine in carbon tetrachloride. The UV spectrum of F shows a $\lambda_{max}^{C_2H_5OH}$ at 257 nm. Deduce the structure for this compound. Is only one structure possible?

7.4. An acetone solution of Compound G ($C_7H_7NO_2$) shows ^{1}H-NMR signals at δ 6.63–7.90 (4H) and at δ 6.55 (3H). The intensity of the δ 6.55 signal is greatly reduced on treatment with heavy water. The UV spectrum of G shows a $\lambda_{max}^{C_2H_5OH}$ at 288 nm. Deduce the structure of compound G. Compound G can be prepared by reducing a nitrobenzoic acid with a mineral acid–metal mixture.

7.5. A Nujol mull of compound H ($C_7H_5BrO_2$) shows, among others, the following IR bands: a broad band, with a number of maxima, from 3100 to 2500 cm^{-1}, and a strong band at 1686 cm^{-1}. The ^{1}H-NMR spectrum (DMSO-d_6/$CDCl_3$) shows signals at δ 7.5–8.0 (4H) and at δ 12.15 (1H). The latter signal is greatly diminished upon heavy water treatment. The UV spectrum shows a $\lambda_{max}^{C_2H_5OH}$ at 245 nm. Deduce the structure of Compound H.

INTRODUCTION TO CHAPTERS EIGHT AND NINE

In practice, identification of an organic compound begins with a history, and large areas are quickly excluded from further consideration. Since, with a few exceptions, we dispense with a history, the limits will be set as follows: The compounds are quite pure; they may contain carbon, hydrogen, oxygen, nitrogen, sulfur, and the halogens in any combination; since the high-resolution mass table (Appendix A, Chapter 2) extends only to a molecular weight of 250, the examples will be limited to this range. Within these restrictions, we can still cover a vast expanse of organic chemistry. Additional information, usually a history, would probably be necessary to identify a compound that contained boron, silicon, or phosphorus in addition to the above elements, but it is hardly likely that a chemist would encounter such compounds without prior knowledge that these elements are present.

The interpreter and correlator of data has always lived on the edge of uncertainty. How pure is his compound, how reliable are his data, how relevant is his reference material? There are few unequivocal data, either spectrometric or chemical; thus, there is no substitute for experience and a broad knowledge of chemistry. Neither is there a prescribed procedure. If a high-resolution mass spectrometer is available, we may obtain directly, the all-important molecular formula and the formulas of the fragments. The more generally available unit-resolution spectrum together with other spectra will at least narrow the choice of a molecular formula to several possibilities. If the molecular ion is very weak or missing, we can probably establish it with chemical ionization, or even "guess" at it by using the nitrogen rule, and by rationalizing the fragmentation pattern (rational fragments) and considering the other spectra. The minimum number of nonequivalent carbon atoms can be obtained from the ^{13}C NMR spectrum. (Coincidence of ^{13}C peaks, though rare, must nonetheless be considered.) The APT or the DEPT spectrum gives the number of protons attached to carbon atoms, which can be compared with the integrated ^{1}H spectrum.

We use the obvious features of one spectrum to bring out the more subtle aspects of another. The power of this methodology lies in the complementary features of the spectra. For example, we can calculate the index of hydrogen deficiency from the molecular formula and determine the presence or absence of certain unsaturated functional groups from the IR spectrum; this information can be confirmed by the ^{1}H and ^{13}C spectra. The UV spectrum quickly establishes the presence or absence of conjugated or aromatic structures. The ^{1}H spectrum is a powerful tool for distinguishing between isomeric possibilities. When enough information is accumulated, a structure is postulated, and spectral features, which are predicted on the basis of the postulated structure, are compared with the spectra actually observed. Appropriate structural modifications are made to accommodate the discrepancies. Confirmation is obtained by comparison with the spectra of an authentic sample. Chapter 8 provides three solved problems in preparation for the problems in Chapter 9.

For most of the compounds in Chapter 9, the complementarity of a unit- or high-resolution mass spectrum, an IR spectrum, an integrated ^{1}H spectrum, and a decoupled ^{13}C spectrum with multiplicities by APT or DEPT will suffice; UV is used for delocalized electron systems. In a number of cases, 2-D NMR spectra are furnished (see Chapter 6). We emphasize again that, with practice, a fair amount of deviation from first order in a proton NMR spectrum may be tolerated (see Section 4.4). To provide practice in the newer techniques, we have indulged in overkill in some of the problems, but other problems should provide compensatory frustration to simulate the real world.

The following recent problem sets are available for further practice.

Sternhell, S. and Kalman, J. R. *Organic Structures from Spectra*. New York: Wiley, 1986.

Davis, R. and Wells, C. H. J. *Spectral Problems in Organic Chemistry*. New York: Chapman and Hall, 1984.

Bates, R. B. and Beavers, W. A. *Carbon-13 NMR Spectral Problems*. Clifton, NJ: Humana Press, 1981.

Fuchs, P. L. and Bunnell, C A. *Carbon-13 NMR Based Organic Spectral Problems*. New York: Wiley, 1979.

Duddeck, H. and Dietrich, W. *Structural Elucidation by Modern NMR. A Workbook*. New York: Springer–Verlag, 1989.

Sander, J. K. M., Constable, E. C., and Hunter, B. K. *Modern NMR Spectroscopy; A Workbook of Chemical Problems*. Oxford: Oxford University Press, 1989.

CHAPTER 8

SETS OF SPECTRA TRANSLATED INTO COMPOUNDS

INFRARED SPECTRUM ***Compound 8.1***

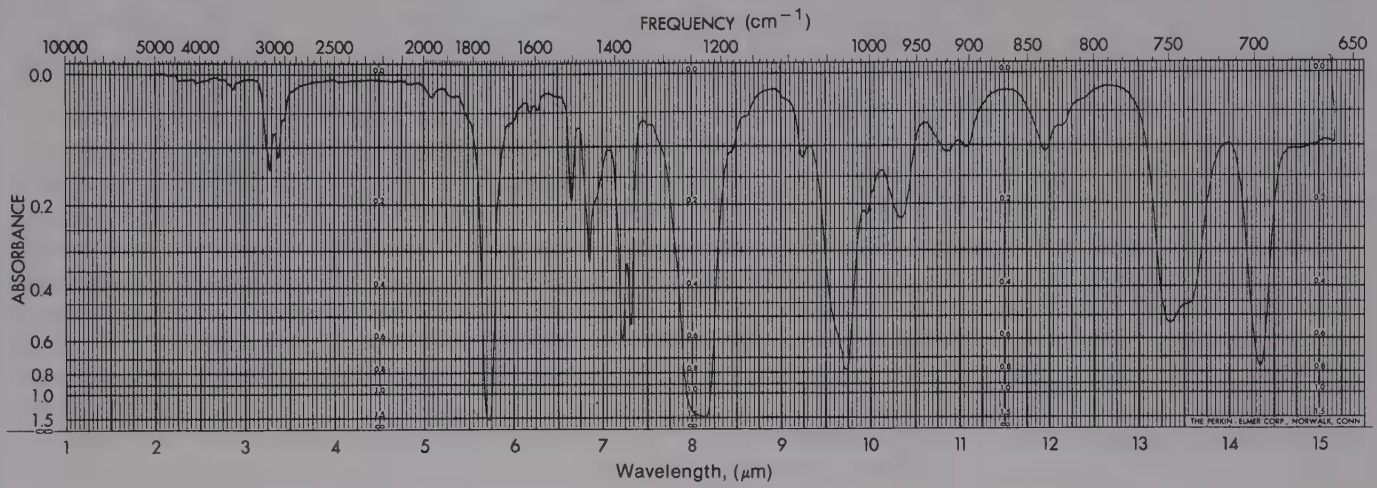

MASS SPECTRAL DATA (Relative Intensities)

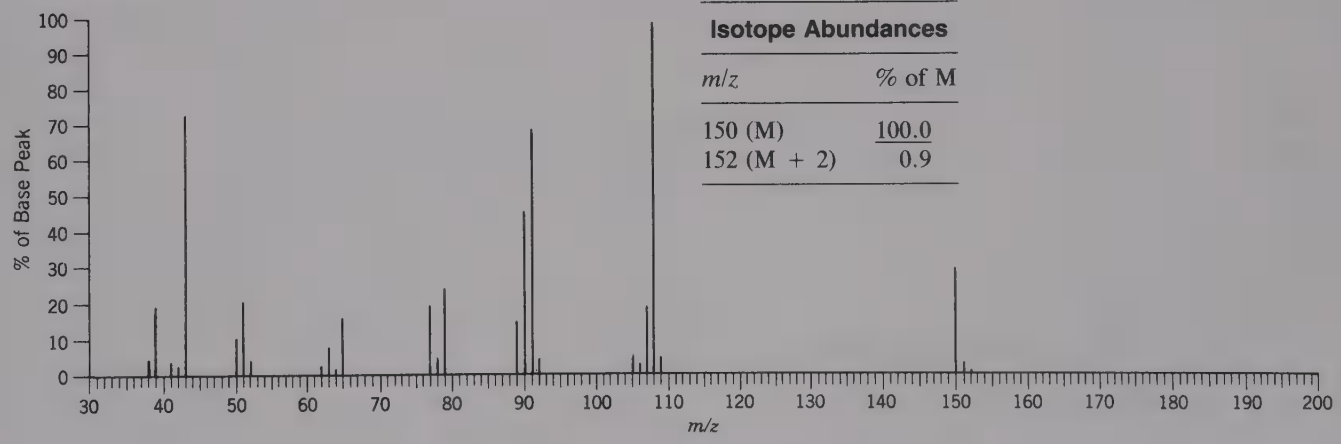

Isotope Abundances

m/z	% of M
150 (M)	100.0
152 (M + 2)	0.9

Ultraviolet Data

λ_{max}^{EtOH} (nm)	ϵ_{max}	λ_{max}^{EtOH} (nm)	ϵ_{max}	λ_{max}^{EtOH} (nm)	ϵ_{max}
268	101	257	194	243 (s)	78
264	158	252	153		
262	147	248 (s)	109		

(s) = shoulder

NMR SPECTRUM (Solvent CCl_4 60 MHz)

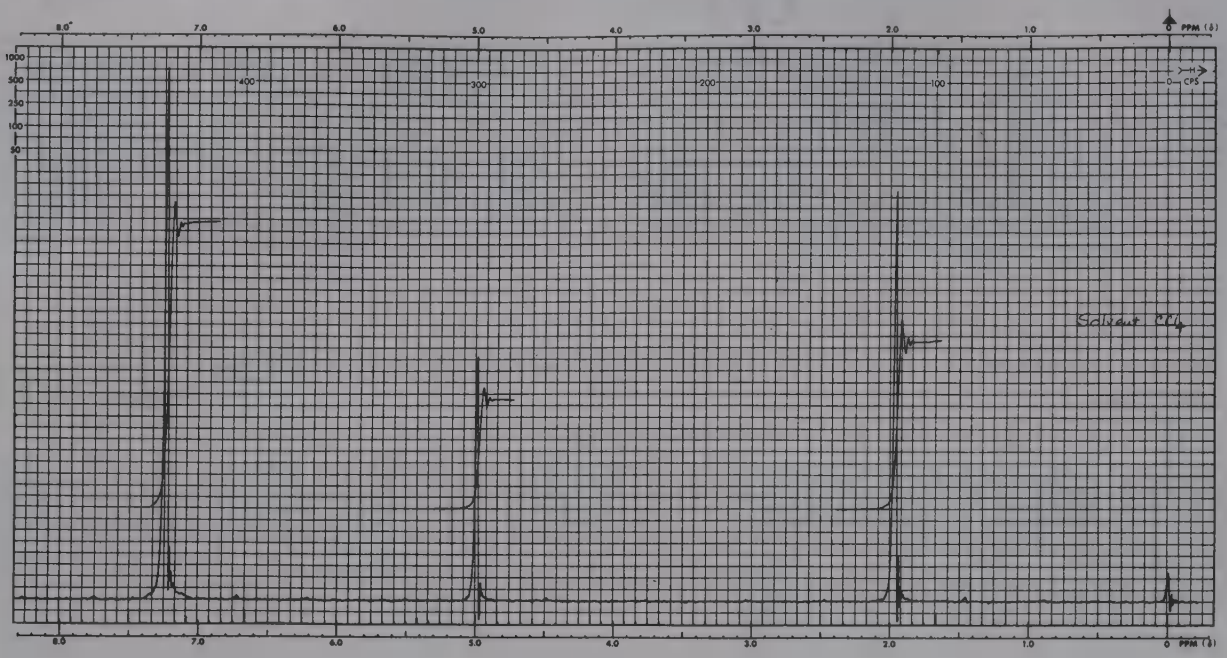

COMPOUND 8.1

The first step in translating these four spectra into a molecular structure is to establish a molecular formula. Since the molecular ion peak (*m/z* 150) is an even number, we are allowed either no nitrogen atoms or an even number of them. The M + 2 peak does not allow for the presence of sulfur, chlorine, or bromine.

The IR spectrum shows a C=O band at 1745 cm^{-1}. The strong, broad band at 1225 cm^{-1} suggests an acetate. Two strong bands at 749 and 697 cm^{-1} suggest a monosubstituted benzene ring. The intensity of the *m/z* 150 peak tends to confirm aromatic structure; further confirmation comes from the aromatic C—H stretching bands at the high-frequency edge of the aliphatic C—H stretching, and from the "ring-breathing" bands between approximately 1600–1400 cm^{-1}. The UV spectrum is in accord with a benzene ring that is not conjugated with the C=O group. The characteristic, intense peak in the mass spectrum at *m/z* 91 is the benzyl (or tropylium) ion formed by cleavage β to the ring; the intense peak at *m/z* 43 confirms the suspected acetate group and leads us to identify the three-proton singlet in the NMR spectrum at δ 1.96 as the CH_3—C=O protons. The five-proton singlet at δ 7.22 must be the aromatic protons, and the two-proton singlet at δ 5.00 must be the benzylic CH_2 group. At this point, we can write the structure

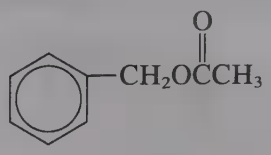

In the excitement of the chase, we have raced past the original modest goal of establishing the molecular formula. Belatedly, we write $C_9H_{10}O_2$ as the only possible choice under the nominal mass 150 in Appendix A of Chapter 2; this formula gives an index of hydrogen deficiency of 5.

Would our postulated structure give the same spectra as those presented? The IR and UV spectra are reasonable. The base peak in the mass spectrum at *m/z* 108 is a predictable McLafferty rearrangement (Sections 2.8 and 2.10.7), and the characteristic peaks for a monosubstituted benzene are present at *m/z* 77–79. The NMR spectrum is completely predictable; higher resolution would show that the downfield peak is really a multiplet. The ultimate test, of course, is peak-by-peak matching against spectra, obtained under the same conditions, of an authentic sample. The student will find it instructive to write the isomeric possibilities for the molecular formula and to eliminate them on spectrometric grounds.

INFRARED SPECTRUM

Compound 8.2

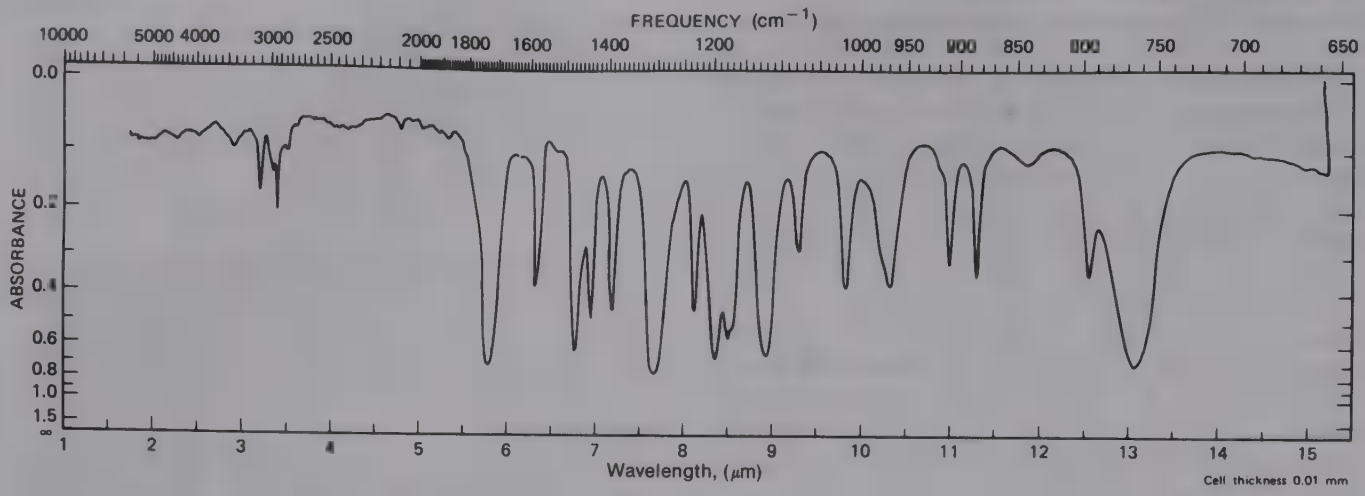

MASS SPECTRAL DATA (Relative Intensities)

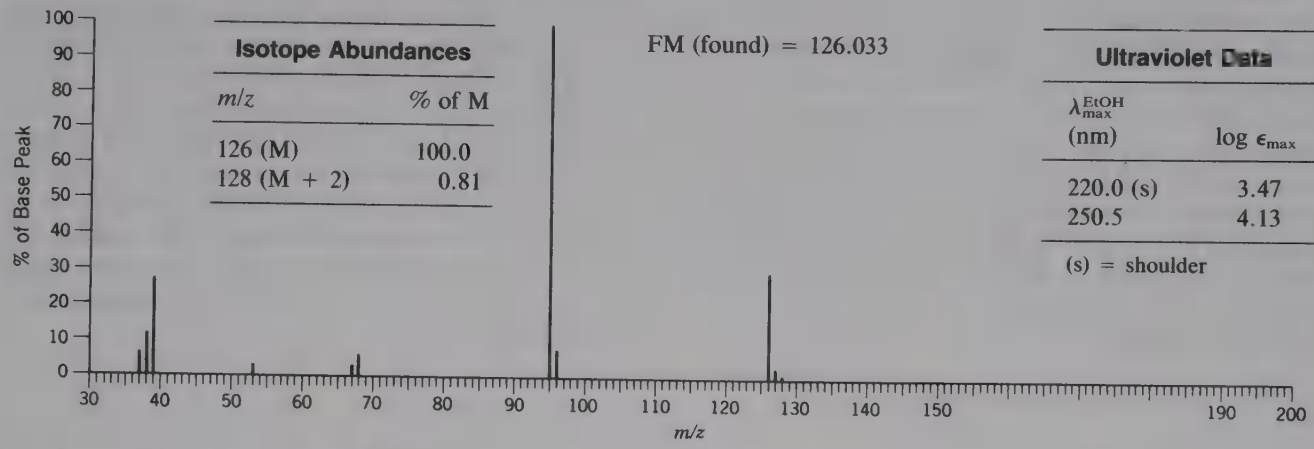

Isotope Abundances	
m/z	% of M
126 (M)	100.0
128 (M + 2)	0.81

FM (found) = 126.033

Ultraviolet Data	
λ_{max}^{EtOH} (nm)	log ϵ_{max}
220.0 (s)	3.47
250.5	4.13

(s) = shoulder

^{1}H NMR SPECTRUM (Solvent CCl_4, 60 MHz)

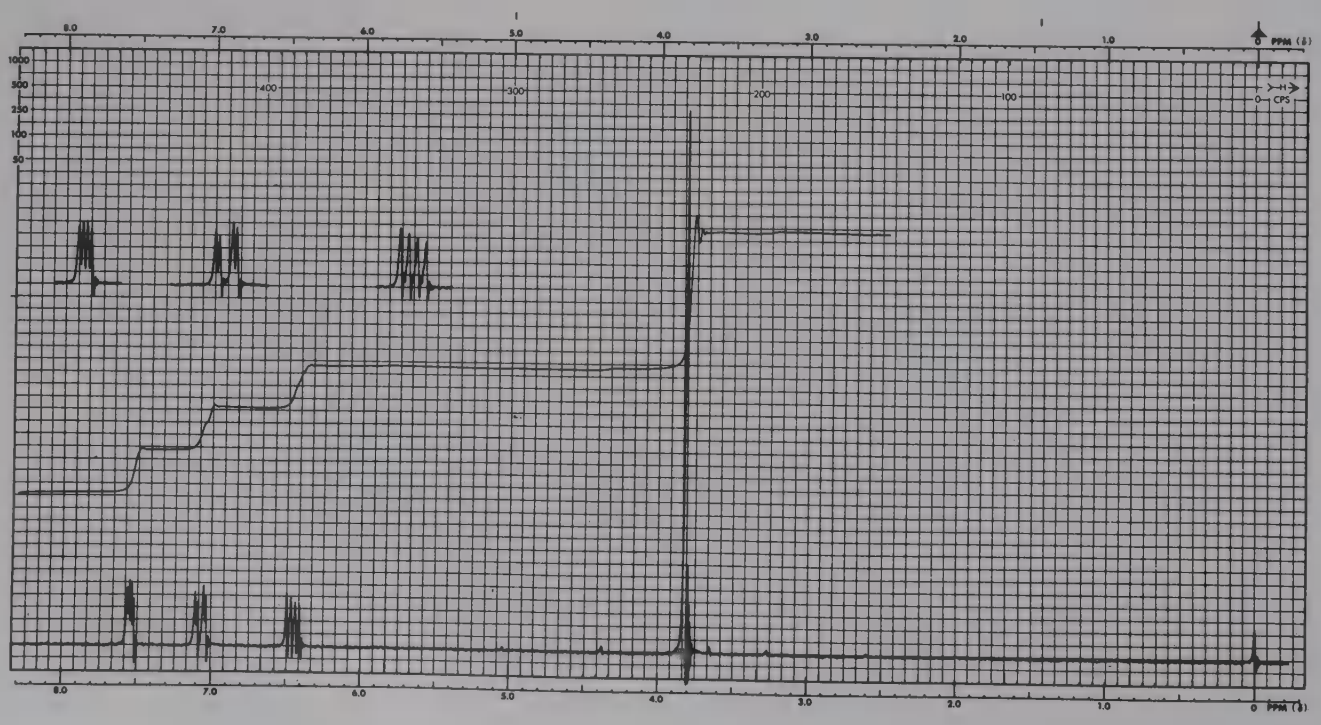

Compound 8.2 (continued)

^{13}C NMR SPECTRUM COMPLETELY DECOUPLED

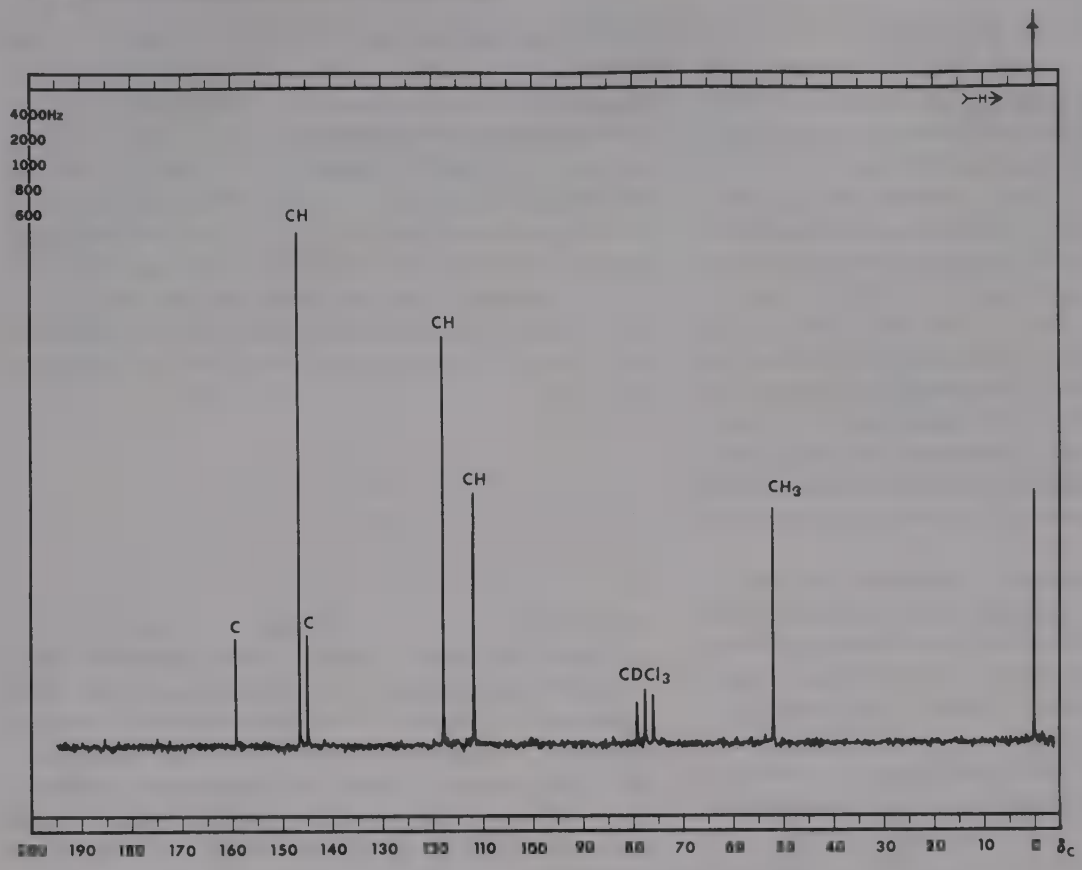

COMPOUND 8.2

The overall impression of this compound with a molecular ion peak at *m/z* 126 is that it is aromatic. Let us start with the very tentative assumption (M + 2 peak and nitrogen rule) that the molecular formula contains only C, H, and O; of course, we cannot rule out absolutely an even number of nitrogen atoms. Integration of the proton NMR spectrum gives, from low-to-high field, 1:1:1:3 for a total of 6 hydrogen atoms. This is supported in the ^{13}C spectrum by the number of protons attached to the carbon atoms (low-to-high field: 0, 1, 0, 1, 1, 3 for a total of 6). If we assume, as a calculated risk, that each peak in the ^{13}C NMR spectrum represents a single carbon atom, we have 6 nonequivalent carbon atoms. This leaves 3 oxygen atoms to accommodate the nominal molecular weight of 126, hence $C_6H_6O_3$ for the molecular formula with an index of unsaturation of 4.

We have made several assumptions for the molecular formula and must assemble more evidence. Aromaticity is evidenced at low field in the NMR spectrum, in the IR spectrum by aromatic C—H stretching bands centered at about 3150 cm^{-1}, intense "ring-breathing" bands between 1600 and 1400 cm^{-1}, and intense bands (out-of-plane aromatic C—H bending) at the low-frequency end of the spectrum. The very conspicuous feature is the intense C=O band at 1730 cm^{-1}; the intense band in the UV spectrum at 250.5 nm strongly suggests conjugation of the C=O group with the aromatic ring, which bears three protons shown at low field in the ^1H NMR spectrum.

We need three O atoms; are we perchance dealing with an ester, which would provide two oxygen atoms? The IR spectrum permits this. Consider the base peak in the mass spectrum at *m/z* 95, which arises from loss of mass 31 from the molecular ion peak—practically diagnostic for a methyl ester; this is speedily confirmed by the three-proton singlet at δ 3.81 in the ^1H NMR spectrum, by the CH_3 peak at δ 51.8, and by the ester–carbonyl peak at δ 159.1 in the ^{13}C spectrum. The *m/z* 95 component must be (C_4H_3O)—C=O resulting from the loss of OCH_3. Surely the molecular formula $C_6H_6O_3$ is abundantly confirmed. All that we need realize is that the C_4H_3O ring represents a monosubstituted furan (a heteroaromatic ring) and the structure becomes

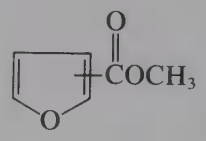

leaving only the decision between substitution at C-2 or C-3. At this point, comparison with published spectra is certainly justified (see Table 5.10 and Table D-5 at the end of Chapter 4). We can confirm the structure as methyl 2-furoate on the basis of the splitting pattern of the ring protons, given the following information: $J_{3,4} = 3.5$, $J_{4,5} = 2.0$, and $J_{3,5} = 1.0$ (long range). From low-to-high field the protons are on C-5, C-3, and C-4, respectively.

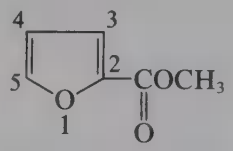

Methyl 2-furoate

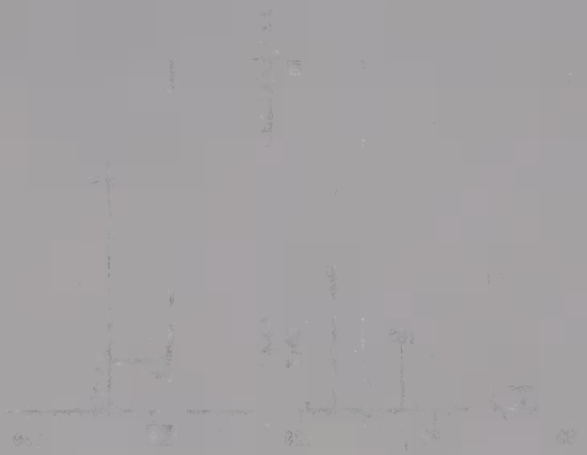

INFRARED SPECTRUM

Compound 8.3

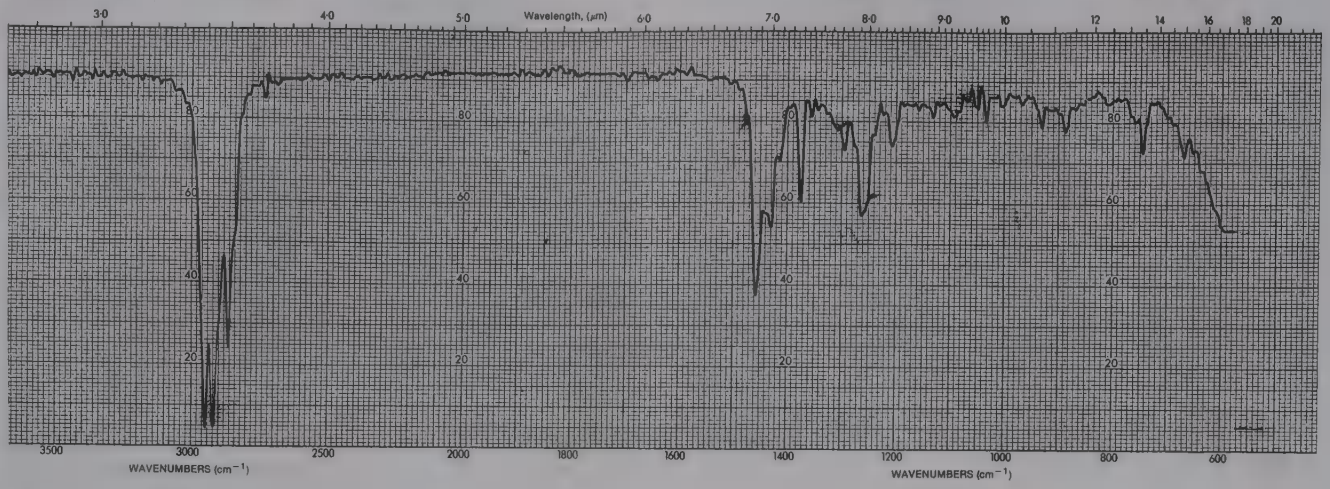

MASS SPECTRUM

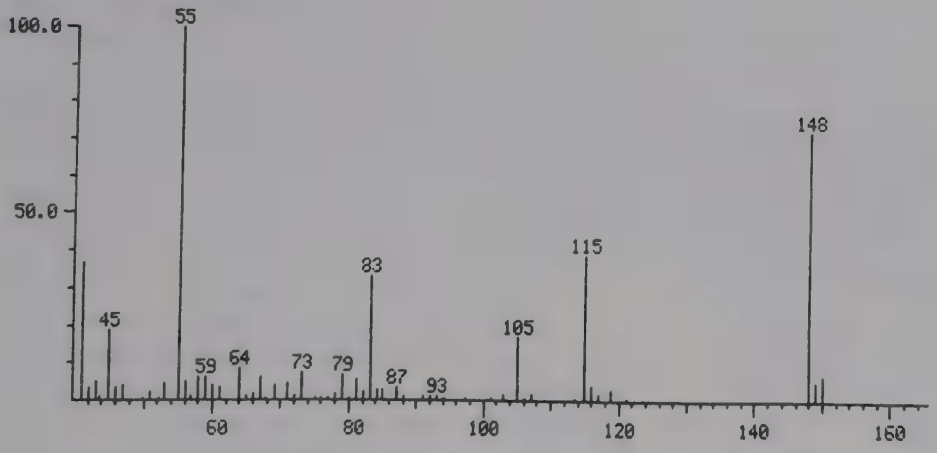

Isotope Abundances	
m/z	% of M
148 (M)	100.0
150 (M + 2)	9.7

^{1}H NMR SPECTRUM $CDCl_3$, 500 MHz

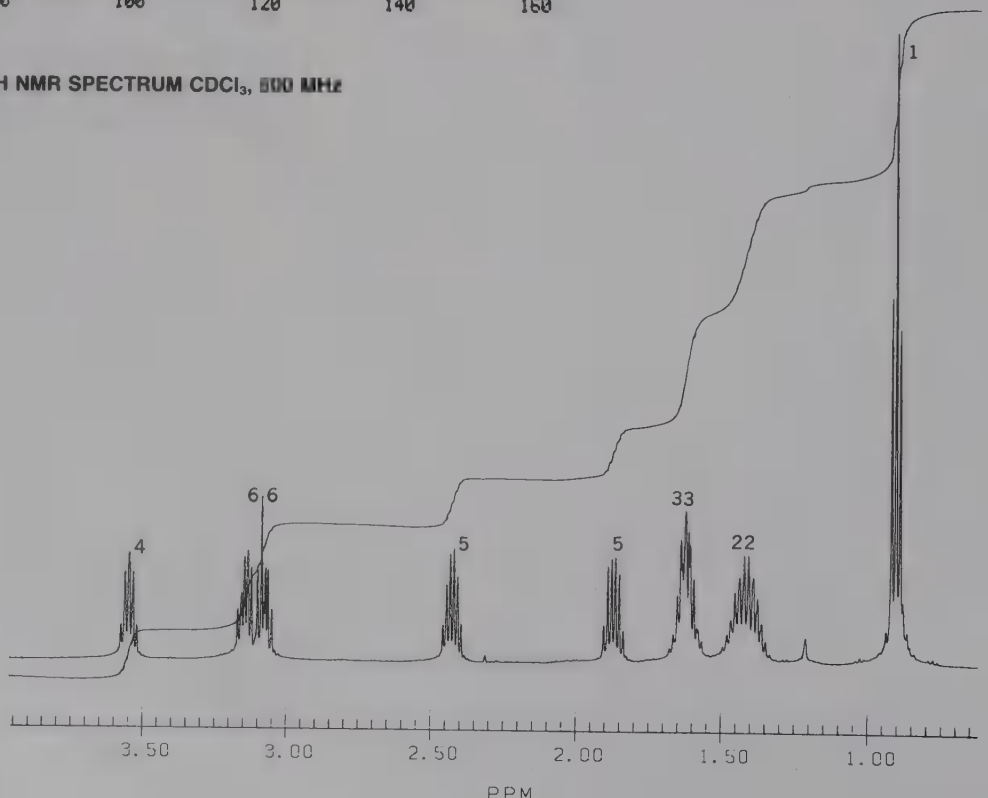

Compound 8.3 (continued)

^{13}C NMR SPECTRUM

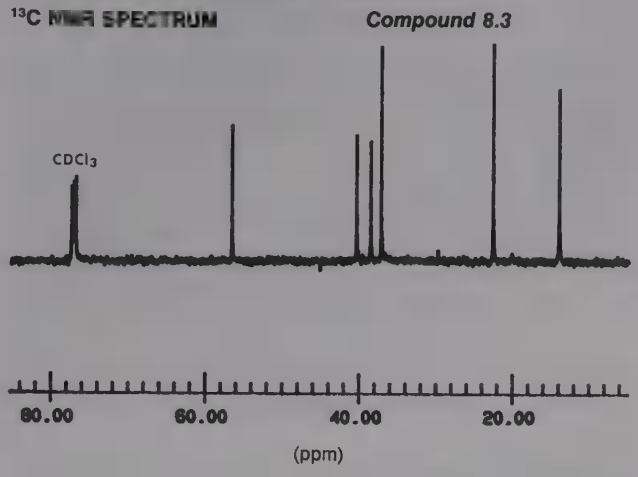

HC–COSY (HETCOR)

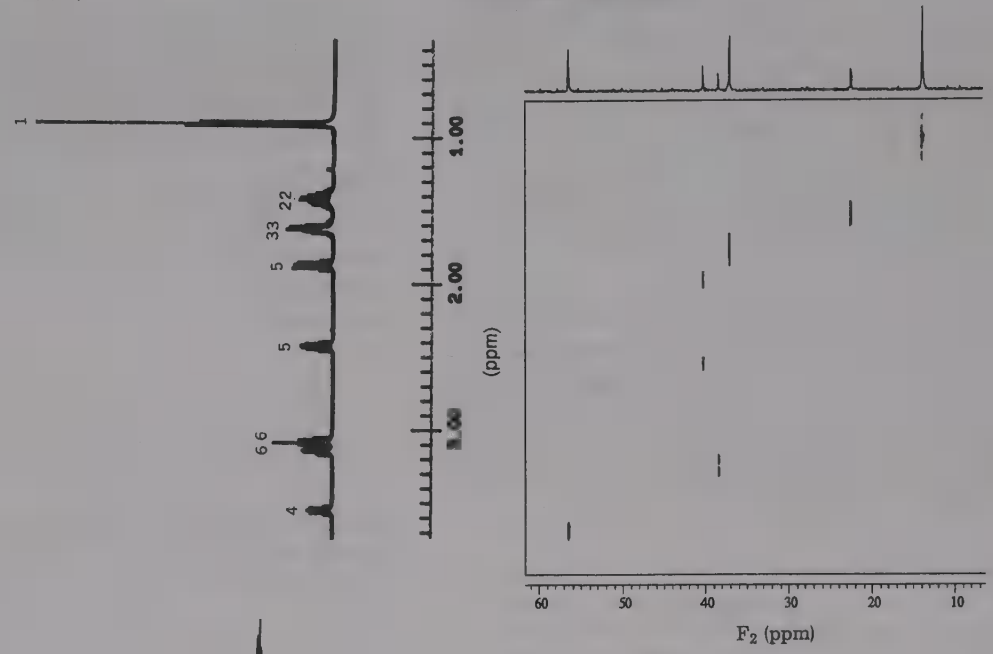

H H COSY

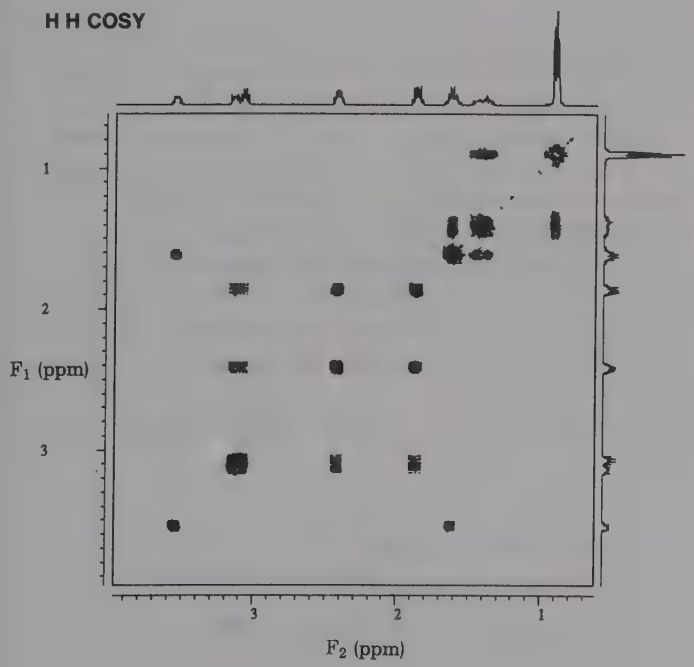

COMPOUND 8.3

The molecular ion peak is 148, and the M + 2 peak is 9.7% of the intensity of M, suggesting the presence of two sulfur atoms. The IR spectrum shows little more than saturated hydrocarbon features; neither the ^1H nor the ^{13}C spectrum shows evidence for *sp* or sp^2 hybridized carbon atoms. The ^1H spectrum integrates for 12 hydrogen atoms and the ^{13}C spectrum shows six peaks. We confidently suggest a molecular formula of $C_6H_{12}S_2$ with an index of hydrogen deficiency of 1, which demands a ring in the absence of evidence for a double bond.

After a few minutes with the ^1H-NMR spectrum (a 500-MHz spectrum), our confidence wanes; there is simply too much of everything: too many different protons, and too many peaks. At first glance, there seems to be 8 different kinds of protons for 6 carbon atoms; the apparent proton integration from high-to-low field is 3:2:2:1:1:1:1:1. In fact, things are even worse since there are really 10 different kinds of protons, as we shall see. To accommodate this situation, we *assume the presence of a chiral center, which would make every methylene group consist of a pair of diastereotopic protons* (i.e., not chemical shift equivalent; Sections 4.7 and 4.10), which couple with each other and with the vicinal protons. The classical CH_3 triplet at δ 0.90 gives us one end of the molecule: $—CH_2CH_3$. The ^1H spectrum obviously cannot be approached on a first-order basis, and we now understand why 2-D spectra are provided for a "simple" 6 carbon compound.

δ	Multiplicity	Number of H Atoms
0.90	*t* (apparent)	3
1.39 (estimated)	*m* (apparently 6 peaks)	1
1.44 (estimated)	*m* (apparently 6 peaks)	1
1.60 (estimated)	*m*	1
1.64 (estimated)	*m*	1
1.87	*m* (apparently 6 peaks)	1
2.44	*m* (apparently 6 peaks)	1
3.07 (estimated)	*m* (apparently 5 peaks)	1
3.14 (estimated)	*m* (apparently 5 peaks)	1
3.55	*m* (apparently 5 peaks)	1
		12

Assuming that the absorptions centered at δ ~1.42, ~1.62, and ~3.10 are all CH_2 groups of diastereotopic protons, we now have seven different kinds of protons—still one too many. We now attempt to summarize the disposition of the protons. Since each proton of a diastereotopic pair has its own chemical shift, we can arbitrarily pick an estimated "center of gravity" on each side of the midpoint (Section 4.4). This is an admittedly crude procedure, but "squinting" gets us quite close to the following assignments, which were estimated by computer simulation of the coupling patterns.

Note that three of the diasterotopic pairs are very strongly coupled, and recall from Figure 4.23 that the inner lines approach each other but do not cross. It also turns out (next paragraph) that the protons at δ 1.87 and δ 2.44 are a weakly coupled diastereotopic pair.

The power of the COSY (HOMCOR) spectrum now becomes obvious. As the point of entry, we start with the terminal CH_3 group at the upper right-hand end of the diagonal and quickly determine the following connectivities:

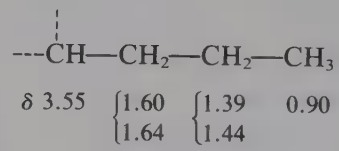

The CH proton shows connectivity to the one-proton signals at δ 1.87 and δ 2.44, but this does not seem reasonable since it must be attached to at least one of the S atoms to account for its low-field shift. The dilemma is resolved if we assume that the signals at δ 1.87 and δ 2.44 represent the well-separated (weakly coupled) diastereotopic protons of another CH_2 group. The lone methine group at δ 3.55 is the chiral center. The δ 1.87 proton and the δ 2.44 proton are in turn coupled to the proton at δ 3.07 and the proton at 3.14; the latter two protons are somewhat less strongly coupled than the other strongly coupled diastereotopic pairs, as is evident in the ^1H spectrum, but the lesser resolution of the 2-D COSY spectrum results in superposition of the contours of all of the diastereotopic pairs except for the pair at δ 1.87 and δ 2.44. At this point, the connectivities of all of the carbon atoms can be shown.

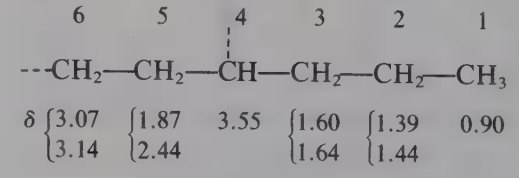

The HETCOR spectrum, with the ^{13}C chemical shifts in the horizontal axis and the ^{1}H chemical shifts in the vertical axis, shows which protons are attached to each carbon. Since the proton connectivities are now established, the HETCOR permits assignments of the carbon atoms; these assignments are left to the student. The diastereotopic protons are clearly differentiated on C-5 and C-6, but the more strongly coupled protons on C-2 and C-3 are not differentiated at this resolution.

It remains only to insert the two sulfur atoms to complete the structural formula

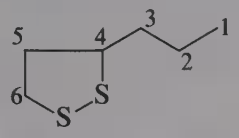

Although the fragmentation pattern of the mass spectrum was not very helpful, it is possible to rationalize the major peaks on the basis of the structure. The molecular ion fragments by two pathways: loss of SH to give *m/z* 115, and cleavage at the ring junction with loss of the $CH_3CH_2CH_2$ radical to give *m/z* 105. The base peak, *m/z* 55, represents a hydrocarbon fragment C_4H_7.

A review of the approach to this problem reveals that the first critical observation was the intensity of the M + 2 peak in the mass spectrum; there is no other spectral clue to the presence of the two sulfur atoms. A modern high-resolution mass spectrometer would have given us directly a readout of the molecular formula. The sulfur atoms in this compound, isolated from the anal gland of the stoat, are quite readily detected by the nose. The second critical observation was that the ^{1}H NMR spectrum was too complex for the number of carbon atoms, and we assumed the presence of a chiral center, which is confirmed by the diastereotopic protons in the HETCOR.

An APT or DEPT spectrum would have told us immediately that there were one CH_3, four CH_2, and one CH groups and would have immediately forced us to realize that all of the CH_2 groups consisted of pairs of diastereotopic protons in order to rationalize the ^{1}H and the COSY spectra. Finally, note that it is the two CH_2 groups in the ring that show the greater difference in chemical shift between the protons of each pair, and the ring CH_2 adjacent to the chiral center shows the greatest difference; the differences in the flexible side chain are smaller because of the averaging effect.

CHAPTER NINE

PROBLEMS

INFRARED SPECTRUM

Compound 9.1

2972.4 1326.9 1015.4
1467.5 1168.9 904.5
1378.8 1111.5 795.5

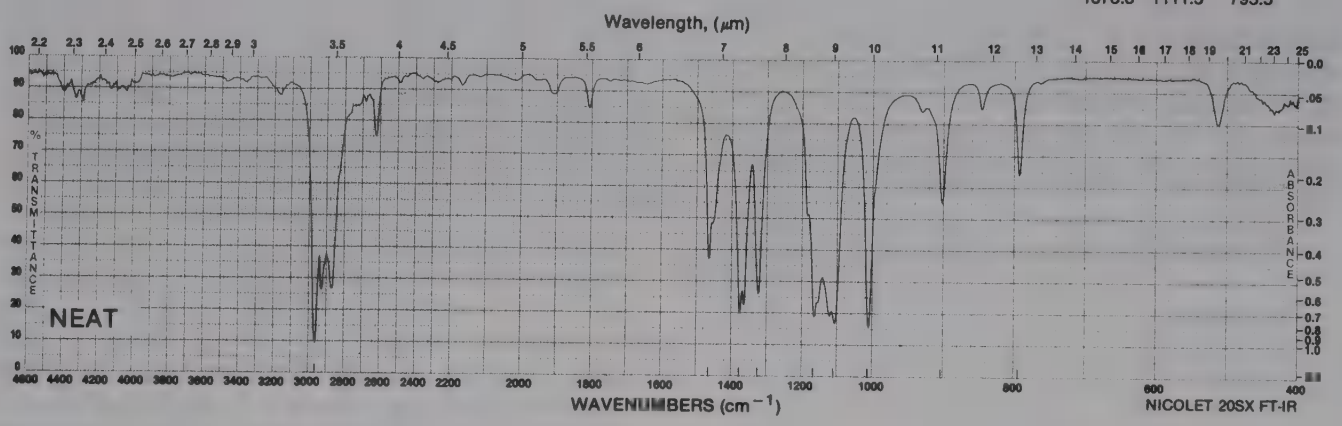

MASS SPECTRAL DATA (Relative Intensities)

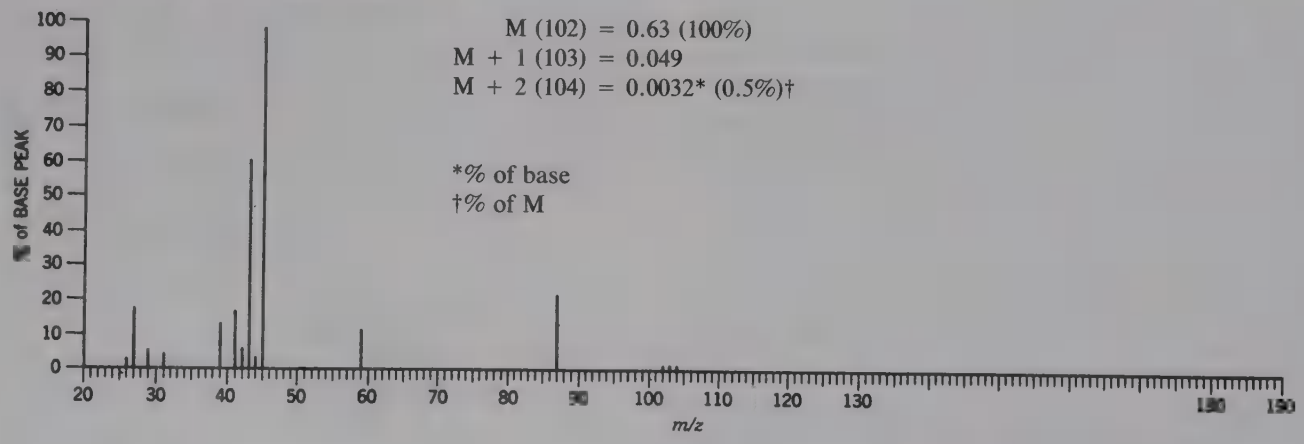

M (102) = 0.63 (100%)
M + 1 (103) = 0.049
M + 2 (104) = 0.0032* (0.5%)†

*% of base
†% of M

Ultraviolet Data

Transparent above 200 nm

Compound 9.1 (continued)

^{1}H NMR SPECTRUM (Solvent $CDCl_3$, 60 MHz)

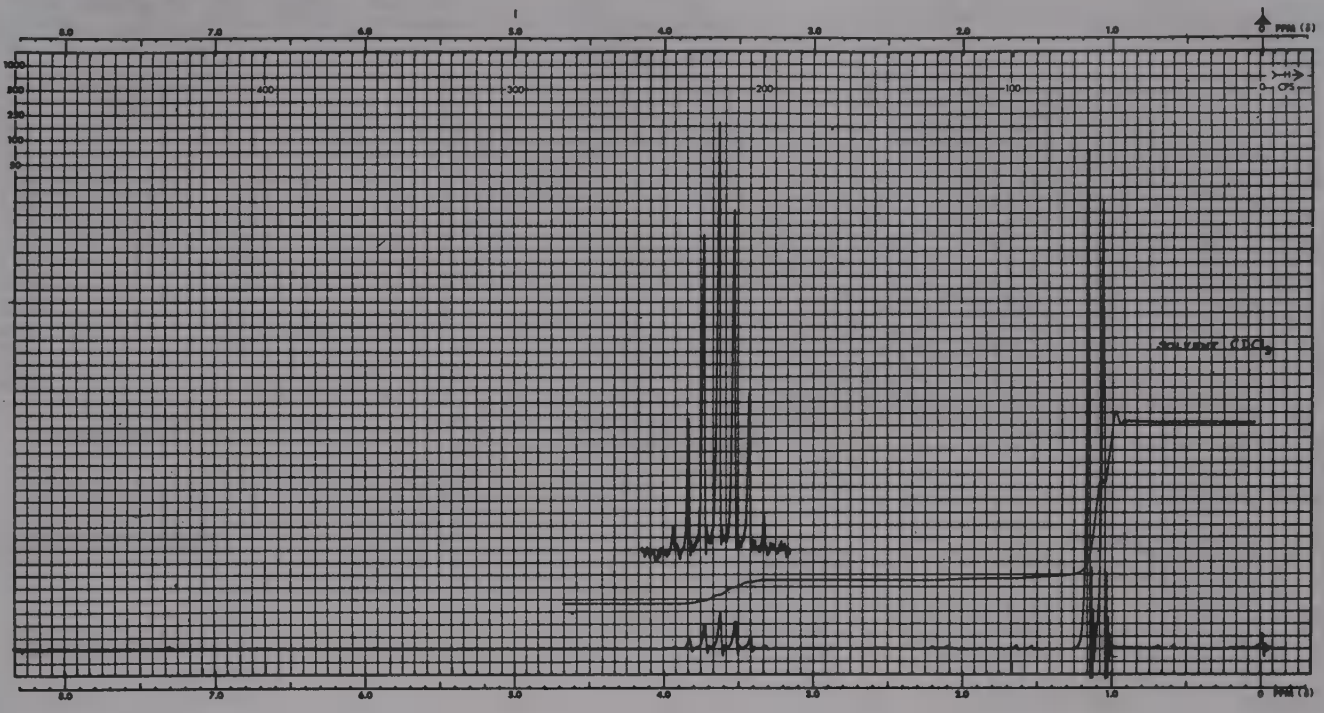

^{13}C NMR SPECTRUM COMPLETELY DECOUPLED

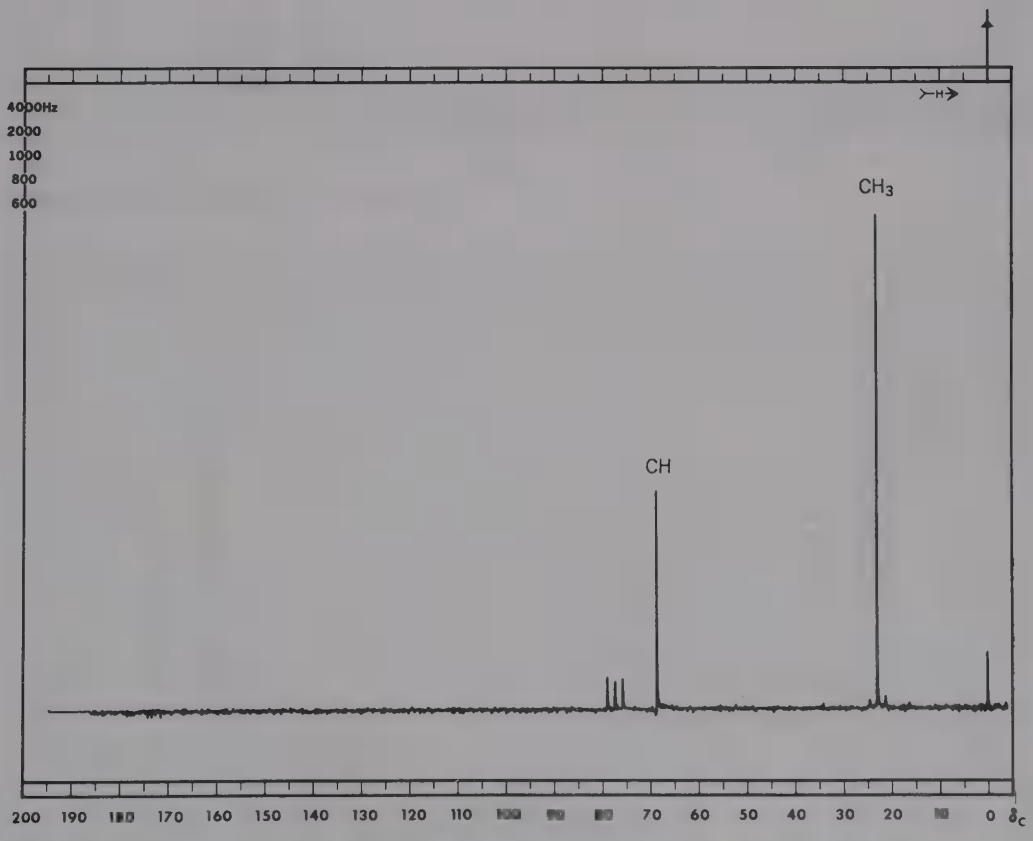

INFRARED SPECTRUM

Compound 9.2

2927.2 1286.8
1466.5 1215.5
1378.5 724.7

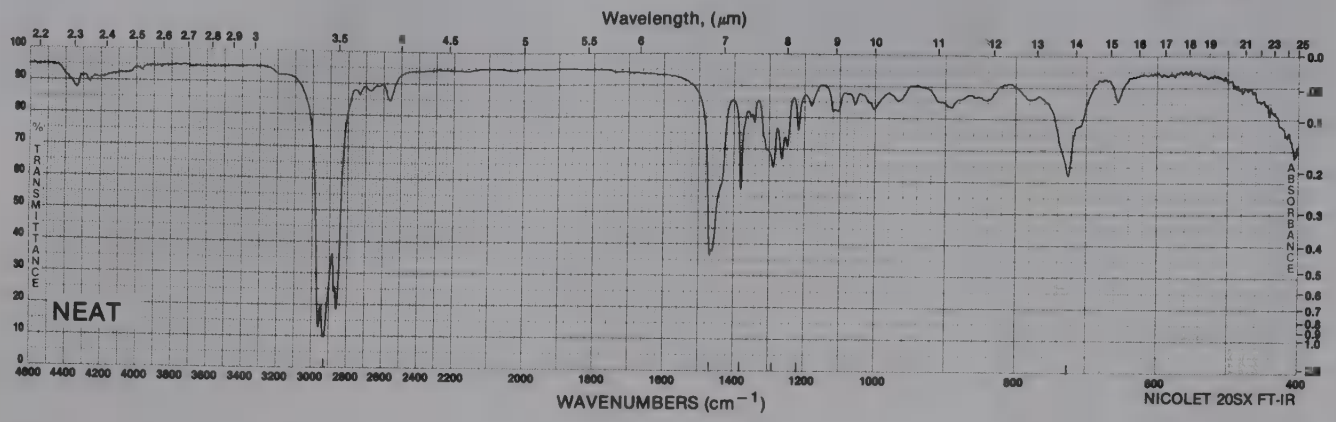

MASS SPECTRAL DATA (Relative Intensities)

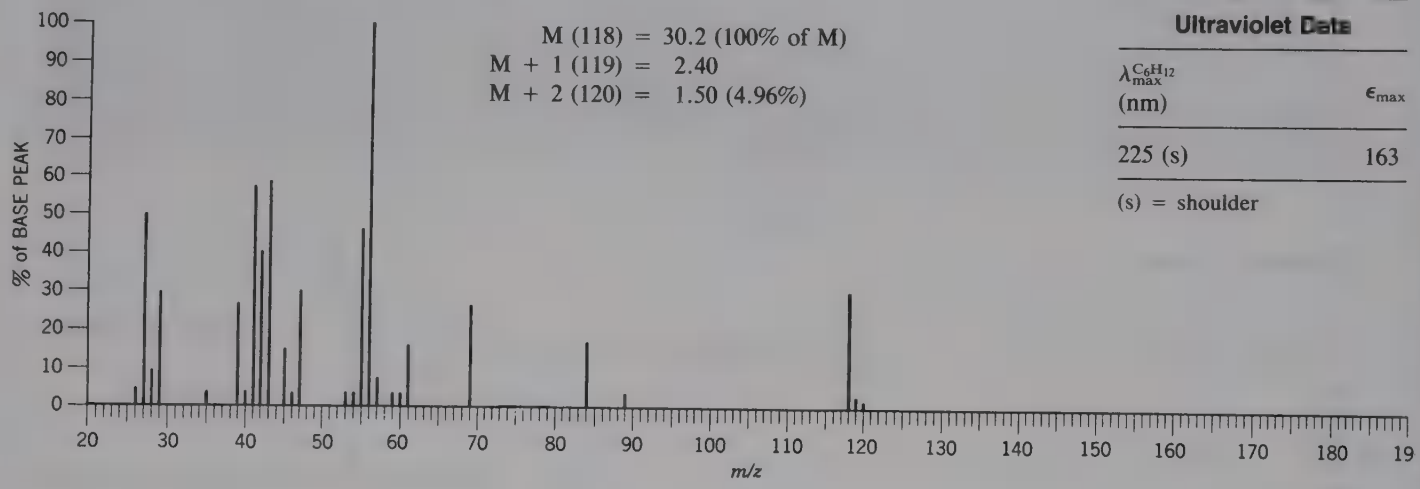

M (118) = 30.2 (100% of M)
M + 1 (119) = 2.40
M + 2 (120) = 1.50 (4.96%)

Ultraviolet Data

$\lambda_{max}^{C_6H_{12}}$ (nm)	ϵ_{max}
225 (s)	163

(s) = shoulder

^{1}H NMR SPECTRUM (Solvent $CDCl_3$, 300 MHz)

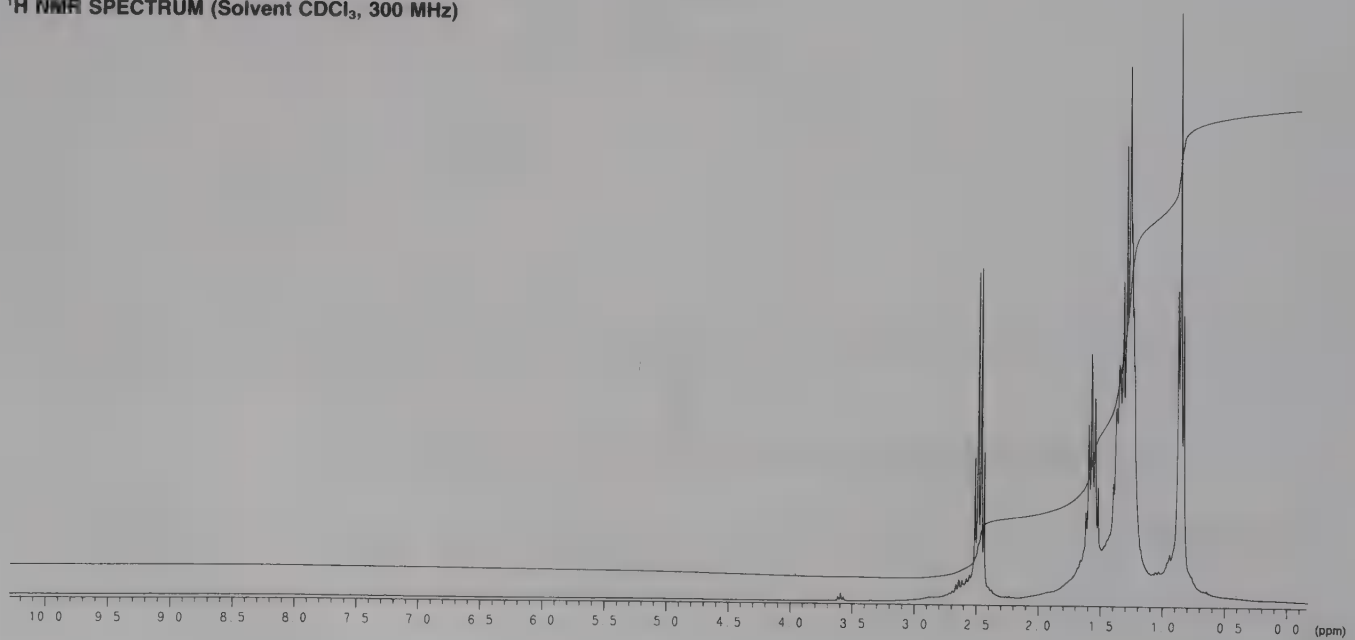

INFRARED SPECTRUM

Compound 9.3

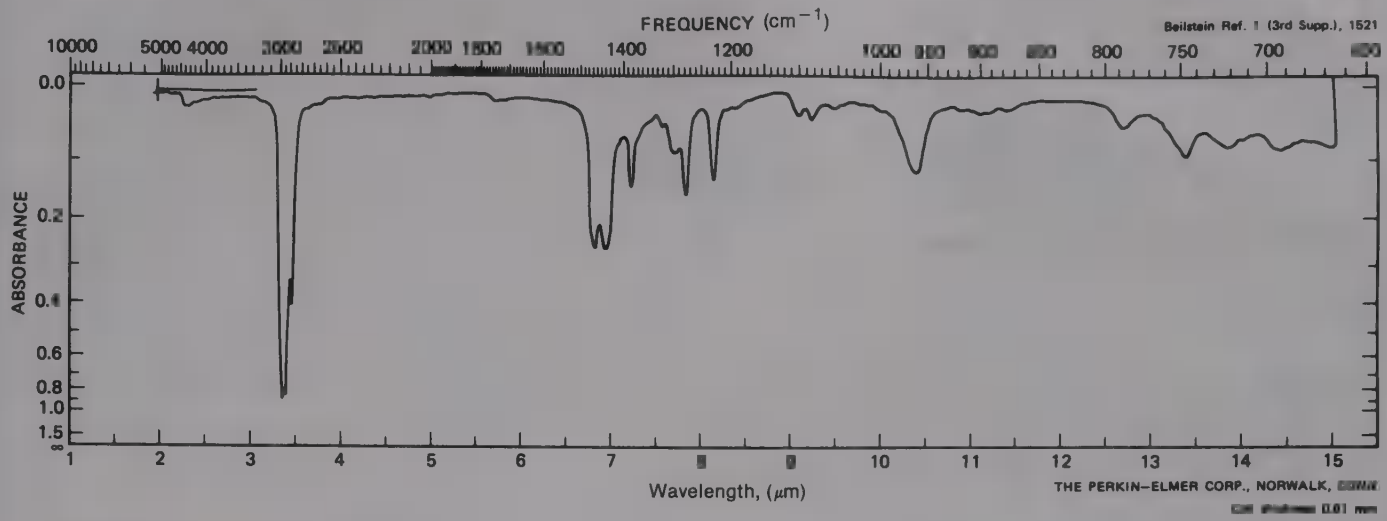

MASS SPECTRAL DATA (Relative Intensities)

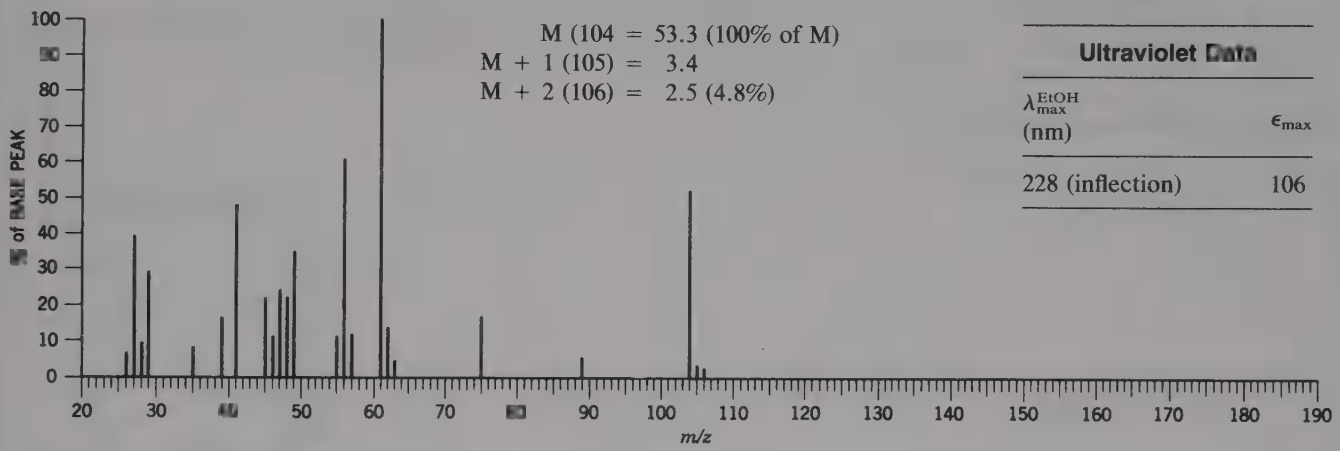

M (104 = 53.3 (100% of M)
M + 1 (105) = 3.4
M + 2 (106) = 2.5 (4.8%)

Ultraviolet Data

λ_{max}^{EtOH} (nm)	ϵ_{max}
228 (inflection)	106

^{1}H NMR SPECTRUM (Solvent $CDCl_3$, 60 MHz)

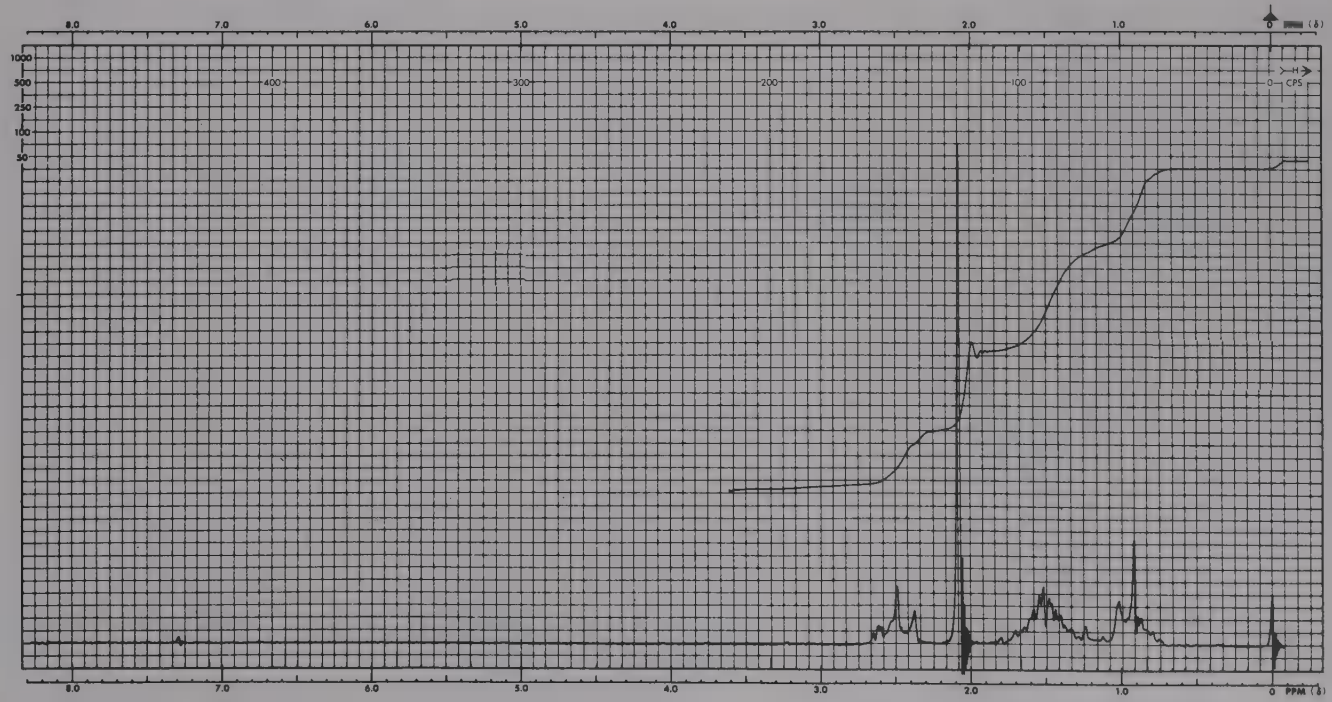

Compound 9.4

MASS SPECTRAL DATA (Relative Intensities)

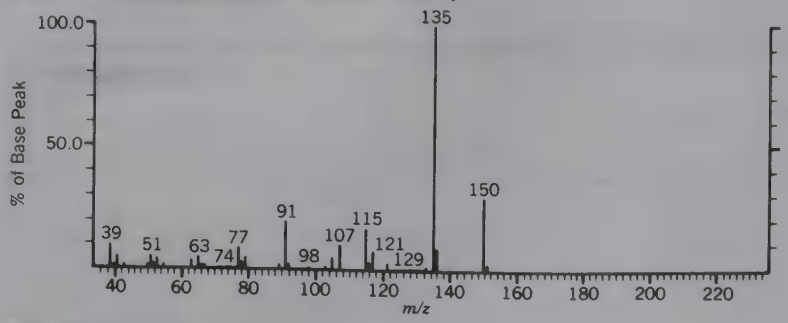

FM (found) = 150.1043

INFRARED SPECTRUM (DILUTE SOLUTION IN CCl_4)

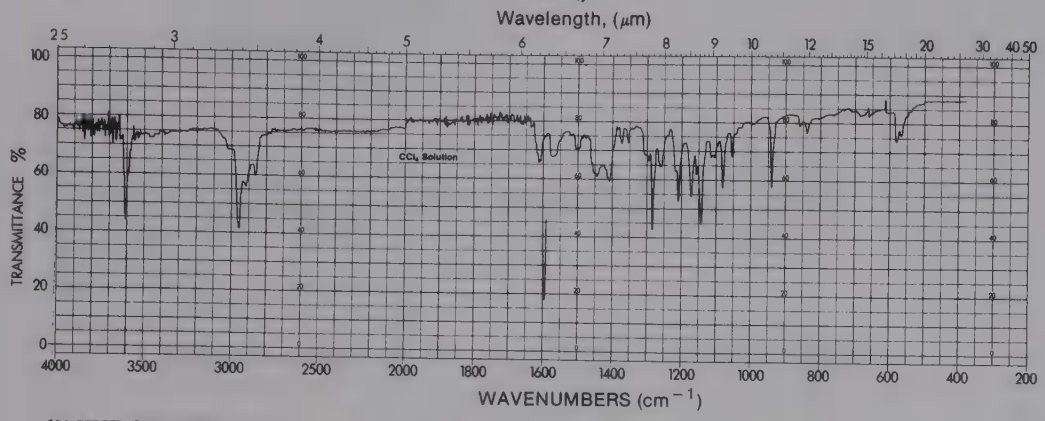

^1H NMR SPECTRUM (Solvent $CDCl_3$, 100 MHz)

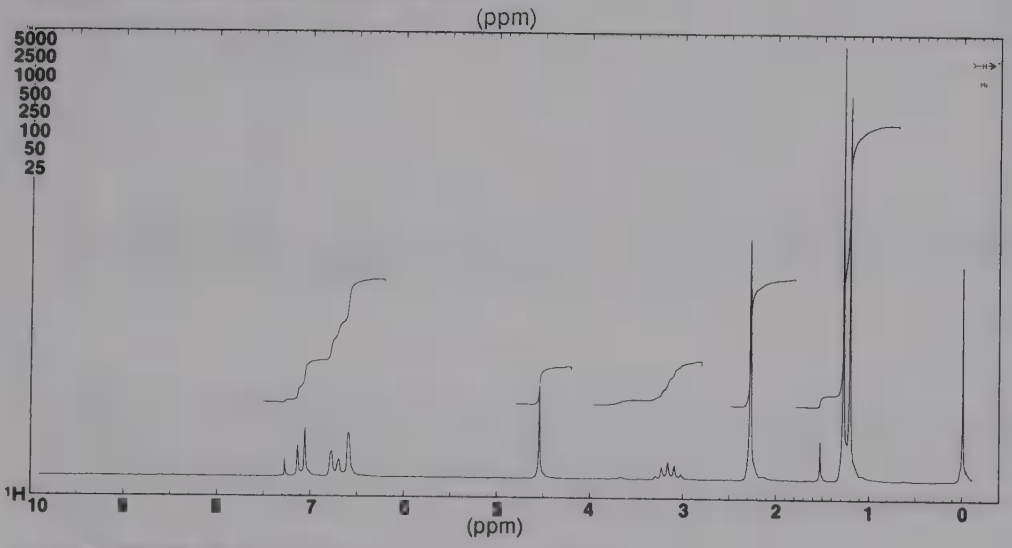

^{13}C NMR SPECTRUM (Completely Decoupled, Solvent $CDCl_3$)

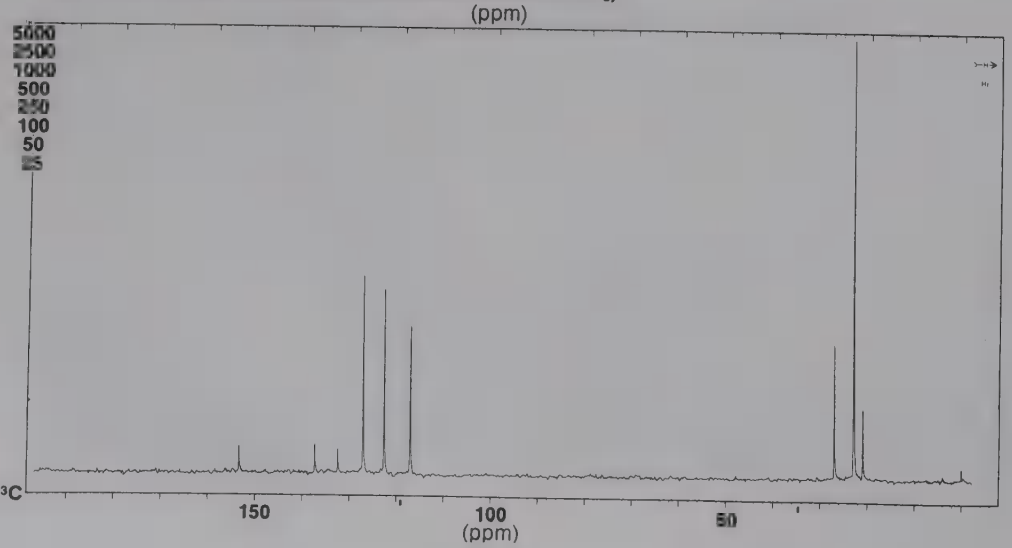

Ultraviolet Data

$\lambda_{max}^{CH_3OH}$ (nm)	log ϵ_{max}
220	3.77
278	3.37
λ_{max}^{NaOH} (nm)	log ϵ_{max}
240	3.95
284	3.78

INFRARED SPECTRUM ***Compound 9.5***

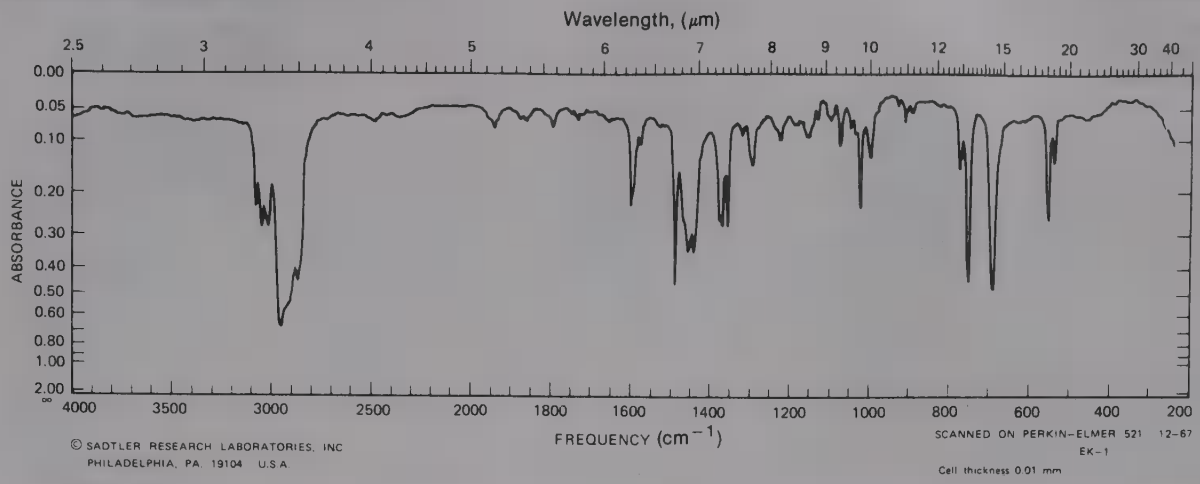

MASS SPECTRAL DATA (Relative Intensities)

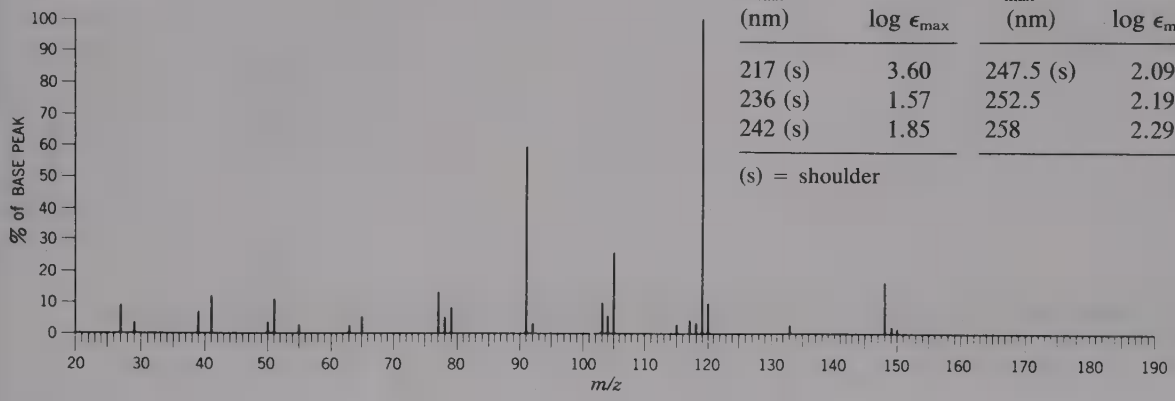

Ultraviolet Data

$\lambda_{max}^{isooctane}$ (nm)	log ϵ_{max}	$\lambda_{max}^{isooctane}$ (nm)	log ϵ_{max}	$\lambda_{max}^{isooctane}$ (nm)	log ϵ_{max}
217 (s)	3.60	247.5 (s)	2.09	261	2.20
236 (s)	1.57	252.5	2.19	264	2.18
242 (s)	1.85	258	2.29		

(s) = shoulder

^{1}H NMR SPECTRUM (Solvent CCl_4, 60 MHz)

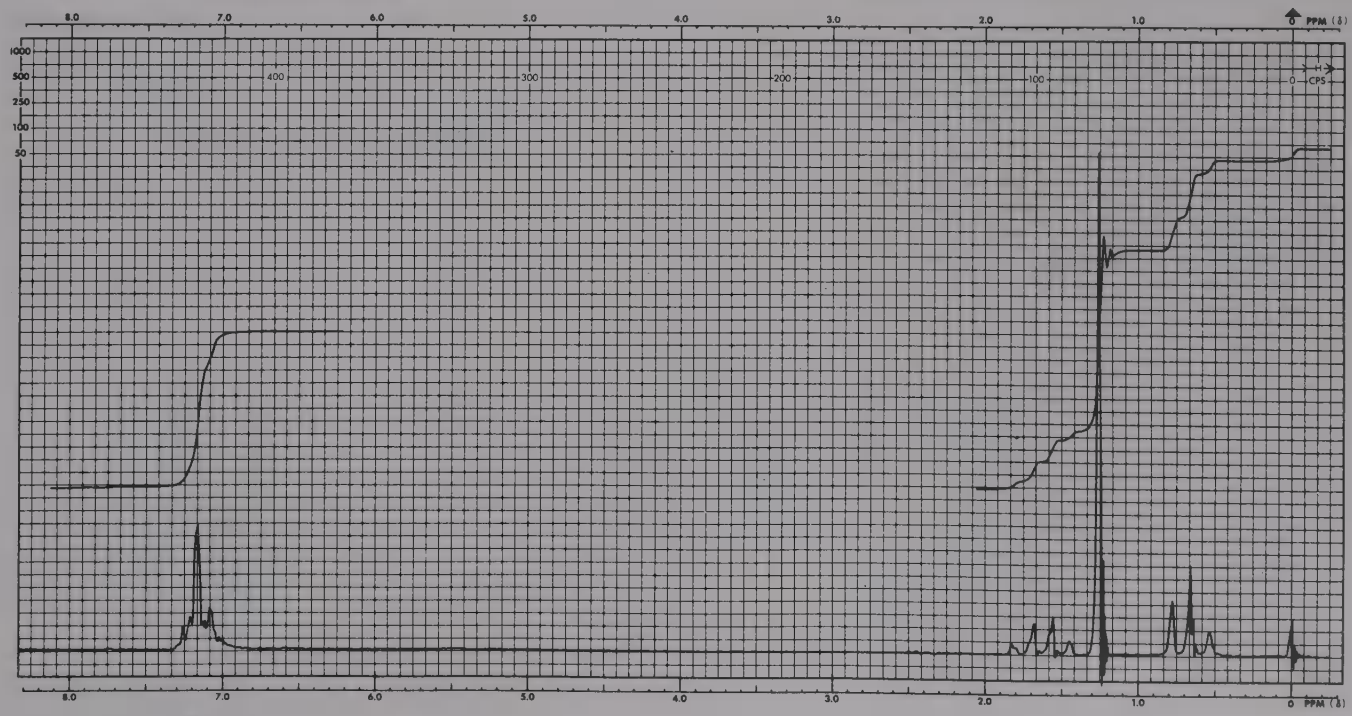

INFRARED SPECTRUM

Compound 9.6

2925.9 1378.3 837.6
1603.5 1081.3 790.6
1465.1 965.8 736.2

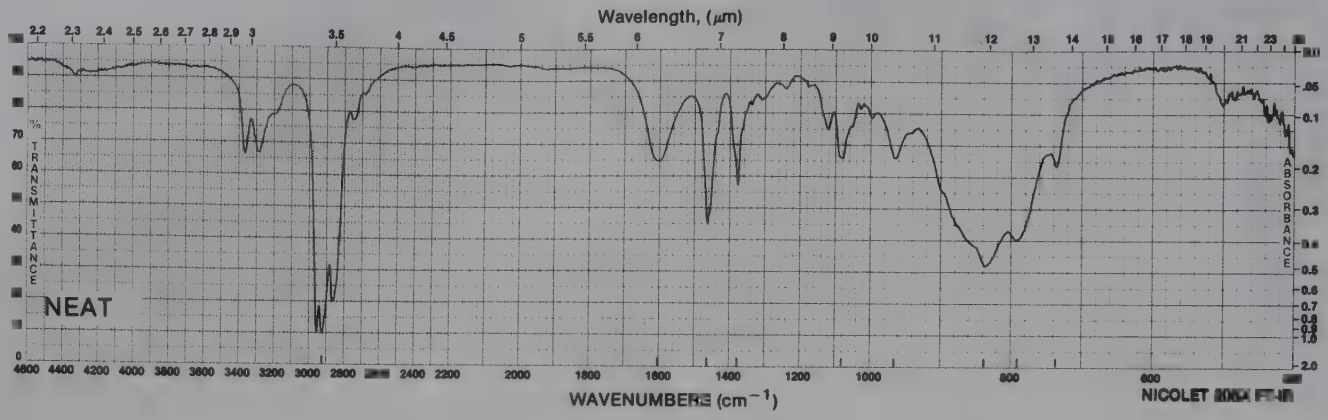

MASS SPECTRAL DATA (Relative Intensities)

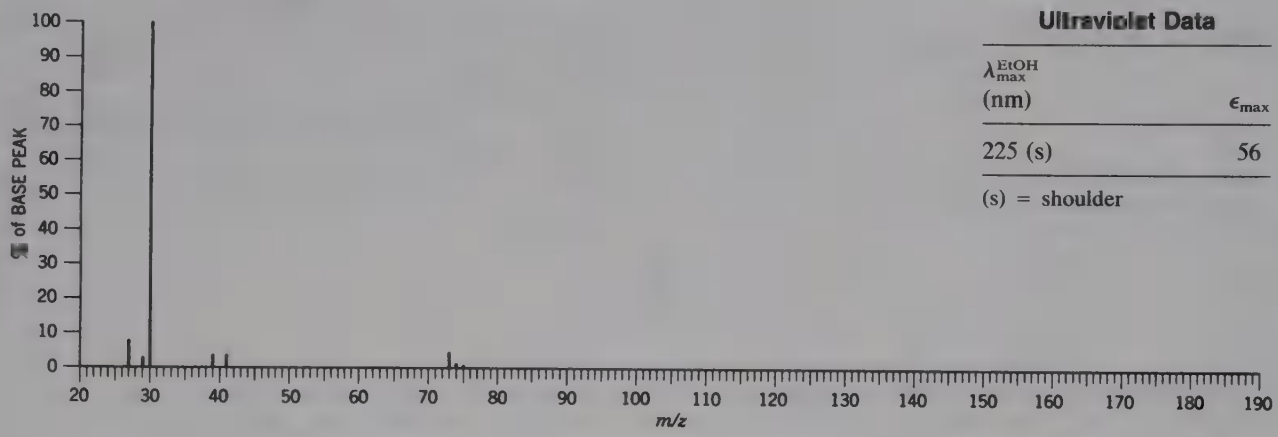

Ultraviolet Data

λ_{max}^{EtOH} (nm)	ϵ_{max}
225 (s)	56

(s) = shoulder

^{1}H NMR SPECTRUM (Solvent $CDCl_3$, 300 MHz)

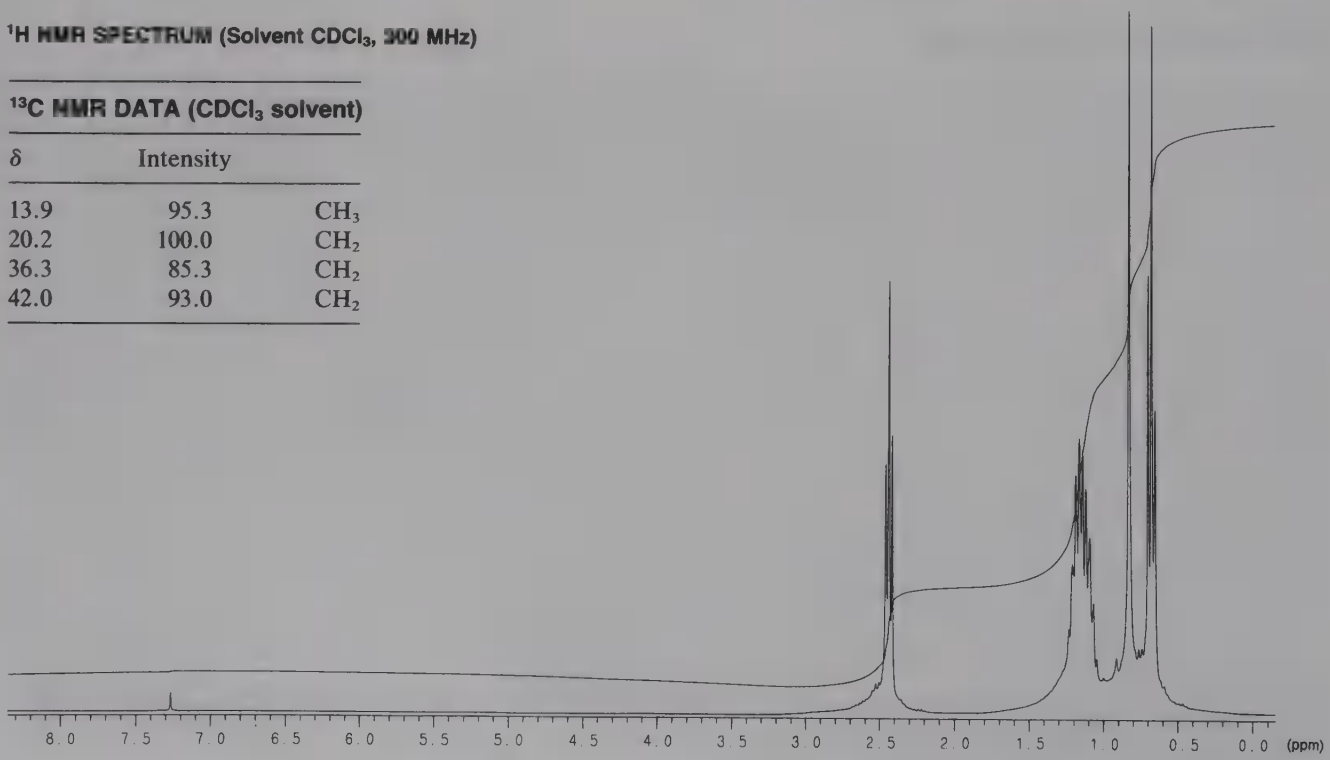

^{13}C NMR DATA ($CDCl_3$ solvent)

δ	Intensity	
13.9	95.3	CH_3
20.2	100.0	CH_2
36.3	85.3	CH_2
42.0	93.0	CH_2

INFRARED SPECTRUM

Compound 9.7

3056.2 1399.4 1155.9
1527.3 1302.6 1020.4
1476.4 1248.4 829.3

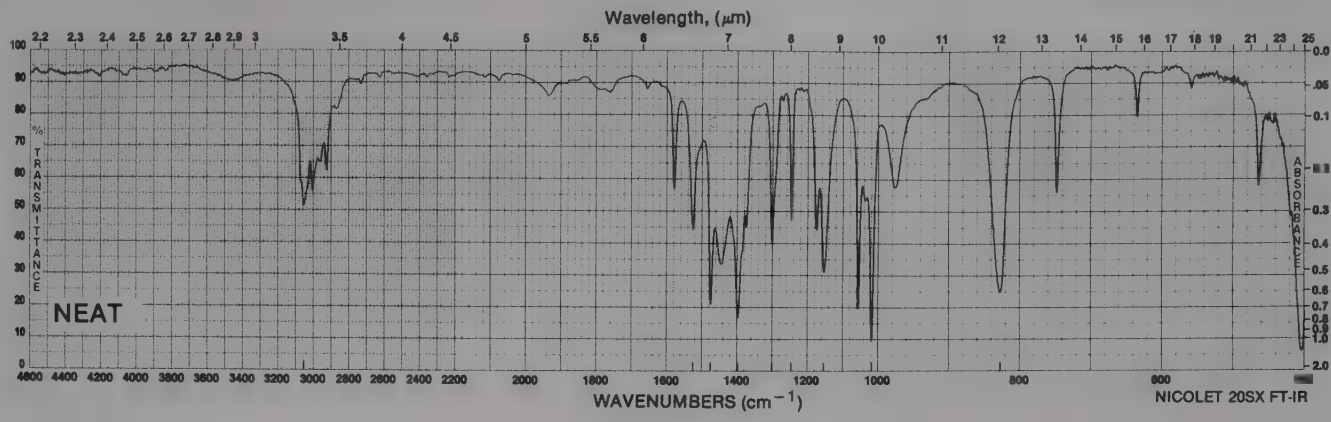

MASS SPECTRAL DATA (Relative Intensities)

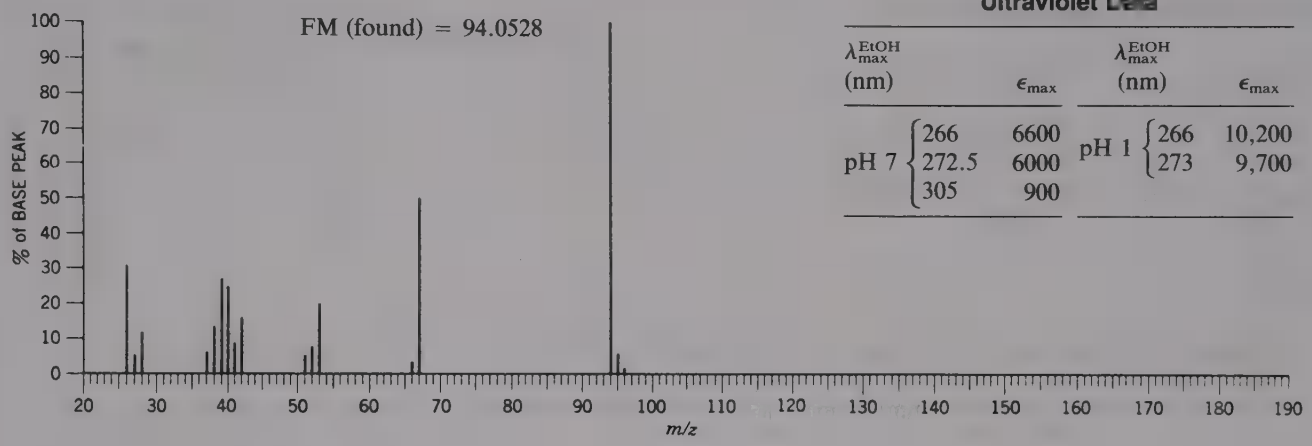

Ultraviolet Data

λ_{max}^{EtOH} (nm)		ϵ_{max}	λ_{max}^{EtOH} (nm)		ϵ_{max}
pH 7	266	6600	pH 1	266	10,200
	272.5	6000		273	9,700
	305	900			

^{1}H NMR SPECTRUM (Solvent $CDCl_3$, 100 MHz)

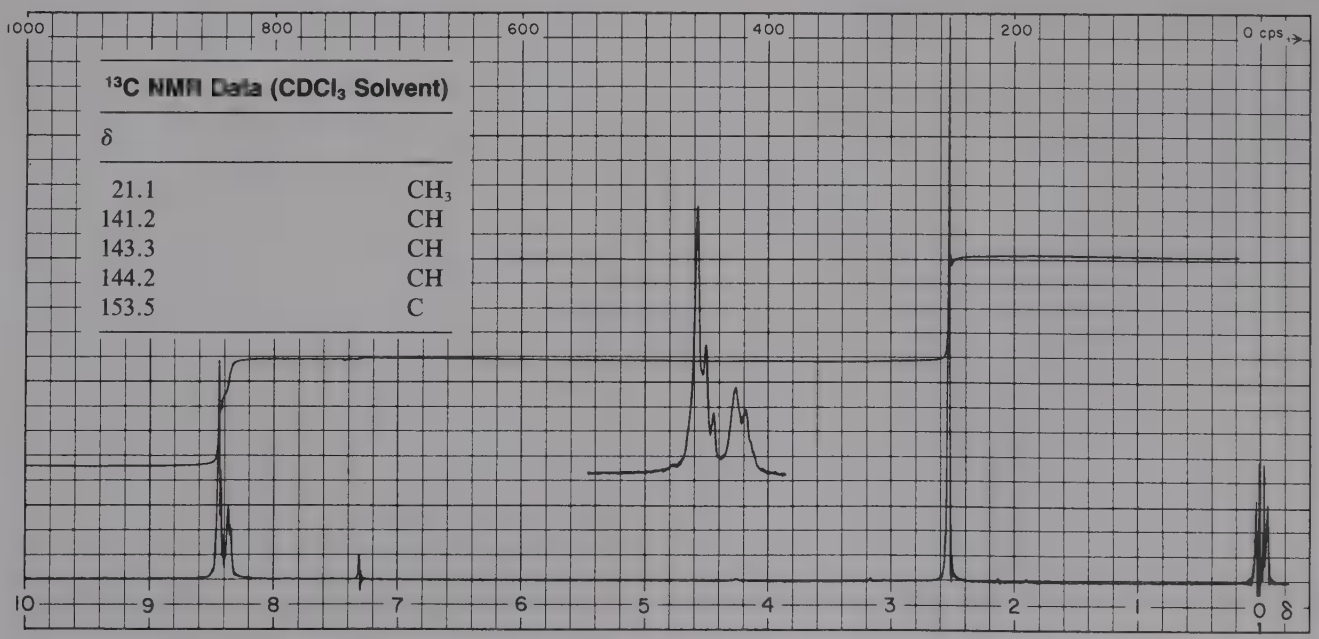

^{13}C NMR Data ($CDCl_3$ Solvent)

δ	
21.1	CH_3
141.2	CH
143.3	CH
144.2	CH
153.5	C

INFRARED SPECTRUM

Compound 9.8

[illegible] 1245.1 1048.9
1601.9 1172.6 753.2
1498.1 1116.0 691.8

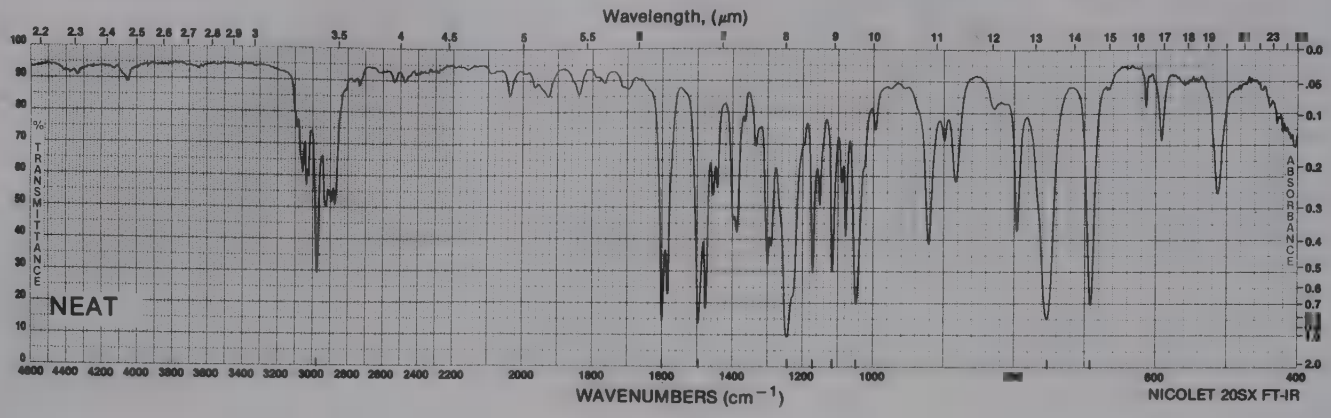

MASS SPECTRAL DATA (Relative Intensities)

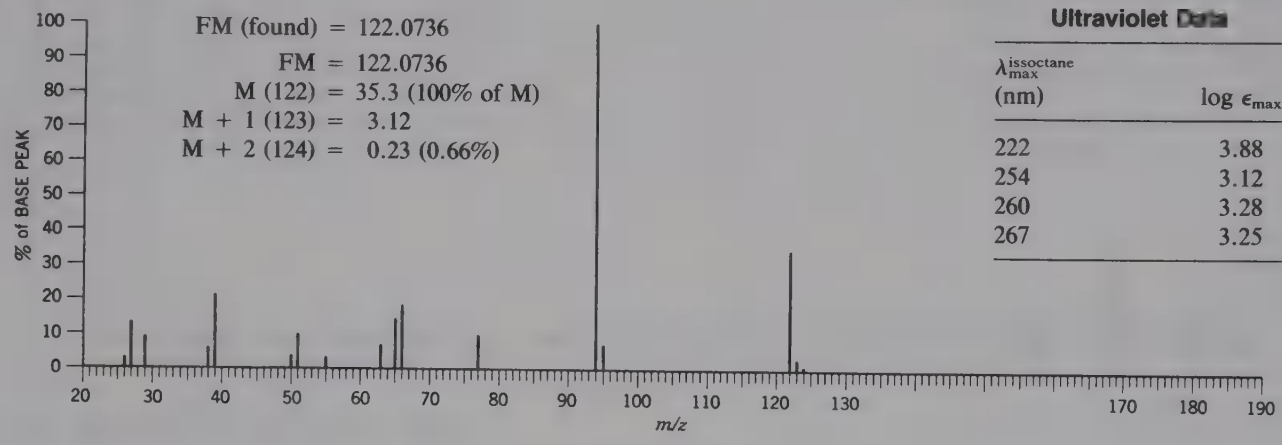

Ultraviolet Data

$\lambda_{max}^{isooctane}$ (nm)	log ϵ_{max}
222	3.88
254	3.12
260	3.28
267	3.25

^{1}H NMR SPECTRUM (Solvent $CDCl_3$, 300 MHz)

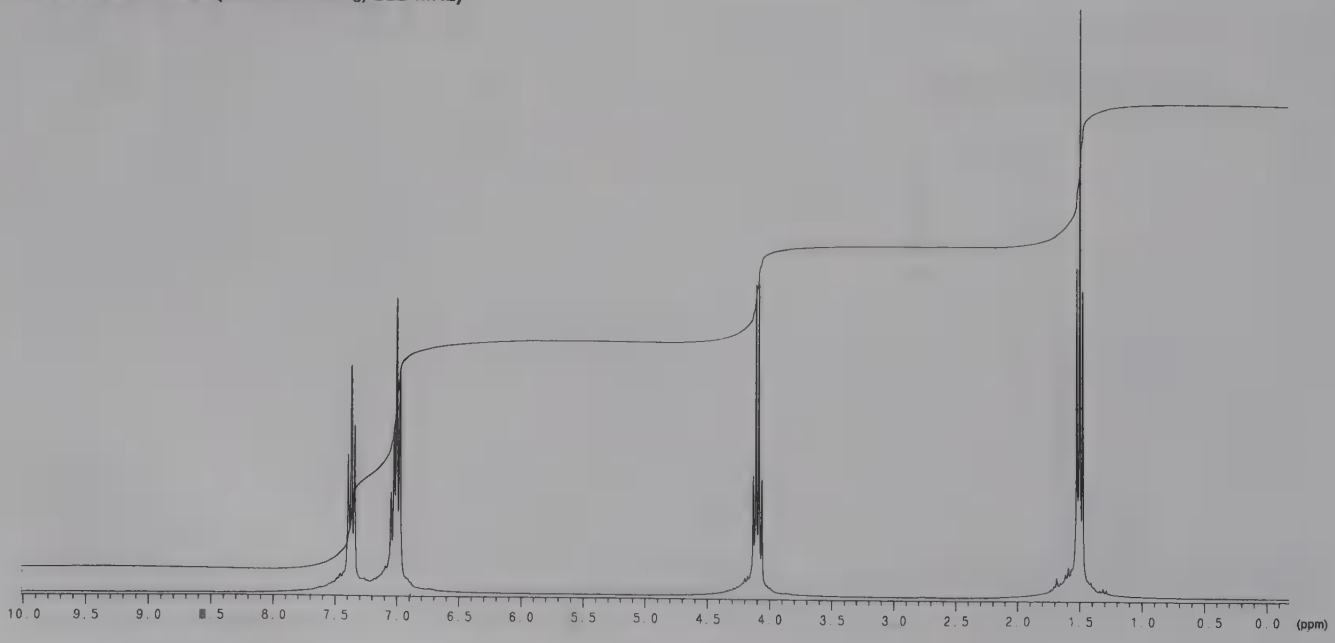

INFRARED SPECTRUM

Compound 3.9

3369.0 1246.4 917.5
1599.1 1173.3 754.4
1497.2 1082.4 692.0

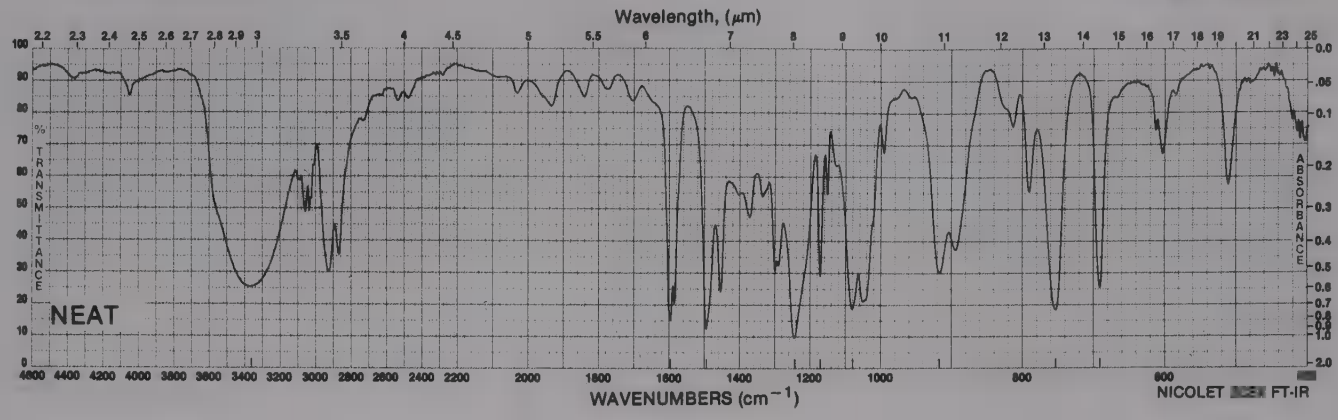

MASS SPECTRAL DATA (Relative Intensities)

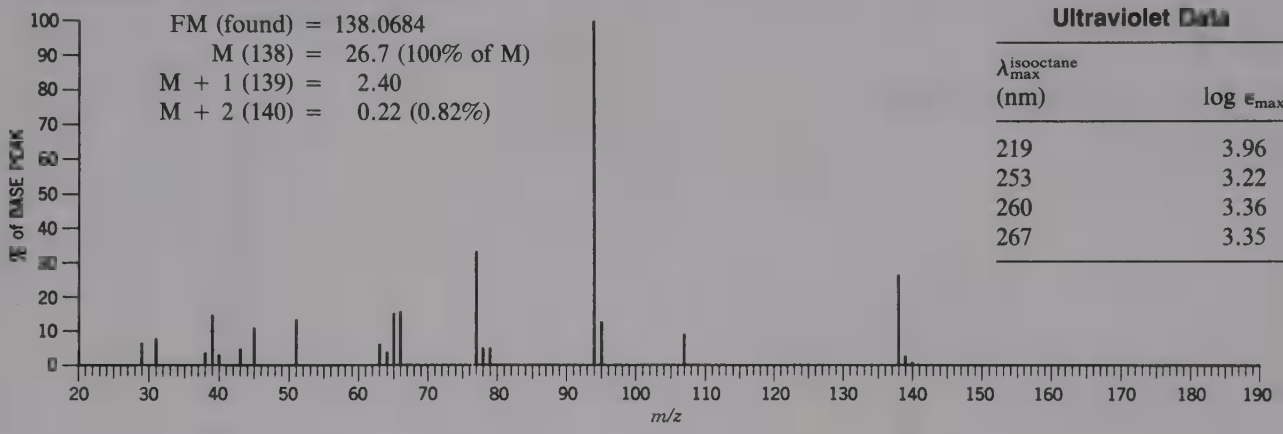

Ultraviolet Data

$\lambda_{max}^{isooctane}$ (nm)	log ϵ_{max}
219	3.96
253	3.22
260	3.36
267	3.35

^{1}H NMR SPECTRUM (Solvent CCl_4, 60 MHz)

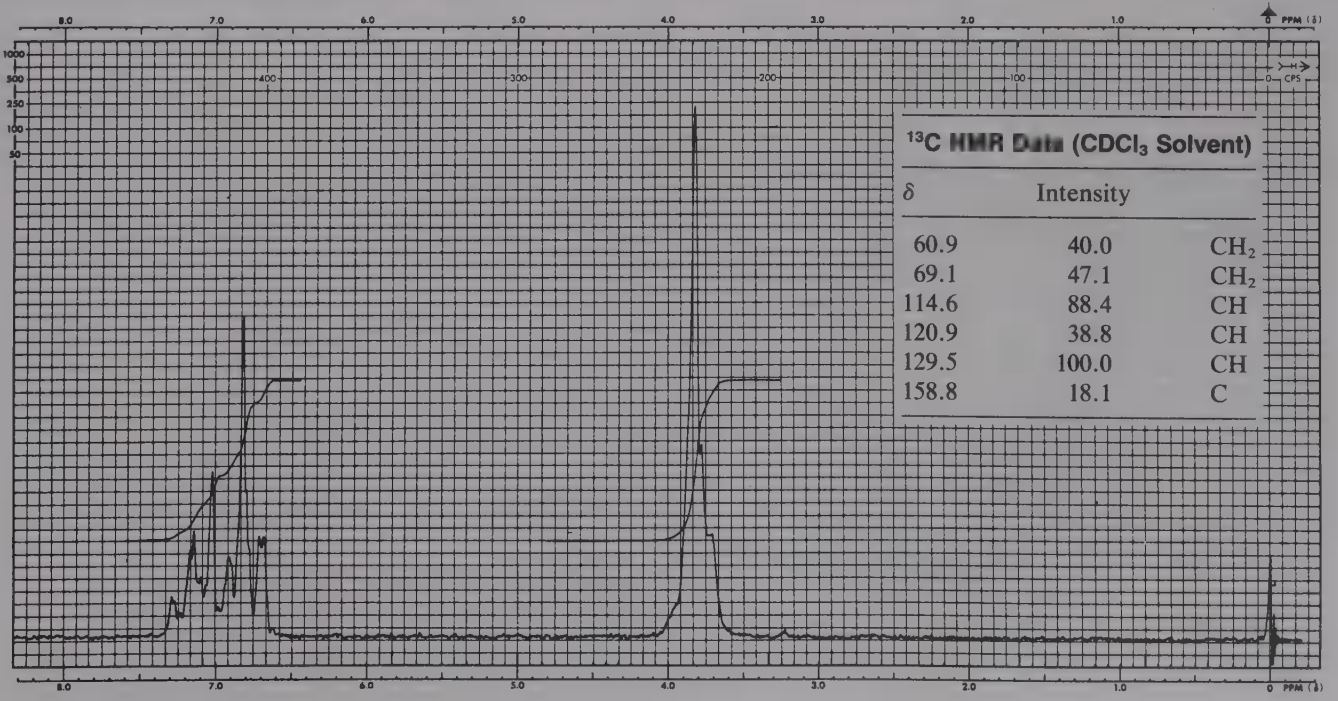

^{13}C NMR Data ($CDCl_3$ Solvent)

δ	Intensity	
60.9	40.0	CH_2
69.1	47.1	CH_2
114.6	88.4	CH
120.9	38.8	CH
129.5	100.0	CH
158.8	18.1	C

INFRARED SPECTRUM

Compound 9.10

3027.8 1603.2 1030.3
2824.8 1496.8 746.7
1724.2 1388.7 700.3

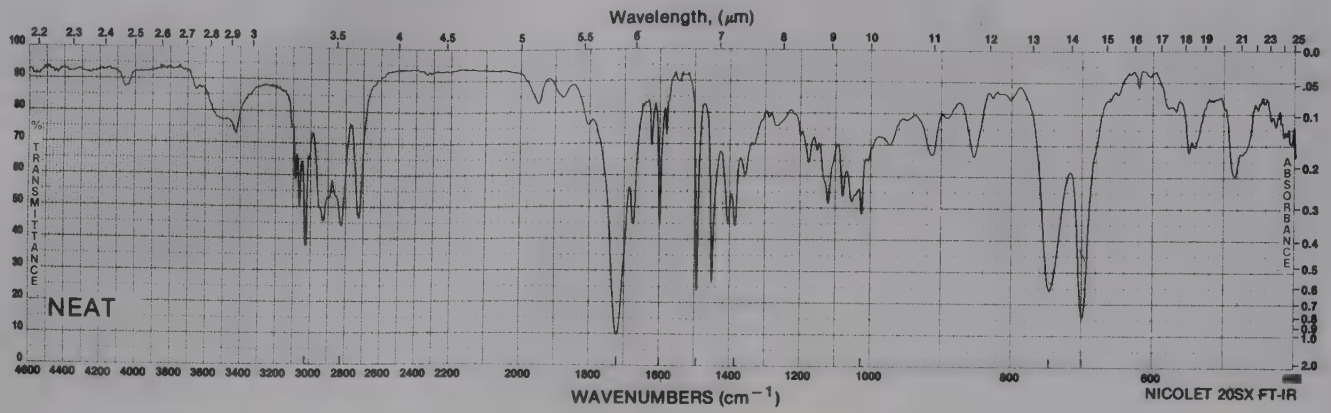

MASS SPECTRAL DATA (Relative Intensities)

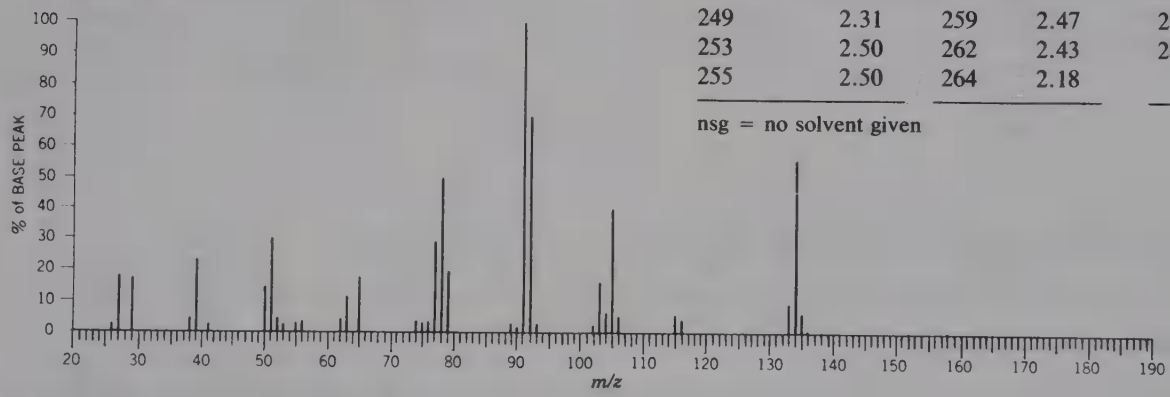

Ultraviolet Data

λ_{max}^{nsg} (nm)	log ϵ_{max}	λ_{max}^{nsg} (nm)	log ϵ_{max}	λ_{max}^{nsg} (nm)	log ϵ_{max}
249	2.31	259	2.47	268	2.25
253	2.50	262	2.43	283	1.59
255	2.50	264	2.18		

nsg = no solvent given

^{1}H NMR SPECTRUM (Solvent $CDCl_3$, 60 MHz)

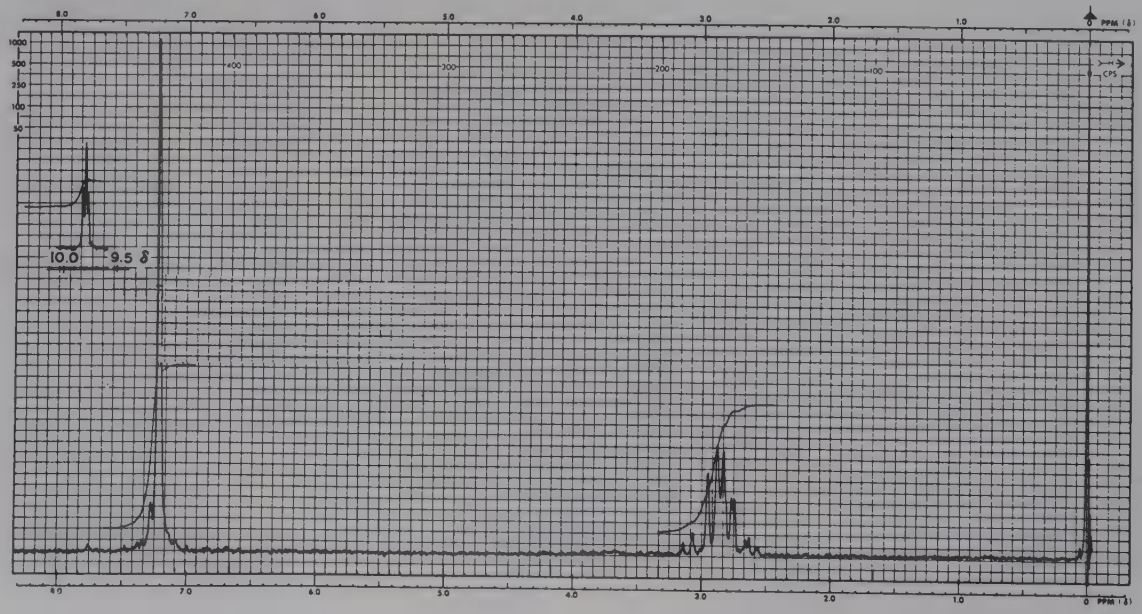

INFRARED SPECTRUM

Compound 9.11

2931.0	1467.1	1123.1
2716.9	1390.3	1052.1
1727.4	1190.7	726.9

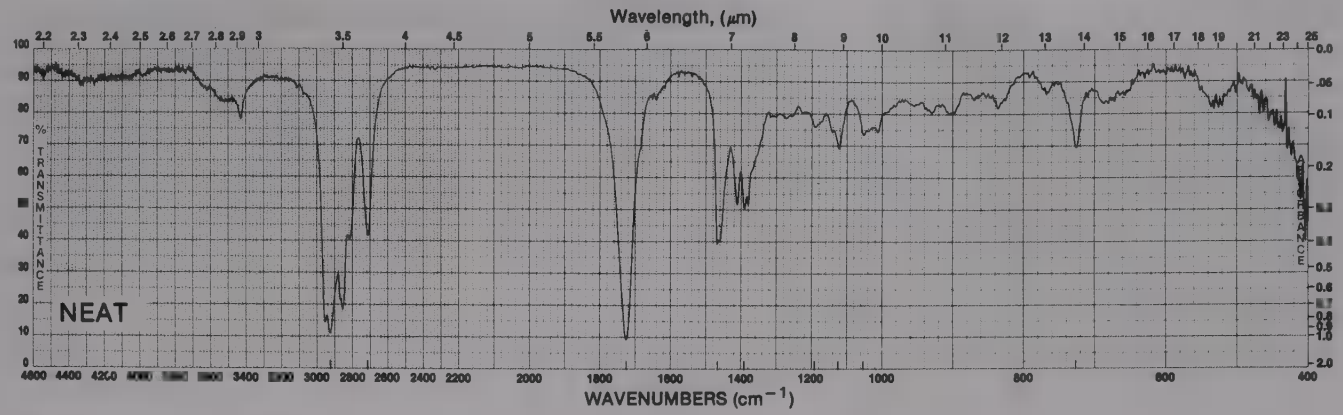

MASS SPECTRAL DATA (Relative Intensities)

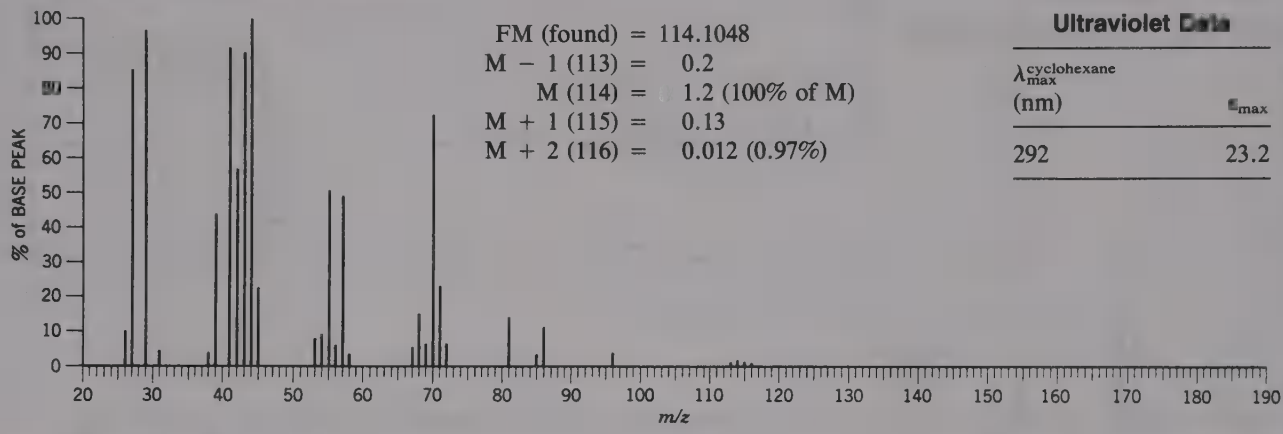

FM (found) = 114.1048
M − 1 (113) = 0.2
M (114) = 1.2 (100% of M)
M + 1 (115) = 0.13
M + 2 (116) = 0.012 (0.97%)

Ultraviolet Data

$\lambda_{max}^{cyclohexane}$ (nm)	ε_{max}
292	23.2

^{1}H NMR SPECTRUM (Solvent $CDCl_3$, 90 MHz)

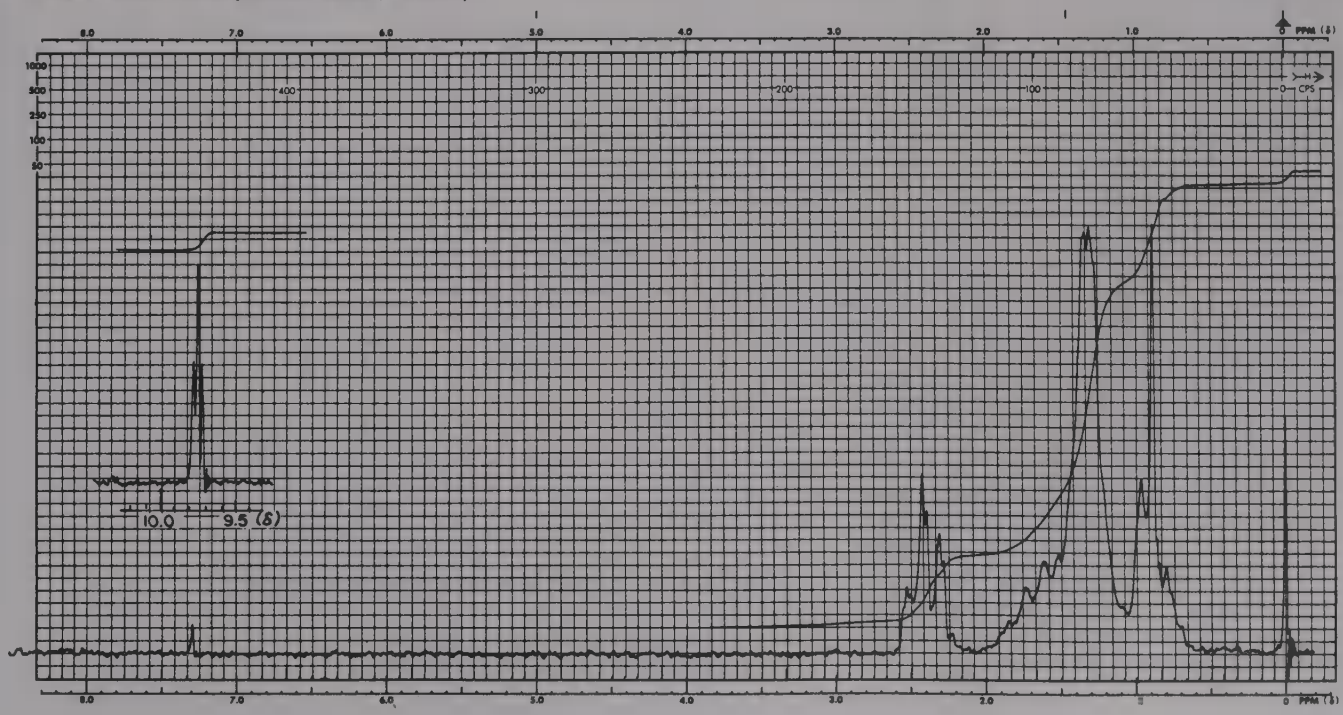

INFRARED SPECTRUM

Compound 9.12

[illegible]	1311.2	[illegible]
1714.0	1221.7	749.8
1449.5	1118.8	489.7

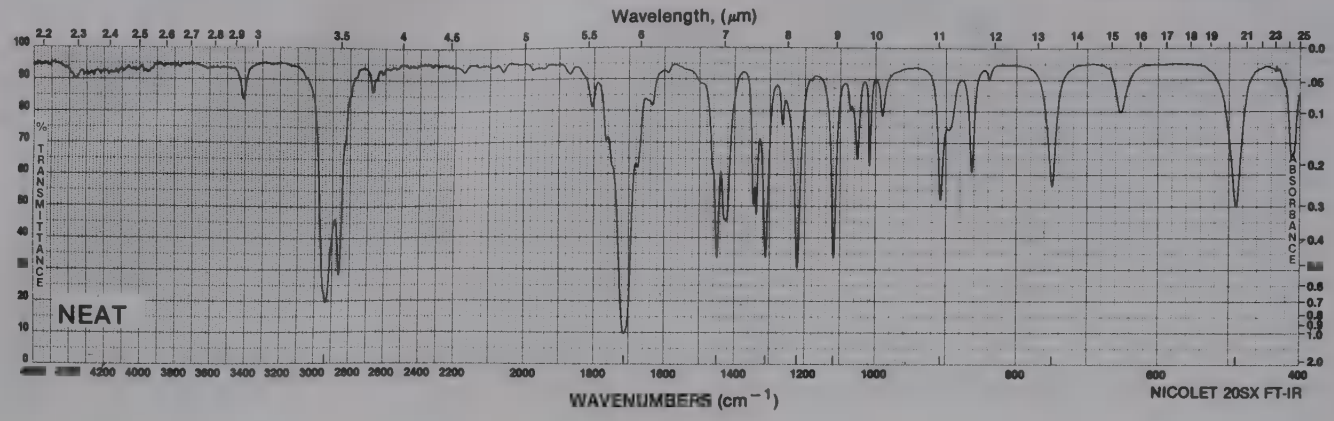

MASS SPECTRAL DATA (Relative Intensities)

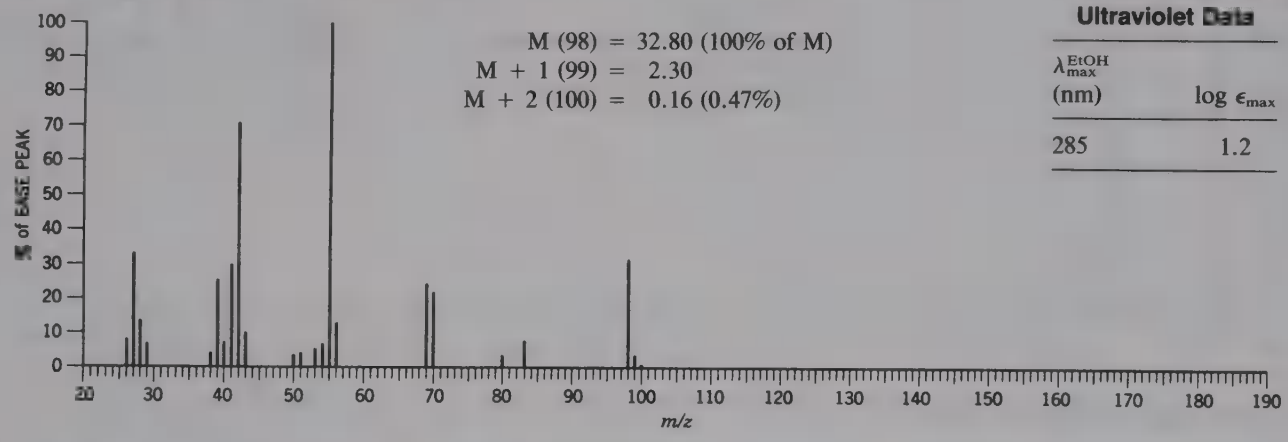

M (98) = 32.80 (100% of M)
M + 1 (99) = 2.30
M + 2 (100) = 0.16 (0.47%)

Ultraviolet Data

λ_{max}^{EtOH} (nm)	log ϵ_{max}
285	1.2

^{1}H NMR SPECTRUM (Solvent $CDCl_3$, [illegible] MHz)

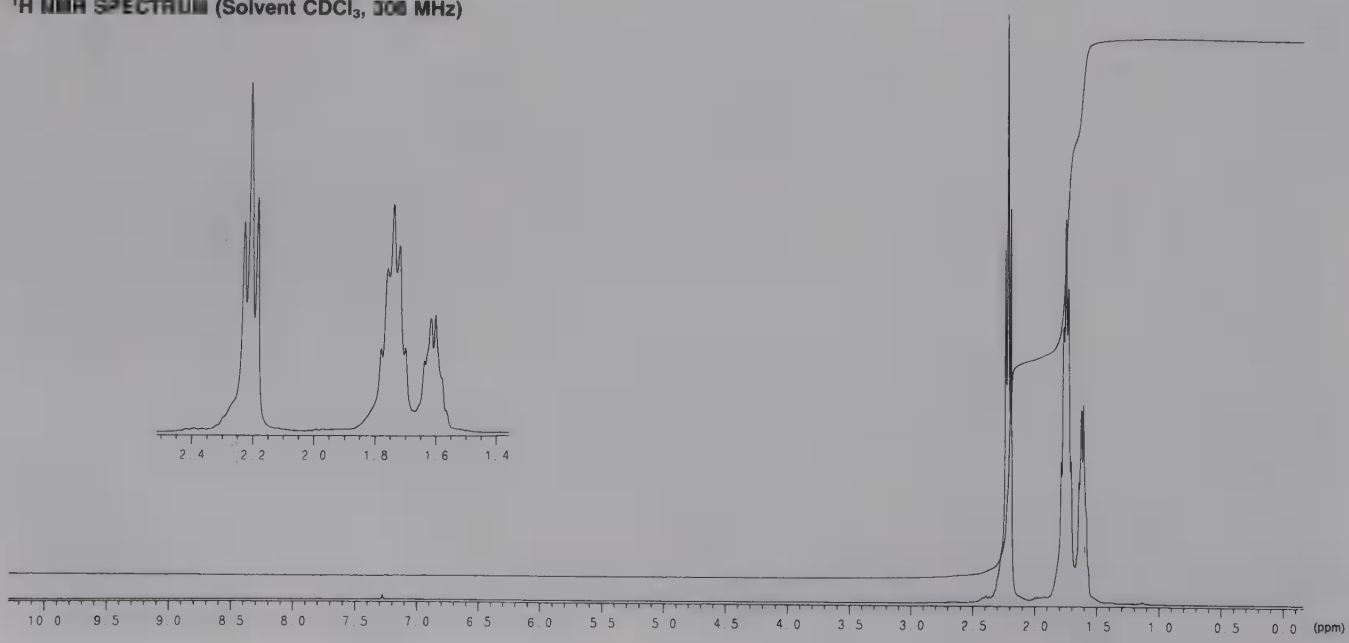

Compound 9.12 (continued)

^{13}C NMR SPECTRUM COMPLETELY DECOUPLED

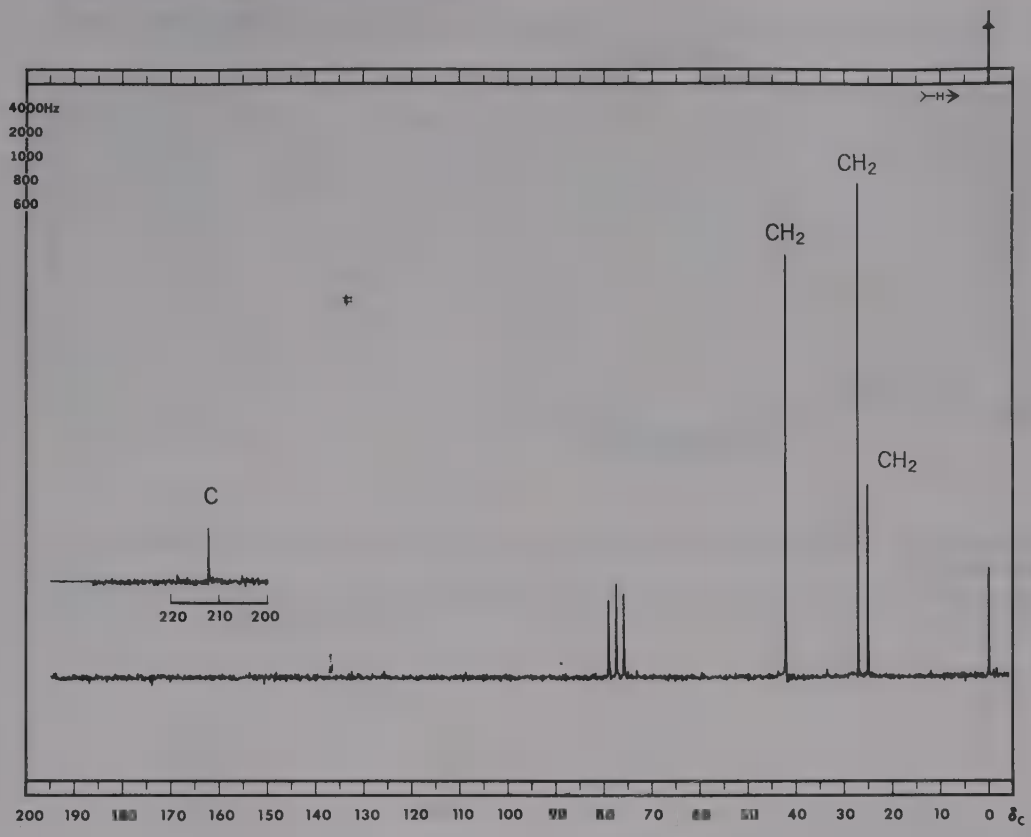

INFRARED SPECTRUM

Compound 9.13

1683.3	1315.4	1024.9
1600.0	1260.6	833.5
1511.0	1160.6	607.6

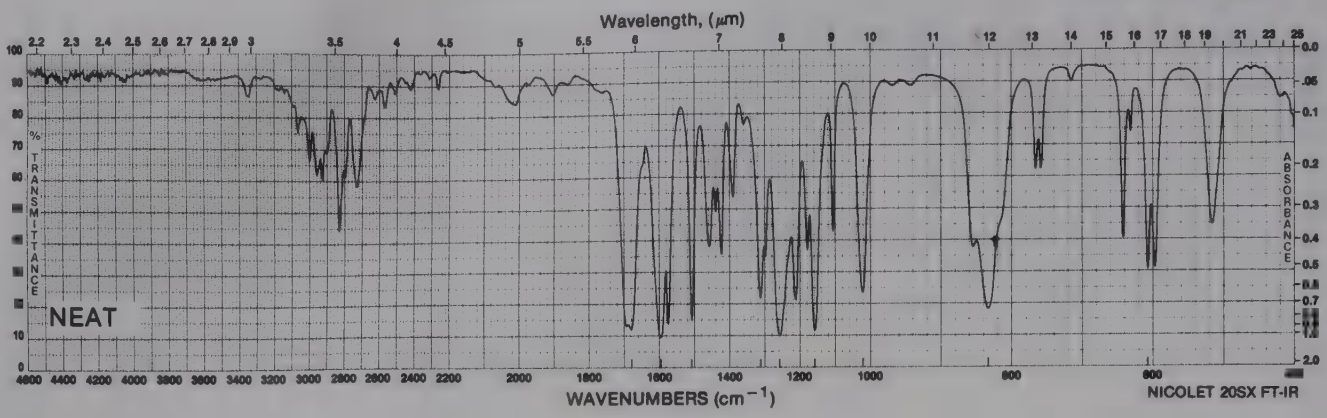

MASS SPECTRAL DATA (Relative Intensity)

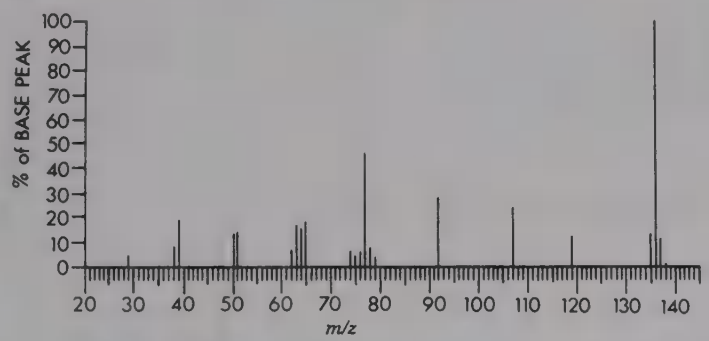

Ultraviolet Data

$\lambda_{max}^{cyclohexane}$ (nm)	ϵ_{max}
215	21,500
221	20,000
266	25,500
288	8,500
312	90
324	83
360	25

^{1}H NMR SPECTRUM (Solvent $CDCl_3$, 100 MHz)

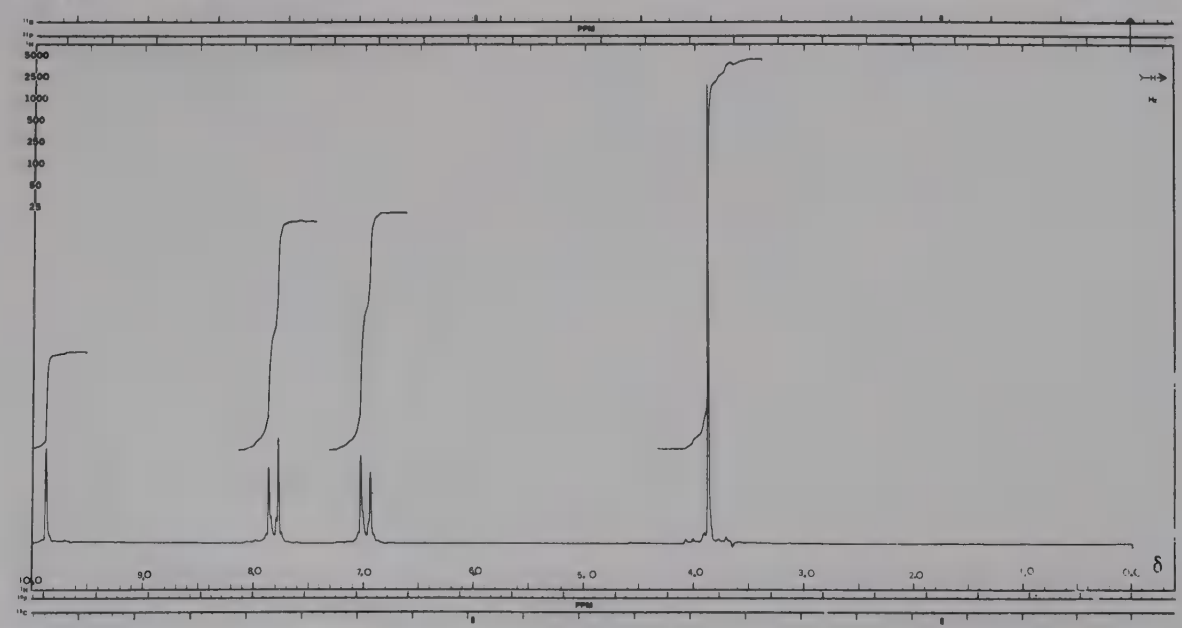

Compound 9.13 (continued)

^{13}C NMR SPECTRUM COMPLETELY DECOUPLED

INFRARED SPECTRUM

Compound 9.14

1662.1	1356.2	857.9
1518.2	1274.0	725.5
1415.2	934.3	591.9

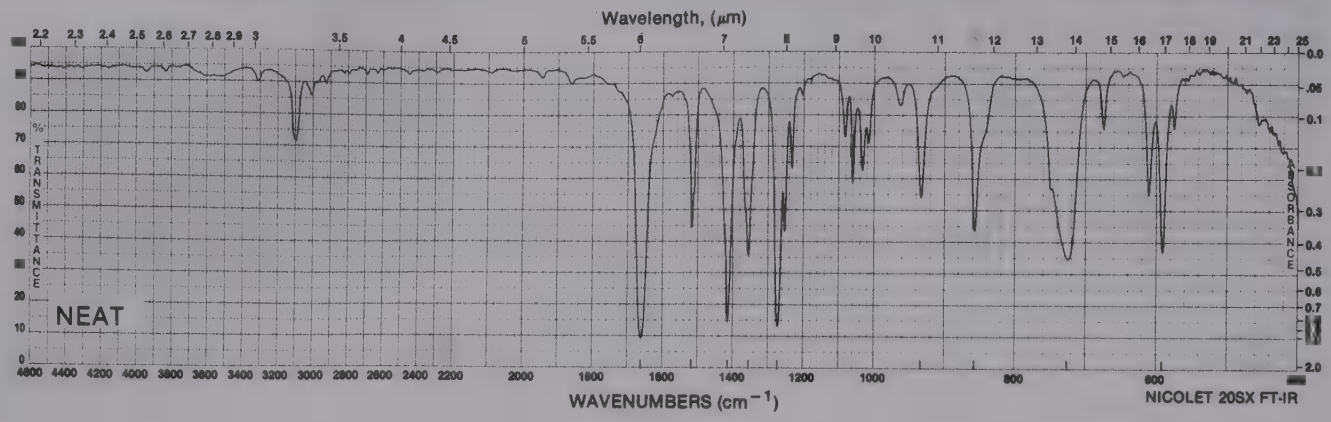

MASS SPECTRA DATA (Relative Intensity)

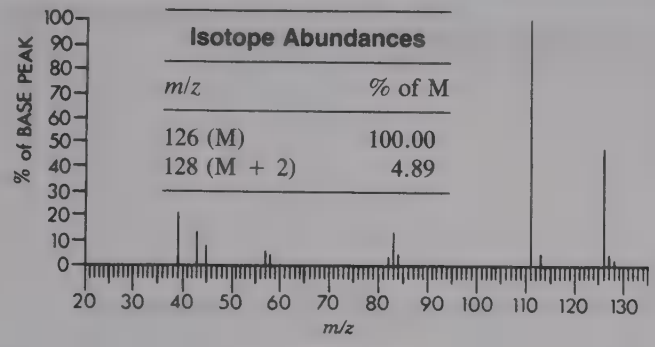

Isotope Abundances

m/z	% of M
126 (M)	100.00
128 (M + 2)	4.89

^{13}C NMR Data ($CDCl_3$ Solvent)

δ	Intensity	
26.6	76.0	CH_3
128.3	89.8	CH
132.8	100.0	CH
133.8	98.4	CH
144.6	25.0	C
190.4	34.9	C

Ultraviolet Data

$\lambda_{max}^{CH_3OH}$ (nm)	ϵ_{max}
257	10,500
280	7,200

^{1}H NMR SPECTRUM (Solvent $CDCl_3$, 60 MHz)

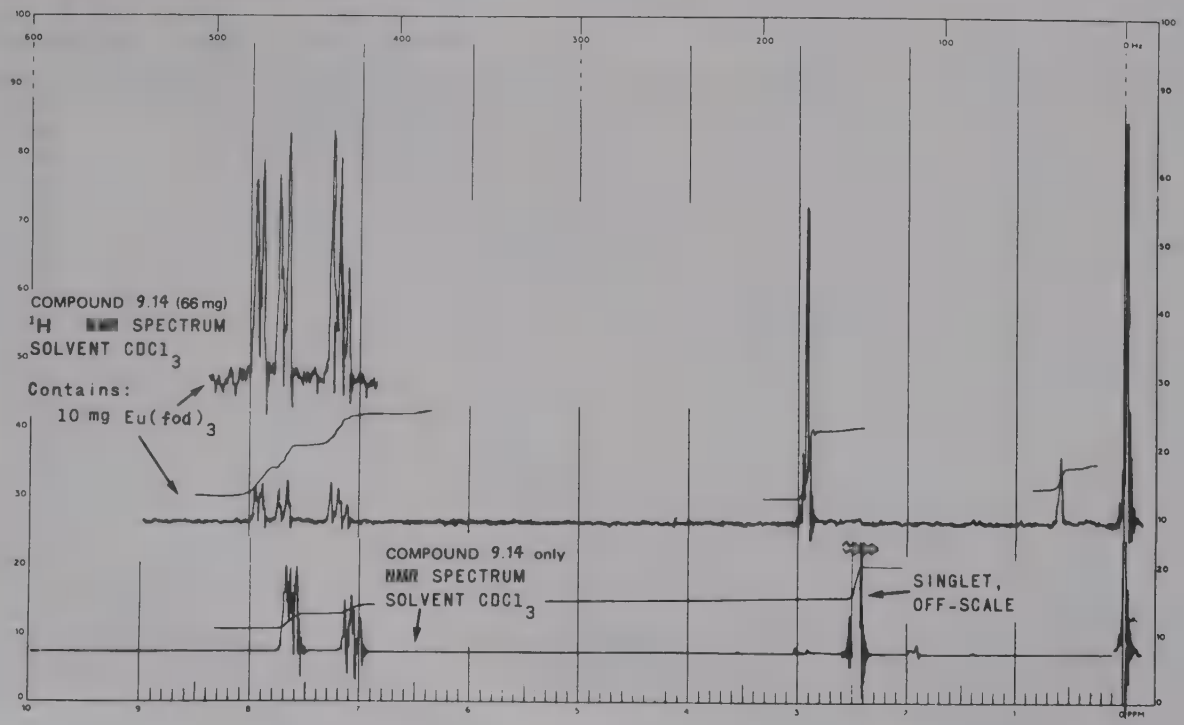

INFRARED SPECTRUM

Compound 9.15

1362.1 1097.7
1741.4 1259.0 996.7
1437.0 1198.0

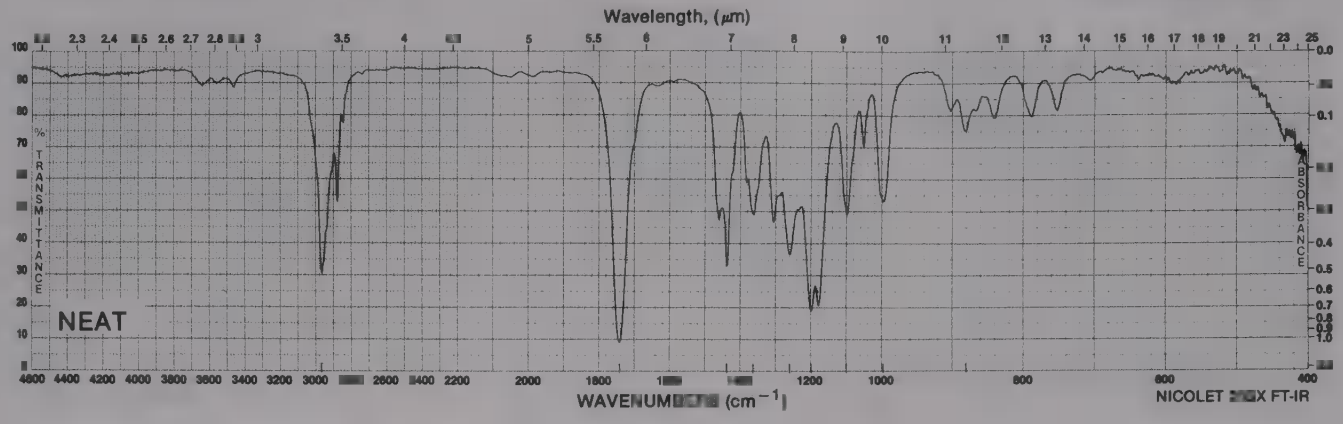

MASS SPECTRAL DATA (Relative Intensities)

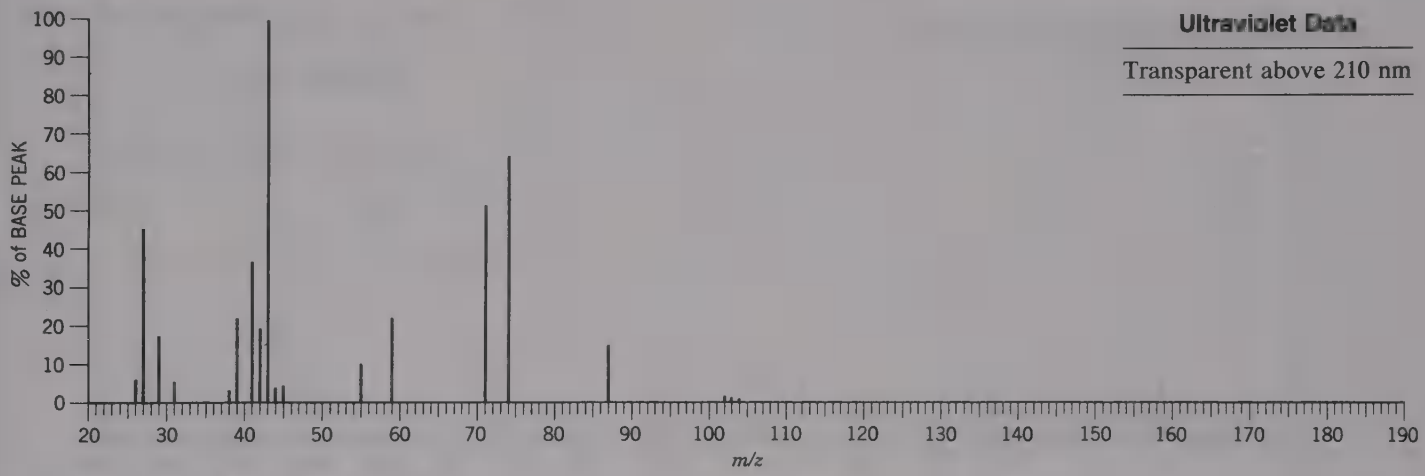

Ultraviolet Data

Transparent above 210 nm

^{1}H NMR SPECTRUM (Solvent CCl_4, 60 MHz)

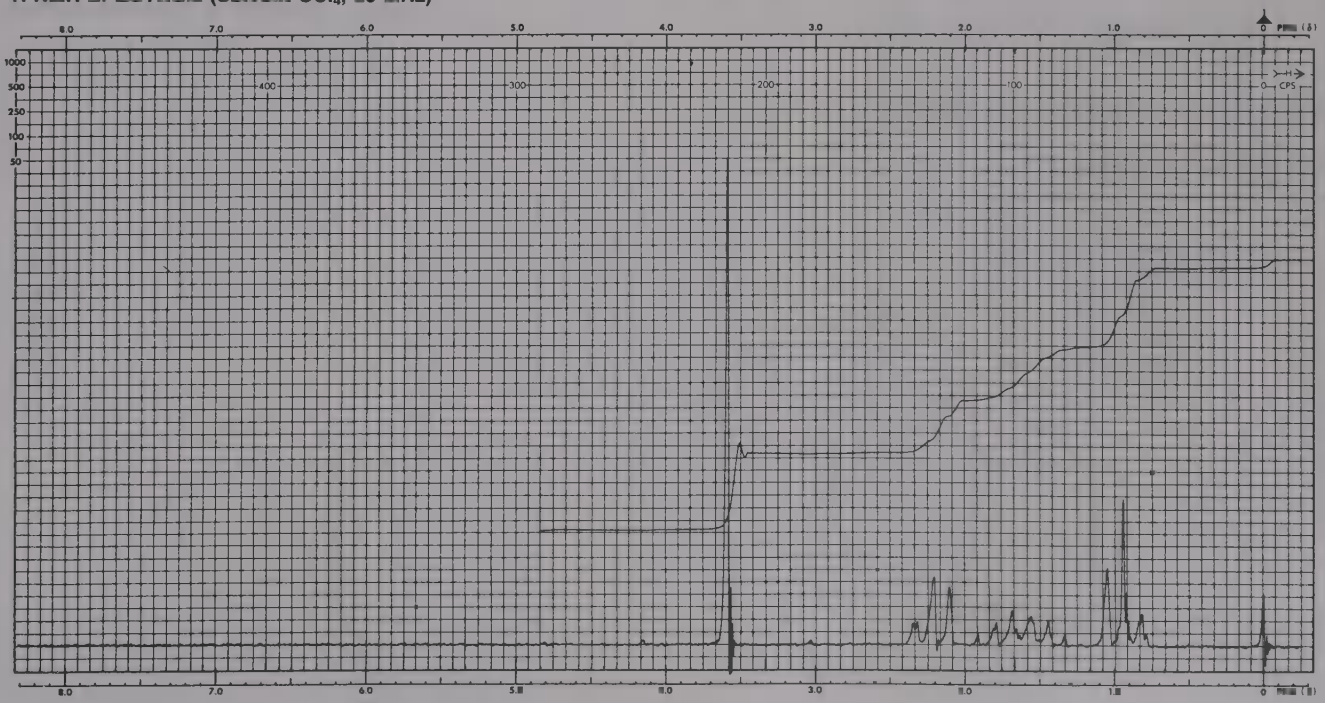

INFRARED SPECTRUM

Compound 9.16

1764.8	1370.6	925.2
1593.8	1193.3	749.0
1493.1	1013.1	691.9

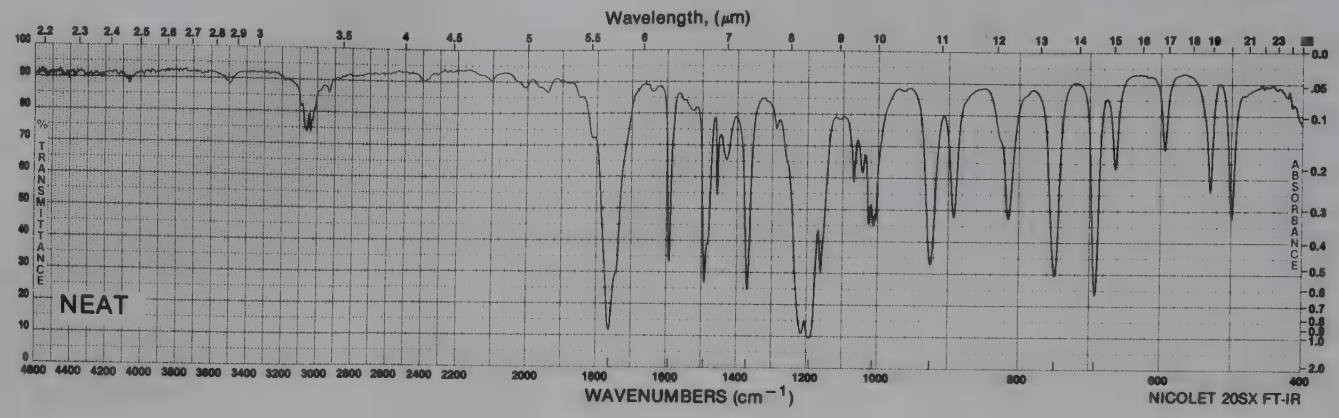

MASS SPECTRAL DATA (Relative Intensities)

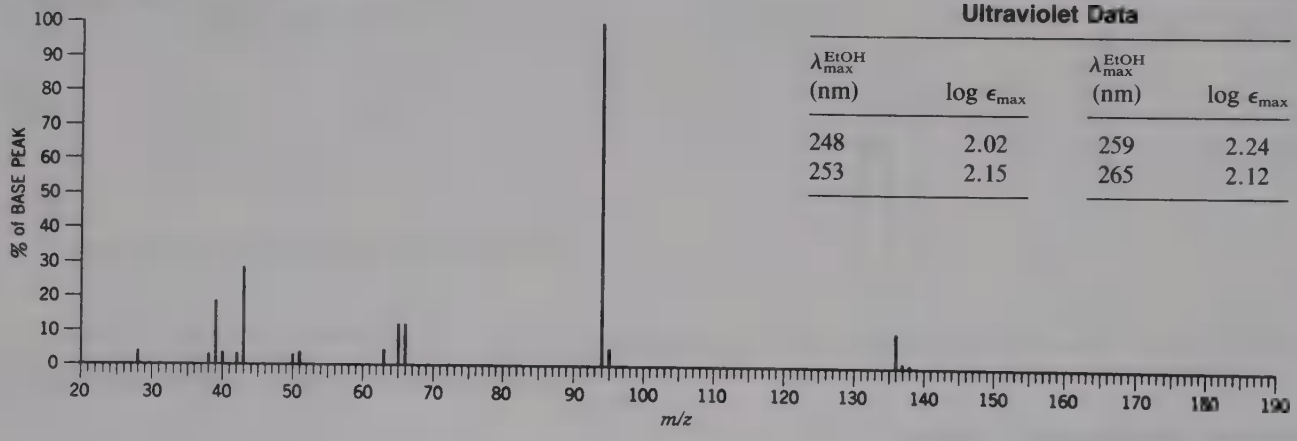

Ultraviolet Data

λ_{max}^{EtOH} (nm)	log ϵ_{max}	λ_{max}^{EtOH} (nm)	log ϵ_{max}
248	2.02	259	2.24
253	2.15	265	2.12

^{1}H NMR SPECTRUM (Solvent $CDCl_3$, 300 MHz)

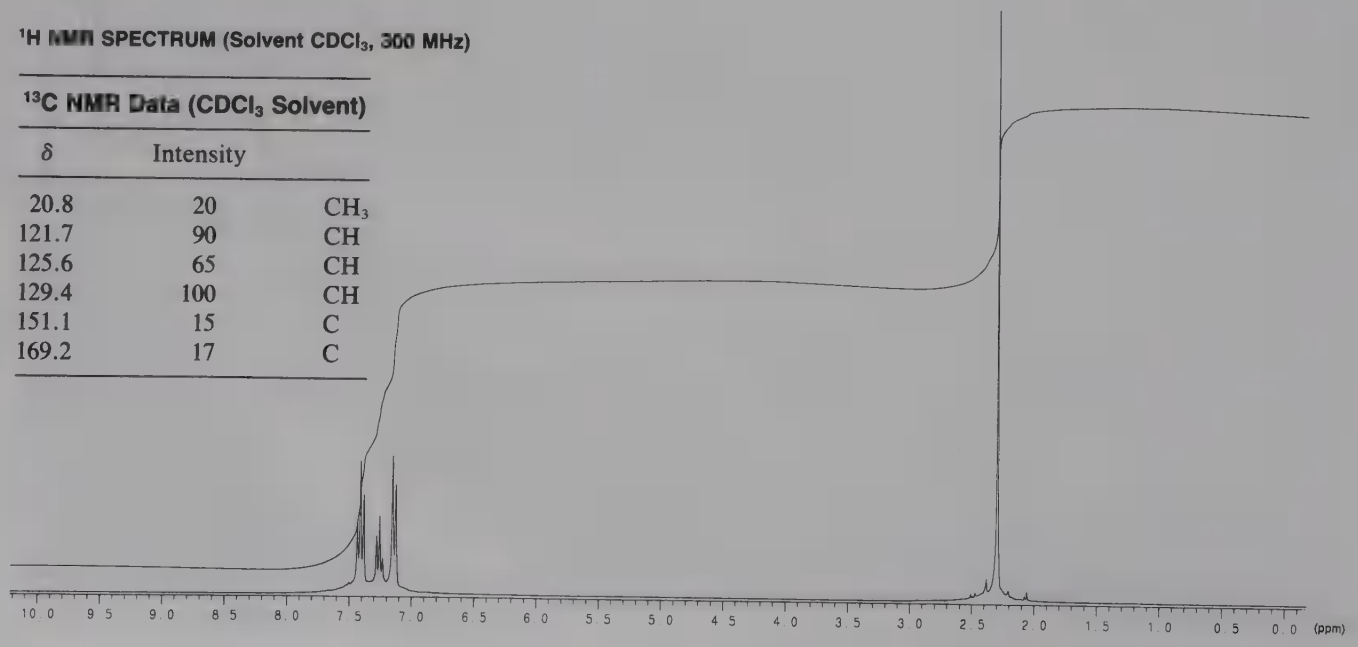

^{13}C NMR Data ($CDCl_3$ Solvent)

δ	Intensity	
20.8	20	CH_3
121.7	90	CH
125.6	65	CH
129.4	100	CH
151.1	15	C
169.2	17	C

INFRARED SPECTRUM

Compound 9.17

[illegible] 1367.2 1108.5
1718.5 1275.8 1028.5
1451.4 1175.2 710.3

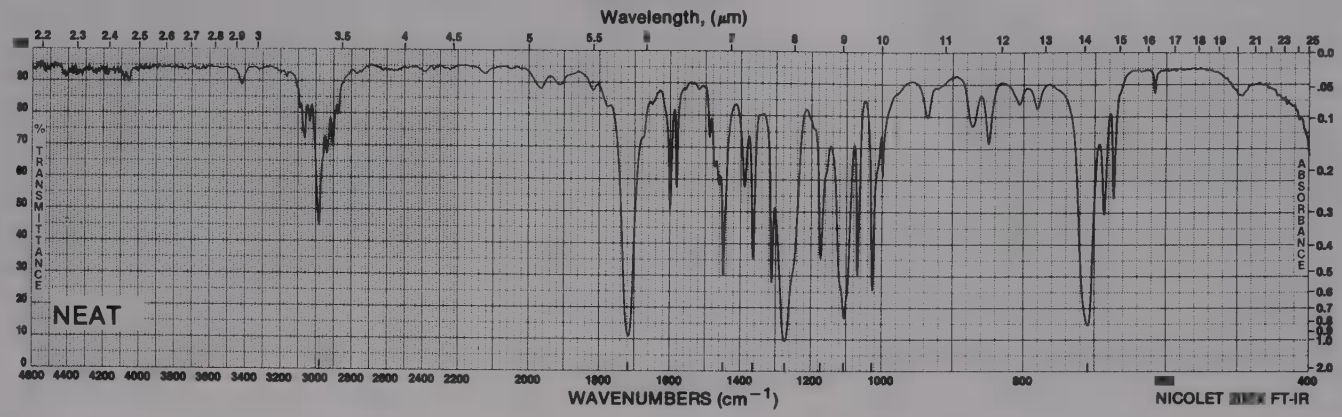

MASS SPECTRAL DATA (Relative Intensities)

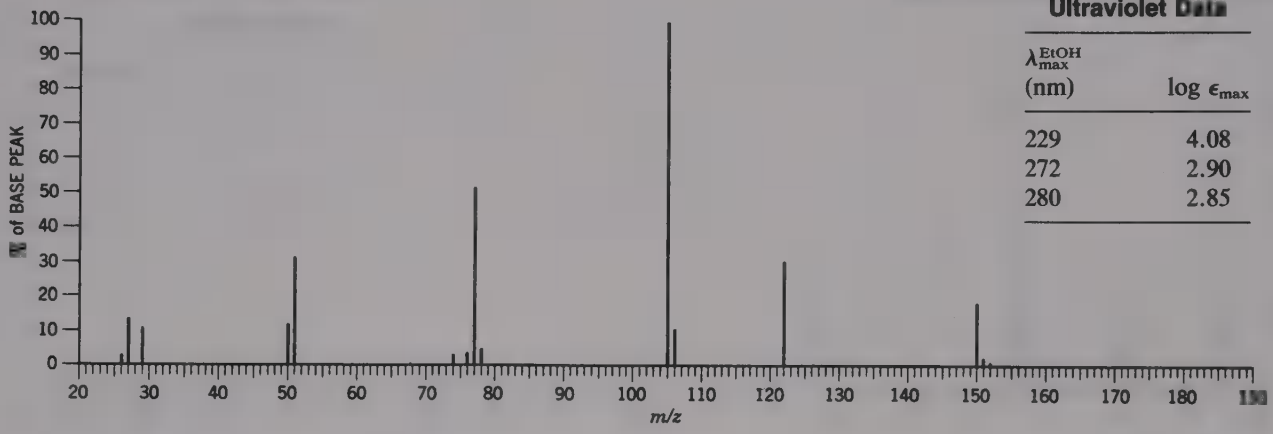

Ultraviolet Data

λ_{max}^{EtOH} (nm)	log ϵ_{max}
229	4.08
272	2.90
280	2.85

^{1}H NMR SPECTUM (Solvent $CDCl_3$, [illegible] MHz)

^{13}C NMR Data ($CDCl_3$ Solvent)

δ	Intensity	
14.4	47.0	CH_3
60.8	39.7	CH_2
128.4	87.0	CH
129.7	100.0	CH
130.9	8.7	C
132.8	50.2	CH
166.3	9.2	C

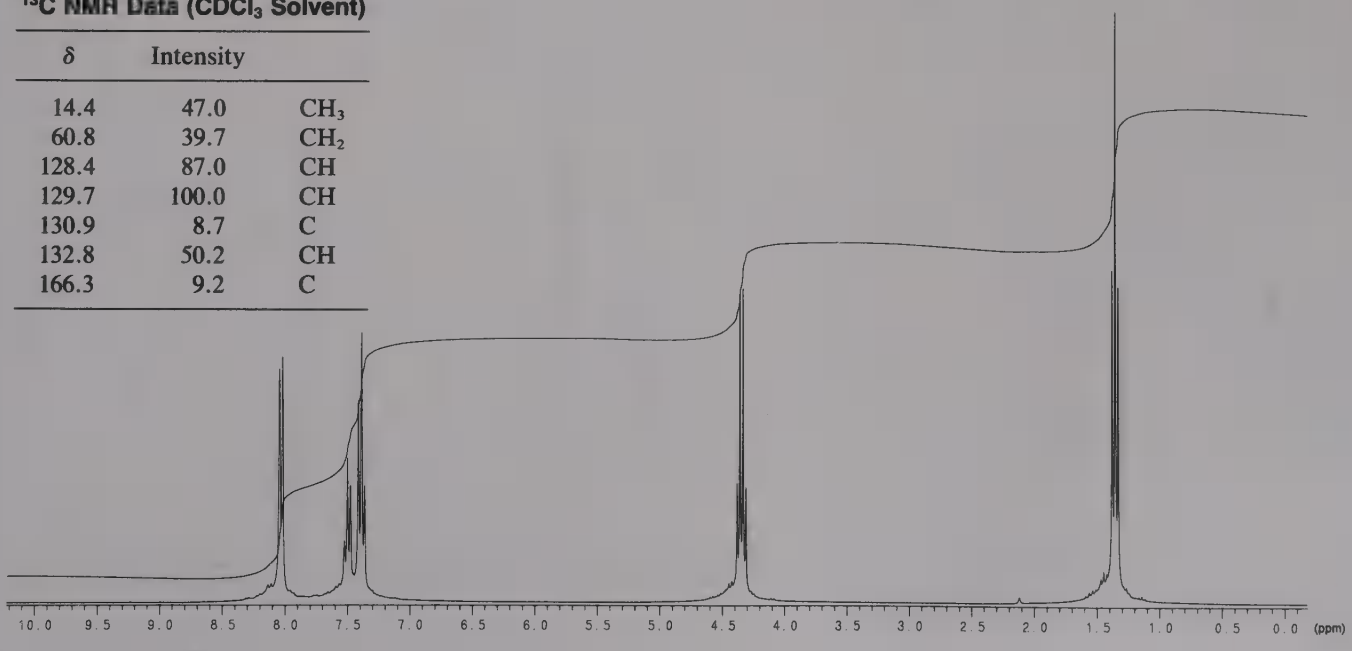

INFRARED SPECTRUM

Compound 9.18

2931.2 1242.1 890.4
1649.0 1070.3 836.0
1447.1 929.9 727.3

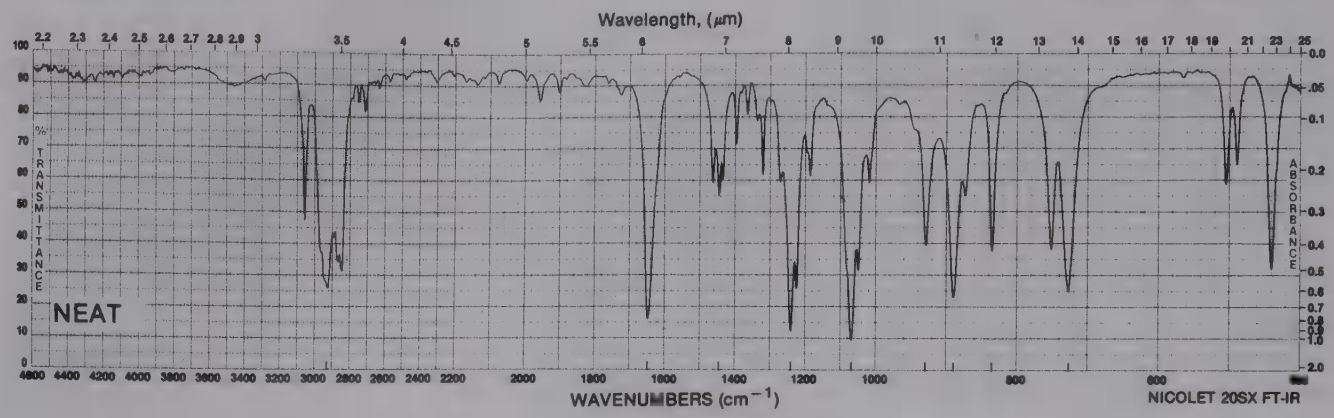

MASS SPECTRAL DATA (Relative Intensities)

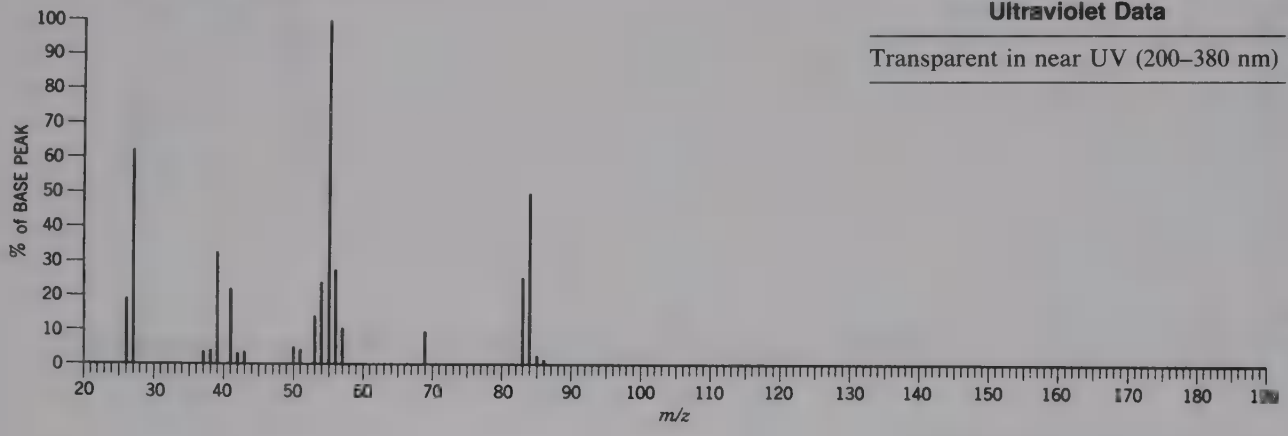

Ultraviolet Data

Transparent in near UV (200–380 nm)

^{1}H NMR SPECTRUM (Solvent $CDCl_3$, 300 MHz)

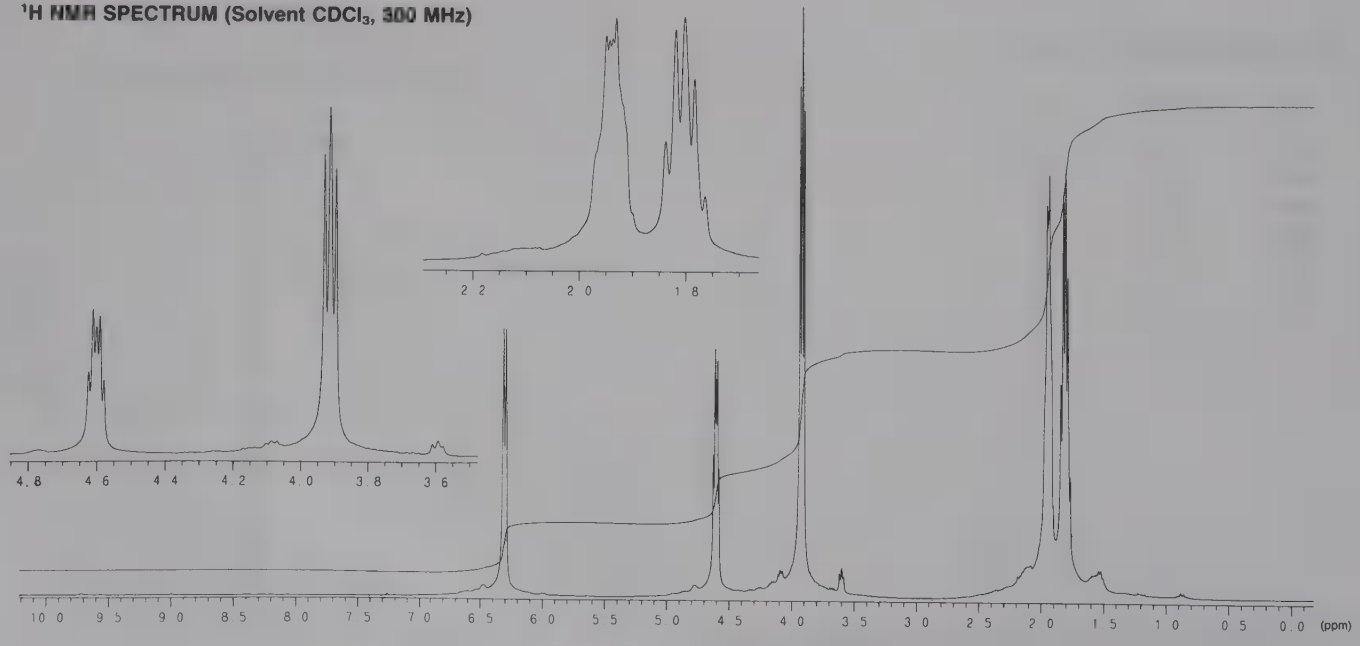

Compound 9.18 (continued)

^{13}C NMR SPECTRUM COMPLETELY DECOUPLED

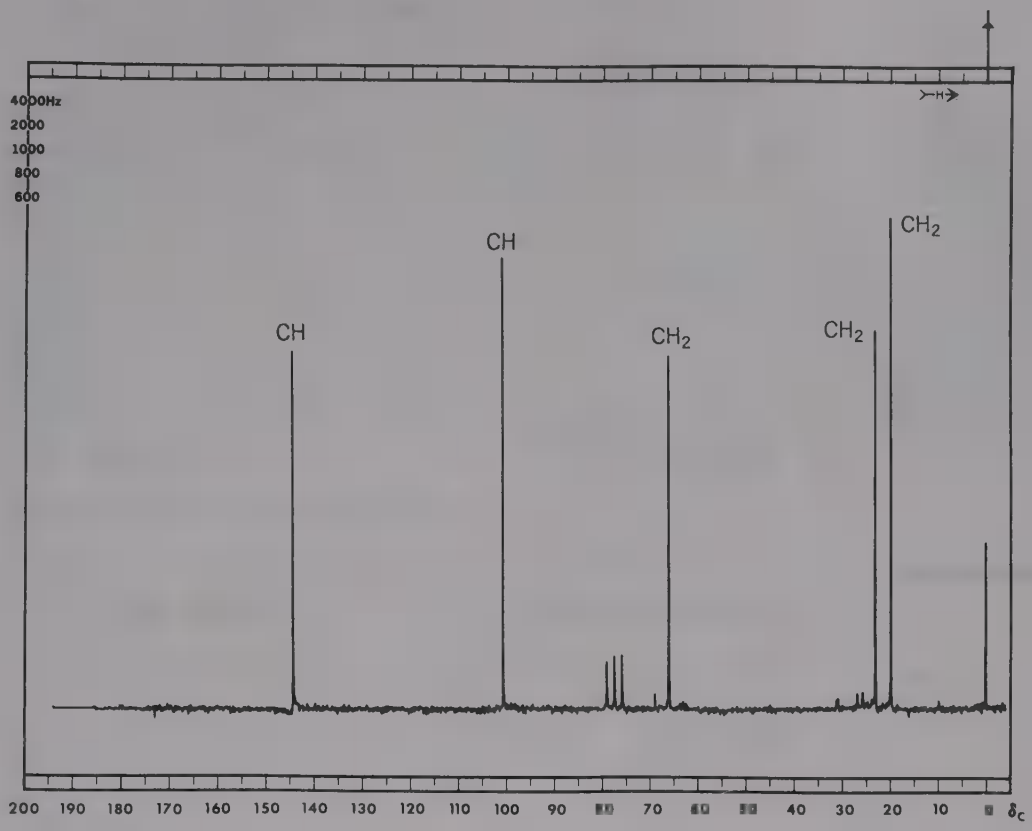

INFRARED SPECTRUM

Compound 9.19

2980.7 1267.2 820.7
1641.1 1211.9 [illegible]
1428.3 [illegible] 563.7

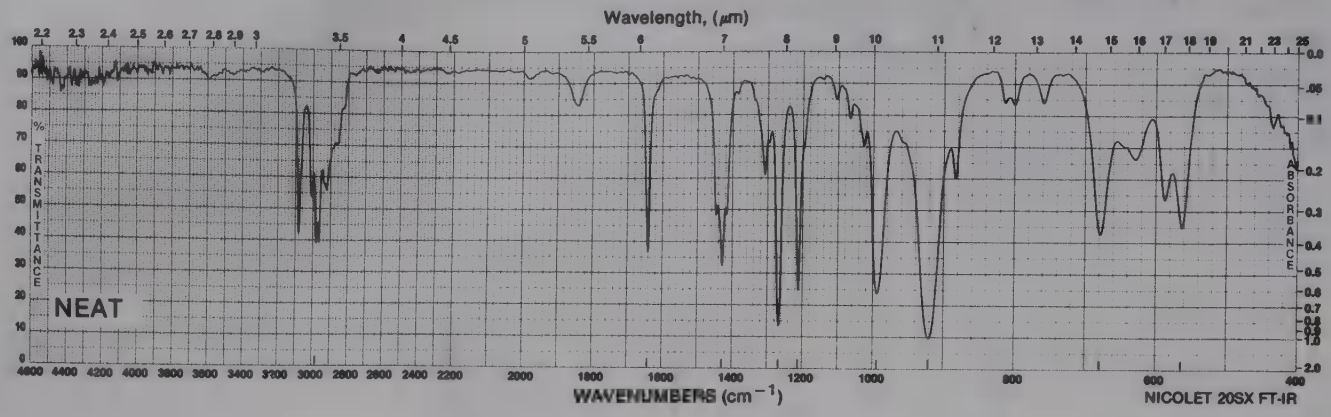

MASS SPECTRAL DATA (Relative Intensities)

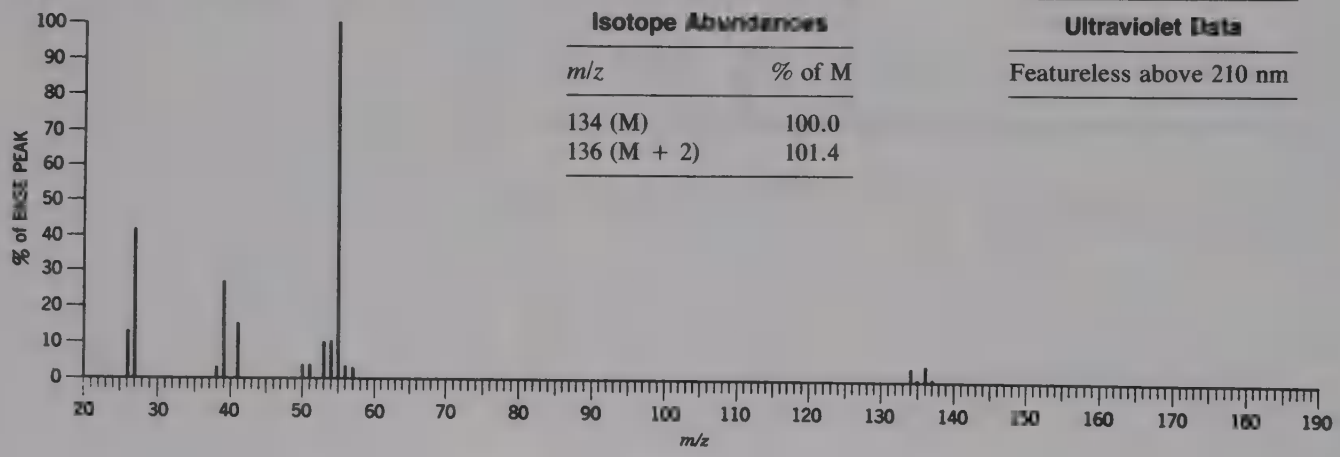

Isotope Abundances	
m/z	% of M
134 (M)	100.0
136 (M + 2)	101.4

Ultraviolet Data
Featureless above 210 nm

^{1}H NMR SPECTRUM (Solvent $CDCl_3$, 300 MHz)

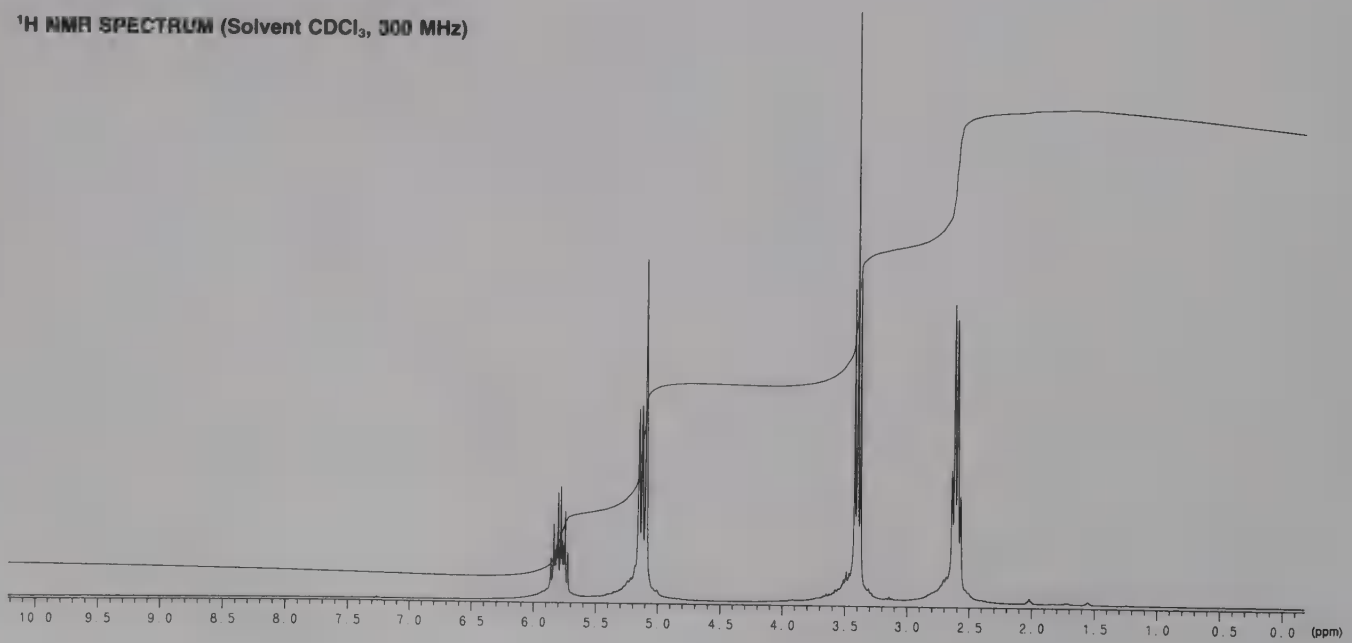

INFRARED SPECTRUM

Compound 9.20

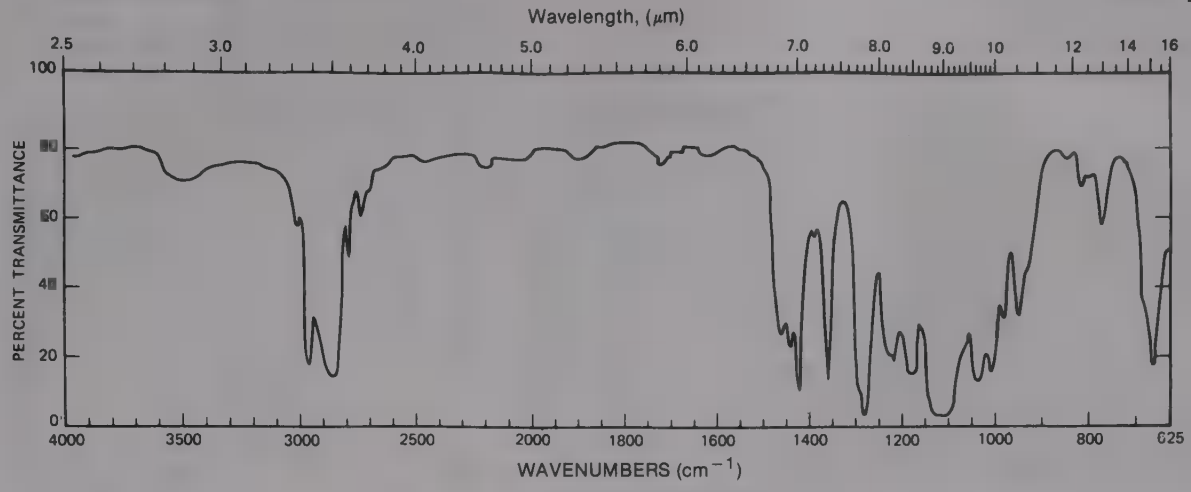

MASS SPECTRAL DATA (Relative Intensities)

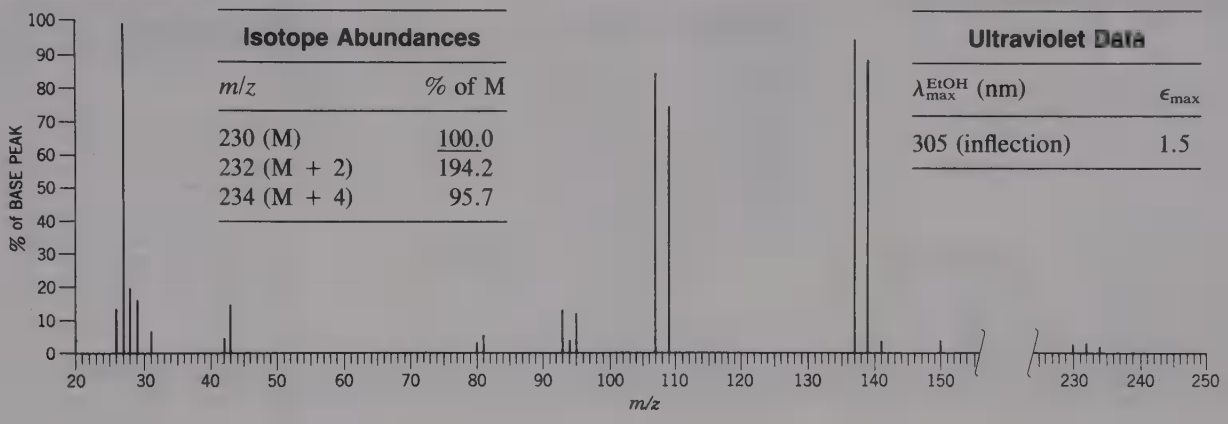

Isotope Abundances

m/z	% of M
230 (M)	100.0
232 (M + 2)	194.2
234 (M + 4)	95.7

Ultraviolet Data

λ_{max}^{EtOH} (nm)	ϵ_{max}
305 (inflection)	1.5

^{1}H NMR SPECTRUM (Solvent CCl_4, 60 MHz)

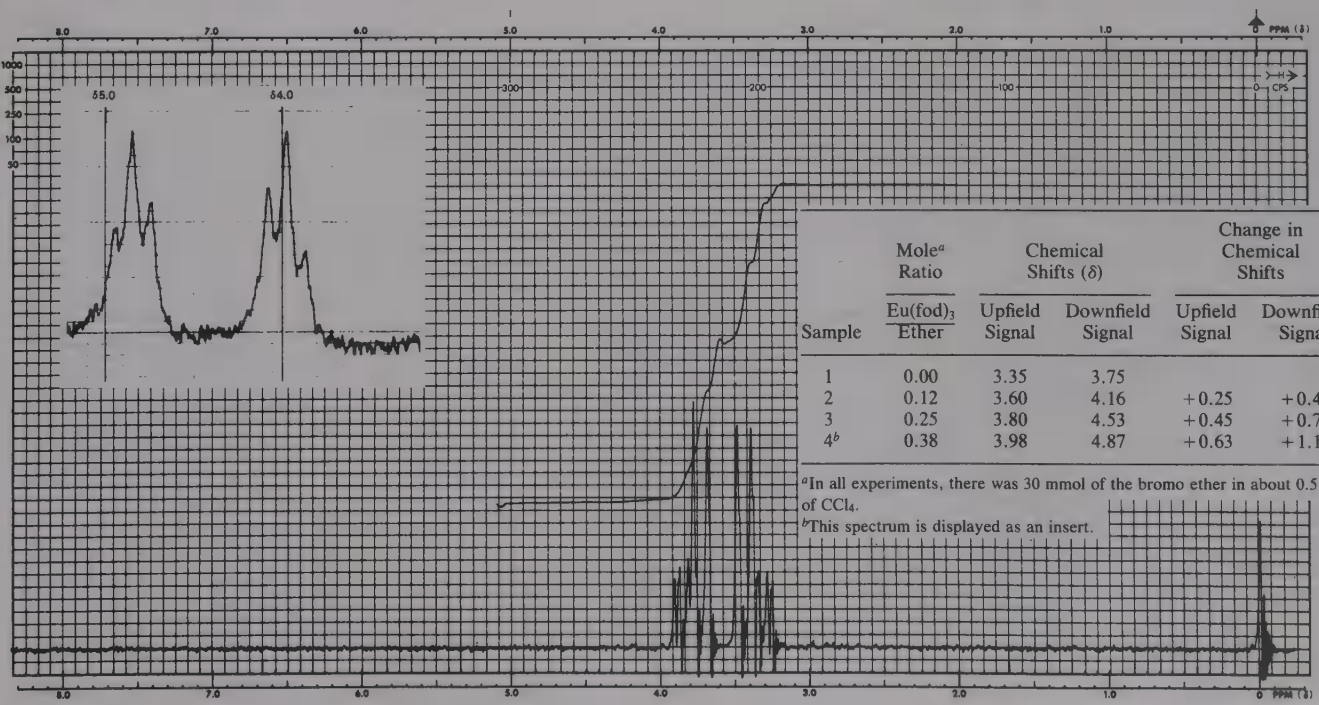

Sample	Mole[a] Ratio $\frac{Eu(fod)_3}{Ether}$	Chemical Shifts (δ) Upfield Signal	Chemical Shifts (δ) Downfield Signal	Change in Chemical Shifts Upfield Signal	Change in Chemical Shifts Downfield Signal
1	0.00	3.35	3.75		
2	0.12	3.60	4.16	+0.25	+0.41
3	0.25	3.80	4.53	+0.45	+0.78
4[b]	0.38	3.98	4.87	+0.63	+1.12

[a]In all experiments, there was 30 mmol of the bromo ether in about 0.5 mL of CCl_4.

[b]This spectrum is displayed as an insert.

INFRARED SPECTRUM

Compound 9.21

1427.7	991.3	719.6
1292.6	900.5	662.5
1219.9	752.9	523.6

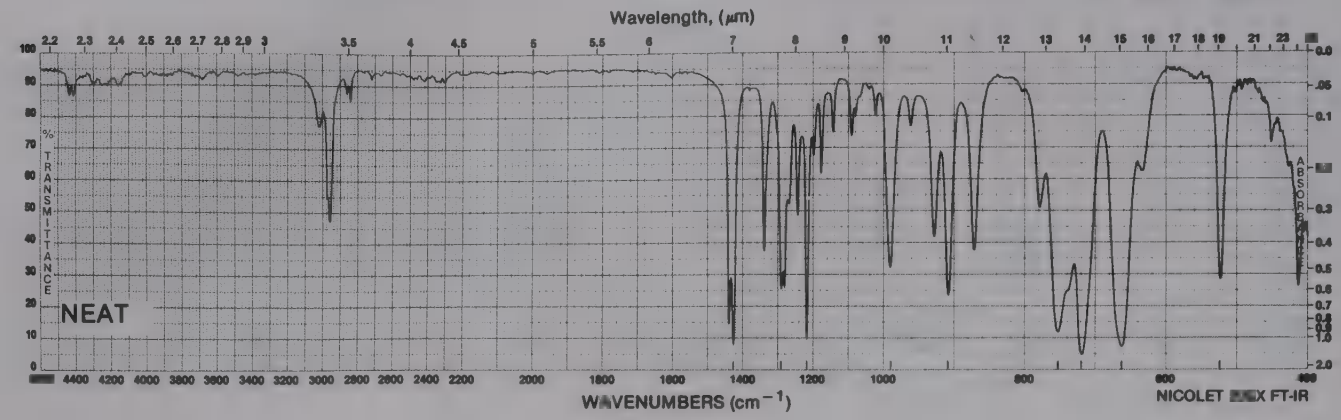

MASS SPECTRAL DATA (Relative Intensities)

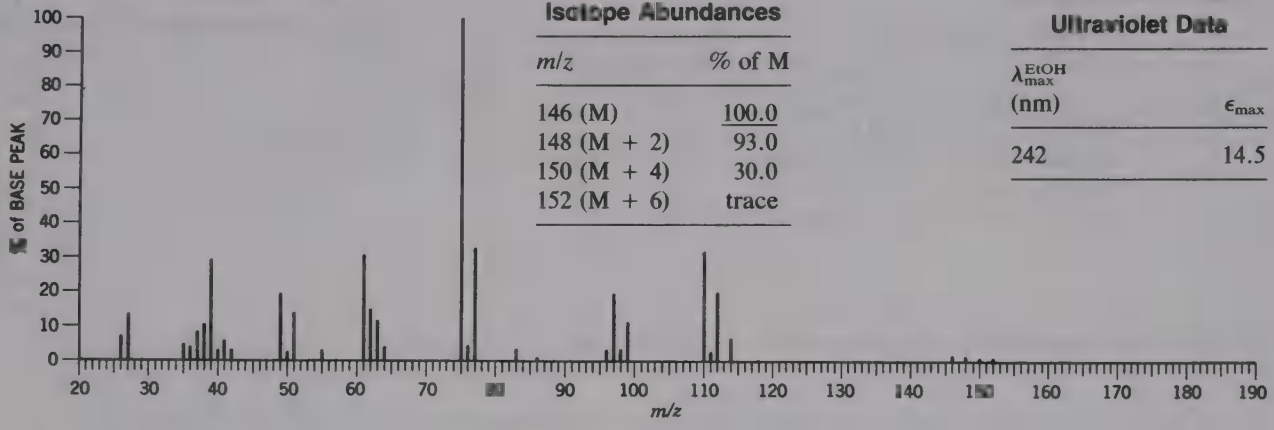

Isotope Abundances

m/z	% of M
146 (M)	100.0
148 (M + 2)	93.0
150 (M + 4)	30.0
152 (M + 6)	trace

Ultraviolet Data

λ_{max}^{EtOH} (nm)	ϵ_{max}
242	14.5

^{1}H NMR SPECTRUM (Solvent CCl_4, 60 MHz)

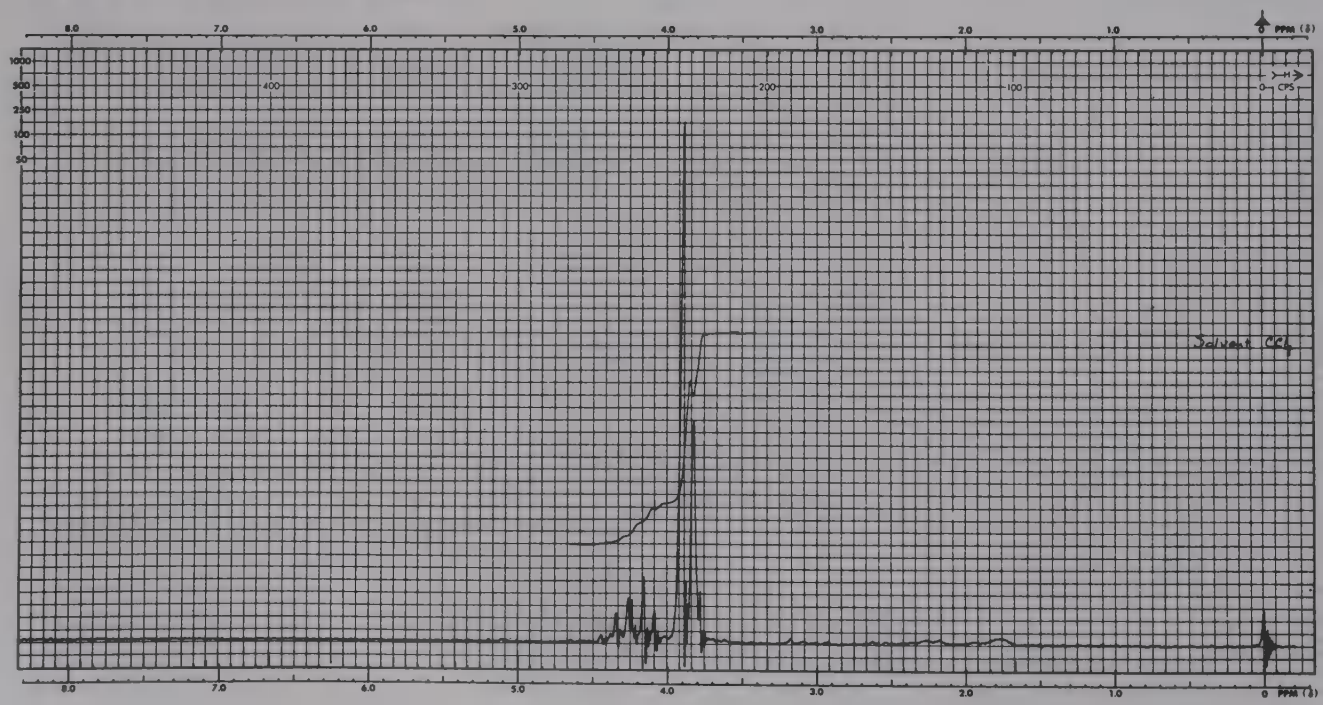

Compound 9.21 (continued)

^{13}C NMR SPECTRUM COMPLETELY DECOUPLED

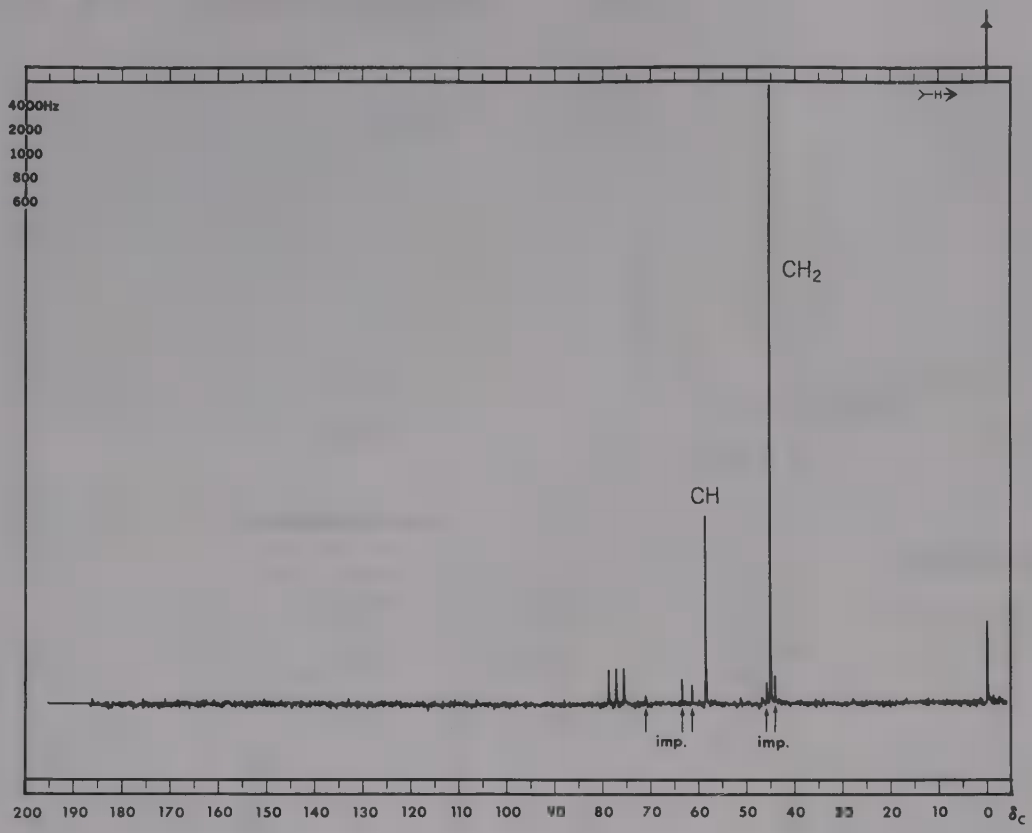

INFRARED SPECTRUM ***Compound 9.22***

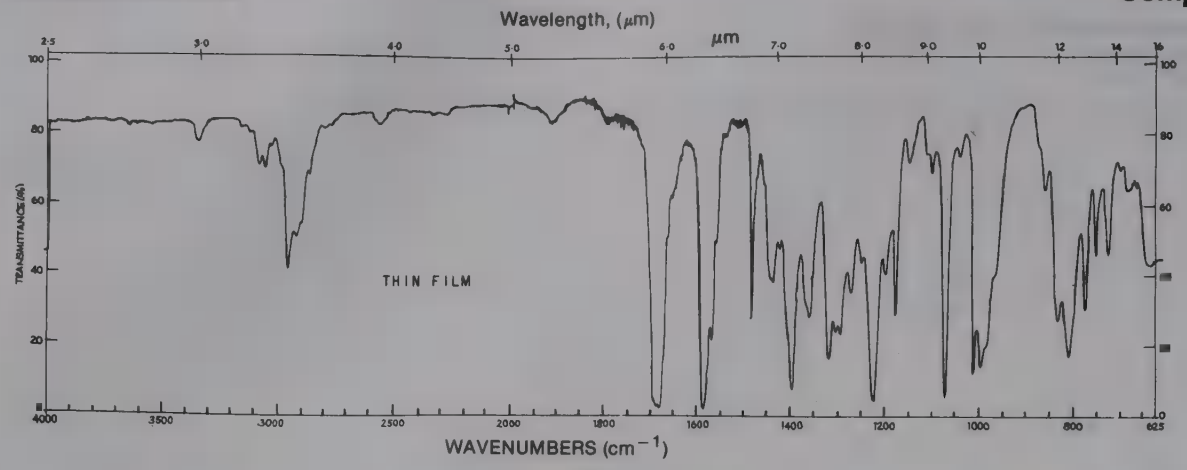

MASS SPECTRAL DATA (Relative Intensity)

FM (found) = 259.9500

Isotope Abundances

m/z	% of M
260 (M)	100.0
262 (M + 2)	127.2
264 (M + 4)	33.0

Ultraviolet Data

λ_{max} (nm)	ϵ_{max}
253	46,400

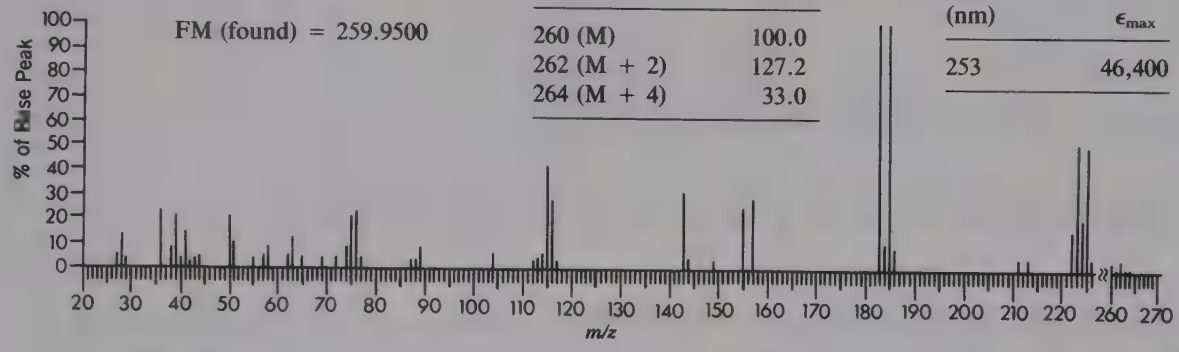

^{1}H NMR SPECTRUM (Solvent $CDCl_3$, 60 MHz)

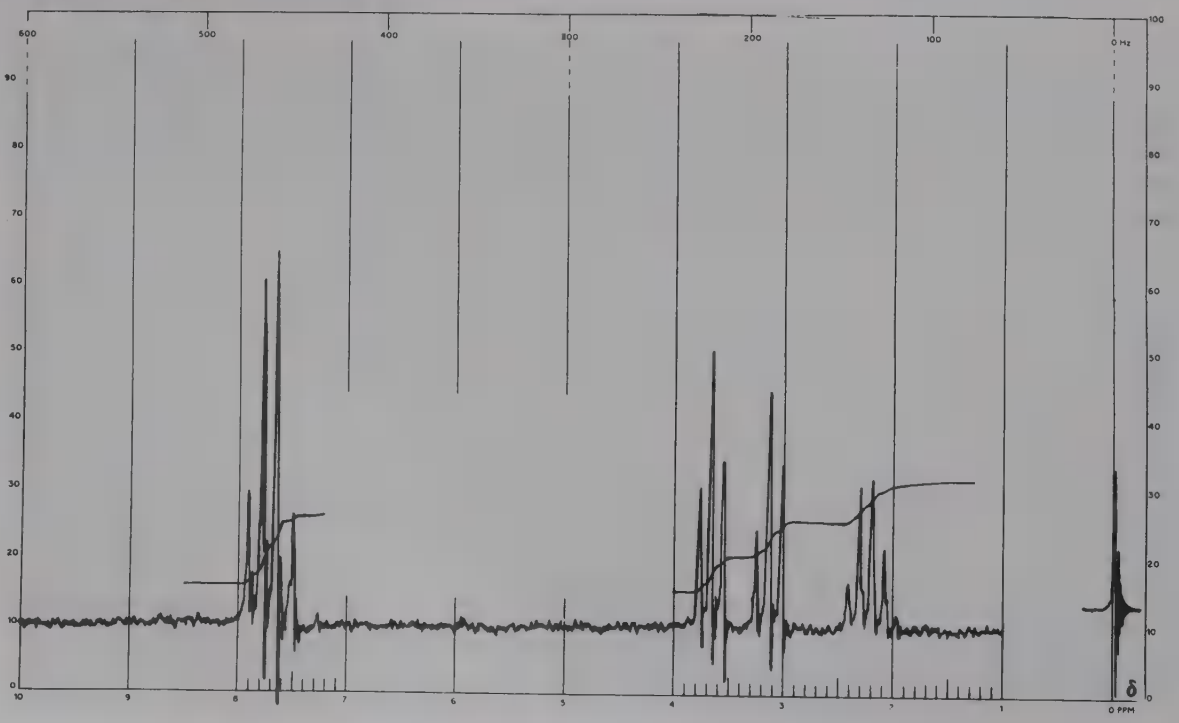

INFRARED SPECTRUM

Compound 9.23

1685.6	1359.5	[illegible].0
1597.5	1266.3	839.2
1506.4	1157.0	565.7

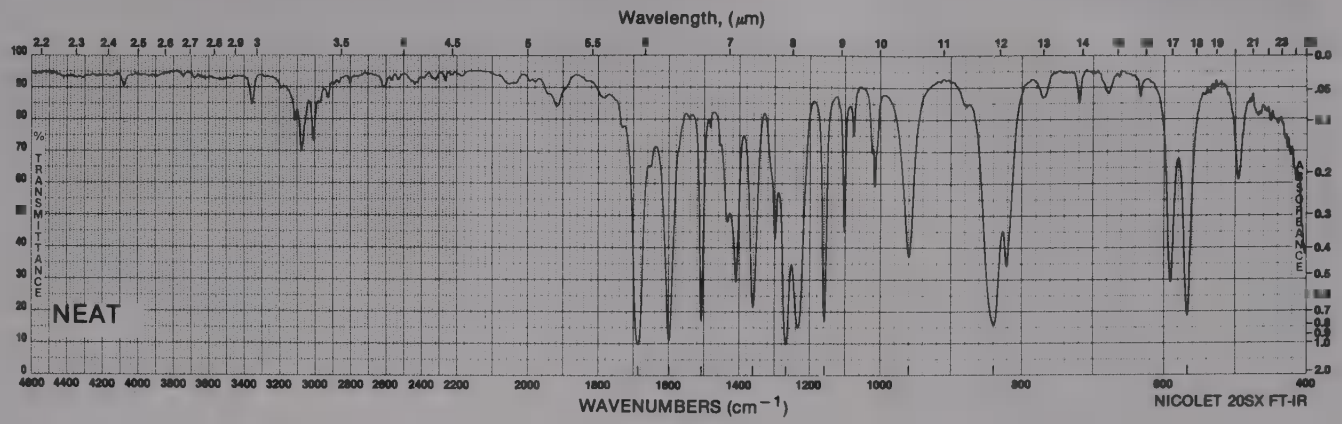

MASS SPECTRAL DATA (Relative Intensities)

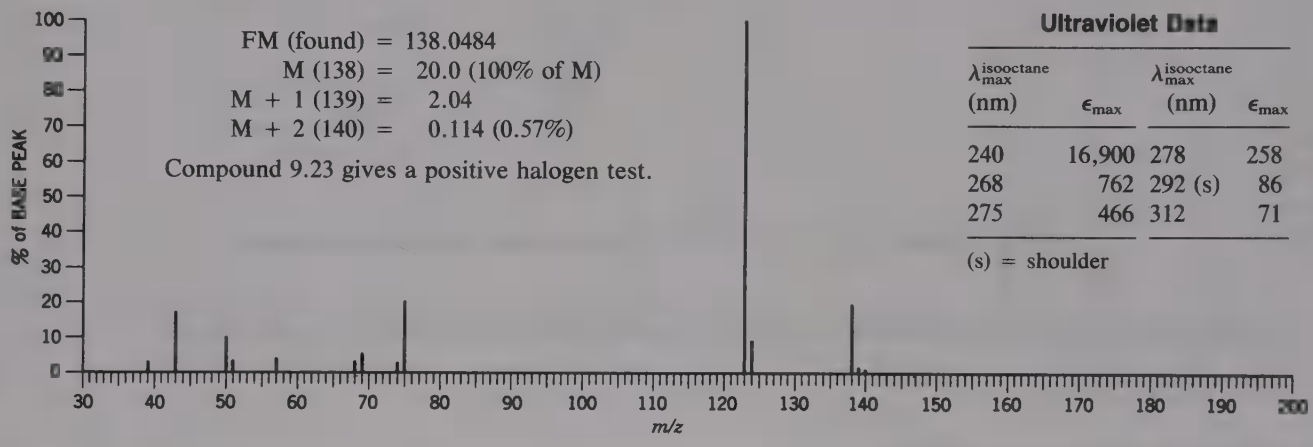

FM (found) = 138.0484
M (138) = 20.0 (100% of M)
M + 1 (139) = 2.04
M + 2 (140) = 0.114 (0.57%)

Compound 9.23 gives a positive halogen test.

Ultraviolet Data

$\lambda_{max}^{isooctane}$ (nm)	ϵ_{max}	$\lambda_{max}^{isooctane}$ (nm)	ϵ_{max}
240	16,900	278	258
268	762	292 (s)	86
275	466	312	71

(s) = shoulder

^{1}H NMR SPECTRUM (Solvent CCl_4, 60 MHz)

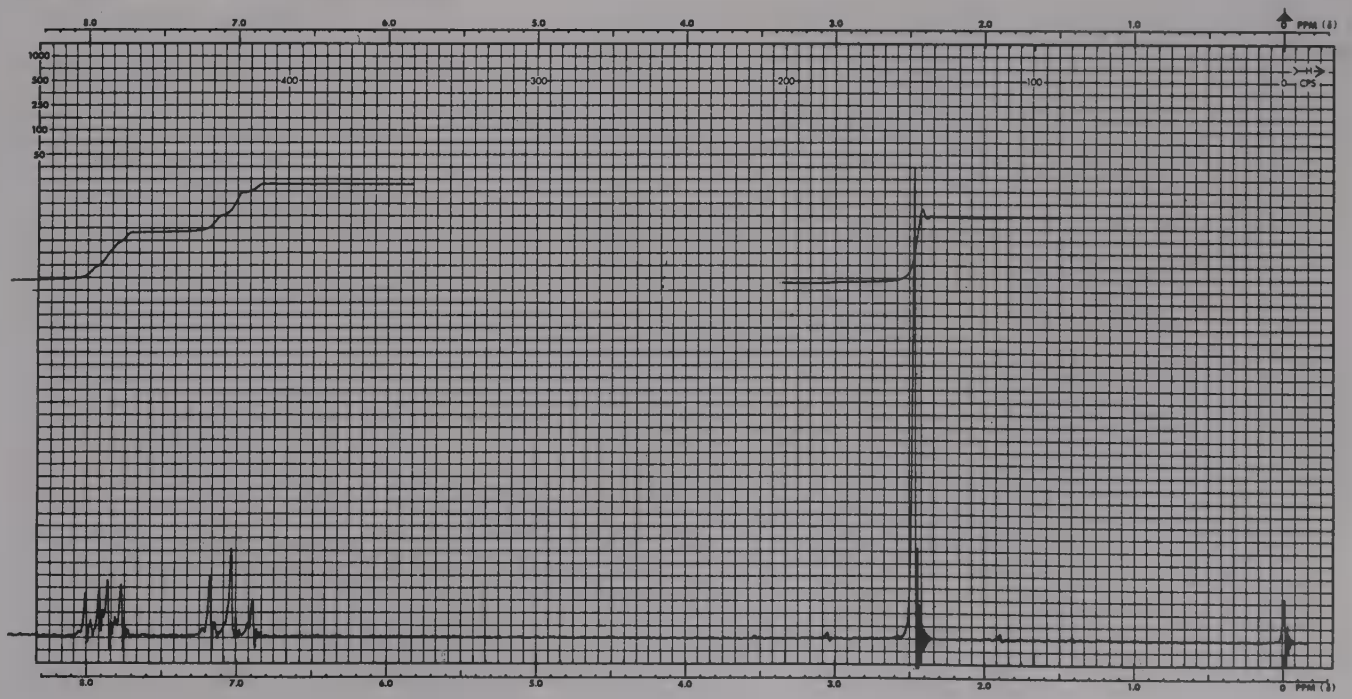

INFRARED SPECTRUM

Compound 9.24

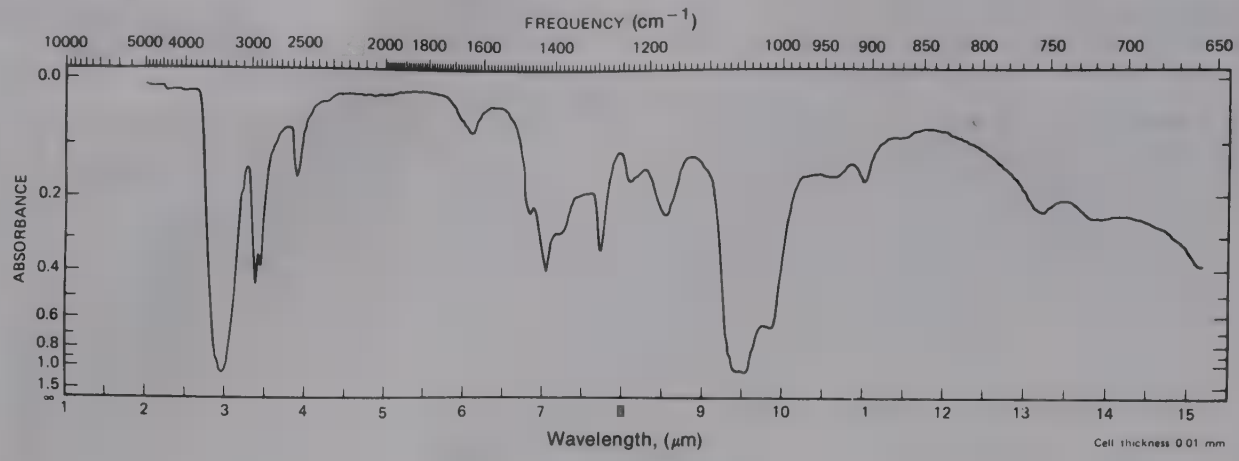

MASS SPECTRAL DATA (Relative Intensities)

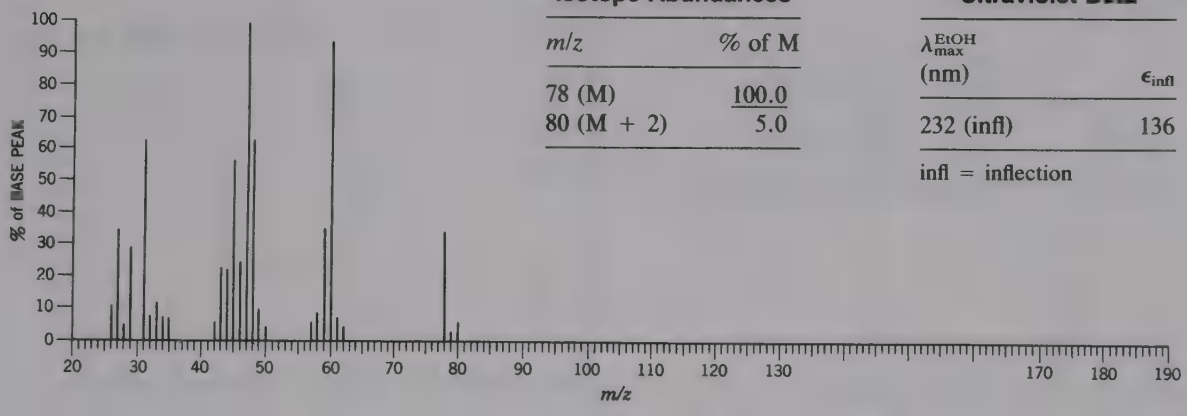

Isotope Abundances	
m/z	% of M
78 (M)	100.0
80 (M + 2)	5.0

Ultraviolet Data	
λ_{max}^{EtOH} (nm)	ϵ_{infl}
232 (infl)	136

infl = inflection

^{1}H NMR SPECTRUM (Solvent $CDCl_3$, 60 MHz)

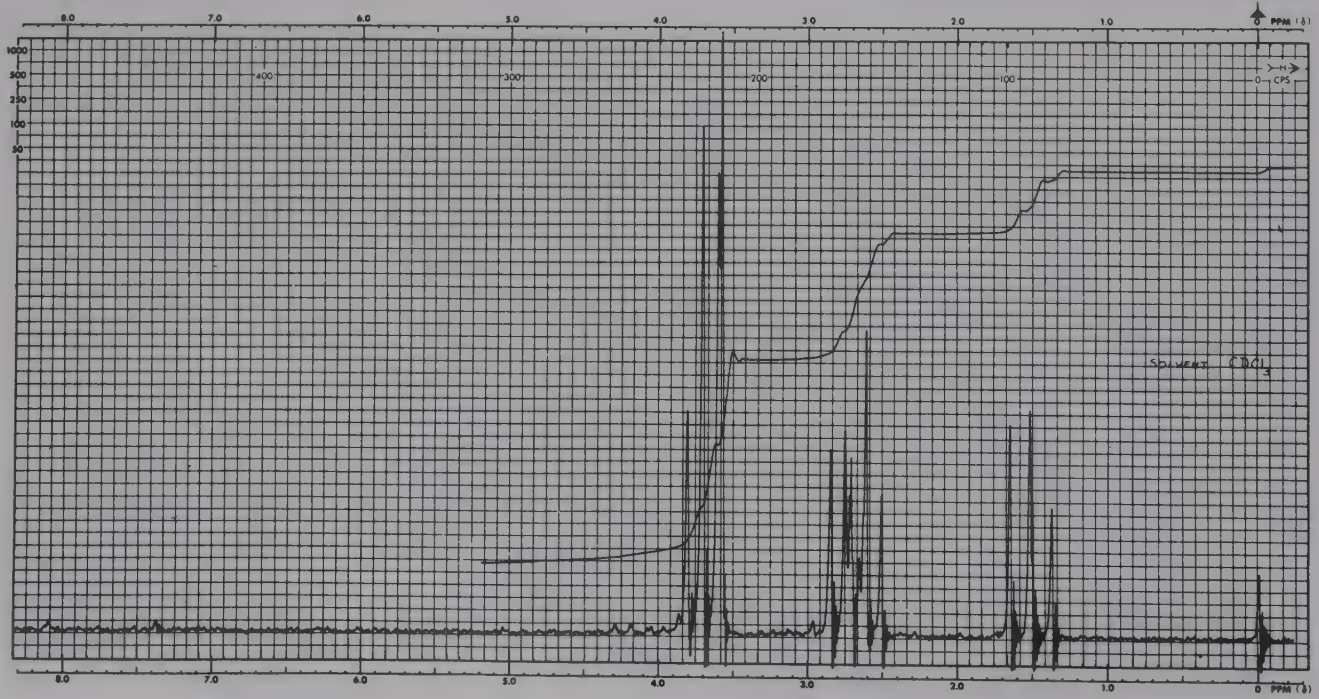

Compound 9.24 (continued)

^{13}C NMR SPECTRUM (Completely Decoupled)

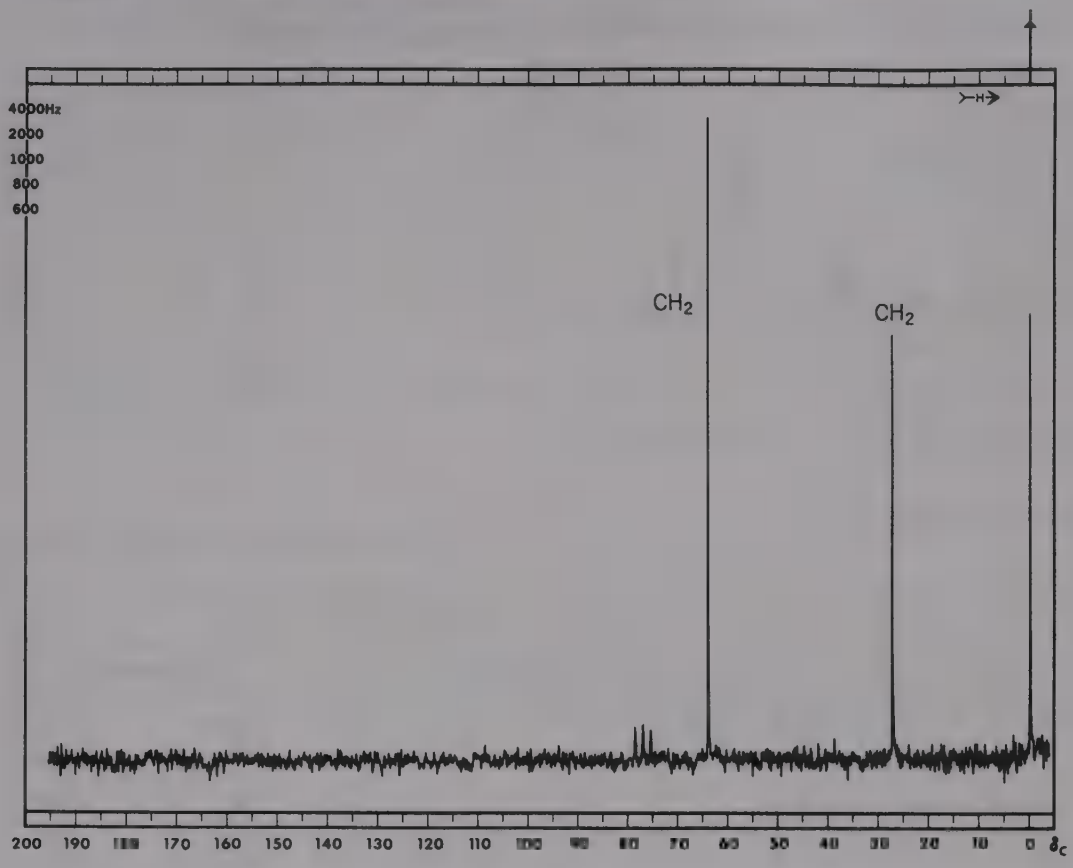

MASS SPECTRAL DATA

Compound 9.25

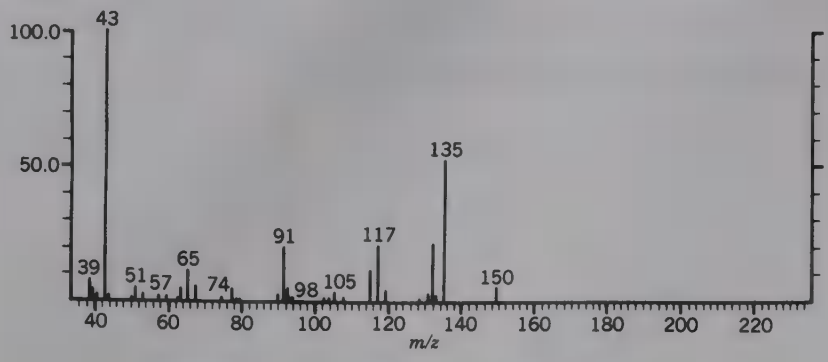

FM (found) = 150.1039

INFRARED SPECTRUM (Dilute CCl_4 Solution)

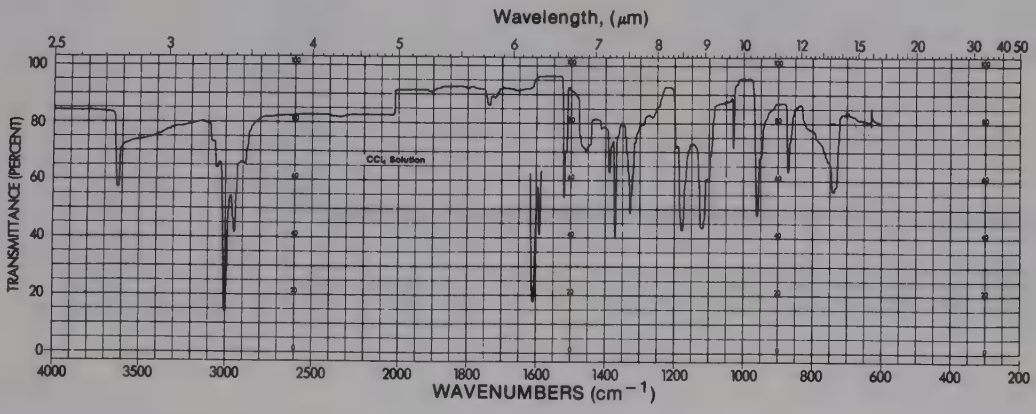

Ultraviolet Data

$\lambda_{max}^{CH_3OH}$ (nm)	$\log \epsilon_{max}$
220	3.86
233	3.24
265	2.58
273	2.56

^1H NMR SPECTRUM (Solvent $CDCl_3$, 100 MHz)

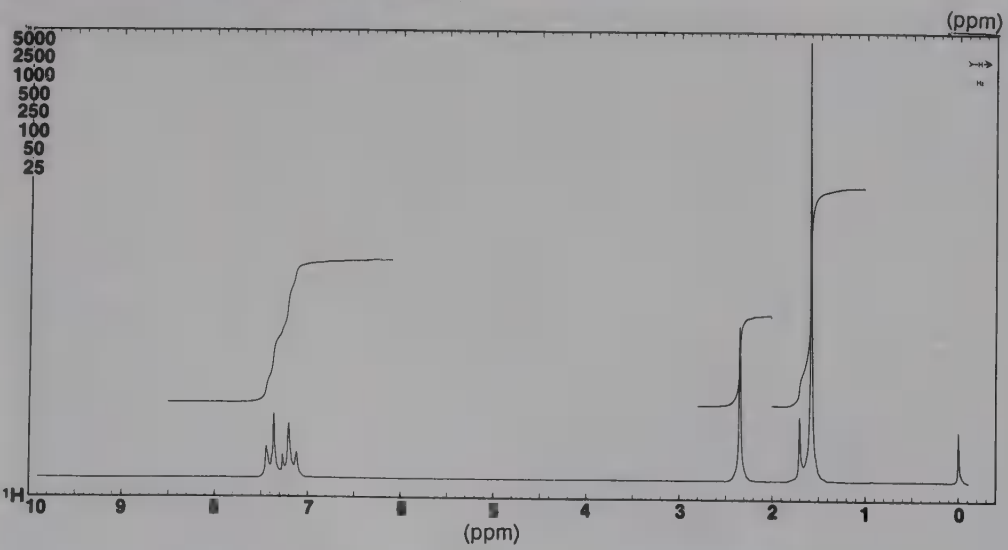

Peak at δ 1.7 disappears upon D_2O treatment.

INFRARED SPECTRUM **Compound 9.26**

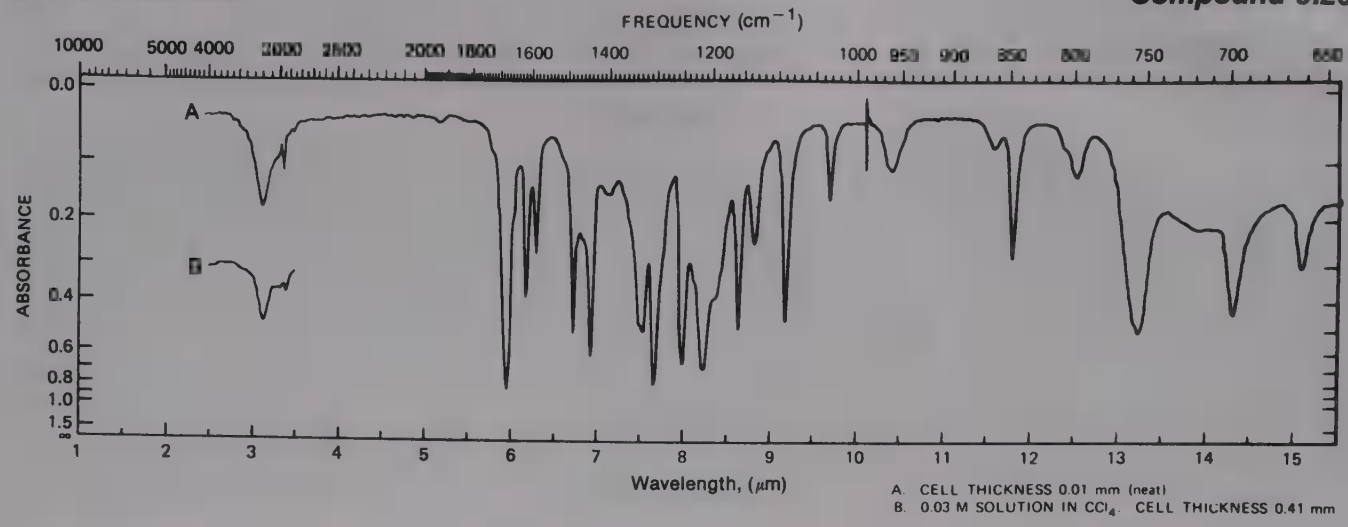

A. CELL THICKNESS 0.01 mm (neat)
B. 0.03 M SOLUTION IN CCl_4. CELL THICKNESS 0.41 mm

MASS SPECTRAL DATA (Relative Intensities)

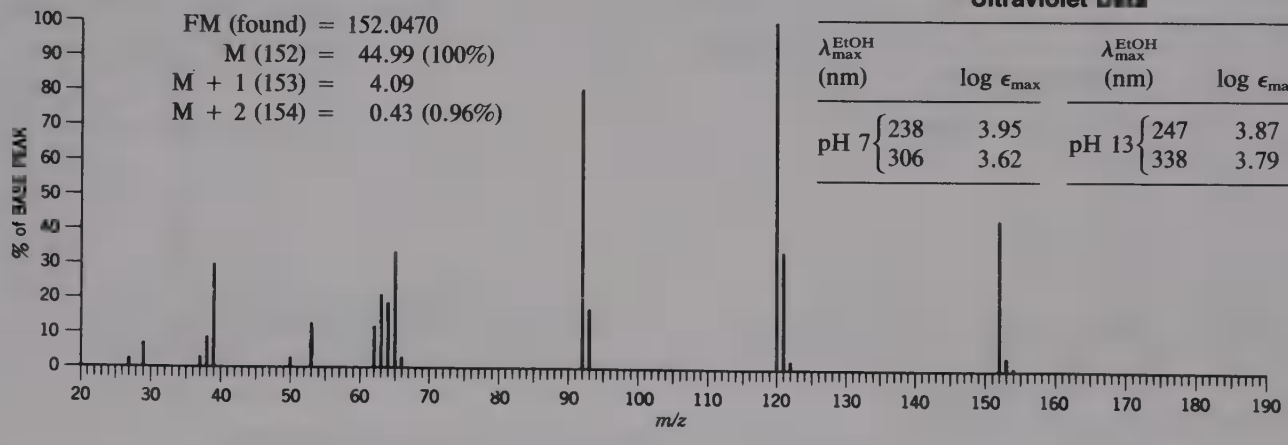

Ultraviolet Data

λ_{max}^{EtOH} (nm)		log ϵ_{max}	λ_{max}^{EtOH} (nm)		log ϵ_{max}
pH 7	238	3.95	pH 13	247	3.87
	306	3.62		338	3.79

^{1}H NMR SPECTRUM (Solvent $CDCl_3$, 300 MHz)

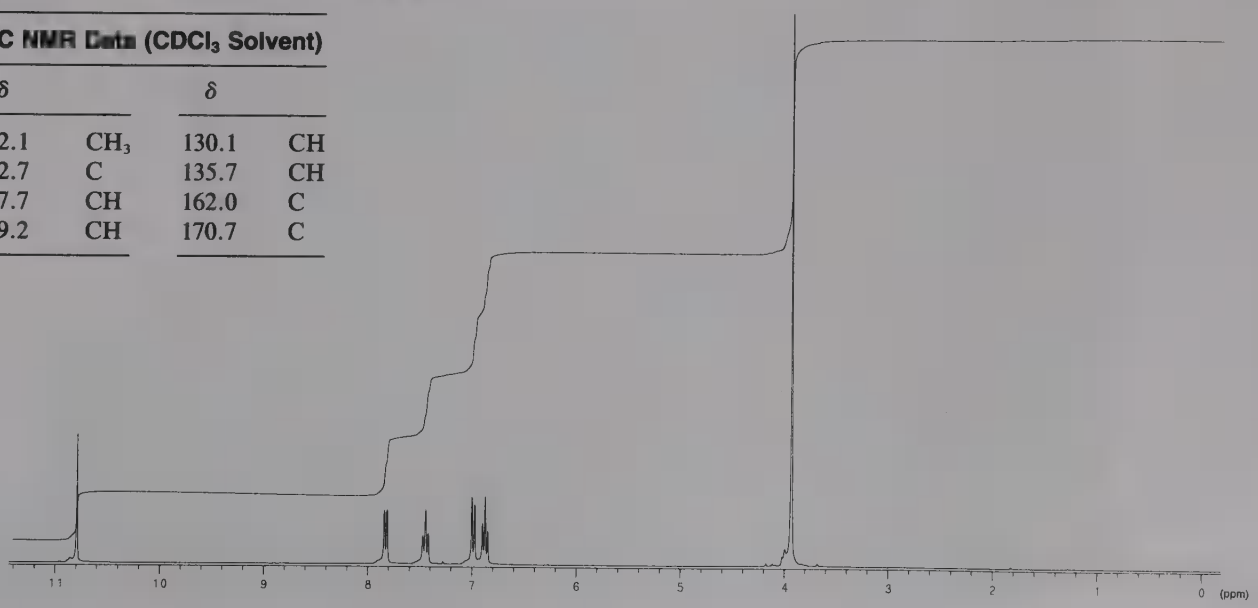

^{13}C NMR Data ($CDCl_3$ Solvent)

δ		δ	
52.1	CH_3	130.1	CH
112.7	C	135.7	CH
117.7	CH	162.0	C
119.2	CH	170.7	C

INFRARED SPECTRUM ***Compound 9.27***

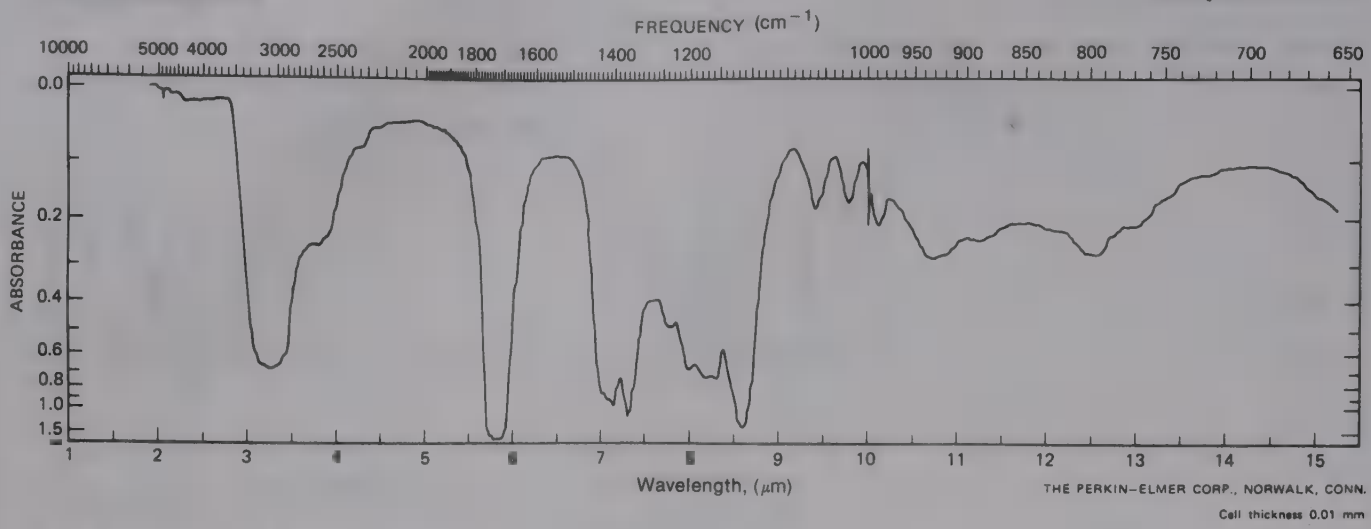

MASS SPECTRAL DATA (Relative Intensities)

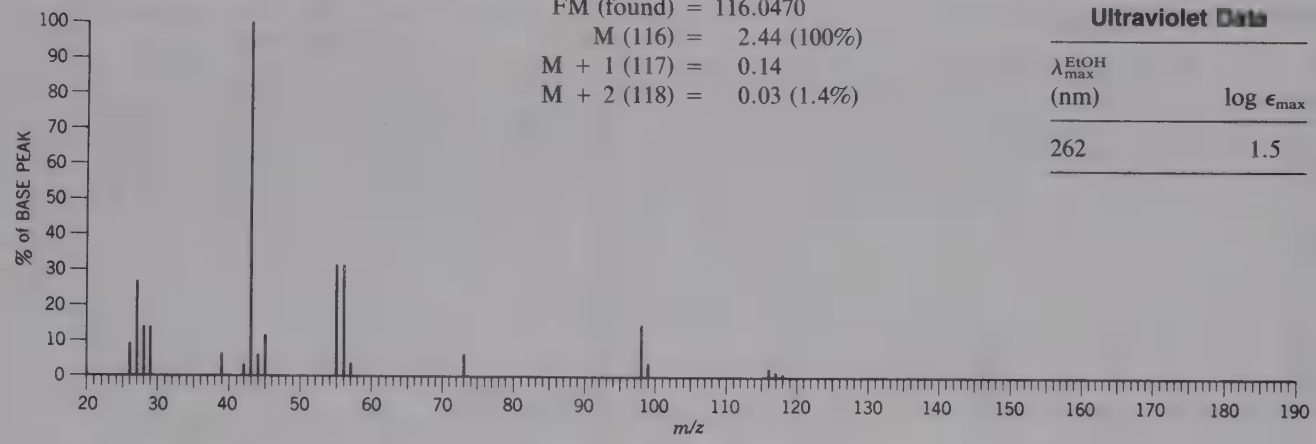

FM (found) = 116.0470
M (116) = 2.44 (100%)
M + 1 (117) = 0.14
M + 2 (118) = 0.03 (1.4%)

Ultraviolet Data

λ_{max}^{EtOH} (nm)	log ϵ_{max}
262	1.5

^{1}H NMR SPECTRUM (Solvent $CDCl_3$, 200 MHz)

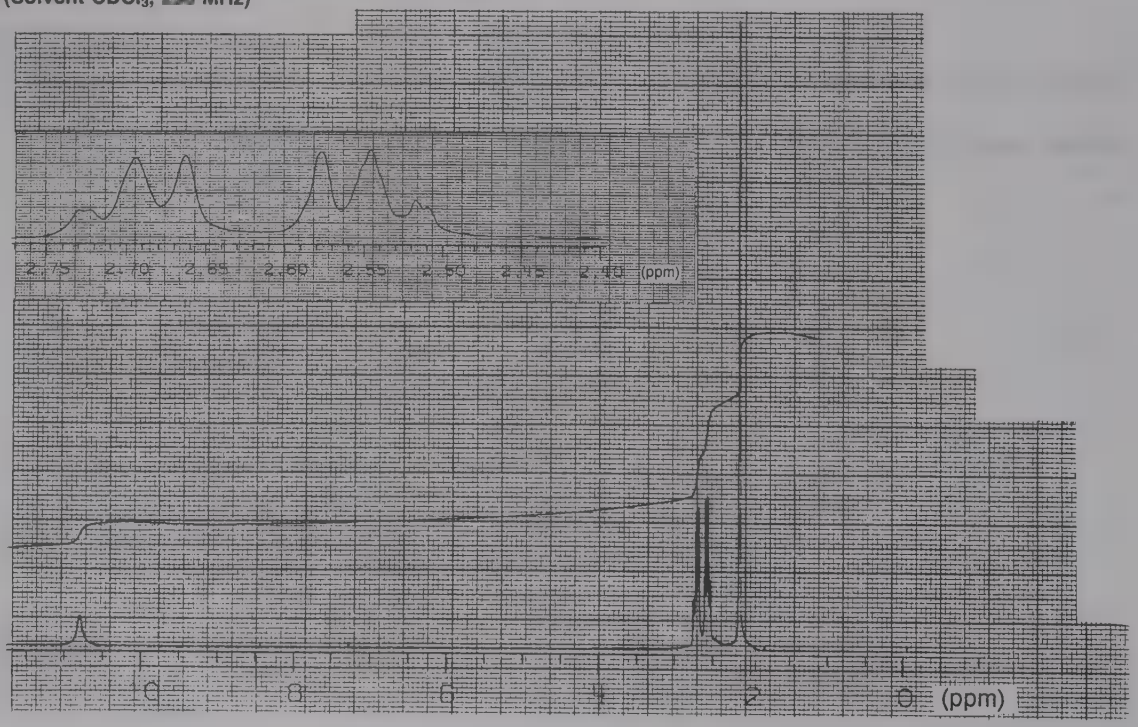

INFRARED SPECTRUM

Compound 9.28

2916.4 1168.4 930.7
1771.3 [illegible] 870.1
1376.9 [illegible] 491.9

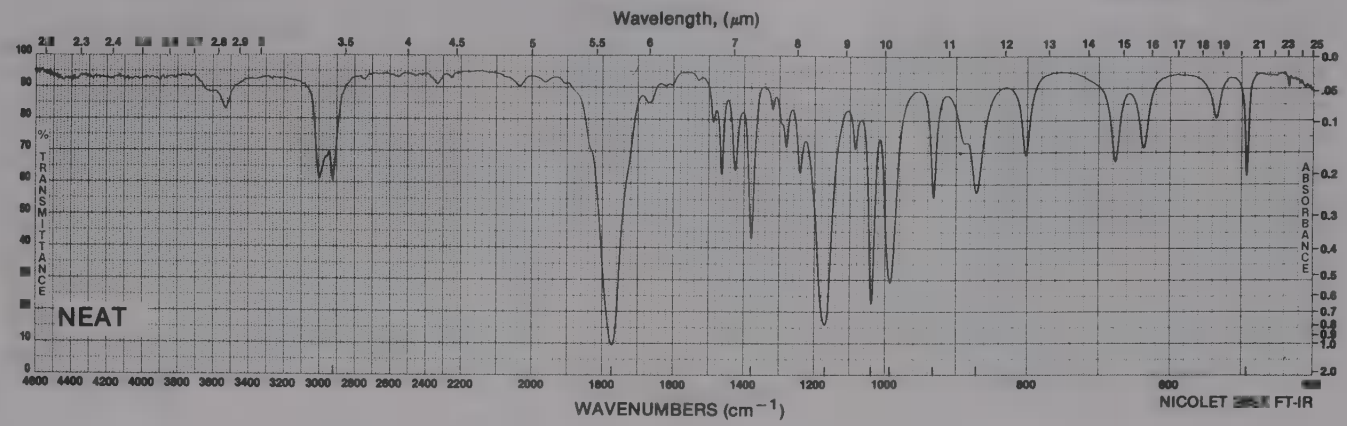

MASS SPECTRAL DATA (Relative Intensity)

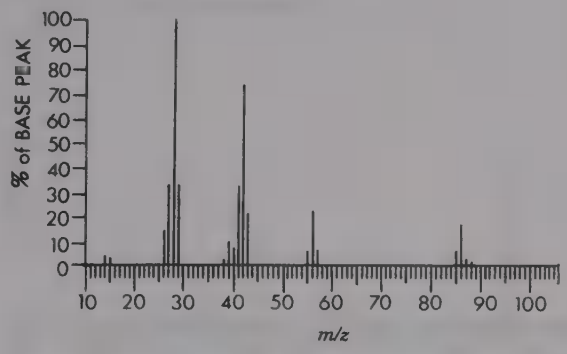

Ultraviolet Data

Transparent above 200 nm

^{1}H NMR SPECTRUM (Solvent $CDCl_3$, 300 MHz)

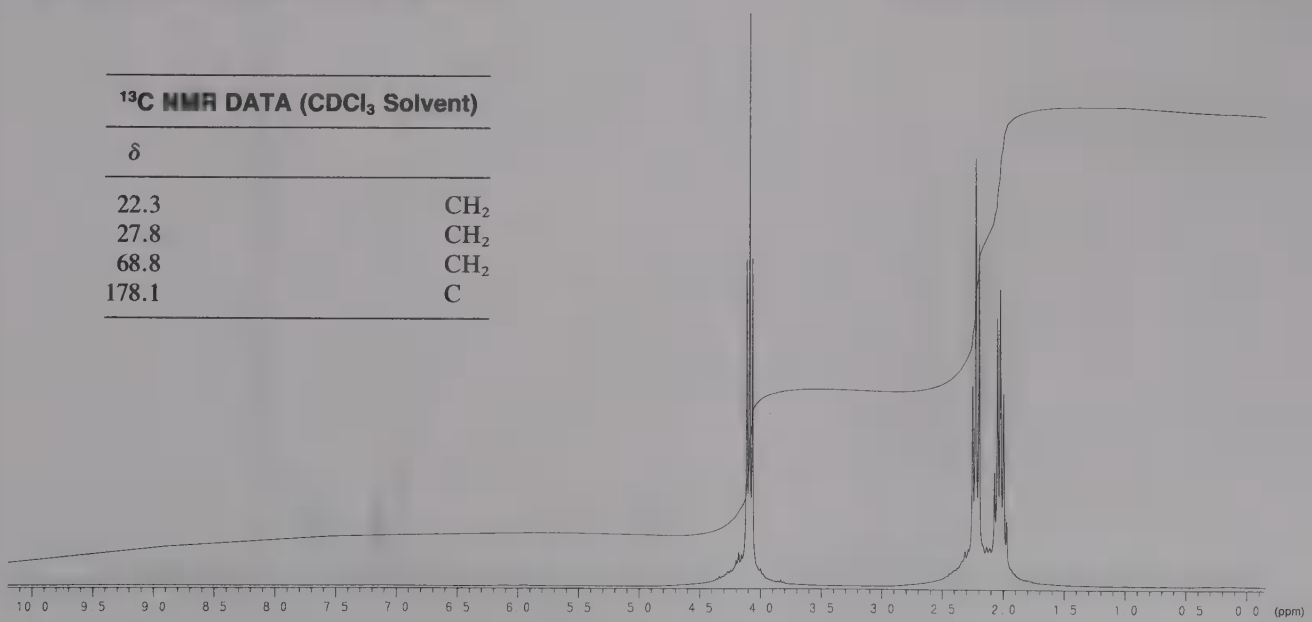

^{13}C NMR DATA ($CDCl_3$ Solvent)

δ	
22.3	CH_2
27.8	CH_2
68.8	CH_2
178.1	C

INFRARED SPECTRUM

Compound 9.29

2980.2 1223.7 1057.8
1773.0 1172.4 941.5
1344.2 1121.6 897.7

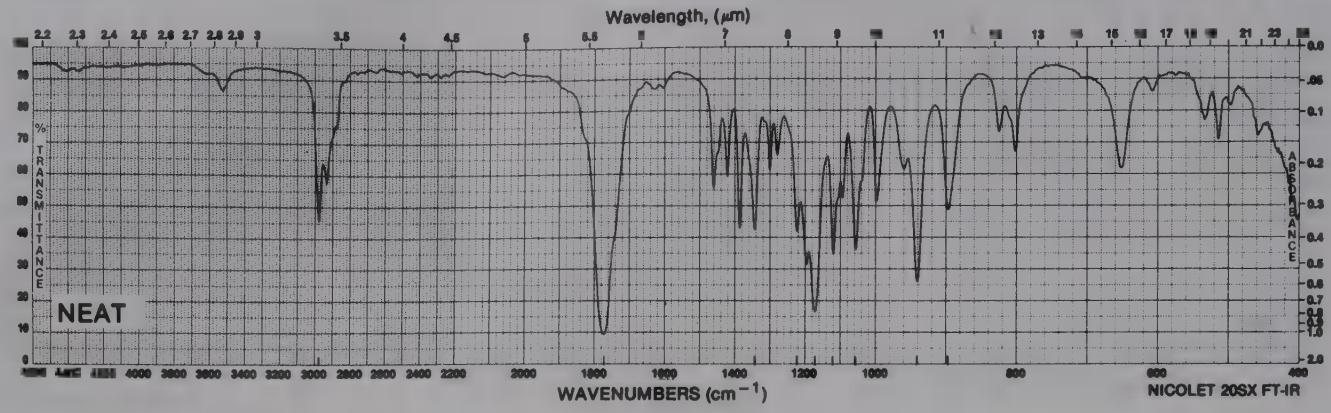

MASS SPECTRAL DATA (Relative Intensities)

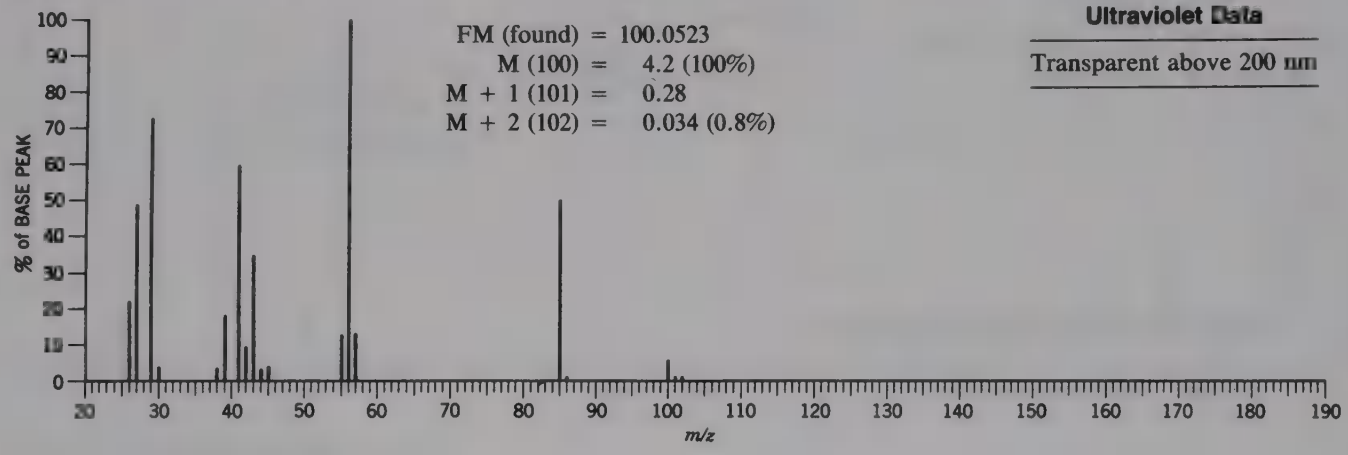

FM (found) = 100.0523
M (100) = 4.2 (100%)
M + 1 (101) = 0.28
M + 2 (102) = 0.034 (0.8%)

Ultraviolet Data

Transparent above 200 nm

^{1}H NMR SPECTRUM (Solvent $CDCl_3$, 300 MHz)

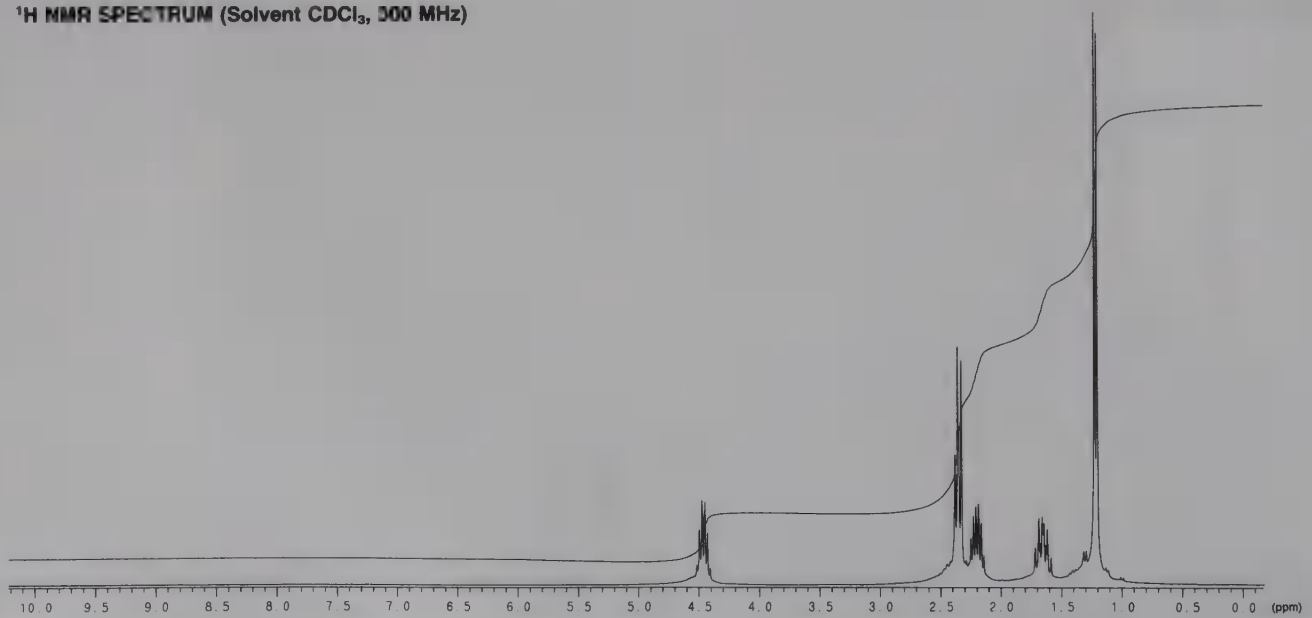

INFRARED SPECTRUM

Compound 9.30

1612.4 1347.3 787.7
1522.7 1149.3 728.1
1460.6 858.7 [illegible]

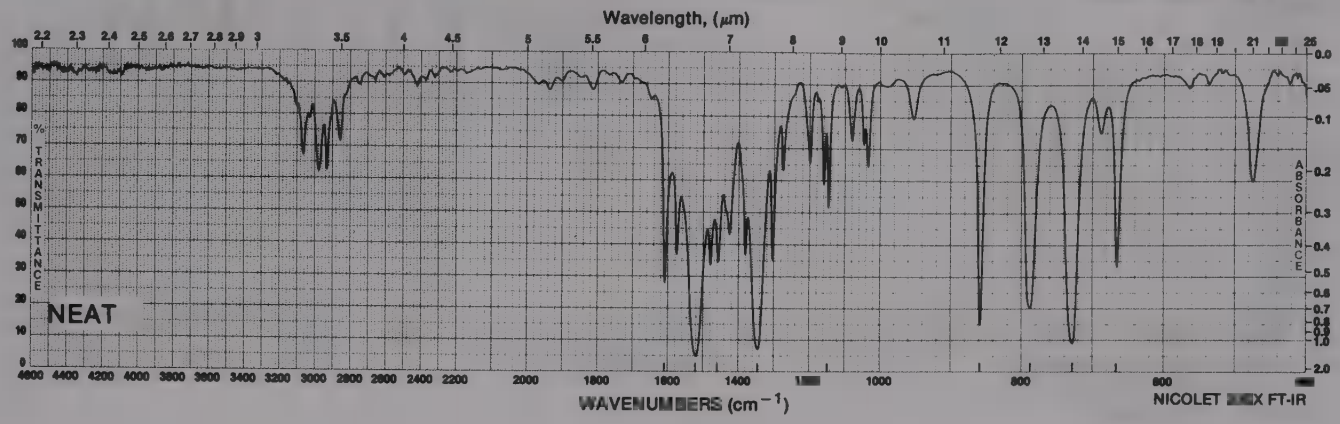

MASS SPECTRAL DATA (Relative Intensities)

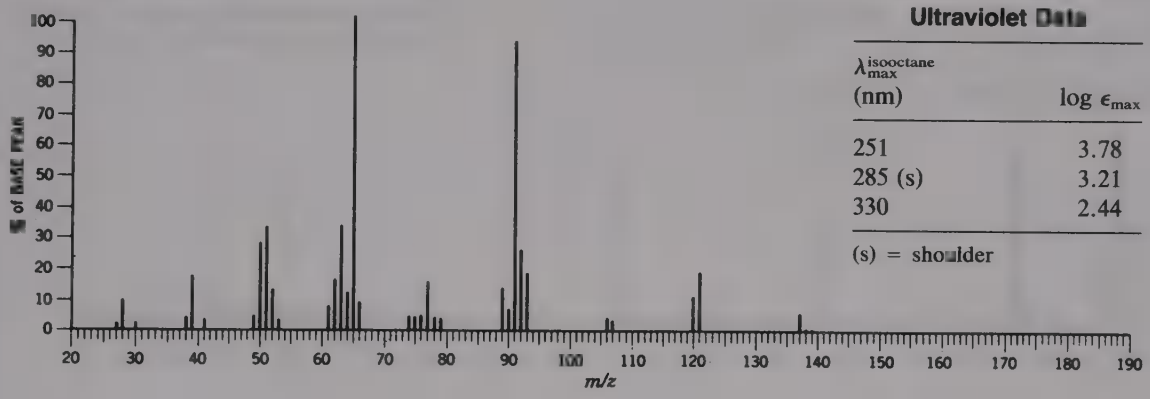

Ultraviolet Data

$\lambda_{max}^{isooctane}$ (nm)	log ϵ_{max}
251	3.78
285 (s)	3.21
330	2.44

(s) = shoulder

^{1}H NMR SPECTRUM (Solvent $CDCl_3$, 300 MHz)

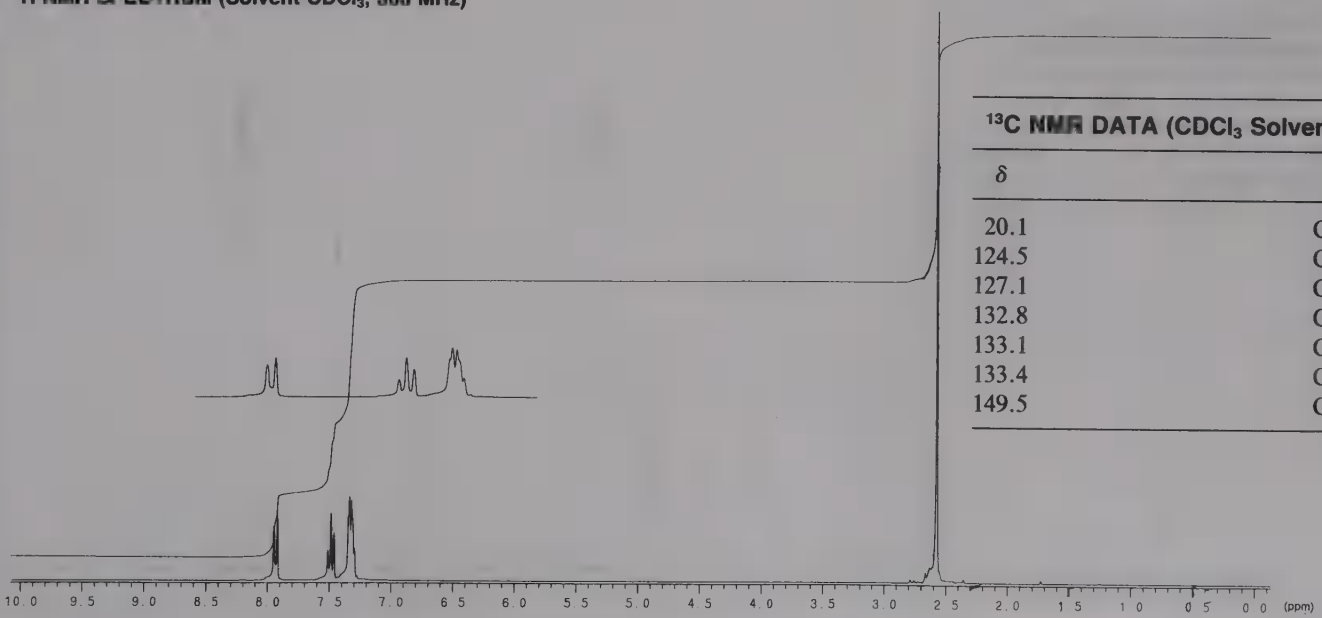

^{13}C NMR DATA ($CDCl_3$ Solvent)

δ	
20.1	CH_3
124.5	CH
127.1	CH
132.8	CH
133.1	CH
133.4	C
149.5	C

INFRARED SPECTRUM

Compound 9.31

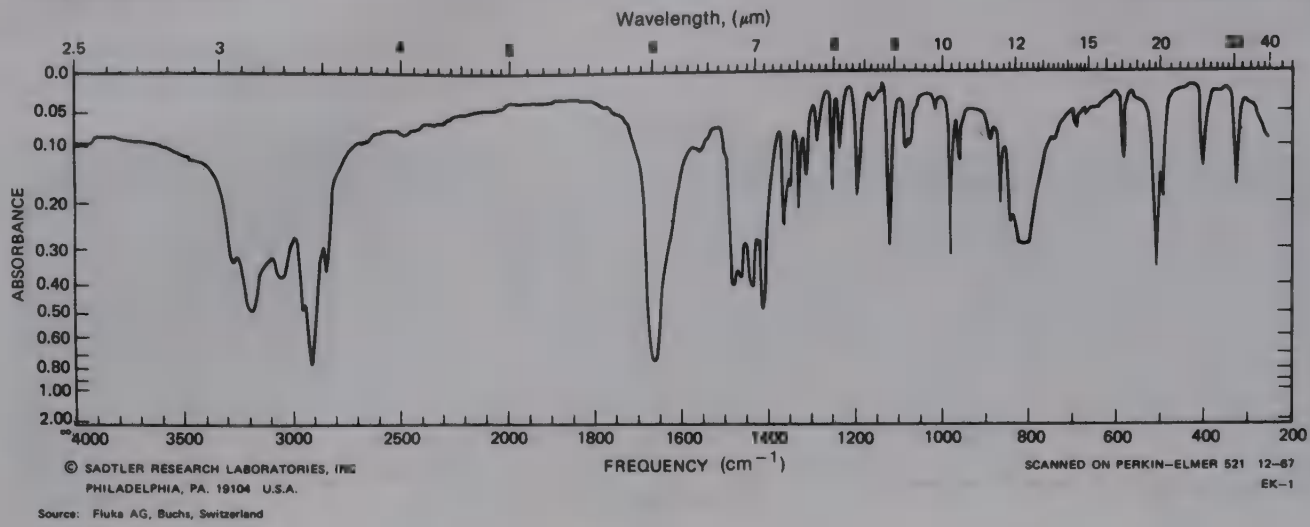

Source: Fluka AG, Buchs, Switzerland

MASS SPECTRAL DATA (Relative Intensities)

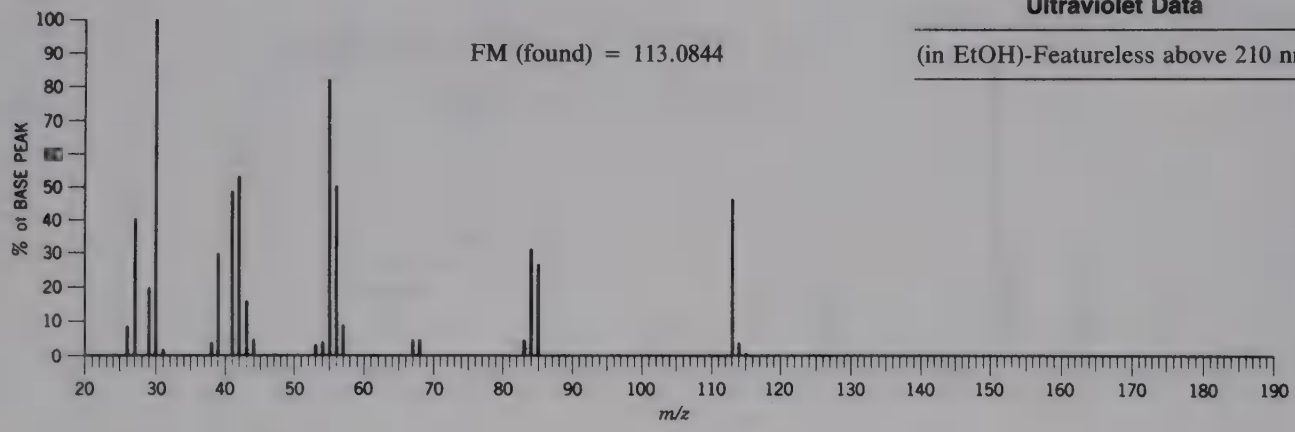

FM (found) = 113.0844

Ultraviolet Data

(in EtOH)-Featureless above 210 nm

^{1}H NMR SPECTRUM (Solvent $CDCl_3$, 300 MHz)

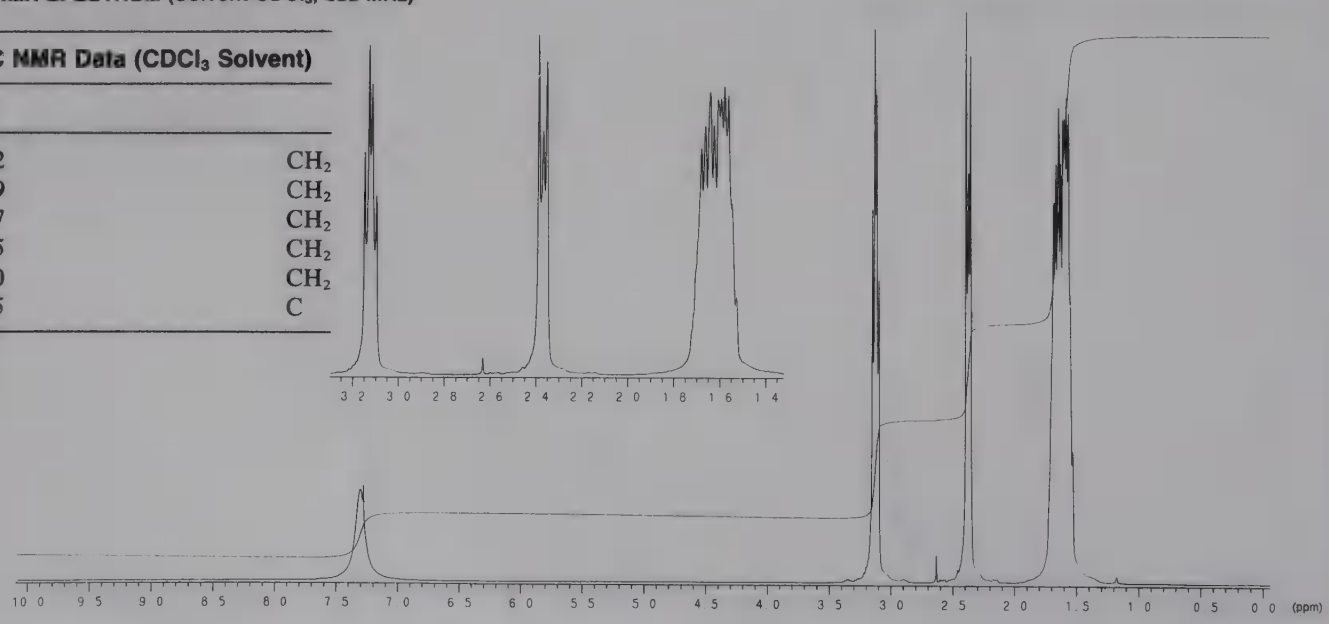

^{13}C NMR Data ($CDCl_3$ Solvent)

δ	
23.2	CH_2
29.9	CH_2
30.7	CH_2
36.5	CH_2
42.0	CH_2
177.5	C

INFRARED SPECTRUM ***Compound 9.32***

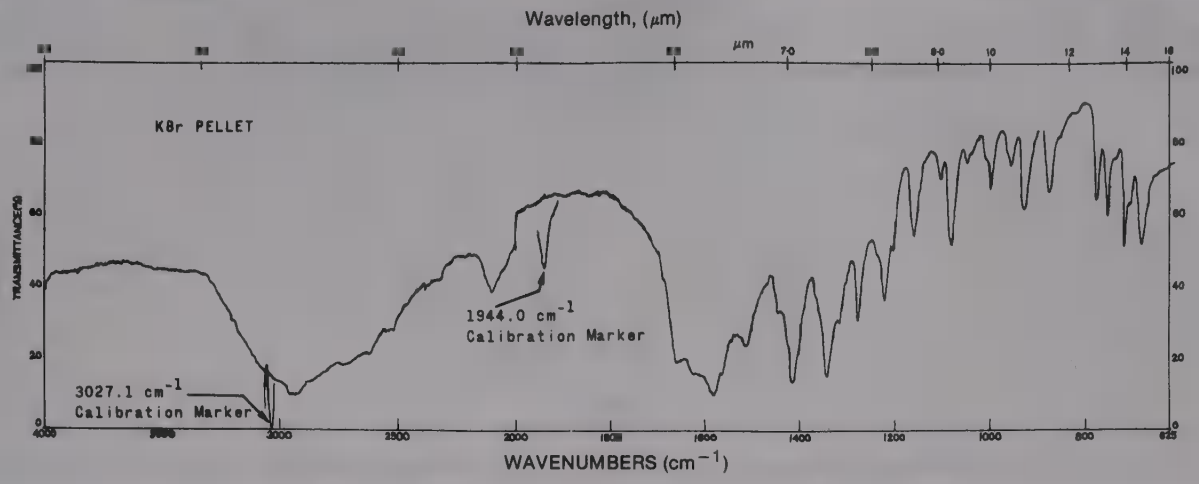

MASS SPECTRAL DATA (Relative Intensity)

FM (found) = 149.0514

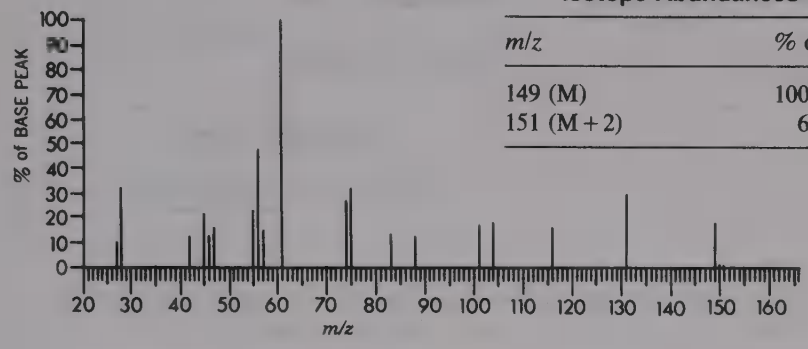

Isotope Abundances	
m/z	% of M
149 (M)	100.00
151 (M + 2)	6.1

Ultraviolet Data
Transparent above 200 nm

^{1}H NMR SPECTRUM (Solvent D_2O, 300 Hz)

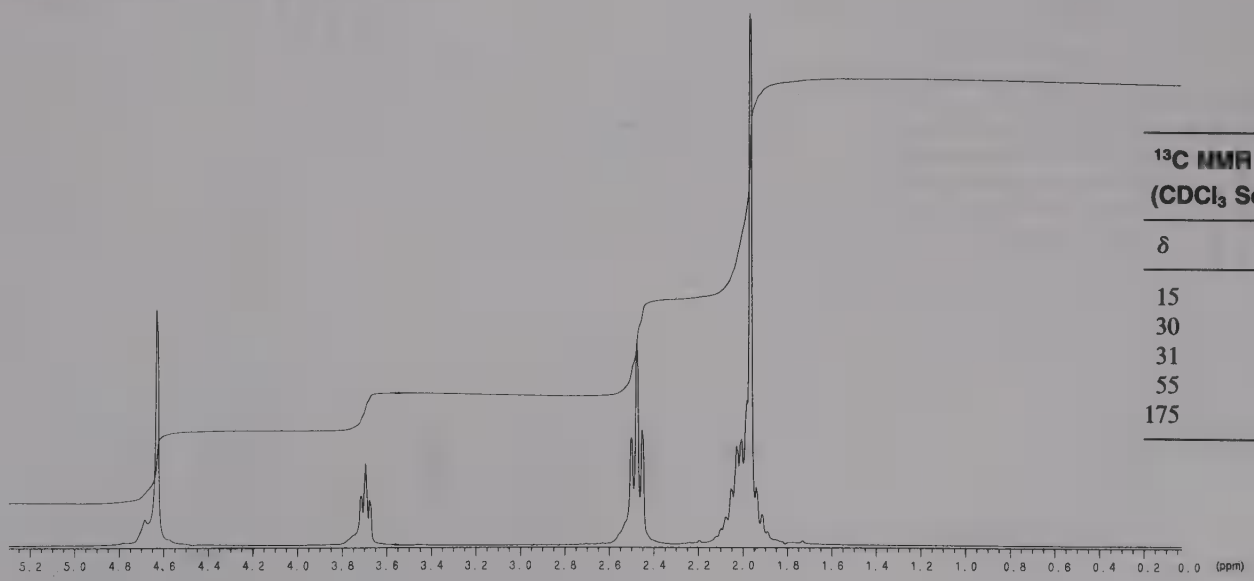

^{13}C NMR DATA ($CDCl_3$ Solvent)	
δ	
15	CH_3
30	CH_2
31	CH_2
55	CH
175	C

INFRARED SPECTRUM ***Compound 9.33***

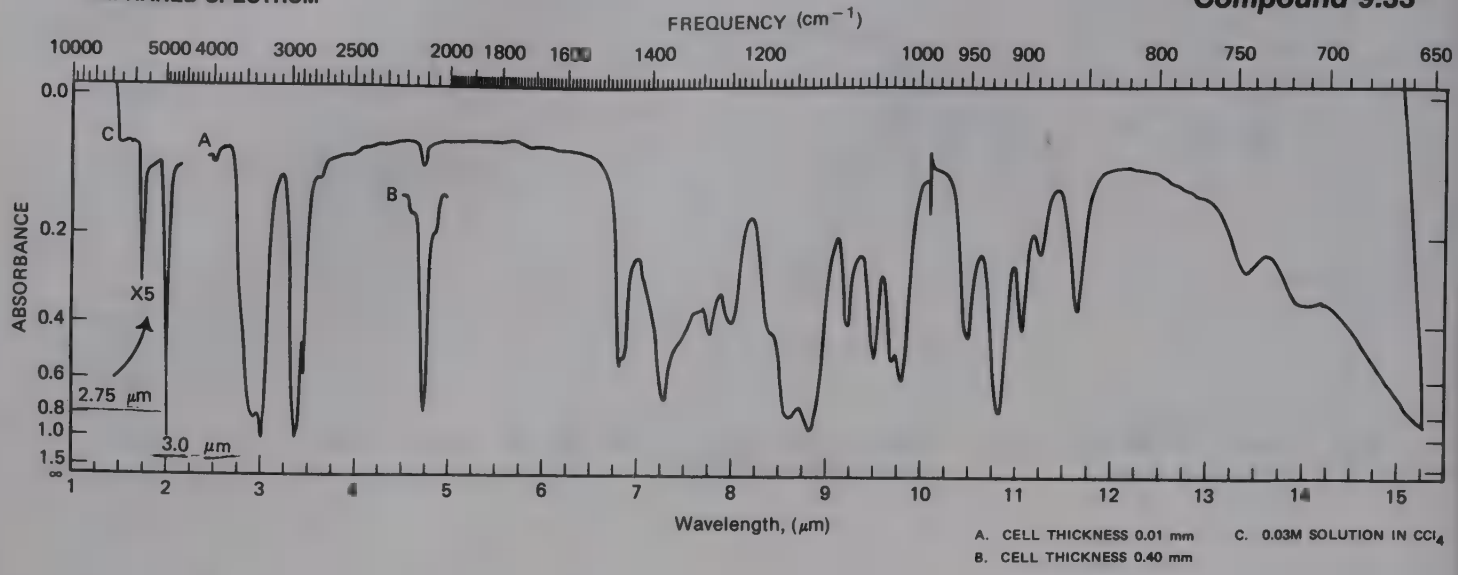

A. CELL THICKNESS 0.01 mm C. 0.03M SOLUTION IN CCl_4
B. CELL THICKNESS 0.40 mm

MASS SPECTRAL DATA (Relative Intensities)

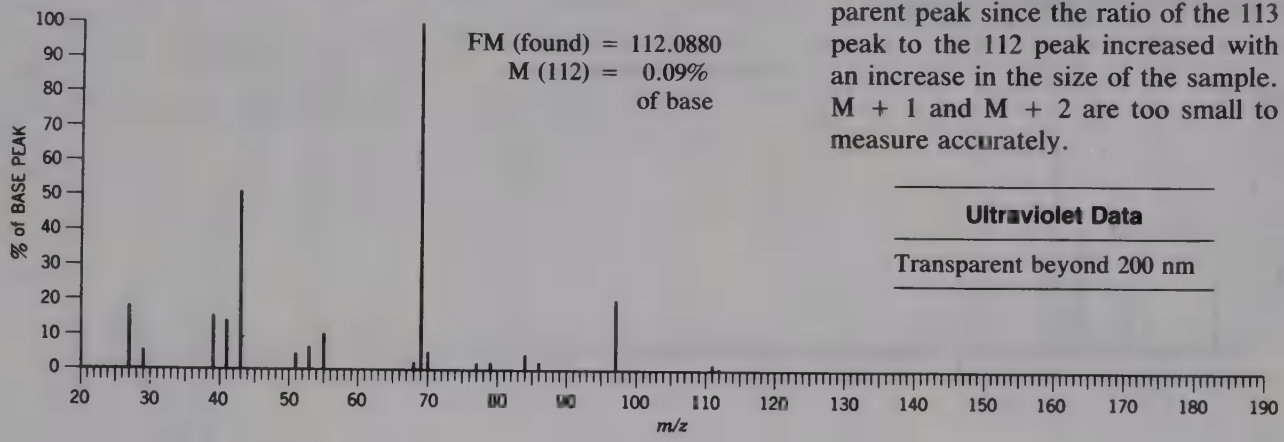

FM (found) = 112.0880
M (112) = 0.09% of base

The 112 peak was established as the parent peak since the ratio of the 113 peak to the 112 peak increased with an increase in the size of the sample. M + 1 and M + 2 are too small to measure accurately.

Ultraviolet Data

Transparent beyond 200 nm

^{1}H NMR SPECTRUM (Solvent CCl_4, 100 MHz)

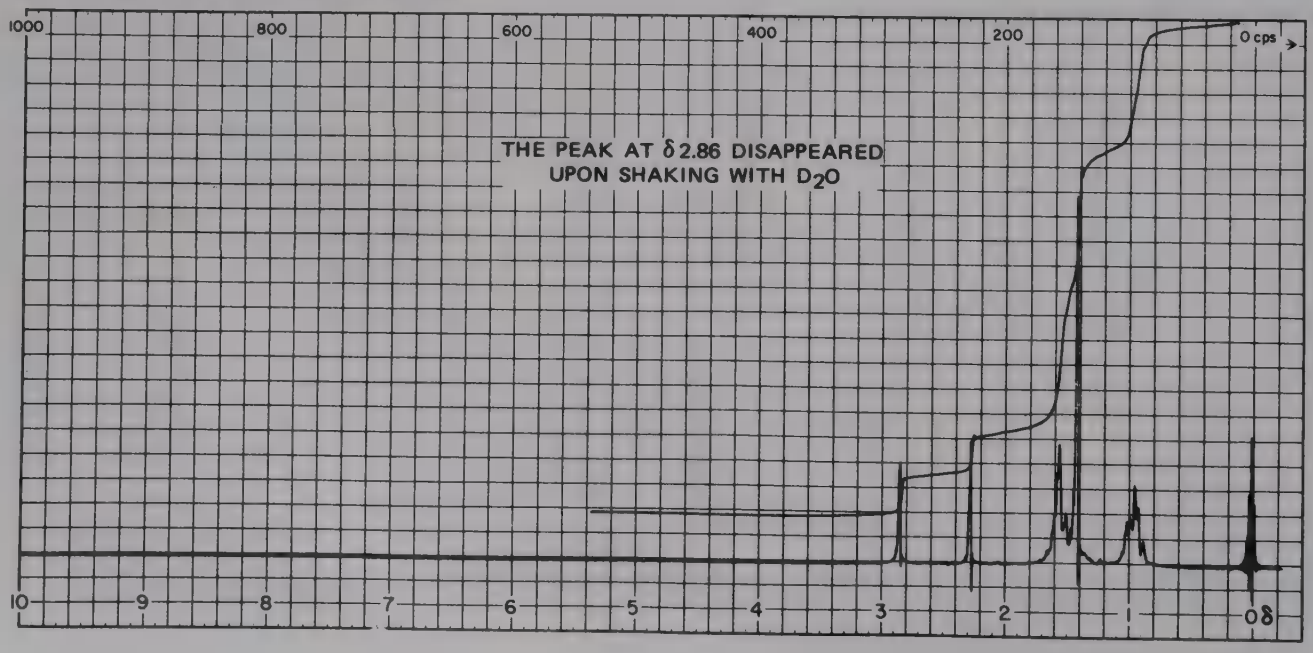

NOTES

Compound 9.34

INFRARED SPECTRUM

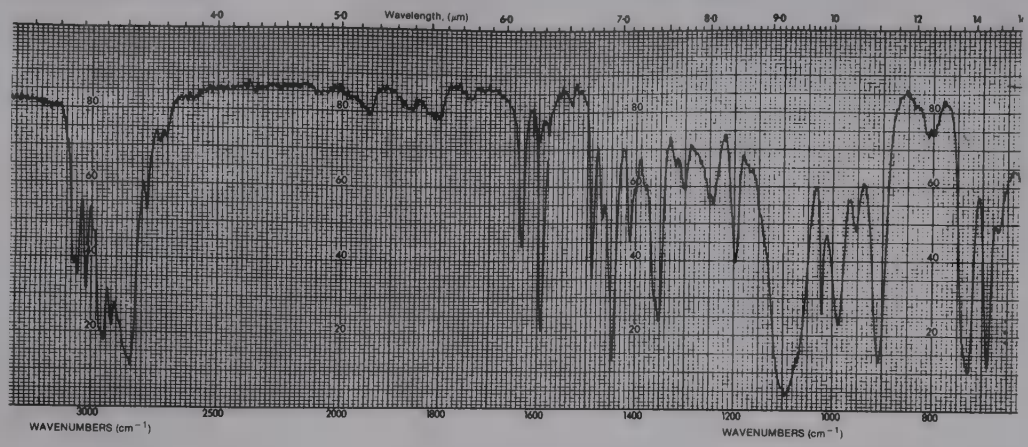

MASS SPECTRAL DATA

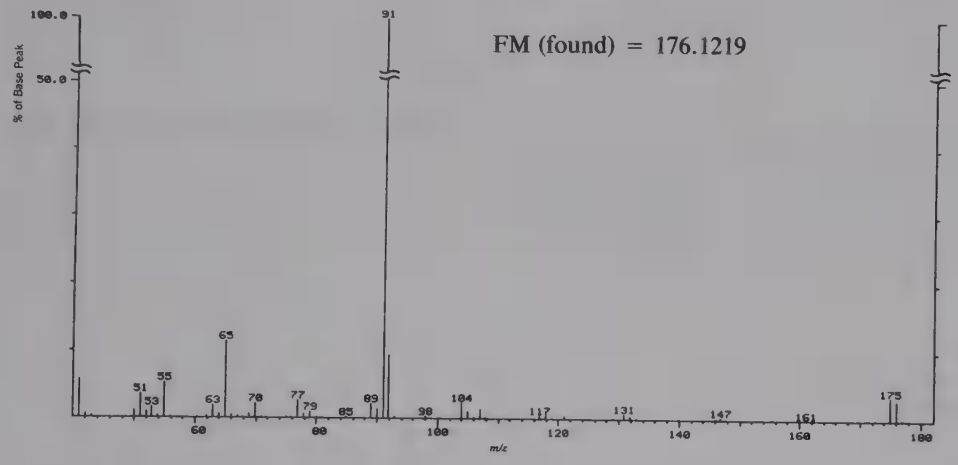

^{1}H NMR SPECTRUM (Solvent $CDCl_3$, 500 MHz)

X = impurity

Compound 9.34 (continued)

^{13}C APT

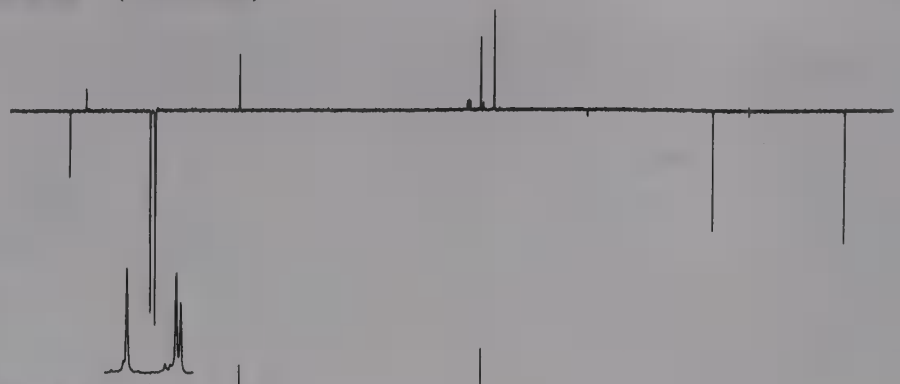

^{13}C NMR SPECTRUM DECOUPLED

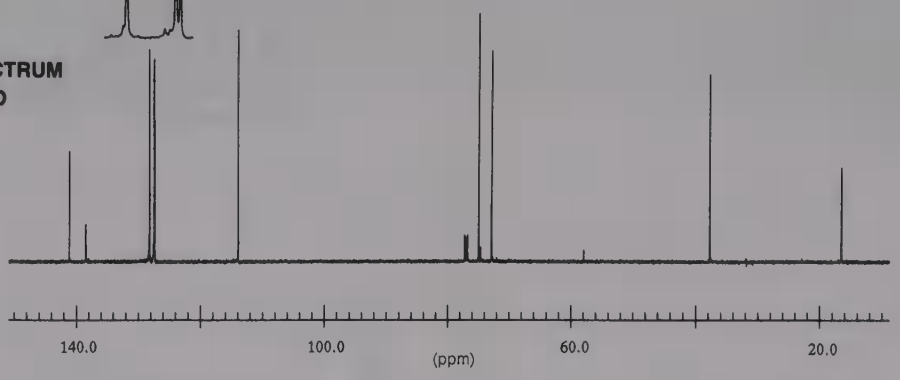

H C COSY (HETCOR)

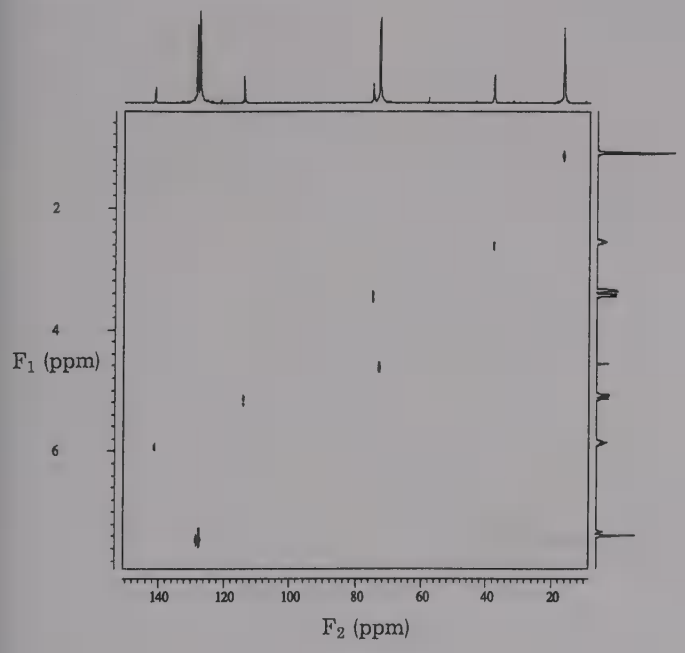

H H COSY

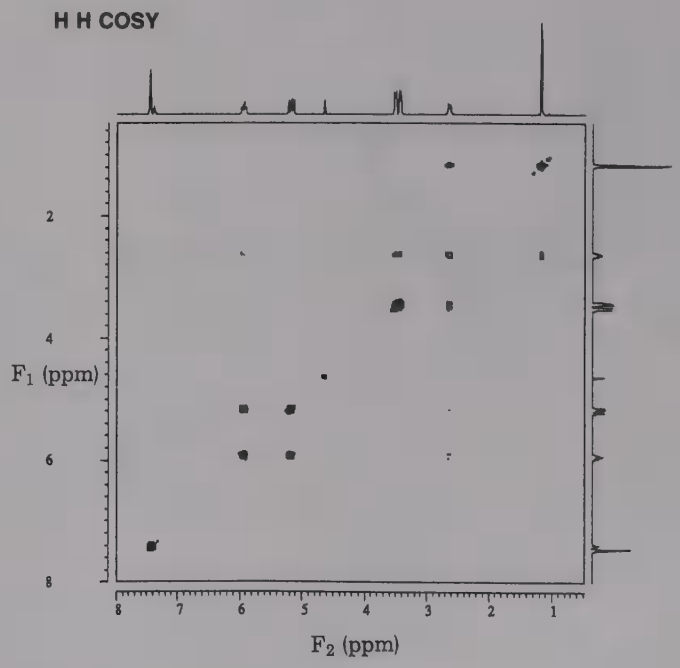

INFRARED SPECTRUM (Neat)

Compound 9.35

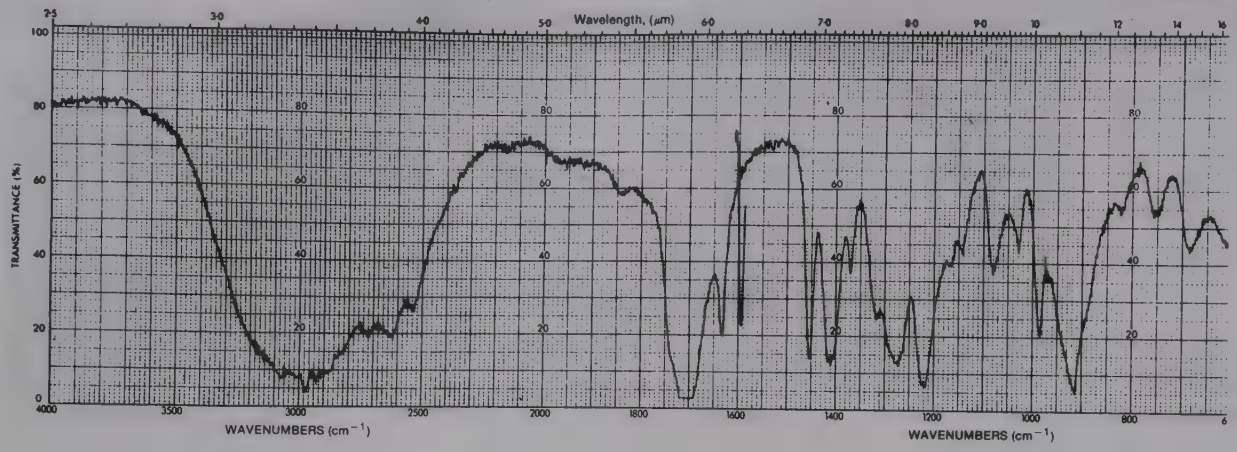

MASS SPECTRAL DATA

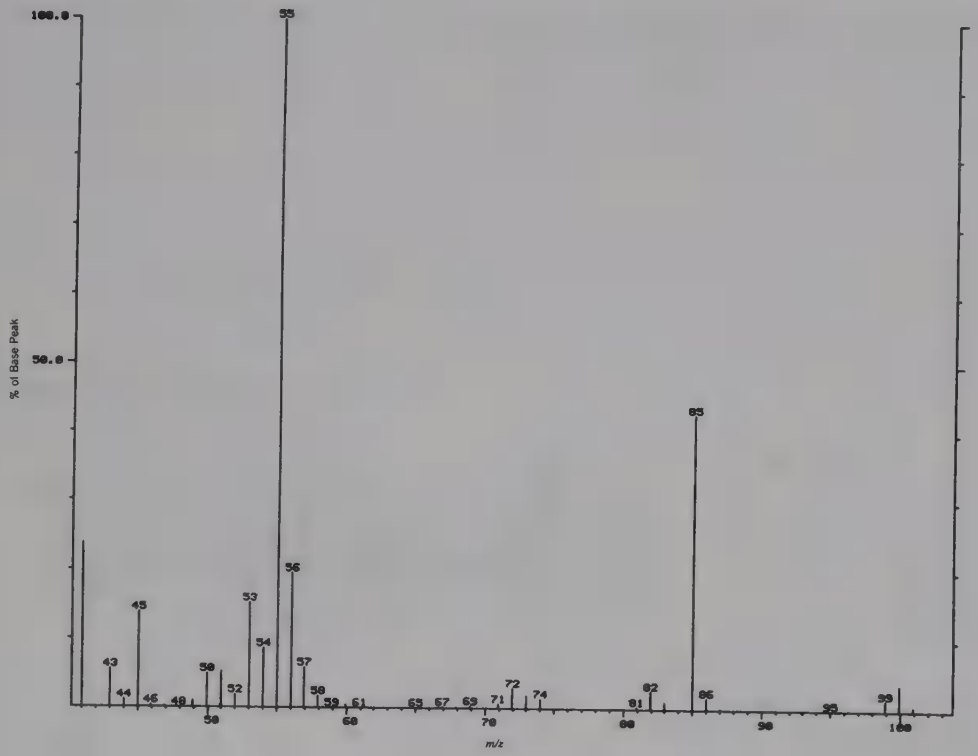

Compound 9.35 (continued)

^{1}H NMR SPECTRUM (Solvent $CDCl_3$, 360 MHz)

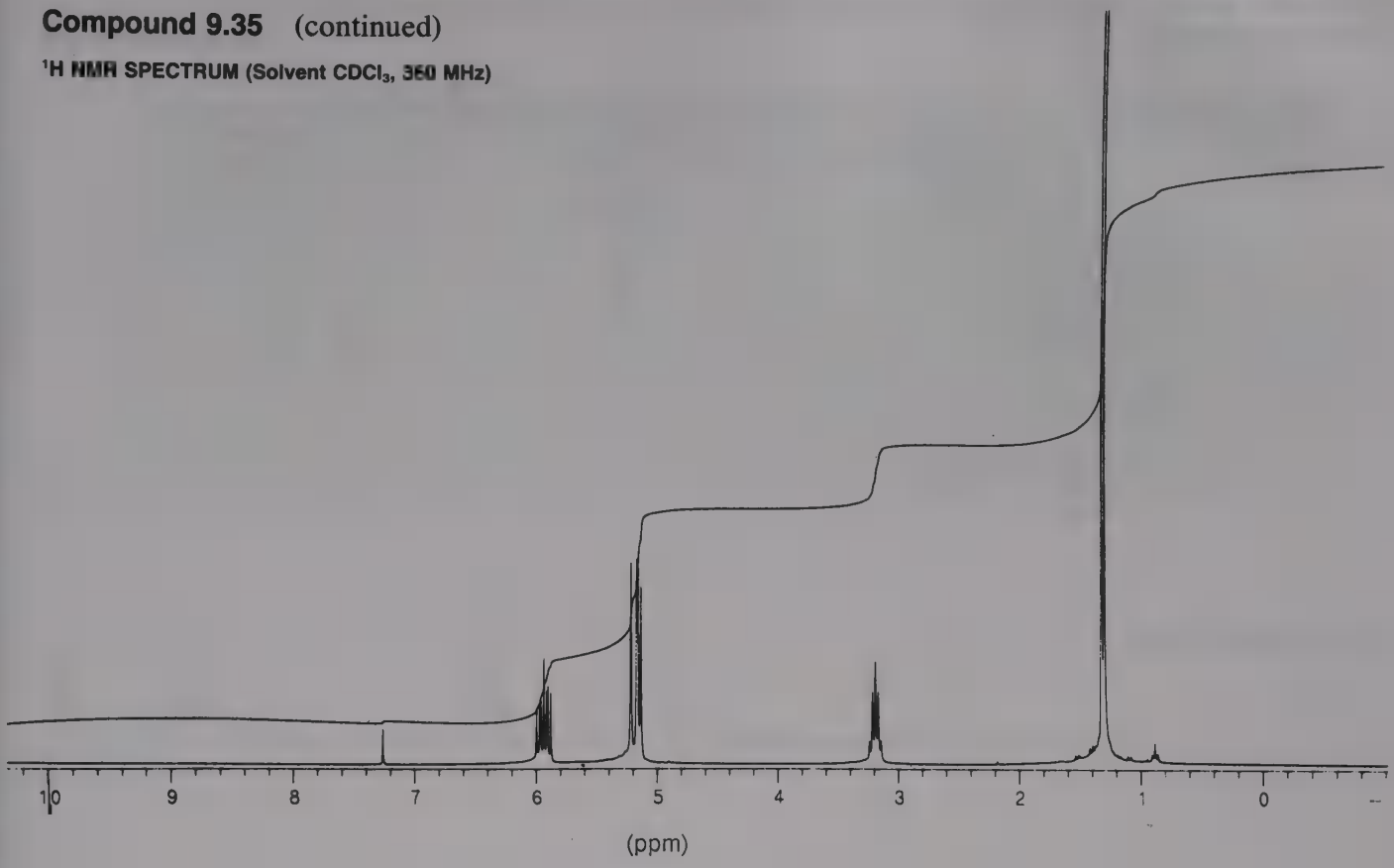

^{13}C NMR SPECTRUM

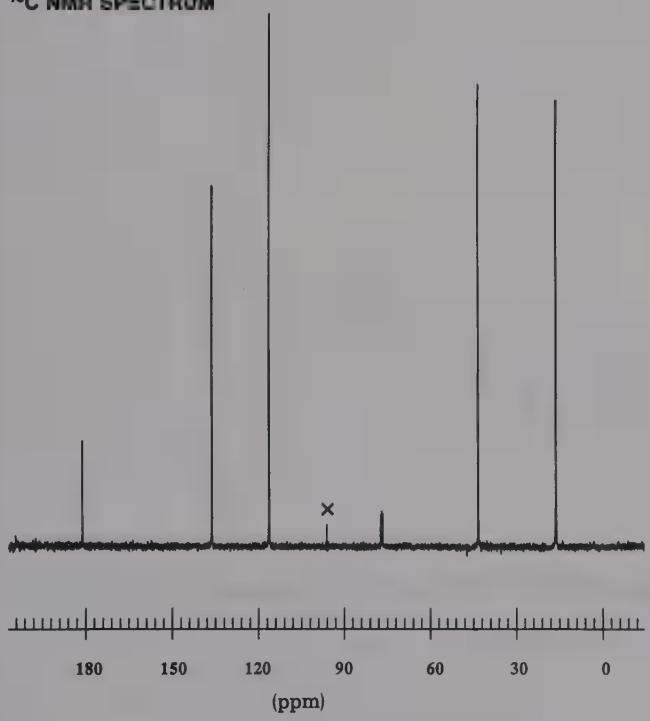

X = Impurity

INFRARED SPECTRUM ***Compound 9.30***

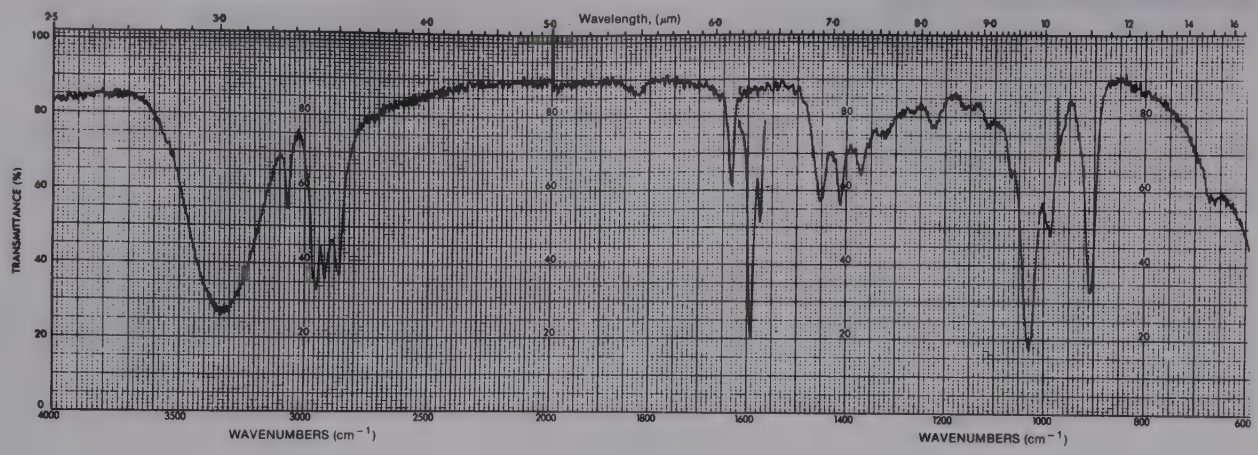

MASS SPECTRAL DATA

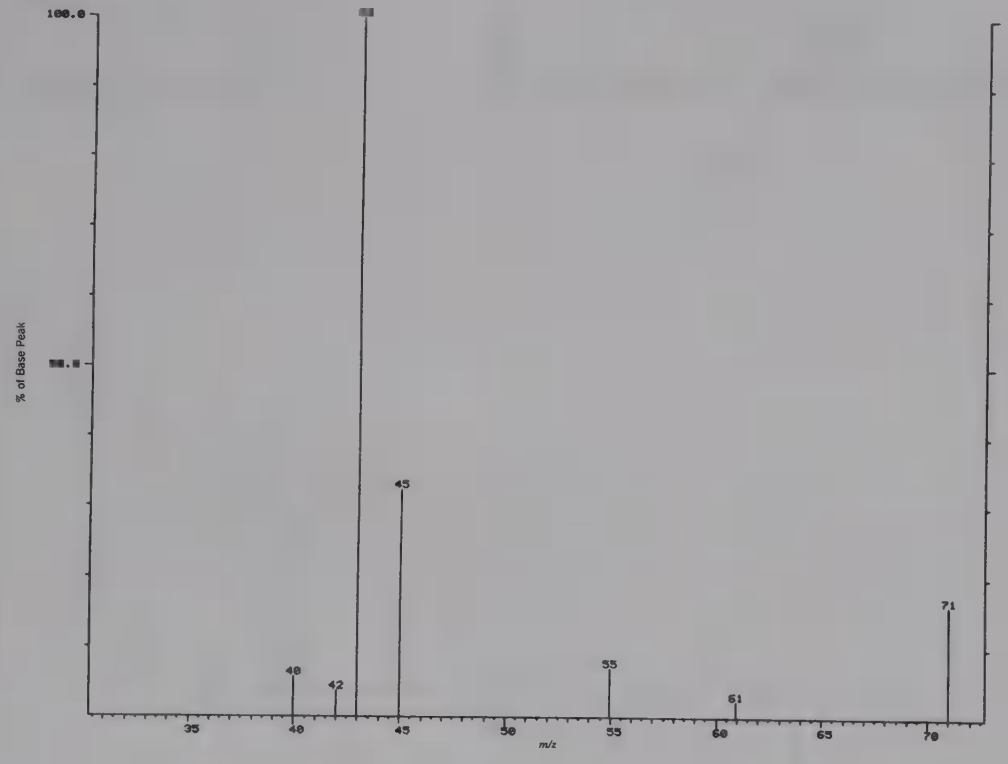

Compound 9.38 (continued)

^{1}H NMR SPECTRUM (Solvent $CDCl_3$, [illegible] MHz)

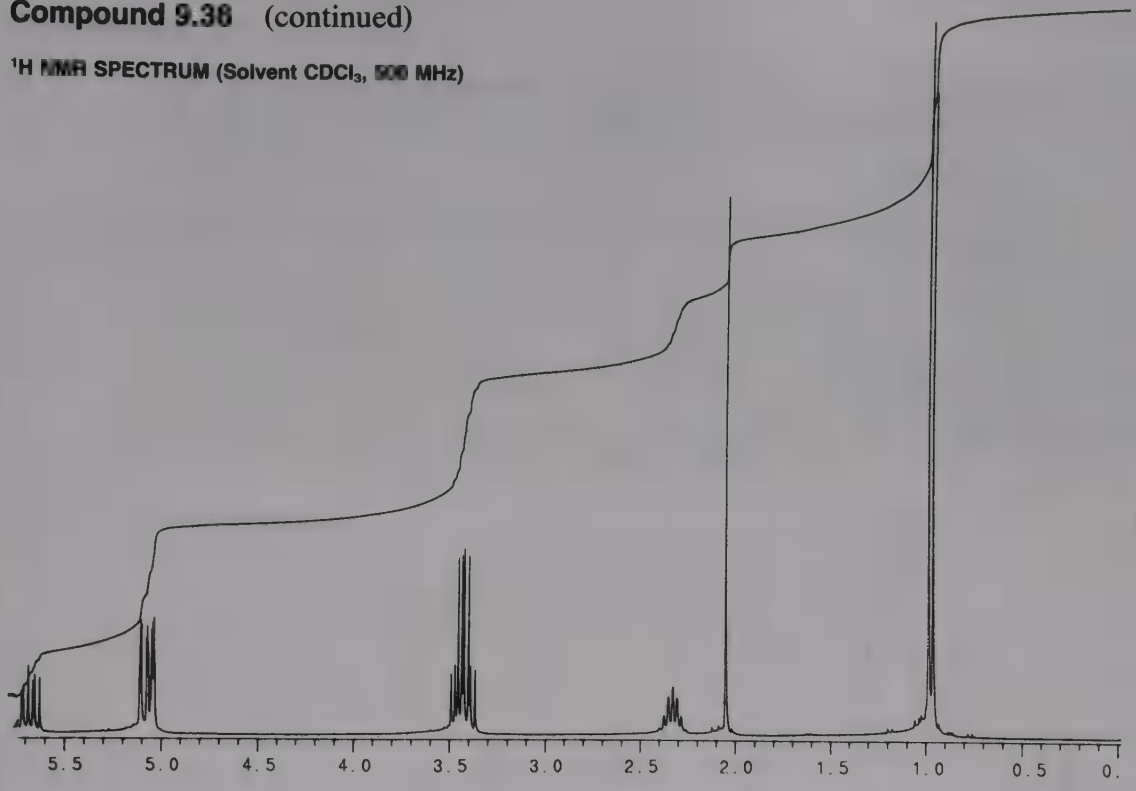

^{13}C NMR SPECTRUM DECOUPLED

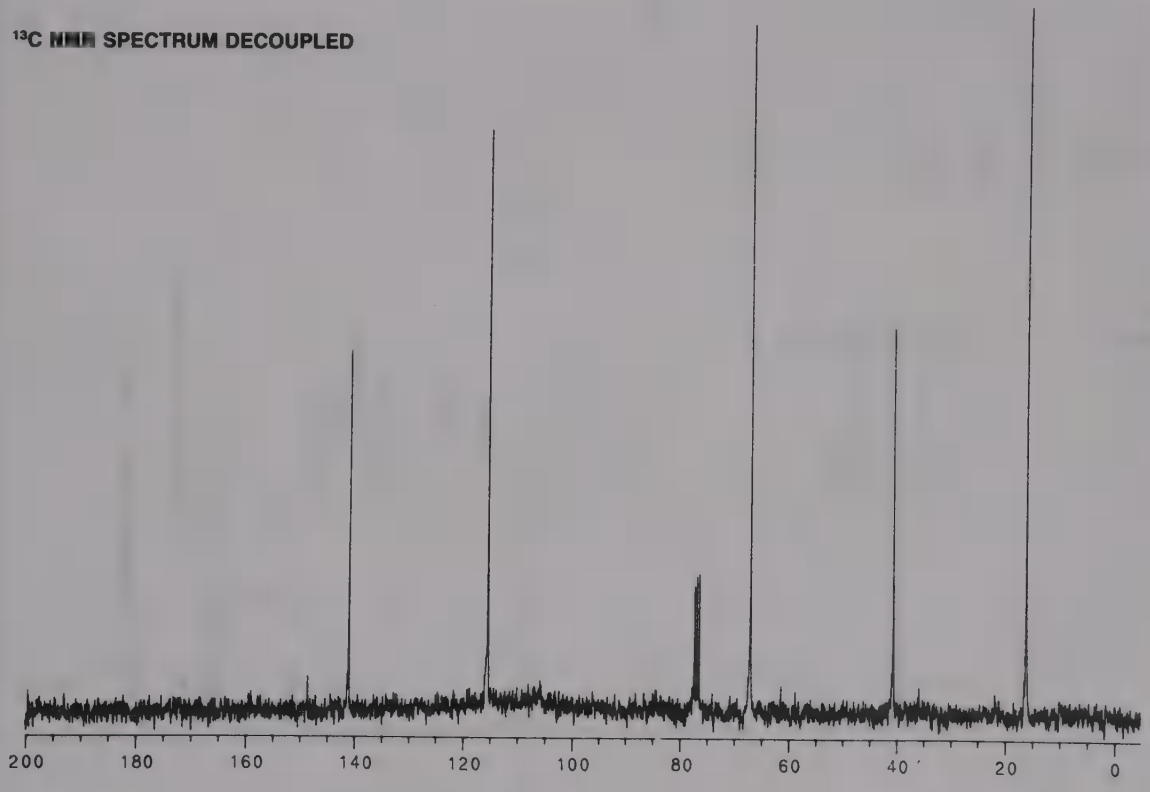

INFRARED SPECTRUM ***Compound 9.37***

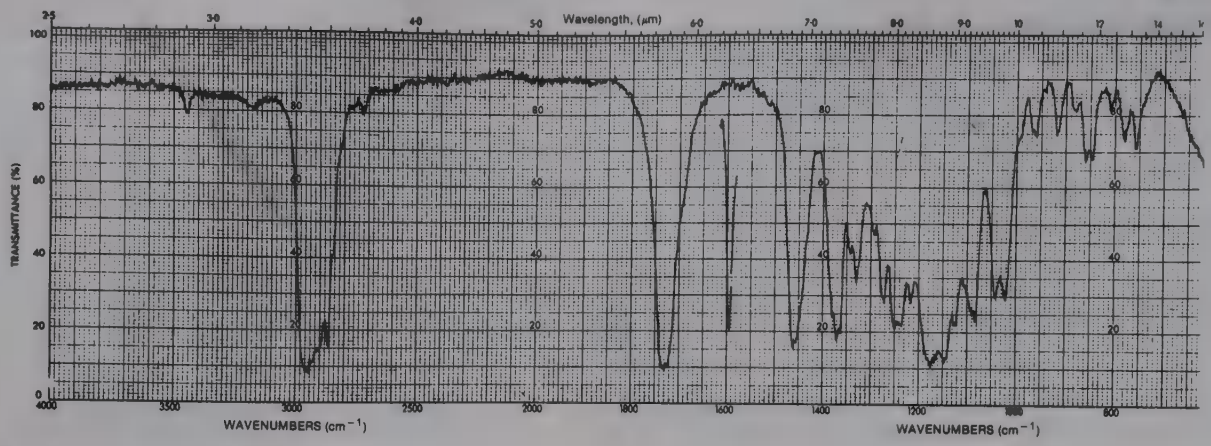

MASS SPECTRAL DATA

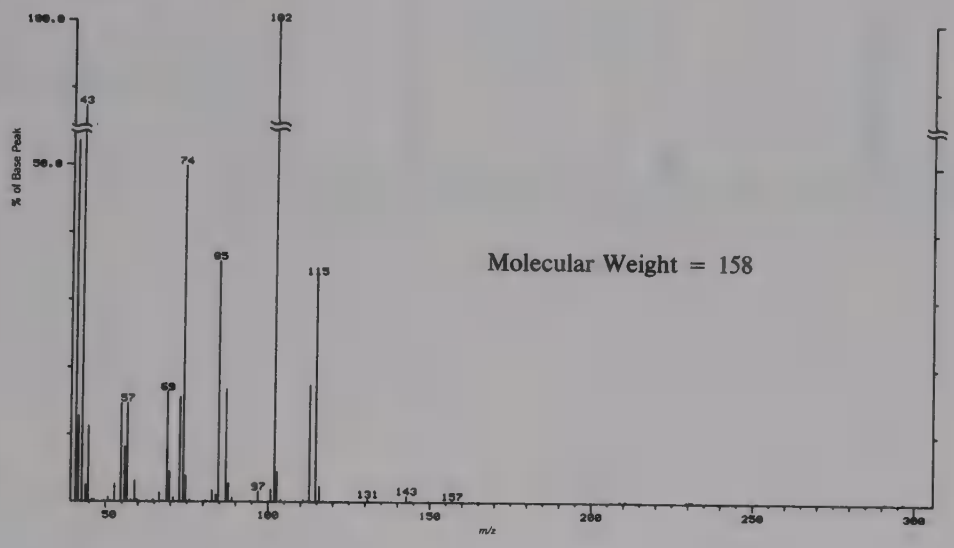

^{1}H NMR SPECTRUM
(Solvent $CDCl_3$, 500 MHz)

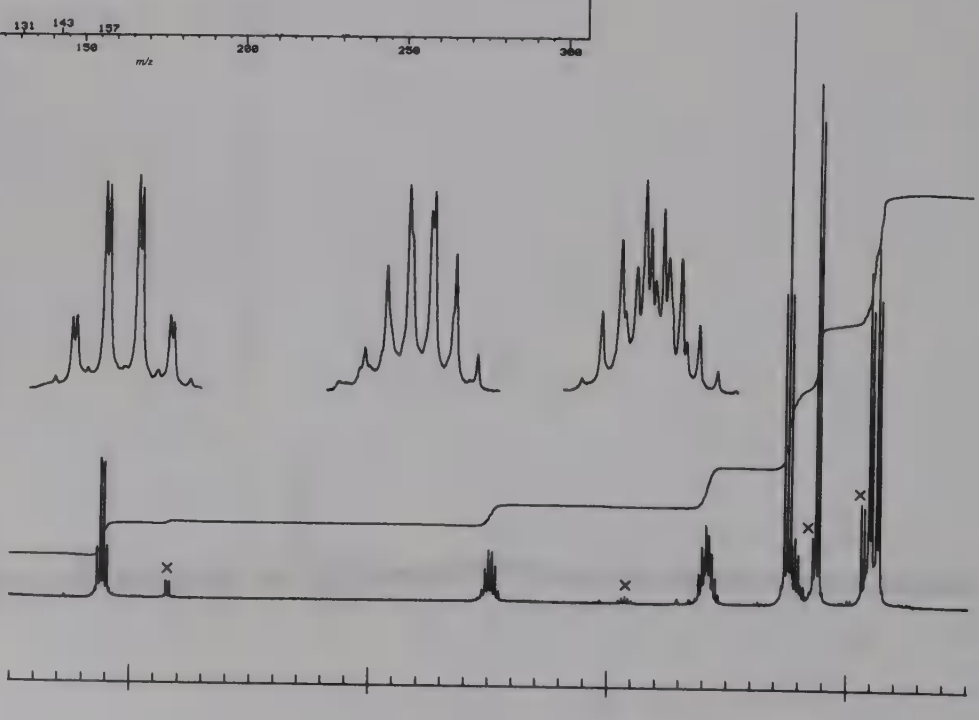

X = Impurity

4.00 3.00 2.00 1.00

(ppm)

Compound 9.37 (continued)

^{13}C APT

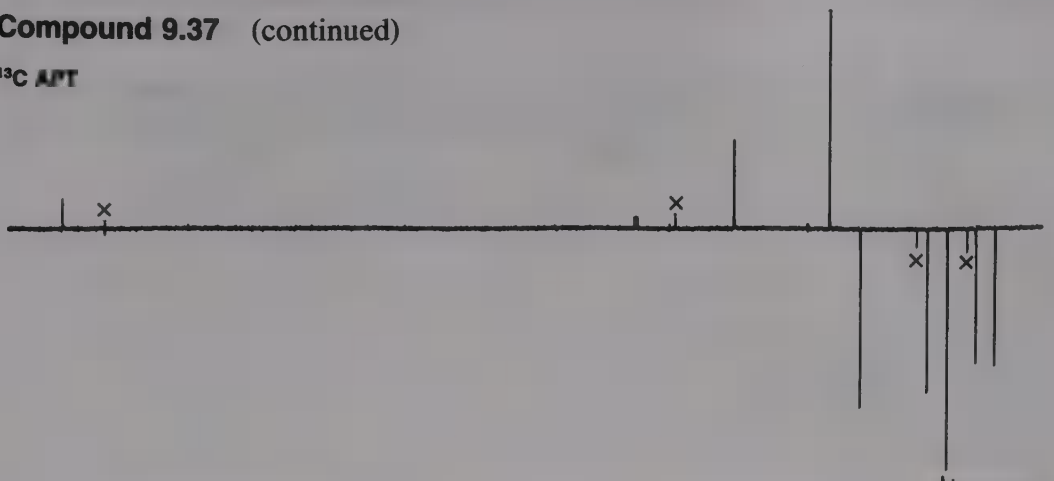

^{13}C NMR SPECTRUM DECOUPLED

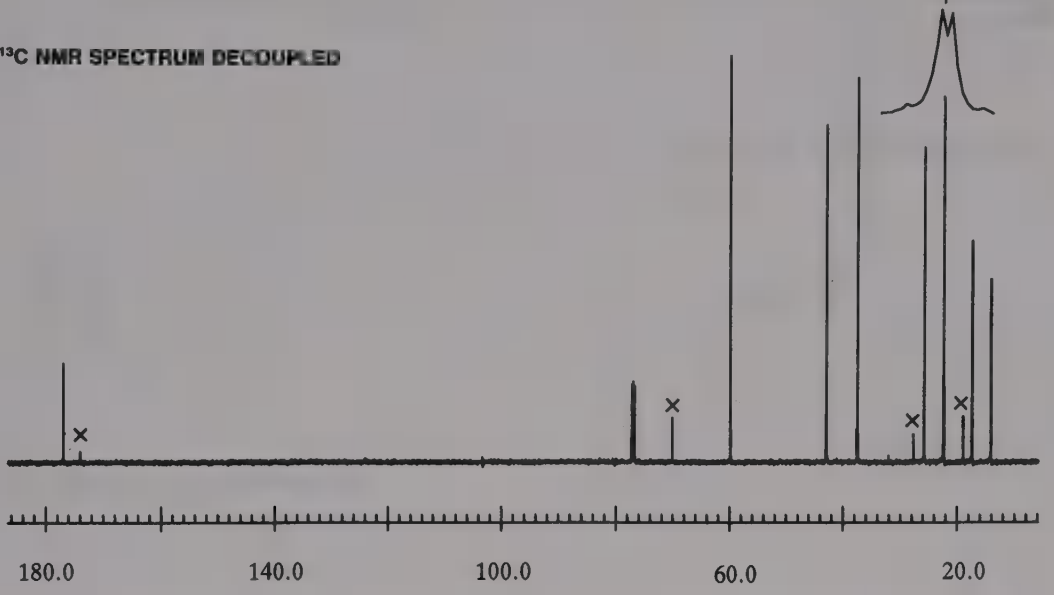

X = Impurity

H H COSY

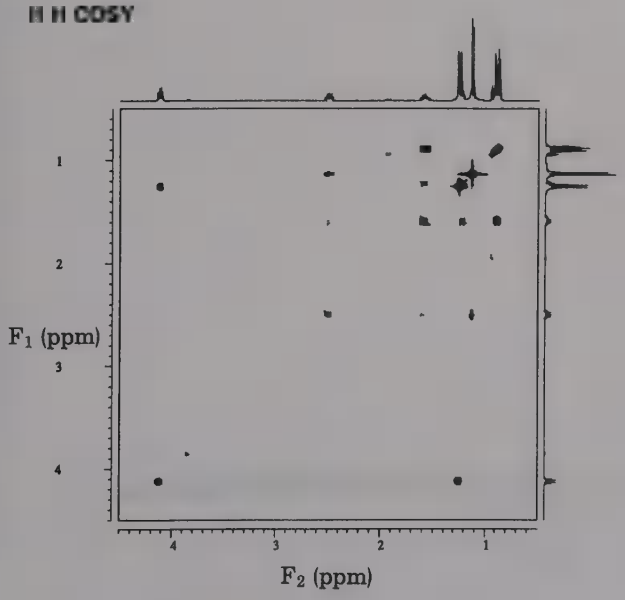

H C COSY (HETCOR)

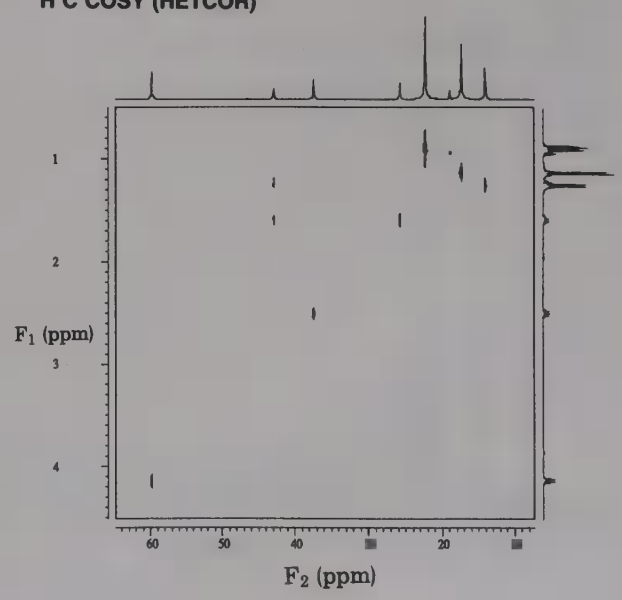

INFRARED SPECTRUM ***Compound 9.38***

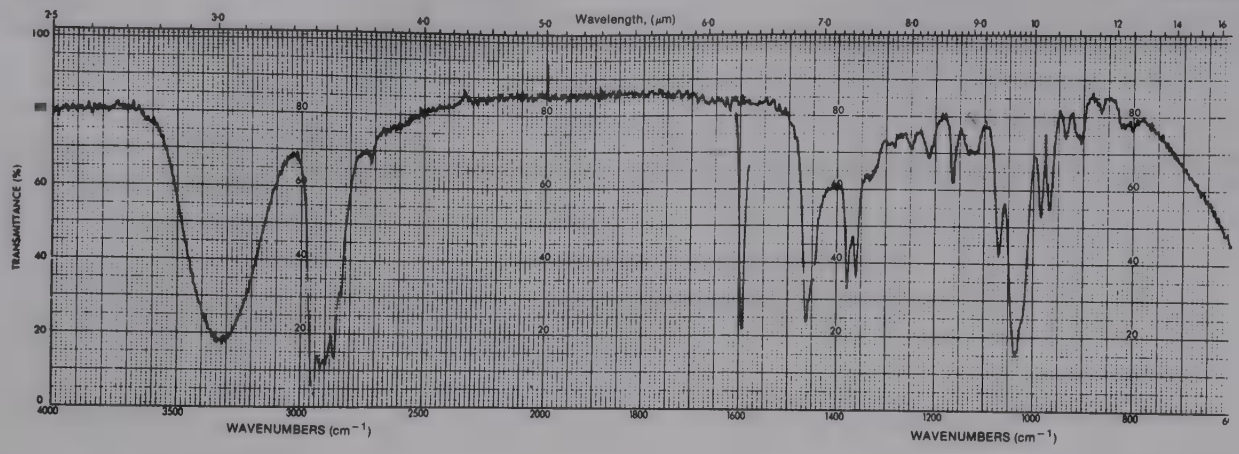

MASS SPECTRAL DATA

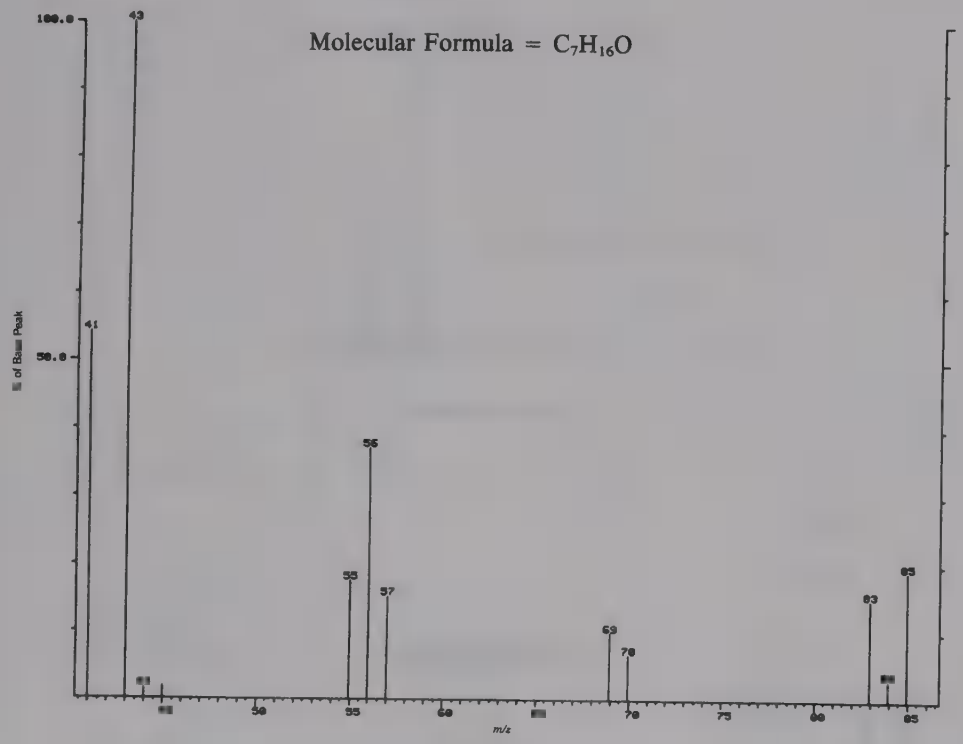

Compound 9.38 (continued)

^{1}H NMR SPECTRA (Solvent $CDCl_3$, 500 MHz)

Signal at δ 1.74 disappears upon shaking with D_2O.

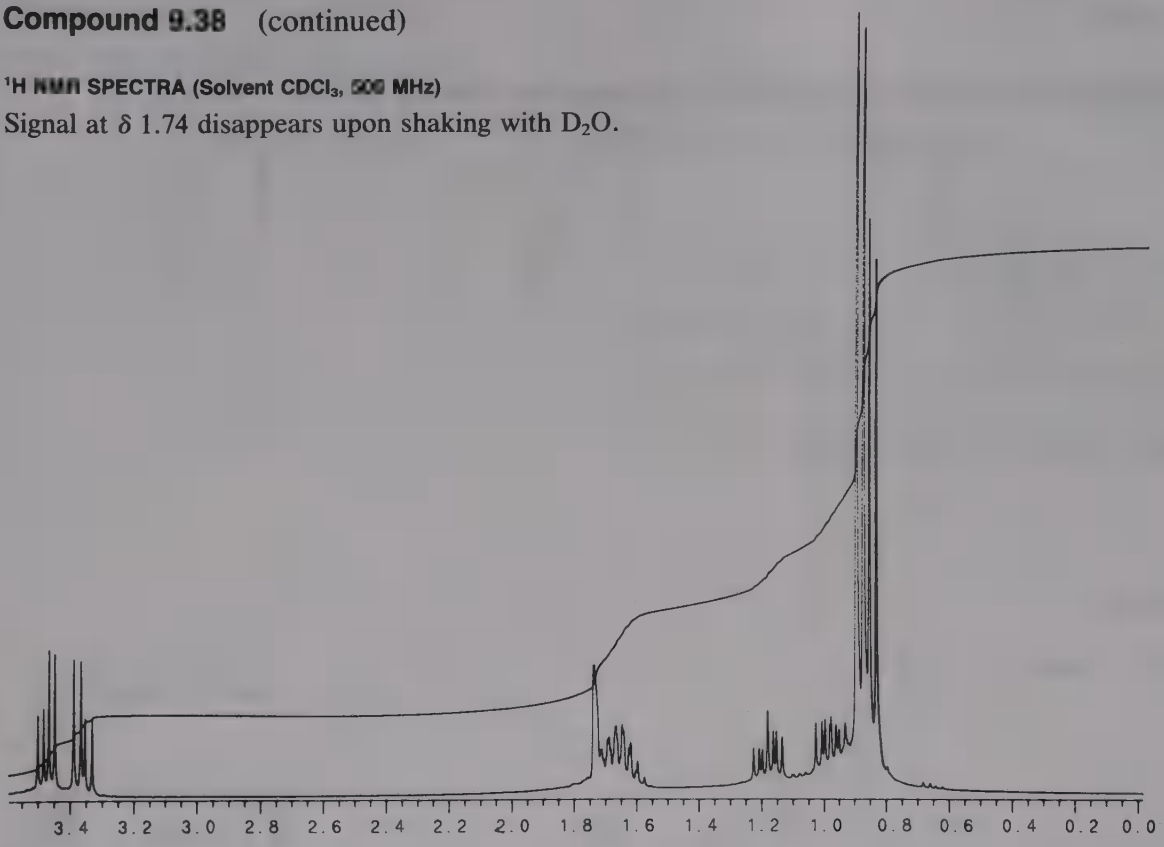

^{13}C NMR SPECTRUM (DECOUPLED)

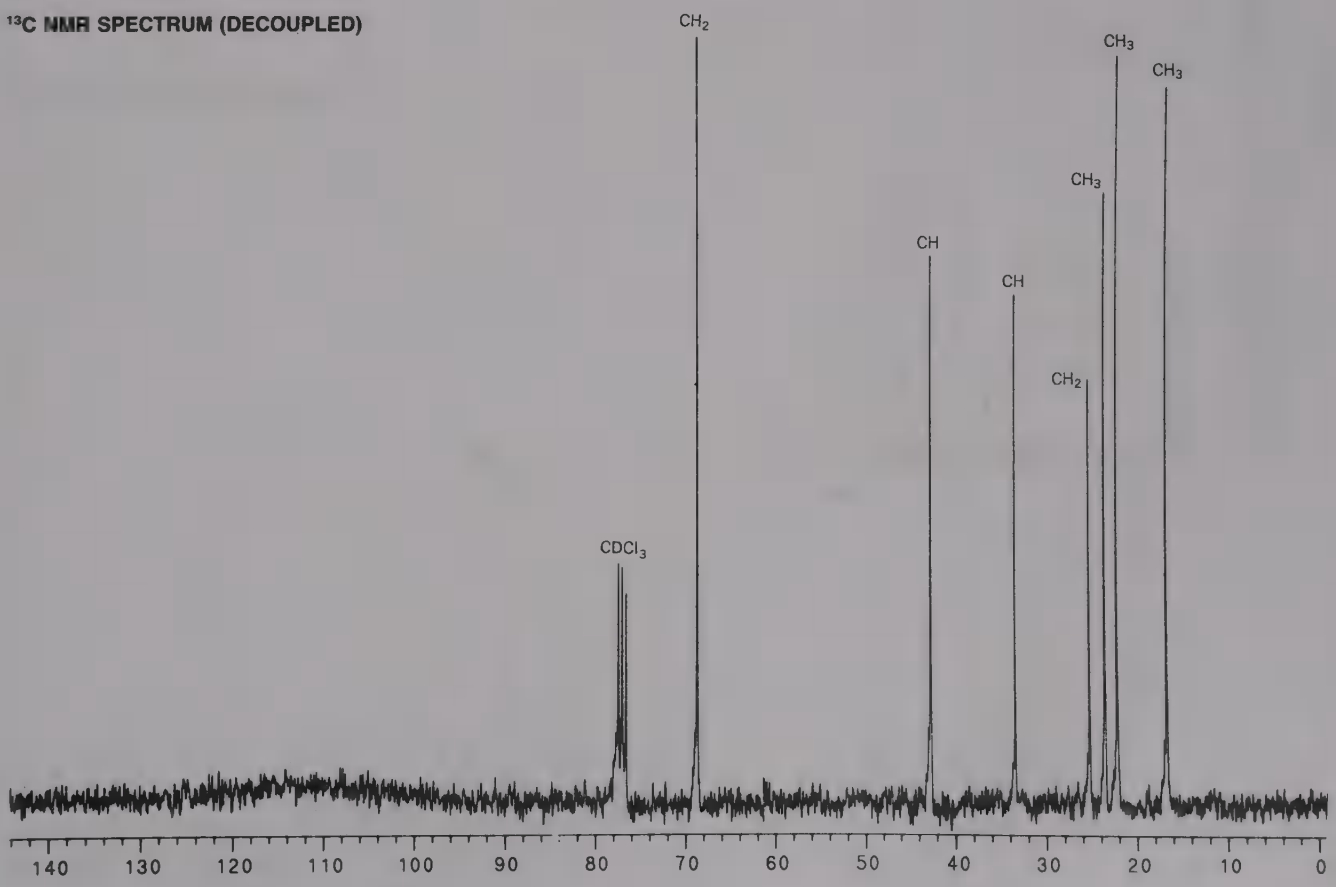

INFRARED SPECTRUM

Compound 9.39

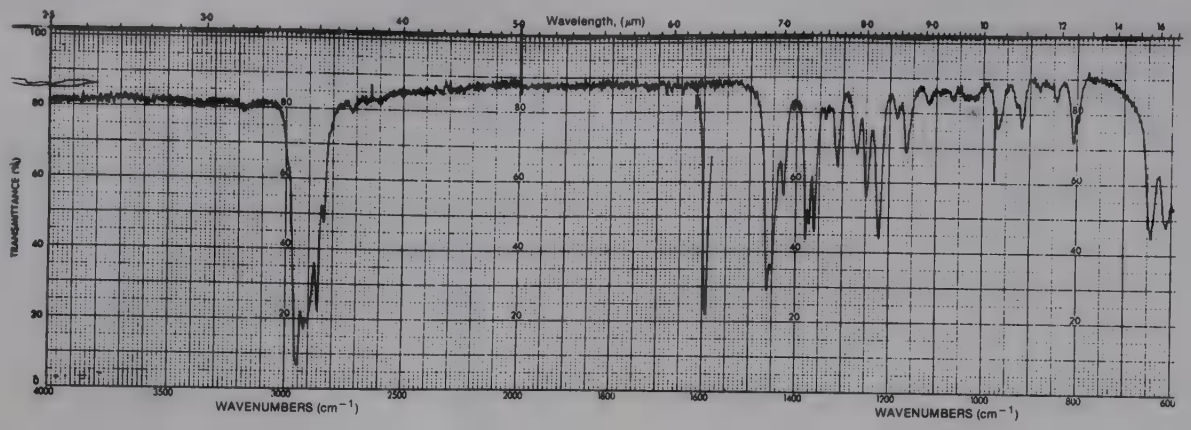

MASS SPECTRAL DATA

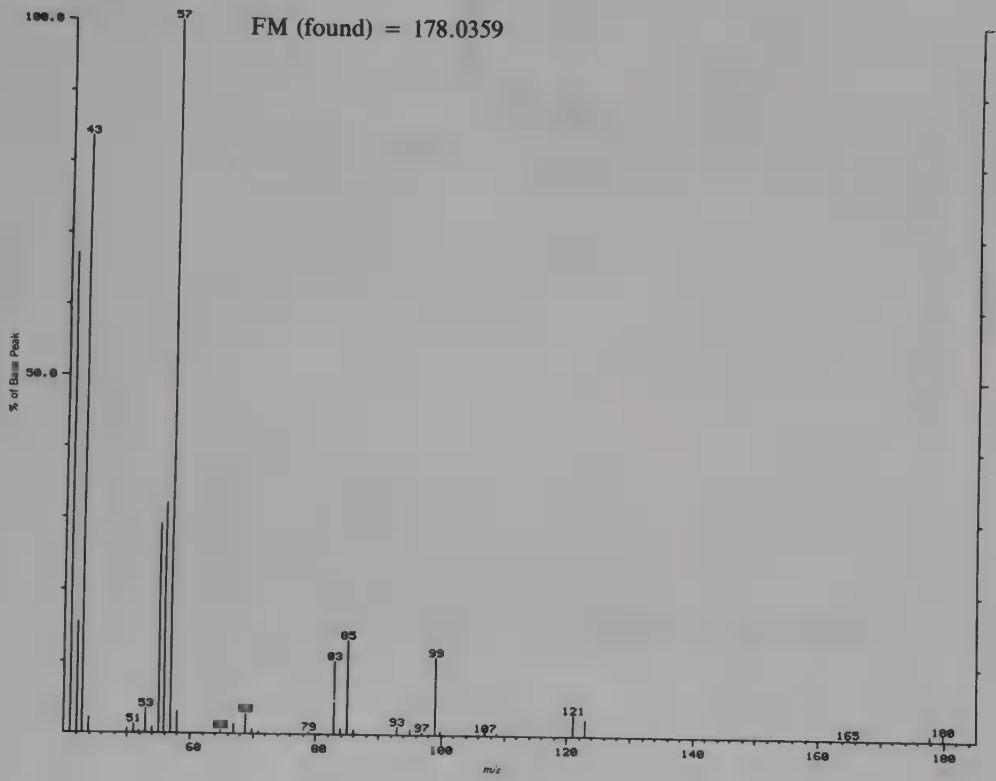

Isotope Abundance	
m/z	% of M
M (178)	100.0
M + 2 (180)	101.0

Compound 9.39 (continued)

^{1}H NMR SPECTRUM (Solvent $CDCl_3$, 500 MHz)

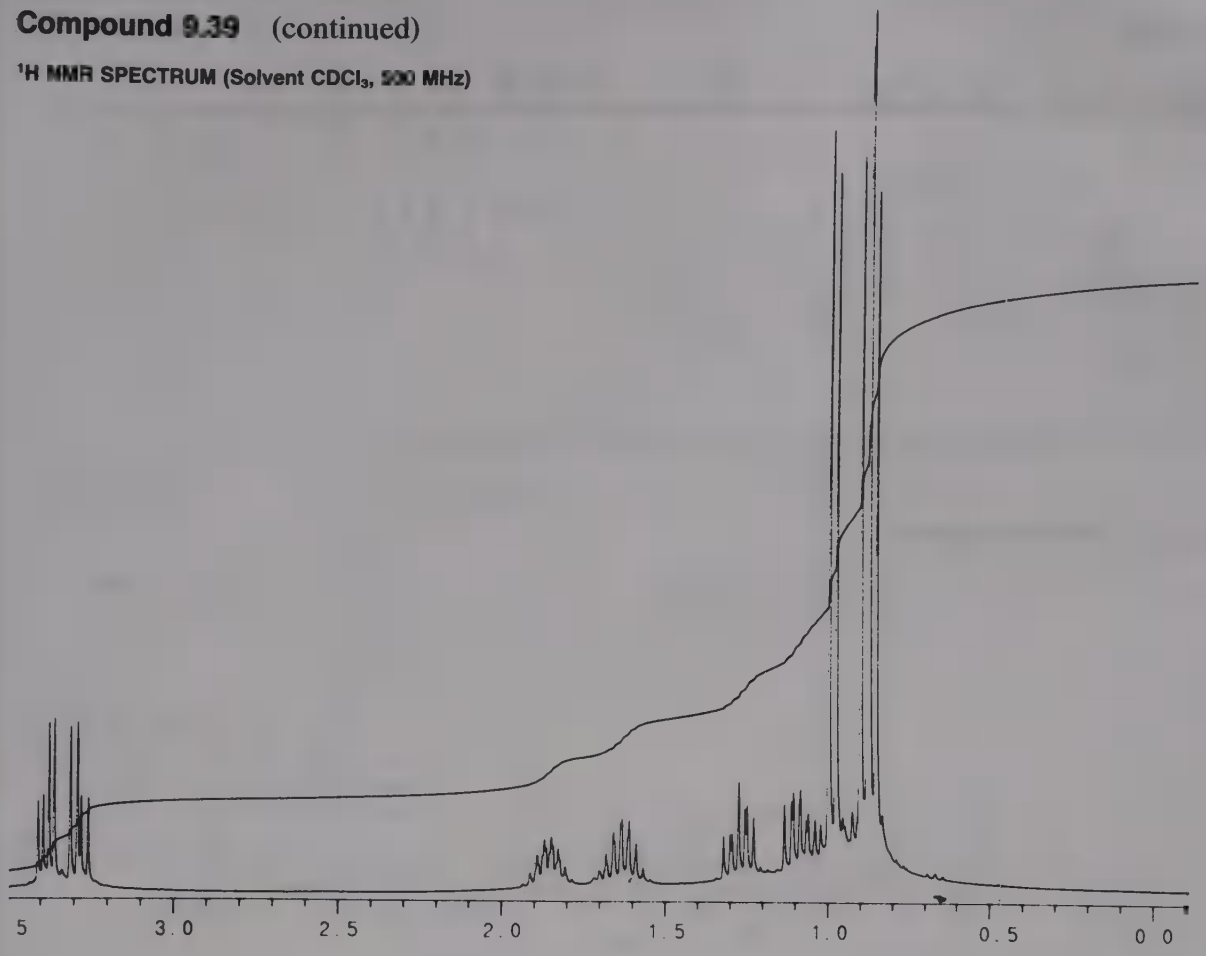

^{13}C NMR SPECTRUM DECOUPLED

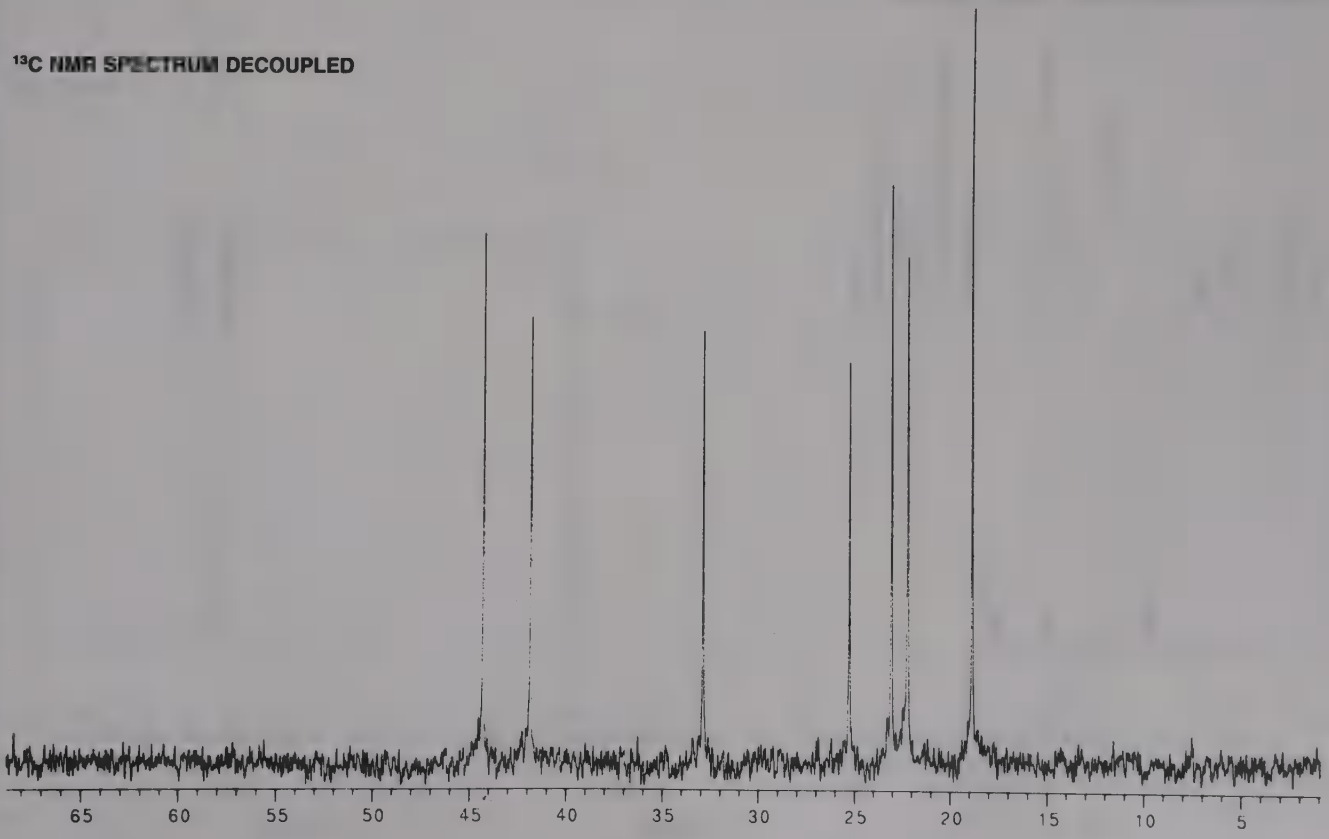

INFRARED SPECTRUM **Compound 9.40**

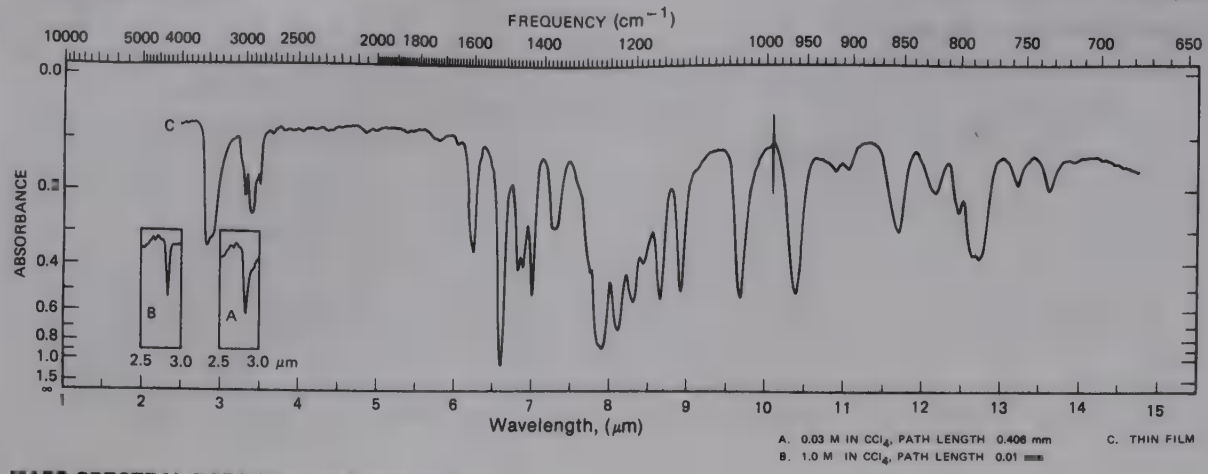

MASS SPECTRAL DATA (Relative Intensities)

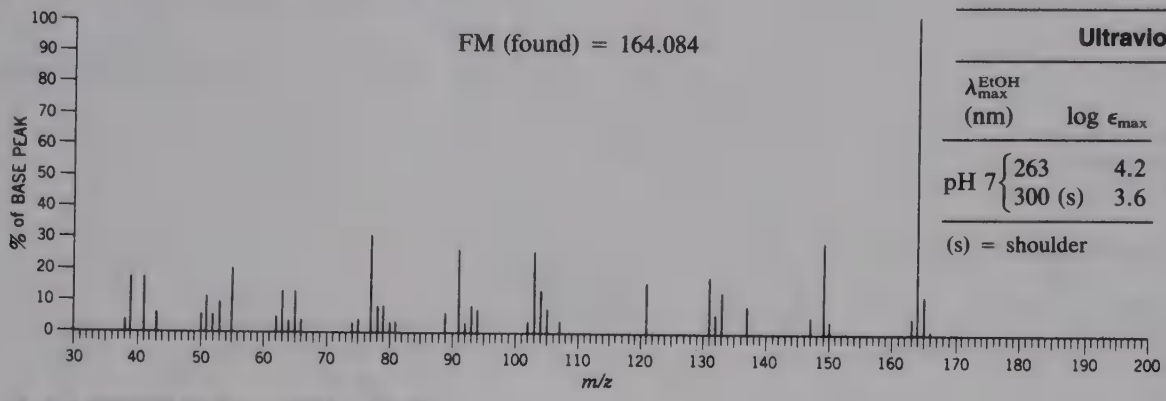

Ultraviolet Data

	λ_{max}^{EtOH} (nm)	log ϵ_{max}		λ_{max}^{EtOH} (nm)	log ϵ_{max}
pH 7	263	4.2	pH 13	288	4.0
	300 (s)	3.6		315 (s)	3.8

(s) = shoulder

^{1}H NMR SPECTRUM (Solvent $CDCl_3$, 500 MHz)

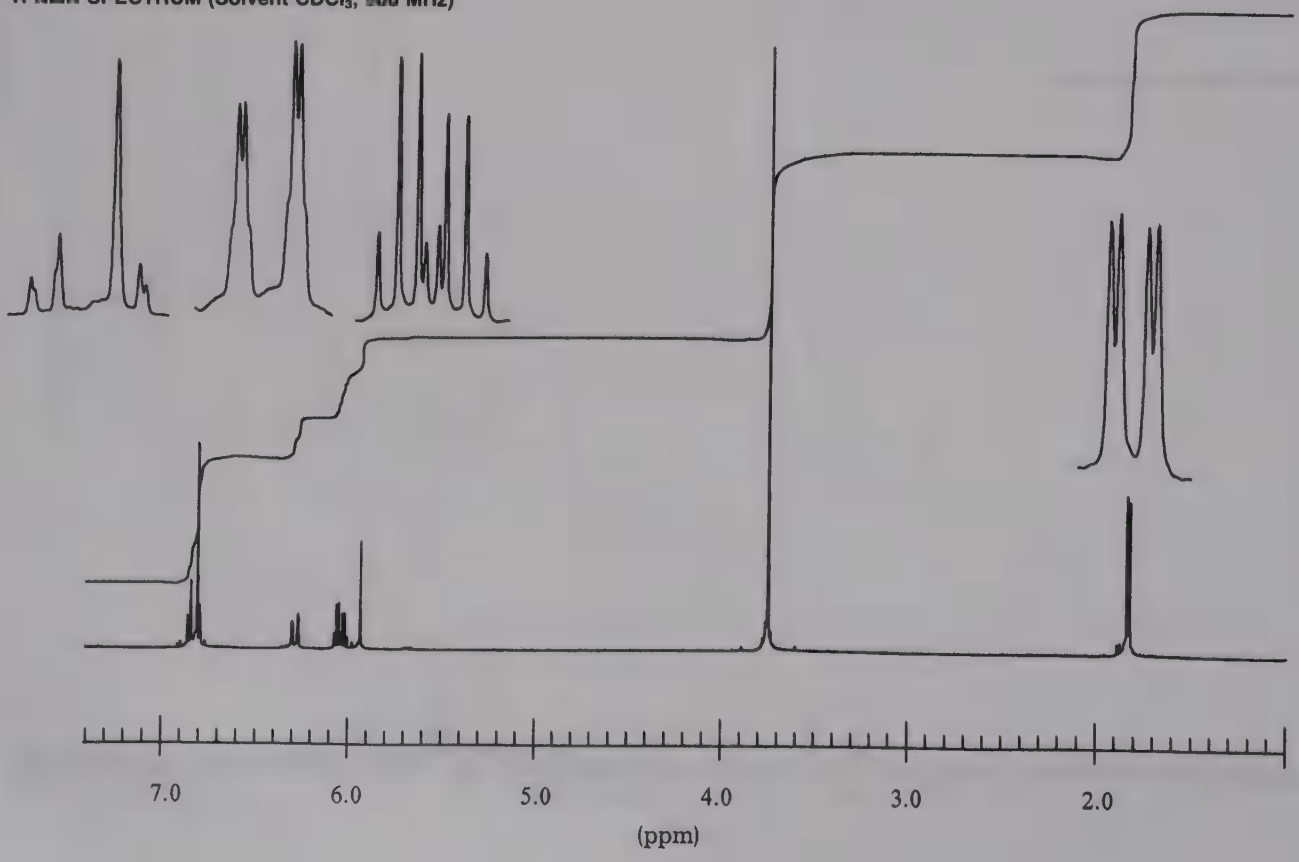

Compound 9.40 (continued)

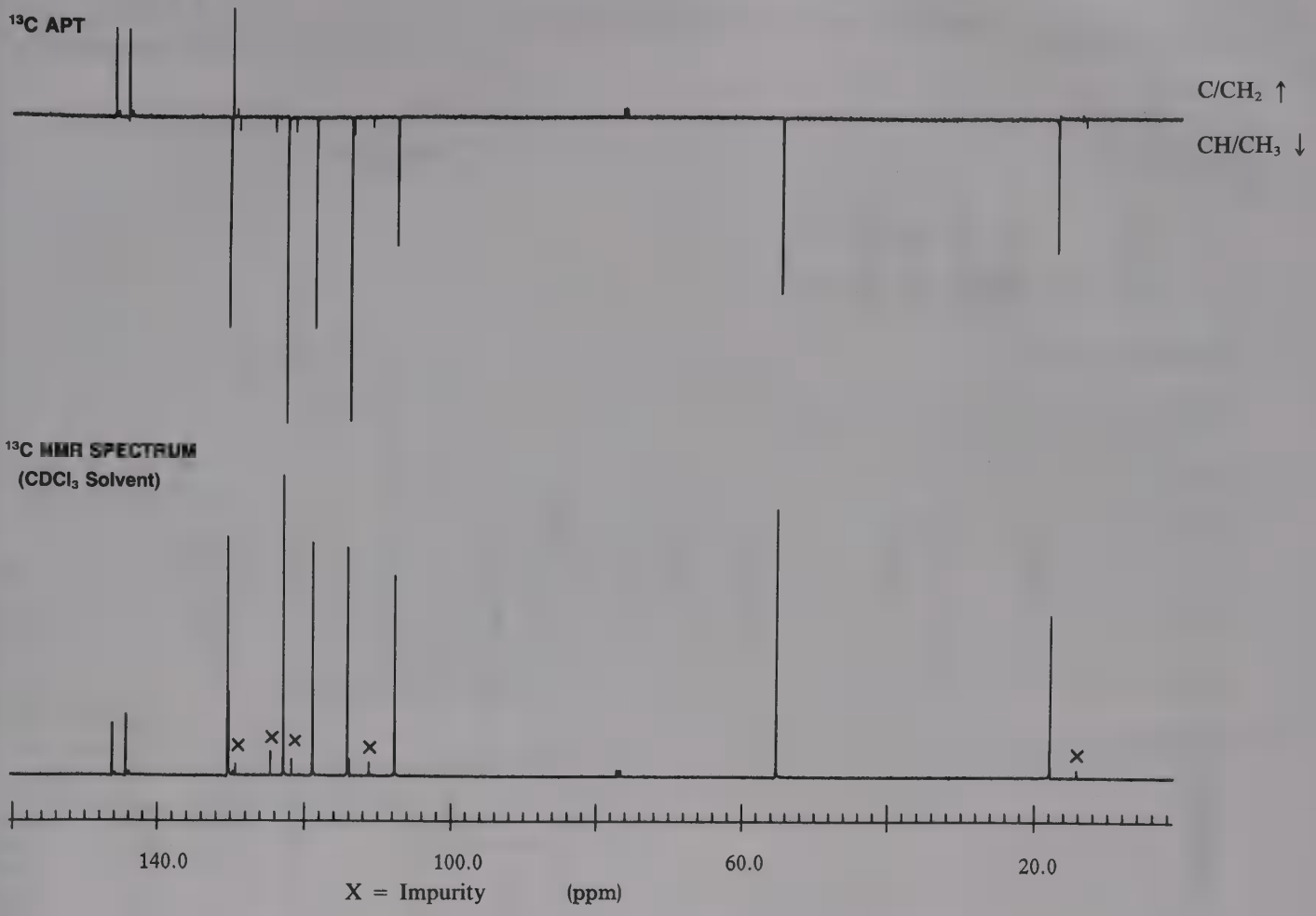

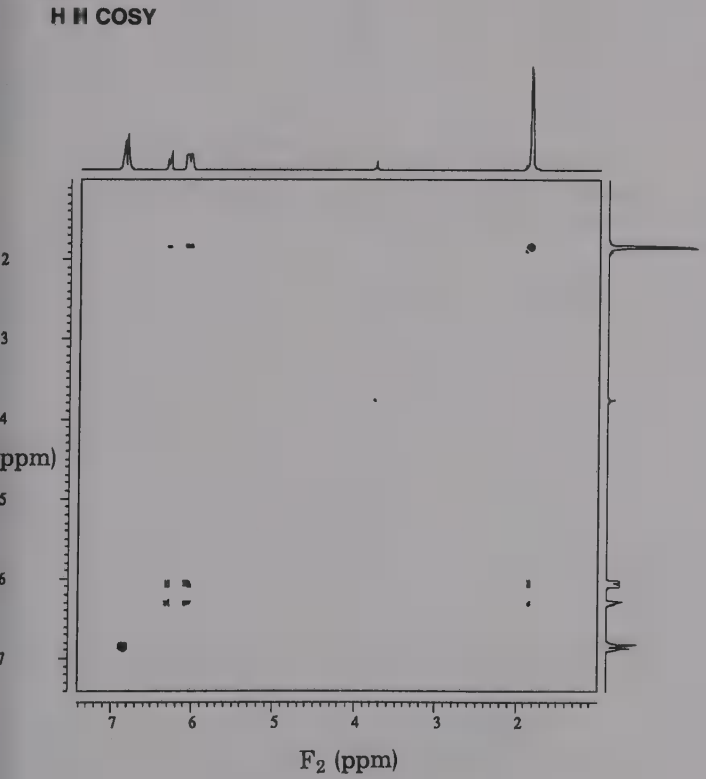

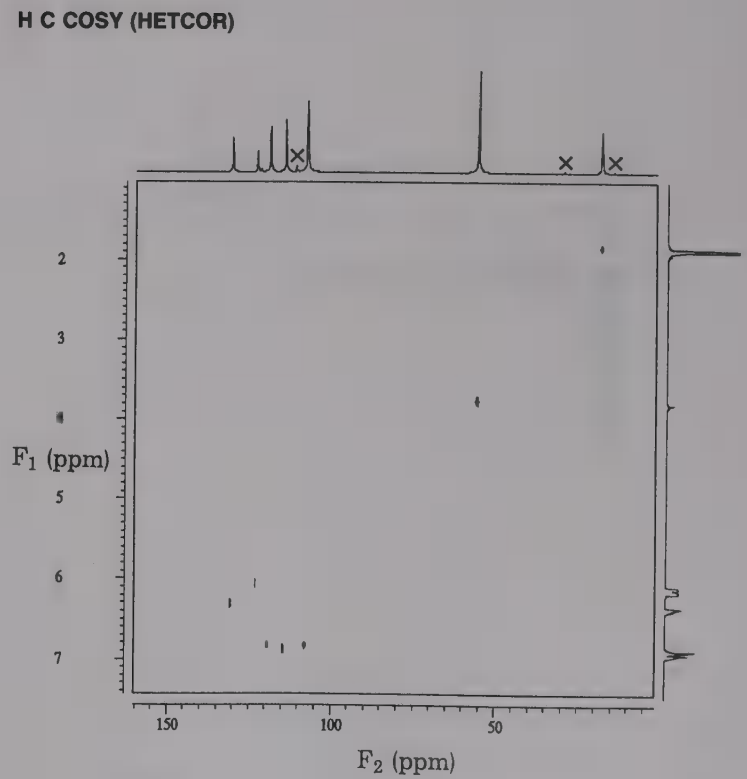

Compound 9.41

MASS SPECTRAL DATA (Relative Intensities)

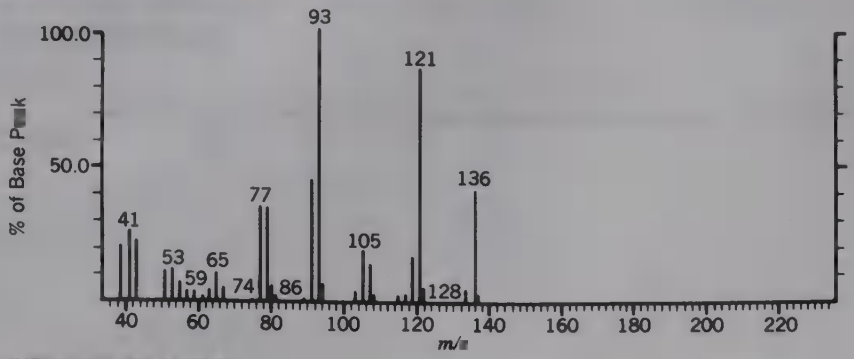

FM (found) = 136.1250

INFRARED SPECTRUM

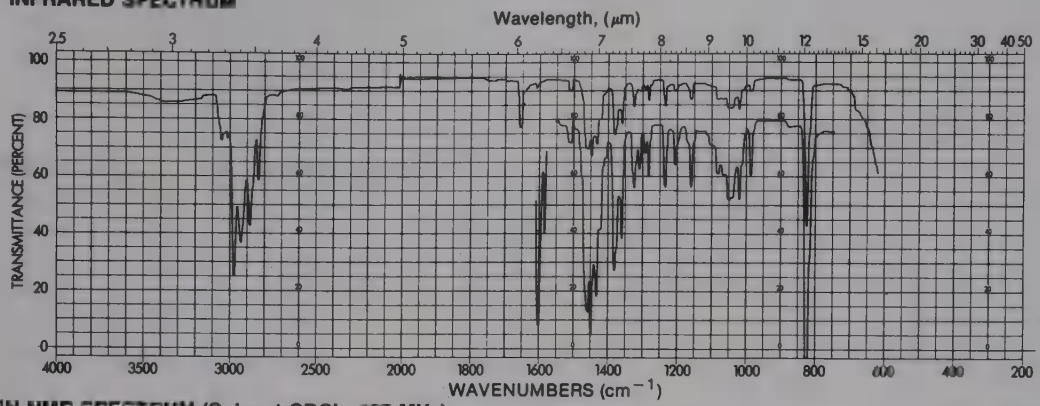

Ultraviolet Data

$\lambda_{max}^{isooctane}$ (nm)	ϵ_{max}
265	6457

^{13}C NMR Data

δ	
20.6	CH_3
22.2	CH_3
24.8	CH_2
28.5	CH_2
34.0	CH
116.5	CH
119.6	CH
131.5	C
140.9	C

^{1}H NMR SPECTRUM (Solvent $CDCl_3$, 100 MHz)

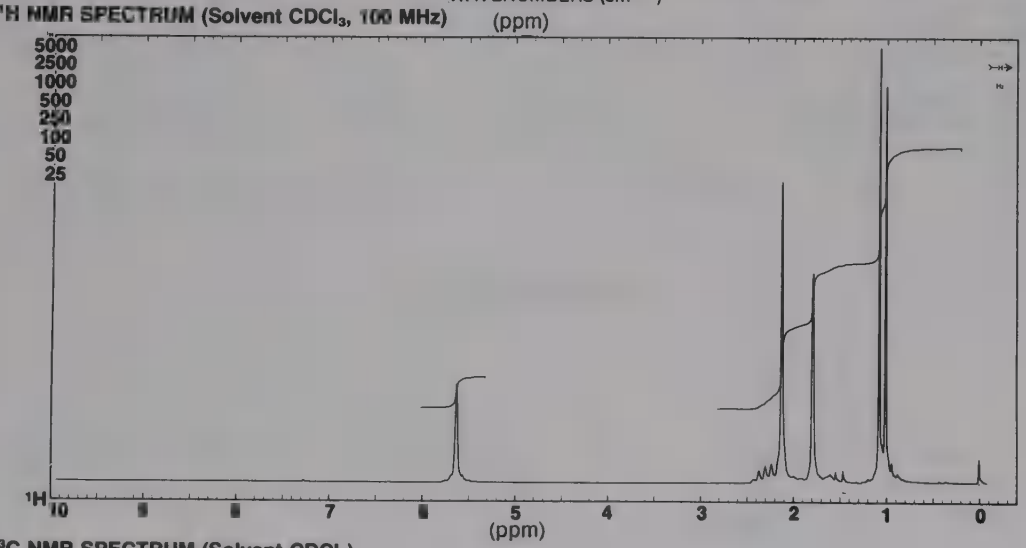

^{13}C NMR SPECTRUM (Solvent $CDCl_3$)

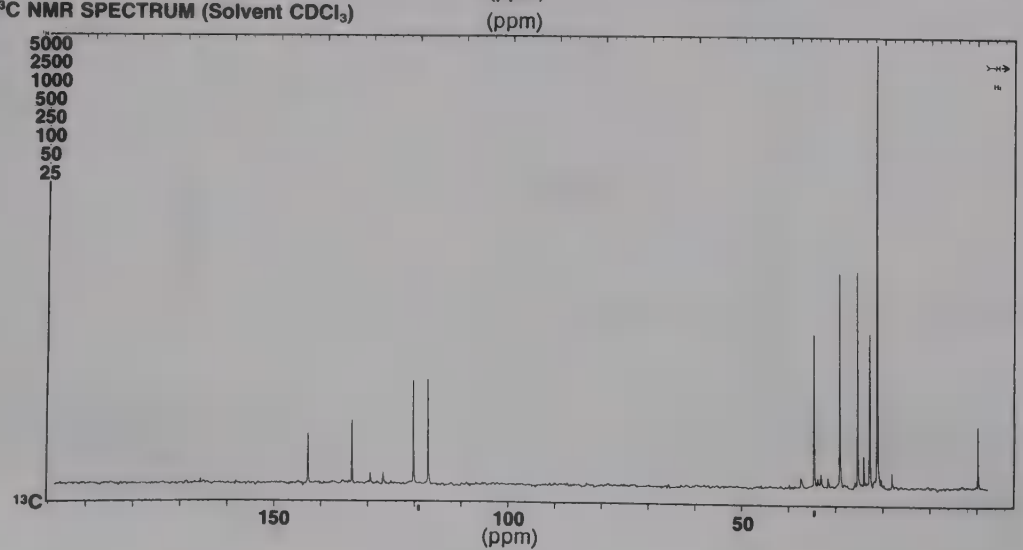

MASS SPECTRAL DATA (Relative Intensities)

Compound 9.42

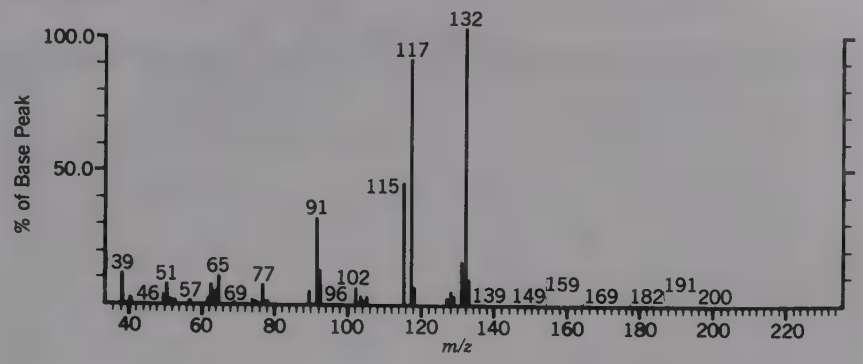

FM (found) = 132.0936

INFRARED SPECTRUM

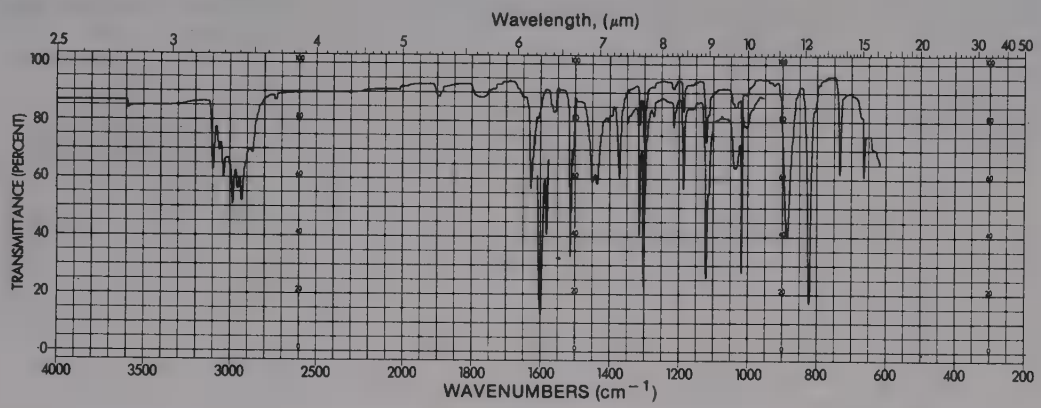

Ultraviolet Data

λ_{max}^{CHOH} (nm)	log ϵ_{max}
247	4.10
283	3.71
294	3.30

^{1}H NMR SPECTRUM (Solvent $CDCl_3$, 100 MHz)

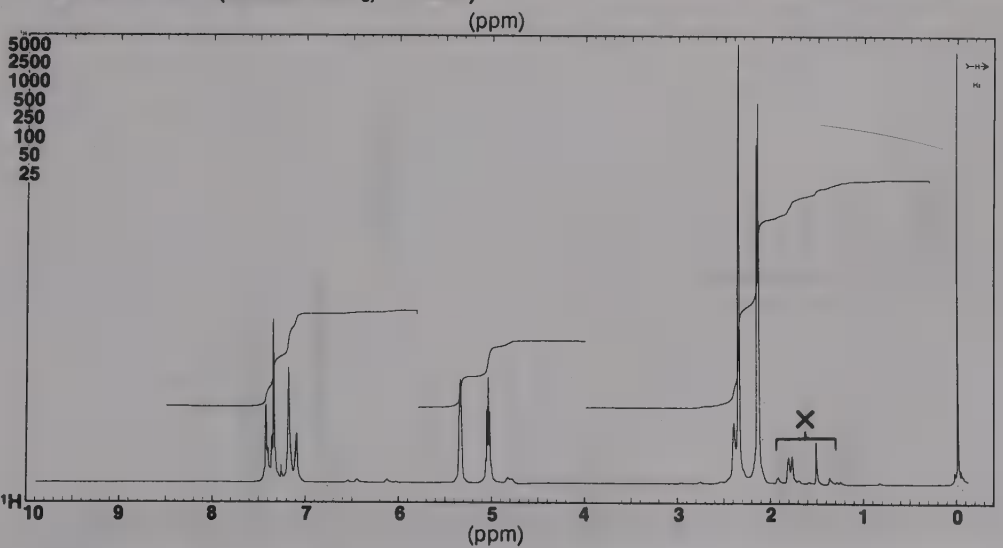

X = Impurities

INFRARED SPECTRUM

Compound 9.43

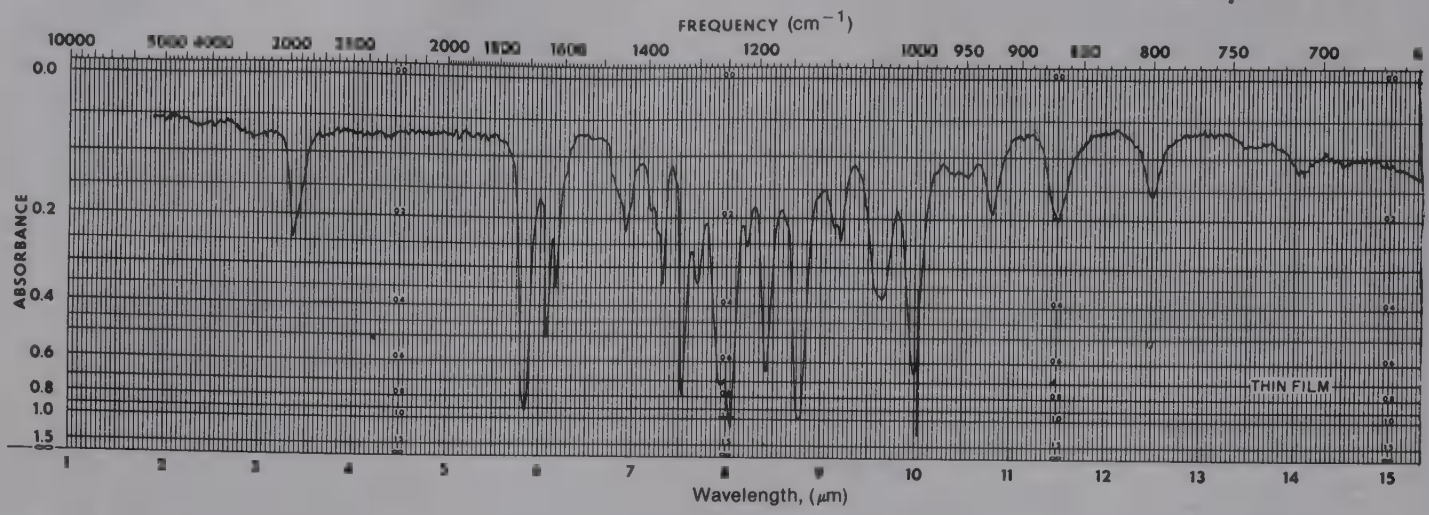

MASS SPECTRAL DATA (Relative Intensities)

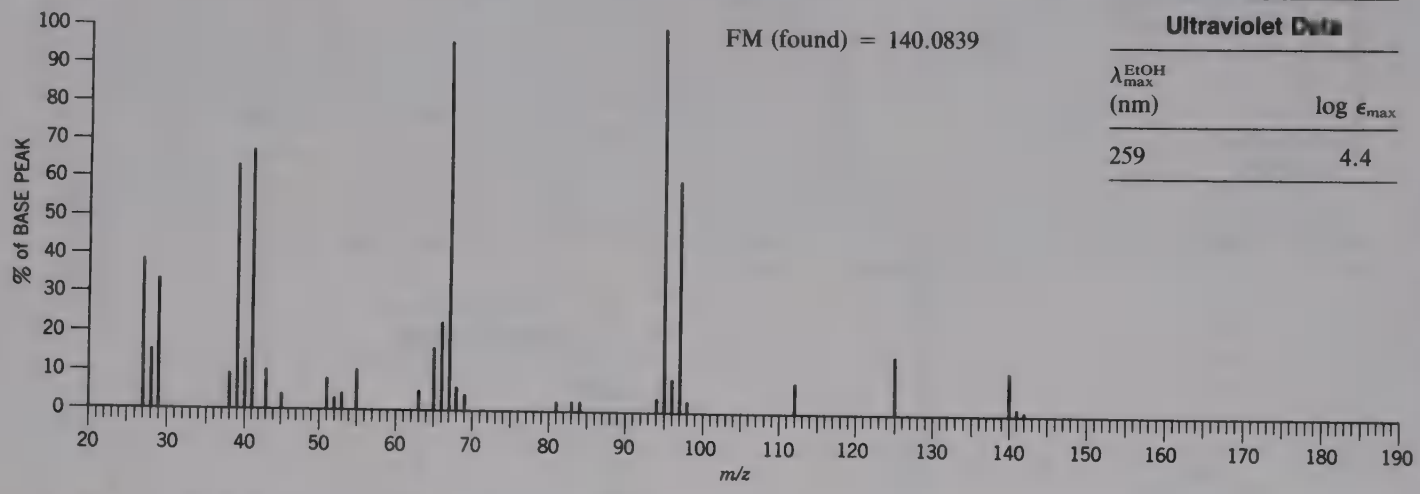

FM (found) = 140.0839

Ultraviolet Data

λ_{max}^{EtOH} (nm)	log ϵ_{max}
259	4.4

^{1}H NMR SPECTRUM (Solvent CCl_4, 100 MHz)

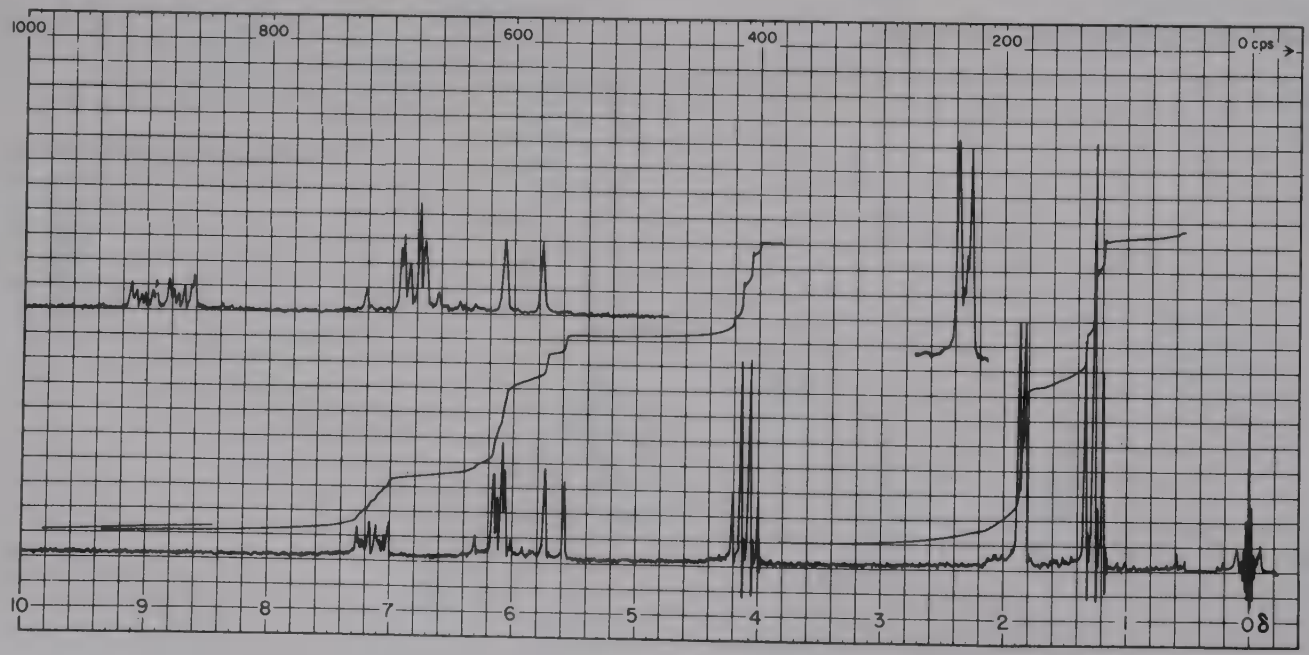

Compound 9.43 (continued)

DECOUPLED ^{1}H NMR SPECTRA

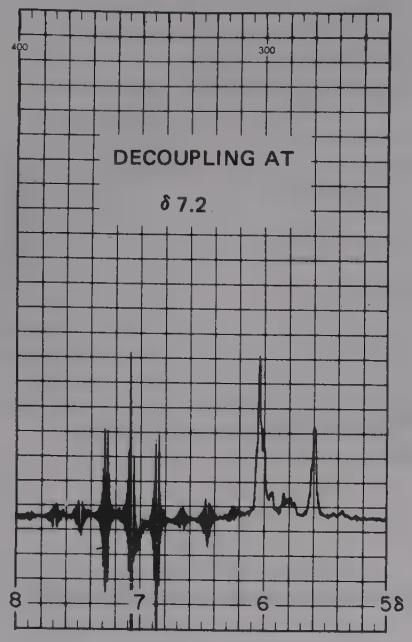

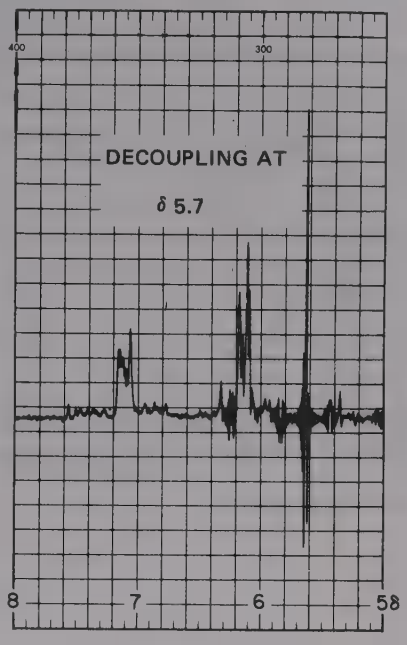

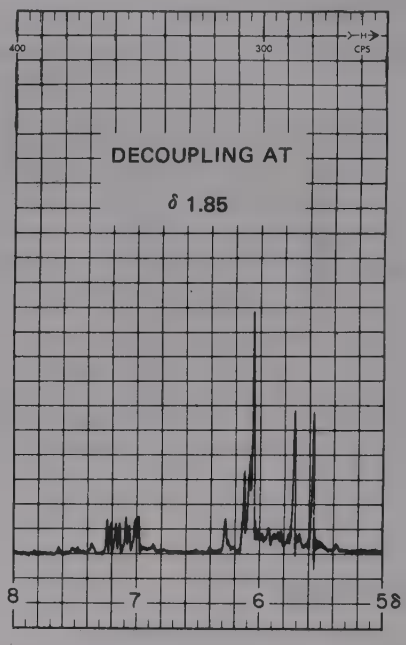

INFRARED SPECTRUM

Compound 9.44

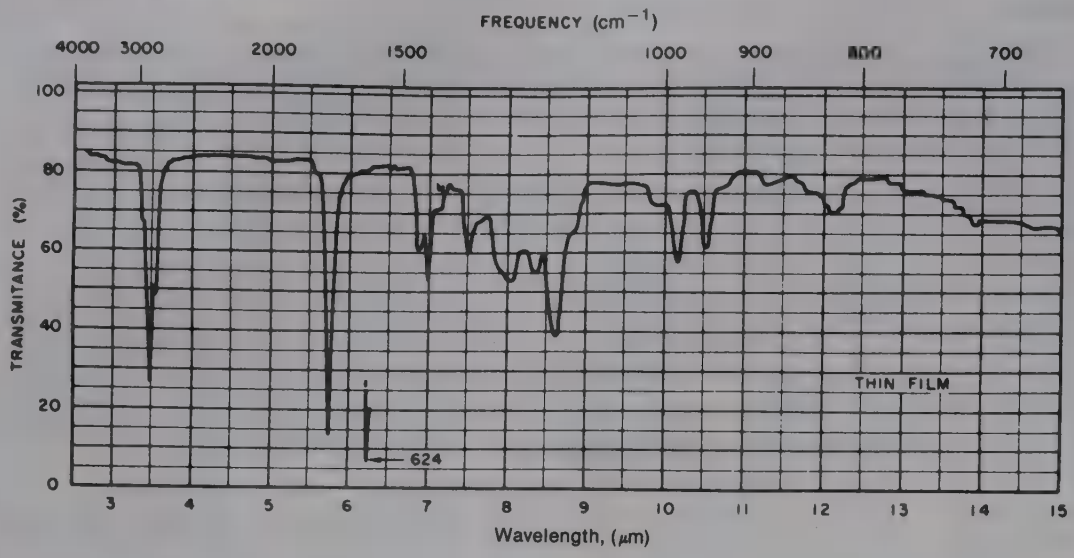

MASS SPECTRUM

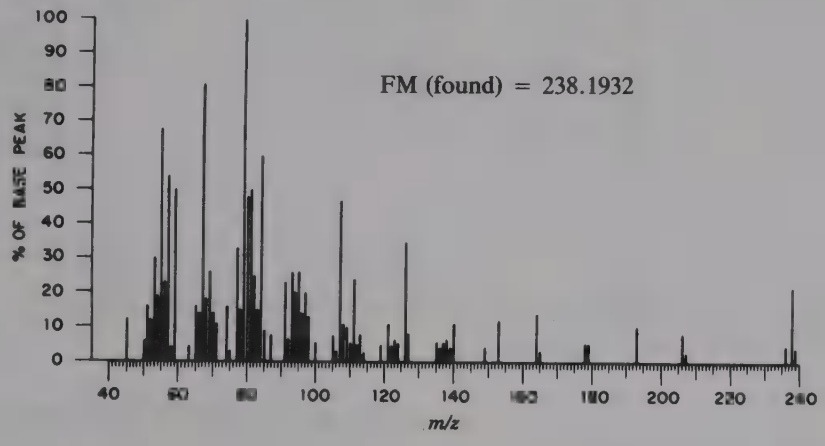

^{13}C NMR Data ($CDCl_3$ Solvent)

δ		δ	
14.0	CH_3	38.0	CH_2
22.6	CH_2	51.8	CH_3
27.7	CH_2	124.3	CH
29.2	CH_2	127.5	CH
29.4	CH_2	129.2	CH
29.5	CH_2	132.4	CH
31.8	CH_2	172.0	C

Ultraviolet Data

$\lambda_{max}^{pentane}$ (nm)	ϵ_{max}
231.5	~30,000

^{1}H NMR SPECTRUM (Solvent CCl_4, 100 MHz)

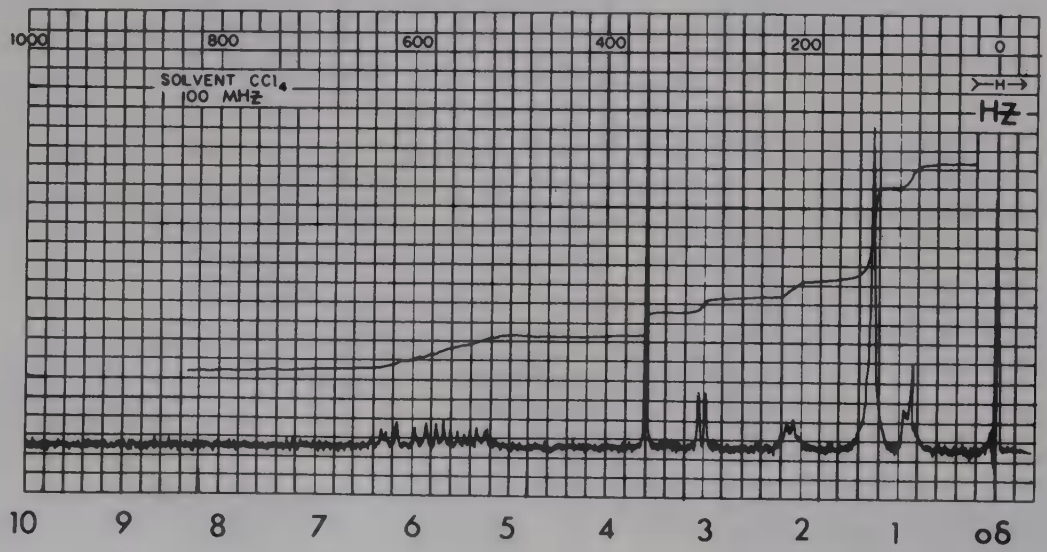

INFRARED SPECTRUM

Compound 9.45

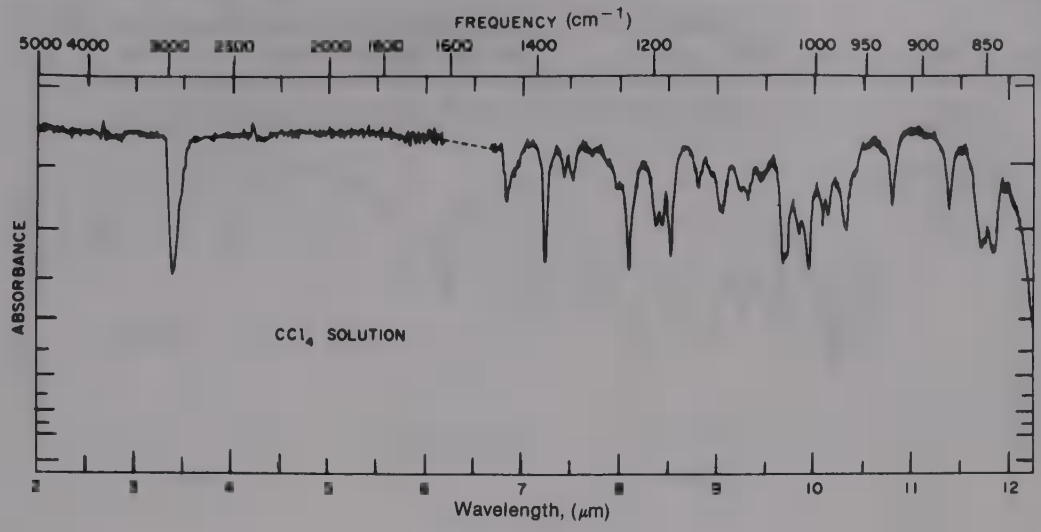

MASS SPECTRAL DATA (Relative Intensities)

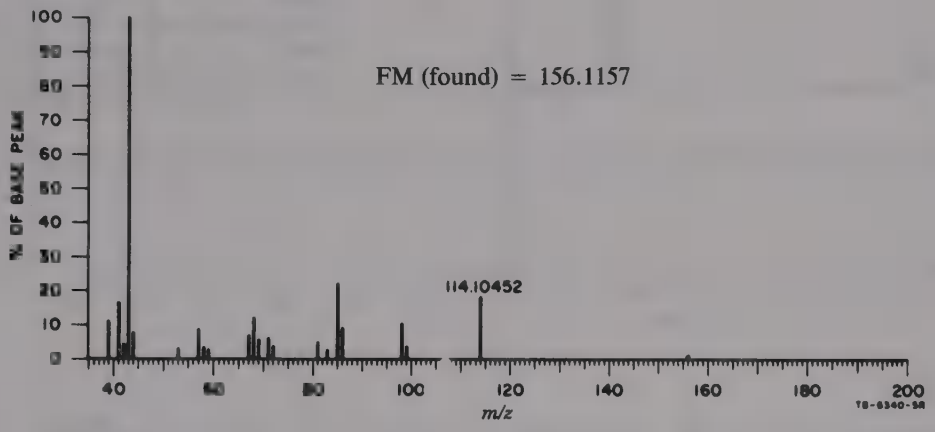

^{13}C NMR Data ($CDCl_3$ Solvent)		
δ	Intensity	
9.7	82.0	CH_3
17.3	97.0	CH_2
25.0	80.0	CH_3
28.0	95.0	CH_2
28.6	100.0	CH_2
35.0	97.0	CH_2
78.3	80.0	CH
81.1	85.0	CH
107.6	35.0	C

Ultraviolet Data
No absorption above 200 nm

^{1}H NMR SPECTRUM (Solvent $CDCl_3$, 100 MHz)

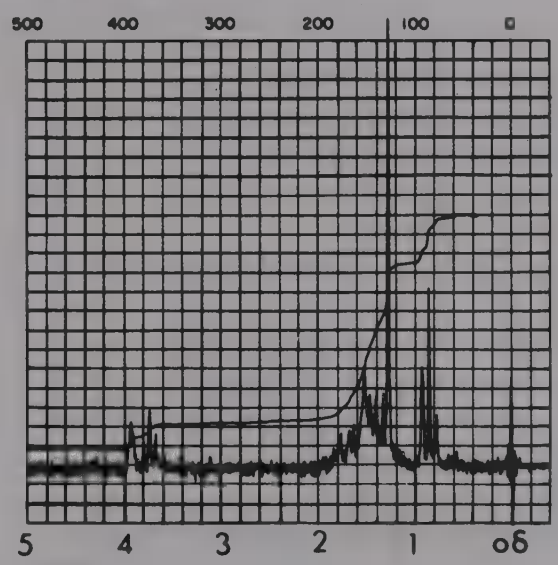

Related Chemical Information

1. Recovered unchanged from treatment with $LiAlH_4$.
2. Catalytic hydrogenolysis (250°C) gave nonane.
3. The compound is part of the aggregation pheromone of a bark beetle.

INFRARED SPECTRUM

Compound 3.46

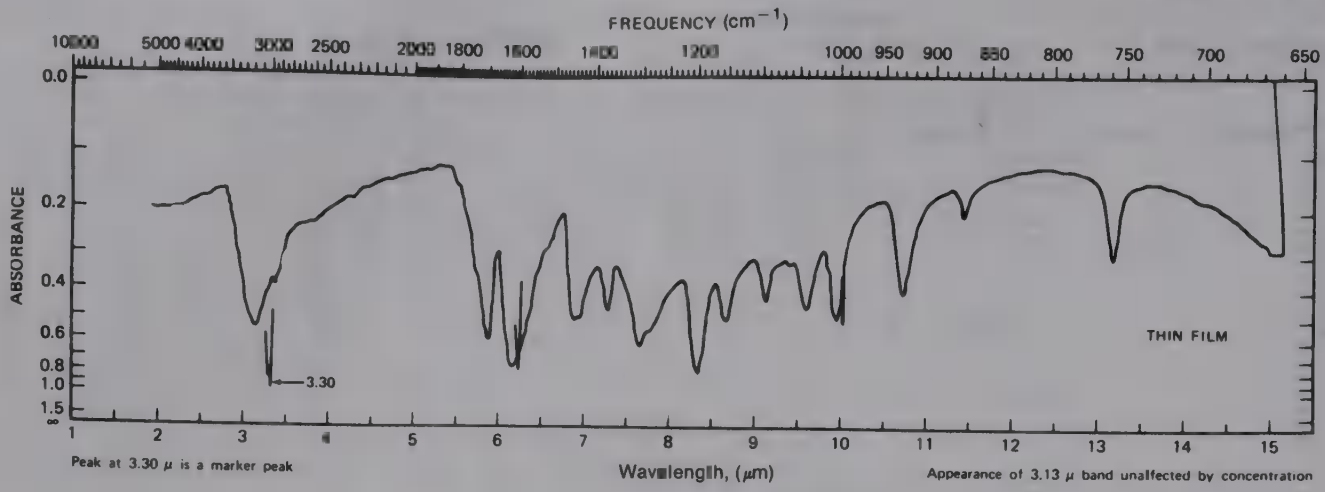

MASS SPECTRAL DATA (Relative Intensities)

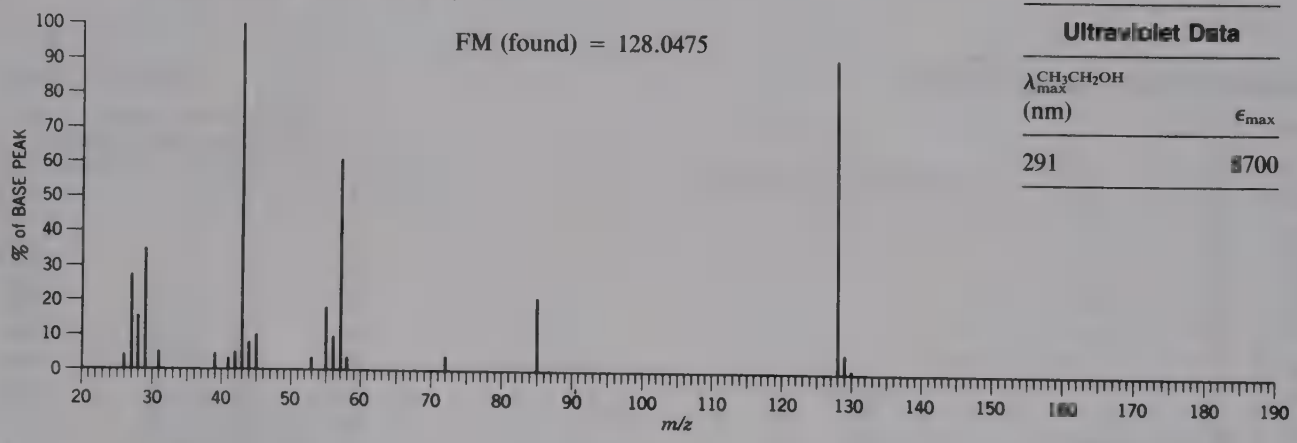

Ultraviolet Data

$\lambda_{max}^{CH_3CH_2OH}$ (nm)	ϵ_{max}
291	5700

^{1}H NMR SPECTRUM (Solvent CCl_4, 60 MHz)

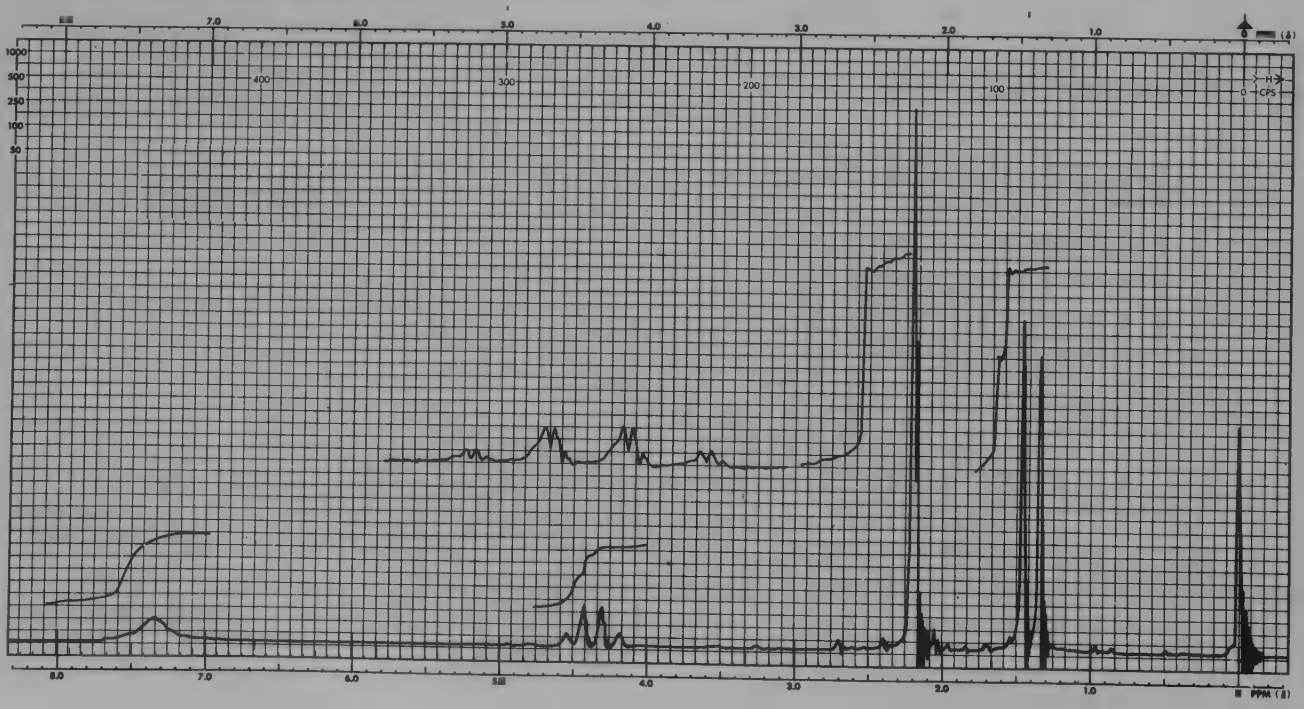

Compound 9.46 (continued)

^{13}C NMR SPECTRUM COMPLETELY DECOUPLED

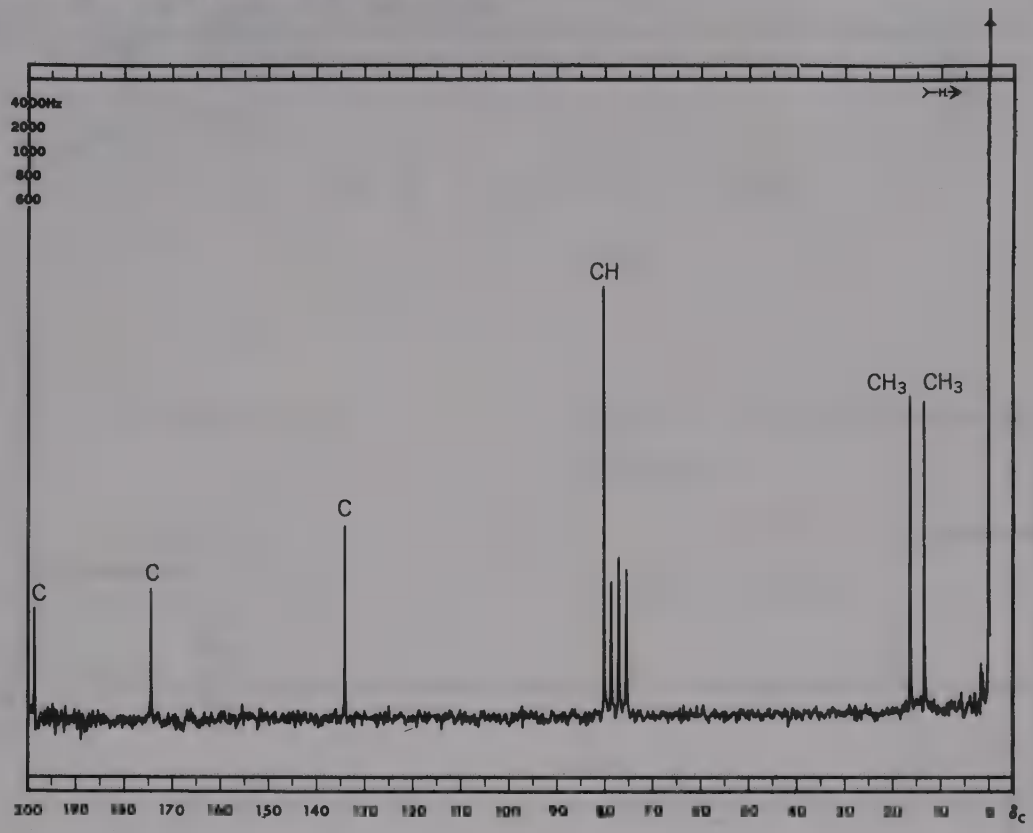

INFRARED SPECTRUM **Compound 9.47**

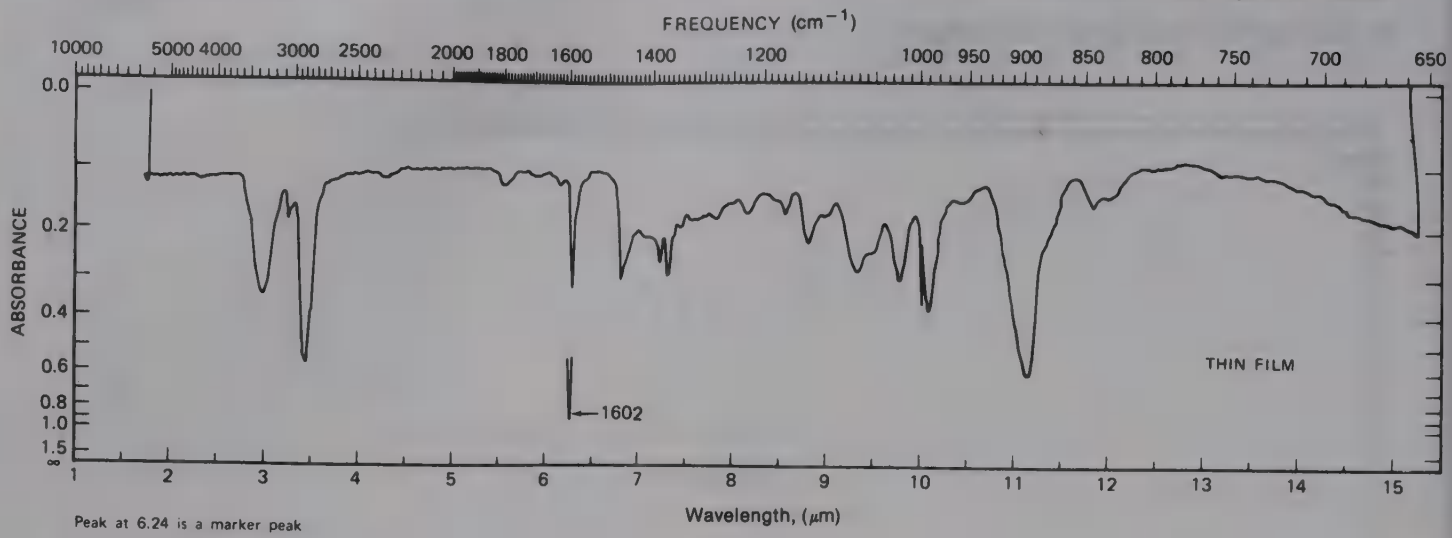

Peak at 6.24 is a marker peak

MASS SPECTRAL DATA (Relative Intensities)

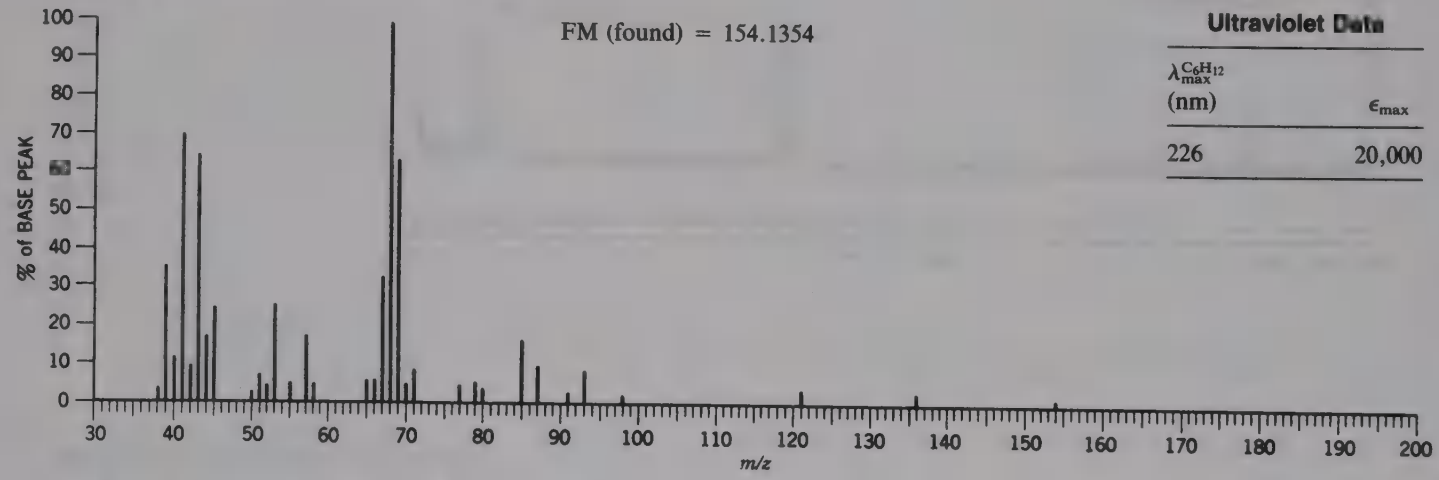

Ultraviolet Data

$\lambda_{max}^{C_6H_{12}}$ (nm)	ϵ_{max}
226	20,000

^{1}H NMR SPECTRUM (Solvent $CDCl_3$, 100 MHz)

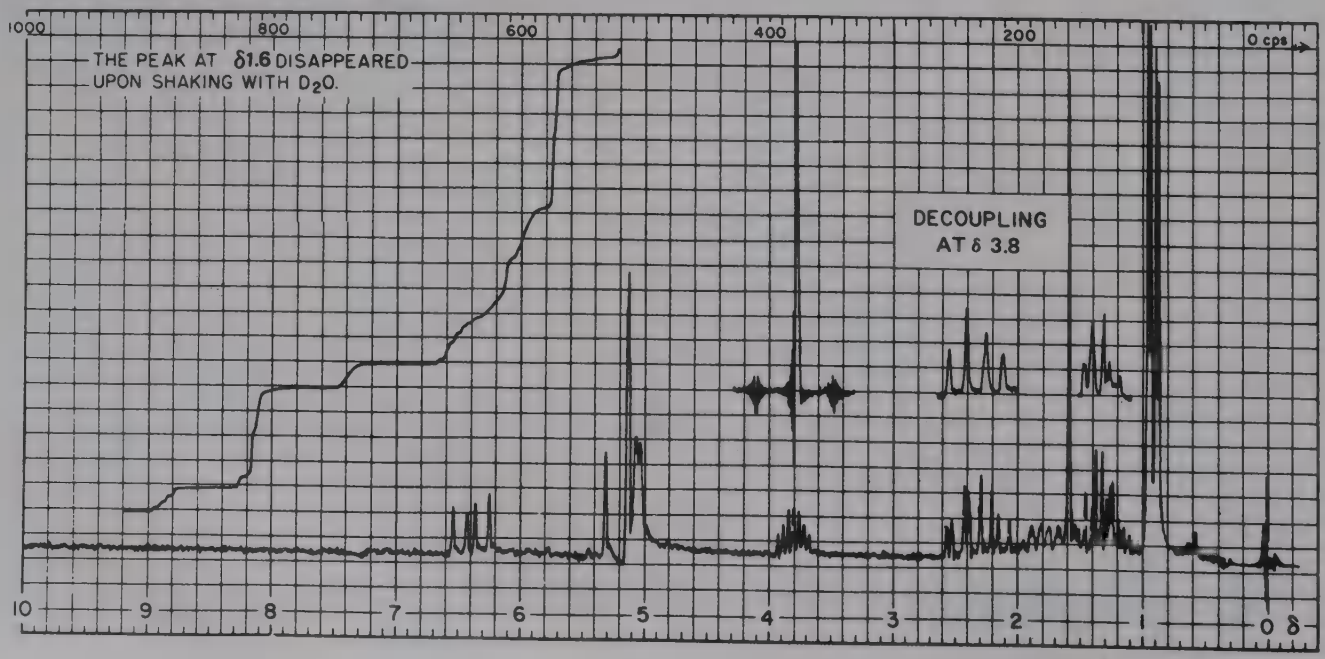

Continued on next page

Compound 9.47 (continued)

^{13}C NMR SPECTRUM COMPLETELY DECOUPLED

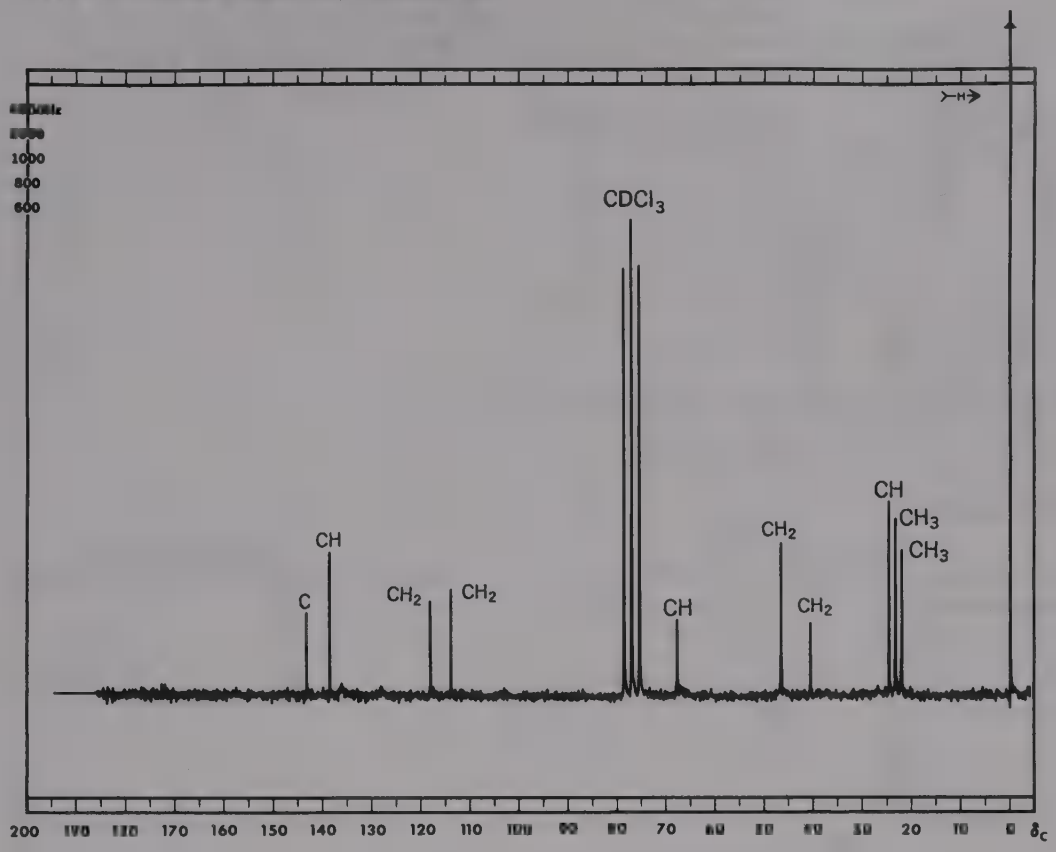

INFRARED SPECTRUM

Compound 9.48
Derivative of Compound 9.47

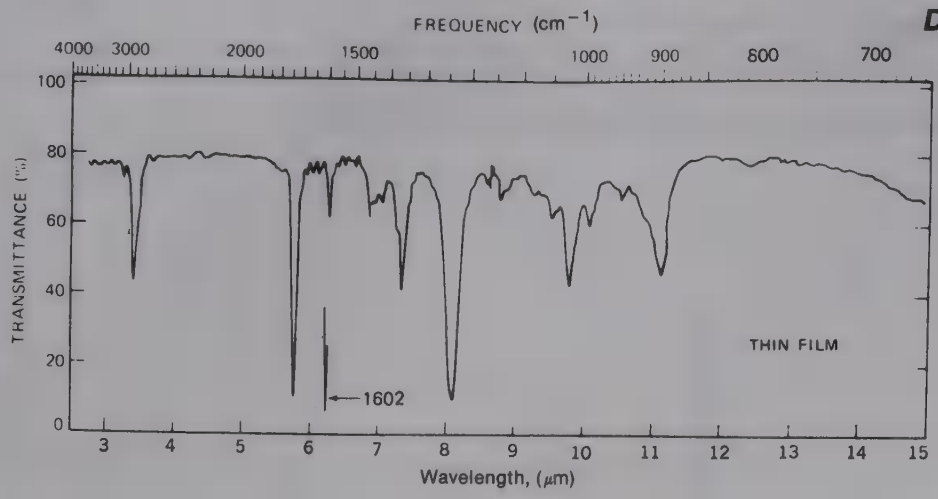

MASS SPECTRAL DATA (Relative Intensities)

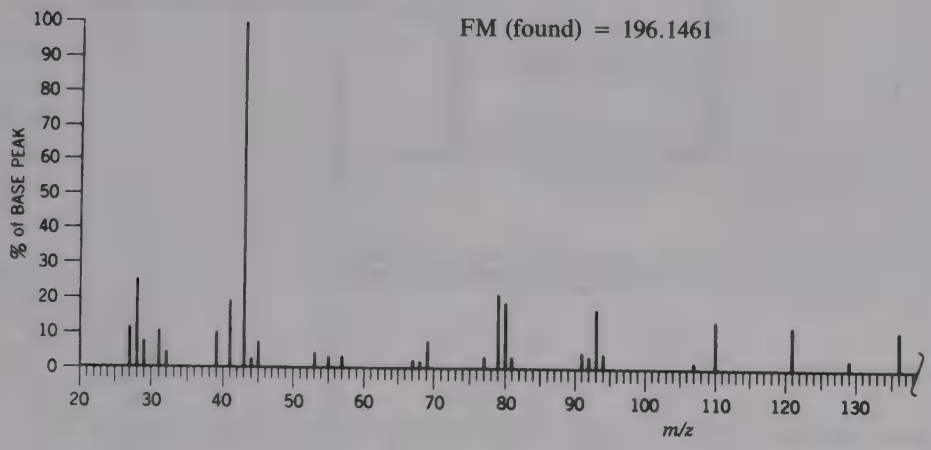

Ultraviolet Data

λ_{max}^{hexane} (nm)	ϵ_{max}
225	26,000

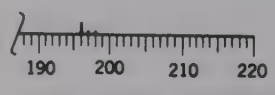

^{1}H NMR SPECTRUM (Solvent $CDCl_3$, 60 MHz)

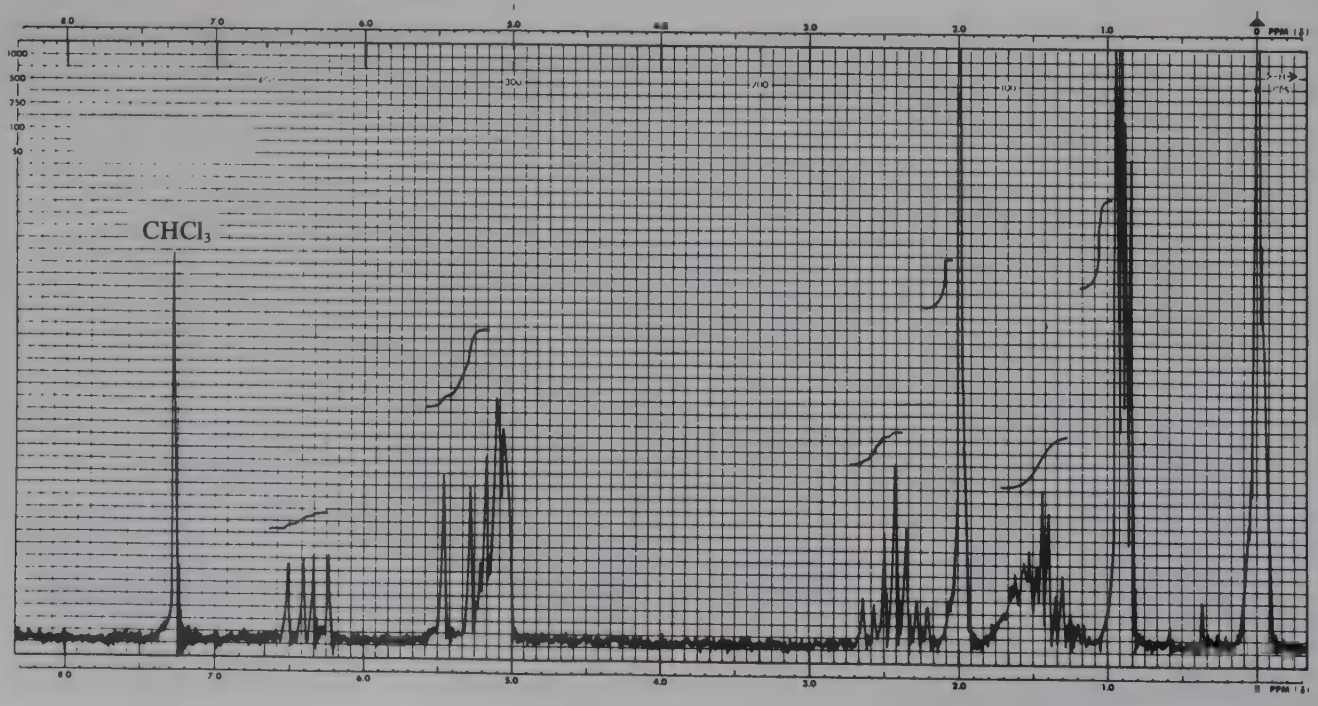

INFRARED SPECTRUM ***Compound 9.49***

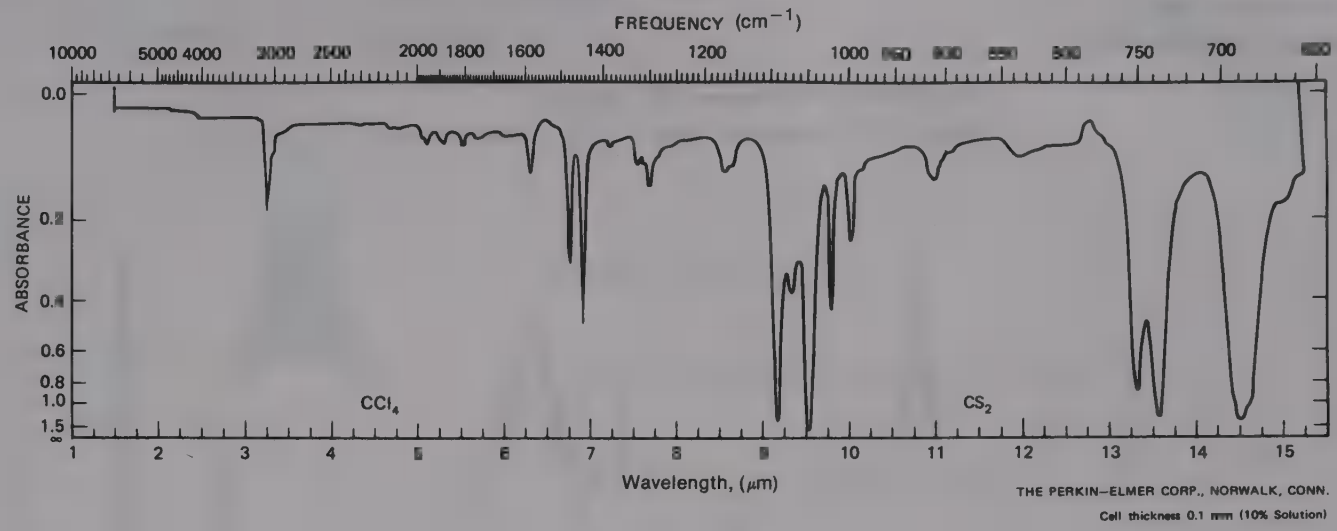

MASS SPECTRAL DATA (Relative Intensities)

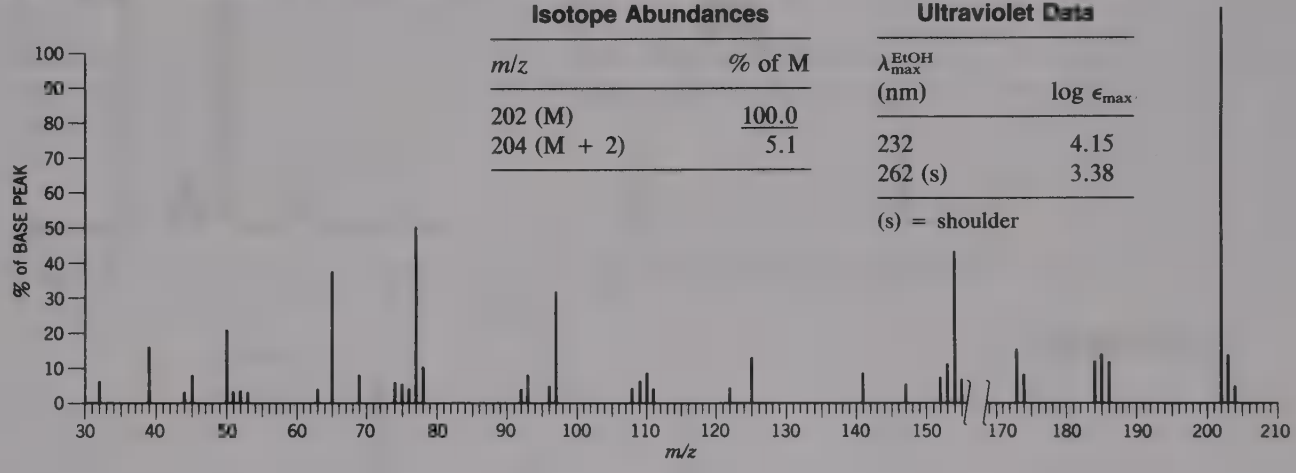

Isotope Abundances

m/z	% of M
202 (M)	100.0
204 (M + 2)	5.1

Ultraviolet Data

λ_{max}^{EtOH} (nm)	log ϵ_{max}
232	4.15
262 (s)	3.38

(s) = shoulder

^{1}H NMR SPECTRUM
(Solvent $CDCl_3$, 300 MHz)

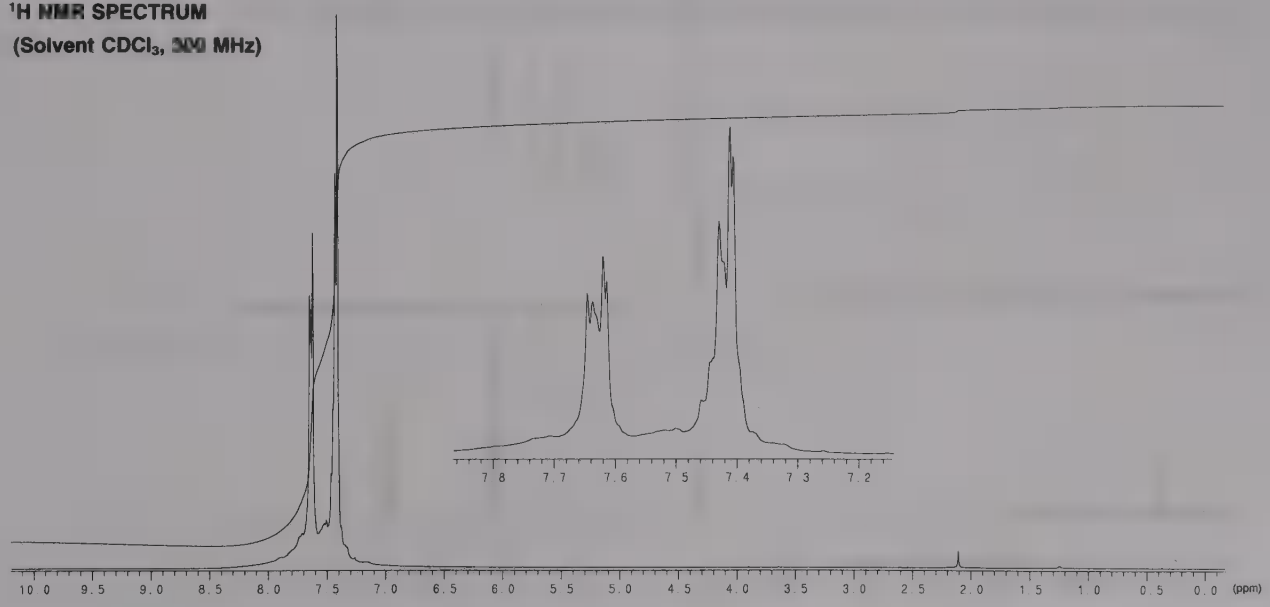

Compound 9.50

MASS SPECTRAL DATA

FM (found) = 128.1203
peaks at *m/z* 128, 113, 110, and 95 (base peak)

INFRARED DATUM

broad, s at ≈ 3300 cm^{-1}

Ultraviolet Data
Transparent above 210 nm

^{1}H NMR SPECTRUM (Solvent $CDCl_3$, 500 MHz)

Peak at δ 2.45 disappears upon shaking solution with D_2O

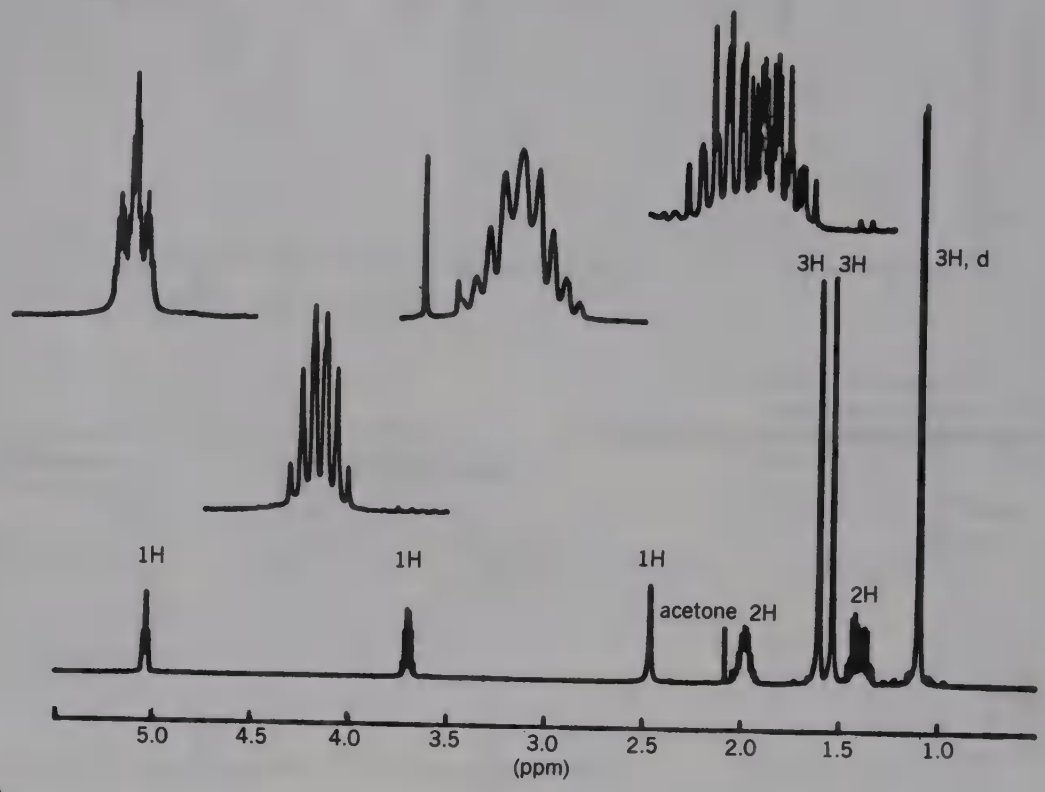

^{13}C NMR SPECTRA

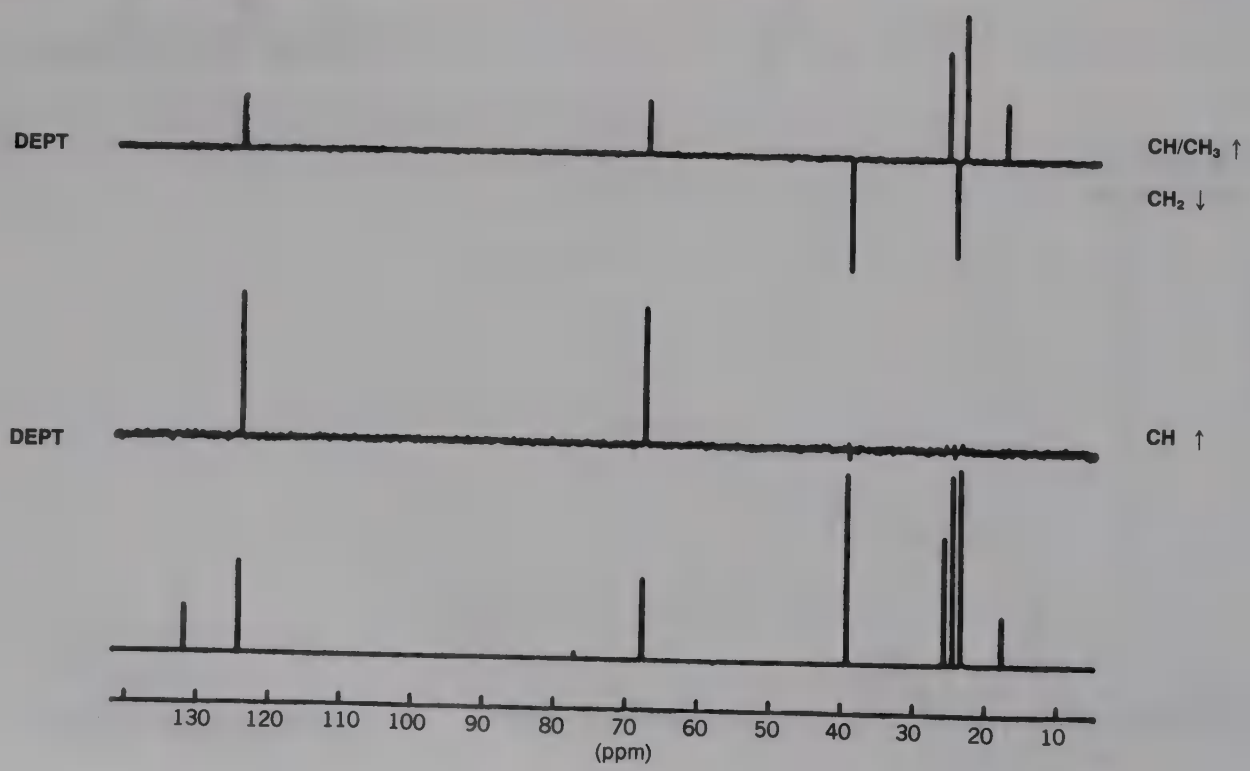

Compound 9.50 (continued)

H H COSY (HOMCOR)

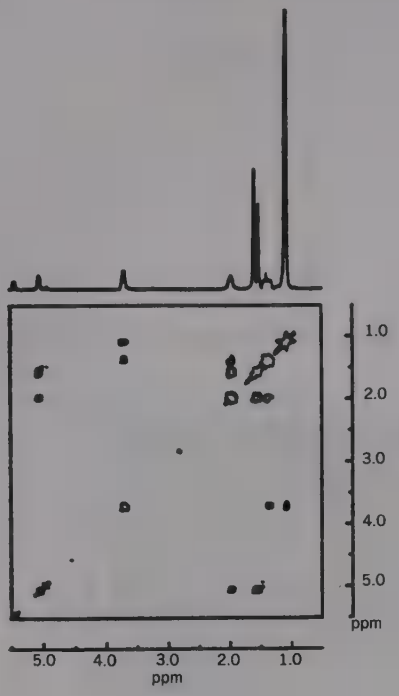

H C COSY (HETCOR)

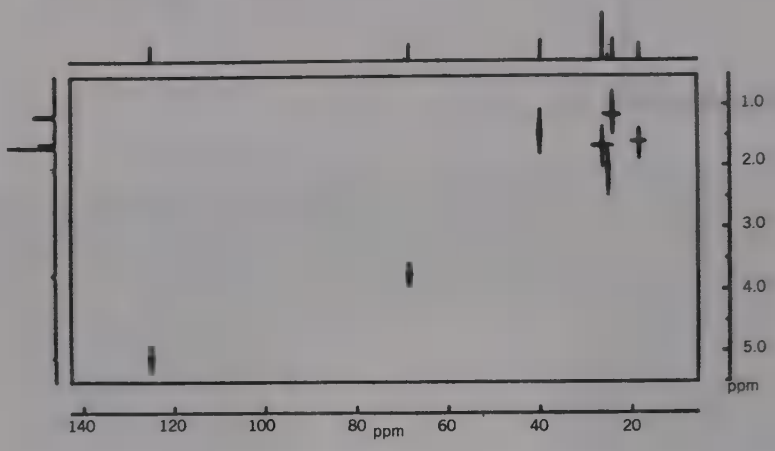

DIFFERENCE NOE

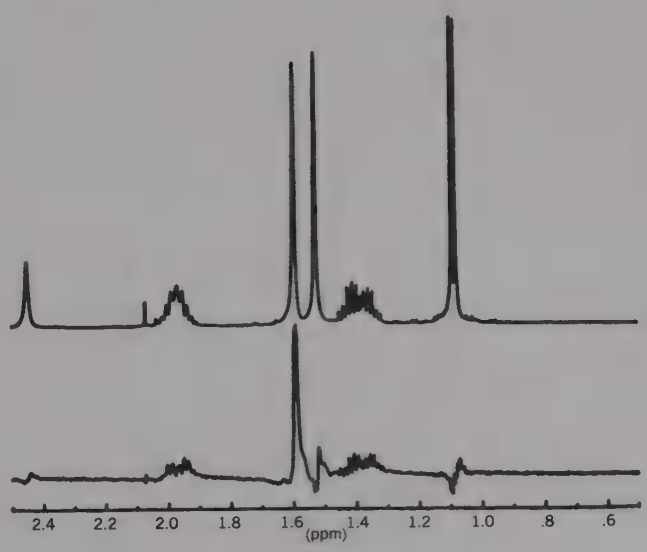

Compound 9.51

$C_4H_2Cl_2O_3$

UV (in alcohol): λ_{max} = 227 nm, ϵ_{max} = 7934

^1H NMR (in CH_3CH_2OH) δ 6.3, 7.5, singlets, 1:1 integration; (in acetone-d_6) δ 6.3, 7.5, 1:1 integration, doublets, J = 8.5 Hz, addition of D_2O results in a singlet at δ 6.3, an HOD peak at $\approx$ δ 3.6 and disappearance of the δ 7.5 peak.

INFRARED SPECTRUM

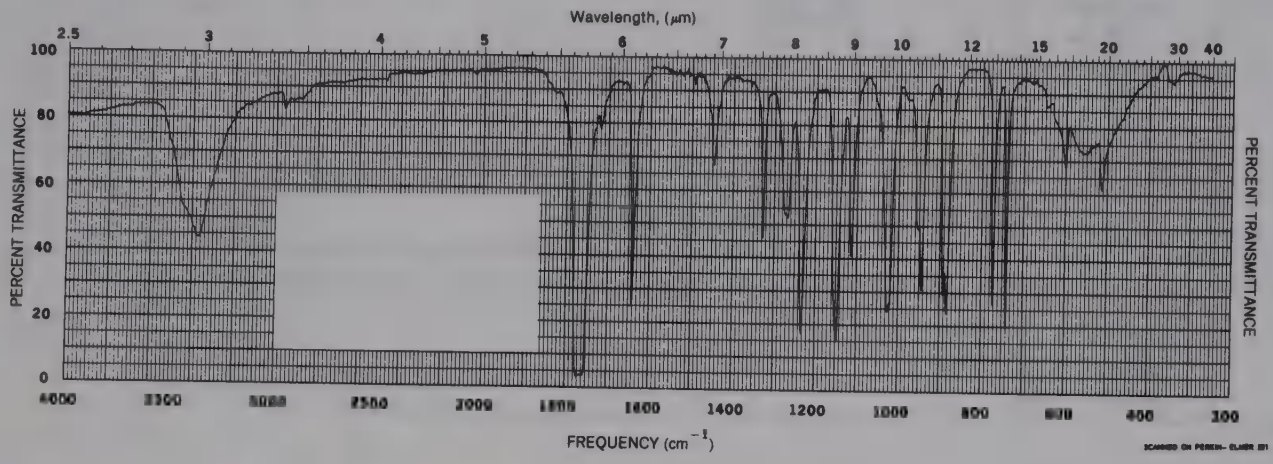

Compound 9.51 (continued)

^{13}C NMR SPECTRUM

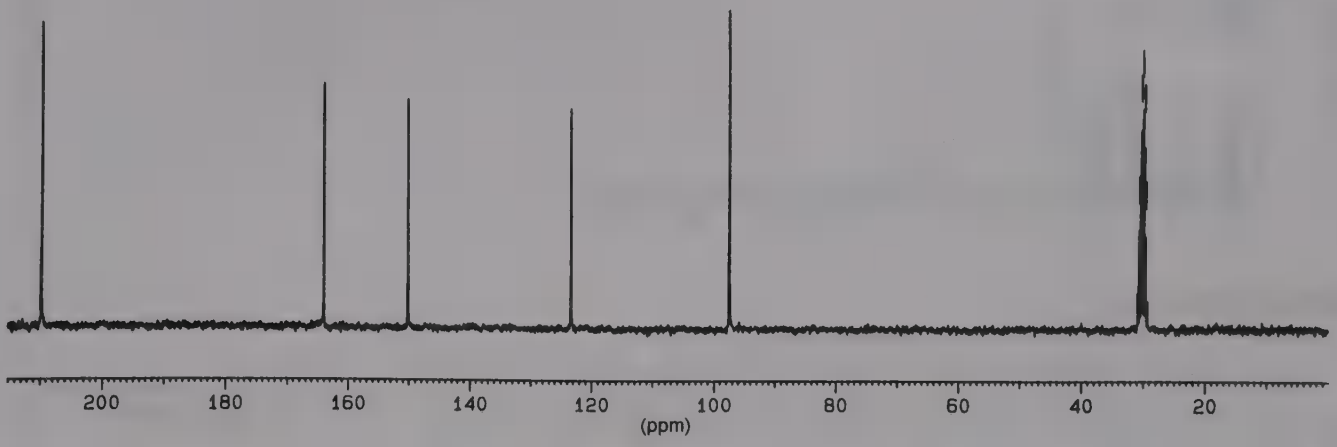

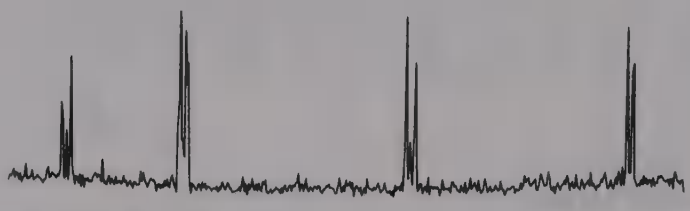

2-D INADEQUATE SPECTRUM

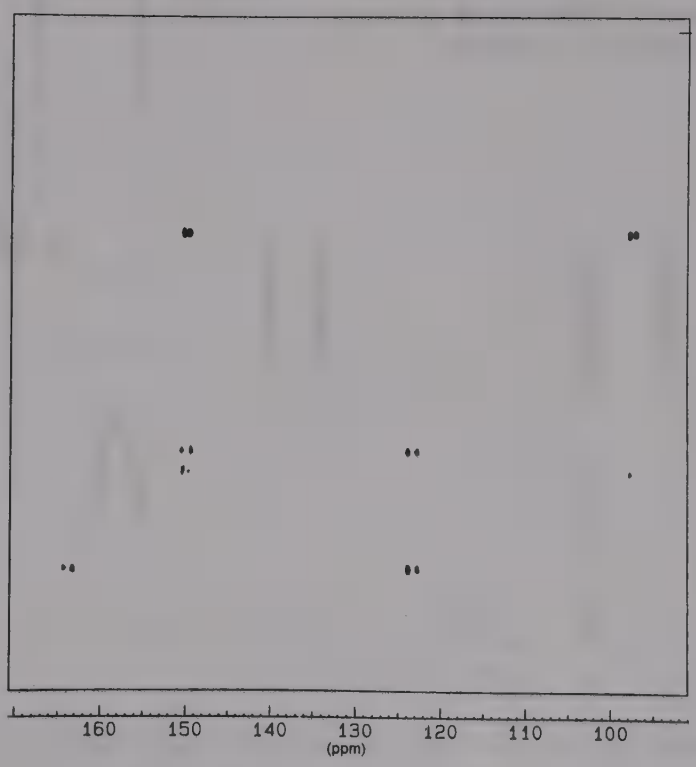

MASS SPECTRAL DATA

Compound 9.52

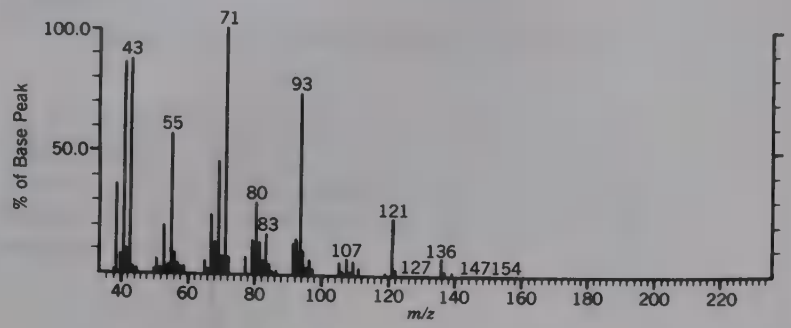

FM (found) = 154.1355

INFRARED SPECTRUM

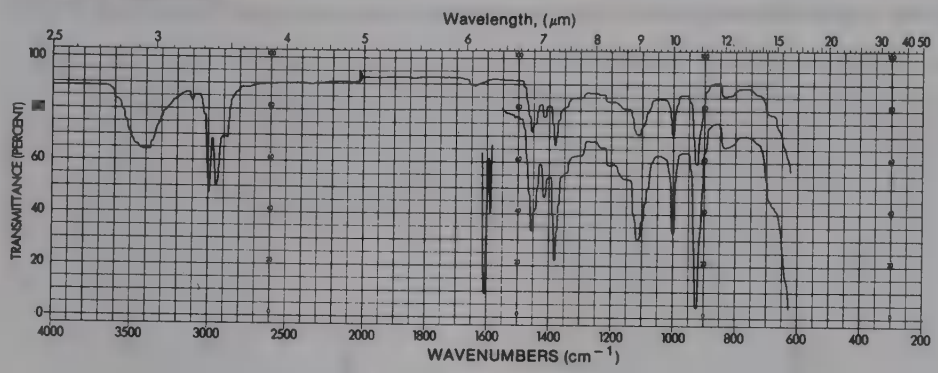

Ultraviolet Data

Transparent above 210 nm

^{1}H NMR SPECTRUM (Solvent $CDCl_3$, 500 MHz)

Singlet marked with arrow (~δ 1.6) moved to lower field when concentration of 9.52 is increased

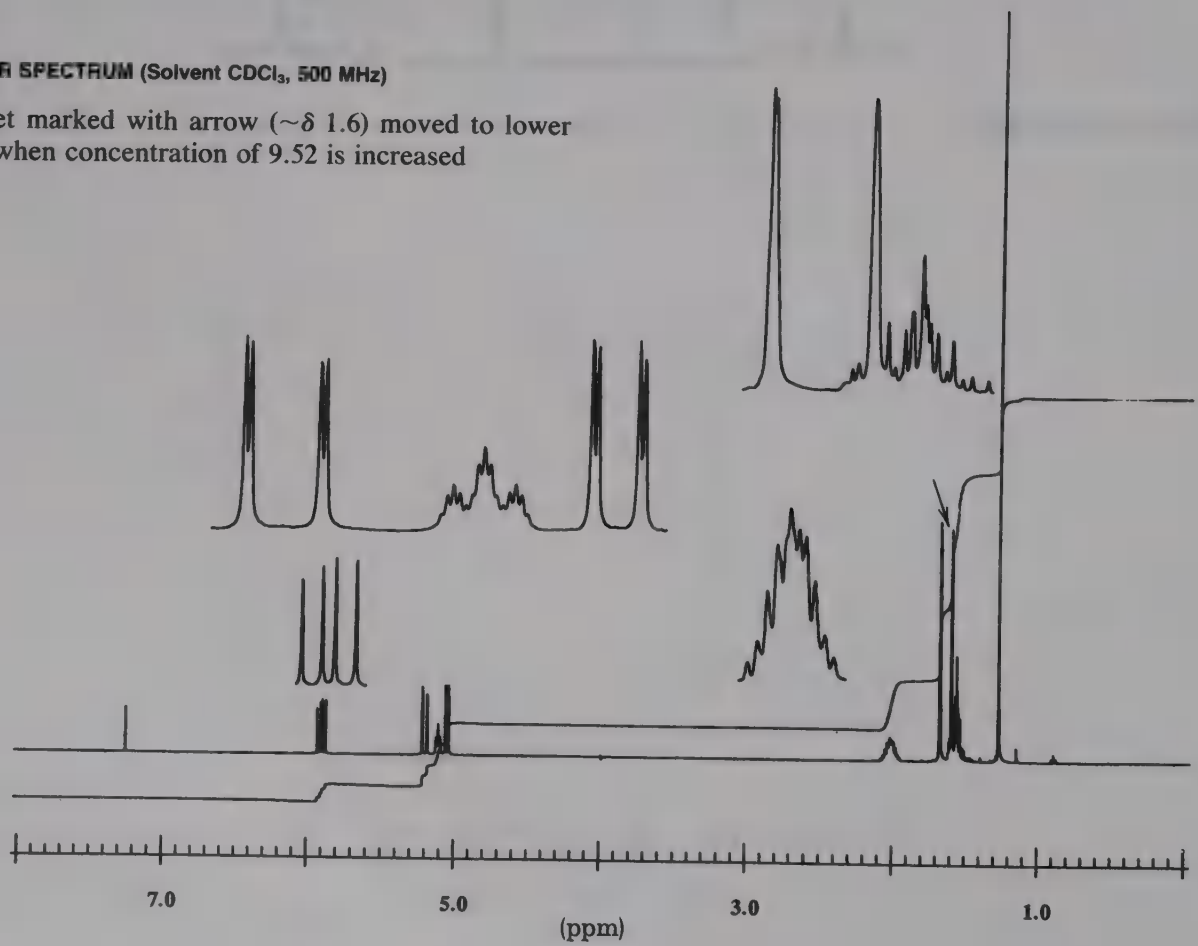

Compound 9.52 (continued)

^{13}C NMR SPECTRUM (Solvent $CDCl_3$)

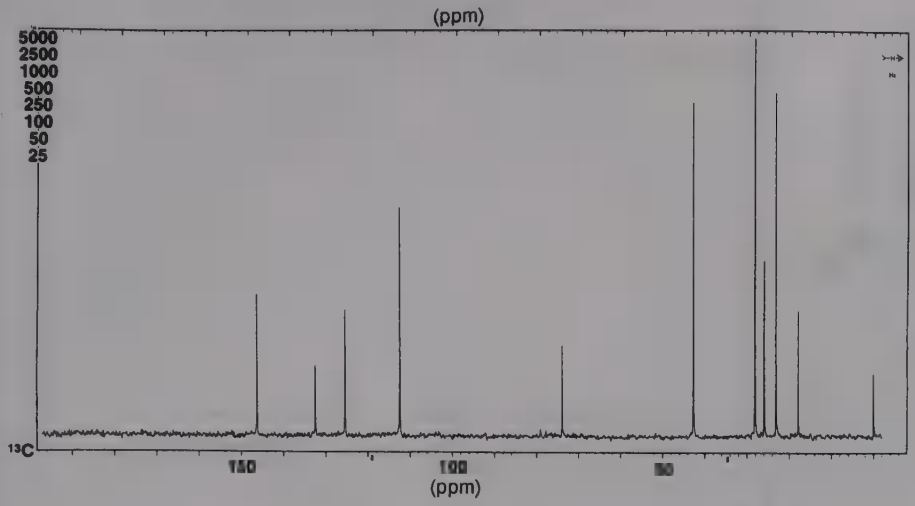

^{13}C NMR Data	
δ	
17.5	CH_3
22.6	CH_2
25.3	CH_3
27.2	CH_3
41.2	CH_2
72.7	C
111.3	CH_2
124.6	CH
130.3	C
145.0	CH

H H COSY

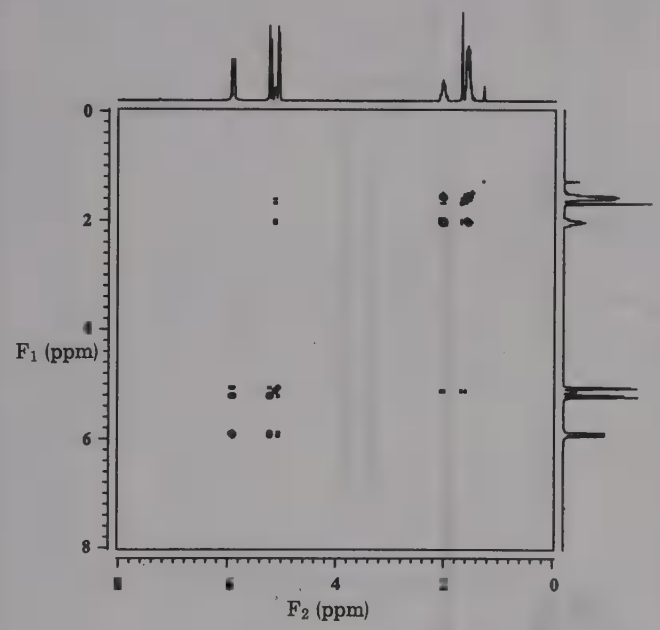

MASS SPECTRAL DATA (Relative Intensities)

Compound 9.53

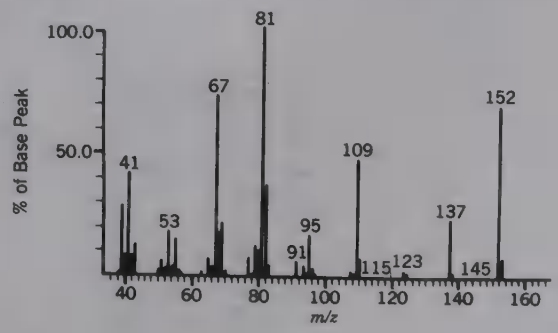

FM (found) = 152.1205

INFRARED SPECTRUM

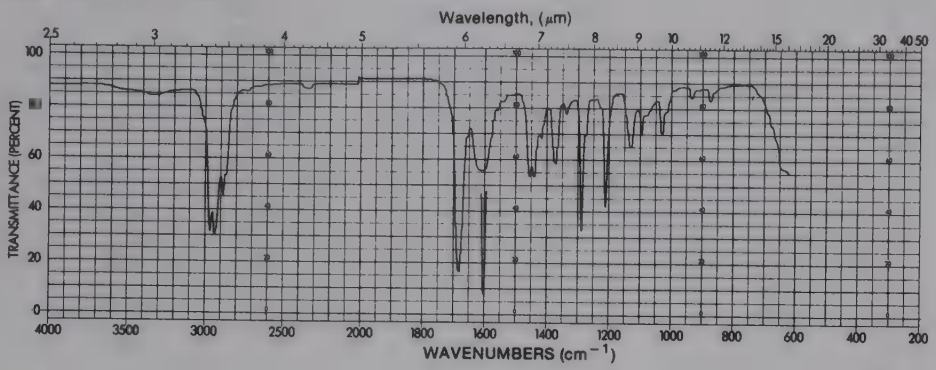

Ultraviolet Data

$\lambda_{max}^{CH_3CH_2OH}$ (nm)	log ϵ_{max}
253	3.86

^{1}H NMR SPECTRUM (Solvent $CDCl_3$, 500 MHz)

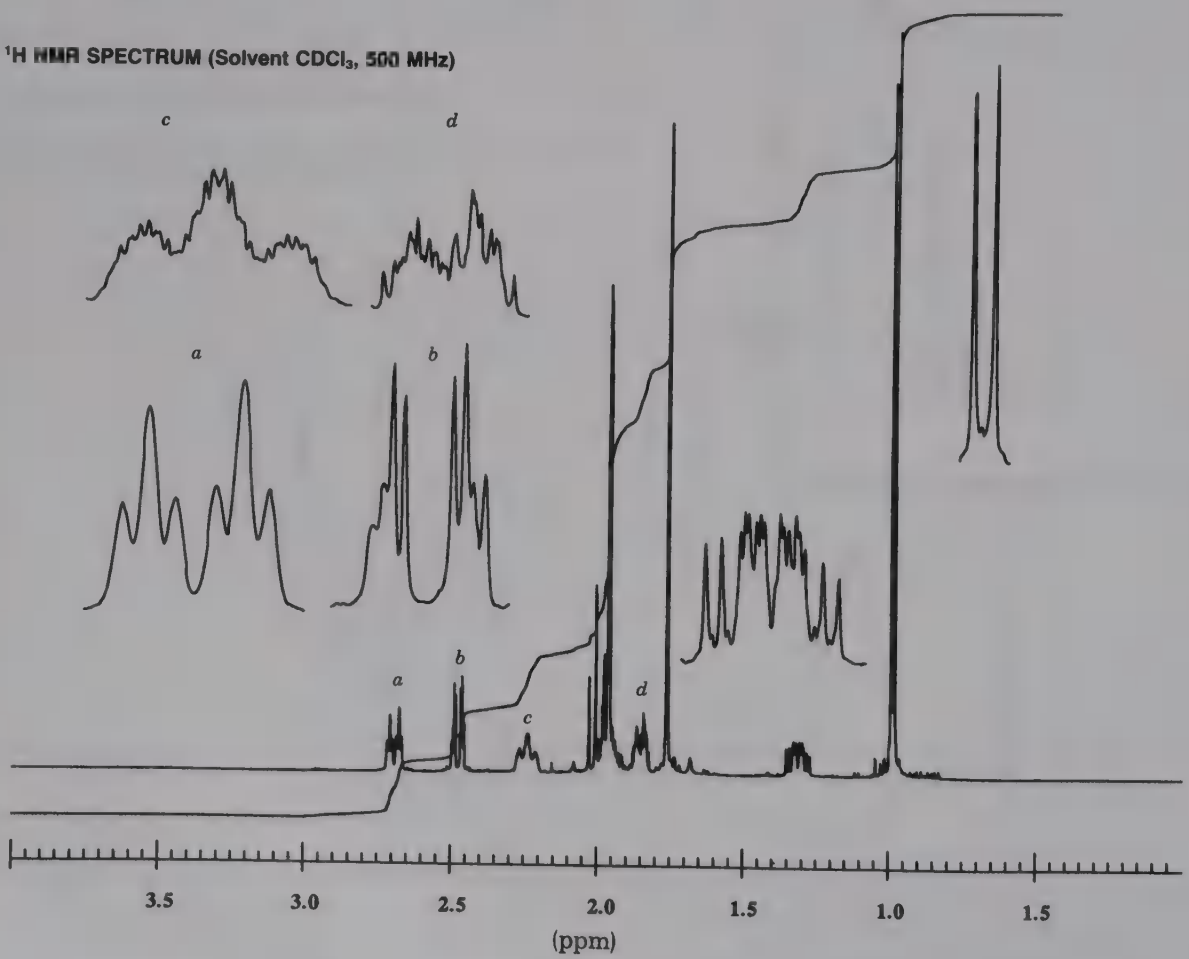

Compound 9.53 (continued)

^{13}C NMR SPECTRUM (Solvent $CDCl_3$, 25 MHz)

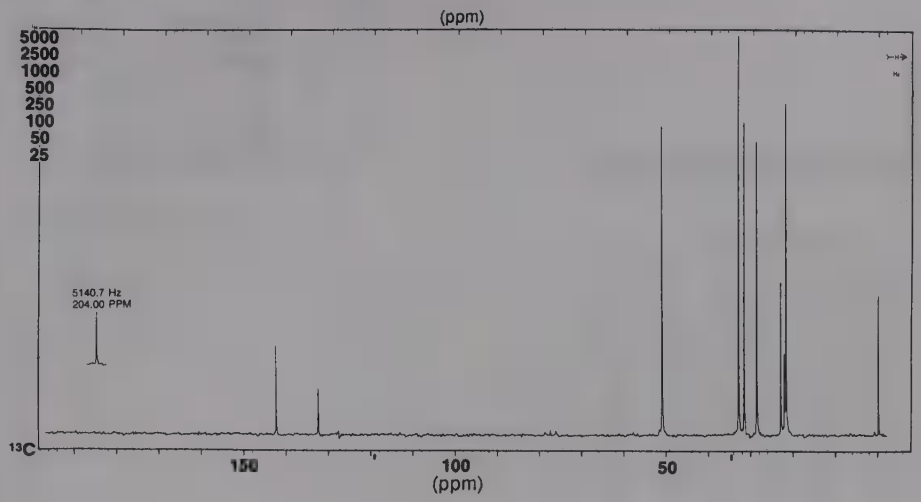

^{13}C NMR Data	
δ	
21.7	CH_3
21.8	CH_3
22.7	CH_3
28.5	CH_2
31.4	CH
32.9	CH_2
50.7	CH_2
131.7	C
140.8	C
204.0	C

H C COSY (HETCOR)

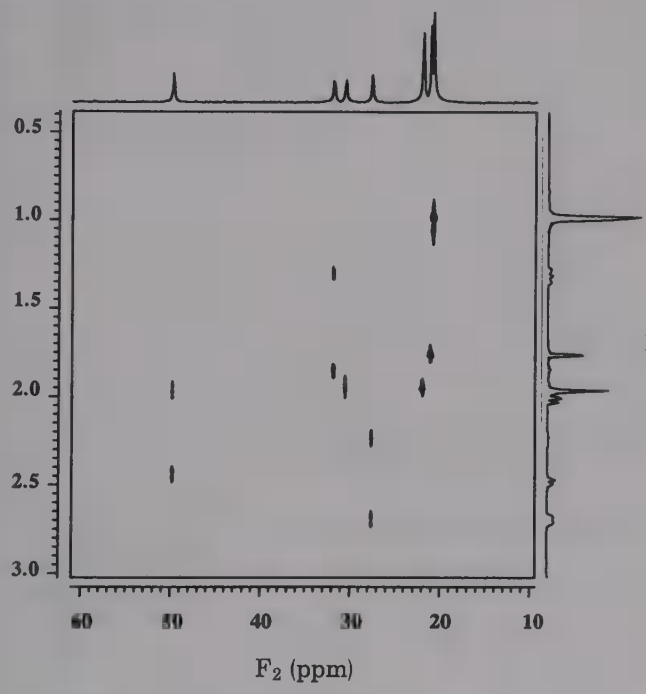

H CH COSY

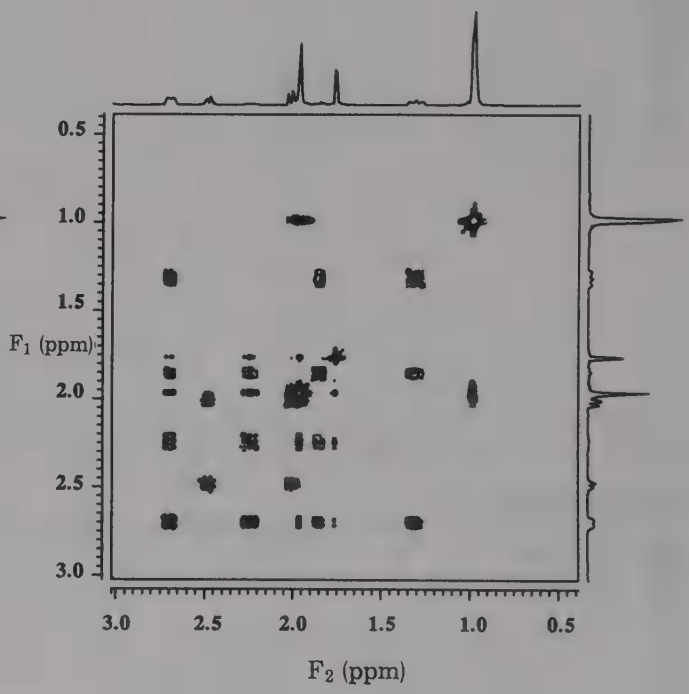

Compound 9.54

MASS SPECTRAL DATA (Relative Intensities)

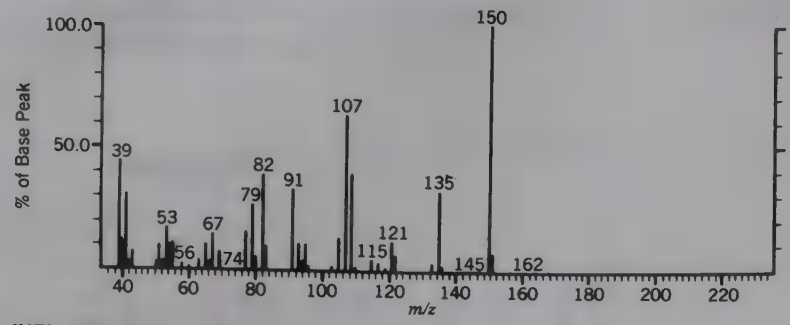

FM (found) = 150.1049

Ultraviolet Data

$\lambda_{max}^{CH_3CH_2OH}$ (nm)	log ϵ_{max}
243	4.00
277	3.90

INFRARED SPECTRUM

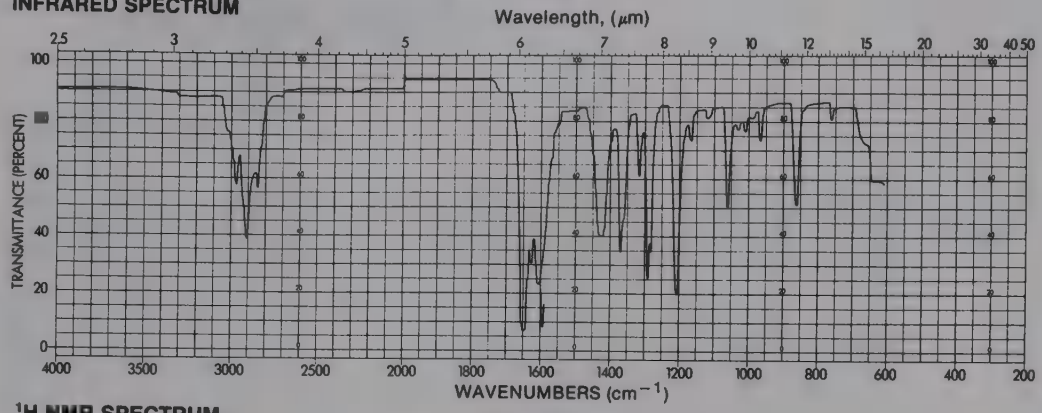

^{1}H NMR SPECTRUM

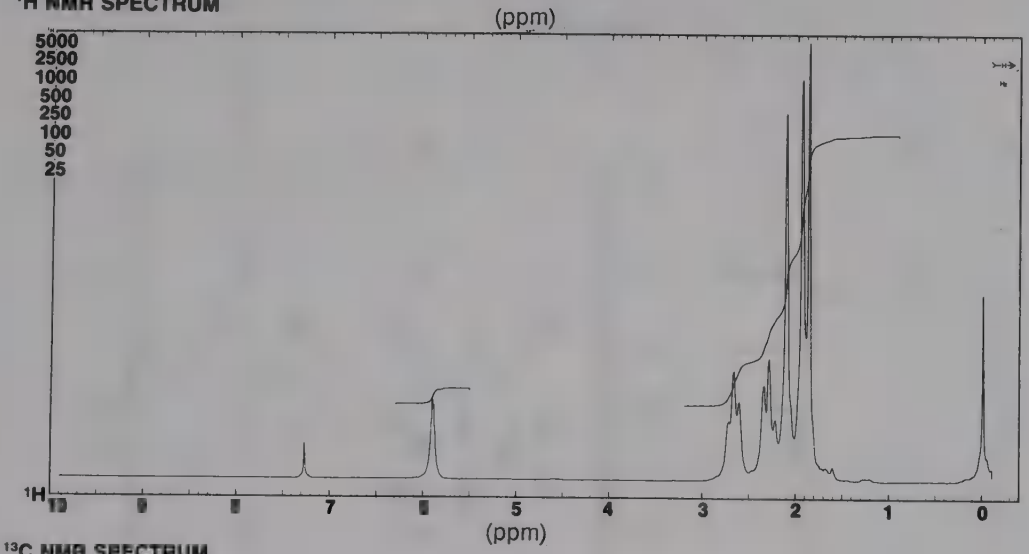

^{13}C NMR SPECTRUM

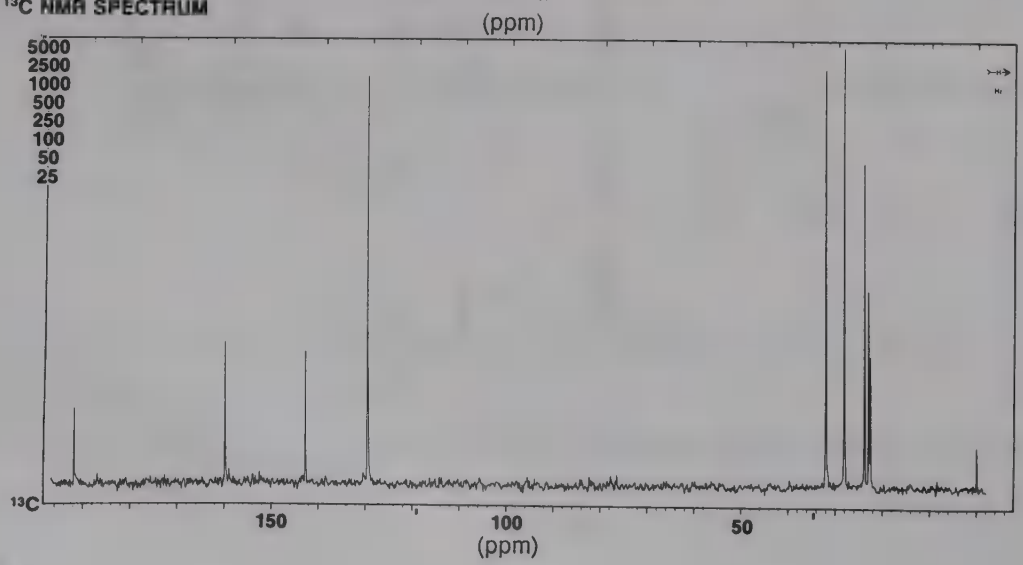

^{13}C NMR Data ($CDCl_3$ Solvent)

δ	
22.4	CH_3
22.7	CH_3
23.7	CH_3
28.0	CH_2
31.8	CH_2
128.8	C
129.0	CH
142.0	C
159.3	C
190.9	C

MASS SPECTRAL DATA (Relative Intensities)

Compound 9.55

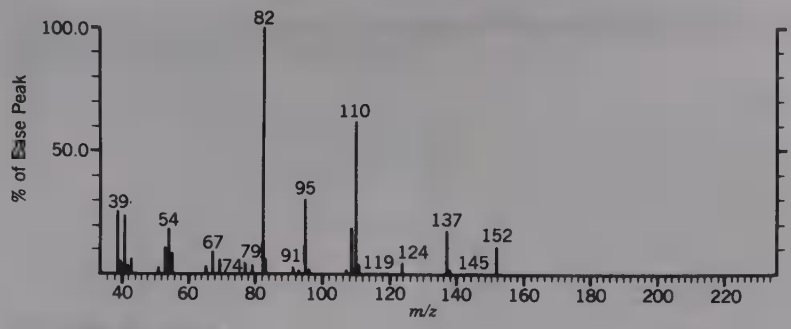

FM (found) = 152.1200

Ultraviolet Data	
$\lambda_{max}^{CH_3CH_2OH}$ (nm)	ϵ_{max}
232.5	13,350

INFRARED SPECTRUM

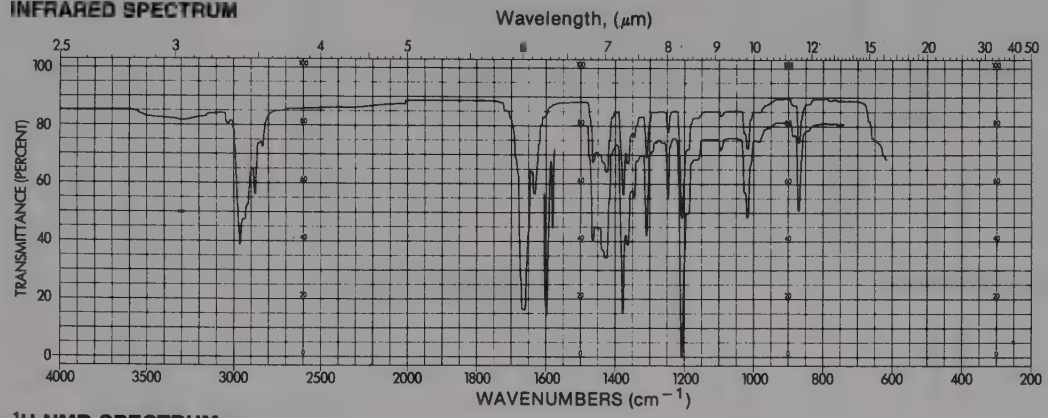

^{1}H NMR SPECTRUM

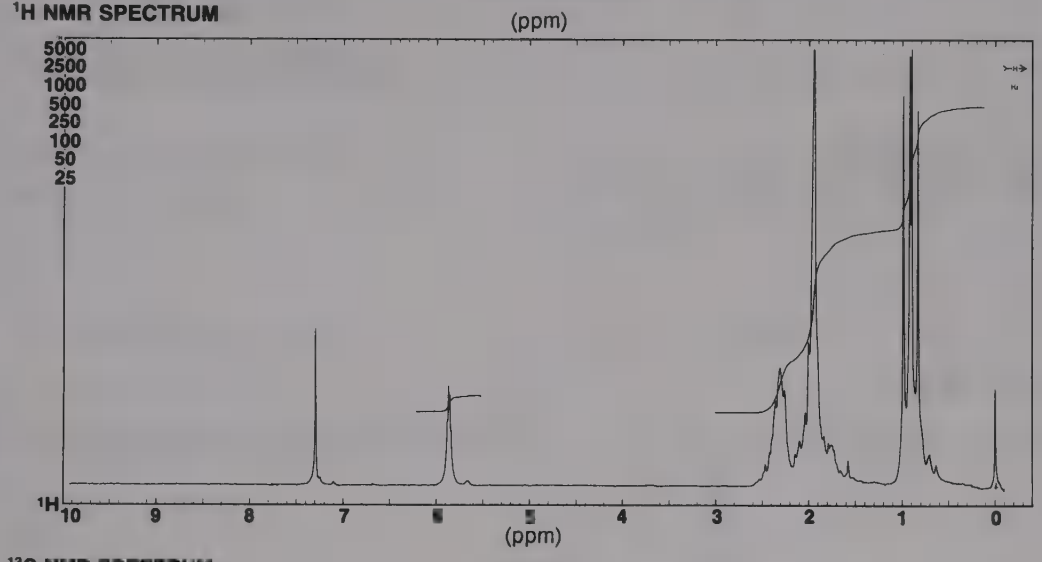

^{13}C NMR SPECTRUM

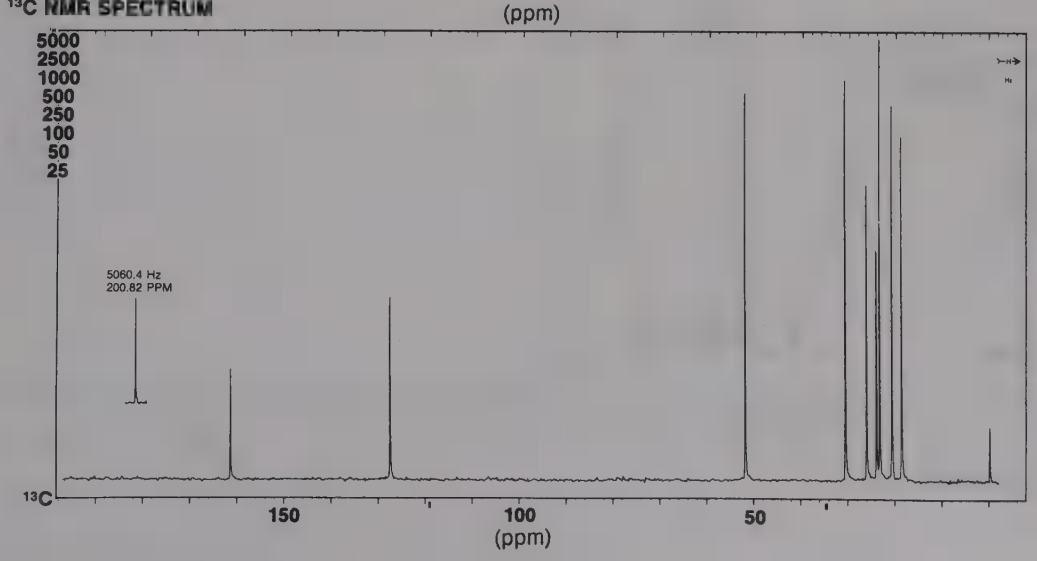

^{13}C NMR Data	
δ	
18.5	CH_3
20.6	CH_3
23.2	CH_2
23.9	CH_3
25.9	CH
30.5	CH_2
51.6	CH
126.8	CH
160.5	C
200.0	C

Compound 9.56

INFRARED SPECTRUM

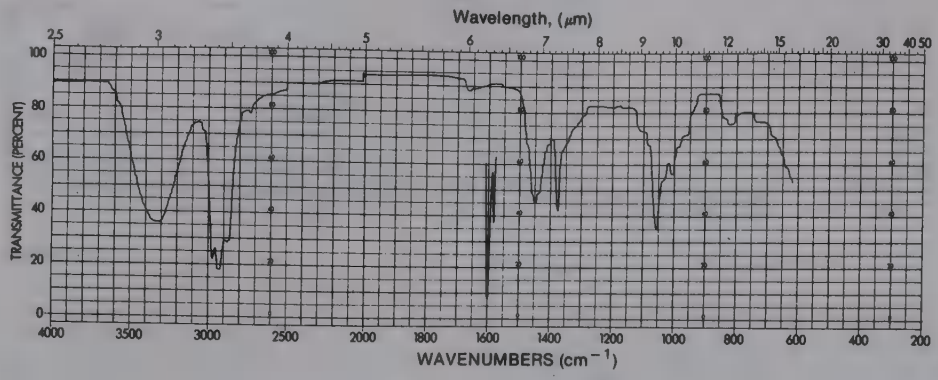

MASS SPECTRAL DATA (Relative Intensities)

FM (found) = 156.1513

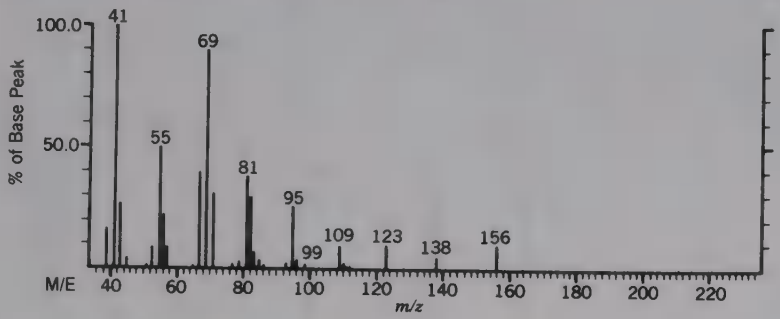

Ultraviolet Data

Transparent above 210 nm

^{1}H NMR SPECTRUM (Solvent $CDCl_3$, 600 MHz)

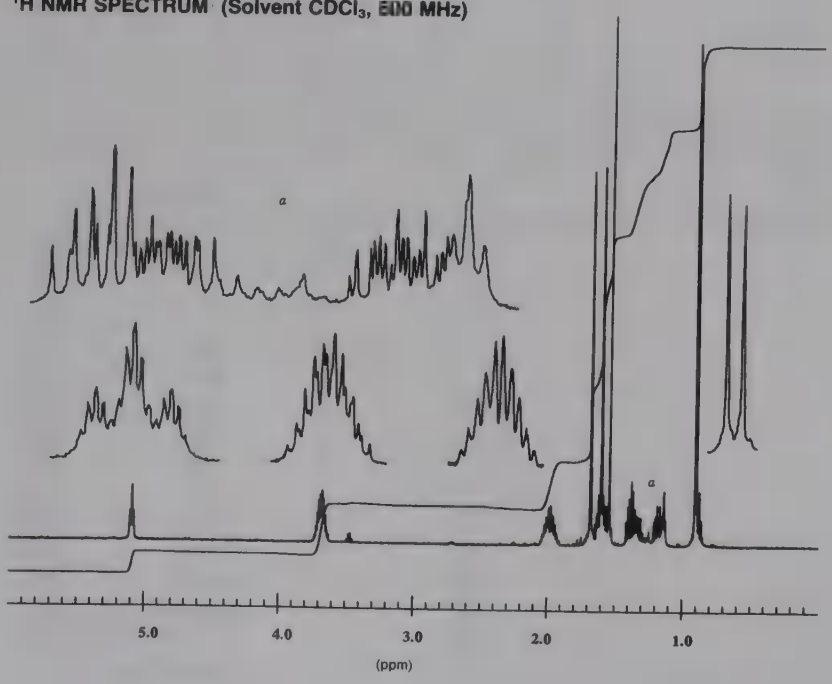

N-H 3300 - 3500
C-N 1180 - 1360
C≡N 2210 - 2260
-NO2 1515 - 1570
1345 - 1385

Compound 9.56 (continued)

^{13}C NMR SPECTRUM

^{13}C NMR Data	
δ	
17.6	CH_3
19.6	CH_3
25.6	CH_2
25.7	CH_3
29.4	CH
37.4	CH_2
39.8	CH_2
60.2	CH_2
125.0	CH
130.7	C

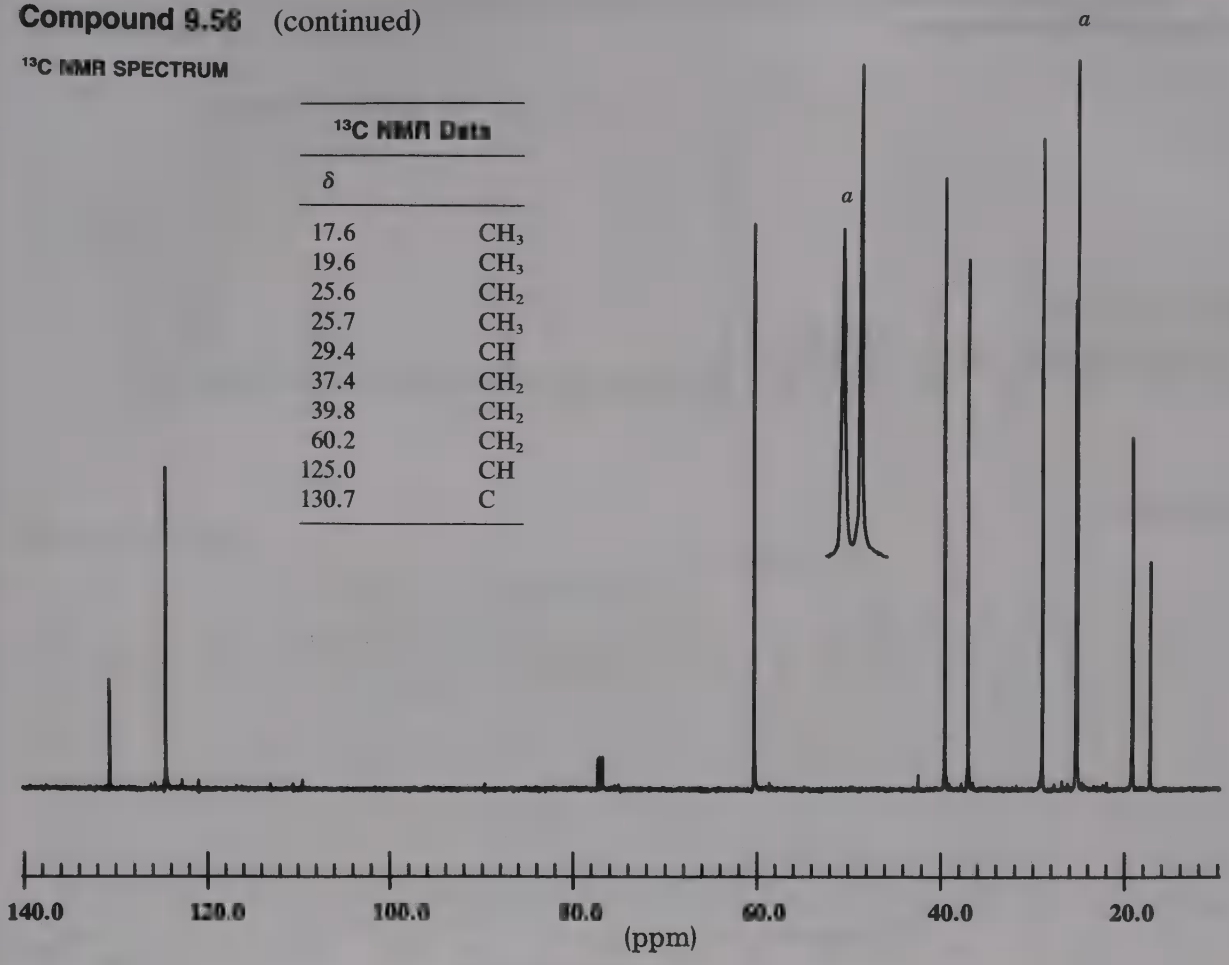

H C COSY (HETCOR)

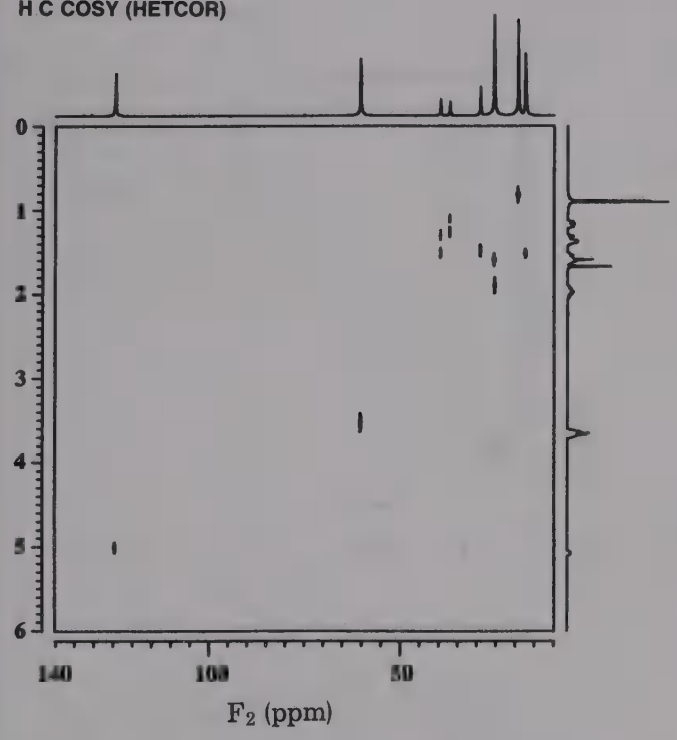

H H COSY

MASS SPECTRAL DATA (Relative Intensities)

Compound 9.57

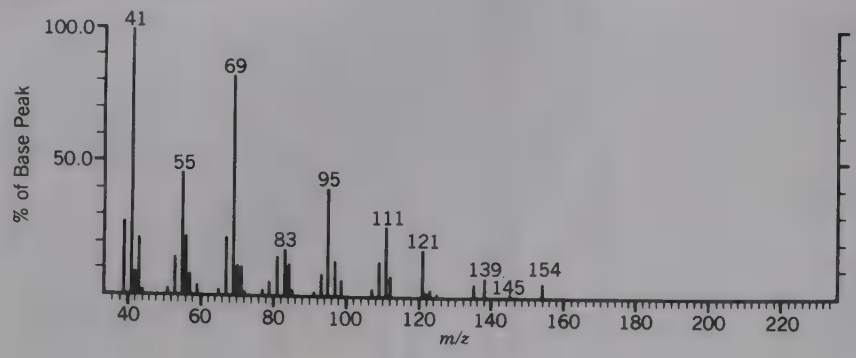

FM (found) = 154.1356

Ultraviolet Data	
$\lambda_{max}^{CH_3CH_2OH}$ (nm)	ϵ_{max}
290	12

INFRARED SPECTRUM

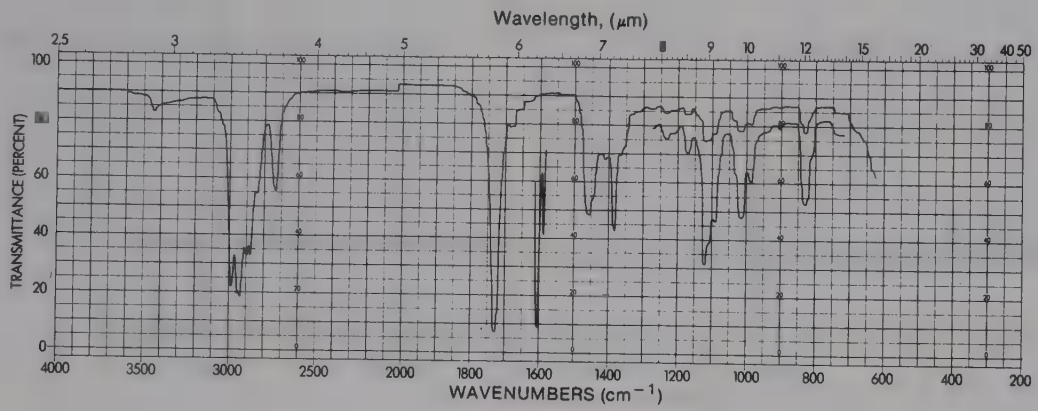

C-O 1080 - 1300

C=O 1690 - 1760

O-H 3610 - 3640

O-H H Bonded 3200 - 3600

COOH 2500 - 3000

^{1}H NMR SPECTRUM (Solvent $CDCl_3$, 100 MHz)

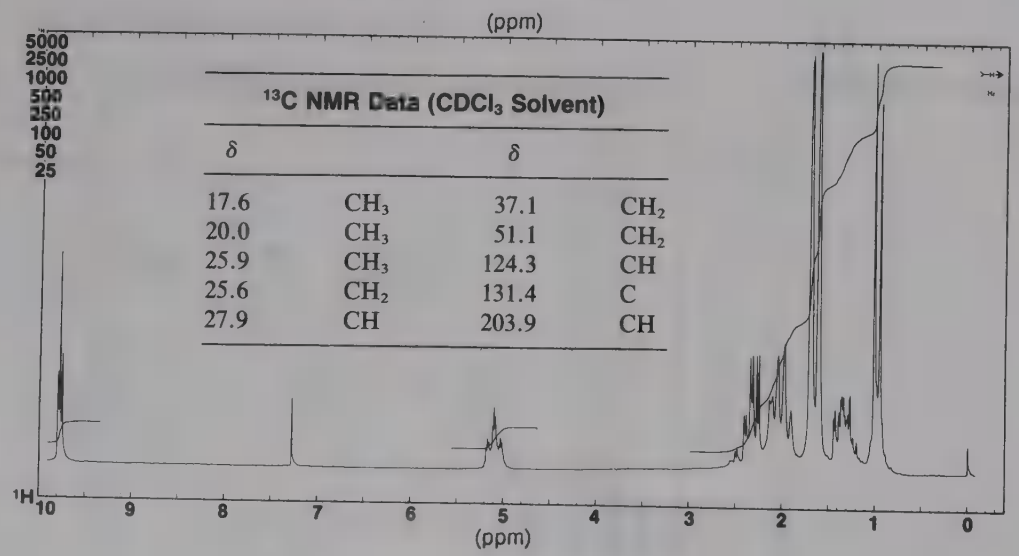

^{13}C NMR Data ($CDCl_3$ Solvent)

δ		δ	
17.6	CH_3	37.1	CH_2
20.0	CH_3	51.1	CH_2
25.9	CH_3	124.3	CH
25.6	CH_2	131.4	C
27.9	CH	203.9	CH

MASS SPECTRUM (Chemical Ionization)

Compound 9.58

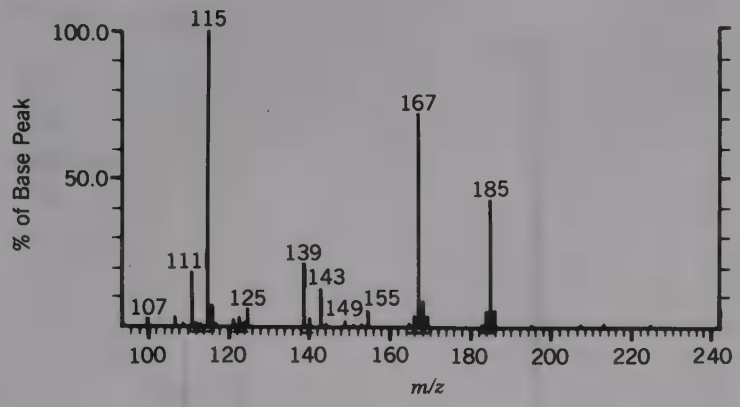

FM (found) = 184.1103 (EI)

Ultraviolet Data
Transparent above 210 nm

INFRARED SPECTRUM

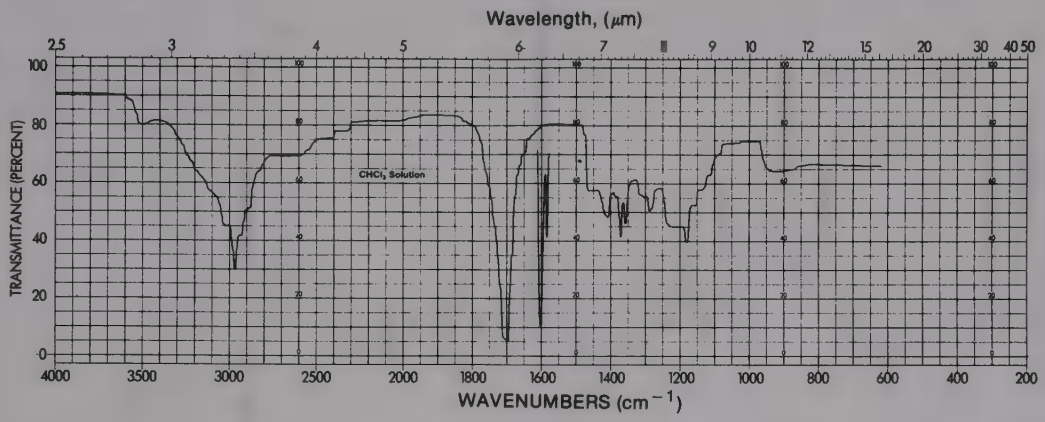

continued on p. 410

Compound 9.58 (continued)

^{1}H NMR SPECTRUM (Solvent $CDCl_3$, 500 MHz)

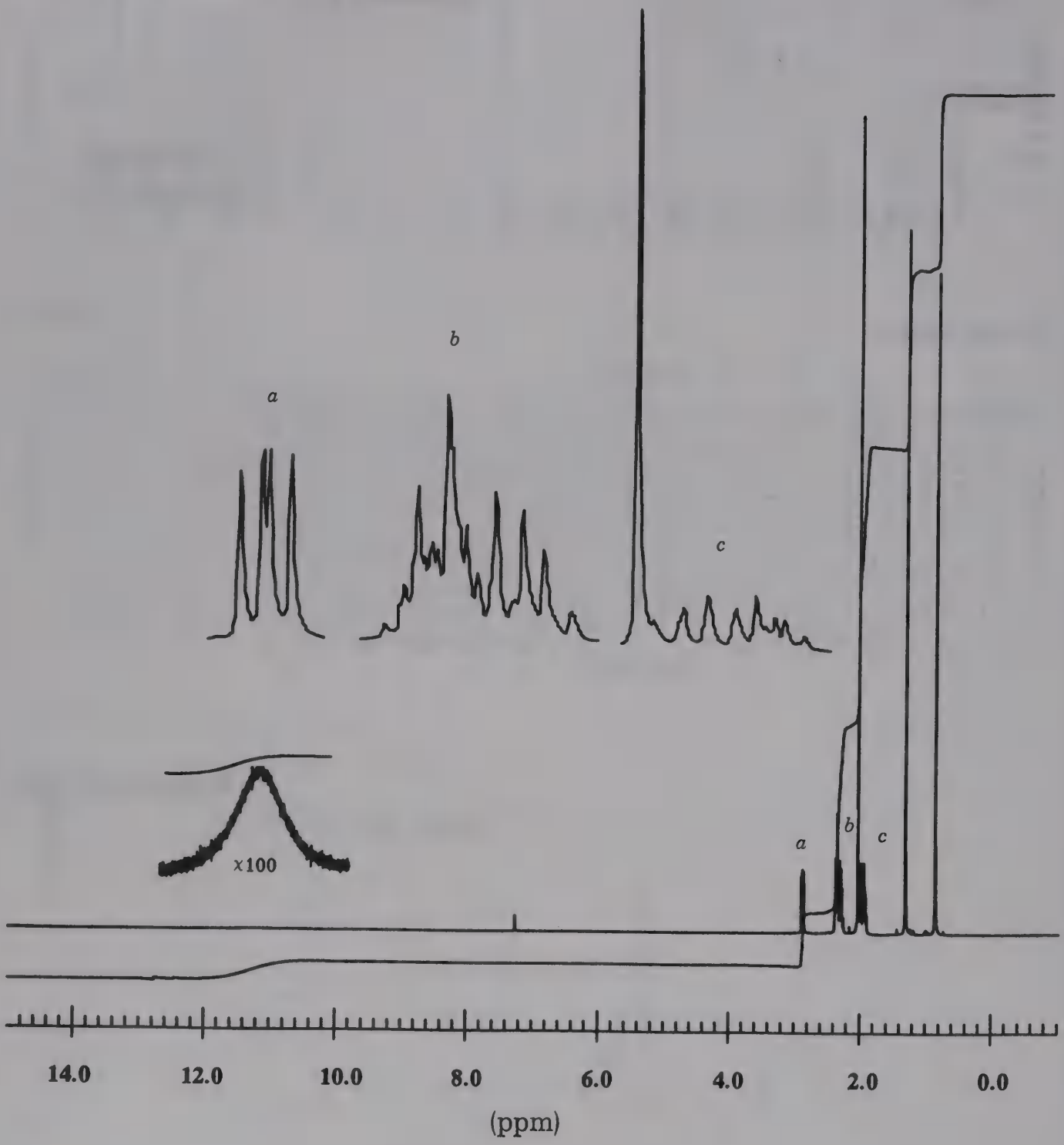

Compound 9.58 (continued)

^{13}C NMR SPECTRUM

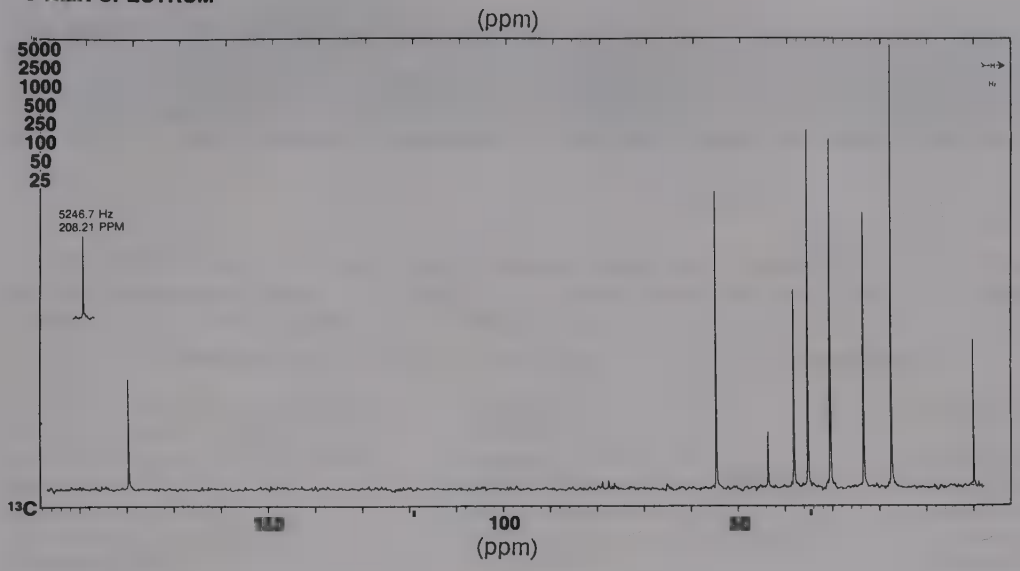

H,H COSY

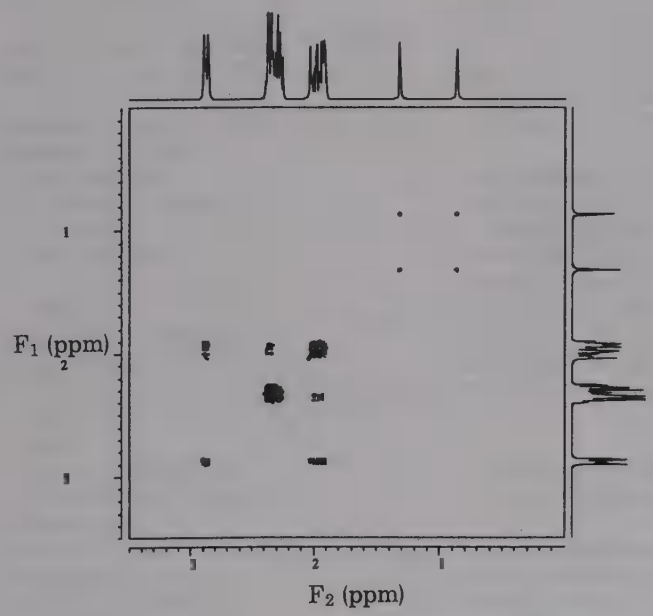

C-H ALKANES 2850 - 2960
1350 - 1470

= 3020 - 3080
675 - 1000

O 3000 - 3100
675 - 870

≡ 3300

C=C = 1640 - 1680

C≡C 2100 - 2250

C=C O 1500, 1600

SUBJECT INDEX

Key: **^{13}C NMR** = Carbon −13 nuclear magnetic resonance spectrometry (Chapter 5); **2D NMR** = Two dimensional nuclear magnetic resonance spectrometry (Chapter 6); **^{1}H NMR** = Proton nuclear magnetic resonance spectrometry (Chapter 4); **MS** = Mass spectrometry (Chapter 2); **UV** = Ultraviolet spectrometry (Chapter 7)

References for complete spectra or spectral data of specific compounds are listed in the Compound Index.

COMPOUND INDEX

For some of the compounds below, complete spectra (of the type denoted in **boldface**) are referenced. Major exceptions are **UV** and **^{13}C NMR** entries. For most of the **UV** entries the λ_{max} and ε_{max} for the major bands are referenced. For many of the ^{13}C entries, shifts for carbons in the molecule are referenced. Listings of compounds in tables, charts and appendixes should also be consulted for additional information.

Printed in Singapore by
Chong Moh Offset Printing Pte Ltd

SIMON
WELCH

This Wiley International Edition is part of a continuing program of paperbound textbooks especially designed for students and professional people overseas. It is an unabridged reprinting of the original edition, which is also available from your bookseller.

Wiley International Editions include titles in the fields of:

Agricultural Engineering & Agriculture
Biochemistry
Biology
Business Administration
Chemistry
Civil Engineering
Chemical Engineering
Computers & Data Processing
Earth Sciences
Economics
Electrical Engineering
Engineering Mechanics
Geography
Industrial Engineering
Mathematics
Materials Engineering
Mechanical Engineering
Medicine
Physics
Physical Chemistry
Polymer Science & Technology
Probability & Statistics
Psychology
Vocational-Technical

JOHN WILEY & SONS, Inc.
NEW YORK • CHICHESTER • BRISBANE • TORONTO • SINGAPORE